CONF-950572--



INTERGAS '95

International Unconventional Gas Symposium

PROCEEDINGS

May 14-20, 1995

Bryant Conference Center & Hotel
The University of Alabama
Tuscaloosa, Alabama U.S.A.



International Unconventional Gas Symposium
May 14-20, 1995
Bryant Conference Center & Hotel
Tuscaloosa, Alabama
U.S.A.

Sponsored by

- **The University of Alabama**
  College of Continuing Studies
  School of Mines and Energy Development
- **Gas Research Institute**
- **U.S. Environmental Protection Agency**
- **U.S. Department of Labor**
  Mine Safety and Health Administration
- **Geological Survey of Alabama**
- **U.S. Department of Energy**

DISCLAIMER

This report was prepared as an account of work sponsored by an agency of the United States Government. Neither the United States Government nor any agency thereof, nor any of their employees, make any warranty, express or implied, or assumes any legal liability or responsibility for the accuracy, completeness, or usefulness of any information, apparatus, product, or process disclosed, or represents that its use would not infringe privately owned rights. Reference herein to any specific commercial product, process, or service by trade name, trademark, manufacturer, or otherwise does not necessarily constitute or imply its endorsement, recommendation, or favoring by the United States Government or any agency thereof. The views and opinions of authors expressed herein do not necessarily state or reflect those of the United States Government or any agency thereof.

DISCLAIMER

Portions of this document may be illegible in electronic image products. Images are produced from the best available original document.

TABLE OF CONTENTS

• Geology & Resources

9501

Coalbed Methane Potential for Alaska and Drilling Results for the Upper Cook Inlet Basin
T.N. Smith, Division of Oil & Gas, Department of Natural Resources, State of Alaska 1

9502

Coalbed Gas Potential of the Greater Green River Basin, Southwest Wyoming and Northwest Colorado
R. Tyler, W.R. Kaiser, A.R. Scott and D.S. Hamilton, Bureau of Economic Geology, The University of Texas at Austin 23

9508

Thin-Skinned Structures Influence Gas Production in Alabama Coalbed Methane Fields
J.C. Pashin, Geological Survey of Alabama; R.H. Groshong, Jr. and S. Wang, The University of Alabama 39

9515

Delineation of Piceance Basin Basement Structures Using Multiple Source Data: Implications for Fractured Reservoir Exploration
T.E. Hoak and A.L. Klawitter, Advanced Resources International, Inc. 53

9516

Gas- and Water-Saturated Conditions in the Piceance Basin, Western Colorado: Implications for Fractured Reservoir Detection in a Gas-Centered Coal Basin
T.E. Hoak and A.D. Decker, Advanced Resources International, Inc. 77

9517

Integrated Exploration Strategy for Locating Areas Capable of High Gas Rate Cavity Completion in Coalbed Methane Reservoirs
A.L. Klawitter, T.E. Hoak, and A.D. Decker, Advanced Resources International, Inc. 97

9549

Characteristics and Economics of Coalbed Methane Production from the Fort Union Formation, Powder River Basin
J.R. Holland, J.R. Holland & Associates, Inc.; and J.W. Kimmons, Torch Operating Company 115

9514

Reconnaissance of Gas Contents and Geological Aspects of the Coalbed Methane Resources in Pennsylvania
A.K. Markowski, Pennsylvania Geological Survey **125**

• Mine Degasification & Safety

9530

The Use of Coalbed Methane Simulators for Coal Mining-Related Applications
M.D. Zuber and M. Semmelbeck, S.A. Holditch & Associates, Inc. **141**

9555

Role of Longwall Gob Formation in Coalbed Methane Emission
S. Patton, Montana Technological University; Y. Jiang, D. Deb, T. Novak, and D. Park, The University of Alabama..... **151**

9538

Evaluation of Methane Drainage from Mining Panel
Kotaro Ohga, Kiyoshi Higuchi, Hokkaido University; Souhei Shimada, University of Tokyo; and Gotai Deguchi, Coal Research Center, Japan **163**

9543

Methods for Forecasting and Reducing Gas Emission in Mine Workings: Improving the Coal Mining Safety
I.V. Sergeev, Skochinsky Institute of Mining, and E.Y. Dikolenko, Rosugol Company, Russia..... **173**

9542

Economical Aspects of Coalbed Methane Extraction and Utilization by Coal Mines in the CIS
V.I. Serov, Skochinsky Institute of Mining, Russia..... **179**

9537

Coal Seam Methane Drainage Through Surface Boreholes
O.I. Kasimov and A.I. Bukhantsov, Makeevka Safety in Mines Research Institute; and V.V. Kasyanov, MakeevkaUgol, Ukraine..... **185**

9504

Sudden Methane Rushes Through the Roadway Floor
I. Bolshinsky, Argonne National Laboratory; A. Morev and S. Kloisner, Makeevka Safety in Mines Research Institute, Ukraine..... **189**

9546

Sudden Methane Outbursts in Mine Workings and Their Prevention by Degassing Methods
Y.L. Khoudin, Skochinsky Institute of Mining, Russia 197

9521

A Brief Overview of the Potential for Development of Coalbed Methane in China
L. Lottman-Craigg, C. Bibler and R.C. Pilcher, Raven Ridge Resources, Incorporated; M. Sun, S. Huang and C. Zhu, Institute of Coal Scientific and Technical Information, Ministry of Coal Industry, People's Republic of China 203

Alternate Paper
9544

Methods and Experience in Intensive Coalbed Methane Recovery at Coal Mines in the CIS
V.S. Zabourdyaev, Skochinsky Institute of Mining, Russia 207

• Well Testing & Completion/Recovery Technology/Innovative Technology

9519

In-Situ Determination of Relative Permeability in Coal Seams Using a Two-Phase Well-Testing Tool
R.A. Koenig, In-Situ, Inc.; S.K. Choi and K.T.A. Meaney, CSIRO Australia 219

9539

The Effect of Fracturing Fluid Damage on Production from Hydraulically Fractured Wells
M.W. Conway, Stim-Lab, Inc.; and R.A. Schraufnagel, Gas Research Institute 229

9533

Openhole Cavity Completions in Coalbed Methane Wells—Modeling of Field Data
M. Khodaverdian, H.H. Vaziri, University of Nova Scotia; I.D. Palmer, Amoco; and J.D. McLennan, TerraTek, Inc. 237

9510

Hydrogeologic Factors Affecting Dynamic Open-Hole Cavity Completions in the San Juan Basin, USA
A.R. Scott and W.R.Kaiser, Bureau of Economic Geology, The University of Texas at Austin 247

9560

Simulation of Coalbed Methane Enhanced Recovery Using Gas Potential and a New Saturation Equation
O.A. Almisned, University of Oklahoma; and R.L. Thrasher, Louisiana Tech University 259

9556

A Micro-Pilot Approach to Coalbed Methane Reservoir Assessment
R. Puri, R. Volz and D. Duhrkopf, Amoco 265

9550

Treatment of Fruitland Coal Production Water with Ion Exchange Media
C. Russell, Agua Vida; and C.P. Richardson, New Mexico Tech, NM 275

9559

The Economics of Converting Coalbed Methane Gas Directly into Liquids
Q. Adams, Earth Resources Technology Services 287

• International Developments

9520

Coalbed Methane Resources in the Carboniferous of Nova Scotia: Canada—An Overview and Update
D.J. MacDonald, Department of Natural Resources, Province of Nova Scotia 297

9505

Evaluation of Coalbed Methane Potential of the Stellarton Basin, Nova Scotia, Canada, Based on Geological, Physical, and Geochemical Properties
P.K. Mukhopadhyay, Global Geoenergy Research Ltd., Nova Scotia; D.J. MacDonald and J.H. Calder, Nova Scotia Department of Natural Resources 311

9506

The Status of Coalbed Methane Research and Development in Australia
J.R. Enever, CSIRO Australia 321

9531

Coalbed Methane Development in the Galilee Basin of Central Queensland, Australia
M.R. Herrington, ENRON Exploration Australia Pty Ltd; and M. Zebrowitz, Advanced Resources International, Inc. 331

9534

Coalbed Methane of the Damodar Valley Coal Fields—Bihar and West Bengal, India
J.L. Cooper, Amoco India Petroleum Company; and P. Kumar, Central Mine Planning and Design Institute, Ranchi, Bihar **341**

9522

Opportunities for the Development and Utilization of Coalbed Methane in Three Coal Basins in Russia and Ukraine
J.S. Marshall, R.C. Pilcher and C.J. Bibler, Raven Ridge Resources, Incorporated **351**

9557

Coalbed Methane Recovery in the Czech Republic
G. Takla, J. Bezdek and Z. Vavrusak, Underground Exploration and Mine Safety, Inc., The Czech Republic **361**

9562

The Resource and Exploration of Coalbed Methane in China
Su Xiaopeng, Natural Gas Laboratory, China National Petroleum Corporation, People's Republic of China **369**

• Reservoir Characterization/Coal Science

9525

Quantitative Evaluation of Coal Seam Gas Content Estimate Accuracy
M.J. Mavor, Tesseract Corporation; T.J. Pratt, Geologic Consultant; and C.R. Nelson, Gas Research Institute **379**

9523

Analysis of Sorption and Thermodynamic Data and a Discussion of an Empirical Model for Sorbed Gases in Coal
J.C. Huddleston, J.S. Marshall and R.C. Pilcher, Raven Ridge Resources, Incorporated **389**

9503

Methane Adsorption on Coals of the Bowen Basin, Queensland, Australia
J. Killingley, J. Levy and S. Day, CSIRO Australia **401**

9528

Numerical Modelling and Verification of Stress and Pore Pressure Dependent Dynamic Permeability Behaviour of Coal Seams Around Wellbores
S. Durucan, T.S. Daltaban, J.Q. Shi and J.M. Wang, Imperial College of Science, Technology and Medicine, Royal School of Mines, England **413**

9509
Limitations and Benefits of Microbially Enhanced Coalbed Methane
A.R. Scott, Bureau of Economic Geology, The University of Texas at Austin **423**

9529
On the Type of Generation and Storage of Coalbed Methane Reservoir
Zhang Xinmin and Zhong Lingwen, Central Coal Mining Reseach Institute, Xian Branch, People's Republic of China **433**

9507
Methane Seeps in the San Juan Basin: Potential Pathways
S.A. Marinello and J.C. Quinn, Colorado School of Mines **441**

9535
Secondary Mineralisation and Its Effect on Coal Permeability
P.J. Tarabbia, J.K. Warren, West Australia Centre for Petroleum Exploration, Curtin University; and P.D. Gamson, CSIRO Australia **451**

9564
Structurally Controlled and Aligned Tight Gas Reservoir Compartmentalization in the San Juan and Piceance Basins
A.D. Decker, V.A. Kuuskraa and A.L. Klawitter, Advanced Resources International, Inc. **461**

• Environmental/Legal & Regulatory

9511
A Comprehensive Assessment of the Potential to Reduce Methane Emissions from U.S. Coal Mines
K. Schultz, Coalbed Methane Outreach Program, U.S. Environmental Protection Agency **477**

9551
Development and Utilization Strategies for Recovery and Utilization of Coal Mine Methane
C.W. Byrer, A.W. Layne and H.D. Guthrie, U.S. Department of Energy, Morgantown Energy Technology Center **483**

9513
Recent Federal Initiatives to Promote Unconventional Gas: High Octane Delivery or Just Hot Air?
M.T. Griff, Berkowitz, Lefkovits, Isom & Kushner, A Professional Corporation **489**

9540

Energy and Environmental Policy Options to Promote Coalbed Methane Recovery
J.L. Lewin, Widener University School of Law 497

9545

Mine Methane and Environment: Ways of Methane Utilization
E.A. Yelchainov, Skochinsky Institute of Mining, Russia 509

9552

Evolution of Severance Tax Policy by Litigation: The Coalbed Methane Industry vs. The State of Alabama
C.D. Haynes, The University of Alabama; and K.P. Hanby, Tom Joiner and Associates 513

9563

Degassing of Methane Bearing Geologic Structures in the Donbass Coal Basin by the Donetsk Coal Association
V.V. Pudak, Donetskugol Coal Association, Ukraine 517

9554

Technical and Economic Feasibility of Coalbed Methane Production and Utilization in the Ukraine
V.L. Saprykin, Gas Institute, Academy of Sciences, Ukraine; Y.A. Boxerman, I.N. Karp and A.I. Pyatnichko, Academy of Sciences of Ukraine 531

9512

International Prospects for Coalbed Methane Recovery at Coal Mines: An Overview of Methane Emissions, Recovery Practices and Key Opportunities
D.W. Kruger, Methane Energy Programs, U.S. Environmental Protection Agency 541

Author Index 557

Committees 559

Advertisements 561

Proceedings Order Form 567

INTERGAS '95

May 15-19, 1995
The University of Alabama
Tuscaloosa, Alabama USA

9501

Coalbed Methane Potential for Alaska and Drilling Results for the Upper Cook Inlet Basin

T.N. Smith, Division of Oil & Gas, Department of Natural Resources, State of Alaska

ABSTRACT

Alaska's estimated coal reserves exceed 5.5 trillion short tons or nearly 1/2 of the U. S. total. Based on analysis performed during this study, I have concluded that these coals could contain up to 1,000 tcf of gas. Most of these coals range in age from Cretaceous to Tertiary and rank from bituminous to subbituminous. This study uses coal rank, present-day burial depth, seam thickness and structure as criteria to evaluate thirteen of Alaska's most promising coal basins. Much of the Cook Inlet, Susitna, North Slope, Middle Tanana, Nenana, Yukon Flats, North Aleutian, Seward Peninsula, and Copper River Basins contain thermally immature coals (Ro<0.5%) with low methane potential. The Upper and Lower Koyukuk, Kobuk, Gulf of Alaska, and the Alaska Peninsula Basins contain bituminous coals with moderate potential for local gas usage. Thermal maturity and coal isopach maps indicate that the Matanuska Valley area of the Cook Inlet Basin and the western foothills belt of the North Slope Basin contain abundant, bituminous, coalbeds up to 50 feet (15 m) thick. These coals have high potential for methane production at depths between 500 and 6,000 feet (150 and 1,800 m). Gas content of coal seams from the first core hole (AK-94CBM-1) drilled in the state to evaluate coalbed methane support this conclusion for the northern portion of Cook Inlet Basin. Coals penetrated by this well show increasing gas content with depth ranging from 63 scf/ton (1.96 cc/g) at 521 feet (159 m) to 245 scf/ton (7.66 cc/g) at 1,236 feet (377 m) on a dry, ash free basis.

INTRODUCTION

Alaska contains vast, lightly explored coal resources that underlie approximately 9% of the land area (Figure 1). Hypothetical coal resources exceed 5.5 trillion short tons, about half of the total United State's coal resources [1]. Most of the coal is Cretaceous to Tertiary in age and bituminous to subbituminous in rank. The North Slope and Cook Inlet Basins contain both subbituminous and bituminous rank coals and constitute the largest coal resources in the state (Figures 1 and 2). The Upper and Lower Koyukuk, Kobuk, Alaska Peninsula and the Gulf of Alaska Basins all contain bituminous coals (Figures 1 and 2). Subbituminous and lignite coals are found in the Susitna, Middle Tanana, Nenana, North Aleutian, Seward Peninsula and Copper River Basins (Figures 1 and 2).

Near-surface coal has been commercially utilized and studied in Alaska for over 100 years and most of the surface coal occurrences have been mapped and studied. Deep coal resources have received considerably less attention. This study focuses on the coal at deeper depths. Information from petroleum production and exploration wells, gravity surveys and surface studies are integrated to provide a coalbed methane resource estimate for Alaska and coalbed methane potential for Alaska's coal basins. Since gas content analyses are available only for the State of Alaska core hole (AK-94CBM-1) in Cook Inlet Basin, established indirect methods using data such as depth, rank and composition [2, 3 and 4] were used to estimate Alaska's coalbed methane resource. The available data suggests that Alaska's coal could contain over 1,000 trillion cubic feet (tcf) of gas. If only 10% is recoverable, the resource would triple the current proven conventional gas reserves for Alaska.

NORTHERN ALASKA PROVINCE

The Northern Alaska Province (North Slope)(Figure 3) contains the largest coal resource in Alaska with hypothetical reserves of 4 trillion short tons [1]. The coals underlie a 400 mile long by 150 mile (640 km by 240 km) wide area (approximately 60,000 square miles (154,000 sq km)). While coals range in age from Mississippian to Tertiary, the primary coal resources occur in the Lower Cretaceous Corwin Formation of the Nanushuk Group (Figure 4).

The North Slope is one of the most thoroughly explored basins in Alaska. Coal was exploited by whaling ships in the late 1800's along the Chukchi Sea coast and the first coal investigation was conducted by Collier [5] in 1906 in that same area. Early explorers also occasionally exploited natural oil seeps for fuel. Oil and gas exploration was initiated in 1919 by geologists of the U. S. Geological Survey and it was this early survey work that led to the

establishment of the Naval Petroleum Reserve No. 4 (now National Petroleum Reserve in Alaska (NPRA)) in 1923. Between 1943 and 1953, early exploratory drilling by the Navy in NPRA found three oil and six gas accumulations. In 1967, the super giant Prudhoe Bay Field was discovered in the central North Slope by ARCO-Humble. This field is now expected to yield 12 billion barrels of oil and eventually over 23 tcf of gas.

The North Slope data base includes more than 350 oil and gas exploratory wells, 2,500 development wells and seismic data from near the Canadian border to the Chukchi Sea. Since NPRA was established, systematic geologic investigations have proceeded on the North Slope and the Brooks Range that include mapping and sampling the coals. Extensive coal studies have been done on Native lands in the area west of NPRA, where large, exploitable deposits are located near tidewater, but lack the infrastructure to commence mining operations.

Mississippian Coal

Mississippian coals are found in the Kapaloak Formation on the Lisburne Peninsula and in the regionally extensive Kekiktuk Formation (Figure 4). The Kapaloak Formation outcrops over a 45 mile (72 km) long belt trending north-south across the Lisburne Peninsula (Figure 3) and contains low-volatile bituminous to semianthracite coals up to 11 feet (3.4 m) thick. A minimum of 13 coal beds have been identified in outcrop along 2,200 feet (670 m) of measured section [6] that is extensively faulted and folded [7].

The presence of the Kekiktuk Formation has been documented across most of the North Slope. It has been described in detail from outcrops in the Brook Range [8] and is the primary petroleum reservoir at the Endicott Field located on the east side of the Prudhoe Bay Complex (Figure 3). In the Endicott Field, multiple, thick (greater than 10 feet (3 m)) coal seams with an average Ro of 0.6% occur at depths greater than 9,500 feet (2,900 m)(Figure 5). Several wells in NPRA have encountered coal beds as thick as 5 feet (1.5 m) in the Kekiktuk Formation [9]. Only minor, thin Kekiktuk Formation coal occurrences are found in the Brooks Range outcrop belt.

Coalbed Methane Potential. The structurally complex and high rank Kapaloak Formation coals on the Lisburne Peninsula may provide gas for local village or mining use. The Kekiktuk Formation coals are generally too deep to be viable for coalbed methane production.

Lower Cretaceous Coal

Most of the coal resources in Alaska are found in the Cretaceous Corwin and the Chandler Formations of the Nanushuk Group (Figure 4) [9]. Both the Corwin and Chandler Formations are dominantly nonmarine strata that were deposited in two separate, but simultaneous prograding delta systems (Corwin delta of western NPRA and Umiat delta of eastern NPRA) [10]. The Corwin Formation contains abundant coal seams up to 20 feet (6 m) thick that underlie most of western and central NPRA and extend farther west under the Chukchi Sea [11]. These coal seams have been documented in outcrop along the Kukpowruk River [12] to the west of NPRA and in wells drilled in NPRA. The Kaolak -1 penetrated 255 feet (78 m) of coal in over 4,500 feet (1,370 m) of Nanushuk section and the Meade -1 encountered 130 feet (40 m) of coal in 2,000 feet (610 m) of Nanushuk Group section. Individual coal beds in these wells reach 20 feet (6 m) with up to 26 coal beds exceeding 5 feet (1.5 m) thick. Mapping by Sable and Stricker [9] shows that the coal-bearing interval lies between the surface and 6,000 feet (1,830 m) in western NPRA (Figure 5). In eastern NPRA, the Chandler Formation contains abundant coals similar to those found in the Corwin Formation. The coal-bearing interval of the Chandler Formation is less than 2,000 feet (610 m) deep (Figure 5). Coal rank increases from north to south, to the foothills of the Brooks Range, and also increases with depth. Most of the coal is high-volatile bituminous with a mean Ro of 0.7% [9].

Coalbed Methane Potential. The area of western NPRA, to the Chukchi Sea coast, has high coalbed methane potential and large possible gas reserves (Figure 5). These coals are in a relaxed tectonic stress regime. The area has been uplifted and stripped of overburden which may allow for open fractures and cleats. In the western NPRA area, the depth to the base of the Nanushuk Group coals exceeds 2,500 feet (760 m), placing a substantial portion of the coal section below permafrost. In eastern NPRA, most of the Nanushuk Group coals lie at depths less than 2,000 feet (610 m), placing them near or in the permafrost zone. It is currently uncertain what effects permafrost and cold temperatures will have on gas flow from these coals.

Upper Cretaceous and Tertiary Coal

The Upper Cretaceous Colville Group and the Tertiary Sagavanirktok Formation (Figure 4) contain substantial coal with coaly intervals and coal beds as thick as 50 feet (15 m) [13 and 14]. However, most beds are thinner and lower in rank than the Nanushuk Group coals. The rank of these coals range from lignite A to subbituminous B. The nonmarine Prince Creek Formation of the Colville Group occurs mostly in northeast Alaska and overlies the Nanushuk Group. The Sagavanirktok Formation conformably overlies the Colville Group [15] and occurs generally northeast of NPRA. In NPRA, distribution of the Sagavanirktok Formation is limited to the northeast corner and northern coastal areas, where it reaches a maximum thickness of 1,500 feet (460 m). East of NPRA, the formation thickens to over 7,000 feet (2,130 m) adjacent to the Arctic National Wildlife Refuge (ANWR)(Figure 3).

Coalbed Methane Potential. The Upper Cretaceous and Tertiary coals represent a large, low rank coal resource that probably contain large gas reserves. However, because of the low rank of these coals and cold subsurface

temperatures (permafrost), they have low potential for coalbed methane production.

COOK INLET-SUSITNA PROVINCE

With hypothetical resources exceeding 1.5 trillion short tons, the Cook Inlet-Susitna Province (Figures 2 and 6) constitute the second largest coal resource in the state. The province covers an area of approximately 14,000 square miles (36,000 sq km), which is bounded by the Kenai Mountains to the east, the Aleutian Range to the west, and extends north to the Alaska Range and the Talkeetna Mountains. Unlike many other areas of the state, portions of the Cook Inlet-Susitna Province are road accessible.

The first major commercial oil discovery in Alaska was made 16 miles (26 km) northeast of Kenai (Figure 6) at Swanson River Field in 1957. Subsequent oil and gas discoveries have produced over 1.2 billion barrels of oil and 5.5 tcf of gas. Seismic, well and production data from within the basin provide an extensive data base which greatly decreases coalbed exploration risk. Additionally, Cook Inlet oil and gas production has created an infrastructure which may enable near term gas development.

Cook Inlet Basin

The Cook Inlet Basin is located in the arc-trench gap between the volcanoes of the Alaska-Aleutian Range and the Aleutian trench. Over 25,000 feet (7,600 m) of Tertiary continental deposits unconformably overlie mostly marine Mesozoic rocks [16]. Although coal is found in the entire Tertiary section, the Oligocene to Miocene Tyonek and the Paleocene Chickaloon Formations (Figure 7) have the highest coalbed methane potential. The Tyonek Formation is widespread across Cook Inlet Basin. Large coal fields have been mapped where it crops out on the west side of Cook Inlet. The Chickaloon Formation is limited to the northeast portion of the Cook Inlet Basin.

Cook Inlet Basin forms a large trough with the basin axis located just west of Kenai and roughly paralleling the current shoreline (Figure 6). Because of post-depositional uplift of the basin margins, older rocks with higher thermal maturity are exposed on the basin margins, while rocks of similar age and thermal maturity occur at significant depths along the axis of the basin. For example, an Ro of 0.6% is reached at a depth of 15,000 feet (4,600 m) near the axis of the basin and at 5,000 feet (1,500 m) near the basin edge (Figure 6). Holocene uplift has brought the thick coals of the Tyonek and the Chickaloon Formations near the surface, making some of the onshore areas of the Cook Inlet basin attractive for coalbed methane exploration.

In 1994, the State of Alaska funded a core hole to sample Tyonek Formation coals near Wasilla, located in the northern portion of Cook Inlet Basin. The core hole (AK-94CBM-1) was drilled on a previously identified prospect [17] (Figure 8) located between the towns of Palmer and Houston and near roads and gas pipelines. In this area, the Tyonek Formation is estimated to have a total thickness in excess of 4,000 feet (1,220 m) with cumulative coal thickness exceeding 100 feet (30 m). High-volatile bituminous coals are expected to be present at depths ranging form 500 to 6,000 feet (150 to 1,800 m).

AK-94CBM-1 was drilled to a total depth of 1,245 feet (380 m), continuously coring the Tyonek Formation from the surface casing shoe at 354 feet (380 m) to total depth. Eighteen seams of high-volatile C bituminous coal were encountered with the thickest being 6.5 feet (3.0 m) and a cumulative thickness of 41 feet (12.5 m). Thirteen of these coal seams were sampled for gas content using 38 gas desorption canisters. Gas content ranges from 63 scf/ton (1.96 cc/g) to 245 scf/ton (7.66 cc/g). Gas content and vitrinite reflectance generally increase with depth, while moisture decreases. Coal moisture contents are low, ranging from 9.02% at 521 feet (159 m) to 4.82% at 1,236 feet (377 m). Gas analyses show that carbon isotopes become slightly heavier with depth indicating an increase in the thermogenic/biogenic gas ratio. The range of -49.3 to -43.2 $\delta^{13}C$ for methane encountered here is indicative of coalbed gas that has both biogenic and thermogenic sources. Gas composition is 98% methane with minor amounts of CO_2 and N_2. Due to cost constraints, the drilling program was designed solely to acquire coal samples for analysis and therefore the well was not flow tested. Porosity and permeability measurements have not been obtained. From visual analysis, coal cleat and fracture density is widely spaced with vertical fractures occurring 1 to 3 inches (2.5 to 7.6 cm) apart. Calcite coating was noted on some of the fracture surfaces which may lower effective permeability. Almost no fractures were noted in the clastic rocks. Figure 9 outlines the coal analyses from core samples for this well.

The coal-bearing Chickaloon Formation occurs only in the Matanuska Valley area north of Palmer (Figure 8). These coals have been mined from 1914 to 1968. Geologists with the Bureau of Mines and the U. S. Geological Survey [18] have mapped the extent of these coals in detail using outcrop, mining and core hole data. Most of the coal is confined to the upper 1,400 feet (426 m) of the Chickaloon Formation, which is greater than 3,000 feet (914 m) thick [18]. The coal in the Chickaloon Formation ranges in rank from high-volatile bituminous to anthracite. Coal beds up to 34 feet (10 m) thick and laterally continuous for up to 5 miles (8 km) have been mapped in faulted synclines that increase in structural severity to the east [18 and 19]. The presence of coalbed gas has been documented by mine explosions which occurred in 1937 and in 1957. In the 1937 incident, a violent methane and dust explosion in the Evan Jones Mine, located 12 miles (19 km) north of Palmer, killed 14 men. The 1957 incident was another methane and dust explosion in the same mine, killing 5 men.

Barnes and Payne [18] estimate that over half of the coal reserves lie beneath 1,000 to 2,000 feet (305 to 610 m) of overburden. Bituminous rank coal at shallow depths and the methane gas problems associated with mining combine

to make the Matanuska Valley area highly prospective for coalbed methane production.

Coalbed Methane Potential. High gas content (up to 245 scf/ton at 1,200 feet (366 m) deep) and large coal resources (hypothetical coal resources exceeding 1.5 trillion short tons), indicate that Cook Inlet Basin contains large gas reserves. Conventional gas production, infrastructure and a local market make near term coalbed gas production possible. The uplifted margins of the basin constitute the best plays.

Cook Inlet coal is very similar to coal found in the Powder River Basin where economical flow rates have been accomplished. However, several significant questions need to be answered to determine the economics of coalbed production from within the basin. These include determination of production flow rates for gas as well as formation water.

Susitna Basin

The Susitna Basin underlies a lowland north of Cook Inlet between the Talkeetna Mountains to the east and the Alaska Range to the north and west (Figures 6 and 8). The Castle Mountain Fault and the Susitna Arch separates the shallower and younger Susitna Basin from the Cook Inlet Basin to the south (Figure 8). The dextral Castle Mountain Fault has offset Mesozoic rocks over 60 miles (97 km) and has almost a 2 mile (3.2 km) vertical throw [20]. The Tertiary coal-bearing section exceeds 13,400 feet (4,080 m) and consists of rocks equivalent to the Sterling, Beluga and upper part of the Tyonek Formations (Kirschner, unpublished report).

Nine exploratory wells have been drilled, plugged and abandoned in the basin, seven of which were drilled near the Castle Mountain Fault. The Trail Ridge -1 was drilled in a deeper part of the basin to 13,708 feet (4,178 m) and encountered Tyonek Formation coals with good gas shows from 11,700 feet to 13,708 feet (3,566 m to 4,178 m). The Tyonek Formation outcrops around the margins of the basin and contains subbituminous coal seams over 20 feet (6 m) thick. One reported seam on Sunflower Creek, located on the northwest side of the basin, measured 55 feet (16.8 m) thick [21].

Coals and sandstones north of the Castle Mountain Fault in the Houston area (Figure 8), where a small coal deposit was mined episodically between 1917 and 1952, appear to have high levels of gas. Five oil and gas exploration wells (Rosetta -1 through Rosetta -4A) and three U. S. Bureau of Mines (USBM) core holes drilled near Houston, encountered gassy coals (Figure 8). The USBM core holes, drilled in 1951, flowed small quantities of gas, possibly from coal seams. The Rosetta wells were drilled between 1954 and 1963 and encountered gas shows while drilling coals and sandstones. In spite of being plugged and abandoned, Rosetta -3 still has some gas escaping from around the surface casing. Some shallow water wells near the Castle Mountain Fault also flow small quantities of gas. Gas analysis results are similar to those from the coals cored in AK-94CBM-1. Gas analyses from a water well located six miles (10 km) north of Wasilla, indicated the gas to be 98% methane, 2% N_2 and the carbon isotope for methane -46.4 $\delta^{13}C$.

Coalbed Methane Potential. Susitna Basin is a smaller, shallower extension of Cook Inlet Basin. Like Cook Inlet Basin, the uplifted basin margins constitute the best potential for gas targets. The area along the Castle Mountain Fault is also highly prospective. This basin lacks the infrastructure of roads and pipelines, however, gas could be exploited for local use or pipelines could be built to connect with the existing gas distribution system in the Cook Inlet Basin.

ALASKA PENINSULA PROVINCE

The Alaska Peninsula contains two distinct coal-bearing basins. Coals in the Cretaceous basin are bituminous rank and the Tertiary (North Aleutain Basin) coals are of bituminous, subbituminous and lignite ranks. The two coal basins have different structural and depositional histories and are separated by a regional angular unconformity. The Cretaceous coal accumulated in an arc-trench gap setting while most of the Tertiary coal-bearing deposits are in a back-arc setting [22].

Cretaceous Basin

All Cretaceous coal occurs in the Upper Cretaceous Coal Valley Member of the Chignik Formation [22]. The Chignik Formation subcrops from Wide Bay in the north to the Herendeen Bay-Pavlof Bay in the south, an area over 200 miles (322 km) long and 50 miles (80 km) wide (Figure 10). The strata is moderately folded and faulted with dips varying from 20 to 35 degrees. The Coal Valley Member is laterally discontinuous in this area. The thickest deposits are found near Herendeen Bay (1,250 feet (381 m)), while this member is absent at other localities. Coal deposition was also variable. An aggregate thickness of 26 feet (7.9 m) of coal [19] was found in one 200-foot (61 m) thick section in the Herendeen Bay area. Other sections within the area contain little coal [23]. Coal beds average 3 feet (0.9 m) thick (the thickest 8 feet (2.4 m)), contain 12 percent ash and have a high (90 percent) vitrinite content. The vitrinite reflectance values of these high-volatile bituminous coals range from 0.57% to 1.76% Ro.

In the subsurface, the Chignik Formation has been penetrated by at least four deep oil and gas wells (Figure 10). The Phillips, Big River A-1 penetrated 27 thin coal seams (maximum thickness of 6 feet (1.8 m) over a 1,345-foot (410 m) interval. The Pan Am, Hoodoo Lake Unit -2 encountered 18 thin coals (maximum thickness of 8 feet (2.4 m)) and the Cities, Painter Cr. -1 encountered 9 coal seams (maximum thickness of 9 feet (2.7 m)). Only the Pan Am, David River 1-A did not encounter any coal seams in the Chignik Formation. All the wells that encountered coals had excellent mudlog gas shows. Coal samples from the

Hoodoo Lake Unit -2 well at depths greater than 8,000 feet (2,438 m), and the David River 1-A at depths between 8,500 to 10,250 feet (2,590 to 3,124 m) (above the Chignik Formation in the overlying Tolstoi Formation) are high-volatile to low-volatile bituminous rank. The Cities Service, Painter Creek -1 encountered a medium-volatile bituminous coal at 1,018 feet (310 m) [24]. Coals of similar rank are found in outcrops at Chignik and Herendeen Bay, indicating that these areas have undergone considerable uplift since maximum burial. The permeability of the cleat system could be enhanced in the uplifted areas.

Coalbed Methane Potential. Cretaceous coal underlies a significant area of the Alaska Peninsula. The variability of the coal development and discontinuous nature of the thin coal beds make subsurface exploration for coalbed methane difficult, particularly for large scale operations. However, if a local energy source is the objective and large reserves and high productivity wells are not necessary, the Chignik Formation coals are viable gas targets for villages towns such as Chignik Lake and Chignik Lagoon.

Tertiary Coal

Alaska Peninsula Tertiary coal occurs in the Tolstoi (Paleocene to Eocene), Stepovak (Oligocene), and Bear Lake (Miocene) Formations. In general, the Bear Lake and Stepovak Formation coals are lignitic to subbituminous rank. Tolstoi Formation coals range from medium- to low-volatile bituminous rank. Most of the coal seams are less than 3 feet (0.9 m) thick. The Bear Lake Formation coals crop out in the area south of Herendeen Bay and on Unga Island (Figure 10). On the north side of the Alaska Peninsula, most of the Tertiary coal-bearing strata subcrop in an area which is over 250 miles (400 km) long and extends at least 35 miles (56 km) offshore to the North Aleutian Cost well in the North Aleutian Basin (Figure 10). Minor to good gas shows are associated with these coals. For example, the Gulf, Port Heiden Unit -1 shows greatly increased mudlog gas in the coaly section in the Bear Lake Formation from depths of 4,000 feet to 5,000 feet (1,219 m to 1,524 m). The mudlog gas levels increased from 20 ppm to over 250 ppm in some of the coal seams. Over this interval, the Port Heiden well encountered approximately 23 coal seams, most of which were less than 5 feet (1.5 m) thick. The David River 1-A well encountered Bear Lake Formation subbituminous coals at similar depths and the Hoodoo Lake Unit -1 penetrated lignitic coals to 5,000 feet (1, 524 m) and subbituminous coals to the well's total depth of 8,049 feet (2,453 m) in the Stepovak Formation [24]. This trend is consistent to the north, where the General Petroleum, Great Basins -1 encountered immature rocks with an average Ro of 0.29% for the Bear Lake Formation and an average Ro of 0.51% for the Stepovak Formation. The Hoodoo Lake Unit -2 encountered a gassy coal section in the Tolstoi Formation between 5,800 feet and 6,500 feet (1,768 m and 1,980 m). Based on the mudlog, this well encountered coal seams to 20 feet (6 m) thick with good mudlog gas shows and trace oil shows. The coal is described as lignitic to subbituminous in rank and is shaly. The rank of these coals must be higher than described in the mudlog since McLean [24] reports the vitrinite reflectance values average 1.15 % (medium-volatile bituminous) for this interval. Geophysical logs do not verify the thick coals noted on the mud log. This may be due to the shale interbeds and/or the nature of the shaly coal beds. The David River 1-A well encountered thin, high-volatile to low-volatile bituminous coal seams between the depths of 8,500 feet and 10,400 feet (2,590 m and 3,170 m) [24].

Coalbed Methane Potential. Structurally high areas where the Tolstoi Formation coals are found above 5,000 feet (1,524 m) in depth have the highest potential. Coal seams in the Bear Lake and Stepovak Formations are too low rank to have good gas potential.

GULF OF ALASKA PROVINCE

The Gulf of Alaska Province consists of the northern Gulf of Alaska onshore area of southern Alaska and is composed of amalgamated tectonic terranes that resulted from both Mesozoic and Cenozoic plate interactions [25]. The Tertiary coal-bearing rocks are found in the Yakutat terrane, the most recently arrived terrane. This terrane is presently moving north with the Pacific plate, colliding with and subducting beneath southern Alaska [26], subjecting the entire area to intense compressional stresses. The tectonism has caused the intense fold and fault deformation present in the Bering River Field [27].

Most of the coal in the Gulf of Alaska Province is found within the Eocene to Early Oligocene Kulthieth Formation [28 and 26]. The coals found in the Bering River Field area (Figure 11) are low-volatile bituminous to meta-anthracite and occur in deformed lenses up to 60 feet (18 m) thick. The coal seams are lenticular both from intense structural deformation and stratigraphic thinning (27) (Merritt, 1986). Coal seams up to 6 feet (1.8 m) thick are found in the Duktoth River District in the Robinson Mountains about 50 miles (80 km) east of the Bering River Field (Figure 11). Thin coal seams are encountered over a much broader and less deformed area in the subsurface from the Bering River field to the Yakutat Bay area, however, none of the thick coal seams found at the Bering River field have been encountered in the subsurface. Onshore exploratory wells (Figure 11) encountered both coal-bearing fluvial and marine strata based on the presence of sparse outer neritic to upper bathyal benthic microfauna in the Kulthieth Formation [29]. Reconstruction of the Kulthieth depositional system indicates that a series of deltas probably deposited sediments directly into a deep marine basin with rapid lateral changes in paleobathymetry [25].

Coalbed Methane Potential. The coals in the Gulf of Alaska Province are subject to intense compressional stress and severely deformed. These coals may be too metamorphosed and compressed to be viable gas targets. However, suitable coalbed methane plays may be found in structurally less deformed areas between the Bering River Field and the coast line.

YUKON-KOYUKUK PROVINCE

The Yukon-Koyukuk Province of western interior Alaska is characterized by maturely-eroded and heavily-vegetated terrain with most of the coal found in outcrops along the Yukon, Koyukuk, and Kobuk Rivers. Three poorly defined coal basins (Upper Koyukuk, Lower Koyukuk, and Kobuk) (Figure 12) have been identified in this province by Merritt and Hawley [1]. Cretaceous and Tertiary volcanic and sedimentary rocks [30] were deposited in a highly mobile basin complex subject to repeated volcanism and plutonism [31]. Up to 25,000 feet (7,620 m) of Cretaceous sedimentary rocks have been documented in this province [31]. This assemblage consists of marine volcanic graywacke and mudstone turbidites overlain by a westward prograding assemblage which includes coal-bearing deltaic deposits at least 10,000 feet (3,048 m) thick [32]. Patton [31] concluded the coal-bearing beds were deposited along a broad shallow trough extending along the eastern margin of the province.

Upper Koyukuk Basin

The thickest coal seams in the Yukon-Koyukuk Province are found in the Tramway Bar Field in the Upper Koyukuk Basin. The Tramway Bar Field is located 35 miles (56 km) above Bettles on the Middle Fork of the Koyukuk River (Figure 12). At this field, three coal seams with thicknesses of 17.5 feet, 3 feet and less than 1 foot (5.3, 0.9, and 0.3 m) have been mapped. These coals are steeply dipping, high-volatile B bituminous, with 38% ash and 6% moisture content [33]. Although these are the only significant coal outcrops in the Upper Koyukuk Basin, abundant coal float has been reported on the John River north of Bettles [34].

Coalbed Methane Potential. The Upper Koyukuk Basin contains bituminous rank coals that could provide gas for local use. Widely scattered outcrops, little surface data, lack of continuity of coal seams, and the structural complexity of the area make drilling targets very elusive.

Lower Koyukuk Basin

Lower Koyukuk Basin coals consist primarily of scattered coal occurrences between Ruby and Anvik on the Yukon River [35] (Figure 12). However, coals in this basin possibly extend much farther south than Anvik as bituminous coals have been reported on the lower Yukon River and Kuskokwim Rivers and Nelson and Nunivak Islands [34]. Between 1890 and 1903, some of these coal occurrences were mined to supply fuel for the steam-powered boats of the Yukon River. The area near Nulato supported several small scale mines in what is now referred to as the Nulato Field. These coals are typically thin (less than 4 feet (1.2 m) thick), high-volatile C bituminous and occur in the Late Cretaceous Kaltag Formation [36]. The thickest coal seam, an 11-foot (3.4 m) bed, is located 12 miles (19 km) upriver from Galena [37]. Thin coal seams were reported at this location by Collier [35] and Chapman [38].

In 1960, the Nulato Unit -1 was drilled to 12,000 feet (3,658 m) and is the only deep well to be drilled in this basin. This well was drilled on a north-east trending surface anticline and penetrated only Cretaceous rocks, yielding little information on the coal-bearing section. Sample descriptions indicate only minor coal was encountered and cores show dips greater than 60 degrees and abundant fractures and brecciation. The entire succession is over mature with respect to oil generation [39] with vitrinite Ro values ranging from 2.62% near the surface to over 4.0% at 6,100 feet (1,859 m) measured depth.

Coalbed Methane Potential. The entire area has undergone moderate to severe structural deformation with some of the coal seams sheared and dipping at steep angles. The complex structure, combined with very limited outcrop control, make predicting reservoir continuity and drillable targets impossible. Gas from bituminous coals for local village usage along the lower Koyukuk and Yukon Rivers may be obtained provided viable drilling targets can be delineated.

Kobuk Basin

Kobuk Basin coals consist of scattered, high-volatile C bituminous occurrences along a 120 mile (193 km) stretch of the Kobuk River between Kiana and Kobuk [21] (Figure 12). Some of these coals were sampled by Clough and others [40] on the west end of the known coal deposition in the Hockley Hills-Singauruk River (near Kiana) areas. Clough and others [40] noted some coal seams up to 6 feet (1.8 m) thick with most of the coal thickness less than 2 feet (0.6 m). Ash contents are high, reaching values of 60%. While the area is slightly less deformed than the Upper and Lower Koyukuk Basins, bed dips exceeding 40 degrees are common. Because of the lack of well and seismic data, no subsurface information on the extent of coal beds is available in this area.

Coalbed Methane Potential. The Kobuk basin lacks the outcrop and subsurface data (well and seismic) to fully evaluate the gas potential of its coals. However, bituminous coals in the basin may be viable exploration targets if they can be demonstrated to subcrop near villages now dependent on imported oil for heating and electricity.

NENANA PROVINCE

The Nenana coal trend is located north of the Alaska Range and includes fields located in the Minchumina, Middle Tanana, and Nenana Basins (Figure 13). These Tertiary coal bearing basins form a discontinuous belt from the Jarvis Creek Field near Big Delta on the east, through Healy, Lignite Creek, and Suntrana Coal Fields in the central portion, to the Farewell-Little Tonzona area (Minchumina Basin) to the southwest. The entire trend extends over 200 miles (320 km) and is over 30 miles (50 km) wide. The coals in these areas are mostly Oligocene to Miocene in age and are subbituminous C or B in rank.

Minchumina Basin

The Minchumina Basin is probably a complex of small, extensional basins [41]. Scattered Tertiary nonmarine sedimentary rocks crop out along stream valleys and river bluffs adjacent to the Alaska Range on the eastern edge of the basin. No subsurface data is available in this area and therefore mapping the lateral extent of coals is problematic. Most outcrops lie along the Farewell Fault Zone and are steeply [42]. The Farewell Fault separates the Minchumina Basin from the Alaska Range. To the west, away from the Farewell Fault, it is conceivable that the dips of these rocks could flatten into the subsurface. Coals in this area range from subbituminous A to high-volatile C bituminous and ash content ranges from 4% to over 26%. Seam thicknesses up to 20 feet (6 m) and multiple coal seams over 3 feet (0.9 m) thick have been mapped [43]. One subbituminous coal seam over 100 feet (30 m) thick has been reported from the Farewell-Little Tonzona Field [44].

Coalbed Methane Potential. The Minchumina Basin contains coal similar to that found in Cook Inlet Basin. Known coal occurrences dip steeply along the major dextral faults in the area. Without subsurface control, the extent and depth to these Tertiary coals is unknown and locating viable coalbed methane targets will be difficult. If found, the coalbed gas could be a useful fuel for local village use.

Nenana Basin

The Nenana Basin contains over 3,000 feet (914 m) of nonmarine Tertiary coal-bearing rocks which unconformably overlie Precambrian and Paleozoic metamorphic rocks. The Nenana Basin is the most explored of the three basins in the Nenana Province and contains a large coal resource (Figures 2 and 13) with coal seams up to 60 feet (18 m) thick. Most of the coal in this basin is subbituminous and is comparable in overall quality to coals found in the Cook Inlet and Wyoming's Powder River Basins [27]. Although the Healy Creek, Suntrana, and Lignite Creek Formations of the Usibelli Group all have significant coal deposits, most exploitable coal is contained within the Suntrana Formation [27]. The Lignite (Hoseanna) Creek Field near Healy is the only active coal mine in Alaska. Here, multiple coal seams that average 20 feet (6 m) thick are being mined from the Suntrana Formation.

Coalbed Methane Potential. The Nenana Basin contains thick coals that are similar to those found in Cook Inlet Basin. If the gas contents are comparable to those in Cook Inlet Basin, these coals could be good gas objectives. This basin contains coalbed methane targets located along the state's road system between Nenana and Healy and in the Big Delta area.

Middle Tanana Basin

The Middle Tanana Basin lies just north of the Nenana Basin and contains about 10,000 feet (3,050 m) of late Cenozoic fill [45 and 41]. Two oil and gas exploratory wells have been drilled in the Middle Tanana Basin. The Unocal, Nenana -1 and the Arco, Totek Hills -1 (Figure 13) were drilled near the margin of the basin. These wells drilled through the Tertiary section, encountering metamorphic basement rocks at 2,090 feet (789 m) and 3,163 feet (963 m) respectively. Both wells encountered coal, with the Totek Hills -1 well encountering numerous coal seams up to 10 feet (3 m) thick. The nonmarine Tertiary sequence in this basin penetrated by these wells consists of the Usibelli Group, which has been described from outcrops in the Nenana Basin to the south. Coals penetrated by both wells produced only minor mudlog gas shows. Cutting descriptions for the wells indicate the coals to be lignite to subbituminous and the section to be poorly to moderately consolidated. Higher rank coals could be encountered in the deeper parts of the Middle Tanana Basin. Stanley and others [46] estimate the top of the oil window (Ro of 0.6%) to be at depths exceeding 4,500 feet (1,370 m).

Coalbed Methane Potential. Wells in the Middle Tanana Basin encountered lignite to subbituminous coal. Higher rank (high-volatile bituminous) coal is projected to be below 4,500 feet (1,370 m) and is probably too deep for good coalbed methane production. Geologically, the low-rank coals are poor to moderate methane drainage targets, although the basin's proximity to the large Fairbanks market makes it attractive from an economic perspective.

NORTHERN YUKON PROVINCE

The Northern Yukon Province encompasses lower to middle Tertiary coal-bearing sedimentary rocks found in the Eagle and Rampart Troughs and the Yukon Flats Basin (Figure 13). Outcrops are scarce in this region occurring only in recently eroded bluffs and stream cutbanks. The area extends west over 400 miles (640 km) from the Canadian border along the Yukon River. Coal rank for the area ranges from lignite A to subbituminous C, though a few localities containing bituminous coal have been reported [47].

Eagle Trough

The Eagle Trough (Tintina Trench) is a northwest-trending basin that lies along the Tintina Fault Zone (Figure 13). This basin is estimated to contain as much as 9,500 feet (3,000 m) of Tertiary fill [48] in the vicinity of the Tintina Fault Zone. The basin contains subbituminous coals, although some coals have been tectonically upgraded in rank near the Tintina Fault Zone [47]. Although coal seams thicker than 30 feet (9 m) have been reported, most seams have a thickness less than 3 feet (0.9 m). In outcrop, many coal beds are highly fractured and steeply dipping [34].

Coalbed Methane Potential. The Eagle Trough contains mainly subbituminous coals which may be too low in rank to be good gas prospects. Gas for local use may be

found in areas near faulting where the coal rank is higher and coal fractures may be better developed.

Rampart Trough

The Rampart Trough is a southwest-trending basin that lies along the Kaltag Fault. Tertiary fill in the trough is estimated to be as much as 6,500 feet (2,000 m) [41] (Figure 13). Coals found in the basin are dominantly subbituminous in rank and generally less than 5 feet (1.5 m) thick. Most of the mapped coal occurrences in the Rampart Trough are found adjacent to the Kaltag Fault and are very tectonically disturbed [47]. As in the Eagle Trough, some of the coals are bituminous in rank due to tectonic rank upgrading along major faults.

Coalbed Methane Potential. The Rampart Trough coals have low gas potential because of their low rank (subbituminous). Near faulting, where coals are fractured and have a higher rank, coalbed methane targets may be more attractive.

Yukon Flats Basin

Covering over 8,500 square miles (22,000 sq km), the Yukon Flats Basin is the largest Tertiary basin in Interior Alaska [47] (Figure 13). The basin is a half-graben complex with about 2 to 3 miles (3 to 5 km) of nonmarine Tertiary fill [49]. The only subsurface control in this large basin is a proprietary oil company seismic survey, shallow core holes, and a 1,200-foot (366 m) core hole drilled in 1994 at Fort Yukon by the U. S. Geological Survey. Bedrock outcrops are rare with the only exposures found along the margins of the basin. These limited exposures indicate coal-bearing rocks probably underlie most of the Yukon Flats Basin. Barker and Goff [47] report augering about 20 feet (6 m) of coal with a rank from lignite A to subbituminous B. The USGS Fort Yukon well encountered a 21+ feet (6.4 m), Middle Miocene, lignitic coal bed at a depth of 1,260 feet (384 m) (Gary Stricker, personnel communication, 1994). The core sample released a significant amount of gas when brought to the surface. This resulted in the termination of drilling (Tom Ager, personnel communication, 1994).

Coalbed Methane Potential. The known coals of Yukon Flats Basin are too low in rank for good gas production. However, higher rank coals found closer to the surface along the uplifted basin margins may have high gas potential.

SEWARD PENINSULA PROVINCE

Lignite and subbituminous coal-bearing rocks of Cretaceous and Early Tertiary age occur in isolated, structurally controlled coal fields on the Seward Peninsula [50] (Figure 12). Some of the coal beds are impressive in thickness reaching 80 feet (24 m) at Chicago Creek Field and 180 feet (55 m) at Grouse Creek [7]. The Tertiary section at Chicago Creek Field is generally less than 200 feet (61 m) thick and unconformably overlies quartz-mica schist of lower Paleozoic or Proterozoic age. Lignite beds in the Unalakleet area are generally less than 2 feet (0.6 m) thick and also dated as early Tertiary [31].

Both the Socal, Cape Espenberg -1, drilled on the north side of the Seward Peninsula, and the Socal, Nimiuk Point -1, drilled south of Kotzebue (Figure 12), penetrated a coal-bearing section in the Selawik Basin. The coal-bearing section penetrated by the wells is Upper Pliocene to lower Pleistocene in age [51] and thermally immature with Ro values less than 0.4%, distinguishing it from the Paleocene coals found in outcrop at Chicago Creek Field [52]. These wells reached total depth in schistose metasandstone and marble that likely correlate with pre-Mississippian schists and marble exposed on the Seward Peninsula. Both wells failed to penetrate the Cretaceous and early Tertiary coal-bearing rocks that outcrop on the Seward Peninsula, possibly indicating that the Seward Peninsula coal-bearing strata occurs as local, isolated basins.

Coalbed Methane Potential. Coals in the Seward Peninsula, Selawik, and Unalakleet areas are too low in rank for good gas production.

OTHER COAL-BEARING AREAS

Southeast Alaska

High-volatile B Bituminous [53] coal occurs near Angoon on the Kootznahoo Inlet (Admiralty Island) throughout an area of about 40 square miles (100 sq km) [54] (Figure 1). The coals are high sulfur, dirty, discontinuous and thin. The prominent structural dip of the rocks in the area is 45 degrees to the southeast. Coal with similar characteristics crops out near Murder Cove at the southern tip of Admiralty Island. Small, isolated outcrops of Tertiary lignite also are present on Prince of Wales, Kuiu, and Kake Islands [34].

Coalbed Methane Potential. The Kootznahoo Inlet coals on Admiralty Island are the only coals in southeast Alaska that hold even low gas potential. However, these coals are thin, discontinuous, dirty and structurally complex, making them unlikely targets.

Copper River

The Copper River Basin (Figure 11) occupies a lowland area in south-central Alaska between the Talkeetna and the Wrangell Mountains. Coal occurs throughout the 3,000 feet (914 m) of nonmarine Tertiary sedimentary basin fill. The coals penetrated in the wells and found in outcrops on the basin margins are lignites. Ten exploratory oil and gas wells have been drilled in the basin. The thickest Tertiary section penetrated in the northeast portion of the basin by Salmon Berry Lake -1 and Rainbow Federal -1 and -2 wells (Figure 11). A high thermal gradient on the eastern side of the basin near the Neogene and Quaternary Wrangell Mountain volcanoes may be present and upgrade the rank of coal in this area. However, coal outcrops in the Wrangell Mountains (Figure 11) are reported to be lignite [1] and Ro

values of Tertiary sediments are generally less than 0.4% in the eastern portion of the basin near the Wrangell Mountains.

Coalbed Methane Potential. The Copper River Basin coals are too low in rank to have good gas potential.

DISCUSSION

Neither a proven reserve base or an export market for coalbed methane has been established in Alaska. However, preliminary analysis suggests that coalbed methane represents a huge, untapped state resource. As Alaska's conventional oil and gas reserves decline, it is critical to locate and identify and catalog potential deposits that can contribute to long term growth. In addition, identifying future energy resources is essential for land use planning.

This report's evaluation of Alaska's coalbed methane potential is based primarily upon the current limited knowledge of the basins and is calibrated with analogs from producing coalbed methane basins, primarily in the lower 48 states. It must be noted, however, that coal is a complex, heterogeneous material that defies simple analysis and comparisons. Predictions of Alaska's coalbed methane potential is fraught with pitfalls and ultimately only exploration drilling and long term well testing can provide definitive results.

For large scale coalbed methane production (involving several tcf) to take place in Alaska, it will have to compete with other gas sources for export to Pacific Rim markets. The economics involved with using coalbed methane as a local energy source may be much more favorable. Alaska's remote communities are currently dependent on large deliveries of diesel fuel for heating and electrical generation. Some areas pay the equivalent of $10 to $15 per mcf in fuel costs. The potential for spills during water-borne transportation of petroleum products is well known, and regulators are making it increasingly expensive. Additionally, using gas for local consumption would eliminate the large oil storage facilities (large enough to sustain the village through the entire winter) that each village must maintain, thus eliminating the potential for oil spills and pollution of ground and surface water. Wells producing 30 mcf per day, that in other situations would be uneconomic, could fill the energy needs of many of Alaska's rural communities.

CONCLUSIONS

Alaska's enormous coal resources provide many opportunities for coalbed methane exploration. Both Northern Alaska (North Slope) and Cook Inlet-Susitna Provinces contain thick coal sequences that hold large coalbed methane resources. The onshore areas in the Matanuska Valley and the uplifted basin margins of Cook Inlet Basin provide the highest potential for near term, large scale coalbed methane development. Large scale coalbed methane development on the North Slope is currently not feasible due to a lack of infrastructure. Bituminous coals in the Upper and Lower Koyukuk, Kobuk, Gulf of Alaska and Alaska Peninsula Basins could provide gas for the rural communities that depend on diesel fuel for power generation. Subbituminous and lignite coals in the North Slope, Cook Inlet, Susitna, Middle Tanana, Nenana, Yukon Flats, North Aleutian, Seward Peninsula and Copper River Basins could provide more opportunities for gas production provided hydrologic conditions and gas contents are suitable.

ACKNOWLEDGMENTS

The author is especially grateful to Michael Pritchard, State Division of Oil and Gas, for preparing all the illustrations in this paper. Thanks to Mark Myers, Don Krouskop, Tim Ryherd, and James Hansen, all from the State Division of Oil and Gas, and Mike Belowich, Consultant, for their review of the manuscript. Thanks to Dave Lappi, Lapp Resources, Inc., for his help and interest in the project from pulling core at the well site to review of this manuscript. Thanks to Matt McCullough and Brad Penn, Marathon Oil Co., and Eric Graven, Unocal, for their help. Thanks to the State of Alaska for providing the funds and time necessary to complete this project and to the U. S. Geological Survey drilling crew (Art Clark, Dan Sweeney, Dean Bohn and Todd Hunter) for all their help and expertise. Special thanks to Don Church for allowing his land to be the drilling site. And finally to my wife, Deborah, for her help and support.

REFERENCES CITED

1. Merritt, R. D. and Hawley, C. C., 1986, Map of Alaska's coal resources: Alaska Division of Geological and Geophysical Surveys Special Report 37, 1 sheet, scale 1:2,500,000.
2. Kim, A. G., 1976, Estimating methane content of bituminous coalbeds from absorption data: U. S. Bureau of Mines Report of Investigations 8245, 22 p.
3. McFall, K. S., Wicks, D. E., Kelso, B. S., Sedwick, K., and Brandenburg, C., 1987, An analysis of the coal and coalbed methane resources of the Piceance Basin, Colorado: SPE/DOE 16418.
4. King, G. R., and Ertekin, T. M., 1989, A survey of mathematical models related to methane production from coal seams, part 1-Empirical and equilibrium sorption models, *in* The 1989 Coalbed Methane Symposium, Proceedings- University of Alabama, Tuscaloosa, April 17-20, 1989: School of Mines and Energy Development, Gas Research Institute, U. S. Mine Safety and Health Administration, and Geological Survey of Alabama, p. 125-138.
5. Collier, A. J., 1906, Geology and coal resources of the Cape Lisburne region, Alaska: U. S. Geological Survey Bulletin 278, 54 p.
6. Tailleur, I. L., 1965, Low volatile bituminous coal of Mississippian age on the Lisburne Peninsula. Northwestern Alaska: U. S. Geological Survey Professional Paper 525B, p. B34-B38.

7. Eakins, G. R., 1986, Investigations of coal resources in northwest Alaska, 1980-1985, *in* Rao, P. D., ed., Focus on Alaska's Coal '86; Proceedings of the Conference: University of Alaska at Fairbanks, Mineral Industry Research Laboratory Report 72, p. 250-265.
8. LePain, D. L., Crowder, R. K., and Wallace, W. K., 1994, Early Carboniferous transgression on a passive continental margin: Deposition of the Kekiktuk Conglomerate, northeastern Brooks Range, Alaska: American Assoc. of Petroleum Geologists Bulletin, v. 78, p. 679-699.
9. Sable, E. G., and Stricker, G. D., 1987, Coal in the National Petroleum Reserve in Alaska (NPRA); Framework geology and resources, *in* Tailleur, I. L., and Weimer, R., eds., Alaskan North Slope geology: Society of Economic Paleontologists and Mineralogists and Alaska Geological Society Book 50, p. 195-216.
10. Ahlbrandt, T. S., Huffman, A. C. , Fox, J. E., and Pasternak, Ira, 1979, Depositional framework and reservoir quality studies of selected Nanushuk Group outcrops, North Slope, Alaska, *in* Ahlbrandt, T. S., ed., Preliminary geologic, petrologic, and paleontologic results of the study of Nanushuk Group rocks, North Slope, Alaska: U. S. Geological Survey Circular 794, 163 p.
11. Tailleur, I. L., and Brosge, W. P., 1975, Coal resources of northern Alaska may be nation's largest, *in* Rao, P. D., and Wolff, E. N., eds., Focus on Alaska's coal '75, Proceedings of the Conference held at the University of Alaska, Fairbanks, October 15-17, 1975: Mineral Industry Research Laboratory Report No. 37, p. 219-226.
12. Warfield, R. S., and Boley, C. C., 1969, Sampling and coking studies of several coal beds in the Kokolik River, Kukpowruk River, Cape Beaufort areas of Arctic Alaska: U. S. Bureau of Mines Report of Investigations 7321, 58 p.
13. Brosge, W. P., and Whittington, C. L., 1966, Geology of the Umiat-Maybe Creek region, Alaska: U. S. Geological Survey Professional Paper 303-H, p. H501-H638.
14. Molenaar, C. M., Kirk, A. R., Magoon, L. B., and Huffman, A. C., 1984, Twenty-two measured sections of Cretaceous-Lower Tertiary rocks, eastern North Slope, Alaska: U. S. Geological Survey Open-File Report 84-695, 19 p.
15. Detterman, R. L., Reiser, H. N., Brosge, W. P., and Dutro, J. T., Jr., 1975, Post-Carboniferous stratigraphy, northeastern Alaska: U. S. Geological Survey Professional Paper 886, 46 p.
16. Calderwood, K. W. and Fackler, W. C., 1972, Proposed stratigraphic nomenclature for Kenai Group, Cook Inlet basin, Alaska: American Assoc. of Petroleum Geologists Bulletin, v. 56, p. 739-754.
17. Smith, T. N., and Clough, J. G., 1993, Coalbed methane potential for Alaska: 1993 American Assoc. of Petroleum Geologists Annual Convention Program, abs., p. 184.
18. Barnes, F. F., and Payne, T. G., 1956, The Wishbone Hill District, Matanuska coal field, Alaska: U. S. Geological Survey Bulletin 1016, 85 p.
19. Alaska's high-rank coals, 1993: State of Alaska, Div. of Geological and Geophysical Surveys Information Circular 33, 36 p.
20. Detterman, R. L., Plafker, G., Hudson, T., Tysdal, R. G., and Pavoni, N., 1974, Surface geology and Holocene breaks along the Susitna segment of the Castle Mountain fault, Alaska: U. S. Geological Survey Miscellaneous Field Studies Map MF-618, scale 1:24,000.
21. Sanders, R. B., 1980, Coal resources of Alaska: *in* Rao, P. D., and Wolff, E. N., eds., Focus on Alaska's coal '80, Proceedings of the Conference held at the University of Alaska, Fairbanks: Mineral Industry Research Laboratory Report No. 50, p. 11-31.
22. Burk, C. A., 1965, Geology of the Alaska Peninsula--island arc and continental margin: Geological Society of America Memoir 99, pts. 1-3, 250 p.
23. Merritt, R. D., and McGee, D. L., 1986, Depositional environments and resource potential of Cretaceous coal-bearing strata at Chignik and Herendeen Bay, Alaska Peninsula: Sedimentary Geology, v. 49, p. 21-29.
24. McLean, Hugh, 1977, Organic geochemistry, lithology, and paleontology of Tertiary and Mesozoic rocks from wells on the Alaska Peninsula: U. S. Geological Survey Open-File Report 77-813, 63 p.
25. Turner, R. F., Risley, D. E., Martin, G. C., Lynch, M. B., Flett, T. O., Larson, J. A., and Horowitz, W. L., 1992, Geologic report for the Gulf of Alaska planning area: OCS Report MMS 92-0065, 302 p.
26. Plafker, George, 1987, Regional geology and petroleum potential of the northern Gulf of Alaska continental margin, *in* Scholl, D. W., Grantz, A., and Vedder, J. G., eds., Geology and resource potential of the continental margin of western North America and adjacent ocean basins - Beaufort Sea to Baja California: Houston, Texas, Circum-Pacific Council for Energy and Mineral Resources, Earth Science Series, v. 6, p. 229-268.
27. Merritt, R. D., 1986, Paleoenvironment and tectonic controls in major coal basins of Alaska, *in* Lyons, P. C., and Rice, C. R., eds., Paleoenvironment and tectonic controls in coal-forming basins of the United States: Geological Society of America, Special Paper 210, p. 173-200.
28. Winkler, G. R., and Plafker, G., 1981, Preliminary geologic map of the Cordova and Middleton Island quadrangles, Alaska: U. S. Geological Survey Open-File Report 81-1164, scale 1:250,000.
29. Rau, W. W., Plafker, G., and Winkler, G. R., 1983, Foraminiferal biostratigraphy and correlations in the Gulf of Alaska Tertiary province: U. S. Geological Survey Oil and Gas Investigations Chart OC-120, 11 p., 3 plates.
30. Patton, W. W., Jr., and Box, S. E., 1989, Tectonic setting of the Yukon-Koyukuk basin and its borderlands, western Alaska: Journal of

Geophysical Research, vol. 94, no. B11, p. 15,807-15,820.

31. Patton, W. W., Jr., 1973, Reconnaissance geology of the northern Yukon-Koyukuk Province, Alaska: U. S. Geological Survey Professional Paper 774-A, p. A1-A17.
32. Patton, W. W., Jr., 1966, Regional geology of the Kateel River quadrangle, Alaska: U. S. Geological Survey Misc. Geol. Inv. Map I-437, scale 1:250,000.
33. Rao, P. D., 1986, Characterization and evaluation of washability of Alaskan coals, fifty selected seams from various coal fields: U. S. Department of Energy Final Technical Report - September 30, 1976 to February 28, 1986 (DOE/PC/62695-T5); University of Alaska at Fairbanks Mineral Industry Research Laboratory Report no. 75, p. 184.
34. Barnes, F. F.,1967, Coal resources of Alaska: U. S. Geological Survey Bulletin 1241-B, 36 p.
35. Collier, A. J., 1903, The coal resources of the Yukon, Alaska: U. S. Geological Survey Bulletin 218, 71 p.
36. Martin, C. G., 1926, Mesozoic stratigraphy of Alaska: U. S. Geological Survey Bulletin 776, p. 396-410.
37. Goff, K. M., and Barker, J. C., 1988, Nulato coalfield: Alaska Division of Geological and Geophysical Surveys Report of Investigations, in press.
38. Chapman, R.M., 1963, Coal deposits along the Yukon River between Ruby and Anvik, Alaska, *in* Contributions to Economic Geology of Alaska: U. S. Geological Survey Bulletin 1155, p. 18-29.
39. Johnsson, M. J., 1992, Vitrinite reflectance and conodont color alteration index data from Alaska (computer file): U. S. Geological Survey Open-file Report 92-409.
40. Clough, J. G., Eakins, G. R., and Menge, M.,1983, Preliminary report on the Hockley Hills-Singauruk River coal occurrence: Alaska Division of Geological and Geophysical Surveys Public-data File 83-3.
41. Kirschner, C. E., 1988, Map showing sedimentary basins of onshore and continental shelf areas, Alaska: U. S. Geological Survey Miscellaneous Investigations Series, Map I-1873, scale 1:2,5000,000.
42. Sloan, E. G., Shearer, G. B., Eason, J. E., and Almquist, C. L., 1981, Reconnaissance survey for coal near Farewell, Alaska, *in* Rao, P. D., and Wolff, E.N., eds., Focus on Alaska's Coal '80: University of Alaska at Fairbanks Mineral Industry Research Laboratory Report 50, p. 152-170.
43. Solie, D. N., and Dickey, D. B., 1982, Coal occurrences and analyses, Farewell-White Mountain area, southwest Alaska: Alaska Division of Geological and Geophysical Surveys Open-file Report 160, 17 p., 1 sheet.
44. Player, Gary, 1976, The Little Tonzona coal bed near Farewell, Alaska; an important extension of the coal field north of the Alaska Range: Gary Player ventures consultant report, Anchorage, 10 p.
45. Barnes, D. F., 1961, Gravity low at Minto flats, Alaska: U. S. Geological Survey Professional Paper 424-D, p. D254-D257.
46. Stanley, R. G., McLean, Hugh, and Pawlewicz, M. J., 1989, Petroleum source potential and thermal maturity of the Tertiary Usibelli Group of Sumtrana, Alaska, *in* Dover, J. H., and Galoway, J. P., eds., Geologic studies in Alaska by the U. S. Geological Survey, 1989: U. S. Geological Survey Bulletin 1946, p. 65-76.
47. Barker, J. C., and Goff, K. M., 1986, Coal resources within the Yukon Drainage, interior Alaska, *in* Rao, P. D., ed., Focus on Alaska's Coal '86; Proceedings of the Conference: University of Alaska at Fairbanks, Mineral Industry Research Laboratory Report 72, p. 336-349.
48. Cady, J. W., and Weber, F. R., 1983, Aeromagnetic map and interpretation of magnetic and gravity data, Circle quadrangle, Alaska: U. S. Geological Survey Open-file Report 83-170C.
49. Magoon, L. B., and Krischner, C. E., 1990, Alaska onshore national assessment program--Geology and petroleum resource potential of six onshore Alaska provinces: U. S. Geological Survey Open-file Report 88-450T, 47 p.
50. Hudson, Travis, 1977, Preliminary geologic map of the Seward Peninsula, Alaska: U. S. Geological Survey Open-file Report 77-167A, scale 1:1,000,000.
51. Turner, D. L., and Olson, D. L., 1978, Preliminary paleontology report, Standard Oil Company of California, Cape Espenberg No. 1 well and Nimiuk Point No. 1 well, Kotzebue Sound--Selawik Basin Area: U. S. Minerals Management Service internal report.
52. Decker, John, Robinson, M. S., Clough, J. G., and Lyle, W. M., 1988, Geology and petroleum potential of Hope and Selawik basins: Alaska Division of Geological and Geophysical Surveys Public-data File Report 88-1, 41 p.
53. Cooper, H. M., Snyder, N.H., Abernathy, R. F., Tarpley, E. C., and Swingle, R. J., 1946, Analyses of mine, tipple, and delivered samples, *in* Analyses of Alaska coals: U. S. Bureau of Mines Technical Paper 682, p. 19-69.
54. Lathram, E. H., Pomeroy, J. S., Berg, H. C., and Loney, R. A., 1965, Reconnaissance geology of Admiralty Island, Alaska: U. S. Geological Survey Bulletin 1181-R, p. R1-R48.

Figure 1. Alaska coal basins and coal occurrences [1].

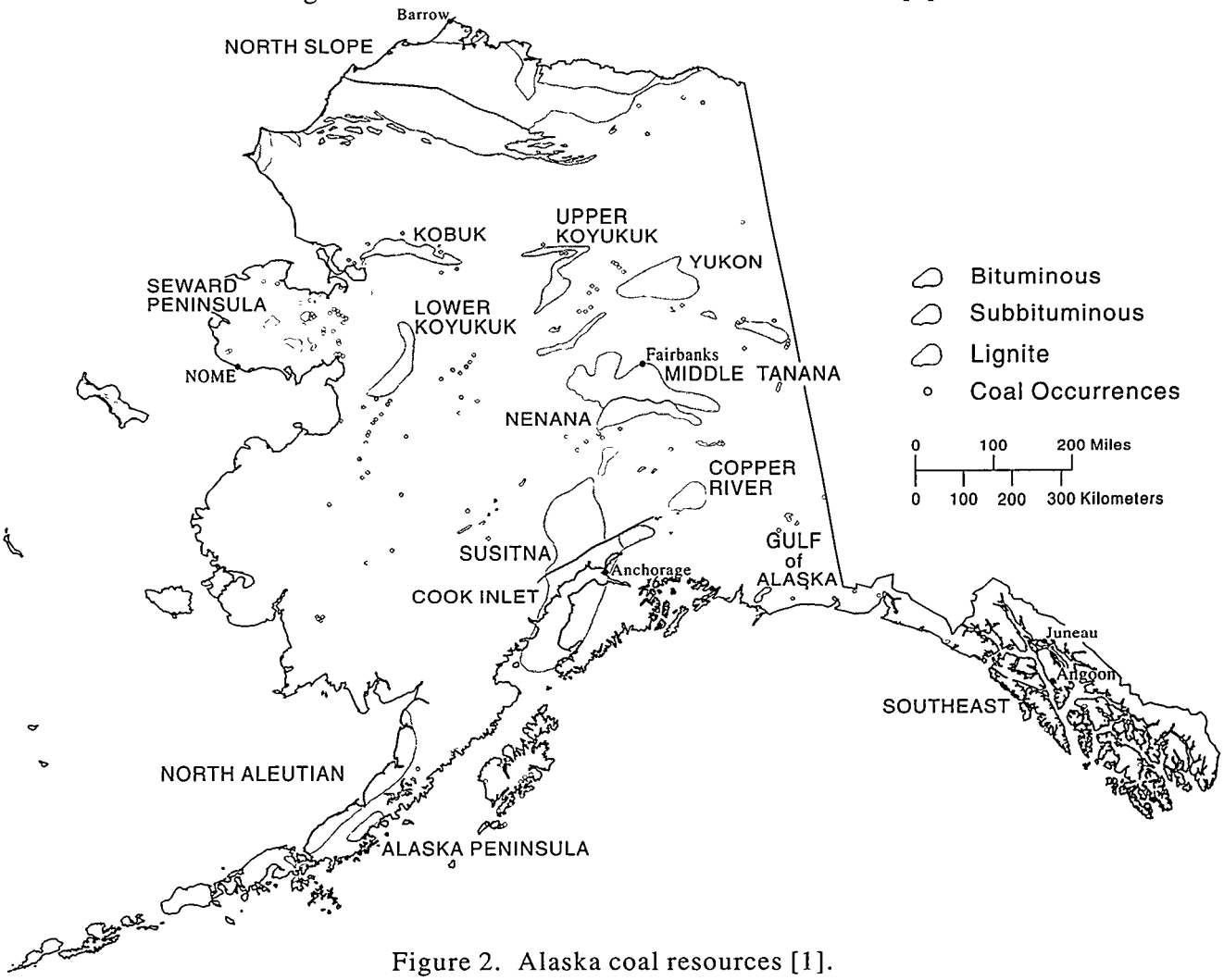


Figure 2. Alaska coal resources [1].

RANK OF COAL	BASIN	HYPOTHETICAL RESOURCES (Billion short tons)
BITUMINOUS COAL		
	North Slope	2,500
	Cook Inlet	500*
	Alaska Peninsula	3
	Gulf of Alaska	4
	Upper and Lower Koyukuk	1
	Kobuk	1
SUBBITUMINOUS COAL		
	North Slope	1,500
	Cook Inlet	1,000
	Nenana	15
	Susitna	3
	Tanana	45
	Yukon	1
	North Aleutian	No Estimate
LIGNITE COAL		
	Copper River	No Estimate
	Seward Peninsula	0.1

*Includes subsurface for Cook Inlet Basin from well data and Matanuska field coals.

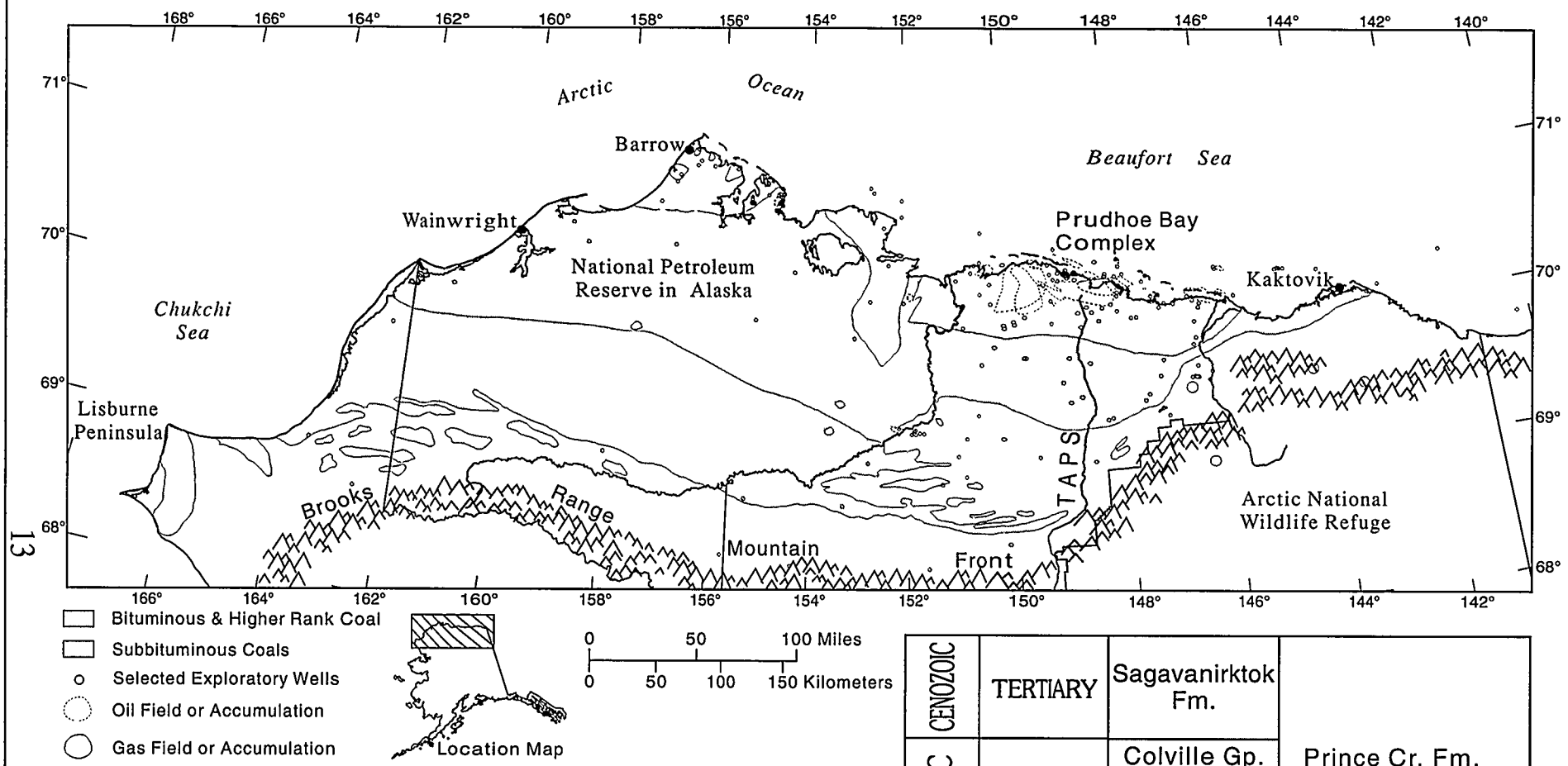


Figure 3. Extent of Northern Alaska Province (North Slope) coals [1].

CENOZOIC	TERTIARY	Sagavanirktok Fm.	
MESOZOIC	CRETACEOUS	Colville Gp.	Prince Cr. Fm.
		Nanushuk Gp.	Corwin Fm.
		Kuparuk Fm.	
	JURASSIC	Kingak Fm.	
	TRIASSIC	Sadlerochit Gp.	
PALEOZOIC	PERMIAN	Lisburne Gp.	
	PENN.		
	MISS.	Endicott Gp.	Kekiktuk Fm.
	DEVONIAN		Kapaloak Fm.

Figure 4. North Slope generalized stratigraphic column.

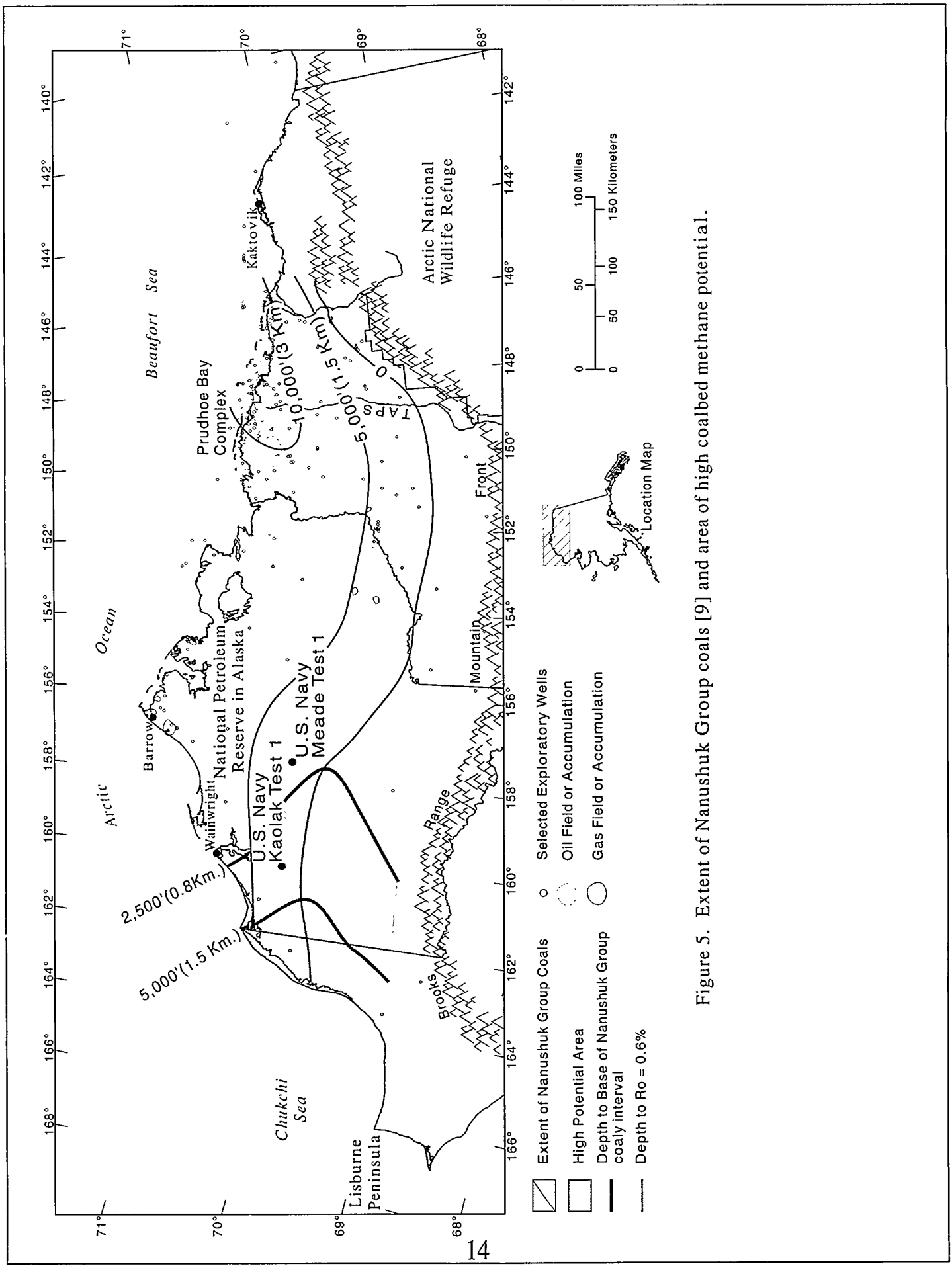


Figure 5. Extent of Nanushuk Group coals [9] and area of high coalbed methane potential.

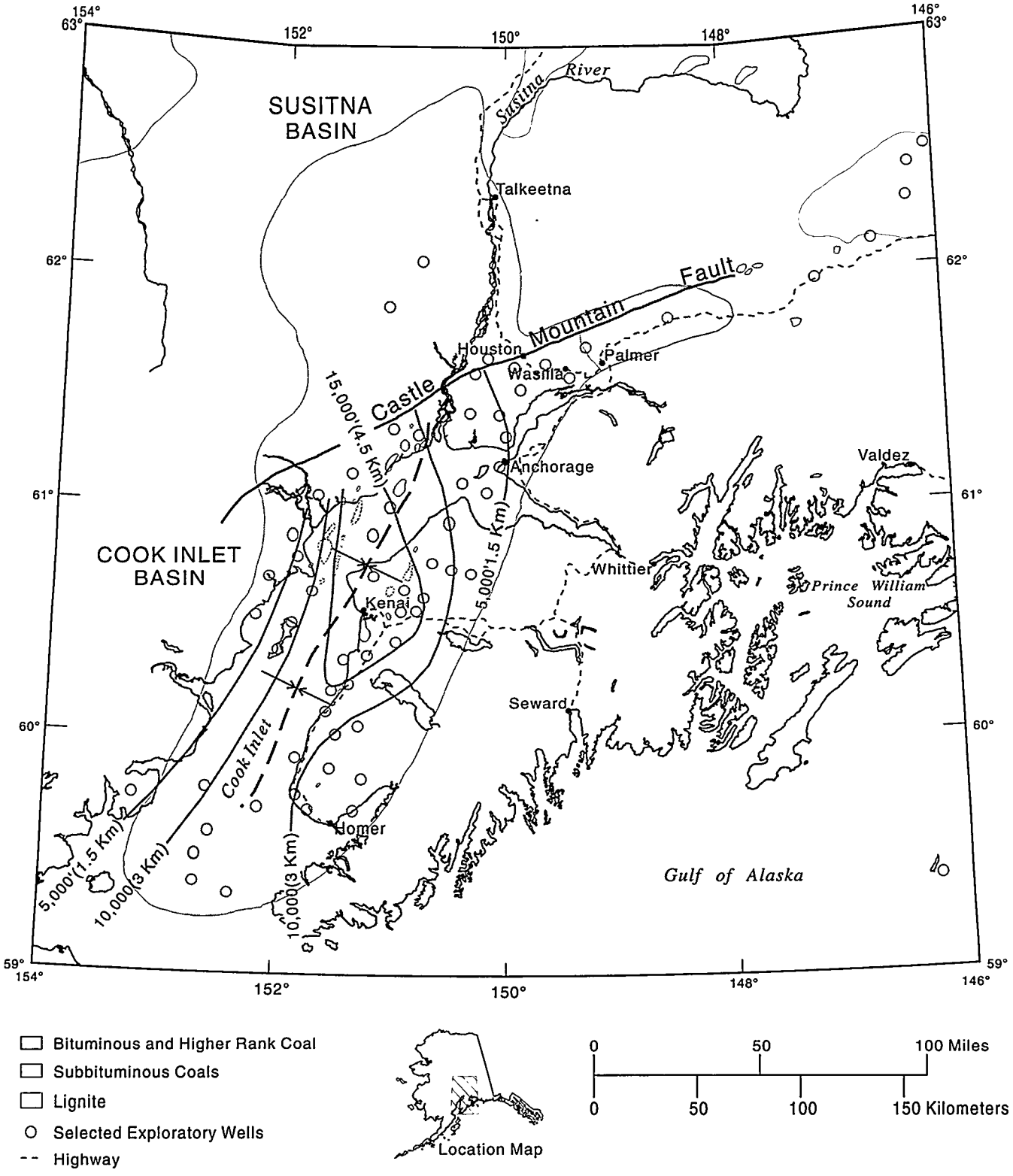


Figure 6. Extent of Cook Inlet-Susitna Province coals [1] showing the basin axis and contours showing depth to Ro = 0.6%.

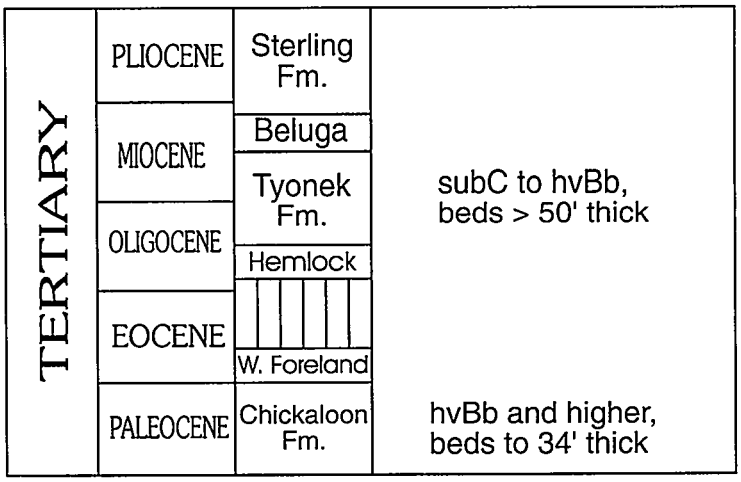


Figure 7. Cook Inlet generalized stratigraphic column.

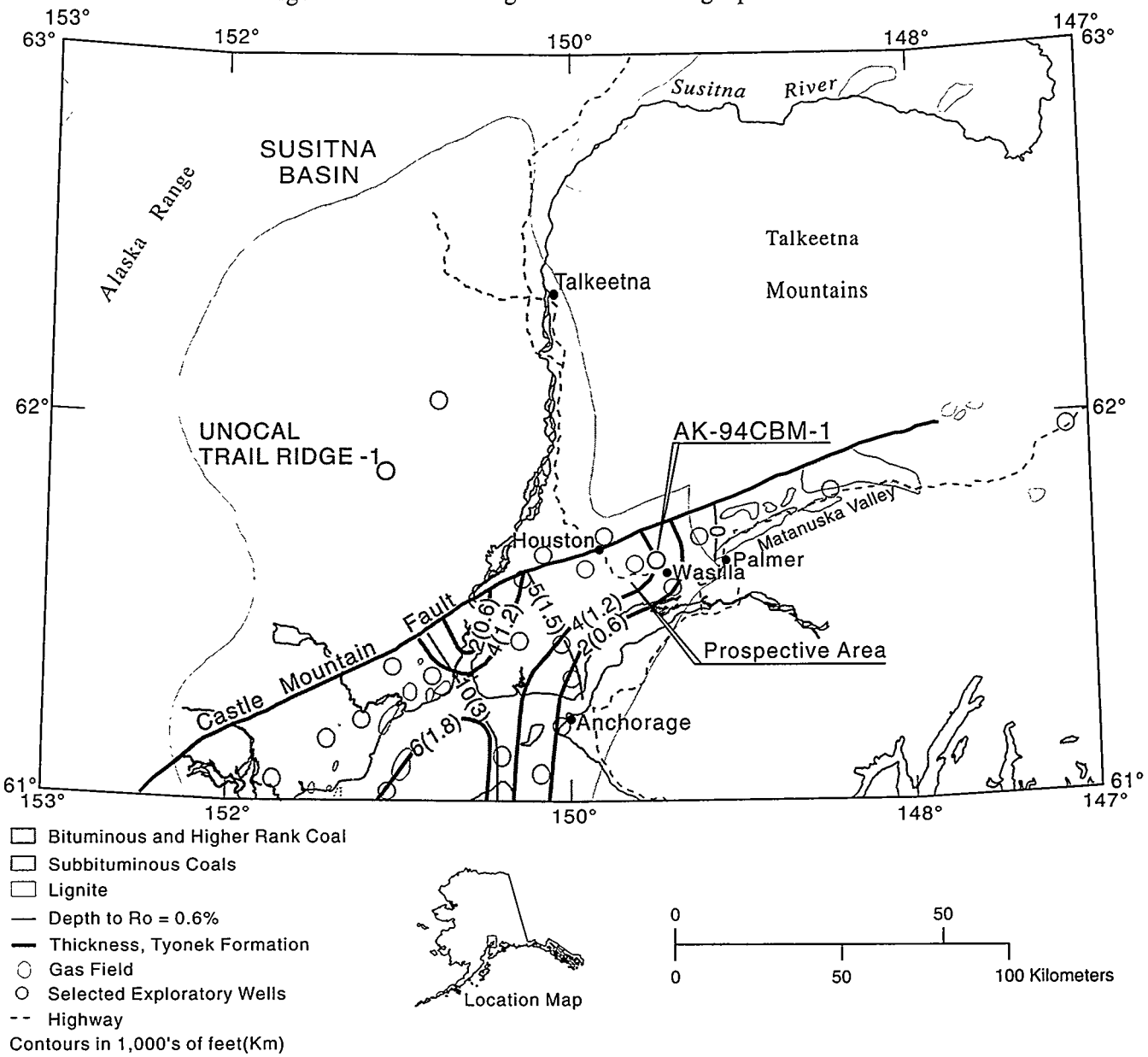
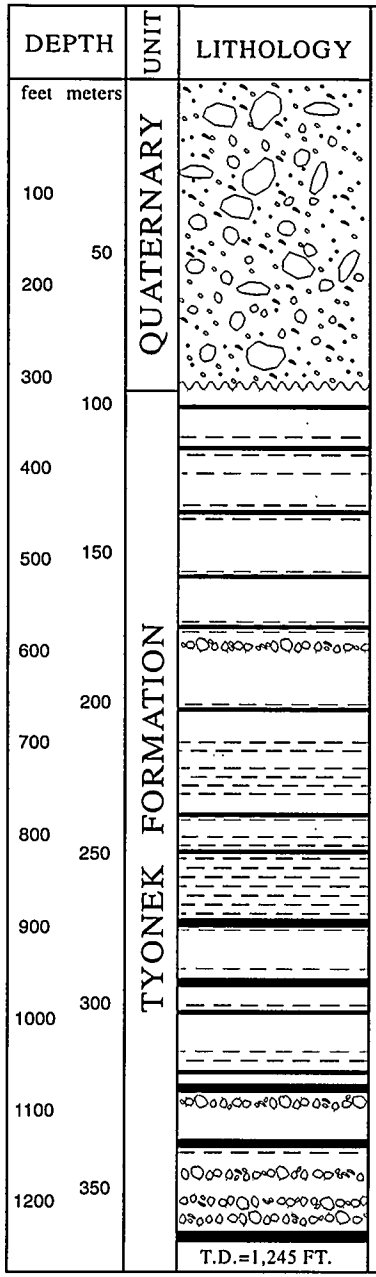


Figure 8. Extent of Susitna and upper Cook Inlet coals [1] showing Tyonek Formation thickness, depth to Ro = 0.6% and prospective area for Tyonek Formation coals.



Legend

- Coal
- Siltstone and mudstone
- Sandstone
- Conglomerate
- Glacial deposits

Seam No.	Gas (DAF) cm^3/gram	Gas (DAF) scf/ton	Moisture %	Ash %	Volatile Matter %	Fixed Carbon %	Ro %	$\delta^{13}C$
1	1.96	63	9.02	8.47	33.80	48.71	0.48	
2	4.14	132	7.13	19.60	32.78	40.49		
3	4.99	160	7.43	11.80	34.34	46/43		-48.9
4	5.31	170	7.96	8.26	34.55	49.23	0.47	
5	5.16	165	5.06	49.80	21.93	23.21		-49.3
6	5.54	177	6.02	14.30	33.84	45.84	0.56	-48.3
7	4.42	141	6.15	26.84	29.47	37.54		-47.0
8	5.94	190	7.17	5.57	37.50	49.76	0.52	
9/10	5.10	163	6.25	14.62	35.18	43.95		
11	5.73	183	5.53	40.18	23.42	30.87		
12	5.72	183	5.23	44.74	22.85	27.18	0.58	-43.3
13	7.66	245	4.82	42.00	30.15	23.03	0.58	-44.0

Figure 9. Coal analyses for AK-94CBM-1.

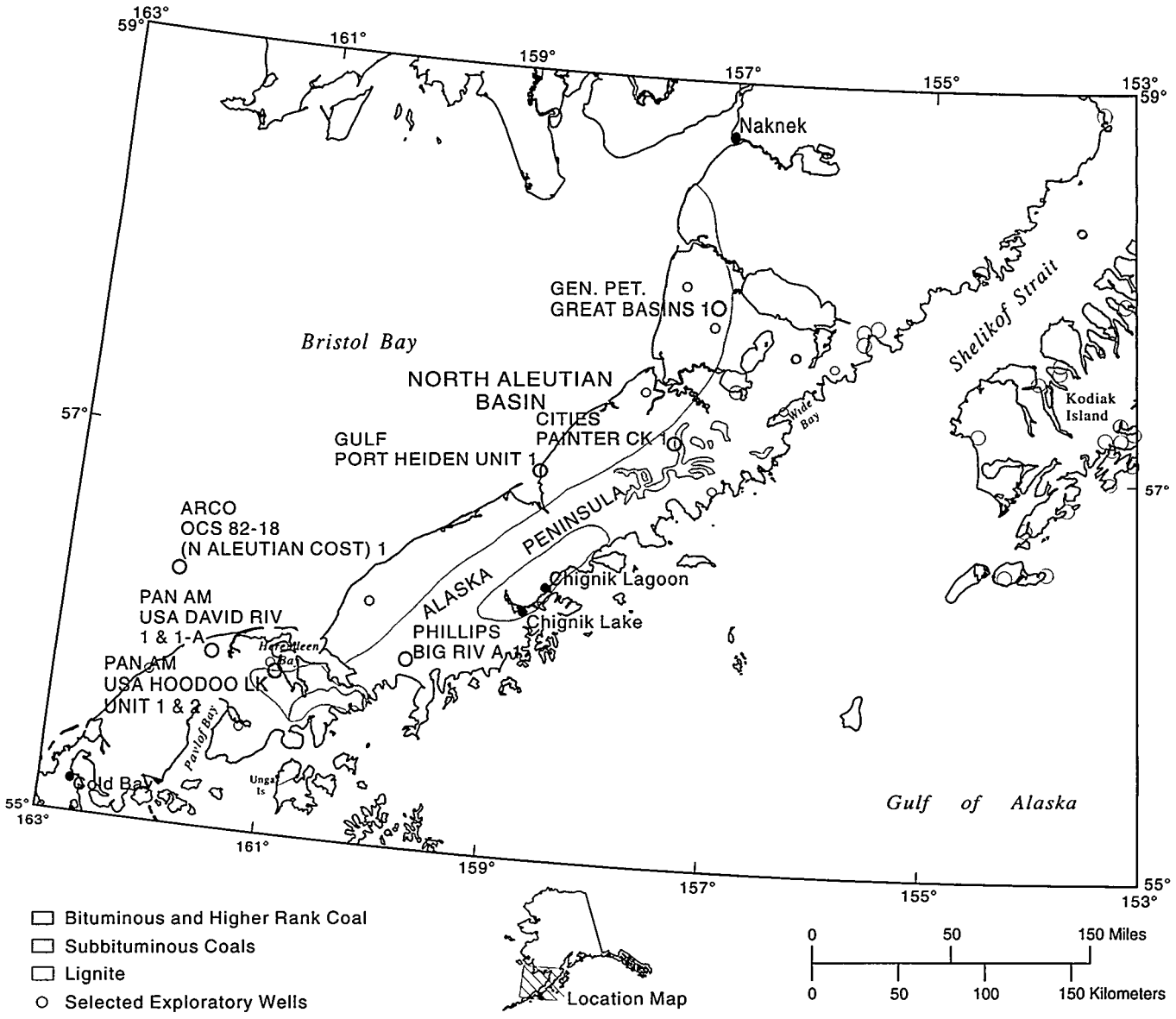


Figure 10. Extent of Alaska Peninsula Province coals [1].

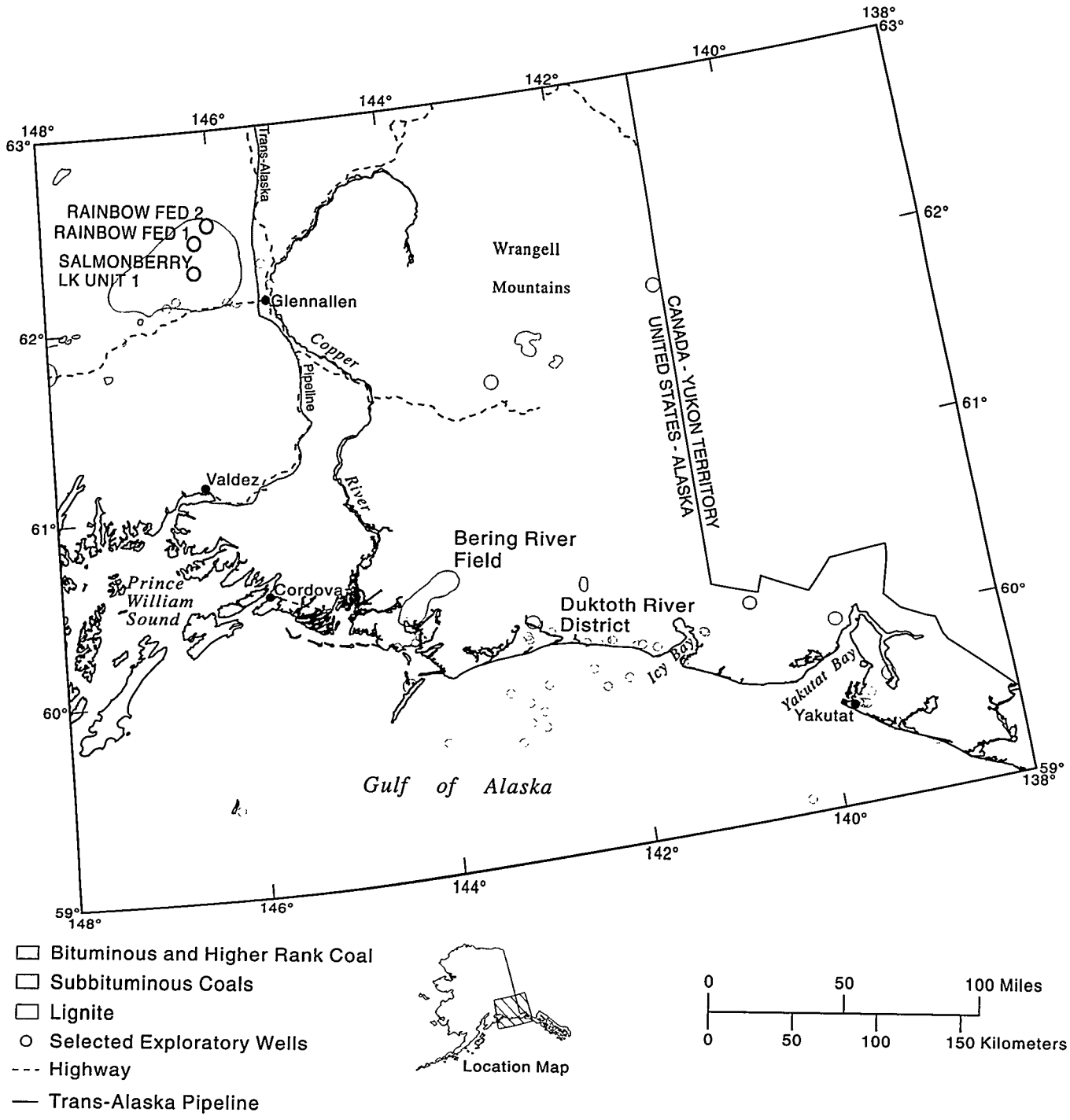


Figure 11. Extent of Gulf of Alaska Province coals and the Copper River Basin [1].

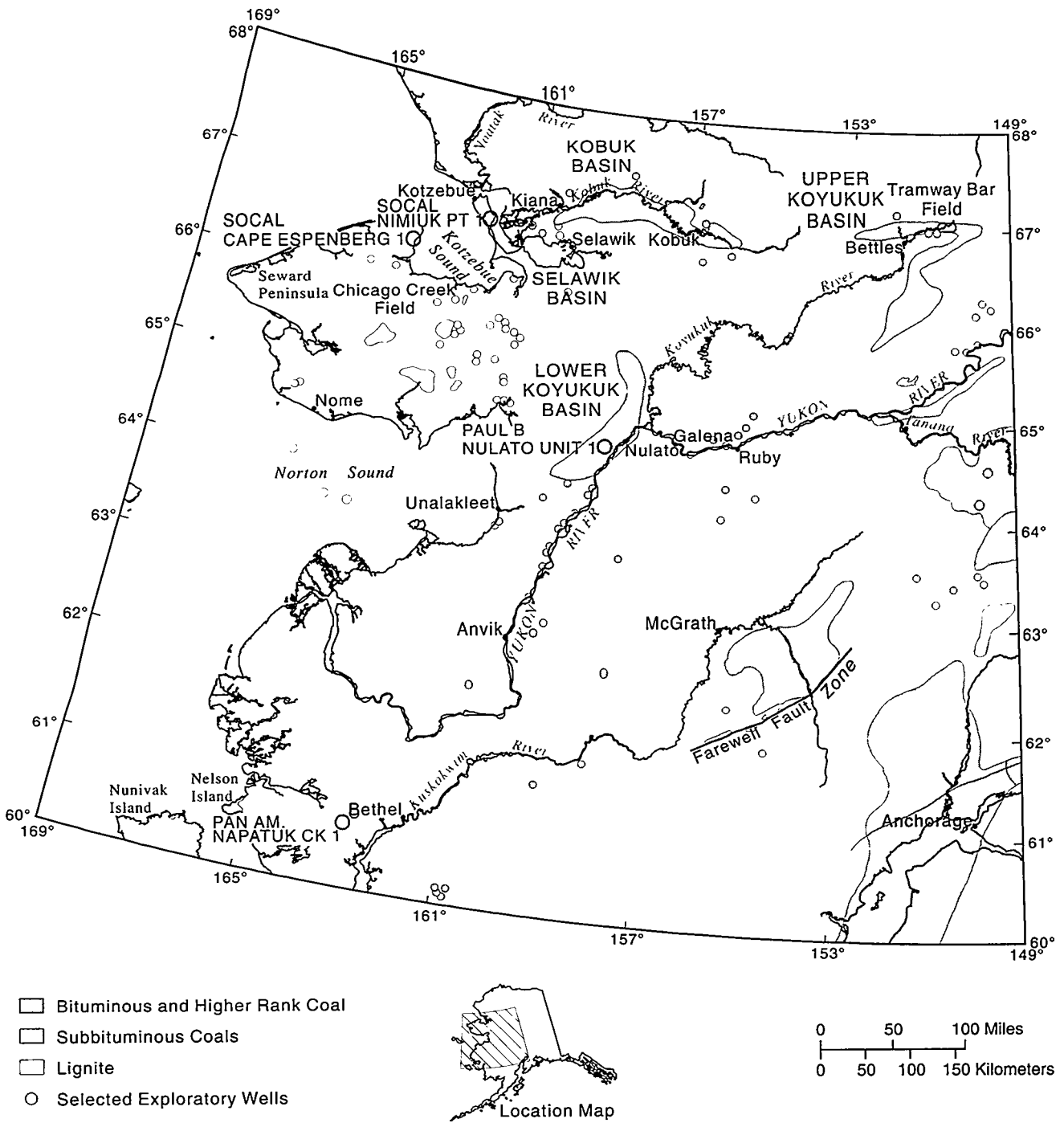


Figure 12. Extent of Yukon-Koyukuk and Seward Peninsula Provinces [1].

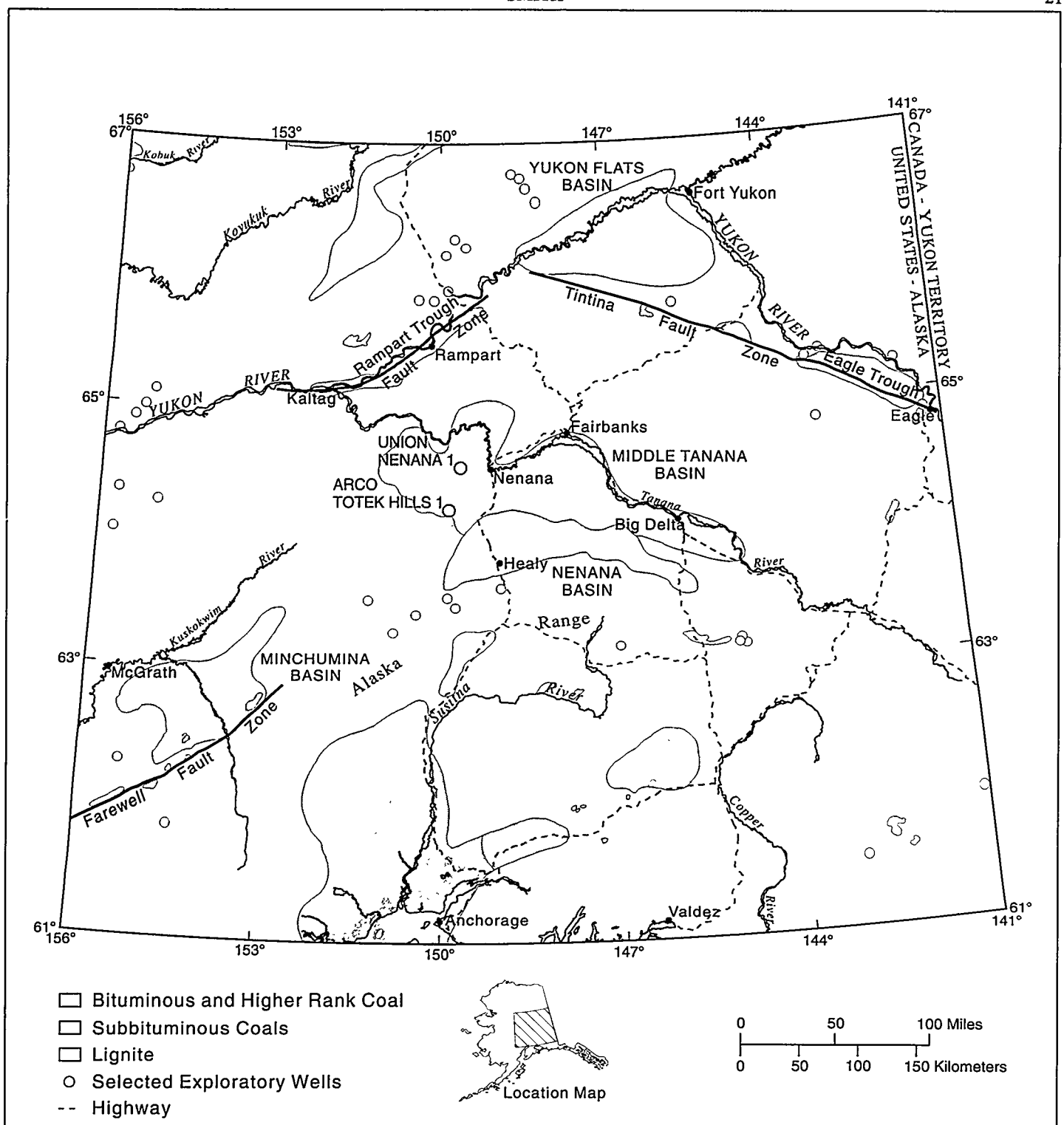


Figure 13. Extent of Nenana Province and Northern Yukon Province coals [1].



NOTES

INTERGAS '95

May 15-19, 1995
The University of Alabama
Tuscaloosa, Alabama USA

9502

Coalbed Gas Potential of the Greater Green River Basin, Southwest Wyoming and Northwest Colorado

R. Tyler, W.R. Kaiser, A.R. Scott and D.S. Hamilton,
Bureau of Economic Geology, The University of Texas at Austin

ABSTRACT

Coalbed gas is an important source of natural gas in the United States. In 1993, approximately 740 Bcf (21 Tm^3) of coalbed gas was produced in the United States, or approximately 4.2 percent of the nation's total gas production. Nearly 96 percent of this coalbed gas is produced from just two basins, the San Juan (615.7 Bcf, 17.4 Tm^3; gas-in-place 84 Tcf, 2.4 Tm^3) and Black Warrior (105 Bcf, 2.9 Tm^3; gas-in-place 20 Tcf, 5.1 Tm^3), and current development represents only a fraction of the nation's estimated 675 Tcf (19.1 Tm^3) of in-place coalbed gas resources. Coal beds in the Greater Green River Basin in southwest Wyoming and northwest Colorado hold almost half of these resources (314 Tcf, 8.9 Tm^3), and coal is an important source of gas for low-permeability sandstones. Because total gas resources in the basin are reported to exceed 3,000 Tcf (85 Tm^3), the basin may substantially increase the domestic gas resource base. Consequently, the coalbed gas potential of the basin was assessed through integrated geologic and hydrologic studies, where tectonic, structural, and depositional setting, coal distribution and rank, gas content, coal permeability, and ground-water flow are critical controls on coalbed gas producibility. Synergism among these geologic and hydrologic controls determines high gas productivity; high productivity is governed by (1) thick, laterally continuous coals of high thermal maturity, (2) basinward flow of ground water through fractured and permeable coals, down the coal rank gradient toward no-flow boundaries oriented perpendicular to the regional flow direction, and (3) conventional trapping of gas along those boundaries to provide additional source gas beyond that sorbed on the coal surface. Using this synergism, Mesaverde Group coalbed gas exploration is justified at the northwestern end of the Cedar Mountain fault system in the Sand Wash Basin, along the eastern margin of the Washakie Basin, and around the northeast flank of the Rock Springs Uplift. In the Fort Union Formation, the Sandy Bend Arch and the Big Piney area are coalbed gas prospective where conventional trapping enhances gas contents in low-rank coals.

INTRODUCTION

Methane from coal beds, an important emerging source of natural gas in the Lower 48 States, is set to make a substantial contribution to the United States domestic gas resource base. Production of coalbed gases has increased nearly fivefold since 1990, accounting for 3 percent of U.S. gas production and 5 percent of proved reserves by the end of 1992 [1]. However, 96 percent of this gas was produced from just two basins, the San Juan and Black Warrior (fig. 1), and current development represents only a fraction of the estimated 675 Tcf (19.1 Tm^3) of coalbed methane resources in place in U.S. basins [2], [3], [4]. The Gas Research Institute (GRI), on behalf of the U.S. natural gas industry, is actively fostering development in other U.S. coal basins. As part of this effort, the GRI has commissioned investigations of the San Juan, Greater Green River, Piceance, Powder River, and Raton Basins, which, by virtue of their tremendous coal tonnages, contain 558 Tcf (16 Tm^3) of methane, or 83 percent of the nation's total coalbed methane resource (fig. 1).

This paper focuses on the Greater Green River Basin and aims at assessing its coalbed methane potential through integrated hydrologic and geologic studies. The Greater Green River Basin report of Tyler and others [5] is the latest of the GRI-sponsored investigations of the Western Interior basins and complements the earlier reports of McCord [6], McFall and others [7], Kelso and others [8], and Stevens and others [9]; the detailed studies of the San Juan [10] and Sand Wash [3], [11] Basins; and the four-basin overview of Tyler and others [12].

This paper also embodies the current ideas of the Bureau of Economic Geology about the geologic and hydrologic conditions necessary for producibility of coalbed methane. The comprehensive studies of the San Juan (containing 88 Tcf) [10], [13] and Sand Wash Basins (containing 101 Tcf) [3], [11] indicate that coalbed methane producibility is profoundly influenced by several key geologic and hydrologic controls, including tectonics, structure, deposition, hydrologic setting, coal rank, and gas

content [14]. These controls and their influence on producibility are discussed in terms of the Upper Cretaceous Mesaverde Group and lower Tertiary Fort Union Formation in the Greater Green River Basin. Their relative importance is assessed in the context of lessons learned in the San Juan and Sand Wash Basins.

RESOURCES AND PRODUCTION

In the Greater Green River Basin, coal and gas resources total 1,277 billion short tons (1,158 billion t) and 314 Tcf (8.89 Tm^3), respectively (table 1) [4]. The Mesaverde Group contains 627 billion tons (569 billion t) and 264 Tcf (7.47 Tm^3), accounting for 49 and 84 percent of the total resources, respectively. The Fort Union Formation contains 649 billion tons (589 billion t) and 50 Tcf (1.42 Tm^3), accounting for 51 and 16 percent of the total resources, respectively (table 1). At depths of less than 7,500 ft (<2,286 m), coal and gas resources are 688 billion tons (624 billion t) and 84 Tcf (2.38 Tm^3), respectively (table 1). At those depths, Mesaverde resources are 243 billion tons (220 billion t) and 56 Tcf (1.58 Tm^3), accounting for 35 and 67 percent, respectively, of the resources at less than 7,500 ft (<2,286 m). Fort Union resources are 445 billion tons (404 billion t) and 28 Tcf (0.79 Tm^3), accounting for 65 and 33 percent of the resources, respectively (table 1).

Coalbed methane production in the Greater Green River Basin has been established only in the Sand Wash Basin, where gas production from the Williams Fork Formation has been minimal and water production excessive. Cumulative gas and water production is 138 MMscf (3.9 MMm^3) and 7.0 MMbbl (1.2 MMm^3), respectively, for a cumulative basinwide gas–water ratio of approximately 20 scf/bbl (~3.6 m^3/m^3). Among the 11 wells in Dixon field, 3 structurally high wells currently produce gas at rates of less than 40 Mcf/d (<1.1 Mm^3/d). Initially, eight wells were flowing artesian and served as dewatering wells; they flowed at rates ranging from 600 to 1,000 bbl/d (95 to 159 m^3/d) for a per-well average of approximately 700 bbl/d (~111 m^3/d) in 1991. Upon production, rates have declined to approximately 500 bbl/d (~64 m^3/d). In Craig Dome field, 16 plugged and abandoned wells produced no gas and large volumes of water (~500 bbl/d [~80 m^3/d] per well) over a 12- to 18-mo test period. Nine Fort Union coalbed wells were completed, production tested, plugged, and abandoned. During test periods ranging from 9 d to 7 mo, the wells made zero to negligible volumes of gas and tens of thousands of barrels of water (thousands of cubic meters). Because of proximity to the recharge area and high permeability, economically dewatering (depressuring) coal beds near the basin margin may be impossible. Disposal costs of large volumes of produced water can adversely affect project economics to the extent that development may be deemed uneconomical.

Along the northeast flank of the Rock Springs Uplift, coals of the Fort Union, Almond, and Rock Springs Formations were tested. Only Rock Springs coals showed commercial promise. Production forecasts predicted recoveries of 1 to 3 Bcf/160 ac (28 to 84 MMm^3/65 ha) and peak rates of 240 to 1,200 Mcf/d (6.79 to 34.00 Mm^3/d). Despite these promising forecasts, test results were disappointing. During a 530-d production test, the most successful well (2 UPRC-1) averaged 78 Mcf/d (2.2 Mm^3/d) and 200 bwpd (32 m^3/d) from a 50-ft (15.3-m) interval [15]. Development was stopped in 1992, primarily by low gas prices and disappointing test results and secondarily by environmental concern over disposal of produced water. A pair of northern wells, completed in Fort Union and Almond coals, were tested for 4 mo and produced less than 100 Mcf/d (<2.8 Mm^3/d); low permeability and low gas content (~200 scf/ton [~6.24 m^3/t]) doomed these wells.

TECTONIC AND STRUCTURAL SETTING

The tectonic and structural setting of a basin is the most fundamental underlying control on coalbed methane resources because it (1) determines the subsidence regime that in turn determines sedimentation patterns and the locus of peat accumulation, (2) dictates whether coalification proceeds to ranks sufficient for thermogenic gas generation through burial and thermal history, (3) orients stress-induced fractures (cleats) in the coal and determines whether the fractures are open to enhance permeability, (4) defines drilling depth to target coalbed reservoirs, and (5) creates structures for conventional trapping of gas [5].

The Greater Green River Basin is located in the Rocky Mountain Foreland, a major tectonic element between the Wyoming–Idaho Overthrust Belt and the North American Craton (fig. 2). During Cretaceous time this foreland was a rapidly subsiding, elongate, asymmetric trough occupied by the Western Interior Seaway, a shallow continental seaway extending from the Gulf of Mexico to the Canadian Arctic [16]. Periodic thrust faulting and uplift in the Overthrust Belt caused sediment to be shed eastward into the seaway, resulting in episodic advancement eastward of the Late Cretaceous shorelines. These wedges of clastic sediment include the thick Mesaverde Group coals that have been targeted for coalbed methane exploration and development. During the Laramide Orogeny, in Late Cretaceous and early Tertiary time, the Rocky Mountain Foreland was broken into a number of smaller basins by thick-skinned thrusting. The Greater Green River Basin became a thrust/fault-bounded, structurally complex intermontane basin that was subdivided into four subbasins (fig. 3). Maximum horizontal compressive stress, orthogonal to thrust fronts, resulted in the genesis of natural fracture domains being oriented in the maximum shortening direction. Face cleat domains strike northeastward over most of the basin, and overlapping cleat domains strike northwestward and northeastward in the Sand Wash Basin, to impose permeability anisotropy on the coal beds. Basement-involved thrusts also elevated basin margin highlands, which shed sediment into the newly formed intermontane basins. Thick sequences of lower Tertiary intermontane fluvial-lacustrine sediments host the Paleocene Fort Union Formation's thickest coal seams, which have been targeted for coalbed methane exploration and development. Organic accumulation and peat preser-

vation were favored by rapid subsidence and syntectonic sedimentation.

The present structural configuration of the Greater Green River Basin began to emerge during the Laramide Orogeny (figs. 2 and 3). Subsequently an episode of erosion occurred, followed by a period of widespread magmatism and volcanism in the Oligocene, and finally an episode of renewed tectonic uplift about 10 m.y.a. By the end of the Pliocene, the basin's present structural configuration, topography, surface drainage, and hydrodynamics were largely established.

Local tectonic and/or compaction-induced folds and faults that are present throughout the basin may be more important controls as sites of fracture-enhanced permeability and conventional trapping of gas. Structural complexity (folds and faults) may favor the presence of fracture-enhanced permeability and conventional trapping of gas, but it also causes steep dips and deep burial of target coal seams. Most of the coal seams are deeply buried except along the southeast margin of the basin (Sand Wash and Washakie Basins), at the Rock Springs Uplift, and on the north end of the Moxa Arch (La Barge Platform), where coals are less than 6,000 ft (<1,830 m) deep (fig. 3).

STRATIGRAPHIC AND DEPOSITIONAL SETTING

The genetic approach to stratigraphic analysis is applied to identify those strata that were deposited during discrete episodes and share a common environment of deposition, or depositional system. Depositional system imposes a strong control on coalbed methane producibility because it determines the size, thickness orientation, and stratigraphy of the coalbed reservoirs. The processes of peat accumulation and its preservation as coal require a delicately balanced subsidence rate that maintains optimum water table levels but excludes disruptive clastic sediment influx. Depositional systems also define the substrate upon which peat growth begins and within which peat swamps proliferate. Size of the coal bed is thus controlled by the area of sediment bypass in the peat swamp, and coalbed thickness is determined by the length of time the swamp remains uninterrupted by sediment influx. Depositional architecture dictates the orientation of the coals. Coastal plain coals, for example, are strike aligned and parallel to the orientation of the shoreline systems [17]. Fluvial coals, in contrast, are commonly dip oriented and closer in geometry to the fluvial-channel belts. Sandstone distribution and coal distribution are generally intimately associated, and an understanding of depositional architecture and sand-body geometry can enable prediction of coalbed distribution throughout a basin. Large net coal thickness is critical to establishing a coalbed gas resource, and individual coalbed thickness indicates productivity.

Although in the Greater Green River Basin the coal-bearing stratigraphic interval extends from the Upper Cretaceous Frontier Formation to the base of the lower Tertiary Wasatch Formation, the Upper Cretaceous Mesaverde Group and lower Tertiary Fort Union Formation are the major coal intervals [12] (fig. 4). Upper Cretaceous depositional systems were predominantly wave-dominated deltas and barrier/strandplains that formed linear clastic shorelines. The thickest coal seams were preserved on the coastal plain landward and parallel to these ancient shorelines. In the Mesaverde Group, the Rock Springs and Williams Fork Formations host thick, continuous, shore-parallel coal beds. The Rock Springs coals reach a maximum net coal thickness of a little more than 100 ft (33 m) in as many as 12 coal beds along an 8.5-mi-wide (13.4-km) zone on the flanks of the Rock Springs Uplift that extends from the town of Rock Springs, Wyoming, northeast for approximately 60 mi (~197 km) and southwest for 40 mi (131 km) (fig. 5) [17]. The coals thin rapidly to the southeast, where they are bounded by shoreline sandstones. By late Mesaverde Williams Fork time, southeastward progradation of the shorelines had established favorable coal-forming conditions in the southeastern Sand Wash Basin in the Craig, Colorado, area. The northeast-oriented Williams Fork coals extend in the subsurface for at least 40 mi (131 km) before being exposed at outcrop along the south and northeast margins of the Sand Wash Basin (fig. 6). Maximum net coal thickness in the Craig area is 220 ft (67 m) in as many as 40 coal beds. The dominant strike-elongate (northeast) orientation of the Rock Springs and Williams Fork coals and their overlap with sandstone-poor coastal plain areas behind the paleo-shorelines indicate that the coastal plain systems provided optimal conditions of subsidence, water table level, and shelter from clastic influx for peat to accumulate and be preserved [17]. The coals thin to the west and northwest in both units, suggesting that peat growth and preservation in that direction was inhibited by disruptive clastic influx and lowering of water table levels associated with the transition landward into slightly elevated fluvial environments.

In contrast to the coals of the Upper Cretaceous, the lower Tertiary coals, hosted by fluvial-lacustrine sediments, show strong evidence of syntectonic control [18]. The lower Tertiary coal beds (lower coal-bearing unit, Fort Union Formation) are thick and widespread. The maximum net coal thickness of 140 ft (42.7 m) occurs in the depositional center of the Green River Basin, but net coal thickness exceeds 80 ft (>24.4 m) in all subbasins (fig. 7). Individually the coal beds can be as much as 40 ft (12.2) thick, extending laterally typically more than 10 mi (>16 km). Syntectonic control is indicated by marked thinning of the coals over the major structural features, the Rock Springs Uplift, Moxa Arch, and Pinedale Anticline, and subtle thinning across the Cherokee and Wamsutter Arches [18]. The syntectonic control is further suggested by the relationship between trends in coal thickness and sandstone distribution of the Fort Union fluvial systems. Net coal is thickest along the depositional axes of the greater basin, and on the basis of detailed studies in the Sand Wash Basin [18], is thought to overlap the trend of high net sandstone. The coals thus occupy the same axial position as the fluvial systems. This suggests that tectonism provided optimal subsidence rates for peat accumulation, periodically shutting down the sediment supply to the intermontane fluvial systems. Channel-fill sandstones focused ground-water flow to initiate peat swamps, maintain water table levels, and preserve peat.

COAL RANK, GAS CONTENT, AND GAS COMPOSITION

In comparison with other Western Interior basins such as the San Juan, Piceance, or Raton Basins, the Greater Green River Basin is characterized by relatively low coal rank. Although reaching semianthracite rank in the deep Washakie Basin, coal ranks at exploitable drilling depths more typically range from high-volatile C to high-volatile A bituminous and have thus barely reached the threshold of thermogenic gas generation (fig. 8). In the Mesaverde Group, coal rank along the basin margins and around the Rock Springs Uplift is subbituminous to high-volatile C bituminous, increasing with depth to high-volatile A bituminous at around 7,500 ft (~2,286 m) (fig. 8). Only below these depths have the coals reached ranks sufficient to generate large volumes of thermogenic gas. Fort Union coal rank is also low, ranging from subbituminous along the basin margins and the Rock Springs Uplift to low-volatile bituminous in the Washakie Basin (fig. 9).

Consistent with the coal rank trends, gas contents of the Greater Green River Basin coals are generally low; dry, ash-free gas content values are typically less than 200 scf/ton (<6.24 m^3/t) in the Mesaverde coals and less than 100 scf/ton (<3.12 m^3/t) in the Fort Union coals (fig. 10). However, despite generally low gas contents, areas of high gas content do exist. Areas having higher Mesaverde gas contents in the Sand Wash Basin are located (1) in an area of artesian overpressure along the Cherokee Arch and (2) along the northwestward-trending Cedar Mountain fault system where ground-water flow turns upward at the transition between hydropressure and hydrocarbon overpressure [3]. Gas contents average 350 scf/ton (10.92 m^3/t) in Rock Springs coals north of the Rock Springs Uplift. The gas content profile in these coals is not fully understood, however, because gas content decreases with increasing depth. This atypical profile is not readily explained, but it may reflect a Pleistocene recharge event and generation of secondary biogenic gases. Gas contents of approximately 500 scf/ton (~15.6 m^3/t) were reported in Fort Union subbituminous coals in the Big Piney area and may reflect conventional trapping of gas.

Greater Green River Basin coalbed gases are early thermogenic, thermogenic, and secondary biogenic [19]. The Mesaverde coalbed gases are early thermogenic and/or secondary biogenic in the hydropressured parts of the basin and predominantly thermogenic in deeper parts of the basin near the hydropressure–hydrocarbon overpressure boundary. Fort Union coals are lower rank, and therefore the coalbed gases are predominantly early thermogenic and/or secondary biogenic, although thermogenic gas may be more important in the deeper parts of the basin, where the coals approach or exceed high-volatile A bituminous rank.

Thermal maturity is the biggest impediment to coalbed methane potential of the Greater Green River Basin. However, mechanisms that enhance gas contents of the generally low rank coals, such as updip gas migration from thermally mature coals at depth, generation of secondary biogenic gas in dynamic flow systems, and conventional trapping at the transition of hydropressure and hydrocarbon overpressure, have been demonstrated in a number of areas. More than likely these same mechanisms have operated in other parts of the basin where data are currently sparse. Exploration and development strategies should allow for these mechanisms.

HYDROLOGY

Hydrology affects coalbed methane producibility in several ways. In a typical coalbed methane reservoir, for example, hydrodynamics promotes sorption of gas on the coal surface by maintaining reservoir pressure. Where the coalbed methane reservoir is dominated by (or has a component of) conventional trapping, vigorous ground-water flow provides the means (in solution or by entrainment) for long distance migration of the coalbed gases to the trap and introduces bacteria for generating secondary biogenic gases. Although hydrodynamics clearly helps enrich gas content for commercial production, it can also be detrimental if production is attempted close to recharge areas and too much water is produced.

Hydrologic characterization can reveal much about reservoir conditions because hydraulic gradient, pressure regime, and hydrochemistry reflect an aquifer's ability to accept and transmit fluid and, thus, regional permeability contrasts. An example in the Fruitland Formation, San Juan Basin, shows enhanced permeability correlating with gentle hydraulic gradients, artesian overpressure, and low-chloride formation waters. We would argue that artesian overpressure requires enhanced permeability and recharge at an elevated outcrop and aquifer confinement in the subsurface. The presence of low-chloride water also indicates active flow and permeable pathways. Underpressure, in contrast, reflects hydrologic isolation, reduced permeability, and limited recharge in the absence of a high-permeability drain. Exceptionally high coal gas production occurs at the transition between pressure regimes.

In our basin-scale conceptual model [14], producibility of coalbed methane is enhanced when hydrodynamics are favorable. We suggest that optimal conditions occur when ground water flows through coals of high rank and gas content orthogonally toward no-flow boundaries (regional hingelines, fault systems, facies changes, and/or discharge areas), enabling efficient sweeping of gas for eventual resorption and conventional trapping basinward [3]. The extent to which these optimal conditions are met in the Greater Green River Basin is assessed in the Mesaverde and Fort Union coal-bearing stratigraphic units.

Recharge to the Mesaverde aquifer occurs primarily at outcrop along the east margin of the Greater Green River Basin, in the foothills of the Sierra Madre Uplift, Park Range, and Williams Fork Mountains (fig. 11). Ground water flows westward, from the wet elevated basin margin, down hydrologic gradient, to discharge eventually basinward along fault systems and facies changes that separate hydropressure from regional hydrocarbon overpressure in the central basin. In the Tertiary aquifer system, recharge occurs primarily along the foothills of the Sierra Madre Uplift and Park Range, Wind River, Wyoming, and Uinta

Mountains. Dynamic flow throughout the greater basin is basinward toward topographically low areas such as the Green River and Little Snake River valleys for eventual discharge. Dynamic flow promotes generation of secondary biogenic gas, migration of it and thermogenic gas, and presumably delivery and concentration at traps when oriented at a high angle to them. Ground-water flow in the Mesaverde aquifer is dynamic in the eastern Sand Wash and Washakie Basins but is restricted off the flanks of the Rock Springs Uplift and in the Green River Basin by low precipitation, high evaporation rates, and faults (fig. 11). Hydrodynamics in the Green River Basin is difficult to assess because the Mesaverde is fault-severed from the wet basin margin and receives little direct recharge. Sluggish ground-water flow is postulated in the basin interior, but data are limited and identification of pressure transition zones that may favor coalbed methane accumulation was impossible.

In the deep central part of the eastern Greater Green River Basin, hydrocarbon overpressuring dominates the Mesaverde aquifer, being flanked by hydropressured strata above approximately 8,000 ft (~2,440 m) (fig. 12). No pressure regime regionally dominates in the hydropressured section, but artesian overpressure occurs locally on the eastern Cherokee Arch and along the east margin of the Washakie Basin. A large fault system, the Savery fault system, separates hydrocarbon overpressured and hydropressured strata along the east margin of the Washakie Basin (fig. 12). The potential for conventional trapping, upward flow at the pressure boundary, and generation of biogenic gas may favor coalbed methane accumulation. The same can be said of the Cedar Mountain fault system in the Sand Wash Basin (fig. 12). The transition zone between hydropressure and hydrocarbon overpressure on the east side of the Rock Springs Uplift may also indicate potential for upward flow and hydrodynamic conditions favorable to coalbed methane accumulation at depth. The transition zone may signify a no-flow boundary caused by extensive diagenesis, where meteoric water moving basinward has mixed with late compactional fluids moving out of the basin. Mixing of chemically disparate waters would favor mineral precipitation and permeability reduction.

Fort Union coals are present throughout much of the basin (fig. 13) but gas contents are low (~100 scf/ton [~3.12 m^3/t] or less), and thus are secondary coalbed methane targets. The possibility of structurally or stratigraphically trapped gas always remains, however. Fort Union coals at 3,500 ft (1,067 m) in a well in the Big Piney area (fig. 13) are reported to have gas contents of approximately 500 scf/ton (~15.60 m^3/t) that may reflect conventional trapping of gas. Fort Union sandstones produce oil and gas from structural, stratigraphic, and combination traps on the La Barge Platform [20]. Hydrocarbons apparently migrated from the nearby deep Pinedale Basin, where coals and shales were thermally mature for hydrocarbon generation [21]. Ranks of high-volatile A bituminous or higher occur in the basin and flank the Big Piney area (fig. 13). Secondary biogenic gas can also be added as a source of gas wherever its generation is favored by active meteoric circulation [19] in the dynamic Tertiary aquifer system. Ground water flows southeastward across the La Barge Platform.

In the northern Green River Basin, more than 100 net ft (>30 m) of coal is present in individual coals as much as 50 ft (15 m) thick. These coals have never been tested and may be prospective on the Sandy Bend Arch, which lies between the La Barge Platform and the northern Rock Springs Uplift (fig. 13). Again, the Pinedale Basin is a potential source of migrated thermogenic gas, and secondary biogenic gas may also be present to increase gas contents. Ground water flows southward, orthogonal to the arch and down the coal-rank gradient, to maximize possible contribution from thermogenic and/or secondary biogenic gas dissolved, entrained, or both, in south-flowing meteoric water. Potential conventional traps may also occur on the downthrown side of the Rock Springs thrust fault.

Finally, along the Cherokee Arch, considerable Fort Union conventional gas and oil production has been established that probably reflects convergent, upward flow as well as structural and stratigraphic trapping. Upward leakage and/or migration updip of water and hydrocarbons from deeper parts of the basin along the Cherokee Arch fault system and flanks of the arch has been postulated [3]. Although Fort Union coals are thinner or less numerous and still of low rank westward along the Cherokee Arch, they may be highly charged with gas and thus be possible candidates for completion in the course of conventional gas development. Such completions have been proposed for the Powder Wash area (fig. 13).

EXPLORATION FAIRWAYS

The Greater Green River Basin is a largely untested, frontier coalbed methane basin, in which deeper drilling will be required to penetrate higher-rank, higher-gas-content Mesaverde and Fort Union coals. Gas contents of the Mesaverde Group, between 6,000 and 7,500 ft (1,830 and 2,286 m), are approximately 350 scf/ton (~10.92 m^3/t) and exceed 500 scf/ton (15.60 m^3/t) below 7,500 ft (2,286 m). Mesaverde and Fort Union coal distribution and steep structural dip limit deeper drilling to the Sand Wash Basin, eastern Washakie Basin, northeast flank of the Rock Springs Uplift, the Sandy Bend Arch, and the La Barge Platform in the Big Piney area (fig. 14).

In the Sand Wash Basin (fig. 14) northwest of Craig, the Cedar Mountain fault system terminates in a zone of convergence along the boundary between hydropressure and regional overpressure. Higher-rank, high-gas-content Mesaverde coals are present in the area, suggesting high production potential. Along the east margin of the Washakie Basin (fig. 14), normally pressured and artesian overpressured coals have gas contents ranging from 250 to 350 scf/ton (7.80 to 10.92 m^3/t). However, although excessive water production has limited producibility, it is predicted to decrease northward coincident with decreasing recharge. On the northeastern Rock Springs Uplift (fig. 14), coals of the Rock Springs Formation have been targeted for development because thickness, resources, and gas content are favorable. Net coal thickness in 5-ft (1.5-m) seams exceeds

40 ft (12 m), gas resources at less than 7,500 ft (<2,286 m) are approximately 9 Tcf (~0.25 Tm^3), rank ranges from high-volatile C bituminous to high-volatile A bituminous, and gas content averages 350 scf/ton (10.92 m^3/t) over a 1,000-ft (305-m) interval. However, an atypical gas-content profile shows decreasing gas content with depth and implies a narrow exploration fairway, which may constrain future development. Thick Rock Springs coals on the southwest flank of the Rock Springs Uplift are probably too deep for economic drilling, thus eliminating these coals as near-term coalbed methane targets.

Although the generally thin Almond coals are not coalbed methane targets, they are possible gas targets in the course of conventional Almond development in the deeper, overpressured parts of the Washakie Basin. Reservoir volumetrics clearly demonstrate that Almond gas production does not originate only from the targeted upper Almond sandstone [22]. Examples are numerous where cumulative gas production has exceeded, or will soon exceed, the total gas in place in the perforated upper sandstone. Iverson [22] attributed the extra gas to laminated sandstones (below the upper sandstone) that were interconnected after hydraulic fracturing. Undoubtedly they contribute gas, but numerous thin coals are present in the upper Almond and may instead be the major contributors and thus should be considered for completion. Completion practices should be reevaluated to consider dual completion of tight sandstones and coals, as is done in the Piceance Basin, for higher-yield, longer-lived gas wells.

Fort Union Formation coals are present throughout much of the basin, but recorded gas contents are low (~100 scf/ton [~3.12 m^3/t] or less) and are thus considered secondary coalbed methane targets. However, structural and/or stratigraphic trapping may enhance gas contents. In the Big Piney area (fig. 14) on the La Barge Platform, where considerable Fort Union conventional oil and gas production has been established, gas contents of approximately 500 scf/ton (~15.6 m^3/t) were reported in subbituminous coals. The coals' low rank and location, flanking the deep Pinedale Basin, are circumstantial evidence of updip migration and conventional trapping of thermogenic gases. In the northern Green River Basin, more than 100 net ft (>30 m) of coal is present, individual coals reaching as much as 40 ft (12.2 m) in thickness. These coals have never been tested and may be prospective on the Sandy Bend Arch (fig. 14). Again, migrated thermogenic gas and secondary biogenic gas are postulated sources of gas. Ground water flows orthogonally to the arch and may bring dissolved and/or entrained gas to the arch for resorption and trapping.

Exploration strategy in the Greater Green River Basin must be to maximize gas content and minimize water production through integrated geologic, hydrologic, and engineering studies. To do so, one must fine-tune three-dimensional modeling of regional system tracts within the regional tectonic, structural, and hydrologic framework. Regional analysis should be coupled with determination of reservoir heterogeneity and properties on a field scale. Greater emphasis should be placed on identifying conventional traps (no-flow boundaries). Conventionally trapped gas and solution gas that can be produced with less associated water are overlooked sources of coalbed methane. Proximity to recharge areas should be avoided because water production has been excessive to date. High water production and depth of drilling are the primary technological challenges facing commercial coal-gas development in the Greater Green River Basin.

CONCLUSIONS

The structurally complex Greater Green River Basin is bounded by the Wyoming–Idaho Overthrust Belt in the west and by basement-cored thrust–faults on the remaining three sides. The basin has four subbasins (Green River, Great Divide, Washakie, and Sand Wash Basins) separated by the Rock Springs Uplift and Wamsutter and Cherokee Arches. Maximum horizontal compressive stress orientations have rotated about a vertical axis with time, a configuration that is reflected in cleat orientations, which are currently northeast in the north and central parts of the basin and are north-northwest in the southeast. The Upper Cretaceous Mesaverde Group and lower Tertiary Fort Union Formation, containing coals that have a maximum combined net thickness of greater than 300 ft (>91.4 m), are the major coalbed methane targets. Coal rank ranges from subbituminous to high-volatile A bituminous, except in deeper subbasins, where coal rank is medium-volatile bituminous and higher. Most of the coalbed gases are thought to be secondary biogenic or migrated thermogenic. Gas contents are less than 200 scf/ton (<6.24 m^3/t) at depths drilled to date. Areas of high gas content (350 to 500 ft^3/ton) reflect conventional trapping of migrated thermogenic or secondary biogenic gases, or both, and correspond to areas of pressure transition and convergent, upward flow of ground water. Conventional trapping will be required to enhance gas content in low-rank coals. Permeable, normally pressured and artesian coal seams occur as deep as 8,000 ft (2,440 m), above regional hydrocarbon overpressure areas. Areas of pressure transition and convergent flow are extensive and are thought to have high production potential. To date, cumulative gas and water production, mostly from Mesaverde (Williams Fork) coals at Dixon field, is 138 MMscf (3.9 MMm^3) and 7.0 MMbbl (1.2 MMm^3) of water, respectively, for a basinwide gas–water ratio of approximately 20 scf/bbl (~3.6 m^3/m^3). Average completion depth is 2,671 ft (814 m). Coal and coalbed methane resources are very large: 1,276 billion short tons (1,158 billion t) and 314 Tcf (8.89 Tm^3). Coal and gas resources in the Mesaverde Group and Fort Union Formation are 627 billion tons (569 billion t) and 264 Tcf (7.47 Tm^3) and 649 billion tons (589 billion t) and 50 Tcf (1.42 Tm^3), respectively. The deeper drilling required to penetrate higher-rank, higher-gas-content coals is thought justified in the Mesaverde Group at the northwest end of the Cedar Mountain fault system in the Sand Wash Basin, along the east margin of the Washakie Basin, and around the northeast flank of the Rock Springs Uplift and in the Fort Union Formation on the Sandy Bend Arch and in the Big Piney area.

ACKNOWLEDGMENTS

This research was funded by the Gas Research Institute under contract no. 5091-214-2261. During the course of the study, our ideas and concepts developed as we discussed research results with operators, other GRI contractors, and our GRI coalbed methane project managers, John Hansen, R. A. McBane, and Dave Hill. Additionally, several operators and pipeline companies supplied data that greatly enhanced the quality of the study; these contributions are gratefully acknowledged. Capable support was also provided by S. E. Laubach, J. S. Yeh, Naijiang Zhou, and R. G. McMurry at The University of Texas at Austin.

This report also benefited from a review by C. M. Tremain, Colorado Geological Survey. The computing staff of the Bureau of Economic Geology, managed by Gerry White, provided guidance in data processing and computer-assisted mapping. Drafting was by the cartographic staff of the Bureau under the direction of Richard L. Dillon, chief cartographer. Word processing was by Susan Lloyd, design by Jamie H. Coggin, and editing by Bobby Duncan.

REFERENCES CITED

1. Oil and Gas Journal, 1993, v. 91, no. 44, p. 89.
2. ICF Resources, 1990, "The United States coalbed methane resource": Quarterly Review of Methane from Coal Seams Technology, v. 7, no. 3, p. 10–28.
3. Kaiser, W. R., Scott, A. R., Hamilton, D. S., Tyler, Roger, McMurry, R. G., Zhou, Naijiang, and Tremain, C. M., 1994a, Geologic and hydrologic controls on coalbed methane: Sand Wash Basin, Colorado and Wyoming: The University of Texas at Austin, Bureau of Economic Geology Report of Investigations No. 220, and Colorado Geologic Survey, Department of Natural Resources, Resource Series 30, 151 p.
4. Scott, A. R., Tyler, Roger, Hamilton, D. S., and Zhou, Naijiang, 1994, "Coal and coal gas resources of the Greater Green River Basin: application of an improved approach to resource estimation," *in* Sonnenberg, S. A., compiler, Natural gas in the western United States, extended abstracts: Rocky Mountain Association of Geologists and Colorado Oil and Gas Association, variously paginated.
5. Tyler, Roger, Kaiser, W. R., Scott, A. R., Hamilton, D. S., McMurry, R. G., and Zhou, Naijiang, 1994, Geologic and hydrologic assessment of natural gas from coal seams in the Mesaverde Group and Fort Union Formation, Greater Green River Basin, Wyoming and Colorado: The University of Texas at Austin, Bureau of Economic Geology, topical report prepared for the Gas Research Institute, GRI-93/0320, 120 p.
6. McCord, J. P., 1984, "Geologic overview, coal, and coalbed methane resources of the Greater Green River coal region—Wyoming and Colorado," *in* Rightmire, C. T., Eddy, G. E., and Kirr, J. N., eds., Coalbed methane resources of the United States: American Association of Petroleum Geologists Studies in Geology Series No. 17, p. 271–293.
7. McFall, K. S., Wicks, D. E., Kuuskraa, V. A., and Sedwick, K. B., 1986, A geologic assessment of natural gas from coal seams in the Piceance Basin, Colorado: topical report prepared for the Gas Research Institute, GRI-87/0060, 75 p.
8. Kelso, B. S., Wicks, D. E., and Kuuskraa, V. A., 1988, A geologic assessment of natural gas from coal seams in the Fruitland Formation, San Juan Basin: topical report prepared for the Gas Research Institute, GRI-88/034, 56 p.
9. Stevens, S. H., Lombardi, T. E., Kelso, B. S., and Coates, J. M., 1992, A geologic assessment of natural gas from coal seams in the Raton and Vermajo Formations, Raton Basin: Advanced Resources International, Inc., topical report prepared for the Gas Research Institute, GRI-92/0345, 84 p.
10. Ayers, W. B., Jr., Kaiser, W. R., Laubach, S. E., Ambrose, W. A., Baumgardner, R. W., Jr., Scott, A. R., Tyler, Roger, Yeh, Joseph, Hawkins, G. J., Swartz, T. E., Schultz-Ela, D. D., Zellers, S. D., Tremain, C. M., and Whitehead, N. H., III, 1991, Geologic and hydrologic controls on the occurrence and producibility of coalbed methane, Fruitland Formation, San Juan Basin: The University of Texas at Austin, Bureau of Economic Geology, topical report prepared for the Gas Research Institute, GRI-91/0072, 314 p.
11. Kaiser, W. R., Scott, A. R., Hamilton, D. S., Tyler, Roger, McMurry, R. G., Zhou, Naijiang, and Tremain, C. M., 1993, Geologic and hydrologic controls on coalbed methane: Sand Wash Basin, Colorado and Wyoming: The University of Texas at Austin, Bureau of Economic Geology, topical report prepared for the Gas Research Institute, GRI-92/0420, 151 p.
12. Tyler, Roger, Ambrose, W. A., Scott, A. R., and Kaiser, W. R., 1991, Coalbed methane potential of the Greater Green River, Piceance, Powder River, and Raton Basins: The University of Texas at Austin, Bureau of Economic Geology, topical report prepared for the Gas Research Institute, GRI-91/0315, 244 p.
13. Ayers, W. B., Jr., and Kaiser, W. R., eds., 1994, Coalbed methane in the Upper Cretaceous Fruitland Formation, San Juan Basin, New Mexico and Colorado: The University of Texas at Austin, Bureau of Economic Geology, Report of Investigations No. 218, Colorado Geologic Survey, Department of Natural Resources, Resource Series 31, and New Mexico Bureau of Mines and Mineral Resources Bulletin 146, 216 p.
14. Kaiser, W. R., Hamilton, D. S., Scott, A. R., Tyler, Roger, and Finley, R. J., 1994b, "Geologic and hydrologic controls on the producibility of coalbed methane": Journal of the Geological Society, London, v. 151, p. 417–420.
15. Stevens, S. H., 1993, "Greater Green River coal region, Washington and Colorado," *in* Coalbed methane—state of the industry: Quarterly Review of Methane from Coal Seams Technology, v. 11, no. 1, p. 13–18.
16. Kauffman, E. G., 1977, "Geological and biological overview, Western Interior Cretaceous basin": Mountain Geologist, v. 14, no. 3–4, p. 75–99.
17. Hamilton, D. S., 1994, "Stratigraphy and coal occurrence of the Upper Cretaceous Mesaverde Group, Sand Wash Basin," *in* Kaiser, W. R., Scott, A. R., Hamilton, D. S., Tyler, Roger, McMurry, R. G., Zhou, Naijiang, and

Tremain, C. M., 1994, Geologic and hydrologic controls on coalbed methane: Sand Wash Basin, Colorado and Wyoming: The University of Texas at Austin, Bureau of Economic Geology Report of Investigations No. 220, and Colorado Geologic Survey, Department of Natural Resources, Resource Series 30, p. 23–49.

18. Tyler, Roger, and McMurry, R. G., 1994, "Stratigraphy and coal occurrence of the Paleocene Fort Union Formation, Sand Wash Basin," *in* Kaiser, W. R., Scott, A. R., Hamilton, D. S., Tyler, Roger, McMurry, R. G., Zhou, Naijiang, and Tremain, C. M., 1994, Geologic and hydrologic controls on coalbed methane: Sand Wash Basin, Colorado and Wyoming: The University of Texas at Austin, Bureau of Economic Geology Report of Investigations No. 220, and Colorado Geologic Survey, Department of Natural Resources, Resource Series 30, p. 79–106.
19. Scott, A. R., 1994, "Composition of coalbed gases": In Situ, v. 18, no. 2, p. 185–208.
20. Dunnewald, J. B., 1969, "Big Piney–La Barge Tertiary oil and gas field," *in* Barlow, J. A., and others, eds., Symposium on Tertiary rocks of Wyoming: Wyoming Geological Association, Twenty-First Field Conference Guidebook, p. 139–143.
21. Curry, W. H., III, 1973, "Late Cretaceous and early Tertiary rocks, southwestern Wyoming," *in* Schell, E. M., ed., Symposium and core seminar on the geology and mineral resources of the Greater Green River Basin: Wyoming Geological Association Guidebook, Twenty-Fifth Field Conference, p. 79–86.
22. Iverson, W. P., 1993, "Mesaverde production and formation evaluation," *in* Natural gas resource characterization study of the Mesaverde Group in the Greater Green River Basin, Wyoming: a strategic plan for the exploration of tight gas sands: Gas Research Institute, contract no. 5091-221-2146, p. 179–200.
23. King, P. B., compiler, 1969, Tectonic map of North America: U.S. Geological Survey, scale 1:5,000,000.
24. Reynolds, M. W., 1968, Geologic map of the Muddy Gap quadrangle, Carbon County, Wyoming: U.S. Geological Survey Geologic Quadrangle Map GQ-771, scale 1:24,000.
25. Blackstone, D. L., Jr., 1979, Geometry of the Prospect–Darby and La Barge faults at their junction with the La Barge Platform, Lincoln and Sublette Counties, Wyoming: Wyoming Geological Survey, Report of Investigations 18, 34 p.
26. Love, J. D., and Christiansen, A. C., 1985, Geologic map of Wyoming: U.S. Geological Survey map, scale 1:500,000.
27. Lickus, M. R., and Law, B. E., 1988, Structure contour map of the Greater Green River Basin, Wyoming, Colorado, and Utah: U.S. Geological Survey Miscellaneous Field Studies Map MF-2031, scale 1:5,000,000.
28. Baars, D. L., Bartleson, B. L., Chapin, C. E., Curtis, B. F., DeVoto, R. H., Everett, J. R., Johnson, R. C., Molenaar, C. M., Peterson, F., Schenk, C. J., Love, J. D., Merin, I. S., Rose, P. R., Ryder, R. T., Waechter, N. B., and Woodward, L. A., 1988, "Basins of the Rocky Mountain region," *in* Sloss, L. L., ed., Sedimentary cover—North American Craton, U.S.: Geological Society of America, Decade of North American Geology, v. D-2, p. 109–220.
29. Scott, A. R., 1993, "Coal rank, gas content and composition, and origin of coalbed gases," *in* Tyler and others, Geologic and hydrologic assessment of natural gas from coal seams in the Mesaverde Group and Fort Union Formation, Greater Green River Basin, Wyoming and Colorado: The University of Texas at Austin, Bureau of Economic Geology, topical report prepared for the Gas Research Institute, GRI-93/0320, p. 69–86.
30. Scott, A. R., Tyler, Roger, Hamilton, D. S., and Zhou, Naijiang (in press), Coal and coal-gas resources of the Greater Green River Basin: The Geological Survey of Wyoming, Public Information Circular.

Table 1. Coal and gas resources in the Greater Green River Basin. From Scott and others [4].

	Resources				
	Coal (billion short tons)	Gas (Tcf)	Percent of total resource Coal	Gas	Average gas content (scf/ton)
Greater Green River Basin	1,277	314	100	100	
<6,000 ft	482	47	38	15	96
6,000 to 7,500 ft	206	37	16	12	185
>7,500 ft	588	230	46	73	390
Upper Mesaverde Group	420	166	33	53	
<6,000 ft	131	25	10	8	189
6,000 to 7,500 ft	65	22	5	7	348
>7,500 ft	224	119	18	38	530
Rock Springs Formation	208	98	16	31	
<6,000 ft	35	5	3	2	128
6,000 to 7,500 ft	12	4	1	1	348
>7,500 ft	161	89	12	28	552
Fort Union Formation	649	50	51	16	
<6,000 ft	316	17	25	5	54
6,000 to 7,500 ft	129	11	10	4	88
>7,500 ft	204	22	16	7	110

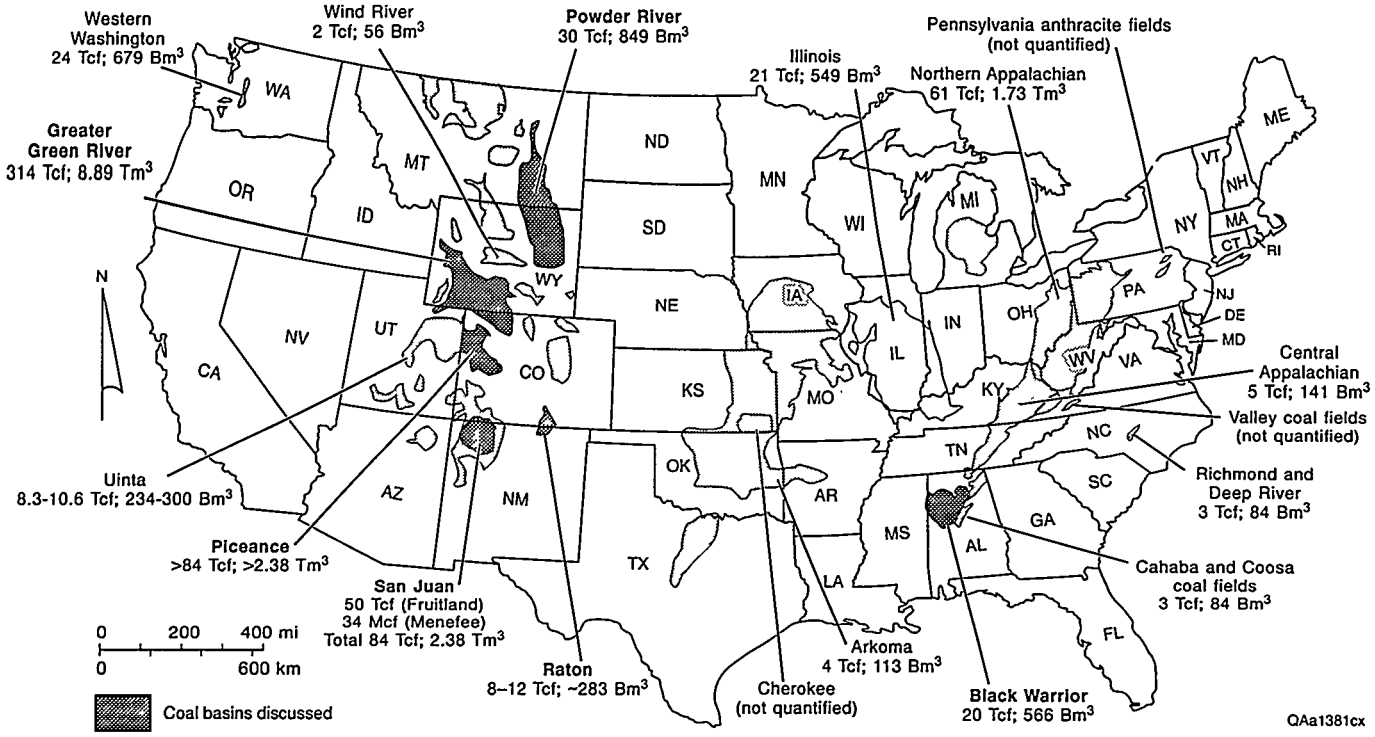


Figure 1. Coalbed gas resources of the United States, totaling 675 Tcf. Data from ICF Resources [2], Ayers and others [10], Stevens and others [9], Scott and others [4], and Tyler and others [5].

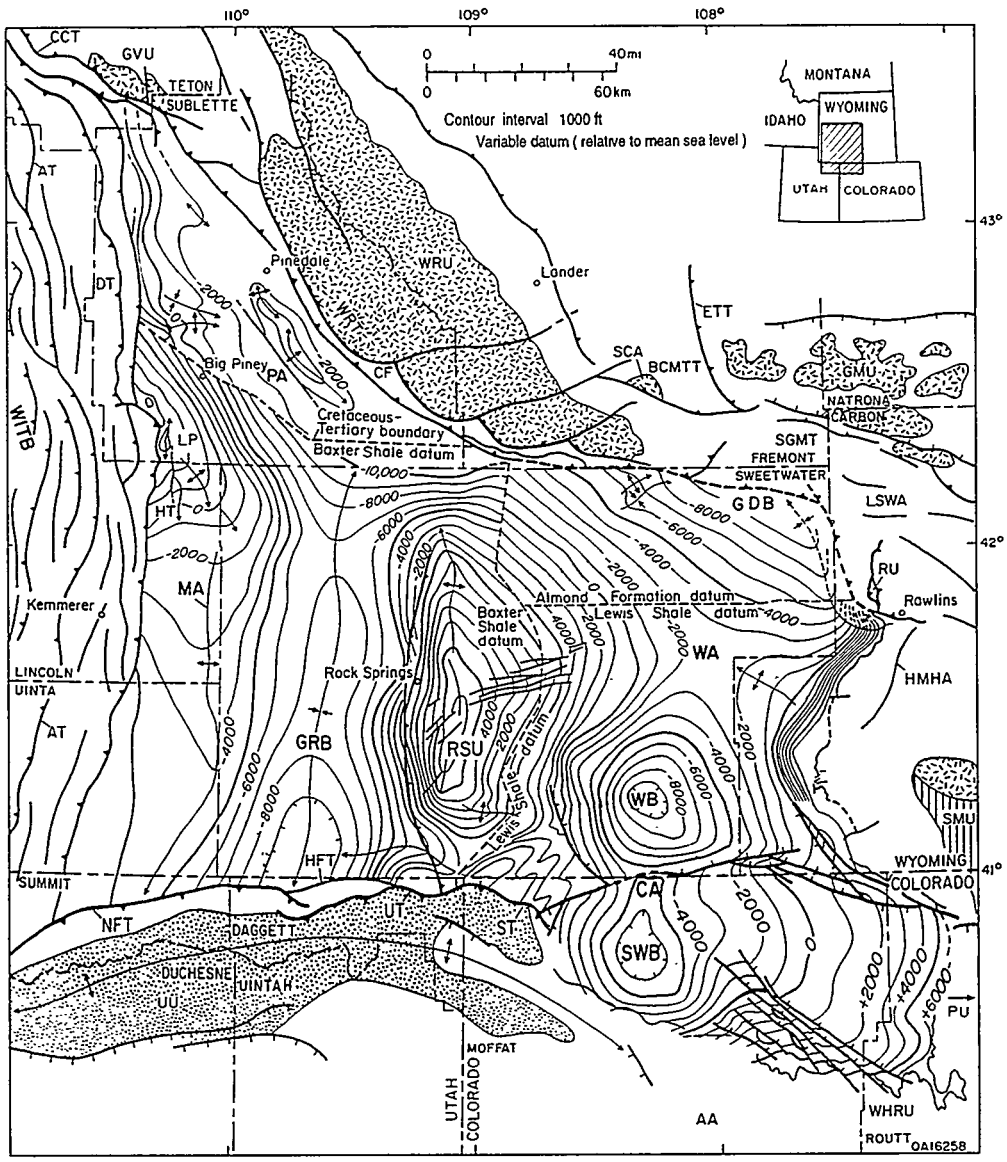


Figure 2. Tectonic map of southwestern Wyoming and adjacent states showing the major tectonic elements of the Greater Green River Basin. The map is taken from King [23] with modifications from Reynolds [24], Blackstone [25], Love and Christiansen [26], Lickus and Law [27], and Tyler and others [5]. Structure contours are drawn on marker horizons in the Upper Cretaceous Formations. Major tectonic features are AA = Axial Arch; AT = Absaroka thrust fault; BCMTT = Beaver Creek and Mormon Trail thrust faults; CA = Cherokee Arch; CCT = Cache Creek thrust fault; CF = Continental Fault; DT = Darby thrust fault; ETT = Emigrant Trail thrust fault; GDB = Great Divide Basin; GMU = Granite Mountain Uplift; GRB = Green River Basin; GVU = Gros Ventre Uplift; HFT = Henry's Fork thrust fault; HMHA = Hatfield and Miller Hill Anticlines; HT = Hogsback thrust fault; LSWA = Lost Soldier and Wertz Anticlines; MA = Moxa Arch; LP = La Barge Platform; NFT = North Flank thrust fault; PA = Pinedale Anticline; PU = Park Uplift; RSU = Rock Springs Uplift; RU = Rawlins Uplift; SCA = Sweetwater Crossing Anticline; SGMT = South Granite Mountains thrust fault; SMU = Sierra Madre Uplift; ST = Sparks thrust fault; SWB = Sand Wash Basin; UT = Uinta thrust fault; UU = Uinta Uplift; WA = Wamsutter Arch; WB = Washakie Basin; WHRU = White River Uplift; WITB = Wyoming–Idaho Overthrust Belt; WRT = Wind River thrust fault; and WRU = Wind River Uplift. Basement rocks are identified as follows: random-dash, vertical-line, and stippled patterns.

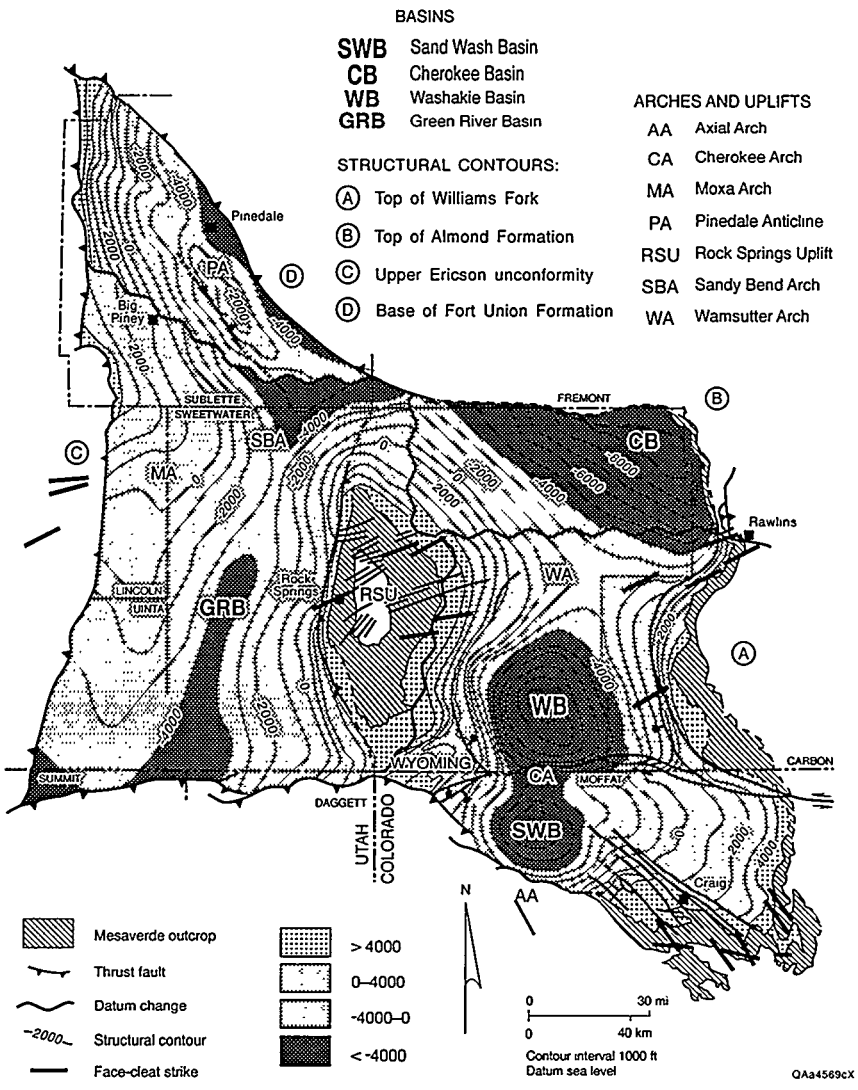


Figure 3. Structural map contoured on various marker beds within the Upper Cretaceous Mesaverde Group and lower Tertiary Fort Union Formation, Greater Green River Basin. Major tectonic features are AA = Axial Arch, CA = Cherokee Arch, MA = Moxa Arch, PA = Pinedale Anticline, RSU = Rock Springs Uplift, SBA = Sandy Bend Arch, and WA = Wamsutter Arch.

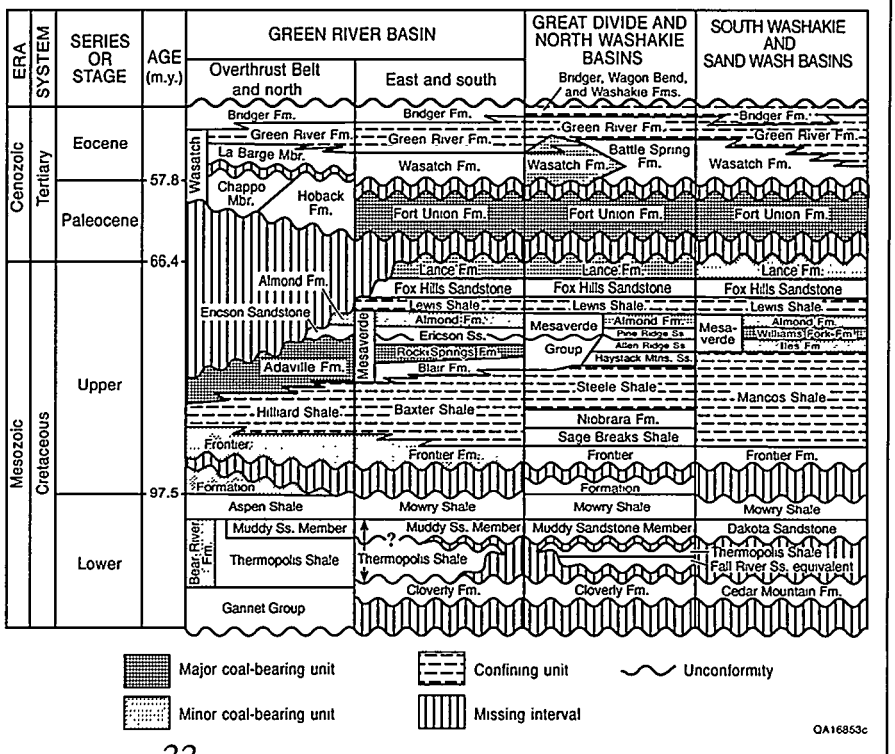


Figure 4. Coal-bearing stratigraphic and hydrologic confining units, Greater Green River Basin. Modified from Baars and others [28].

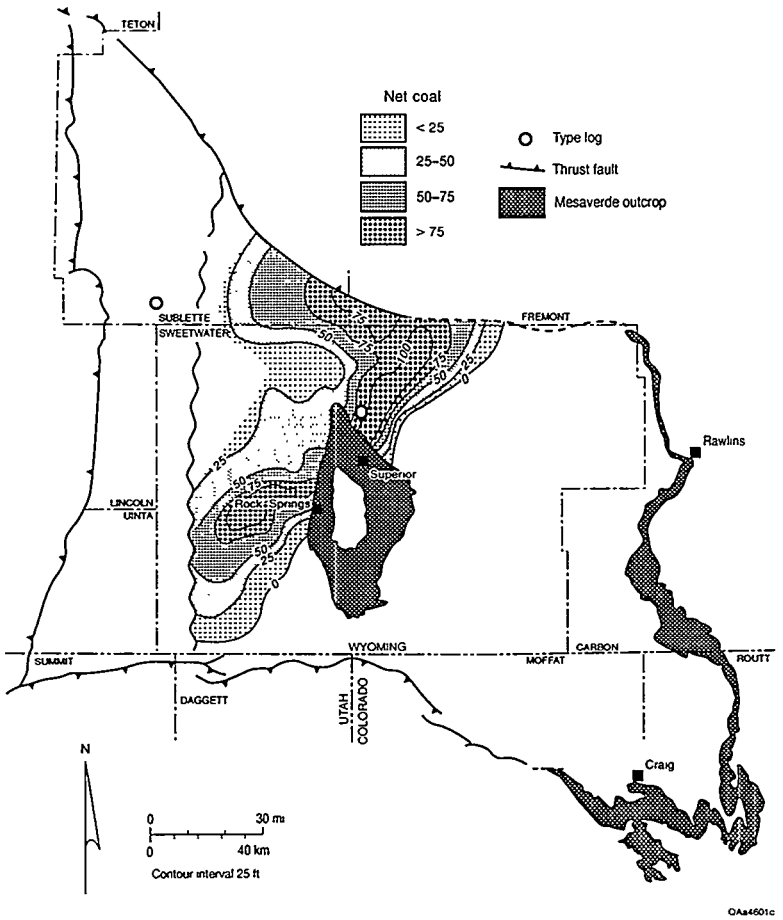


Figure 5. Net-coal-thickness map, Rock Springs Formation. Thickest net coal occurs in a strike-oriented (northeast) trend across the Rock Springs Uplift. The coals thin abruptly to the southeast, coincident with the paleoshoreline.

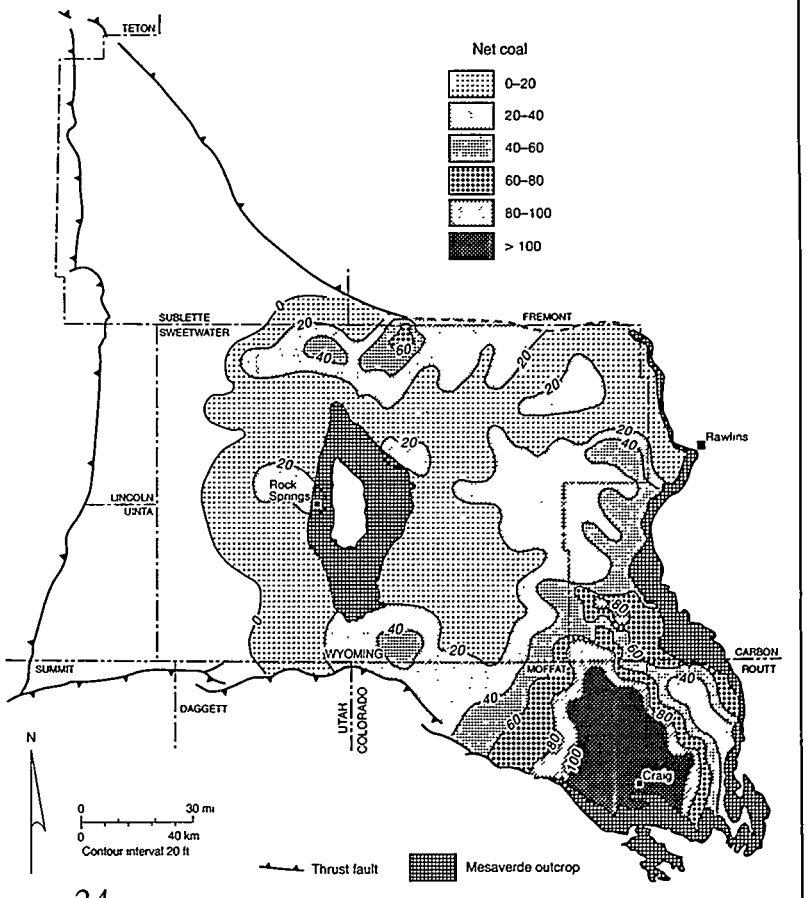


Figure 6. Net-coal-thickness map, Williams Fork Formation. Thickest coals in the Sand Wash Basin are associated with the shoreline and coastal-plain systems. The coals thin to the north and west onto the ancient alluvial piedmont.

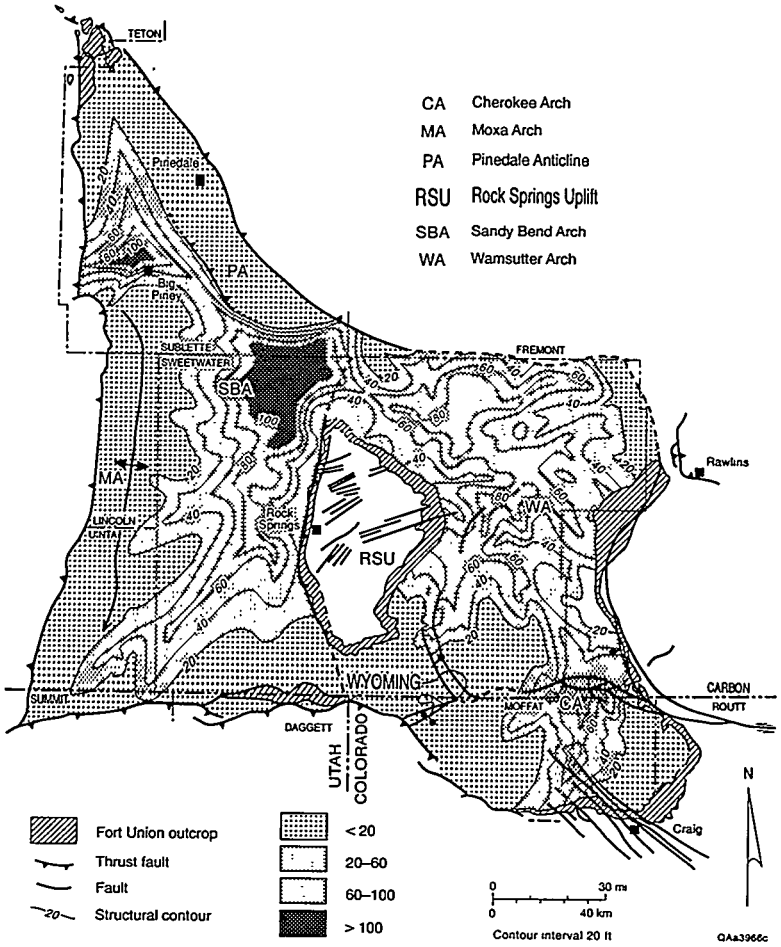


Figure 7. Net-coal-thickness map of the lower coal-bearing unit, Fort Union Formation, Greater Green River Basin. Thickest net coal development (>100 ft, >30.5 m) occurs above and alongside a south-north-oriented fluvial system along the west and east flanks of the Rock Springs Uplift and along a northwest-southeast-oriented fluvial system along the west flank of the Pinedale Anticline.

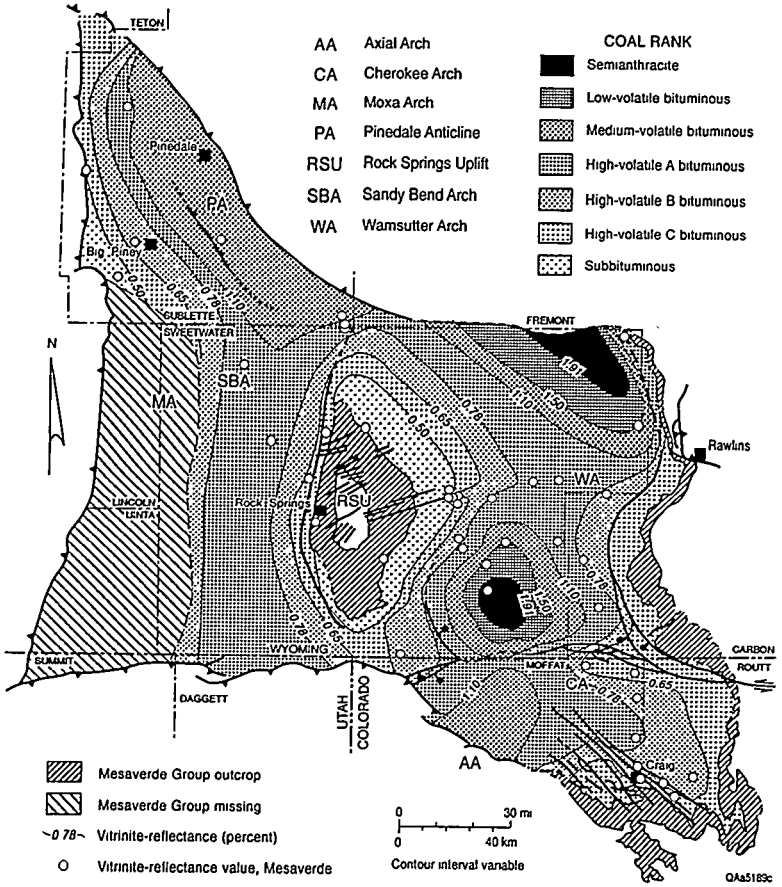


Figure 8. Coal-rank map, top of the Mesaverde Group. Vitrinite-reflectance and coal-rank trends were estimated by combining several types of data. Coal rank increases away from basin margins and the Rock Springs Uplift toward high-volatile A bituminous and higher rank coals in deeper subbasins. From Scott [29].

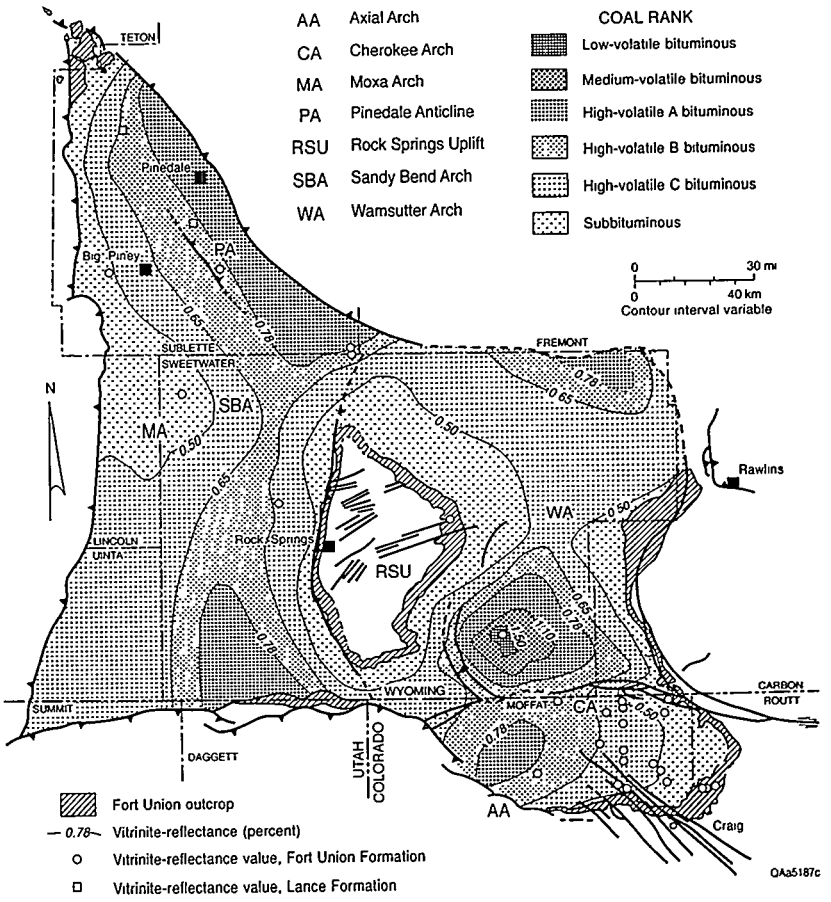


Figure 9. Coal-rank map, base of the Fort Union Formation. Subbituminous coals around basin margins and the Rock Springs Uplift indicate that these structures developed before, or syntectonically with, coalification. Net coal and coalification trends suggest that although the Wamsutter and Cherokee Arches also formed syntectonically with coalification, they did not become as pronounced as the major uplifts. From Scott [29].

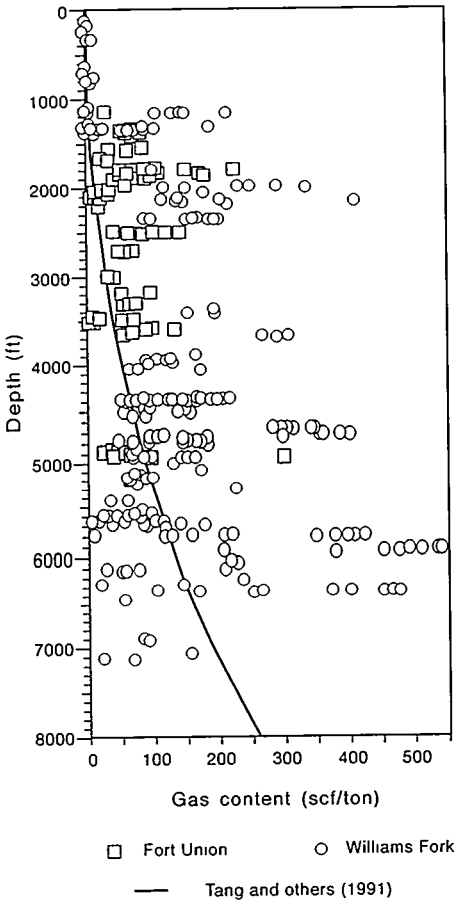


Figure 10. Gas-content profile of the upper Mesaverde Group and Fort Union Formation, Sand Wash Basin. Gas content increases with depth as in other western U.S. basins. Gas content values vary widely at any particular depth. Sidewall cores and cuttings generally have lower gas contents than do whole cores. Ash-free values for coals lacking proximate analysis were calculated from average ash contents of adjacent coal beds. From Scott and others [30].

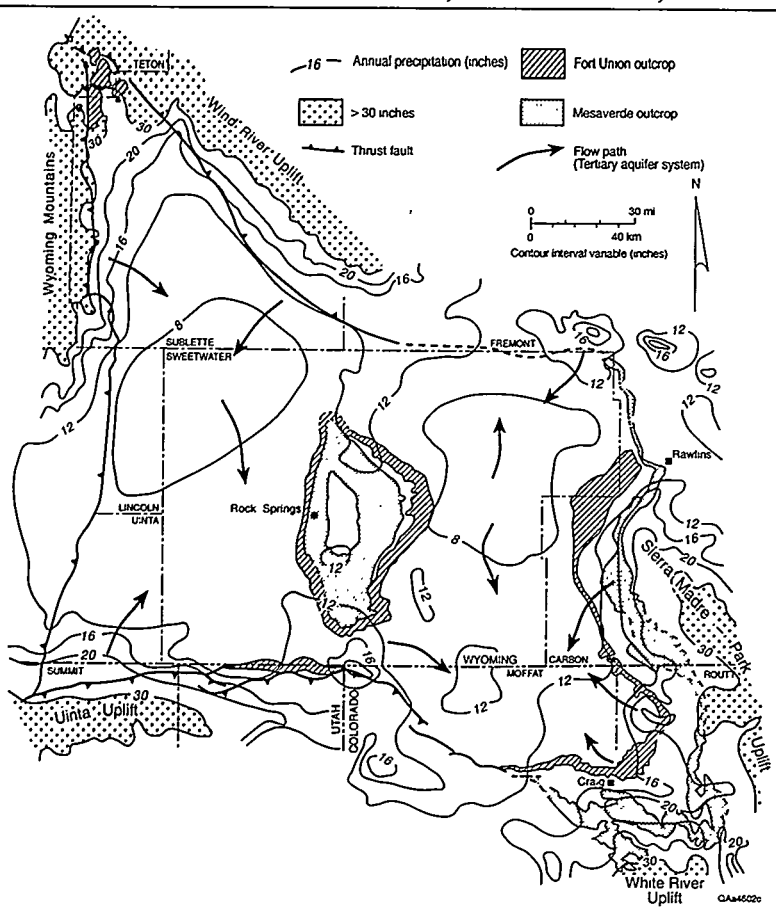


Figure 11. Mean annual precipitation, Greater Green River Basin. Precipitation is highest over highlands on the southeast, northwest, and southwest margins of the basin. Outcrop-related recharge occurs along the foothills of those highlands. In the Tertiary aquifer system, water flows from the wet, elevated basin margins to discharge into major river valleys and basin centers, and flow is dynamic throughout the basin.

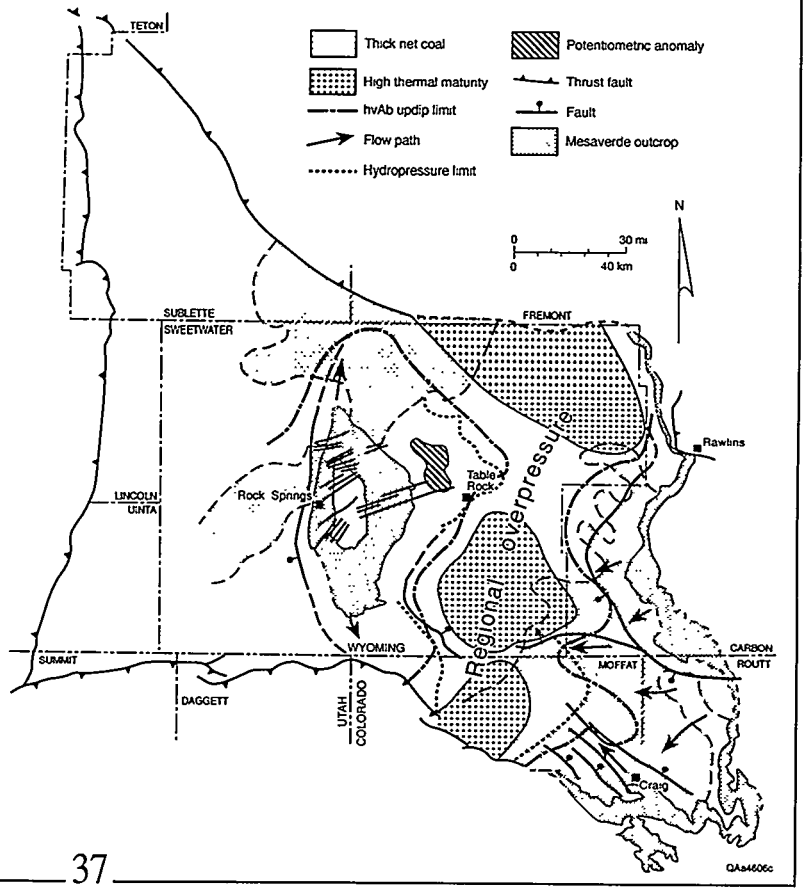


Figure 12. Geologic and hydrologic characterization of the Mesaverde Group, Greater Green River Basin. Because of high overall permeability, the permeability floor for coalbed methane exploration may be lower than normally expected in western coal basins. Deeper drilling to test higher rank, higher gas content coals may be in order at the (1) termination of the Cedar Mountain fault system northwest of Craig, (2) east margin of Washakie Basin, and (3) northeast flank of the Rock Springs Uplift. Prime targets are the northeast Rock Springs Uplift, eastern Washakie Basin, and southeastern Sand Wash Basin.

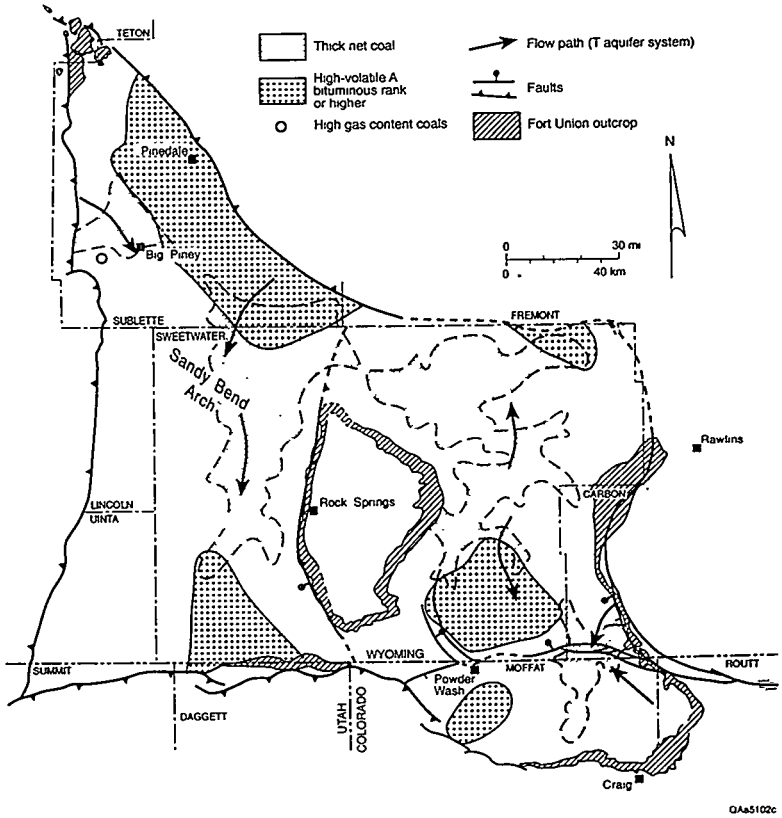


Figure 13. Geologic and hydrologic characterization of the Fort Union Formation, Greater Green River Basin. Prime targets are in the Big Piney area and on the Sandy Bend Arch.

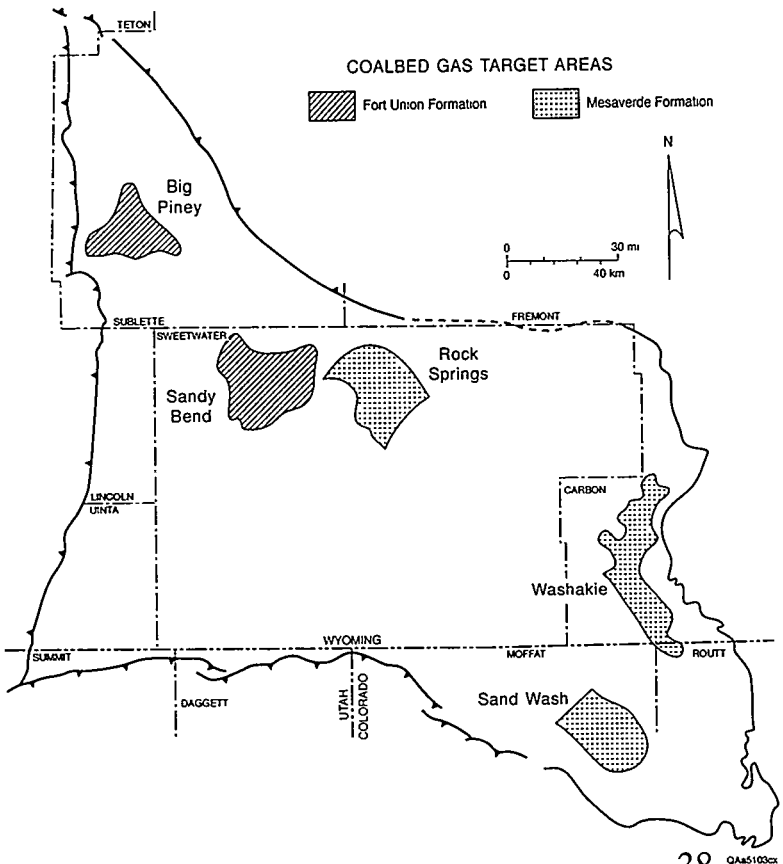


Figure 14. Mesaverde Group and Fort Union Formation exploration fairways, Greater Green River Basin.

INTERGAS '95

May 15-19, 1995
The University of Alabama
Tuscaloosa, Alabama USA

9508

Thin-Skinned Structures Influence Gas Production in Alabama Coalbed Methane Fields

J.C. Pashin, Geological Survey of Alabama;
R.H. Groshong, Jr. and S. Wang, The University of Alabama

ABSTRACT

Thin-skinned structures are abundant in the Alabama coalbed methane fields and affect the production of gas and water from coal. Extensional structures in Deerlick Creek and Cedar Cove fields include normal faults and hanging-wall rollovers detached in the Pottsville Formation. Compressional folds in Gurnee and Oak Grove fields, by comparison, are interpreted to be detachment folds formed above decollements at different stratigraphic levels. Patterns of gas and water production reflect the structural style of each field and further indicate that folding and faulting have affected the distribution of permeability and the overall success of degasification operations.

INTRODUCTION

Folds and faults control the distribution and producibility of conventional hydrocarbons, but the effect of these structures on coalbed methane production has been elusive. This is because conventional trapping mechanisms play a minimal role in coal, which is a self-sourced reservoir that holds gas in an adsorbed state. Consequently, the fundamental requirements for producing gas from coal are, first, having an economically feasible gas resource and, second, being able to reduce reservoir pressure sufficiently for gas to desorb. The way reservoir pressure is reduced, moreover, is by removing formation water that must be disposed of safely and economically.

These basic relationships raise questions regarding the significance of folding and faulting in developing strategies for exploration and production of coalbed gas, as well as for production and disposal of produced water. More than 4,500 coalbed methane wells have been drilled in west-central Alabama since 1980, and 20 fields are now established (fig. 1). Eighteen of these fields are in the eastern part of the Black Warrior foreland basin, and the remaining two are in the Cahaba coal field, the southernmost coal basin of the Appalachian thrust belt. Cumulative production of coalbed gas from Alabama now exceeds 450 Bcf and, along with the gas, more than 400 MMbbl of water have been produced. Throughout the region, gas is produced from coal in the Lower Pennsylvanian Pottsville Formation, which contains coalbed methane resources exceeding 20 Tcf (McFall and others, 1986; Telle and Thompson, 1987).

The Pottsville Formation includes a multitude of geologic structures of extensional and compressional origin. This diversity of geologic structure, as well as the large number of wells with a long production history, makes west-central Alabama an ideal place to test for structural controls on coalbed methane production. With this in mind, we chose four areas for detailed study (fig. 1). Southeastern Deerlick Creek and eastern Cedar Cove fields contain numerous extensional structures, specifically normal faults and rollover folds, which are characteristic of extensional terranes worldwide. By contrast, northern Gurnee and central Oak Grove fields contain broad, open folds of compressional origin, which are common in foreland thrust belts.

We had two major objectives while conducting this study. The first was to analyze the geometry of geologic structures in the Alabama coalbed methane fields. Structural geometry is an important key to the origin of fold and fault systems and further controls the depth, attitude, and continuity of coalbed reservoirs. In the coalbed methane fields, most structures appear to be thin-skinned; that is, the structures are detached within the sedimentary cover above crystalline basement (Wang and others, 1993; Pashin and others, 1995). Our second objective was to determine the effect of geologic structures on gas and water production. Do folding and faulting affect gas and water production, or is production more responsive to regional fracturing and engineering procedures? In the following section we review some of the theory relating to the geometry and kinematics of extensional and compressional structures. In the subsequent sections we document those structures in west-central Alabama. We then demonstrate the effects of these structures on gas and water production and conclude by synthesizing the results into a conceptual model.

The primary tools we used were geophysical well logs and production data. Structural contour maps of key marker beds, including coal beds and cycle boundaries (Pashin, 1994a, b), were made for each study area and are based on interpretations of gamma ray and density logs on file at the Alabama State Oil and Gas Board. Cross sections are also based on well logs and were constrained using the area balancing techniques described in the next section. Outcrop data compiled by Pashin and others (1995) were used to constrain the cross section in Gurnee field. Folds were then classified using the limb-dip diagrams of Jamison (1987). Records of gas and water production were also obtained from the State Oil and Gas Board; monthly values were divided to obtain daily rates. To elucidate structural controls on production, bubble maps of peak gas and peak water production were superimposed on the structural contour maps. Additional maps and cross sections of Deerlick Creek field are available in Wang and others (1993) and Wang (1994). Structure and production maps of Cedar Cove field are from Sparks and others (1993).

AREA BALANCE IN THIN-SKINNED STRUCTURES

The geometry of thin-skinned structures (fig. 2) can be quantified using some simple area balancing techniques. Area balancing provides a means of constraining structural cross sections, because layer-parallel transport and the position of the basal detachment can be calculated (Groshong, 1990, 1994; Epard and Groshong, 1993). To employ these techniques, only basic stratigraphic data are required, preferably from several marker beds; these data can be obtained by correlating geophysical well logs. We applied these techniques to extensional structures in Deerlick Creek field and to compressional structures in Gurnee field.

Two fundamental assumptions are used when area balancing thin-skinned structures. The first is that the cross-sectional area of a body of rock remains constant during deformation; this is the primary tenet of area balance. The second assumption, which applies specifically to thin-skinned structures, is that the structure must terminate downward at a basal detachment. The theory is outlined briefly here, and thorough discussions are in Epard and Groshong (1993), Groshong (1994), and Groshong and Epard (1994).

If the cross-sectional area of a structure is constant, then the area displaced above the basal detachment is equal to the area uplifted or downdropped relative to the original level, termed regional, so that:

$$S = DH, \quad (1)$$

where S is displaced area , D is displacement distance of the block on the lower detachment, and H is depth to detachment. The area downdropped below regional in extensional structures is termed lost area, whereas the area uplifted above regional in compressional structures is termed excess area. The sign convention is that displacement distance and the displaced area are negative in extensional structures and are positive in compressional structures. The cross section must obey the area-depth relationship at every structural level given by the depth, h, to a common reference level. Plotted on an area-depth graph (fig. 3), the relationship between structural levels is the straight line,

$$S = Dh + S_a, \quad (2)$$

where S_a is the area intercept of the line. The slope of this line is the displacement distance on the lower detachment, and the detachment itself is located where lost or excess area projects to zero; the detachment may be above or below the arbitrary reference level. In a typical example, the displaced areas from multiple stratigraphic markers are plotted to define the area-depth line from which the displacement and depth to detachment are determined (fig. 3).

EXTENSIONAL STRUCTURES

Extensional structures, specifically normal faults, are common in foreland basins and have been proposed to form by flexural extension of the upper lithosphere in response to differential subsidence during deformational loading (Bradley and Kidd, 1991). Normal faults and hanging-wall rollover structures are abundant in the Black Warrior basin and help form traps for conventional hydrocarbons in the northwestern part of the basin (Semmes, 1929; Bearden and Mancini, 1985; Epsman, 1987). However, little is known about the effect of these structures on the production of coalbed gas, and many questions remain regarding the geometry of the faults and the associated rollovers. Many of the faults in the western part of the basin penetrate deep into the sedimentary cover and are possibly detached in basement (Thomas, 1988; Pashin, 1993). However, short fault length and limited vertical separation in the eastern part of the basin suggest development of shallow detachments in some coalbed methane fields.

Deerlick Creek Field

Recent work in southeastern Deerlick Creek field by Wang and others (1993) and Wang (1994) has fostered a new perspective of faulting in the eastern part of the Black Warrior basin. The map area contains six normal faults that strike northwest and define a horst and graben system (fig. 4). A horst and full graben are in the central part of the map area and are bound on the east and the west by half grabens with westward polarity. Most of the faults extend beyond the map area, and vertical separation along the faults is generally between 100 and 300 feet. Data in Wang (1994) indicate that the faults dip between 50° and 70° and have a planar to listric geometry (fig. 5). Strata between the faults are folded into a series of gentle rollover structures. In the Strip Mine graben, Pottsville strata roll over into the opposed faults, thus forming an anticline with nearly 50 ft of closure (figs. 4, 5).

Area-depth plots were made for each Pottsville cycle boundary in the full graben and the two half grabens (fig. 6). Plots for the Strip Mine graben and the Holt Lake half graben yielded similar results and predict detachment between 50 ft above and 400 ft below the reference level. Thus the detachment appears to be in the lower part of the Pottsville Formation, probably near the top of the Boyles Sandstone Member, which is a structurally stiff unit that forms the basal 300 ft of the formation. The area-depth plot for the Franklin Hill half graben is less well constrained but suggests detachment between the top of the Boyles Sandstone and the base of the Pottsville Formation. Slope of the regression lines indicates that layer-parallel displacement at the detachment is approximately 300 ft in the Strip Mine graben and in the Holt Lake half graben and is approximately 125 ft in the Franklin Hill graben.

Cedar Cove Field

Eastern Cedar Cove field contains diverse structures of extensional and compressional origin (fig. 7). The field is developed along the upturned southeastern margin of the Black Warrior basin, where strata dip steeply and are truncated by a major thrust fault that in places superposes Cambrian-Ordovician carbonate rocks on the coal-bearing Pottsville Formation. Some minor thrust faults are developed in the northeastern part of the field as much as 5 mi northwest of the basin margin. Normal faulting predominates in the remainder of the field and, overall, the structural style resembles that in Deerlick Creek field.

A swarm of normal faults traverses the central part of the map area from northwest to southeast (fig. 7). The fault swarm forms a half graben with polarity toward the southwest, which is characteristic of normal fault systems in the Black Warrior basin. Most faults within the swarm have a vertical separation of less than 100 feet, and cumulative vertical separation across the swarm is generally less than 200 feet. Immediately southwest of the main swarm is a major rollover complex. The northwestern part of the rollover complex contains normal faults with a left-stepping, en echelon map pattern. Some of the faults have vertical separation approaching 150 feet, and strata between the faults have second-order rollover folds. South of the en echelon faults, strata dip gently southwest and are deformed into a syncline near the basin margin. We have yet to make estimates of detachment depth and lateral displacement for the normal faults, but the limited plan length and vertical separation of most faults suggests a shallow detachment similar to that in Deerlick Creek field.

COMPRESSIONAL STRUCTURES

Appalachian folds have been recognized as detached structures since early this century and have been used to develop basic models of thin-skinned compressional structures in thrust belts (Chamberlin, 1910; Rich, 1934). Rodgers (1950) was first to suggest that the Sequatchie anticline, one of the dominant structures in Oak Grove field, is detached in Cambrian Shale, as are most other first-order Appalachian folds. Success producing conventional hydrocarbons from the Appalachian thrust belt has been limited, but coalbed gas holds great promise for widespread economic production in foreland thrust belts worldwide (Pashin and Carroll, 1993). Gurnee and Oak Grove fields contain more wells than any other fields in the Appalachian thrust belt and thus present an unparalleled opportunity to evaluate the geometry and kinematics of thin-skinned folds and the effect of these structures on the production of coalbed methane and water.

Gurnee Field

Wells in northern Gurnee field have been completed in a series of folds with variable geometry and orientation (fig. 8). Wells along the northwest margin of the map area penetrate the backlimb of the Tacoa anticline, which has a curvilinear axial trace and plunges southwest. Immediately southeast of the Tacoa anticline are the Dry Creek syncline and the Woods Creek anticline. Axial traces of these structures are approximately 4 mi long; the Dry Creek syncline plunges southeast and shares limbs with the Tacoa and Woods Creek anticlines. The Woods Creek anticline, by contrast, is a doubly plunging structure that narrows toward the northeast; a thrust fault emerges in the broad western part of the structure (figs 8, 9). Bedding is steeper than 40° in parts of the Tacoa and Woods Creek anticlines. In the southeastern part of the map area, the Maylene syncline, Dogwood anticline, and Pea Ridge syncline are extremely gentle, open folds with limbs generally dipping less than 10°.

Abundant outcrop and subsurface data make it possible to apply area balancing techniques to the Woods Creek anticline, so excess area plots were made for the full anticline, as well as the ramp anticline of the thrust fault emerging near the crest of the structure (fig. 10). The plot for the full anticline suggests that, where the backlimb of the structure terminates, the basal detachment is at an approximate elevation of -5,000 feet. Thus, with 90 percent confidence, we suggest that the detachment is between the middle of the Nunnally coal zone and the base of the Pottsville Formation. The excess area plot for the ramp anticline, however, suggests that the thrust fault is shallower than the basal detachment. Thus, caution must be applied when interpreting compressional structures in the Pottsville Formation, because thrust faults observed at the surface can be mistaken for ramps of basal detachments.

Oak Grove Field

Oak Grove field contains numerous structures of extensional and compressional origin (fig. 11). Normal faults similar to those in Deerlick Creek and Cedar Cove fields are present in the western part of the field. Compressional folds, including the Sequatchie anticline and the Coalburg syncline, dominate structure in the eastern part of the field. The Sequatchie and Coalburg structures plunge southwest and terminate at a series of right-stepping, en echelon tear faults that traverses the central part of the field (Pashin, 1994c). The Sequatchie anticline shares a common limb with the Coalburg syncline, and the forelimb and backlimb of the anticline dip less than 2°. In the north-central part of the field, the Sequatchie anticline contains a crestal uplift with more than 400 ft of relief. The Oak Grove mine, which is where the modern coalbed methane industry was born, is southwest of the crestal uplift in the main backlimb of the anticline. Note that a localized syncline is developed immediately northwest of the mine along the hinge separating the crestal uplift from the main backlimb.

The broad, open nature of the Sequatchie anticline, as well as the other compressional uplifts discussed in this paper, raises questions about the geometry and kinematics of folds in the Alabama coalbed methane fields. Geometric and kinematic models of thin-skinned compressional folds, including fault-bend folds, fault-propagation folds, and detachment (decollement) folds have been developed by several workers (Suppe, 1983, 1985; Jamison, 1987; Suppe and Medwedeff, 1990). The diagrams of Jamison (1987) are especially useful, because folds can be classified by plotting backlimb dip and interlimb angle (fig. 12). None of the anticlines considered plot as fault-bend or fault-propagation folds with constant bed length and thickness, nor do they reasonably fit models incorporating thickening of the forelimb (e.g., Jamison, 1987). Instead, we suggest that the folds are best classified as detachment folds in which the value of fold amplitude divided by detachment depth (a/h) is less than 1. Interestingly, the limb-dip data appear to plot along a line of decreasing interlimb angle and increasing backlimb dip. One possibility is that this line defines a general evolutionary pathway along which folds grow by limb rotation from extremely open structures, like the Sequatchie anticline, into tighter structures, like the Tacoa anticline.

STRUCTURAL CONTROLS ON PRODUCTION

Having established the structural style of the four study areas, the relationship between structure and production can be evaluated. In the following sections we review the basic production characteristics of the four fields investigated and relate the production of gas and water to structure. In so doing, it should become apparent that folds and faults can effect gas and water production in a variety of ways. However, we defer detailed interpretations of why these structures affect production to the conceptual model.

Deerlick Creek Field

Deerlick Creek is the fourth most productive coalbed methane field in the Black Warrior basin. By the end of 1993 the field had produced 38 Bcf of gas and 22 MMbbl of water. As with all coalbed methane fields in Alabama, gas and water production are quite variable, as is readily apparent in the bubble maps (fig. 4). However, exceptionally productive wells are restricted to parts of specific fault blocks.

In most of the map area, peak gas and peak water production were less than 300 Mcfd and 750 Bpd, respectively (fig 4). Exceptionally productive wells with peak gas production higher than 300 Mcfd and peak water production higher than 750 Bpd have been drilled in two general areas. Most of these wells have been drilled in the Holt Lake half graben. The two exceptionally productive wells near the eastern edge of the Strip Mine graben penetrate the fault and, thus, are also completed in the Holt Lake half graben. Exceptionally productive gas wells appear to be dispersed sporadically between the faults defining the half graben, whereas exceptionally productive water wells are clustered in the west-central part of the area.

The other area of exceptional gas and water production is in the eastern part of the Franklin Hill half graben (fig. 4). Wells with peak gas production greater than 300 Mcfd are concentrated in the northeast part of the half graben, whereas wells with peak water production greater than 750 Bpd are dispersed in the southeast part. Only one well in the east-

central part of the structure produces large quantities of both gas and water.

Cedar Cove Field

Cedar Cove is ranked third among coalbed methane fields in Alabama, with cumulative gas production exceeding 68 Bcf. Cedar Cove has produced more water than any other field and, at the end of 1993, cumulative water production exceeded 113 MMbbl, accounting for 30% of the total water produced from the Alabama coalbed methane fields. Gas and water production within the field are strongly influenced by normal faulting and by Appalachian folding (fig. 7).

A northwest-elongate fairway of exceptional gas production is defined where average gas production exceeded 200 Mcfd in June, 1991 (fig. 7). Nearly all the highly productive gas wells are in the hanging-wall rollover complex southwest of the fault swarm. The largest area of exceptional gas production is in the north-central part of the map area between the fault swarm and the left-stepping, en echelon faults. South of this area, exceptionally productive wells have a patchy distribution, and the two southern patches appear to correspond with flexures within the rollover.

A northwest-elongate fairway is also apparent where average water production exceeded 500 Bpd in June, 1991 (fig. 7). Within the fairway, water production has a patchier distribution than gas production. Also, many of the wells that produced more than 500 Bpd were drilled into the fault swarm and into the western part of the en echelon fault system. An even stronger northeast-elongate fairway of water production is apparent in the map; the northeast fairway is not associated with voluminous gas production. The northeast fairway corresponds with structures along the southeast margin of the Black Warrior basin. Northeast of the fault swarm, a large quantity of water has been produced from steeply dipping strata at the basin margin. In the fault swarm, the northeast-elongate fairway appears to join the northwest-elongate fairway. Southwest of the swarm, most water is produced from the synclinal axis between the rollover complex and the upturned basin margin.

Gurnee Field

Gurnee field contains more than 400 wells, which is more than any other gas field in the Appalachian thrust belt, yet less than one-third of the wells have been completed. Completed wells are restricted to the northern part of the field, and only 2.3 Bcf of gas and 2.7 MMbbl of water have been produced since establishment of the field in 1990. Whereas structural control of gas and water production are readily discerned in Deerlick Creek and Cedar Cove fields, relationships are less clear in Gurnee field.

Of the wells completed in Gurnee field, only 7 have reported peak gas production exceeding 100 Mcfd (fig. 8). Most of those wells are clustered in the western parts of the Woods Creek anticline and the Dry Creek syncline. The other two wells with peak production greater than 100 Mcfd are in the southern part of the map area in the Pea Ridge syncline. These wells are the most productive in the field, both having peaked higher than 300 Mcfd; they are the only wells in Gurnee field with peak production comparable to that of the exceptional wells in Deerlick Creek and Cedar Cove fields. The least productive wells are those drilled in the Maylene syncline. Admittedly, those wells were pumped for only a short time, but maximum production reports were typically less than 10 Mcfd.

Water production is also limited in Gurnee field (fig. 8). Whereas some of the most favorable gas production comes from the western parts of the Woods Creek anticline and the Dry Creek syncline, only a few wells have had peak water production exceeding 200 Bpd, and none of the wells have peak water production exceeding 400 Bpd. In the Maylene syncline, where the least gas has been produced, very little water has also been produced, save for one well that peaked at an anomalous 439 Bpd. The wells that have produced the most water are clustered between the backlimb of the Tacoa anticline and the axis of the Pea Ridge syncline. These are the southwesternmost wells that have been completed in the field and are in the area of the two wells with the highest peak gas production.

Oak Grove Field

The first coalbed methane wells in Alabama were drilled in a closely spaced pattern immediately east of the Oak Grove mine (fig. 11), and Oak Grove field, which was established in 1980, was the first coalbed methane field recognized by the State Oil and Gas Board. At the end of 1993, Oak Grove ranked second among the coalbed methane fields in total gas production, with 76 Bcf accounting for 19% of the coalbed gas produced in Alabama. The field also ranked second in total water production, with 87 MMbbl accounting for 23 percent of the water produced from the coalbed methane fields.

An extremely strong linear trend of exceptional gas production is less than 1 mi northwest of the Oak Grove mine. Here, most wells with peak gas production greater than 300 Mcfd are aligned along the minor synclinal axis that marks the hinge between the crestal uplift of the Sequatchie anticline and the main backlimb containing the mine (fig. 11). Interestingly, no obvious control of water production by structure was identified. Instead, water production simply increases northwest away from the underground mine, reflecting the prolonged activity of mine dewatering (Pashin, 1991). However, salinity of the formation water is lower along the synclinal axis than in adjacent areas.

CONCEPTUAL MODEL

Having established basic structural controls on gas and water production, a conceptual model can be formulated using the observations from each field (fig. 13). Furthermore, explanations can be offered for why specific production patterns exist. Results from all four fields indicate that thin-skinned structures influence gas and water production, but the effect is different in each area. Establishing structural controls on production can be satisfied using a comparative approach, but providing viable explanations for the relationship between production and structure can be extremely difficult. This is especially true in coalbed reservoirs, in which traditional trapping mechanisms are of questionable importance, and in which economic gas production is dictated by the ability to effectively lower reservoir pressure.

Patterns of gas and water production in Deerlick Creek field provide evidence for structural segmentation of coalbed methane reservoirs by normal faulting (figs. 4, 13). Exceptional production of both gas and water in parts of the Holt Lake and Franklin Hill half grabens indicates local enhancement of permeability and may also indicate a heterogeneous distribution of gas and water (fig. 4). For these reasons the performance of individual wells is difficult to predict. We doubt that our results indicate that half grabens are inherently superior to horsts and full grabens. For example, well performance has been poor near faults in the western part of the Franklin Hill half graben, although part of the problem may be low coal rank (Winston, 1990). Additionally, Wang (1994) calculated that stretching strain and hence, permeability, should be greatest in the deep parts of full grabens. Consequently, we think that additional work is required before a predictive

template can be developed for siting wells in coalbed reservoirs segmented by faulting.

In Cedar Cove field, the northwest-elongate fairway of enhanced gas production appears to be related to rollover folding (figs. 7, 13). Rollover structures localize extensional strain in the hanging wall of normal fault systems (Groshong, 1994; Withjack and others, 1995) and thus may be important targets for coalbed methane exploration. The distribution of exceptional gas production in the northern part of the map area suggests that segmentation by faulting is locally effective. Association of some productive patches in the south with minor anticlinal and synclinal flexures further indicates that enhanced permeability related to curvature may in places favor gas production. Curvature has also been suggested to be associated with increased fracturing and coalbed gas production in part of the San Juan basin of New Mexico (Decker and others, 1989). Rollover folding may have also affected the modern distribution of stress in Cedar Cove field, because in-situ stress appears to be lower in the northwest production fairway than in adjacent areas (Sparks and others, 1993). Water production also appears to be enhanced by rollover folding in Cedar Cove field, but a considerable amount of water is also produced from the fault swarm, which suggests enhanced permeability. Clayton and others (1994) measured a significant amount of gas issuing from a fault in western Oak Grove field, so faults in the Black Warrior basin can be effective conduits for fluid.

In Gurnee field, concentration of wells with peak gas production exceeding 100 Mcfd in the Woods Creek anticline and the Dry Creek syncline suggests that detachment folding can influence gas production (figs. 8, 13). Why those wells are concentrated in the western, up-plunge parts of those structures, however, is a matter for speculation. One possibility is that folding and faulting have increased curvature and permeability, but little water has been produced from this area. Another possibility is that, over geologic time, gas has diffused toward the up-plunge end of the structures. Indeed, migration of gas may have also occurred in the Black Warrior basin, which has undergone multiple episodes of burial, uplift, and gas generation (Carroll and others, 1993; Rice, 1993; Scott, 1993). Significant gas and water production in the southwestern part of the Gurnee map area appears not to be related to folding. Even so, production some of these wells rivals that from exceptionally successful wells in the Black Warrior basin. Thus, completing some of the more than 200 wells in the southern part of Gurnee field may hold economic promise.

A fourth style of structurally influenced gas production, which we term the hinge effect (fig. 13), appears to be effective in Oak Grove field, where exceptionally productive wells are aligned along the syncline separating the crestal uplift of the Sequatchie anticline from the broad backlimb of the structure (fig. 11). The syncline is a zone of intense curvature, and presence of low-salinity water along the axis of the structure indicates enhanced fracture permeability (Pashin, 1991). Mapping fold hinges, as has recently been done in the California Borderland by Shaw and others (1994), may be an effective way of identifying areas prospective for drilling for coalbed gas. A hinge effect is also apparent in Cedar Cove field where, southwest of the fault swarm, a large quantity of water has been produced from the synclinal axis separating the upturned basin margin from the backlimb of the rollover complex (fig. 7B). Exceptional water production in the absence of significant gas production in this area, however, may indicate inability to effectively depressurize the reservoir because of rapid hydrologic recharge.

CONCLUSIONS

Area balancing indicates that thin-skinned structures of extensional and compressional origin are widespread in the Alabama coalbed methane fields. Comparison of structure and production further indicates that these structures have a significant effect on the production of gas and water. Extensional structures in Deerlick Creek and Cedar Cove fields include normal faults and hanging-wall rollovers that appear to be detached within the lower part of the Pottsville Formation. In Cedar Cove field, faulting has segmented coalbed reservoirs, with exceptional volumes of gas and water having been produced from parts of two half grabens. In Cedar Cove field, rollover folding southwest of a normal fault swarm has apparently contributed to permeability and, hence, gas and water production. Much water but little gas have been produced from the fault swarm proper.

Compressional folds in Gurnee and Oak Grove fields are interpreted to be detachment folds that grew primarily by limb rotation. Area balance of the Woods Creek anticline in Gurnee field indicates that the structure is developed above secondary detachments within the Pottsville Formation. The Sequatchie anticline, by contrast, is probably developed above a major basal detachment in Cambrian shale. Detachment folding seems to have affected gas production in both fields. In Gurnee field, productive wells are concentrated in the up-plunge parts of the Woods Creek anticline and the complementary Dry Creek syncline. In Oak Grove field, exceptionally productive gas wells are aligned in a small syncline that marks the hinge between the crestal uplift of the Sequatchie anticline and the main backlimb of the structure. Hinge effects are also visible in Cedar Cove field, where water production is enhanced along the axial trace of a syncline that follows the upturned southeast margin of the Black Warrior basin.

Results of our investigation indicate that structure mapping and area balancing are powerful techniques that can be used to identify controls on the production of coalbed methane and water. The apparent thin-skinned nature of structures in the coalbed methane fields indicates that structure within the upper part of the Pottsville Formation does not reflect structure deep in the sedimentary cover. Indeed, it is below the inferred detachment for the normal faults where most water disposal wells are drilled and where conventional hydrocarbon traps may be sought in the eastern Black Warrior basin. Structural control of coalbed gas and water production indicates that the structures have a strong influence on the distribution of fractures and, hence, permeabilty in the Pottsville Formation. However, the production potential of specific structures can be difficult to predict in advance of drilling, completion, and pumping, because economic extraction of coalbed gas depends on more than permeability. A viable gas resource must be present, and dewatering must effectively reduce reservoir pressure.

REFERENCES CITED

Bearden, B. L., and Mancini, E. A., 1985, Petroleum geology of the Carter sandstone (Upper Mississippian) in the Black Warrior basin of Alabama: American Association of Petroleum Geologists Bulletin, v. 69, p. 361-377.

Bradley, D. C. and Kidd, W.S.F., 1991, Flexural extension of the upper continental crust in collisional foredeeps: Geological Society of America Bulletin, v. 103, p. 1416-1438.

Carroll, R. E., Pashin, J. C., and Kugler, R. L., 1993, Burial history and source-rock characteristics of Mississippian and Pennsylvanian strata, Black Warrior basin, Alabama, *in* Pashin, J. C., ed., New Perspectives on the Mississippian

System of Alabama: Alabama Geological Society 30th Annual Field Trip Guidebook, p. 79-88.

Chamberlin, R. T., 1910, The Appalachian folds of central Pennsylvania: Journal of Geology, v. 18, p. 228-251.

Clayton, J. L., Leventhal, J. S., Rice, D. D., Pashin, J. C., Mosher, Byard, and Czepiel, Peter, 1994, Atmospheric methane flux from coals—preliminary investigation of coal mines and geologic structures in the Black Warrior basin, Alabama, *in* Howell, D. G., ed., The Future of Energy Gases: U.S. Geological Survey Professional Paper 1570, p. 471-492.

Decker, A. D., Close, J. C., and McBane, R. A., 1989, The use of remote sensing, curvature analysis, and coal petrology as indicators of higher reservoir permeability: Tuscaloosa, Alabama, University of Alabama, 1991 Coalbed Methane Symposium Proceedings, p. 325-340.

Epard, J.-L, and Groshong, R. H., 1993, Excess area and depth to detachment: American Association of Petroleum Geologists Bulletin, v. 77, p. 1291-1302.

Epsman, M. L., 1987, Subsurface geology of selected oil and gas fields in the Black Warrior basin of Alabama: Alabama Geological Survey Atlas 21, 255 p.

Groshong, R. H., Jr., 1990, Unique determination of normal fault shape from hanging-wall bed geometry in detached half grabens: Eclogae Geologicae Helvetiae, v. 83, p. 455-471.

___1994, Area balance, depth to detachment and strain in extension: Tectonics, v. 13, p. 1488-1497.

Groshong, R. H., Jr., and Epard, J.-L, 1994, The role of strain in area-constant detachment folding: Journal of Structural Geology, v. 15, p. 613-618.

Jamison, W. R., 1987, Geometric analysis of fold development in overthrust terranes: Journal of Structural Geology, v. 9, p. 207-219.

McFall, K. S., D. E. Wicks, and V. A. Kuuskraa, 1986, A geological assessment of natural gas from coal seams in the Warrior basin, Alabama: Gas Research Institute Topical Report GRI 86/0272, 80 p.

Pashin, J. C., 1991, Regional analysis of the Black Creek-Cobb coalbed-methane target interval, Black Warrior basin, Alabama: Alabama Geological Survey Bulletin 145, 127 p.

___1993, Tectonics, paleoceanography, and paleoclimate of the Kaskaskia sequence in the Black Warrior basin of Alabama, *in* Pashin, J. C., ed., New Perspectives on the Mississippian System of Alabama: Alabama Geological Society 30th Annual Field Trip Guidebook, p. 1-28.

___1994a, Flexurally influenced eustatic cycles in the Pottsville Formation (Lower Pennsylvanian), Black Warrior basin, Alabama, *in* Dennison, J. M., and Ettensohn, F. R. eds., Tectonic and eustatic controls on sedimentary cycles: Society of Economic Paleontologists and Mineralogists Concepts in Sedimentology and Paleontology, v. 4, p.89-105.

___1994b, Cycles and stacking patterns in Carboniferous rocks of the Black Warrior foreland basin: Gulf Coast Association of Geological Societies Transactions, v. 44, p. 555-563.

___1994c, Coal-body geometry and synsedimentary detachment folding in Oak Grove coalbed-methane field, Black Warrior basin, Alabama: American Association of Petroleum Geologists Bulletin, v. 78, p. 960-980.

Pashin, J. C., and Carroll, R. E., 1993, Origin of the Pottsville Formation (Lower Pennsylvanian) in the Cahaba synclinorium of Alabama: genesis of coalbed reservoirs in a synsedimentary foreland thrust system: Tuscaloosa, Alabama, University of Alabama, 1993 International Coalbed Methane Symposium Proceedings, p. 623-637.

Pashin, J. C., Carroll, R. E., Barnett, R. L., and Beg, M. A., 1995, Geology and coal resources of the Cahaba coal field: Alabama Geological Survey Bulletin 163, 49 p.

Rice, D. D., 1993, Composition and origins of coalbed gas: American Association of Petroleum Geologists Studies in Geology 38, p. 159-184.

Rich, J. L., 1934, Mechanics of low-angle overthrust faulting as illustrated by the Cumberland thrust block, Virginia, Kentucky, and Tennessee: American Association of Petroleum Geologists Bulletin, v. 18, p. 1584-1596.

Rodgers, John, 1950, Mechanics of Appalachian folding as illustrated by the Sequatchie anticline, Tennessee and Alabama: American Association of Petroleum Geologists Bulletin, v. 34, p. 672-681.

Scott, A. R., 1993, Composition and origin of coalbed gases from selected basins in the United States: Tuscaloosa, Alabama, University of Alabama, 1993 International Coalbed Methane Symposium Proceedings, p. 207-222.

Semmes, D. R., 1929, Oil and Gas in Alabama: Alabama Geological Survey Special Report 15, 408 p.

Shaw, J. H., Hook, S. C., and Suppe, John, 1994, Structural trend analysis by axial surface mapping: American Association of Petroleum Geologists Bulletin, v. 78, p. 700-721.

Sparks, D. P., Lambert, S. W., and McLendon, T. H., 1993, Coalbed gas well flow performance controls, Cedar Cove area, Warrior basin, U.S.A.: Tuscaloosa, Alabama, University of Alabama, 1993 International Coalbed Methane Symposium Proceedings, p. 529-548.

Suppe, John, 1983, Geometry and kinematics of fault-bend folding: American Journal of Science, v. 284, p. 684-721.

___1985, Principles of Structural Geology: Englewoood Cliffs, New Jersey, Prentice Hall, 537 p.

Suppe, John, and Medwedeff, D. A., 1990, Geometry and kinematics of fault-propagation folding: Eclogae Geologicae Helvetiae, v. 83, p. 409-454.

Telle, W. R., and Thompson, D. A., 1987, Preliminary characterization of the coalbed methane potential of the Cahaba coal field, central Alabama: Tuscaloosa, Alabama, University of Alabama, 1987 Coalbed Methane Symposium Proceedings, p. 141-151.

Thomas, W. A., 1988, The Black Warrior basin, *in* Sloss, L. L., ed., Sedimentary cover —North American craton: Geological Society of America, The Geology of North America, v. D-2, p. 471-492.

Wang, Saiwei, 1994, Three-dimensional geometry of normal faults in southeastern Deerlick Creek coalbed methane field, Black Warrior basin, Alabama: Tuscaloosa, Alabama, University of Alabama, unpublished Master's thesis, 77 p.

Wang, Saiwei, Groshong, R. H., Jr., and Pashin, J. C., 1993, Thin-skinned normal faults in Deerlick Creek coalbed-methane field, Black Warrior basin, Alabama, *in* Pashin, J. C., ed., New Perspectives on the Mississippian System of Alabama: Alabama Geological Society 30th Annual Field Trip Guidebook, p. 69-78.

Winston, R. B., 1990, Preliminary report on coal quality trends in upper Pottsville Formation coal groups and their relationships to coal resource development, coalbed methane occurrence, and geologic history in the Warrior coal basin, Alabama: Alabama Geological Survey Circular 152, 53 p.

Withjack, M. O., Islam, Q. T., and La Pointe, P. R., 1995, Normal faults and their hanging-wall deformation: an experimental study: American Association of Petroleum Geologists Bulletin, v. 79, p. 1-18.

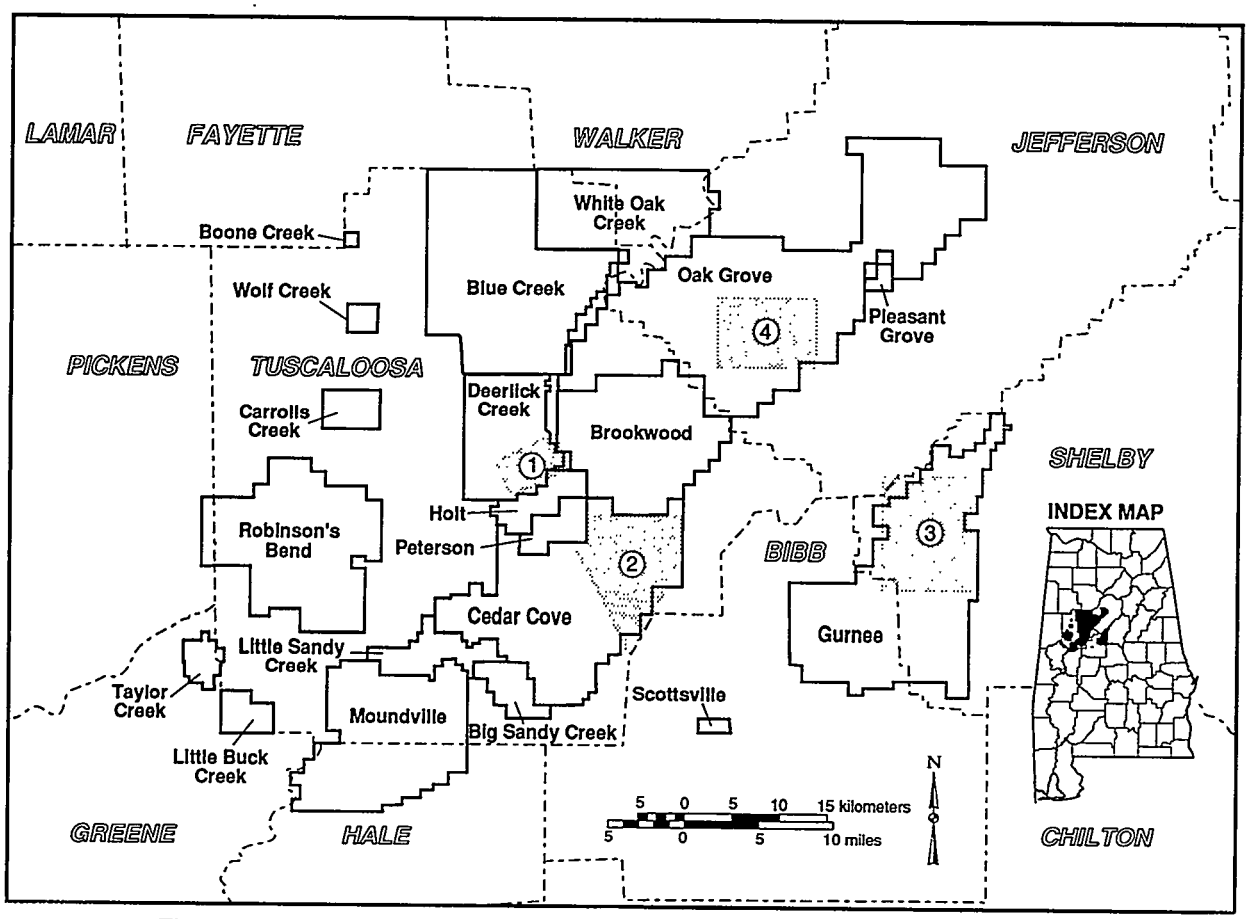


Figure 1. Coalbed methane fields in west-central Alabama. Shaded areas mark the four areas investigated, and circled numbers indicate those areas in order of discussion.

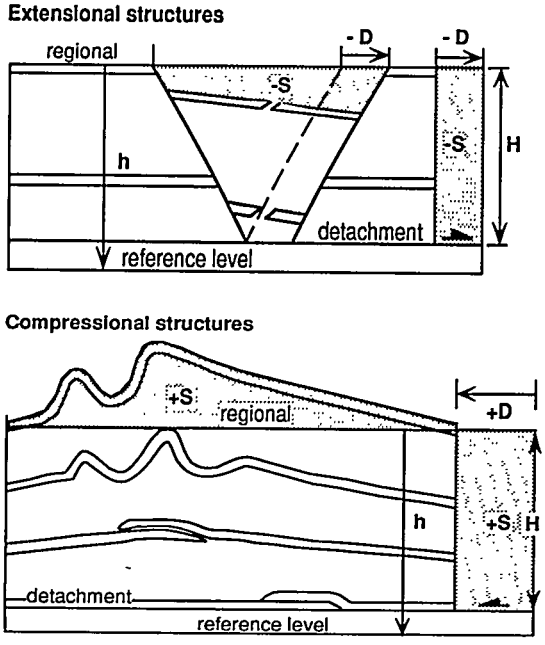


Figure 2. Geometry of extensional and compressional thin-skinned structures and terms required for area balance. S = area displaced, D = displacement distance, H = depth of detachment, and h = depth from marker bed regional to reference level.

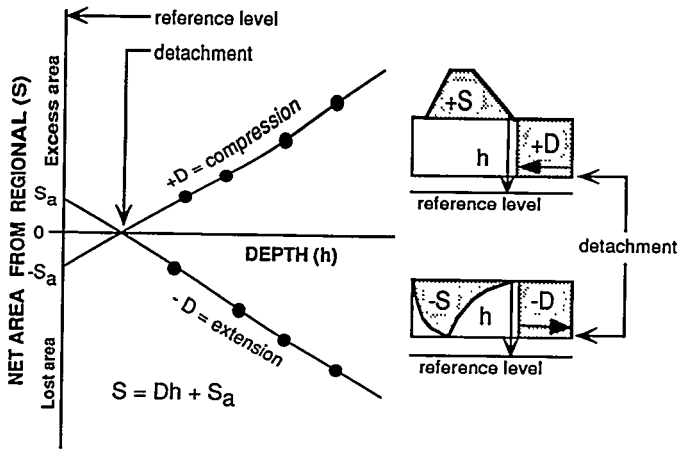


Figure 3. Idealized area-depth plots for extensional and compressional structures.

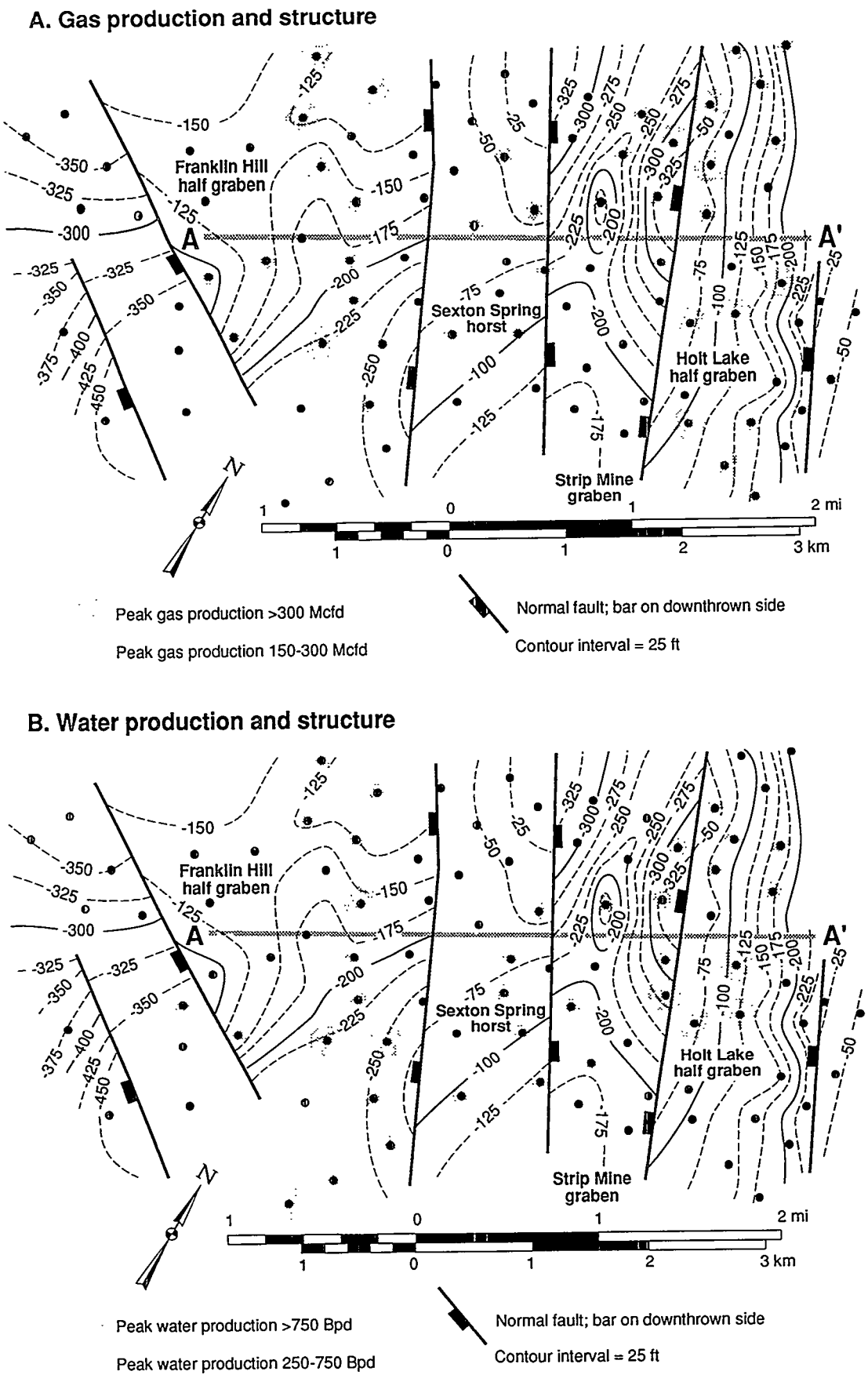


Figure 4. Relationship between structure and production in southeastern Deerlick Creek field. See Figure 1 for location. Structure contours represent elevation of top of Gwin cycle.

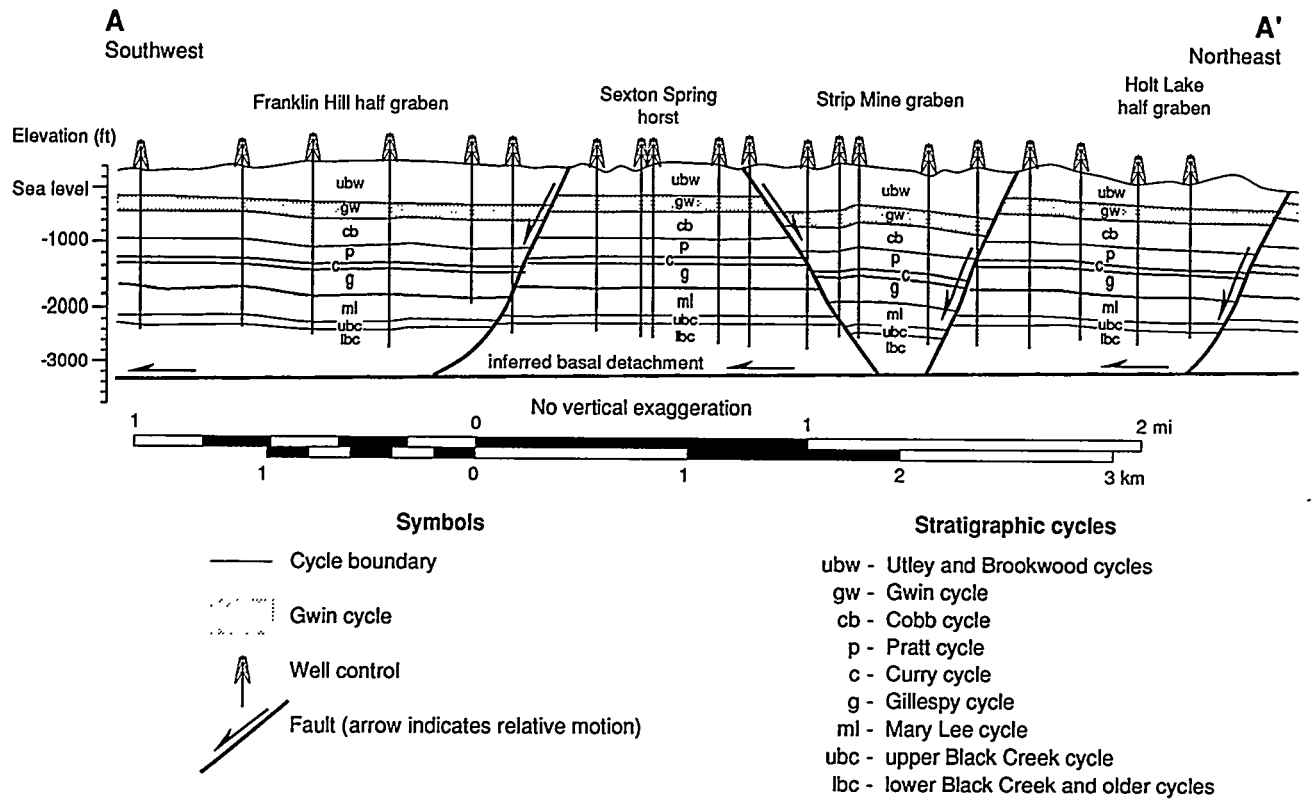


Figure 5. Structural cross section of the Pottsville Formation in southeastern Deerlick Creek field (modified from Wang, 1994). See Figure 4 for location.

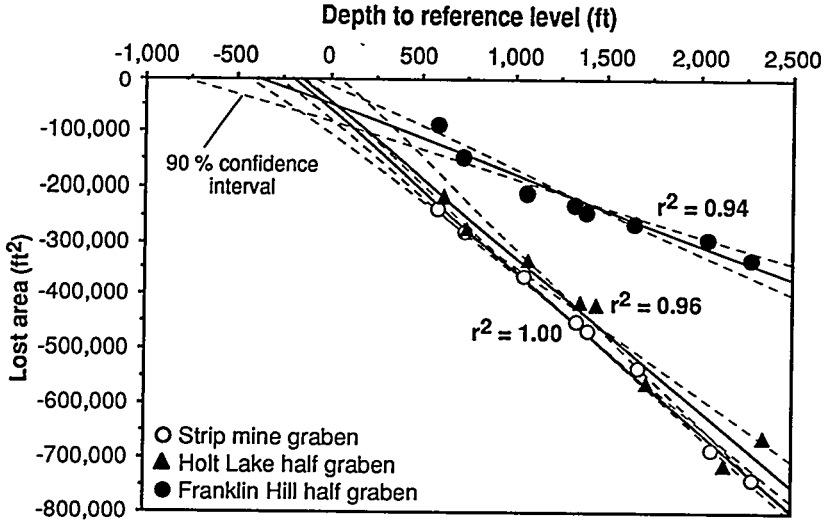


Figure 6. Area-depth plot for extensional structures in southeastern Deerlick Creek field.

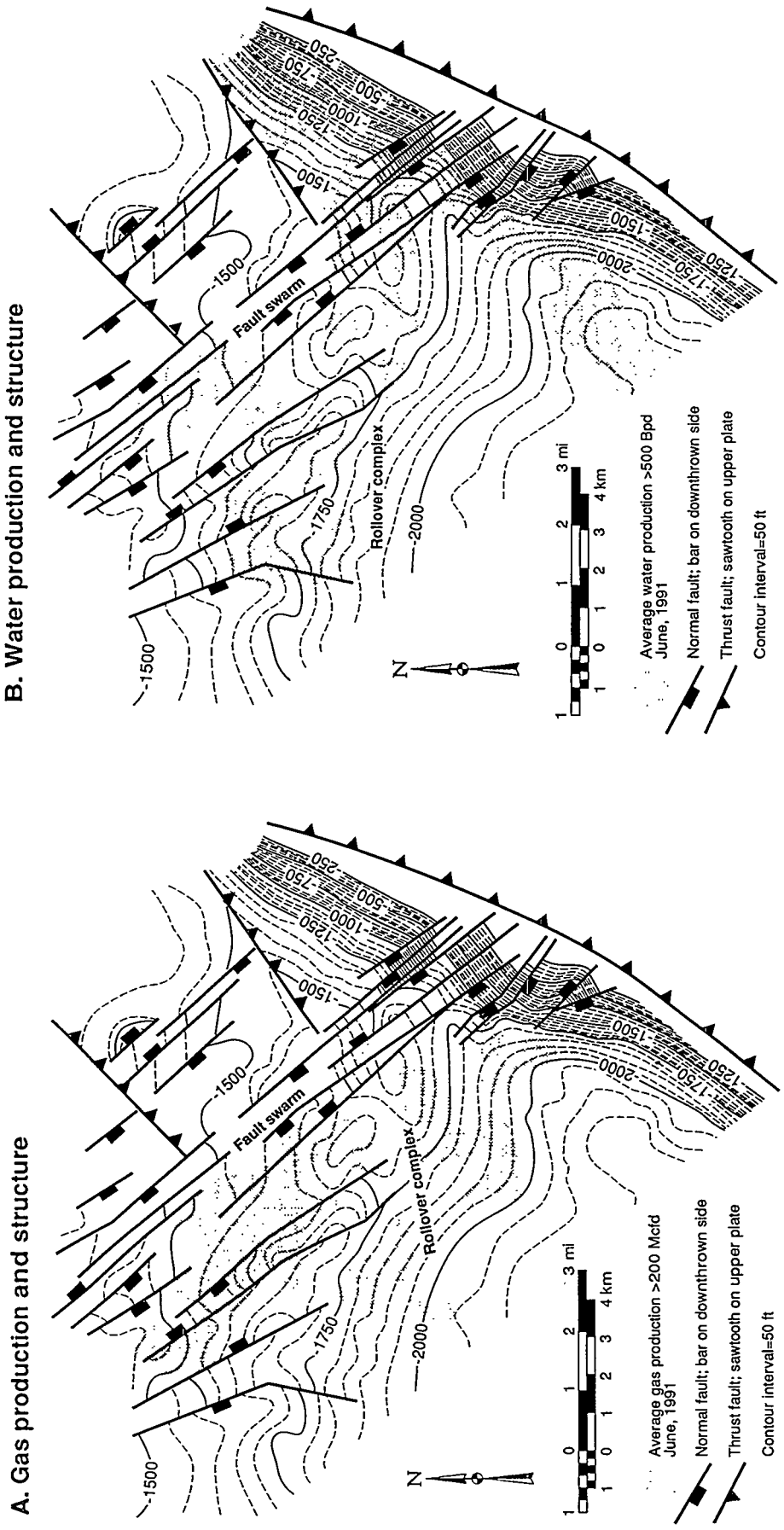


Figure 7. Relationship between structure and production in eastern Cedar Cove field (modified from Sparks and others, 1993). See Figure 1 for location. Structure contours represent elevation of top of New Castle coal, Mary Lee cycle.

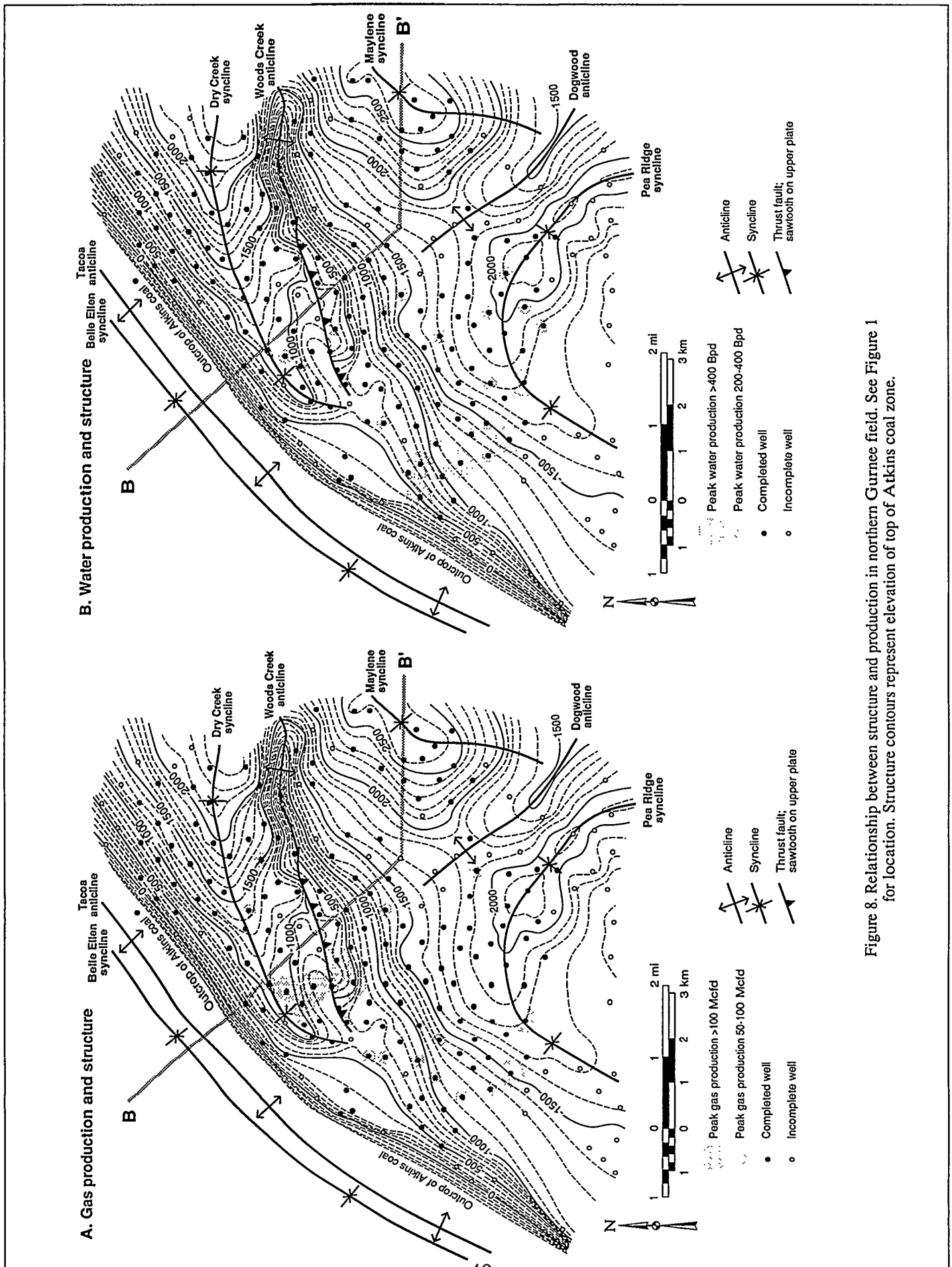


Figure 8. Relationship between structure and production in northern Gurnee field. See Figure 1 for location. Structure contours represent elevation of top of Atkins coal zone.

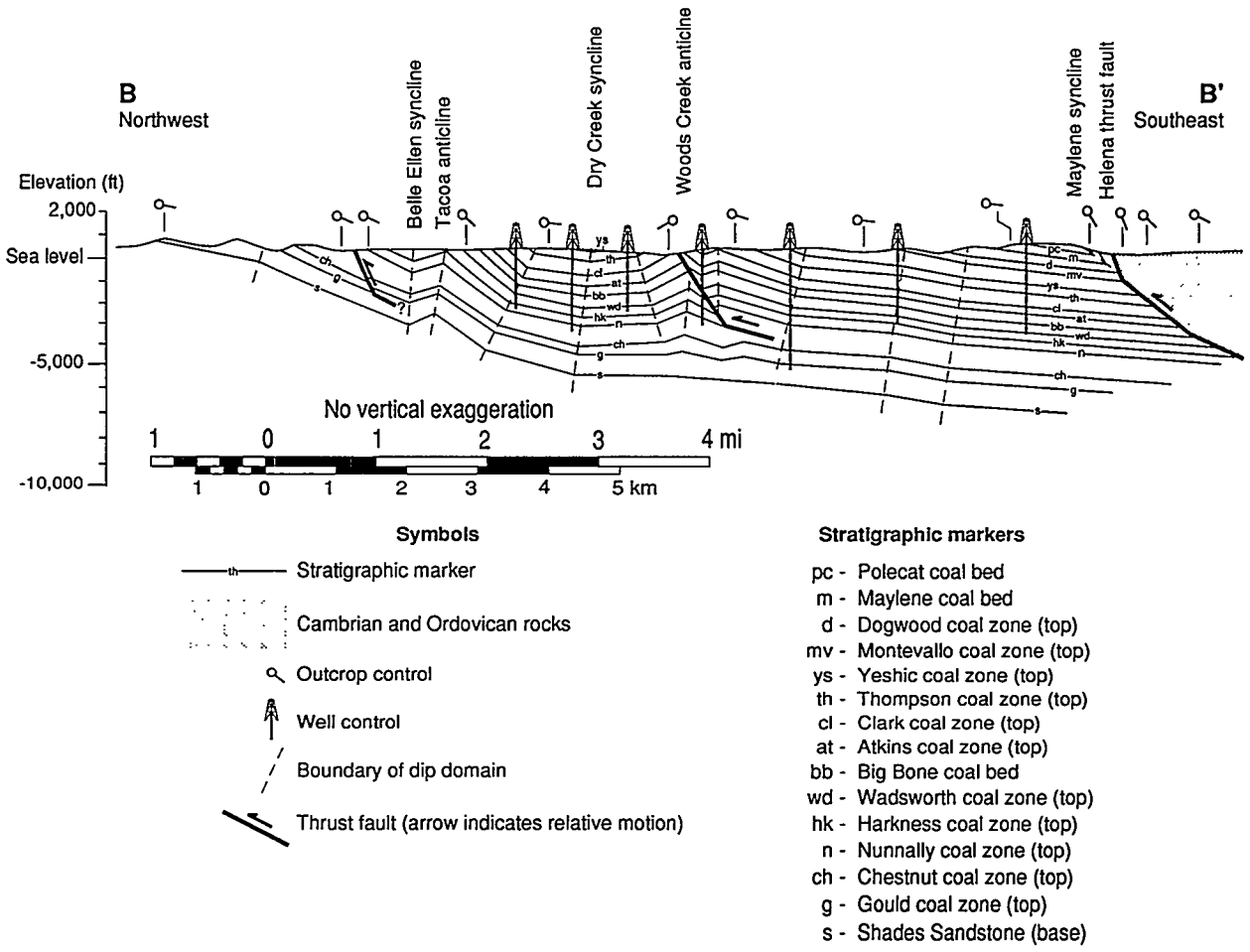


Figure 9. Structural cross section of the Pottsville Formation in Gurnee field (modified from Pashin and others, 1995).

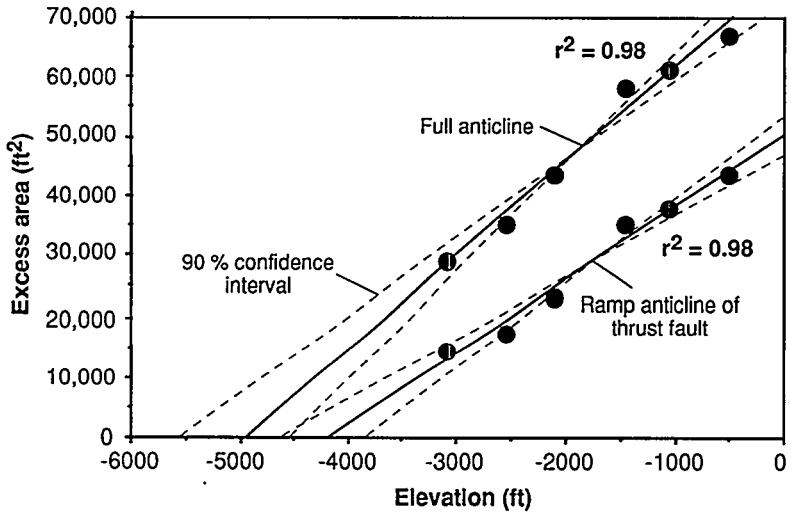


Figure 10. Excess area plots of the Woods Creek anticline in Gurnee field.

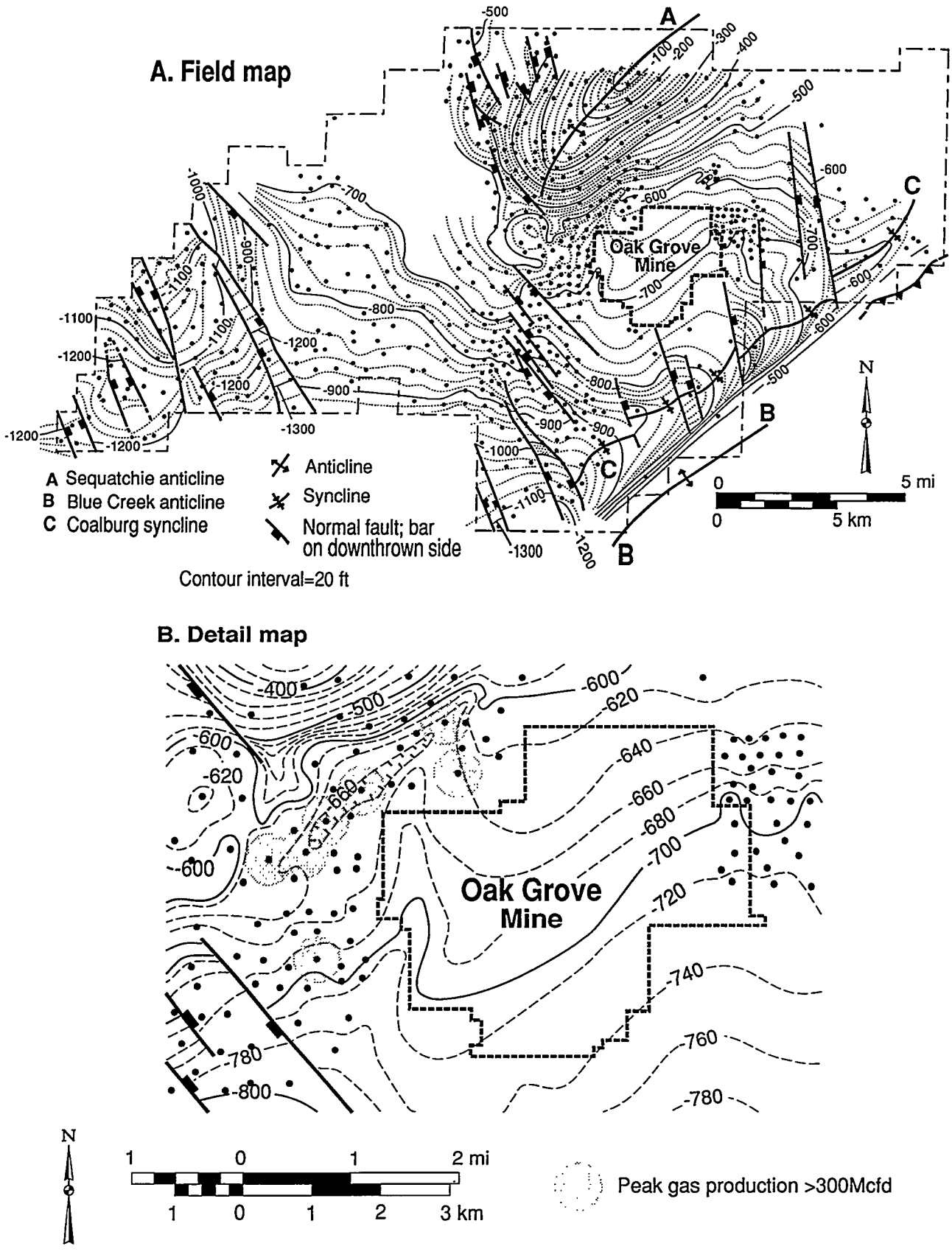


Figure 11. Relationship between gas production and structure in Oak Grove field (modified from Pashin, 1991, 1994c). Structure contours represent elevation of top of Mary Lee coal.

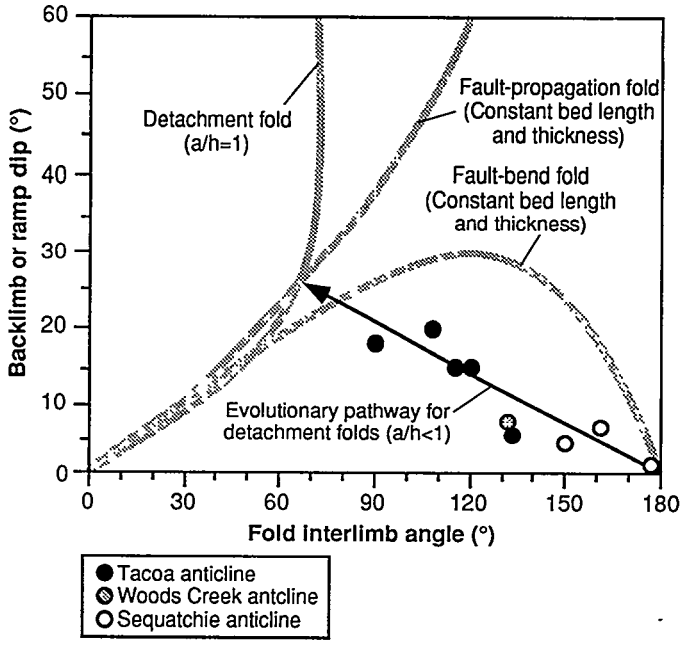


Figure 12. Classification of compressional folds in Alabama coalbed methane fields using diagram of Jamison (1987). a = fold amplitude, h = detachment depth. Detachment folds with a/h < 1 plot to right of line, whereas detachment folds with a/h > 1 plot to left of line.

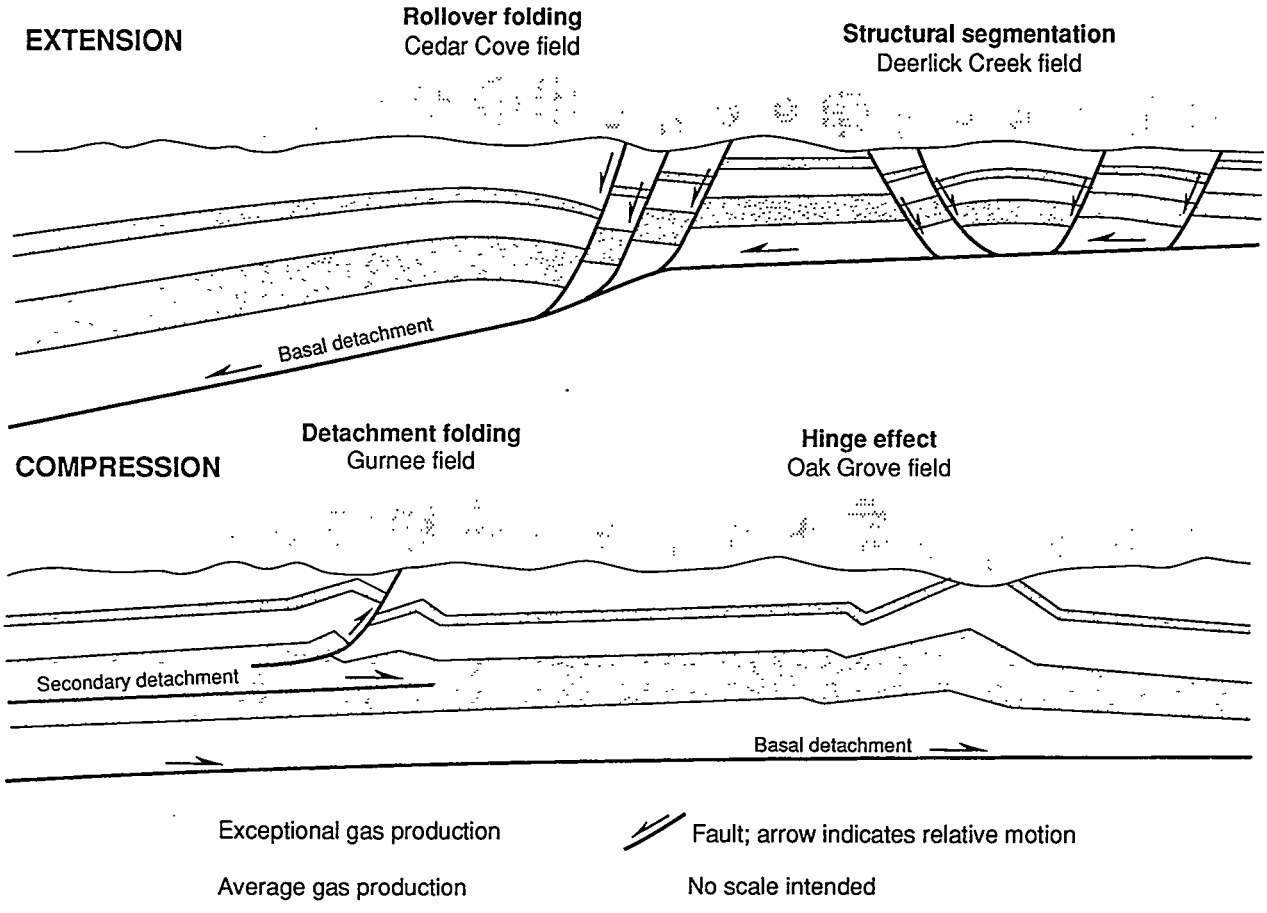


Figure 13. Conceptual model of structurally controlled gas production in Alabama coalbed methane fields.

INTERGAS '95

May 15-19, 1995
The University of Alabama
Tuscaloosa, Alabama USA

9515

Delineation of Piceance Basin Basement Structures Using Multiple Source Data: Implications for Fractured Reservoir Exploration

T.E. Hoak and A.L. Klawitter,
Advanced Resources International, Inc.

ABSTRACT

Fractured production trends in Piceance Basin Cretaceous-age Mesaverde Group gas reservoirs are controlled by subsurface structures. Because many of the subsurface structures are controlled by basement fault trends, a new interpretation of basement structure was performed using an integrated interpretation of Landsat Thematic Mapper (TM), side-looking airborne radar (SLAR), high-altitude, false color aerial photography, gas and water production data, high-resolution aeromagnetic data, subsurface geologic information, and surficial fracture maps. This new interpretation demonstrates the importance of basement structures on the nucleation and development of overlying structures and associated natural fractures in the hydrocarbon-bearing section. Grand Valley, Parachute, Rulison, Plateau, Shire Gulch, White River Dome, Divide Creek and Wolf Creek fields all produce gas from fractured tight gas sand and coal reservoirs within the Mesaverde Group. Tectonic fracturing involving basement structures is responsible for development of permeability allowing economic production from the reservoirs. In this context, the significance of detecting natural fractures using the integrated fracture detection technique is critical to developing tight gas resources.

Integration of data from widely-available, relatively inexpensive sources such as high-resolution aeromagnetics, remote sensing imagery analysis and regional geologic syntheses provide diagnostic data sets to incorporate into an overall methodology for targeting fractured reservoirs. The ultimate application of this methodology is the development and calibration of a potent exploration tool to predict subsurface fractured reservoirs, and target areas for exploration drilling, and infill and step-out development programs.

INTRODUCTION

The objective of this investigation is to provide a perspective into the dynamics of an integrated fracture detection methodology applied to the Piceance Basin tight gas sands and coals. The integrated methodology involves the parallel interpretation and ultimate integration of conventional subsurface data (wells), aeromagnetic, seismic, and remote sensing imagery interpretation, integrated within the context of a detailed regional tectonic synthesis (Decker et al., 1994). To illustrate the approach, several gas fields from the Piceance Basin are used as examples to demonstrate the power of the method as it applies to understanding production trends and the controls on gas production in fractured fields in the Piceance Basin. Previously, few Piceance Basin fields were thought to contain fractured reservoirs (Brown et al., 1986). Those fields known to contain fractures include White River Dome, Divide Creek and Wolf Creek anticlines and the Rulison Anticline (Brown et al., 1986). Additional fractured reservoirs have subsequently been documented by fractured cores from Grand Valley Field (Reinecke et al., 1991), Parachute Field (Reinecke et al., 1991), Plateau and Piceance Creek fields (T. Barrett, Personal communication, 1994). Given the extremely small permeabilities observed in central Piceance Basin tight gas sands (5-30 microdarcies, Reinecke et al., 1981) commercial production cannot be achieved unless natural fractures are present in these fields. Data collected at the MWX site has confirmed that a 100 fold increase in reservoir permeability is achieved when natural fractures are present (Lorenz et al., 1991; Lorenz and Finley, 1991).

This paper is organized into several sections. After a brief basin overview, we demonstrate the relationship between production, and structural geology and stratigraphy. Because production trends are structurally controlled, we describe areas of the basin where regional subsurface structural mapping suggests that other fractured regions may exist. Because of the basement control on subsurface structure, we have used high-resolution aeromagnetics to delineate basement structures, confirmed by seismic, that control the shallower structures and production trends. Finally, we demonstrate how remote sensing imagery analysis provides a cost-effective method to rapidly define regional structural trends and to delineate zones of enhanced fracturing. Confirmation of the reservoir scale complexity of these fractured zones requires additional, more detailed analysis to clearly understand the nature of the fracture anisotropy using seismic or other advanced geophysical methods. However, the integrated methodology represents the most cost-effective system to minimize potential exploration area while maximizing the opportunity for success.

BASIN OVERVIEW

The Piceance Basin is an elongate, NNW-trending structurally-downwarped region that formed as a result of Laramide contractional tectonics. The northern boundary of the basin is defined by the thrust-cored structures of the Axial Arch

and the Uinta Uplift. The sinuous eastern margin is formed by the "S"-shaped, thrust-cored, Grand Hogback Anticline lying along the flank of the White River Uplift. The western boundary, formed by the Douglas Creek Arch, separates the Uinta Basin from the Piceance basin. The southwestern boundary is formed by the Uncompahgre Uplift. The West Elk Mountains and the Gunnison Uplift form the southeastern boundary of the basin. All uplifts surrounding the basin have experienced multiple phases of tectonic deformation ranging from Precambrian tectonism through Pennsylvanian-Permian deformation, culminating in the Laramide thrusting that defines the present-day basin geometry. Additional details regarding the tectonic evolution of the basin will be discussed later in the paper.

STRUCTURAL AND STRATIGRAPHIC CONTROLS ON GAS PRODUCTION

To assess the importance of fractured reservoirs on production trends, detailed structure and production mapping was performed in Grand Valley, Parachute, Rulison, Shire Gulch and Plateau fields (see Figure 1 for locations) to determine the relationship between production and structure. These fields produce gas from the Tertiary-age Wasatch Formation (primarily Grand Valley, Parachute, Rulison), the Cretaceous-age Williams Fork (all fields), and the underlying Cretaceous-age Iles Formation (primarily Shire Gulch and Plateau). In these zones, gas is trapped in regionally-extensive, structurally-enhanced gas-centered basin-type traps. A large percentage of Williams Fork gas is produced from vertically-stacked fluvial sand channels, and from thick coals in the Cameo Coal section located below the fluvial interval. Production from marine sands in the Cozzette-Corcoran sandstones (Iles Formation) is dominated by shoreface sands in the transition between the marine and continental facies. Plateau and Shire Gulch fields straddle the transition zone between the two facies. For discussions of reservoir sedimentology and regional stratigraphy, see Johnson and Nuccio (1986) for the Williams Fork, and Brown et al. (1986) for the Rollins, Cozzette and Corcoran sandstones.

The primary objective of this section is to characterize the relationship between production trends in these fields, regional stratigraphy and structure, most notably the influence of structural and stratigraphic trends on reservoir productivity.

Production Trends in Grand Valley, Parachute and Rulison Fields

To understand production controls, gas production data for the best six months during the life of the well were contoured and normalized by the total days of production. By normalizing the best six months production, it is possible to minimize reporting inaccuracies and the effects of variable seasonal production. To assess the controls on production, production contours were overlaid with depositional systems information and structural geology (Figures 2a and 2b). Figure 2a illustrates the relationship between structure and production trends in the three fields. The structure contours are drawn on the top of the Rollins Sandstone Member (Iles Formation). The production trends lie parallel to local structure trends in the three fields. To examine the effect of stratigraphic variation, a total sand isochore map was compared to production trends for Parachute and Rulison fields (Figure 2b). The depositional system consists of vertically-stacked fluvial channels. In general, it is extremely difficult to predict the location of thick Williams Fork Formation reservoir sands due to complex internal variability in the meander belt system. The overall depositional trend of the fluvial meander belt trends to the northeast (Peterson, 1984). The NW-striking production trend lies perpendicular to the depositional systems trends (Figure 2b), strongly confirming the structural control on production in these fields. Natural fractures measured from fracture detection logs and oriented core in the three fields lie oblique (WNW-trend) to the production trends observed in the central basin (Lorenz and Finley, 1991).

Grand Valley, Parachute and Rulison fields illustrate the importance of structural controls on production trends. It is interesting to note that the NW-striking production trends and local structure lie oblique to the dominant WNW or E/W fracture trends measured during the MWX coring program in vertical and horizontal wells (Lorenz and Finley, 1991). There are several possible explanations for this relationship. The most plausible is that local tectonic deformation caused by structures, such as the Rulison Anticline, generates enhanced dilatancy along "regional" fracture sets oriented oblique to the structure. In such a scenario, the fractures cored at MWX are not necessarily the trend controlled by the local structure. Instead, the local structure, possessing its own strike-parallel fracture set merely dilates the MWX set and increases its connectivity. If this is true, and the regional fractures formed first, the MWX fractures would likely show minor amounts of shear displacement during formation of the anticline. Alternatively, if they formed later, they would not necessarily show any surface ornamentation characteristic of shear displacement (e.g. slickensides). Given that there is no obvious surficial ornamentation on the mineralized fracture planes cored in the MWX wells, it suggests that these fractures may post-date formation of the anticline. A further complexity is introduced by the small NE-trending normal fault found in the MWX #2 well (Sattler et al., 1985; Branagan et al., 1985). This fault lies orthogonal to the NW-striking production trend and the dominant measured fracture orientation. It is possible that the MWX and SHCT coring program fortuitously cored only the E/W or WNW fracture trend and did not manage to intersect a more dominant set that controls production. It is also possible that E/W fractures are localized and are restricted to the E/W-trending section of the Colorado River while the other fields lie along NW-trending structures that control the NW-striking drainages. Available data are presently unable to resolve this complexity.

Production Trends in Plateau and Shire Gulch Fields

Production data from Corcoran and Cozzette Sandstones (Iles Formation) were contoured and compared with structural contours to investigate the relationship between the two parameters (Figures 3a and 3b). Production trends in Plateau and Shire Gulch fields strike northwest, parallel to the trend of mapped surface faults. Interestingly, there is a slight obliquity between the trend of field structure (contoured on top of the Rollins Sandstone Member of the Iles Formation) and production contours in these two fields (Figure 3a). Instead, the production trends lie parallel to the trend of mapped surface faults (Donnell et al., 1984) and basement fault zones to be discussed below. Structure contours on the Rollins Sandstone Member of the Iles Formation show that the regional structure

in this area is a WNW-trending series of broad, open and upright anticlines and synclines. Eastward, these folds die out into the regional NW-trending east-dipping western synclinal limb of the basin. The WNW-trending folds appear to have formed late in the tectonic evolution of the basin. These folds are probably related to differential subsidence over basement fault zones. The Rollins structural datum is used in these two fields to maintain regional consistency and because of the greater number of Rollins penetrations. The Corcoran structure is nearly identical to that of the Rollins, only deeper. This relationship is confirmed by isopachs or isochores of the Rollins-Corcoran interval that shows a monoclinally southeastward-dipping surface.

Corcoran-Cozzette depositional strandlines trend northeast (Zapp and Cobban, 1960; Brown et al., 1986), perpendicular to the trend of the production axes (Figure 3b). The strandline differentiates between nearshore continental and offshore marine facies. The boundary between the two facies is primarily delineated by the presence of coal in the continental facies. There appears to be little stratigraphic variation in the depositional system along the northeast strandline trend (Zapp and Cobban, 1960; Warner, 1964; Brown et al., 1986). Some complexity appears to occur in the continental facies regarding the relative influence of fluvio-deltaic vs. wave-dominated facies (Warner, 1964). There is some evidence that some of the wave-dominated sediments have been reworked (Warner, 1964). This reworking destroys the diagnostic internal geometry of the sediments and makes it difficult to characterize the log response of the facies.

REGIONAL STRUCTURE MAPPING

Detailed structural mapping of the Plateau-Shire Gulch and Grand Valley-Parachute-Rulison fields clearly demonstrates the structural control on production trends (Figure 4). To focus regional or basin-scale exploration efforts, regional structure mapping was used to locate other areas where local structure controls fractured production trends. Such regional structural trends are readily observable on regional structure maps constructed on the Rollins Sandstone Member (top of the Iles Formation). Although the Rollins Sandstone Member is a progradational system, shingled toward the southeast, the magnitude of the shingling is small ($< 100'$) such that regional structure maps are not greatly affected by this geometry. Detailed structural studies of gas fields throughout the basin are even less affected because the vertical variation caused by shingling is generally imperceptible within the boundaries of most typical Piceance Basin gas fields.

Three dominant regional structural trends persist throughout the basin. In the eastern basin, the NW-trending Divide Creek, Wolf Creek and Coal Basin anticlines have been formed by WSW-directed thrusting. In the western basin, several broad, low amplitude anticlines have formed with dominant E/W trends. These anticlines include the Debeque, Unnamed (here designated Bull Creek Anticline, located to the south of the Debeque anticline in Plateau Field) and the Douglas Creek Anticline. The latter anticline has an WNW trend. The northern boundary of the basin, the Axial Arch, is a WNW-trending fault-bend fold formed during south-directed Laramide thrusting (Stone, 1986). The last significant trend is the N/S trend typified by the sections of the Hogback between Meeker and Rio Blanco, and from Carbondale to the Elk Mountains.

Preliminary overview of the basin suggests that fractured reservoir conditions should be present in several of the anticlines along the eastern flank of the Douglas Creek Arch. In addition, the northern basin contains the Powell Park and Sulphur Creek structures that are likely to be fractured. Limited well control, combined with a lack of high-resolution aeromagnetic data and seismic confirmation, makes additional effort into understanding the fracture potential of these structures a future priority for regional exploration efforts.

The thrust-cored structures in, and adjacent to, the Piceance Basin include the Grand Hogback (Gries, 1983), Wolf Creek Anticline (Grout, 1990) and Divide Creek Anticline (Grout, 1990; Gunneson et al., 1994), Rangely Anticline (Stone, 1986), Axial Arch and Maudlin Gulch (Richard, 1986), and the White River Dome, and Powell Park Anticlines. Thrust involvement or basin fault inversion is also evident in the Rulison Anticline, a Pennsylvanian-age paleohorst (Waechter and Johnson, 1986), and along the margins of older horst blocks including the Grand Hogback (Waechter and Johnson, 1986).

The tectonic evolution has been assessed using published sources integrated into a dynamic structural analysis. To perform this synthesis, a tectonic chart (see Figure 5) was prepared that tracks the evolution and development of major structures (see Figure 6) throughout the geologic evolution of the Piceance Basin and precursor basins and uplifts located in the region. At the initiation of the Late Cretaceous-Early Tertiary Orogeny, there were two dominant regional anisotropies that formed during extensional tectonics that were part of the Precambrian and the Pennsylvanian-age Ancestral Rockies Orogeny. The Precambrian anisotropy trends WNW in the Uinta Uplift and trends NW in the Uncompahgre Uplift. The Pennsylvanian-age structural grain trends more NW and forms the Rulison paleohorst (beneath Rulison Field) and a paleohorst beneath the Grand Hogback Monocline (Waechter and Johnson, 1986). It is important to note that recent seismic interpretation in the central Piceance Basin shows that many, if not most, of the basement faults show reverse sense of displacement. This relationship is valid for all basement faults, not just those reactivated during Laramide contraction. This is contrary to older interpretations of Precambrian tectonics that emphasized the dominance of extensional tectonics (Tweto, 1975). Given the complexity and timeframe involved in Precambrian deformation throughout Colorado, complete understanding of this problem requires extensive additional research.

These two anisotropy trends were reactivated during the Laramide Orogeny. Initially, the compression axis was oriented NNE. Structures formed during this phase include the Rangely, White River Dome, and Uinta Uplift features. Later, the overall compression axis shifted and was oriented NE/SW to form major NW-trending thrust-cored folds such as the Divide Creek Anticline, Wilson Creek Anticline, the Axial Arch and related structures. As this phase of tectonism abated, the compression axis shifted to a more easterly trend and a broad gentle regional uplift occurred resulting in the formation of the Douglas Creek Arch.

Following the end of Laramide contraction, the region has experienced slight WNW to E/W compression that persists to the modern day. During the transition period, the White River and Dudley Gulch grabens formed and basaltic dikes were emplaced in the southeast basin.

During Laramide tectonics, the thrust geometries that were initiated were locally complex. Exclusive seismic data from throughout the basin center have recently been interpreted. These data show three primary detachment levels in the basin. The deepest level is an intrabasement detachment that allows thrust duplication within the Precambrian basement. In the eastern basin, where the Pennsylvanian-age Eagle Valley Evaporite is best developed, the evaporite forms a Paleozoic-level detachment surface. The uppermost detachment is found in the Cretaceous-age Mancos Shale. Locally, imbricate thrust systems fan off this detachment and cause local, dekameter-scale, thickening in the Iles Formation sandstones (Rollins Cozzette, Corcoran). The complex thrust geometry in the eastern basin has been documented in high-resolution seismic data across the Divide Creek Anticline by Gunneson et al., (1994) but these relationships have not been previously demonstrated to extend into the basin center. We are attempting to obtain permission to publish seismic data from the basin center that illustrates the multi-level detachments. Work in progress is assessing the influence of these multiple displacements on production.

BASEMENT CONTROL OF SHALLOWER STRUCTURES

The critical relationship in the Piceance Basin is the relationship between shallow and intermediate (< 10,000 feet depth) fractured structures and deeper basement structures. To assess this relationship, high-resolution aeromagnetic data, calibrated with published and proprietary seismic data was used to establish the relationship between basement structures and the shallower structures that delineate fractured production trends. By delineating the geometry of basement structures, we appear to have confirmed our ability to predict fractured reservoirs in shallow structures in other areas of the basin using the integrated approach.

There are several areas where this relationship is extremely clear and unequivocal. The Grand Valley-Parachute-Rulison area clearly demonstrates the basement control on shallower structures that control production trends. A detailed view of a seismic line under Parachute and Rulison fields demonstrates that the Rulison Anticline lies above a reactivated or inverted fault system lying along a basement horst block (Figure 7). The timing of the extensional tectonics that formed the horst are clearly Paleozoic (Pennsylvanian) in age because the Paleozoic section shows evidence of syntectonic deposition. Other proprietary seismic lines in the central Piceance Basin seismic grid more clearly illustrate this relationship. From this grid (see Figure 8 for line locations) we have interpreted the geometry of basement fault systems. The fault systems show a complex interplay of normal and thrust faults (Figure 9). It appears that many of the normal faults may represent older structures, whereas the thrusts are generally younger, thought to be formed during Laramide deformation. Work in progress is refining the temporal and spatial evolution of the faults in the context of a detailed tectonic evolution. The critical and confirming relationship is the similarity in trends of the production contours, shallower subsurface structure and the basement fault orientations.

The correspondence of basement faults to structures mapped on the regional Rollins map, reveals the close relationship between the shallower subsurface structures and the deep fault systems (Figure 9). There is excellent correspondence between basement and shallower structures in Grand Valley-Parachute-Rulison similar to relationships found to the southwest in the Plateau and Shire Gulch fields. Seismic-interpreted basement faults in the Divide Creek-Wolf Creek anticlines also show similar relationships (Gunneson et al., 1994) although Cozzette-Corcoran production data from this area in the public domain is extremely limited due to the mid-late 1950's age of the original production and drilling activity. Work in progress is attempting to collect production information from these fields to confirm basement control on fractured reservoir production trends.

Calibration With High-Resolution Magnetics

High acquisition costs, especially in the Piceance Basin, associated with regional seismic surveying effectively prohibits its use for regional reconnaissance studies. In addition, single seismic lines generally do not satisfactorily explain complex structural geometries. To obviate this problem, we have calibrated a newly-acquired high-resolution aeromagnetic survey against the seismic grid. Aeromagnetic surveying was chosen for several reasons. Existing NURE data demonstrated that aeromagnetics provided important basement information; the survey is relatively low-cost; and the data can be rapidly acquired. In addition, analysis and digital reprocessing of regional, lower-resolution NURE aeromagnetic data (Grauch and Plesha, 1989) (Figure 10) appeared to define gross boundaries between basement domains. From this information, we attempted to maximize new data acquisition in the transitional areas between these domains. In addition, we wanted to clearly image the magnetic basement beneath the majority of producing fields in the southern Piceance Basin. The aeromagnetic survey was flown with N/S flight lines at four hundred meter spacing with perpendicular tie lines acquired at sixteen hundred meters. This is in sharp contrast to the NURE aeromagnetic data acquired at three mile E/W flight line spacing with twelve mile N/S tie line spacing.

Detailed aeromagnetic contours clearly identify regions in the basin corresponding to differences in basement structure. In general, basement fault zones with significant throw correspond to steep magnetic gradients. Detailed examination of the regional map reveals numerous areas where basement faults are likely to be present (see Figure 11). We will focus our attention on the Grand Valley-Parachute-Rulison and Plateau-Shire Gulch areas.

The Grand Valley-Parachute-Rulison area in the basin center lies on the margin of a large E/W trending basement high recognized on the aeromagnetic survey. The magnetic high corresponds to a missing Paleozoic section confirmed by drilling (Barrett Resources-Arco Deep #1-27). Along the northeast margin of this structure, there are numerous NW-trending normal and thrust faults evident on the aeromagnetic maps that have been confirmed by seismic surveying (Figure 12). In this area of the basin, basement faults trend NW, parallel to the structural trends observed in the shallow

subsurface and parallel to production trends observed in subsurface reservoirs. The magnitude of the displacements associated with the basement faults are difficult to establish from the aeromagnetic data. Seismic data suggest that the displacements vary from 500-2500 feet at the basement level.

In the Plateau-Shire Gulch area, it appears that some of the high-angle normal faults observed in the basement propagate to the surface as evidence by surface mapping discussed earlier. Seismic lines in this area show several normal faults that drop the hangingwall down to the northeast (Brown et al., 1986). In this field, the trend of basement faults in the aeromagnetic data is the same as the trend of faults mapped on the surface (Figure 13). We have already demonstrated how production trends in these fields lie parallel to the subsurface and surface fault trends. The aeromagnetic data suggest that these fault trends continue down to the basement level. In addition, using this information, we can extrapolate or predict fracture-controlled production trends using aeromagnetic data for areas lacking other subsurface controls.

REMOTE SENSING IMAGERY ANALYSIS

A key component of any basin fracture analysis is the relationship between surficial features and subsurface and basement structures. Basement control of shallow subsurface structures has been previously demonstrated. To extrapolate or calibrate this information against surficial geology requires the recognition of subsurface and basement fractures on the surface. To investigate the relationship between surficial data sets and subsurface structures, remote sensing imagery analysis was integrated with surficial mapping to evaluate the relationship between these two data sets and the relationship between the surface and subsurface data sets.

The Plateau-Shire Gulch area contains several NW-trending normal faults that lie parallel to the production trends. These trends are also recognized by remote sensing imagery analysis of this area. To determine the relationship between regional subsurface structure and surficial trends observed on remote sensing imagery, remote sensing imagery analysis was performed using Thematic Mapper (TM) data, Side-Looking Airborne Radar (SLAR) and high-altitude, high-resolution, false-color infrared aerial photos (NHAP). Figure 14 presents linear features interpreted from aerial photos and TM data registered onto a regional structure map constructed using the top of the Rollins Sandstone Member. To verify the nature of these linears, interpreted linears were compared to published maps of surface geology (USGS MF- and GQ- map series for the area of the fields). Remote sensing imagery analysis accurately locates the surface fault locations. In addition, numerous parallel linear features are noted that may also represent faults or fault-parallel fractures. These linear features were not recognized during field mapping. There appears to be little relationship between the fracture orientation or density and the location of the linears on the fold geometry. This relationship, combined with the apparent absence of oblique-slip slickenlines on these fractures, suggests that the fractures formed after the fold. Additional fieldwork is necessary to confirm the regional persistence of these limited field observations.

The relationship between production and linear features is shown in Figure 15. Production trends directly correlate to trends and locations of surficial linears. All linears are shown in Figure 15. Because of the trend of surface faults and the production trends, a rose diagram (Figure 16) was constructed that shows the dominant linear features trends in the field. There is a wide range of orientations. We know, however, that the WNW-NW range of linears corresponds to mapped surface faults. Because of this, we filtered the data set to only contain these trends (Figure 17). From this map, the excellent correspondence between linear features interpreted from remote sensing imagery analysis can be seen. Nearly all significant production trends are overlain by a surficial linear. The confirmation of subsurface production trends by remote sensing imagery analysis suggests that we should be able to use a combination of high-resolution aeromagnetic data to locate basement faults and remote sensing imagery analysis to identify the surficial manifestation of these same zones. From this information, we are able to predict the orientation and location of subsurface production trends.

REGIONAL ASSESSMENT OF SURFICIAL FRACTURES

Because of the relationships established at Plateau and Shire Gulch fields, a regional assessment of the relationship between surficial linears and mapped surface faults was conducted. It was hoped that this effort would clearly establish the dominant surficial fracture patterns in a time and cost-effective manner. To accomplish this objective, data regarding timing relationships between fracture sets and trends were compiled from the extensive work on regional fractures and joints collected by Grout and Verbeek (1985; 1989). This data set has also been compared against the remote sensing imagery analysis linear features interpretation (see Figure 18 for example areas). Overall, there is excellent agreement between the remote sensing-based interpreted linear features, and the surficial mapping. It is important to note that remote sensing analysis is generally unable to fully determine the structural sequence in which fracture sets formed. For this reason, it is essential that remotely-sensed interpreted linear features be ground-checked to verify the characteristics of the linears.

There are numerous examples of the ability of remote sensing image analysis to document trends verified by field mapping of joint systems. In the White River Dome area and the Douglas Creek Arch area in the northern Piceance Basin, remote sensing imagery analysis recognizes all of the surface-mapped linear trends (Figure 18). In the Douglas Creek area, surface faults possess a dominant NE-trend (Figure 18). There are considerably lesser number of NW-trending faults. Remote sensing imagery analysis accurately identifies the location and trend of the surface structures. Similarly in the White River Dome, surface mapping shows three dominant joint trends. These trends (NW, NNW and NNE) are also confirmed by the remote sensing imagery analysis (Figure 18).

The surface joints at Rifle Gap are also identified in the remote sensing data set (Figure 18). In the Colorado River and Debeque areas, the remote sensing analysis identifies additional linear trends that do not correspond to the dominant surface mapped joint trends. The significance of these additional linear trends requires ground confirmation to identify their significance. It is important to stress, however, that the remote sensing imagery analysis does correctly identify the abundant

surface mapped joints.

In general, there is excellent agreement between the orientation of the significant trends determined from imagery analysis and ground-based studies. Given the similarity of the two data sets, this outcome is not surprising. It is important to emphasize, however, the cost-efficacy of remote sensing analysis compared to field mapping. The rapidity of remote sensing analysis provides an extremely rapid process to recognize the dominant structural trends in the basin. Timing relationships, of course, still require surficial field work to confirm crosscutting relationships. Remote sensing analysis, however, readily identifies those areas where these relationships are best-expressed.

CONCLUSIONS

Fractured production trends in Piceance Basin Cretaceous-age Mesaverde Group gas reservoirs are controlled by subsurface structures. Many, if not most, of the subsurface structures are controlled by basement fault trends.

These basement faults can be interpreted using an integrated interpretation of remote sensing imagery data (Landsat TM), airborne radar (SLAR), high-resolution aerial photography, gas and water production data, high-resolution aeromagnetic data, subsurface geologic information, and surficial fracture maps. This new interpretation demonstrates the importance of basement structures on the nucleation and development of overlying structures and associated natural fractures in the hydrocarbon-bearing section.

Parachute, Rulison, Divide Creek and Wolf Creek fields produce gas from fractured tight gas sand and coal reservoirs within the Mesaverde Group. Tectonic fracturing involving basement structures is responsible for development of economic permeability within the reservoirs. In this context, the significance of detecting natural fractures using the integrated fracture detection technique is critical to developing tight gas resources.

Remote sensing imagery analysis appears to provide a cost and time-effective method to locate regional structures and surficial manifestation of basement-controlled fracture systems. Confirmation and delineation of the internal reservoir-scale characteristics of the fracture systems can then be performed by the application of more expensive exploration methods in a greatly-reduced area of interest.

Integration of data from widely-available, relatively inexpensive sources such as high-resolution aeromagnetics, remote sensing imagery analysis and regional geologic syntheses provide excellent data sets to incorporate into an overall methodology for targeting fractured reservoirs. The ultimate application of this methodology is the development and calibration of a potent exploration tool to predict subsurface fractured reservoirs and target areas for exploration drilling, and infill and step-out development programs

ACKNOWLEDGEMENTS

The authors would like to acknowledge financial support for this paper and the associated Fractured Reservoir Detection Optimization project from the Department of Energy-Morgantown Energy Technology Center (DOE-METC contract DE-AC21-93MC30086). Royal Watts (DOE-METC) is thanked for project management and encouragement. Seismic data were obtained from Barrett Resources, our industry partner in the project. Special thanks to Terry Barrett for helpful discussions and generous cooperation. Seismic interpretation was by Stuart Squires (Advanced Resources International). The aeromagnetic survey was performed by World Geoscience, Houston, Texas. Linear features analysis of the Plateau and Shire Gulch fields was by Peter Blomquist (Advanced Resources International), production trend mapping in all fields was conducted by Grant Carnie (Advanced Resources International).

REFERENCES

1. Bredehoeft, J.D., Wolff, R.G., Keys, W.D., and Shuter, E., 1976, Hydraulic Fracturing to Determine the Regional In Situ Stress Field, Piceance Basin, Colorado, Geological Society of America Bulletin, 87 250-258.

2. Brown, C.A., Smagala, T.M., and Haefele, G.R., 1986, Southern Piceance Basin Model-Cozzette, Corcoran and Rollins Sandstones, In: Spencer, C.W. and Mast, R.F. eds., *Geology of Tight Gas Reservoirs*, AAPG Studies in Geology #24, 207-219.

3. Decker, A.D., Klawitter, A.L., Hoak, T.E., Kuuskraa, V.A., 1994, Development of an Exploration Strategy Designed for Identifying Regions Capable of High Gas Rates Utilizing the Open-Hole Cavitation Technique, SBIR Phase I-Final Report for DOE-METC SBIR Contract No. DE-FG03-93ER81502, 124 p.

4. Donnell, J R., Yeend, W.E., and Smith, M.C., 1984, Preliminary Geologic Map of the Mesa Quadrangle, Mesa County, Colorado, USGS MF-1698 map.

5. Eckert, A. D., 1982, The Geology and Seismology of the Dudley Gulch Graben and Related Faults, Piceance Creek Basin, Northwestern Colorado, Unpub. M.S. Thesis, Univ. of Colorado-Boulder 139 p.

6. Gries, R. R., 1983, Oil and Gas Prospecting Beneath Precambrian of Foreland Thrust Plates in Rocky Mountains, American Association of Petroleum Geologists Bulletin, 67 1-28.

7. Grout, M.A., 1990, Fracture History of the Southern Piceance Basin and Tectonic Development of Intrabasin Folds, Northeastern Colorado Plateau, Colorado, Unpub. Ph.D. Dissertation, Univ. of Colorado-Boulder 232 p.

8. Grout, M.A., Abrams, G.A., Tang, R.L., Hainsworth, T.J., Verbeek, E.R., 1991, Late Laramide Thrust-related and Evaporite-domed Anticlines in the Southern Piceance Basin, Northeastern Colorado Plateau, American Association of Petroleum Geologists Bulletin, 75 (2) 205-218.

9. Grout, M.A., and Verbeek, E.R., 1985, Fracture History of the Plateau Creek and Adjacent Colorado River Valleys, Southern Piceance Basin-Implications for Predicting Joint Patterns at Depth, U.S. Geological Survey Open File Report 85-744, 17 p.

10. Grout, M.A., and Verbeek, E.R., 1989, Prediction of Fracture Networks at Depth in Low-Permeability Reservoir Rocks, Piceance and Washakie Basins, Western U.S., American Association of Petroleum Geologists Bulletin, 73 (9) p. 1158

11. Gunneson, B., Wilson, M., and Labo, J., 1994, A structural history of the Divide Creek Anticline, Piceance Basin, Northwest Colorado, Poster Session, AAPG Annual Meeting, Spring 1994, p. 160.

12. Harper, M.L., 1964, Mechanics of Basement Deformation in Glenwood Canyon, Colorado, Unpub. Ph.D. Dissertation, Univ. of Colorado-Boulder 102 p

13. Johnson, R.C., and Nuccio, V.C., 1986, Structural and Thermal History of the Piceance Creek Basin, Western Colorado, in Relation to Hydrocarbon Occurrence in the Mesaverde Group, In: Spencer, C.W. and Mast, R.F. eds., *Geology of Tight Gas Reservoirs*, AAPG Studies in Geology #24, 165-205.

14. Johnson, R.C., and Finn, T.M., 1986, Cretaceous Through Holocene History of the Douglas Creek Arch, Colorado and Utah, In: D.S. Stone, ed., *New Interpretations Northwest Colorado*, Rocky Mountain Association of Geologists Publication, 77-98.

15. Lorenz, J., 1985, Predictions of Size and Orientation of Lenticular Reservoirs in the Mesaverde Group, Northwestern Colorado, Society of Petroleum Engineers SPE/DOE 13851, In: Proceedings of the 1985 SPE/DOE Joint Symposium on Low Permeability Reservoirs, 23-28.

16. Lorenz, J., Warpinski, N.R., Teufel, L., Branagan, P. T., Sattler, A.R., and Northrop, D.A., 1988, Results of the Multiwell Experiment, EOS (Transactions of the American Geophysical Union) v. 69 (35), 817, 825-826

17. Lorenz, J. C., Teufel, L. E., and Warpinski, N. R., 1991, Regional Fractures II: Fracturing of Mesaverde reservoirs in the Piceance Basin, American Association of Petroleum Geologists Bulletin, 75, 1738-1757.

18. Lorenz, J., Teufel, L., and Teufel, N., 1991, Regional Fractures I: A mechanism for the formation of regional fractures at depth in flat-lying reservoirs, American Association of Petroleum Geologists Bulletin, 75, 1714-1737.

19. Murray, F.N., 1966, Stratigraphy and Structural Geology of the Grand Hogback Monocline, Colorado, Unpub. Ph.D. Dissertation, Univ. of Colorado-Boulder, 218 p.

20. Osmond, J.C., 1986, Petroleum Geology of the Uinta Mountains-White River Uplift, Colorado and Utah, In: D.S. Stone, ed., *New Interpretations Northwest Colorado*, Rocky Mountain Association of Geologists Publication, 213-222.

21. Peterson, R.E., 1984, Geological and Production Characteristics of the Nonmarine Part of the Mesaverde Group, Rulison Field Area, Piceance Basin, CO, SPE/DOE/GRI Joint Symposium on Unconventional Gas Recovery, SPE 12835, 47-56.

22. Poole, F.G., 1955, Geology of the Grand Hogback Area, Garfield and Pitkin Counties, Colorado, Unpublished M.S. Thesis, Univ. of Colorado-Boulder 128 p.

23. Reinecke, K. M., Rice, D. D. and Johnson, R. C., 1991, Characteristics and Development of Fluvial

Sandstone and Coalbed Reservoirs of Upper Cretaceous Mesaverde Group, Grand Valley, Colorado, In: *Coalbed Methane*, Rocky Mountain Association of Geologists Publication, 209-225.

24. Richard, J.J., 1986, Interpretation of a Seismic Section Across the Danforth Hills Anticline (Maudlin Gulch) and Axial Arch in Northwest Colorado, In: D.S. Stone, ed., *New Interpretations Northwest Colorado*, Rocky Mountain Association of Geologists Publication, 183-190.

25. Sattler, A.R., Raible, C.J., and Gall, B.R., 1985, Integration of Laboratory and Field Data for Insight on the Multiwell Experiment Paludal Simulation, SPE/DOE 1985 Low Permeability Gas Reservoirs, SPE 13891, 397-409.

26. Stone, D.S., 1986, Geology of the Wilson Creek Field, Rio Blanco County, Colorado, In: D.S. Stone, ed., *New Interpretations Northwest Colorado*, Rocky Mountain Association of Geologists Publication, 229-246.

27. Tweto, O., 1975, Laramide (Late Cretaceous-Early Tertiary) Orogeny in the Southern Rocky Mountains, In: B.F. Curtis, ed., *Cenozoic History of the Southern Rocky Mountains*, Geological Society of America Memoir, 144, 1-44.

28. Tweto, O., 1980, Tectonic History of Colorado, In: H.C. Kent and K.W. Porter, eds., *Colorado Geology*, Rocky Mountain Association of Geologists, 5-9.

29. Waechter, N.B., Johnson, W.E., 1986, Pennsylvanian-Permian Paleostructure and Stratigraphy as Interpreted From Seismic Data in the Piceance Basin, Northwest Colorado, In: *New Interpretations Northwest Colorado*, Rocky Mountain Association of Geologists Publication, 51-64

30. Warner, D.L., Mancos-Mesaverde (Upper Cretaceous) Intertonguing Relations, Southeast Piceance Basin, Colorado, American Association of Petroleum Geologists Bulletin, 48 (7) 1091-1107.

31. Zapp, A.D., and Cobban, W.A., 1960, Some Late Cretaceous Strand Lines in Northwestern Colorado and Northeastern Utah, USGS Geological Survey Research-Short Papers in the Geological Sciences, B246-B249.

FIGURE 1

SELECTED CRETACEOUS GAS FIELDS AND BASIN LOCATION MAP

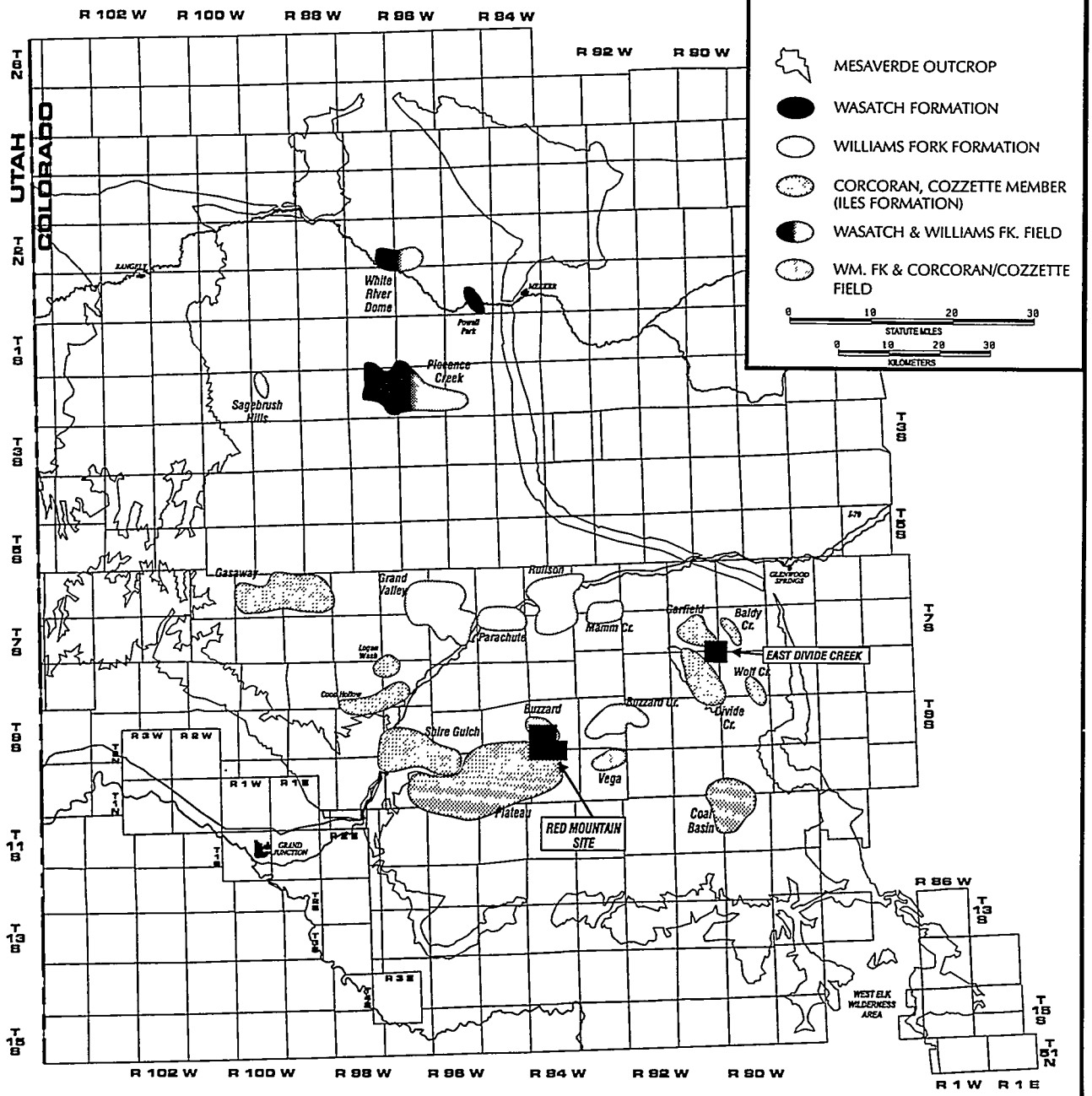


FIGURE 2A

RELATIONSHIP BETWEEN STRUCTURE AND PRODUCTION
Grand Valley, Parachute and Rulison Fields, Piceance Basin

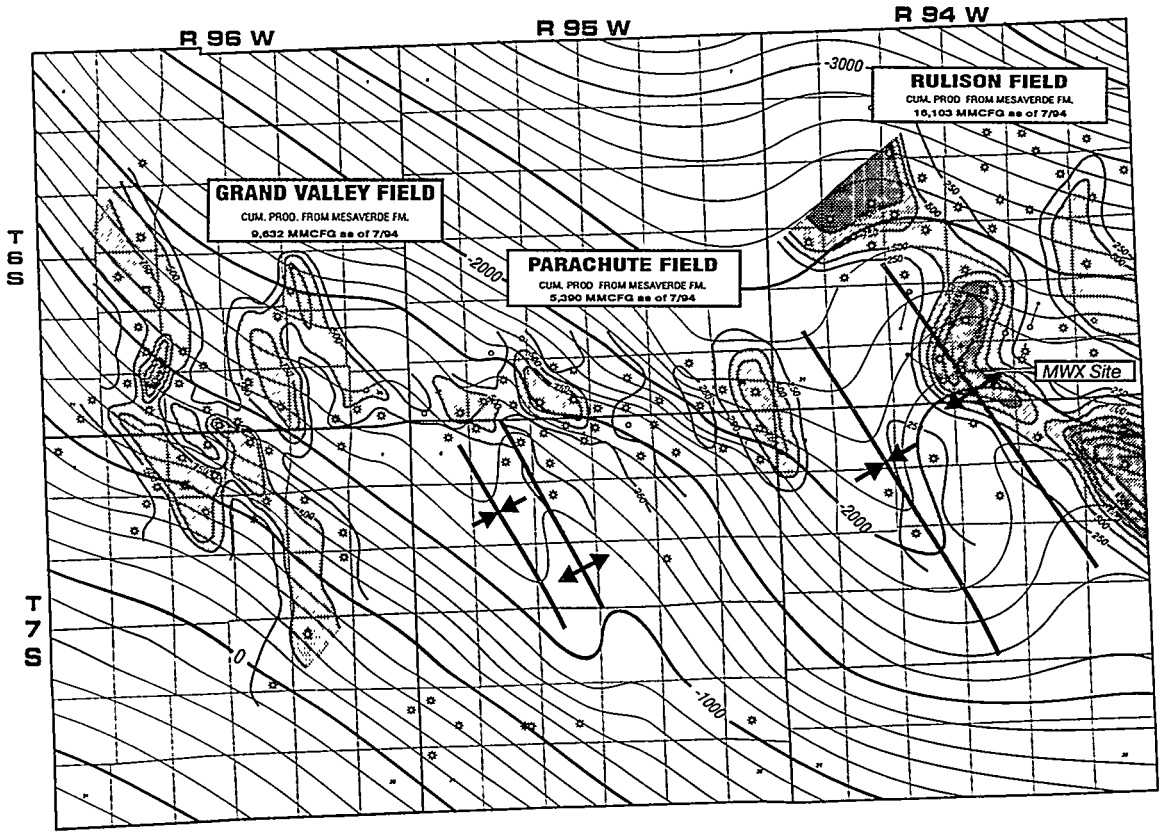
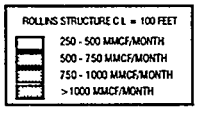
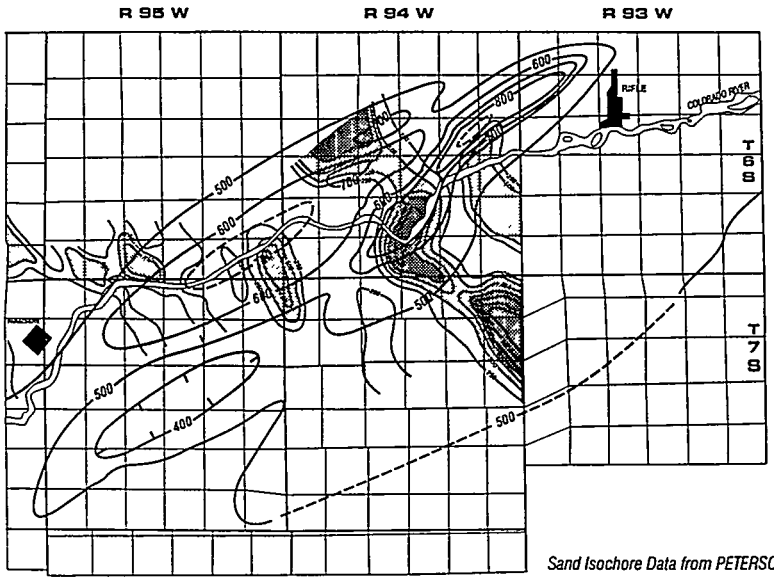


FIGURE 2B

PARACHUTE - RULISON FIELD
Sand Isochore and Production Relationship

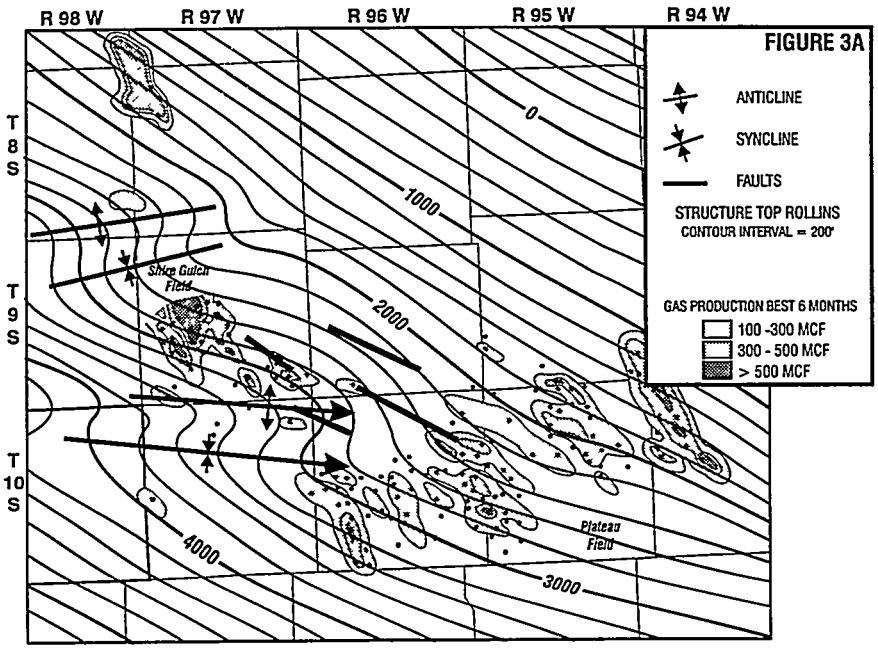
BEST 6 MONTHS PRODUCTION OF THE MESAVERDE FM
(Upper/ Middle Williams Fork and Cameo Sand)



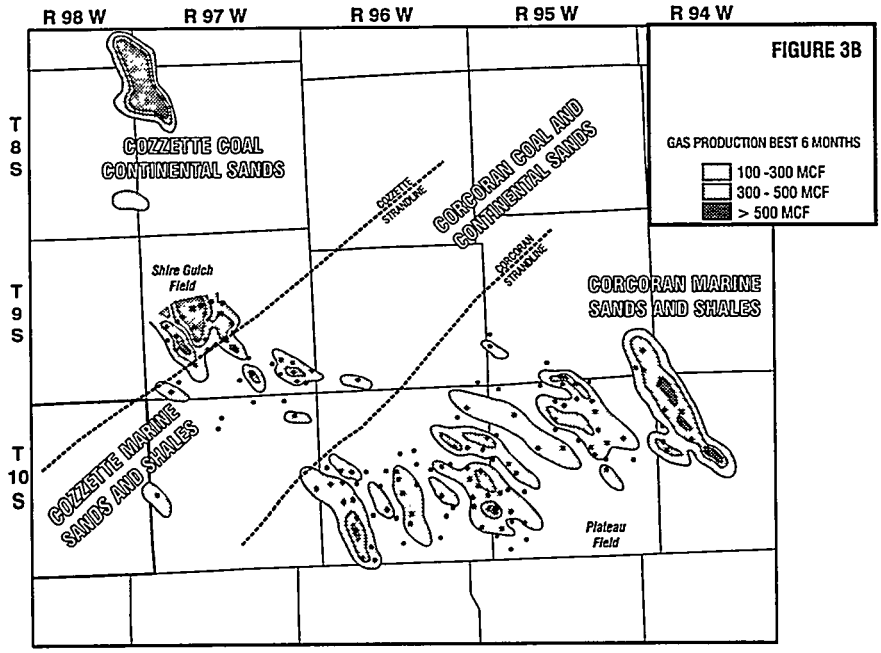


Sand Isochore Data from PETERSON, 1984

PLATEAU - SHIRE GULCH RELATIONSHIP BETWEEN STRUCTURE AND PRODUCTION



PLATEAU - SHIRE GULCH RELATIONSHIP BETWEEN STRATIGRAPHY AND PRODUCTION



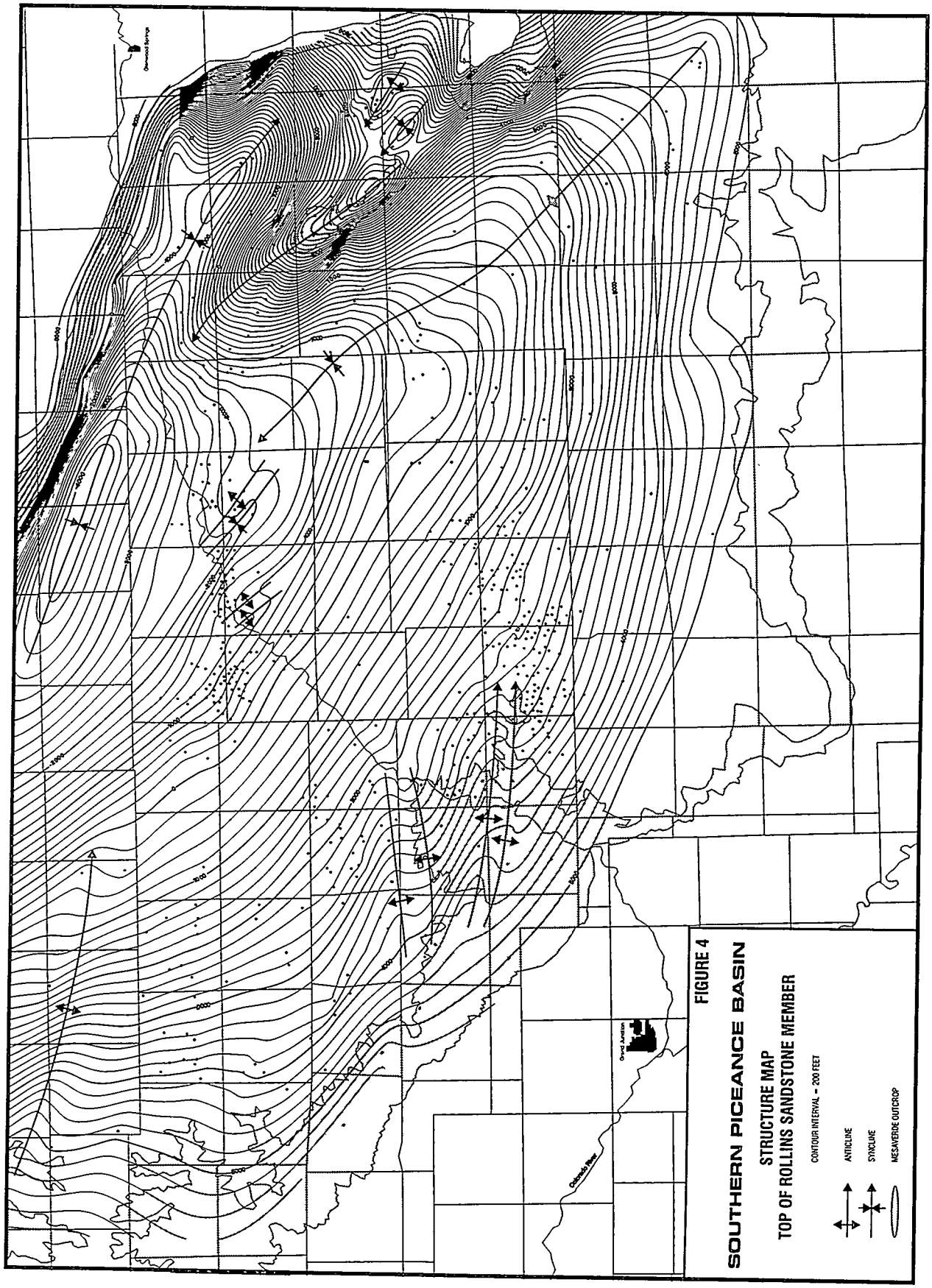

FIGURE 4
SOUTHERN PICEANCE BASIN
STRUCTURE MAP
TOP OF ROLLINS SANDSTONE MEMBER
CONTOUR INTERVAL = 200 FEET
ANTICLINE
SYNCLINE
MESAVERDE OUTCROP

FIGURE 5

PICEANCE BASIN TECTONIC EVOLUTION

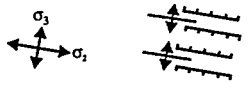
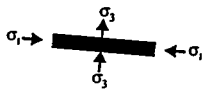
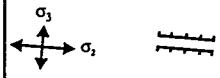
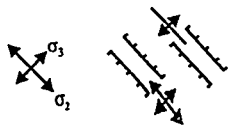
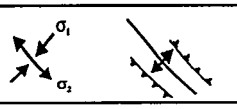
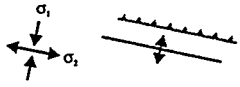
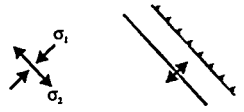
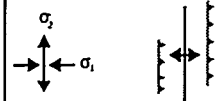
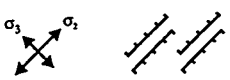
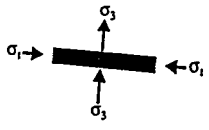
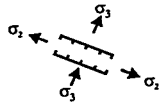
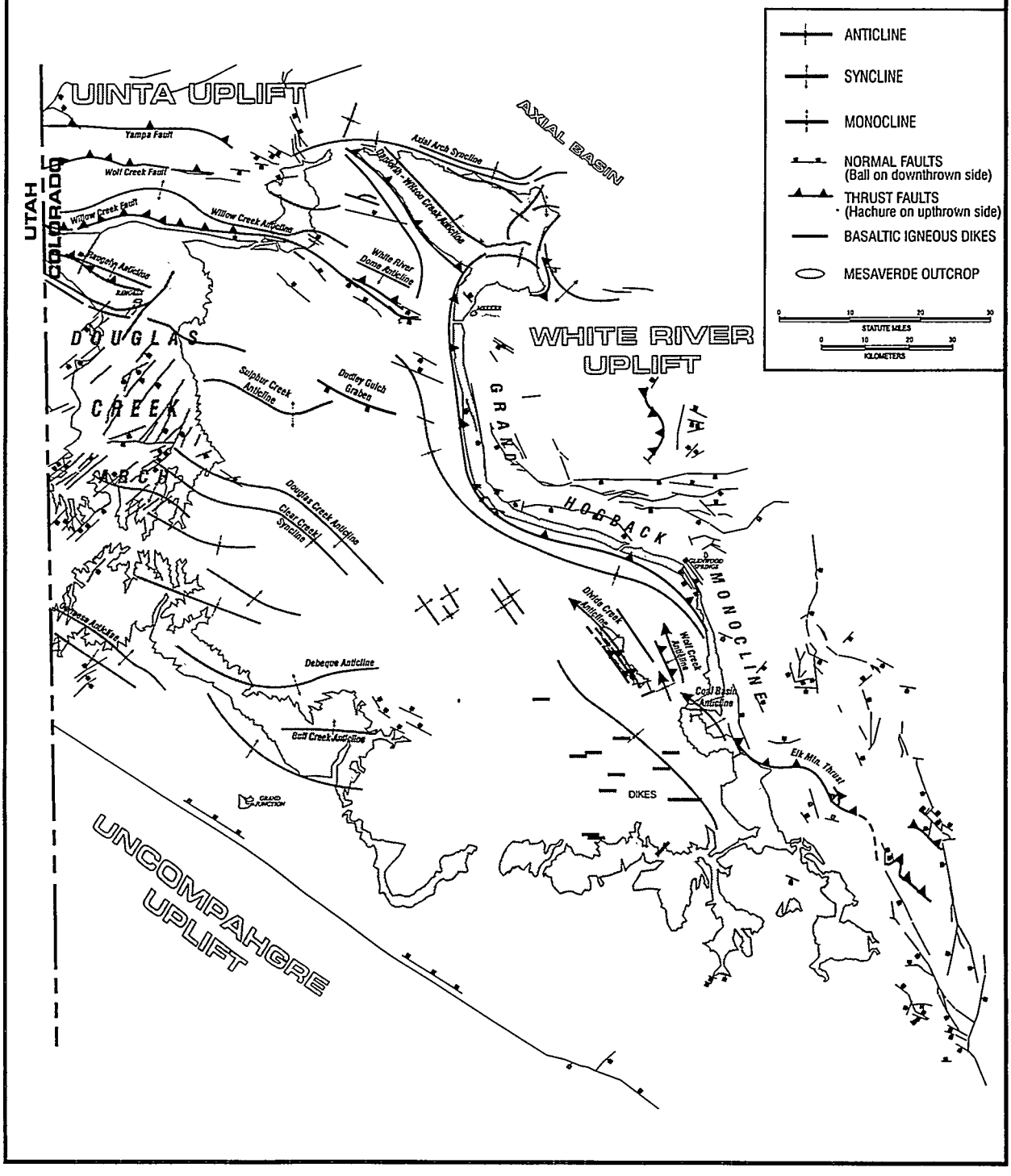
M.Y.A.	AGE	STRESS REGIME	STRUCTURES	REFERENCES
	PRECAMBRIAN		Uncompahgre Uplift elements Horsts, grabens, forced folds	Tewksburry, 1989 Tweto, 1980 Heyman et al., 1986
	CAMBRIAN		Basaltic dikes along N. Uncompahgre	Tweto et al., (map) 1976
	MISS.		Block faulting	Landis and Tschauder, 1990
	PENNSYLVANIAN		Horsts, grabens, forced folds Hogback Paleohorst (Des Moines and Morrowan-age)	De Voto et al., 1986 Waechter & Johnson, 1986
	LATE PERMIAN		Thrust inversion along older horsts (SW Uncompahgre and Eagle Basin)	De Voto et al., 1986 Waechter & Johnson, 1986
65 57.8	LATE CRETACEOUS -PALEOCENE		Uinta Uplift Rangely Anticline Uncompahgre Uplift White River Dome	Osmond, 1986; Hansen, 1986 Richard, 1986 Tweto, 1975 Quigley, 1965
	EARLY - MID EOCENE		White River Uplift, Grand Hogback Divide Creek Anticline Elk Mountain Thrust, Wilson Creek Anticline, Axial Arch Mesaverde maximum burial Lake Uinta formed-oil shale deposited	Johnson & Nuccio, 1986 Richard, 1986 Bryant, 1966 Stone, 1986 Johnson, 1987
36.6	LATE EOCENE EARLY OLIGOCENE		Douglas Creek Arch Piceance Creek Dome	Osmond, 1986 Johnson & Nuccio, 1986 Tweto, 1975; Johnson, 1987
	MID-LATE OLIGOCENE		NE-trending faults on Douglas Creek Arch SE basin volcanics commence	Johnson & Finn, 1986
23.7	MIOCENE-PLIOCENE		Basaltic dikes in SE basin 10 Ma - Colorado River downcutting and Basin-wide unconformity 9.7 Ma - Grand Mesa Basalt	Tweto, Muench & Reed, 1978 Osmond, 1986 Johnson, 1987
5.3	PLIOCENE-PLEISTOCENE		Dudley Gulch Graben White River Graben Debeque Anticline Bull Creek Anticline	Eckert, 1982 Johnson & Nuccio, 1986
0.01	HOLOCENE		Volcanics in SE basin (4,150 years ago) N 70° W hydraulic fracture stimulations N 50°-70° W breakouts in central basin	Giegengack, 1962 Bredehoeft et al., 1976 Industry sources

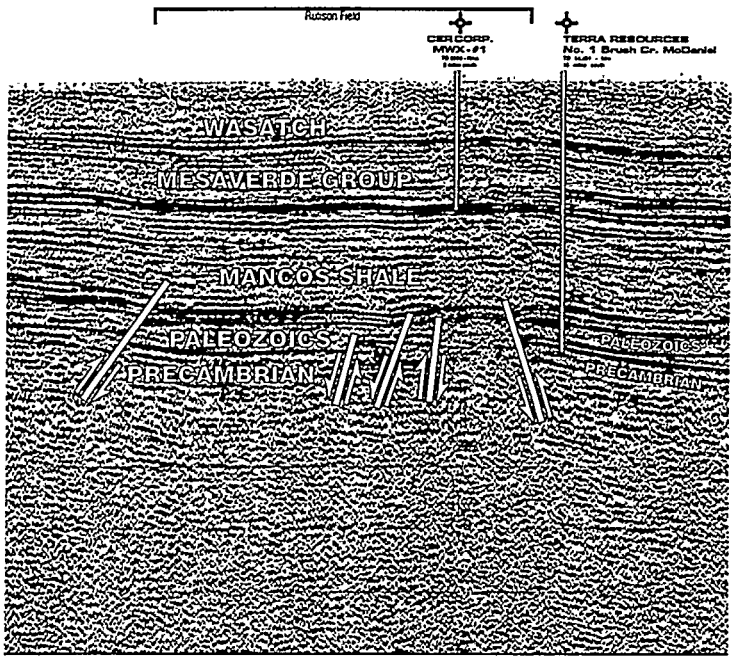
FIGURE 6

TECTONIC MAP
PICEANCE BASIN, WESTERN COLORADO

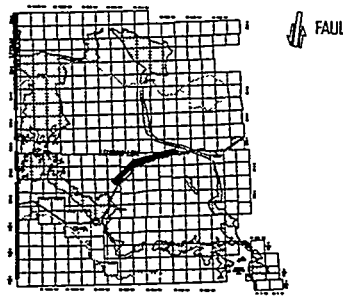


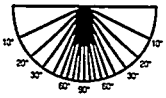
BASEMENT STRUCTURE BELOW RULISON FIELD

FIGURE 7



Modified after WAECHTER and JOHNSON, 1985





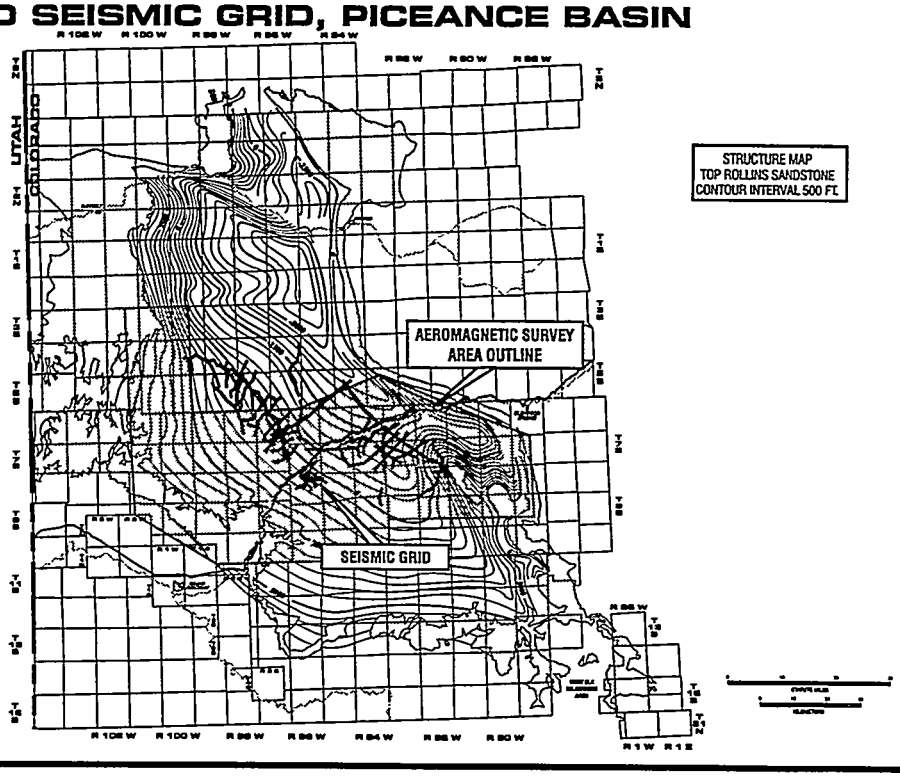


Approximate Vertical Exaggeration
2.4 at 2 Seconds

NOTE: Some Pennsylvanian-Permian normal faults were reactivated during Laramide contraction as thrusts.

AEROMAGNETIC SURVEY AREA AND SEISMIC GRID, PICEANCE BASIN

FIGURE 8



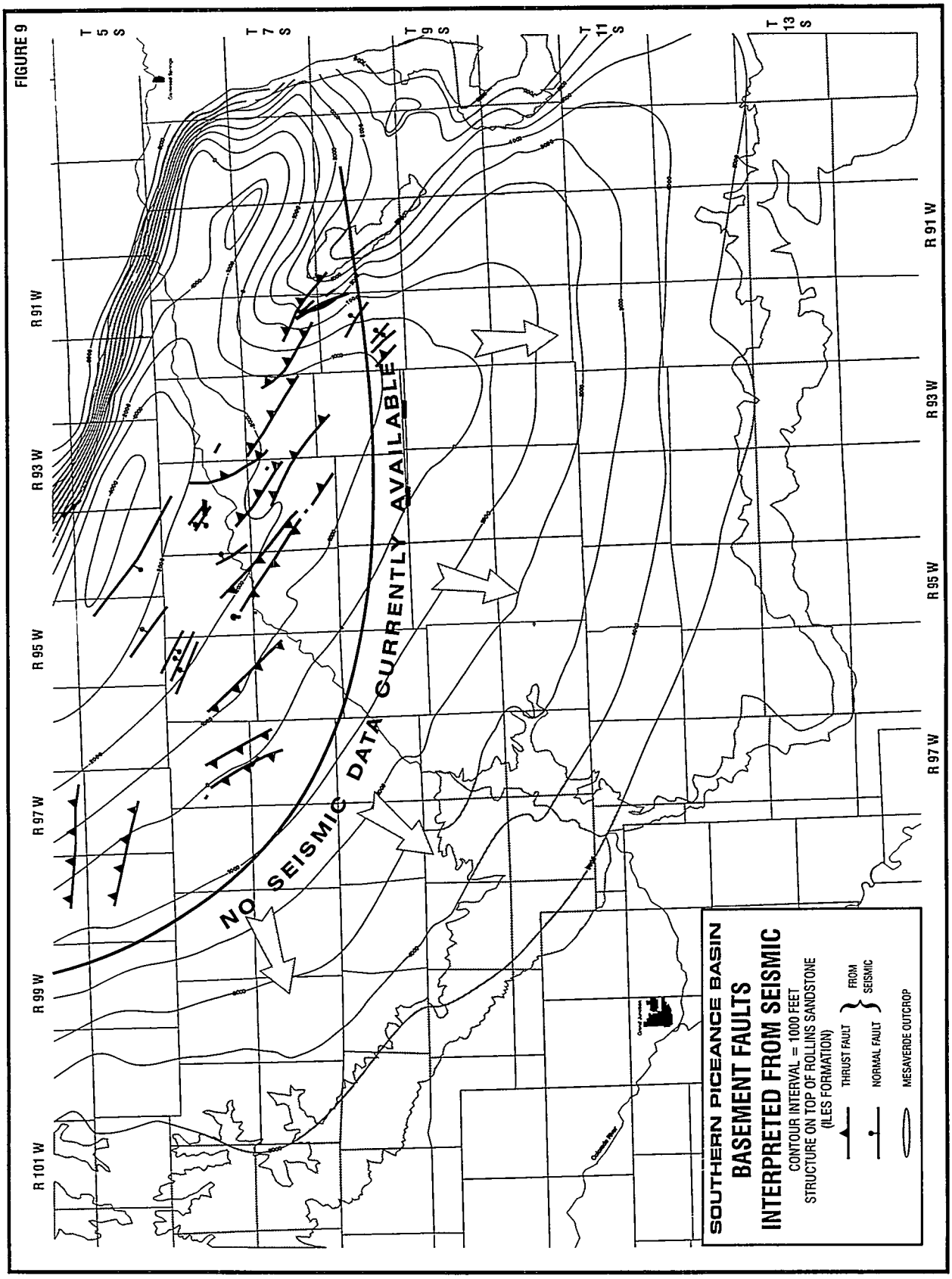

FIGURE 9
T 5 S
T 7 S
T 9 S
T 11 S
T 13 S
R 101 W
R 99 W
R 97 W
R 95 W
R 93 W
R 91 W
NO SEISMIC DATA CURRENTLY AVAILABLE
SOUTHERN PICEANCE BASIN
BASEMENT FAULTS
INTERPRETED FROM SEISMIC
CONTOUR INTERVAL = 1000 FEET
STRUCTURE ON TOP OF ROLLINS SANDSTONE
(ILES FORMATION)
THRUST FAULT
NORMAL FAULT
FROM SEISMIC
MESAVERDE OUTCROP

FIGURE 10

NURE REGIONAL RESIDUAL MAGNETIC INTENSITY

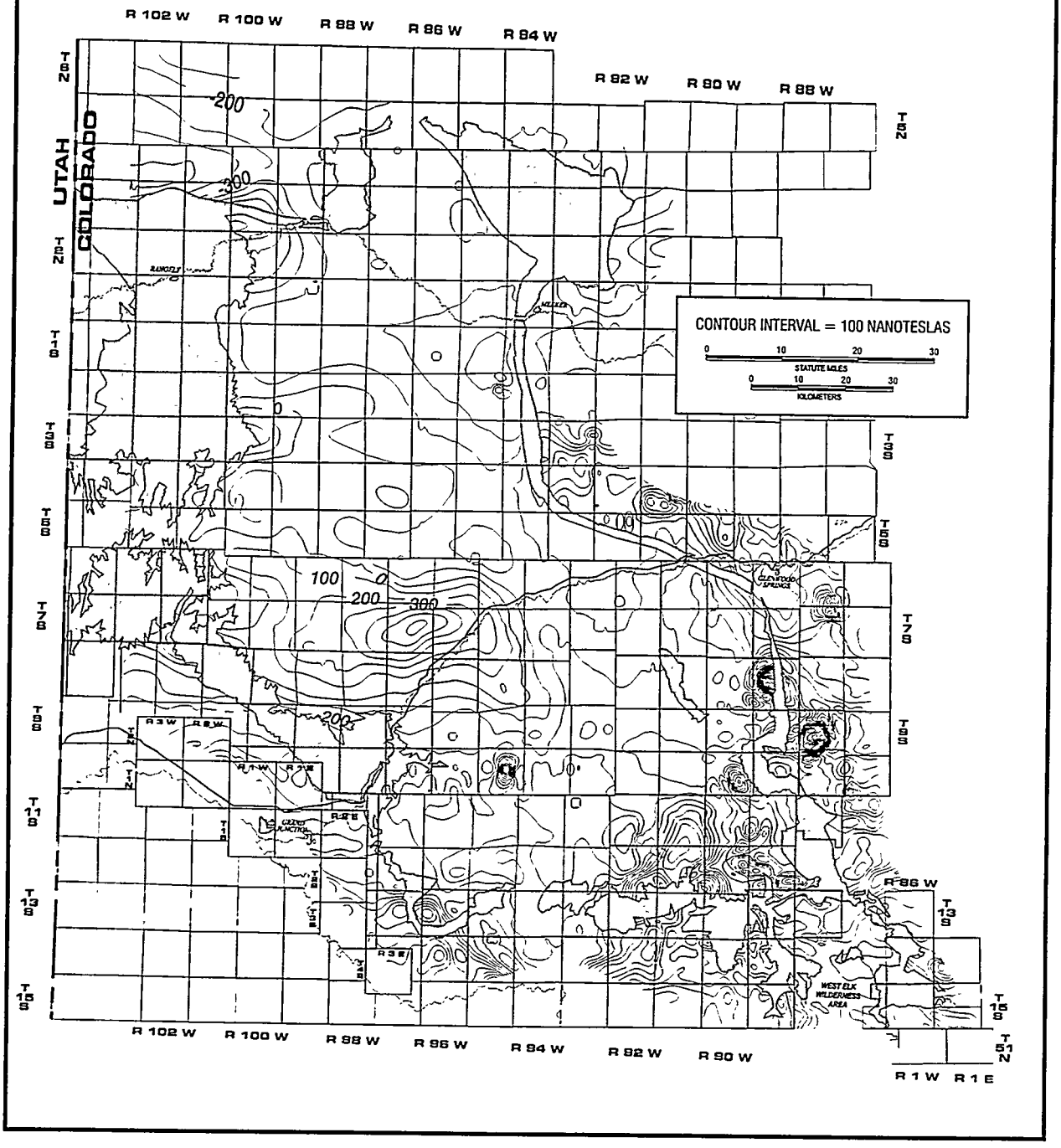


FIGURE 11

REGIONAL HIGH-RESOLUTION TOTAL FIELD MAGNETIC INTENSITY WITH INTERPRETED FEATURES

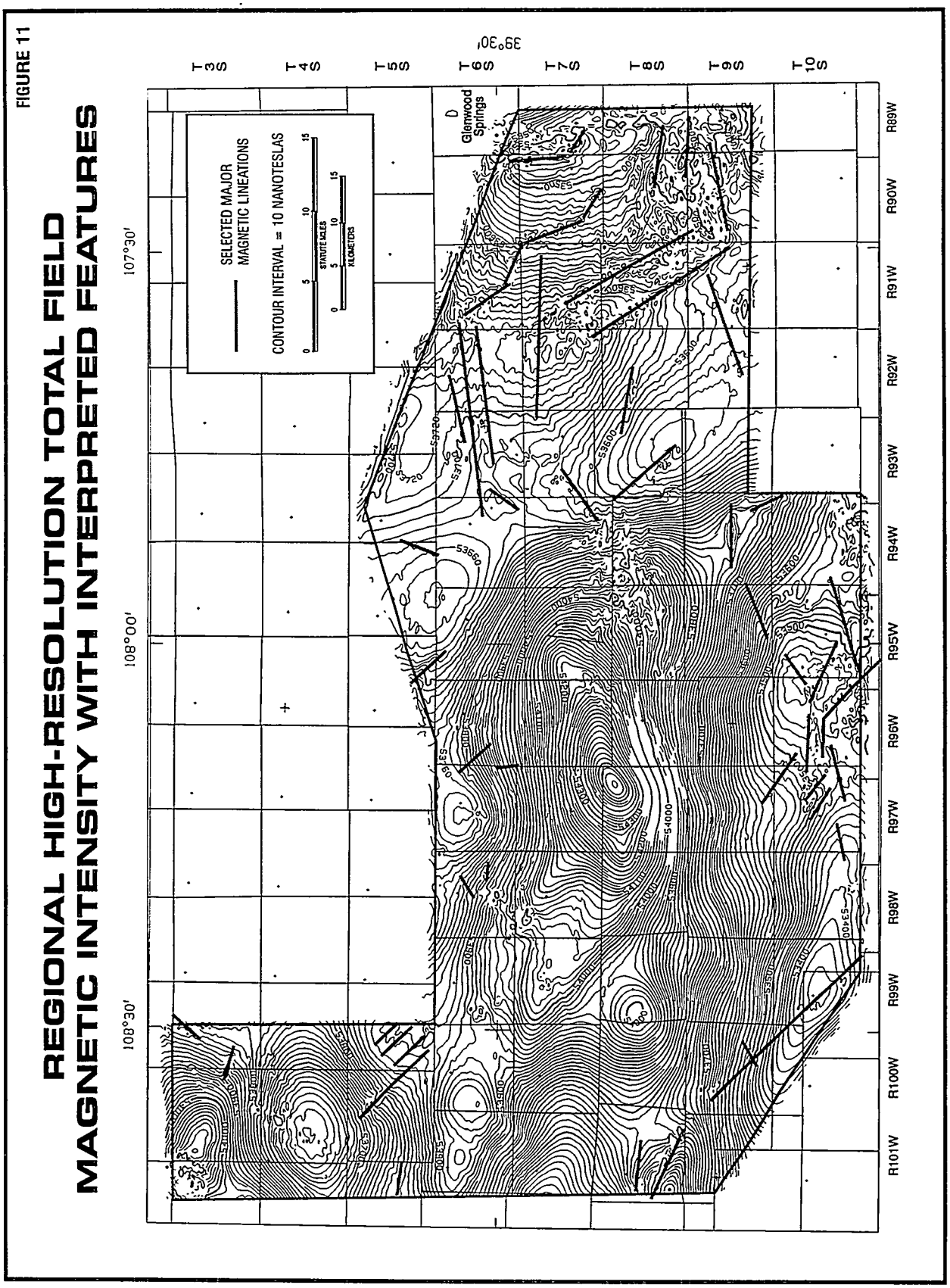
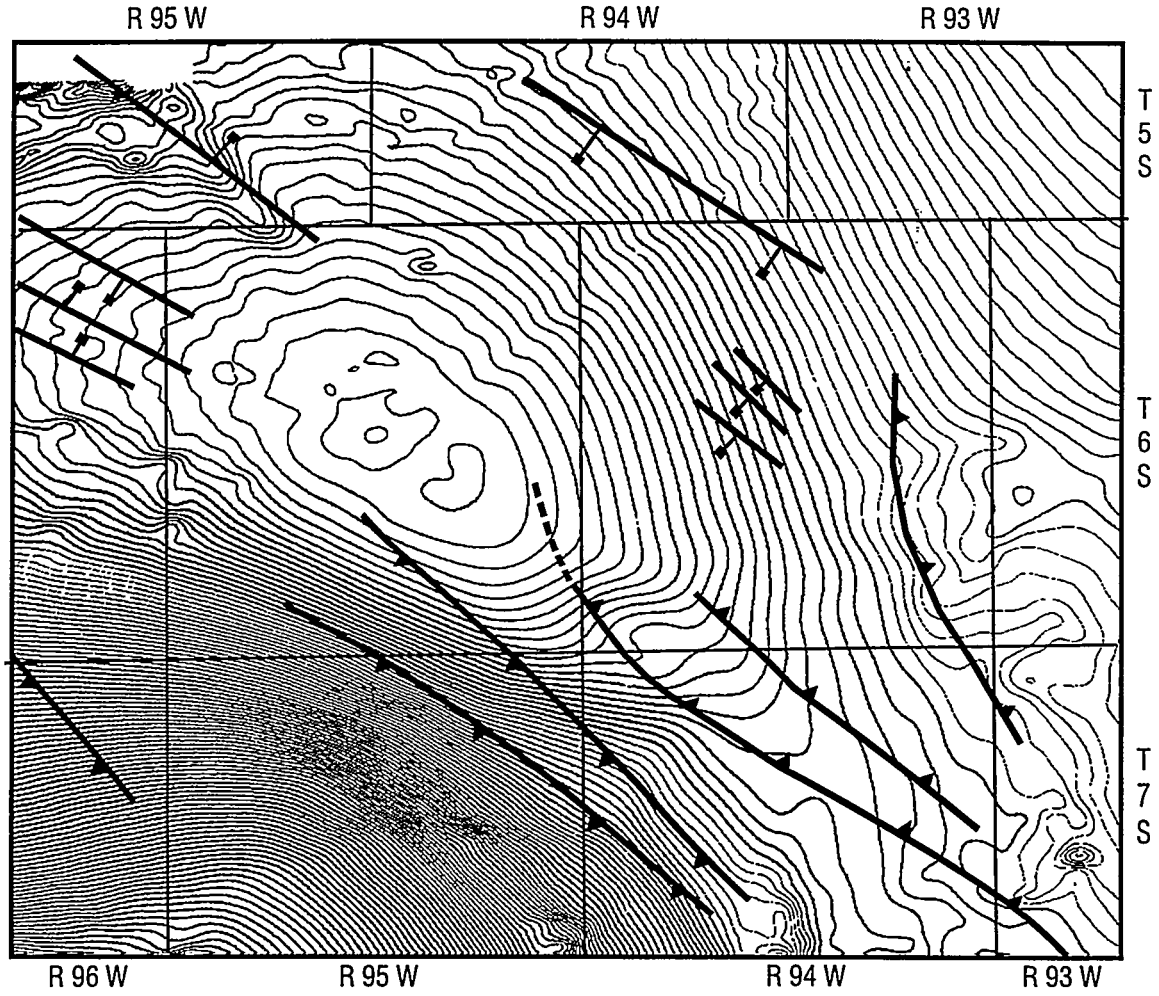


FIGURE 12

AEROMAGNETIC STRUCTURE RULISON ANTICLINE AREA



Total Field Magnetic Intensity
Contour Interval = 5 nanoteslas

BASEMENT FAULTS FROM SEISMIC

THRUST FAULT (hachure on upper plate)

NORMAL FAULT (tick on downthrown block)

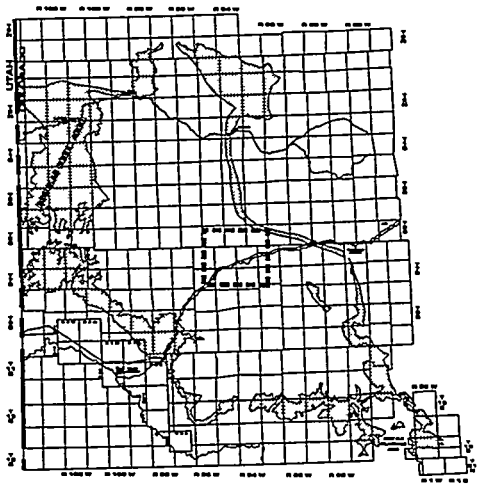
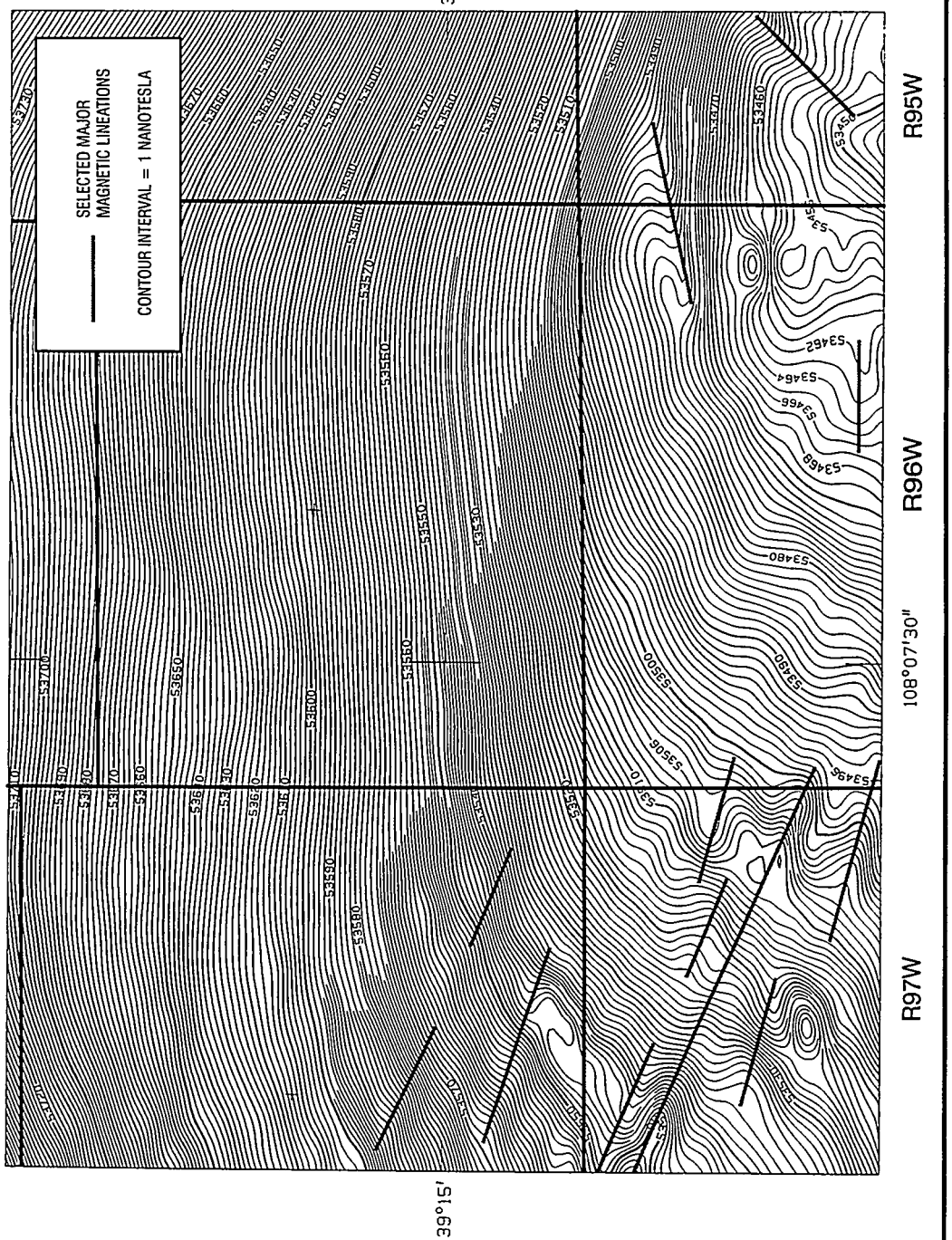


FIGURE 13

HIGH-RESOLUTION REDUCED-TO-POLE MAGNETIC INTENSITY WITH INTERPRETED FEATURES OF PLATEAU-SHIRE GULCH AREA



PLATEAU - SHIRE GULCH
RELATIONSHIP BETWEEN INTERPRETED THEMATIC MAPPER LINEARS AND STRUCTURE

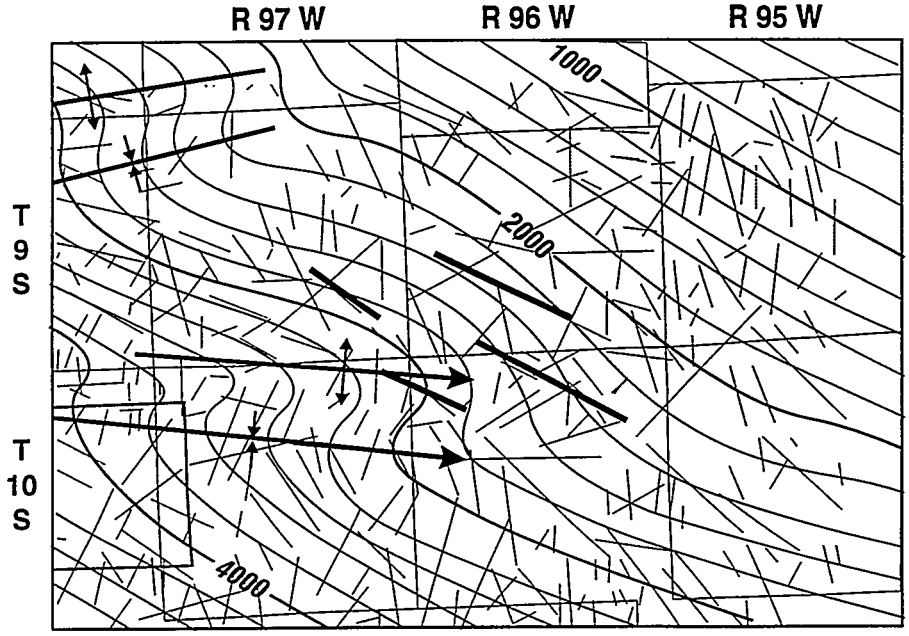


FIGURE 14

ANTICLINE
SYNCLINE
FAULTS
LINEAR FEATURES INTERPRETED FROM THEMATIC MAPPER

STRUCTURE TOP ROLLINS
CONTOUR INTERVAL = 200'

PLATEAU - SHIRE GULCH
RELATIONSHIP BETWEEN INTERPRETED THEMATIC MAPPER LINEARS AND PRODUCTION

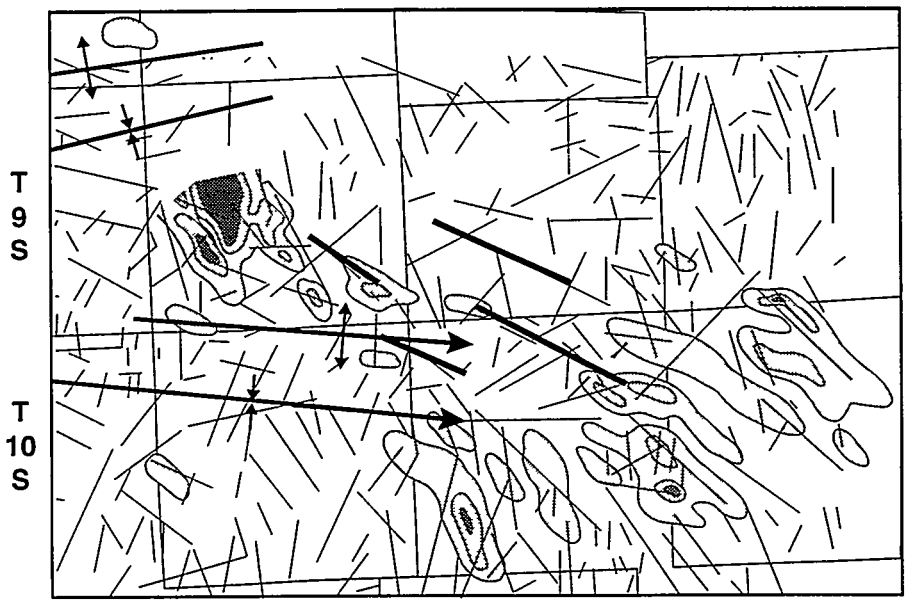


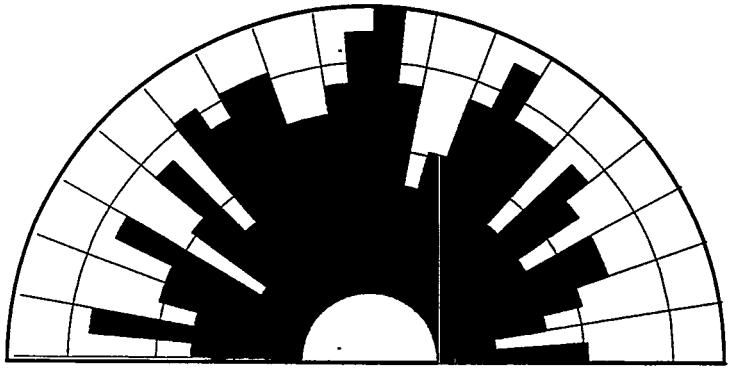
FIGURE 15

ANTICLINE
SYNCLINE
FAULTS
LINEAR FEATURES INTERPRETED FROM THEMATIC MAPPER

DAILY GAS PRODUCTION
BEST 6 MONTHS / TOTAL DAYS PRODUCED
100 - 300 MCF
300 - 500 MCF
> 500 MCF

FIGURE 16

PLATEAU - SHIRE GULCH
INTERPRETED LINEAR FEATURES FROM THEMATIC MAPPER (TM) DATA



Unweighted Frequency

N = 144

PLATEAU - SHIRE GULCH
N 90 W - N 45 W INTERPRETED THEMATIC MAPPER LINEARS AND PRODUCTION

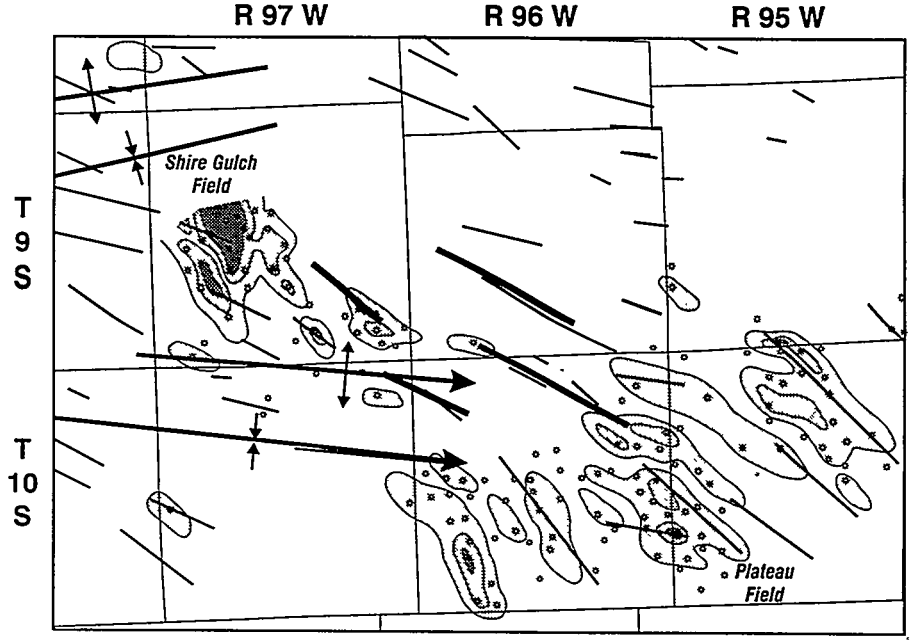


FIGURE 17

ANTICLINE

SYNCLINE

FAULTS

LINEAR FEATURES INTERPRETED FROM THEMATIC MAPPER

DAILY GAS PRODUCTION
BEST 6 MONTHS / TOTAL DAYS PRODUCED

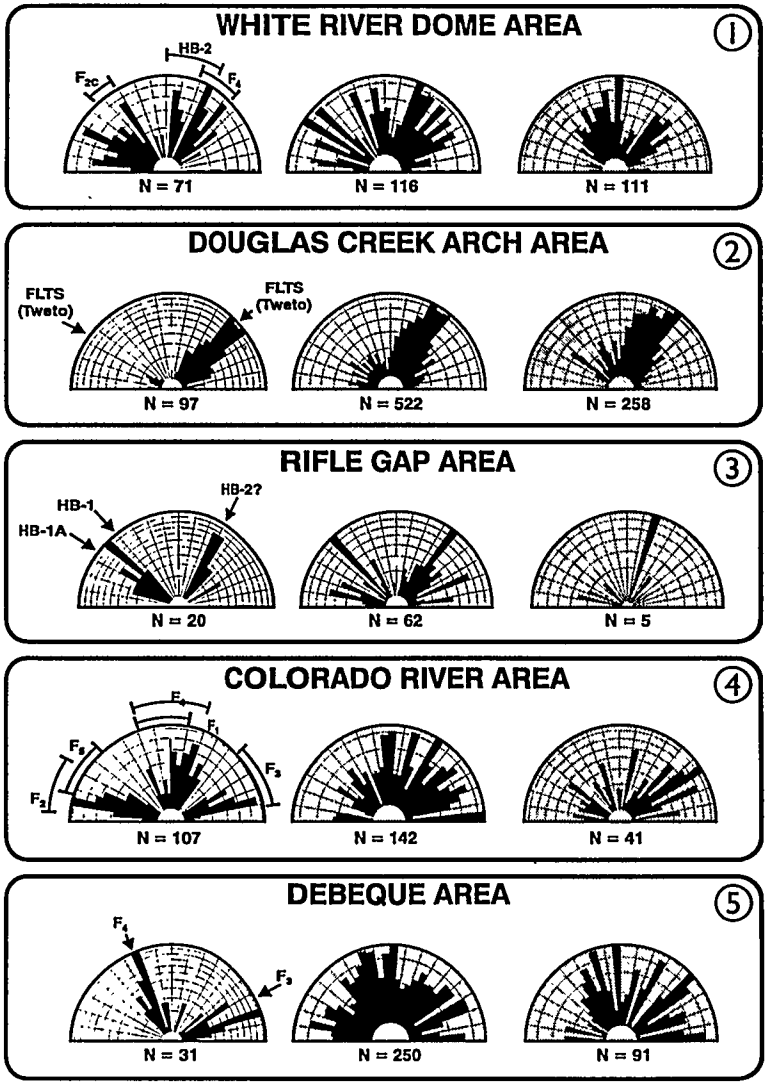
100 - 300 MCF

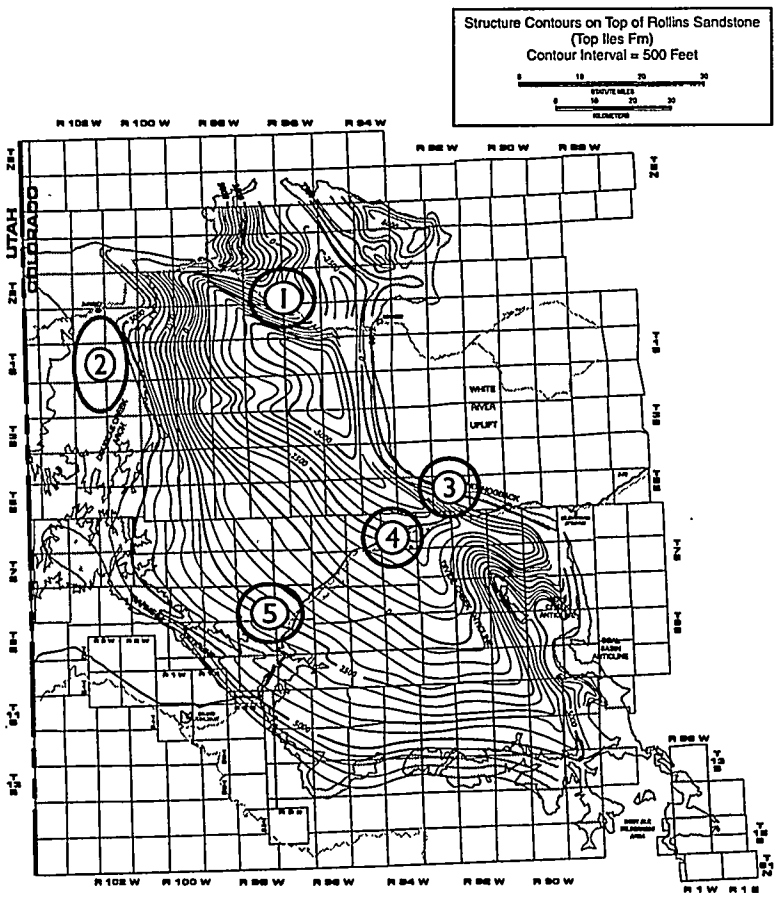
300 - 500 MCF

> 500 MCF

FIGURE 18

COMPARISON OF LINEAR FEATURE ORIENTATIONS INTERPRETED FROM IMAGERY TO MAPPED JOINTS AND FAULTS - PICEANCE BASIN





MEASURED JOINT ORIENTATIONS FROM PUBLISHED SOURCES (GROUT, 1990)

LINEAR FEATURE ORIENTATIONS FROM LANDSAT THEMATIC MAPPER (TM) ADVANCED RESOURCES INTERNATIONAL

LINEAR FEATURE ORIENTATIONS FROM SIDE-LOOKING AIRBORNE RADAR (SLAR) ADVANCED RESOURCES INTERNATIONAL



NOTES

INTERGAS '95

May 15-19, 1995
The University of Alabama
Tuscaloosa, Alabama USA

9516

Gas- and Water-Saturated Conditions in the Piceance Basin, Western Colorado: Implications for Fractured Reservoir Detection in a Gas-Centered Coal Basin

T.E. Hoak and A.D. Decker,
Advanced Resources International, Inc.

ABSTRACT

Mesaverde Group reservoirs in the Piceance Basin, Western Colorado contain a large reservoir base. Attempts to exploit this resource base are stymied by low permeability reservoir conditions. The presence of abundant natural fracture systems throughout this basin, however, does permit economic production. Substantial production is associated with fractured reservoirs in Divide Creek, Piceance Creek, Wolf Creek, White River Dome, Plateau, Shire Gulch, Grand Valley, Parachute and Rulison fields. Successful Piceance Basin gas production requires detailed information about fracture networks and subsurface gas and water distribution in an overall gas-centered basin geometry. Assessment of these three parameters requires an integrated basin analysis incorporating conventional subsurface geology, seismic data, remote sensing imagery analysis, and an analysis of regional tectonics.

To delineate the gas-centered basin geometry in the Piceance Basin, a regional cross-section spanning the basin was constructed using hydrocarbon and gamma radiation logs. The resultant hybrid logs were used for stratigraphic correlations in addition to outlining the trans-basin gas-saturated conditions. Mud weight, DST and bottomhole pressure data show that the present-day overpressured zone in the basin is concentrated within Williams Fork fluvial sandstones overlying the Cameo Coal section. The basin overpressured zone corresponds to the area where the maximum vitrinite reflectance is greater than 0.9. In this same area, the marine Iles Formation sandstones (Rollins, Cozzette and Corcoran) also exhibit overpressured conditions although the magnitude of the overpressure is less than in the overlying fluvial and paludal sections. The magnitude of both pressure gradients (paludal and marine intervals) is greater than can be generated by a hydrodynamic model.

To extend cross-sectional observations laterally into the third dimension, gas and water production data were used to evaluate gas and water-saturated areas throughout the basin. Several structurally positive areas (Divide Creek Anticline, Bull Creek Anticline) are breached to meteoric influx and are water-saturated. The Corcoran and Cozzette are largely gas-saturated, however, breached conditions are locally present for the Corcoran in the western basin. The Cozzette Member shows complex water-gas saturated conditions in the transitional area between the water-saturated eastern basin and gas producing horizons in the western region.

To investigate the relationships between structure and production, detailed mapping of the basin (top of the Iles Formation) was used to define subtle subsurface structures that control fractured reservoir development. The most productive fields in the basin possess fractured reservoirs. Detailed studies in the Grand Valley-Parachute-Rulison and Shire Gulch-Plateau fields indicate that zones of maximum structural flexure on kilometer-scale structural features are directly related to areas of enhanced production. These smaller structures, common throughout the basin, represent excellent targets for additional field development because most larger structures in the basin have been extensively drilled.

INTRODUCTION

The following paper describes part of a multi-year fracture detection program calibrated using the Piceance Basin (see Figure 1 for location map) sponsored by the Department of Energy. Initial efforts have identified gas and water-saturated intervals in the Piceance Basin and the relationship between basement structure and production from fractured tight gas reservoirs. The fracture detection program is an integrated study involving detailed geologic characterization of the basin. To geologically characterize the basin, remote sensing imagery analysis, 2D seismic interpretation and newly-acquired, high-resolution, aeromagnetic data have been synthesized with a detailed tectonic/structural analysis to identify zones of enhanced fracturing. Production analyses of the larger gas fields in the basin have been performed to document the presence of fractured reservoir conditions. A parallel effort to numerically model the fracture genesis of the basin is being conducted at Indiana University by Dr. Peter Ortoleva using a self-consistent, reaction-transport forward model. In this model, an initial protolith is progressively varied using mathematically-consistent reaction equations to generate the final geologic characteristics observed in the basin. The results from these two efforts will be used to identify areas predicted to be contain fractured zones. In these areas, a 3D multi-component survey will be acquired, processed, and interpreted to more fully characerize subsurface fracture geometries in advanced of drilling. Barrett Resources will drill or recomplete several wells to verify the results of the 3D survey, the geologic predictions and the predictions of the numerical model.

This paper delineates the location of gas and water-saturated areas in order to establish the geometry of the gas saturated zone and the controls on production throughout the

basin. The geometry of the gas and water-saturated areas is critical because it permits operators to avoid water-prone fractured areas and also provides insight into the basin hydrodynamics and the relationship between hydrodynamics and production. Knowledge of gas-saturated areas permits operators to develop exploration strategies to maximize production from these areas and restrict their prospect generation efforts to areas most likely to contain gas. A more complete integration of production, remote sensing, aeromagnetic, seismic and regional tectonic syntheses is provided in a companion paper (Hoak and Klawitter, this volume).

BASIN OVERVIEW

The Piceance Basin is an elongate, NNW-trending structurally-downwarped region that formed as a result of Laramide contractional tectonics (See Figure 2 for basin structure map). The northern boundary of the basin is defined by the thrust-cored structures of the Axial Arch and the Uinta Uplift. The sinuous eastern margin is formed by the "S"-shaped thrust-cored, Grand Hogback Anticline lying along the flank of the White River Uplift. The western boundary, formed by the Douglas Creek Arch, separates the Uinta Basin from the Piceance basin. The southwestern boundary is formed by the Uncompahgre Uplift. The southern boundary is formed by the Gunnison Uplift and the West Elk Mountains in the southeast basin. All of these uplifts have experienced multiple phases of tectonic deformation ranging from Precambrian tectonism through Pennsylvanian-Permian deformation, culminating in the Laramide thrusting that defines the present-day basin geometry.

Three dominant regional structural trends persist throughout the basin. In the eastern basin, the NW-trending Divide Creek, Wolf Creek and Coal Basin anticlines have been formed by WSW-directed thrusting. In the western basin, several broad, low amplitude anticlines have formed with dominant E/W trends. These anticlines include the Debeque, Unnamed (here designated Bull Creek Anticline, located to the south of the Debeque anticline in Plateau Field) and the Douglas Creek Anticline. The latter anticline has a WNW trend. The northern boundary of the basin, the Axial Arch, is a WNW-trending fault-bend fold formed during south-directed Laramide thrusting (Stone, 1986). The last significant trend is the N/S trend typified by the sections of the Hogback between Meeker and Rio Blanco, and from Carbondale to the Elk Mountains.

The Cretaceous-age Mesaverde Group stratigraphy is pervasively gas-saturated and is overlain by the tremendous oil shale reserves of the Green River Formation. The focus of this report is the gas found within the Cretaceous-age Mesaverde Group (Williams Fork Formation) coals and interbedded sandstones. Additional significant gas resources are found within underlying marine sandstones of the Cretaceous-age Iles Formation, and within overlying fluvial sandstones in both the upper Williams Fork Formation, and the Tertiary-age Wasatch Formation (see Figure 1 for gas fields and producing horizons). The largest hydrocarbon resource (>13 trillion barrels, Taylor, 1987) is found within the lacustrine, Tertiary-age Green River Formation oil shale that overlies the northern half of the basin. Oil shale production from the Green River shales has gone through several periods of evaluation to develop extraction methods that can economically produce oil in an environmentally acceptable manner. The oil shale deposits, coupled with the gas resources hosted by Cretaceous-age sediments, represent one of the world's largest hydrocarbon accumulations.

GAS- AND WATER-SATURATED CONDITIONS IN THE PICEANCE BASIN

A critical first step during basin exploration is to locate gas-bearing zones in the subsurface. Further partitioning of the exploration area can then be performed using integrated studies of remote sensing, high-resolution aeromagnetics, seismic, and structural geology to locate fractured reservoirs. To analyze the location of gas-bearing zones, water and gas data were assembled from initial production, and monthly and cumulative production data collected throughout the Piceance Basin. Production data were then used to delineate the areal distribution of the gas and water-saturated zones. A cross-section was constructed using gas volumes from mud logs to illustrate cross-sectional basin hydrodynamics. Recognition of subsurface fracture-related permeability caused by tectonic structures is a more complex problem. To determine zones or orientations of enhanced subsurface permeability, remote sensing imagery analysis was used to constrain regional macrostructures and related fracture trends. The results of this analysis are reported in a companion paper (see Hoak and Klawitter, this volume).

The following discussion of gas-and-water saturation is organized into two sections. The first section outlines the characteristics of typical gas-centered basins and then assesses water and gas-saturated conditions throughout the Piceance Basin. The second section outlines the relationship between subsurface structure and production.

Basin-Centered Gas Model

Numerous models relating basin subsidence and hydrocarbon generation and retention have been proposed by such authors as Barry (1959) and Meissner (1978). Recently, Law and Dickinson (1985) have further extended this model and described the process by which thermal influences result in abnormal pressure in low-permeability systems. The central idea of this model is the dynamic relationship between thermal maturity, permeability changes and burial depth. In this model, there are four primary phases (Figure 3). The generation and existence of overpressured conditions is a key piece of data to be used in regional fracture studies. By knowing the timing of overpressure generation and the mechanical state of the host rock mass, the geometry of natural fractures that formed during this phase can be much more accurately predicted. Available data from the Piceance and other basins suggest that overpressuring may initiate and/or facilitate regional natural fracture development in many tight gas sand reservoirs (Lorenz et al., 1991).

In the gas-centered basin model of Law and Dickinson (1985), the first phase involves sediment deposition and basin dewatering. During this phase, sediments show high porosity (up to 40%) and elevated permeability. Throughout this initial phase, porosity is reduced by compaction and precipitation of early pore-filling cement, and the sediment mass experiences an increase in Young's modulus (a measure of rock stiffness).

The second phase is characterized by thermally-induced carbon dioxide generation commencing at a temperature of approximately 120^0 F. Carbon dioxide produced during this phase reacts with existing water to form carbonic acid. The net effect is a lowering of the pH of the formation fluids that

dissolves some of the early cement phases and causes the precipitation of other cements. The increase in carbon dioxide also serves to increase the overall fluid or gas pressure in the system.

The third phase commences when organic materials within the host sediments commence gas generation. During this phase, cementation causes a reduction in permeability and porosity because water mobility and mixing are reduced. Mechanical compaction is considered minimal at this stage. Water is forced up dip and/or up section when gas pressure exceeds the local hydrostatic value and more gas is generated than can be stored in the available pore space. The fluid migration direction is dependent on local pressure gradients.

In theory, provided sufficient quantities of organic materials, gas generation should continue as long as thermal cracking can occur. However, because of uplift and declining thermal gradients, combined with fracturing and concomitant leakoff, the overpressured zone generally cannot be sustained. As the overpressured zone experiences decay (a gradual decline in gas pressure due to cessation of gas generation combined with regional uplift), meteoric recharge is able to breach the reservoir and flush hydrocarbons from the system. This phase represents the present-day conditions in most gas basins that had a gas-centered origin. Thick, thermally mature coals interbedded within lenticular sand bodies are a common feature in many gas-centered basins. This geometry is also found in the Piceance Basin where the isolated hydrodynamics of lenticular sandstone reservoirs maintain unbreached and overpressured conditions.

Piceance Basin Gas Genesis

In order to assess the present state of gas generation in the basin and the location of areas possessing sufficient thermal maturity for gas generation, thermal modeling using vitrinite reflectance data from Piceance Basin coals was used to construct the chronology of thermal maturation in the basin (Decker and Horner, 1987). The model used in this analysis was a fourteen layer model using appropriate layer thermal conductivity values to better reflect the thermal stratification and evolution of the system. A representative example of vitrinite reflectance profiles (thermal history plot) from the Red Mountain and East Divide Creek sites (see Figure 1 for location) are shown in Figure 4. These curves show that active gas generation (defined as the point at which the coals passed through a vitrinite reflectance value of 0.75) at all three sites commenced nearly simultaneously approximately 52 million years ago, suggesting a rapid and uniform subsidence of the central and eastern basin. These curves also indicate that the central and eastern Piceance Basin reached maximum thermal maturity and gas generation ceased approximately 22 million years ago when regional uplift occurred and thermal maturation ceased.

Vitrinite reflectance and basin thermal modeling also provide a mechanism to calibrate significant events during basin evolution such as fracture genesis and uplift chronology. Previous efforts to determine a fracture chronology have largely relied on relative age determination based on crosscutting relationships. Through the use of vitrinite reflectance and thermal modeling, we have a framework for assigning an absolute age to basin events. A typical burial history from the MWX location is shown in Figure 5. A basinwide distribution of thermal maturity values (Figure 6) shows that the majority of the basin center experienced a thermal maturity of 0.8 R_o or larger and entered the gas generation window at approximately 0.75 R_o.

The geometry of the overpressured zone was delineated using calibrated mud weight information. Maximum mud weights during drilling in excess of 11.0 lbs./gallon were used to delineate the boundaries of the overpressured zone. This information is shown on Figure 6 as a shaded area. Several localities show mud weights in excess of 11.0 lbs/gallon, however, careful review of drilling records showed that heavier mud weights were used for hole stability problems, not to control overpressured conditions. Inside the overpressured area, several wells have been drilled under balance. Mud weights from these wells were disregarded in construction of the overpressured boundary. Extrapolation of the boundary along the basin axis to the northwest is precluded by the lack of drilling activity on the high mesas in that area. Complete definition of the overpressured zone requires data collection in this area.

Cross-Sectional Gas and Water-Saturation, and Overpressured Conditions

A critical element in the gas-centered basin model is the thermal generation of gas and maintenance of overpressure due to low permeability reservoir conditions. In the Piceance Basin, the overpressured zone (as determined by drilling mud weights and calibrated against known bottomhole pressure data) has been identified in the lower section of the Williams Fork Formation within the Rulison Field. In this field, the top of the overpressured zone lies just above the Cameo Coal, and appears to have a gradational lower boundary along the top of the laterally continuous marine Rollins sandstone of the Iles Formation. Decayed or remnant overpressure is also present in the Cozzette and Corcoran sandstones, separated from the overlying Rollins sandstone by a tongue of the Mancos "A" shale in Rulison Field. It is difficult to determine from available data if the Rollins sandstone is also overpressured. The limited tests that have been performed on the Rollins suggest that it is gas-bearing but that it tends to also be water-saturated. The regional persistence of this relationship is known only anecdotally. Figure 7 illustrates the gas-centered basin geometry across the Piceance Basin. The geometry of this zone roughly parallels the vitrinite reflectance isotherm of 0.8 along the western boundary and the basin outcrop to the east.

This cross-section or basin profile was created from the digitized total gas curve from hydrocarbon logs, and wireline log gamma log traces from the same well. The combined gas and gamma log traces for these wells were hung on a structural datum (Top Mesaverde or Cretaceous/Tertiary boundary) to illustrate the basin geometry. Relevant information such as the location of the overpressured zone, stratigraphic correlations, and vitrinite reflectance values (isotherms) were added to the section. From this cross-section, lateral and vertical water/gas transitions are located in the basin. The east/west cross-section defines the overpressured zone as being restricted to Rulison field and approximately one-half township to the east. Parachute field is normally pressured except along the transitional eastern field margin where it grades into Rulison field. From hydrocarbon log traces, the lower Williams Fork Formation appears gas-saturated across the basin interior. The discontinuous, lensoidal geometry of the Williams Fork, combined with its low matrix permeability, requires natural fractures for economic gas recovery. The importance of fracture detection

is to identify areas capable of economic production from this reservoir horizon. In sharp contrast to the Williams Fork lensoidal stratal geometries, the marine Iles Formation sandstones (lying underneath the Williams Fork Formation) are laterally continuous. However, the low-permeability conditions in these sands also require fracture permeability for economic gas yields.

In cross-section, the Cozzette and Corcoran Member sandstones in the Iles Formation appear to be gas-saturated across the basin and were probably once overpressured in the basin center. The Cozzette member sandstones are water-saturated along the eastern basin margin. The Rollins member sandstone is water-saturated across the basin except for scattered localities along the western basin margin where isolated tests have shown it to be dry and gas-bearing. In the gas-centered basin model, the discontinuous nature of the fluvial sandstones in the Williams Fork has enhanced the preservation of overpressured conditions. In the underlying Rollins sandstone, lateral continuity across the basin may allow this member to serve as a regional aquifer. The Cozzette member has probably behaved in a similar fashion although it appears to have greater internal complexity and may contain flow boundaries that impede ready migration of water through these sands. The Corcoran member has a relatively thin outcrop exposure on the eastern margin so that the area of potential meteoric influx is small compared to the other two Iles Formation sandstones.

A primary control on fluid flow through the basin subsurface has been thought to be the approximately two thousand feet of hydraulic head difference between the eastern and western margins of the basin. In this flow regime, artesian flow will occur from east to west (Figure 8). However, there are several problems with this model. The first, is the presence of overpressured conditions in the basin center that inhibits flow of fluids across the overpressured interface. Lithologic flow barriers are also created by the lensoidal geometry of the Williams Fork fluvial channels and the low-permeability of these sands and the underlying marine sandstones. The Rollins, Cozzette and Corcoran sands possess microdarcy permeability and regional flow regimes through these low-permeable systems seem untenable.

From the basin cross-section, an excellent perspective is gained into the origin and evolution of basin subsurface hydrodynamics. Determination of the areal extent of the water- and gas-saturated zones is the next step.

Lateral Variability in Piceance Basin Water and Gas-Saturated Zones

Lateral variation in the geometry of the gas and water-saturated zones is most useful to explorationists and those creating basin syntheses. This perspective permits the cross-sectional information described above, to be expanded into the third dimension and then projected into plan view. To assess gas and water-saturated conditions, gas-saturated conditions were initially screened by the presence of gas fields producing from a particular reservoir horizon. This was confirmed by verifying the presence and magnitude of gas shows in mud logs from that area. Mud logs are often considered preferable to neutron density logs in the Piceance Basin because the "gas effect" or neutron crossover is commonly suppressed in tight gas sands despite the presence of high gas saturation. Numerous examples are available where significant gas shows are observed on the hydrocarbon log but the neutron density logs do not show any crossover effect.. Because of this observation, the cross-over effect is not always a reliable tool for identifying gas-bearing sands.

Initially, all publically-available hydrocarbon (mud) logs from throughout the basin were collected and the location of the gas-saturated zone was determined on these logs. From a subset of these logs, the cross-section described previously (Figure 7 & schematically in Figure 8) was constructed.

Water-saturation was determined by using initial production data (generally calculated by operators after approximately three months of flow to remove hydraulic fracture stimulation fluid returns from production information) and flagging all wells in the basin flowing greater than 5 barrels of water per day (BWPD). Production data for these wells were then examined to determine if the wells flowed more than 10 BWPD over time. By identifying wells as either "wet" or "dry", the boundaries of the gas and water-saturated zones were delineated. Because many areas show complex water production, those areas with increasing or variable water production over time were labeled as transitional.

In the Piceance Basin, the vast majority of Williams Fork Formation fields are gas-saturated (Figure 9). Significant local breaching of the system is evidenced by water-saturated conditions such as within the Divide Creek Anticline in the southeast area of the basin. Differential amounts of meteoric recharge occur along the basin margins where the Williams Fork Formation or its equivalent crops out. To date, the most productive Williams Fork fields appear to lie in an overpressured zone along the basin axis. If gas is sourced from the Cameo Coal group within the low-permeability Williams Fork, this is the logically the most likely zone for gas entrapment in a basin-centered gas model. Also, the majority of gas would have been generated at the most thermally mature, deepest part of the basin. Water produced in the Williams Fork is variable. In Divide Creek and the basin center, water appears to be sourced from the coal interval (Sattler et al., 1985).

Very limited production and test data are available for the Rollins Member sandstone. There are less than a half dozen wells in the south half of the basin that have reported tests in the Rollins. Most operators consider the Rollins to be water-saturated throughout the basin. Only along the western quarter of the basin (where significant facies changes occur in the Rollins and equivalent sands) does the Rollins appear to be gas-saturated, though the test data suggest uneconomic volumes. The source of water produced from the Rollins is unknown. Because of limited available information, a regional map of gas-saturation in the Rollins has not been constructed.

The Cozzette Member of the Iles Formation is a shingled, southeastward-prograding, laterally continuous, marine sandstone (Figure 10). The sandstone was deposited along approximately NE/SW trending strandlines with depositional limits present along the northern and southern boundaries (Brown et al., 1986). Meteoric influx occurs along both eastern and western basin margins. However, influx along the western margin is limited due to the semi-arid conditions that prevail in that region. The source of the Cozzette water is unknown.

Gas and water production from the Corcoran Member of the Iles Formation show that most of the Corcoran

sandstone is gas-bearing (Figure 11). Only along the basin margins where subsurface depths are relatively shallow does the Corcoran produce water. There are several Corcoran producers that have apparent associated water, however, it is unclear from the reporting of the commingled production data whether the water is sourced from overlying reservoir horizons or from the Corcoran. Possibly, some of this water may be fracture flow water sourced from adjacent reservoir horizons. Similar to the Cozzette sandstone, the Corcoran is also breached along the Bull Creek Anticline structure just to the south of Debeque Canyon. The geology of the Corcoran and the Cozzette sandstones are both quite similar and represent regressive shoreline sequences. Like the Cozzette, the Corcoran also prograded to the southeast. The source of the Corcoran water is unknown.

Complex water-saturated relationships are particularly evident in the Cozzette Member of the Iles Formation. In this reservoir horizon, wells producing no water are often surrounded by wet wells. One possible explanation is that water is sourced from fractures that connect wet zones while gas is trapped in less-connected fractures. The presence of a small normal fault in MWX #2 providing communication between the Cozzette and Rollins sandstones suggests that the Cozzette water may be sourced from the overlying Rollins sandstone and transported along the fault. If this small-scale faulting is prevalent in the gray transitional area (see Figure 10), it may provide an explanation for the complex boundary between the gas and water-saturated zones in the basin center.

A major problem for most gas producers in the southern Piceance Basin is that high permeability zones are commonly water-saturated. Work in progress is attempting to determine if water production is controlled by fracturing and whether these zones are natural extension fractures or shear fractures/fault zones. In addition, ongoing efforts are underway to characterize the source of water and geochemical evolution of the basin.

FRACTURED RESERVOIR ANALYSIS

To assess the importance of fractured reservoirs on production trends, detailed structure and production mapping was performed in Grand Valley, Parachute and Rulison fields to determine the relationship between production and structure. This section represents an abbreviated geologic and production synthesis of Grand Valley, Parachute and Rulison fields (see Figure 9 for field locations). These fields produce gas from the Tertiary-age Wasatch Formation, the Cretaceous-age Williams Fork, and the underlying Cretaceous-age Iles Formation. In these zones, gas is trapped in structurally-enhanced stratigraphic traps. A large percentage of Williams Fork gas is produced from fluvial sand channels, and from thick coals in the Cameo Coal section located below the fluvial interval. Limited production (approximately three wells) is contributed from marine sands in the Cozzette-Corcoran sandstones (Iles Formation).

The primary objective of this study is to understand the relationship between production trends in the three fields and regional structure, most notably the influence of structural trends on subsurface permeability and reservoir productivity.

Reservoir Stratigraphy

Producing zones in the Rulison and Parachute fields can be dissected into three primary reservoir horizons. Most successful Williams Fork wells produce from fluvial sand channels. Extensive research at the MWX site in Rulison field demonstrated that the widths of these sand channels (approximately 300-500' wide, 20-50' thick; Lorenz, 1985) are significantly less than regulated well spacing. Recently, with new field rules (80 acre spacing, 2/94), additional production should be achieved from these lenticular, isolated channel sand reservoirs.

In the Piceance Basin, reservoir thickness is directly related to depositional environment. In the Iles Formation, shallow marine, shoreline deposits are composed of homogeneous, widespread blanket-type sandstones possessing sub-microdarcy permeability. Similar clean sands are found within fluvial channels and in the paludal (coal-bearing) interval of the Williams Fork Formation. These fluvial and paludal Williams Fork sands, especially where fractured, represent the best exploration targets. However, these zones are generally more complex targets because of the anastamosing, discontinuous nature of the reservoir. The complexity is further magnified by the complex internal structure of the reservoir sediments.

Limited production is also sourced from the marine sediments composing the Cozzette-Corcoran lying immediately underneath the Williams Fork Formation. In general, these sediments prograde to the southeast and have an internal shingled geometry typical of a transgressive systems tract.

Production Trends in Grand Valley, Parachute and Rulison Fields

To develop an understanding of the controls on production, production data for the best six months during the life of the well were contoured. Figure 12 illustrates the relationship between production trends in the three fields. Production trends correlate to local structure trends in the three fields. To examine the effect of stratigraphic variation, a total sand isochore map was compared to the production trends for Parachute and Rulison fields (Figure 13). The production trend lies perpendicular to the depositional systems trends, strongly confirming the structural control on production in these fields. Work in other fields confirms these relationships (see Hoak and Klawitter, this volume).

These three fields illustrate the importance of structural controls on production trends. It is interesting to note that the NW-trending production trends and local structure lie oblique to the dominant WNW or E/W fracture trends documented by the MWX coring program (Lorenz and Finley, 1991). There are several possible explanations for this relationship. The most plausible is that local tectonic deformation caused by structures, such as the Rulison Anticline, generates enhanced dilatancy along fracture sets oriented oblique to the structure.

REGIONAL STRUCTURE AND TECTONICS

Regional structural mapping, integrated with ancillary data, delineates the location of fracture prone areas. Linear features analysis using remote sensing imagery is used as a reconnaissance tool to locate regional structures and the surficial manifestation of deeper subsurface features. In those locations where local structures are breached to meteoric incursion, remote sensing imagery linear features analysis is used to recognize these zones to avoid local water-saturated areas. Prominent linear features proximal to seismic anomalies are also indicative of possible basement faulting.

Analysis of surficial structures from remote sensing imagery can also recognize subtle, subsurface structures such as the Rulison Anticline that are controlled by basement structures. These basement features can be clearly imaged on aeromagnetic data and confirmed by seismic data through these areas. Figure 14 demonstrates the geometry of the subsurface structure defined by aeromagnetic data in the Rulison Field. Note the presence of a NW-trending basement structure parallel to the trend of the shallower subsurface structure and the production trends that lie within this structure. This structure is confirmed by seismic. Seismic data, integrated with ancillary wellbore data in the southern Piceance Basin, clearly image the geometry of subsurface structure and the complex deformation history of the basin. A published E/W seismic line through Grand Valley, Parachute and Rulison fields has been interpreted by Waechter and Johnson (1986). Figure 15 is a reinterpreted portion of the seismic line interpreted by Waechter and Johnson. It is important to note that the primary focus of these authors was documentation of Paleozoic structural features. Because of this focus, an interpretation of Laramide contractional features has been added to this section. It is essential not to neglect the strong Laramide overprint superimposed on the older extensional horst and graben system because it is the tectonic event that dominates and was responsible for most of the major structures in the basin.

As shown by Waechter and Johnson (1986), a NW-trending, Pennsylvanian-age horst block is present underneath Rulison field. This block lies parallel to the Pennsylvanian-age tectonic grain, well documented in uplifted blocks flanking the margins of the Piceance Basin.

Southeast of the Rulison area is the Divide Creek Anticline, a fault-propagation-fold structure that plunges to the northwest. The explanation for the northwestward plunge and dissipation of the Divide Creek fold is probably related to the termination and/or decreased displacement of a thrust fault in the fold core whose displacement dies out along-strike to the northwest. The termination of the thrust and related fold probably is an analogous geometry to the termination of smaller-scale thrusts into folds common in both the Appalachian and Alberta fold-and-thrust belt. These thrust terminations and related folds represent the source of the fractures common in the Rulison field. The thrust tip termination requires regional strain to be accommodated by internal deformation of the rock (i.e. fractures) because strain cannot be accommodated by additional thrust displacement, or by folding or other ductile processes.

CONCLUSIONS

Most of the Williams Fork Formation, and the Cozzette and Corcoran sandstones of the Iles Formation are gas-saturated throughout the Piceance Basin. Water-saturated conditions are present along the basin margins and where structural uplift and erosion have breached the reservoirs. The majority of Piceance Basin reservoirs require significant natural fractures to permit economic production from low permeability sandstones.

The model of thermal gas generation and preservation of overpressure for the Piceance Basin can be readily applied to other western coal-bearing basins that contain thick, thermally-mature coals and interbedded, low-permeability, vertically-stacked, lenticular sands.

Mud weight, DST and bottomhole pressure data show that the present-day overpressured zone in the basin is concentrated within Williams Fork fluvial sandstones lying above the Cameo Coal section. The basin overpressured zone corresponds to the area where the maximum vitrinite reflectance is greater than 0.9. In this same area, the marine Iles Formation sandstones (Rollins, Cozzette and Corcoran) also show overpressured conditions although the magnitude of the overpressure is less than in the overlying fluvial and paludal sections. Low permeability conditions in these sands allow the preferential preservation of overpressured conditions. In this context, the low permeability sands of the Williams Fork and Iles formations are best modeled as regional aquitards rather than major hydrodynamic flow units of a regional artesian system.

Williams Fork gas-saturated conditions extend from approximately eight miles basinward of the Mesaverde Group outcrop belt surrounding the basin. Several structurally positive areas are breached by meteoric influx and are water-saturated. The Corcoran and Cozzette members show similar relationships although breached conditions are only locally present for the Corcoran in the western basin. The Cozzette Member exhibits complex water-gas-saturated conditions in the transitional area between the water-saturated eastern basin and the gas-producing horizons in the western region. Some of this complexity may be the result of fault systems connecting the water-prone areas of the Rollins Sandstone to underlying, lower-pressured zones in the Cozzette.

The most productive fields in the basin represent fractured reservoirs. Detailed studies in the Grand Valley-Parachute-Rulison and Shire Gulch-Plateau fields indicate that zones of maximum flexure on kilometer-scale structural features are directly related to areas of enhanced production. These smaller structures, common throughout the basin, represent the best focus for additional field development because most larger structures in the basin have been extensively drilled.

To determine the complex tectonics of the Piceance Basin, significant information about burial and uplift history can be determined through the use of thermal modeling using vitrinite reflectance data from the abundant coals seams throughout the basin. By placing fracture genesis in the context of thermal gas generation and basin maturity, an appropriate window of fracturing can be determined and tectonic events related to this fracturing can, in turn, be calibrated against an absolute time frame. This approach represents a tremendous improvement to previously-utilized relative timing methods based on crosscutting relationships.

Detailed analysis of regional structure and gas and water production can be used to determine fractured reservoir conditions, the relationship between fractures, structure and producibility, basin hydrodynamics, overpressured zones and the geometry of a structurally-influenced, gas-centered basin. Integrated with remote sensing analysis of the basin, seismic data and numerical modeling of the basin evolution, these analytical tools represent a powerful means of understanding and predicting fracture-controlled hydrocarbon production.

ACKNOWLEDGEMENTS

The authors would like to acknowledge financial support for this paper and the associated research project from the Department of Energy-Morgantown Energy Technology

Center (DOE-METC contract DE-AC21-93MC30086). Special thanks to Royal Watts (DOE-METC) for project management and encouragement.

REFERENCES

1. Brown, C.A., Smagala, T.M. and G.R. Haefele, 1986: Southern Piceance Basin Model-Cozzette, Corcoran and Rollins Sandstones, *in:* Spencer, C.W. and Mast, R.F. eds., *Geology of Tight Gas Reservoirs,* AAPG Studies in Geol. No. 24, 207-219.

2. Decker, A.D. and D.M. Horner, 1987: "Origin and Production Implications of Abnormal Coal Reservoir Pressure," *in:* Proc. of the 1987 Coalbed Methane Sym., Tuscaloosa, AL, Nov. 16-19, p. 51-62.

3. Law, B.E. and W.W. Dickinson, 1985: "Conceptual Model for Origin of Abnormally-Pressured Gas Accumulations in Low-Permeability Reservoirs, Am. Assoc. of Pet. Geol. Bull. 69 (8) p. 1295-1304.

4. Lorenz, J., 1985: "Predictions of Size and Orientation of Lenticular Reservoirs in the Mesaverde Group, Northwestern Colorado," Soc. of Pet. Eng. SPE/DOE 13851, *in*: Proc. of the 1985 SPE/DOE Jt. Sym. on Low Perm. Reservoirs, p. 23-28.

5. Lorenz, J., Warpinski, N.R., Teufel, L., Branagan, P.T., Sattler, A.R. and D.A. Northrop, 1988: "Results of the Multiwell Experiment," EOS (Transactions of the Am. Geophy. Union) V. 69 (35), 817, p. 825-826

6. Lorenz, J., Teufel, L. and Warpinski, N., 1991: "Regional Fractures I: A Mechanism for the Formation of Regional Fractures at Depth in Flat-Lying Reservoirs," Am. Assoc. of Pet. Geol. Bull. 75, p. 1714-1737.

7. Lorenz, J.C., Teufel, L.E. and N.R. Warpinski, 1991: "Regional Fractures II: Fracturing of Mesaverde Reservoirs in the Piceance Basin," Am. Assoc. of Pet. Geol. Bull. 75, p. 1738-1757.

8. Martinez, C. and H. Duey, 1982, Rulison Field, in: Crouch, M.C., ed., *Oil and Gas fields of Colorado, Nebraska and Adjacent Areas,* Rocky Mtn. Assoc. of Geol., V. 2, p. 444-449.

9. Meissner, F.F., 1978: "Patterns of Source-Rock Maturity in Nonmarine Source-Rocks of some Typical Western Interior Basins," in: *Nonmarine Tertiary and Upper Cretaceous Source Rocks and the Occurence of Oil and Gas in West-Central U.S.*, Rocky Mtn. Assoc. of Geol., Continuing Education Lecture Series, 1-37.

10. Mercer, J.C., K.H. Frohne, 1986: "Production Characterization of Tight Lenticular Gas Sands in the Rulison Area of Western Colorado," SPE Unconventional Gas Tech. Sym. Proc., SPE 15248, p. 1-6.

11. Peterson, R.E., 1984: "Geological and Production Characteristics of the Nonmarine Part of the Mesaverde Group, Rulison Field Area, Piceance Basin, CO," SPE/DOE/GRI Joint Sym. on Unconventional Gas Recovery, SPE 12835, p. 47-56.

12. Reinecke, K.M., Rice, D.D. and R.C. Johnson, 1991: "Characteristics and Development of Fluvial Sandstone and Coalbed Reservoirs of Upper Cretaceous Mesaverde Group, Grand Valley, Colorado," in: *Coalbed Methane*, Rocky Mtn. Assoc. of Geol., p. 209-225.

13. Sattler, A.R., Raible, C.J. and B.R. Gall, 1985: "Integration of Laboratory and Field Data for Insight on the Multiwell Experiment Paludal Simulation," SPE/DOE 1985 Low Perm. Gas Res., SPE 13891, p. 397-409.

14. Spencer, C.W., 1987: Hydrocarbon Generation as a Mechanism for Overpressuring in Rocky Mountain Region," Am. Assoc. of Pet. Geol. Bull., 71 (4) 368-388.

15. Stone, D.S., 1986: "Geology of the Wilson Creek Field, Rio Blanco County, Colorado," in: *New Interpretations Northwest Colorado*, Rocky Mtn. Assoc. of Geol. p. 229-246.

16. Taylor, O.J., 1987: "Oil Shale, Water Resources, and Valuable Minerals of the Piceance Basin, Western Colorado: the Challenge and Choices of Development," U.S. Geol. Survey Prof. Paper No. 1310, 143 p.

17. Waechter, N.B., W.E. Johnson, 1986: "Pennsylvanian-Permian Paleostructure and Stratigraphy as Interpreted from Seismic Data in the Piceance Basin, Northwest Colorado," in: *New Interpretations Northwest Colorado*, Rocky Mtn. Assoc. of Geol., p. 51-64.

FIGURE 1

SELECTED CRETACEOUS GAS FIELDS AND BASIN LOCATION MAP

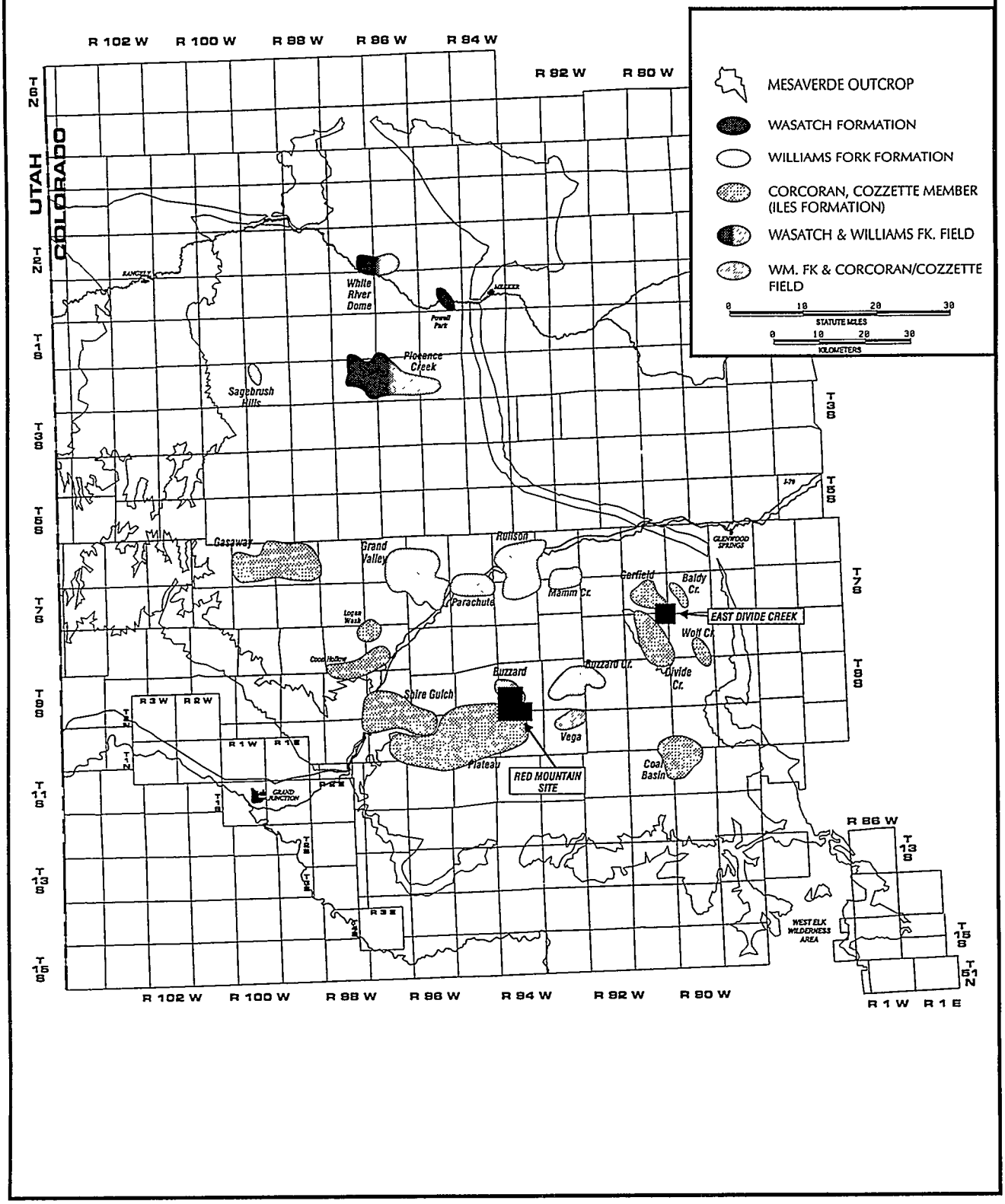
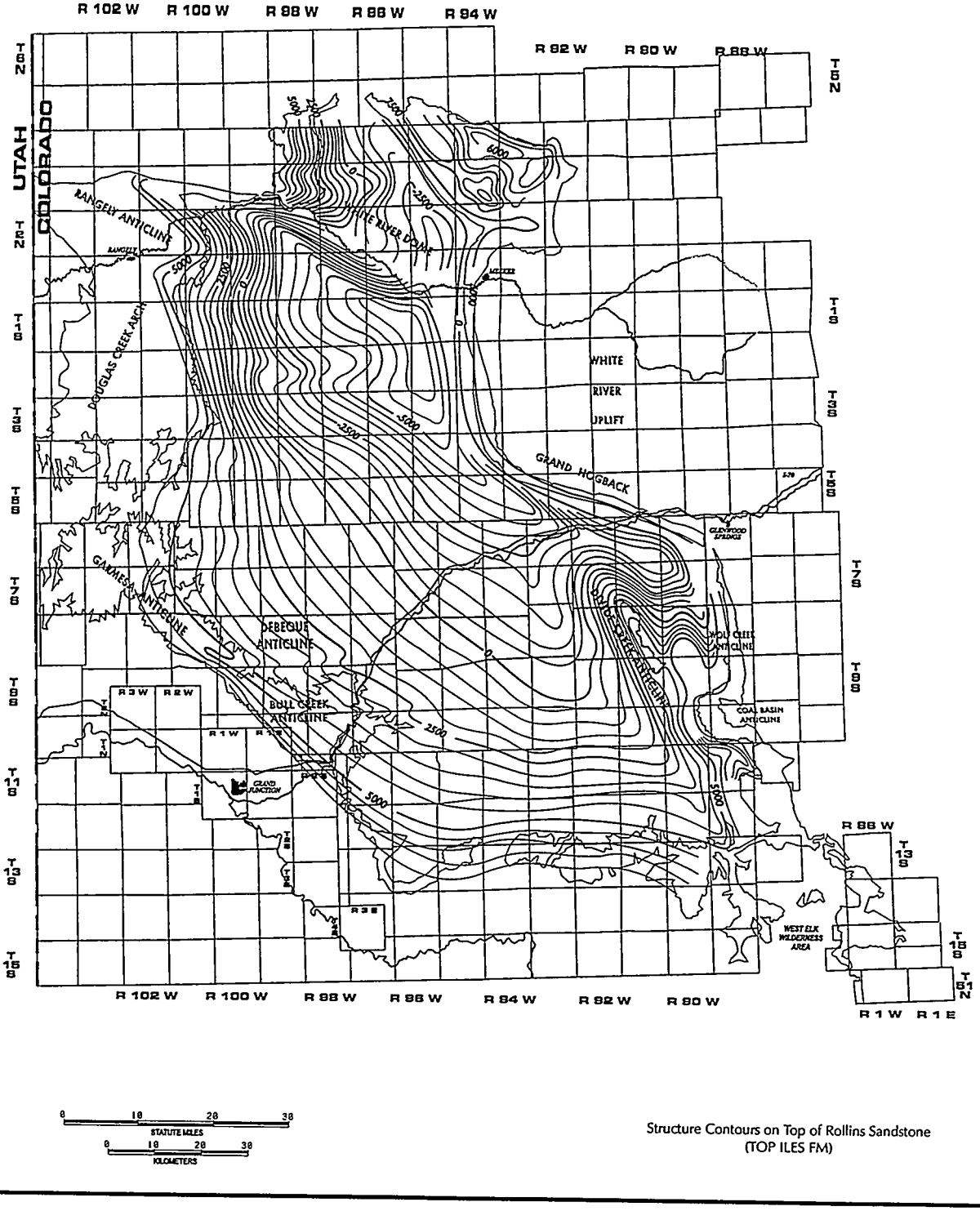


FIGURE 2

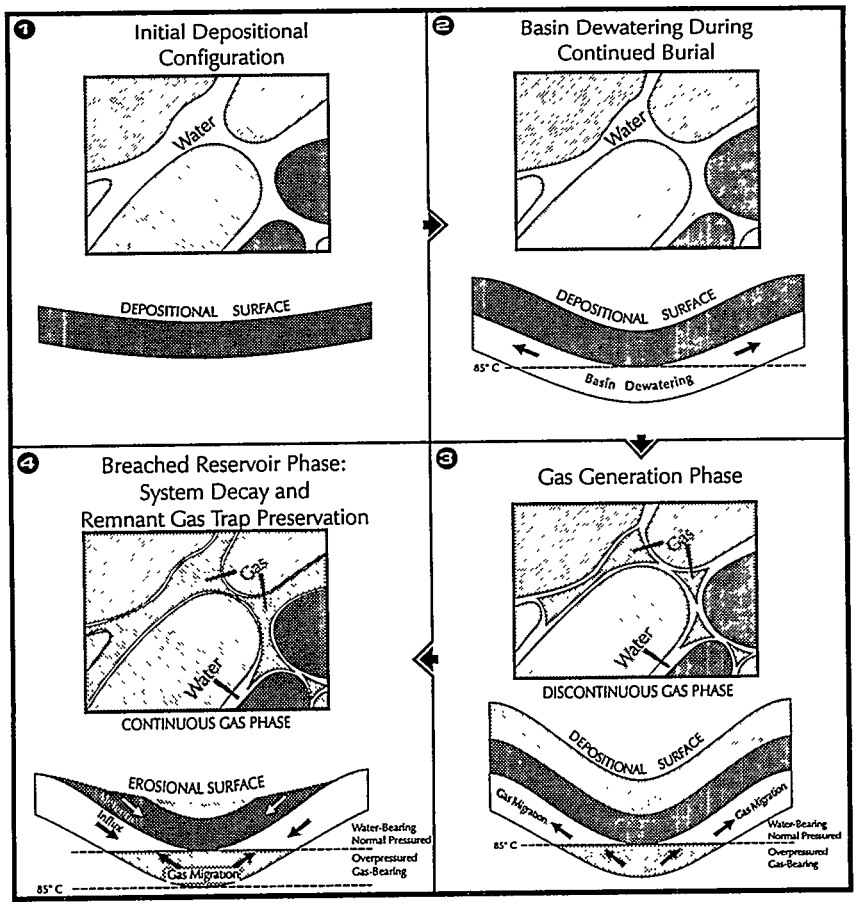
PICEANCE BASIN
REGIONAL STRUCTURE MAP



Structure Contours on Top of Rollins Sandstone
(TOP ILES FM)

FIGURE 3

EVOLUTION OF A GAS-CENTERED BASIN



Modified after LAW & DICKINSON, 1985

FIGURE 4

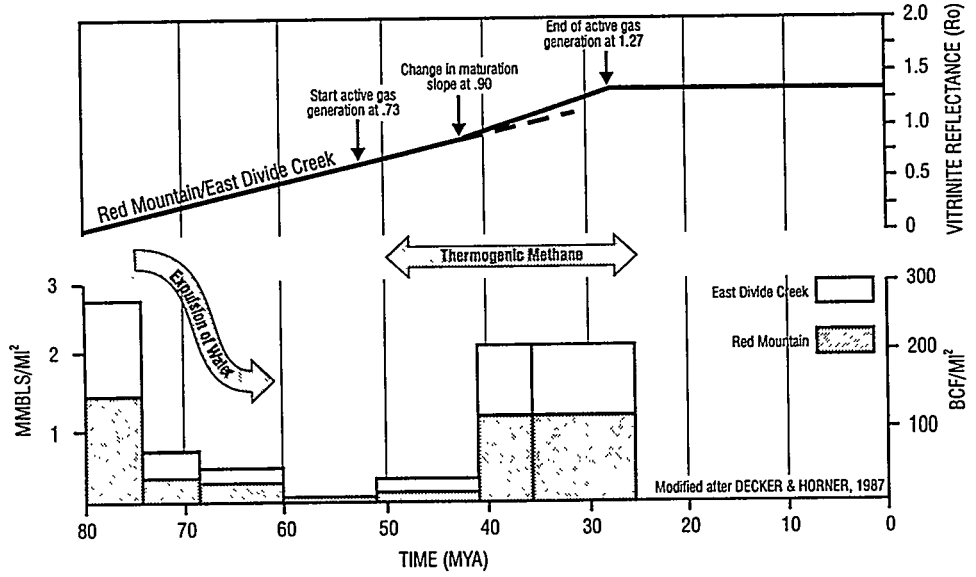


FIGURE 5

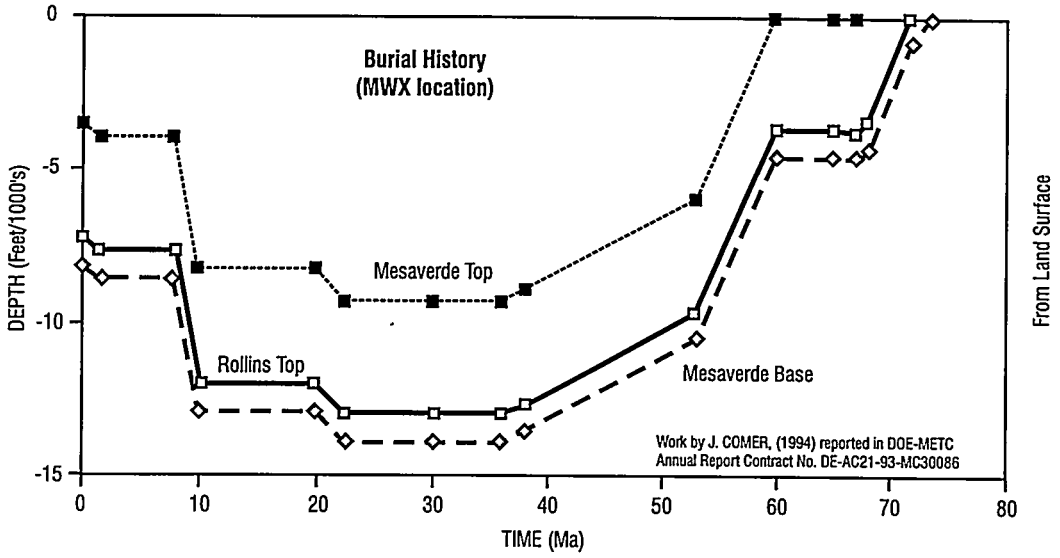


FIGURE 6

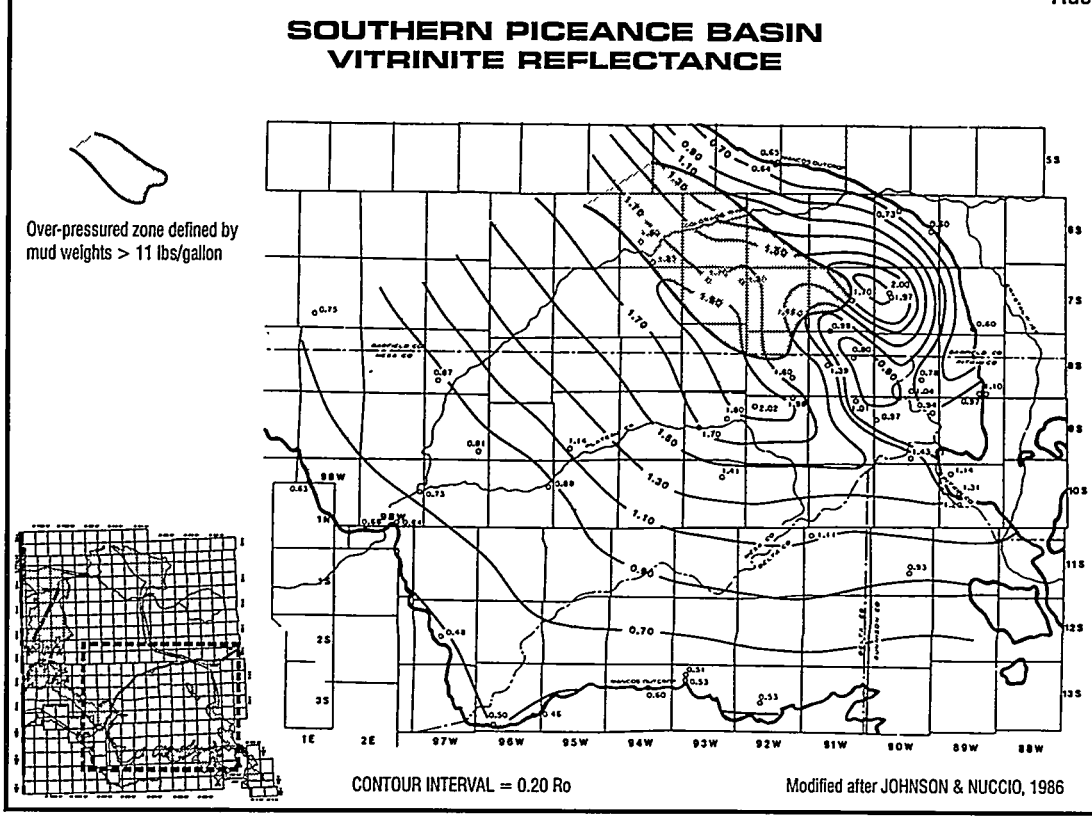
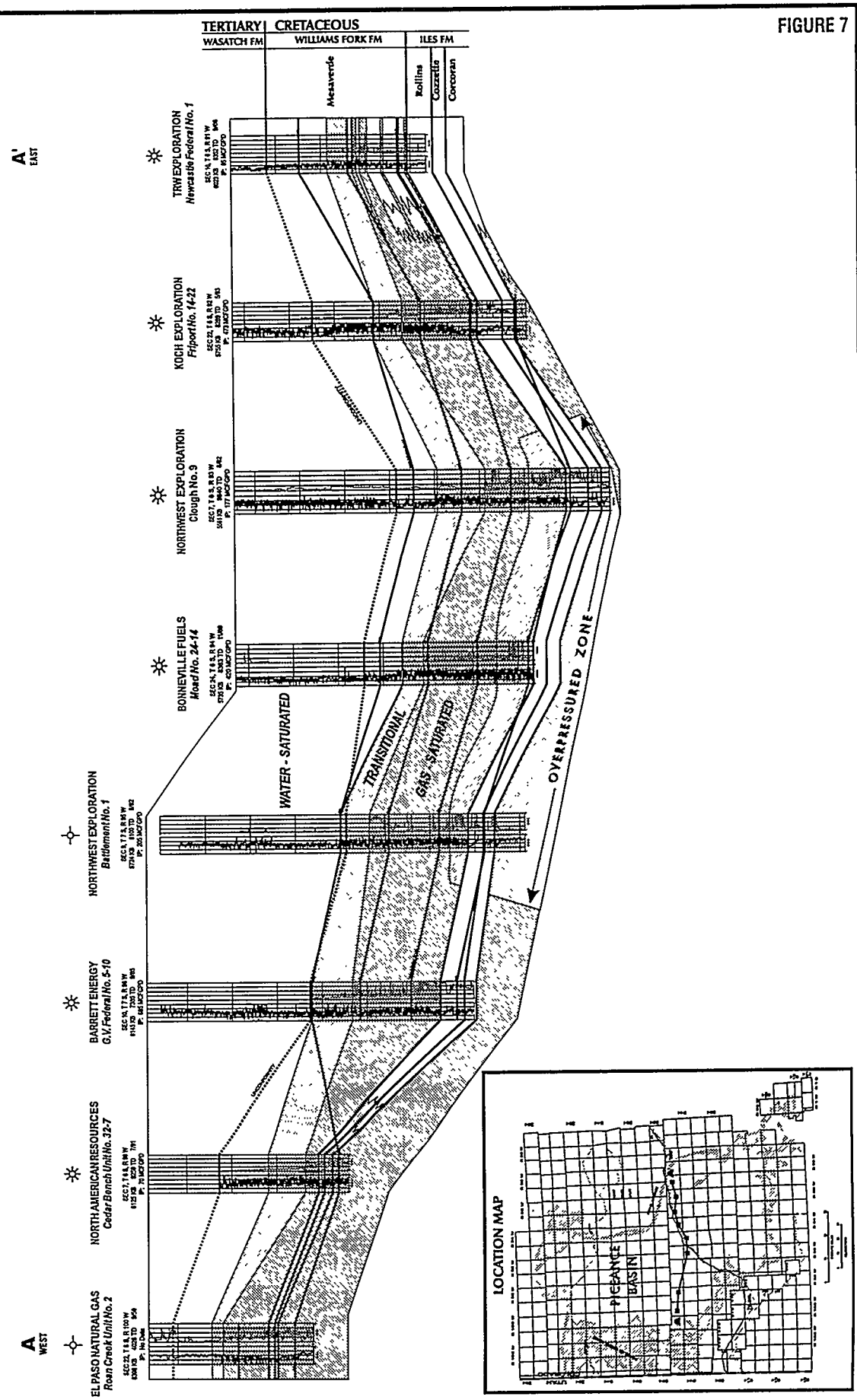


FIGURE 7

HYDROCARBON - GAMMA LOG CROSS SECTION ACROSS THE PICEANCE BASIN ILLUSTRATING GAS - CENTERED BASIN GEOMETRY



SCHEMATIC CROSS SECTION ACROSS PICEANCE BASIN

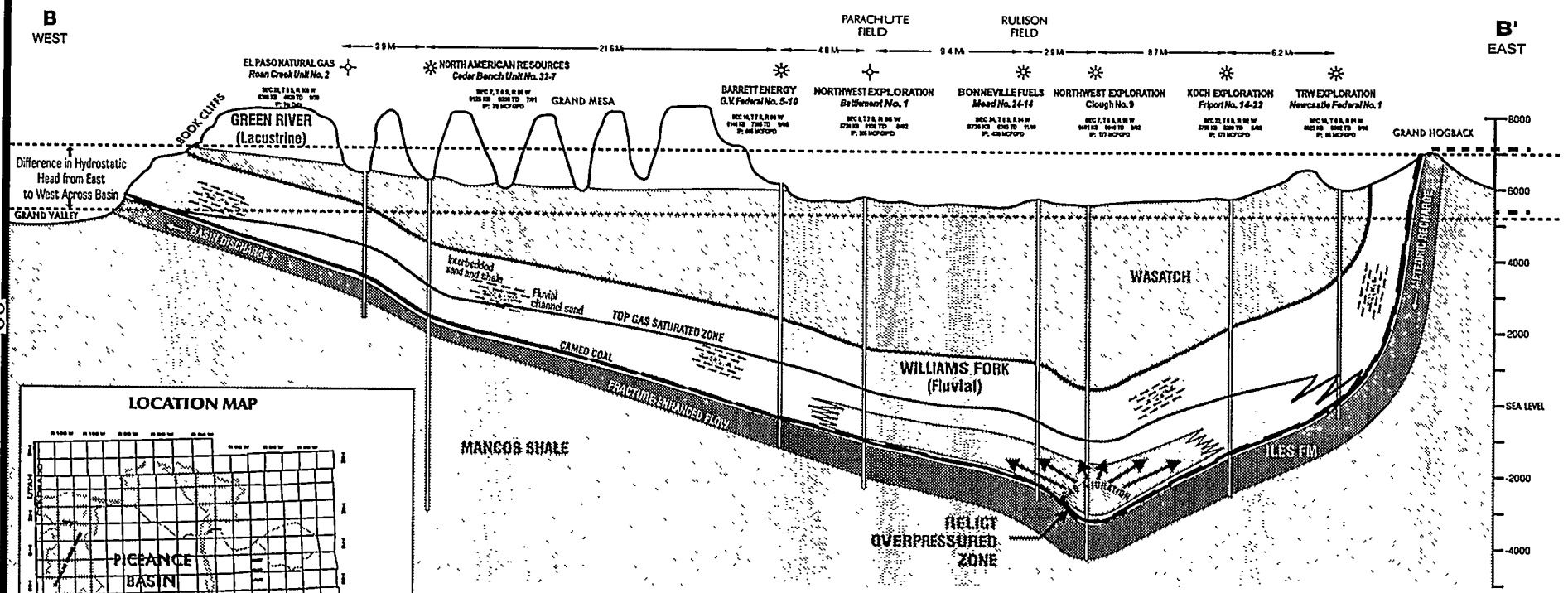


FIGURE 8

FIGURE 9

WILLIAMS FORK FORMATION GAS-SATURATED ZONE, PICEANCE BASIN

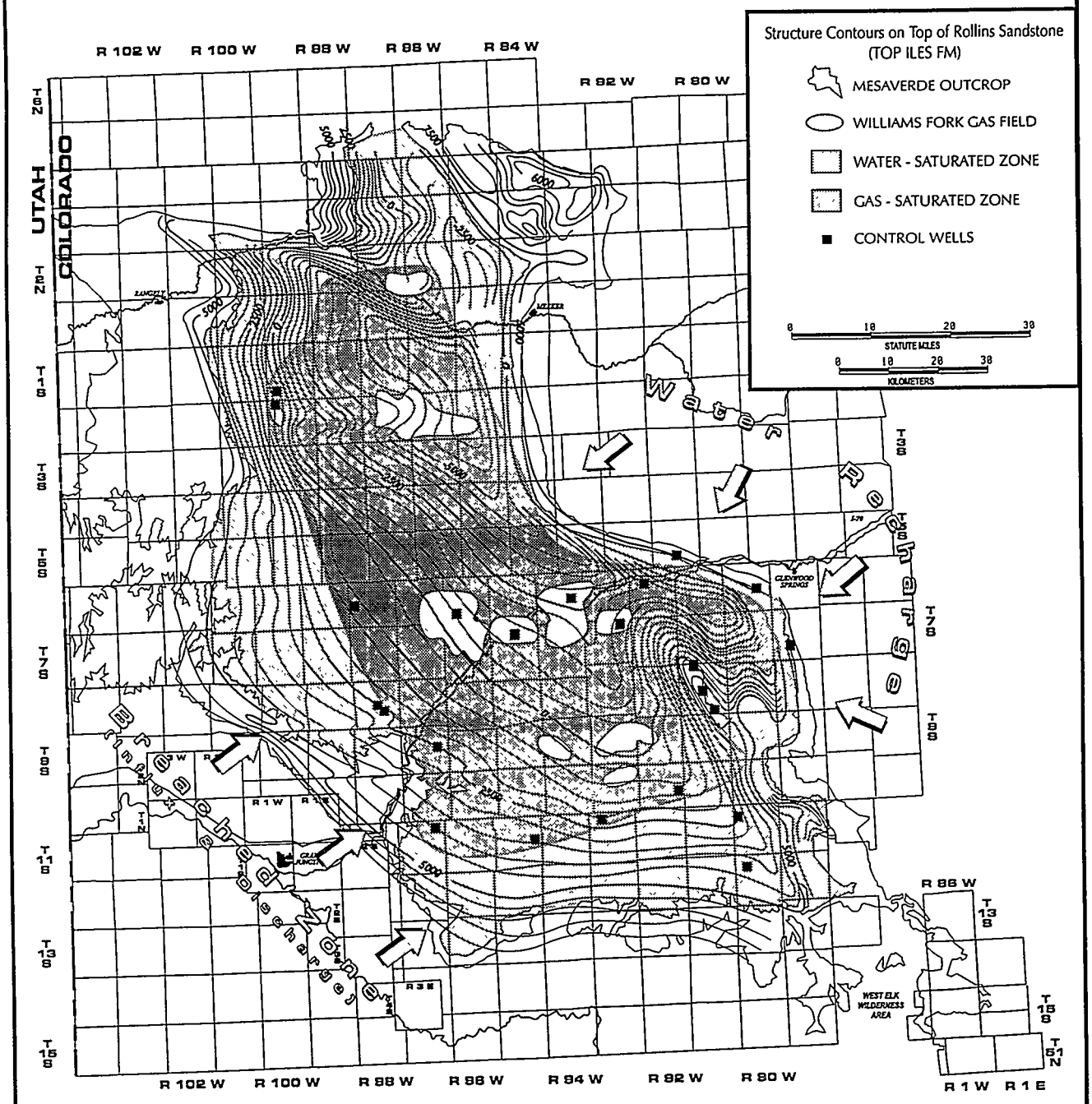


FIGURE 10

COZZETTE SANDSTONE - ILES FORMATION GAS-SATURATED ZONE, PICEANCE BASIN

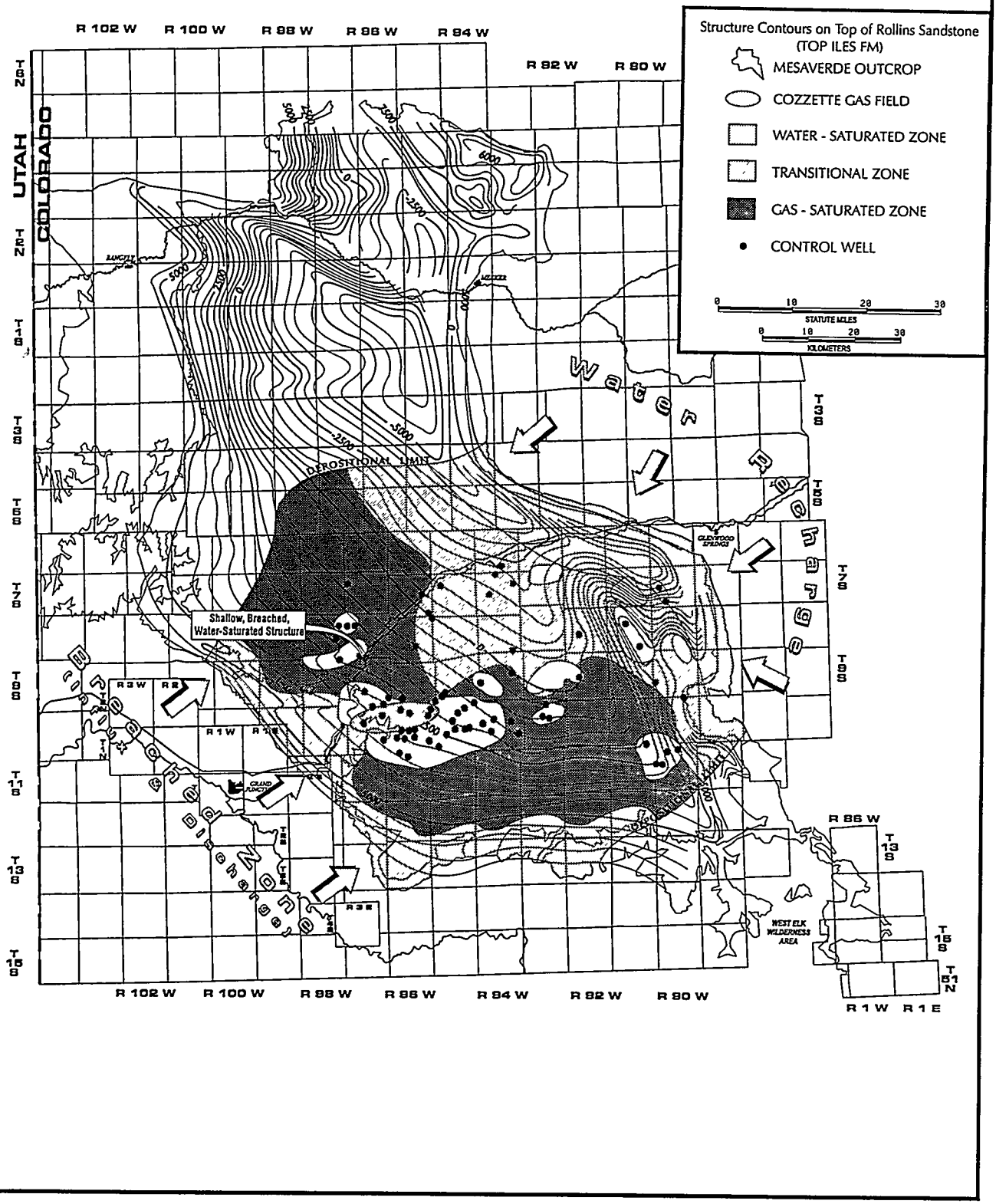


FIGURE 11

CORCORAN SANDSTONE - ILES FORMATION GAS-SATURATED ZONE, PICEANCE BASIN

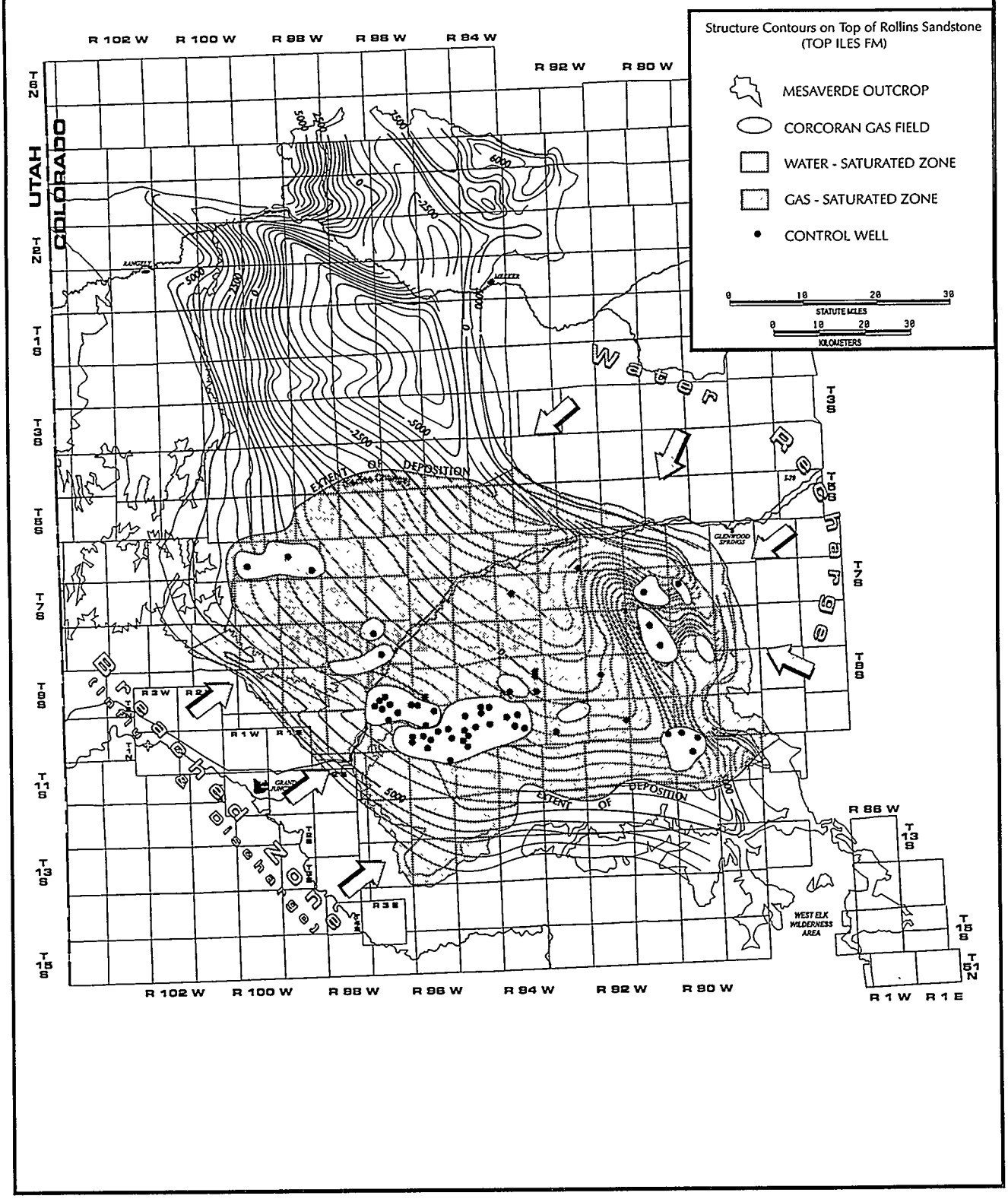


FIGURE 12

RELATIONSHIP BETWEEN STRUCTURE AND PRODUCTION
Grand Valley, Parachute and Rulison Fields, Piceance Basin

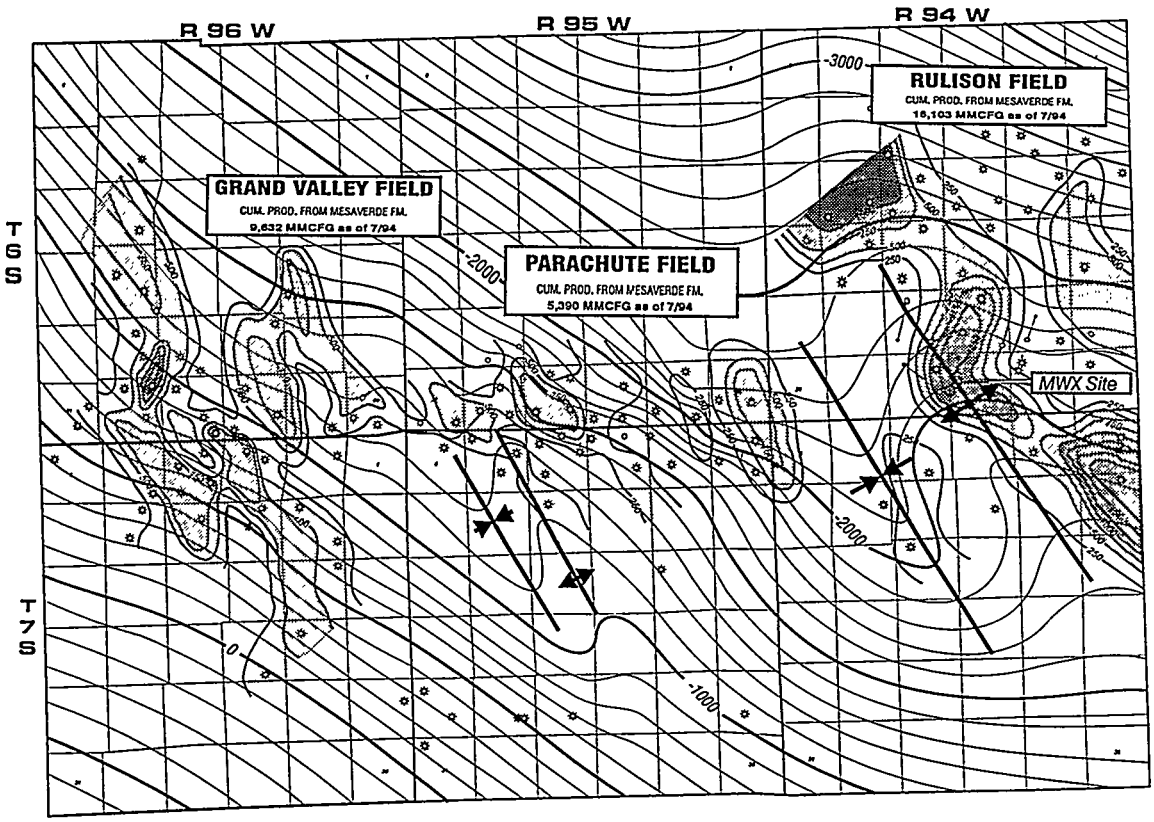
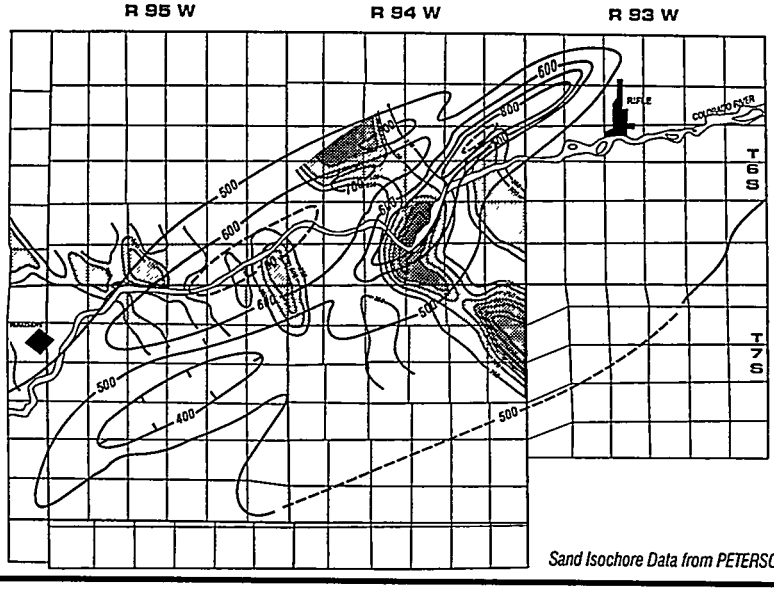


FIGURE 13

PARACHUTE - RULISON FIELD
Sand Isochore and Production Relationship



BEST 6 MONTHS PRODUCTION OF THE MESAVERDE FM
(Upper/ Middle Williams Fork and Cameo Sand)

ROLLINS STRUCTURE C.I. = 100 FEET
250 - 500 MMCF/MONTH
500 - 750 MMCF/MONTH
750 - 1000 MMCF/MONTH
>1000 MMCF/MONTH

Sand Isochore Data from PETERSON, 1984

FIGURE 14
AEROMAGNETIC STRUCTURE
RULISON ANTICLINE AREA
R 95 W
R 94 W
R 93 W
R 96 W
T 5 S
T 6 S
T 7 S
Magnetic Intensity
Contour Interval = 5 nanoteslas
BASEMENT FAULTS FROM SEISMIC
THRUST FAULT (hachure on upper plate)
NORMAL FAULT (tick on downthrown block)

FIGURE 15
BASEMENT STRUCTURE BELOW
RULISON FIELD
Rulison Field
CARDOAR, INC. #21
TERRA RESOURCES NO. 1 Orum Cr. McDaniel
WASATCH
MESAVERDE GROUP
MANCOS SHALE
PALEOZOIC
PRECAMBRIAN
FAULTS
Modified after WAECHTER and JOHNSON, 1985
0
5 Kilometers
5 Miles
Approximate Vertical Exaggeration
2.4 at 2 Seconds
NOTE: Some Pennsylvanian-Permian normal faults were reactivated during Laramide contraction as thrusts.

Dinosaur Ridge
Grand Junction
Colorado River
UNCOMPAHGRE UPLIFT
FIGURE 16
SOUTHERN PICEANCE BASIN
STRUCTURE MAP
TOP OF ROLLINS SANDSTONE MEMBER
CONTOUR INTERVAL = 200 FEET
ANTICLINE
SYNCLINE
MESAVERDE OUTCROP



NOTES

INTERGAS '95

May 15-19, 1995
The University of Alabama
Tuscaloosa, Alabama USA

9517

Integrated Exploration Strategy for Locating Areas Capable of High Gas Rate Cavity Completion in Coalbed Methane Reservoirs

A.L. Klawitter, T.E. Hoak, and A.D. Decker,
Advanced Resources International, Inc.

ABSTRACT

In 1993, the San Juan Basin accounted for approximately 605 Bcf of the 740 Bcf of all coalbed gas produced in the United States. The San Juan "cavitation fairway" in which production occurs in open-hole cavity completions, is responsible for over 60% of all U.S. coalbed methane production. Perhaps most striking is the fact that over 17,000 wells had penetrated the Fruitland formation in the San Juan Basin prior to recognition of the coalbed methane potential. The exploration maturity of this basin, prior to the recognition and exploitation of one of the nation's largest resource bases, bodes well for exploration and development efforts in other coal-bearing basins.

To understand the dynamic cavity fairway reservoir in the San Juan Basin, an exploration rationale for coalbed methane was developed that permits a sequential reduction in total basin exploration area based on four primary exploration criteria. One of the most significant criterion is the existence of thick, thermally mature, friable coals. In general, these conditions can be evaluated using a combination of coal thickness maps, desorption data, and information about basinal distribution of coal rank and ash content. Clean coals possessing a rank of 0.75% R_o or greater have adequate thermal maturity for sufficient gas generation and mechanical properties for cavitation.

A second criterion is the existence of fully gas-charged coals. Evaluation of this criterion requires reservoir geochemical data to delineate zones of meteoric influx where breaching has occurred. Infiltrating meteoric fluids will transport dissolved solids and will also strip adsorbed gas from within the coal and its fracture systems. Reservoir simulations in conjunction with field studies have shown that the extent of gas charge is critical. In this context, thin, fully-charged coals can yield gas production as significant as thick coals possessing less than fully-charged properties.

A third criterion is the presence of adequate reservoir permeability. Natural fracturing in coals is due to cleating and tectonic processes. Because of the general relationship between coal cleating and coal rank, coal cleating intensity can be estimated by analysis of regional coal rank maps. To augment this data and provide additional information about natural fractures and related permeability in coal, regional remote sensing imagery analysis is used to assess domains of enhanced fracturing as manifest in surficial geology. Remote sensing imagery analysis is particularly effective in recognizing basement structural influence on overlying stratigraphic successions.

The final criterion is determining whether natural fractures are open or closed. To make this determination, remote sensing imagery interpretation is supported by ancillary data compiled from regional tectonic studies. Extensional tectonic regimes appear to possess favorable conditions for cavitation, especially where the differential stress is high. The effect of confining stress is less significant than coal fracture intensity and dependent on reservoir pressure conditions.

Application of these four criteria to the San Juan Basin in a heuristic, stepwise process resulted in an overall 94% reduction in total basin exploration area. Application of the first criterion reduced the total basin exploration area by 80%. Application of the second criterion further winnows this area by an additional 9%. Application of the third criterion reduces the exploration area to 6% of the total original exploration area. Most significantly, this tiny percentage encompasses the majority of the cavitation fairway. At the same time, by following the methodology, we have increased our chance of drilling success to 8 out of 10, or 80%, of wells drilled. The successful application of this exploration rationale suggests widespread application of the methodology to other coal basins.

INTRODUCTION

In the San Juan Basin, significant coalbed methane reserve increases have been achieved using cavity completion methods in Cretaceous-age, Fruitland Formation coal seams (Figure 1). The region of maximum production corresponds to a NW-trending, elongate "fairway", Figure 2, where cavity completions best exploit the available resource. Inside the fairway, cavity completions perform five times better than hydraulic stimulations. Outside the fairway, hydraulic stimulations are preferred since the rock mechanical/stress properties do not allow successful cavity completions. Limited cavity completions outside the fairway and in other basins may be due to a failure to place wells in areas favorable to cavitation. The objective of this investigation was to delineate fundamental controlling parameters of an economically successful coalbed methane exploration program. These parameters were required to be available, and/or attainable at minimal cost, in order to use these criteria to explore globally for coalbed methane fairways in other coal

bearing basins. Using this information, an exploration rationale was developed. The exploration rationale developed during this investigation integrates engineering, conventional subsurface petroleum geologic studies, seismic surveying, remote sensing imagery analysis, and regional tectonic studies. By integrating these subspecialties into a cohesive exploration strategy, we are able to achieve significantly improved exploration success compared to older conventional approaches. To test the success of the exploration rationale, these parameters were mapped around the San Juan Basin.

This paper is subdivided into five sections. The first section outlines the economic significance of locating open-hole, cavity completion fairways. The second section describes the development of the exploration rationale used in the San Juan Basin. The third section outlines our remote sensing imagery analysis approach to determining zones of enhanced basin permeability. The fourth section integrates the remote sensing imagery analysis into the regional tectonic evolution, and makes additional predictions on subsurface permeability controls. The final section summarizes the overall conclusions and future research objectives that will be addressed in subsequent work.

SIGNIFICANCE OF PRODUCTION FAIRWAYS AND CAVITATION TECHNOLOGY

The growth of coalbed methane has been dramatic, and of great value to the domestic and international natural gas industry. The great bulk of this growth has taken place in the San Juan Basin, particularly following the discovery of the geologically favorable "cavity fairway" and its development with open-hole cavitation technology. Production data show that the San Juan Basin dominates coalbed methane production, with this single basin accounting for about 80% of total coalbed gas produced in the U.S. in 1993 (Figure 3). Within the San Juan Basin, the small number of open-hole cavity wells (600) accounts for 60% of U.S. coalbed methane production (Table 1). The majority of U.S. coalbed methane production (1.2 Bcfd out of a total of 2 Bcfd), is provided by less than 10% of the wells, the highly prolific open-hole cavity wells located in the San Juan Basin "cavity fairway". This fact emphasizes the central thrust for future growth of the U.S. coalbed methane industry. Finding and efficiently developing other coalbed methane "fairways" is a top priority for an expanding coalbed methane industry.

Coalbed methane was first produced in the San Juan Basin from the Fruitland formation by the Phillips #6-17 in 1953. The well was a conventional open-hole completion and produced at rates between 70-400 Mcfd stabilizing at 180 Mcfd with no co-produced water. Forty years later, the well has continued to flow at the same gas rate. Current cumulative production is 1.4 Bcf. For years prior to this completion, blowouts and lost circulation were encountered in the Fruitland coals. Common drilling practices were to drill with mud to the top of the Pictured Cliffs, set casing, then proceed to targets within the Mesaverde or Dakota while drilling with air. For many years, the potential of the Fruitland coals was unknown and untested. The first cavity completion within the basin was accomplished in 1987 by Meridian, 8 miles southeast of the Phillips #6-17. The well initially produced at rates between 200-1,100 Mcfd. The present size of the cavitation fairway as defined by the 1 MMcfd contour is slightly more than 300 sq. mi. and contains 10 Tcf of proven reserves. Although the basin has an average drilling density of almost 3 wells per square mile, the Fruitland coals were considered a nuisance rather than a resource until the late 1980's.

EXPLORATION CRITERIA

The objectives of this research were to establish basic criteria to delineate mappable geologic characteristics that would cost effectively delineate potential coalbed methane fairways. The most important geologic characteristics of the are:

1. Friable coals, vitrinite reflectance greater than .75%,
2. Fully gas charged coals,
3. Reservoir permeability enhanced by tectonic fracturing, and
4. Dilatant fracture network.

The exploration rationale has been designed to evaluate each of these four characteristics. In the San Juan Basin, over 17,000 conventional wells had been drilled prior to discovery of the fairway and the successful utilization of the cavity completion method in that area. Because of the relatively mature nature of this basin, significant data existed for this basin that may not be available in frontier basins. In applying the exploration rationale to frontier areas, some preliminary data must be collected to evaluate the four primary basin geologic characteristics outlined above.

Criteria 1: Coal Rank, and Thickness

Because of the importance of cavity completion methods to coalbed methane production, special emphasis has been placed on the requirements for successful cavitation in the exploration strategy. There is some data available to suggest that cleating is dependent on thermal maturity. In general, cleat spacing decreases with increasing coal rank (Mingzhu, 1993). Figure 4 graphically illustrates this point. The mechanical properties of coal change with increasing cleat density. Generally, coals with vitrinite reflectances less than .75% and low in vitrinite content are blocky and will not cavitate, whereas, coals with R_o greater than .75% and high in vitrinite content are more friable and will cavitate. Ash content also affects the ability of coal to cavitate. Low ash content coals are more highly cleated and cavitate better than high ash content, poorly cleated coals. To determine coal purity requires some assessment of the amount of interbedded ash or tonstein layers. In this investigation, thickness, thermal maturity, and coal purity were determined by consulting published geologic literature. Thermal maturity, as measured by vitrinite reflectance of the Fruitland coals, is presented in Figure 5. This figure accurately portrays the orientation and asymmetry of the basin. Note the strong correlation between successful cavity completions that define the southern San Juan Basin fairway and the .75% vitrinite reflectance contour on Figure 5.

Another important parameter is the presence of thick coals that can generate economic volumes of gas. The total coal thickness of the Fruitland formation within the cavity fairway averages over 60 feet (Figure 6). Anomalously thick coals, over 70 feet, are aligned along a NW-trending zone coincident with a basinal hingeline delineated in the gravity data (Figure 8), and an interpreted zone of weakness from the imagery analysis detailed in a later section. The location of the coals

in relationship to the location of the hingeline suggest that vertical movement along the hingeline was synchronous with the deposition of the Fruitland coals causing the anomalous thick zone. Reactivation of this structure is thought responsible for tectonic fracturing of the coals in the cavity fairway.

Although thick coals, greater than 30 feet, with adequate gas contents greater than 500 cubic feet per ton, are often the prime exploration criteria pursued by some parts of the industry, our view is that these parameters should rate lower in importance. Coals are inherently a rich gas reservoir compared with conventional gas sources. If the coals are fully gas-charged, coals with lower gas content (on the order of 200 to 300 cubic feet per ton), or coals with low to moderate thickness (10 to 20 feet), can provide an attractive "fairway" containing gas concentrations of 10 to 20 Bcf per section, and gas reserves of 3 to 5 Bcf per well. Figure 7 shows the difference in gas production from a "fairway" setting of fully gas charged, naturally fractured, low confining stress coals with: (1) good gas content and coal thickness (Base Case); (2) lower gas content, thick coals (with one-half the gas content), as might be found in lower rank coals of the Green River or Piceance basin; and, (3) high gas content moderately thin coals (with one-third the net thickness), such as might be found in the Appalachian Basin.

Criteria 2: Fully Gas Charged Coals

The second exploration criterion is the existence of fully gas charged coals. When breached by meteoric water or escape through fractures that have ruptured the reservoir seal, gas saturated coals can be partially flushed of gas. Coals that produce water containing high total dissolved solids (TDS), indicate original connate water and fluid isolation over geologic time. In contrast, coals with low TDS waters often indicate a breached system in which connate waters have been diluted by meteoric recharge. Systems that allow water influx typically show enhanced gas migration and diffusion that leads to undersaturated gas conditions, and therefore, are not fully gas charged. In spite of breached conditions, successful cavitation may still be achieved, however, little gas production and significant associated water will generally be produced. A typical map of breached conditions revealed by a chlorinity map is shown in Figure 8. This map shows that significant meteoric influx occurs in the northwest corner of the basin. The cavity fairway is located in a region of high chlorinity indicating isolation from recharge occurring along the outcrop. Low water to gas ratios, herein defined as "dry" coalbed methane production, Figure 9, is another characteristic of the cavity fairway that supports the conclusion that minimal amounts of water migrate to the basin interior. A strong correlation is evident between "dry" coalbed methane production and the cavity fairway.

To assess the extent of overpressuring, an indicator of possible gas-charging and reservoir isolation in the basin, drilling mud weight and fresh-water potentiometric surface maps were obtained. The fresh-water potentiometric surface, Figure 10, reveals an isolated pod of overpressure coincident with "dry" coalbed methane production in the cavity fairway. One explanation of this relationship is that this pod represents an isolated region within the Fruitland where the coals have become fully gas-charged and an effective reservoir seal has been maintained. The pod lies south of areas of recharge defined by the potentiometric surface and chlorinity of produced Fruitland coal water.

Criteria 3: Delineation of Fracture Permeability Using Integrated Exploration Methods

The third criteria, permeability, exerts the ultimate control on methane producibility in coal basins. Permeability is a reflection of the ability of the reservoir to deliver gas to the wellbore. Deliverability is accomplished through fractures within the reservoir. Some fractures in coals, termed cleats, represent one source of permeability. Tectonically induced natural fractures create additional permeability and may be essential to cavitation efforts. All fracture conduits, whether cleats or tectonically-induced, exert greater influence on production in high differential stress environments where fractures remain dilatant.

To assess fracture permeability, remote sensing imagery analysis was performed to identify regional and local structures. We are not targeting the structures themselves, but the fracturing which may be associated with the structures. Features identified on imagery were integrated with surficial and subsurface geological, geophysical potential field, and seismic data to determine structural significance. In many cases, structures are genetically related to underlying basement structures that can be identified on magnetic, gravity, and seismic data. Regional tectonic analysis of mapped structures and literature searches provided estimates of present and paleostress orientations. Regional tectonics also provided guidance interpreting the remote sensing imagery analysis.

The sources of subsurface permeability in the San Juan Basin coals are primarily natural fractures and secondarily, cleat systems in the coal. Because fractures in this region are dominantly structurally controlled, remote sensing imagery was used to delineate surficial manifestations of the subsurface structures that control fracturing. The ultimate objective was to use remote sensing imagery analysis to define naturally fractured, high-permeability regions where production could be enhanced, and development of cavity completion wells could be most successful. Fracture mapping through linear feature and imagery analysis proved to be the most efficient and cost-effective method of determining fracture geometries and related permeabilities. The objectives of linear feature and imagery analysis were to:

1. Interpret linear features from remote sensing imagery;
2. Perform statistical linear feature analysis of interpreted linear features;
3. Interpret regional lineaments;
4 Compare lineaments to available geophysical potential field and geological data to establish structural significance; and
5. Identify areas thought to possess characteristics indicative of subsurface permeability.

Linear features are herein defined as distinct, non-cultural linear elements interpreted from imagery. Lineaments are zones of aligned and concentrated linear features. The analytical techniques used to interpret lineaments from linear features were developed by Sawatzky and Raines (1981). Lineaments are recognized as representative of important structural and tectonic elements (O'Driscoll, 1981, Knepper, 1982, Marrs and Raines, 1984, and Perry, 1985). By

comparing lineaments, surficial expressions, gravity and magnetic data, subsurface expressions, and previously mapped features, structural significance may be determined (Gutman and Heckman, 1977).

The techniques used for deriving lineaments closely follow the methods described by Sawatzky and Raines (1981). The process is divided into three phases. The first phase was image interpretation. Linear features are mapped through conventional photogeologic methods. All non-cultural elements were included. In the second phase, the linear features were digitized and directional trends established. Significant trend intervals were determined and plots of linear features within the significant intervals were generated. Contour plots of the frequency, number of linear features, and concentrations of features were created. Finally, lineaments were interpreted and compared to available ancillary data to establish geologic conclusions. This method was designed to reduce the subjectivity of the image interpreter.

Digital Landsat Thematic Mapper (TM) and Multispectral Scanner (MSS) imagery were acquired for the San Juan Basin of Colorado and New Mexico. Thematic Mapper coverage was limited to the northern portion of the basin overlying the fairway. Thematic Mapper imagery provided additional spatial resolution, 30 meters, necessary to interpret linear features not apparent on the Multispectral Scanner imagery, 79 meters. However, Multispectral Scanner data provided regional coverage that allowed interpretation of linear features and extension of these lineament trends into outcrop surrounding the basin where they are most prominently developed. The reader is referred to Sabins (1987) for additional information regarding imagery characteristics and digital image processing of satellite data.

Interactive digital image processing is essential for producing optimal images for linear feature interpretation. Un-enhanced imagery is more difficult to interpret and subtle features are more easily missed. High pass spatial filtering using a nine kernel, modified Laplacian filter enhanced slight spectral differences crucial to linear feature identification. A TM false-color infrared composite of bands 5, 4, 1 in red, green, and blue was selected since it displayed maximum spectral diversity for this area. An intensity-hue-saturation, IHS, transform was performed to maximize the color representation of the spectral differences inherent in the imagery. The regional MSS imagery mosaic was comprised of four scenes. A standard false-color infrared composite of bands 7, 5, 4 in red, green, and blue, respectively, was processed similarly to the TM imagery.

Linear features were interpreted using standard photogeologic techniques, delineation based upon distinct color-textural-tonal changes, on clear mylar overlays. 1,191 linear features were interpreted on Landsat TM transparencies. Most linear features were expressions of stream segments, escarpments, ridges, and cliffs. Some, however, were derived from tonal and textural differences and are not related to topography. These linear features arose from spectral differences between rock/soil type, vegetation type density, and/or moisture content. Linear feature end points were digitized and linear features plots were generated at identical scales to the interpretation overlays to correct for digitization and duplication errors. Vellum plots of the linear features interpreted from TM were generated at 1:250,000 and 1:100,000 scale. These plots were then registered on USGS topographic maps of equivalent scales and cultural features were eliminated.

The objective of strike-frequency analysis is to determine if statistically significant azimuthal trend intervals exist within a set of interpreted linear features. Significant trend intervals have been shown to represent regional structural trends (Sawatzky and Raines, 1981; Knepper, 1982; and Perry, 1985). A Monte Carlo simulation was used to determine the orientations of mathematically significant linear feature frequency trends, and a modified Monte Carlo simulation was used to determine the orientations of mathematically significant length-weighted linear feature frequency trends. Length-weighted frequency, as well as frequency of linear features, must be accounted for since a single long feature could be represented as numerous linear feature segments.

Significant trend intervals interpreted in this investigation were; N55-50W, N0-5E, N40-45E, and N60-70E (Figure 11). Knepper (1982) identified five important trend intervals in a Landsat MSS study of the Four Corners area; N10W-N16E, N35-72E, N33-59W, N74-83W, and N89-90W - N89-90E. Baumgardner (1991) reported significant trends at N0-10E and N60-80E in Landsat TM imagery of the San Juan Basin. Wandrey (1989), working in the northwestern portion of the basin with aerial photography, reported important trends at N60-80E and N35-70W. Significant regional structural trends identified through linear feature analysis are consistent with previous imagery investigations, dominant face cleat, and paleostress configurations (Figure 14). Figure 11 graphically depicts the relationship between statistically significant trend intervals and an orientated core extracted from the Fruitland coal within the cavity fairway at a depth of slightly more than 3000 feet. The average face and butt cleat trends as well as average open fracture trends are similar to imagery derived surficial trends in the northern San Juan Basin.

Trend interval maps describe the spatial distribution and concentration of linear features. Patterns recognized in these maps define lineaments that may indicate important geologic features. Three types of maps were produced. Linear features within each trend interval were plotted and reveal patterns not evident in the original linear feature interpretation. Contoured frequency and length-weighted frequency plots for each interval depict spatial and density relationships between linear features within the interval. Contoured linear feature maps used in conjunction with the corresponding linear feature maps were used to interpret lineaments.

Lineaments refer to zones of concentrated and aligned linear features. They may be kilometers wide and may offset potential field anomalies or mapped features due to; contouring, component of dip, flight line spacing, and/or interpreter subjectivity. Criteria for lineament interpretation established by Perry (1985) were used. Interpreted lineaments are presented on Figure 12. Six lineaments were interpreted, five from TM data only, and one from a combination of TM and MSS data (NE-2). Lineament designation was determined by the general trend of the lineament, and the order from west to east or south to north.

Ancillary data confirm that some imagery derived

lineaments represent regional and local structural features. NW-2 lies on a gravity defined basinal hingeline that displays dip reversals on the time-structure map of the basement, (Figure 12). This lineament also corresponds to the southern boundary of anomalous coal thicknesses, Figure 6, and the overpressured zone, (Figure 10). Normal faults and fractures mapped at the surface are also coincident with NW-2. NW-1 also correlates well with potential field anomalies and mapped basement faults. N-2 is coincident to recently discovered gas seeps in the Pine River Ranches area and faults in the Hogback Monocline (ARI, 1994). N-1 is proximal to normal faults south of Durango. All interpreted lineaments have some correlation to mapped structures, geophysical discontinuities, and/or stratigraphic anomalies. However, due to the resolution and location of ancillary data, field verification of mapped lineaments is necessary.

Lineaments correlate to subsurface fracture permeability trends. NW-2 defines the southern boundary of prolific production of methane from the Fruitland coals within the basin (Figure 2). Figures 13a and 13b depict the correlation between fluid production from Fruitland coals which is indicative of formation permeability and therefore, presence of reservoir fractures and interpreted structural zones. Fluid production values were generated by an empirical "permeability proxy" relationship of 5 Mcfd gas is equivalent to 1 Bwpd established for the cavity fairway. On Figure 13a, NE-1 is coincident with prolific water production from the Fruitland coals parallel to the Hogback Monocline. A series of gas seeps occur along N-2 at its northern tip in the Pine River Ranches area. Intersections of lineaments are proximal to either prolific production of gas or water from Fruitland coals. An alternative method of displaying the correlation between interpreted imagery features and fluid production is presented in Figure 13b. This figure helps illustrate the point that interpreted lineaments are zones and not lines of determinable width. Linear features within each significant trend interval were gridded according to frequency and length-weighted frequency. These eight grids were then added with equal weighting to form a new grid. This contoured grid has been superimposed on top of fluid production. Again, the correlation between interpreted linear features and fluid production from the Fruitland coals is evident. Units on contours are relative and relate to grid cell size. Areas adjacent to the interpreted lineaments and at their intersections are suspected of possessing characteristics of possible subsurface permeability, since they appear to represent regional structures and fracturing that may be associated with these regional structures.

Criteria 4: Prediction and Confirmation of Subsurface Permeability

The fourth criteria is to determine the present stress regime in the area of interest. The key to understanding the importance of lineament analysis and its relationship to subsurface structure and related fracture permeability comes from understanding the tectonic evolution of the basin. The present-day structural configuration of the San Juan Basin (Figure 14) results from the superposition of Laramide tectonics onto older NW-trending Paleozoic and Precambrian structural trends. Most constraints on basin tectonics comes from detailed studies of the uplifts flanking the basin since there is little basement data from within the basin.

Because of the strong anisotropy that exists in the San Juan Basin, support for a strain partitioning model is found within the modern-day stress configuration. In strain partitioning, regional deformation (e.g. extension), preferentially occurs along pre-existing anisotropies. Instead of continuous regional deformation, strain is partitioned along the dominant anisotropy trends. Such behavior is reflected in the modern stress configuration of the basin. The modern stress configuration varies between the Four Corners Platform and the southeast corner of the San Juan Basin (Wong and Humphrey, 1989). Microseismicity analyses throughout the northwestern San Juan Basin clearly indicate that NE-oriented extension has occurred on NW-trending fault systems. In contrast, microseismicity in the southeastern basin shows NW-oriented extension on NE-trending zones. This orthogonal change in the direction of regional extension probably reflects the controlling influence of the nearest major tectonic features. In the Four Corners region, the dominant influence is Basin-and-Range extension, while the southeastern basin is dominated by Rio Grande rifting. The boundary of the two strain regimes is presently unknown and requires additional investigation. Most importantly, modern seismicity occurs along pre-existing anisotropies/faults throughout the San Juan basin and surrounding regions. Such fault reactivation and opportunistic partitioning of regional strain along older trends has typified structural deformation and regional tectonics in this region since the Proterozoic.

The strain history of the three primary lineament trends recognized by remote sensing imagery analysis (NE, NW, and N-S trends) can be determined using a dynamic structural analysis. By putting the lineament zones into the stress state that existed during a given tectonic phase, it is possible to determine the displacement history of the basement faults that are thought to underlie the lineament zones. The NW-trending linears, NW-1 and NW-2, experienced regional contraction across these trends during the Laramide Orogeny. The Hogback Thrust System (Huffman and Condon, 1993) shows dominant Laramide-age thrust displacement acting on NW-trending structures. NE-trending linears, NE-1 and NE-2, should show some amount of Laramide thrusting, although the obliquity of the linears to the regional principal compressive stress should cause significant sinistral wrench deformation along these trends. The strain history along the NE-trending linears should also show some thrust deformation because proprietary seismic data across the NE-trending segment of the Grand Hogback, parallel to and just west of the NE-1 linear, show thrusting on these trends. The magnitude of the thrusting is less significant than is observed on NW-trending structures. The N-S trending lineaments should also show wrench deformation along these trends. These trends should show dextral offset during the Laramide Orogeny. Careful field documentation of the fault displacement history on minor faults associated with the regional lineaments should confirm the dynamic tectonic interpretation presented above.

During the transition from Laramide tectonism to the modern-day stress regime in the basin, the Laramide contractional, thrust and wrench, tectonics in the basin were reactivated as normal faults in a complex extensional regime dominated by the Basin-and-Range tectonics in the northwest basin, and by the Rio Grande Rift in the southeastern and eastern basin. It is the modern-day stress state that controls which fault and fracture systems are presently dilatant. In the

San Juan Basin, these dilatant trends are the NE and NW-trends. Some dilatancy is probably present along the N-S trending lineaments due to their location in the transition zone between the two regional stress regimes (Basin-and-Range and Rio Grande Rift).

Subsurface permeability in the San Juan Basin coal is a composite of intrinsic permeability (i.e. face cleat and butt cleat), and tectonic fractures. Figure 14 clearly outlines the probable orientations of regional fracture systems. Orientations of face cleat have been mapped throughout the San Juan Basin (Tremain et al., 1991). For most of the basin interior and the southern margin of the basin, the face cleats strike to the northeast, approximately parallel to the axis of Laramide shortening axis. In the northern portion of the basin, the majority of face cleats strike to the northwest. These face cleats appear unrelated to any Laramide shortening, unless they form perpendicular to the shortening axis. A related possibility is that NW-trending face cleats lie parallel to the uplift margins and formed later in the evolution of the basin and are more closely related to thrust deformation along the northern margin of the basin. In this context, the cleats may represent longitudinal fracturing parallel to the regional monocline axes.

The key to understanding the relationship between cleats and tectonic structures lies in understanding the timing of cleat formation. Cleat orientations are always perpendicular to the enclosing strata, despite regions where strata inclination is present (e.g. the Hogback Monocline - Figure 14; Tremain et al., 1991). This observations suggest that cleats form late in the diagenetic history but prior to tectonic deformation. This is confirmed by observations of tectonic fractures crosscutting cleats at most localities (Tremain et al., 1991). In this context, it appears that the most plausible explanation for the polymodal orientations in the basin is that cleats form during the late diagenesis, early deformation phase. Cleats at the northern end of the basin likely reflect the greater warping that occurred in this area. Cleats in the southern basin reflect the far-field regional shortening conditions. Cleat trends in the southeast basin reflect the competing influences of the NW/SE extension axis of the Rio Grande system and the N/S oriented anisotropy of the Nacimiento fault zone.

The San Juan Basin has experienced a complex tectonic history resulting from the early development of a strong regional anisotropy, which has been reactivated during subsequent tectonic phases (Figure 14). Superposition of different regional strain states onto these older structures results in complex strain partitioning along preferred regional orientations. Complex fracture networks, folds and fault zones, which experienced multiple slip events throughout the tectonic evolution of the San Juan basin support this interpretation. Close spatial and orientation relationships between lineaments, core data, structural events, and cleating suggest lineaments are of structural origin and should be related to fracturing and stress settings.

RESULTS AND CONCLUSIONS

Significant findings were the delineation of four easily mappable parameters necessary for successful cavitation programs in the San Juan Basin. These parameters were: 1) friable coals, vitrinite reflectance greater than .75%; 2) fully gas charged coals; 3) reservoir permeability enhanced by tectonic fracturing; and 4) dilatant fracture network.

Exploration target areas were screened using an iterative, heuristic process, set forth on Figures 15, 16, 17, 18 and summarized on Figure 19, based on criteria detailed in the previous sections. Fruitland coal maturity data were available from numerous sources, chiefly, published values by the USGS (Fassett & Hinds, 1971). A thermal maturity cutoff corresponding to a vitrinite reflectance of .75% was selected as a minimum value for acceptable coal strength, thermal maturity, and cleating intensity properties necessary for successful cavitation. Coal thickness and gas contents throughout the northern portion of the basin were sufficient for economic exploitation. Figure 15 depicts locations and completion type of producing coalbed methane wells drilled prior to 12/93. Vitrinite reflectance values greater than 0.75% are represented within the shaded portion of Figure 16. The shaded area encompasses 1,345 square miles, a reduction in basinal exploration area of 80%.

Formation water geochemistry and hydraulic potentiometric surfaces were then used to define areas within the basin where the Fruitland coals have been breached and are being flushed by meteoric waters. Shaded areas of Figure 17 present areas within the basin where vitrinite reflectance is greater than or equal to 0.75%, and where formation fluid composition, greater than 700 mg/l chlorine, and hydrostatic head, greater than 7,000 feet, indicate that the coals have not experienced fresh water infiltration. Formation fluid composition and formation pressure are indicators of open or sealed reservoirs. The shaded area in Figure 13 is 748 square miles, which represents an additional reduction of basinal exploration area by 44%.

Linear feature analysis of digitally enhanced Landsat imagery resulted in the interpretation of six major lineaments within the San Juan Basin. Interpreted lineaments directly correspond to prolific coalbed methane production, previously mapped structural zones (Dart, 1992), surficial and basement faults, and geophysical discontinuities. Statistically significant azimuthal trends depicted by the linear features also represent expected fracture orientations. These fracture orientations result from present and past stress regimes, which were determined from a regional tectonic analysis. Regions adjacent to geologically significant lineaments and at their intersections are more likely than other areas to exhibit subsurface fracturing.

Figure 18 shows shaded areas that possess acceptable coal ranks, which have not been breached, and which are spatially associated with structurally significant lineaments. Gridded linear feature frequency and length-weighted frequency data for each significant trend interval were added with equal weighting. The resultant value was gridded and contoured. This value represents concentrations of linear features within statistically defined geologically significant trend intervals. A cut-off value was determined empirically. The value is dependant upon grid cell size. This area represents 6% of the total area of the San Juan Basin. It is also apparent from comparing Figure 15 and Figure 18 that the overwhelming majority of cavity completions lay within the shaded area.

Figure 19 graphically summarizes the results and accuracy

of the criteria for locating coalbed methane cavitation production fairways. The San Juan Basin encompasses an area of approximately 6,760 square miles measured along the Fruitland Formation outcrop. Fruitland coals with a vitrinite reflectance greater than 0.75% account for an area of approximately 1,345 square miles. Of this 1,345 square miles, only 748 square miles appear to have unbreached reservoir characteristics. Additional refinement of the 748 square miles by assessing the probable extent and interconnected nature of the subsurface fracture network, results in an exploration target area of approximately 404 square miles. The exploration target area represents less than 6% of the basinal exploration area.

Within the San Juan Basin, the ratio of coalbed methane cavity wells that produce more than one million cubic feet of gas per day per well to all coalbed methane wells is approximately 1 to 4. In areas limited to coals with a vitrinite reflectance of .75% or greater, the ratio is 1 to 3. Restricting the exploration areas to coals with vitrinite reflectance of 0.75% and higher, with an unbreached reservoir, increases the ratio to 2 to 3. Further limitation of the exploration areas utilizing integrated imagery interpretations increases the ratio to 8 to 10. By using the exploration criteria outlined in the technical approach section, a 94% reduction in the amount of potential exploration area to be considered was achieved. The benefit is a more than a three fold increase in the probability of drilling a successful coalbed methane well than could have been achieved by using conventional exploration methods.

The easily mappable geologic parameters outlined above assist in delineating potential economic cavity fairways in coal-bearing basins. The necessary data are readily available for most domestic and international basins. As part of an integrated exploration effort that considers dynamic rock mechanical properties, the methodology and criteria developed in this paper provide the essential framework for establishing a successful coal cavity completion development program. The successful application of this program to the San Juan Basin has spawned additional exploration programs in other basins. Success to date in these other basins indicates the widespread utility of the multi-criteria, integrated approach to exploration and development programs in other unconventional reservoirs such as tight gas sands and fractured shales.

ACKNOWLEDGMENTS

The authors would like to acknowledge financial support for this paper and the associated research project from the U.S. Department of Energy, Morgantown Energy Technology Center, SBIR Phase I contract DE-FG03-93ER81502. We also thank Anderson Geoconsultants for providing image processing and hardcopy generation services.

REFERENCES

1. ARI, 1994: "Gas Seepage in the Pine River Area, Colorado," prepared for Colo. Oil and Gas Comm., Nov., 1994.

2. Ayers, W.B., et al, 1991: "Geologic and Hydrologic Controls on the Occurrence and Producibility of Coalbed Methane, Fruitland Formation, San Juan Basin," The Univ. of Texas at Austin, Bur. of Eco. Geol., Topical Report prepared for GRI under contract 5087-214-1544.

3. Baumgardner, R.W., 1991: "Comparative Lineament Analysis of the San Juan Basin: Relationships between Lineament Attributes and Coalbed Methane Production in Upper Cretaceous Fruitland Formation, San Juan Basin, Colorado and New Mexico: Implications for Coalbed Methane Exploration and Development," *in* Ayers, W.B., et al, 1991, Geol. and Hydro. Controls on the Occurrence and Producibility of Coalbed Methane, Fruitland Formation, San Juan Basin, The Univ. of Tex. at Austin, Bur. of Eco. Geol., Topical Rpt. prepared for GRI under contract 5087-214-1544, p. 153-179.

4. Dart, S.W. Jr., 1992: "Evaluation of San Juan Basin Fractured Reservoirs from Surface Data," *in:* J.W. Schmoker, E.B. Coalson, and C.A. Brown, eds., Geol. Studies Relevant to Horizontal Drilling: Examples from Western N. Am., RMAG 1992 Guidebook, p. 95-114.

5. Decker, A.D., Close, J.C., and R.A. McBane, 1989: "The Use of Remote Sensing, Curvature Analysis, and Coal Petrology as Indicators of Higher Coal Reservoir Permeability," Proc., 1989 Coalbed Methane Sym., the Univ. of Alabama, Tuscaloosa, p. 325-340.

6. Fassett, J.E. and J.S. Hinds, 1971: "Geology and Fuel Resources of the Fruitland Formation and Kirtland Shale of the San Juan Basin, New Mexico and Colorado," U.S. Geol. Sur. Prof. Paper 676, 76 p.

7. Gutman, S.I., and G.A. Heckman, 1977: "An Integration of Landsat and Geophysical Data in Northeastern Arizona," GS Laboratories, Rpt. of Invest., U.S. Geol. Sur. contract 94599, 47 p.

8. Huffman, A.C. and S.M. Condon, 1993: "Stratigraphy, Structure and Paleogeography of Pennsylvanian and Permian Rocks, San Juan Basin and Adjacent Areas, Utah, Colorado, Arizona, and New Mexico," U.S. Geol. Sur. Bull. 1808-0, 44 p.

9. Kaiser, W.R., Swartz, T.E., and G.J. Hawkins, 1991: "Hydrology of the Fruitland Formation, San Juan Basin," *in:* Ayers, W.B., et al., Geol. and Hydro. Controls on the Occurrence and Producibility of Coalbed Methane, Fruitland Formation, San Juan Basin, The Univ. of Tex. at Austin, Bur. of Eco. Geol., Topical Rpt. prepared for GRI under contract 5087-214-1544, pp. 195-241.

10. Knepper, D.H., 1982: "Lineaments Derived from Analysis of Linear Features Mapped from LANDSAT Images of the Four Corners Region of the Southwestern United States," U.S. Geol. Sur. Open-File Rpt. 82-849, 79 p.

11. Marrs, R.W., and G.L. Raines, 1984: "Tectonic Framework of the Powder River Basin, Wyoming and Montana, Interpreted from Landsat Imagery," Am. Assoc. of Pet. Geol. Bull., v. 68, p. 1718-1731.

12. Mingzhu, Fan, 1993: Presentation Coalbed Methane Symposium, December 10, Lakewood, Colorado.

13. O'Driscoll, E.S.T., 1981: "Structural Corridors in Landsat

Lineament Interpretation," Mineral Deposits, v. 16, 85-101.

14. Perry, S.L., 1985: "Lineaments of the Northern Denver Basin and their Paleotectonic and Hydrocarbon Significance," unpublished M.S. theses, Colo. School of Mines, 111 p.

15. Sabins, F.F. Jr., 1987: "Remote Sensing - Principles and Interpretation," Second Ed., NY, W.H. Freeman and Co.

16. Sawatzky, D.L., and G.L. Raines, 1981: "Geologic Uses of Linear Feature Maps Derived from Small-Scale Images," *in* O'Leary, D.W., and J.L. Earle, eds., International Conf. on Basement Tectonics, Third, Durango, CO 1978.

17. Scott, A.R., Kaiser, W.R., and W.B. Ayers, Jr., 1991: "Thermal Maturity of Fruitland Coal and Composition and Distribution of Fruitland Formation and Pictured Cliffs Sandstone Gasses," *in:* W.B. Ayers, et al., Geol. and Hydro. Controls on the Occurrence and Producibility of Coalbed Methane, Fruitland Formation, San Juan Basin, The Univ. of Tex. at Austin, Bur. of Eco. Geol., Topical Rpt. prepared for GRI under contract 5087-214-1544, pp. 243-270.

18. Stevenson, G.M., 1983: "Paleozoic Rocks of the San Juan Basin: An Exploration Frontier," *in*: Four Corners Geol. Soc. pub., Oil and Gas Fields of the Four Corners Area, 780-788.

19. Suits, V.J., and L. Cordell, 1981: Bouguer Gravity Map of the San Juan Basin Region, Colorado, Arizona, and New Mexico, U.S. Geol. Sur. Open-File Rpt. 81-657, Scale 1:500,000.

20. Tremain, C.M., Laubach, S.E. and N.H. Whitehead, III, 1991: "Coal Fracture (Cleat) Patterns in Upper Cretaceous Fruitland Formation, San Juan Basin, Colorado and New Mexico: Implications for Coalbed Methane Exploration and Development," *in*: W.B. Ayers et al., 1991, Geol. and Hydro. Controls on the Occurrence and Producibility of Coalbed Methane, Fruitland Formation, San Juan Basin, The Univ. of Tex. at Austin, Bur. of Eco. Geol., Topical Rpt. prepared for the GRI under contract 5087-214-1544, 97-117.

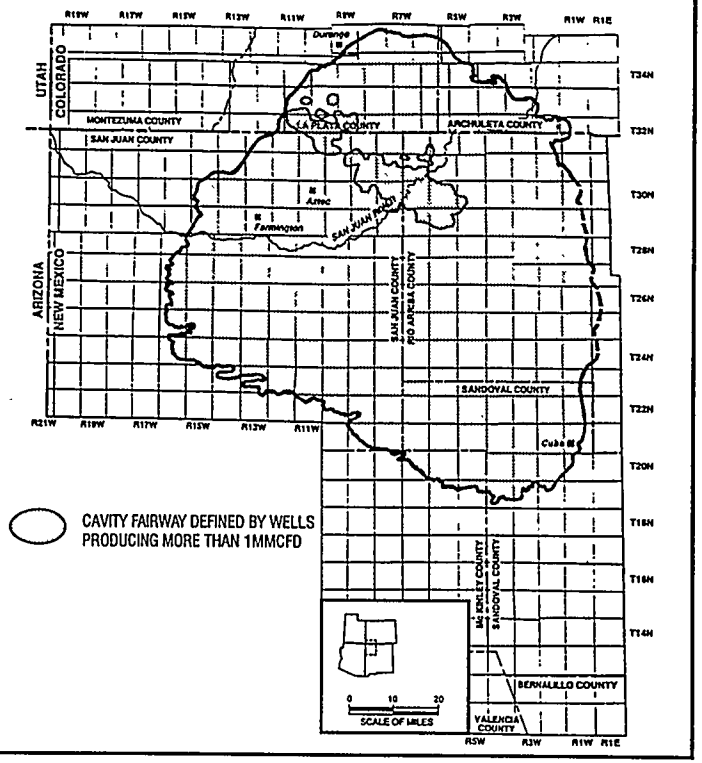
21. Wandrey, C.J., 1989: Lineament Map of Part of the Southern Ute Reservation, San Juan Basin, Southwestern Colorado, U.S. Geol. Sur. Open File Rpt. 89-112, Scale 1:100,000.

22. Welte, D.H., et. al., 1981: "Application of Organic Geochemistry and Quantitative Analysis to Petroleum Origin and Exploration - an Approach for a Quantitative Basin Study," *in:* G. Atkinson and J.J. Zucherman, eds., Origin and Chem. of Pet., Pergamon Press, Elmsford, N.Y., pp. 67-88.

23. Wong, I.G. and J.R. Humphrey, 1989: "Contemporary Seismicity, Faulting and the State of Stress in the Colorado Plateau," Geol. Soc. of Am. Bull. 101, 127-1146.

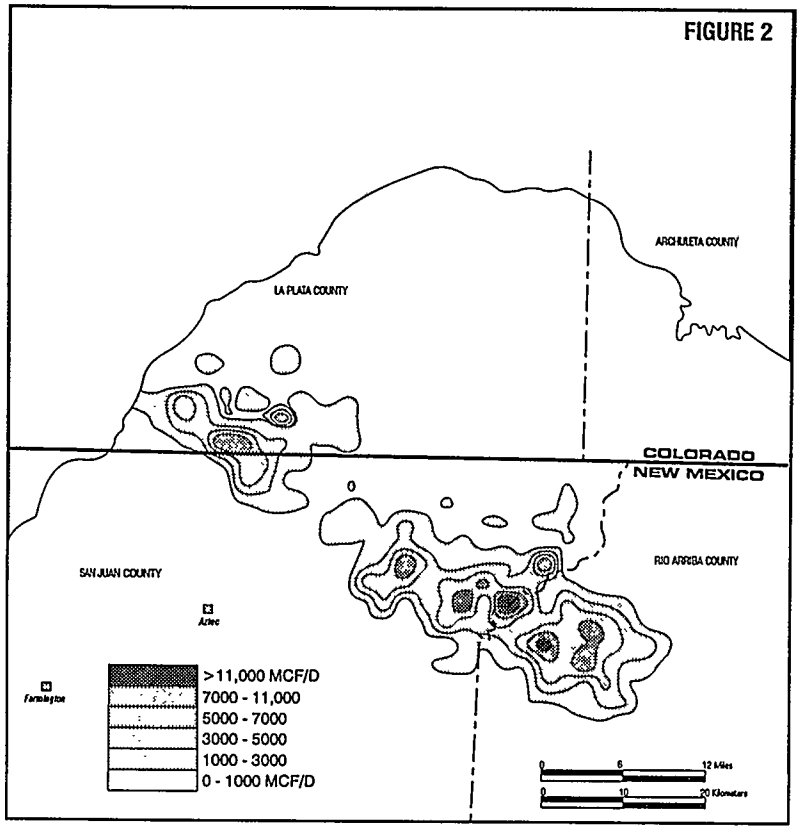
SAN JUAN BASIN LOCATION MAP

FIGURE 1



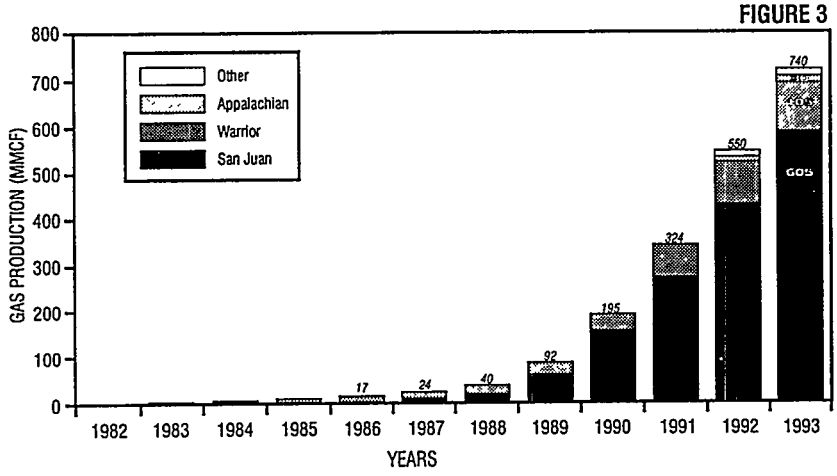
AVERAGE DAILY GAS PRODUCTION FROM FRUITLAND COALS IN CAVITATION FAIRWAY

FIGURE 2



GROWTH IN COALBED METHANE GAS PRODUCTION

FIGURE 3



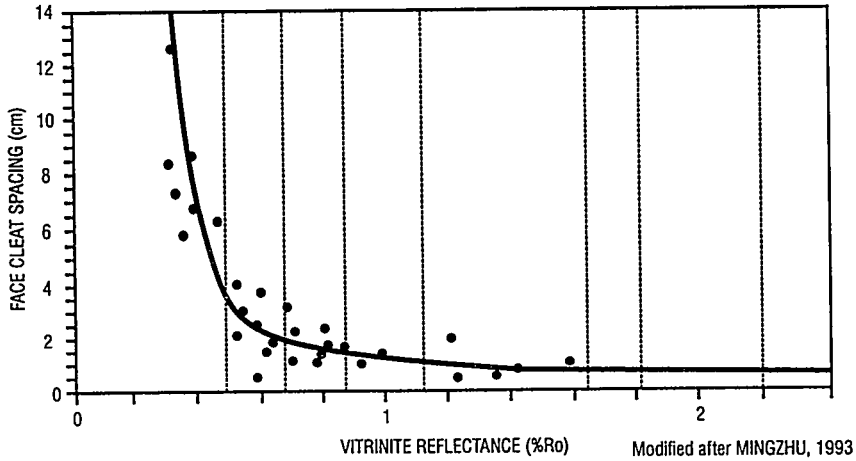
INFLUENCE OF CAVITY COMPLETIONS UPON COALBED METHANE PRODUCTION

TABLE 1

	SAN JUAN BASIN						OTHER BASINS	TOTAL ALL BASINS
	Open-Hole Cavity		Other		Total			
	#	%	#	%	#	%		
Currently Producing Wells	600	9	2,100	32	2,700	41	3,900	6,600
	BCF/D	%	BCF/D	%	BCF/D	%	BCF/D	%
1993 Estimated Gas Production	1.2	60	0.4	20	1.6	80	0.4	2.0

RELATIONSHIP BETWEEN VITRINITE REFLECTANCE VALUES AND FACE CLEAT SPACING

FIGURE 4



Modified after MINGZHU, 1993

VITRINITE REFLECTANCE OF THE FRUITLAND COALS

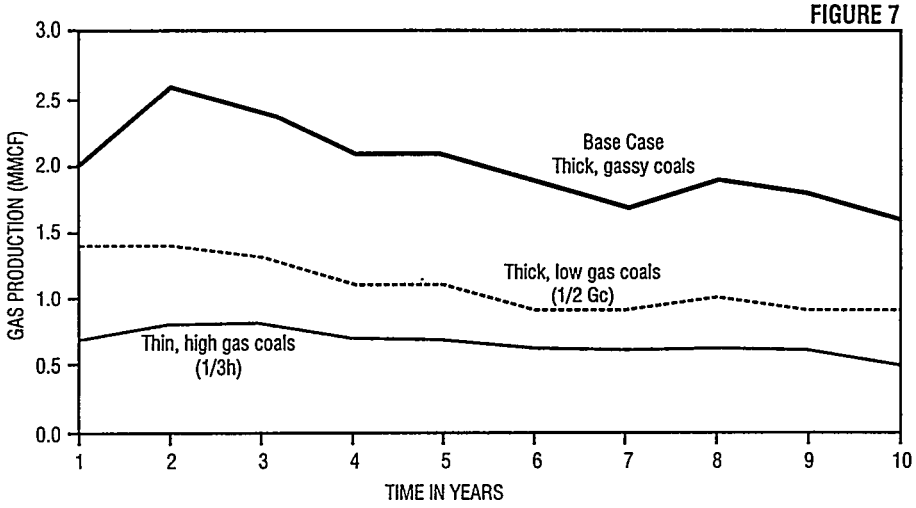
FIGURE 5

NET COAL THICKNESS OF FRUITLAND FORMATION

FIGURE 6

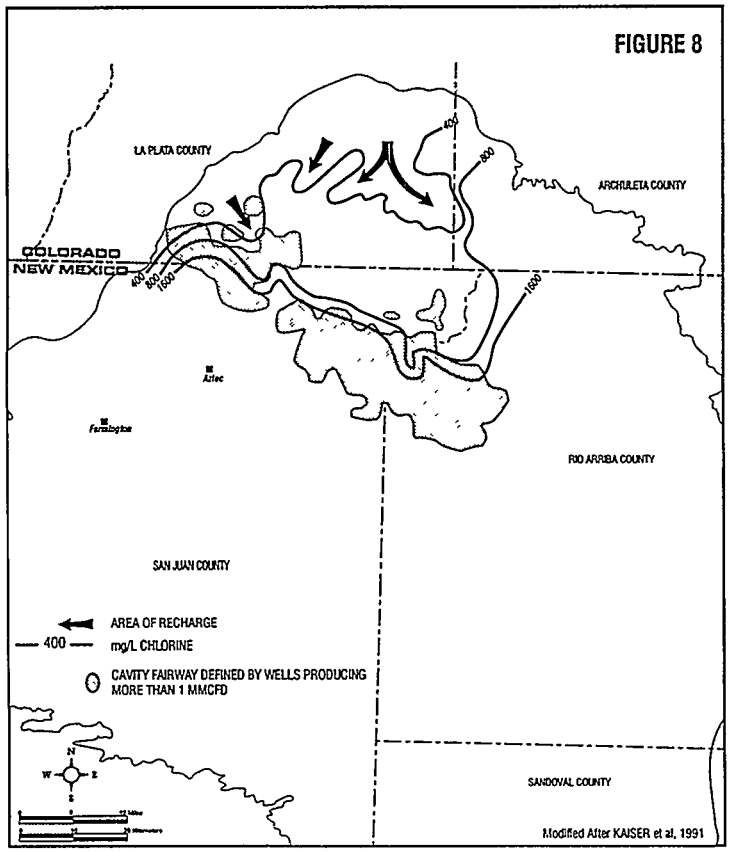
DIFFERENCE IN GAS PRODUCTIVITY DUE TO GAS CONTENT AND COAL THICKNESS

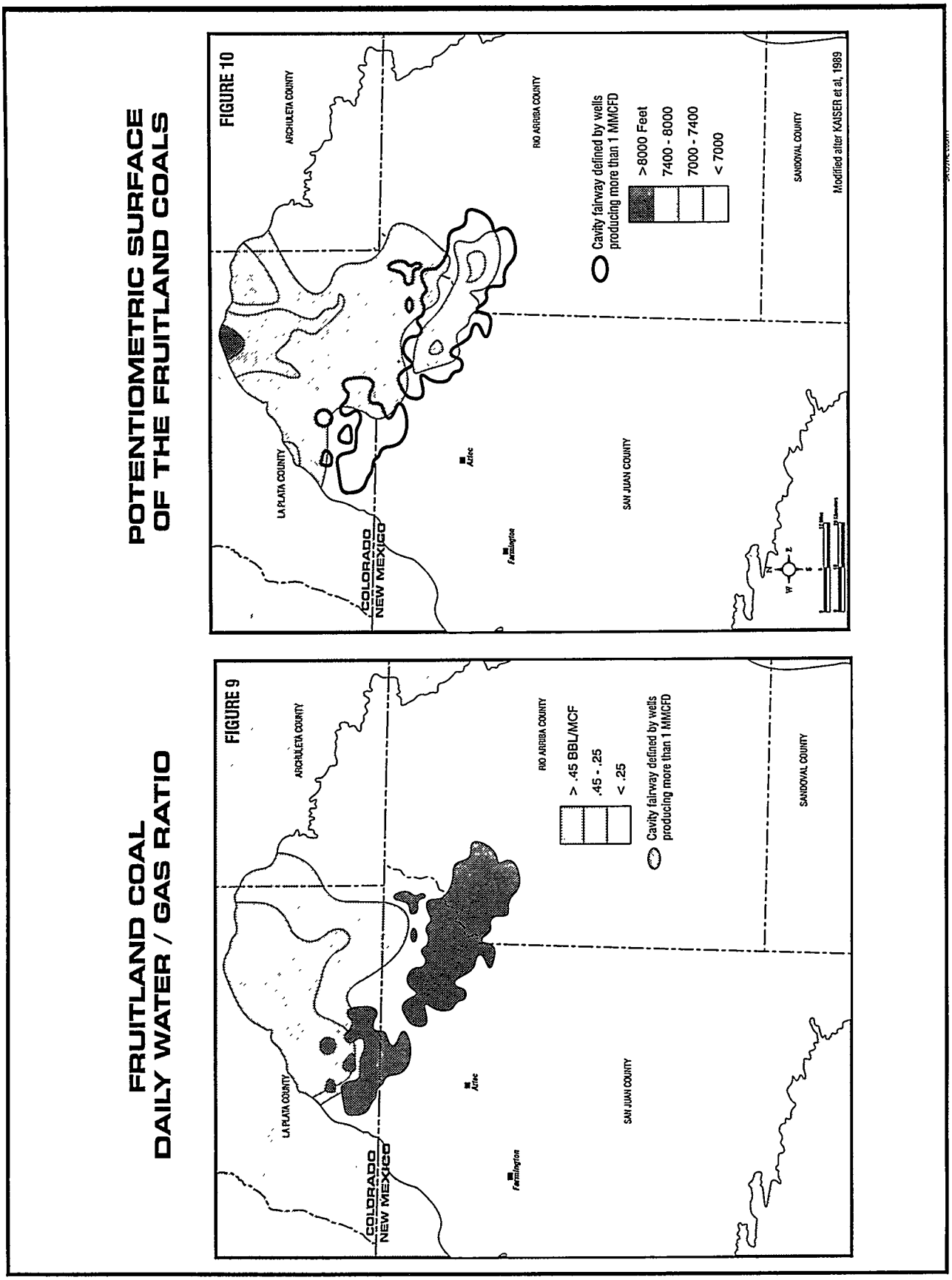
FIGURE 7



NORTHERN SAN JUAN BASIN
CHLORINITY CONTENT OF WATERS PRODUCED FROM FRUITLAND COALS

FIGURE 8




FRUITLAND COAL
DAILY WATER / GAS RATIO
FIGURE 9
ARCHULETA COUNTY
LA PLATA COUNTY
RIO ARRIBA COUNTY
SAN JUAN COUNTY
SANDOVAL COUNTY
COLORADO
NEW MEXICO
Aztec
Farmington
> .45 BBL/MCF
.45 - .25
< .25
Cavity fairway defined by wells producing more than 1 MMCFD
POTENTIOMETRIC SURFACE
OF THE FRUITLAND COALS
FIGURE 10
>8000 Feet
7400 - 8000
7000 - 7400
< 7000
Modified after KAISER et al, 1989

RESIDUAL BOUGUER ANOMALY MAP OF THE SAN JUAN BASIN WITH INTERPRETED LINEAMENTS

FIGURE 12

Modified After SUITS and CORDELL, 1981

FIGURE 11

SIGNIFICANT LINEAR FEATURE, AZIMUTHAL TRENDS NORTHERN SAN JUAN BASIN

Length-Weighted Frequency of Interpreted Linear Features From Landsat TM Imagery

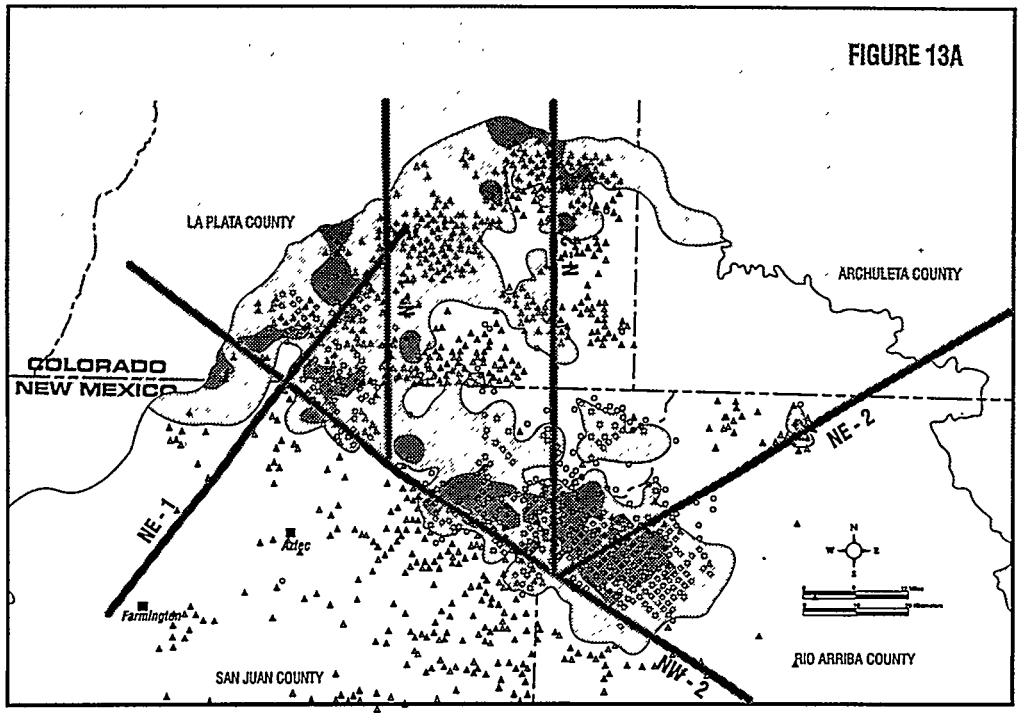
Number of Linear Features = 1191
Corrected to True North

FRUITLAND COAL CLEAT TRENDS FROM ORIENTATED CORE FRACTURE ANALYSIS CEDAR HILL FIELD, HAMILTON NO. 3

DECKER, CLOSE & McBANE, 1989

NORTHERN SAN JUAN BASIN
FLUID PRODUCTION FROM FRUITLAND COALS

FIGURE 13A



NORTHERN SAN JUAN BASIN
FLUID PRODUCTION FROM FRUITLAND COALS
WITH CONTOURED LINEAR FEATURES

FIGURE 13B

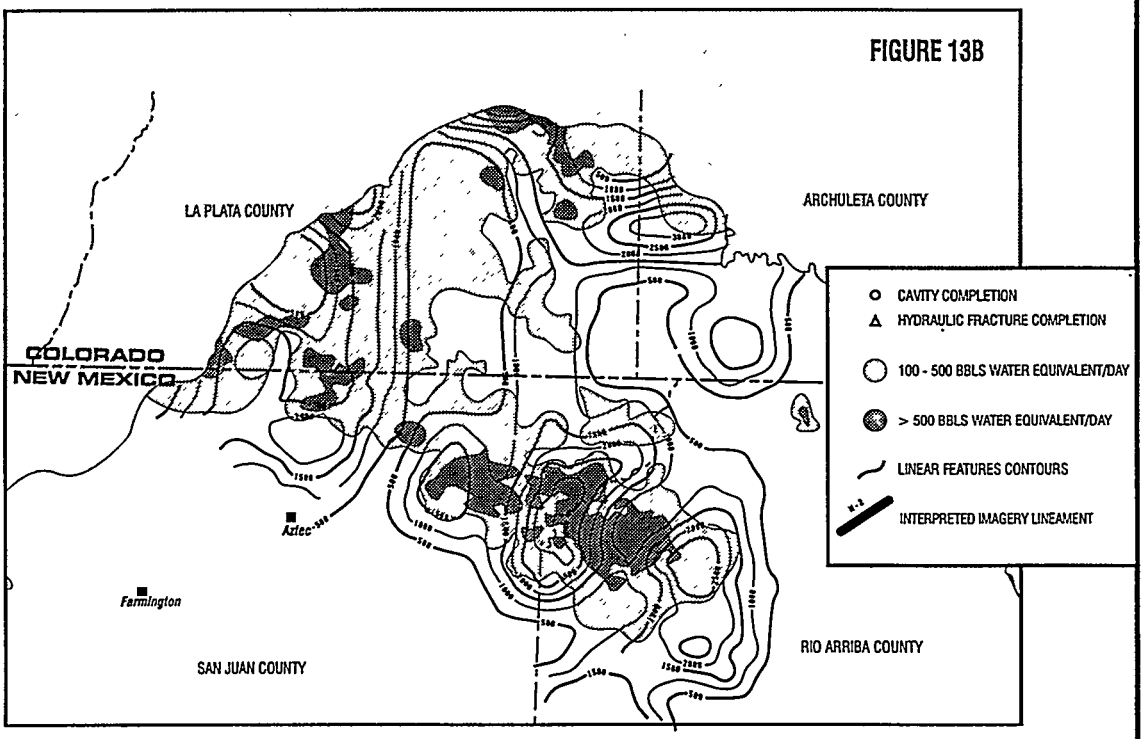
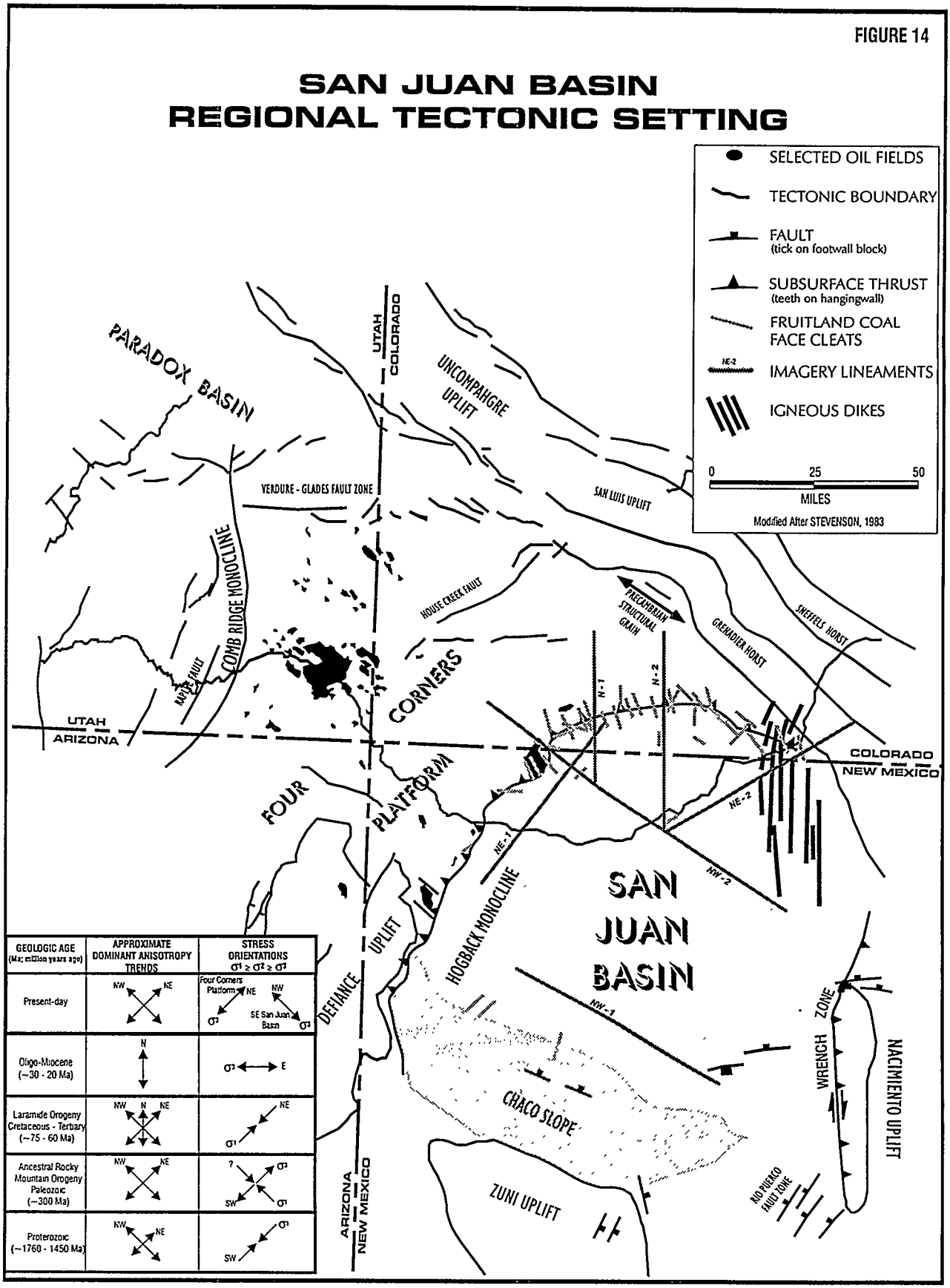
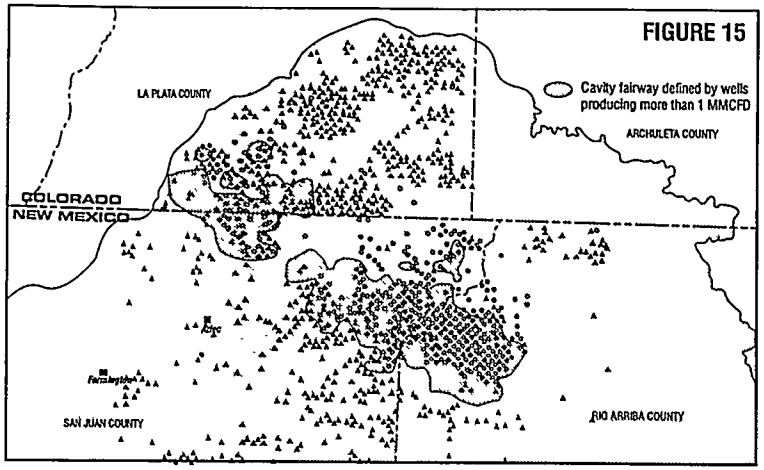


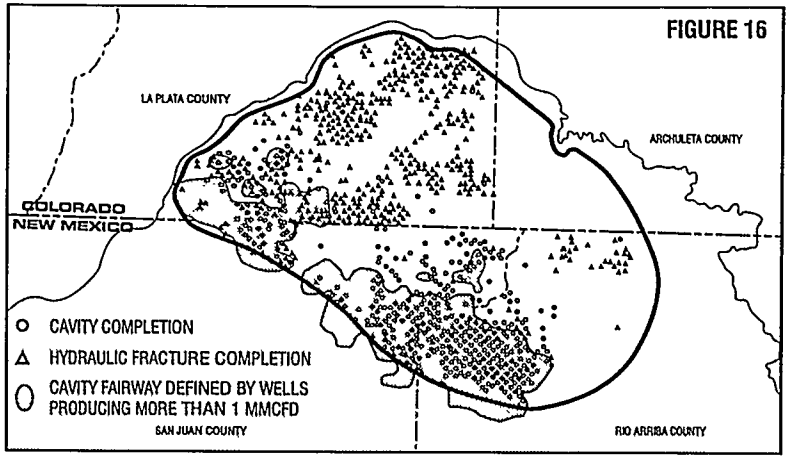
FIGURE 14


SAN JUAN BASIN
REGIONAL TECTONIC SETTING
SELECTED OIL FIELDS
TECTONIC BOUNDARY
FAULT
(tick on footwall block)
SUBSURFACE THRUST
(teeth on hangingwall)
FRUITLAND COAL FACE CLEATS
NE-2
IMAGERY LINEAMENTS
IGNEOUS DIKES
0 25 50
MILES
Modified After STEVENSON, 1983
PARADOX BASIN
UTAH
COLORADO
UNCOMPAHGRE UPLIFT
VERDURE - GLADES FAULT ZONE
SAN LUIS UPLIFT
COMB RIDGE MONOCLINE
HOUSE CREEK FAULT
PRECAMBRIAN STRUCTURAL GRAIN
GRENADIER HORST
SHEEFELS HORST
NOOSE FAULT
UTAH
ARIZONA
CORNERS
FOUR
PLATFORM
COLORADO
NEW MEXICO
N-1
N-2
NE-2
NE-1
NW-2
SAN
JUAN
BASIN
DEFIANCE
UPLIFT
HOGBACK MONOCLINE
NW-1
WRENCH ZONE
NACIMIENTO UPLIFT
CHACO SLOPE
ZUNI UPLIFT
RIO PUERCO FAULT ZONE
ARIZONA
NEW MEXICO
GEOLOGIC AGE (Ma; million years ago)
APPROXIMATE DOMINANT ANISOTROPY TRENDS
STRESS ORIENTATIONS σ1 ≥ σ2 ≥ σ3
Present-day
Four Corners Platform
SE San Juan Basin
Oligo-Miocene (~30 - 20 Ma)
Laramide Orogeny Cretaceous - Tertiary (~75 - 60 Ma)
Ancestral Rocky Mountain Orogeny Paleozoic (~300 Ma)
Proterozoic (~1760 - 1450 Ma)

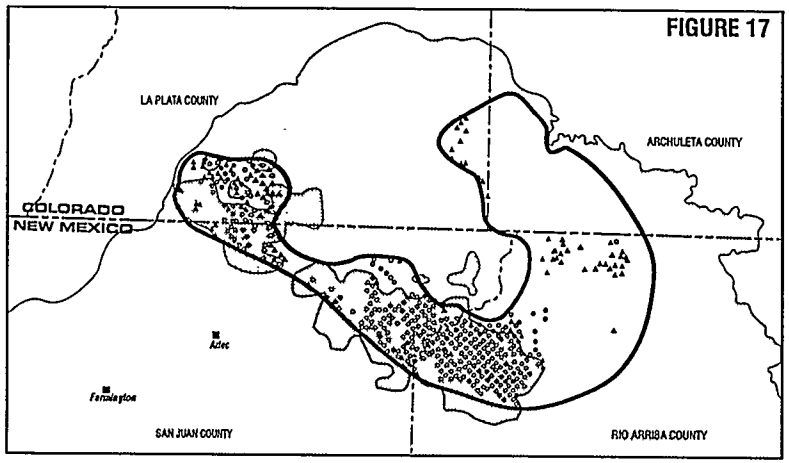
LOCATION OF COALBED METHANE WELLS BY COMPLETION TYPE



NORTHERN SAN JUAN BASIN AREAS WHERE FRUITLAND COAL VITRINITE REFLECTANCE >0.75



NORTHERN SAN JUAN BASIN AREAS WHERE FRUITLAND COAL VITRINITE REFLECTANCE > 0.75 AND RESERVOIR IS NOT BREACHED



NORTHERN SAN JUAN BASIN PARTITIONING BY VITRINITE REFLECTANCE, RESERVOIR INTEGRITY, AND IMAGERY ANALYSIS CRITERIA

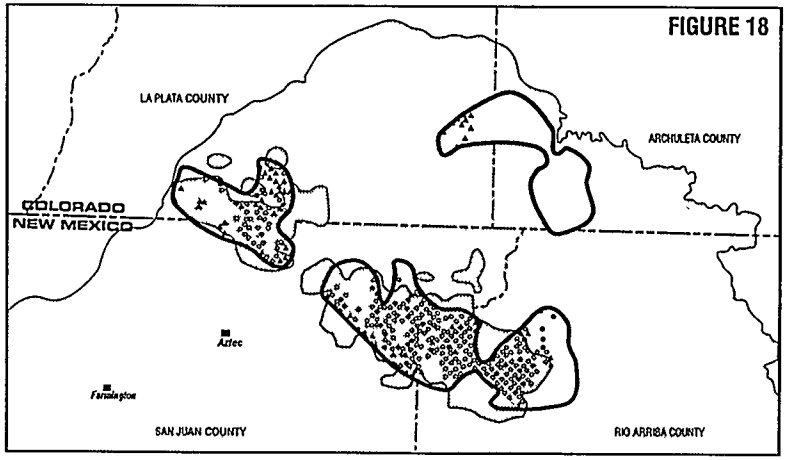
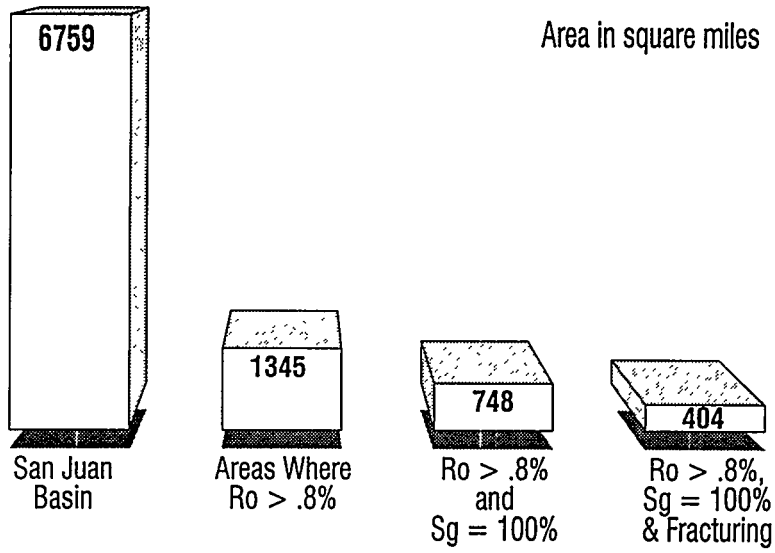


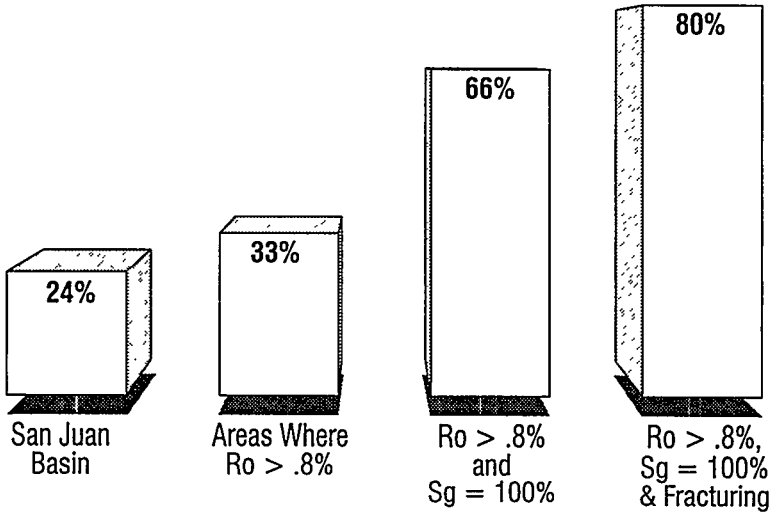
FIGURE 19

GRAPHIC SUMMARY OF RESULTS AND ACCURACY OF EXPLORATION CRITERIA IN THE SAN JUAN BASIN

SELECTION AND PARTITIONING OF CAVITATION FAIRWAY BY GEOLOGIC AND IMAGERY CRITERIA



PERCENTAGE OF CAVITATED WELLS PRODUCING GREATER THAN 1MMCF/D TO TOTAL NUMBER OF WELLS IN PARTITION



INTERGAS '95

May 15-19, 1995
The University of Alabama
Tuscaloosa, Alabama USA

9549

Characteristics and Economics of Coalbed Methane Production from the Fort Union Formation, Powder River Basin

J.R. Holland, J.R. Holland & Associates, Inc.; and J.W. Kimmons, Torch Operating Company

ABSTRACT

The Fort Union Formation contains thick deposits of subbituminous coals over a large area of eastern Wyoming and Montana. These low rank coals appear to contain relatively low volumes of methane, probably less than 100 scf/ton. The coals are thick, over 100 feet in many areas, and hold large volumes of gas. In Campbell County, Wyoming, the Fort Union coals are relatively shallow and the costs of drilling are low.

Betop Inc., Martens & Peck and Wyatt Petroleum have been the most active operators in Campbell County. Prior to December 31, 1992, Martens & Peck drilled 78 wells near Gillette, Wyoming into the Anderson-Wyodak coal seams. This coal outcrops along a north-south line just east of Gillette. Coalbed methane wells in this area are typically 300' to 800' deep. The Martens & Peck wells south of Gillette began producing gas in May 1993. In April 1994 these wells were bought by Torch Operating Company.

The production from these Torch wells, and recent estimates of the development and operating costs, are used to evaluate the economic performance of this coalbed methane project. These new projections are then compared with the earlier projections (1990) made by Hobbs who used data from the Rawhide Butte Field north of Gillette. These projections indicate that new shallow coalbed methane wells drilled in Campbell County, Wyoming should have favorable economic performances if low capital and operating costs can be achieved.

INTRODUCTION

The Powder River Basin of northeastern Wyoming and southeastern Montana covers an area of 25,800 square miles and is the largest intermontane basin east of the thrust belt. The Basin contains a vast resource of coal. The Paleocene coals in the Tongue River Member of the Fort Union formations, have been estimated by Ayers to total 1.16 trillion short tons of low sulfur, subbituminous coal to a depth of 3000 ft. [1]. The methane gas contained in these coals also represents a large potential resource even though the gas content per ton of coal is relatively low. The basin has been estimated to have generated as much as 1,500 trillion cubic feet of biogenic methane. It is estimated that up to 39 trillion cubic feet of this gas is stored in the coalbeds in the basin. Also, some of the gas generated has migrated into the associated shales and sandstones and much of this gas may be still retained in structural and stratigraphic traps and at structural highs in or near the coal. A large volume of the gas generated has escaped over geologic time to the upper atmosphere.

Much of the 39 TCF stored in the coals occurs at relatively shallow depths, less than 2,500 ft. Because of the shallow depth, and the occurrence of individual coalbeds of 100 ft. or greater in thickness, and sequences of coalbeds to 250-300 ft. in net thickness, the Powder River Basin appears to provide an excellent opportunity for the economic recovery of coalbed methane. These Fort Union coals have permeabilities in the range of 10 md to several darcys with many of coals apparently being in the range of approximately 50-100 md.

The eastern and northeastern margins of the Basin (see Figure 1) appear to offer the greatest potential for methane recovery for the following reasons:

a) The Wyodak, Anderson, Dietz, Canyon, Cook, Wall, Pawnee, and Cache coalbeds are relatively shallow.

b) In some areas near Gillette, Wright, Recluse and Buffalo, Wyoming, these coals are very thick. Near Gillette, the Wyodak, Anderson, Canyon and Dietz beds converge to form a superbed with thickness ranging from 50 to over 150 ft. Near Buffalo the Wasatch coals (Eocene) are reported to be over 200 ft. thick.

c) The Wyodak-Anderson bed is being actively strip mined along the eastern margin in the central portion of the Basin near Gillette, Wyoming.

d) The Anderson, Dietz, Canyon and Wall beds are being strip mined to a lesser extent, along the northeastern margin of the Basin in southeastern Montana.

e) Proximity of strip mining should aid in water removal, if the mines are updip from a coalbed methane development. However, if the development is too close to the mine there may be a significant loss of gas.

f) Existing coalbed methane wells near the eastern margin have water initial rates of production (IP's) typically in the range of 300 to 600 bbls/day.

g) Gas pipelines generally run along or across the eastern and northeastern margins of the Basin.

h) Historically the eastern margin has been an active area for oil and gas developments below 5000 ft. in the upper and lower Cretaceous and Pennsylvanian formations.

i) The coalbeds on the eastern and northeastern flanks of the basin dip at 0.4 to 1.0 degrees westward toward the Basin center (near the Powder River).

j) Surface topography is generally favorable.

Prior Methane Developments

Much of the earlier efforts to recover biogenic methane have focused either on the Fort Union sandstones in the vicinity of Recluse and Spotted Horse, Wyoming, or on very thick coals nearer to the Basin axis (see Figure 1). By year end 1992, approximately 250 wells had been drilled. These drilling activities have been described by Larsen [2], Jones and DeBruin [3], Randall [4, 5], the Quarterly Review of Methane [6], and Tyler et al. [7]. The wells near Recluse reported early success, and, apparently many coalbed methane wells in the Carson, Chan, Oedekoven, Recluse, and Spotted Horse gas fields have been moderately successful.

The deeper wells drilled nearer the basin axis, e.g. in T49N, R75W and in T48N, R77W and 76W, have, by and large, been either shut in or abandoned because of the large volumes of water produced. Water IP's from these wells are reported to be as high as 3000 bbl/d, and average about 1500 bbl/d. Gas production from these wells was low.

WELLS STUDIED

In the spring of 1994, Torch Energy purchased a 66.67% working interest in two coalbed methane producing properties in Campbell County, Wyoming [8]. These properties were drilled and developed by Martens and Peck Operating Company of Denver, Colorado. A total of 78 wells were drilled into the Wyodak-Anderson coals on these properties between 1989 and the end of 1992. These two properties will be referred to in this paper as the Rawhide Butte Field and the Marquis Field. The Rawhide Butte Field is adjacent to the airport which is just north of Gillette. This field contains over 30 wells; 15 of these were drilled by Martens and Peck prior to 1991. Most of the other wells were drilled by Betop, Inc. Many of the wells in the Rawhide Butte Field were drilled only into the upper levels of the Wyodak-Anderson coal seam; approximately 10 to 15 feet of this coal were drilled. This coal is estimated to be over 70 feet thick in this area. Historically the wells in the Rawhide Butte Field were not pumped, but have produced water and gas from unassisted flow from the wells. Artesian flow is a frequent occurrence in Campbell County. These Rawhide Butte wells will require pumps to achieve their full economic life. Because most of the coal seam was not penetrated and the Rawhide Butte Field production is largely unaided by pumping, we consider these 15 wells to be atypical of the coalbed methane wells in the Powder River Basin. We have not included them in this study.

More recently, Martens and Peck drilled 63 wells in the Marquis Field which lies in parts of three townships (T48N, R72W; T47N, R71 and 72W) south of Gillette, see Figure 1. This field extends some 8 to 9 miles in a north-south direction along the eastern margin of the Powder River Basin. Most of these wells were drilled prior to the end of 1992; 55 out of the 63 wells qualify for the Section 29 Tax Credits. These wells were drilled through the Wyodak-Anderson coal seam. The coals were left open hole and were not stimulated. The wells were equipped with submersible pumps similar to those used in water wells in the region. In this study we have assumed that this group of 63 wells in the Marquis Field is prototypical of coalbed methane development and expected production along the eastern margin of the Powder River Basin.

METHODOLOGY

In making this evaluation of the production characteristics and economics of coalbed methane development in the Powder River Basin, we analyzed the gas and water production data, and the lease operating costs supplied by Torch Energy for their 63 wells in the Marquis Field. Historical production data for the 63 wells and the operating conditions in the field were reviewed in order to prepare a suitable gas production curve for the Marquis Field. Our estimates of the production were then compared with estimates prepared by others for similar coalbed methane production.

The difficulties encountered in preparing a gas production/decline curve for the Marquis Field arise from two factors, (a) the short production history (wells began to come on line in May 1993) and (b) gas production was severely constrained by the compressor capacity. It is expected that this constraint will be removed early in 1995. In this study we have assumed that since April 1994, when Torch acquired these wells, the gas production has not been constrained by the compressor capacity. The period for this study is from April 1994 through the year 2008.

The economic model used for this study estimated the gross revenues for the Marquis project from the production/ decline curve and a gas price scenario. The capital cost for the Marquis project was estimated from public information concerning the acquisition costs. Operating costs for the Marquis Field were estimated based on the cost of Torch operations in 1994. Engineering estimates for additional expenses for well maintenance and workovers were made on the basis of prior experience with coalbed methane wells operations.

The Marquis Field was assumed to be burdened with a 25% interest in royalties and over-rides, leaving a 75% net revenue interest for the working interests (100%). Torch purchased 66.67% of this working interest. The net revenues and tax credits to this interest were determined and compared with the estimated acquisition (or developmental) costs. The internal rates of return, return on investment and present values were estimated for the fifteen year period.

MODEL INPUTS

Reserves

Wells in the study are on nominal 40 acre spacings. The wells were drilled in clusters or pods, which were on structural highs. The separation between clusters varies, but typically is greater than one mile. These well pods are elongated along a north-south axis and, usually, are only 1 to 3 spacings wide. Almost all wells are on the perimeter of these elongate patterns and are able to drain an area much greater than the nominal well spacing, see Figure 2. These pods contain from 4 to 15 wells. In Figure 2, the pod contains 9 wells on 40 acre spacings or 360 acres total. Considering the high permeability of the coal, estimated to be over 100 md, the actual drainage area for the pod is probably much closer to the shaded area. This total drainage area is estimated to be approximately 1100 acres; the average drainage per well is just over 120 acres. For the purpose of estimating in place reserves per well, a drainage area of 120 acres per well was used in this study. This may be less than the area eventually drained over the economic life of these wells, but allows for a conservative estimate of reserves, see Table I.

Original gas in place per well was calculated based on an average coal thickness of 75 feet, gas content of 55 scf per ton of coal, a drainage area of 120 acres, and 1700 tons of coal per acre-foot. The calculated in place reserves per well were 841,500 mcf.

Production/Decline Curve

The production/decline curve was developed starting from April 1994 when Torch took over operation of the wells. At that time the Marquis Field was producing 4400 mcfd or approximately 70 mcfd per well and the gas production was constrained. From this point we estimated the production on an unconstrained basis. The gas production was projected, see Figure 3, from this initial point, through the three production stages usually experienced with coalbed methane wells, i.e. Stage I - dewatering with rising gas production, Stage II - stable gas production, and Stage III - declining gas production. From the initial production of 70 mcfd/well in April 1994, gas production was projected to monotonically rise for eight months (to the end of 1994), corresponding to Stage I. For calendar year 1995, the production was projected to be stable at 150 mcfd/well, corresponding to Stage II. The decline from the stable Stage II was adjusted to a rate that would recover 50% of the estimated reserves per wells, by the end of year 2008. For this scenario, a decline rate of 10% per year is calculated to recover 50.67% of the reserves, and this decline rate was used for Stage III.

Gas Prices and Tax Credits

The gas price projections were based on the wellhead price received by Torch. The wellhead price is determined by a Wyoming index price less a charge for compression, transportation and marketing. In 1994 the average wellhead price was $1.08/mcf of gas. This starting price was escalated five percent per year to account for anticipated future increases in gas price. Tax credits were assumed to be $1.03/mcf for 1994 and were escalated four percent per year. The acquisition costs for the project were estimated to be $9,135,000 or $145,000/well. This estimate was made based on available public information concerning the acquisition [8]. Of this total $1,575,000 was assigned to tangible equipment and $7,560,000 was assigned to the leasehold cost.

In 1994, the lease operating expenses, including administration, averaged approximately $700/month per well. This cost includes extensive repairs and rework of facilities including the installation of 21 new pumps. Operating costs for 1995 are projected to be less, at $600/month per well. These costs were considered to be fixed costs and from 1995 forward these operating costs were held flat. The costs of compression, transportation and marketing were accounted for by the use of wellhead gas pricing as previously discussed. The costs for major maintenance and well rework were estimated to average $750/year per well for the second year of operation (1995) and $400/year per year for subsequent years. These estimates were based on the assumption that these wells should have a very low frequency of major maintenance or rework.

The water disposal costs were minimal because the produced water is fresh, e.g. less than 250 ppm total dissolved solids. The water in the Marquis Field is being used by the ranchers in the area and is discharged into the ranchers' stockponds or tanks.

FISCAL MODEL ASSUMPTIONS

The economic model for the Torch interest was based on a 66.67% working interest (WI) in a 75% net revenue interest (NRI) for the Marquis Field. The Torch net revenue interest was 50%. It was assumed that the wells are on line 95% of the time, i.e. the deliverability per well was 95% for the year. Gross annual gas production was calculated from the average daily production per well, the number of wells on line, the deliverability factor and 365 days/year. The gross annual production in mcf and the actual or projected gas price/mcf and tax credits/mcf were used to calculate the gross annual production revenues and tax credits. These gross figures were reduced by the royalty and over-riding interests to yield an adjusted project gross for the 100% working interest (75% NRI in this case). From this point, calculations were made either on a project basis (100% working interest) or to a participant's working interest. This adjusted gross was reduced by the lease operating costs, maintenance costs, applicable severance and ad valorem taxes, to arrive at a before taxes net for the project or participant. Severance and ad valorem taxes were assumed to be 12% for these wells. Taxable income was calculated after deducting the depletion allowance and depreciation. The depletion allowances for the project were calculated on a unit of production basis.

Depreciation of the equipment costs in this case were taken over 5 years, on a straight line basis. A corporate tax rate of 39.8% was applied to net taxable income. It was assumed that the full amount of Section 29 Non-Conventional Fuels Tax Credit was used in the year earned. The Tax Credit for 1994 was assumed to be $1.03/mcf and escalated along with the inflation rate (assumed to 4% per year) until the tax credit expires at the end of the year 2002.

RESULTS

Production and Reserve Depletion

The cumulative production of the Marquis Field over the fifteen year period was estimated to be 26.8 BCF, or an average of 426,000 mcf per well. The original gas in place per well was calculated to be 841,550 mcf.

Project Economics

The economic analysis is summarized in Table II. On a cash on cash basis, the before federal income tax (BFIT) undiscounted profit to the participant (Torch) is $10,685,000 from an investment of $9,135,000 for a return on investment (ROI) of 1.17 to 1; an internal rate of return (IRR) of 2.349%, and present value (worth), discounted 15%, of $4,646,000 (i.e. the net present value then is a negative $4,489,000). When depletion, depreciation and Section 29 tax credits are fully utilized, the after net undiscounted profit increases markedly to $28,305,000. The ROI is 3.10 to 1; the IRR is 29.19% and the present value, at a 15% discount rate, rises to $14,330,000. Payout occurs in 2.84 years on an after tax basis and in 11.45 years on a before tax basis.

DISCUSSION OF RESULTS

Under these production and price scenarios the acquisition of the Marquis Field represents an attractive after tax return on investment for a moderate risk, gas production acquisition, if the tax credits, depletion and depreciation can be fully utilized.

Earlier projections were made by Hobbs [9] for shallow coalbed methane wells along the eastern margin of the Powder River Basin. Using a development cost per well of $60,000, an operating cost of $500/well per month, a wellhead gas price of $1.01/mcf, peak production of 160 mcfd/well, Hobbs projected economic returns that are more favorable than the results from the present study. For example, this earlier study indicated on a before tax basis, an IRR of 51%, a ROI of 2 to 1 and a payout of 2.1 years. On an after tax basis, using a 34% corporate tax rate, and with full use of the Section 29 tax credits, depletion allowances and depreciation, the IRR was over 100%, the P/I (or ROI) ratio was 5 to 1 and payout was 1.3 years. These earlier projections of economic returns appear to be much more attractive than the results from the present study. These differences in economic returns stem largely from the large difference between the acquisition costs for the Marquis Field and the development costs estimated by Hobbs. A development cost of $60,000 per well appears to be closer to the true development costs, with full infrastructure, at current prices. It is likely in the Marquis Field that original development costs were much less than the acquisition costs, but the Section 29 tax credits were a powerful upward influence on the market value of this producing property.

The favorable after tax economic parameters on this project, as compared with the low returns for the cash on cash case, i.e. before taxes, credits, depreciation and depletion, clearly show the strong influence of these tax credits and allowances on economic performance. Without the tax credits the Marquis Field would have a much, much lower market value. However, in the earlier work, Hobbs [9] reached the conclusion that with lower development and operating costs Powder River Basin coalbed methane projects can have attractive economic returns. This conclusion appears to be valid for the present study if current estimates of development and operating costs can be achieved.

REFERENCES

[1] Ayers, W.B., Jr., 1986: "Coal Resources of the Tongue River Member, Fort Union Formation (Paleocene), Powder River Basin, Wyoming and Montana"; Geological Survey of Wyoming-Report of Investigations No. 35.

[2] Larsen, V. E., 1989: "Preliminary Evaluaton of Coalbed Methane Geology and Activity in the Recluse Area, Powder River Basin, Wyoming"; Quarterly Review Methane from Coal Seams (GRI) June, p. 2-10.

[3] Jones, R.W. and R.H. DeBriun, 1990: "Coalbed Methane in Wyoming"; Geological Survey of Wyoming, Public Information Circular No. 30.

[4] Randall, A.G., 1989: "Shallow Tertiary Gas Production, Powder River Basin, Wyoming"; Wyoming Geological Association Guidebook, Fortieth Field Conference.

[5] Randall, A.G., 1991: "Shallow Teriary Gas Production, Powder River Basin, Wyoming:" Proceedings of the 1991 Coalbed Methane Symposium, University of Alabama, Tuscaloosa, Alabama. p. 509-525.

[6] "Powder River Basin, Wyoming and Montana"; Quarterly Review of Methane from Coal Seams, August 1993, p. 28-32, pub. by the Gas Research Institute.

[7] Tyler, R., Ambrose, W.A., Scott, A.R., et al., 1991: "Coalbed Methane Potential of the Greater Green River, Piceance"; GRI Topical Report, GRI-91/03125, December, 244 p.

[8] "Rocky Mountain Region, Coalbed Methane Report"; Petroleum Information Corporation, V. 5, No. 5, May 1994.

[9] Hobbs, G.W., 1990: "Coalbed Methane Development in the Powder"; Western Oil World, August, p. 17-20.

POWDER RIVER BASIN
MARQUIS FIELD
RESERVE/ PRODUCTION MODEL

Well Depth:	300 to 800 feet
Average Coal Thickness:	75 feet
Estimated Gas Content:	55 scf/ ton
Coal Density:	1700 tons/acre-foot
Coal Permeability, estimated:	100 millidarcies
Well Drainage Area, estimated:	120 acres
Original Gas in Place:	841,500 mcf/ well
Initial Production Rate:	70 mcfd/ well
Stage I Duration:	8 mos, beginning April 1994
Average Peak Production Rate:	150 mcfd/ well
Stage II Duration:	12 mos.
Production Decline Rate, Stage III:	10% / year
Gas Recovered in 15 Years:	426,000 mcf/ well
Depletion of Reserves:	50.67%

TABLE I

POWDER RIVER BASIN
MARQUIS FIELD

ECONOMIC RESULTS

	Before Taxes & Credits (BFIT)	After Taxes & Credits (AFIT)
Investment	$ 9,135,000	$ 9,135,000
Future Net Profits, undiscounted	$10,685,000	$28,305,000
Return on Investment , ROI	1.17 to 1	3.10 to 1
Internal Rate of Return, IRR	2.34%	29.19%
Present Value, at 15% disc.	$ 4,646,000	$14,330,000
Payout	11.45 yrs.	2.84 yrs.

TABLE II

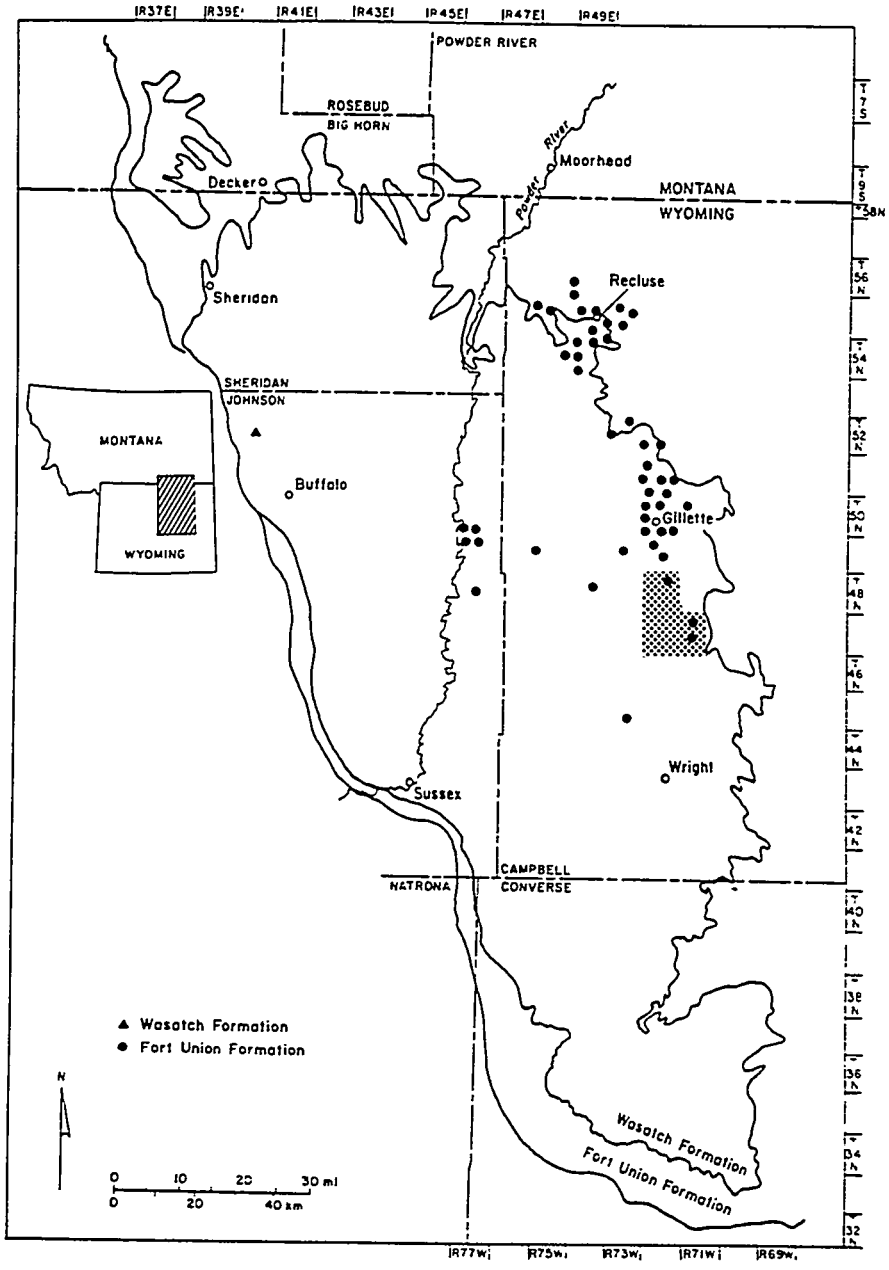


Figure 1. Map of the Powder River Basin, showing coalbed methane wells drilled through 1991. The majority of the wells were drilled along the easter margin, from just north of Recluse to South of Gillette. Modified from Tyler [7]. The approximate location of the Marquis Field is indicated by the shaded area.

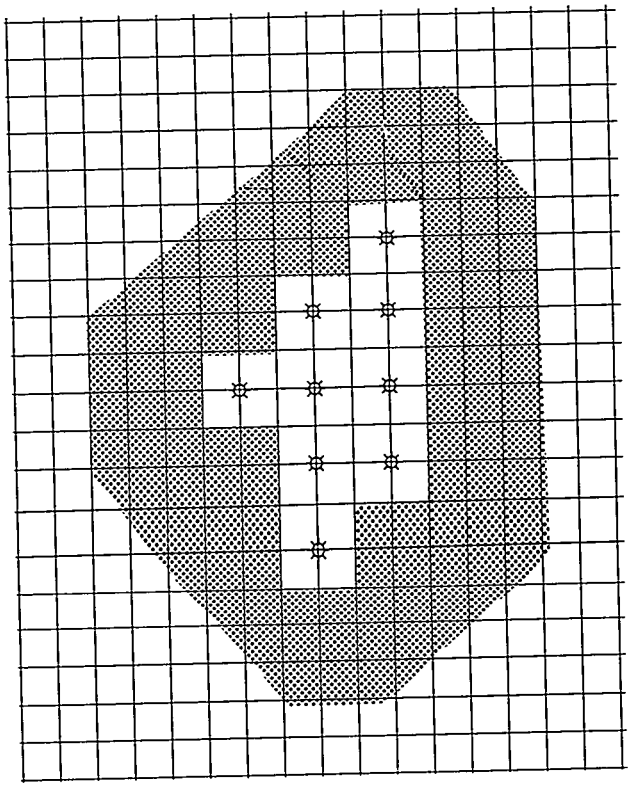


FIGURE 2. Schematic of typical pod of wells in the Marquis Field. The nine wells are on 40 acre spacings. An estimated drainage area for these wells is indicated by the shaded area. This drainage area is approximately 1100 acres for an average drainage area per well of just over 120 acres.

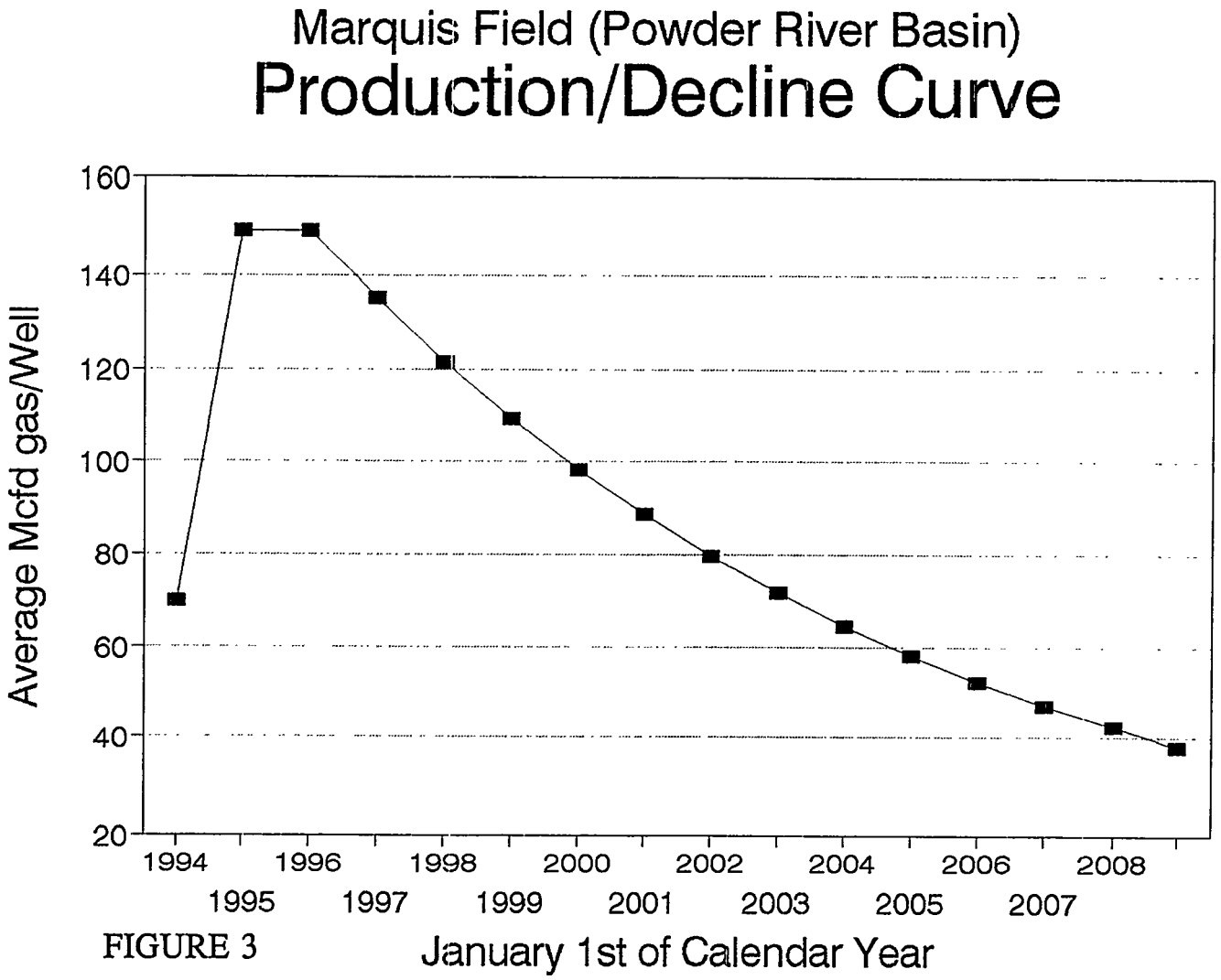

Marquis Field (Powder River Basin)
Production/Decline Curve
Average Mcfd gas/Well
160
140
120
100
80
60
40
20
1994
1995
1996
1997
1998
1999
2000
2001
2002
2003
2004
2005
2006
2007
2008
January 1st of Calendar Year

FIGURE 3



NOTES

INTERGAS '95

May 15-19, 1995
The University of Alabama
Tuscaloosa, Alabama USA

9514

Reconnaissance of Gas Contents and Geological Aspects of the Coalbed Methane Resources in Pennsylvania

A.K. Markowski, Pennsylvania Geological Survey

A compilation of coalbed methane gas content data from approximately 360 coal samples was obtained from a variety of sources including exploratory drillholes, pre-mining degasification drillholes, and methane recovery test projects from the Main Bituminous Coal Field of Pennsylvania. Exploratory coal cores studied ranged in age from the Pennsylvanian-Permian Dunkard Group to the Middle Pennsylvanian Allegheny Group. The tests on these coal cores revealed that the greater the depth and rank the greater the total and cumulative gas content. Average gas composition and Btu values were also determined for 14 selected samples.

Additionally, the Pennsylvania Geological Survey and the West Virginia Geological and Economic Survey conducted a joint mapping investigation of coalbed methane resources in the Northern Appalachian (Dunkard) Coal Basin to better understand the influence regional geology has on coalbed methane potential. Regional cross sections focusing on the correlation of Pennsylvanian-age strata and results of total and cumulative gas contents are presented.

Two units thought to have the greatest economic potential to produce coalbed methane in southwestern Pennsylvania are the stratigraphic intervals: 1) from the base of the Clarion coal (lower Allegheny Group) to the top of the Mahoning coal (lower Conemaugh Group); and 2) from the base of the Pittsburgh coal to the top of the Sewickley coal (lower Monongahela Group).

There is more of a challenge than just understanding the geologic aspects of coalbed methane before significant development will occur. Economic, legal, and environmental issues unique to Pennsylvania will also help to determine the fate of this usually wasted and much maligned, but potentially valuable resource.

INTRODUCTION

Historically, in the Northern Appalachian Coal Basin, coalbed methane has endured a negative hazardous reputation in the mining industry and generally been overlooked by the oil and gas industry. However, in about the last 25 years, interest in the economic value of coal seam gas has attracted the oil and gas industry. In the 1970's, various industries, the U.S. Bureau of Mines, and the U.S. Department of Energy launched a series of pilot methane recovery projects whose success paved the way for potential commercial development.

Objectives

The principal objective of this report is to identify and evaluate the natural gas resource potential of the major coal seams in southwestern Pennsylvania from existing and new data. Assuming that the resource potential is promising, additional objectives include: 1) identification of key areas with a high coalbed methane content; 2) correlation of gas contents with the stratigraphy of various coal seams, their thicknesses, ranks, and behavior of the gas with time; 3) subsurface delineation of the coal-bearing intervals, especially the Allegheny Group coalbeds and associated reservoir-quality sandstones through use of public domain subsurface information; interpretation of coal data and coal-sandstone relationships; and 4) assessment of the implications of exploiting coalbed methane as a supplemental and/or alternative energy source for the Commonwealth.

Scope

This report is generally a compilation and summary of previous work, some of which was completed in a cooperative study with the West Virginia Geological and Economic Survey. It represents data collected from the Main Bituminous Coal Field of Pennsylvania consisting of up to approximately 30 different coal seams ranging in age from Pennsylvanian-Permian to early Pennsylvanian.

The information provided in this report does indicate, however, the presence of very gassy coals in certain parts of the basin. Their resource potential deserves serious consideration.

GENERAL GEOLOGY

The Northern Appalachian Coal Basin is a symmetrical, oval basin covering approximately 43,700 square miles (Figure 1). Structure controls the basin configuration on the east with late Middle Pennsylvanian-age coal cropping out on the flanks of northeast/southwest trending folds [2]. The major coal-bearing units of the study area include the Pennsylvanian- and/or Permian-age

Dunkard Group and the Pennsylvanian-age Monongahela, Conemaugh, Allegheny, and Pottsville Groups (Figure 2). Although most of the coals in the basin are only locally continuous, some seams, like the Pittsburgh coal, are regionally continuous because of long, consistent environments of deposition and slow subsidence rates.

Regional Setting and Structure

The study area (Main Bituminous Field) is located in southwestern Pennsylvania in the central part of the Appalachian Plateau (Figures 1 and 3). Extending from central and eastern New York to central Alabama, the plateau occupies the western part of the Appalachian Basin, also known as the Appalachian Coal Basin. Paleozoic rocks in and around the study area have been deformed into long, gentle open folds. These folds formed during the main phase of the Alleghanian orogeny. This orogeny occurred after the Pennsylvanian and before the Late Triassic-Early Jurassic rifting in eastern North America. Fractures and faults, the presence or absence of which are so important in the transmission and storage of fluids in coalbeds, formed before, during, and after the main phase of Alleghanian folding.

Tight to moderate folding interrupts the otherwise undeformed Northern Appalachian Coal Basin. These features trend northeast to southwest with dips generally between 10 and 20 degrees [5]. In some cases, these folds bring the coalbeds to the surface, thus causing the gas to be lost by updip migration over time. Examples of this are the coals that lie near the Chestnut Ridge and Laurel Hill anticlines (Figure 4). Coal-bearing strata in the central part of the basin are relatively flat, covered by thick overburden. The deepest part of the Northern Appalachian Coal Basin is alternately called the Dunkard Basin and the Pittsburgh-Huntingdon synclinorium [3]. The Dunkard Basin measures 35 miles wide by 250 miles long and contains coals generally buried up to 1500 feet deep [5]. Adams and others [2] reported some coals to have a maximum overburden thickness of about 2300 feet in Greene County.

The relatively high rank, total effective coal thickness, and deep burial of the coal in the Dunkard Basin suggests that this area has great potential for production. The higher rank coals formed in a more deeply buried portion of the basin which experienced higher pressures and temperatures [2]. Coal ranks in the study area increase from northwest to southeast with the medium- to low-volatile bituminous ranks fringing the southeast (Figure 3).

COALBED METHANE IN PENNSYLVANIA

Existing Coalbed Methane Pools and Production

Currently, there are nine coalbed methane pools in Pennsylvania (Figure 4), but the number of reported wells and pools is increasing as of this writing. Three of the nine pools are located in Greene County, three are in Westmoreland County, and the others are in Cambria, Indiana, and Washington counties. Wells drilled from 1970 to 1994 are described by county below. Production and interval depths were taken from public well records and completion reports.

The first and oldest coalbed methane pool in Pennsylvania, an unnamed pool in Gump field, Greene County, is located about one-quarter mile west of the Bellevernon anticlinal axis on the Oak Forest 7.5-minute quadrangle (Figure 4). The three methane degasification wells in this pool, drilled by Carnegie Natural Gas Co., produced from the Pittsburgh coal seam of the Monongahela Group (Figure 2). Deepest productive intervals occurred between 624 and 760 feet, natural open flows ranged from 0.19 to 14.9 Mcfd, and total depths ranged from 828 to 1250 feet. The wells are plugged and abandoned.

The Blairtown pool in Waynesburg field, is located about one-half mile southeast of the Waynesburg synclinal axis on the Waynesburg 7.5-minute quadrangle in Greene County (Figure 4). The main coalbeds in the quadrangle include the Pittsburgh, Sewickley, and Waynesburg coals (Figure 2). The main seam of the Pittsburgh coal is about 68 inches thick with a thick lower main bench accompanied by one or more thinner beds and partings.

Emerald Mines Corp. (now known as Cypress Emerald Resources Corp.) drilled 18 wells in Blairtown pool between July 1970 and December 1979. These pre-mining degasification wells penetrated the Washington, Waynesburg, Uniontown, and Pittsburgh coals, and the coals of the Conemaugh Group (Figure 2). Natural open flows ranged from 0 to 100 Mcfd mainly from the Pittsburgh coal, with deepest productive intervals ranging from 586 to 1022 feet. Production was not reported for about half of the wells. Traces of brackish water were found at the depth of the Pittsburgh coal. Total depths ranged from 616 to 1022 feet with a maximum slant hole depth of 4802 feet. The wells are plugged and abandoned.

Also in Greene County, the Windy Gap pool in New Freeport field is located about one-half mile southeast of the Nineveh synclinal axis on the New Freeport 7.5-minute quadrangle (Figure 4). CNG Producing Co. drilled five coalbed methane wells in the New Freeport field from late March to early April of 1991 as part of a project. The gas wells penetrated the Waynesburg coal to the Sharon coal (Figure 2). Total depths ranged from 1348 to 3600 feet. Deepest productive intervals ranged from 1140 to 1756 feet. Natural open flows were too small to test, but after hydraulic fracture stimulation, the open flows were estimated to be 50 Mcf. The gas was relatively free of contaminants and yielded a Btu value acceptable for pipeline quality control. Traces of fresh water were found at some of the shallower coal depths in three of the five wells. CNG reported brackish water near a deep coal in one of the wells. The wells are now plugged and abandoned.

The South Franklin pool in Lagonda field, Washington County, is located one-half mile northwest of the Washington anticlinal axis on the Washington West 7.5-minute quadrangle (Figure 4). Jesmar Energy, Inc. reported a natural open flow of 3000 Mcfd from the Pittsburgh gob zone in a gas well spudded June 18, 1991. The gas had a low Btu value and contained 10 percent nitrogen, the productive interval ranged from 485 to 490 feet, and total depth was 504 feet. The well is

producing and on line.

Westmoreland County currently has three coalbed methane pools. The Waltz Mill pool in Oakford field is located about two miles southwest of the Grapeville (Jacksonville) anticlinal axis on the Smithton 7.5-minute quadrangle (Figure 4). Two wells penetrated Pennsylvanian rocks exclusively, one as an observation well, the other as a methane gas well. The gas well produced from the Freeport, Kittanning, Clarion, Brookville, Mercer, Quakertown, and Sharon coals (Figure 2). Deepest productive intervals ranged from 551 to 658 feet and total depths were 741 and 750 feet, respectively.

Gas contents in the Waltz Mill pool ranged from 13 to 102 cf/t with a weighted average of 37 cf/t [2]. Desorption values indicate an average content of 186 cf/t, yielding a computed coalbed resource estimate of 1.85 MMcf/acre following Kiel hydraulic fracture stimulation [12]. Core analyses suggested an in-place resource estimate of 8 MMcf/acre [2]. The average natural open flow was 28 Mcfd. Water production dropped from a maximum of 240 barrels/day to 120 barrels/day [2]. These wells were part of a project initiated by Westinghouse Electric Company to test for the supply of gas for space heating in a nearby facility. Although the wells are still active, no production has been reported to date.

The two most recently discovered coalbed methane pools in Pennsylvania, the Orchard Hill pool in Hoggs field and the Morewood pool in Mayfield field, also occur in Westmoreland County. Orchard Hill pool is located about one-third mile southeast of the Uniontown (Latrobe) synclinal axis on the Mount Pleasant 7.5-minute quadrangle (Figure 4). As of this writing, Equitable Resources Exploration drilled one well that perforated the Brush Creek, Upper Freeport, Upper Kittanning, Mercer "A", and the Mercer "B" coals (Figure 2). Deepest productive intervals ranged from 688 to 1116 feet. The operator was unable to gauge the natural open flow, but after treatment open flow was about 10 Mcfd. Total depth was 1275 feet.

Moorewood pool is located about one mile west of the Uniontown (Latrobe) synclinal axis on the Mount Pleasant 7.5-minute quadrangle (Figure 4). Equitable Resources drilled two wells and perforated the Conemaugh, Allegheny, and Pottsville coals (Figure 2). Deepest productive intervals of the first well ranged from 683 to 1096 feet. The natural open flow was too small to test, but the after treatment open flow was 146 Mcfd. Total depth was 1163 feet.

The second well penetrated Allegheny and Pottsville coals (Figure 2). Deepest productive intervals ranged from 848 to 1086 feet. After treatment open flow was 40 Mcfd. There was no natural open flow. Total depth was 1220 feet. The Orchard Hill and Morewood pool wells are currently shut in.

To date only one pool occurs in Indiana County. The Campbells Mill pool in Blairsville field, is located on the Blairsville and Bolivar 7.5-minute quadrangles. The Latrobe synclinal axis cuts through the eastern half of the pool and the Fayette anticlinal axis lies about one mile west of the pool (Figure 4). At this writing, Campbells Mill pool has the largest number of known coalbed methane wells drilled (23), by O'Brien Methane Production, Inc. (now owned by Belden and Blake Inc.) and Lee E. Minter. The O'Brien wells, drilled inside Homer City Mine, produced pipeline quality gas at an average after treatment open flow of 40 Mcfd. The gas was sold to Peoples Natural Gas Co. Water production was 115 barrels/day/well. The Minter wells produced from the Lower Conemaugh to Pottsville Group coals (Figure 2). Deepest productive intervals ranged from 475 to 1132 feet, natural open flows ranged from 120 to 140 Mcfd, and total depths ranged from 434 to 1500 feet. Two of the three Minter wells are producing and on line.

The Powell pool in Carrolltown field, Cambria County, is located about three-quarters of a mile southeast of the Laurel Hill anticlinal axis, on the Colver 7.5-minute quadrangle (Figure 4). CNG Producing Co. completed one well on June 12, 1993 in an abandoned mine. The well reached total depth in the Upper Freeport coal at 254 feet. A natural open flow yielded 84 Mcfd. The well continues to be monitored.

Compilation Data

Most of the coal samples used in this report are high-volatile A in rank. The graph in Figure 5 shows a slight visual correlation between gas content and depth among high-volatile A bituminous coal cores from Pennsylvania. This graph represents data from 360 samples compiled from methane recovery projects, the U.S. Department of Energy, the U.S. Bureau of Mines, the Pennsylvania Geological Survey, and supporting data from industry.

Selected Sampling Sites

Note: Total gas contents in Figures 6 and 8 are based on the entire coalbed. The coal core samples in Figures 7 and 9 show the top portion of the coal sample only because the cores were divided into three parts for ease of handling.

Greene County. Five coalbeds were sampled from two drillholes, one in Wayne Township on the Oak Forest 7.5-minute quadrangle, the other in Washington Township on the Waynesburg 7.5-minute quadrangle. Coal rank in both areas is high-volatile A bituminous. The Wayne Township site was located about 0.7 mile west of the Bellevernon anticlinal axis (Figure 4). The coalbeds encountered here ranged in depth from the Waynesburg A at 510 feet to the Pittsburgh at 934 feet. Total gas contents ranged from 51 cf/t for the Waynesburg A to 216 cf/t for the Sewickley coal.

The Washington Township site was located about 1.25 miles west-southwest of the deep mined-out areas of the Pittsburgh coal. It occupies a position 0.83 miles east of the Amity anticlinal axis and 1.4 miles west of the Waynesburg synclinal axis (Figure 4). The coalbeds encountered in the drillhole ranged in depth from the thin Ten Mile coal at 351 feet to the Sewickley coal at 938 feet. Total gas contents ranged from 32 cf/t for the Ten Mile coal to 117 cf/t for the Sewickley coal (Figure 6). The gas composition at this site averaged from 95 percent methane for the Ten Mile

coal to 86 percent methane for the Sewickley coal. The sampling period ranged from six to eleven months, respectively.

Figure 6 reveals gas content that generally tends to increase with depth. The exception is the Little Washington coal. There was no apparent relationship between total gas content and thickness, atmospheric pressure, or temperature. Cumulative gas, however, appeared to increase slightly with an increase in atmospheric pressure and temperature. The amount of cumulative gas in the top part of the Sewickley coal also increased proportionally with elapsed time, and the gas continued to increase over a period of approximately 350 days after which time testing was terminated (Figure 7).

Cambria County. A drillhole in Cambria Township on the Ebensburg 7.5-minute quadrangle encountered the Upper and Lower Freeport coalbeds at 724 and 771 feet. Although this site was about thirty miles east of the study area, it is included because the results were impressive. The site lies about one mile west of the Wilmore synclinal axis and 3.4 miles east of the Ebensburg anticlinal axis [11]. Locally, it is about one mile from a mine dump and 4.5 miles west-northwest of a strip mine. Total gas contents ranged from 203 cf/t for the Upper Freeport to 395 cf/t for the Lower Freeport (Figure 8). The Upper Freeport was the thicker of the two seams at 5.27 feet compared to the Lower Freeport at 2.77 feet. Coal rank is medium-volatile bituminous. The gas composition averaged 99 percent methane for each coal seam.

Thickness of the coal and total gas content show no relationship. There also was no apparent correlation between total gas content and atmospheric pressure or temperature. Cumulative gas appeared to increase slightly with an increase in atmospheric pressure and temperature. The amount of cumulative gas in the top part of the Lower Freeport coal also increased steadily with elapsed time, but stabilized after 200 days (Figure 9).

Results of Testing

Variables such as barometric pressure, temperature, and time were initially plotted against the cumulative gas calculated at standard temperature and pressure for data collected during this study. Thickness was also plotted against total gas content. Because there appeared to be no significant correlation between barometric pressure and temperature versus cumulative gas and thickness versus total gas content, these data are not included in this report. Most of the data used for this report suggest a direct correlation between depth of the coalbed and an increase in total gas content (additional data on other coal seams can be obtained from the Pennsylvania Geological Survey).

The rate of cumulative desorbed gas versus time depends on the degree of fracture networking. That is, if the coal is blocky and dense with a poor fracture network, there will be a slow rate of cumulative gas desorption. If the coal is friable with a good fracture network, there will be a measurably rapid rate of cumulative gas released.

Gas Composition and Btu. Fourteen coal cores (sampled from seven coalbeds) retrieved from two exploratory drillholes were monitored for their gas composition from as little as one month to as long as eleven months. Analyses of gas composition reveal that the coals sampled below at least 300 feet generally have about 90 percent or greater methane content. Samples with low methane values indicate either a shallow coal sample or the introduction of nitrogen to the sample with time. For example, methane contents will be lower if the drillhole or well is within 2000 to 3000 feet of an active mine. Previous studies from the U.S. Bureau of Mines revealed that over time, higher molecular weight hydrocarbons like ethane, propane, butane, pentane, and associated isomers tend to increase in the later stages of desorption. This suggests that large volumes of these gases might have been generated in certain coalbeds, and in such cases would seem to desorb more slowly due to a larger molecule size [14]. The Greene County samples, for example, contained from 0.03 to 2.91 normalized percent of the higher hydrocarbons over a six month desorption period. Residual gas from some of these samples ranged from 0.10 to 5.94 normalized percent over an 11 month period.

Heating values of various ranks of coal from across the United States generally range from 4500 to 14,350 Btu/scf [15]. Coal samples from this study averaged 15,209 Btu (daf). Heating values from gas samples in this study averaged about 1000 Btu/scf, comparable to conventional natural gas values. The samples with lower methane contents also had very low heating values and gas contents. High methane contents, on the other hand, do not always guarantee high gas contents.

GEOLOGIC EVALUATION OF PREVIOUS STUDIES

Introduction

The Pennsylania Geological Survey and the West Virginia Geological and Economic Survey conducted a joint mapping investigation of coalbed methane resources in the Northern Appalachian (Dunkard) Coal Basin to better understand the influence regional geology has on coalbed methane potential. Regional cross sections focusing on the correlation of Pennsylvanian strata are presented.

Phase I of this cooperative study evaluated the coalbed methane potential of the entire Pennsylanian coal-bearing interval within the Northern Appalachian Coal Basin. The data set for Phase I was derived mainly from drillers' logs of oil and gas wells. Phase I concentrated on the Monongahela prospect interval (Monongahela Group) (Figure 2). The Pittsburgh coal acted as a datum because it is regionally continuous and is commonly noted on the drillers' records. Most drillers use the Pittsburgh coal as a reliable stratigraphic marker on their logs. Oil and gas operators typically do not log shallow Pennsylvanian-age rocks because they are interested in casing off these rocks as soon as possible due to caving and problems associated with the Conemaugh redbeds. Gamma ray logs can be run through casing [3].

Phase II of the cooperative study focused on subsurface delineation of the Allegheny Group coalbeds (Figure 2) and associated reservoir-quality sandstones. Methodology included

the use of coal cores and oil and gas records and logs; correlation of coals and sandstones for regional cross sections; and interpretation of coal-sandstone relationships. Numerous oil and gas wells and coal cores, (Figure 10) were the source of data for the regional cross sections presented in Figures 11-14.

Monongahela Prospect Interval

The Pittsburgh and Sewickley coals, the most commonly reported coals in Greene and Washington counties, are the primary targets for methane production in the Monongahela Group (Figure 2). The Pittsburgh and Sewickley are also the most commonly reported coals in Greene and Washington counties with the Waynesburg and Washington coals being subordinate.

Cumulative coal thickness as determined from oil and gas data generally ranges from 10 to 19 feet. The Pittsburgh coal, which becomes progressively thicker from west (4 feet) to east (8 to 10 feet) within the study area, generally accounts for most of the coal thickness indicated. Net coal thickness in excess of 10 feet normally indicates the added presence of either the Sewickley and/or Waynesburg coalbeds.

Maximum thickness of the thickest individual coalbed reported per well ranges from 4 to 7 feet. A progressive easterly thickening of the Pittsburgh coal occurs along most of the southwestern border of Pennsylvania.

Defining the Allegheny Group

As commonly defined, the Allegheny Group extends downward from the top of the Upper Freeport coalbed to the top of the Homewood Sandstone (Figure 2). For mapping purposes, however, the need for definition of an "operational" Allegheny arose because the Upper Freeport coalbed cannot always be identified from subsurface data, or is not always present [3]. The "operational" Allegheny Group as used here extends from the base of the Brush Creek marine zone and/or coal to the top of the Pottsville Group (Figure 2). Thickness is about 400 feet in southwestern Pennsylvania [3].

The Brush Creek, one of several marine zones in the overlying Conemaugh Group, proved to be a useful correlation horizon [3]. It commonly occurs about 450 feet below the Pittsburgh coal and about 110 feet above the Upper Freeport coal [3]. The Brush Creek marine zone and associated coal, where they exist, can be determined on geophysical logs with the aid of nearby core hole data. Similarly the stratigraphic positions and identity of the Pittsburgh coal and Conemaugh Group red mudrocks, which operators commonly report in their well records, can also be determined from geophysical logs.

Definition of the base of the Allegheny Group/top of the Pottsville Group is less clear because the Clarion sandstone (adjacent to the Clarion coal at the base of the Allegheny Group) commonly merges with the Homewood and Connoquenessing sandstones (Pottsville Group) (Figure 2). Most of these thick sandstones were noted on drillers' logs and identified in cores and gamma ray logs as the Salt sands or Homewood Sandstone, depending on geographic region and the number of sandstones encountered. If a very thin sandstone or no sandstone is present, the top of the Pottsville must be chosen by estimation through nearby data points.

Allegheny Prospect Interval

The coalbed methane potential of the Allegheny Group is thought to exceed that of the Monongahela Group because Allegheny Group coals have higher rank and greater total gas content per ton of coal. Allegheny Group coals are typically thin and discontinuous and are commonly associated with sandstones. Most of the study area contains at least four Allegheny coals greater than 2 feet thick, having an average total coal thickness of 10 to 15 feet. For a depositional model, Oldham and others [3] suggested that thick coal pods commonly occur offset from thick fluvial sandstone zones. Areas where differential compaction has been the primary influence tend to have offset channel systems. Erosional contacts have formed between coalbeds and overlying channel-fill sandstones, thus forming potential coalbed methane traps [3]. Areas influenced by tectonics may exhibit stacked channel-fill sandstones. Repetitive sequences of peat (coal) accumulation are also stacked, commonly with shale interburden. These areas should be a prime target for completion of coalbed methane wells [3].

CROSS SECTIONS

Figures 11 and 12 show a cross section index map and an explanation, respectively, for selected cross sections. Gamma ray logs and a corresponding strip log showing lithologic picks represent the wells in the cross sections (Figures 12-14). These cross sections show coalbeds only where both gamma ray and density logs, or coreholes, are used. They also show tentative correlations of the Mahoning Sandstone, individual Allegheny and Pottsville coalbeds, and redbeds of the Conemaugh Group and Mauch Chunk Formation (Figure 2). Wells with only gamma ray logs were used to fill in areas where core and/or gamma ray/density logs were unavailable [3].

Cross section A_2-A' (Figure 11) trends from north-central Greene County northeast to central Indiana County, Pennsylvania and includes the interval from the Pittsburgh coal to the Loyalhanna Formation. The operational Allegheny generally thickens to the northeast whereas the Pottsville Group/ Mauch Chunk Formation interval becomes thinner. Several Allegheny Group coalbeds appear to be present everywhere, but, they are very discontinuous, making correlation difficult [3].

The Pittsburgh coal and Conemaugh Group disappear along the line of cross sections A_2-A_3 and A_3-A' (Figures 12-13) because of erosion. Although the Mahoning Sandstone becomes more discontinuous, the lowermost Allegheny coals become more continuous. Mauch Chunk redbeds occur between Pottsville Group sediments and the Loyalhanna Formation, providing alternative correlation tools [3].

Cross sections E-E' through G-G' (Figure 11) trend northwest to southeast across the study area. Representative cross section F-F' (Figure 14) shows

the "operational" Allegheny interval, from the Brush Creek marine zone/coal to just below the top of the Pottsville Group. The coalbeds display much variation in thickness and discontinuity. The Mahoning Sandstone and selected coalbeds, where present, were tentatively correlated.

RESULTS OF MAPPING COAL DATA

A series of maps was constructed for the cooperative study from data derived from cores and gamma ray/density log combinations (only coals greater than 2 feet in thickness were used). Isopleth maps of the number of Allegheny coalbeds, net Allegheny coal thickness, and thickest individual Allegheny coalbeds can be obtained from the Pennsylvania Geological Survey.

Most of the study area contains at least four coals greater than 2 feet thick each, with as many as 10 individual beds in localized areas. Total thickness of all seams averages 10 to 15 feet over much of the area with thicker pods in the northeastern part of the Pennsylvania study area.

The thickest individual coalbed averages 4 to 5 feet over much of the area, with localized thicknesses of up to 11 feet. Field and core observations suggest that coals thicker than 7 feet may contain multiple thin partings that do not show up on oil and gas geophysical logs because of logging speed [3].

Field, core, and geophysical log interpretations have shown that many coal-sandstone contacts in the Allegheny Group are erosional in nature, where ancient channels cut into or through the peat. If differential compaction dominated, the channels which occupy topographically low areas would immediately overlie the previously deposited inter-channel peat. This scenario seems to fit most of the Pennsylvania cross sections. No apparent evidence of tectonic influence is shown in this study. However, Kertis [16] identified areas of stacked channel sandstones and offset channel sandstones in the Freeport-Kittanning coal interval in Indiana and Armstrong counties. She noted that stacked channel deposits occur if active tectonic control predominates, and that offset channels occur if differential compaction is the predominant control. Kertis based her study on detailed mine information and individual sandstone bodies in a local area, whereas this study was regional in nature.

ASSESSMENT OF POTENTIAL

Selected correlations presented in this report and throughout the literature show that the gas content of Pennsylvania's bituminous coal increases with increasing rank and depth. The greater the depth of overburden, the higher the methane content. Most identified coalbeds occurring in western Pennsylvania between approximately 600 and 1500 feet deep are optimum economic targets.

Thickness of the coalbed, according to communication from various industrial sources, is also important for economic production of coalbed methane, although, it is not evident in this study. Combined production from stimulating multiple coalbeds in a single well is common in Pennsylvania because of the prevalence of relatively thin cyclical beds. There was no significant correlation between gas content and thickness, temperature, or barometric pressure.

Within different ranks of coal, however, variations in gas content occur based on variations in coal chemistry. The physical nature of the coal also dictates the rate of gas release. Friable coals having a more pronounced fracture network emit more gas during desorption than a blocky, dense coal.

The presence of a fracture or cleat system in the coalbed is necessary for establishing permeability and hydrostatic/hydrodynamic conditions. These may be faults, fold-induced fracturing, or stress fractures due to differential compaction properties of coal seams and adjacent shales. It is inferred that favorable geologic structure and permeability occurs preferably on the flanks of anticlines or synclines where the orientation and degree of jointing is more evident than on the structural axes [17], as reported by a company exploring in the Campbells Mill Pool, Indiana County (Figure 4).

Coal in general is an ideal reservoir rock. Its retention capacity is superior to that of a conventional natural gas sandstone or carbonate reservoir. Different ranks of coal have different capacities to store gas. In most cases, higher rank (and deeper) coals have a higher adsorptive or retentive capacity for methane gas storage than lower rank coals.

The target area for commercial development in Pennsylvania describes a rough ellipse in the southwestern part of the state (Figure 1). This is where the deepest flat lying coalbeds occur compared to other parts of the state. Pennsylvania's nine coalbed methane pools are located in this target area (Figure 4). Overall estimates of coalbed methane resources in the Northern Appalachian Coal Basin indicate there may be 61 Tcf of gas contained in the coal of the basin [5]. This includes portions of Pennsylvania, Ohio, West Virginia, and a small part of Maryland.

REGULATORY ISSUES

Legal ownership of coalbed methane is still contested, despite a 1983 legal settlement in which the court concluded that "any gas found within a coalbed must necessarily belong to the owner of the coal!" [18]. Until clear ownership is established, any successful development of coalbed methane will likely depend on agreements among the oil and gas developer, the landowner, and the coal company. Federal legislation proposed to stimulate development includes the concept of forced (involuntary) pooling. Modeled after Virginia's 1990 oil and gas law, forced pooling requires the landowners to pool and develop their lands as a unit prior to ownership of coalbed methane determination.

CONCLUSIONS

In the last 25 years, the economic value of coal seam gas has attracted oil and gas industry interest. In the 1970's, various industries, the U.S. Bureau of Mines, and the U.S. Department of Energy launched a series of pilot methane recovery

projects whose success helped pave the way for future projects.

The information provided in this report indicates the presence of very gassy coals in certain parts of the Dunkard Basin. Their resource potential deserves serious consideration. The target area for commercial development in Pennsylvania occurs in the southwestern part of the state, within an elliptical region of the Northern Appalachian Coal Basin. The deepest coals that exist here, and other coals near mines with known high emission rates, are potentially the most attractive to develop. Overall estimates of coalbed methane resources indicate there may be 61 Tcf contained in the Northern Appalachian Coal Basin.

Historically, the Pittsburgh coal of the Monongahela Group is considered to be a prime target for coalbed methane. Gas shows are reported on many drillers' logs and estimated gas emission volumes are often large. Currently, gob gas from the Pittsburgh is being produced via converted pre-mine ventilation wells.

The operational Allegheny prospect interval contains the following target beds: Mahoning, Upper and Lower Freeport, Upper, Middle, and Lower Kittanning, Clarion, and Brookville coals. Average gas content for Allegheny Group coalbeds ranged from 183 Scf/ton for Kittanning coals to 227 Scf/ton for the Clarion/Brookville coals. Associated sandstones may also be gas targets.

Analyses of coalbed depth and thickness versus total gas content from previous studies and supporting literature suggested there is a direct positive relationship between depth and gas content. Coal's retention capacity is superior to that of a conventional natural gas sandstone or carbonate reservoir. Different ranks of coal have different capacities to store gas. In most cases, higher rank (and deeper) coals have a higher adsorptive or retentive capacity for methane gas storage than lower rank coals.

When the severance of mineral ownership rights among different owners exists, there is potential for conflict. Several options exist to address this issue. These include requiring the coalbed gas lessee to designate proposed wells and get the coal owner's approval or the coalbed gas lease should specifically address the issue of conflicting uses. Any successful development will depend on compromises between the oil and gas developer and landowner with the coal company. Unless Pennsylvania can develop its own coalbed methane program to encourage development by October 1995, federal legislature will effect a cooperative "forced (involuntary) pooling" of methane ownership.

NOMENCLATURE

Btu/scf	British thermal units per standard cubic feet
cf/t	cubic feet per ton
daf	dry ash free basis
ft	feet
gob	The coal and surrounding strata above the coal that has collapsed due to longwall mining.
isomer	A compound, radical, or ion containing the same numbers of atoms of the same elements but differ in structural arrangement and properties.
Kiel fracture	Type of hydraulic stimulation that pumps pulses of water and proppant into the coalbed at a specified low flow rate [2].
Mcfd	thousand cubic feet per day
MMcf	million cubic feet
on line	Gas that is transported via a pipeline for commercial use.
residual gas	The gas trapped in the coal matrix.
shut in	A temporary halt in gas well operations.

ACKNOWLEDGEMENT

This report would not have been possible without the substantial contributions of Anne V. Oldham, Thomas E. Repine, Jr., Kimberly J. Timberlake, Joseph F. Schwietering, Douglas G. Patchen, and Katharine L. Avary (West Virginia Geological and Economic Survey). Additionally, the valuable technical and editorial contributions of John A. Harper and assistance in field equipment assemblage by Leslie T. Chubb (Pennsylvania Topographic and Geologic Survey) is greatly appreciated. Other valuable editorial contributions from Kathy J. Flaherty, Christopher D. Laughrey, Samuel W. Berkheiser, and Donald M. Hoskins (Pennsylvania Geological Survey) are gratefully acknowledged. The core project this report is based on was coordinated by William R. Kaiser of the Texas Bureau of Economic Geology and funded by the Gas Research Institute of Chicago.

Acknowledgements also go to personnel of Bethenergy Mines, Inc.; Gateway Coal Co.; U.S. Bureau of Mines Ground and Methane Control; and Mine Safety and Health Administration for their time, information, and friendly cooperation.

REFERENCES CITED

1. Byrer, C. W., Mroz, T. H., and Covatch, G. L., 1984: "Production Potential for Coalbed Methane in U.S. Basins", paper SPE/DOE/GRI 12832, Proceedings of the Unconventional Gas Recovery Symposium, Pittsburgh, Pennsylvania, 1984, p. 15-28.

2. Adams, M. A., Eddy, G. E., Hewitt, J. L., Kirr, J. N., and Rightmire, C. T., 1984: "Geologic Overview, Coal Resources, and Potential Methane Recovery from Coalbeds of the Northern Appalachian Coal Basin - Pennsylvania, Ohio, Maryland, West Virginia, and Kentucky", p. 15-43, in Rightmire, C. T., Eddy, G. E., and Kirr, J. N., eds., Coalbed Methane Resources of the United States: American Association of Petroleum Geologists Studies in Geology Series 17, 378 p.

3. Oldham, A. V., Repine, T. E., Jr., Markowski, A. K., and Harper, J. A., in review: "Geological Aspects of Coalbed Methane Occurrence in the Northern Appalachian Coal Basin"; GRI Contract 5091-214-2261 (April

1992-August 1993), Gas Research Institute, 86 p.

4. Pennsylvania Geological Survey, 1992: "Distribution of Pennsylvania Coals", Map 11, third edition, scale 1:2,000,000, 8.5" x 11".

5. Kelafant, J. R., Wicks, D. E., and Kuuskraa, V. A., 1988: "A Geologic Assessment of Natural Gas from Coal Seams of the Northern Appalachian Basin"; Topical Report GRI 88/0039, Gas Research Institute, Chicago, IL, 86 p.

6. Markowski, A. K., in review: Reconnaissance of the Coalbed Methane Resources in Pennsylvania: Pennsylvania Geological Survey, 4th ser.

7. Dodge, C. H., and Glover, A. D., compilers, 1984: Coal Resources of Greene County, Pennsylvania: Pennsylvania Geological Survey, 4th ser., Mineral Resource Report 86, Part 1, 67 p.

8. Skema, V. W., compiler, 1987: Coal Resources of Washington County, Pennsylvania: Pennsylvania Geological Survey, 4th ser., Mineral Resource 93, Part 1, 96 p.

9. Skema, V. W., compiler, 1988: Coal Resources of Westmoreland County, Pennsylvania: Pennsylvania Geological Survey, 4th ser., Mineral Resource Report 94, Part 1, 127 p.

10. Glover, A. D., compiler, in press: Coal Resources of Indiana County, Pennsylvania: Pennsylvania Geological Survey, 4th ser.

11. Glover, A. D., compiler, 1990: Coal Resources of Cambria and Blair Counties, Pennsylvania: Pennsylvania Geological Survey, 4th ser., Mineral Resource Report 96, Part 1, 129 p.

12. Westinghouse Electric Corporation, 1979: "Coalbed Methane Extraction and Utilization"; 7th monthly progress report: contract EW-78-C-21-8332, Dept. of Energy Contract Office, Oak Ridge Ops., in U.S. Dept of Energy report WAESD-TME-2940, Advanced Energy Systems Division, "First Phase of a Coalbed Methane Extraction and Utilization Program", April, 1979; also from the National Technical Information Service (NTIS), U.S. Dept. of Commerce, Springfield, Virginia 22161.

13. Diamond, W. P., LaScola, J. C., and Hyman, D. M., 1986: "Results of Direct Method Determination of the Gas Content of U.S. Coalbeds"; U.S. Bureau of Mines Information Circular 9067, 95 p.

14. Ulery, J. P., and Hyman, D. M., 1991: "The Modified Direct-Method (MDM) Determination of Gas Content", paper 9163, Proceedings of the 1991 Coalbed Methane Symposium, The University of Alabama, Tuscaloosa, 12 p.

15. Edmunds, W. E. and Koppe, E. F., 1968: Coal in Pennsylvania: Pennsylvania Geological Survey, 4th ser., Educational Ser. 7, 29 p.

16. Kertis, C. A., 1984: Recognition and Prediction of Coalbed Discontinuities, Indiana and Armstrong Counties, Pennsylvania: unpublished M.A. thesis, University of Missouri, Columbia, Missouri, 88 p.

17. Ayers, W. B., Jr., and Kelso, B. S., 1989: "Knowledge of Methane Potential for Coalbed Resources Grow, But Needs More Study"; Oil and Gas Journal, V. 87, No. 43, p. 64-67.

18. Johnson, E. C., 1992: "Who Owns Coalbed Methane?"; Appalachian Pipeline, V. 3, No. 2, p. 5-7.

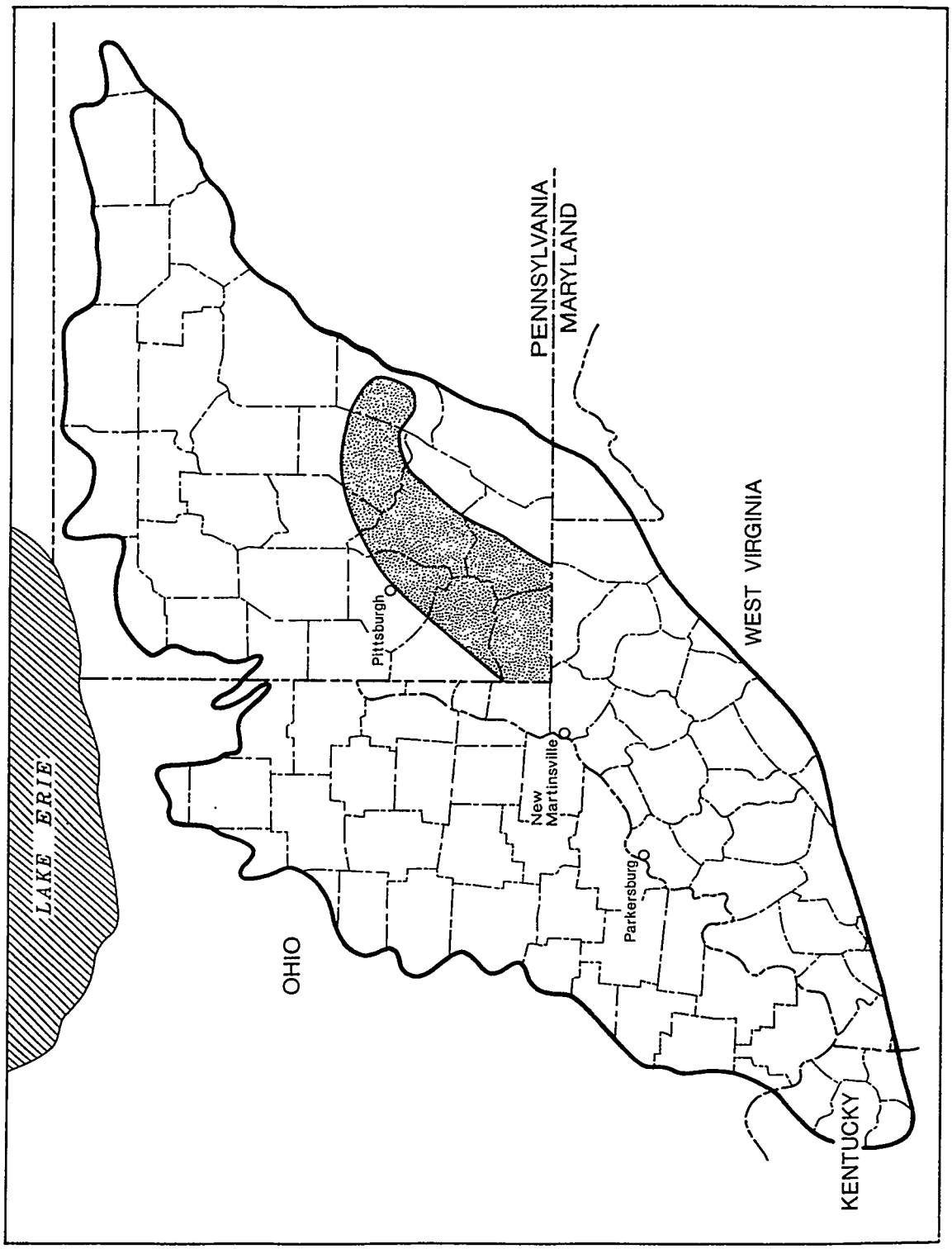


Figure 1. Map of the Northern Appalachian Coal Basin showing county lines, study area for the gas content reconnaissance, and general target area for exploration (stippled) (modified from [1]).

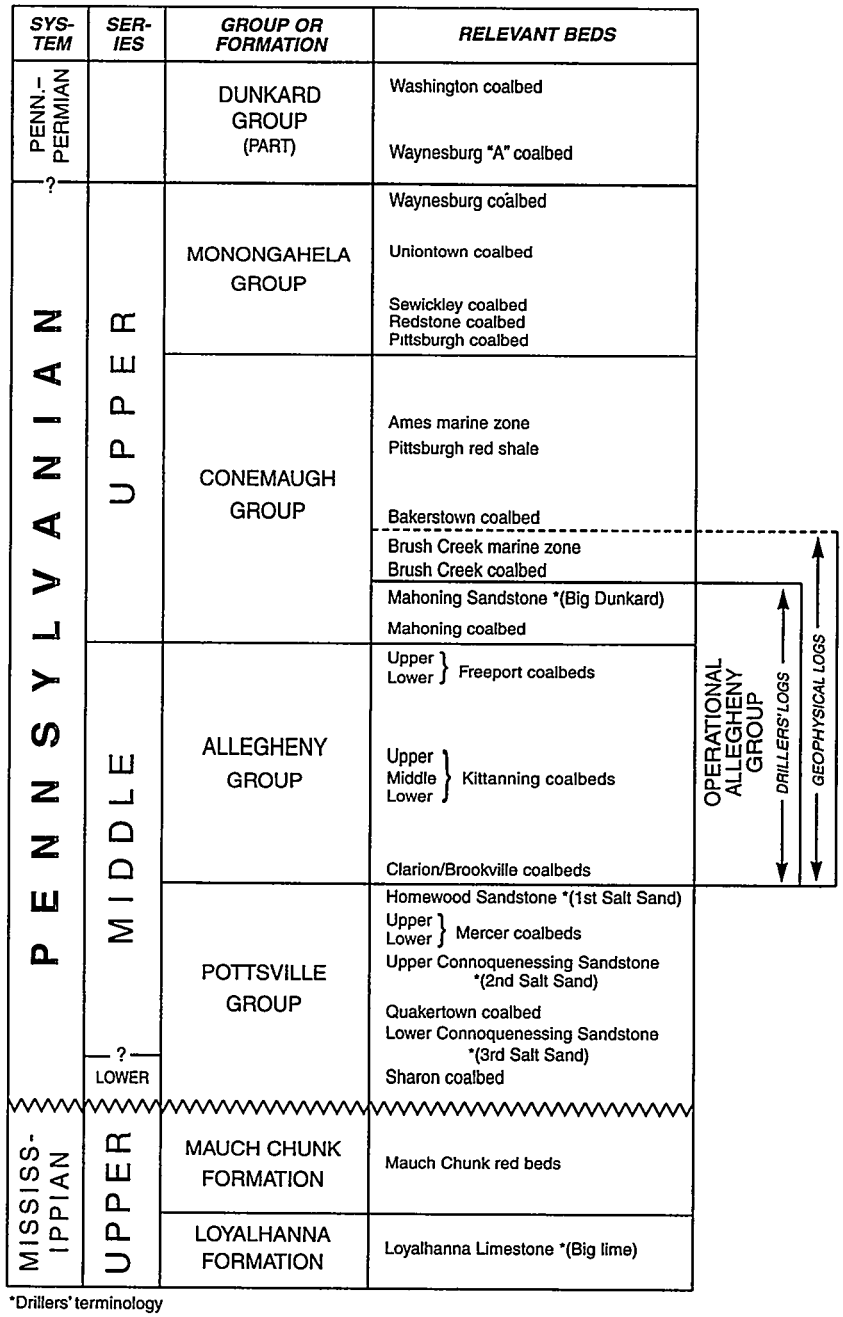


Figure 2. Subdivisions of the Pennsylvanian System and the stratigraphic position of beds important to this study (modified from [3]).

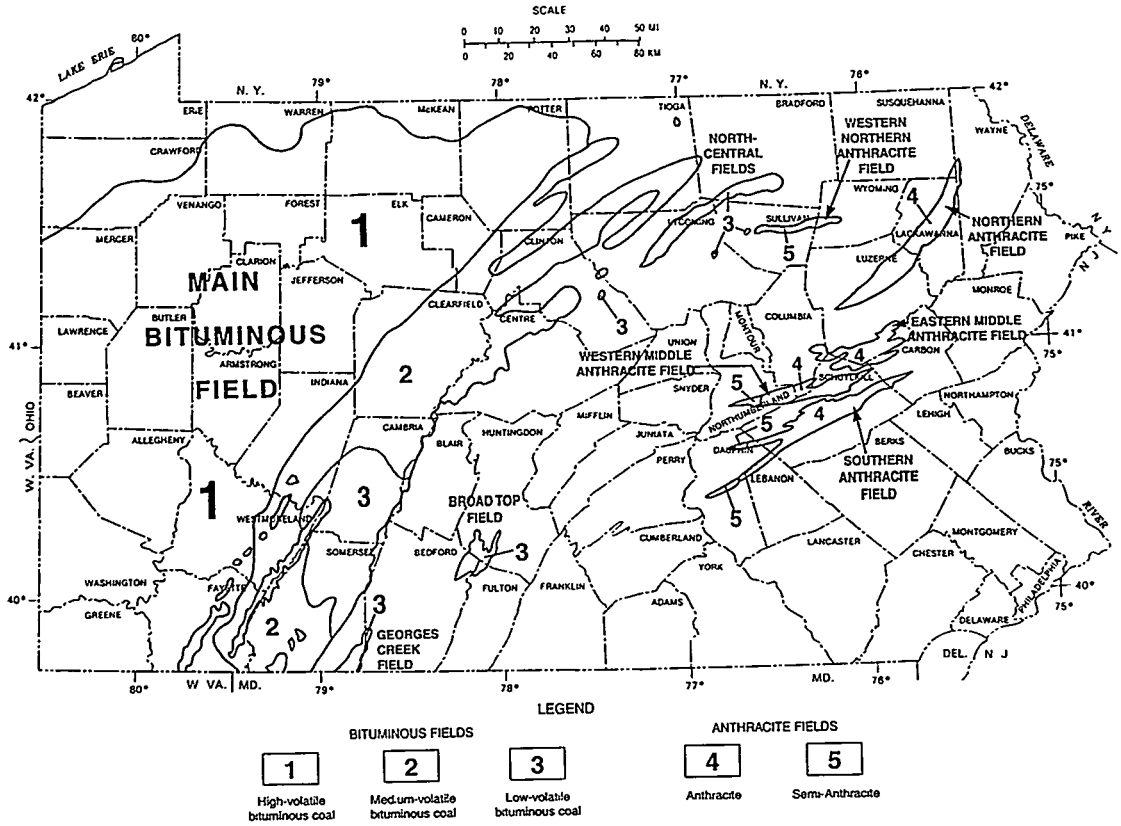


Figure 3. Location of coal-bearing rocks and coalfields across Pennsylvania (modified from the Pennsylvania Geological Survey, 1992, third edition [4]).

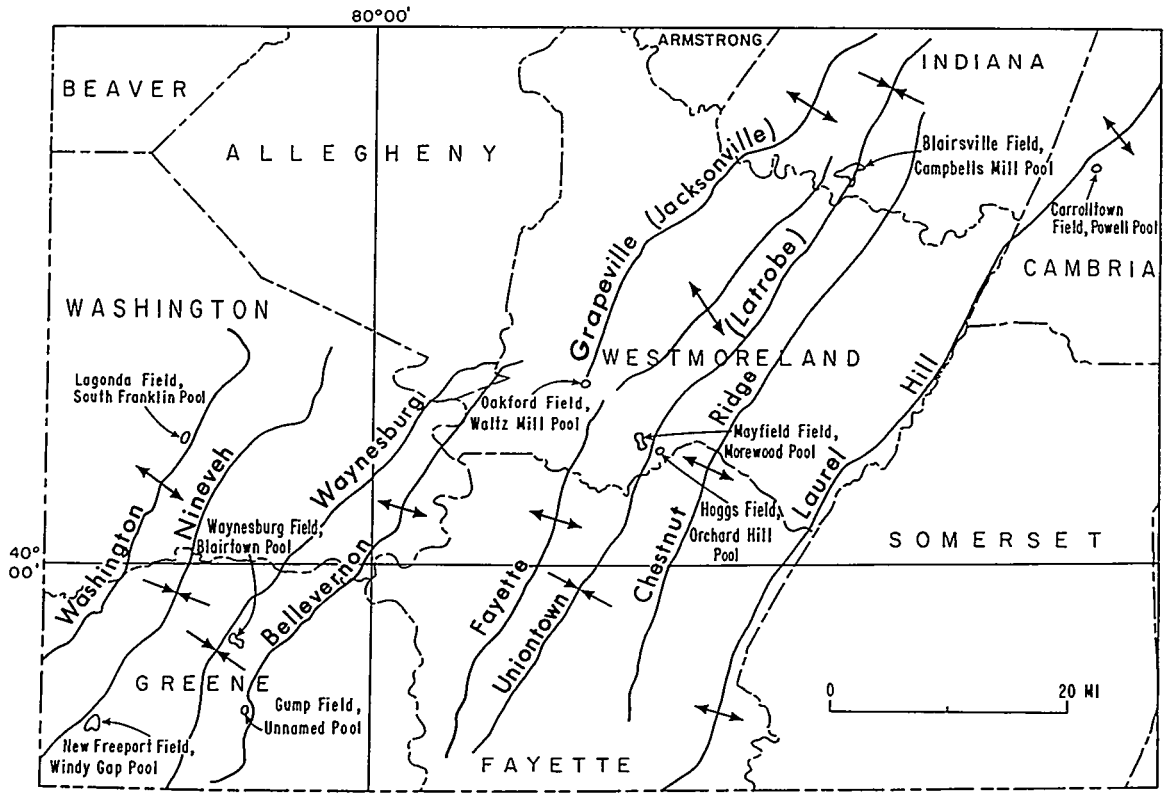


Figure 4. Coalbed methane pools and major fold axes in Pennsylvania [6]; fold axes from [7,8,9,10,11].

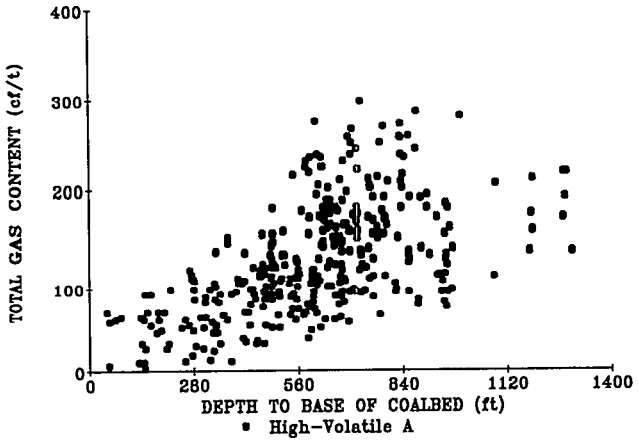


Figure 5. Total gas contents for Pennsylvania high-volatile A bituminous coals versus depth to the base of the coalbed [6, modified from 13].

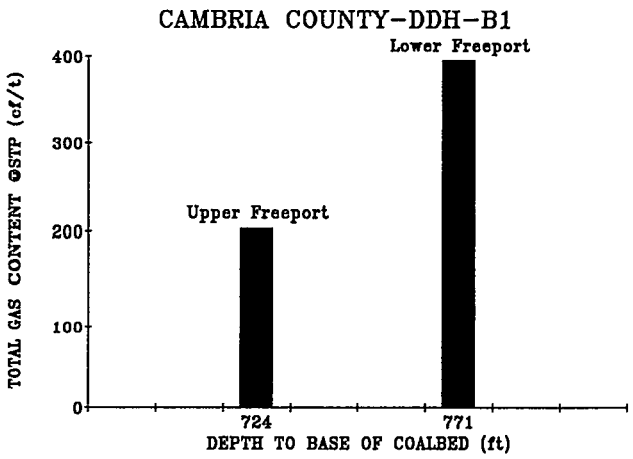


Figure 8. Total gas contents for the Upper and Lower Freeport coals in Cambria County based on depth to the base of the coalbed [6].

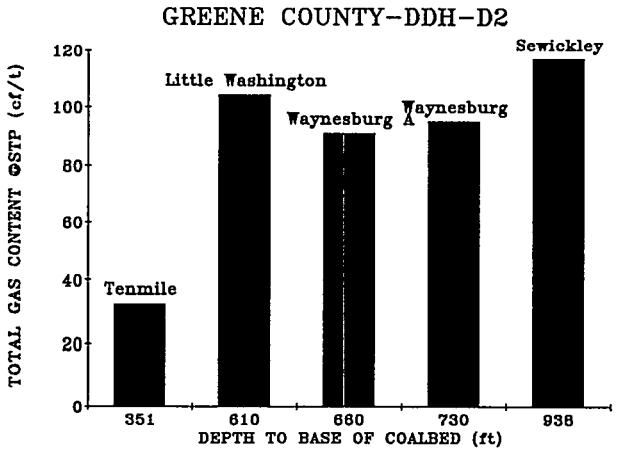


Figure 6. Total gas contents for the Dunkard and Monongahela Group coals in Greene County based on depth to the base of the coalbed [6].

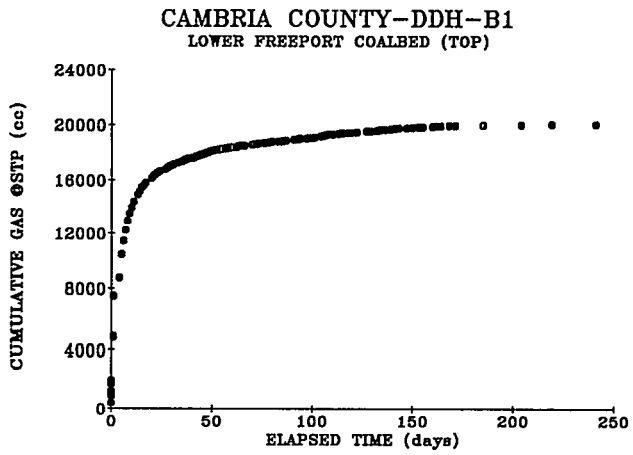


Figure 9. Cumulative gas content versus elapsed time for the top portion of the Lower Freeport coalbed in Cambria County [6].

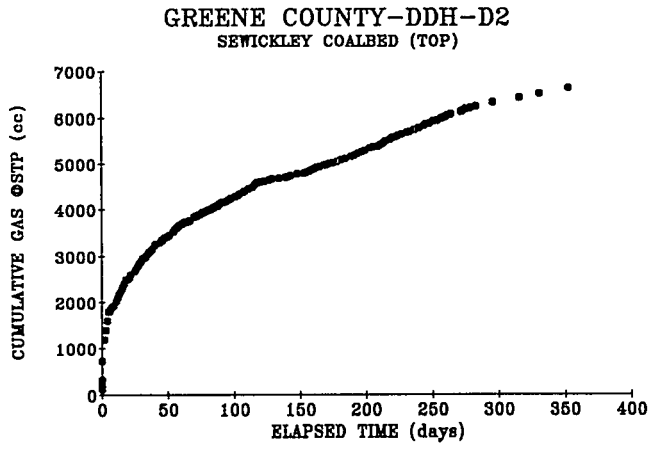


Figure 7. Cumulative gas content versus elapsed time for the top portion of the Sewickley coalbed in Greene County [6].

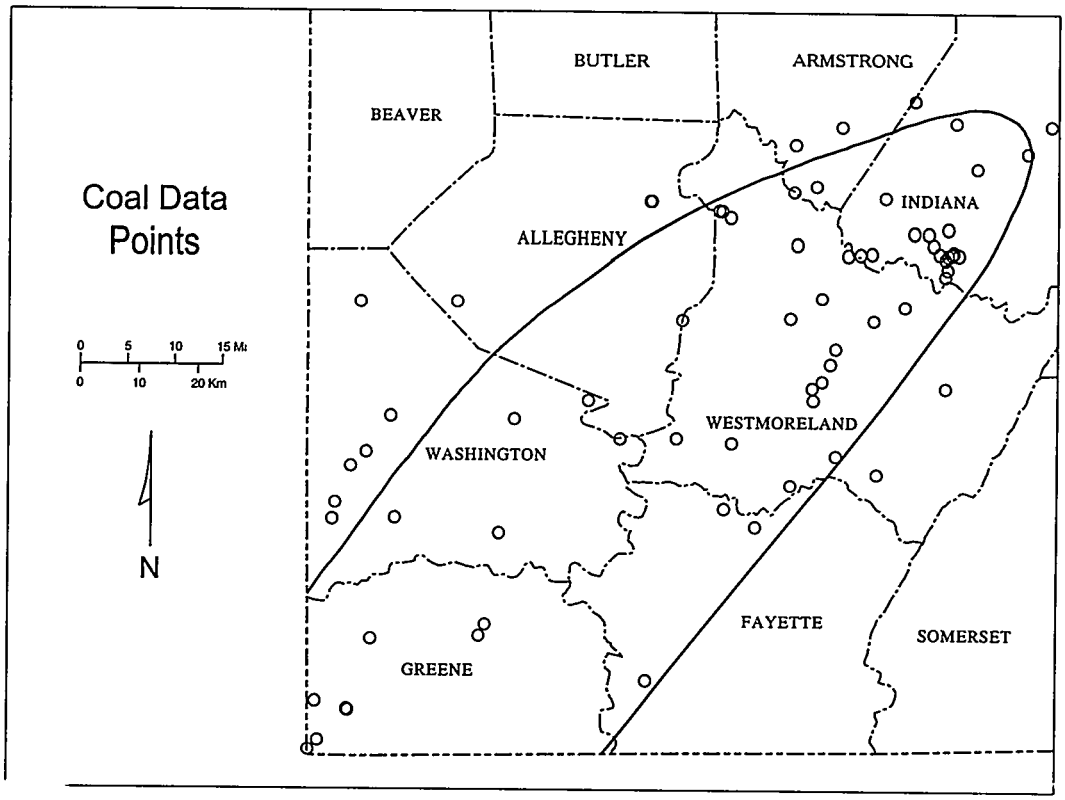


Figure 10. Location of wells with core and gamma ray/density log suites used for coal mapping (modified from [3]).

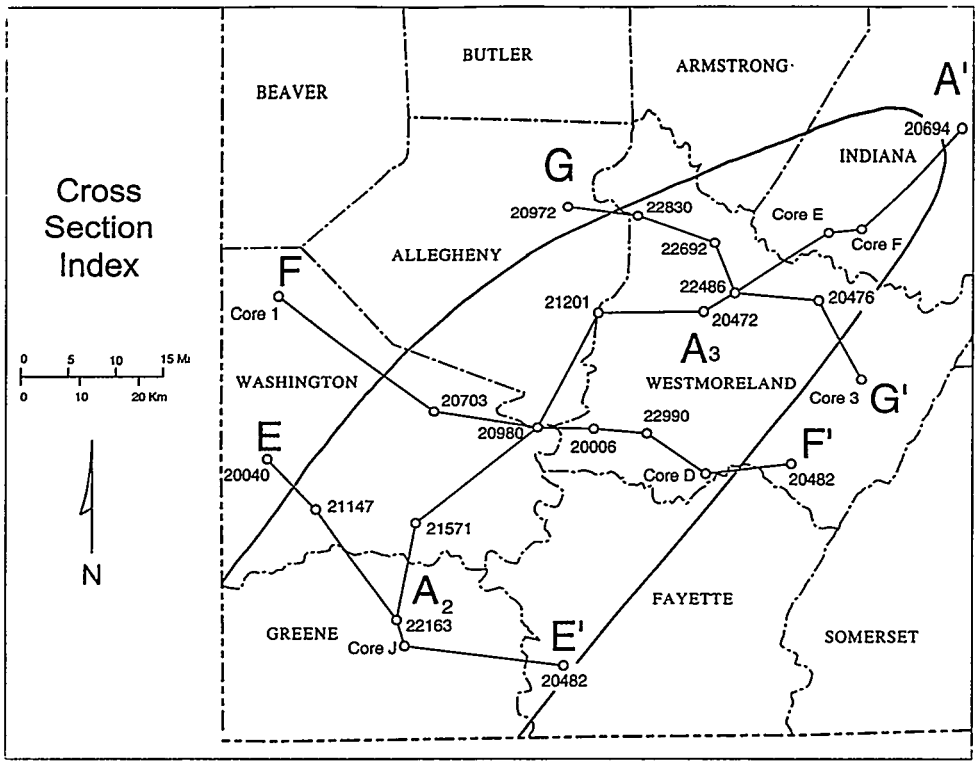


Figure 11. Cross section index map (modified from [3]).

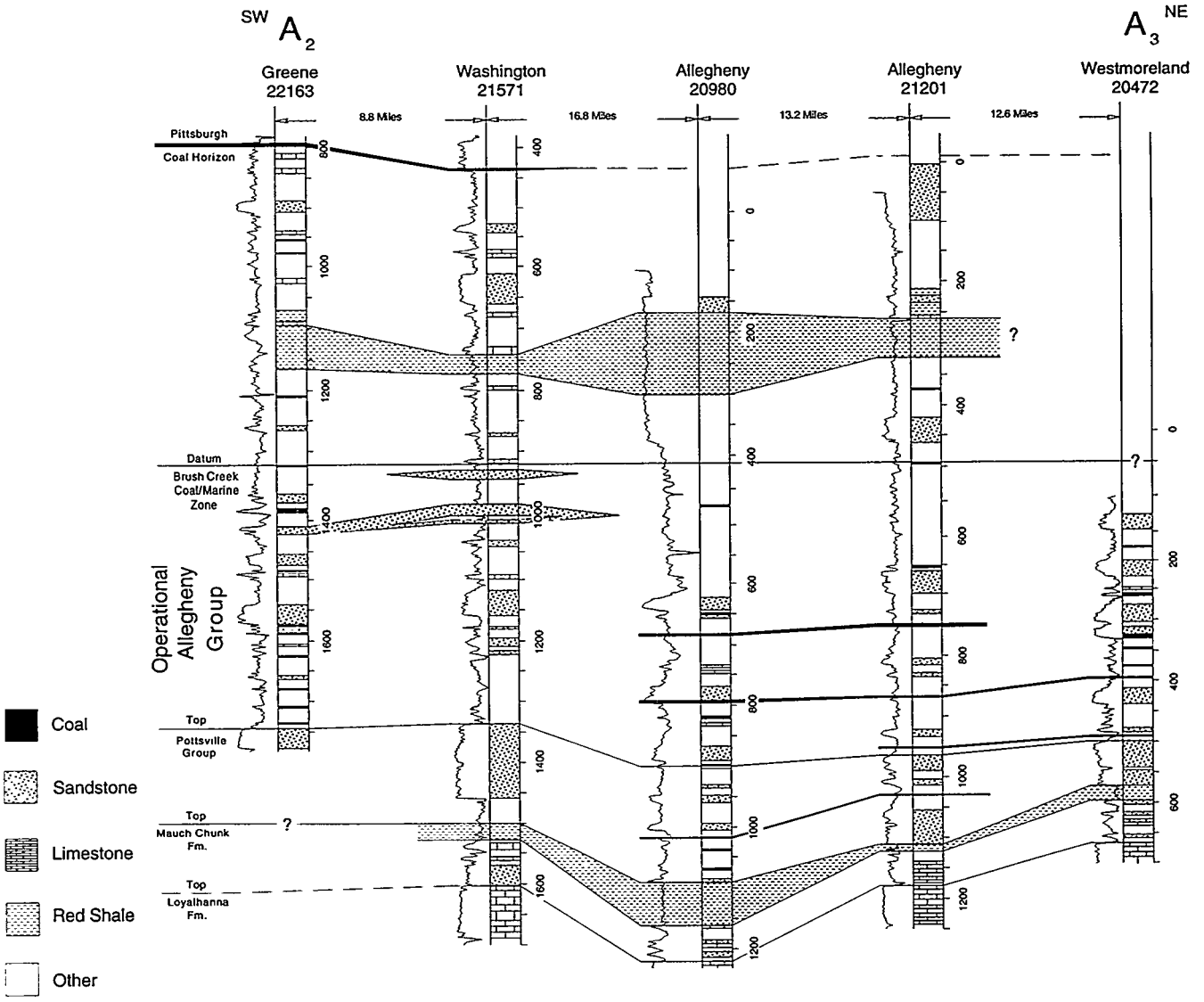


Figure 12. Explanation with cross section A_2-A_3 showing the Pittsburgh coal to Loyalhanna Formation interval in Greene, Washington, Allegheny, and Westmoreland counties, Pennsylvania (modified from [3]).

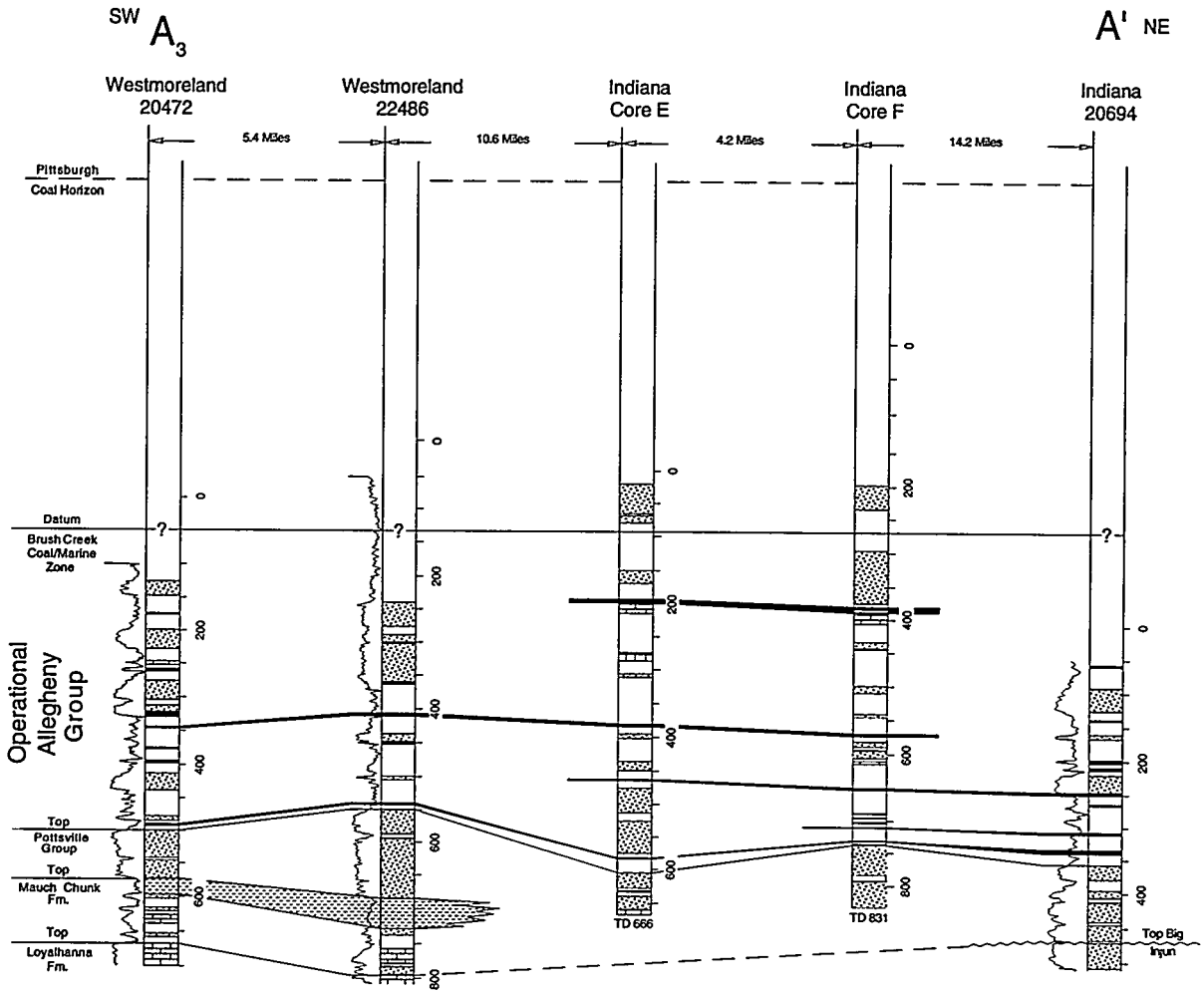


Figure 13. Cross section A_3-A' showing the Pittsburgh coal to Loyalhanna Formation interval in Westmoreland and Indiana counties, Pennsylvania (modified from [3]). Refer to Figure 12 for explanation.

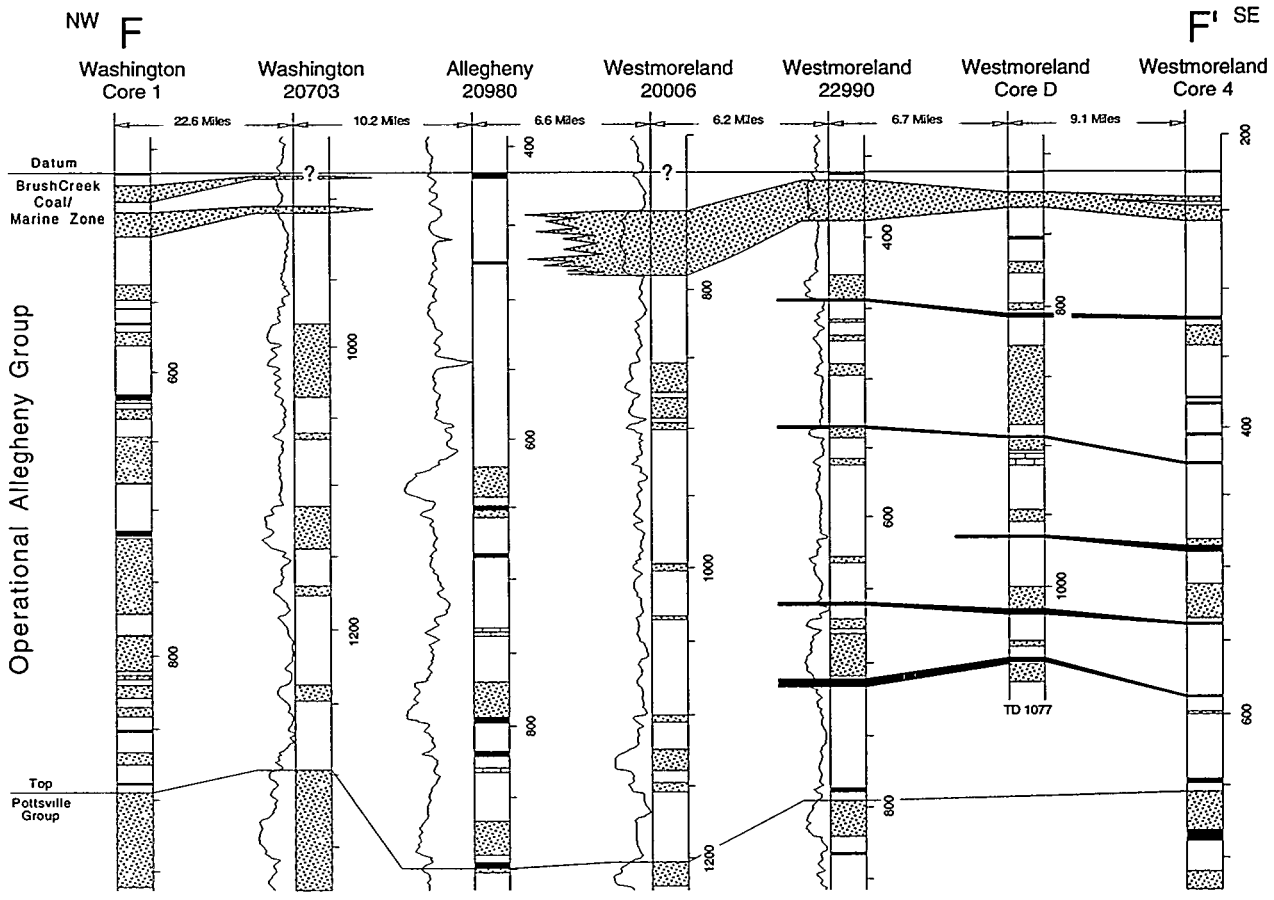


Figure 14. Cross section F-F' showing the operational Allegheny Group in Washington, Allegheny, and Westmoreland counties, Pennsylvania (modified from [3]). Refer to Figure 12 for explanation.

INTERGAS '95

May 15-19, 1995
The University of Alabama
Tuscaloosa, Alabama USA

9530

The Use of Coalbed Methane Simulators for Coal Mining-Related Applications

M.D. Zuber and M. Semmelbeck,
S.A. Holditch & Associates, Inc.

ABSTRACT

This paper discusses the use of a coalbed methane simulator that has been modified to account for the removal of grid blocks as a function of time to estimate gas emission and production for a variety of mine-associated problems. The specialized features of the simulator are presented. Example applications illustrate the models' use in estimating methane emission rates during mine roadway development, and estimation of longwall panel degasification by horizontal boreholes.

INTRODUCTION

Coalbed methane simulators have been developed for solving a variety of well problems.[1-5] These simulators are designed for analysis of coalbed methane production wells and include the reservoir mechanisms significant to gas and water flow in coals, including desorption, diffusion, and two-phase flow in the coal fracture system.[1] Wide-spread application of coalbed methane models has demonstrated the usefulness to engineers of these tools for analyzing and estimating production from coalbed methane wells.[5-7] However, most existing simulators are restricted to modeling flow into wells, either vertical or horizontal.

The coalbed methane production industry is expanding rapidly into the northeastern United States and Eastern Europe. In these areas, development is likely to be associated with active mining projects. The need for analytic tools that can be used to predict, design, and evaluate production of mine-associated coalbed gas is obvious. Mining companies are increasingly viewing coalbed methane as a potential resource. Mine-gas problems can have a significant impact on the ability of a mining operation to profitably operate. Therefore, it is important for a mine plan to incorporate accurate estimates of methane emissions and design appropriate methane mitigation techniques.

Longwall mining poses many problems which may be addressed by simulation. Longwall mining removes large volumes of coal from the seam very rapidly. Methane is released into the mine workings as the mined coal is ground from the seam face. In addition, methane flows into the mine workings across the exposed mine faces. In an active mine, the area of exposed mine face is continually expanding. The rate of gas flow across any specific area of exposed mine face depends primarily upon the gas content, permeability, and pressure of the coal, as well as the cumulative time of exposure to the mine workings. To accurately predict mine-associated methane emissions, a coalbed methane simulator must account for these dynamic reservoir changes. **Fig. 1** shows schematically the developments associated with a typical longwall project. The following problems are of particular importance in estimating methane emission and/or production.

- Methane emissions during roadway development. This is particularly important because the mine workings are encountering the coal at virgin reservoir conditions (the seams contain the maximum amount of gas).
- Methane drainage potential of inseam horizontal wells (drainholes) drilled into the longwall panels.
- Gob well production from seams and other gas-bearing strata above the mined coal seam in the areas of relaxed stress.

The primary limitation of well-based coalbed methane reservoir simulators for application to mine-related problems is the inability to account for the removal of coal as the mine workings progress through time. We have modified a coalbed methane simulator to dynamically account for the removal of reservoir blocks as a function of time, the concurrent expansion of exposed mine face area as a function of time and the methane production associated with this process. We have found that this simulator is capable of accurately estimating methane emissions in coal mines. The purpose of this paper is to discuss the enhanced capabilities of a coalbed methane simulator (COALGAS™)[8] developed specifically for mine-related applications. We discuss the formulation of this coalbed mine simulator, focusing specifically on the features associated with the capability to model the dynamic removal of coal reservoir as a function of time. We then present example applications of this simulator for estimating methane recovery from roadway developments and for estimating gas pre-drainage for horizontal wellbores. A variety of other applications of coalbed simulators for mining related problems, such as estimating gob well

production are possible. However, these are beyond the scope of this paper, and are not addressed.

MINE SIMULATOR FORMULATION

This section discusses the features of coalbed methane simulators, and the specialized features of COALGAS™[8], the coalbed simulator developed by S. A. Holditch & Associates, Inc. for modeling mining processes.

FEATURES OF COALBED METHANE SIMULATORS

Coalbed methane simulators have been developed to account for the complexities of the coal reservoir.[1,3] These simulators are used to analyze well tests, predict well performance, estimate well reserves, and optimize reservoir performance. All currently available coalbed methane simulators are based on the same set of basic theories regarding the storage and flow of both methane and water in coals.[1] Most of these theories were developed by mining research organizations (the U.S. Bureau of Mines, etc.) in an effort to understand methane flow in coals, and to determine ways to minimize the occurrence of mine explosions. The current understanding of the mechanisms that govern gas and water storage and flow in coals are schematically illustrated in **Fig. 2.**

Currently available coalbed methane simulators handle the processes of methane and water flow in coals as a three stage process where:

- Methane flows through the coal matrix by diffusion;
- Methane transitions (desorbs) from the adsorbed state to the free state at the matrix cleat interface; and
- Gas and water flow in the bulk cleat system in response to pressure gradients as described by Darcy's Law (see **Fig. 2**).

The equations incorporated in coalbed simulators to model these mechanisms have been discussed in detail in the literature.[1,3,4,5] Currently available coalbed methane simulators are designed to be flexible enough to allow the user to solve a variety of problems.

COALGAS™, a reservoir simulation tool developed by S. A. Holditch & Associates, Inc. (SAH), is a three-dimensional finite-difference reservoir simulator. To use this model for simulating production from coal reservoirs, the reservoir is divided into discrete blocks. Each grid block is assigned reservoir properties such as permeability, porosity, adsorbed gas content, water saturation, etc. using available geologic and engineering data. Wellbores, either vertical or horizontal, can be placed in each grid block and assigned properties to emulate actual well conditions, such as wellbore radius, degree of skin damage or stimulation, flowing pressure, specified flowing rates, etc.

Data Used in Simulation

Because coalbed methane simulators simultaneously model several flow mechanisms, much data is required to accurately model these processes. A list of the data required to simulate production using a coalbed methane reservoir simulator is shown in **Table 1.**

TABLE 1

DATA INPUTS FOR COALBED RESERVOIR SIMULATION

Matrix
Adsorbed Gas Content
Desorption Isotherm
Bulk Fracture System
Average Permeability
Average Fracture Spacing
Average Effective Porosity
Initial Water/Gas Saturations
Relative Permeability Relationship
General
Drainage Area
Net Coal Thickness
Reservoir Pressure
Flowing Bottomhole Pressure
Gas/Water PVT Data
Hydraulic Fracture Half-Length
Bulk Density of Coal

Most of the key data items can be determined from core tests, well logs, or pressure transient tests. Significant effort in terms of sample gathering, lab testing, and well testing is required to gather these data. However, for mine associated problems, many of these data are typically available from core data obtained from coreholes drilled as a routine part of the mine development process.

MINING MODEL FORMULATION

COALGAS™[8] has been modified to include features specifically for coal mining applications. Grid blocks that represent parts of the coal seam which will be removed by mining can be removed from the simulation at the appropriate times, without re-starting the simulation run. Consider a part of a simulation grid where a new roadway is about to be driven. **Fig. 3** shows a plan view of part of the grid with a well located in the first gridblock which is to be removed. As the simulation proceeds, each movement of the roadway is simulated by removing part of the grid. As the simulation proceeds, the model estimates the gas production rate off the roadway face. In addition, the volume of gas in the removed coal blocks is recorded. This provides an estimate of the potential gas volume that may be liberated, in addition to gas flow across the roadway face, due to the grinding of the mined coal.

As the simulation progresses, new wells are added to account for flow at the new portions of the seam which are opened by progress of the mine. This is shown in **Fig. 4**, where 17 well completions are used to represent flow at the mine face along this roadway. This simulation can be extended to include drainholes drilled from the roadway into adjacent panels which are to be mined at a later date. All of these activities can be modeled in a single simulation run.

The primary purposes of these simulations is to determine the amount of gas that can be removed from the coal seam and estimate the amount of methane that must be handled by a mines' ventilation system. **Fig. 5** illustrates the actual flow of gas at the mine face that is being represented by wells within the unmined coal seam. Like all simulations, however, the accuracy is dependent on the accuracy of the reservoir data specified to the simulator.

DEGASIFICATION OF LONGWALL PANELS

One of the mining related issues that can be addressed using a coalbed simulator is the estimation of the number of drainholes required to sufficiently drain the gas from a longwall panel prior to mining the panel. In some mines, the coal may have a high enough gas content that longwall panels cannot be safely mined at an economic rate without prior drainage of at least some of the methane in the panels.[10-12] Several criteria may be used to evaluate the sufficiency of panel drainage, depending on the specifics of a particular project. Common criteria are:

1. Reduction of the panel gas content of the coal by a specified fraction, or
2. Reduction of the panel gas content below a specified acceptable level.

These criteria should be determined based on mining experience, and using the results of core data available from the coal seams to be mined. The timing of the panel gas drainage to the specified criteria is an important factor in the drainhole development plan. This will depend primarily on the panel dimensions, and key reservoir properties such as permeability and initial gas content.

An example of the simulation grid used to evaluate this problem is shown in **Fig. 6**. Our assumed typical longwall panel dimensions are 5,500 ft in length, 630 ft in width, and a coal thickness of 5.3 ft. We used coal reservoir properties similar to those reported for the Pocahontas No. 3 coal.[12-17] These data are provided in **Table 2.**

TABLE 2

SUMMARY OF PROPERTIES USED FOR LONGWALL MODEL

Reservoir Property	Value Used
Panel Dimensions	
Length, ft	5,540
Width, ft	630
Horizontal Wellbore Length, ft	530
Coal Seam Thickness, ft	5.30
Initial Reservoir Pressure, psia	700
Water Saturation, fraction	0.70
Initial Gas Content, scf/ton	440
Base Permeability, md	1.0
Cleat Porosity, %	1.0
Langmuir Volume, scf/ton, DAF	536
Langmuir Pressure, psia	255
Ash Content, %	0.13

The following simplifying assumptions are made for the purposes of estimating gas drainage requirements using horizontal drainholes in the panel.

- A representative section of the panel is utilized (200 ft in this case).
- The drainhole wellbores are 530 ft in length, 3-in in diameter, with completed skin factors of +1.5. The first 50 ft from the mine face is cemented, and therefore non-productive.
- All wells are produced simultaneously.
- Flow across both ends of the panel into the mine workings is allowed. This assumes that roadway development is completed on both sides of the panel at the time when the horizontal drainholes are completed in the panel.

We conducted a series of simulations for this representative 200-ft section of longwall panel assuming no wells are drilled in the panel, and for well spacings of 200, 100, 67, and 29 ft. All simulations were made for period of 2 years (730 days). We generated this series of runs using reservoir permeabilities of 1 md and 5 md.

Fig. 7 and **8** illustrate the results of these simulation runs using plots of the percentage of initial gas in place in the longwall panel drained as a function of time. These figures show that drainage from the panel is accelerated as the number of wells in the panel is increased (closer well spacing is utilized). These results also indicate the impact of formation permeability on drainage times, with more rapid drainage capabilities at higher permeabilities.

The results shown in **Figs. 7** and **8** are used to estimate the time to drain a specified portion of the gas contained in the longwall panel. For this example, we chose a threshold of 75% of the initial gas in place as an acceptable level of drainage. The time

to drain 75% of the initial gas in place for each of the simulation cases described above is shown in **Fig. 9**. This graph can be used to determine time requirements for pre-draining longwall panels at a specified drainhole spacing or to determine the drainhole spacing necessary to meet pre-drainage requirements. For example, in the case illustrated here, a drainhole spacing of 62 ft would be required to drain 75% of the gas from a panel in a lead time of 200 days, if the formation permeability is 1 md.

The techniques shown in this example could be applied to any mine design plan where longwall panels are being developed and gas emissions from longwall panels are problematic. The key reservoir factors in this problem are the initial gas content of the coal, the coal thickness, and the seam permeability. Coal thickness and gas content are generally readily available from core data. Permeability can be estimated from a production history match of test drainholes developed prior to full scale development of the target coals, or from well tests conducted on vertical wellbores.

Note that this example assumes no pre-drainage of the longwall panel due to flow of gas across the exposed panel faces into the mine workings. A more rigorous analysis would include estimation of this pre-drainage using the methods illustrated in the following example.

GAS INFLOW DURING ROADWAY DEVELOPMENT

Another significant problem in the development of mine programs which can be addressed by a coalbed simulator is the ability to estimate the volume of gas inflow which will occur during roadway development. In this case, the reservoir simulator is used to estimate the rate of gas emission into the advancing roadway. This is important because there will be a maximum safe rate of gas emission that can be handled by the ventilation system designed for the mine development project. Based on the parameters of the ventilation system, the maximum allowable methane emission rate can be estimated using the legal limitations of methane content in the ventilation air stream. The simulator is then used to estimate the rate at which mining can safely proceed, or provide data to re-design the ventilation system.

Fig. 10 shows a schematic of a typical roadway for longwall development. The mine coalbed simulator described in this paper is capable of estimating the volume of gas emission into the mine workings as the roadway is advanced. The rate of gas influx into the roadway ventilation systems will be dependent on the initial gas content of the coal, the permeability of the coal, and the rate of development. Obviously, the goal of the mining process is to establish the maximum development rate which can be used to develop the roadway systems.

As an example of how the coal simulator is used to address this problem, we calculated the methane emissions during the development of a 4,000 ft roadway. As in the previous example, we utilized the reservoir properties consistent with data reported for the Pocahontas No. 3 seam.[13-17] The assumed coal thickness for this problem is 5.3 ft, and the width of the pillar between the dual advancing roadways is assumed to be 60 ft. The roadway width is assumed to be 20 ft. For simplicity, the simulation includes calculations for one of the dual advancing roadways. It is assumed that both roadways are developed simultaneously. The effects of the cut-throughs developed periodically between the roadways for the purposes of circulating ventilation air are ignored.

A series of simulation runs was made for the problem described above assuming roadway advance rates of 25, 50, and 100 ft per day, and reservoir permeabilities of 1 md and 5 md. The simulator calculates the methane emission rate across the sidewalls of the advancing roadway as a function of time. The results from these simulations are compared using plots of gas emission rate as a function of the roadway development distance. The results of these simulations are shown in **Fig. 11** for the 1 md case, and **Fig. 12** for the 5 md case.

These results illustrate that gas influx rate is highly dependent on the roadway advancement rate and coal permeability. Simulations such as these provide valuable information for use in designing mine ventilation and evaluating the economic relationship between ventilation capacity and mine development rate. For example, in the case illustrated here, if the maximum influx rate that the ventilation system could handle and maintain the air methane content below the legal limit is 750 Mscf/D, a 4,000 ft roadway could be developed at a rate of 50 ft/day (see **Fig. 11**) if the coal permeability is 1 md, and 25 ft/day if the coal permeability is 5 md.. Conversely, these results could be utilized to design a ventilation system such that a desired roadway advanced rate could be achieved.

Although not presented here, the impact of fractured zones, which could lead to periods of short-term high-rate gas inflows into the ventilation system could be estimated by this model by including areas of higher permeability intersecting the advancing roadway. This would provide estimates of the short-term effects of contact with fracture zones in the mine seams. In addition, the effect of horizontal drainholes on mine emissions could be estimated by the addition of drainholes to the simulation case described above. This could be accomplished in a single simulation run.

SUMMARY

A specialized formulation of a coalbed methane simulator that allows dynamic removal of coal blocks to simulate continuous mining operations, and estimate methane emissions due to pulverization of coal during mining has been presented. Example applications of this model for (1) estimating gas drainage of a longwall panel by horizontal drainholes, and (2) estimating gas emissions during roadway development have been illustrated. Based on the results of these example applications, the following conclusions have been drawn.

1. The lead-time necessary to achieve a specified percentage of gas drainage of a longwall panel using horizontal drainholes is a strong function of coal seam permeability and drainhole spacing. The drainhole spacing required to achieve a specified amount of pre-drainage prior to mining can be

estimated using the coalbed methane reservoir model described in this paper.
2. Methane inflow into mine workings are a strong function of coal seam permeability and the mining rate. The relationship between maximum safe mining rate and ventilation capacity can be estimated using the coalbed reservoir model described in this paper.

REFERENCES

1. Zuber, M. D. and Semmelbeck, M. E.: "Simulators Analyze Coalbed Methane," *The American Oil and Gas Reporter* (September 1990), 40-44.
2. King, G. R., Ertekin, T., and Schwerer, F. C.: "Numerical Simulation of the Transient Behavior of Coal Seam Degasification Wells," *Formation Evaluation*, (April 1988), 165-183.
3. Schwerer, F. C.: "Development of Coal-Gas Production Simulators and Mathematical Models for Well Test Strategies", Final Report to Gas Research Institute, May, 1986.
4. Sawyer, W. K., Paul, G. W., and Schraufnagel, R. A.: "Development and Application of a 3D Coalbed Simulator", paper 90-119 presented at CIM/SPE International Technical Meeting, Calgary, Alberta, June 10-13.
5. Young, G. B. C., Paul, G. W., Saulsberry, J. L., and Schraufnagel, R. A.: "Characterization of Coalbed Reservoirs at the Rock Creek Project Site, Alabama", Proceedings of the 1993 International Coalbed Methane Symposium, Birmingham, 705-714.
6. Zuber, M. D., Sawyer, W. K., Schraufnagel, R. A., and Kuuskraa, V. A.: "The Use of Simulation and History Matching to Determine Critical Coalbed Methane Reservoir Properties," paper SPE/DOE 16420 presented at the 1987 SPE/DOE Low Permeability Reservoirs Symposium, Denver, May 18-19.
7. Sawyer, W. K. *et al.*: "Using Reservoir Simulation and Field Data to Define Mechanisms Controlling Coalbed Methane Well Production," paper 8763 presented at the 1987 Coalbed Methane Symposium, Tuscaloosa, Nov. 16-19.
8. COALGAS: A Comprehensive Coalbed Methane Simulator, User's Manual, Version 3.1, S. A. Holditch & Associates, Inc., College Station, TX, Jan. 1990.
9. Gray, I: "Reservoir Engineering in Coal Seams: Part I - The Physical Process of Gas Storage and Movement in Coal Seams", *SPERE* (Feb. 1992) 1-4.
10. Diamond, W. P., Ulery, J. P., and Raab, D. E.: "Evaluation of the Source and Migration of Longwall Gob Gas - Lower Kittanning Coalbed, Cambria County, Pennsylvania", The 1991 Coalbed Methane Symposium Proceedings, Tuscaloosa, AL, May 13-17, 1991, Gas Research Institute, May 1991, p. 171-180.
11. Ulery, J. P. and Hyman, D. M.: "The Modified Direct Method of Gas Content Determination: Application and Results", The 1991 Coalbed Methane Symposium Proceedings, Tuscaloosa, AL, May 13-17, 1991, Gas Research Institute, May 1991, p. 489-500.
12. Baker, E. C. *et al.*: "Economic Evaluation of Horizontal Borehole Drilling for Methane Drainage from Coalbeds," 1986, USBM IC 9080.
13. Schatzel, S. J. *et al.*: "Underground Gob Gas Drainage During Longwall Mining," 1982, USBM RI 8644.
14. Krickovic, S. *et al.*: "Methane Emission Rate Study in Deep Pocahontas No. 3 Coalbed Mine in Conjunction with Drilling Degasification Holes in the Coalbed", 1972, USBM RI 7703.
15. Kissell, F. N.: "Methane Migration Characteristics of the Pocahontas No. 3 Coalbed", 1972, USBM RI 7649.
16. Reznik, A. A. *et al.*: "Air-Water Relative Permeability of Pittsburgh and Pocahontas Coals", *SPEJ* (Dec. 1974) 556-562.
17. Kim, A. C.: "Estimating Methane Content of Bituminous Coalbeds from Adsorption Data", U.S. Bureau of Mines, RI 8245 (1977).

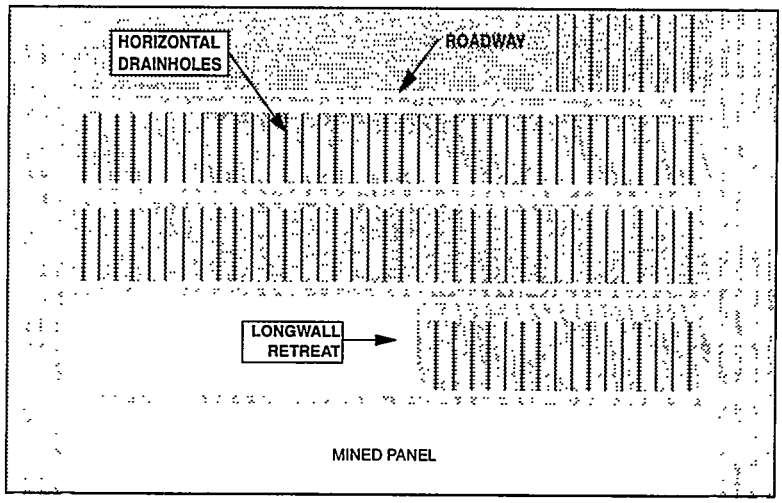


Fig. 1 -Schematic of longwall mine workings.

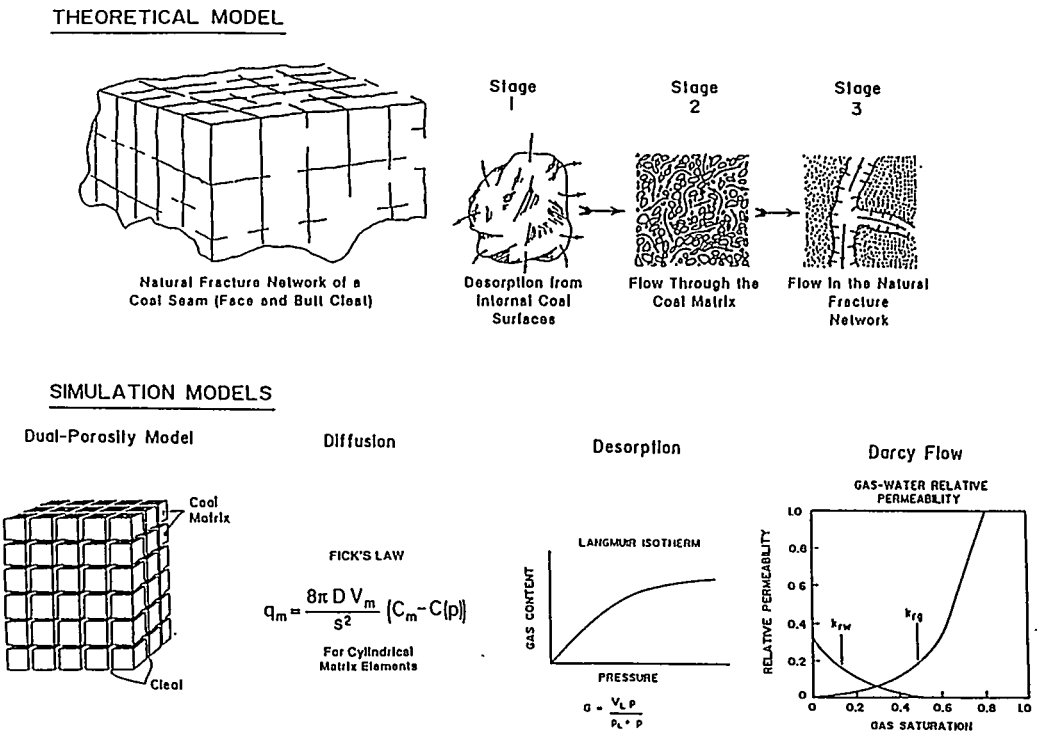


Fig. 2 -Mathematical representation of coal storage and transport mechanisms in coalbed simulators.

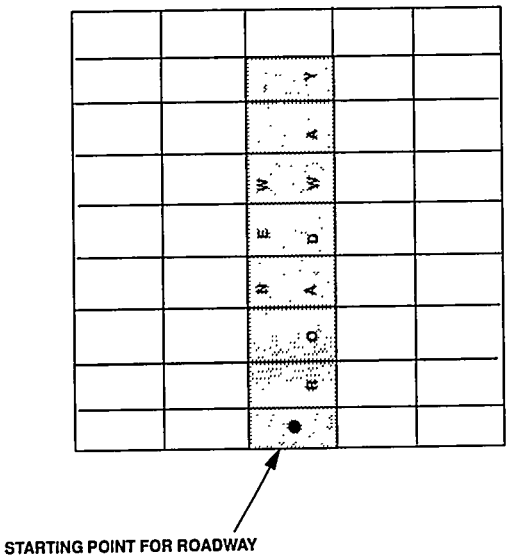


Fig. 3 -Plan view of simulation grid for roadway development with well at starting point of new roadway.

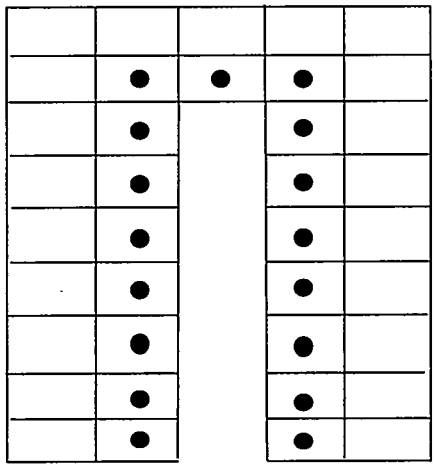


Fig. 4 -Grid with roadway cells removed and wells to account for flow into the roadway from the mine face.

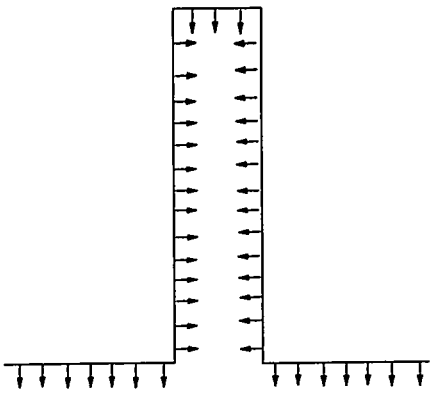


Fig. 5 -Flux at all open wall faces of the mine can be modeled by COALGAS.

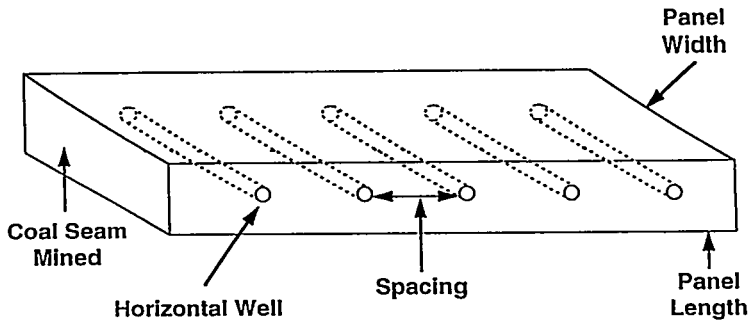


Fig. 6 -Schematic of simulation model used to estimated longwall panel degassification using horizontal drainholes.

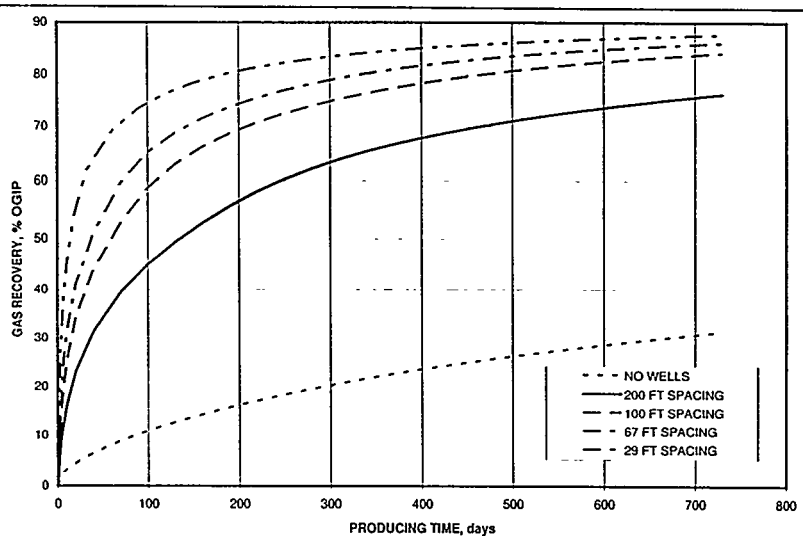


Fig. 7 -Simulated gas drainage from a 200-ft panel section for a 2-year drainage time as a function of drainhole spacing; 1 md Case.

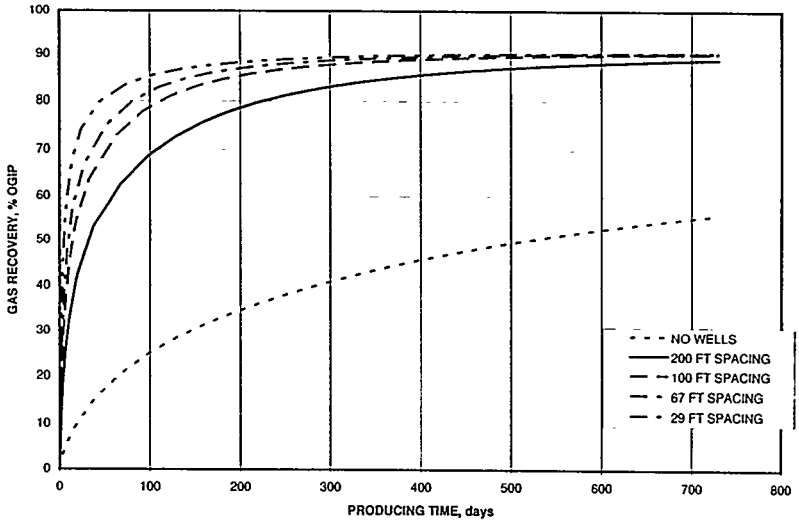


Fig. 8 -Simulated gas drainage from a 200-ft panel section for a 2-year drainage time as a function of drainhole spacing; 5 md Case.

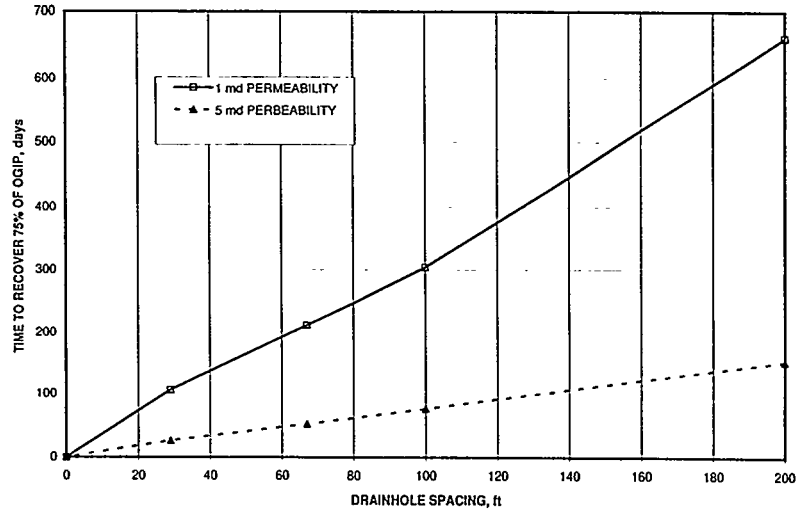


Fig. 9 - Estimated time to recover 75% of in place gas from a longwall panel as a function of drainhole spacing; permeability's of 1 md and 5 md.

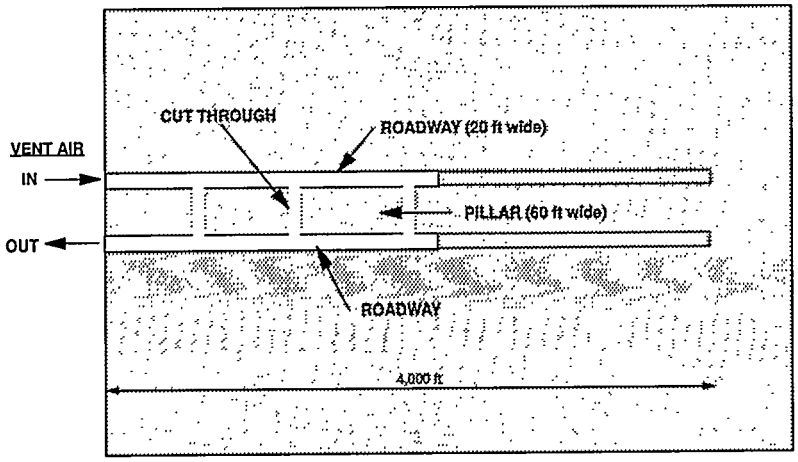


Fig. 10 -Schematic of roadway development (includes dimensions used in example problem).

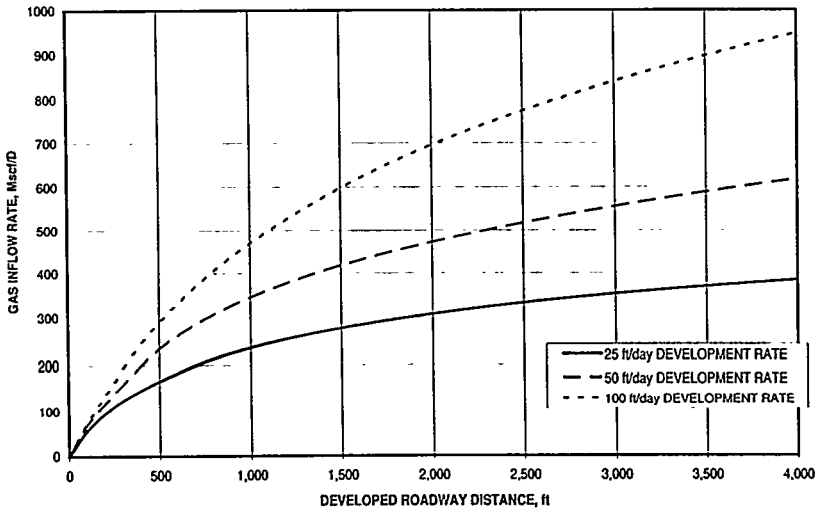


Fig. 11 -Simulated gas inflow into roadway during roadway development as a function of roadway advance rate; 1 md case.

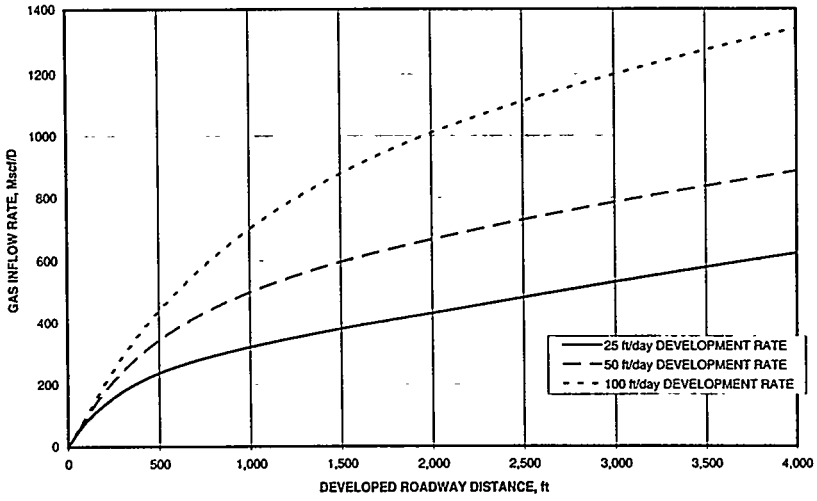


Fig. 12 -Simulated gas inflow into roadway during roadway development as a function of roadway advance rate; 5 md case.



NOTES

INTERGAS '95

May 15-19, 1995
The University of Alabama
Tuscaloosa, Alabama USA

9555

Role of Longwall Gob Formation in Coalbed Methane Emission

S. Patton, Montana Technological University;
Y. Jiang, D. Deb, T. Novak, and D. Park,
The University of Alabama

ABSTRACT

Because of increased scrutiny by the Environmental Protection Agency (EPA), more coal mines in the future may be forced to consider methane collection as a means to reduce methane emissions to the atmosphere, in addition to degasification for safety purposes. With increased need for collection, the importance of quantifying the gas emission zone of a mine becomes apparent. Methane can enter the mining area from the coal seam being mined and from the surrounding coalbeds as a result of fracture development and caving. The actual emission zone is a three-dimensional area surrounding the working face, including the caving zone (gob area), fracture zone, and yielding zone. There is evidence that methane is emitted from nearby seams when the roof falls and floor heaves. Thus, the degree of methane emission is closely related to geomechanical characteristics, such as strata yielding due to pressure, fracture development in the overlying strata, and roof caving. This paper presents the initial phases of an investigation into the correlation between the geomechanical behavior of the gas emission zone with methane liberation.

INTRODUCTION

Methane is contained under pressure within the micropores, joints, and fractures of coalbeds. Fractures are formed in the highly stressed or relaxed zone of the mining area (Diamond and Ulery, 1991; Layne et al., 1987), and gas flows, by Darcy flow, through the network of cracks contained within the coal structure and adjacent strata toward a low pressure region (working face or gob area). Methane liberation is closely linked to coal face movement in longwall mining (McCulloch and Daurice, 1973) and is dependent on development of fractures in roof strata (McPherson, 1975). Furthermore, the permeabilities in the emission zone are increased because of mining and may be the principal factor controlling gas emission into the working and gob areas.

An investigation of the geomechanical behavior of the gob gas emission zone is being conducted within the Warrior Basin of Alabama, where the Blue Creek and Mary Lee seams are being mined and horizontal and gob well degasification are practiced. Extensive data were collected from the site, including monthly or daily gob gas production, geological information, and mining activities. The location of gob wells and the face advancement for three typical panels are illustrated in Figure 1 (face locations as a function of time are indicated by dashed lines). The panels studied range from 3200 to 6120 ft in length and 575 to 840 ft in width. Gob wells are identified by their section, township, and range, and are represented by a hatched circle at the panel centerline. Figure 2 gives the stratigraphic column (S-310-4) of coal groups near the three panels shown in Figure 1. Detailed information about the surrounding coal seams is shown in Figure 3.

Three coal groups, Cobb, Pratt, and Black Creek, are considered major contributors to gob gas production. The focus of this study is to characterize the geomechanical behavior in the emission zone with respect to methane liberation and gob gas production. The overall objectives are to correlate methane liberation, migration, and gob well production with coal production, panel characteristics, stress redistribution, roof deformation, fracture development in the overburden, roof falls, strata and pillar yielding, and floor heaving as related to longwall mining. The initial work performed in this study is presented here and includes collection and correlation of the data related to methane emission, such as gob well production, horizontal well production, gas emission to the ventilation system, mining advance rate, camera surveys of prior gob wells for fracture information, and the monitoring of free gob-well casing movement relative to the set casing with face advancement over time.

MONITORING AND DATA COLLECTION

Gob Well Production

Gob wells are drilled to a depth of 30 ft above the mined coal seam near the centerline of the longwall panels. The holes have typical depths of 1600-2000 ft. The upper half of the hole is cased while the bottom is left open. Three or four holes are drilled per panel and are concentrated mostly in the first half of the panel. Gob well production is reported in thousands of cubic feet at standard temperature and pressure, and has been collected on a daily or monthly basis.

Horizontal Well Production

Horizontal wells are drilled to a depth approximately 75% of the panel width at a spacing interval based on experience. A typical panel in the study area has approximately 20 to 25 wells with a total footage in the range of 7500 to 10,000 ft. The data for horizontal well production were also collected and used for evaluation of the total amount of methane emission.

Mining Advance Rate and Mining Height

Daily or monthly mining advance rates are collected as indicated in Figure 1 by dashed lines. The corresponding coal seam thickness and mining height are also collected. With the use of computer modeling and camera surveys, the volume of void area in the coal seam horizon can be estimated.

Ventilation System

The mine ventilation system must be taken into account when considering overall gas emission. Gas emission rates are not recorded throughout the mine on a continuous basis. Monthly data is collected for state reports on emission in the development sections, longwall face, and at the fan. An estimation of the gas emitted from the gob zone into the ventilation system is determined by subtracting the mining face emission from the fan emission. This should be representative of the percentage contribution of gob gas.

Camera Surveys of Gob Well

Downhole information can be obtained by using a small diameter camera encased in a housing and connected to the end of an armored cable. The cable includes a transmitter cable and electric conductors. The electric conductors provide power to the camera, lights, and camera control. The transmitter cable conveys the information to the surface for recording on VHS tapes. The depth is recorded as the survey progresses. The depth of fracturing, fracture spacing, and density of fractures can be obtained from the surveys. Indications of gas and water are also available by viewing casing separation points. At the present time, this information is being used to verify hypotheses concerning gob formation for modeling purposes.

Relative Casing Movement

A diagram of a typical gob well cross-section is included as Figure 4. Gob wells are typically drilled to a depth of 2000 ft, stopping at a marker bed some distance (approximately 30 ft) above the seam being mined. A large diameter (17-1/2") hole is drilled to approximately 150 ft, cased, and cemented in place. A smaller diameter (12-1/4") hole is then drilled to the marker bed or required distance. This hole is cased approximately half its depth and cemented only the bottom 124 ft. Thus, the inner and outer casings move with ground movement, independent of each other. The relative displacement between two casings was monitored along with subsidence for a gob well in the same geologic setting as the well from which methane data was obtained.

The displacement measuring apparatus is shown in Figure 5. A ruler was fixed to the outer casing and a pointer to the inner casing to measure relative displacement between the two as mining progresses. Relative displacement, after correcting for subsidence, is the measurement of ground movement or bed separation between the bottom of the outer casing and the bottom of the inner casing. Due to field problems unrelated to monitoring, the measurements are not currently being recorded.

CHARACTERIZATION OF GEOMECHANICAL BEHAVIOR IN THE METHANE EMISSION ZONE

Stratigraphic Zones Due to Longwall Mining

As a longwall face advances, four different stratigraphic zones, i.e., yielding, caved, fractured, and continuous deformation, are formed due to stress redistributions (Figure 6). The caved zone, which ranges in thickness from 2 to 8 times the mining height, falls on the main floor in an irregular manner with material of various sizes. The expansion ratio or bulking factor plays an important role in determining the height of the caved zone. In the fractured zone, the strata are broken into blocks by vertical and/or sub-vertical fractures and horizontal cracks develope due to bed separation. The behavior of this zone can be compared with a force-transmitting beam of broken strata. The thickness of the fractured zone is 28 to 42 times that of mining height. In the continuous deformation zone, the strata are deformed without any major cracks.

It is believed that the permeabilities of the seam being worked, overburden, and surrounding strata, the main controlling parameters for methane flow, are affected by stress redistribution (Ediz and Edwards, 1990). The fracture system of the caved, yielding, and fractured zones will directly control methane production of gob gas wells. The range of those zones depends on a combination of geologic and mining factors, such as mining height, in-situ stresses, and rock properties of the overburden. As a result, a proper understanding of stress-permeability characteristics and geomechanical properties of strata will significantly contribute to research concerning the methane production of gob gas wells. Finite element modeling is being conducted to estimate the extent of gob formation and fracture development in the overburden strata. This should lead to a better understanding of the geomechanical behavior of rock strata.

Finite Element Models in Estimating Gob Formation

Finite element modeling is being performed to simulate stress distribution, gob formation phenomena, and surface subsidence as the longwall face advances. Figure 7 shows a two-dimensional finite element mesh including the Blue Creek seam, immediate and main roof, overburden, and other overlying coal seam groups (Pratt and Cobb). The depth of the mine being modeled is 1856 ft (566 m) below the surface. Three coal seam groups, located on top of the Cobb group as shown in the geological logs (Figure 2 and 3), were not included in the modeling, since the camera survey of gob wells indicated that the fracture system extends only up to 900 ft (274 m) on an average from the coal seam after the panel is mined out. Thus, in the finite element mesh, the working seam depth is 856 ft (264 m) and another 1000 ft (305 m) of overburden load is applied externally.

The first model is developed with 69 ft (21 m) of face advanced from the starting point. In all subsequent models, the face is advanced 40 ft (12 m) at a time and includes the cumulative gob zone created by previous models. Figure 7 shows the condition of the mine when the face is at 551 ft (168 m) from the starting point. The gob zone extends vertically 435 ft (132.5 m) from the working seam and suggests that the tensile cracks and fractures will be far beyond this height.

A progressive failure technique (Park and Gall, 1989) using Hoek and Brown failure criteria is applied for compressive failure of coal and rock. Simple tensile failure criteria are considered for these models. Any element having horizontal tensile stress is considered failed and immediately taken from the model. Since rock is weak with respect to tensile stress, the criteria provide a steady progression of tensile zone which extends the gob in each model. For the subsequent models, the face will be advanced 40 ft (12 m) and the same process will be continued. These models will produce detailed stress distributions in the yielded, fractured, and caved zones with further face advancing.

PRELIMINARY RESULTS AND DISCUSSION

Gob Well Production

Figure 8 illustrates total gas production for the three panels, G, H, and I. It can be seen that the production of methane from the gob wells reaches numerous peaks. In the early stages of mining, gas production at the gob wells is low because the emission zone in the gob is not yet formed. With face advancement, fractures initiate from the immediate roof to the main roof and gradually move toward upper layers, resulting in a large emission zone. Consequently, gas from the overlying seams are released into the ventilation system or stored in the gob zone. As the face intersects with the first gob well, it provides a low pressure gradient to initiate the release of methane from the storage location through the cracks and

fractures. Gas production increases with the increase in size of the emission zone, which is dependent on the development of fractures and caving in the mining area. The first peak in well production is thought to be attributed to the storage capacity of the fractured gob zone before communication is established with the first gob well. The remaining peaks result from fracturing into coal bearing zones above the immediate roof. The cumulative production per panel is compared in Figure 9. A relatively stable gob gas production, from 130 to 210 MCF per foot of face advancing, was reached after 2000 ft from the start of the panel. Panel I does not appear to follow the consistent behavior of the previous mined panels and is not shown in the figure. This inconsistent behavior could be attributed to placement of wells and/or operational problems.

Total Methane Emission

The following table lists individual contributions of gas emission for the G and H Panels. It can be seen that greater than 50% of the gas in the ventilation system can be attributed to the gob zone.

Longwall Panel	G-Panel	H-Panel
Gob to Ventilation System*	3,240	3,240
Active Face*	1,620	1,080
Horizontal Wells	**	178
Gob Well	1,507	1,962

*Estimated
**Data set not complete

Gob Gas Migration

An interesting case occurred during the months (7/25/91 - 10/25/92) when mining was conducted simultaneously in two adjacent panels (Panels G and H). The gob wells of Panel G show an increasing trend in gas production, which indicates the interaction that exists between the panels, even at great distance.

A comparison of the gob gas production for each well in the H Panel is shown in Figure 10. From analyses of gas production from each well, it can be seen that the methane emitted from mining mostly flows to the surface through the well nearest the face (after the face has passed the well). After passing the last well, 4-2-5, methane emitted from the remaining half of the panel migrates to the last well, resulting in higher production in that well. Also, it indicates that methane is highly mobile over a large range of the gob zone, and reveals that removing wells 33-10-9 and 33-15-10 may not reduce total gob gas production at Panel H although the removal rate may not be adequate to alleviate gas production at the face during mining. The same comparison for Panel G was conducted, and the results, similar to those in Panel H, are shown in Figure 11. However, production of the last well, 4-1-4 in Panel G, is less than expected. Obviously, gas leakage to the ventilation system or through cracks to the surface occurred. Further investigations will be directed toward the optimization of gob well design, including well spacing and location, and panel dimensions.

Effect of Face Width

In recent work, the monthly production data of 72 gob wells were analyzed in an attempt to established a correlation with panel width. The results are not conclusive at this time but do show an interesting trend that will be investigated further. The panel production per square foot was correlated for three ranges of panel widths, less than 650 ft, between 650 and 750 ft, and greater than 750 ft. The analysis results are presented in Figure 12, which show that gas production has a significant decreasing trend with increasing panel widths.

Initially, this phenomenon is being explained by the relationship between a competent sandstone layer (150-300 ft thick) located in the roof approximately 900 ft above the working seam. The gas-bearing coal seams are all located below this layer. It is thought that as the panel width is reduced, the sandstone does not fracture extensively, thus the gob gas is directed horizontally to the gob wells. As the panel width increases, the sandstone undergoes increasing tensile stresses which cause fractures and fissures to form within it. This in turn causes gas to migrate into the sandstone bed where it is possibly held as in a conventional reservoir. These results are preliminary and subject to further investigation. Data from an additional 190 wells will be collected for further analysis. Finite element modeling of the gob creation process will be used to identify panel width at which the competent sandstone is affected in an attempt to corroborate these findings.

Effect of Mining Face Advancing Rate

Variation in face advancement rates will affect the emission area created by mining as well as gob gas production. Figures 13 and 14 show a relationship between gob gas production and face advancement rate. It is clear that daily production is increased with face advancement rate, but gas production per volume of coal seam mined has a decreasing trend with an increase in face advancement rate.

SUMMARY AND CONCLUSIONS

A large amount of data related to this project has been collected, but much has yet to be assimilated into a usable format. It should be noted that the study area was not degasified in advance of mining through the use of vertical wells. What this data will reveal about formulating models for gob gas production and gob formation is left to be determined in the remainder of the project. Quantifying the amount of gas that can be collected in an economical manner before it reaches the ventilation system and is exhausted to the atmosphere is important information for mining companies. Preliminary analyses show there is an obvious relationship between the mining process and production of gob gas. A good understanding of geomechanical behavior in the methane emission zone will contribute greatly to gob gas recovery.

REFERENCES

1. Diamond, W.P., J.P. Ulery, "Evaluation of Source and Migration of Longwall Gob Gas—Lower Kittanning Coalbed, Cambria County, Pennsylvania," *Proceedings, 1991 Coalbed Methane Symposium*, Tuscaloosa, AL, May 13-16, pp. 171-180.

2. Dunmore, R., "Gas Flow Through Underground Strata," *Mining Engineer*, Vol. 128, No. 100, January 1969, pp. 193-199.

3. Ediz, I.G. and J.S. Edwards, "Numerical Simulation of Time-Dependent Methane Flow," *Mining Science and Technology*, Elsevier Science Publishers, Amsterdam, No. 12, pp. 1-15.

4. Kissell, Fred N.,"The Methane Migration and Storage Characteristics of the Pittsburgh, Pocahontas No. 3, and Oklahoma Hartshorne Coalbeds," RI 7667, *Bureau of Mines Report of Investigations*, 1972, 22 pp.

5. Lambert, S.W. and A.T. Michael, "Using Vertical Boreholes to Remove Methane from the Mary Lee Coalbed, Warrior Basin, Alabama—A Case Study," *Proceedings, 1991 Coalbed Methane Symposium*, Tuscaloosa, AL, May 13-16, 1980, pp. 257-264.

6. Layne, A.W., H.J. Siriwardane, and C.W. Byrer, "Factors that Influence the Effective Placement of Coalbed Methane Drainage Wells for Removel of Gob Above Longwall Panels," *Proceedings, 1987 Coalbed Methane Symposium*, Tuscaloosa, AL, Nov. 16-19, pp. 255-270.

7. McCulloch, C.M. and M. Daurice, "Geologic Factors Causing Roof Instability and Methane Emission Problems," RI 7769, *Bureau of Mines Report of Investigations*,1973, 25 pp.

8. McPherson, M.J., "The Occurrence of Methane in Mine Working," *Journal of the Mine Ventilation Society of South Africa*, August 1975, Vol. 28, No.8, pp. 118-126.

9. Mordecai, M. and L.H. Morris, "The Effects of Stress on the Flow of Gas Through Coal Measure Strata,", July 1974, *Mining Engineer*, Vol. 133, No. 9, pp. 435-443.

10. Park, D.W. and Y.M. Jiang, "Analysis of a Deep Longwall Face and Support System," 9th Annual Workshop, Generic Mineral Technology Center, Mine System Design and Ground Control, Lexington, KY, November 1991.

11. Park, D.W. and Gall, V., "Supercomputer Assisted Three-Dimensional Finite Element Analysis of a Longwall Panel," *Proceedings, 30th U.S. Symposium on Rock Mechanics*, West Virginia University, Morgantown, 1989, pp. 141-148.

12. Peng, S.S., H.C. Li, and Y.M. Jiang, "Large Scale Simulation Model as a Longwall Design Tool, A Case of Shallow Longwalling," Longwall USA Conference, June 2-4, 1987, Pittsburgh, PA.

13. Vinson, R.P., E.D. Thimons, and F.N. Kissell, "Methane Accumulations in Coal Mine Roof Cavities," RI 8267, *Bureau of Mines Report of Investigations*, 1978, 15 pp.

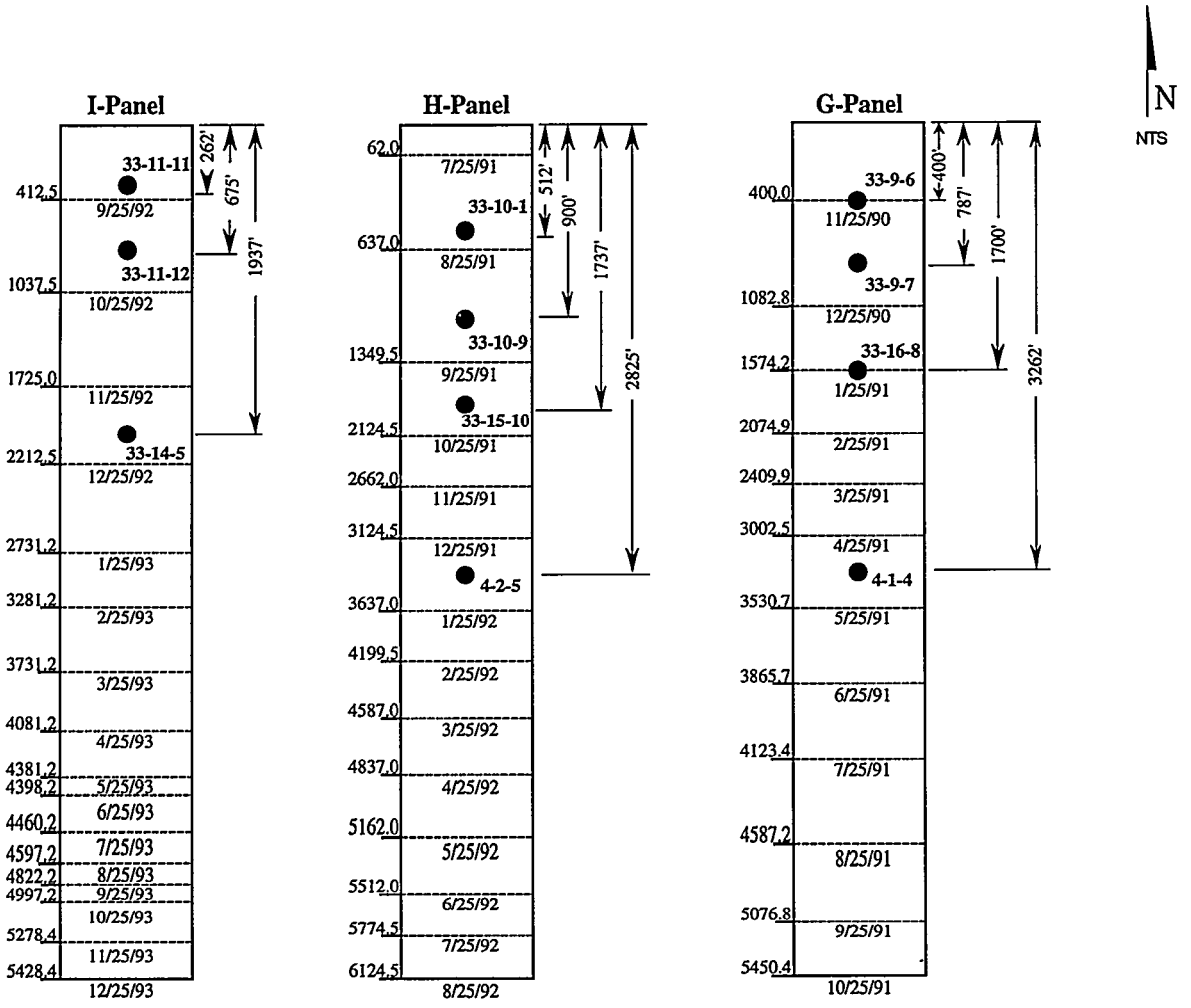


Figure 1. Location of gob wells and face advancement for three investigated panels, G, H, and I.

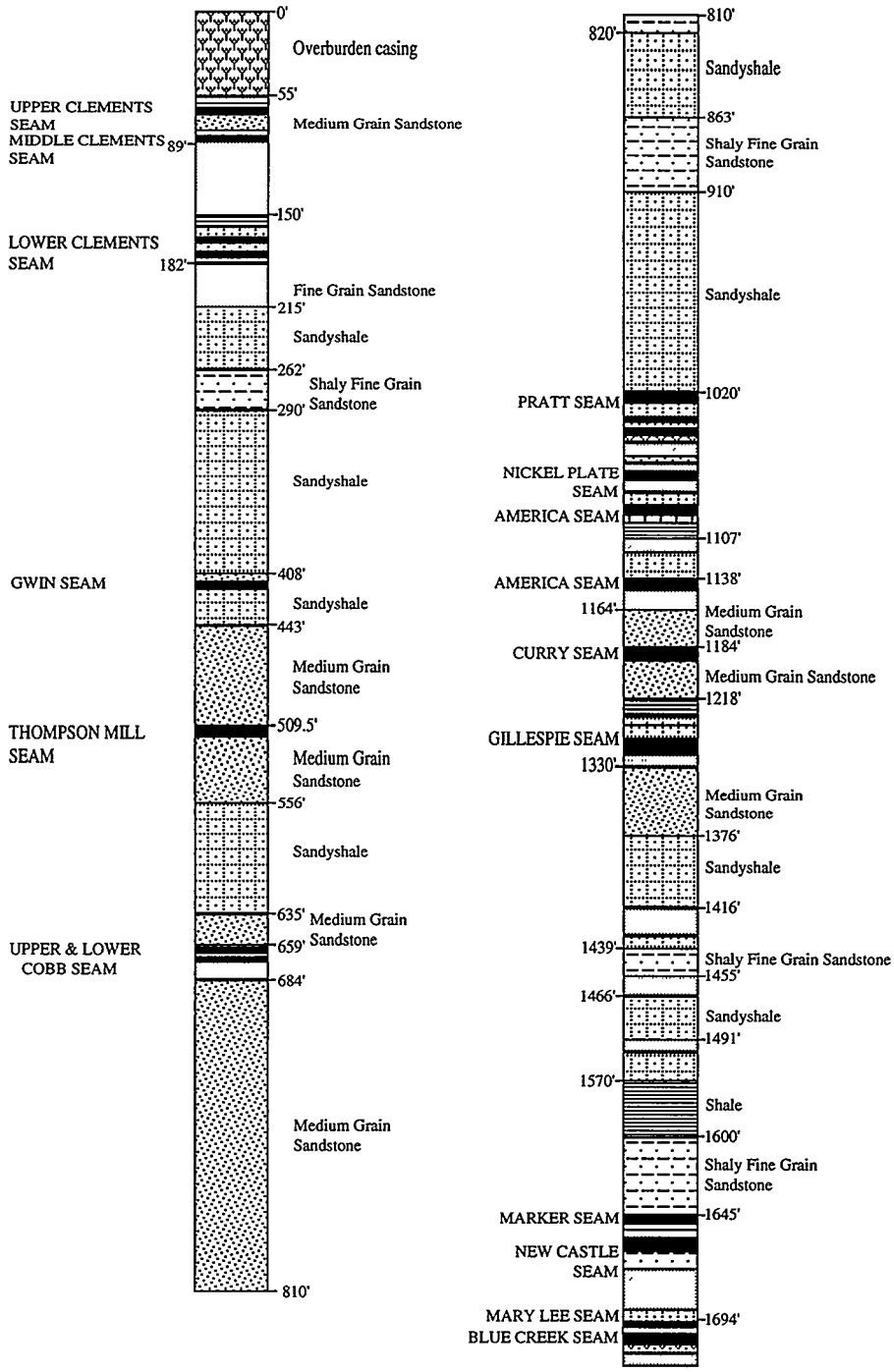


Figure 2. Stratigraphic column of S-310-4 near three panels shown in Figure 1.

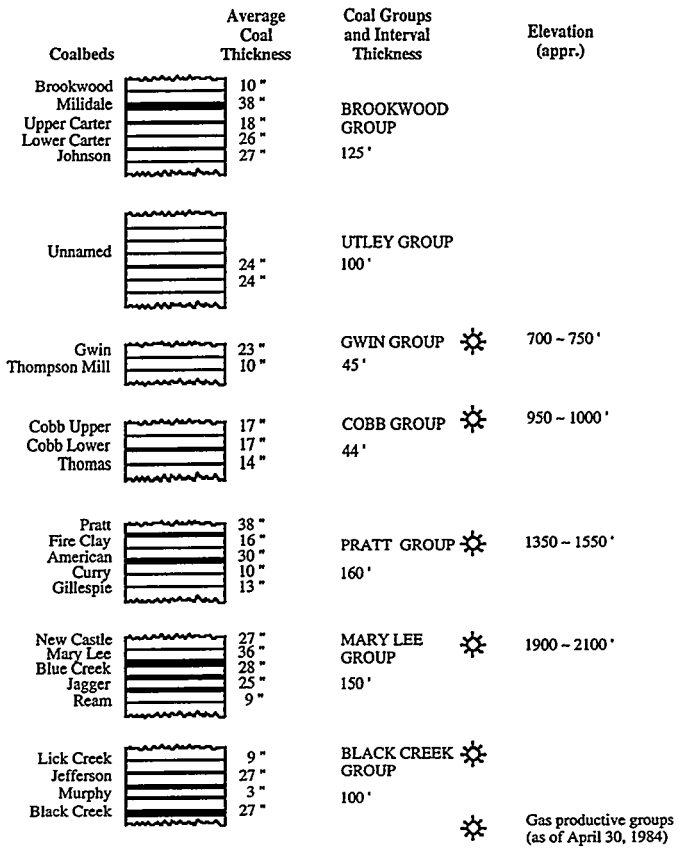


Figure 3. Stratigraphic column of coal groups in the Warrior coal basin (modified from Geological Survey of Alabama, 1977).

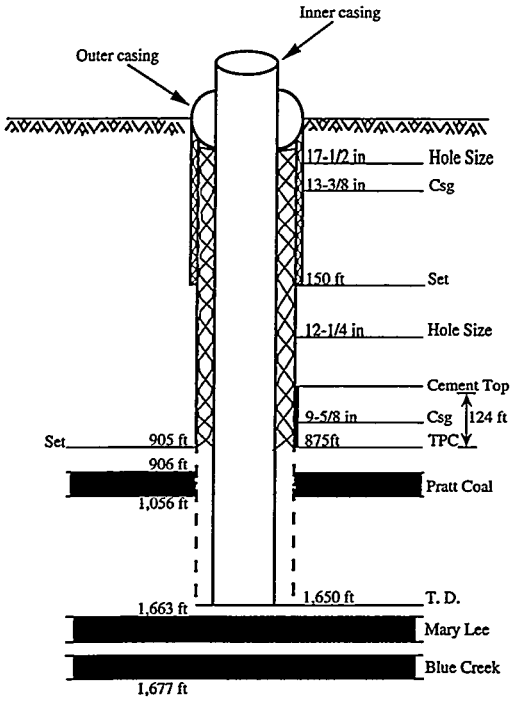


Figure 4. Typical cross-section of a gob gas well (source: Jim Walter Resources, Inc.).

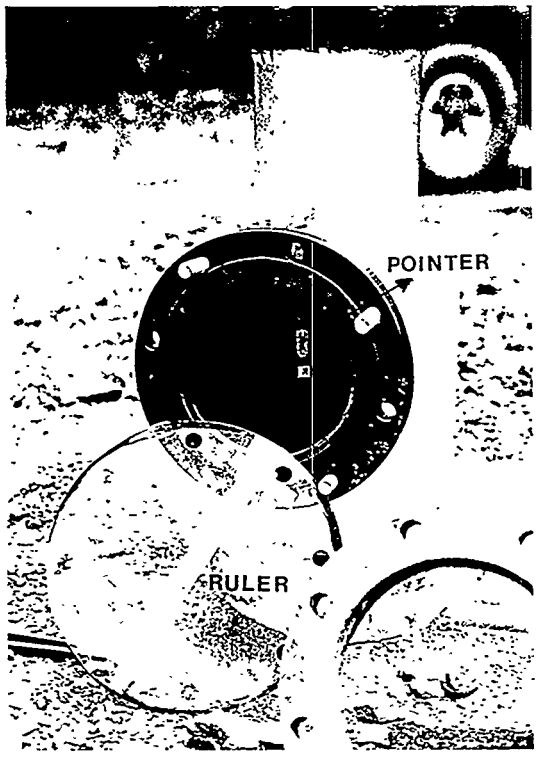


Figure 5. A diagram of a typical gob well cross-section.

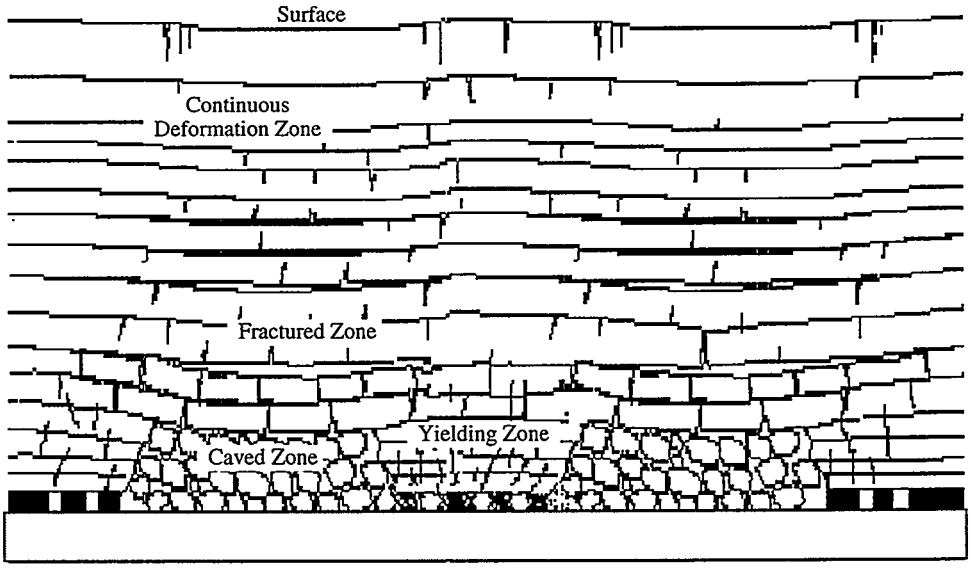


Figure 6. Strata movement and four zones in overburden of two longwall panels.

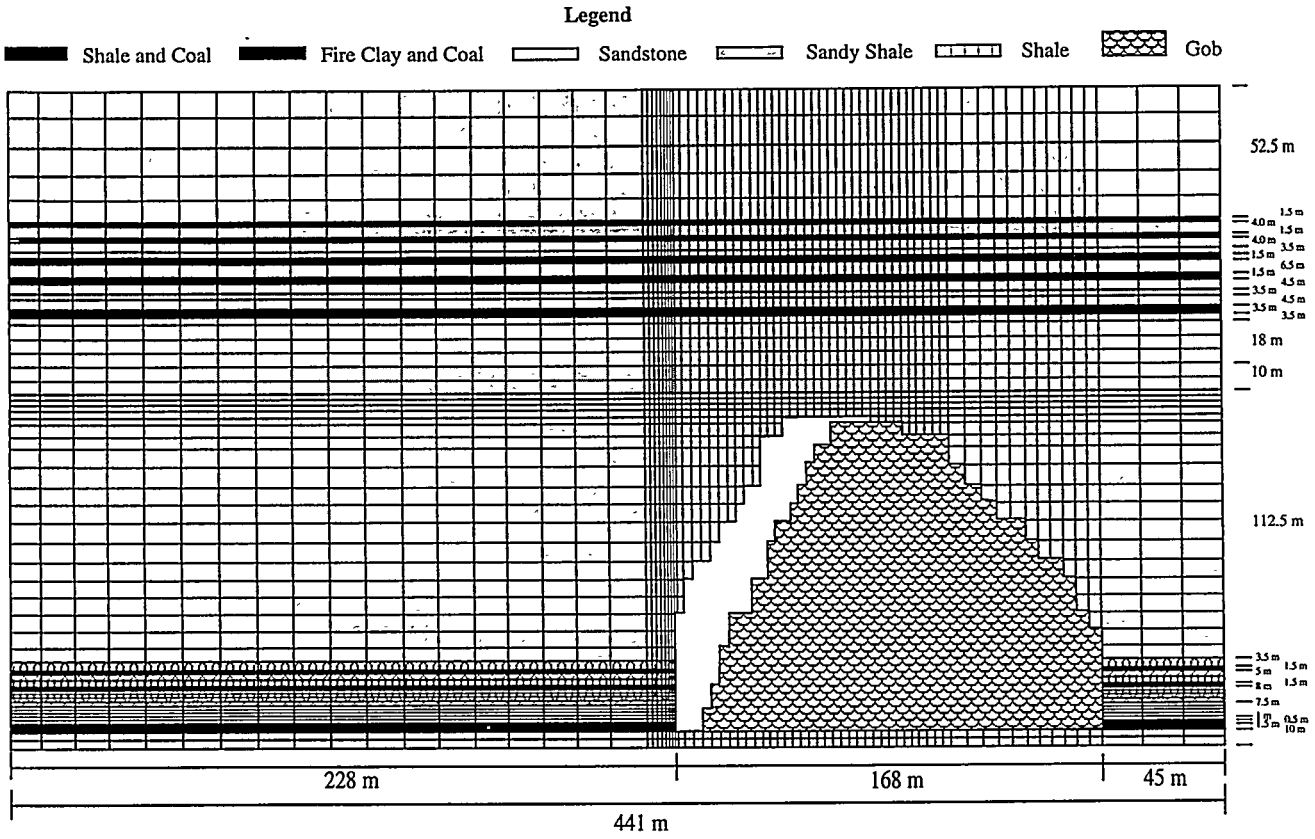


Figure 7. Finite element modeling for simulating geomechanical behavior of gob emission zone.

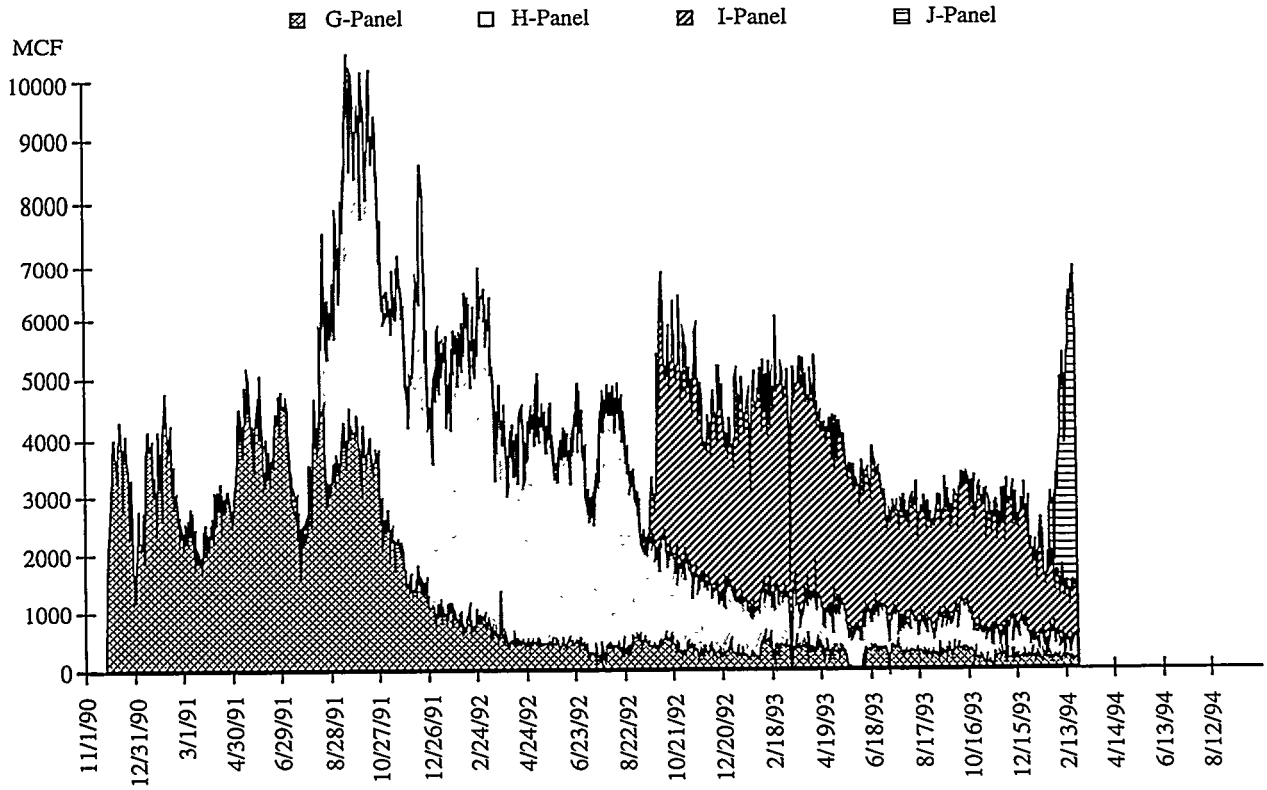


Figure 8. Total gas production from vertical gob wells in panels G, H, and I.

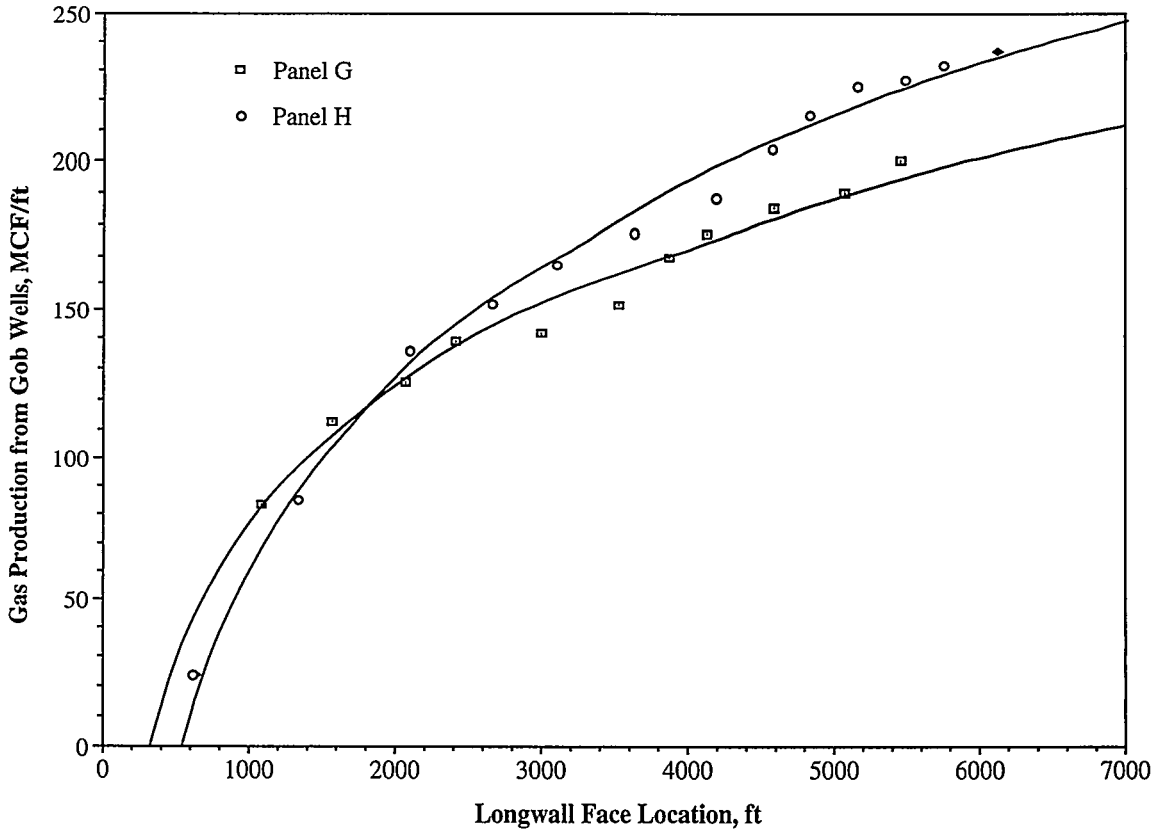


Figure 9. Cumulative gas production from gob wells in panels G and H.

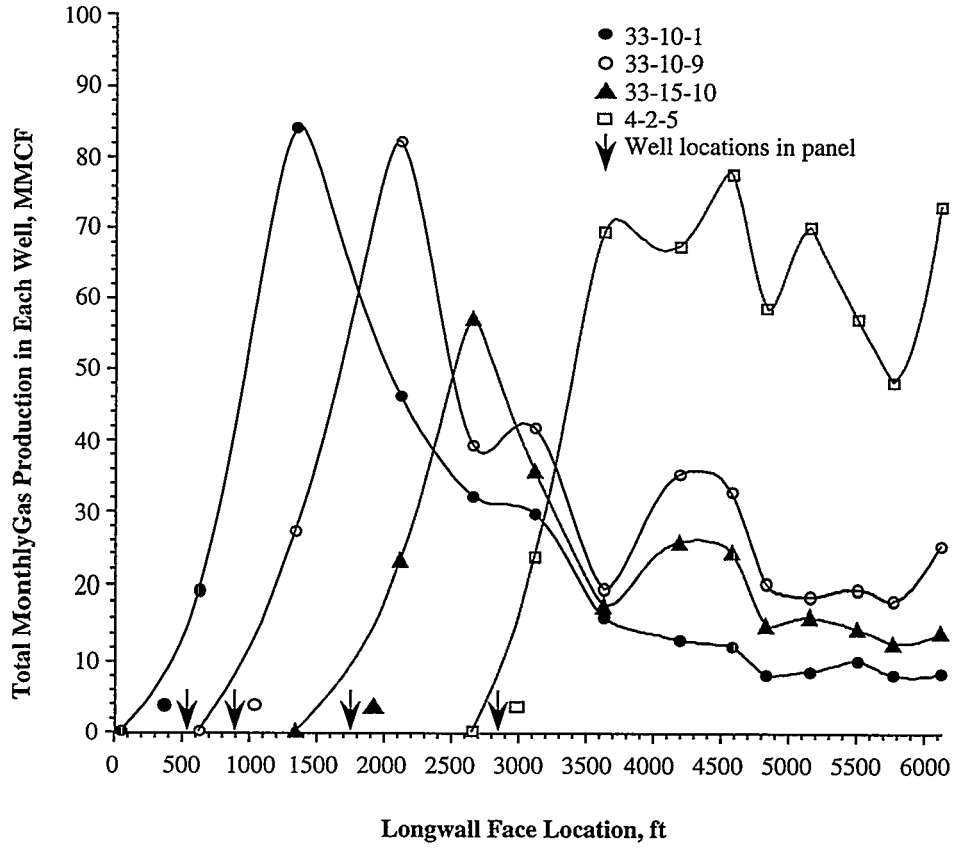


Figure 10. A comparison of the gas production of each well in Panel H.

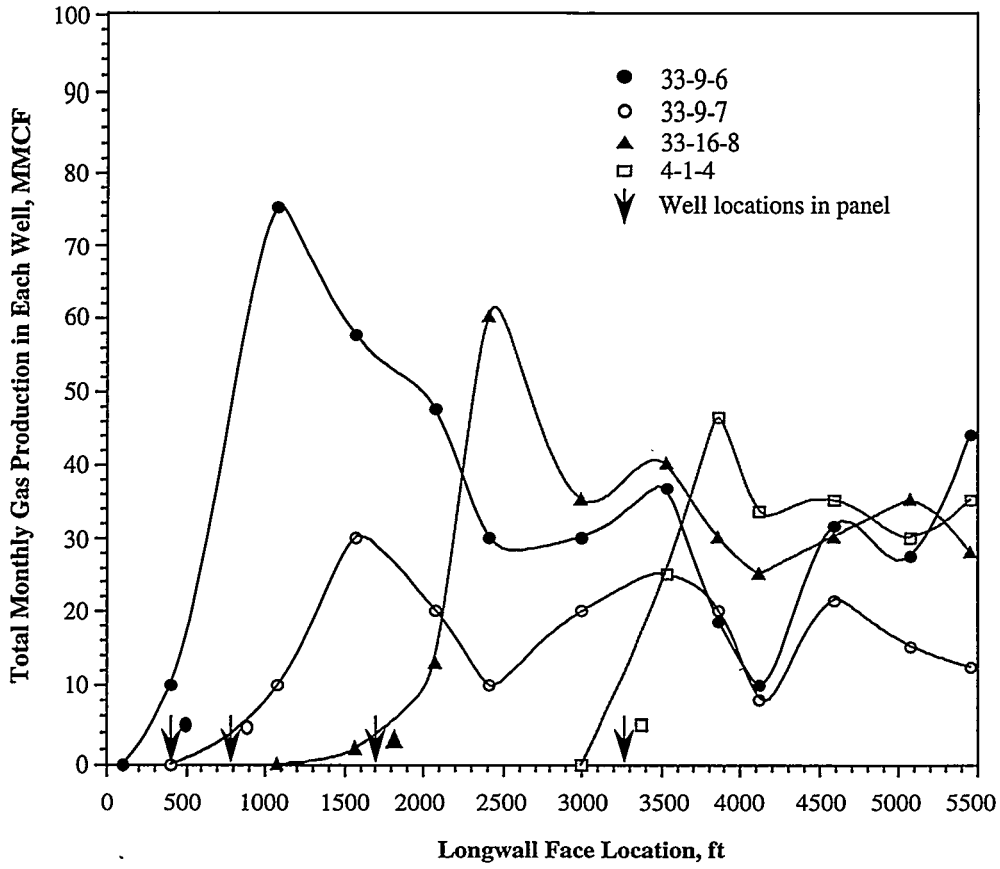


Figure 11. A comparison of the gas production of each well in Panel G.

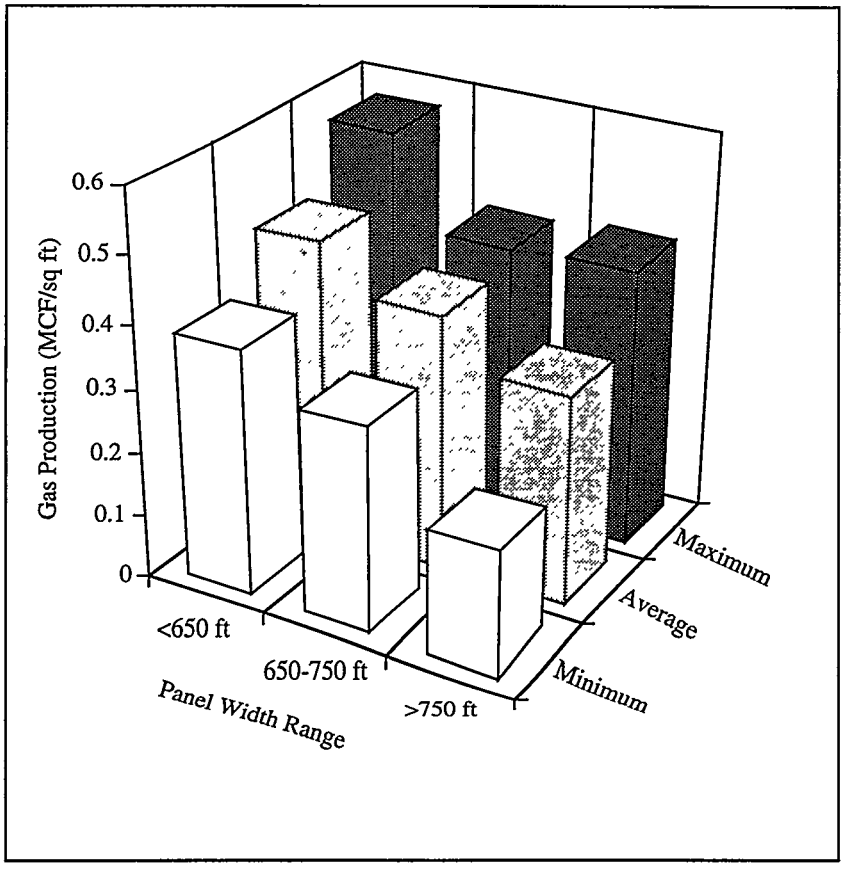


Figure 12. Comparison of gas production in different ranges of panel widths.

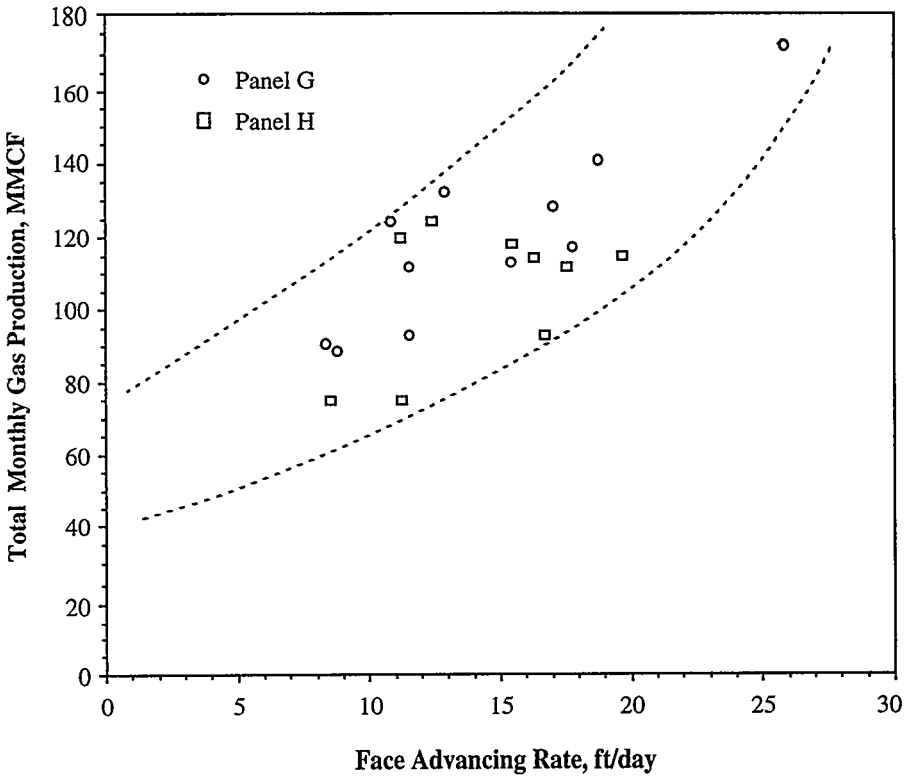


Figure 13. Relationship between monthly gas production and face advancement rate.

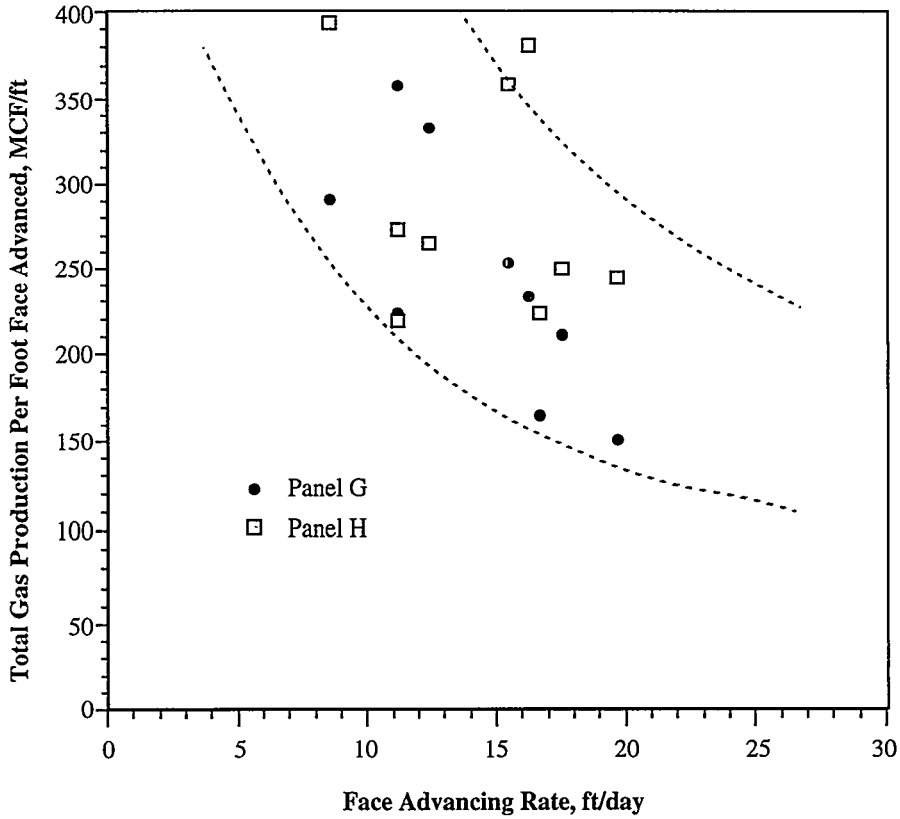


Figure 14. Relationship between gas production in unit volume of coal seam mined and face advancement rate.

INTERGAS '95

May 15-19, 1995
The University of Alabama
Tuscaloosa, Alabama USA

9538

Evaluation of Methane Drainage from Mining Panel

Kotaro Ohga, Kiyoshi Higuchi, Hokkaido University;
Souhei Shimada, University of Tokyo;
and Gotai Deguchi, Coal Research Center, Japan

ABSTRACT

In order to reduce the cost of coal production, mining by the longwall method, which is more than 250m was attempted at the Taiheiyo Coal Mine. To get successful results by this mining method, the control and prediction of gas emission from the mining panel is most important . At the Taiheiyo Coal Mine, different methods of methane drainage from the mining panel have been carried out to reduce the methane concentration at the mining face.

To evaluate the effect of these drainage methods, different lengths of boreholes for methane drainage were drilled into the mining panel and the flow rate from each borehole was measured.

The results of data analysis showed that the conventional methane drainage method, which uses long- and middle-length boreholes, is very effective as a drainage method from disturbed coal seams, and the efficiency of methane drainage from undisturbed coal seams depends on the location of the borehole drilled in the coal seam.

INTRODUCTION

In order to reduce the cost of coal production, the mining by the longwall method, which is more than 250m, was used with successful results in the Taiheiyo Coal Mine. As the mining area of this coal mine is under the sea, the air flow rate for ventilation is restricted. In order to get successful results by this mining method, the control and prediction of gas emission from the mining panel is most important things. At the Taiheiyo Coal Mine , different methods of methane drainage from the mining panel have been carried out to reduce methane concentration at the mining face.

To evaluate the effect of these drainage methods, different lengths of boreholes for methane drainage were drilled into the mining panel and the flow rate from each boreholes was measured. In this paper, the results of analysis carried out on this data are described.

METHANE DRAINAGE METHOD FROM LONGWALL PANEL

Draining methane gas from virgin coal seams is difficult due to the low permeability of coal. Therefore, methane drainage from the upper relaxed area using long-, middle- and short-length boreholes is usually carried out. Fig.1 shows the outlines of the methane drainage methods for different lengths of boreholes. Methane drainage by long-length boreholes with a length of more than 500m, is carried out from the drainage station excavated in the rock seam above the mined coal seam. The number of boreholes are usually 3 or 4, as shown in Fig.1-A. Methane drainage by middle-length boreholes with a length from about 200m to 300m, is carried out from the drainage station in the rock seam, as shown Fig.1-B. Methane drainage by short-length boreholes with a length 100m, is carried out from the tail gate of the longwall panel, as shown in Fig.1-C. Usually, combination of the above three length boreholes is used .

TEST FIELD AND LAYOUT OF METHANE DRAINAGE BOREHOLES

Test were carried out at the CW9 No.3 Longwall Panel of the Taiheiyo Coal Mine. Fig.2 shows a localized map of the test field. The mining panel is 650m below the sea, the width and length of longwall are 250m and 750m, respectively.

Five long length boreholes and six middle-length boreholes were drilled for methane drainage in this panel, as shown in Fig.2. Above this panel, there is a old road way which is not used. This

road way was sealed at two places as shown in Fig.2, and used as a methane drainage sealed road way. Attempts were especially made to use short length boreholes for methane drainage from the virgin coal seam. A total of 20 short-length boreholes were drilled into the main coal seam from the tail gate and one other was drilled into the underlying coal seam.

MEASUREMENT OF METHANE DRAINAGE FLOW RATE

Measurement of the Flow Rate of Methane Drainage by Long- and Middle- Length Boreholes

The flow rates of methane drainage by long- and middle-length boreholes were measured by flow rate sensors and methane concentration sensors fitted to the inside of the main drainage pipe in the methane drainage stations. Mark • A in Fig.2 shows the location of sensors for the measurement of the flow rate from the long-length boreholes and methane concentration, and mark • B shows the location of sensors for the measurement of flow rate from the middle-length boreholes and methane concentration.

Measurement data was transmitted to the personal computer at the surface and recorded. Measurements were carried out for a period of 136 days, from September 5,1992 to January 19,1993.

Measurement of the Flow Rate of Methane Drainage from the Sealed Road Way

W No.1 Road Way in the rock seam above the overlying coal seam was sealed at two locations, as shown in Fig.2, and emission gas between the sealed locations was drained by the methane drainage pipe. The flow rate of methane drainage was measured in the same way as described above. Mark • C shows the location of sensors for the measurement of flow rate and methane concentration. The period of measurement was also the same as above.

Measurement of the Flow Rate of Methane Drainage from a Virgin Coal Seam

The short length boreholes for methane drainage from a virgin coal seam were drilled into the main coal seam and the underlying coal seam. Fig.3 shows the outline of the measurement of methane flow rate from these boreholes. A special polyethylene pipe protects against static electricity was inserted into the boreholes to a depth of about 20m, and cement was injected into the gape between the pipe and the borehole to set it in place. The diameter of the pipe was 80mm and a gas flow meter for house use was connected to the pipe by a rubber hose The flow rate from each borehole was measured by an inspector in each working shift.

MEASUREMENT RESULTS

Methane Drainage Flow Rate

Fig.4 shows the flow rate of methane drainage from the long-length boreholes, the middle-length boreholes and the sealed road way, and the advancing distance of the mining face from the starting point. The flow rate from the long-length boreholes increases on December 26,1993, when the advancing distance of the mining face was about 300m. At this time, the mining face was more than 100m below the bottom of the long-length boreholes. This suggests that the coal and rock seams above the mined coal seam were disturbed, and methane gas flowed through the disturbed zone from the overlying coal seam or underlying coal seam to the long-length boreholes. The amount of methane drainage from the long-length boreholes was about 0.45 million m3 for the measurement period. The average flow rate of methane drainage was about 2.0 m3/ min.

The flow rate from the middle-length boreholes was very low value at the beginning of the measurement period, but increased rapidly on November 18,1993, when the advancing distance of the mining face was 180m. The middle-length boreholes were drilled in a lower part of the overlying seams than the long-length boreholes, which meant that the development of fractures reached the area surrounding the middle-length boreholes earlier than the long-length boreholes. In this panel, an increase in the flow rate of methane drainage was seen when the mining face had passed 30m bellow the end of the boreholes.

The amount of methane drainage from the middle-length boreholes was about 0.3 million m3, and the average methane drainage flow rate was about 4.0 m3/min in this panel.

The flow rate from the sealed road way increased at the beginning of measurement period and reached a maximum when the advancing distance of the mining face was about 40m. After that, the flow rate from the sealed road way decreased, and fluctuating between 1.5 and 4.0 m3/min. The amount of methane drainage from the sealed road way was about 0.27 million m3 and the average methane drainage flow rate from the sealed road way was about 1.8 m3/min.

The measurement results of methane drainage from the virgin coal seams are shown in Table 1. Borehole number 21 is the borehole which was drilled into the underlying coal seam and the other number indicate the boreholes which were drilled into the main coal seam. The highest level of methane drainage (6900m3) was recorded at No.1 boreholes.

Typical examples of methane drainage flow rate change with time are shown in Fig.5 and Fig.6. As seen in Fig.5, the flow rate of borehole No.1 fluctuated around 0.1 m3/min at the beginning of measurement period and increased when the distance from the mining face to the borehole was about 65m (September 28) . After that, it decreased when the distance from the mining face to the borehole was less than 30m (October 3).
The flow rate of borehole No.15 increased for a few days at the beginning of the measurement period and then decreased. When the distance between the mining face and the borehole was about 70m (October 9), it increased again and when the distance between the mining face and the borehole was less than 35m (October 26), drainage from the borehole was stopped owing to a smashed casing pipe.

The fluctuations in the methane drainage flow rate with time can be classified into two types, such as the above examples. One type is a flow rate which has a relatively low value at the start of drainage and increases as the mining face approaches the boreholes. The other type is a flow rate which increases for a few days at the start of drainage and then increases again as the mining face approaches the borehole. The amount of methane drainage in the former type is more than the later type.

Amount of Methane Drainage per Unit of Borehole Length

Table 2 shows the amount of methane drainage, the total borehole length and the amount of methane drainage per unit length of borehole, for each drainage method.
The results of a comparison of the amounts of methane drainage per unit length of borehole show that the highest level of methane drainage is by the middle-length boreholes and second highest level is by long-length boreholes. The amount of methane drainage per unit length of borehole was the smallest for the drainage method from the virgin coal seams. The level of drainage depends on boreholes. The level of methane drainage per unit length of borehole for each boreholes is shown in Fig.7. As seen in Fig.7, the value of No.1 borehole is the relatively high ,but the other level are vary different. L.B. and M.B. in Fig.7 indicate the values of the long-length boreholes and the middle-length boreholes.

Amount of Methane Drainage per Unit Length of Borehole and Unit time of Drainage Period

The period of methane drainage differs according to drainage method. Therefore, the amount of methane drainage per unit length and unit time for each drainage method was calculated and the results are shown in Fig.8. The highest level of methane drainage per unit length and unit time was in No.21 borehole, which was drilled into the underlying coal seam. The second highest level was in No.18 borehole. Thus, the results showed that some of the boreholes drilled into the virgin coal seam drained methane from the coal seam efficiently.

Methane Drainage Ratio of Each Drainage Method

To obtain the methane drainage ratio of each drainage method, we assumed the following; methane drainage by the long length boreholes, the middle-length boreholes and the sealed road way drained methane gas from the disturbed coal seams which are the overlying and the underlying coal seams. The area from which methane gas was drained was a little larger than the actual mined area during the measurement period. The width of the calculated region was 290m and the length, 500m. The thickness of the underlying and overlying coal seams was 2.0m and 0.5m, respectively. The methane content and the density of each coal seam were measured and the measured values of methane content and the density were 3.0 m3/t and 1.35 g/cc respectively.
On the basis of these assumptions, the calculated methane content of region of each coal seam were as follows: the amount of methane contained in the region of the underlying coal seam was 11,745,000 m3 and in the overlying coal seam, 2936,250 m3.
The methane drainage ratios were obtained by dividing the amount of methane drainage for each method by the total amount of methane contained in the underlying and overlying coal seams. The results are as follows; the methane drainage ratio was 30.1% for long-length boreholes, 20.5% for the middle-length boreholes ,and 18.4% for the sealed road way . The total ratio of these three methods was about 70%. Thus, 70% of methane gas contained in the overlying and underlying coal seams was drained by these three methods.
For the methane drainage from the virgin coal seam , the calculated region of the main coal seam was defined as the area surrounding the drilled area of the coal seam. The width and length of the region were calculated as 250m and 200m, respectively. The methane drainage ratio from the virgin coal seam was obtained in the same manner as the above. The value was about 4%.

Conclusion

1) Methane drainage using the long and the middle-length boreholes is effective as a drainage method for disturbed coal seams.
2) The results of a comparison of the amounts of methane

drainage and methane drainage ratios show that the methane drainage by short-length boreholes drilled into the main coal seam is not an effective drainage method for a virgin coal seam. However, the results of a comparison of the methane drainage per unit length of boreholes and unit time of each borehole show that there were some effective boreholes, such as No.1 or No.18 borehole.

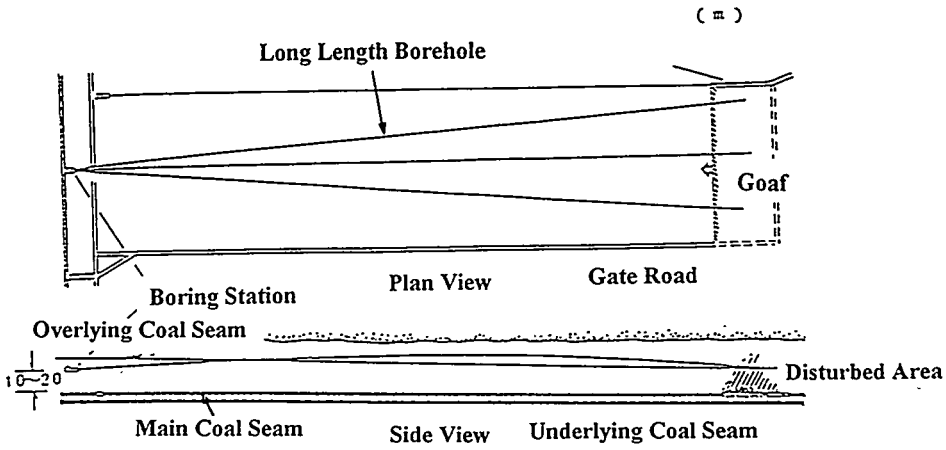
3) The efficiency of methane drainage from virgin coal seams depends on the location of the boreholes drilled in the coal seam.

Reference

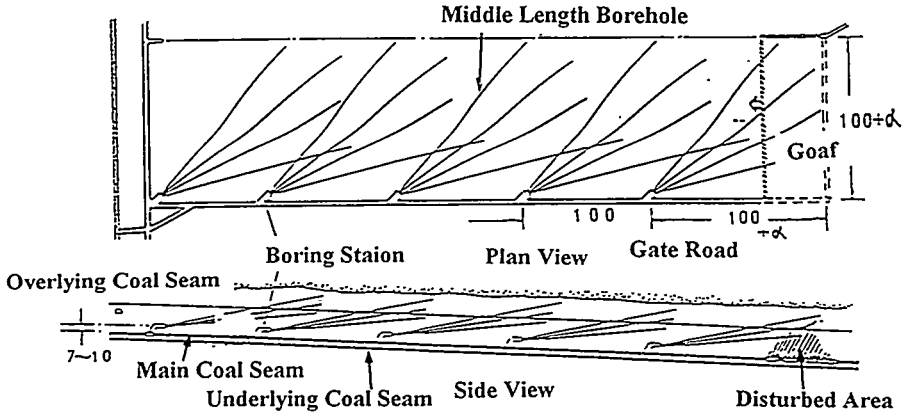
1. K.Ohga and K.Higuchi, 1987 : " The Practice of Methane Drainage in Japan"; Proceedings of the 3rd Mine Ventilation Symposium, The Pennsylvania State University, Pennsylvania, P261-270.

2. K.Ohga, K.Higuchi and V.J. Hucka, 1991:" A New Technique of Determining the Methane Content In-Situ"; Proceedings of 5th Mine Ventilation Symposium, West Virginia University, West Virginia, P494-499.

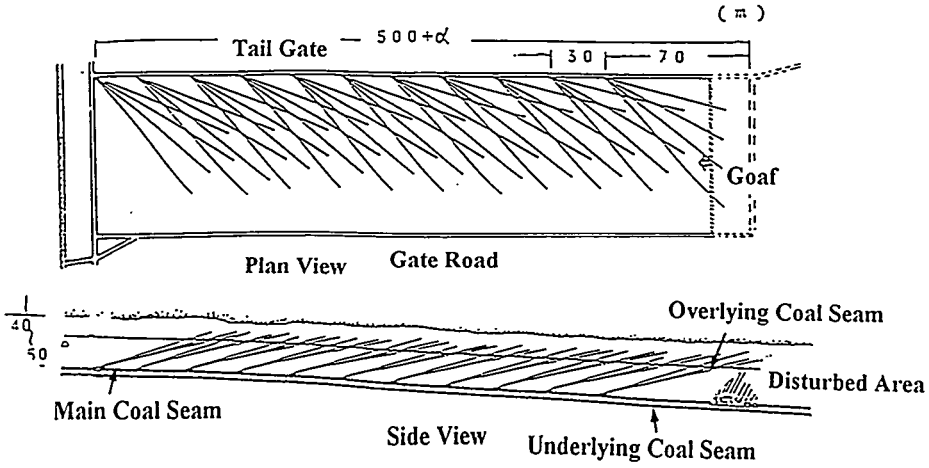
3. K.Ohga, K.Higuchi and G.Deguchi, 1993 :" Countermeasures and Prediction of Gas Emission from Longwall Panel"; Proceedings of 6th Ventilation Symposium, The University of Utah, Utah, P9-104/



(A) Methane Drainage By Long Length Boreholes



(B) Methane Drainage By Middle Length Boreholes



(C) Methane Drainage By Short Length Boreholes

Fig.1 Outline of Methane Drainage Methods at Taiheiyo Coal Mine

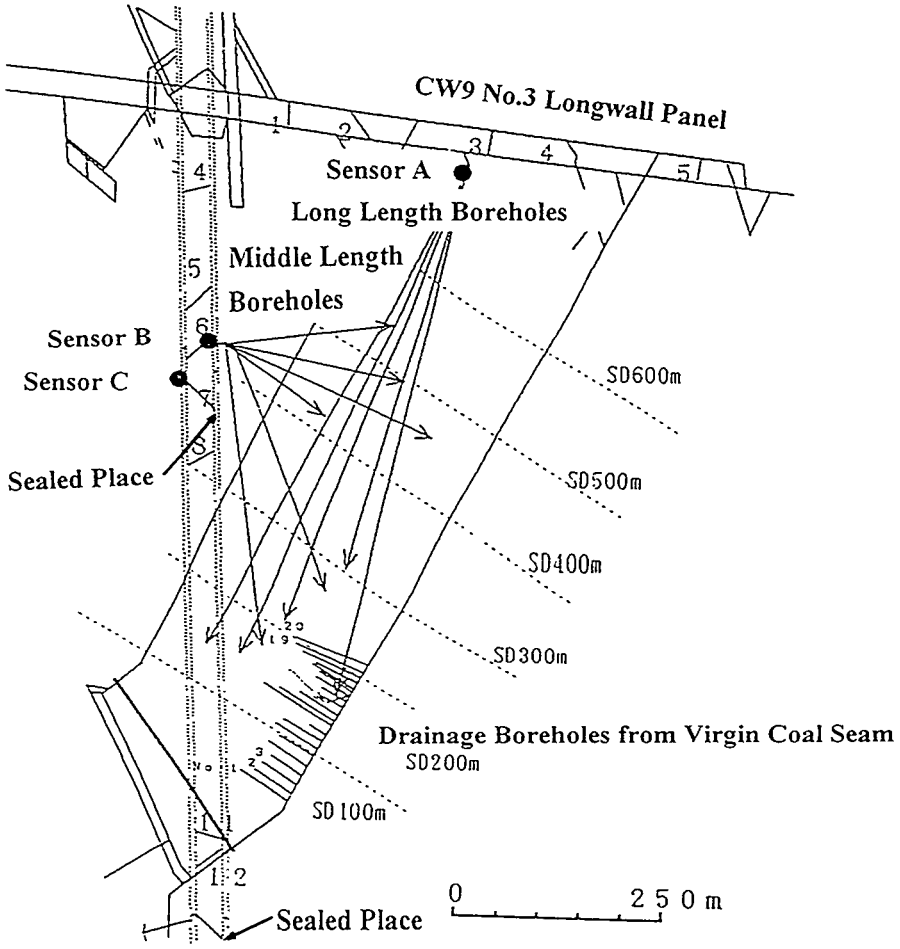


Fig.2 Localized Map of Test Field

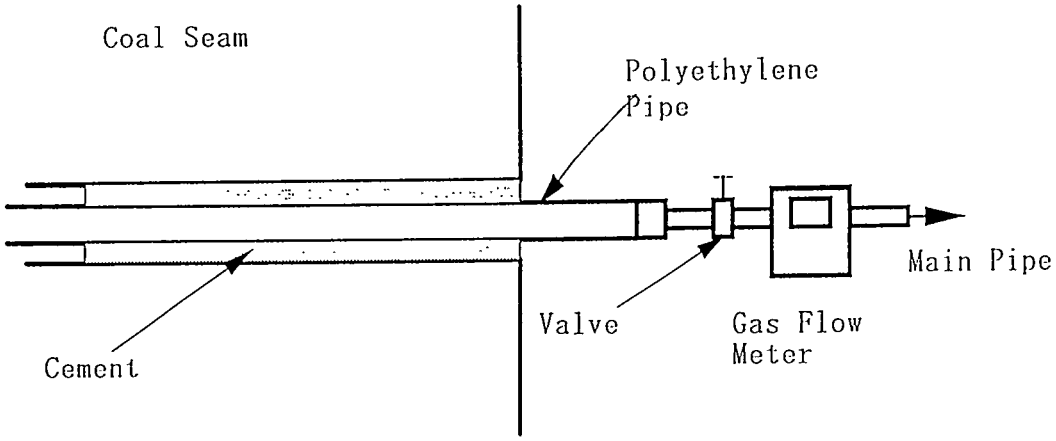


Fig.3 Outline of Measurement of Methane Flow Rate from Virgin Coal Seam

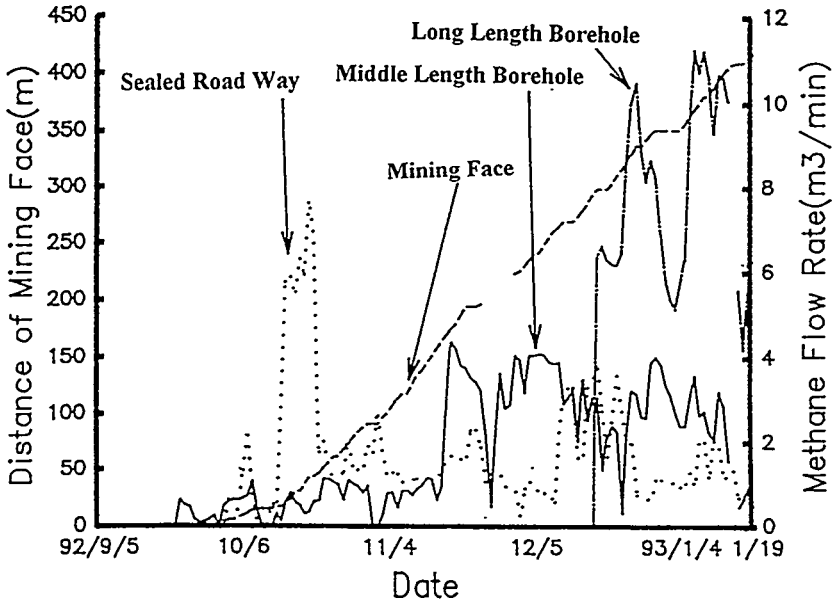


Fig.4 Flow Rate of Methane Drainage by Each Methods

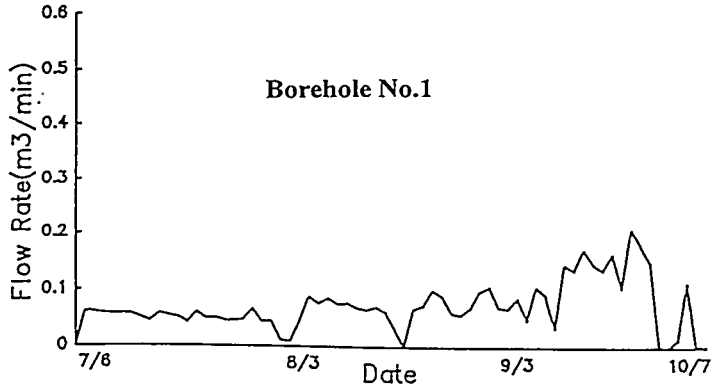


Fig.5 Methane Drainage Flow Rate from Virgin Coal Seam

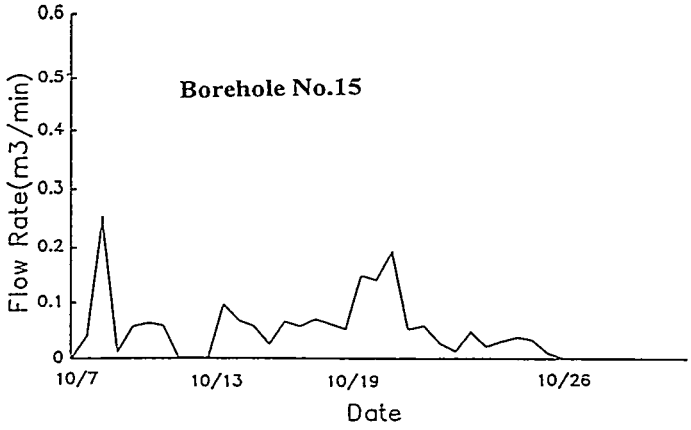


Fig.6 Methane Drainage Flow Rate from Virgin Coal Seam

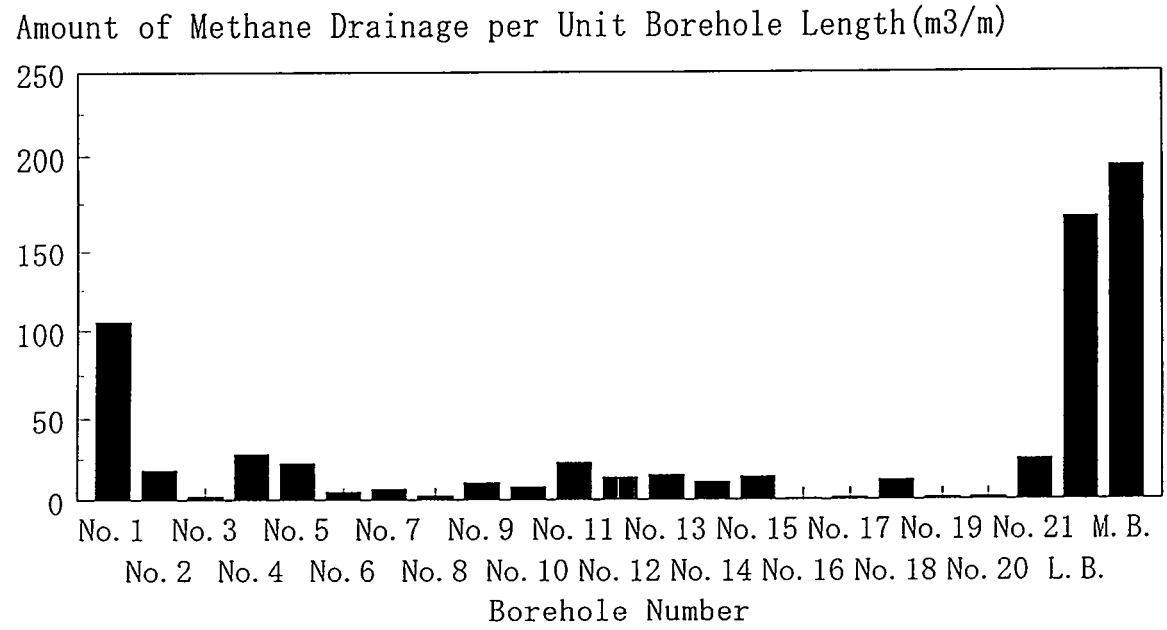


Fig.7 Amount of Methane Drainage per Unit Length of Borehole

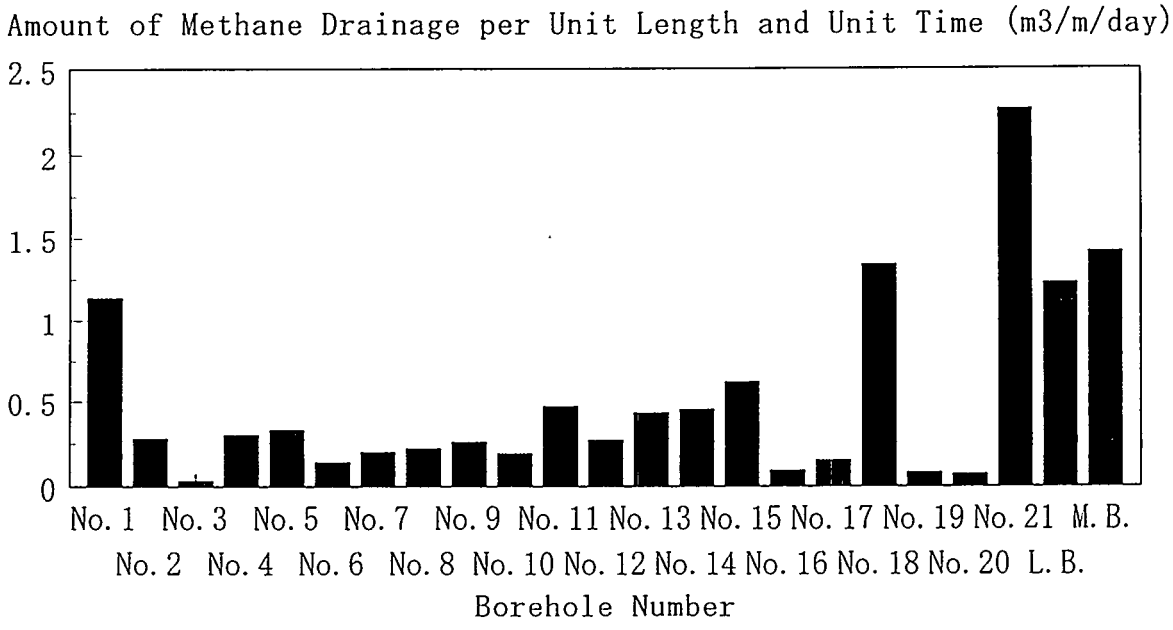


Fig.8 Amount of Methane Drainage per Unit Length of Borehole and Unit Time of Drainage Period

Table 1 Measurement Results of Methane Drainage from the Undisturbed Coal Seams

Borehole No.	Location of Borehole (distance from the starting point of the mining face m)	Borehole Length (m)	Drainage Period (day)	Amount of Drained Methane (m3)
No.1	72.6	65.5	93	6891.75
No.2	84.4	42.5	65	778.82
No.3	97.6	38.0	65	82.13
No.4	107.4	41.0	95	1163.97
No.5	117.5	50.5	70	1150.57
No.6	123.2	43.0	34	205.19
No.7	134.0	53.5	34	360.00
No.8	143.5	48.0	12	126.24
No.9	152.7	17.5	40	183.74
No.10	162.9	80.0	42	622.70
No.11	168.2	65.0	49	1501.99
No.12	173.0	50.5	51	700.82
No.13	183.4	29.5	36	452.69
No.14	192.8	32.0	24	347.41
No.15	202.8	44.0	23	624.96
No.16	212.6	47.0	8	33.94
No.17	219.4	43.0	10	64.09
No.18	223.5	52.0	9	625.03
No.19	228.5	76.0	14	88.92
No.20	240.8	74.5	21	116.19
No.21	202.8	20.5	11	512.25
Total				16,633.38

Table 2 Amount of Methane Drainage per Unit Borehole Length

	Methane Drainage by Long Length Boreholes	Methane Drainage by Middle Length Boreholes	Methane Drainage from Undisturbed Coal Seam
Total Borehole Length (m)	2718 (5)*	1,554 (6)*	1014 (21)*
Total Methane Drainage (m3)	454,305	301,098.8	16,833.4
Amount of Methane Drainage per Unit Borehole Length (m3/m)	167.2	193.8	16.6

* the number in parenthesis indicate to the number of borehole.



NOTES

INTERGAS '95

May 15-19, 1995
The University of Alabama
Tuscaloosa, Alabama USA

9543

Methods for Forecasting and Reducing Gas Emission in Mine Workings: Improving the Coal Mining Safety

I.V. Sergeev, Skochinsky Institute of Mining,
and E.Y. Dikolenko, Rosugol Company, Russia

ABSTRACT

Coal seams when mined, undermined and overmined as well as their interlayers and enclosing rock are sources of coal-bed methane released in coal faces, workings and developments of collieries.

Methane emission is a multiform process depending on a lot of natural and technical factors. First of all it depends on the speed of advance of roadheaders and shearers. With the data obtained the methane emission process can be simulated in order to forecast and reduce gas release into mine workings as well as to improve safety in mines.

Coal-bed methane degassing is obtained by drilling barrier holes and boreholes from the surface. Depending on the system of mining used one can resort to different methods of degassing described in detail in the paper.

* * *

Sources of methane released in mine workings include the coal seams and interlayers being mined, undermined and overmined as well as the enclosing rock out of which methane is emitted both in the developments and mine workings.

The gas emission process is diverse and depends on several natural and technical factors while concrete gas manifestation and its quantitative evaluation depend upon concrete conditions. Methane emission in a development takes place because of degassing of a coal seam with an exposed surface of the seam and methane desorption from the coal cut while in the coal face it happens due to degassing of coal seam mined and adjacent undermined and overmined coal seams and interlayers as well as the enclosing rocks within the zone of coal mining operations.

Gas emission in the developments depends on the natural methane content of the coal seam, on time spent and speed of driving of the development. Analysis of these factors has made it possible to obtain some analytical dependences describing the process of methane release out of a coal seam and to work out a method of calculating the volume of expected gas emission.

Absolute methane content of a development being driven consists of two components such as methane emission from the exposed surfaces of a coal seam and from the coal cut during driving the development.

Methane emission from the surfaces of a development L m long driven with a speed r will be equal to:

$$q_1 = an\ m\ r\ Q\ (2\sqrt{\frac{L}{2}} - 1),\ \text{cu.m/min} \qquad (1)$$

Methane content of a development conditioned by the gas emission from the coal cut can be determined from the expression:

$$q_2 = m\ r\ \gamma\ b\ (x - x_1),\ \text{cu.m/min} \qquad (2)$$

where, Q_o - initial intensity of gas emission, cu.m/sq.m.min
γ - volumetric weight of coal, t/cu.m
b - width of development, m
x - natural gas content of a coal seam, cu.m/t
x_1 - residual gas content of coal mined, cu.m/t

Total absolute gas content of a development will be equal to:

$$q = m\ r\ [an\ Q_o\ (2\sqrt{\frac{L}{2}} - 1) + \gamma\ b\ (x - x_1)],\ \text{cu.m/min} \qquad (3)$$

One of the main parameters determining the gas emission from exposed coal surfaces is the initial intensity of gas emission which depends on the seam gas content and the physical and mechanical properties of coal.

The value Q_o is determined with gas emission measurements with insulating membranes and gas survey in the development. In case there are no such measurements, the value can be determined according to the formula:

$$Q_o = 0.026 \times [0.0004\ (V^r)^2 + 0.16],\ \text{cu.m/sq.m.min} \qquad (4)$$

where, V^r - volatile matter emission out of coal referred to combustible mass, per cent.

Gas content of a development is determined by the speed of driving. According to the formula (3) it is possible to determine in each concrete case the permissible speed of driving depending on the gas content of the seam and the type of partial ventilation fan applied.

The amount of air necessary for ventilation with one per cent of methane permissible concentration limit is determined according to the expression:

$$\frac{W}{100} = m\ r\ [an\ Q_o\ (2\sqrt{\frac{L}{2}} - 1) + \gamma\ b\ (x - x_1)],\ \text{cu.m/min} \qquad (5)$$

The data given show that the greater is the gas content permissible according to the gas factor the slower must be

the speed of driving.

Gas balance of a development depends on its length and speed of its driving. The diagram (Fig. 1) compares the amount of methane emitted in the development out of coal cut and from the exposed surfaces of the seam during different speed of driving. The data obtained show that the gas content in the development during slow speed of driving is conditioned mainly by the gas emission from the exposed surfaces of the coal seam while, provided the speed of driving is great, the main role in the gas balance of the development is played by gas emission from coal mined.

Taking into acount these particularities of gas emission and necessity of uninterrupted supply of air to the near-face space to dilute the methane emitted down to a safe concentration at any moment of time, it is expedient to calculate the gas content of a blind section of development and the projected amount of air according to the real speed of advance of the roadheader.

So the speed of driving a development in gassy seams with a single face will be determined by the amount of air which is possible to deliver to the development with a partial ventilation fan. When driving with twin faces the ventilation can be carried out by a total mine depression. In this case only ventilation of the blind section of the development with a partial ventilation fan is a limiting factor. The amount of air necessary for ventilation of this section of the development depends on its length, speed of driving and gas content of the seam.

Results of experimental observations as far as the character of methane emission in the coal faces from coal seams and goaf is concerned indicate that the absolute values of methane emission depend on many factors, and first of all on the advance speed of the shearer. On the basis of the data obtained a model was built to demonstrate the process of methane emission depending on the main factors. This made it possible to develop a method for forecasting methane content in workings during mining. Briefly the propositions of this method are given below.

Relative gas content of the workings is determined by mining and statistical method together with calculations of the natural gas content of coal seams.

The results of regular every-ten-days measurements as well as data of special gas survey together with information about actual output of coal faces and districts serve as the basic data for the methane content forecast by the first method. While according to the second method it is the natural methane content of coal seams determined directly during prospecting.

Relative methane content of a coal face or a mine district by both methods is a constant value which is characterized by the ratio of the amount of methane emitted during a long period of time to the coal output during the same period of time.

In order to determine the relative methane content according to the mining and statistical method, the absolute methane emission is found out by processing the measurement data during the entire time of district coal extraction. The ten-days measurements are plotted on a graph with coordinates Q and t while $Q_{ср}$ is determined either graphically or as an average value. Then:

$$\Sigma Q = 1440\ t\ Q_{ср},\ \text{cu.m} \qquad (6)$$

This value is to be divided by the output during t days to get the relative methane content.

Forecast of methane emission of a mine district according to the natural methane content is done in the following way.

Total relative methane emission of a mine district is expressed as a sum of methane emissions from separate sources such as

$$q_{уч} = q_{пл} + q_{в.п} + q_{п},\ \text{cu.m/t} \qquad (7)$$

where, $q_{пл}$ - relative methane emission in workings of the seam being extracted, cu.m/t

$q_{в.п}$ - relative methane emission conditioned by the gas emitted from overmined and undermined coal seams, cu.m/t

$q_{п}$ - relative methane emission due to methane release from enclosing rock, cu.m/t

$$q_{пл} = (x - x_1)\frac{m_п}{m_в}(k_{пл} + k_у),\ \text{cu.m/t} \qquad (8)$$

where, $m_п$, $m_в$ - total and extracted thickness of a coal seam, m

$k_у$ - coefficient to determine methane emission from pillars left

$k_{пл}$ - coefficient of the seam being drained with developments.

Relative methane emission of workings in the coal seam being extracted, conditioned by the gas emission from the adjacent seams, is equal to:

$$q_{в.п} = \frac{m_c}{m_в}(x - x_c)\left(1 - \frac{h_c}{h_p}\right),\quad \text{cu.m/t} \qquad (9)$$

where, m_c - thickness of the overmined and undermined adjacent coal seams, m

x_c - residual gas content of an adjacent coal seam after its overmining or undermining, cu.m/t

h_c, h_p - distance to the adjcent seam and maximum distance for influence of overmining and undermining operations, m

Value of h_p depends on rock structure, seam thickness being extracted, roof rock control, seam occurrance angle and other factors. Besides, the more the seam is released from the rock pressure, the more gas is emitted, while the greater is the normal component of the gravity force acting on the seam, the more efficient is the seam unloading. In general,

$$h_p = Nm_в(1.2 \pm \cos\alpha),\ \text{m} \qquad (10)$$

where, N - undermining and overmining coefficients equal to 60 and 30 (plus and minus correspond to undermining and overmining operations).

Relative methane content of workings due to methane emission from enclosing rock is considered equal to 5-10 per cent of $q_{пл}$ depending on actual data.

The processes of methane emission during development driving and mining operations described analytically above determine the qualitative values of methane emission. On this basis it is possible to recommend some means for reduction of methane content to provide for permissible (explosion-safe) methane concentration in the mine outgoing air flow.

Besides the better operation safety in coal faces as fas as the gas factor is concerned, the means to reduce methane content must provide for efficient methane release from a rock massif to be utilized for heat and electric power production.

As we have pointed out before, it is considered expedient to obtain methane from rock massif and to utilize it. Simultaneously one should take into account the following priority aims such as a provision of safe labour conditions in mine by reducing catastrophy and explosion hazard, reduction of gas release in the atmosphere, as well as economical profits due to methane combustion as an energy carrier and improvement of mining operation parameters.

Methane release with boreholes drilled along the contour of the workings provides for efficient degassing when driving in-seam developments (barrier boreholes). This method helps reduce the methane content of developments by 40-50 per cent. Resorting to some artificial means to increase gas yield from the seams - being tested at present - increases efficiency of degassing as high as to 60-70 per cent. In this case during driving a development the rate of gas yielding from massif reaches 10 and more thousand cu.m per day which enhances the field of its application as fuel. The recommended schemes of degassing are given in Fig. 2 and 3.

The main method of reducing methane emission in workings is different means of degassing coal seams and rock massif disturbed with mining operations. Under the conditions of rock massif disturbance it is possible to get the maximum effect for methane removal with the help of boreholes both drilled from the workings and from the surface to the massif undermining (or overmining) zones. These methods are determined according to the dependences described by the formulae (9) and (10). The recommended patterns for degassing are given in Fig. 3, 4, 5.

While considering these patterns it is necessary to point out a possible efficiency of methane removal from the disturbed zones with the help of gas-accumulating workings as well as with boreholes drilled from the surface to the disturbed rock massif. In both cases it is necessary to mark thoroughly the disturbance boundaries of rock massif, the upper section of which is sure to accumulate considerable amounts of methane.

CONCLUSION

Safety in mines with high gas content, reduction of methane and coal dust explosion hazard can be provided by the correct detection of the sources and probable accumulation of methane as well as by resorting to a reliable method to forecast methane emission. With this initial data present one chooses the means for reducing the methane emission from rock massif into the workings. The most effective methods are the degassing methods described in the paper. These methods are to be applied both to provide safety and to obtain methane as fuel.

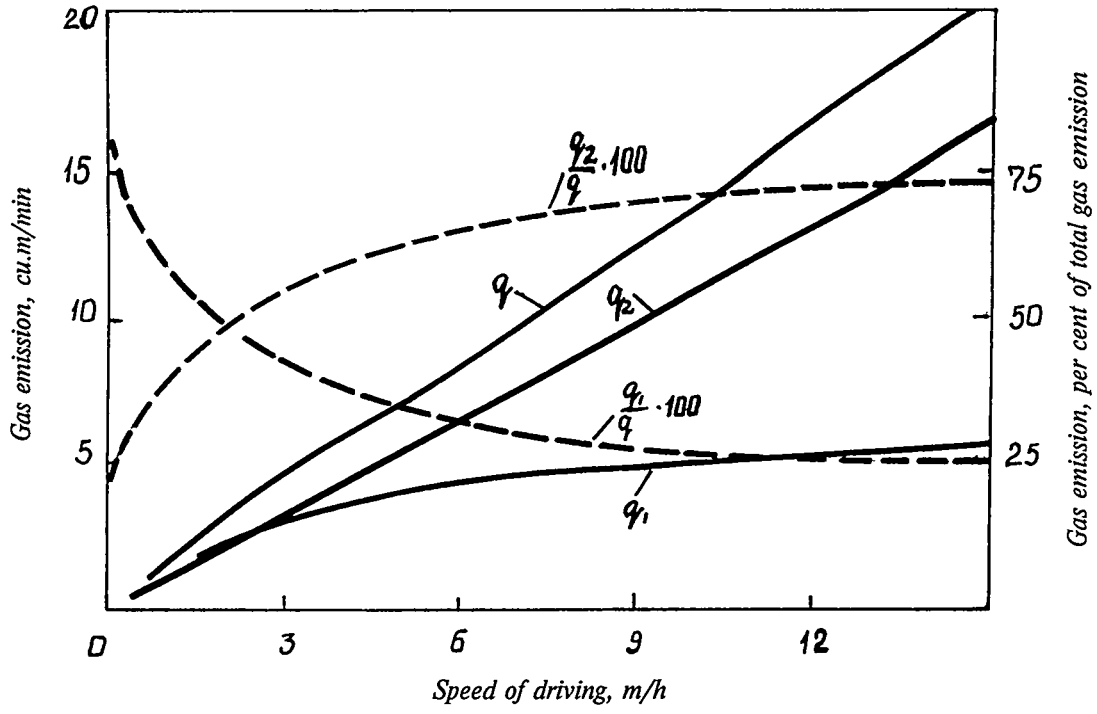


Fig. 1. Gas balance of development depending on speed of driving

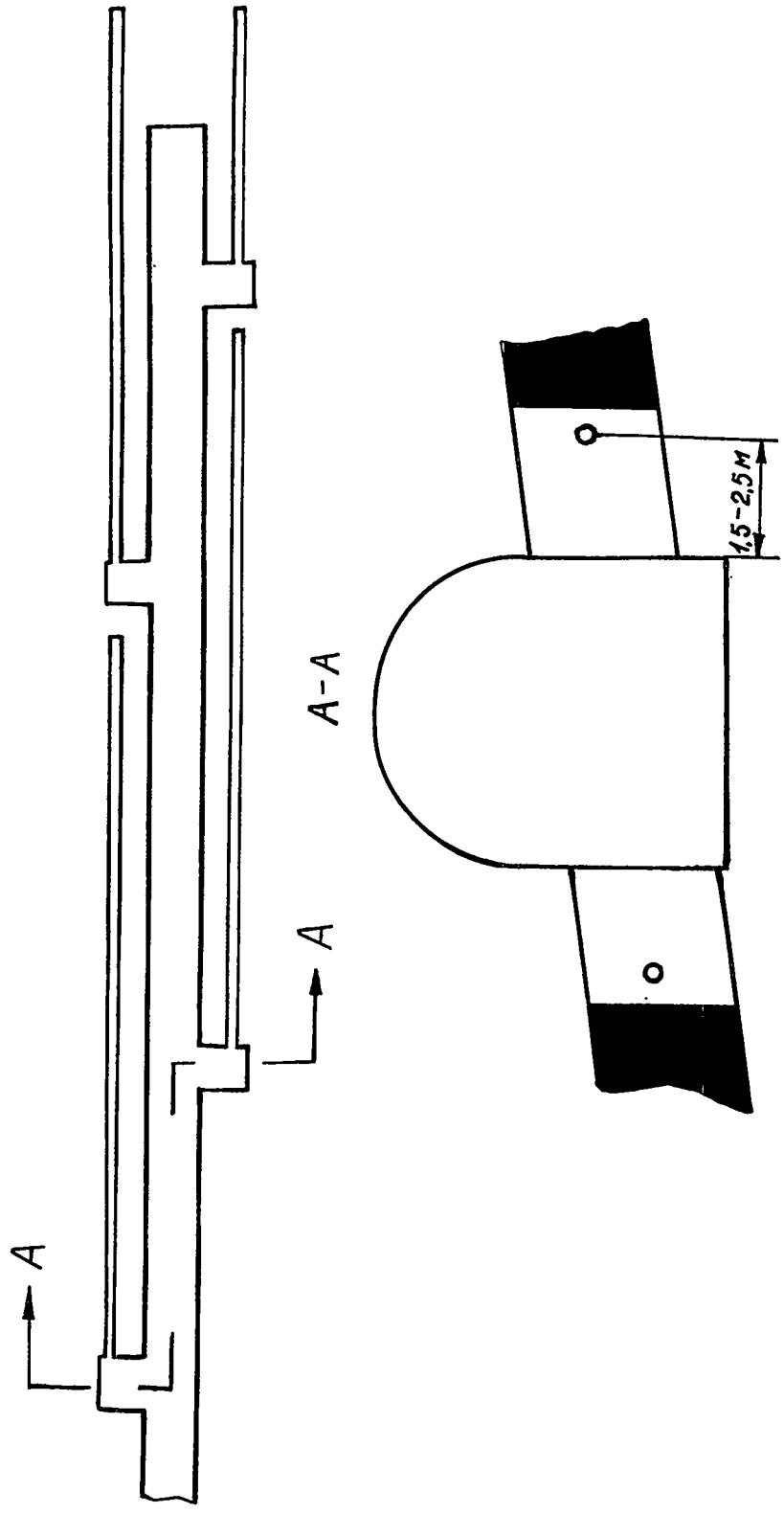


Fig. 2. Barrier borehole pattern for driving in-seam developments

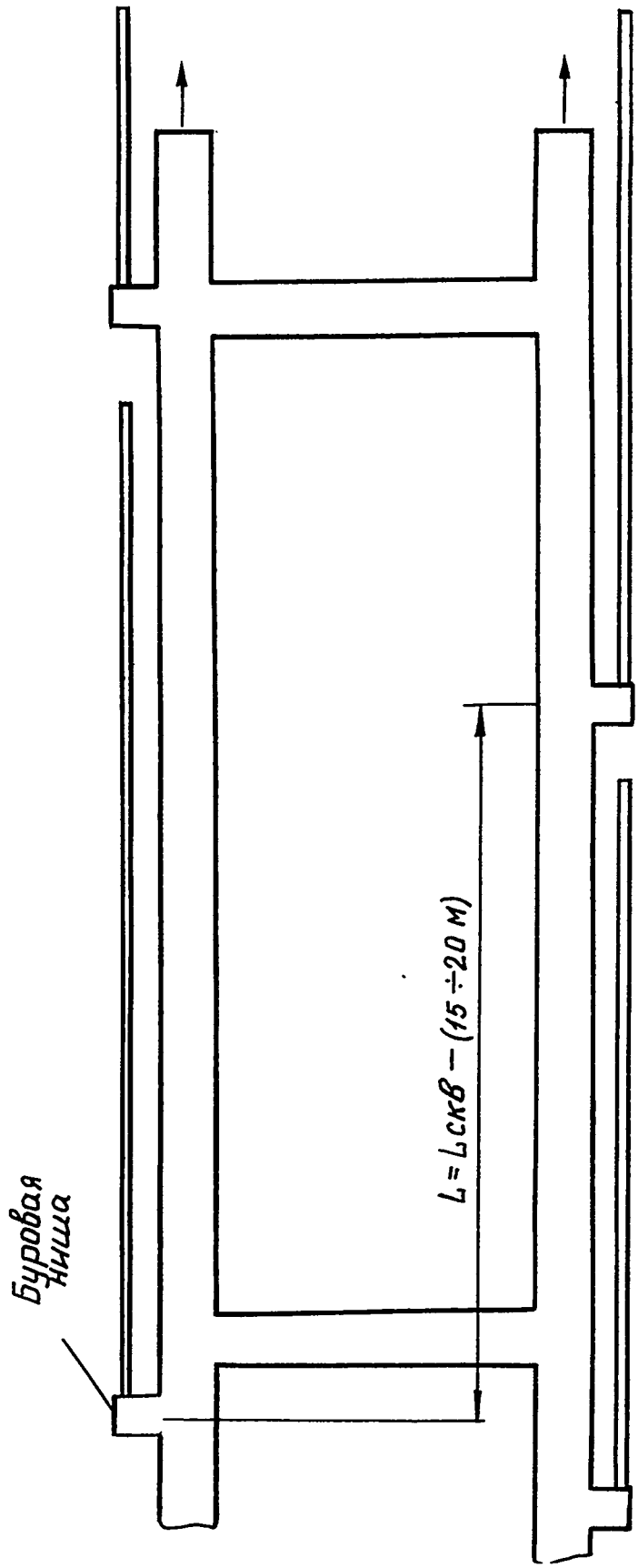
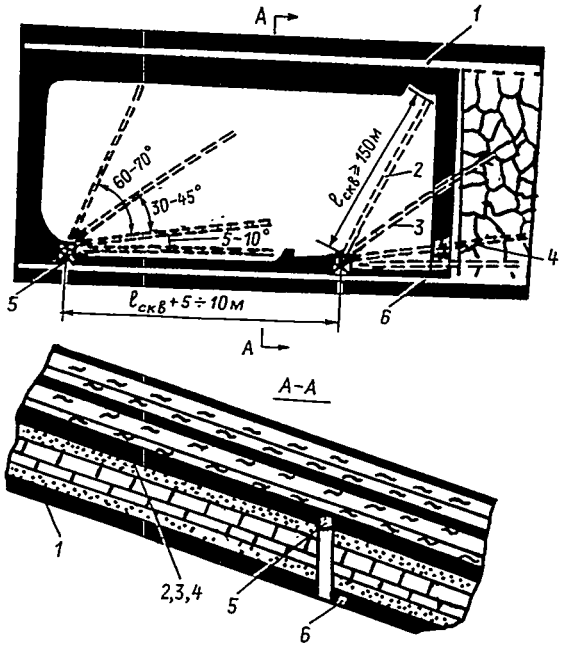


Fig. 3. Pattern of coal massif degassing with barrier boreholes when driving twin developments Borehole stable

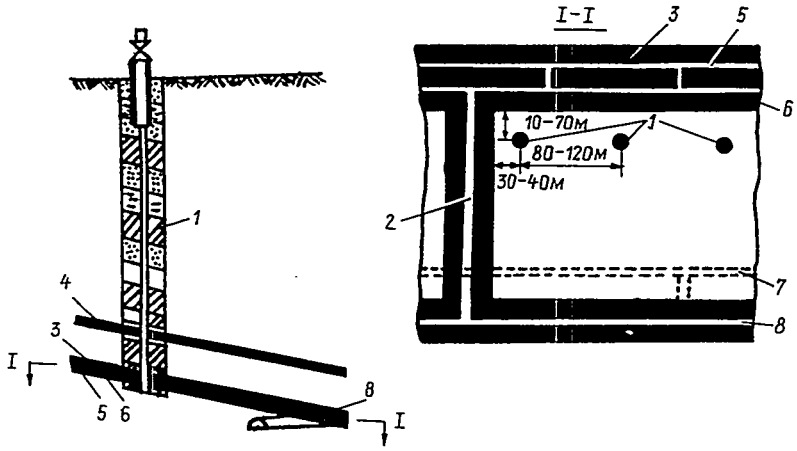
Pattern for degassing of undermined coal seams with the help of big-diameter gas-accumulating boreholes

Fig. 4



1 - ventilation entry, 2, 3, 4, - gas-accumulating boreholes, 5, 7, - winze with borehole stable, 6 - haulage gallery

Pattern for degassing of undermined coal seams and goaf with boreholes drilled from the surface



1 - borehole, 2 - cross-cut, 3 - seam being mined, 4 -seam to be degassed, 5 - ventilation entry, 6 - ventilation cross-cut, 7 - field haulage gallery, 8 - transportation cross-cut.

INTERGAS '95

May 15-19, 1995
The University of Alabama
Tuscaloosa, Alabama USA

9542

Economical Aspects of Coalbed Methane Extraction and Utilization by Coal Mines in the CIS

V.I. Serov, Skochinsky Institute of Mining, Russia

ABSTRACT

The paper deals with the most profitable way of the drained methane utilization as a part of the general problem of coalbed methane.

* * *

The coal present in the greater part of the coal mines in Russia, Ukraine and Kazakhstan is highly gassy: Average methane gas emissions, caused by coal mining in these areas, amount to approximately 25-30 normal cubic meter per tonne (880-1060 cf/t) of coal extracted.

The coalbed methane resource in the coal basins of the CIS (including Russia with the Kuznetsk and Pechora coal fields; Ukraine, with the Donetsk coal field; Kazakhstan, with the Karaganda coal field), down to a depth of 1800 m (5900 ft), amounts to $17 \cdot 10^{12}$ m³ (600 Tcf), with $13 \cdot 10^{12}$ m³ (460 Tcf) out of that amount present in Russia.

The increase in operating depths at the coal mines in the course of the years was accompanied by an increase in methane emissions. This development eventually required the application of the degassing systems.

The installation of degassing systems started in 1952, when the average depth of the coal mines was at 248 m (813 ft) and the daily emissions of methane at 2 million m³ (70 MMcf). The main purpose of the methane drainage by the degassing systems was to prevent explosion hazards and delays due to methane problems at the working face.

In 1989, average depth of the coal mines reached 550 m (1804 ft), and daily methane emissions went up to 24 million m³ (848 MMcf). At that time 195 mines were equipped with degassing systems: 116 in the Donetzk coal field; 45 in Kuznetzk; 24 in Karaganda, and 10 in Pechora.

In 1988, the volume of coalbed methane extracted by degassing systems reached 1.36 billion m³ (48 Bcf), with a net content of methane of about 30%. Out of that amount 115 million m³ (4 Bcf) were burned in boiler houses. The rest with 1.245 billion m³ (44 Bcf) was vented into the atmosphere. At that time, total coalbed methane emission, caused by coal extraction, amounted to 8 billion m³ (283 Bcf).

In 1993, total methane emissions in all coal fields of the CIS combined were 6.7 billion m³ (236.6 Bcf). Out of this volume, 1.15 billion m³ (40.6 Bcf) were drained, and 0.23 billion m³ (8.1 Bcf) burned in boiler houses as a fuel. Presently, problems with coalbed methane are more complicated, with three aspects to consider:

- The safety of coal mine operations, in view of intensive coal extraction, with the goal to prevent the hazard of methane explosions in the mines.
- The moderation of the greenhouse effect, dy reducing emissions of coalbed methane into the earth's atmosphere caused by coal mines.
- The recovery and utilization of the methane as a valuable and ecologically relatively clean fossil fuel.

Under present financial conditions in the CIS, the only reliable way to solve the methane emission problem, is to use the drained methane now available for power generation. This solution reguires moderate initial investments and allows a short pay-out time for the capital invested. The profitability of such an undertaking should gain the attention of coal mine management regarding the quantity and quality of the coalbed methane drained and accordingly, it should also attract the investments required.

There are different ways for using the coalbed methane drained:

- To pump the methane into distributing pipelines by compressors and to sell it to customers. However, a larger part of the drained methane now available is considerably diluted by air and cannot be used without expensive, highly efficient gas separators, able to maintain pipeline quality of the methane produced.
- To burn the methane in local boiler houses for heat production. This method is simple and easy regarding performance, and it is presently used by some coal mines. Bit the demand of heat depends on the seasons, and this fact prevents to use all the methane drained, as it should be required for safety reasons. The only partial utilization of the methane resource, and the relatively low price caught for the heat produced, render this method unprofitable.
- To use the methane gas as a fuel for local power stations located at the mines, for producing both electricity and heat.

The last method described is the most attractive one: It corresponds to the state of the art regarding degassing technology, that causes the low quality of the gas drained and high market prices of electric energy. The power can be continuously fed into the local grid of mines, thereby reducing expenses for power purchases, or it can be fed into regional power grids for sale to outside consumers.

The generator sets of local power stations connected to the public electric power grid of practically unlimited capacity are able to consume the drained methane quantity as it is required for maintaining the safety in mines.

For choosing the appropriate type of power generating sets, the following factors must be taken into account:

- The methane produced by mine degassing systems is considerably diluted by air. The content of methane in the methane-air mixture can range from 10 to 60%;
- The methane-air mixture contains a humidity of 100%, caused by the water ring vacuum pumps, used in degassing systems;
- The outlet pressure of water-ring pumps is only 0.05-0.5 bar (0.7-7 psi).

These characteristics are determibed by the state of current technology of degassing systems. A rapid change of this situation is not expected, and so long distance transport of drained methane in pipelines must be avoided for above-mentioned reasons. Accordingly, olny one reliable way for using the drained methane remains, namely to use it as a fuel in power stations. These should be placed close to the vacuum pumps in operation at the mines, using all the gas produced at the site.

The power set of a typical power plant consist of a prime drive engine (a gas turbine or an internal combustion engine), with a heat-exchanger and an alternator.The most suitable type for a power set drive for local power stations is a four-stroke gas engine, or a dual fuel diesel engine, with the fuel-air mixer placed ahead of the charging turbo-compressor. Such a type of engine setup is basically able to work equally efficiently with coal mine gas of a methane content varying between 5-100%, without requiring prior concentration of the methane content or prior compression.

Present safety rules valid for mines allow to use coalbed methane in boiler houses and power plants only, if the methane content of the gas delivered remains above 25%. In the case of four-stroke internal combustion engines, this rule is appliied to prevent the risk of explosions in an emergency, provoked e.g. by faults in the inlet valve of the engine, followed by an ignition of the gas in the manifold and a propagation of the explosion along the feeding pipeline. The limitation in the use of gas mixtures could be abolished however, with the introduction of a reliable barrier against the propagation of such explosions as soon as this method becomes available and is officially certified.

Alternatives to four-stroke internal combustion engines are two-stroke engines and gas turbines. But their common shortcoming is their requirement to compress the gas prior its use and the limitation to feed gas with a methane content within the explosion range (which is between 4-16%).

An inevitable precondition for solving the coalbed methane problem in the CIS countries successfully, is to secure sufficient financial means for the initial investments and to restrict the investments required to the minimum. Under present technical and economical conditions, the key to solving this problem is to install local power stations at the coal mines, equipped with four-stroke internal combustion engines, that are fuelled by otherwise wasted coalbed methane,of a quality, as delivered by existing degassing systems. The moderate initial investments for this first step of using fuel available for free, must help to provide the means for the further steps in solving the methane problem related to coal mining in the CIS.

Regarding the Russian part of the Coalbed Methane Utilization Program, it is envisaged to install the types of power sets as listed in Table 1. The power stations equipped with these sets will be fuelled by methane as delivered by the degassing systems of the coal mines. At the mines, the methane will be drained by a number of boreholes drilled from underground works or from the surface.

The drive engines of the power sets are fitted with automatic gas feeding devices, which adjust the fuel-air mixture according to the methane content and pressure of the fuel gas, just as it is delivered by the degassing systems. This allows to operate the sets steadily, despite of rapid changes in the methane content of the fuel gas between 25-100%, and despite its low pressure, fluctuating between 0.01-0.5 bar (0.15-7.2 psi).

The power sets have heat exchangers installed for using the waste heat produced by the engines. The combined efficiency of such sets, taking into account the output of both the electric power and the heat energy, can reach up to 85%. The four types of power sets listed in Table 1 are suited to satisfy the needs of the coal industry for using the methane drained as required.

Figures of the expecetd effect of applying these concepts in Russia, Ukraine and Kazakhstan for the volumes of the methane drained at present and expected, are shown on Table 2.

Russian coal mines, using drained methane now available for free in amounts of 700 m^3/min (35.6 MMcf/d), can generate electric power at a rate of 145 MW, and in addition 143 Gcal/h (572.5 million Btu/h) of heat. This corresponds to $1.27 \cdot 10^6$ MWh of electricity and $1.25 \cdot 10^6$ Gcal of heat (5 trillion Btu) per year. Under present market conditions, the value of this energy corresponds to 90 billion Rubles.

At an expected price for power sets fuelled by gas and manufactured in Russia of some $1.5 \cdot 10^6$ to $1.7 \cdot 10^6$ Rubles per kW, the cost of power stations with a total power capacity of 145 MW would amount to approximately 250 billion Rubles. The time required for repaying such investments would range from 3-3.5 years. However, present prices for energy and equipment are not stable, and they do not always reflect the real value of these items. As a comparison, a similar calculation made only two years ago arrived at a repay time of 1.5-2 years.

By improving the existing degassing systems, the rate of methane drained could be increased from 700 m^3/min to 1800 m^3/min (35.6 to 91.5 MMcf/d). This rate would allow to generate 379 MW of electric power with an additional 320 Gcal/h (1.27 billion Btu/h) of heat power.

In Russia, the most successful coalbed methane drainage and utilization system is operating in the Vorkuta coal fields (Table 3). There, twelve mines are present, out of which eight are equipped with degassing systems, with 115 suction pumps installed. The suction pumps are placed at the surface and connected by steel pipes of a diameter

of 219-235 mm (8.6-12.8 in.) to a number of wells drilled from underground works. The total length of the pipeline systems is 232 km (144 miles).

The application of such technical means in 1994 resulted in a flow of drained methane of about 400 m³/min (20.3 MMcf/d). Half of that quality (196 m³/min = = 10 MMcf/d) is burned in boiler houses in close proximity to the suction pump stations. The other half of the methane drained (195 m³/min = 9.9 MMcf/d), is presently vented into the atmosphere, although it would be suitable as a fuel for generating elctric and heat power. Using presently wasted methane during the winter months would allow to produce 41 MW of electric power and 37 Gcal/h (146 million Btu/h) of heat.

In Vorkuta, in addition to fuelling boiler houses, drained methane is also being used for directly heating air for the mines' ventilation systems and for coal drying.

During the summer, when the entire flow of drained methane is available as a fuel for power sets, it is possible to generate 82 MW of electric power and 75 Gcal/h (298 million Btu/h) of heat. This is sufficient to approximately cover the average energy requirements of the mines in the Vorkuta area.

The coal mine Severnaya has the most perfected system for degassing and use of the methane drained. There, about 51% (130 m³/min) of the total volume of methane emitted due to coal extraction is drained by the vacuum pumps and partly burned in boiler house covers entire present heat demand of the mine can already be covered now of the mine, with the additional possibility for the future to also cover the entire electric power demand. The delivery of the equipment for power stations is already progressing there.

Experiences at the coal mine Severnaya show the potential to drain half of the total methane emissions caused by coal mining. If similar results could be achieved in general, relative to the specific methane content of coal in Russian mines of 18.6 m³/tonne (657 scf/t), it would be possible to generate 32 kWh of electric power per metric tonne of coal. Compared to that potential, presently the coal industry in Russia as an average consumes 52 kWh of electric power per tonne of coal extracted. These considerations show how necessary it is to install local power plants in the coal mines foe economic and ecologic reasons. This view agrees with the general policy of energy production in the CIS.

The concept of centralized systems for energy production and distribution followed in the past had forced out small power stations. The reasons for the advance of large power stations at the cost of small local ones relates to the greater efficiency of the large ones, the availability of cheap prime energy bearers, and the absence in the past of ecological restrictions for mining them and burning them as a fuel. Meanwhile, fossil fuel resources are no longer considered as unexhaustable, and their exploitation is becoming increasingly expensive. Additionally, ecological reservations are increasing too regarding the mining of conventional energy bearers and their use in large power stations.

All these factors combined lead to the development of decentralized auxilliary systems of energy generation, based on the concept of small power stations that are fuelled by small and unconventional resources of prime energy.

The introduction of small power stations as a general rule requires a higher specific investment per kW of power installed, with the smaller powersets often having a lower efficiency. However, small power stations equipped with internal combuston engines that use drained coalbed methane as a fuel, represent an exception : The specific investments for the construction of power stations based on internal combustion engines are less than half of those required for conventional large steam power stations of comparable efficiency regarding maintenance costs. At the end, the high level of automation in small plants renders the electric power produced by them cheaper than the power supplied by the large plants.

SUMMARY

1. Coal fields in the CIS, with their substantional reserves of coal deposits, contain significant quantities of coalbed methane that can be used for energy production.

2. Systems of methane drainage as presently installed were originally developed only as an effective means to improve the safety and productivity in coal mines by avoiding delays, caused by the risk of an excessive methane content of the air at the working face. The contamination of the methane drained by a high air content renders that sort of gas unsuited for transportation by pipeline to potential consumers.

3. The most efficient way of dealing with the coal mine methane under present conditions is to use it as a fuel for the generation of electric power and heat in local power plants, equipped with four-stroke internal combustion engines.

4. The profitability of this method of using methane otherwise wasted, promises to stimulate the further development of the technology for methane drainage. This will eventually result in increasingly larger volumes of methane captured, thereby improving the safety and productivity of mine operations. Additionally, this approach will provide the mines with energy, and it will also reduce methane emissions into the earth's atmosphere.

5. The further development in the utilization of methane from mines should be directed towards increasing the proportion of methane captured and towards improving its quality, by implementing modern technology. A further step towards a better utilization of the methane and prevention of pollution of the earth's atmosphere, should be to develope an appropriate technique for oxydizing the methane emanating from outlets of ventilation systems of coal mines. The low methane concentration of such outlet gas allows to predict that this goal will be expensive and technically difficult to achieve.

REFERENCES CITED

1. Serov V.I., Bernstein A.E. and Tuzhikov V.F., 1994: «Development of non-traditional power generation in Vorkuta coal field: Experience and outlook»; Ugol, №4

2. Zabourdyaev V.S., Dmitriev A.M., Pak V.S., 1992: «Resources, volumes of recovery and utilization of methane in mines»; Ugol, №12.
3. TsNIEIugol Review, 1986: «Complex degassing of high-efficient mining areas;» Moscow.

Table 1: Types of Power Plants, Envisaged for Russia

№	Electric power, kW	Type of drive engine	Rev/min	Rated voltage of alternator, V	Frequency of electric current, Hz	Heat output, Gcal/h	Fuel	Specific fuel consumption, kJ/kWh	Methane contents in air-methane mixture used as fuel, %
1.	2500	Gas Disel	500	6300	50	2,4	methane 94% + oil 6%	9800	25-100
2.	1000	Gas Engine	1000	6300	50	0,96	methane 100%	10300	25-100
3.	500	Gas Engine	1500	6300/400	50	0,48	methane 100%	10100	25-100
4.	200	Gas Engine	1500	6300/400	50	-	methane 100%	10700	25-100

Conversion Factor: 1 Gcal/h = 1.1628 MW = 3.9683 million Btu/h

Table 2: CBM Potential in the CIS

	Total methane emissions caused by coal extraction, m³/min	Specific methane emission, m³/t	Drained methane output (flow), m³/min	Drained methane flow used in boiler houses, m³/min	Flow of methane vented into the atmosphere (available for use), m³/min	Expected flow of drained methane, m³/min	Energy potential of drained methane			
							Year 1994		Expected	
							Electrical power MW	Heat power Gcal/h	Electrical power MW	Heat power Gcal/h
Russia	4230	18,6	900	200	700	1800	146	125	375	321
Ukraine	6450	24,5	914	323	591	1800	123	106	375	321
Kazakhstan	2110	26,0	346	123	323	690	65	57	134	120
former USSR	12790		2160	646	1614	4290	334	288	884	762

Conversion Factor: 1 m³/min = 50.853 Mcf/d
1 Gcal/h = 3.9683 Btu/h = 1162.8 kW

Table 3: CBM Drainage and Utilization Systems, Vorkuta Coal Fields

Names of Vorkuta Coal Mines	Methane drained, m^3/min	Methane content in drained methane-air mixture, %	Part used in boiler houses, m^3/min	Part available for electricity generation, m^3/min	Electric power, that can be generated using methane available MW
1. Severnaya	130	41	60	70	14,6
2. Juzhnaya	40	25	0	40	8,3
3. Vorkutinskaya	55	37	45	10	2,0
4. Komsomolskaya	60	43	60	-	-
5. Zapolarnaya	50	27	30	20	4,2
6. Jur-Shor	7	25	0	7	1,5
7. Zentralnaya	43	40	0	40	9,0
8. Promishlennaya	6	35	0	6	1,3
Total	391		195	193	40,9

(See Conversion Factors, Tables 1-2)



NOTES

INTERGAS '95

May 15-19, 1995
The University of Alabama
Tuscaloosa, Alabama USA

9537

Coal Seam Methane Drainage Through Surface Boreholes

O.I. Kasimov and A.I. Bukhantsov, Makeevka Safety in Mines Research Institute; and V.V. Kasyanov, MakeevkaUgol, Ukraine

ABSTRACT

Methane production from minable coal seams is dealt with in the paper. 26 surface drainage holes at 6 Donbass mines have been tested to determine the portion of gas that can be captured through them when the gas is released while mining.

Many years of surface hole drainage at Donbass mines show that an additional gas makes up over 40% of hole output. This is the gas usually remaining in the rock after stoping operations. In view of energy problems in the Ukraine we suggest to produce methane through the surface holes.

Assumingly, a certain part of methane can be produced from coal and gas-containing seams before stoping, with the help of hydrofracturing. The remaining gas will be captured through the surface holes after stoping. Prospect holes, provided they are properly equipped, can be used to this end, thus enabling some savings.

It has been experimentally demonstrated that the portion of gas, able to be removed from undermined strata intersected by gas-taking hole sections, is determined mainly by the gob area per a hole. Gas-taking hole length should be at least 120 times of minable seam thickness.

The relationship we suggest enables to determine gas amount that can be produced in particular conditions with known gas content values in coal/rock, and given hole design and distribution over the minable area.

PRACTICE OF SURFACE HOLE DRAINAGE

Hard energy situation in Ukraine awoke great interest to methane, associating coal mining operations. According to Donbassgeologiya PO estimates the proven mining fields in Donbass contain 645 bln m^3 of mehane including operating mines with 239 bln m^3. About 90% of methane is trapped by coal and can be removed only when rock stability is changed.

Efforts to remove methane before mining operations showed the best results when seam permeability was increased by hydrofracturing. Coal seams being hydraulically treated with further water pumping are able to produce 13 to 43% of methane (see Table 1). The borehole output rate, however, is not enough to make effective use of the gas captured, though the results show the prospect for hydraulic treatment of coal beddings and gas rocks to significantly improve the time and volumes of drainage. An extensive programme is carried out to identify experimentallythe feasibility of methane drainage from coal seams not relieved from rock pressure yet with enough output to be utilised.

Surface boreholes used for drainage of coal seams and rock that are relieved with mining show that output and rate of the gas removed are quite enough to compensate utilisation costs. More over, the holes appeared to produce "additional" methane, that is to provide more extensive drainage of undermined strata compared with underground workings and boreholes. Comparison of gas emission values at Khrustalskaya mine, working the same seam at various stopes with about the same coal output showed that with surface holes methane emission increased on the average by 11.4 m^3/min making up 44.7% of the average discharge rate (Table 2).

Therefore the surface boreholes produce significant portion of methane which without the holes of this kind could remain trapped.

DETERMINATION OF SURFACE HOLE GAS REMOVAL COEFFICIENT

To develop methane production projects for working mines it is necessary to have a method to determine minable coal reserves. Drainage experience in mines suggests that gas can be drawn from coal seams and rocks when they are relieved in the process of coal extraction. As many studies of rock stability and physical and chemical properties of undermined seams show [1,2,3] the changes of those are significant at the point of inersection of seams with the planes that are perpendicular to the bedding and run across non-advancing boundaries of the coal strata around the goaf. Beyond the boundaries coal seams are actually impermeable, rock at the boundaries being additionally compressed, porosity and permeability much decreased. All those factors together assume that methane can be only remoned from the zone

limited to the dip and strike by the boundaries mentioned.

Studies of methane inflows into surface holes demonstrated [4] their upward travelling with the rock movement along an uncased length of the hole up to the upper level of methane zone.

Gas pressure in undermined strata, as is proved by experiments [5], is decreased due to drainage holes. Ideally it can be assumed that with sufficient number of holes gas pressure in undermined strata can be reduced down to atmospheric pressure by several times.

Following from the above a method is given below to determine methane reserves that can be removed by surface boreholes.

$$V_{v.h} = (V_c + V_r) d_{v.h}, \quad (1)$$

$$V_c = \sum_1^k S m_i \gamma_i (x_i - x_0), \quad (2)$$

$$V_r = \sum_1^{k_i} S m_j \gamma_j x_j \quad (3)$$

All parameters in the equations except the coefficient of removal can be easily determined. The latter needs experimental check, which has been done at seven stopes of six coal mines in Donbass where surface boreholes were drilled for drainage purposes (Table 3). During the operation period the holes discharge rate was being monitored. At the same time the gob area was measured. The coefficient of removal is expressed by the following ratio:

$$d_{v.h} = \frac{V_{v.h}}{V_c + V_r} \quad (4)$$

The results obtained show that gob area per one hole is the most critical factor (Table 4 and Fig. 1).

When the area decreases the coefficient tends to unity, thus enabling to describe its relation to the specific area by the following eguation, if $15 \times 10^3 \le S_s \le 60 \times 10^3$:

$$d_{v.h} = \frac{1}{1 + 52 \times 10^{-6} S_s} \quad (5)$$

The amount of gas captured by holes can be calculated by:

$$V_{v.h} = \frac{V_c + V_r}{1 + 52 \times 10^{-6} S_s} \quad (6)$$

Hole pumping can increase the discharge rate but does not significantly influence the total output of methane produced.

Thus, critical factors influencing the amount of methane to be removed by vertical holes of 100-127 mm diameter are the removable methane reserves intersected by the uncased length of hole (or the pipes are perforated) and holes spacing within stoping area.

The method we suggest to calculate the amount of methane to be removed by surface boreholes enables to make up plans for methane production through the holes mentioned and to estimate whether it is cost effective provided the gas-taking length equals at least the value of a 120-fold thickness of a working seam.

Further investigations are pursuing the aim to determine how hole discharge rates are related to mining conditions.

NOMENCLATURE

$V_{v.h}$ - amount of methane captured by surface holes at a given stope, m^3.

V_c, V_r - removable gas reserves in coal and rock seams (amount of gas capable to releasefrom coal and rock seams intersected by gas-taking hole lengths at atmospheric pressure), m^3.

$d_{v.h}$ - coefficient of gas removal by vertical holes (portion of removable gas reserves, captured by holes).

S_s - average gob area per a hole, m^2.

REFERENCES

1. Morev A.M. and I.I.Yevseyev, 1975: Methane recovery from adjacent coal seams: Moscow, Nedra, 167 p.

2. Voloshin N.K., 1963: Advance mining of protective inclined seams: Moscow, Nedra, 63 p.

3. Novichikhin I.A., Khilko V.V. and M.A.Ilyashov, 1990: Mining of outburst coal seams: Kiev, Tekhnika, 74 p.

4. Kasimov O.I. and V.V.Kasyanov, 1994: "Gas reserves in undrmined strata and the prospects of removal."; Ugol Ukrainy, No. 2, p. 5-7.

5. Airuni A.G.,1981: Theory and practice of mine gas control at great depths: Moscow, Nedra, 335 p.

Table 1.
Results of methane drainage from unrelieved seams after hydraulic fracturing.

Mine	Number of holes	Discharge rate, m^3/min		Average volume of CH_4/ hole, thou m^3	Average time of drainage	Percentage of CH_4 removed
		average	max			
Severnaya	7	0.4	1.8	383	665	28
10-bis	3	0.54	2.2	650	837	42
Communist	10	0.52	1.3	104	139	18
Zuevskaya	5	0.45	1.2	101	156	27
Pochenkova	1	0.6	1.1	52	87	13

Table 2.
Surface boreholes effect for methane emission from working stope.

Mine, face	Average discharge rate (m3/min) emitted in			Total
	workings	underground holes	surface holes	
Khrustalskaya				
1 West, seam	19.7	24.6	-	44.3
5 West, seam	20.2	30.6	-	50.8
average	20.0	27.6		47.6
1 East, seam	12.0	16.8	25.4	54.2
5 East, seam	12.9	25.0	27.5	65.4
6 East, seam	12.4	22.1	24.5	59.0
average	12.4	21.0	25.6	59.0

Table 3.
Holes parameters

Mine, face	Hole depth, Hh,mm	Case diam., d ,mm	Final hole diam., d, mm	Casing length, Hc,m	Length of gas-taking part of hole, Hg-t,m	Hole face to working seam distance, Hs,m
Khrustalskaya 1 East	370	127	76	40	330	30
Chaikino 3 and 4 North	560	108	93	400	160	30
Ukraine 2 South	455	127	112	350	105	40
Communist F 48 bis	528	114	114	400	128	0
Stakhanov 2 North	1128	200	130	810	318	0
Vostochnaya 2 East	724	108	108	70	254	30

Table 4.
Methane removed by vertical holes

Mine, face	Nos of holes	Field area per hole, thou m^3	Gas reserves in roof, mln m^3	Average discharge rate	Amount of gas captured,mln m^3		Percentage of gas captured, %
					total	one hole	
Khrustalskaya 1 East	10	18.7	20.7	2.2	10.0	1.0	48.3
Chaikino 3 and 4 North	5	47.6	26.6	2.8	7.4	1.48	27.8
Communist F 48 bis	6	41.2	10.7	2.4	4.2	0.7	39.2
Ukraine 2 South	2	38.8	14.2	9.7	4.2	2.1	29.6
Stakhanov 2 North	2	57.5	22.6	5.6	5.7	2.85	25.2
Vostochnaya 2 East	1	57.0	10.0	4.5	2.5	2.5	25.0

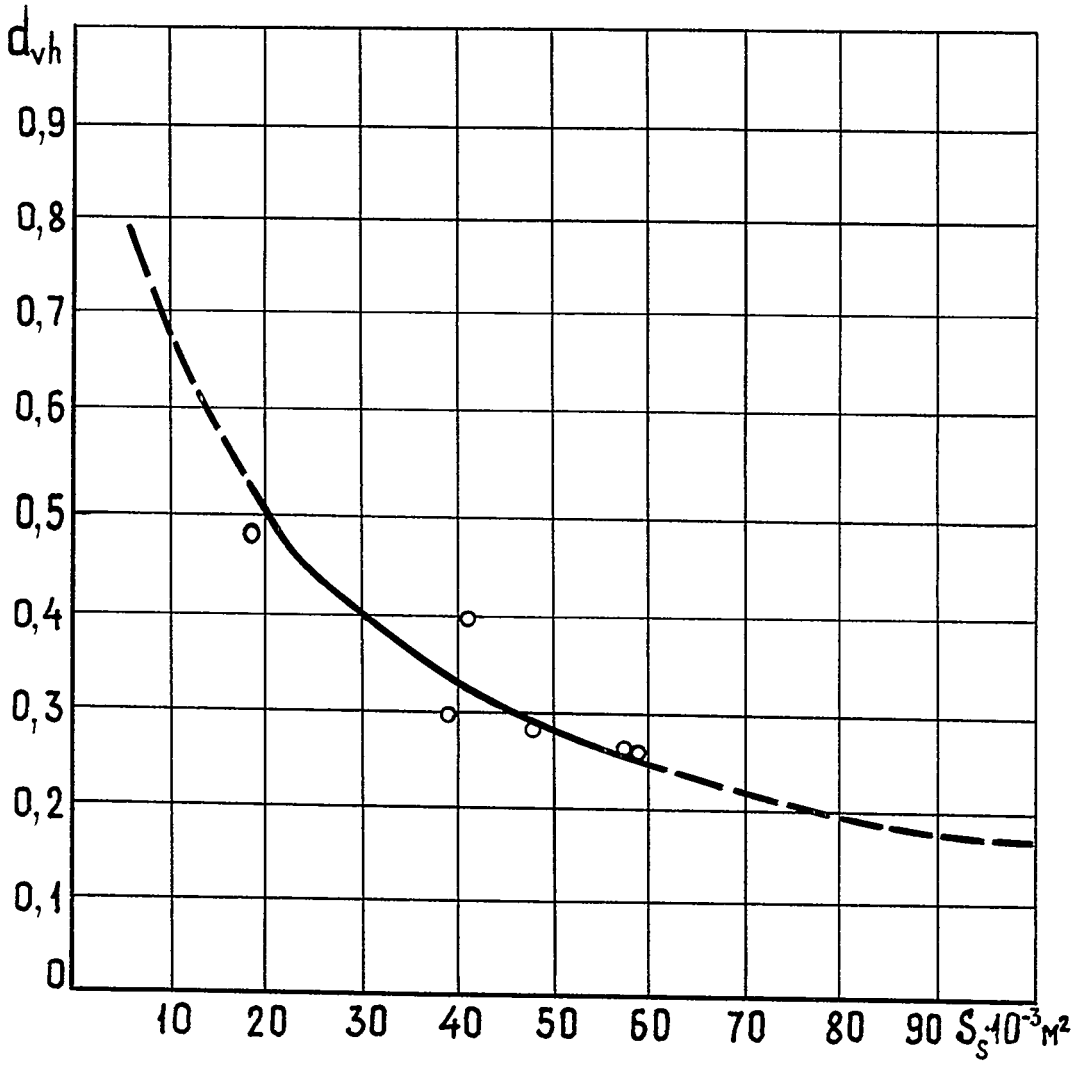


Figure 1. Coefficient of vertical hole methane removal versus average gob area per a surface hole.

INTERGAS '95

May 15-19, 1995
The University of Alabama
Tuscaloosa, Alabama USA

9504

Sudden Methane Rushes Through the Roadway Floor

I. Bolshinsky, Argonne National Laboratory;
A. Morev and S. Kloisner, Makeevka Safety in Mines Research Institute, Ukraine

ABSTRACT

Methane rush through the roadway floor is a short time process of floor rock heaving and breaking with subsequent rushing of methane into the roadway atmosphere. Some cases of sudden methane rushes through roadway floor had catastrophic effects.

Physical and mathematical models of floor rock breaking are suggested. Maximum stress value in floor rock was taken as a criteria to identify this phenomena occurrence. The problem is reduced to evaluating the stressed state of elastic, homogeneous isotropic rectangular slab lying on elastic Winkler basement and influenced by random transverse load. The method of evaluation of maximum methane emission and total methane emission during sudden ruches are also developed.

The safety of miners in the case of a sudden rush through the roadway floor can be assured by a special system of measures, which includes:

- prediction of methane rushes;
- protection against sudden methane rushes;
- measures to insure safety in the workings.

To prevent sudden methane rushes in the Former Soviet Union the following techniques are applied:

- degasification of the overworked rock mass by boreholes drilled from workings;
- protective overworking or underworking;
- changing the roadway location relative to the gas emission sources.

In the Former Soviet Union the methods of working in mines dangerous because of sudden methane ruches are regulated by "Instruction on Prediction and Prevention of Sudden Methane Ruches Through Roadway Floors" [1].

INTRODUCTION

At the present more than 20% of mines in the Former Soviet Union are deeper than 700 m, of these, 6% are deeper than 1000 m. Deep mineral mining in mines is unfavorably affected by gas-dynamic phenomena generated within rocks due to mining operations which have become the most dangerous factors giving rise to emergency cases. These phenomena include coal, rock and gas outbursts, rock bursts, sudden methane rushes through the roadway floor.

Different gas-dynamic phenomena appear at different depths of mining. So their nature depends on the depth of mine as well. Sudden methane rushes through the roadway floor and coal and gas outbursts appear first at a depth of 100-450 m depending of the coal rank. The minimum depth of sandstone outbursts is 650-700 m. Outbursts of rock and gas may happen not only in mines but also while driving tunnels. For example, in the Former Soviet Union while driving the Arpa-Sevan tunnel there were outbursts of porphyrite and gas at the depth of 600-650 m.

Currently more than 200 sudden methane rushes are on record. They have occurred practically all major coal basins of the Former Soviet Union, as well as in Germany, Great Britain and other countries Sudden methane rushes occur in all kinds of roadways, but most often in transportation workings. In many mines these phenomena are linked with geological dislocations.

Rock displasment into the working during methane rushes may reach a few tens of centimeters, resulting in damage to supports and machines and a safety hazard to miners. In horizontal and slope workings the maximum displasment takes place in the middle of the workings. In long roadways the length of displacement my reach 30-40 m. The time of gas emission in case of sudden rushes is about a few hours. During a relatively short period of time methane emission reaches a maximum and then decreases slowly.

With an increase in the depth of mines the quantity of methane emitted increases during rushes. For example, at a depth of 93 m maximum methane emission was 15.5 m^3/min.. At a depth of 270 m it was 57 m^3/min. and at a depth of 743 m it was 200 m^3/min.

NATURE AND CAUSES OF SUDDEN METHANE RUSHES

An extensive analysis of all known sudden methane rushes cases, recorded by Makeyevka Safety in Mines Research

Institute (MakNII), enables to highlight some characteristic properties of this phenomena. Better understanding of these characteristics helps to describe how the process originates and develops, and to present in as follows.

Drivage operations promote rock pressure relief in a working floor accompanied by deformation and stress redistribution in the vicinity of the working. Around the working an abutment pressure zone is generated due to concentrated weight transfer by rock mass being underworked. If one or more layers of extra-hard rocks overlay less hard, yielding rock layers, the layers flex upwards at the working boundaries under abutment pressure influence. Different elastic properties of rock contribute to separations (cavities formation) at hard rock-yielding rock boundary; these cavities, being filled with methane desorbed from gaseous layers, if any, in floor. The layer that is band to working is the place of differently signed increased stresses and bending moments. This, in turn, is associated with opening and development of cracks that play the role of stress concentrators. With certain mining versus geological conditions relationship stresses in the layer being bent exceed its strength. In such cases the layer breaks and gas rushes into the working (Fig. 1).

Since in most cases when sudden methane rushes occur the breaking layer thickness to typical working size ratio does not excess 0.5 m, we can assume that elastic rock layers in the floor are devolved like a plate (a slab) bending under load normal to its surface. Then, more yielding rocks adjacent to elastic rocks may function as a elastic basement satisfies an elementary Winkler-Zimmerman hypothesis which states that the basement reactions in some point are proportional to slab bending in this point. Practically without loss of generality, we suppose that elastic slab is located horizontally and is rectangle in plan. Contour rigid fixing is taken as a boundary condition. The mentioned above enables to reduce the problem of stressed floor to the following problem of elasticity theory: to determine stressed state of elastic, homogeneous isotropic rectangular slab lying on elastic Winkler basement, rigidly fixed along the contour, with random transverse load influencing the upper basement of the slab.

Laying OX axis of Cartesian rectangular coordinate system along the strike line, and OY axis along the face line we write the differential equation for the bent slab surface as follows:

$$\frac{\partial^4 W}{\partial x^4} + 2\,\frac{\partial^4 W}{\partial x^4 \partial y^4} + \frac{\partial^4 W}{\partial y^4} = -D^{-1}(q - K(W_0 - W)) \qquad (1)$$

where: D - slab rigidity under bending; q = q(x, y) - transverse load function; K - elastic basement modules (bed ratio); W_0 - slab edge bending flexure, and W = W(x, y)- slab arbitrary point-to-edge bending flexure.

Boundary conditions in this case are simplified to:

$$W\big|_{\substack{x=0\\x=a}} = W\big|_{y=0}^{y=b} = 0; \quad \frac{\partial W}{\partial x}\Big|_{x=0}^{x=a} = \frac{\partial W}{\partial y}\Big|_{y=0}^{y=b} = 0 \qquad (2)$$

where: **a** and **b** denote liner sizes of the slab along the face line and in the direction perpendicular to it.

Bending moments and stresses occurring in the slab can be found by the known equations:

$$M_x = -D\left(\frac{\partial^2 W}{\partial x^2} + \nu\,\frac{\partial^2 W}{\partial y^2}\right); \quad \sigma_X = \frac{\delta M_X}{h^2};$$

$$M_y = -D\left(\nu\,\frac{\partial^2 W}{\partial x^2} + \frac{\partial^2 W}{\partial y^2}\right); \quad \sigma_Y = \frac{\delta M_Y}{h^2}. \qquad (3)$$

where: ν - Poisson's ratio of slab material, h - slab thickness.

To solve the problem we express the bending flexure function in the following form:

$$W = W_1(x, y) + \bar{W}(x, y) \qquad (4)$$

where: W_1 - function, satisfying the equation (1) and boundary conditions:

$$W_1\big|_{\substack{x=0\\x=a}} = W_1\big|_{y=0}^{y=b} = 0; \quad \frac{\partial W_1}{\partial x}\Big|_{x=0}^{x=a} = \frac{\partial W_1}{\partial y}\Big|_{y=0}^{y=b} = 0 \qquad (5)$$

which correspond to simply supported slab.

W(x, y) function is bending flexures of the slab being affected by moments distributed along its edges so that W = W(x, y) function satisfies boundary conditions (2).

W_1 bending flexure function of simply supported slab we determine through Navier method [2].

The proposed mathematical model of overworked rock stressed state enables both to estimate bending flexures, stresses and bending moments occurring in the floor, to reveal how these variable are related to various mining parameters and evaluate the potential parameters contributing to sudden floor rock breaking.

A program package has been developed to investigate numerically how mining parameters influence the stresses state of floor rock. It helps to evaluate bending flexures (W), stresses (σ_x and σ_y)and bending moments (M_x and M_y) at any point of the slab, maximum values of these variable and position of points where these values are reached. The output data may be tabulated or plotted as distribution of bending flexures, stresses and bending moments along the length and width of workings.

The extensive numerical investigations enable to conclude that slab thickness, mining depth, rank of coal and host rock, lithology and elasticity of floor rock, and geometry of long workings are major contributory factors to floor stressing.

Specifically, the results of investigations show that maximum stress-versus-slab thickness curve has its maximum. Therefore, it is possible to eliminate sudden floor breaking hazard through changing the slab thickness in either directions (i.e. by changing a working location). Yet another results show that increased width of a working involves higher maximum values of bending flexures stresses occurring in the floor. However, width above 100 m change of the values has no effect upon bending flexure and stress quantities.

PREDICTION AND PREVENTION OF SUDDEN METHANE RUSHES

Better knowing of relationships that determine floor stressed state dependence upon mining and geological conditions results in a new method developed to predict sudden methane rushes in active workings and in the workings planning stage.

As we mentioned above, the cavities formatted in the working floor may be filled with methane desorbed from the gaseous layers, if any, in floor.

The maximum methane emission from these cavities during the floor rock breaking can be determined from the following equation:

$$I_m = \varphi \eta P_1 \qquad (6)$$

where: φ - experimental coefficient depending on methane parameters and the relative open size of cavity, $\varphi = 0.0162*10^{-5}$ $m^4/(min.*N)$; η - size of the working, m; P_1 - methane pressure in the cavity, Pa.

Total methane emission (I) during the methane rush through the roadway floor is determined by three components:

$$I = I_1 + I_2 + I_3 \qquad (7)$$

where: I_1 . primary emission of desorbed gas from the cavity;
I_2 - emission from the surface of the cavity;
I_3 - methane emission in the working before the methane rush.

Primary emission of desorbed gas from the cavity can be found from the following equation:

$$I_1 = \varphi \eta P_1 \exp\left(-\frac{P_a \varphi \eta t}{V}\right) \qquad (8)$$

where: V- size of the cavity, m^3.

Methane emission from the surface of the cavity is equal to:

$$I_2 = \frac{aS(x - x_t)}{(1 + t)^b} \qquad (9)$$

where: x - gas content of the gaseous layer, m^3/T; S - size of cavity, m^2; a and b -experimental coefficients.

The method for predicting sudden methane rushes through the roadway floor was in-field tested and demonstrated its high effectiveness. This method is now successfully used in Donetsk coal basin mines.

To prevent sudden methane rushes in the following techniques were developed:

- degasification of the overworked rock mass by boreholes drilled from workings
- protective overworking or underworking;
- changing the roadway location relative to the gas emission source (cavity).

Gas drainage by boreholes is most widely used. In this case the boreholes are drilled to the nearest coal seam in the working floor and they have to cross it. The schemes of degasification of overworked strata are shown in Fig. 2, 3, 4. The boreholes are drilled at a distance of 20 m from each other.

The degasification boreholes should be connected with the degasification network draining methane from the mine by surface or underground assembly [3].

Protective overworking or underworking are the best technological means to protect against sudden methane rushes. As a result of rock pressure relief and increase of permeability of strata in the are of influence of the protective seam, there is natural degasification. In Fig. 5 the boundaries of protective zones are shown.

Changing the roadway location relative to the gas emission source is the most efficient method during the design stage.

CONCLUSIONS

Successful experience of predicting and preventing of sudden methane ruches through the roadway floors in Donbass coal mines has shown that the danger of sudden methane emission through floors can be significantly decreased and, in many cases, fully eliminated by a special system of measures developed by Makeevka Safety in Mines Research Institute, Ukraine.

REFERENCES

1. Morev A. and Sklayrov L., eds., 1987: Instruction on Prediction and Prevention of Sudden Methane Ruches Through Roadway Floors: Makeevka, Donbass, 30 p.

2. Timoshenko S. P., Woinowsky-Kriger S., 1959: Theory of Plates and Shells: New York, McGraw-Hill Book Company, Inc., 590 p.

3. Morev A. and Kasimov O., eds., 1990: Manual on Degasification of Coal Mines: Moscow, Nedra, 120 p.

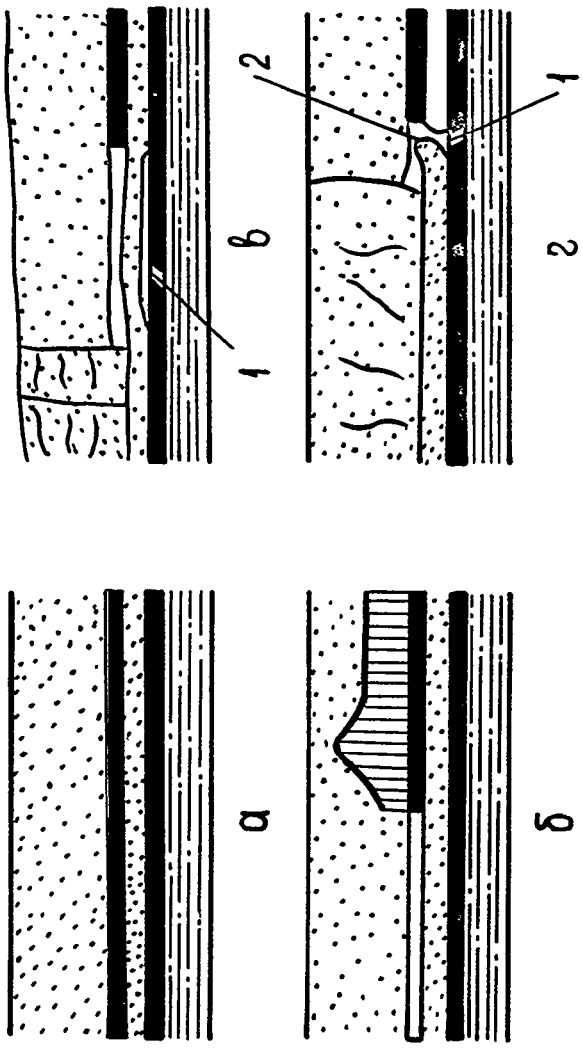


Figure 1. Scheme of origination and development of the sudden methane rush through the roadway floor

а - before mining operations;
б - generating of the abutment pressure zone;
в - creating of the cavity;
г - floor rock breaking and methane rushing.

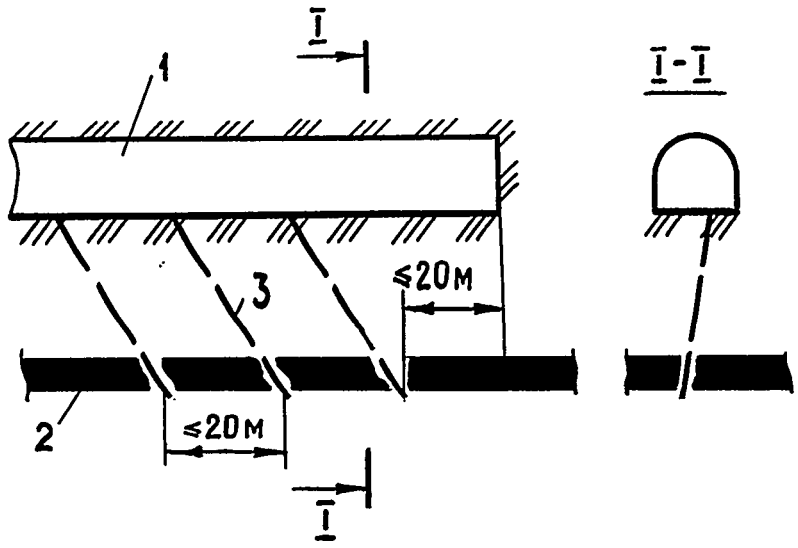


Figure 2. Scheme of degasification of underworked rock mass during drivage of horizontal and slope roadways

1 - working;
2 - potential methane source;
3 - drainage boreholes.

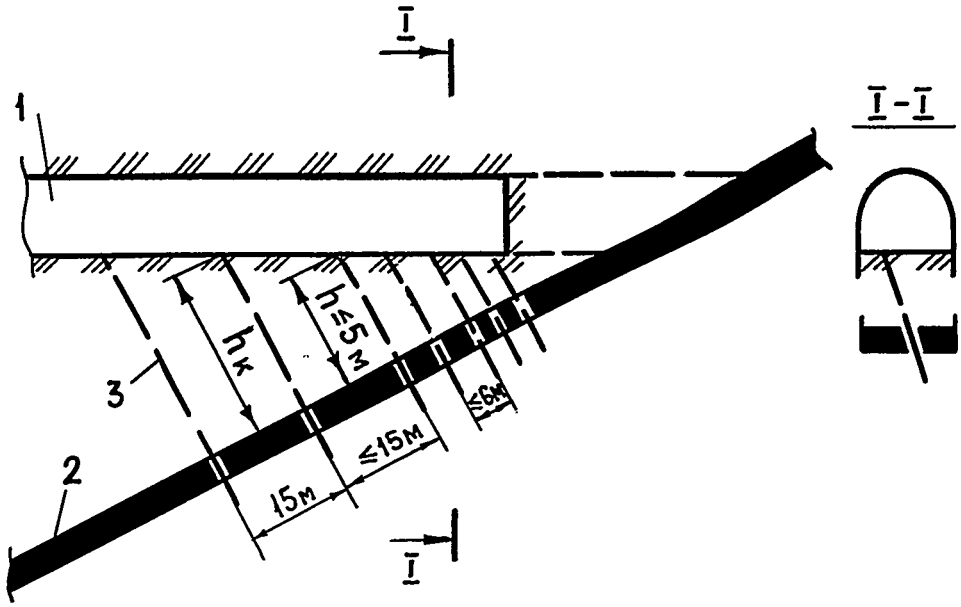


Figure 3. Scheme of degasification of underworked rock mass during crosscut drivage

1 - crosscut;
2 - potential methane source;
3 - drainage boreholes.

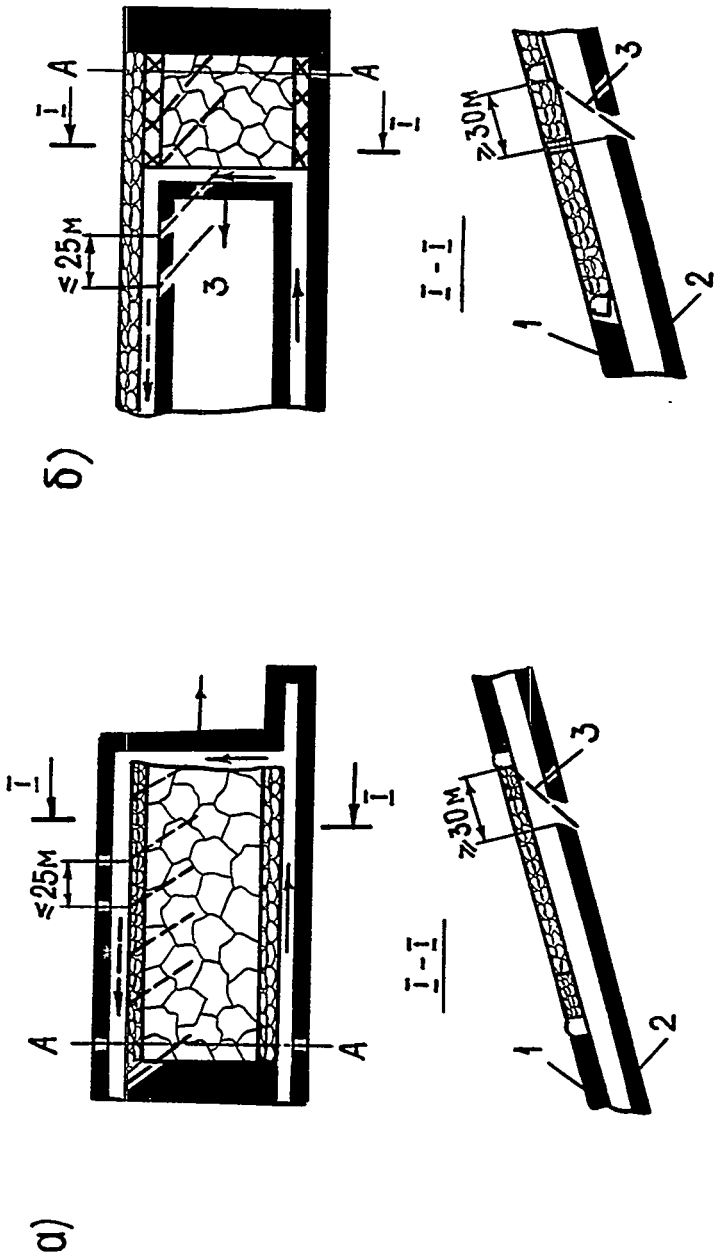


Figure 4. Scheme of degasification of underworked rock mass during longwall mining

1 - working seam;
2 - potential methane source;
3 - drainage boreholes.

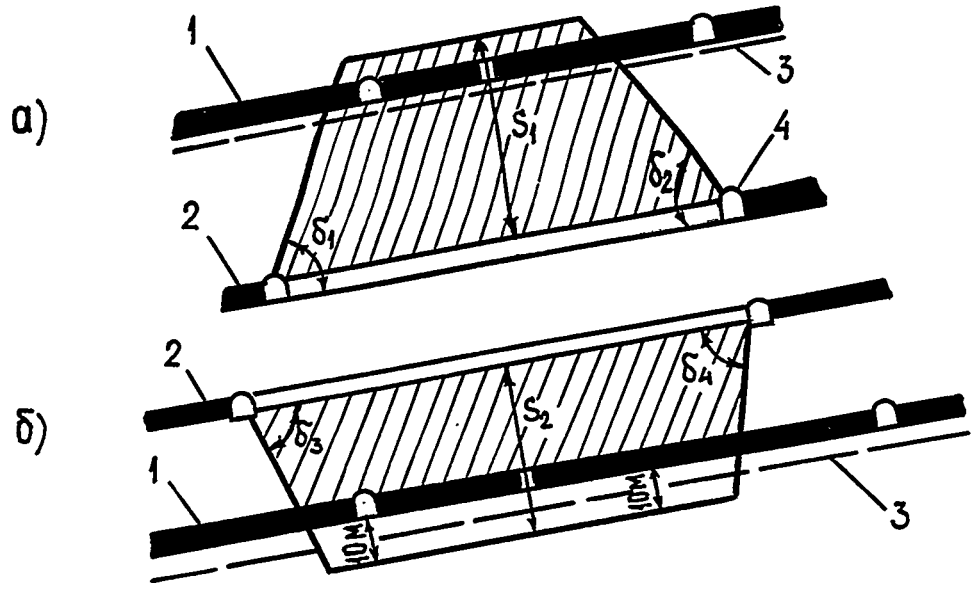


Figure 5. Boundaries of the protective zone from methane rushes during overworking (a) and underworking (b)

1 - working coal seam;
2 - protective coal seam;
3- working.



NOTES

INTERGAS '95

May 15-19, 1995
The University of Alabama
Tuscaloosa, Alabama USA

9546

Sudden Methane Outbursts in Mine Workings and Their Prevention by Degassing Methods

Y.L. Khoudin, Skochinsky Institute of Mining, Russia

ABSTRACT

Sudden gas (methane) outbursts in mine workings have been registered lately at coal and some metallic minerals mines causing the floor rocks and workings failure with emission of up to 300 m^3/min. of methane over a period of 10-30 minutes. This results in raising methane content in mine air for a long time, and in some cases, in decreasing 02 content in it to less than 12 %. Most of such outbursts have been registered at a depth of more than 300 m, and as a rule in the presence of a shielding layer of sandstone in the stratigraphic section of the deposit. These phenomena are also observed in the zones of geological faults.

* * *

The main causes of the floor rocks failure associated with an important gas emission are local concentrations of strains and stresses in the zones of support pressure and desorbed gas accumulation in these zones. The methane desorbed from coal seams and interlayers fills the pockets in the laminated rocks applying an additional pressure to the surrounding massif.

From the standpoint of methane explosion hazards at mines a phenomenon of roof hard rocks hanging up over a large area is of a specific importance. A great amount of methane is accumulated there, and when this gas collector fails the amount of methane released in mine workings cannot be deluted to admissible concentrations.

In the paper the methods of forecasting and preventing the described phenomena are examined.

Sudden gas outbursts /rushes/ from the rocks of the floor can be prevented by degassing the rock massif situated in the floor. The parameters of this method implementation under concrete conditions have been established.

The methods for the roof rocks strength decreasing and the overlying rock massif degassing for carrying out mining operations under conditions of roof hanging over a large area have been suggested.

Today sudden floor heaving with fractures formation and high methane emission into the workings is more often encountered at coal and other mines. This phenomenon is called «sudden failure of the floor rocks» and is understood as instantaneous lift and breaking down of rocks at the bottom of mine workings.

If such a phenomenon takes place in the working at the bottom of which the coal seam occurs, it differs from coal and gas outbursts, because it does not produce finely dispersed broken material and does not throw it off at a great distance. Should gas-bearing coal seams or interlayers, or coal shales occur in the zone of the bottom rock failure high methane emission in the workings will take place resulting in a long-term gas presence in the workings, and in some cases, in oxygen content decrease to dangerously low level, people injuries, mine support and mining equipment damage. As mining operations go deeper methane emission from the massif being overmined into the workings increases at sudden failure of the bottom rocks and the consequences of this failure redouble.

In the world practice there is no a universally recognized method of prediction and prevention of sudden failure of rocks of the bottom and methane inrushes (outbursts) through the overmined massif. The cause of it is that the researchers have no a unique opinion on the nature and the mechanism of these phenomena and there are no scientifically founded and fiable methods for their prediction and prevention.

The up-to-date ideas on this complex phenomenon and the methods of its prediction are presented below.

Most of sudden methane rushes (outbursts) were observed when mining of flat seams at a depth of over 300 m. 80% of such cases were registered in the seams at the bottom of which hard sandstones or aleuroliths were deposited in a layer being over 2.5 m thick, and remaining 20% of cases were registered in the zones of geological faults.

The most wide spread and dangerous phenomenon is the one of bottom heaving with formation of fissures being 10-20 mm wide and more and with the subsequent high methane emission into the workings (50%). In 25% of cases there was no noticeable gas emission, and in other cases only some gas

release was observed , that did not increase gas content in the air of the workings. Methane rushes usually take place at the sites of the face connection with headings and at the face area. Floor heaving was also observed in the headings, lateral horizontal and inclined workings and shafts.

The main cause of this effect is local concentration of stresses in the zones of support pressure. Depending on the geometry of the exposed area of mine working and the methods of mine supporting and rock pressure control the stresses are generated there that exceed the bending, shear and tensile strengths of rocks at the bottom of the working.

The presence of large gas volumes can be attributed to the fact, that at coal seam mining the coal series being overmined is unloaded (relaxed) from pressure over large areas, and the gas released from the adjacent coal seams and enclosing rocks (in case of hard rocks presence at the bottom) is accumulated in this zone in great quantities. The factor that enhances gas accumulation in the relaxed zone is the presence of pillars around the working that prevent from methane penetration into the goafs.

In the unloaded zone the stresses at contacts of weak seams with more hard ones and the pressure of gas contained in the pockets of the coal seams being overmined and enclosing rocks produce rock lamination with cavities formation. Gas from coal seams and enclosing rocks rushes into the cavities formed in the laminated series and in a short time (from several hours to several days) gas pressure in the cavities becomes approximatively equal to natural gas pressure in the seam.

The rocks of the bottom up to the nearest laminated part can be considered as a beam fixed along the contours of its end parts and to which a uniformly distributed load is applied from the side of the cavity, the said load being a function of gas pressure in the cavity and the counter pressure of the weight of the overmined seams situated over the cavity. At a certain distance from the face in the direction of the goaf this plate (beam) supports an additional load of converged roof rocks. The highest tensile strains are generated in the rocks of the bottom along the face in the adjacent workings.The floor of the working fails when tensile strains of rocks exceed their tensile strength. Through the fissures formed in the seam gas from the cavity rushes into the mine workings.

Thus, the methane rushes from the overmined massif into the workings if there is a cavity formed in the laminated section of the overmined rocks and when the rocks occurring over the cavity of lamination fail with formation of fissures connecting the cavity with the working. The rocks of the bottom of mine workings fail if at their bending the tensile strains are generated that are equal in value to their tensile strength parallel to bedding.

Sudden gas rushes can be predicted based on the following initial data: type of working; its geometrical dimensions: for the face - stope length and its distance from the raise entry; for the shafts of circular cross section - excavated diameter; for other workings - excavated length and width; coal seams features evaluated according to volatile matters liberation, sorption capacity and gas pressure; mining depth; distance along the normal from the prognosis point to the plane of shift of the nearest disjunctive fault; depth of the zone of gas weathering; air consumption in the working; methane release into the return current up to the gas dynamic effect.

Before rocks failure begins methane in the cavities of laminated series is present in free state and its pressure is close to natural. Total gas quantity that can get released during gas rushes into the mine workings can be calculated as follows. Based on the analysis of stratigraphic profiles the gas-bearing zones are determined that are bounded with impermeable screen-forming rocks which are often represented by sandstones and aleuroliths. We can assume, that within the determined zones during many centuries of coal formation gas migration from coal seams into enclosing rocks permeable to gas resulted in equalizing of gas pressure in them. Hence, based on known gas sorption capacity of coals the value of pressure is determined at which the sorptional balance is obtained. The same value should characterise free gas pressure, the said gas being present in the coal pockets in gas-bearing enclosing rocks. Then, gas-bearing capacity of enclosing rocks of every lithological facies is calculated as a function of rocks porosity and methane compression ability. Proceed that the dimensions of the overmined rock mass and gas content of all lithological facies of enclosing rocks and coal seams in the zone being overmined are known, it is possible to evaluate methane reserves contained in them, and thus, total gas quantity released at sudden gas inrushes.

At several mines including those of Karagandinsky coal basin in addition to sudden gas and coal outbursts the instantaneous gas rushes from the floor of development workings are observed. These effects are also encountered at mining of thick seams in Kuzbas. Gas rushes from the floor of mine workings are registered during the workings drivage by shearers in the upper layer of thick and outburst hazard seams should the lower part of the seam contain faulted coal series with high gas content. Gas rushes arise without any marked preliminary indications during the shearer operation and are practically instantaneous. They are associated with squeezing out of large masses of coal from the bottom of the working and high gas emission. Because of specific nature of these phenomena they were classified as a separate group called «sudden gas rushes with dynamic fracture of the floor of mine working». They interfere with the development workings drivage and create emergency situations.

These phenomena were observed at Lenin and «Saranskaya» mines. Very often they are registered at Lenin mine when seam d6 mining at a depth over 300 m or development workings drivage in the upper layer of the thick and outburst hazard seam.

Sudden floor heaving is due to the presence of 1-2 m thick faulted gas-bearing coal layer at the bottom of the seam characterized by low strength and high gas emission. The

upper coal layer having a higher strength is 2.4-4.0 m thick. Natural gas content of the seam varies from 14 to 28 m^3/t. Specific feature of the seam is high content of free gas in the rock mass relaxed from rock pressure. The initial rate of gas emission of the lower part of the seam is much higher than that of the upper layer.

The mechanism of floor heaving and gas emission may be represented as follows. In the floor of the working the coal mass gets unloaded under the effect of rock pressure, and this results in increased permeability to gas and gas emission rate of the lower coal layer. Under the effect of variable static and dynamic loading arising from the weight, vibrations and additional loading generated during the shearer operation an intensive fissuring takes place in the coal layer under the shearer and the cavities are formed at the boundary between the rock band and the faulted coal layer. As gas pressure increases the cavities in the laminated part of the seam grow and join between them, and thus the area at which gas pressure is applied to the bottom of the working extends. Gas pressure acting through the rock band at the coal layer situated under the shearer fractures the coal layer along the walls of the working. It fails like a fixed beam at the edges of which bending moments have maximum values. Gas from the lower layer together with coal fines rushes into the fissures formed.

The condition of sudden outburst realization from the development working, found based on comparison of active and passive forces, may be used as that of sudden gas inrush, if we assume that the zones of the face area at the coal seam are consequently the layer of high strength coal under the shearer, the zone of lamination at the boundary between the underlying layer and rock band, and the underlying layer of the seam. At bottom heaving from 0.3 to 1.3 m the active forces exceed the passive ones by 1.1-3.6 times, and at bottom heaving from 1.3 to 3.3 m they are 3.7-6.7 times higher than passive forces.

Gas inrushes arise without any preliminary indications both in the zones of high rock pressure and outside of them. The probability of gas inrushes increases with the depth of mining and extention of the exposed area of the floor of mine working. Along the working the zones susceptible to gas inrushes correspond to the areas of high gas content in the underlying layer. The initial rate of gas emission from the blast-holes can serve as an indirect indication to a degree of risk. So, gas inrush hazard prediction for the lower underlying layer can be performed using a well-known method by measuring the initial rate of gas emission at 1 m intervals in the blast-holes drilled into the lower layer of the seam.

Standard index used ocurrently for prediction of sudden outbursts serves as an indicator of gas inrushes risk in the zone of dynamic fracturing of the bottom of mine working. To obtain critical value of index the initial rate of gas emission from the reference blast-hole at 1 m interval is assumed to be 6 l/min.m. At a lower gas emission value the zone is considered as not gas inrushes hazard, and at a higher value the zone is considered as gangerous.

At face advance of 2.5 m the blast-holes used for gas inrushes prediction are drilled from the face to the bottom of the seam at an angle of 50 degrees to the vertical. The blast-holes being 4.5 m long are situated at a distance of 1.0 m from the walls and 0.5 m from the bottom of the working. At face advance of 3.5 m the blast-holes being 5.5 m long are drilled from the face to the bottom of the seam at an angle of 60 degrees. In both cases the blast-holes should be at least 1 m longer than the face section advanced. The prediction is performed with an interval of 2.5 and 3.5 m for the cycle of advance, respectively.

Owing to prediction of sudden gas inrushes according to critical value of gas emission (6 l/min.m) at Lenin mine more than 1 km of experimental development workings were driven, 7 dangerous zones were revealed and gas drainage wells of 250 mm diameter were drilled along 107 m of the working. During this period there was no sudden inrushes with dynamic fracturing of the floor of the working registered there. Monthly face advance was 80 m.

Sagging of high strength rocks of the roof at large areas, and thus, gas accumulation in the «collector» formed is a factor of risk as to methane explosions. If this gas collector fails the quantity of methane released is so important that it cannot be diluted to acceptable level. These phenomena have been registered at mines in South Kuzbas.

Sudden gas inrushes from the floor can be prevented by one of the following methods, that have been approbated at mines: protective overmining (undermining) of seams; degassing of the massif being overmined and consisting of high-strength rocks and adjacent coal seams and interlayers; changing of wokings position relative to the seam being overmined. The first method is very effective from the standpoint of unloading-degassing, but its use is very restricted because of mining and geological conditions and difficulties in chosing of optimal sequence of coal seams mining in the series.

According to the today's situation in mine fields development at productive mines the most effective and wide spread is the method of degassing of the overmined coal seams, interlayers and enclosing rocks. Figures 1 and 2 show two possible schemes of degasification. On the whole, the choice of a scheme depends upon concrete conditions of seams occurring and mining.

It should be noted, that the preference is given to the method of degassing, because it allows to prevent (or reduce) methane accumulation in the collector formed in the massif being overmined by methane drainage during a long period though at a low flow rate. Actual data show, that methane discharge from a well ranges 0.3-0.6 $m^3/min.$, as a rule, and the duration of this process may be 20-40 days (Fig.1) and 100-120 days (Fig.2).

To operate effectively the wells at a practical realization of this method the following conditions and requirements should be satisfied: the well should be drilled into the unloaded zone, by the time when overmining of the well

4

begins at least two wells should be in operation in the zone of unloading; the distance between the wells is selected by calculation, based on the quantity of methane to drain. In practice this distance varies from 20 to 30 m. At face length over 100-120 m it is reasonable to drill the wells from two drifts.

Methane inrushes from the bottom of development workings driven in the thick seam can also be prevented by degassing of the lower seam layer with unloading-degassing wells that reduce the volume of the methane accumulated at the bottom of the working.

Several methods have been suggested that allow to prevent roof sagging and forcing of high methane quantities out of goafs. These are the methods of roof weakening with caving by blasting and water pumping under a high pressure in the wells. The first of these methods is unsufficiently safe, and the second is unsufficiently effective and not technologically correct. Hence, the most perspective is the use of degassing to decrease methane accumulation in the goafs. At present a method is being developed and its parameters are being established for methane drainage through the wells drilled from the surface and equipped with special ventilators.

CONCLUSIONS

This paper reports on the phenomena that take place in gas-bearing coal seams and are characterized by methane release in great quantities: sudden floor rocks heaving in productive and development workings with large fractures formation; sudden methane rushes from the bottom of development workings at their drivage in thick seams; sudden methane rushes out of goafs into the workings at roof sagging over large areas.

The nature and the mechanism of such phenomena can be explained by manifestation of two factors acting at the same time. These are geomechanical and gas-dynamic processes that accompany many other processes when mining the deposits of mineral resources. It is necessary to predict them with a high degree of certainty, because they may result in people injuries and mine workings failure. The methods of these processes prediction presented in the paper are approximative, and further studies of sudden gas inrushes phenomena are underway at research centers of Russian Federation.

Prevention of the floor rocks failure and methane release in high volumes into mine workings can be performed by localization of dangerous manifestations of geomechanical and gas-dynamic processes, first of all, by decreasing of the stressed state of the massif and by its degassing.

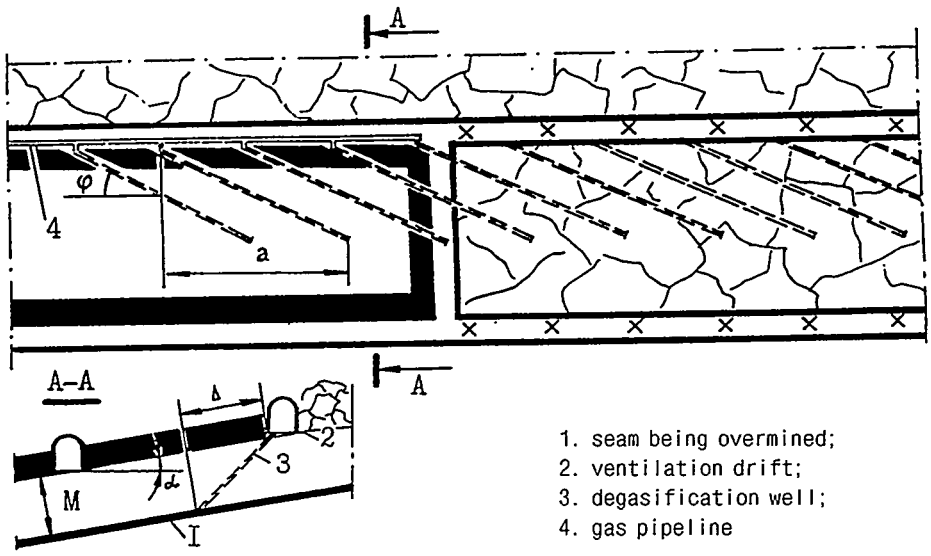


Fig.1. Scheme of degasification of the seam being overmined with the wells drilled from the working to be caved behind the coal face

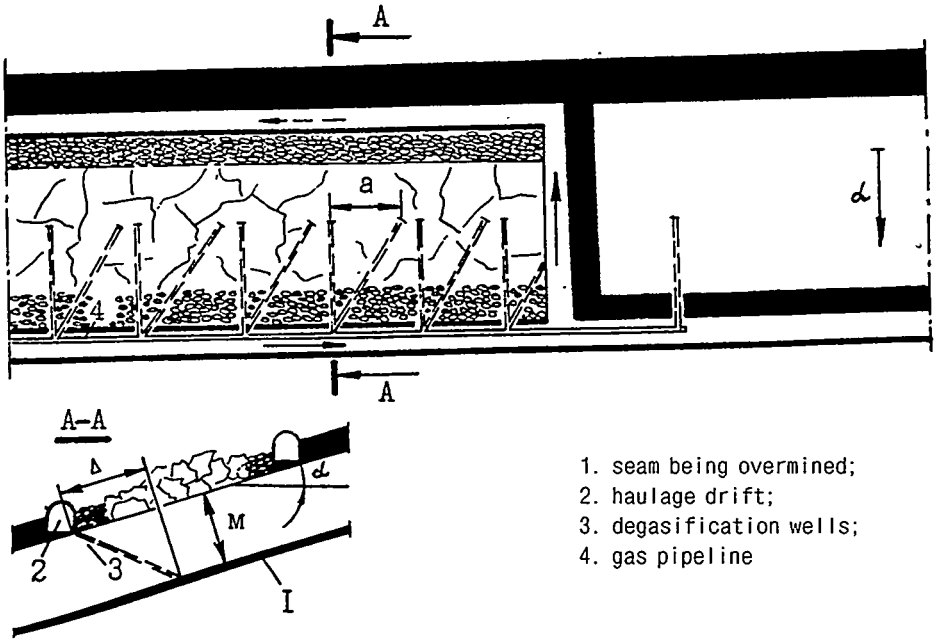


Fig. 2. Scheme of degasification of the seam being overmined with the wells drilled from the working being maintained behind the face



NOTES

INTERGAS '95

May 15-19, 1995
The University of Alabama
Tuscaloosa, Alabama USA

9521

A Brief Overview of the Potential for Development of Coalbed Methane in China

L. Lottman-Craigg, C. Bibler and R.C. Pilcher, Raven Ridge Resources, Incorporated; M. Sun, S. Huang and C. Zhu, Institute of Coal Scientific and Technical Information, Ministry of Coal Industry, People's Republic of China

ABSTRACT

China faces serious challenges in its energy sector. The nation's unprecedented economic growth is creating demand for energy that is outpacing China's ability to produce it. Coal is the dominant fuel, comprising three-quarters of China's fuel mix, and growth in coal consumption is expected to continue. Oil is China's second largest energy source, comprising 19 percent of its energy mix. Demand for oil exceeds production, necessitating imports. Methane emissions from Chinese coal mining account for one-third of the world's total from this source. China liberates an estimated 13-19x10^9 cubic meters of methane annually, about two percent of which is utilized. Recently initiated coal industry reforms will provide incentives for increased recovery and utilization of coalbed methane, as this can increase mine productivity, efficiency, profitability and safety. China is also recognizing the potential environmental benefits of using coalbed methane to offset coal use at mines and surrounding communities, where coal burning creates severe air quality problems. An estimated 30x10^{12} cubic meters of methane are contained in China's coal resources. Increased recovery and utilization of methane would help China's energy economy, as well as benefiting the regional and global environment.

INTRODUCTION

This paper summarizes preliminary findings of a report for the U.S. EPA that is currently in progress. The U.S. EPA is interested in reducing methane missions in China as methane is a potent greenhouse gas affecting the global climate. The report, to be published late in 1995, is a collaborative effort between Chinese and U.S. experts, and will represent the most comprehensive public sector evaluation of China's coalbed methane potential to date.

Half of China's underground mines are classified as high gas or outburst mines. Approximately one-third of the mines that produce more than one million tons per annum are classified as high gas mines. Although greater than 60 percent of the 434x10^6 m^3 of gas recovered from degasification systems is used, this amounts to less than three percent of the total gas liberated during coal mining.

ENERGY PRODUCTION AND CONSUMPTION

China is currently the fastest growing major economy in the world. Energy production and consumption are increasing steadily, with coal providing three quarters of the nation's energy. China produced 1.1x10^9 tons of coal in 1992, more than any other nation in the world [1]. Of the other primary energy sources, oil provides 19 percent, hydroelectricity five percent; and natural gas two percent of the total fuel mix [2]. The industrial sector consumes two-thirds of the available energy, with coal being the dominant source. The domestic sector (primarily residential energy use) is currently the fastest growing consumer of energy, as coal is replacing traditional rural (biomass) fuels for heating and cooking.

The outlook for coal consumption in China is continued growth, approximately three percent per year until 2010. Much of the growth will be in the power generation sector. In order to meet the projected growth in coal consumption, the Chinese government has set a target for annual coal production of 1.4x10^9 tons for the year 2000 [3].

Oil is China's second largest energy source; the nation produced 141x10^6 tons in 1992. According to the Oil & Gas Journal, proven reserves are 2.4x10^9 barrels [4]. China is the fifth largest oil producing country, with one to three percent of the world's reserve base. In the past, China exported some oil; however, demand has increased sharply, and preliminary data indicate that in 1994, China became a net importer of crude oil for the first time since the 1960's.

Of the other major energy sources of China, conventional natural gas is the most underutilized. Although proven reserves are estimated at 850-990x10^9 cubic meters, total resources may be in excess of 1.5x10^{12} cubic meters [4]. Natural gas production averages 15x10^9 cubic meters (530x10^9 cubic feet) annually [5]; this is barely enough to keep pace with demand. The industrial sector is the major consumer of natural gas in China, using it for a variety of purposes including feedstock and fuel for chemical manufacturing and ammonia plants. Production is centered in Sichuan Province in southern China. Recent discoveries in the Tarim Basin of northwest China and Hainan Island show great potential. There are barriers to increased production, however, including inadequate pipeline and gathering systems to transport gas from fields to markets. As shown in Figure 1, there are only two major gas pipelines in China.

COAL: THE DOMINANT FUEL

Organization of China's Coal Industry

Currently, each mine in China is operated under one of three types of management systems: *State-run* (government); *Locally-controlled*; and *Township*. State-run mines are large (producing 500,000 tons to 30 million tons per annum), relatively modern, and highly mechanized, with

many using longwall mining methods. There are currently about 650 state-run mines in China, managed by more than 100 Coal Mining Administrations (CMA's).

Locally-controlled mines produce coal that is used locally, with a portion allocated to the state coal distribution plan. Township mines are collective and privately financed. Through the 1970's, state-run mines accounted for all coal production in China. Since the 1980's, local and township mines have become increasingly important in China, and now over one-half of the nation's coal is produced from these smaller mines [2].

For several years prior to 1993, the coal industry in China was administered by the China National Coal Corporation, a company overseen by the Ministry of Energy. Coal prices were based on artificially low levels, and disparities between in-plan and market coal prices resulted in mines operating at a loss, receiving large government subsidies.

In March, 1993 the Ministry of Coal Industry was established for the purpose of restructuring the coal industry, including liberalization of coal prices. Its main purpose is to develop policies to encourage efficient and cost-effective use of China's coal resources, and to eliminate existing barriers to increased coal utilization.

Coal Resources, Production, and Consumption

Proven coal reserves for China range from 800 to 900 x 10^9 tons; of this, 250-300x10^9 tons are considered economically mineable [6]. About 70 percent of the reserves are bituminous, 16 percent anthracite, and 14 percent lignite. In general, coal seams are thick and laterally continuous. These expansive coal deposits are diverse in age, structure, and rank, and occur in all of China's provinces. Though widely distributed throughout the country, a large percentage of the coal reserves are in the northern, eastern and northeastern regions of China (Figure 1), which are also the most heavily populated, polluted, and energy-intensive.

Principal bituminous and anthracite deposits which developed in the Paleozoic and Mesozoic Eras occur in the northern portion of China. Large deposits of mineable reserves with economically important coal seams occur within Carboniferous, Permian, Jurassic, and Tertiary-age sediments.

Based on similarities in structural and depositional history among coal basins, China is divided into three coal mining provinces: North, Northeast, and South. Of the more than 40 mechanized coal mines producing more than one million tons per annum, most are located in the North and Northeast coal mining provinces.

Over 95 percent coal production is from underground mines throughout China. There are more than two thousand underground mines, producing more than 30 thousand tons of coal annually. from depths of 300 to 500 meters, with some mines over 800 meters deep. In contrast to other major coal producing countries, about two-thirds of China's coal is utilized for direct burning; only one-third of the coal is converted to secondary energy [7]. The dependence on underground coal has serious environmental impacts, both globally and locally, including high levels of SO_2, NO_X, and particulate emissions.

THE POTENTIAL FOR COALBED METHANE DEVELOPMENT IN CHINA

It is estimated that China currently accounts for approximately one-third of worldwide methane emissions from coal mines. The U.S. EPA estimates that 8 to 13 teragrams (12-18x10^9 cubic meters) of methane are liberated from coal mines in China annually [10], and most of this gas is vented to the atmosphere. The total resource, moreover, is vast; China's Ministry of Energy estimated that its coal basins contain up to 30x10^{12} cubic meters of methane [6].

Expanded methane drainage has multiple economic benefits, which include reduced ventilation requirements, quicker, more efficient coal extraction, and the potential for utilizing the produced methane. This largely untapped resource could help China meet its rapidly growing energy needs.

Coalbed Methane Recovery

The Chinese coal industry has extracted gas from its mines for over forty years, using in-mine techniques. Current methods used for drainage are pre-mining degasification from working and adjacent seams, and in-mine gob recovery. There are 110 state-run mines with methane recovery systems. In 1990, about 434x10^6 cubic meters of methane were recovered from China's coal mines, representing just two to three percent of the 13-19x10^9 cubic meters liberated [8].

Recovery efficiencies could increase significantly with updated technologies, including vertical pre-drainage, in-mine drainage using longholes or fracturing, surface gob wells, and advanced equipment. In the near term, basic technical improvements could increase the quality and quantity of gas recovered and utilized. In the longer term, an integrated approach to mine drainage could maximize the recovery of methane and improve mine profitability and safety.

Coalbed Methane Utilization

Of the 434 million cubic meters of methane recovered from China's coal mines in 1990, 270x10^6 cubic meters (approximately 60 percent) were used. While this is a relatively high utilization rate compared to some countries, it represents only a small fraction of the methane that could potentially be utilized if the quantity and quality of recovered methane were increased. In 1990, fewer than one-half of the mines with recovery systems used any of the methane they drained.

Currently, the primary residential consumers of coalbed methane in China are employees of the state-run mines, who use it for cooking in their homes; it is also sold as a commodity to urban residents outside the CMA's. Current principal industrial uses for coalbed methane are small carbon black plants run by the CMA's, and a small gas turbine generator at Fushun.

The most attractive options for increasing methane utilization from mines varies regionally, depending on the quality and quantity of the gas and local energy markets. In general, China's coal producing regions are well-suited to on-site gas use, due to the close proximity of industrial and residential users to the mines. Increased methane recovery could displace coal use in the growing residential sector. Incentives to implement a more economic methane recovery system include policies to substitute methane for coal; expanded gas storage facilities; expanded pipeline infrastructure; use of methane for electricity generation; and additional gas turbines.

Coalbed methane could be used for many purposes, including:

- drying coal in preparations plants;
- heating or refrigeration of mine ventilation air;
- generating electricity and steam for use in mine facilities and nearby communities; and
- as a vehicle fuel, to meet China's rapid growth in motorized vehicle use.

There are several ways in which coalbed methane can be used to displace the use of coal for power generation. These include:

- converting boilers to intermittent use of gas;
- gas turbines;
- internal combustion engines; and
- cofiring with natural gas.

Policies to Encourage Coalbed Methane Development in China

Numerous barriers currently prevent China from achieving its full potential for reducing methane emissions from coal mining. These include the lack of an appropriate policy framework, limited capital for project investments and equipment, and the need for additional information and experience with technologies. Artificially low gas prices set by the government and the difficulty with repatriation of profits create barriers for development of foreign investment in joint ventures to produce domestic energy resources.

Positive changes have occurred recently which should help expand coalbed methane recovery in China. Foremost of these is the development and implementation of a conversion factor policy, under which coalbed methane recovered during coal mining is counted toward a coal mine's production quota. It should be noted that most existing international policies, such as the Unconventional Fuels Tax Credit and resolution of gas ownership issues in the U.S., focus on incentives for recovery of coalbed methane from vertical wells in unmined areas. In China, the optimal method to reduce methane emissions and gain an additional source of natural gas is through government policies which provide incentives for utilization of coalbed methane. Once potential gas markets are identified in key mining areas, the best utilization options can be selected for specific mines.

CONCLUSIONS

Many regions in China are facing serious coal shortages, and need additional local sources of energy. Coal is also a major source of local air pollution, and China is thus interested in developing clean-burning natural gas resources. Conventional natural gas fields are distant from potential markets, however, the nation currently lacks adequate infrastructure to transport and distribute this gas. Coalbed methane, on the other hand, is distributed throughout China's industrial areas, and relatively little investment in infrastructure would be required to distribute it to consumers.

Currently, only about two percent of all methane liberated from coal mining activities in China is utilized. Given the size of the resource and number of large, active underground coal mines, tremendous opportunities exist to increase the quality and quantity of methane recovered in China. Recent reforms in China's energy policy reflect a strong interest in expanding methane utilization, both regionally and locally.

Based on China's unique energy needs, air quality issues, and lack of pipeline infrastructure, the most likely opportunities for coalbed methane utilization are centered around the increased substitution of methane for coal, particularly in industries and residences near large coal mines, or as a vehicle fuel.

REFERENCES

1. China Coal Industry Yearbook 1993, China Coal Industry Publishing House, 132 p.

2. Sinton, J.E. (Ed), 1992, China Energy Databook, Lawrence Berkeley Laboratories, LBL 32822/UC350.

3. UNDP (United Nations Development Program), 1992, Project of the Government of the Peoples Republic of China: Development of Coalbed Methane Resources in China, Project #CPR/92/G32/A/1G.

4. Oil & Gas Journal, "Worldwide Production Falls as Market Plays Its Wild Cards", p. 37-54

5. DOE/EIA, 1994, International Energy Annual 1992, DOE-EIA 0219, Washington, DC, 196 p.

6. MOE, 1991, Coalbed Methane Recovery in China: An Information Report for the Consultants of UNDP, 11/91, 5 p.

7. JP International, 1990, Opportunities for Coalbed Methane Recovery and Utilization in China, Prepared for USEPA, 52 p.

8. USEPA, 1993, Options for Reducing Methane Emissions Internationally, Volume II (International Opportunities for Reducing Methane Emissions: Report to Congress), Chapter 4, p. 4-1 to 4-12.

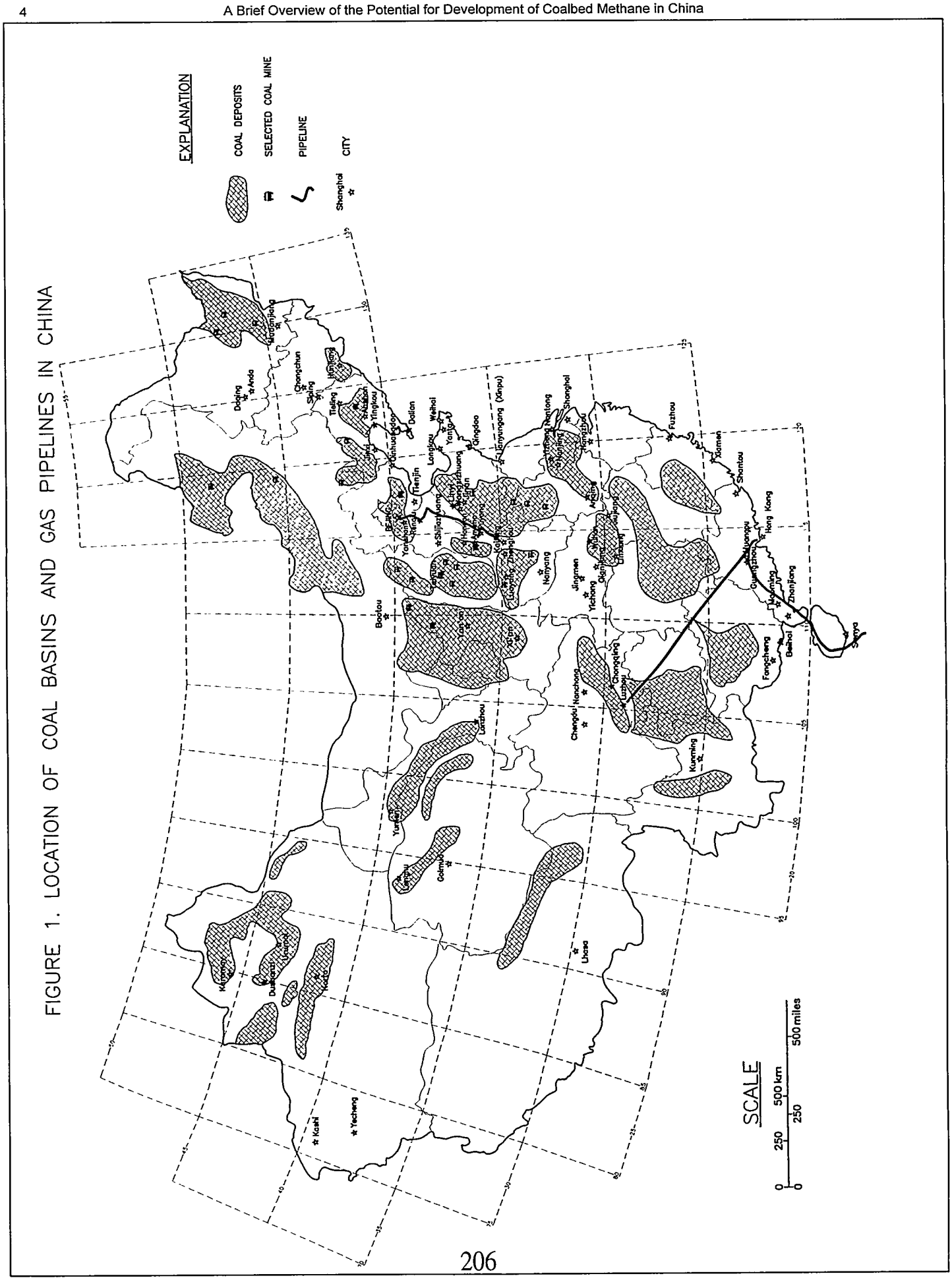


FIGURE 1. LOCATION OF COAL BASINS AND GAS PIPELINES IN CHINA

INTERGAS '95

May 15-19, 1995
The University of Alabama
Tuscaloosa, Alabama USA

9544

Methods and Experience in Intensive Coalbed Methane Recovery at Coal Mines in the CIS

V.S. Zabourdyaev, Skochinsky Institute of Mining, Russia

ABSTRACT

Mining practice in the CIS shows that the requirement to extract coal at progressively greater depths creates the situation where very high levels of methane emission are generated in the underground workings estimated to be as high as 200-250 m³/min at some more gassy mines. These volumes of methane emitted underground represent, first, a serious danger because of not rare damages of mine ventilation systems, and second, this methane is lost from energy standpoint and harmful for the environment as almost all of it is vented to the atmosphere. A rather bad situation as to the recovered methane utilisation exists in Kouznetsky coal basin, where none of 33 mines equipped with degasification systems utilizes methane-air mixtures drained.

Factors have been studied that affect the dilution of coalbed methane emissions with mine air. Conditions and parameters for methane-air mixture recovery through surface and underground wells in advance to mining and during mining have been analysed. The methods of intensive methane recovery from working seams with crossing wells have been studied and introduced at mines in Donetsk and Karaganda basins. A method suggested is 1.5-2.5 times more effficient than the traditional one at equal volumes of drilling.

The paper reviews the cases and results of application of conventional and new methods of degasification of working seams and those adjacent to them under conditions of different mines in the CIS. The regularities existing in the processes of methane recovery have been revealed, and based on them the recommendations on the methods to be used, selection of regimes and parameters of the intensive coal seams degasification have been formulated.

INTRODUCTION

Our experience of many years in exploitation of gassy coal deposits in the Commonwealth of Independent States (the CIS), particularly, in Russia, Ukraine and Kazakhstan, shows that the emission of methane during underground coal mining increases with mining depth and makes up to 200-250 m³/min at the most gassy mines.

A drop in productivity of coal mines registered in the recent years resulted in a certain decrease in methane emission into the mine workings, but it still remains high at gassy mines. Thus, in 1992-1993 methane emission per one gassy mine in Kouznetsky, Donetsky, Pechorsky (Vorkouta deposit) and Karagandinsky coal basins averaged 45-120, 45-140, 85-220 and 40-215 m³/min, respectively. These amounts of methane liberated in mines are, first, associated with the hazards because of not rare damages of mine ventilation systems, and second, this methane is lost from energy production standpoint and harmful for the environment.

Table 1 shows the data on annual average methane emission in mines, the amounts of CH_4 utilized and vented to the atmosphere in 1992-1993. According to these data almost all mine methane in the CIS countries is emitted to the atmosphere.

The main causes of this are:

1. lack of a reliable equipment manufactured in the country being able to utilize the methane-air mixtures drained from mines at different flow rate and having various methane content;
2. non time-constant flow rate of methane, and
3. parameters and operating conditions of degasification wells that do not always allow to recover gas mixtures with a sufficient gas content.

First of all it is the case of all mines at which degasification of goafs was implemented.

A rather bad situation as to the recovered methane utilization exists in Kouznetsky coal basin where none of 33 mines equipped with degasification systems utilizes methane-air mixtures captured using vacuum pumps or purpose designed ventilator VMTsG-7, though there are there rather gassy and perspective for methane recovery mines, for example, the ones of «Kouznetskugol», «Leninskugol» and «Belovougol».

METHODS

To get at the root of causes that unfavourably affect the recovery of methane of standard grade the conditions, regimes and parameters of methane-air mixtures recovery with different degasification methods at Kouzbass, Donbass, Vorkouta and Kazakhstan mines have been analyzed. The parameters of degasification of working and adjacent coal seams and of goafs have been studied based on published, archive and actual data for mines. The factors

have been examined that affect methane emission from coal seams in mine workings and degasification wells, as well as conditions and causes of methane flows dilution with mine air. The processes of methane recovery from coal seams through surface and underground wells in advance to mining have been investigated, and a method of optimisation of degasification parameters has been developed.

Special attention has been paid to investigation of coal seams permeability to gas and gas emission into mine workings and degasification wells /1-5/. The studies performed were essentially as follows.

To describe the process of gas emission q_s from the exposed surface of the seam the following equation was adopted:

$$q_s = \frac{K}{\mu} \frac{P_\infty^2 - P_o^2}{\sqrt{K_o^*}\, 2\sqrt{\pi}\, \sqrt{t}\, P_o}, \qquad (1)$$

where

$$K_o^* = \frac{K}{\mu \Pi^*} 0.8 P_\infty ; \quad \Pi^* = \Pi + \frac{\gamma a \beta P_o}{(1+\beta P^*)^2};$$

$$P^* = 0.66 P_\infty$$

K - coefficient of permeability to gas, m^2;
μ - methane viscosity, kg/(s.m);
P_∞ - gas pressure in vergin massif, Pa;
P_o - atmospheric pressure, Pa;
Π - seam porosity in fractions of unit;
γ - volume weight of coal, t/m^3;
a - maximum methane sorption capacity of coal, m^3/t;
β - sorption constant of isothermic line, 1/Pa;
t - time, s.

To determine the coal seam permeability to gas a gas-air survey in blind development workings has been performed. At working advance rate v in the seam the thickness of which does not exceed the hight of the working gas emission from the seam into the working having the length ℓ per 1 m of the seam thickness is found from the formula:

$$G_s = 2\int_o^\ell \frac{A}{\sqrt{\ell / v}} d\ell = 4A\sqrt{v}\ \sqrt{\ell} \qquad (2)$$

where ℓ length of the working at the moment of gas emission;

$$A = \frac{K}{\mu} \frac{P_\infty^2 - P_o^2}{\sqrt{K_o^*}\, 2\sqrt{\pi}\, P_o}$$

As $\ell = vt$, where t is the time from the moment of the working drivage,

$$G_s = 4Av\sqrt{t} \qquad (3)$$

or at $A = \frac{B}{4}$

$$G_s = BV\sqrt{t} \qquad (4)$$

where $B = 2\sqrt{\frac{K}{\mu}} \frac{P_\infty^2 - P_o^2}{\sqrt{P^*}\, P_o\, \sqrt{\pi}} \qquad (5)$

The prmeability of coal seam to gas K can be found provided the values of Π, a, β, γ and P_∞ are known and the value of B is determined from the formula (5).

Specific methane flow rate q_w, m^3/m a day from the wells drilled across the strike of the coal seam was found from the following formula:

$$q_w = \frac{\pi}{\ln(1+\sqrt{\pi\tau}/1.1)} \frac{K}{\mu} \frac{P_\infty^2 - P_o^2}{P_o^2} \qquad (6)$$

where $\tau = \frac{K}{\mu}\sqrt{P_\infty^2 - P_o^2} \cdot \frac{\Pi^*}{r_o^2} t$, and r_o - diameter of the well, m.

To describe the process of gas emission q, m^3/(m^2 day), into the degasification wells drilled in the plane of unloaded seam a relation found experimentally was used:

$$q = \frac{q_o}{a^* t + 1} \qquad (7)$$

where q_o - intensity of initial gas emission from the seam into the well, m^3/(m^2.day), at the beginning of plane-parallel gas flowing in the direction of the well; a^* - rate of gas emission decrease with time, t, day^{-1}.

Gas emission indices q and a^* are interrelated as follows:

$$a^* = K_p q_o$$

where K_p is a characteristic of coal seam permeability to gas found based on experimental data using the following equation:

$$\frac{1}{q} = K_p t + b_o \qquad (8)$$

The methods of K_p value evaluation are described in papers /1, 3, 5/. It has been established that gas emission into the wells from the moment when plane-parallel gas flow starts is similar to gas emission into the workings at practically equal values of K_p. This allows to accelerate determining gas emission indices of the coal seams to be used in the projects of degasification of working seams with wells.

The processes of methane emission into the wells drilled from the underground workings and from the surface to adjacent seams have been studied according to known methods /6-8/.

RESULTS

Initial data used to determine the permeability to gas of coal seams in Leninsk and Belovo regions of Kouzbass were: P_∞ = 1.7 MPa, a = 15.3 m^3/t, β = 0.25 (kgp/cm^2)$^{-1}$, γ = 1.35 t/m^3, Π = 0.05. The results of determination of gas permeability of 6 coal seams are summarized in Table 2, from which it can be seen, that the coefficient of permeability to gas varies from 0.005 to 0.045 mD.

At known gas permeability coefficient equation (6) was transformed into equation (9), which describes with a sufficient accuracy the time - related evolution of gas emission q'_w from the wells drilled across the strike of the coal seam:

$$q'_w = \frac{C}{\ln\left[1 + \frac{D}{r_o}\sqrt{t}\right]} \qquad (9)$$

where C and D are coefficients, for which the values are given in Table 2; t - time, days.

Relation $q'_w(t)$ was used to calculate gas emission from coal seams in Kouzbass. Table 2 gives average dayly methane flow rates which can be expected when degassing of unloaded coal massif using the wells drilled from the surface.

The results of studies show, that under conditions of mines in Leninsk and Belovo regions of Kouzbass degasification of unrelaxed seams with the wells drilled across the strike is not rational because of rather low methane flow rates and high cost of vertical wells.

METHANE RECOVERY FROM WORKING COAL SEAMS

From technical and economical standpoint the most effective methods of working coal seams degasification are the ones with long wells drilled from the in-seam workings. But at deep mines (more than 600 m from the surface) traditionally used degasification schemes with wells parallel to the face allow to recover only 0.5 - 1.5 m^3 of methane per 1 t of degassed coal reserves for 180-360 days, that is unsufficient for deep degasification of coal massif. That's why in the recent years investigations were carried out in order to develop and justify new methods of working coal seams degasification allowing for more intensive gas recovery from the seam.

There were two directions in the study performed: a) determining the effect produced on the coal massif by water being pumped into the seam in a pulse mode through the underground wells /5, 9-11/, and 2) development of a rational pattern of in-seam wells /4, 12, 13/.

For the first direction of the study the folllowing has been established.

To obtain a required degree of gas content decrease calculated for every specific case based on the productivity of the face planned according to gas factor or conditions of instantaneous coal and gas outburst prevention, the measures are to be taken to stimulate gas emission from the seam into the wells. The value of the coefficient of gas emission intensification is determined from the relation of the required degree of coal seam degasification to that actual (forecasted).

The coefficients of gas emission from coal seams with different filtration characteristics, as well as the required degree of seam degasification,obtainable owing to the wells drilled parallel to the face, and the coefficient of gas emission intensification allowing to obtain the required degree of seam degasification have been determined for conditions of Karaganda and Donetsk basins. The results of these investigations are given in Table 3, from which it can be seen, that only in one case (seam m_3) degasification to non-hazard gas content could be obtained without enhancing gas emission from the coal massif (specific gas emission G_k = 80.3 m^3/m^2).

For safe mining of gas-bearing coal deposits a 1.5 - 3 times increase in gas emission of the coal massif is required, and in the seams liable to sudden outbursts gas emission rate should be increased up to 5.5 times.

Conditions and parameters of degasification of the seam using the wells drilled parallel to the face as a function of coal seams permeability to gas are given in Table 4. The given scheme can be used in the seams with permeability to gas of 10^{-3} mD or more. Degassing of coal seams with permeability to gas of 10^{-3} - 10^{-4} mD or less without artificial enhancement of gas emission is not reasonable.

Pulse methods of coal seams treatment are promissing for enhancement of methane recovery efficiency. They allow to treat the coal seam in a more uniform way and for shorter periods to increase its permeability. The energy of hydraulic pulse action at the coal massif depends on the amplitude of pressure and the time for which it is applied. At compressive strength of coal ranging from 3 to 7 MPa, the radius of fracturing being of 10 m and the radius of the well being of 0.05 m minimum stresses along the contour of the well should be of 43-100 MPa. Such values of pressure of liquid in the well can be obtained owing to explosive-hydraulic-pulse and explosive methods of treatment of the massif.

When mining at depths of 1000-1200 m to break down coal seams by pulse action applied through the long wells the shock wave pressure of 100 MPa and more should be generated. In the period of quasi-static water infusion it should be at least 40 MPa. In this case the time of explosive-pulse action of liquid at the coal massif is 1.5 - 2.0 s., and the flow rate of liquid is at least 0.1 m^3/s.

Based on the results of investigations according to the second approach to intensification of gas emission from coal massif into degasification wells the following conclusions have been made.

Positive results of coal seam degasification with the wells drilled in the direction of the face are due to the wells location in the zone of technogenous fracturing, where the coal seam permeability to gas is several times higher than that outside the zone being under the influence of the working face. The suggested scheme of degasification is on the average 1.8 times more effective than the standard one owing to a higher productivity of wells in the zone of technogenous fracturing in front of the face at a distance of 30 m. In the seam having a sufficient natural permeability to gas these schemes are practically equivalent at equal volumes of drilling.

The methods of coal seams degasification with crossing wells (Fig. 1.) are developed taking into account the coal massif unloading (relaxing) close to the wells at the points of the wells crossing, where two systems of vertical crossing fissures are formed. The fractures formed assure the aerodynamic connection between the wells drilled at a certain angle relative to each other. Specific quantity of methane captured from the seam (the volume of methane recovered is related to 1 m of the well length and 1 t of coal reserves being degassed) with crossing wells is 2.1 times higher in thick and medium-thickness seams (Karagandinsky basin) and 1.5 times higher in medium-thickness seams (Donetsky basin) as compared to degasification with the wells parallel to the face. In the seams susceptible to outbursts and containing less hard coals gas recovery is increased by 2.2 times, and in the seams containing hard coals it is only increased by 1.2 times .

The schemes of degasification of working seams with crossing wells are very promissing, that was confirmed by actual data /4, 12/. Thus, at a distance of 8-10 m between the heads of crossing wells some 4.4 - 5.3 m^3 of methane per 1 t of coal was recovered in the outburst hazard seams for 150-180 days ("Komissarovskaya" mine, Donbass, and «Sokourskaya» mine, Kazakhstan; mining depth was 370

and 520 m, respectively).

The efficiency of degasification evaluated according to decrease in gas emission from the seam into the face was 35% after 180 days in the zone ,where crossing wells were drilled at 10 m interval («Komissarovskaya» mine) and 45% after 150 days in the zone where the wells were drilled at an interval of 8 m («Sokourskaya» mine). Gas content of the district was decreased, peak concentrations of methane were smoothen during mining set operation that produced favourable conditions according to gas emission factor for extraction of 965 and 1480 t/day of coal in the faces of the above-mentioned mines. After introduction of degasification of working seams with crossing wells the productivity of face at 7 mining districts increased by 18% on the average.

Experience in degasification of working coal seams of Karaganda and Donetsk basins using crossing wells was taken into account when implementing the new method in Kouzbass. The indices of gas emission in several seams of Leninsky, Belovsky and Tom-Ousinsky coal bearing regions found experimentally as well as the values calculated prove that degasification of working seams in Kouzbass with crossing wells is rather promissing (Table 5).

RECOVERY OF METHANE FROM ADJACENT SEAMS

Most investigations aimed at evaluation of the efficiency of adjacent seams degasification and methane-air mixtures drainage through the wells drilled from the surface have been performed at mines of Leninsky and Belovsky regions of Kouzbass based on the data published /14/ and collected during the recent 10-15 years. The data on « Baydayevskaya» mine (A/O «Kouznetskugol») and several mines of Karagandinsky basin were also used /8/.

The practice of mines degasification through the wells drilled from the surface has shown the following.

There is a direct relation between the coefficient $K_{d.v}$ and the value of relation of total thickness of adjacent seams being degassed $\Sigma m_{a.s}$ to working thickness of the seam m_w. For «Kirov», »Komsomolets» and «Oktyabrskaya» mines («Leninskugol»), where pillar-and-room mining system with roof caving and return current ventilation scheme is used (Fig. 2) this dependence can be described by the following equation:

$$K_{d.v} = \alpha\left(\sum_{i=1}^{n} m_{a.s} / m_w\right) + \beta \quad \text{unit fractions} \quad (10)$$

where α and β are empirical coefficients.

Provided that there are partly degassed coal seams occuring in the roof of the working seam, for example, in case they have been overcut when mining the overlying seam, it is necessary to take into account their degree of natural degasification replacing in formula (10) the value of $\sum_{i=1}^{n} [m_{a.s.i}(1 - K_{n.i})]$ for $\sum_{i=1}^{n} m_{a.s}$ where $K_{n.i}$ - degree of natural degasification of the i-th adjacent seam. The same substitution should also be made if the overcut seams being degassed by other methods, but in this case coefficient $K_{n.i}$ is substituted by the coefficient of induced degasification of the i-th methane source $K_{d.i}$.

The truthworthiness of equation (10) with coefficients $\alpha = 0.15$ and $\beta = 0.15$ under different conditions has been evaluated for mines of Karaganda and Kouzbass basins (Table 6).

The analysis of actual data shows, that though degasification of adjacent seams and goafs with the wells drilled from the surface is very efficient, methane content in the gas mixture recovered is not high with rare exeption. First of all it is due to the fact that degasification wells were drilled into the goaf being actively ventilated (Fig. 3,a).

It has been established, that there is a regularity in methane content increase in the mixture captured in the wells at methane discharge rise. The lower is the number of wells operated at the same time, the higher is methane concentration in the mixture (Fig. 3,c). Air-methane mixture of acceptable quality (more than 30% of methane) was recovered if methane discharge from the wells was higher than 7 m³/min. This level of methane emission is observed, as a rule, when the well being operated is situated in the zone of active unloading relaxing) of adjacent seams, i.e. in the zone of higher gas emission. The variation of methane concentration C_M in the mixture captured in vertical wells as a function methane discharge J_M, m³/min, is described by the equation:

$$C_M = K_N J_M \quad (11)$$

where K_N proportionality factor, that depends on the number of vertical wells operated at the same time at the mining district.

Fig. 3,d shows the variation of K_N coefficient found based on actual data for Kouzbass conditions. The value of this coefficient can be calculated using the following formula:

$$K_N = \frac{1}{0.11N + 0.1} \quad (12)$$

where N is the number of vertical wells being operated at the same time at the mining district.

Operation of vertical wells drilled from the surface depends to a great extent on vacuum pumps used, depth of the wells and their inside diameter, construction of casing string and condition of the site being degassed (Fig.4).

The scheme of degasification of adjacent seams shown in Fig. 3,b, allows to recover methane of acceptable quality. According to experimental data methane content in the air-methane mixture captured at mine «Oktyabrskaya» was 35-60%. This scheme permits to decrease the costs of degasification and to create favourable conditions for utilization of the methane recovered.

Wide use of direct current ventilation schemes with the return current dilution with fresh air and gas suction through vertical wells of large diameter situated at the boundary of mining districts resulted in intensive ventilation of goafs at mining districts because of the artificially induced (by gas exhaust ventilators VMTsG-7) air leakages. Owing to this the probability of methane accumulation near the face was considerably decreased, and at the same time methane content in the air-gas mixture captured dropped. Methane concentration in the wells drilled according to the scheme shown in Fig. 3,a, with rare exception, did not exceed 10-15%.

The results of degasification of adjacent seams and goafs at 11 active mining districts performed using vertical wells, side wells located over the rising entry and gas suction out of goafs using VMTsG-7 ventilators are as follows:

- the efficiency of vertical wells at return current ventilation scheme (mines «Chertinskaya», «Komsomolets» and «Oktyabrskaya») is of 67% on the average, and at direct current ventilation (mine «Baydayevskaya») it is of 62%;
- the efficiency of side wells drilled over the rise entry (mines «Chertinskaya» and «Abashevskaya») is of 48%;
- vertical wells operating in the zone of influence of side wells have a considerably higher efficiency as to methane recovery compared to side wells (mine «Chertinskaya»);
- in case of simultaneous use of vertical wells and VMTsG-7 at the mining district (mine «Chertinskaya») the efficiency of degasification with vertical wells is 2.5 times higher than that with gas suction means.

ECONOMICAL CONSIDERATIONS

The algorithm for calculation of a relationship between the costs of degasification and the coefficient of degasification has been developed taking into account the statements cited in paper /15/, regularities of methane-air discharge from degasification wells, efficiency of different methods and schemes of degasification for various sources of methane emission, and recommendations on determining the parameters and the number of degasification wells to be operated /16/.

Specific costs of degasification, Z_v, roub./t, of adjacent seams and goafs with the wells drilled from the surface can be found from the formula:

$$Z_v = 0.0061 \frac{K_{d.v}\ P_v}{(1 - K_{d.v})\ L_f} \sqrt{\frac{H^3}{m_s^3\ B_v}} \qquad (13)$$

Specific costs of degasification of adjacent seams and goafs with underground wells, including the costs of the gas line laying, Z_u, roub./t, can be found from the formula:

$$Z_u = \frac{0.19\ K_{d.u}\ P_u\ \ell^{3/2}}{N_c\ R_c\ L_f\ m_s\ (1 - K_{d.u})\sqrt{d^{3.1}\ B_u}} \qquad (14)$$

Specific costs of degasification of working seams with wells, Z_s, roub/t, can be determined using the formula:

$$Z_s = \frac{1.3\ K_{d.s}\ P_s\ q_s}{K_B\ G_h} \qquad (15)$$

In formula (13) - (15) the following symbols are used: $K_{d.v}$, $K_{d.u}$ - coefficient of degasification of adjacent seams and goafs with the wells drilled from the surface and underground wells, respectively, unit fractions; $K_{d.s}$ - coefficient of degasification of working seam, unit fractions; P_v, P_u, P_s - costs of drilling and equipment of 1 m of vertical, underground or in-seam well, respectively, roub./m; L_f - face length, m; H - depth of the seam occuring (length of vertical well), m; m_s - seam thickness, m; B_v, B_u - vacuum at vertical and underground wells heads, respectively, mm of mercury column; ℓ - length of underground wells, m; N_c - number of degasification chambers operated simultaneously, pieces; R_c - distance between degasification chambers, m; d - diameter of underground wells, m; q_s - gas emission from working seam, m³/t; K_B - coefficient of influence of vacuum on methane discharge from working seam into the wells; G_h - quantity of methane recovered per 1 m of well and 1 m of seam thickness, m³/m².

Specific costs of degasification by different methods or schemes are calculated using numerical minimization of costs function. As a result of these calculations a relationship $Z(K_{deg})$ is established. To calculate it at a preset K_{deg} value a series of degasification coefficients for different methane emission sources has to be considered.

The method of degasification parameters optimisation has been implemented under conditions of «Abayskaya» mine (Production Association «Karagandaugol»). In Table 7 are given the results of calculation of optimal indices of degasification of the mining district in the seam K_{11}, and in Fig. 5 is shown the variation of profit P (prices of 1989) as a function of the efficiency of degasification.

CONCLUSIONS

At coefficient of permeability to gas of coal seams in Kouzbass being equal to 0.005 - 0.045 mD methane emission in the wells drilled from the surface is 3-24 m³/ /day, so, it is evident, that this scheme of degasification of unloaded coal massif is not rational. High cost of drilling and equipment of vertical wells at a very low level of methane discharge and low coal-bearing capacity of the deposit does not allow for industrial use of surface method of degasification.

Underground methods of degasification of unloaded (being under rock pressure) coal seams are more effective as compared to surface ones. Up to 1.5 m³ of methane per 1 t of coal reserves being degassed is captured using the wells drilled in the plane of working seam parallel to the face, and up to 5-5.3 m³/t of methane is recovered when crossing wells are used.

Further increase in volumes of methane recovered from unloaded seams is possible through an artificial enhancement of the coal massif permeability to gas and its methane discharge into degasification wells. To achieve this, the methods of hydrodynamic action at coal massif of working fluid pumped in it in a pulse mode are very promissing. They produce an artificial fracturing of coal seam.

Methane recovery from the coal seams undercut when mining is rather productive both in case of degasification with underground wells and with the ones drilled from the surface.

Based on the regularities established for undermined seams degasification with vertical wells a nomograph has been developed to determine the efficiency and conditions of degasification assuring a recovery of air-methane mixtures of acceptable quality as to methane content that can be effectively utilized.

The method of optimization of parameters of mines degasification allows to determine a rational (from economical standpoint) efficiency of degasification under concrete conditions of coal seams mining. It also permits to make prompt and economically justified decisions

concerning the variation of the efficiency and parameters of degasification of different methane emission sources at mining districts.

REFERENCES

1. Lidin G.D., Sergeev I.V., and Zabourdyaev V.S., 1971: «Calculation of parameters of working coal seams degasification with wells»; Labour Safety in Industry, Moscow,» Nedra», №3, p. 33-36.
2. Sergeev I.V., Boukhny D.I., and Fitterman A.E., 1988: *Theoretical and experimental methods of investigation of gas condition of coal massif:* Moscow, «Nauka» Publishers, 110 p.
3. Zabourdyaev V.S., 1975: « Degasification of coal seam with development workings and wells», Scientific Reports. Skochinsky Institute of Mining, №126, p. 179-184.
4. Zabourdyaev V.S., 1990: *New methods of degasification and gas emission control at coal mines*: Moscow, TsNIEIugol, 65 p.
5. Zabourdyaev V.S., Sergeev I.V., Vilchitskky A.V. et al, 1988: *Degasification of coal seams using the methods of gas emission stimulation:* Moscow, TsNIEIugol, issue 1, 50 p.
6. Zabourdyaev V.S., 1979: « Mines degasification at different mining methods», Ugol, №9, p. 38-40.
7. Sergeev I.V., Zabourdyaev V.S., Ayrouni A.T. et al., 1992: *Gas emission control at coal mines when stoping:* Moscow, «Nedra», 256 p.
8. Zabourdyaev V.S., 1994: «Methods of high quality methane recovery at coal mines», Labour Safety in Industry, №3, p.12-16.
9. Zabourdyaev V.S., 1983: «Selection of technological schemes of Hydrolic impulse action at coal seam during its degasification», Problems of aerology at coal mines: Scientific Reports, Skochinsky Institute of Mining, №222, p. 48-53.
10. Zabourdyaev V.S., Vilchitsky A.V., Roudakov B.E., 1985: « Enhancement of degasification of coal seams at deep levels», Labour Safety in Industry, №9, p. 48-53.
11. Zabourdyaev V.S., Roudakov B.E., Boukhny D.I. et al., 1989: «Investigation of parameters of explosive-pulse treatment of the seam for the purpose of its degasification»; Sudden coal ans gas outbursts, mine aerology: Scientific Reports. Skochinsky Institute of Mining, p. 148-157.
12. Sergeev I.V., Zabourdyaev V.S., Boukhny D.I. et al., 1989: *Practice of intensive degasification of mining districts,* Moscow, TsNIEIugol, 36 p.
13. Zabourdyaev V.S., 1992:» Degasification of gassy and liable to sudden outbursts coal seams with wells»; Labour Safety in Industry, №3, p.27-30.
14. Gaybovitch F.M., Dianov G.M., Doubov G.P. et al., 1988: *Degasification at mines of Leninsky and Belovsky regions of Kouzbass:* Moscow, issue 9, 40p.
15. Zabourdyaev V.S., Boukhny D.I., Roudakov B.E., 1991: «Method of optimisation of mines degasification parameters»; News of Skochinsky Institute of Mining, issue 1, p. 98-102.
16. *Instructions on degasification of coal mines,* 1990, Moscow, 186 p.

Table 1. Methane emission at coal mines in the CIS

Country	Number of mines		Methane emission, Bt m³/year				Methane utilization, Bt m³/y
	total	with degasification	total	in mine workings	in degasif. system	into atmosphere	
Russia	177	57	2.21	1.73	0.48	2.16	0.05
Ukraine	244	100	3.39	2.90	0.49	3.22	0.17
Kazakhstan	26	21	1.11	0.93	0.18	1.10	0.01
Total	477	178	6.71	5.56	1.15	6.48	0.23

Table 2. Gas emission into the wells drilled across the strike of unloaded coal seam

Seam	Seam thickness, m	B value, $m^3/(m.day)$	Coeffic. of permeability to gas, mD	Coefficients from equation (9)		Average gas emission (m^3/day) into the wells with a dia of (m):	
				C	D	0.1	0.2
Polysayevsky-2	3.2	9.0	0.036	22.7	0.72	17.0	20.2
Polysayevsky-1	2.6	9.2	0.038	24.4	0.74	14.6	17.4
Nadbaykaimsky	3.7	9.2	0.037	23.4	0.73	20.1	24.0
Breevsky	2.9	9.0	0.005	3.1	0.26	2.7	3.4
Tolmachevsky	2.3	9.5	0.013	6.1	0.43	4.9	6.0
Seam 4	1.5	10.0	0.045	28.5	0.92	9.1	10.8

Table 3. Results of study of coal seams degasification degree

Coal basin	Seam	Gas content of the seam, m^3/t	Seam thickness, m	Gas emission indices		Degasification degree, unit fractions	Required degree of degasification, unit fractions	Coefficient of gas emission intensification
				initial gas emission $m^3/(m^2.day)$	rate of decrease of gas emission, day^{-1}			
Karagandinsky	K_{12}	15	4.5	0.77	0.012	0.35	0.5	1.45
" - "	K_{13}	16.5	1.8	0.52	0.012	0.2	0.35	1.76
Donetsky	m_3	13.5	1.4	0.78	0.01	0.4	0.4	1
" - "	m_3	15	1.7	0.5	0.01	0.25	0.4	1.6
	K_3	18	0.8	0.55	0.014	0.2	0.55	2.75
	K_3*	18	0.4-1.7	1.1	0.16	0.1	0.55	5.5

*In the zone of seam plication.

Table 4. Conditions of coal seam degasification with wells drilled parallel to the face

Seam permeability to gas, mD	Required efficiency of degasification, unit fractions	Conditions of seam degasification	
		Degasification period, days	Hydroimpulse treatment of the seam
Over 10^{-3}	0.3	360	-
	0.4	360	In 180 days from the start of degasification
10^{-3} - 10^{-4}	0.3	360	same
	0.3	180	At the beginning of degasification process
	0.4	180	same
	0.4	360	same
Under 10^{-4}	0.3	180	same
	0.4	360	At the beginning and during degasification process

Table 5. Indices of gas emission of coal seams in Kouzbass

Mine (association)	Seam	Depth, m	Seam thickness, m	Gas emission indices			
				K_p	g_o	a^*	G_h
Oktyabrskaya («Leninskugol»)	Polysayevsky-1	300	2.6	0.0303	0.33	0.010	34.0
	Nadbaykaimsky	245	3.7	0.0472	0.36	0.017	29.7
Chertinskaya («Belovougol»)	4	450	1.5	0.0220	0.50	0.011	49.6
	5	570	2.1	0.0105	0.38	0.005	64.2
Tomskaya («Kouznetskugol»)	III	285	9.2	0.0034	0.17	0.0006	29.1
	VI	365	4.7	0.0033	0.39	0.0013	63.1

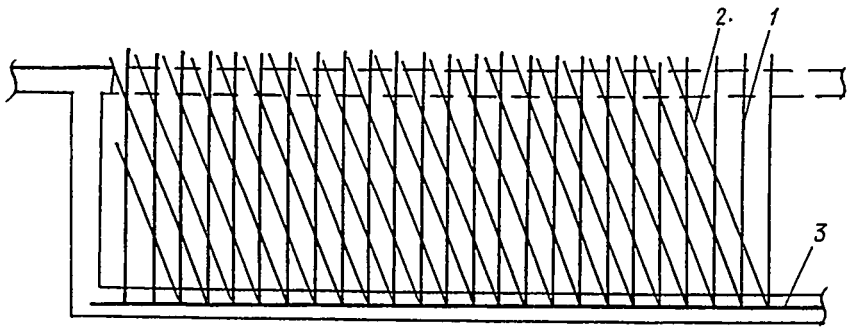
Table 6. Results of approbation of equation (10)

Mine	Seam	Seam thickness, m		Thickness of the seams being undermined, m	Efficiency of degasification, unit fractions			
		total	working		Underground method	According to equation (10)	Actual limit	Actual average
				Kouznetsky basin				
"Chertinskaya"	5	2.3	2.1	6.55	-	0.62	0.45-0.75	0.61
	3	2.8	2.5	5.80	0.10	0.57	0.4-0.6	0.46
				Karagandinsky basin				
"Chourou-bay-Nourinskaya"	K_{13}	6.4	2.2	5.1	0.14	0.46	0.4-0.5	0.42
"Stakhanovskaya"	K_{10}	2.7	2.5	7.7-7.8	0.41	0.42	0.3-0.5	0.36

Table 7. Optimal indices of degasification of mining district in seam K_{11}

Indices	Optimal values of indices				
	for mining district	for different sources of gas emission			
		Working seam	Goaf		
			total	vertical wells	underground wells
Coefficient of degasification, unit fractions	0.62	0.49	0.70	0.40	0.50
Specific costs of degasification, roub./t (prices of 1989)	2.38	0.53	1.85	1.72	0.13

Fig.1. Scheme of coal seam degasification with crossing wells



1 - wells drilled parallel to the face
2 - wells drilled in the direction of the face
3 - degasification pipeline

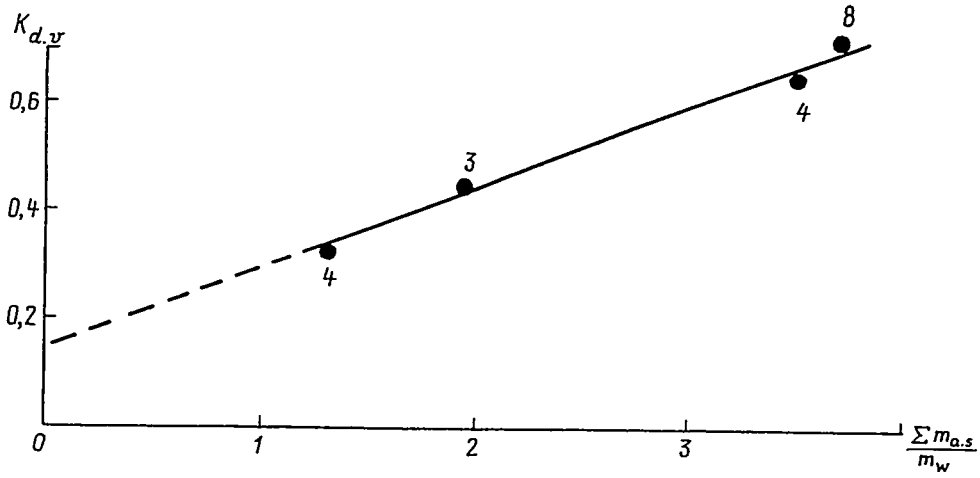


Fig.2. Relationship: $K_{d.v} = f(\Sigma m_{a.s} / m_w)$

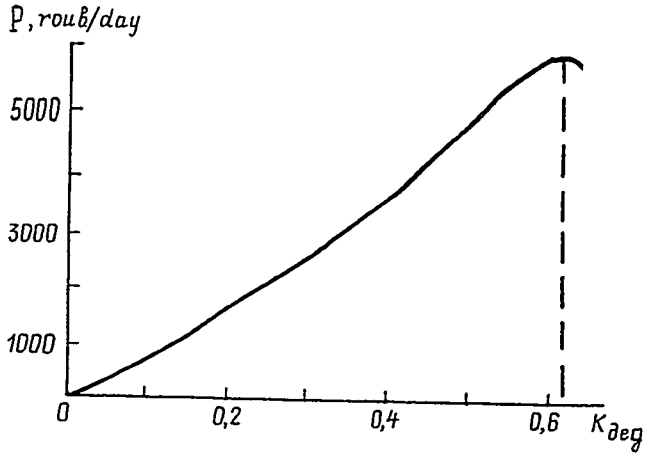
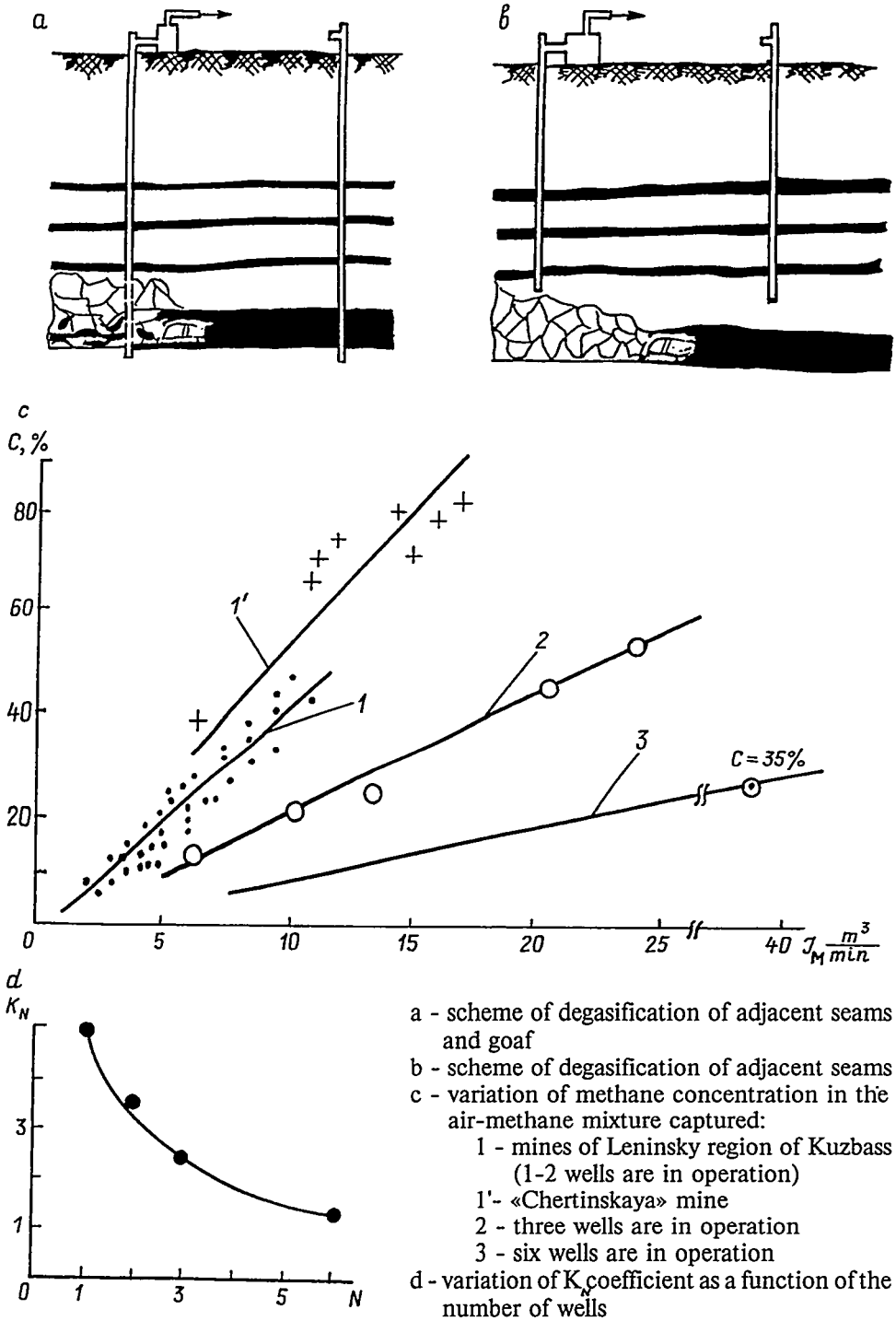


Fig.5. Relationship: $P = \varphi(K_{deg})$

Fig.3. Schemes and results of degasification of adjacent seams with vertical wells



a - scheme of degasification of adjacent seams and goaf
b - scheme of degasification of adjacent seams
c - variation of methane concentration in the air-methane mixture captured:
1 - mines of Leninsky region of Kuzbass (1-2 wells are in operation)
1'- «Chertinskaya» mine
2 - three wells are in operation
3 - six wells are in operation
d - variation of K_N coefficient as a function of the number of wells

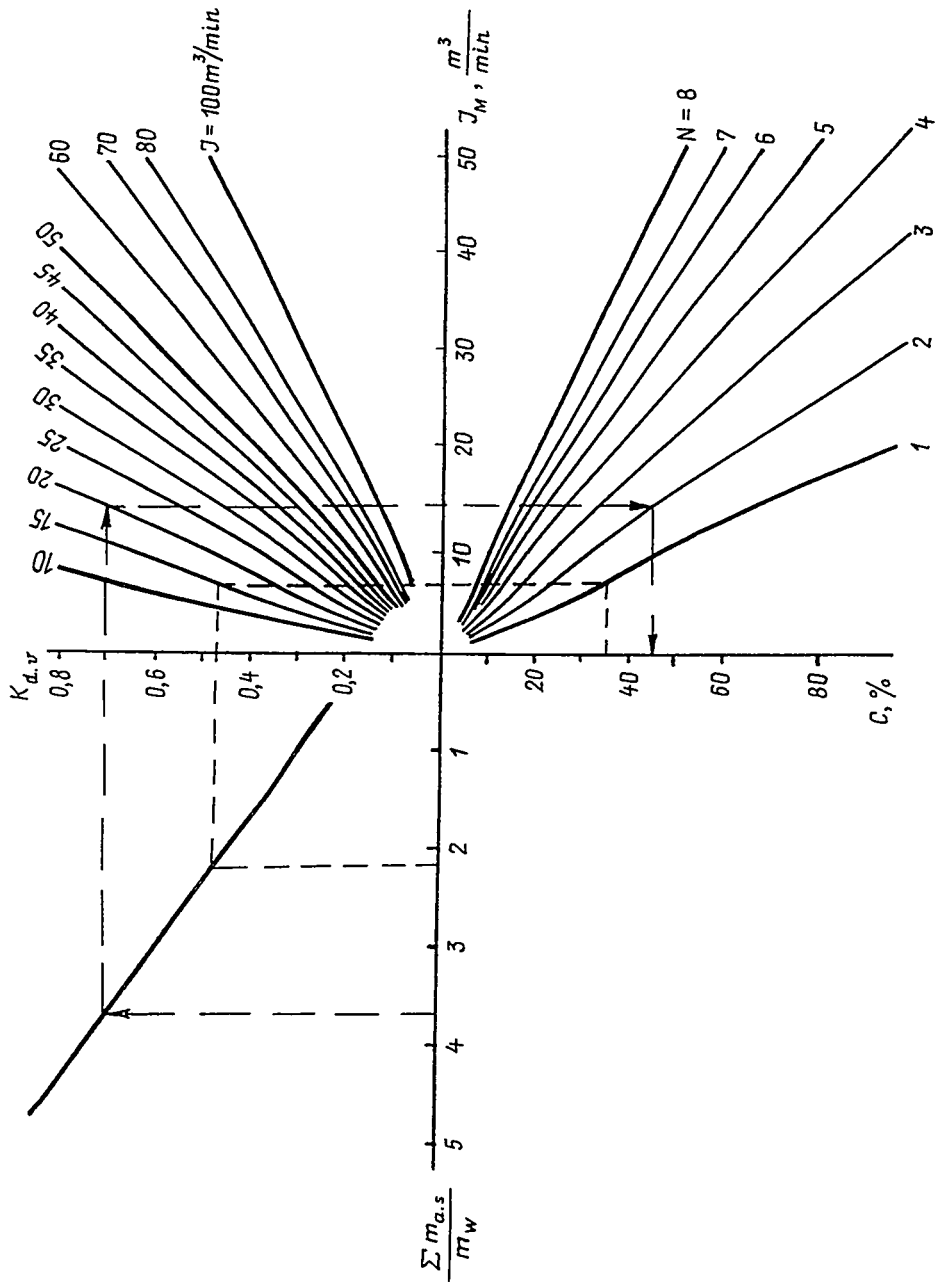


Fig.4. Nomograph for selection of operating regime for vertical wells

INTERGAS '95

May 15-19, 1995
The University of Alabama
Tuscaloosa, Alabama USA

9519

In-Situ Determination of Relative Permeability in Coal Seams Using a Two-Phase Well-Testing Tool

R.A. Koenig, In-Situ, Inc.; S.K. Choi and K.T.A. Meaney, CSIRO Australia

ABSTRACT

The Commonwealth Scientific and Industrial Research Organisation (CSIRO), Division of Petroleum Resources, Melbourne, Australia, has developed a two-phase well testing tool along with field procedures and data analysis methods. This effort addresses laboratory and field experience in measuring formation properties related to producing methane gas from coal seams. Water in coal has an extreme limiting effect on the effective permeability to gas in the coal. Adequate dewatering of coalbed methane reservoirs is crucial to successful gas production, and satisfactory measurement of relative permeability curves for particular sites is essential to accurately assess their production potential. Descriptions of the two-phase tool, procedures for collecting appropriate data using the tool, and data analyses using a coalbed methane simulator appear in this paper. Also discussed are examples of tests conducted in a coal seam in the Hunter Valley of New South Wales, Australia. The results of history-matching field data using the simulator include relative permeability curves and gas desorption pressures at particular locations in the coal seam.

DESCRIPTION OF THE TWO-PHASE TOOL

A schematic diagram of the two-phase tool appears in Figure 1. The tool operates in an HQ—96 mm (3.8 in) diameter—borehole to test variable-length intervals to depths of 700 m (2,300 ft). Two inflatable packers isolate the target interval. Various lengths of BQ-size drill rods serve to adjust the distance between the packers to fit the thickness of the target coal seam.

A positive-displacement pump, mounted in a stainless steel chamber above the upper packer, withdraws water at a constant rate from the isolated test interval to conduct a test. A hydraulically powered air compressor supplies pressure to control the pneumatically powered pump at a rate suitable for the seam conditions.

A pressure transducer, mounted in a stainless steel chamber above the upper packer, monitors the pressure in the borehole above the test interval to detect any communication between the test interval and the upper portion of the borehole. Two other pressure transducers, mounted in a stainless steel chamber below the lower packer, monitor pressure in: (1) the test interval and (2) the borehole below the test interval. The lower pressure transducer detects any communication between the test interval and the lower portion of the borehole.

A sensor mounted near the top of the lower packer measures the temperature in the test interval. Temperature is an important factor for computing both gas flow rates and water viscosity downhole.

A specially manufactured tubing bundle—external diameter of about 30 mm (1.2 in)—connects the surface facilities with the downhole tool. Contained in the tubing bundle are:

- an air-inlet and an air-exhaust line to power the pump;
- a pump discharge line to carry produced water and gas to the surface separating and metering facilities;
- a high-pressure hose for inflating and deflating the packers;
- power and signal cables to operate the downhole sensors and carry the impulses to the data acquisition system at the surface.

A personal computer at the surface controls the data acquisition system to process and record signals from the pressure transducers, temperature sensors, and flow meters. Commercial software provides a continuous display of real-time data to keep the operator fully informed throughout the test. Other commercial software is useful for processing and beginning to analyze the acquired data.

An important feature of the tool is its ability to discharge gas and water simultaneously. The onset of gas production does not prevent the pump from continuing to produce water. The relatively small volume of the isolated test interval

practically eliminates borehole storage effects. Thus the tool provides essential data from all three stages of fluid production (single-phase water flow, unsaturated water flow, and two-phase flow of water and gas) in a short time—usually a matter of hours instead of days, weeks, or months.

OPERATIONAL PROCEDURES

A truck-mounted reel handles the tubing bundle using hydraulic power to lower or raise the tool inside an HQ rod string that protects the tool. Figure 2 shows the tool operating at Dartbrook in the Hunter Valley, New South Wales. The HQ rod string is precisely th right length to position the packers at the desired test interval. The tool engages inside the core bit with the packers projecting into the open borehole.

With the tool locked in place, the packers deflated, and all systems connected, the data acquisition system monitors the pressure and temperature sensors until readings stabilize. The pump then operates long enough to fill the discharge line, the separator, and the meter run with borehole water, while purging any stored gas from the system. The total internal volume of the system is about 25 l (6.6 gal). A final period of operating the pump with the packers deflated allows the operator to adjust the pressure applied to the pump so that it runs at a predetermined discharge rate suitable for the particular test interval. After stopping the pump, the operator inflates the packers to a pressure about 2 MPa (290 psi) above the hydrostatic pressure outside the packers. With the packers securely set, another period of monitoring pressure and temperature occurs during equilibration to static reservoir conditions—usually ten minutes to an hour depending on seam permeability.

The test begins by starting the pump at the previously set rate. The data acquisition system records test data as the downhole pressure declines with discharge of water from the test interval. When the downhole pressure declines to the gas desorption pressure, methane gas begins to desorb from the coal and alters the relative permeability to water. The operator observes this change of relative permeability by an increased rate of downhole pressure decline. Eventually two-phase flow of gas begins, and the separator at the surface allows the operator to measure the flow rates of both gas and water. Analyses of fluid samples collected during the pumping period can provide additional chemical information about the water and gas contained in the coal seam. This information can be significant in cases where methane is not the only species adsorbing on the coal. On the basis of examining the data displayed during the pumping period, the operator can decide when to stop the pump and end the test.

DATA ANALYSIS

A coalbed methane simulator developed at the University of New South Wales, Australia, was the primary tool for analyzing the test data. Some of the important features of the simulator include:

- two-phase flow of gas and water;
- three dimensional geometry;
- single- or dual-porosity reservoir;
- multiple adsorbing gas species;
- hydraulic fracture modeling;
- variable permeability, porosity, and girds;
- internal phase behavior;
- matrix shrinkage option;
- fully implicit formulation.

Conventional straight-line analysis (downhole pressure versus the logarithm of time), during the period of single-phase water flow, yields intrinsic coal permeability as input for the simulator. In the examples discussed below, additional information about intrinsic seam permeability comes from previously conducted injection/falloff tests in the same test intervals. A value for static reservoir pressure comes from direct measurement of the equilibrated pressure after setting the packers. A value for gas desorption pressure comes from observing the deflection point on the straight-line plot showing downhole pressure versus logarithm of time.

History matching the test data requires additional input derived from knowledge of local geology, well drilling logs, geophysical logs, and core samples. Values for gas content, Langmuir parameters, coal density, coal porosity, and coal compressibility come from laboratory analyses of coal samples taken from the tested interval. Seam location and thickness come from drilling information and geophysical logs. In the absence of laboratory analyses yielding capillary pressure versus water saturation for the coal discussed below, curves came from Dabbous and others [1] based on physical similarity of the coal to Pittsburgh coal.

EXAMPLES OF TWO-PHASE TESTS

To date the two-phase tool has performed 18 drawdown tests in 10 wells in Australia. The purpose of each test was to characterize a coal seam. Two of the tests were in two wells in the Bowen Basin, Queensland. Four of the tests were in one well in the Gloucester Basin, New South Wales. Twelve of the tests were in seven wells in the Hunter Valley, New South Wales.

Described below are three tests selected as examples of two-phase testing in coal seams. The tests occurred in two wells at the Dartbrook Coal Mine near Muswellbrook, New South Wales, in the Hunter Valley. The coal seam there is generally 24 m (79 ft) thick. Local geological data suggests a division of the seam by coal characteristics into three layers: a

lower layer 4 m (13 ft) thick, with very low permeability; a middle layer 4m (13 ft) thick, with higher permeability; and an upper section having two 8-m (26-ft) layers, with intermediate permeability.

For convenience the two host wells appear in the following discussion as DB1 and DB2. The first two tests occurred in well DB1 in November 1993 and the third test in well DB2 in March 1994.

DB1—180 to 193 m

With the packers isolating a test interval from 180 to 193 m (591 to 633 ft) in well DB1, the pump discharged water at an average rate of 0.75 l/min (6.8 bbl/d) for a period of 4.8 hours. Figures 3 through 5 display the pressure drawdown and flow rates during the test. Pressure in the test interval declined from a static reservoir pressure of about 1.79 MPa (259 psi) to about 0.48 MPa (69 psi) at the end of the test—a total drawdown of 1.31 MPa (190 psi). The plot in Figure 5 shows a deflection in the rate of drawdown after about 15 min (900 s) of pumping. That deflection may indicate the onset of gas desorption at a pressure of about 0.93 to 1.07 MPa (135 to 155 psi). Gas first appeared at the surface after 1.9 hours (6,850 s) of pumping. The gas production rate increased steadily to a maximum of 3.5 l/min (180 SCF/d) at the end of the test. Conventional analysis of earlier pressure drawdown yields a permeability of 1.1 md. Conventional analysis of recovery data taken for 1.5 hours after stopping the pump yields a permeability of 0.7 md. Conventional analysis of a previous injection/falloff test in the same interval, using water injected at 0.99 l/min (9.0 bbl/d), gave a permeability of 0.7 md.

After the onset of gas production, the nature of flow in the whole system changed from continuous to discrete. The produced gas and water appeared at the surface in discrete parcels that, when integrated over the elapsed time between events, yield a constant water rate and an increasing gas rate. This pattern appeared in every test involving gas production.

The coalbed simulator produced the match of the field data appearing in Figure 6. The geometry employed consisted of 18 grid blocks in each of four layers as described above. The blocks were distributed radially with increasing radii at greater distances from the wellbore. A uniform horizontal permeability was assigned to each block based on the results of previous injection/falloff tests and the two-phase tests. Uniform vertical permeability of about 10 to 15% of the horizontal permeability in each block was assumed. The fluid species simulated included water, methane, and carbon dioxide, each with suitably defined properties. The extended Langmuir model simulated the adsorbing species of methane and carbon dioxide using parameters based on adsorption isotherms determined in the laboratory. Table 1 contains the main input values used to derive the match appearing in Figure 6. The relative permeability curves that produced the match appear in Figure 7.

Attempting to match the field data revealed considerable sensitivity to some of the input parameters. The time at which gas production starts in the model is sensitive to the input value of gas desorption pressure. The shape of the gas production curve is sensitive to the relative permeability curves. The maximum gas rate is sensitive to the intrinsic permeability. Figure 8 shows the effect of changing only the intrinsic permeability from 0.95 to 0.96 md. A very small change causes a significant pressure response.

DB1—193.5 to 197.5 m

With the packers isolating a test interval from 193.5 to 197.5 m (635 to 648 ft) in well DB1, the pump discharged water at an average rate of 0.87 l/min (7.9 bbl/d) for a period of 6.5 hours. Figures 9 and 10 display the pressure response during the test. Pressure in the test interval declined from a static reservoir pressure of about 1.76 MPa (256 psi) to about 0.39 MPa (56 psi) at the end of the test—a total drawdown of 1.38 MPa (200 psi). The plot in Figure 9 shows a deflection in the rate of drawdown after about 20 min (1,200 s) of pumping. That deflection may indicate the onset of gas desorption at a pressure of about 1.14 MPa (165 psi). Gas first appeared at the surface after 1.2 hours (4,300 s) of pumping. The gas production rate increased steadily to a maximum of 2.5 l/min (130 SCF/d) at the end of the test. Conventional analysis of earlier pressure drawdown yields a permeability of 1.5 to 2.0 md. Conventional analysis of recovery data taken for 1.5 hours after stopping the pump yields a permeability of 1.3 md. Conventional analysis of a previous injection/falloff test in the same interval, using water injected at 0.68 l/min (6.2 bbl/d), gave a permeability of 1.3 md.

The coalbed simulator produced the match of the field data appearing in Figure 10. The geometry employed was the same as described above. Table 1 summarizes the main input values used to derive the match appearing in Figure 10. The relative permeability curves that produced the match appear in Figure 11.

DB2—251 to 256.6 m

A longer test was arranged in another well at the Dartbrook site. The objective was to see whether a longer test could yield data that would better define the gas production curve and hence refine the history match. With the packers isolating a test interval from 251 to 256.6 m (823 to 842 ft) in well DB2, the pump discharged water at a rate of 0.21 to 0.44 l/min (1.9 to 4.0 bbl/d) for a period of 122.5 hours. Figure 12 displays the pressure and rate response during the test. Pressure in the test interval declined from a

static reservoir pressure of about 2.45 MPa (355 psi) to about 0.46 MPa (67 psi) at the end of the test—a total drawdown of 1.99 MPa (288 psi). The plot in Figure 12 shows no definite deflection in the rate of drawdown. Gas first appeared at the surface after 3.6 hours (13,000 s) of pumping. The gas production rate increased rapidly to about 0.6 l/min (30 SCF/d) and then steadily increased to a maximum of 1.0 l/min (51 SCF/d) at the end of the test. Conventional analysis of earlier pressure drawdown yields a permeability of 0.6 md. Conventional analysis of a previous injection/falloff test in the same interval, using water injected at 2.1 l/min (19.3 bbl/d), gave a permeability of 0.6 md. The pressure response to injection, plotted on a log-log scale, definitely followed a half-slope trend indicating linear flow. This is a strong indication that a fracture intercepts the wellbore at that horizon.

The coalbed simulator produced the match of the field data appearing in Figure 12. The geometry employed was the same as described above except that a vertical fracture intercepting the wellbore—half-length = 2.77 m (9.09 ft); width = 0.013 m (0.043 ft); height = 1.52 m (4.99 ft)—was assumed. Table 1 summarizes the main input values used to derive the match appearing in Figure 12. The relative permeability curves that produced the match appear in Figure 13.

OBSERVATIONS AND CONCLUSIONS

Koenig and others [2] give additional information describing the two-phase tool and its operation. The tool has successfully completed 18 tests in Australian coal seams. Data analyses and history matching for some of those tests are in progress. Responses have varied over a wide range. Some test intervals, where adsorbed gas is known to reside, have shown no indication of gas production after many hours of pumping. Other intervals have produced up to 2,500 SCF/d of gas after as little as 30 minutes of pumping.

History matching to date indicates that each test interval produces a different set of relative permeability curves. Given that relative permeability has a significant influence on ultimate gas production, it may be important to obtain site specific relative permeability curves to accurately forecast gas production. Use of generic relative permeability curves may give misleading results in some cases.

Experience to date with history matching of short-term drawdown tests in coal seams indicates that patience is a key factor. The analyst may have to change the input data set many times to achieve a satisfactory match. The simulated response is particularly sensitive to gas desorption pressure, the relative permeability curves, and the intrinsic permeability. For the key parameters, however, there is a surprisingly small range of values that will give a good match while honoring the other measured parameters.

The twelve tests conducted at Dartbrook included intervals isolating various portions of a thick coal seam. This suggests that testing subintervals of a single coal seam is possible, at least in some coal seams, by using inflatable packers.

ACKNOWLEDGMENT

The authors wish to thank Dartbrook Coal Pty. Ltd. for the opportunity to use the two-phase tool and for their valuable assistance during the testing activities.

REFERENCES CITED

1. Dabbous, M. K., A. A. Reznik, B. G. Mody, P. F. Fulton, and J. J. Taber, Oct. 1976: "Gas-Water Capillary Pressure in Coal at Various Overburden Pressures"; Soc. of Pet. Eng. Journal, V. 6, No. 5, p. 261-268.

2. Koenig, R. A., A. K. Dean, and G. Lupton, 1993: "A Two-Phase Well Testing Tool to Measure Relative Permeability of Coal", paper 9337, Proceedings of the 1993 International Coalbed Methane Symposium, Birmingham, Alabama, p. 257-262.

TABLE 1. INPUT VALUES FOR HISTORY MATCH

	DB1 180 - 193 m	DB1 193.5 - 197.5 m	DB2 251 - 256.6 m
Fluid property description			
Water reference pressure	1.0 atm	1.0 atm	1.0 atm
Water density at reference pressure	1.0 g/cm^3	1.0 g/cm^3	1.0 g/cm^3
Water compressibility	4.4×10^{-10} /Pa	4.4×10^{-10} /Pa	4.4×10^{-10} /Pa
Water formation volume factor at ref. pressure	1.002 cm^3/cm^3	1.002 cm^3/cm^3	1.002 cm^3/cm^3
Water viscosity at reference pressure	8.0×10^{-10} Pa·s	8.0×10^{-10} Pa·s	8.0×10^{-10} Pa·s
Rock/Fluid/Adsorption data			
Radial permeability layer 1	0.35 md	0.35 md	0.35 md
Radial permeability layer 2	0.95 md	1.70 md	0.80 md
Radial permeability layer 3	0.95 md	1.70 md	0.80 md
Radial permeability layer 4	0.95 md	1.70 md	0.80 md
Vertical permeability layer 1	0.05 md	0.05 md	0.05 md
Vertical permeability layer 2	0.10 md	0.30 md	0.30 md
Vertical permeability layer 3	0.10 md	0.30 md	0.30 md
Vertical permeability layer 4	0.10 md	0.30 md	0.30 md
Coal density	1.40 g/cm^3	1.40 g/cm^3	1.40 g/cm^3
Coal porosity	2%	2.5%	2%
Coal compressibility	2.9×10^{-8} /Pa	1.45×10^{-8} /Pa	2.9×10^{-8} /Pa
Langmuir adsorption volume (methane)	16.4 m^3/tonne	16.4 m^3/tonne	16.4 m^3/tonne
Langmuir adsorption volume (carbon dioxide)	36.8 m^3/tonne	36.8 m^3/tonne	36.8 m^3/tonne
Langmuir pressure (methane)	1.95 MPa	1.95 MPa	1.95 MPa
Langmuir pressure (carbon dioxide)	1.12 MPa	1.12 MPa	1.12 MPa
Initial conditions			
Temperature in coalbed	29.4 °C	29.4 °C	29.4 °C
Depth to centre of test interval	186.5 m	197.5 m	253.7 m
Reservoir pressure	1.79 MPa	1.76 MPa	2.45 MPa
Gas desorption pressure	1.28 MPa	1.16 MPa	1.66 MPa
Well definition			
Wellbore radius	0.048 m	0.048 m	0.048 m
Skin factor	1.0	-1.3	-1.9
Average water discharge rate	0.75 l/min	0.63 l/min	0.35 l/min
Fracture half-length	—	—	2.77 m
Fracture width	—	—	0.013 m
Fracture height	—	—	1.52 m

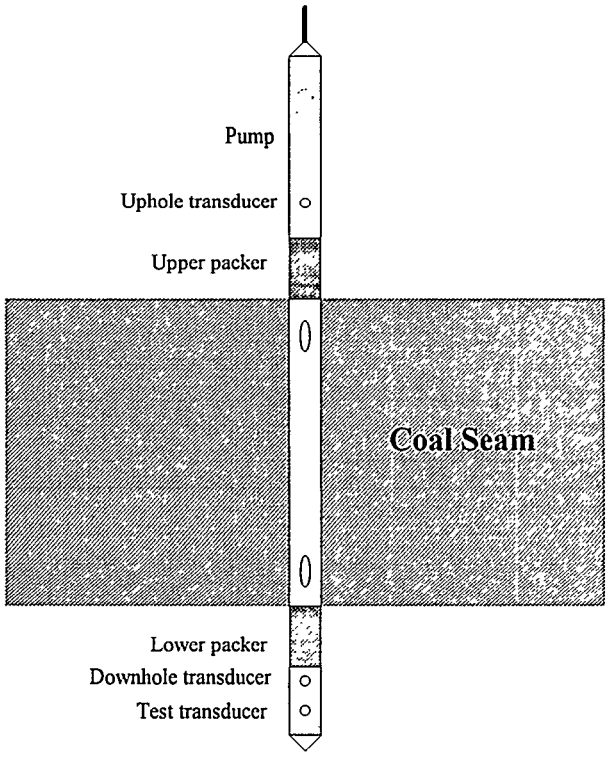


Figure 1. Schematic diagram of the two-phase well testing tool.

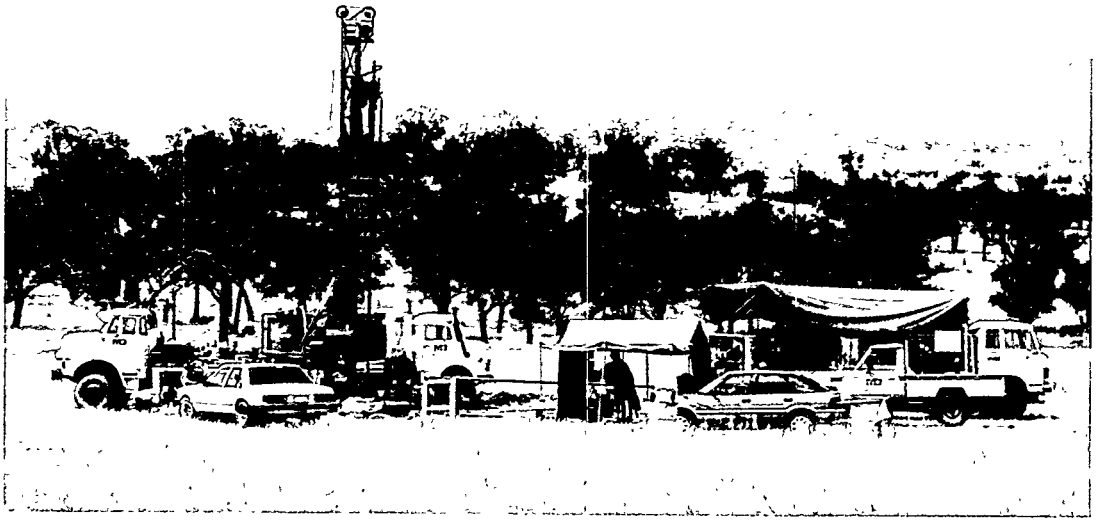


Figure 2. The two-phase tool operating at Dartbrook in the Hunter Valley, New South Wales.

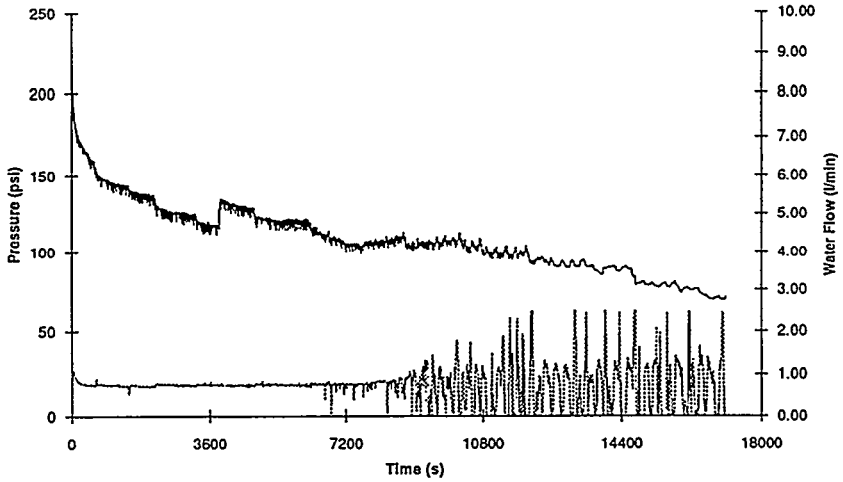


Figure 3. DB1—180 to 193 m. Pressure and water flow versus time.

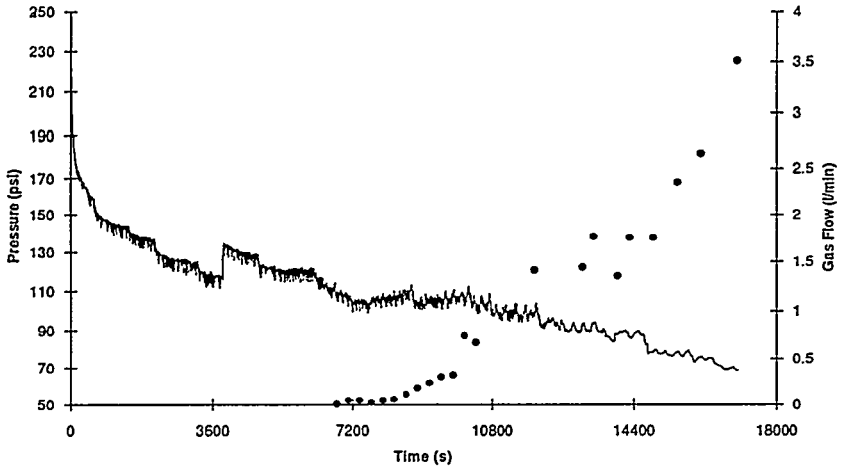


Figure 4. DB1—180 to 193 m. Pressure and gas flow versus time.

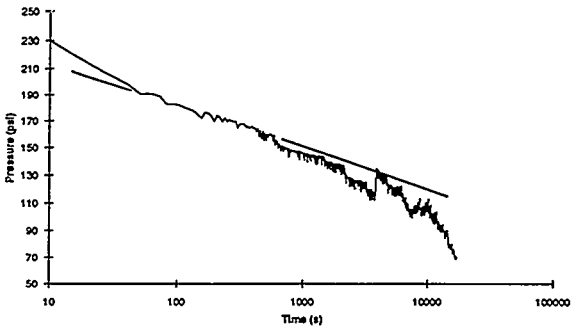


Figure 5. DB1—180 to 193 m. Pressure versus logarithm of time during pumping.

q = 0.75 l/min
m = 6.3 m/cycle
h = 13 m
μ = 0.9 cp
p_o = 259 psi
p_{1s} = 216 psi
kh/μ = 1.6×10^{-7} m^2/s
k = 1.1 md
$skin$ = 1.0

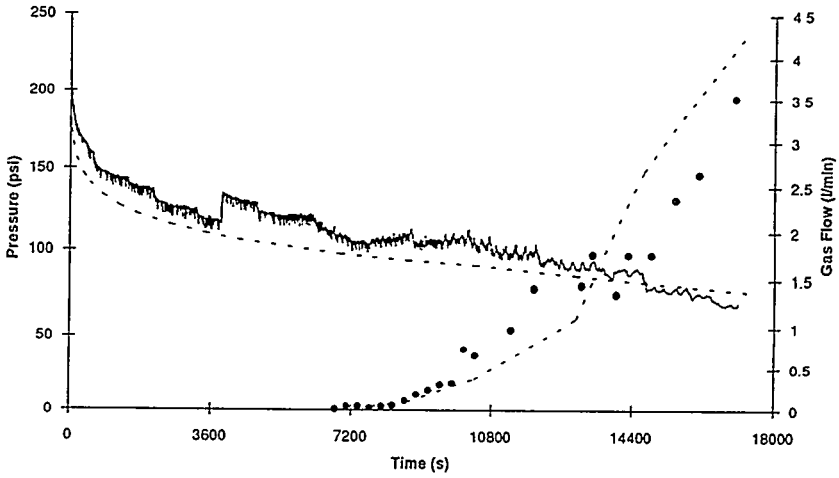


Figure 6. DB1—180 to 193 m. Best-fit history match of pressure decline and gas production using a permeability of 0.95 md in the test interval.

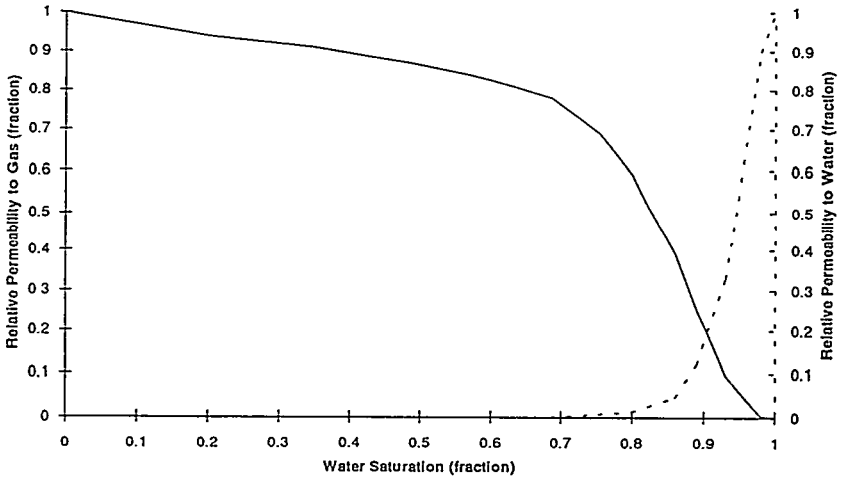


Figure 7. DB1—180 to 193 m. Relative permeability curves used to derive the best-fit history match.

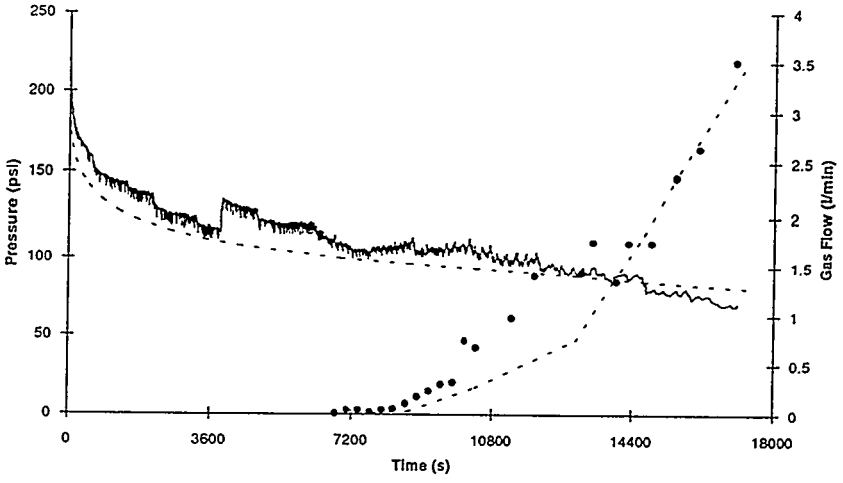
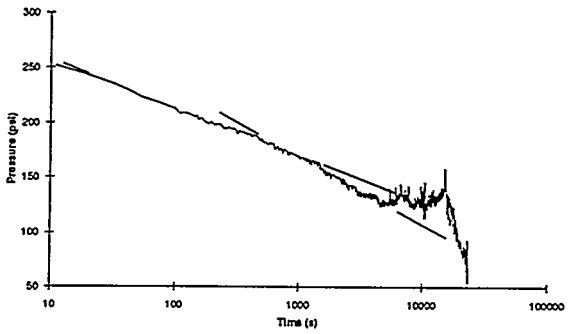


Figure 8. DB1—180 to 193 m. Best-fit history match of pressure decline and gas production using a permeability of 0.96 md in the test interval.



q = 0.87 l/min
m = 13.4 to 20.1 m/cycle
h = 4 m
μ = 0.9 cp
p_o = 256 psi
p_{1s} = 301 psi
kh/μ = 5.8×10^{-8} to 8.6×10^{-8} m^2/s
k = 1.5 to 2.0 md
$skin$ = -1.3 to -2.3

Figure 9. DB1—193.5 to 197.5 m. Pressure versus logarithm of time during pumping.

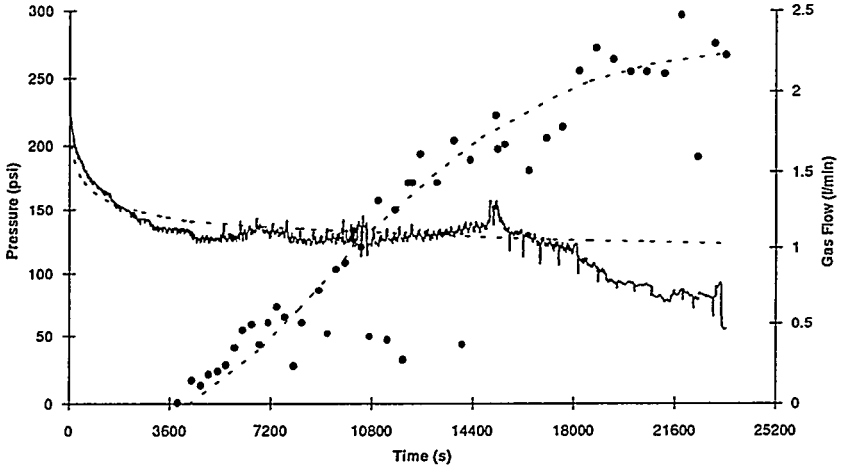


Figure 10. DB1—193.5 to 197.5 m. Best-fit history match of pressure decline and gas production.

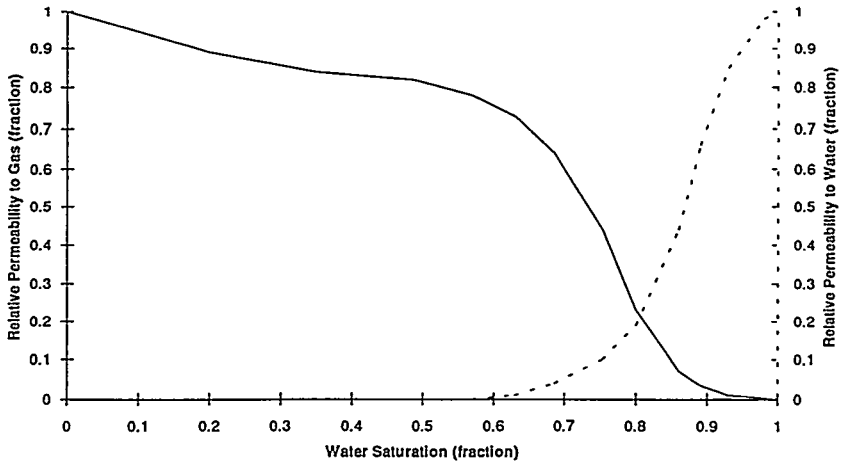


Figure 11. DB1—193.5 to 197.5 m. Relative permeability curves used to derive the best-fit history match.

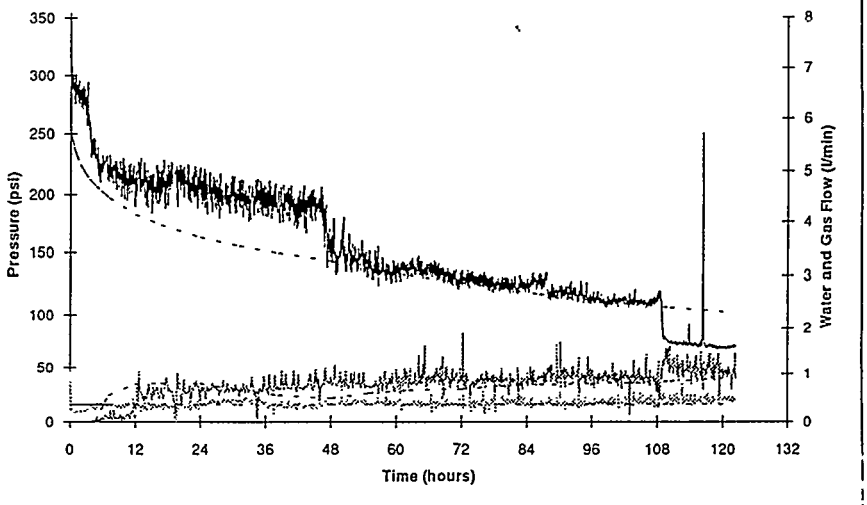


Figure 12. DB2—251 to 256.6 m. Best-fit history match of pressure decline and gas production.

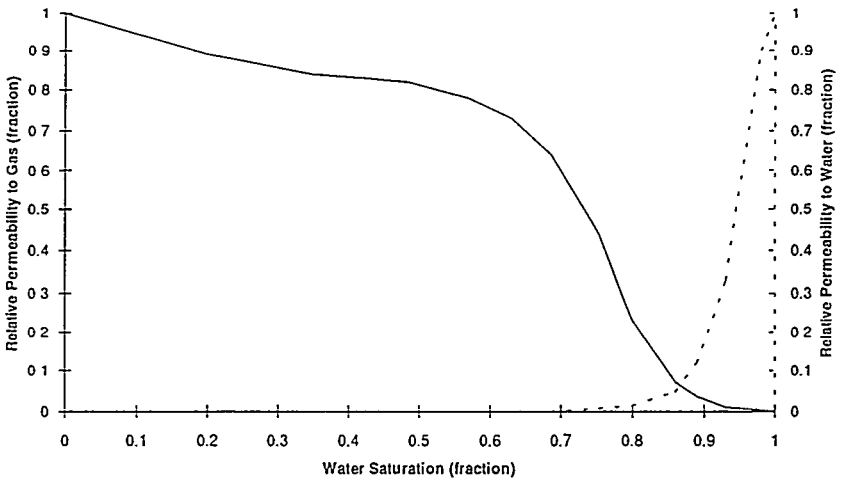


Figure 13. DB2—251 to 256.6 m. Relative permeability curves used to derive the best-fit history match.

INTERGAS '95

May 15-19, 1995
The University of Alabama
Tuscaloosa, Alabama USA

9539

The Effect of Fracturing Fluid Damage on Production from Hydraulically Fractured Wells

M.W. Conway, Stim-Lab, Inc.; and R.A. Schraufnagel, Gas Research Institute

ABSTRACT

Many coalbed methane wells have failed to produce the expected quantities of gas. Recent laboratory studies have shown that the stimulation fluids used to complete the wells can create permeability damage and alterations in the relative permeability curve that impair the production of gas much more than the production of water. This study demonstrates that computer simulations of the adverse effects of stimulation fluids on the producibility of coalbed methane wells can explain many of the production profiles observed in the field.

INTRODUCTION

Laboratory data from studies with coal shows a significant formation damage potential to coalbed methane wells from many stimulation fluids and additives.[1] We feel there are some fundamental facts that have been learned from coalbed methane production which have a high potential for improving gas production from both coalbed methane wells and conventional gas wells. The impact of formation damage on production has been largely under estimated; first because it has not been studied in much detail and secondly because it is quite difficult to use single phase production simulators to predict the clean up behavior from gas wells hydraulically fractured with water based fluids.

The original work on formation damage by Holditch *et al.*[2] has recently been updated[3] and acknowledges the necessity of properly considering the non-propped fracture tip. Unless extreme care is used in performing these simulations and the simulator characteristics are well known, little loss in production is predicted from formation damage in hydraulically fractured wells.[4] This result has been very comforting to many well stimulation experts. The fact remains that the production from many wells has been improved by remedial treatments which reduced damage, indicating the need to be concerned about the damage potential of stimulation fluids.

Unfortunately, many of the newer, supposedly less damaging fracturing fluids have not resulted in improved production. Recent studies in a number of reservoirs have shown that the wells treated with fluids used in the early 1980's had similar or better production records than wells treated with newer fluids developed more recently. This phenomena has been clearly documented in the Moxa Arch.[5,6] There is some controversy about some of the conclusions of the study.[7] However, it can be safely concluded that the benefits of other significant technological improvements such as high strength proppants can be obscured by the fluid effects.

The latest proppant and formation damage studies have shown that the identified damage potential depends on both the fluid (brine, gas or oil) used to assess the permeability damage and the flow rate used in the study. During return permeability testing in the laboratory, high flow rates, which may not be possible in many real wells,[8] are one of the best ways to remediate damage. This shows the importance of calibrating the testing method to field conditions and validating the predictions of the laboratory tests.

There is a significant issue in laboratory testing of multi-phase flow permeability that is not encountered in measuring absolute permeability. Absolute permeability is a state function, but relative permeability is not. It is a statistical representation of the flow properties occurring under a defined set of flow conditions. Capillary end effects can generate a laboratory artifact of capillary pressure effects which cannot be translated to the field.[9] In real wells, there is discontinuity at the wellbore-fracture interface and at the fracture-formation interface where capillary pressure effects can create anomalous pressure effects. However, the magnitude of the pressure drop in the formation should be great enough to make these effects negligible in producing wells. This is distinctly different from the laboratory test where the short finite core length results in pressure losses due to end effects

which may be very significant compared to the flow characteristics occurring in the core.

There are two types of damage that can occur. The first is absolute permeability damage. Fracturing polymers are the most obvious source of this type of damage during stimulation.[11] Limiting the depth of reservoir penetration is one of the best ways to limit the production reduction from this type of damage. The second type of damage is to the relative permeability to the hydrocarbon present in the reservoir. Some surfactants are the best example of additives which can adversely alter the relative permeability curve to gas, which may limit production.[11]

The production from a hydraulically fractured well depends on both the created and propped fracture geometry and the permeability of the propped fracture, and the permeability of the reservoir in contact with the fracture. The basic message to be presented in this paper is that fluid damage can be equally or more important than adverse fracture geometry in dictating the production from hydraulically fractured wells. The issues have been identified, but solutions to the fluids problems are far from solved at this time.

POST-STIMULATION PRODUCTION PREDICTIONS

All service companies use single phase simulators to predict the production expected from a proposed stimulation treatment. Frankly, this has been one of the major factors that has inhibited the development of a clear understanding of the effect of stimulation fluid additives on production. Multi-phase production simulations require additional information about the fluids and the reservoir which will only begin to become available if the service companies need the information on a routine basis in order to design stimulation treatments.

The additional information required is the effect of the fracturing fluid on the relative permeability to brine and gas in the invaded zone as well as the native relative permeability of the formation. Unfortunately, relative permeability measurements are difficult and expensive to determine in the laboratory. The limited measurements in coalbed methane[12,13] have been quite variable and differences in testing methodology have been implicated. A GRI supported project to develop standard methods for relative permeability measurements did not successfully resolve all the issues.[14]

Field derived relative permeability curves have all shown that the water permeability drops much faster and the gas permeability increases faster than is measured in the laboratory. Recently, a laboratory determined relative permeability curve was obtained that has come much closer to the shape of the field derived curves. This curve was successfully used to predict an absolute permeability from multi-phase well tests that was in general agreement with other estimates of absolute permeability measured on the same well.[15]

The purpose of post-treatment simulations is to try to determine whether the reservoir characteristics are dictating performance and the production cannot be significantly improved on an economic basis by redesigned stimulation treatments, or if the treatments are not optimizing production. A series of post-treatment simulations were performed to quantify the types of production gains that might be obtained by redesigned stimulation treatments.

The simulations performed examined the two potential types of treatment fluid effects. The first is absolute permeability damage and the second is an alteration to the relative permeability curve. The Comet PC-3D™ Coalbed Methane simulator was used to explore the potential impact of these two effects on the cumulative production after 2 years. The major effects studied were a 50% reduction in the fracture conductivity, a 99% reduction in matrix permeability 5 ft around the fracture (figure 1) and an extensive alteration in the relative permeability curve due to additives used in the treatment that invaded deep into the formation.

A micro-model described previously[16] was used to determine relative permeability curves with a foaming surfactant ("foam relative permeability") and without a foaming surfactant ("native relative permeability") to use in the simulation (figure 2). These curves do not resemble those derived from field data, but the differences in these curves is believed to be representative of the effect that could occur in the field. The simulator results are shown in figure 3 and are quite revealing regarding the differences in the production rates of gas and water which can occur from formation damage. The alterations in the relative permeability curve alone reduced the predicted cumulative gas production after 2 years by 14%, but simultaneously resulted in a 31% increase in the water production. Ultimate recovery differences may be much reduced. This observation is in agreement with field experience that has demonstrated increased water production rates in wells with disappointing gas production rates.

Simulator results with the "native" relative permeability curve show that severe permeability damage around the fracture only results in a 9% reduction in the produced water volume. This is similar to the predictions normally obtained with single phase simulators. Gas production, however, is reduced by 42%.

The most dramatic prediction was an increase in water production (24%) from the well with an altered relative permeability curve with severe damage compared to the simulation for a well with the native relative permeability curve with no damage. Gas production under the same conditions was reduced by 69%. There are far too many field cases that could be explained by these two factors.

The most dramatic field example of widely varying gas rates and similar water rates are is seen in the production around the GRI/Amoco/REI COAL site

well in the San Juan Basin.[17] Six wells, including the COAL site well, were initially hydraulically fracture stimulated and then recompleted either by sidetracking or drilling replacement wells to be treated by installing a cavity. Examples of the production rates are given in figure 4. In all cases water production rates were identical between the pairs of completions, but gas rates were dramatically different. At the COAL site, the hydraulically fracture stimulated well produced 45 thousand cfd compared to the current production rate of 11 million cfd being produced from the cavitated well. The COAL site well, Southern Ute Tribal #2, initially produced 1.2 mmcfd gas after cavitation and has slowly increased up to the current production rate of 11 mmcfd.

Studies supported by GRI have shown that there are many additives used in stimulation treatments that impair the return permeability to gas and brine.[10] These data were obtained with the standard procedure developed to examine the effect of stimulation additives on permeability. Examples of the types of changes in permeability that can occur after treatment are given in figures 5 to 7.

Foamers reduce the permeability to both gas and brine due to gas trapping as well as alter the relative permeability curve (figure 5). Surface tension reducing surfactants typically reduce gas permeability without changing the brine permeability (figure 6). Acid corrosion inhibitors are also examples of additives that reduce both brine and water permeability. The degree of permeability impairment varies widely; thus, there is an opportunity to optimize treatment results by the judicious selection of the fluids used to stimulate coalbed methane wells.

However, this procedure does not provide the necessary data for computer simulation of the expected production with two phase simulators. The development of relative permeability curves that represent the "damage" seen in the above laboratory tests is still in progress.

Micro models show promise as a means to conduct such studies because water saturation can be easily quantified and the mechanism of the permeability alteration visually described simultaneously with the acquisition of the data required for simulation studies. Further work is currently under way to define the reasons why the current data does not agree with relative permeability curves defined by other laboratory studies and the relative permeability derived from field production data.

CONCLUSIONS

1. Production results from reservoirs producing both gas and water show that water can be very successfully produced from fractures which will not produce acceptable quantities of gas.
2. Laboratory studies show that many stimulation additives adversely affect gas permeability and their properties should be carefully evaluated.
3. Production simulations of hydraulically fractured wells show that formation damage around the fracture can have a much more severe effect on production than previously recognized.
4. Many wells in both coalbed methane and tight gas reservoirs have shown substantial production increases from post-fracture remedial treatments which substantiates the improved production possible from reduced damage to the proppant pack and the formation.

REFERENCES

1. Puri, R., King, G.E., and Palmer, I.D.: "Damage to Coal Permeability During Hydraulic Fracturing," paper SPE 21813 presented at the 1991 Rocky Mountain Regional and Low Permeability Reservoirs Symposium held in Denver, CO, April 15-17.
2. Holditch, S.A.: "Factors Affecting Water Blocking and Gas Flow From Hydraulically Fractured Gas Wells," *JPT* (Dec. 1979) 1515-1524.
3. Sherman, J.B. and Holditch, S.A.: "Effect of Injected Fracture Fluids and Operating Procedures on Ultimate Gas Recovery," paper SPE 21496 presented at the 1991 Gas Technology Symposium held in Houston, Texas, Jan. 22-24, 1991.
4. Wright, T., RES, personal communications.
5. Cipolla, C.L. and Kyte, D.G.: "Infill Drilling in the Moxa Arch: A Case History of the Frontier Formation," paper SPE 24909 presented at the 67th Annual Technical Conference and Exhibition held in Washington, DC, October 4-7, 1992.
6. Cipolla, C.L., Meehan, D.N. and Stevens, P.L.: "Hydraulic Fracture Performance in the Moxa Arch Frontier Formation," paper SPE 25918 presented at the 1991 Rocky Mountain Regional Meeting/Low Permeability Reservoirs Symposium held in Denver, Colorado, April 26-28, 1993.
7. Schubarth, S.K. and Chabaud, R.A.: "Moxa Arch Frontier Formation Development Success Through Increased Fracture Conductivity," paper SPE 28610 presented at the 69th Annual Technical Conference and Exhibition held in New Orleans, Louisiana, September 25-28, 1994.
8. Penny, G.S. and Conway, M.W.: "Report on the Investigation of the Effects of Fracturing Fluids Upon the Conductivity of Proppants, Proppant Flowback and Leakoff," 1994 STIM-LAB Proppant Consortium.
9. Whillhite, P.G.: *Waterflooding*, Society of Petroleum Engineers, Richardson, TX, (1986), SPE Textbook Series, **3**, 55-59.
10. Penny, G. S., and Conway, M. W., "Coordinated Studies in Support of Hydraulic Fracturing of Coalbed Methane", Annual Report No. GRI-93/0215 (January 1993 - April 1994), prepared for the Gas Research Institute under contract no. 5090-214-1983, August 1994.

11. Huh, D.G. and Handy, L.L.: "Comparison of Steady- and Unsteady-State Flow of Gas and Foaming Solution in Porous Media," SPE Reservoir Engineering, February 1989, 77-84.
12. Gash, B. W., Volz, R. F., Potter, G., and Corgan, J. M., "The Effects of Cleat Orientation and Confining Pressure on Cleat Porosity, Permeability and Relative Permeability in Coal", paper 9224 presented at the 33rd Annual Symposium of the Society of Professional Well Log Analysists, Society of Core Analysts Symposium Volume III, Oklahoma City, OK, June 15-17, 1992.
13. Puri, R., Evanoff, J. C., and Brugler, M. L., "Measurement of Coal Cleat Porosity and Relative Permeability Characteristics", paper 21491 presented at the SPE Gas Technology Symposium, Houston, TX, January 23-25, 1991.
14. Felber, B. J., and Daneshjou, D. H.: "Improved Evaluation of Coal Reservoirs Through Specialized Core Analysis", Final Report GRI-92/0343 (January 1989-December 1991), prepared for the Gas Research Institute under contract no. 5089-214-1868, November 1992.
15. Conway, M.W., Mavor, M.J., Saulsberry, J., Barree, R.B. and Schraufnagel, R.A: "Multi-Phase Flow Properties for Coalbed Methane Wells: A Laboratory and Field Study," paper SPE 29576 to be presented at the 1995 Joint Rocky Mountain Regional Meeting/Low Permeability Reservoirs Symposium held in Denver, CO, March 20-22, 1995.
16. Conway, M.W., Smith, K., Thomas, T. and Schraufnagel, R.A.: "The Effect of Surface Active Agents on the Permeability of Brine and Gas in Porous Media," paper SPE 28982 to be presented at the SPE International Symposium on Oilfield Chemistry held in San Antonio, TX, February 14-17, 1995.
17. Conway, M.W.: "Is It Time to Put the Final Nail in the Fraccing Coffin," Quarterly Review of Methane from Coal Seams Technology, **11**, 3-4, (April 1994) 7-12.

RESERVOIR CHARACTERISTICS for the SIMULATION STUDIES

Property	"Initial"	"Damaged"
Permeability (x, y, z, md)	50,10,5	1% of original
Initial Pressure (psi)	420	420
Fracture Conductivity (md-ft)	5000	50% of original
Initial Water Saturation	100%	100%
Porosity	0.5%	0.5%
Langmuir Volume (scf/cu ft)	25.	25.
Langmuir Pressure (psia)	561	561
Total Compressibility (1/psi)	1 E-5	1 E-5

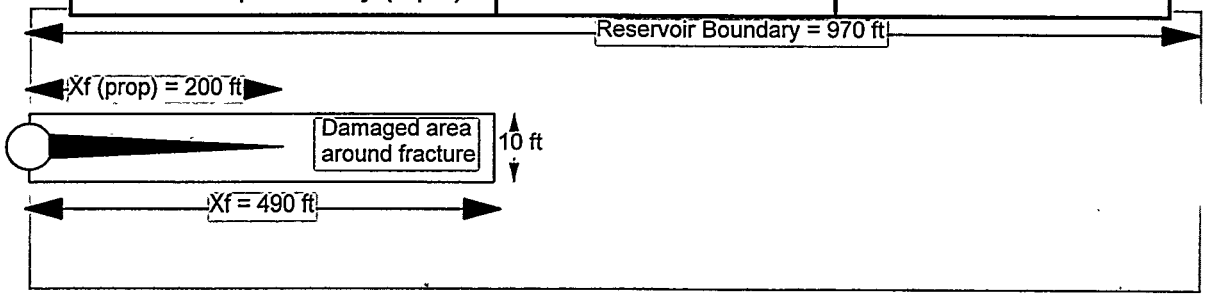


Figure 1. Reservoir characteristics used in the Coment PC-3D production simulation studies to evaluate the effects of damage and relative permeability curve alterations on production.

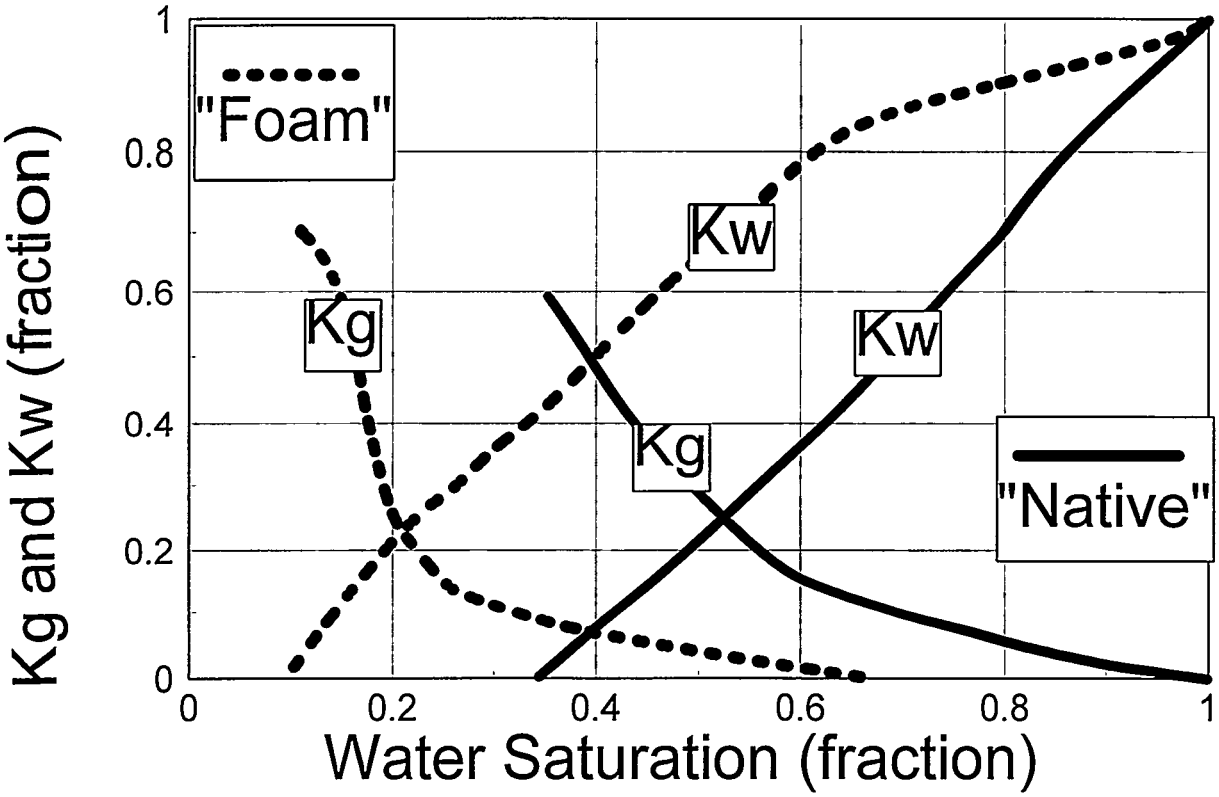


Figure 2. Micro-slot relative permeability curves determined with ("Foam") and without ("Native") a foaming surfactant.

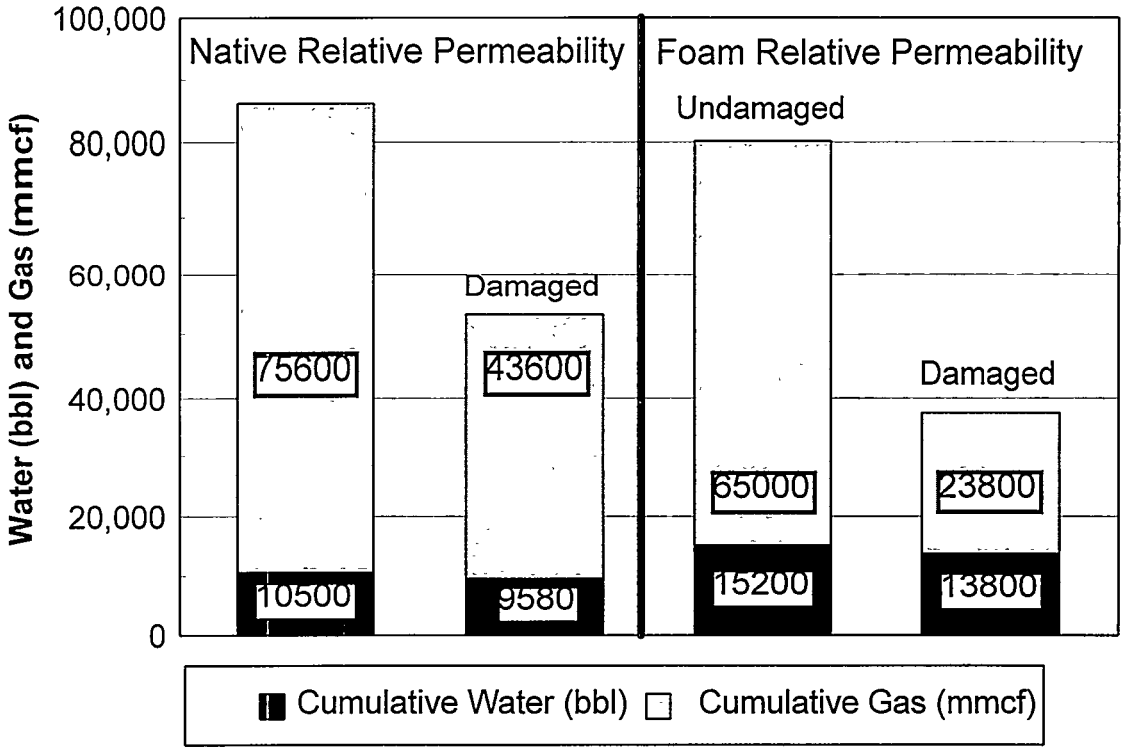


Figure 3. Predicted 2 year cumulative gas and water production from wells with and without relative permeability curve alterations and damage around the fracture.

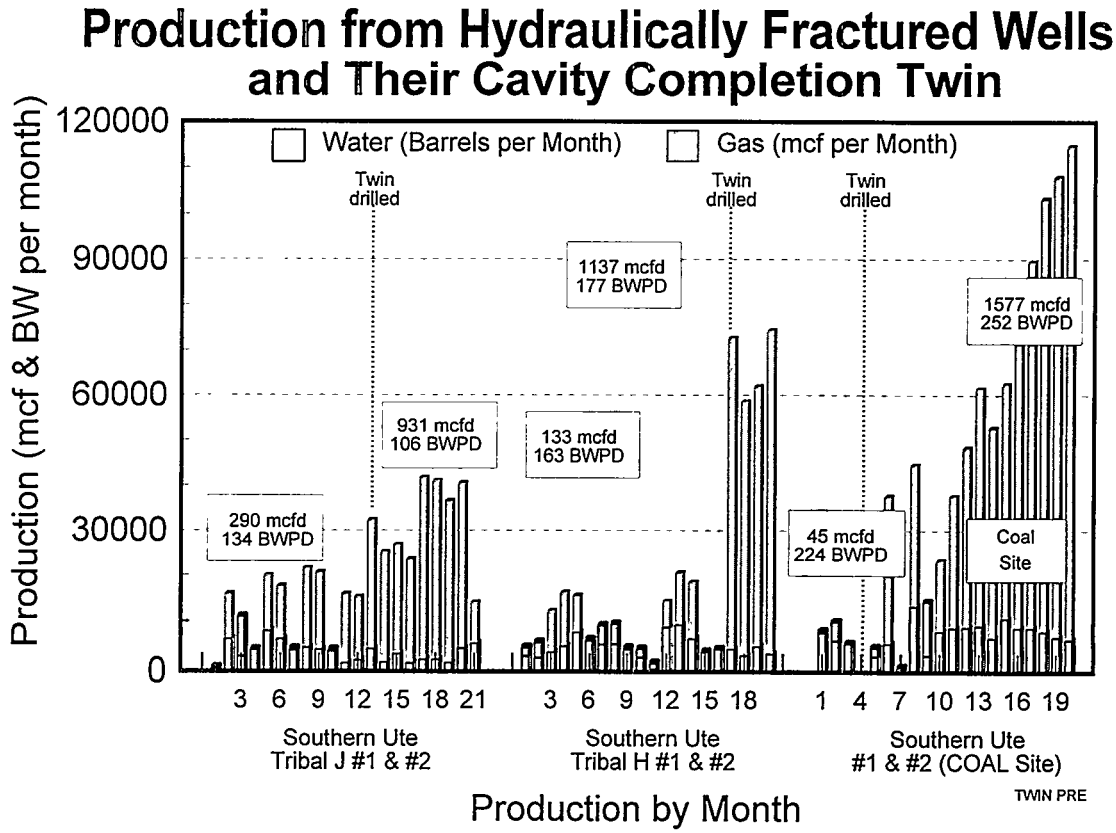


Figure 4. Monthly gas and water production rates from hydraulically fractured wells and their cavitated twins in the San Juan Basin.

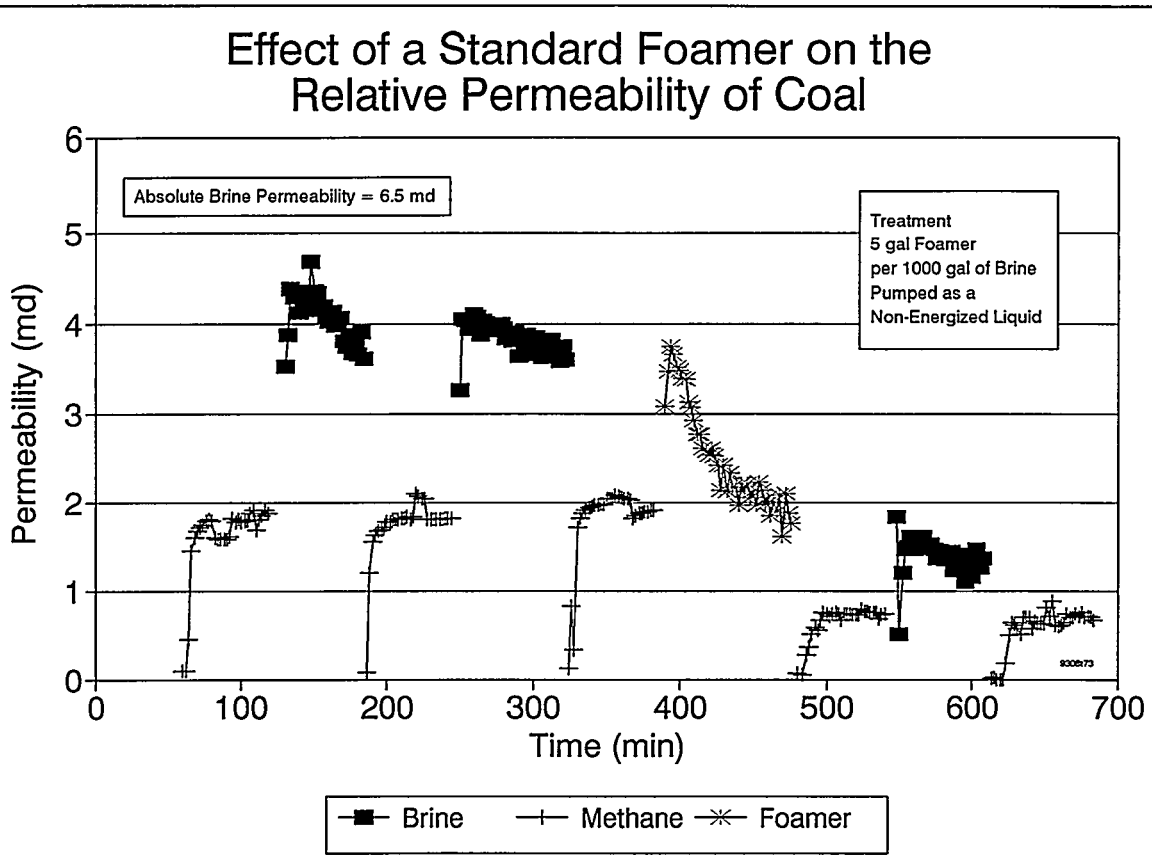


Figure 5. Effect of a standard foaming agent on the relative permeability to gas and water of Blue Creek coal using the standard GRI core flow test. The relative permeability curve determined with the micro-model using the same foaming surfactant was presented in figure 2.

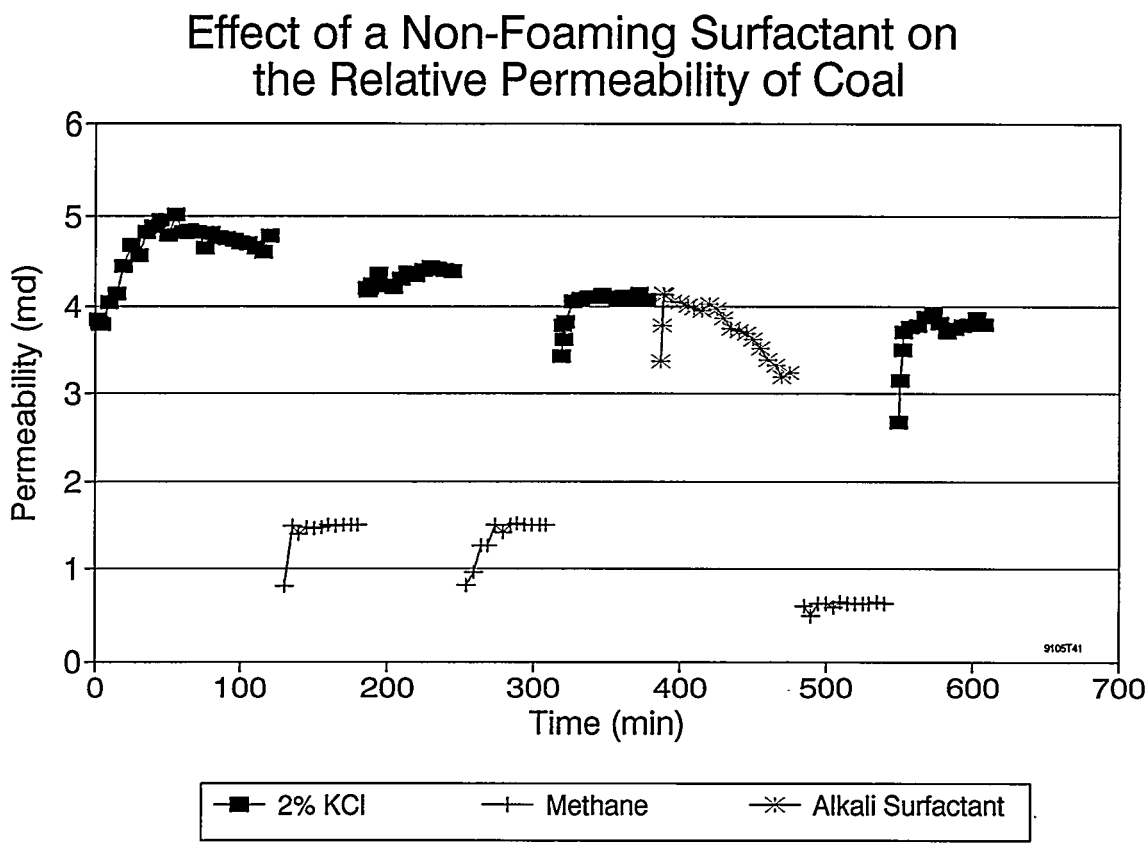


Figure 6. Effect of adding 5 gal/1000 gal of a surface tension reducing surfactant on the relative permeability of gas and water of Blue Creek coal using the standard GRI core flow test.

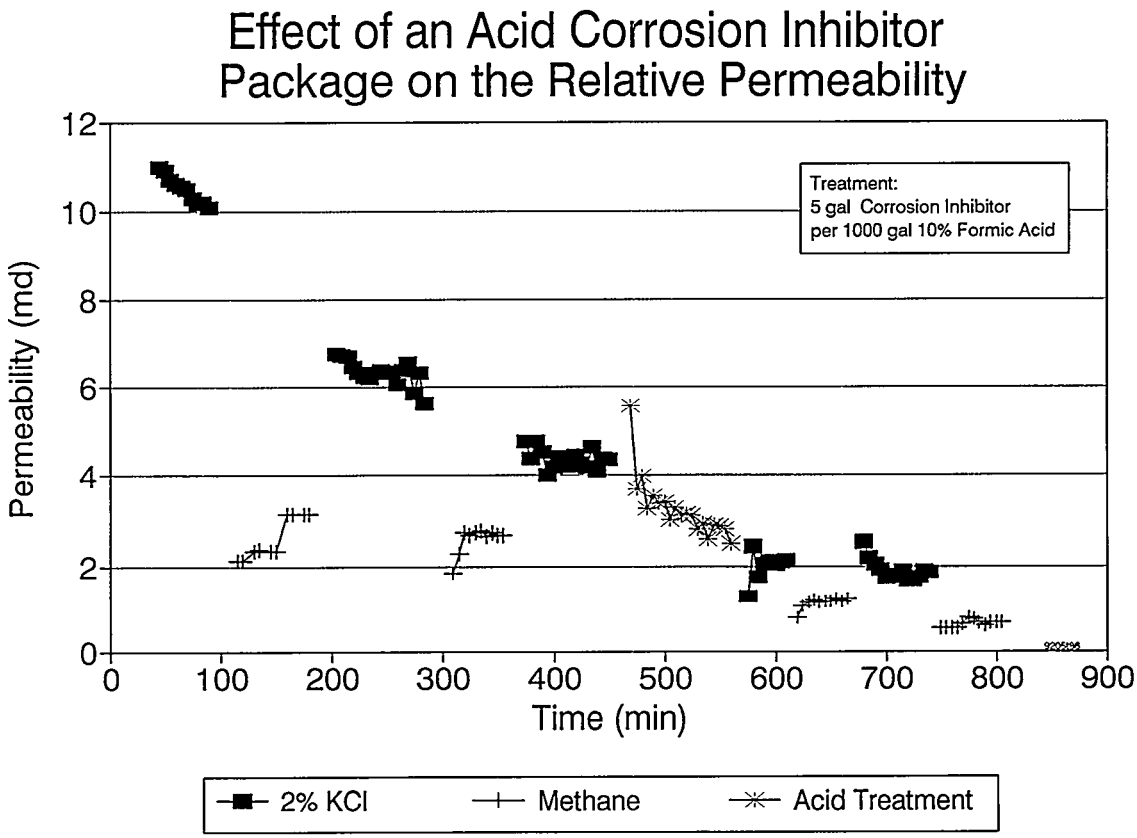


Figure 7. Effect of a standard corrosion inhibitor in formic acid on the relative permeability to gas and water of Blue Creek coal using the standard GRI core flow test.

INTERGAS '95

May 15-19, 1995
The University of Alabama
Tuscaloosa, Alabama USA

9533

Openhole Cavity Completions in Coalbed Methane Wells—Modeling of Field Data

M. Khodaverdian, H.H. Vaziri, University of Nova Scotia; I.D. Palmer, Amoco; and J.D. McLennan, TerraTek, Inc.

ABSTRACT

Cavity completions, also referred to as dynamic openhole completions, have been successfully performed in the "fairway" region of the San Juan Basin, for coalbed methane production. The cavity wells in this region generally yield production levels several folds greater than analogous hydraulically fractured wells. Meanwhile, outside of the "fairway" region, cavity completed wells have not been as effective as hydraulically fractured wells. The discrepancy between post-cavity production within and outside of the "fairway" has prompted an investigation of the mechanisms leading to successful cavity completions and their relation with the reservoir properties.

Earlier analyses of the field data strongly indicated that the size of the physical cavity (i.e., normally between 4 and 5 feet in radius) cannot account for the post-cavity production levels achieved within the "fairway" region. This suggests that cavity completions in coal induce a "zone of enhanced permeability" beyond the cavity wall which effectively connects the wellbore to the reservoir, thus leading to "high" production rates. In the current work, a series of numerical analyses were performed for several cavity wells in the San Juan Basin to verify the existence of the "enhanced permeability zone" and to determine the size of this zone as well as its contribution to the overall production. These analyses have shown that the radius of the "plastic" failure zone, with significant permeability enhancement, is less than 50 feet, but permeability enhancement can occur beyond this distance. The increased permeability within this zone is due to material plasticity and shear failure induced during the injection/surging cycles.

INTRODUCTION

Openhole cavity completion techniques use a series of air injections (or shut-ins for natural cavitation) and flowbacks to create a cavity and to stimulate the formation. The injection/surging cycles are typically performed over a one- to two-week period. During surging, the well is rapidly opened to the atmosphere to create high rate depressurization (actually a controlled blowout). Coal fails and sloughs into the wellbore, and is ejected from the well, leading to creation of a cavity.

These techniques have been used with overwhelming success in the "fairway" region (sweet spot) of the San Juan Basin (Figure 1). Some wells in this region, at depths of approximately 3000 ft, with 40 ft gross coal thickness, produce in excess of 10 MMCFD. The average cavity radius for typical wells in the fairway region has been determined to be 5 ft. However, the production rates observed require formation stimulation within a radius of over 100 feet from the wellbore. A number of potentially applicable mechanisms have been cited in explaining these substantial production rates [2,10,12,13]. The most prominent of these mechanisms (in addition to physical hole enlargement) are:

- The permeability in the formation around the cavity is increased due to material plasticity and shear failure during the injection/surging cycles.
- Natural, fractures and discontinuities within the formation are connected to the wellbore through the shear failure zone, i.e., cavity completions enhance formation connectivity to the wellbore. This mechanism may be potentially applicable if the bulk of the flow is through large-scale, isolated fractures within the formation.

Based on the previous work [2,10,13], the post-cavity formation may include three distinct zones, as illustrated in Figure 2. These include the physical cavity, a "plastic" zone immediately around the cavity, and an "intact" zone extending beyond the plastic zone. The physical cavity is induced as the drag forces during surging cause material tensile failure at the cavity wall. Repeated surging cycles enhance this process by weakening the coal in the vicinity of the cavity. The "plastic" zone around the cavity may be generated due to material shear failure. This is expected to result in significant permeability enhancement within the affected region. The formation outside of the "plastic" zone remains nominally intact; it does however probably experience changes in the stresses and, therefore, permeability.

Numerical evaluation of the mechanics of cavity completion has embraced the following goals:

- Verify the existence of a "permeability enhanced zone" around the cavity.

- Calculate the size of the permeability enhanced zone and its contribution to the overall well productivity.

Finite Element analyses of formation response during cavity completions have been performed using data from two GRI cooperative wells in the San Juan Basin. These are well I#2 at the COAL site, located within the "fairway" region, and the Amax Southern Ute Well #5-7, outside of the "fairway" region. These wells were selected for numerical analysis because of the differing in-situ conditions of the coal seams as well as the availability of fairly complete data sets. In well I#2, a 45 ft thick coal seam was stimulated at an approximate depth of 3150 ft. In Well #5-7, three coal seams, within a depth interval of 1320 ft to 1470 ft, were simultaneously treated; the thickness for each seam was between 15 and 20 ft.

NUMERICAL MODELING PROCEDURE

Numerical Model Description

A Finite Element program, ENHANS3 [13,16], was used for numerical modeling of the aforementioned cavity wells. This program is capable of real-time modeling of cavity wells using elasto-plastic analysis, coupled with single phase fluid flow (liquid or gas). The formation around the wellbore was modeled using a 2-D axisymmetric grid with the wellbore axis collinear with the vertical axis-of-symmetry. This grid allows representation of the various formations below and above the coal seam and, therefore, can be used for the analysis of multiple-seam cavity completions. With this grid, the material properties in the horizontal direction can only be varied as a function of the distance, r, from the wellbore, i.e., horizontal formation anisotropy is not included in the model.

The grid used for modeling each well extended to a radial distance of approximately 1900 ft from the wellbore to minimize boundary effects. The grid was composed of either eight-noded quadrilateral elements or six-noded triangular elements. Since material failure and plasticity occur in the near-field (close to the wellbore/cavity), the element sizes were varied as a function of the distance from the wellbore, with the finer elements allocated to the immediate vicinity of the wellbore.

Coal Physical and Mechanical Properties

As discussed, the model developed for the current analyses reflects three distinct concentric zones in the post-cavity formation, including the physical cavity, a "plastic" zone immediately around the cavity, and an "intact", but altered zone extending beyond the plastic zone. Numerical analyses of these zones require careful specification of the formation's physical and mechanical properties under various loading regimes up to and beyond failure. A material failure criterion was needed to determine the cavity size as well as the size of the plastic zone. A stress-dependent permeability criterion was also required to calculate the permeability within the plastic and intact zones during and after various injection/surging cycles.

To develop a failure criterion for coal, triaxial compression tests were initially performed at various confining stresses and pore pressures on coal samples representative of the San Juan Basin. The square samples used for these tests had a 4 in^2 cross-sectional area (2 inches in each dimension) and were 4 inches long. A Mohr-Coulomb failure envelope was constructed from these data, resulting in linear cohesion of 245 psi and an angle of internal friction of 50°, for mean effective stresses below 500 psi. However, when this failure criterion was used in the numerical model, the predicted cavity radii were much smaller than those typically observed in the "fairway" region. Therefore, it was speculated that the scale difference between the field and the laboratory specimens (used for triaxial tests) might have led to overprediction of the coal strength applicable on a field scale. It was further speculated that, while on a small scale (i.e., laboratory triaxial tests) the failure plane primarily passes through the intact coal, coal disturbance and failure in the field may occur along the cleats, thus leading to lower strength.

These observations led to the development of an alternate failure criterion for coal, based on the "cleat" shear strength. This was carried out by performing "direct shear tests" on coal samples. In these tests, the cleat shear strength was measured at different normal stress levels. Figure 3 shows the failure envelope (dashed line) constructed from individual direct shear test results (solid circles) performed on a representative medium volatile bituminous coal. This coal was well cleated, with a face cleat spacing of less than 0.5 inch. A bilinear Mohr-Coulomb failure envelope (i.e., the solid lines in Figure 3) was developed for use in the numerical model. In this approximation, the failure envelope is defined by the friction angle, ϕ, and cohesion, c, at "low" normal stresses and by ϕ' and c' at "high" normal stresses. *This bilinear failure envelope is an extremely important deviation from the conventional simplistic representations used for coal. It incorporates the lower cohesion and higher friction angle at low normal stresses (characteristic of dilatant materials) and incorporates cleat properties rather than the behavior of intact coal.* The values of ϕ, c, and ϕ' used in the current analyses were 50°, 0 psi, and 30°, respectively. Different values of c', ranging between 5 psi and 15 psi, were used to match the cavity radii to those observed in the field.

The cleat dilation data (i.e., increase in cleat width) from the direct shear tests was used to develop a permeability enhancement criterion for prediction of post-cavity formation permeability [3]. It has been long speculated that dilatant cleat behavior due to shearing stress is an important component in permeability change with stress, in addition to any changes strictly caused by variations in the effective mean stress such as those shown by Seidle [15]. Equation (1) estimates the coal permeability (md) as the material is subjected to deviatoric (i.e., shear) and hydrostatic stresses:

$$k_s(\sigma',T) = \frac{0.00833}{a}\left\{4.933\sqrt[3]{\frac{a\,k_i(\sigma')}{2}} + d_s(T)\right\}^3 + \frac{k_i(\sigma')}{2} \qquad (1)$$

where $k_i(\sigma')$ is the absolute permeability function (md) at a mean effective stress of σ', "a" is the average cleat spacing (cm), and $d_s(T)$ is the cleat dilation function given as:

$$d_s(T) = 56.41\,T^3 - 2.714\,T^2 - 5.580\,T \qquad (2)$$

In Equation (2), "T" is the normalized shear stress defined by:

$$T=\frac{\tau}{\tau_f(\sigma')} \quad (3)$$

where $\tau_f(\sigma')$ is the cleat peak shear strength at a normal stress of σ', determined from the failure envelope in Figure 3. The function $k_i(\sigma')$ in Equation (1) is defined by [15]:

$$k_i(\sigma') = k_o e^{-0.00288(\sigma'-\sigma'_o)} \quad (4)$$

in which k_o is the absolute permeability at the mean effective stress of σ'_o. Given the in-situ stresses and the average absolute permeability for a seam, the value of k_o can be determined from Equation (1). *The permeability criterion given by Equation (1) is an important concept because it indicates that even if the effective mean stress is increasing, as may happen during surging, the permeability may be increased, depending on the associated deviatoric stresses.*

Other coal mechanical properties required for Finite Element modeling are the Young's modulus, E, and Poisson's Ratio, ν. A hyperbolic stress-strain relation was used to represent deformation up to failure [1]. The parameters used in the hyperbolic relation incorporate an implied initial (peak) Young's modulus, E_i, of 100,000 psi. Based on laboratory triaxial test data, the value of Poisson's ratio for coal is in excess of 0.30 (at low deviatoric stresses), approaching 0.5 at failure, where the material can undergo shear deformation with little to no volume change. The hyperbolic stress-strain relations represent an initial (i.e., lower bound) Poisson's ratio, ν_i, of 0.30 at zero deviatoric stress and a value of 0.49 at failure.

Sensitivity Analysis

A limited parametric study was performed to determine the model sensitivity to several of these physical and mechanical properties; the results are summarized in Table 1. The parameters evaluated in the sensitivity analyses include the formation in-situ permeability, the cohesion, c′ (refer to Figure 3), Young's modulus, and Poisson's ratio. The "reference" values used in these analyses (base case) were 25 md for the in-situ permeability, c′=15 psi, E_i=100,000 psi, and ν_i=0.30. It should be noted that the typical cavity radius in the "fairway" is between 4 and 5 ft; similar to that obtained for the base case with c′=15 psi.

The numerical sensitivity to formation permeability was evaluated by analyzing a typical cavity well in the "fairway" region using in-situ permeability values of 2.5 md, 25 md (base case), and 250 md, respectively. These permeability values resulted in cavity radii of approximately 6.4 ft, 4.5 ft, and 3.1 ft, respectively. For the case with an in-situ permeability of 250 md, the maximum cavity radius did not increase after the third surging cycle, possibly indicating equilibration of the formation stresses at the cavity wall with the seepage (tensile) stresses induced during surging. The larger cavity radius for the in-situ permeability of 2.5 md is attributed to a larger near-wellbore pressure gradient during surging, resulting in increased seepage tensile stresses. The calculated plastic zone radii for the aforementioned permeability values were approximately 46 ft, 34 ft, and 30 ft, respectively.

The influence of cohesion, c′, on the cavity size and the size of the plastic zone was considered by performing additional analyses using cohesion values of 2 psi and 35 psi. These resulted in cavity radii of 6.4 ft and 2.0 ft, respectively. The plastic zone radii for these cohesion values were 52 ft and 12 ft, respectively.

The effect of Young's modulus was determined by performing parametric analyses, with E_i ranging between 30,000 psi and 450,000 psi. These analyses indicate that the magnitude of stiffness (E_i) does not have any significant influence on the size of the cavity and/or the plastic zone. The influence of Poisson's ratio on the cavity and plastic zone radii was evaluated by performing an analysis in which ν_i was set to 0.49 (in addition to the base case with ν_i=0.30). This resulted in a cavity radius of 7.5 ft and plastic radius of 38 ft. Considering that the base case (i.e., ν_i=0.30) resulted in cavity and plastic radii of 4.5 ft and 34 ft, respectively, it may be concluded that Poisson's ratio has a significant influence on the cavity size, but not necessarily on the size of the plastic zone.

NUMERICAL MODELING RESULTS

COAL Site I#2 Well

Well I#2 at the COAL site was cavitated during July 12-21, 1991. The COAL site is located in the north-west corner of the "fairway" (see Figure 1). A total of 49 cavity surging cycles were performed; twenty involved injecting a mixture of air and water pills prior to surging, and 29 followed wellbore shut-in to allow pressure buildup (i.e., natural cavitation) for periods of more than 10 minutes. Figure 4 shows the gamma log and the post-stimulation cavity dimensions, as measured using sonar caliper logging after the completion of all surging cycles.

During the first day of surging (i.e., the first six injection/surging cycles), the gas production rate was estimated to have increased from 107 MSCFD to over 560 MSCFD, both at a bottomhole pressure of 700 psi [8,9]. Peak gas production, 2200 MSCFD, was achieved during the fifth day of cavitation. During the eighth day of cavitation, significant interference (up to 20 psi pressure rise) was recorded in an observation well located 178 ft away, in the butt cleat direction. Interference time delay was determined to be between 1 and 5 minutes [8].

Finite Element analysis was performed to determine the formation response after the first day of surging in the I#2 well. Figure 5 shows the bottomhole pressure/surging history used in the numerical model. These data were constructed from the available field information, primarily daily reports; the injection pressures and rates had been periodically measured but were not monitored continuously. As is suggested in Figure 5, the minimum bottomhole pressure during surging was maintained at 80 psi. The basic parameters used in the model were:

Coal Seam Interval	3150-3195 ft
Vertical Stress Gradient (σ_v/d)	1.00 psi/ft
Horizontal Stress Gradient (σ_h/d)	0.70 psi/ft
Pore Pressure Gradient (p/d)	0.48 psi/ft
Absolute Permeability	25 md
Cohesion (c′)	15 psi
Gas Viscosity	0.0146 cp
Drilled Radius	0.5 ft

Figures 6 and 7 show the calculated profiles for the near-wellbore zone before surging (i.e., after drilling and drawdown) and immediately after the first day of surging (i.e., after the sixth surging cycle), respectively. The data in these figures include the formation effective stresses (radial, circumferential or hoop, and vertical), pore pressure, and absolute permeability as functions of the radial distance from the wellbore. These data represent the calculated values at the seam mid-height.

The data in Figure 6 suggest that some spalling and wellbore failure probably occurred as a result of drilling and drawdown (before surging), with the cavity radius increasing from 0.5 ft (drilled diameter) to approximately 1.2 ft. Figure 7 indicates that a cavity radius of 4.5 ft was predicted after all the surging cycles on the first day. As was suggested earlier, significant permeability enhancement is expected within the "plastic" zone where the material undergoes shear failure. The radius of the plastic zone increased from 12 ft before surging to approximately 34 ft after. Figure 8 compares the calculated permeability before and after surging. This figure indicates that permeability enhancement is not limited to the plastic zone; after the first day of surging, permeability values of more than twice the virgin value are predicted for radial distances between 34 and 60 ft.

In order to evaluate the formation response to continued surging in this well, numerical analysis was performed for a second day of stimulation. The stimulation included one natural cavitation cycle and three injection/surging cycles, all performed over a time period of four hours. The analysis resulted in a stable cavity radius of 5 ft and a plastic radius of approximately 40 ft after the first three surging cycles on the second day of cavitation (these values were 4.5 ft and 34 ft, respectively, after the first day of cavitation); there was no further change in these quantities during the fourth surging cycle. Therefore, it may be concluded that both the cavity size and the plastic zone stabilize after a certain number of surging cycles. This is not to say that further formation alteration did not occur subsequently, as obviously was represented by the peak production on the fifth day and the interference first encountered on the eighth day. It suggests however that much of the process of cavity creation occurred rapidly, that the plastic zone stabilized fairly quickly, and that far-field permeability alterations occurred more slowly.

Amax Southern Ute #5-7

The Amax Southern Ute #5-7 well was completed during September 18-21, 1992 [5,6,8]. This well is located outside of the north-west corner of the "fairway" region. Pre-stimulation production testing indicated marginal gas rates and 150 BPD of water. Nineteen injection/surging cycles were performed in this well, of which fourteen were performed with air injection only and 5 with air/water combinations [5,8]. The density log and the post-stimulation cavity dimensions are shown in Figure 9. Production testing after the first day of stimulation resulted in 5 MSCFD of gas; the water production rates are unknown. After the completion of all cavity cycles, the production rates increased to 17 MSCFD of gas and 380 BWPD. The average gas and water production rates during 1993 were 81 MSCFD and 159 BPD, respectively. These rates are several folds smaller than those of nearby hydraulically fractured wells [6].

Figure 10 shows the surface injection pressure (shaded line) and the air injection rate (solid line) for seven (7) injection/surge cycles performed during the first day of stimulation. These data were used for numerical modeling of this well. The various parameters used in the model are as follows:

Coal Seam Intervals	
Seam A	1320-1336 ft
Seam B	1342-1360 ft
Seam C	1450-1470 ft
Vertical Stress Gradient (σ_v/d)	1.00 psi/ft
Horizontal Stress Gradient (σ_h/d)	
Seams A and B	0.79 psi/ft
Seam C	0.66 psi/ft
Pore Pressure Gradient (p/d)	0.44 psi/ft
Absolute Permeability	
Seams A and B	25 md
Seam C	12 md
Cohesion (c')	
Seams A and B	5 psi
Seam C	15 psi
Gas Viscosity	0.0146 cp
Drilled Radius	0.5 ft

The different values of cohesion (c') for the three seams were determined by matching the calculated cavity radii with the measured values which are shown in Figure 9. Figures 11 and 12 show the numerically calculated data for seam B, before and after cavitation, respectively; Figures 13 and 14 show the same data for seam C. The post-cavitation numerical predictions show cavity radii of 5.3 ft, and 2.5 ft, respectively, for seams B and C. These radii are in fairly good agreement with the measured values in Figure 9. The corresponding calculated plastic failure radii for these seams are approximately 22 ft, and 16 ft, respectively.

Figure 15 shows a composite plot of the calculated absolute permeability for seams B and C after drilling (dashed line) and after surging (solid line). Comparison between the permeability data for seams B and C indicates a larger permeability enhanced zone for seam B, both before and after surging. Low production from seam C has been proposed as a possible cause of the poor productivity for this well [6].

WELL PERFORMANCE

The absolute permeability data calculated from the numerical model were analyzed to rationalize the effect of formation permeability improvement on post-cavity production. The analyses included calculation of the "average" formation permeability and the wellbore skin factor to compare with the measured field values.

Equation (5) is a simplistic representation of the equivalent (average) permeability between the cavity wall, r_1, and a distance of r_n from the wellbore in the post-cavity formation [11]. The formation around the wellbore was modeled as concentric rings with a constant permeability of k_i within each ring bounded by radii r_{i-1} and r_i.

$$k_{avg}(r_n) = \frac{\ln(\frac{r_n}{r_1})}{\sum_{i=2}^{n} \frac{1}{k_i} \ln(\frac{r_i}{r_{i-1}})} \quad (5)$$

This equation was applied to the calculated permeability data for the COAL site (Figure 8). The resulting "average" permeability data after drilling and after surging are plotted in Figure 16. This shows that k_{avg} between the cavity wall and a location 178 ft away from the wellbore (i.e., the offset observation well GRI#1 at the COAL site) was 77 md after the first day of surging; the in-situ permeability for the COAL site is approximately 25 md.

Typical post-cavitation permeability values predicted by the numerical model have also been observed for the Barnes B21 well, located in the northwestern portion of the "fairway" [14]. This well had been previously cavity completed, resulting in post-stimulation production of 6,000 MCFD. After two years of production, the average gas rate declined to 1,500 MCFD at which stage it was decided to recavitate the well. Prior to restimulation, an old Pictured Cliffs well, located 242 ft from the cavity well in the approximate direction of the maximum regional horizontal stress, was reconfigured to serve as an observation well. Two sets of injection/surging cycles were performed in the B21 well, at 4 days apart. During both sets of surges, a response was clearly seen at the observation well. Pulse analysis was performed on the interference data between the cavity well and the observation well to determine the "average" permeability [14]. These analyses resulted in an interwell absolute permeability of 27.6 md after the first set of surges and 48.1 md after the second set, an improvement ratio of 1.7. From Figure 16, the pre- and post-stimulation value of k_{avg}, within a radius of 240 ft from the I#2 well, were 40 md and 65 md, respectively, a ratio of 1.6.

The "average" permeability profiles were also calculated for the three coal seams in the Amax #5-7 well (using the permeability profiles shown in Figure 15); these data are shown in Figure 17. The predicted pre-stimulation (i.e., after drilling and a drawdown before cavitation) values of k_{avg} within 240 ft from the wellbore were approximately 27 md and 15 md for seams B and C, respectively. The post-stimulation values were 40 md and 21 md, respectively, yielding permeability enhancement ratios of 1.5 and 1.4, respectively. It is evident that the permeability enhancement ratio determined from pulse analyses for the Barnes B21 well is within the range of the predicted values for the I#2 well and the Amax #5-7 well.

The skin factor for the post-stimulation formation is approximated by Equation (6). In this equation, k_u is the "unaltered" formation permeability, the interval between r_{N-1} and r_N represents the outer most zone with altered permeability k_N, r_0 is the drilled diameter, and the interval between r_0 and r_1 is the cavitated zone with a permeability of $k_1 = \infty$ [9].

$$s_t = \sum_{i=1}^{N} (\frac{k_u}{k_i} - 1) \ln(\frac{r_i}{r_{i-1}}) \quad (6)$$

Application of Equation (6) to the COAL site data (Figure 8) results in steady state skin factors of -2.82 after drilling, and -4.67 after surging. The skin contributions due to the presence of the enlarged cavity alone before and after surging are -0.90, and -2.20, respectively. The post-stimulation skin factors for the Amax #5-7 well are -3.75, and -3.56 for seams B, and C, respectively.

The pseudo-steady-state flow efficiency (i.e., ratio of the reservoir fluid flow after stimulation to that of unstimulated reservoir) for single phase flow is given by Equation (7). In this equation, r_e represents the drainage radius [9].

$$R_q = \frac{\ln(\frac{0.473 r_e}{r_0})}{\ln(\frac{0.473 r_e}{r_0}) + s_t} \quad (7)$$

Assuming a drainage radius of 2106 ft (320 acre drainage area) and drilled radius of 0.5 ft, the predicted flow efficiency for the COAL site I#2 well is calculated to be 2.60

Using a single phase flow model, the short-term productivity ratio (i.e., production after surging to that after drilling and drawdown) for the I#2 well was calculated to be 3.0; a ratio of approximately 5.0 was determined from short-term productions in the field. A potential reason for the discrepancy between these ratios is that the numerical modeling of the pre-cavity wellbore involved pressure drawdown to 80 psi while the field bottomhole pressure was maintained at a minimum of 700 psi. The lower bottomhole pressure for numerical simulation may have resulted in larger pre-stimulation wellbore failure, thus a larger production rate. Reservoir modeling using the predicted permeability profiles is in progress to formalize the accuracy of the numerical cavitation modeling and provide more accurate predictions of the short-term and long-term wellbore productivity.

CONCLUSIONS

Numerical modeling of cavity stimulation described here and elsewhere [13] provides an unique approach to predicting the post-cavity formation properties and production levels. The procedures used in the analysis are complex and have not been detailed here. Regardless, certain critical aspects have been identified that must be considered in numerical modeling of cavities.

For example, two material-dependent factors which overwhelmingly regulate cavity formation and numerical predictions are the coal failure characteristics and the permeability enhancement criterion. A standard Mohr-Coulomb failure envelope, constructed from laboratory triaxial test data on coal, results in gross over-prediction of the coal shear strength applicable on a field scale, leading to underestimation of cavity dimensions and formation deliverability. It is speculated that this is due to scale differences between the laboratory and the field. To overcome this, a "cleat" shear failure criterion was developed which is believed to be more representative of the coal strength characteristics (e.g., cohesion) on a field scale.

Another extremely important development is a permeability enhancement criterion that uses the cleat dilational characteristics (under shear stress) to predict coal permeability at elevated shear stresses, up to failure. This criterion

effectively incorporates cleat dislocation during shearing to allow for permeability enhancement, even under certain loading conditions leading to increased mean effective stresses; this material response may be part of the reason why permeability reduction with depletion has not always been observed.

Numerical modeling of two wells has clearly shown that cavity completions induce a zone of enhanced permeability beyond the cavity wall; this is for predicted cavity sizes similar to those observed in the field. The permeability enhancement is particularly significant within a "plastic" zone induced by material shear failure during surging. However, increased permeability may also be achieved outside of the shear failure zone due to changing stress conditions. For the wellbores analyzed, the radius of the "plastic" zone appears to be no more than ten times the physical cavity radius, e.g., less than 50 ft for a typical well in the "fairway" with a cavity radius of 5 ft. The predicted size of this zone is highly dependent on the failure criterion applied in the model.

Preliminary evaluation of short-term production for the well I#2 at the COAL site, using a single phase flow model, indicated a production increase ratio of approximately 3 (i.e., ratio of the production after drilling and drawdown to the production after stimulation); the observed ratio for this well was 5. Short and long-term production simulation, using the predicted formation permeability data, is in progress.

ACKNOWLEDGEMENTS

This research project was funded by the Gas Research Institute (GRI) under Contract No. 5091-214-2220, "Spalling and the Development of a Hydraulic Fracturing Strategy for Coal." Dr. Richard Schraufnagel was the GRI Project Manager. The authors wish to thank GRI for supporting this project. We also gratefully acknowledge Mr. Matthew Mavor's (Tesseract Corporation) reservoir engineering support for this work.

REFERENCES

1. Duncan, J.M., Byrne, P.M., Wong, K.S., and P. Mabry, 1980, "Strength, Stress-Strain and Bulk Modulus Parameters for Finite Element Analyses of Stresses and Movement in Soil Masses," Report No. UCB/GR/78-02, Dept. of Civil Eng., U. of Cal., Berkeley, CA, 80p.

2. Khodaverdian, M.F., and J.D. McLennan, 1993, "Cavity Completions: A Study of Mechanisms and Applicability," Proceedings of the 1993 International Coalbed Methane Symposium, Tuscaloosa, Alabama, May 17-21.

3. Khodaverdian, M.F., Palmer, I.D., and H.H. Vaziri, 1994, "Spalling and the Development of a Hydraulic Fracturing Strategy for Coal," TR 95-34, October Monthly Progress Report to GRI.

4. Logan, T.L., Mavor, M.J., and M.F. Khodaverdian, 1993, "Optimization and Evaluation of Open-Hole Cavity Completion Techniques for Coal Gas Wells," SPE 25859, Joint Rocky Mountain Regional and Low Perm. Reservoirs Symposium, Denver, CO, April 26-28.

5. Logan, T.L., Mavor, M.J., and M.F. Khodaverdian, 1993, "Western Cretaceous Coal Seam Project," Quarterly Review of Methane from Coal Seams Technology, Volume 10, Number 4, GRI, Chicago, IL.

6. Logan, T.L., 1993, "Preliminary Results of Cooperative Research Efforts with Phillips Petroleum Company and Amax Oil and Gas, Inc., San Juan Basin" Quarterly Review of Methane from Coal Seams Technology, Volume 11, Number 4, GRI, Chicago, IL.

7. Mavor, M.J., 1991, "Evaluation of Coalbed Natural Gas Openhole Cavity Completion Productivity," Report to GRI, GRI-91/0374, Chicago, IL.

8. Mavor, M.J., Logan, T.L., Close, J.C., Pratt, T.J., and J.R. Robinson, 1993, "Western Cretaceous Coal Seam Project," Gas Research Institute Annual Report, GRI-93/0245, Chicago, IL.

9. Mavor, M.J., 1994, "Coal Gas Open-Hole Well Performance," SPE 27993, Centennial Petroleum Engineering Symposium, Tulsa, OK, August 29-31.

10. McLennan, J.D., Khodaverdian, M.F., and A.H. Jones, 1994, "Creation of an Open-Hole Cavity - Theory and Laboratory Results" Quarterly Review of Methane from Coal Seams Technology, Volume 11, Number 4, Gas Research Institute, Chicago, IL.

11. Monicard, R.P.,1, 1980: Properties of Reservoir Rocks: Core Analysis: Houston, TX, Gulf Publishing Co., 64 p.

12. Palmer, I.D., Mavor, M.J., Spitler, J.L., and R.F. Volts, 1992, "Openhole Cavity Completions in Coalbed Methane Wells in the San Juan Basin," SPE 24906, SPE 67th Annual Technical Conference, Washington, DC.

13. Palmer, I.D., and H.H. Vaziri, 1994, "Modeling of Openhole Cavity Completions in Coalbed Methane Wells," SPE 28580, SPE Annual Technical Conference and Exhibition, New Orleans, LA, September 25-28.

14. Palmer, I.D., and P.A. Edwards, 1995, "Pressure Interference and Pulse Analysis at Barnes B21 Well in Fairway of San Juan Basin," Internal Report, Amoco Production Company, Tulsa, OK.

15. Seidle, J.P., Jeansonne, M.W., and D.J. Erickson, 1992, "Application of Matchstick Geometry to Stress Dependent Permeability in Coal," SPE 24361, Proc. Rocky Mtn. Reg. Conference, Casper, WY.

16. Vaziri, H.H., 1994, "Finite Element Code ENHANS3 - User's Manual," Internal Report, Technical University of Nova Scotia, Halifax, Nova Scotia, Canada.

Table 1. Summary of the numerical model sensitivity analyses.

Parameter	Cavity Size	Plastic Zone Size
Absolute Permeability	Increases with decreasing permeability, assuming that the strength properties remain unchanged	Increases with decreasing permeability, assuming that the strength properties remain unchanged
Cohesion c′ (ranges between 5 and 15 psi for the seams evaluated)	Increases with decreasing cohesion	Increases with decreasing cohesion
Young's Modulus, E_i	Second order effect	Second order effect
Poisson's ratio, ν_i	Increasing Poisson's ratio leads to a significant increase in cavity radius.	Relatively insensitive

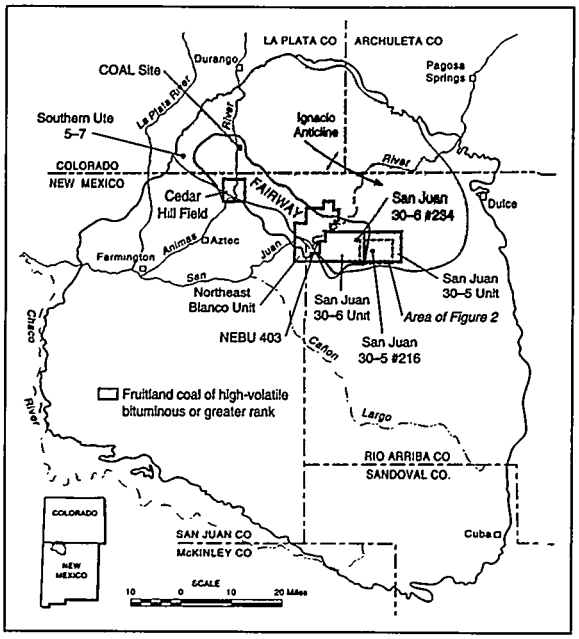


Figure 1. Map of the San Juan Basin showing the "fairway" region [6].

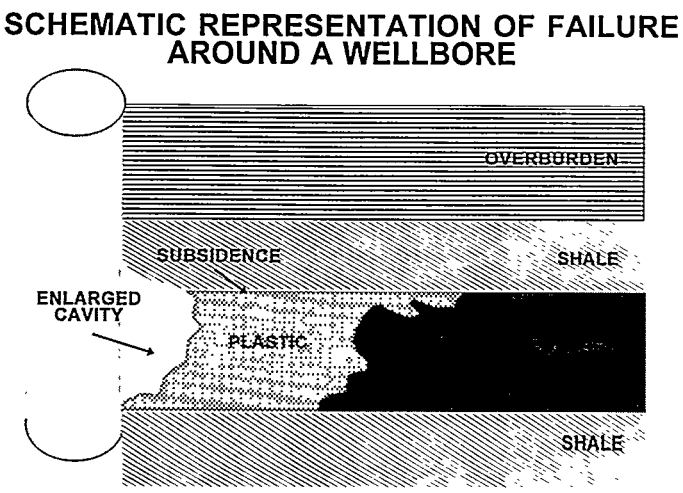


Figure 2. Conceptual schematic of the cavity and the "plastic" failure zone after cavitation.

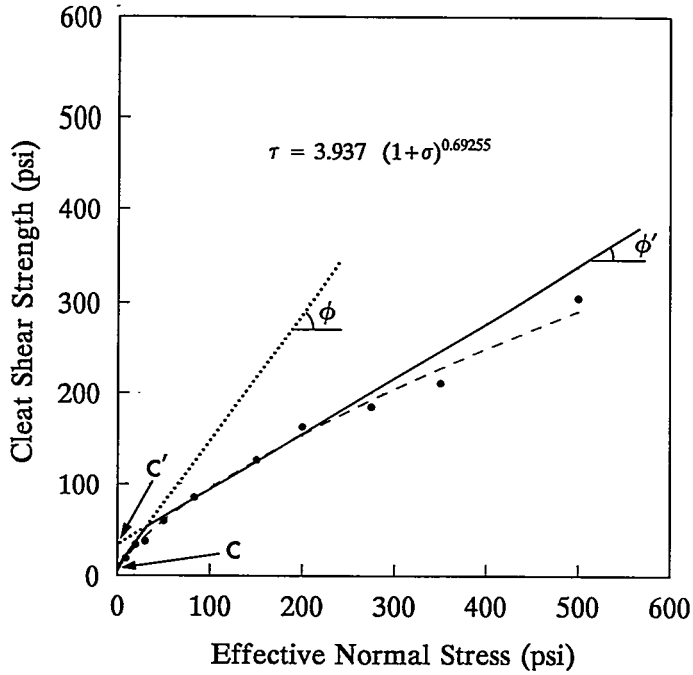


Figure 3. Shear failure envelope constructed using direct shear test data for coal.

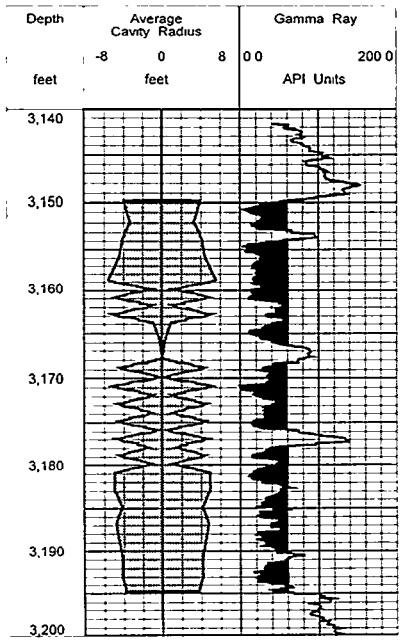


Figure 4. Gamma ray log and post-stimulation cavity dimensions for the COAL site I#2 well.

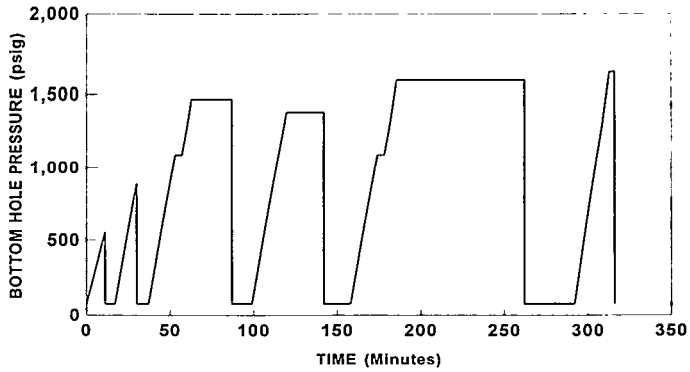


Figure 5. Bottomhole pressure data used for numerical modeling of I#2 well at the COAL site; data represents the first day of cavitation.

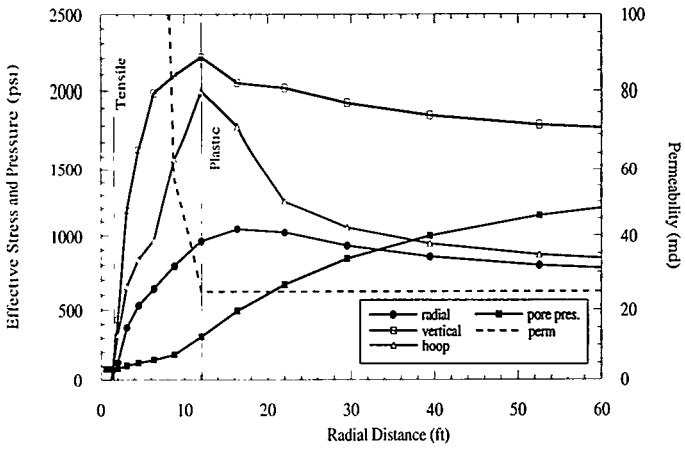


Figure 6. Calculated data for I#2 well after drilling (before surging).

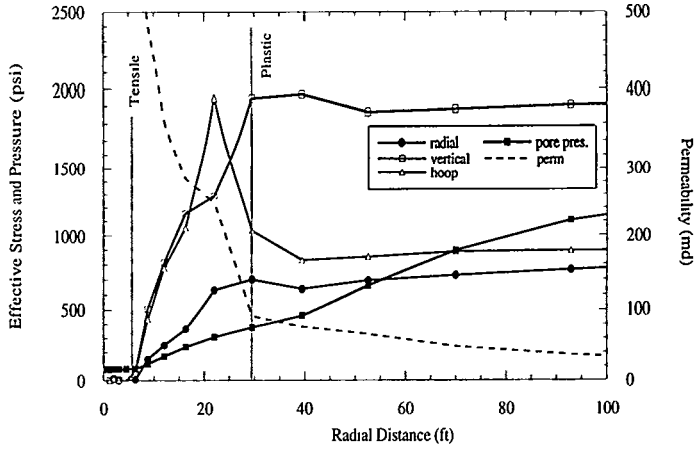


Figure 7. Calculated data for I#2 well after the first day of surging.

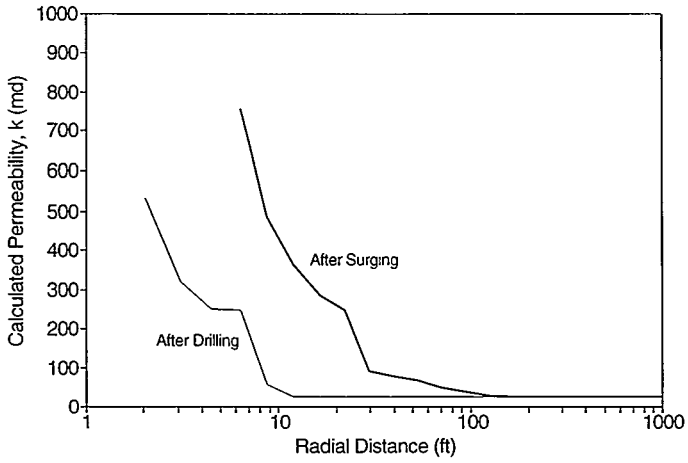


Figure 8. Comparison of the calculated permeability profile for I#2 well before and after surging.

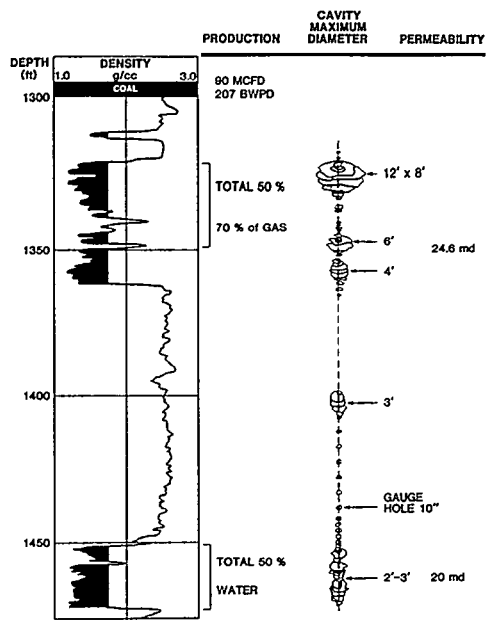


Figure 9. Density log and post-stimulation cavity dimensions for the Amax Well #5-7 [8].

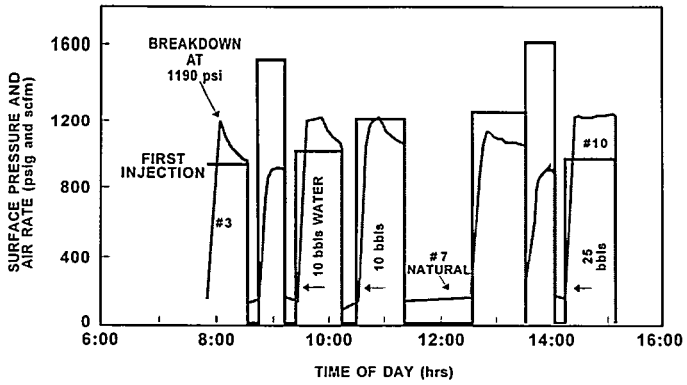


Figure 10. Surface pressure and injection data used for numerical modeling of the Amax Well #5-7; data represents the first day of cavitation.

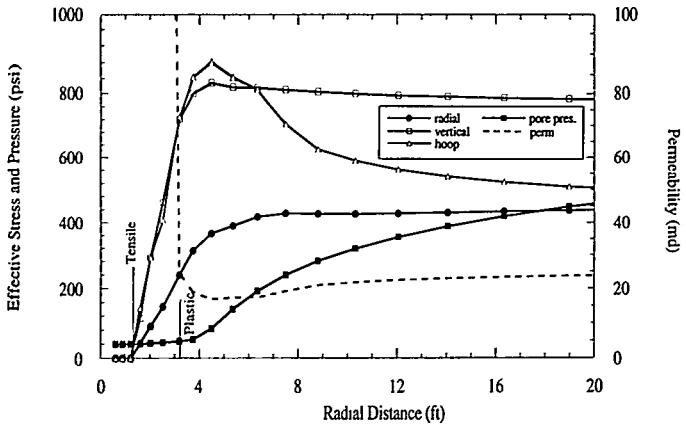


Figure 11. Calculated data for seam B in Well #5-7 after drilling (before surging).

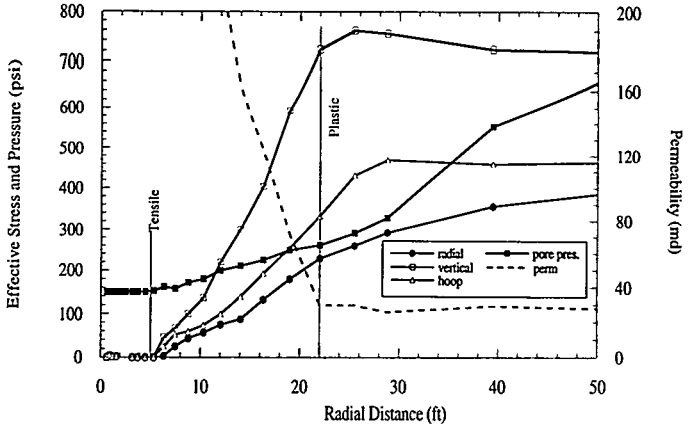


Figure 12. Calculated data for seam B in Well #5-7 after the first day of surging.

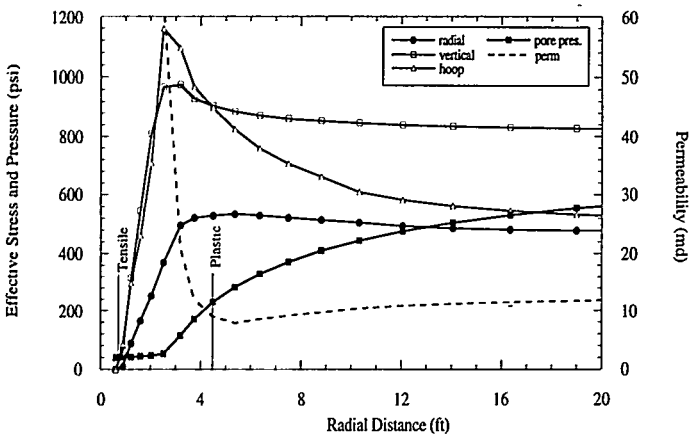


Figure 13. Calculated data for seam C in Well #5-7 after drilling (before surging).

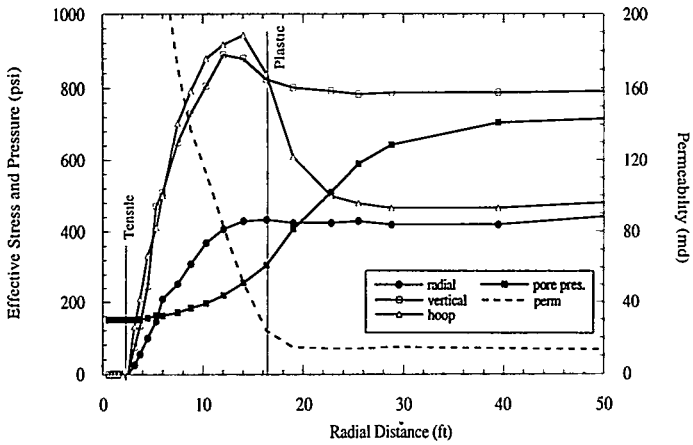


Figure 14. Calculated data for seam C in Well #5-7 after the first day of surging.

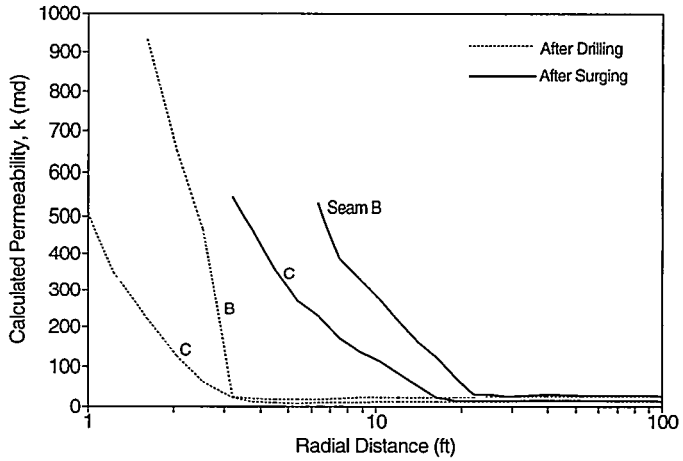


Figure 15. Calculated absolute permeability for seams B and C in the Amax Well #5-7 before surging (dashed lines) and after surging (solid lines).

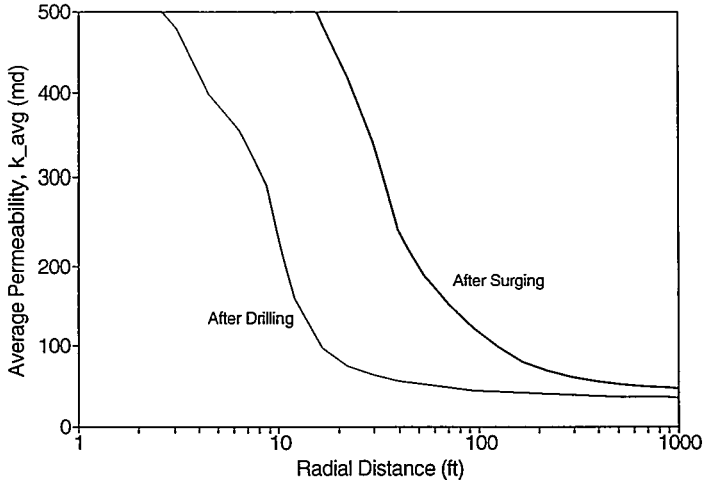


Figure 16. Calculated "average" permeability between the cavity and the specified radial distance - I#2 well at the COAL site.

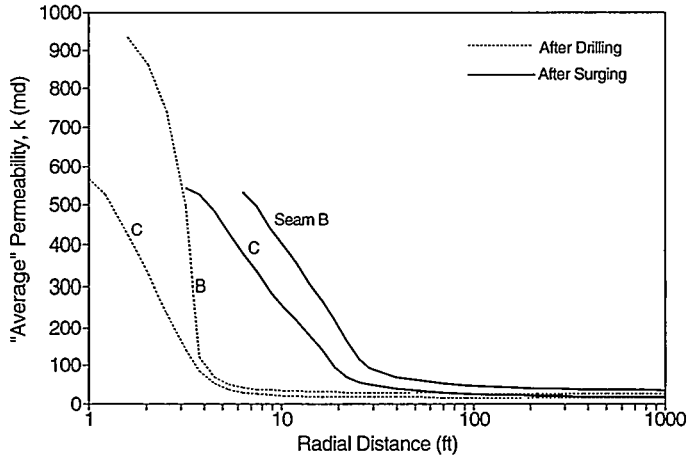


Figure 17. Calculated "average" permeability between the cavity and the specified radial distance - Amax Well #5-7 (Seams B and C).

INTERGAS '95

May 15-19, 1995
The University of Alabama
Tuscaloosa, Alabama USA

9510

Hydrogeologic Factors Affecting Dynamic Open-Hole Cavity Completions in the San Juan Basin, USA

A.R. Scott and W.R. Kaiser, Bureau of Economic Geology, The University of Texas at Austin

ABSTRACT

The most successful area for dynamic open-hole cavity completions in the San Juan Basin is the northwest-trending high-productivity fairway in the north-central part of the basin, defined by wells producing more than 1,000 Mcf/d and relatively small volumes of water. No single factor explains cavitation, which is a complex process controlled by a poorly understood interplay among many variables. Successful completions are dependent on basin hydrogeology where high permeability, high reservoir pressures, and fully gas-saturated coals are the critical factors in successful completions. However, other factors, such as carbon dioxide content of coal gases, reservoir heterogeneity, coal properties (ash content, hardness, etc.), coal rank, in-situ stress, and cleat domains, are also important. The generation and conventional trapping of secondary biogenic gases may contribute to successful cavity completions and high productivity.

The high-productivity fairway corresponds to the southern and eastern limits of regional artesian overpressure. The northern boundary of the fairway corresponds to maximum net coal and the northern limit of upward flow as defined hydrodynamically, whereas the southeastern margin of the fairway is controlled by a major northeast-trending channel sandstone belt that disrupts laterally continuous coal beds. The southern boundary of the fairway is probably controlled by pinch-out and/or offset of coal beds by faults along a structural hingeline and possibly by permeability barriers within laterally continuous coals.

INTRODUCTION

Most coalbed methane wells require some type of stimulation to connect the wellbore to the natural fracture system. Dynamic open-hole completions have been attempted with varying degrees of success in the San Juan, Piceance, and Black Warrior Basins in the United States and in the Southern Bowen Basin in Australia in coals ranging in rank from high-volatile C bituminous to low-volatile bituminous (T. L. Logan, personal com., 1993). Although hydraulic fracturing is the most common technique for stimulating coalbed methane production in the northern and southern parts of the San Juan Basin [1], dynamic open-hole cavity completions are used with variable success in the north-central part of the basin, indicating that some combination of factors results in successful open-hole cavity completions (fig. 1). However, hydraulic fracturing is more successful than dynamic open-hole cavity completions in certain areas of the basin, whereas dynamic open-hole cavity completions outperform hydraulic fracturing in other parts of the basin. The area of most successful dynamic open-hole cavity completions has been the northwest-trending high-productivity fairway, in the north-central part of the San Juan Basin, defined by wells producing more than 1,000 Mcf/d and relatively small volumes of water [1] (fig. 1). Nearly 80 percent of the wells within the high-productivity fairway were stimulated using some type of dynamic open-hole cavity completion technique [2]. However, the area of successful dynamic open-hole cavitations extends north of the high-productivity fairway (fig. 1). The objectives of this study, supported by the Gas Research Institute, are to (1) discuss hydrogeologic factors that affect successful open-hole cavitation in the north-central San Juan Basin and (2) evaluate geologic factors affecting high production rates in the high-productivity fairway.

DYNAMIC OPEN-HOLE COMPLETIONS

One of the first attempts to complete in Fruitland coals was performed by Stanolind Oil & Gas Company (now Amoco Production Company) in 1953 [3]. The forerunner of modern dynamic open-hole cavity completions was the Cahn No. 1 well, which was completed by Amoco in 1977. Coal was allowed to slough naturally into the wellbore for a long time and after completion produced 2,000 Mcf/d (57 Mm^3/d) [1, 4]. In the late 1980's, Meridian, Inc., began using a similar method in completing wells in the high-productivity fairway. Since then, numerous coalbed methane wells in the high-productivity fairway have been stimulated using dynamic open-hole completions. A dynamic open-hole cavitation is considered successful in a mechanical sense if a physical cavity is created, whereas the cavitation can also be considered a success if the well

produces gas at a rate higher than would be expected if other completion techniques were used [2]. However, it is important to remember that a mechanically successful cavitation does not necessarily guarantee a high production rate because there are other hydrogeologic factors affecting coalbed methane producibility [5] that may or may not influence the physical process of cavitation.

Wells completed in the high-productivity fairway, using the dynamic open-hole cavity technique, have significantly higher production (1,700 Mcf/d; 48 Mm^3/d) than fracture-stimulated wells that average 400 Mcf/d (11 Mm^3/d) [2]. According to Kelso [2], 10 coalbed methane wells originally completed using hydraulic fracturing were recompleted using dynamic open-hole cavitation, resulting in a 30-fold increase in production. The increase in production rate does not correspond to the size of the cavity, which may exceed 10 ft (3 m) in diameter, but rather with the development of shear fractures that are usually perpendicular to the face cleat direction. For example, at one location in the north-central San Juan Basin, cavitation increased gas production 13 times and water production 3.3 times over pre-stimulation production [6, 7]. The physical cavity increased production only 1.6 times, indicating that most of the production increase was due to shear and tensile fracture development.

The lower production rate of hydraulically fractured wells is attributed to the interaction of the coal with fracturing fluids, sorption-induced swelling, and possible plugging of the cleat system by residual gels that reduce permeability [1, 7–9]. Additionally, changes in the relative permeability of gas to water may occur during dynamic open-hole cavitation, resulting in higher gas production [1].

HYDROGEOLOGIC FACTORS AFFECTING DYNAMIC OPEN-HOLE CAVITATION

Previous studies have suggested that high permeability, high reservoir pressures, and fully gas-saturated coals are major factors affecting the success of dynamic open-hole cavitations in the high-productivity fairway [1, 2, 4]. However, no single factor explains cavitation, which is a complex process controlled by a poorly understood interplay among many variables (fig. 2). However, other influences, such as cleat domains, coal rank, in-situ stress, carbon dioxide content of coal gases, coal properties (ash content, hardness, etc.), and reservoir heterogeneity, are also important.

Permeability

Permeability is one of the key factors for successful open-hole cavitation completions, and previous studies suggest that a minimum of 2 to 10 md is required to achieve a mechanically successful cavitation [2, 4, 9]. Horizontal and vertical permeability anisotropy are also important for successful cavitation and producibility [1]. Low-permeability reservoirs with a poorly developed natural fracture system or well-cleated coals with relatively high permeability and associated high-water production will not have exceptionally high gas production rates [5], regardless of how mechanically successful a dynamic open-hole cavitation is. Water production in coalbed methane reservoirs is often an indicator of sufficient permeability for coalbed methane producibility [5, 10] and may also indicate sufficient permeability for successful cavitation.

Pressure Regime

Another key parameter for successful dynamic open-hole cavitation is overpressure [1, 11]. Although a hydrocarbon origin of overpressure has been proposed, a basinward sloping potentiometric surface, downflow chlorinity gradient, strata-bound overpressure, and geologically young (33,176 years), isotopically light water indicate that Fruitland Formation waters are meteoric and that overpressure is artesian in origin [10] (fig. 3). Pinch-out of coal beds, faulting along a structural hingeline, and permeability barriers within coal beds inhibit the basinward movement of meteoric water through laterally continuous coals. High pore pressures associated with overpressured conditions in the northern part of the San Juan Basin may facilitate shear and tensile fracture development during cavitation and increase producibility. Additionally, vertical pressure gradients in the high-productivity fairway are near or above the coal fracture gradient, which may enhance cavitation and fracture development.

Gas Saturation

Coals that are saturated to oversaturated with respect to gas may also be important for successful dynamic open-hole cavitation (D. Decker, personal com., 1993). The internal energy of the combined coal and sorbed gas system decreases during gas desorption, suggesting that the gas must store some energy such that work is performed during coal outbursts [12]; the work performed by the desorbing coal gas may contribute to cavity formation. The maximum amount of work that can be performed by a gas during desorption is a function of the sorption isotherm and can be described thermodynamically. Although successful cavitation may depend on fully gas-saturated coals, gas saturation may be more critical to high coalbed methane producibility.

Coals are saturated to oversaturated with respect to methane during active gas generation, suggesting that a minimum level of thermal maturity (high-volatile A bituminous) is required for fully gas saturated coals. However, as temperature decreases during uplift and erosion, the sorption isotherm of the coal changes such that the coals become undersaturated with respect to methane [13]. Therefore, the presence of high-volatile A bituminous and higher rank coals does not necessarily indicate the presence of fully gas-saturated coals. Relatively little thermogenic methane is generated from the coals after uplift and basinal cooling, indicating that the methane required to saturate the coals must be derived from other sources. Scott and others [14] suggested that secondary biogenic gases generated by bacteria transported in

meteoric water through permeable coal beds and the migration and conventional trapping of thermogenic and/or secondary biogenic gases are responsible for the presence of fully gas saturated coals in the northern San Juan Basin.

Cleat Domains

Permeability in the north-central San Juan Basin is highest in the high-productivity fairway and decreases abruptly to the southwest. Tremain and others [15] recognized the presence of northwest- and southeast-trending cleat domains in the northern San Juan Basin and suggested that the region of cleat-domain overlap may be an area of enhanced permeability. The region of cleat-domain overlap generally corresponds to the area of mechanically successful dynamic open-hole cavity completions (fig. 1) and also extends southwestward to include at least part of the high-productivity fairway. The area where dynamic open-hole cavity completions are successful from a production standpoint is smaller than the region where dynamic open-hole cavities are considered successful from a mechanical standpoint. Therefore, although permeability is important for mechanical and production success in dynamic open-hole cavitation, other factors are required to achieve high coalbed methane producibility. However, areas of cleat domain overlap or structurally enhanced permeability may be favorable for successful dynamic open-hole cavitations.

Coal Rank

Coals in the high-productivity fairway are generally high-volatile A bituminous (vitrinite reflectance values between 0.78 and 1.10%) (fig. 4), and previous studies suggest that coal rank may be important in dynamic open-hole cavitation and coalbed methane producibility in the northern part of the San Juan Basin [2, 16]. Palmer and others [1], recognizing that the minimum compressive rock strength of coal does not correspond to the high-volatile A bituminous coal rank, suggested that other parameters are more important than coal rank in mechanically successful dynamic open-hole cavitation. Furthermore, if coal rank were a dominant factor in successful dynamic open-hole cavitations, then the technique would work consistently well in other basins containing high-volatile A bituminous and higher rank coals.

Significant quantities of gas are not generated from coal until a certain threshold of thermal maturity is reached during the high-volatile A bituminous rank. Thus, large volumes of thermogenic gas are not generated from lower rank coals, indicating that saturation of the coal with respect to methane does not occur without migration and conventional trapping of thermogenic gases in low-rank coals.

In-Situ Stress

The orientation of in-situ stress will determine the direction of shear and tensile fractures and cavity geometry formed during dynamic open-hole cavity completions. The following discussion of the geomechanics of dynamic open-hole cavity completions is summarized from the work of Palmer and others, Logan and others, and McLennen and others [1, 4, 17]. The tensile failure zone developed during hydraulic fracturing is parallel to the maximum horizontal stress direction, which may be in the face or butt cleat direction. This zone may contain numerous connected parallel fractures that may extend as much as 100 to 200 ft (30 to 60 m) from the wellbore. As pressure is decreased during cavitation, shear failure zones, developed in a manner similar to wellbore breakout, are perpendicular to maximum horizontal stress. Fractures formed during shear failure are perpendicular to the more permeable face cleat direction and are believed to be one of the major reasons for the success of dynamic open-hole cavitations.

A more connective cleat network will develop if the difference between maximum and minimum horizontal stresses is small or where fluid pressure in the cleat system is high. Low effective stress, resulting from overpressured conditions and/or low in-situ stresses, enhances cleat movement, promotes self-propping of shear and tensile fractures, and induces larger apertures to allow for improved fluid flow. Additionally, low cohesion promotes the development of larger cavities and permeability modification at greater distances from the wellbore.

Carbon Dioxide Content

The distribution of wells producing coalbed gases with high carbon dioxide contents corresponds to areas of highest production in the fairway, suggesting that carbon dioxide may be important during cavitation (fig. 5). As reservoir pressures decrease during cavitation, the energy released during carbon dioxide exsolution from bicarbonate-rich formation waters, coupled with changes in coal volume during desorption, may enhance shear and tensile fracture development during cavitation.

Previous studies have documented that coal volume increases when carbon dioxide is sorbed onto the coal, suggesting that desorption of carbon dioxide from the coal will result in coal matrix shrinkage and increased permeability. Laboratory experiments performed by Harpalani and Chen [18] found that coal volume increased by 0.2 to 1.6% as pressure increased to 2,200 psi (15.2 MPa). Additional experiments found that permeability increased more than 16 times as pressures were decreased from 900 to 90 psi (6.2 to 0.6 MPa); 75% of the permeability increase was attributed to matrix shrinkage during desorption. Produced gas from Fruitland coal beds in the high-productivity fairway have high carbon dioxide contents that may exceed 10% [19] (fig. 5). Because proportionally more carbon dioxide is sorbed onto coal surfaces than is in the produced gas [20], matrix shrinkage during desorption may affect dynamic open-hole cavitation. A minimum carbon dioxide threshold for successful cavitation has not been established, although the area of successful dynamic open-hole cavitations in the northern San Juan Basin (fig. 1) corresponds to a carbon dioxide content of more than 3% (fig. 5). The decrease in reservoir pressure

during cavitation may also result in carbon dioxide exsolution from bicarbonate-rich formation waters, which may assist cavitation. This process is analogous to the pressure release when a bottle of carbonate water is opened. However, exsolution of carbon dioxide may not release enough energy to significantly enhance cavitation, and a detailed evaluation of the process may be warranted.

Coal Properties

Dynamic open-hole cavitation may be affected by ash content and grindability (hardness) [21] as well as by cleat spacing. Coal is compositionally complex and varies within individual coal beds and laterally between wells [22]. Therefore, changes in maceral composition, ash-content, and hardness may affect cavity development and the formation of tensile and shear fractures. Maceral composition may also affect the amount of gas sorbed to the coal surface, resulting in the situation where some parts of a coal bed may be saturated with methane, whereas other parts are undersaturated.

Coal is often sensitive to fracture fluids introduced into the well during completion [8], and the volume and types of fluid that are in contact with the coal vary significantly between dynamic open-hole cavitation and hydraulic fracturing techniques [1]. The effect that wettability has on cavitation (water or gas wet) remains uncertain, although Palmer and others [1] suggested that injection of incompatible water could change wettability and alter the relative permeability of gas to water in a coal bed, thereby affecting production. Breakage of coal during cavitation could result in a fresh coal surface's having different wettability relative to previous fractures contacted by injection fluids. Additionally, fractures generated during cavitation remain propped open by coal fines and/or rotation of coal blocks [9], suggesting that coal properties such as hardness and ash content may affect the size and quantity of material mobilized during the cavitation process.

Reservoir Heterogeneity

Reservoir heterogeneity exists on several scales in coalbed methane reservoirs. Heterogeneity can exist on a microscopic scale, as evidenced by maceral variability, on a macro scale, where significant changes in fracture development, gas content, hardness, and ash content occur on the order of several feet (1 m) [21], and on a basinwide scale, as shown by production heterogeneity in the high-productivity fairway in the northern San Juan Basin (fig. 1). Anisotropy within individual seams and between seams may significantly affect the size of the cavity and the production success of dynamic open-hole cavitations; individual coal beds may respond differently to cavitation [9, 21]. Permeability anisotropy due to variable cleat spacing and aperture width occurs in many coal reservoirs [6, 23]. Variability of cleat spacing, and cleat aperture width locally, may also affect the mechanical properties of coal and the success of cavitations.

HYDROGEOLOGIC CONTROLS ON CAVITATION AND THE HIGH-PRODUCTIVITY FAIRWAY

Recent studies by Kelso [2, 24] determined that the 600 producing open-hole cavity wells, representing 34% of the total coalbed methane wells in the basin, account for more than 73% of current coalbed methane production. Over 225 open-hole wells produce at rates of more than 1 MMcf/d (28.2 Mm^3/d). Many factors affect successful dynamic open-hole cavities and high coalbed methane producibility. However, a distinction must be made between high coalbed methane producibility due to completion technique and high producibility due to favorable geologic settings. The area of mechanically successful dynamic open-hole cavity completions extends north of the high-productivity fairway, suggesting that high production rates in the high-productivity fairway are not entirely the result of completion techniques but are influenced by geologic and hydrologic setting as well. The high-productivity fairway corresponds to the southern and eastern limits of regional artesian overpressure (figs. 3 and 6), and the transition zone between overpressure and underpressure is characterized by the presence of overpressured and underpressured coal beds within the same well. The width of this transition zone depends on the type of permeability barrier (fig. 7).

The southern margin of the high-productivity fairway is characterized by a distinct northwest-trending boundary separating mechanically successful natural cavitation attempts from failures [2]. This boundary also separates artesian overpressure from underpressure, highly productive (>1,000 Mcf/d) wells from lower productive (<250 Mcf/d) wells, high-gas-content coals (>500 scf/ton; 15.6 cm^3/g) from low-gas-content coals (<200 scf/ton; 6.3 cm^3/g), well-cleated, higher permeability (5 to 65 md) coals from poorly cleated, lower-permeability (<2 md) coals, and chemical dry, carbon dioxide-rich (>6%) coal gas from chemically wet, carbon dioxide-poor(<2%) coal gas [10, 14, 16, 25] (fig. 8). The southern boundary also corresponds to the transition from high-volatile B to high-volatile A bituminous coals, leading previous researchers to suggest that coal rank is a critical parameter for successful open hole cavitation and high producibility [2, 16]. Although the transition to high-volatile A bituminous coal rank corresponds to the southern boundary of the high-productivity fairway, coal rank and producibility do not correspond along the eastern margin of the high-productivity fairway [1] (fig. 4), suggesting that factors in addition to coal rank are probably more important for high coalbed methane producibility.

Ayers and others [26] and Kaiser and others [10] suggested that pinch-out of coal beds and/or faulting along a structural hingeline inhibited the basinward movement of meteoric water. Although some coal beds are continuous

across the southern boundary of the high-productivity fairway, permeability barriers may also exist within individual coal beds. Permeability anisotropy within individual coal beds and/or precipitation of calcite from bicarbonate-rich formation waters are two examples of intercoal permeability barriers. Scott and others [14] suggested that coal gases in the high-productivity fairway were derived from multiple sources: (1) thermogenic gases generated in-situ during coalification (25 to 50%), (2) secondary biogenic gas generated by bacteria introduced into the coal beds by meteoric water after coalification (15 to 30%), and (3) migrated thermogenic gases (12 to 60%). Therefore, exceptionally high coalbed methane producibility and successful dynamic open-hole cavity completions are influenced by conventional and hydrodynamic trapping of thermogenic and secondary biogenic gases along the southern margin of the high-productivity fairway.

The northern boundary of the fairway corresponds to decreasing net coal thickness and the northern limit of upward flow as defined hydrodynamically, whereas the southeastern margin of the fairway is controlled by a major northeast-trending channel sandstone belt that disrupts laterally continuous coal beds (figs. 4 and 6). The reasons for permeability decrease northeastward of the high-productivity fairway remain uncertain [1], although permeability anisotropy may be linked to the generation of secondary biogenic gases. Previous research indicates that a significant amount (15 to 30%) of coal gases in the high-productivity fairway were generated by bacteria introduced by meteoric water [14, 25]. Bioconversion of coal to methane and carbon dioxide may enlarge cleat apertures and thereby increase permeability [27], suggesting that higher permeabilities in the high-productivity fairway may be partially attributed to permeability enhancement by bacteria.

CONCLUSIONS

(1) No single factor explains cavitation, which is a complex process controlled by a poorly understood interplay among many variables. However, permeability, high reservoir pressures, and fully gas saturated coals are major influences on cavitation success.

(2) Other factors such as cleat domains, coal rank, in-situ stress, carbon dioxide content of coal gases, coal properties (ash content, hardness, etc.), and reservoir heterogeneity are also important in successful dynamic open-hole cavitation.

(3) Basin hydrogeology directly or indirectly influences nearly all of the factors affecting successful dynamic open-hole completions. The combination of successful dynamic open-hole completions and exceptionally high coalbed methane producibility probably requires an active hydrodynamic system.

(4) The area of mechanically successful dynamic open-hole cavity completions extends north of the high-productivity fairway, suggesting that high-coalbed methane production rates are not entirely due to completion techniques but are also influenced by geologic and hydrologic setting.

(5) The high-productivity fairway corresponds to the southern and eastern limits of regional artesian overpressure. Pinch-out of coal beds, faulting along a structural hingeline, and permeability anisotropy within coals are permeability barriers along the southern margin of the high-productivity fairway.

(6) The northern boundary of the fairway corresponds to decreasing net coal thickness and the northern limit of upward flow as defined hydrodynamically, whereas the disruption of laterally continuous coals by a major northeast-trending channel sandstone belt defines the eastern margin of the fairway.

(7) Successful dynamic open-hole cavitation and high gas production rates in the high-productivity fairway were enhanced through the generation and conventional trapping of methane and carbon dioxide during secondary biogenic gas generation. Enlargement of cleat aperture widths during the bioconversion of coal to methane and carbon dioxide may contribute to higher permeabilities and successful cavitation in the fairway.

ACKNOWLEDGMENTS

This research was funded by the Gas Research Institute under contract number 5091-214-2261. Several of the concepts developed in this paper originated from a September 1993 meeting organized by the Bureau of Economic Geology for the Gas Research Institute that was attended by Rich McBane (GRI), Andrew Scott, W. R. Kaiser, S. E. Laubach, and R. J. Finley (Bureau of Economic Geology), R. H. Meek (Conoco, Inc.), T. L. Logan and J. C. Close (Resource Enterprises, Inc.), A. D. Decker (Advanced Resources International, Inc.), and Magell Candelaria (ARCO). All these individuals contributed to our understanding of the factors affecting successful dynamic open-hole cavitations, and their efforts are gratefully acknowledged. Critical reviews by Muhammad Razi and Tucker F. Hentz improved the manuscript. Word processing was by Susan Lloyd and layout was by Jamie H. Coggin. Editing was by Amanda R. Masterson. Drafting was provided by the cartographic staff of the Bureau of Economic Geology under the direction of R. L. Dillon. This publication was authorized by the Director, Bureau of Economic Geology, The University of Texas at Austin.

REFERENCES CITED

1. Palmer, I. D., Mavor, M. J., Spitler, J. L., Seidle, J. P., and Volz, R. F., 1992, "Openhole cavity completions in coalbed methane wells in the San Juan Basin": Society of Petroleum Engineers paper SPE 24906, presented at the 67th Annual Technical Conference and Exhibition, Washington, D.C., October 4–7.
2. Kelso, B. S., 1994, "Geological control on open-hole cavity completion in the San Juan Basin": Quarterly Review of Methane from Coal Seams Technology, v. 11, no. 3 & 4, p. 1–6.
3. Dugan, T. A., and Williams, B. L., 1988, "History of gas produced from coal seams in the San Juan Basin": *in* Fassett, J. E., ed., Geology and coalbed methane resources of the Northern San Juan Basin, Colorado and

New Mexico: Rocky Mountain Association of Geologists Guidebook, p. 1–9.
4. Logan, T. L., Mavor, M. J., and Khodaverdian, M. K., 1993, "Optimizing and evaluation of open-hole cavity completion techniques for coal gas wells": Proceedings, 1993 International Coalbed Methane Symposium, v. II, p. 609–622.
5. Kaiser, W. R., Hamilton, D. S., Scott, A. R., Tyler, Roger, and Finley, R. J., 1994, "Geologic and hydrologic controls on the producibility of coalbed methane": Journal of the Geological Society of London, v. 151, p. 417–420.
6. Mavor, M. J., 1991, "Evaluation of coalbed natural gas open-hole cavity completion productivity": Gas Research Institute Topical Report, GRI-91/0374, variously paginated.
7. Mavor, M. J., Close, J. C., and Pratt, T. J., 1991, "Western Cretaceous coal seam project summary of the Completion Optimization and Assessment Laboratory (COAL) site": Gas Research Institute Topical Report, GRI 91/0377, variously paginated.
8. Puri, R., King, G. E., and Palmer, I. D., 1991, "Damage to coal permeability during hydraulic fracturing": Proceedings, 1991 International Coalbed Methane Symposium, p. 247–255.
9. Logan, T. L., 1994, "Improving dynamic open-hole completion techniques in the San Juan Basin": Quarterly Review of Methane from Coal Seams Technology, v. 11, no. 3 & 4, p. 13–18.
10. Kaiser, W. R., Swartz, T. E., and Hawkins, G. J., 1991, "Hydrology of the Fruitland Formation, San Juan Basin," *in* Ayers, W. B., Jr., and others, Geologic controls on the producibility of coalbed methane, Fruitland Formation, San Juan Basin: Gas Research Institute Topical Report, GRI-91/0072, p. 195–241.
11. Palmer, I. D., Mavor, M. J., Spitler, J. L., Seidle, J. P., and Volz, R. F., 1993, "Openhole cavity completions in coalbed methane wells in the San Juan Basin": Journal of Petroleum Technology, November, p. 1072–1080.
12. Jagiello, Jacek, Lason, Mieczyslaw, and Nodzenski, Adam, 1992, "Thermodynamic description of gas liberated from a coalbed": Fuel, v. 71, p. 431–435.
13. Jüntgen, H., and Karweil, J., 1966, "Formation and storage of gas in bituminous coals—part 1, gas storage" (English translation): Erdol und Kohle-Erdgas-Petrochimie, v. 19, p. 339–344.
14. Scott, A. R., Kaiser, W. R., and Ayers, W. B., Jr., 1994, "Thermogenic and secondary biogenic gases, San Juan Basin, Colorado and New Mexico—implications for coalbed gas producibility": American Association of Petroleum Geologists Bulletin, v. 78, no. 8, p. 1186–1209.
15. Tremain, C. M., Laubach, S. E., and Whitehead, N. H., III, 1991, "Coal fracture (cleat patterns in Upper Cretaceous Fruitland Formation, San Juan Basin, Colorado and New Mexico: implications for coalbed methane exploration and development": *in* Ayers, W. B., Jr., and others, Geologic controls on the producibility of coalbed methane, Fruitland Formation, San Juan Basin: Gas Research Institute Topical Report GRI-91/0072, p. 97–117.
16. Meek, R. H., and Bowser, P. D., 1993, "The transition between the low-rate and the high-rate producing areas of the Fruitland coal, San Juan Basin, New Mexico" (abs.): American Association of Petroleum Geologists Bulletin, v. 65, p. 1455.
17. McLennan, J. D., Khodaverdian, M., and Jones, A. H., 1994, "Creation of an open-hole cavity theory and laboratory results": Quarterly Review of Methane from Coal Seams Technology, v. 11, no. 3 & 4, p. 27–34.
18. Harpaloni, S., and Chen, G., 1993, "Gas slippage and matrix shrinkage effects on coal permeability": Proceedings, 1993 International Coalbed Methane Symposium, v. I, p. 285–294.
19. Scott, A. R., 1993, "Composition and origin of coalbed gases from selected basins in the United States": Proceedings, 1993 International Coalbed Methane Symposium, v. I, p. 207–216.
20. Arri, L. E., Yee, Dan, Morgan, W. D., and Jeansonne, M. W., 1992, "Modeling of coalbed methane production with binary gas sorption": Society of Petroleum Engineers paper SPE 24363, presented at the SPE Rocky Mountain Regional Meeting, Casper, Wyoming.
21. Pratt, T. J., and Close, J. C., 1993, "Integrated methods for coal gas completion zone selection": Society of Petroleum Engineers paper SPE 26630, presented at the 68th Annual Technical Conference and Exhibition of the Society of Petroleum Engineers, Houston, Texas, October 3–6, p. 217–232.
22. Levine, J. R., 1992, "Geochemical and petrologic controls on gas generation, storage, and producibility": *in* Ayers, W. B., Jr., Kaiser, W. R., and Levine, J. R., Coalbed methane: depositional, hydrologic, and petrologic characteristics of coal beds: American Association of Petroleum Geologists Energy Minerals Division Short Course #13, 1992 Annual Convention, Calgary, Alberta, variously paginated.
23. Young, G. B. C., McElhiney, J. E., Paul, G. W., and McBane, R. A., 1991, "An analysis of Fruitland coalbed methane production, Cedar Hill Field, Northern San Juan Basin": Society of Petroleum Engineers paper SPE 22913, presented at the 66th Annual Technical Conference and Exhibition, Dallas, Texas, October 6–9.
24. Kelso, B. S., 1993, "Geological control on open-hole cavity completion in the San Juan Basin": Notes from GRI Coalbed Methane Open-Hole Cavity Completion Workshop, Denver, Colorado, April 25, 20 p.
25. Scott, A. R., Kaiser, W. R., and Ayers, W. B., Jr., 1991, "Composition, distribution, and origin of Fruitland and Pictured Cliffs Sandstone gases, San Juan Basin, Colorado and New Mexico": *in* Schwochow, S., ed., Rocky Mountains Association of Geologists Guidebook, p. 93–108.
26. Ayers, W. B., Jr., Ambrose, W. A., and Yeh, J., 1991, "Depositional and structural controls on coalbed methane occurrence and resources in the Fruitland Formation, San Juan Basin": *in* Ayers, W. B., Jr., and others, Geologic controls on the producibility of coalbed methane, Fruitland Formation, San Juan Basin: Gas Research Institute Topical Report, GRI-91/0072, p. 9–46.
27. Scott, A. R., 1995, "Limitations and benefits of Microbially Enhanced Coalbed Methane": this proceedings.

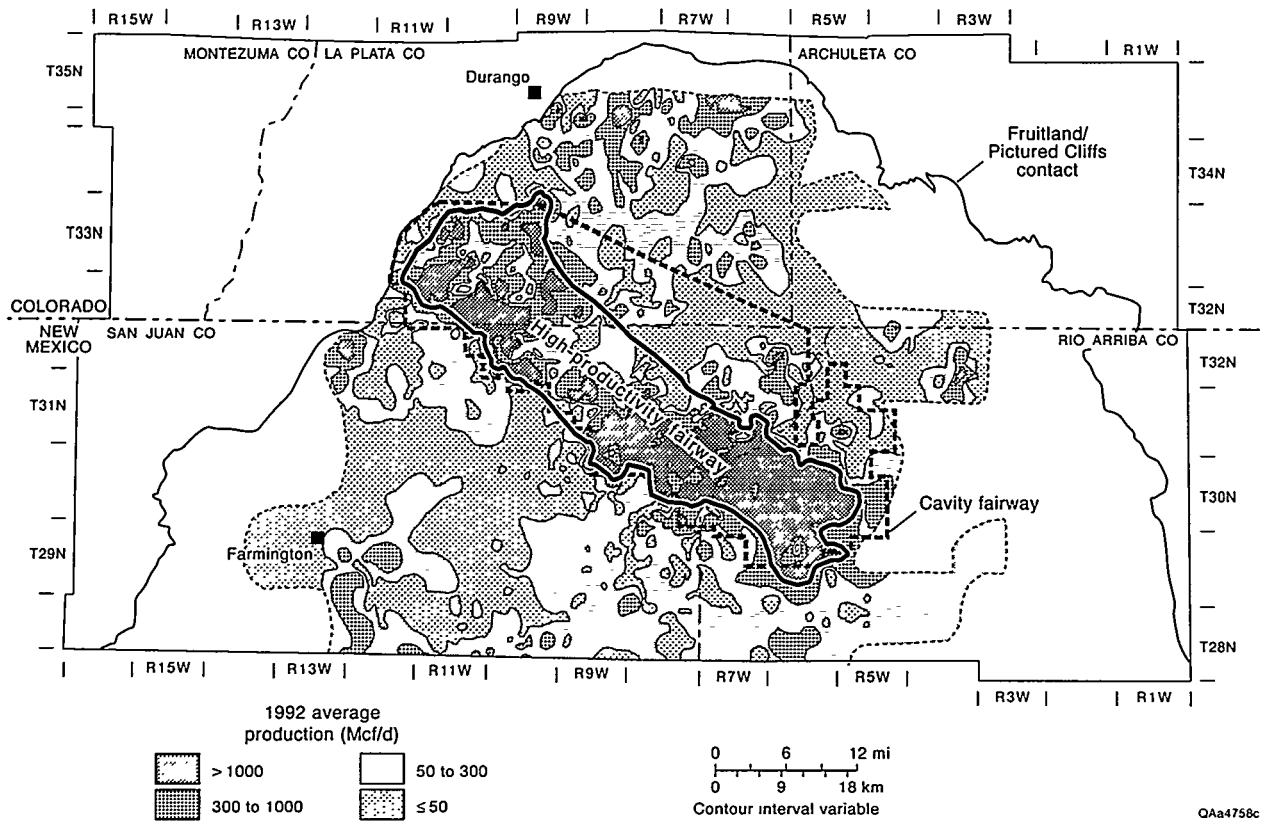


Figure 1. Average daily production and location of the high-productivity fairway and dynamic open-hole cavity fairways. Average daily production courtesy of R. H. Meek of Conoco, Inc. Locations of high-productivity and cavity fairways are from Palmer and others [1] and Kelso [2], respectively.

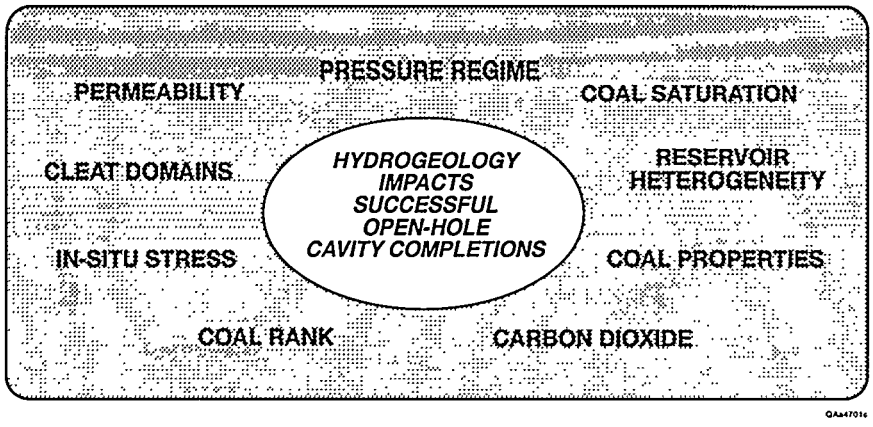


Figure 2. Geologic and hydrologic factors controlling successful dynamic open-hole completions. No single factor explains cavitation, which is complex process controlled by a poorly understood interplay among many variables.

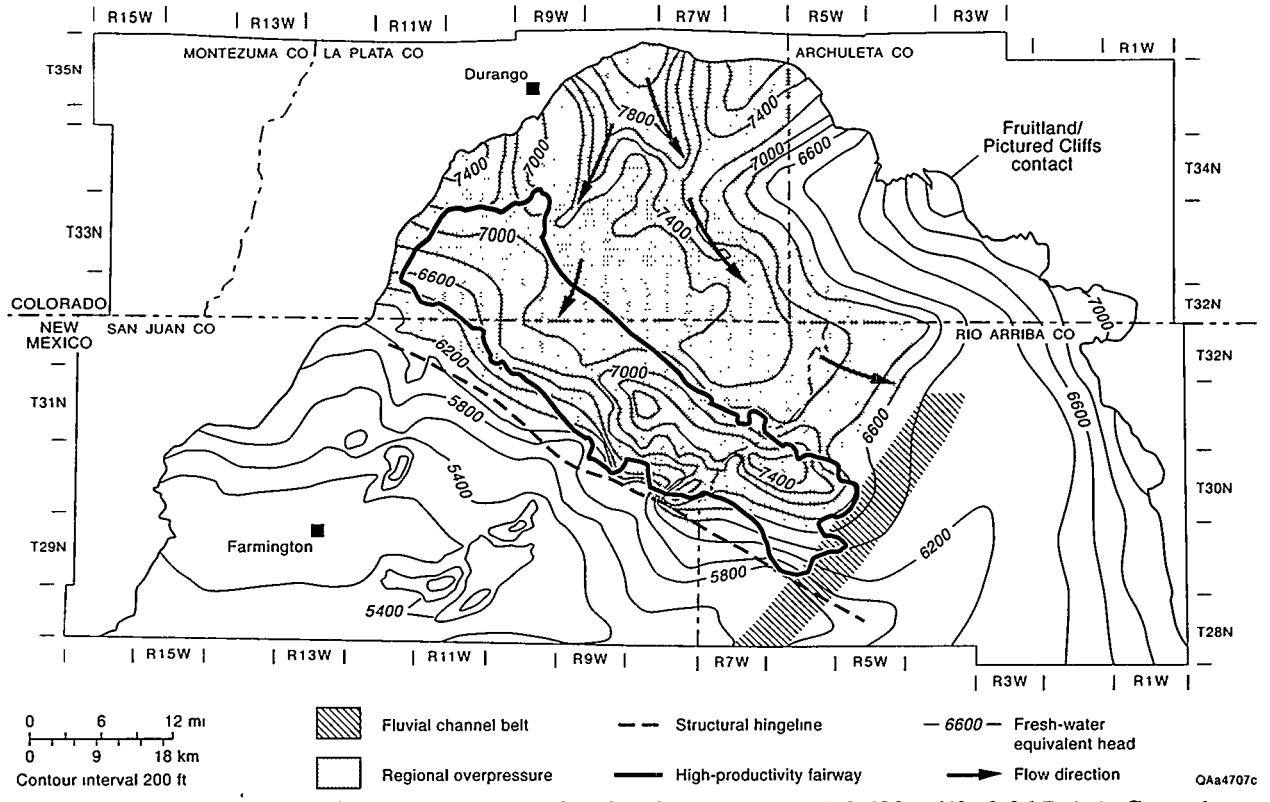


Figure 3. Fruitland potentiometric surface map and area of regional overpressure (>0.433 psi/ft; 9.8 kPa/m). Ground water flows southward from the northern margin of the basin perpendicular to head contours. Potentiometric ridge showing higher head values corresponds to the high-productivity fairway. Modified from Kaiser and others [10].

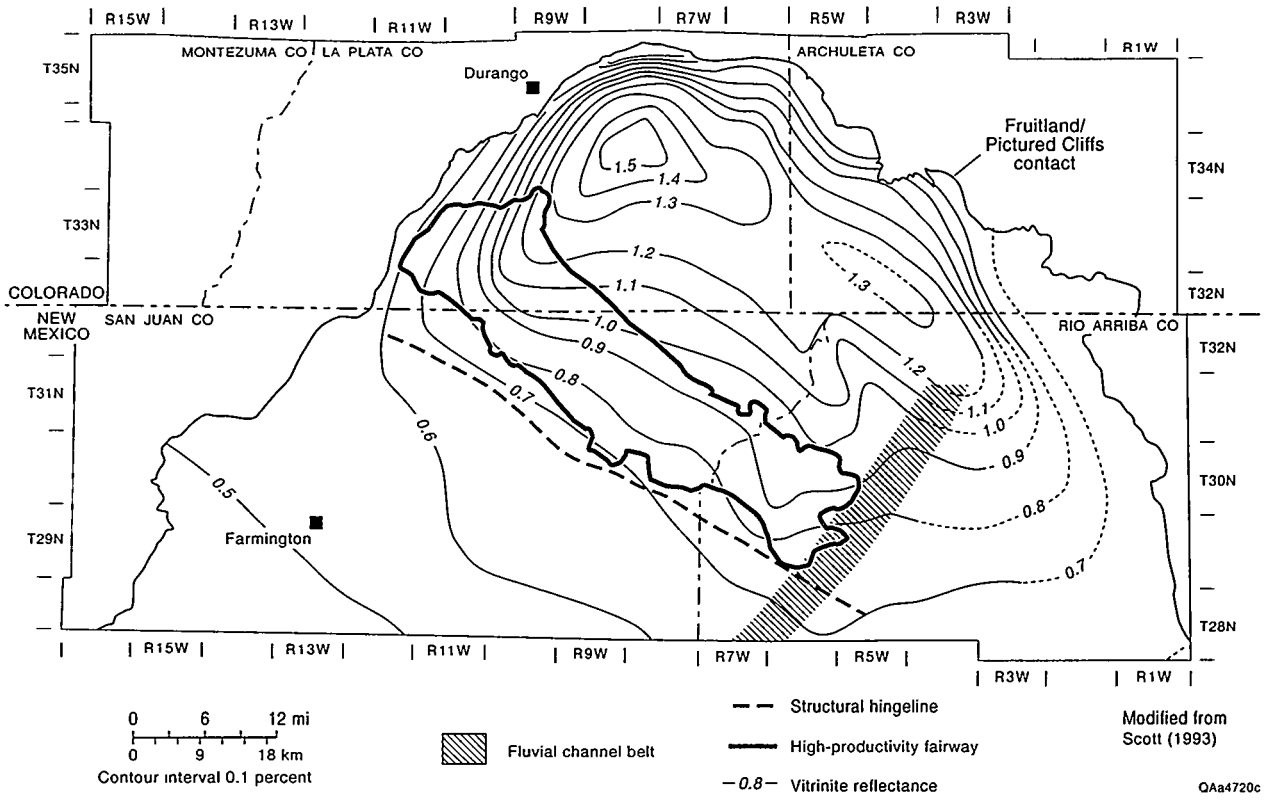


Figure 4. Regional coal-rank map, northern San Juan Basin. The southern boundary of the high-productivity fairway corresponds to that of the high-volatile A bituminous rank (VR of 0.78%), where gas contents are predicted to be less than 250 scf/ton (7.8 g/cm^3). However, gas contents in Fruitland high-volatile A bituminous coal approach 700 scf/ton (21.9 g/cm^3), suggesting that factors other than the coalification jump control the area of high-producibility. Modified from Scott and others [14].

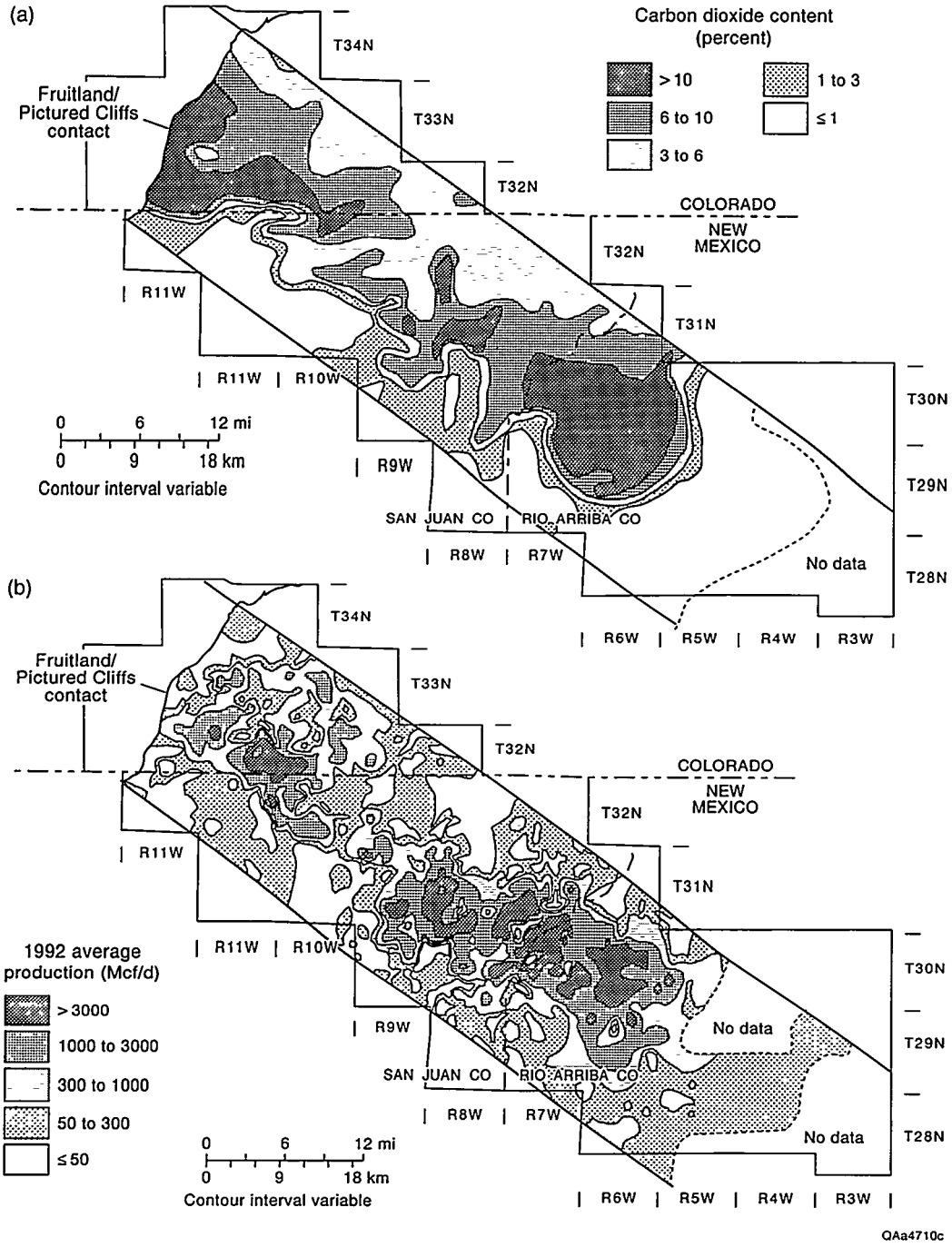


Figure 5. Carbon dioxide content of coalbed gases (a) and average daily production (b). The carbon dioxide content of coalbed gases corresponds to areas of high production, suggesting that there is a correlation between carbon dioxide and producibility in the high-productivity fairway. Average daily production courtesy of R. H. Meek of Conoco, Inc. Coal gas carbon dioxide content modified from Scott and others [14].

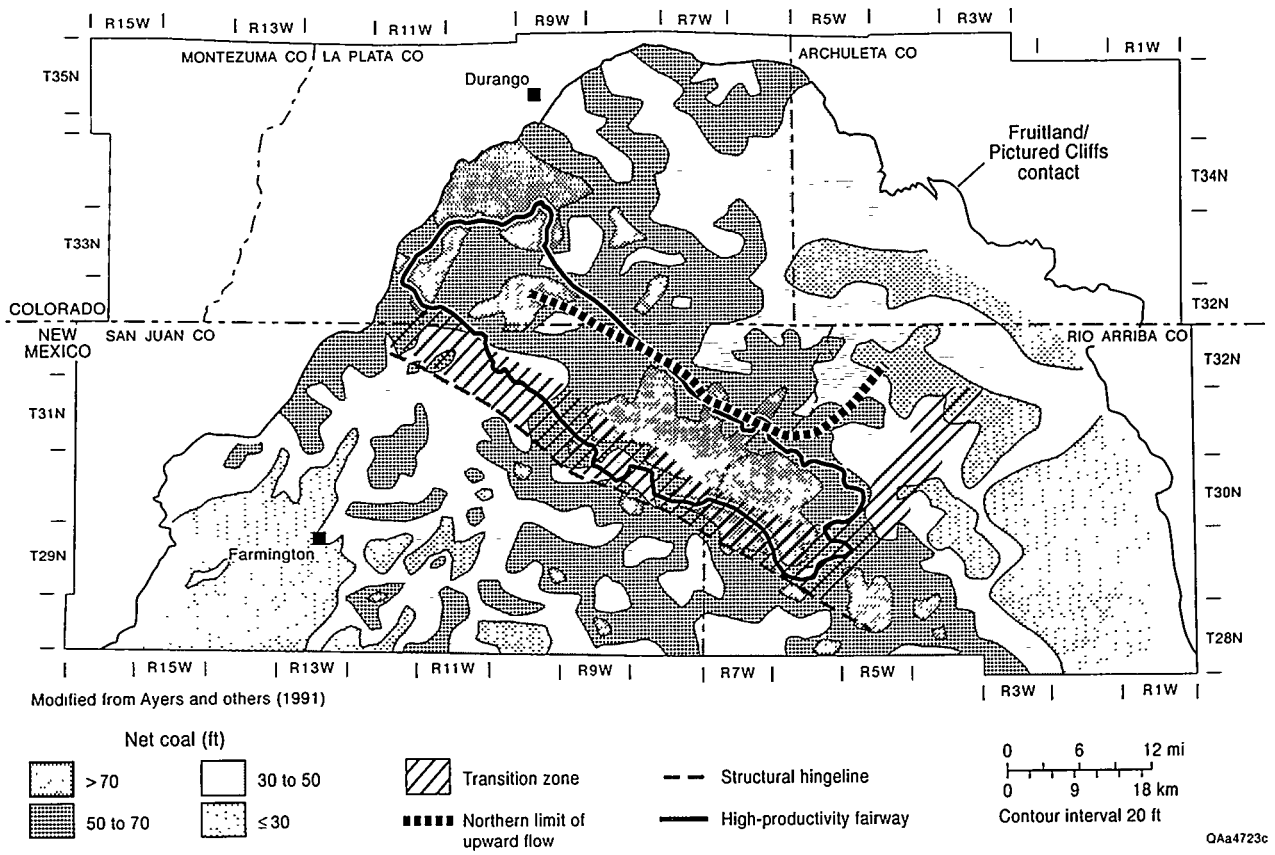


Figure 6. Fruitland net-coal map showing the high-productivity fairway. The high-productivity fairway corresponds to areas of upward-flow potential, maximum net coal, and high-carbon dioxide content. The southern boundary is controlled by pinch-out and/or faulting of permeable coal beds along a structural hingeline, whereas the northern boundary corresponds to maximum net coal and the northern limit of regional upward flow. Net coal map from Ayers and others [26].

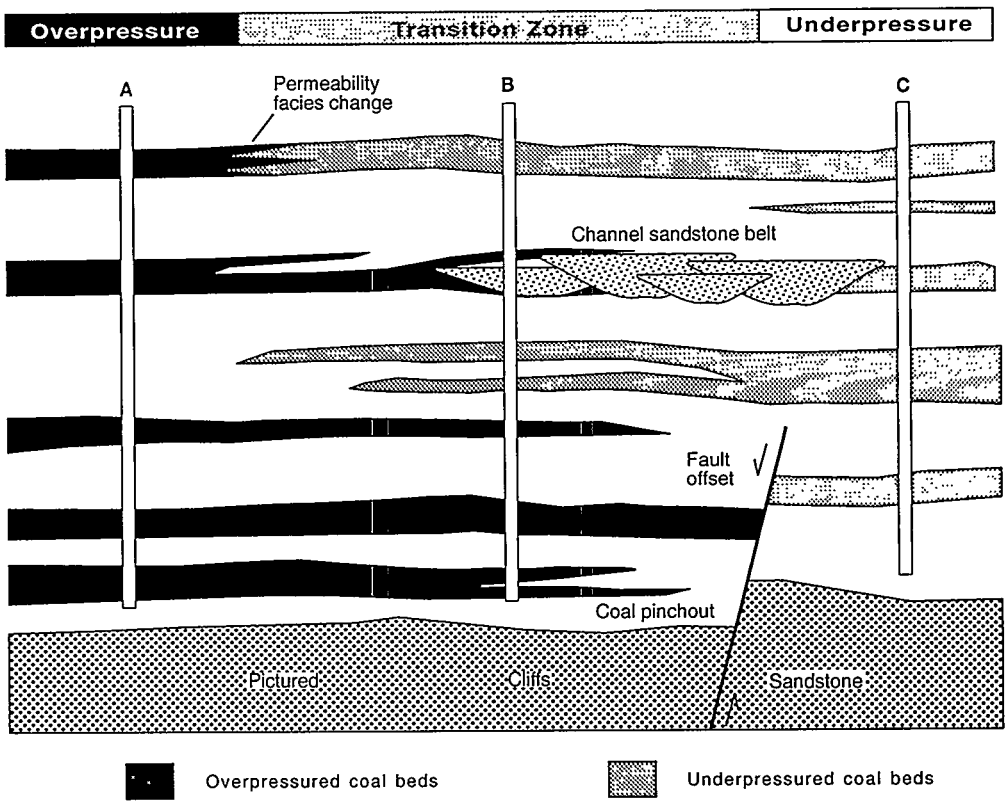


Figure 7. Schematic diagram of a transition zone. This zone often contains overpressured and underpressured coal beds within the same well. Width of this transition zone depends on coalbed geometry and the type of permeability barriers present.

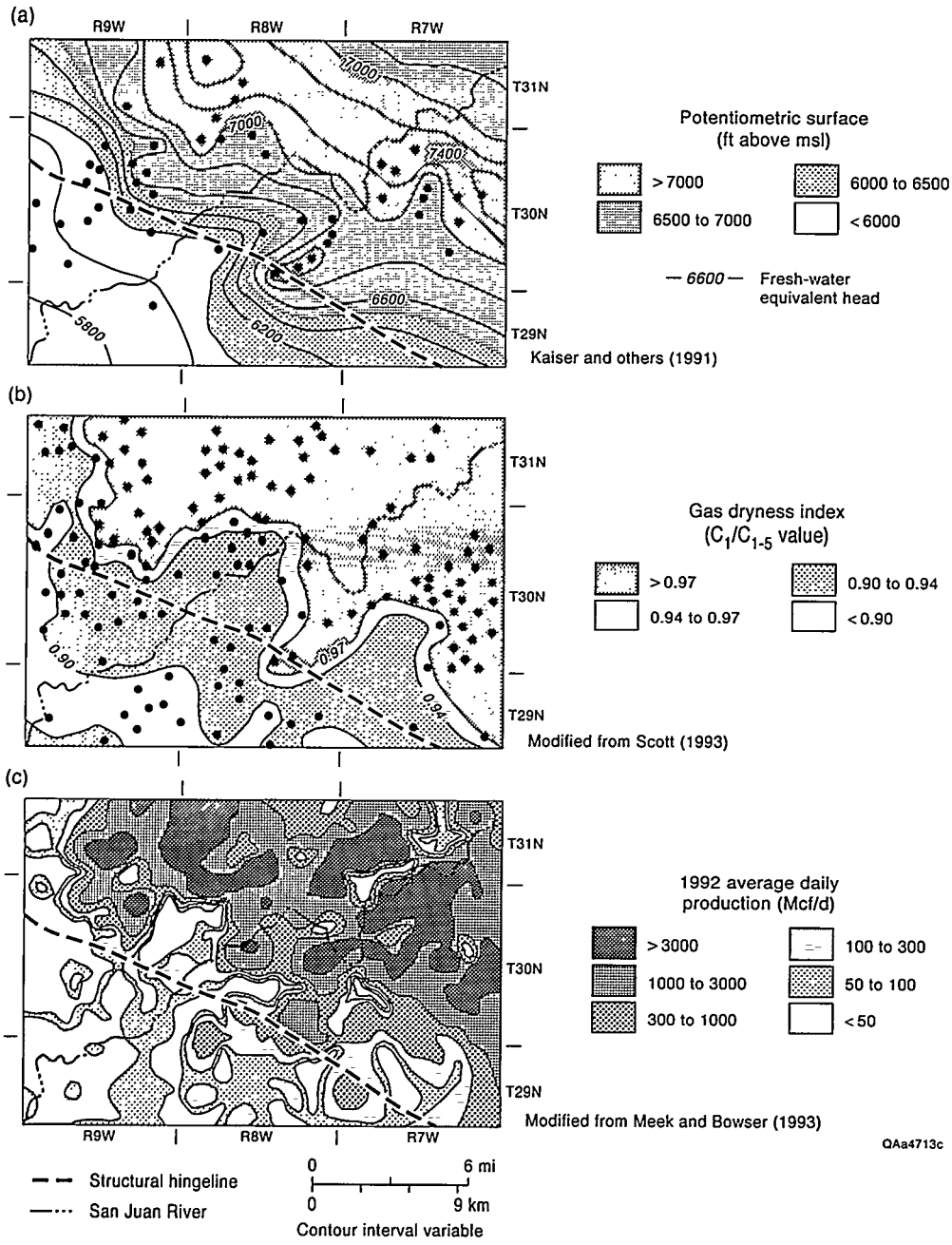


Figure 8. Southern boundary of high-productivity fairway, potentiometric surface (a), coalbed gas composition (b), and average daily production (c). Steepening of the potentiometric surface and abrupt changes in gas chemistry and average daily production indicate that there is a true southern boundary, which is attributed to basin hydrogeology. The northwest-trending potentiometric mound in T30N, R7W corresponds to wells producing more than 3,000 Mcf/d. Data from Kaiser and others [10], Scott and others [14], and Meek and Bowser [16].

NOTES

INTERGAS '95

May 15-19, 1995
The University of Alabama
Tuscaloosa, Alabama USA

9560

Simulation of Coalbed Methane Enhanced Recovery Using Gas Potential and a New Saturation Equation

O.A. Almisned, University of Oklahoma;
and R.L. Thrasher, Louisiana Tech University

ABSTRACT

A two-dimensional, two-phase coalbed methane degasification computer simulator was developed. The water, gas, and pore volumes used in the saturation equation were corrected by the inclusion of water, gas and pore compressibilities in the calculations. This correction is new to the conventional saturation equation calculations. The gas potential was generalized to include all pressure dependent factors, including Klingkenberg effect, viscosity, compressibility factor and stress dependent permeability. After the simulator was validated, a nitrogen injection capability was introduced in which the sorption isotherm was redefined to account for two gases adsorbing on the coal.

INTRODUCTION

Drilling into coalbeds and degasification of coalseams is a production and use of the valuable resource methane. The degasification of methane gas can maximize mining safety, speed up mining operation and minimize ventilation cost [1]. Coal seams have a dual porosity nature consisting of micropores within the coal matrix plus a natural fracture network composed of face and butt cleat systems that are perpendicular to each other. The cleat system permeability is anisotropic, and the transport of gas within the fractures is laminar and controlled by Darcy's Law:

$$\overline{v} = \frac{q}{A} = \frac{k_{ref}}{\mu}\frac{dP}{dL} \qquad (1)$$

The transport of gas in the micropores is governed by diffusion due to the concentration gradient. The adsorbed gas moves through three stages before being produced at the surface. First, gas is desorbed from coal grains. Second, it diffuses through the solid coal matrix. Third, it travels through the fracture system.

Many coalbed methane degasification models with different features and capabilities have been developed in the last three decades [2]. These features [3] include: stress dependent porosity and permeability; the Klinkenberg slippage effect, and; the effect of desorption on porosity and permeability (i.e. shrinkage of the coal matrix due to desorption)[4]. In this paper a gas potential, rather than pressure, equation that includes these features is introduced, and a new accurate saturation equation is developed and used in the developed nitrogen injection, enhanced coalbed methane recovery simulator.

GAS POTENTIAL EQUATION

Under normal reservoir pressure and flow conditions, the absolute permeability is dependent on the porous medium regardless of the flowing fluid. However, in the real gas case, at low pressure, the gas molecules tend to slip against the walls of the pores which results in an increase in the absolute permeability. This dependency of permeability on the nature of the fluid and its pressure is called the Klinkenberg effect and is accounted for by the correction to the absolute permeability.

$$k = k_\infty\left(1 + \frac{b}{P_g}\right) \qquad (2)$$

Due to the natural fracture network in coal seams, both the macropore porosity and permeability are dependent on the effective stress

$$\sigma_e = \sigma_{OB} - P_g \qquad (3)$$

where σ_{OB} is the overburden pressure.

The relationship between permeability and porosity is

$$\frac{k}{k_{ref}} = \left(\frac{\phi}{\phi_{ref}}\right)^{N_c} \qquad (4)$$

The value of the exponent Nc is usually 3 or greater [5]. ϕ is a function of the gas phase pressure.

The shrinkage of coal matrix due to methane desorption was confirmed by Harpalani and Schrautnegel [4,6], and the porosity equation was derived to account for both pore volume compressibility and matrix shrinkage compressibility:

$$\phi = \phi_{ref} - C_p\phi_{ref}(P_{ref} - P) + C_m(1 - \phi_{ref})P_{ref}\left(1 - \frac{V}{V_{ref}}\right) \qquad (5)$$

where V is the adsorbed gas volume and V_{ref} is the adsorbed gas volume at P_{ref}. Equation (5) is used to calculate the porosity term of Equation (4) so that the reduction of permeability due to stress and enhancement of permeability due to coal matrix shrinkage are accounted for [4,6]. The gas flow between any two points in the coal seam is controlled by the difference in potential between these two points. Equations (2) and (4) were combined with Darcy's Law and a real gas potential equation, Equation (6), was derived for the model (See Appendix for complete derivation).

$$\Phi = \int_{P_*}^{P}\frac{(\phi_E/\phi_{ref})^{N_c}(P+b)}{\mu Z}dP \qquad (6)$$

This potential equation accounts for stress dependent porosity and permeability.

Since flow rate is proportional to gas potential gradient, using gas potential yields flow equations that are more nearly linear and thus more efficient to solve. However, the formulation results in a more complicated code.

THE SATURATION EQUATION

Fluid volumes in a reservoir block should satisfy the equations:

$$V_g + V_w = V_p \tag{7}$$

and

$$V_w = S_w V_p \tag{8}$$

However, after solving the pressure equations,

$$V_g = m_g/\rho_g$$

$$V_w = m_w/\rho_w$$

and

$$V_w = V_B\phi$$

the equation

$$V_g + V_w = V_p$$

is not satisfied. Usually, this fact is ignored and S_w is defined as either

$$S_w = V_w/V_p$$

or

$$S_w = V_w/(V_w + V_g)$$

In our approach, we introduce the pressure correction ΔP necessary to make the fluid volumes balance:

$$\left(V_g + \frac{\partial V_g}{\partial P}\Delta P\right) + \left(V_w + \frac{\partial V_w}{\partial P}\Delta P\right) = \left(V_p + \frac{\partial V_p}{\partial p}\Delta P\right) \tag{9}$$

and

$$\left(V_w + \frac{\partial V_w}{\partial P}\Delta P\right) = S_w\left(V_p + \frac{\partial V_p}{\partial P}\Delta P\right) \tag{10}$$

Solving for ΔP in Equation (9) gives:

$$\Delta P = -\frac{V_g + V_w - V_p}{\frac{\partial V_g}{\partial P} + \frac{\partial V_w}{\partial P} - \frac{\partial V_p}{\partial P}} \tag{11}$$

and solving for ΔP in Equation (10) gives:

$$\Delta P = -\frac{V_w - S_w V_p}{\frac{\partial V_w}{\partial P} - S_w\frac{\partial V_p}{\partial P}} \tag{12}$$

Equating the two equations and solving for S_w one gets the Almisned-Thrasher saturation equation:

$$S_w = \frac{V_w\left(\frac{\partial V_g}{\partial P} - \frac{\partial V_p}{\partial P}\right) - \frac{\partial V_w}{\partial P}(V_g - V_p)}{V_p\left(\frac{\partial V_g}{\partial P} + \frac{\partial V_w}{\partial P}\right) - \frac{\partial V_p}{\partial P}(V_g + V_w)} \tag{13}$$

NITROGEN INJECTION

From their laboratory studies, Puri and Yee [7] concluded that methane partial pressure controls adsorption to and desorption from the coal matrix. Since the coalbed methane desorption is dependent on the partial pressure and not the total pressure, introducing nitrogen to the coalbed seam will lower the partial pressure of methane gas and maintain the total pressure constant (if not increase it). This process is called "the inert gas stripping method" [7] where desorption of coalbed methane is accelerated due to partial pressure reduction when nitrogen is injected. It is worth mentioning here that the increased production is not due to displacement of nitrogen in the cleat system.

In order to accommodate the two components, methane and nitrogen in the gas phase, Langmuir's Isotherm has been redefined for two gas components:

$$V_E(P_g) + \frac{V_L P_g}{P_L + P_g} \tag{14}$$

DISCUSSION OF RESULTS

In order to test the validity of the model, it was essential to compare its results to an existing numerical model. The model developed by Ertekin, King and Schwerer [8] was chosen for the comparison. The run was compared against the two-phase, one-dimensional results.

The validation results for gas and water in terms of rate versus time are shown in Figure 1. The agreement shown in the figure is satisfactory considering the differences in grid system (2D, rectangular) and the numerical solution procedure (IMPES) of the proposed model and those of Ertekin, King and Schwerer's model (1D, radial, fully Implicit). Also, the differences in selection of time and step sizes can be responsible for the slight differences in the results.

A hypothetical, 10-acre, 10x10 block areal simulation grid reservoir was used for the sensitivity runs. The simulated area was selected so that, with appropriate calculations of productivity indices, it represents a quarter of a 40-acre total drainage area with five-spot pattern wells [9].

A base case with one production and one injection well, and no nitrogen injection, was set up and run by the simulator. The reservoir was placed on pressure depletion with a constant bottom hole pressure of 20 psi in the producer. Results of the run of the base case are shown in Figure 2 which shows a typical coalbed methane degasification pattern. After 20 years of pressure depletion, 63,366 MCF of methane is recovered from the total drainage area. The cumulative produced methane is 30% of the initial gas-in-place.

In order to test the theory of adsorbed methane stripping by nitrogen flooding, the reservoir was initially placed on pressure depletion after 4 1/2 years of production. When the produced methane rate started declining, nitrogen was injected into the coal seam while maintaining a fixed injection pressure of 600 psi in the injector well. Nitrogen injection continued for six months before being terminated.

Figure 3 shows the nitrogen injection run compared to the base case. Even after injection of nitrogen was stopped at the end of the fifth year of the life of the reservoir, the methane production rate was significantly increased due to nitrogen injection. A 74,606 MCF of methane was recovered which represents 36% of the initial gas-in-place. All of the simulation results were obtained using the gas potential and the new saturation equations.

CONCLUSIONS

A coalbed methane degasification model has been developed with an improved saturation equation and a gas potential equation that accounts for stress-dependent porosity and permeability, the Klinkenberg slippage effect, and the effect of desorption on porosity and permeability. The improved saturation equation and the generalized gas potential function have successfully been used in this coalbed methane simulator. The results of the

developed simulator were compared against an existing numerical model and showed a positive agreement between the two models.

Without reducing the total gas phase pressure, nitrogen injection into the coal seam is shown to reduce the methane concentration and consequently enhance the coalbed methane recovery. The simulation results reported in this study confirm the work of Puree and Yee[7] which concluded that adsorption/desorption of methane to the coal matrix is dependent on partial pressure of the gas and not the total pressure of the system.

APPENDIX - DERIVATION OF GAS POTENTIAL EQUATION

The real gas equation is:

$$PV = ZnRT \tag{A-1}$$

where V is volume, R is the gas constant, and n is the number of moles of gas. And, since

$$\rho = m/V \tag{A-2}$$

or

$$\rho = mP/ZnRT \tag{A-3}$$

one can write:

$$\rho = \frac{PM}{ZRT} \tag{A-4}$$

In Darcy's law:

$$\bar{v} = -\frac{k\,dP}{\mu\,dx} \tag{A-5}$$

Since the mass flow rate $\dot{m}=\rho\bar{v}$, we can write:

$$\dot{m} = \frac{k\rho\,dP}{\mu\,dx} \tag{A-6}$$

Substituting for ρ from Equation (A-4),

$$\dot{m} = -\frac{k\,PM\,dP}{\mu\,ZRT\,dx} \tag{A-7}$$

To get $\dot{m}=-d\Phi/dx$, we define the potential as follows:

$$\Phi = \int_{P_*}^{P}\frac{k\,M}{\mu\,ZRT}dP \tag{A-8}$$

The Klinkenburg effect can be included in the potential by substituting for k of Equation (2) in Equation (A-8):

$$\Phi = \int_{P_*}^{P}\frac{k_\infty(1+b/P)MP}{\mu ZRT}(dP) \tag{A-9}$$

or

$$\Phi = \int_{P_*}^{P}\frac{k_\infty(P+b)M}{\mu ZRT}(\Delta dP) \tag{A-10}$$

Since the stress dependent permeability equation is:

$$\left(\frac{k}{k_{ref}}\right) = \left(\frac{\phi}{\phi_{ref}}\right)^{N_\phi} \tag{2}$$

we can include the stress effect in the potential equation. Therefore Equation (A-10) becomes:

$$\Phi = \int_{P_*}^{P}\frac{k_{ref}(\phi/\phi_{ref})^{N_\phi}(P+b)M}{\mu ZRT}dP \tag{A-11}$$

we can write:

$$\left(\frac{\phi}{\phi_{ref}}\right)^{N_\phi} = \left(\frac{\phi}{\phi_E}\right)^{N_\phi}\left(\frac{\phi_E}{\phi_{ref}}\right)^{N_\phi} \tag{A-12}$$

where

$$\left(\frac{\phi}{\phi_E}\right)^{N_\phi}$$

is a history dependent term and

$$\left(\frac{\phi_E}{\phi_{ref}}\right)^{N_\phi}$$

is a pressure dependent term.

Equation (A-11) becomes:

$$\Phi = \int_{P_*}^{P}\frac{k_{ref}(\phi/\phi_e)^{N_\phi}(\phi_E/\phi_{ref})^{N_\phi}(P+b)M}{\mu ZRT}dP \tag{A-13}$$

or

$$\Phi = \frac{Mk_{ref}(\phi/\phi_E)^{N_\phi}}{RT}\int_{P_*}^{P}\frac{(\phi_E/\phi_{ref})^{N_\phi}(P+b)}{\mu Z}dP \tag{A-14}$$

Redefining the potential:

$$\Phi = \int_{P_*}^{P}\frac{(\phi_E/\phi_{ref})^{N_\phi}(P+b)}{\mu Z}dP \tag{6}$$

Darcy's equation becomes:

$$\dot{m} = \frac{Mk_{ref}(\phi/\phi_E)^{N_\phi}}{RT}\frac{d\Phi}{dx} \tag{A-15}$$

Equation (6) is the final form of the gas potential equation.

NOMENCLATURE

A	Area	m^2
b	Gas slippage factor	Pa
C_m	Matrix shrinkage compressibility	Pa^{-1}
C_p	Pore volume compressibility	Pa^{-1}
k	Permeability	Darcy
k_{ma}	Macropore permeability	Darcy
k_{ref}	Reference permeability	Darcy
k_∞	Liquid permeability (permeability at infinite pressure)	Darcy
L	Length	m
m	Mass	kg
M	Molecular weight	kg/mol
p	Pressure	Pa
P_g	Gas phase pressure	Pa
P_L	Langmuir pressure	Pa
P_{ref}	Reference pressure	Pa
q	Volumetric flow rate	m^3/s
S_w	Water phase saturation	fraction
T	Temperature	°C

V	Volumetric concentration	scm/m^3
$\overline{v}$	Velocity (Volumetric flux)	m/s
V_E	Equilibrium volumetric concentration	scm/m^3
V_L	Langmuir volumetric concentration	scm/m^3
X	Distance	m
Z	Gas compressibility factor	fraction
μ	Dynamic viscosity	Pa-s
ρ	Density	kg/m^3
ρ_g	Gas phase density	kg/m^3
ρ_w	Water phase density	kg/m^3
σ_e	Effective stress	Pa
σ_{ob}	Overburden stress	Pa
Φ	Gas phase potential	Pa
ϕ	Porosity	fraction
ϕ_{ref}	Reference porosity	fraction

Subscripts

B	Bulk property
E	Equilibrium property
g	Gas phase property
o	Initial condition property
p	Pore volume property
w	Water phase property

REFERENCES CITED

1. Sung, W., 1987: "Development, Testing, and Application of a Multiwell, Numerical Coal Seam Degasification Simulator," Ph.D. Dissertation, The Pennsylvania State University.

2. King, G.R. and Ertekin, T.M., 1989: "A Survey of Mathematical Models Related to Methane Production from Coal Seams, Part I: Empirical and Equilibrium Sorption Models," Proc., 1989 Coalbed Methane Symposium, Tuscaloosa, Alabama, April 17-20.

3. King, G.R. and Ertekin, T.M., 1989: "A Survey of Mathematical Models Related to Methane Production from Coal Seams, Part II: Non-Equilibrium Sorption Models," Proc., 1989 Coalbed Methane Symposium, Tuscaloosa, Alabama, April 17-20.

4. Harpalani, S. and Schraufnagel, R.A., 1990: "Influence of Matrix Shrinkage and Compressibility on Gas Production from Coalbed Methane Reservoirs," paper SPE 20729 presented at the 1990 SPE Annual Technical Conference and Exhibition, New Orleans, Sept. 23-26.

5. King, G.R. and Ertekin, T., 1989: "State-of-Art in Modeling of Unconventional Gas Recovery," paper SPE 18947 presented at the 1989 SPE Joint Rocky Mountain Regional/Low Permeability Reservoirs Symposium and Exhibition, Denver, CO, March 6-8.

6. Harpalani, S. and Schraufnagel, R.A., 1989: "Permeability Changes Resulting from Gas Desortion," Final Report under GRI contract Number 5088-215-1666.

7. Puri, R. and Yee, D., 1990: "Enhanced Coalbed Methane Recovery," paper SPE 20732 presented at the 1990 SPE Annual Technical Conference and Exhibition, New Orleans, Sept. 23-26.

8. Ertekin, T., King, G.R. and Schwerer, F.C., 1986: "Development of Coal Gas Production Simulators and Mathematical Models for Well Test Strategies," Final Report under GRI contract Number 5081-321-0457.

9. Almisned, O.A., 1993: "Construction of A Coal-Bed Methane Simulator with Nitrogen Injection Capability", M.Sc Thesis, Mississippi State University.

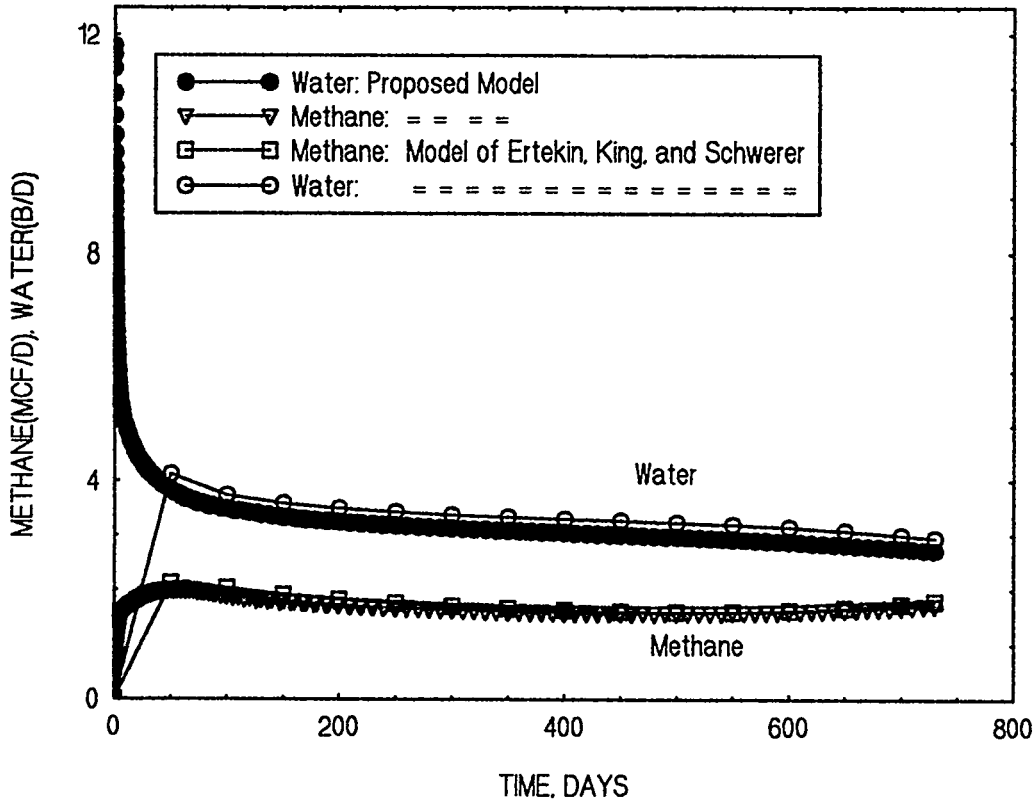


Figure 1: **Comparison of Proposed Model and Model of Ertiken, King and Schwerer [8]: Methane Gas and Water Production Rate Vs. Time**

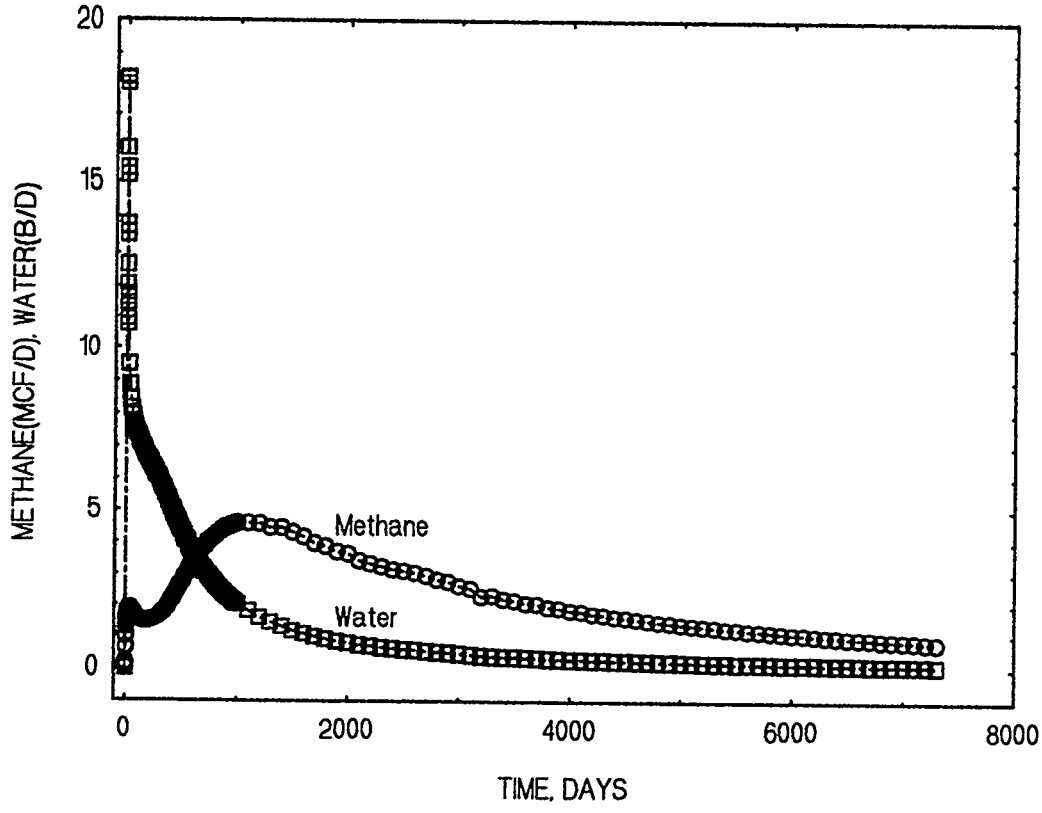


Figure 2: **Base Case: Methane and Water Production Rate Vs. Time**

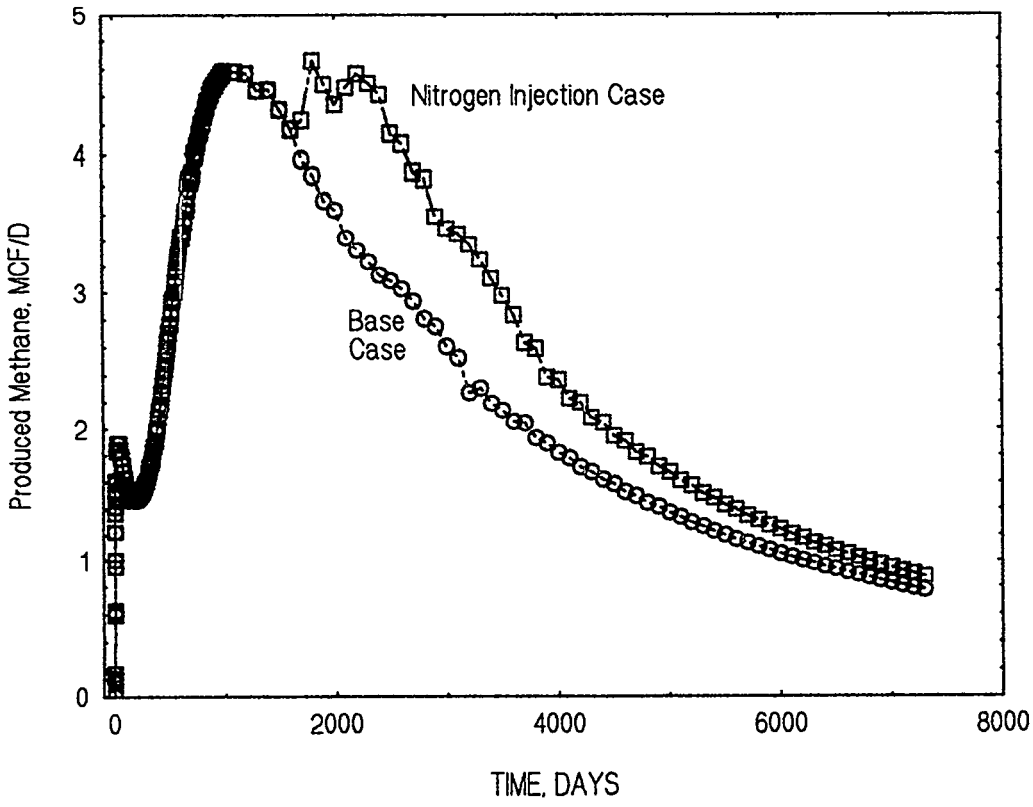


Figure 3: Effect of Nitrogen Injection on Methane Production Rate

INTERGAS '95

May 15-19, 1995
The University of Alabama
Tuscaloosa, Alabama USA

9556

A Micro-Pilot Approach to Coalbed Methane Reservoir Assessment

R. Puri, R. Volz and D. Duhrkopf, Amoco

ABSTRACT

Determination of the technical and economic feasibility of coalbed methane production by means of pressure depletion (CBM) or enhanced recovery by injection of desorbing gases such as nitrogen and carbon dioxide (ECBM) is expensive and time consuming. A new methodology of coalbed methane reservoir quality assessment has been developed and applied recently, resulting in drastic reductions in evaluation cycle time and cost. This new approach, referred herein as a "Micro-pilot," uses a combination of direct field measurements and numerical simulations to match perturbations in bottom hole pressures, injection and production flow rates, and gas compositions created by a brief air huff'n puff procedure on a coal seam.

The injected air during a Micro-pilot releases methane adsorbed to coal near the wellbore by means of partial pressure reduction. The concurrent pressure transient and gas composition data during flow back yields critical reservoir properties such as coal seam gas content, diffusivity, injectivity, stress dependent permeability, etc. Results from three coal basins in the United States prove that the Micro-pilot technology is a valuable resource assessment tool for coalbed methane prospects. Although the Micro-pilot is not as comprehensive as the traditional method of coalbed methane reservoir quality assessment, the time and cost savings are substantial.

This paper discusses the Micro-pilot test procedure, details field data analysis and interpretation, and presents actual results from a coalbed methane reservoir evaluation study conducted recently in the San Juan Basin of New Mexico, USA. Key parameters that impact the Micro-pilot tests, along with their relative effects, are addressed. When Micro-pilot results are used appropriately, engineering estimates of CBM and/or ECBM field performances can be estimated. This knowledge, coupled with project cost data, enables an early determination of the commercial viability of alternative production technologies.

BACKGROUND

Coalbed methane is a relatively new unconventional natural gas play in the United States. Large scale coalbed methane commercial projects started in about 1989, and by early 1994, over 6600 wells had been drilled, of which 5400 are currently producing. The two dominant basins in the U.S. are the San Juan Basin in Colorado/New Mexico, and the Black Warrior Basin of Alabama. It is estimated that U.S. coal deposits may contain as much as 400 Trillion cubic feet of gas in place, most of which has not been developed due to poorer economics. By year end 1994, coalbed methane production in the U.S. approached 2 Billion cubic feet per day.

Coal As A Reservoir Rock

Coalbed methane gas is composed primarily of methane, typically between 90 and 99% by volume. Unlike conventional gas reservoirs, methane in coal is not stored as free gas in void volume. Rather, natural gas is adsorbed to the internal surface area of the micro-porous coal, at near liquid densities.

The gas storage capacity of coal is expressed as Standard Cubic Feet (SCF) per ton of coal. The ability of a particular coal to hold a gas, such as methane, is a function of pressure at a given temperature. A typical adsorption isotherm for a coal sample from the San Juan Basin is shown in Figure 1.

Since many coalbed methane projects in the United States have been commercially successful, exploration for coalbed methane in other parts of the world has begun. At present, reservoir quality assessment efforts are underway in several countries, including China, India, Australia, United Kingdom, and Poland.

COALBED METHANE RECOVERY METHODS

There are fundamentally two distinct commercial options for recovering methane gas from coal seams:

Pressure Depletion (CBM)

At present, coalbed methane is being recovered exclusively by means of reservoir pressure depletion. After a coal well is drilled, and the bottom hole pressure is reduced, water and gas in the coal cleat system surrounding the wellbore are recovered. In accordance with the sorption isotherm relationship (example shown in Figure 1), the coal surrounding the production wellbore desorbs gas to reach an equilibrium with the new reduced reservoir pressure. The free gas diffuses from the coal matrix to the cleats, and flows to the wellbore as per Darcy's Law. Consequently, the reservoir pressure of the formation continually decreases over time as methane is recovered from the coal deposit.

While reservoir depletion is simple and effective, it is not necessarily the most efficient or economic. Reduction in reservoir pressure deprives the fluids of the energy necessary to flow to the wellbore and may even result in a reduction of permeability. Furthermore, there is a practical and economic limit on the extent to which reservoir pressure can be reduced. In most cases, reservoir pressure depletion method of coalbed methane production permits the recovery of 40-60% of the original gas-in-place over a very long period of time, usually several decades. The recovery rate of gas from coal, and the percentage of the original gas-in-place that can be economically recovered, is dependent on the reservoir properties of the formation.

Injection Enhanced Recovery (ECBM)

An alternate method of coalbed methane recovery currently under testing and development consists of injecting desorbing gases, such as nitrogen, air, flue gas, or carbon dioxide, into the coal formation.[1] In the case of nitrogen or nitrogen rich gases, the desorbing fluid reduces the partial pressure of methane in the cleats, and causes methane to desorb from the coal matrix. In the case of carbon dioxide or carbon dioxide rich gases, the coal has much greater affinity for the injected gas than methane, thereby leading to displacement desorption of methane. Once methane diffuses into the cleat system, it migrates to the production wellbore as per Darcy's Law.

Unlike CBM, methane desorption during ECBM is either by partial pressure reduction, or displacement desorption, and sometimes both. Compared to CBM, ECBM can significantly accelerate gas production rates and increase recoverable reserves. Although the technology and economics of ECBM are not yet as well established as those of CBM, any prudent coalbed methane exploration program needs to evaluate the feasibility of both of the production alternatives.

RESERVOIR QUALITY ASSESSMENT

Determination of the quality of a coal reservoir for a CBM or ECBM commercial project is difficult, expensive and time consuming. Given the large up-front capital exposure of coalbed methane projects, it is imperative that the reservoir characteristics of the coal and the surrounding formations be adequately understood. Knowledge of coal seam reservoir parameters, coupled with numerical simulation studies, can help forecast gas and water production rates and reserves from a basin or project area.

Traditional Approach

A traditional coalbed methane exploration program generally consists of: (1) a preliminary geological and engineering evaluation, (2) drilling of core holes and laboratory analysis of coal cores and cuttings samples, (3) delineation of project areas by drilling one or more closely spaced pilot wells, (4) well testing using pressure transient analysis, (5) gathering production data from pilot(s) for a period of at least one year, and typically more, (6) numerically simulating and history matching pressure depletion performance of pilot(s), and (7) forecasting full field CBM performance and economic viability. Similar approaches for a traditional coalbed methane exploration program have been discussed by Decker (1991), Semmelbeck & Lee (1990) and others.[2][3]

Although an elaborate exploration program of core holes and pilot wells can sometimes lead to a reasonable determination of the coal reservoir quality for commercial CBM production operation, it is not always efficient in terms of time, cost and effort. Typically, a coalbed methane exploration and reservoir assessment program can take 2-3 years, and cost as much as 5-10 million dollars. Unfortunately, since coals are quite heterogeneous and anisotropic, even a well executed reservoir assessment program may not lead to a successful commercial project. Furthermore, if an ECBM project is contemplated, injectivity and stress dependent permeability of a coal seam cannot be inferred from a traditional production pilot.

Over the past decade, Amoco Production Company has explored at least a dozen coal basins in the United States. To date, our exploration program has been along the lines of the traditional approach described above. In the San Juan, Warrior, and Raton Basins, we drilled dozens of core holes and a number of closely spaced 5-spot production pilots. A considerable amount of money, time, and effort was spent analyzing the production data from pilot projects using laboratory tests and a state-of-the-art numerical simulator. The results were then used in the design and forecasting of large scale drilling programs.

Although the reservoir description obtained by the pilot programs has generally been satisfactory, there has also been a realization that drastic reductions in cycle time and costs are needed. Furthermore, due to variations in coal seam properties over relatively short distances, there were inherent difficulties in extrapolating results of core and

pilot wells to the entire basin or project area. Given a fixed exploration program budget, the value of a closely spaced multiple production well pilot, as compared to widely spaced single wells, appears questionable.

Micro-Pilot Approach

In recent months, we have developed a novel approach to coalbed methane reservoir quality assessment that has drastically reduced the cycle time and costs associated with forecasting gas rates and reserves of a potential CBM or ECBM project. This methodology, herein referred to as a "Micro-pilot," uses a combination of direct field measurements and numerical simulations to match behaviors of bottom hole pressures, injection and production flow rates, and gas composition during a brief air huff'n puff on a coal seam.[4]

Although the Micro-pilot approach is not as comprehensive as the more traditional approach to coal reservoir quality assessment, the time and cost savings are substantial. While a traditional pilot test program takes 1-2 years, and costs millions of dollars, a Micro-pilot test can be conducted and analyzed at 1/10th or less cost, and in a matter of months. From a limited number of field tests we have conducted to date, it appears that a few Micro-pilot tests over a large basin or project area would yield a better assessment of the CBM or ECBM potential of a coal deposit.

A secondary benefit of a Micro-pilot approach is the tremendous saving in time and effort involved with permitting a multi-well depletion or gas injection pilot operation. Although the basic procedure of a Micro-pilot test is in some ways similar to a normal injectivity and pressure fall-off test, use of air (a coalbed methane desorbing gas), and the measurement of gas compositions and/or flow rates during flow-back, are some of the novelties that make a Micro-pilot test procedure unique.

MICRO-PILOT METHODOLOGY

In broad terms, the Micro-pilot test can be conducted in a core hole or a well. The region of the wellbore that penetrates the coal formation can be completed open-hole or it can be completed with casing which is perforated into the formation to allow fluid to flow between the formation and the wellbore. It is preferable to utilize a wellbore which is completed with casing and perforations if there are several coal seams that are vertically separated from one another.

If an existing producing well is used, it is preferred that the well be shut in for a couple of weeks to allow the pressure in the formation near the wellbore to approach stabilization. A desorbing gas, preferably air, is then injected for a period ranging from as little as a week, to as many as three to four weeks. During this air injection stage, the surface pressure and volumetric rate is frequently recorded. Upon termination of air injection, the down hole pressure fall-off is carefully monitored for about two weeks. Finally, the well is put back on production. The post injection flow rate, gas composition, and surface/bottom hole pressures are monitored for several weeks to months. Overall, the actual time required to conduct a Micro-pilot test is generally two months or more.

The general procedure for a Micro-pilot test outlined herein is only a guide. Special considerations may be required, depending upon where the actual Micro-pilot test is conducted. For example, the volume of injected gas will dictate the areal extent of the reservoir to be investigated. It is highly recommended that if there are any offset wells, they be monitored for rates, pressures, and gas composition. Changes observed in any neighboring well will be important in understanding the flow characteristics of the reservoir.

Micro-Pilot Test Analysis

The direct field observations of pressures, injection rates, production rates, and gas compositions are used in a comprehensive coalbed methane numerical simulator to history match well performance. As contrasted with a simple pressure transient test using water, a Micro-pilot test creates a perturbation in the reservoir using air, which has the ability to desorb methane from coal.

The nitrogen in air desorbs methane from coal, while the oxygen is mostly lost to coal due to rapid oxidation. The amount of methane released by coal due to air injection, and the subsequent pressure fall-off rate will be largely dependent on the reservoir properties such as permeability, wellbore skin, cleat porosity, gas content, etc. In a similar manner, the flow back of gases after a brief shut in period will also be highly dependent on the reservoir characteristics of the coal and surrounding formations.

By adjusting the coal seam properties that are unknown, a match can be obtained of the Micro-pilot test data. Although as with a traditional multiple well production pilot, the history match of a Micro-pilot is not expected to be unique, but subject to some interpretation.

MICRO-PILOT FIELD EXAMPLE

The first Micro-pilot test was conducted in the New Mexico portion of the San Juan Basin. The test well was drilled to a depth of 2975 feet and cased. Two major coal seams are present which total 55' in net thickness. The initial completion consisted of a slick water frac using 150,000 lbs of 40/70 and 20/40 mesh sand. Following the completion, the well was brought on line and gas sales began.

Approximately one year later, a well head compressor was placed on this well in an attempt to lower the well head pressure and increase production. Cumulative production prior to beginning the Micro-pilot test totaled 63.9 MMCF of gas.

The primary reason for conducting the Micro-pilot test was to determine the CBM and ECBM potential of the project area. The test well was shut-in for approximately three weeks prior to commencement of air injection. The pressure response during the shut-in period is shown in Figure 2.

Air was injected in two steps. During the first step, air was injected at a rate of 800,000 SCF/day at a bottom-hole injection pressure of approximately 800 psia. After five days, the air injection rate was increased to 1,400,000 SCF/day at a bottom-hole injection pressure of 1,400 to 1,600 psia. Air injection was ceased after approximately three weeks of injection.

The wellbore was shut-in after the injection was ceased, and the pressure fall-off was monitored, as depicted in Figure 3. After approximately 30 days, the wellbore was reopened and allowed to flow-back to the surface. During the flow-back period, the surface pressure and gas composition were measured. The cumulative injected air volume totaled 27.6 MMSCF, which is 43% of the total produced gas volume prior to injection.

Model Strategy

A coalbed methane simulator was used to history match the production and injection phases of the Micro-pilot well. A single well, radial model, with logarithmically spaced grid points was used in this simulation, as shown in Figure 4. The actual model input parameters for all simulations are included in Table I.

Reservoir Description

To capture the performance of the Micro-pilot test, it was necessary to incorporate many reservoir parameters into the model, i.e., rock compressibility, stress dependent permeability, etc. For this particular effort, a large amount of actual field data and lab measured data was available. The field and lab data have been honored as much as possible, and any exceptions are addressed within this paper.

MODEL INPUT PARAMETERS

Although a detailed discussion of the model input parameters would be impractical, some discussion of the important history matching effort is hereby provided:

Layering

As stated earlier, there were two distinct coal layers present in the test well. A two-layer model was found to be no more accurate than a single layer model in simulating the history of production and injection pressures. Therefore, for simplicity, the two layers were combined into a single layer.

Permeability

The pressure transient analysis (PTA) test was analyzed for permeability, fracture half length, skin, and reservoir pressure. The PTA test was conducted with both seams in direct communication with each other and resulted in an average permeability of 0.37 md. Furthermore, the wellbore skin was determined to be -5.15 (fracture half length of 95 ft).

Relative Permeability

Since the Micro-pilot test well was a very low water producer, gas-water relative permeability effects were ignored. The initial water rate from this well was 6 Barrels per day (BPD). As explained next, not incorporating water production data into the model may have impacted the stress-dependent permeability relationship used in the simulation.

Stress Dependent Permeability

Of primary importance to this particular history match was stress dependent permeability which has been shown to decrease exponentially as net confining stress increases.[5][6] The published stress dependent permeability relationship shown in Figure 5 did not provide an acceptable history match of the Micro-pilot test. Modifications to the stress dependent permeability curve (also shown in Figure 5) were made until an acceptable history match of the production phase was achieved. The discrepancy between the theoretical and fitted stress-dependent permeability ratio curves is believed to have been caused by relative permeability effects which are being accounted for here, rather than in the relative permeability calculations. This explanation was later validated by performing a scoping model run which incorporated a very low initial water production rate. In this particular case, the stress-dependent permeability ratio behaved very similar to the theoretical curve.

Lack of lab measurements of stress permeability above initial reservoir pressure required an assumption that stress permeability would continue to follow the exponential function. This was found to be true, up to a point. Again, adjusting the stress-dependent permeability ratio curve for the injection phase, also shown in Figure 5, reveals an exponential growth up to a maximum value of 1.35.

At lower pore pressures, the actual permeability ratio curves also deviated from the theoretical curve. In fact, minimum values are reached as shown in Figure 5.

With an acceptable history match of both the initial production and air injection phases, the post injection reservoir performance was analyzed. As shown in Figure 5, the stress-dependent permeability ratio curve was adjusted to match field performance. Note that there is a hysteresis effect, and the permeability ratio declines from its maximum value of 1.35 to a minimum value of 0.55.

Hysteresis effects, similar to those observed in this Micro-pilot test, have also been observed in past studies.[7]

It is also worth noting, the permeability ratios observed in this history matching effort are believed to be low. The ability to capture diffusional effects, which are discussed later and is a limitation of the simulator, would result in higher permeability ratios than those being shown here.

Isotherm

The actual methane and nitrogen adsorption isotherms for the coal from the test well were not available. Therefore, a lab measured isotherm from a nearby well had to be used, and is shown in Figure 1. Note that the coal can hold about 2.5 times more methane than nitrogen. Due to model limitations, the oxygen in air was assumed to have the same properties as nitrogen. Based on a qualitative relationship of each component's adsorption strength and boiling point, pure oxygen isotherm would fall somewhere between those for pure nitrogen and methane.[8]

Diffusivity

The inability of the numerical simulator to match (1) the early time pressure response observed during flow back, and (2) composition during flow back, is believed to be due to the lack of short term diffusional effects in the simulator. The gas analysis of samples taken during flow-back revealed that the methane is produced from the very outset at a concentration of 30%. It appears that the nitrogen fails to reach an equilibrium with the adsorbed methane near the wellbore, as is assumed in the numerical simulator. Consequently, the by-passed adsorbed methane is released during the initial flow-back period, as observed in the Micro-pilot.

Laboratory diffusivity measurements of coals similar to that in the test well have shown that 20 days is not sufficient to allow the coal to come to an equilibrium with the injected nitrogen. This fact was not contradicted by the Micro-pilot.

Since the Micro-pilot test on the test well showed the importance of incorporating coal diffusivity and multi-component gas injection capabilities, the simulator is being modified to handle these relationships in the future.

HISTORY MATCH RESULTS

A Micro-pilot test for the test well was history matched in three distinct stages: (1) initial production, (2) air injection, and (3) flow-back. This approach was used since each stage was contingent on the results of the preceding stage(s), and each history match may have required changes to the model input parameters. Overall, this approach was worthwhile, and the results are in very good agreement with historical data. The history match results are presented as the four individual plots in Figures 6 through 9.

The model predicted pressure response observed in the initial production and injection phases is excellent. However, some deviation in the pressure response was observed in the post-injection production phase. We believe this deviation is primarily caused by diffusional effects which could not be addressed due to limitations of the simulator.

PERFORMANCE PREDICTIONS

The Micro-pilot is aimed at better defining the reservoir quality of a coal formation, and in turn, predicting CBM and ECBM project performances. The model parameters obtained in achieving a successful history match of the Micro-pilot test well provided an excellent basis for an engineering scoping prediction of long term CBM and ECBM performance. Both the primary depletion and nitrogen injection scenarios were evaluated using one-quarter (1/4) of a nine-spot pattern as shown in Figure 10.

To simulate nitrogen enhanced coalbed methane, the injection pressure was assumed to be 20% more than the maximum pressure during the Micro-pilot test. However, the maximum injection pressure was limited to 2000 psia, the estimated parting pressure derived during previous fracture stimulation treatment of the test well. Simulated injection began and the ten-year predicted injection profile is shown in Figure 11.

The methane production rates and cumulative recoveries for simulated CBM and ECBM projects are shown in Figures 12 and 13. Due to the conversion of one producer to injector, methane production under nitrogen injection (ECBM) is less than primary depletion case (CBM) for almost two years. However, after three years of nitrogen injection, cumulative gas recovery using ECBM exceeds CBM. Since diffusional effects and coal heterogeneity are ignored during ECBM, the simulation results are perhaps pessimistic in the response time, and optimistic on nitrogen breakthrough. Therefore, the performance predictions based on a Micro-pilot results are best viewed as good scoping estimates.

Since coal seam injectivity is highly sensitive to the native coal seam permeability and the stress dependent relationship, ECBM results were recalculated using a higher permeability of 0.5 md, instead of 0.35 md. Table II compares the key difference in reservoir responses during ECBM with respect to changes in permeability.

Although we have pointed out some shortcomings of a Micro-pilot test if the model used to analyze the test has limitations, it is our opinion that the Micro-pilot test provided extremely useful data that was valuable in providing a scoping prediction of CBM and ECBM field performances. These results when used in conjunction with project costs can be helpful in determining the economic viability of CBM and ECBM options.

If a quick and inexpensive Micro-pilot test suggests that the coal reservoir is suitable for a commercial project, further reservoir characterization or pilot test program may be justified. In fact, the speed and cost of a Micro-pilot may justify several Micro-pilot tests in core holes and wells across the basin. This strategy may provide sufficient data to eliminate or select a portion of the field for a more detailed evaluation.

DIFUSSION TIME

It may be possible to detect a diffusion limited coal seam from Micro-pilot test results. Although this has not been performed on field data, it is our belief that a comprehensive coalbed methane simulator with diffusional capabilities would be able to distinguish the response of a diffusion limited coal seam, from one that is not diffusion limited.

VERTICAL COMMUNICATION

Micro-pilot data from the test well provided an extremely valuable diagnostic procedure which may perhaps be the most cost effective and reliable method of determining the presence and extent of vertical communication between the coal seams and the surrounding non-coal formations.

Although air was used as a desorbing fluid during the Micro-pilot test, it was observed that the oxygen in the air was trapped by the coal seam and not recovered during flow back. That is, the oxygen content of the gas sampled during the flow back period was extremely low relative to the nitrogen concentration.

Since coal is a known scavenger of oxygen, and the surrounding sand and shale formations are not, the ratio of oxygen to nitrogen in the flow back gas stream is a very good indicator of the presence or absence of vertical communication between the coal and the surrounding formation. In other words, if most of the air injected into a wellbore flows into a sandstone instead of a coal seam, the loss of oxygen will be minimal; the ratio of nitrogen to oxygen will be relatively closer to that of air (4:1).

For this reason, air is a preferred gas for a Micro-pilot test, more so than nitrogen or flue gas. The magnitude of oxygen loss to the formation would be directly correlated to the vertical communication that exists between coal and the surrounding formations. This knowledge is valuable in assessing the quality of a coal reservoir for a commercial CBM or ECBM project. Knowledge of the presence or absence of vertical communication between coal and other formations becomes specially important if the coal well is a prolific water producer.

If a Micro-pilot test data shows almost complete loss of oxygen to coal, it is an excellent indication that the produced water is from the coal and with further dewatering, will lead to higher gas rates in the future. On the contrary, if the injected oxygen flows right back during a Micro-pilot, the water flow into the well is most likely from a fracture system or surrounding non-coal aquifer. If so, the water rate may not represent future gas producing potential that has been observed in other coal wells which produce similar volumes of water from only the coal seam.

THEORETICAL POSSIBILITIES

In theory, a Micro-pilot test can be used as a diagnostic tool to determine if a coal seam is undersaturated in gas. Gas undersaturated coal seams have to be depressured (dewatered) extensively to allow commercial quantities of methane to flow to the wellbore. If a Micro-pilot test data cannot be history matched without assuming that it is undersaturated, adequate care must be taken in evaluating the prospects of a commercial CBM project.

Although the Micro-pilot concept is a new concept and has only been tested a few times in the field, it appears to be a cost and time effective alternative to the traditional method of reservoir quality assessment. Further improvements to the Micro-pilot test procedure and analysis method may be possible in the future.

RESULTS AND CONCLUSIONS

1. A novel "Micro-pilot" procedure for assessing coalbed methane reservoir quality has been developed and field tested.

2. It appears that the Micro-pilot approach to coalbed methane resource assessment can supplement, if not eliminate, the need for a traditional exploration program consisting of drilling and producing closely spaced pilot wells.

3. The greatest benefit of a Micro-pilot test program is its ability to drastically reduce coalbed methane exploration cycle time and costs.

4. A Micro-pilot test has the unique capability of detecting the source of water or gas in a coalbed methane well. That is, it is now possible to determine if there is vertical communication between coal and the surrounding formations, at least near the wellbore.

5. In theory, Micro-pilot tests can indicate the presence of under saturated or diffusion controlled coal seams.

6. Although a Micro-pilot test is not comprehensive, it can provide sufficient data for an engineering estimation of future production rates and reserves by means of pressure depletion or nitrogen/carbon dioxide injection enhanced recovery.

7. To fully evaluate Micro-pilot test results, a comprehensive computer simulator is essential, especially one that is capable of modeling diffusion limited desorption, multi-component sorption, and stress dependent permeability.

8. A Micro-pilot test is a valuable reservoir evaluation tool for determining coal seam injectivity and stress dependent permeability relationship.

METRIC CONVERSION

m = 0.3048 feet
MPa = 0.0068948 psia
cm3/g = 32.037 SCF/ton

REFERENCES

1. Puri, R., and Yee, D., 1990: "Enhanced Coalbed Methane Recovery", paper SPE 20732, 65th Annual Technical Conference and Exhibition of the Society of Petroleum Engineers, New Orleans, LA,..

2. Decker, A.D., White, J. & Reeves, S.R., 1991: "Coalbed Methane Exploration Strategies Applied in the Bowen Basin, Queensland, Australia", Coalbed Methane Symposium, Tuscaloosa, AL.

3. Semmelbeck, M.E., Lee, W.J., 1990: "Well Test Requirements for Evaluation of Coalbed Methane Development Potential", paper SPE 20669, 65th Annual Technical Conference of the Society of Petroleum Engineers, New Orleans, LA.

4. Puri, R., "A Method for Determining the Reservoir Properties of a Solid Carbonaceous Subterranean Formation", U.S. Patent Application, 1994.

5. Puri, R., and Seidle, J.P., 1991: "Measurement of Stress Dependent Permeability in Coal and Its Influence on Coalbed Methane Production", Coalbed Methane Symposium, Tuscaloosa, AL,.

6. Seidle, J.P., Jeansonne, M.W., and Erickson, D.J., 1992: "Application of Matchstick Geometry to Stress Dependent Permeability in Coals", SPE Rocky Mountain Regional Meeting, Casper, WY.

7. Harpalani, S., and McPherson, J.M., : "Effect of Stress on Permeability of Coal", 26th U.S. Symposium on Rock Mechanics in Rapid City, SD.

8. Ettinger, I., Eremin, I., Zimakov, B., and Yanovskaya, M., : Natural Factors Influencing Coal Sorption Properties I-Petrography and Sorption Properties of Coals, Fuel, Vol. 45, pp.267-275,.

TABLE I
History Match Reservoir Description
From Micro-Pilot Test

ϕ, porosity (%)	0.20
k, horizontal permeability (md)	0.35
h, reservoir thickness (ft)	55
c_w, water compressibility (psi^{-1})	3×10^{-6}
water density @ 14.7 psia (lb/ft^3)	62.43
μ_w, water viscosity (cp)	1.0
r_w, wellbore radius (ft)	0.23
s, skin factor	-5.2
r_{weff}, effective wellbore radius (ft)	39.7
p_i, initial reservoir pressure (psia)	60
bulk density (gm/cc)	1.53
V_{mCH4}, maximum sorption capacity-methane (SCF/ton)	475
b_{CH4}, Langmuir constant - methane (psi^{-1})	0.0139
V_{mN2}, maximum sorption capacity - nitrogen (SCF/ton)	194
b_{N2}, Langmuir constant - nitrogen (psi^{-1})	0.000734
L, layers	1
c_f, rock compressibility (psi^{-1})	9.61×10^{-4}

TABLE II

Comparison of key points of long term nitrogen injection with respect to changes in permeability

	Permeability (md)	
Key Factor Observed	0.35	0.50
1. Time to reach max. inj. pressure (2000 psia) at an injection rate of 1600 MCFD (years)	0.5	3.9
2. Time of N2 breakthrough at nearest producer (years)	1.0	0.8
3. Time to reach peak methane rate (years)	8.5	6.6
4. Peak methane rate (MMCFD)	1.44	2.03
5. Time to reach break-even point with primary depletion (years)	2.8	2.3
6. Cumulative methane produced within approximately 10 years	3.3	4.9

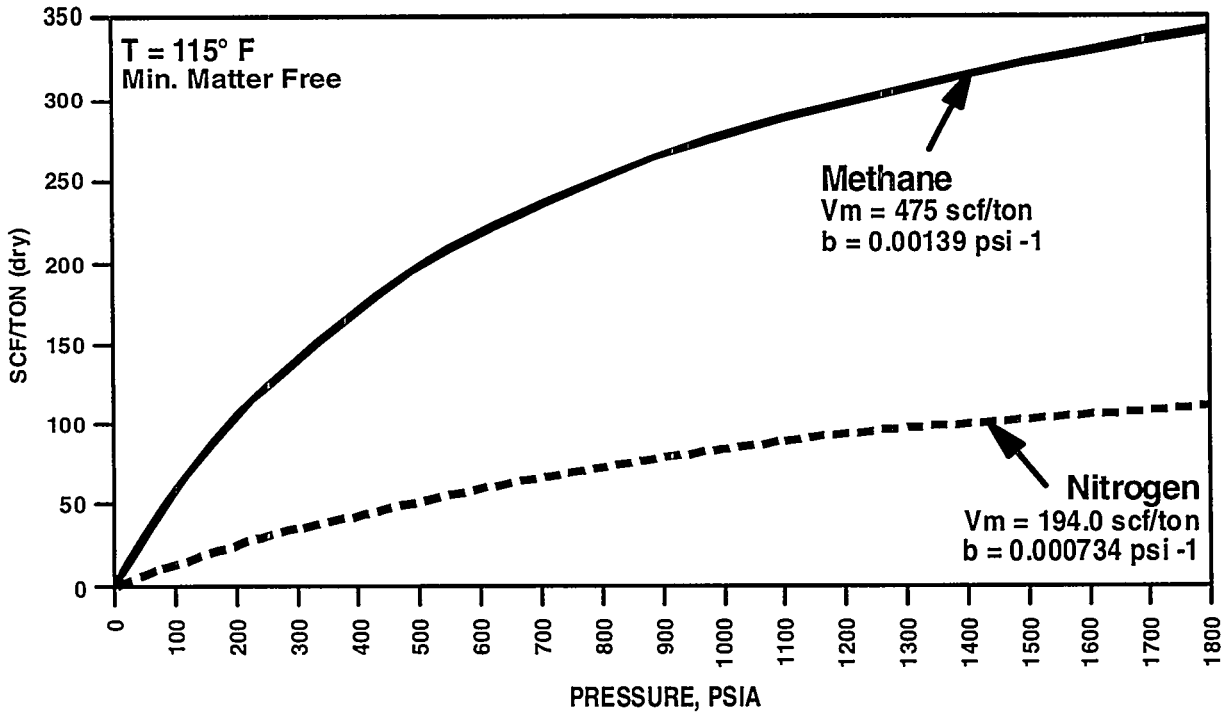


Figure 1: Sorption isotherm for methane and nitrogen.

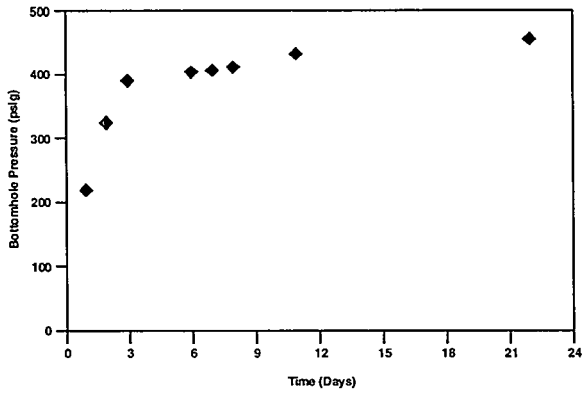


Figure 2: Bottomhole pressure response during shut-in period preceeding air injection.

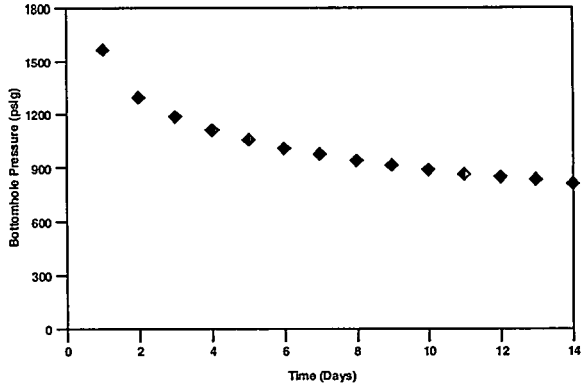


Figure 3: Bottomhole pressure response during shut-in period following air injection.

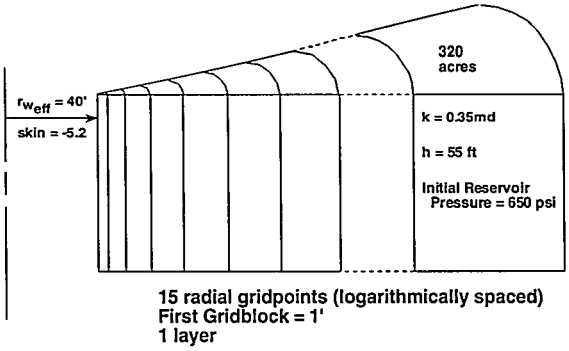


Figure 4: Grid and model parameters used in the history match.

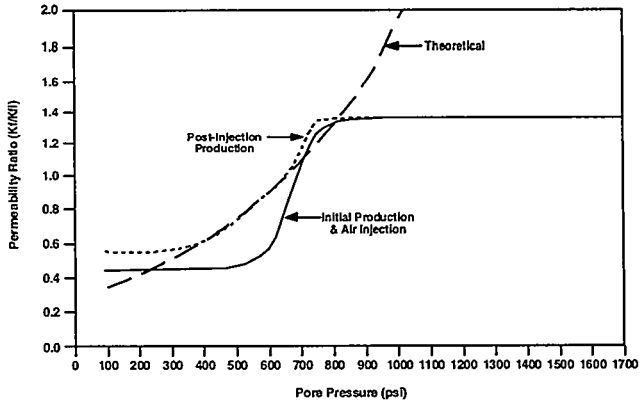


Figure 5: Permeability relationship to pore pressure used in the history match.

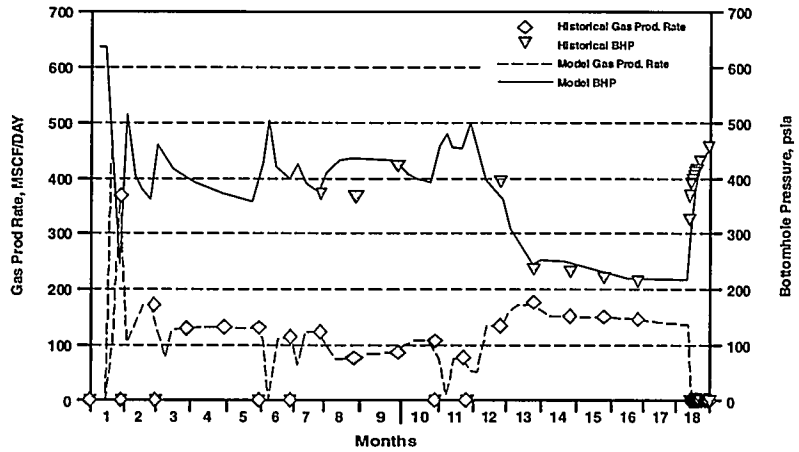


Figure 6: History match of Initial Production Phase.

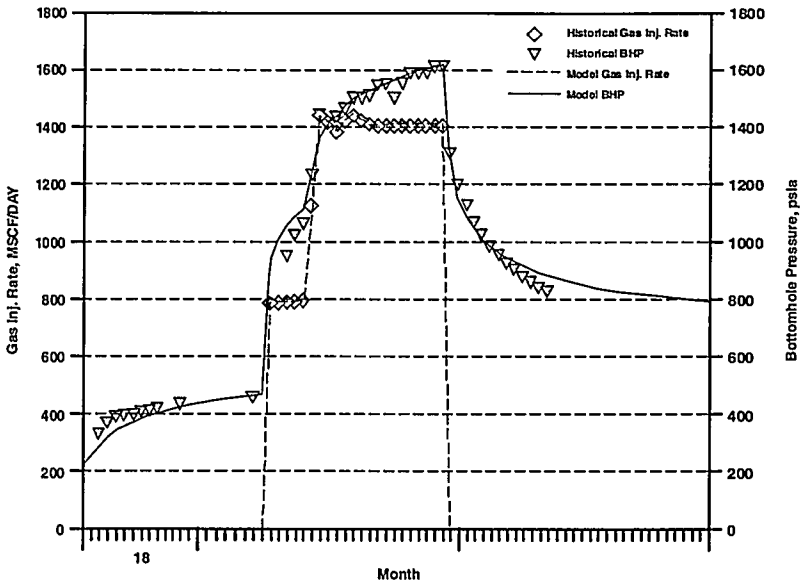


Figure 7: History match of Air Injection Phase.

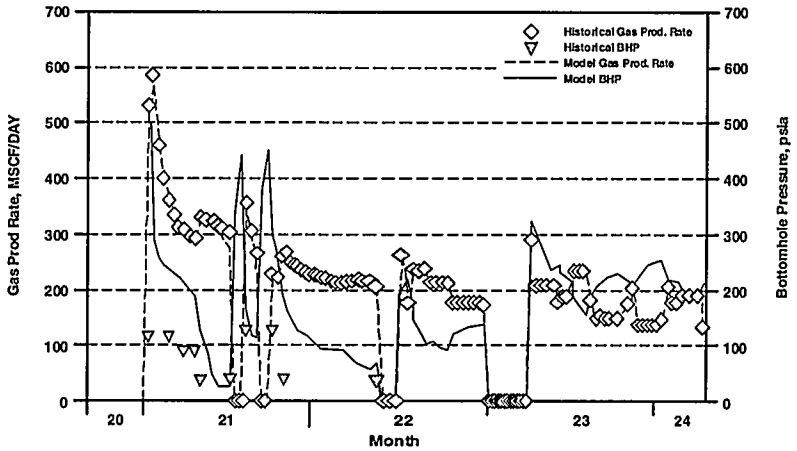


Figure 8: History match of Flowback Period.

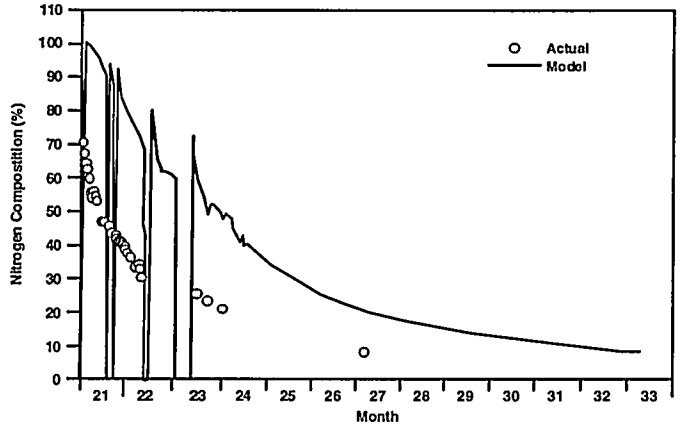


Figure 9: History match of nitrogen composition during Flowback Period.

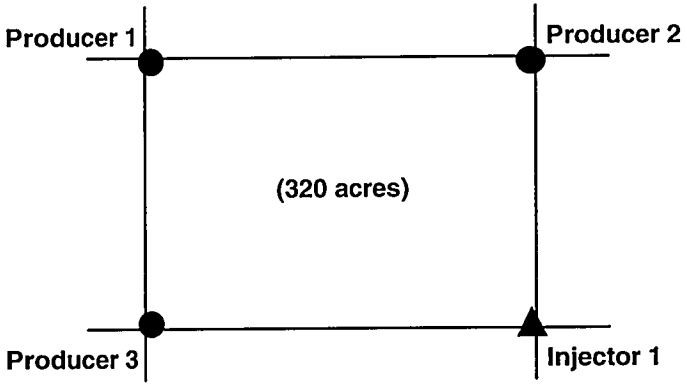


Figure 10: Quarter nine-spot injection pattern.

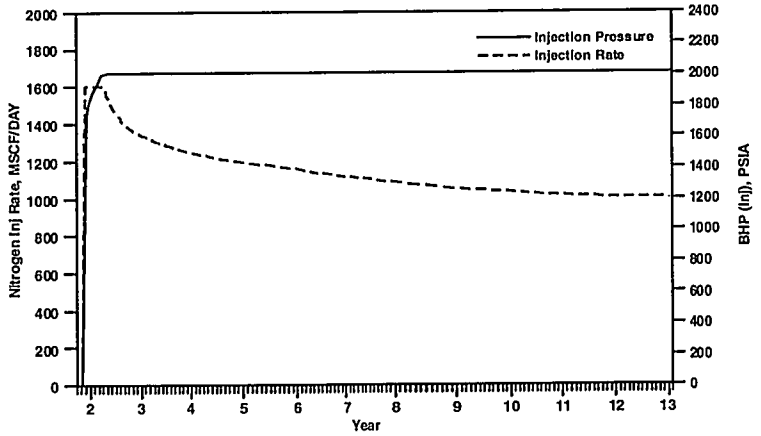


Figure 11: Model predicted nitrogen injection rate and pressure for full nine-spot pattern.

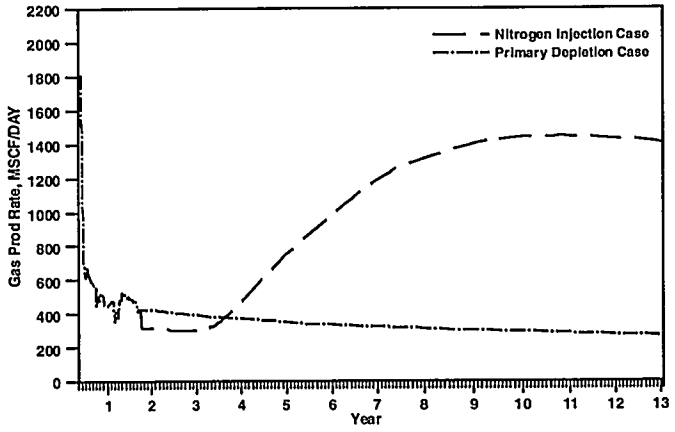


Figure 12: Model predicted methane production rate for full nine-spot pattern under primary depletion and nitrogen injection.

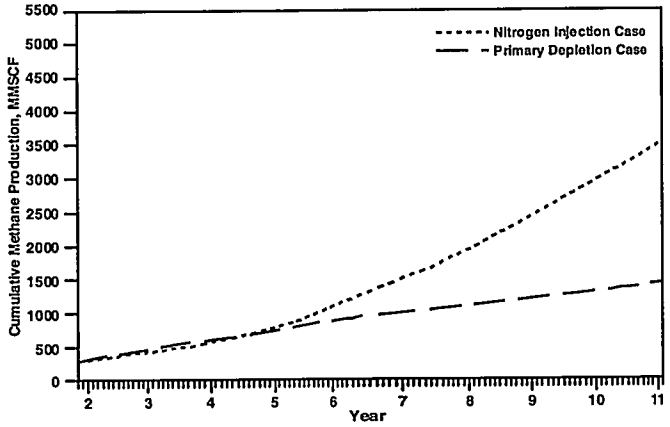


Figure 13: Model predicted cumulative methane production for a full nine-spot pattern under primary depletion and nitrogen injection.

INTERGAS '95

May 15-19, 1995
The University of Alabama
Tuscaloosa, Alabama USA

9550

Treatment of Fruitland Coal Production Water with Ion Exchange Media

C. Russell, Agua Vida; and C.P. Richardson, New Mexico Tech, NM

ABSTRACT

This paper presents ion exchange as an economic desalination method for water produced from oil and gas wells. Presently, industry uses Class II disposal wells, reverse osmosis, and evaporative techniques to discard this water in an environmentally responsible way. The oil and gas operator's selection of a method for disposal is driven by economics. Traditionally, pumping untreated water into injection wells has proven most cost effective considering the large volumes and regulatory requirements. Produced water, currently an exempt waste, may be reclassified nonexempt. As such, the treatment of production water to a set standard for beneficial use may prove to be the alternative of choice. The findings of this study indicate that ion exchange can be employed exclusively to reduce the total dissolved solids concentration. A specific case of production water is presented. The water is produced from the Fruitland Coal in the San Juan Basin of northwestern New Mexico. It has a high content of sodium bicarbonate (10,000 ppm) with all other constituents occurring in relatively minor amounts. The method described involves pretreating the production water in a bicarbonate anion exchange column, where noncarbonate anions are removed and replaced by the bicarbonate. The final step involves processing in an aerated and fluidized hydrogen cation exchange resin. Here, the hydrogen ion is replaced on the resin by another cation, typically sodium. The released hydrogen then reacts with a bicarbonate anion producing both water and carbon dioxide gas. Upon completion, the finished water can contain less than 500 ppm total dissolved solids. Because of the aeration, a reduction in residual dissolved hydrocarbons may also be realized. The design is simple, easy to implement, and economically competitive with other presently used methods of treatment and disposal.

INTRODUCTION

Produced water may be used in a beneficial way once it is treated to remove constituents that occur in excess of critical standards. The standards vary depending on the needs of the end user and are dictated by the EPA. Although the EPA prescribes the standards to be met, oil and gas operators must ultimately choose the disposal system for their wells based on cost and liability. The environmental liabilities presented in the 1990's are increasingly forcing more oil and gas operators to work abroad. This paper explores the feasibility of using ion exchange media for treating Fruitland Coal production water. The process has not been previously identified for this purpose. It is hoped that this work and other research aimed at the area of desalinizing produced water will help oil and gas operators in the United States to comply with present and future environmental regulations and still remain competitive at home.

Produced Water in New Mexico

In 1993, produced water, as it is commonly referred, reached nearly 71.6 million cubic meters (450 million barrels) in New Mexico [2]. If treated for end use, this yearly volume of water can serve all the needs for a city of 300,000 people or support farming on 20,000 acres of land [25,26]. In New Mexico, gas and oil producing areas are found in the San Juan Basin of northwestern New Mexico and the Permian Basin in the southeastern portion of the state. The San Juan Basin primarily produces natural gas; it accounted for 5.82 million cubic meters (36.6 million barrels) of produced water in 1993 [2]. Of this amount, 2 million cubic meters (12.6 million barrels) were produced from the Fruitland Formation as a result of coal degas operations. The water analysis found in Table 1 represents Fruitland Coal water with a total dissolved solids (TDS) content of 16,500 ppm. The average Fruitland well has a TDS of 10,000 ppm [14]. The water quality analysis shown is quite comprehensive as compared to most tests that quantify only the ions present. In desalination, the prevalent consumptive (TDS< 500 ppm) water recovery rate is 75%. The waste stream column in Table 1 is based on the this recovery rate. A molar balance of ions in Table 1 indicates a 10% differential between the anion and cations. Presumably, this may be accounted for in unreported or underreported ions.

In order for an operator to continue to produce, water from their well must either be disposed, or treated for further use. The word disposal is used to describe that operation in which the water is released with no intention of beneficial use. A treated water denotes that the water is processed for beneficial use. The operator will rightfully use a method of disposal or treatment that serves the operation's best interest. The EPA's Resource Conservation and Recovery Act (RCRA) does give allowances to companies actively involved in recovering produced wastes from their operations [15]. These

allowances, as applied to the wellsite, will in some instances justify treatment over disposal.

Disposal Methods

Currently, the oilfield uses the following methods to dispose of the produced water:

- Deep Well Injection
- Evaporation
- Waterflooding

While waterflooding is not considered a disposal method, it becomes one as oil is no longer economically recoverable.

Producers have found that Class II deep well injection is the most cost effective method for produced water disposal. The water is trucked or pumped to a central site and then injected into a deep formation. Regulations require this formation not to have gas or oil in commercial quantities nor have water present that is deemed usable in the future (200 years) [2,3]. In the San Juan Basin, these formations generally have a low saturation of highly saline water with minor amounts of hydrocarbons present. The average injection rates of these wells are at present 400 m^3pd (2500 bwpd) with calculated average ultimate storage capacities of 31.8 million cubic meters (200 million barrels) [1]. The wells are usually completed at an initial capital outlay of approximately $500,000 with variable transportation costs. Operators often quote an average injection cost of $6.29/m^3 ($1.00/bbl) and compare other methods to this benchmark price, although the method of amortization may vary widely. At present, Class II disposal wells require limited regulatory intervention initially and in the daily operating process. Recent proposals by the EPA have been suggested to change produced water's current status as an exempt hazardous waste, whereby regulatory intervention would inevitably be increased [18].

Natural evaporation is utilized primarily in the Permian Basin. The major disadvantages to this process are the large area required for viable rates and the formation of a highly salinized water which lowers the evaporative efficiency. In the San Juan Basin, several companies rent "steamers", where the produced water is contained in heated tanks and the formed water vapor is vented to the atmosphere. The process is driven by natural gas at an expected rate of 14.2 cubic meters of gas consumed per cubic meter of water evaporated (0.5 mcf/bbl) [27].

Desalination

The TDS content of production water may be lowered in a number of ways at the wellsite:

- Distillation
- Ion Exchange
- Electrodialysis
- Reverse Osmosis
- Freezing
- Chemical Precipitation

Neither freezing nor chemical precipitation are considered economic for brine water desalination. Reverse osmosis (RO) and electrodialyisis (ED) are currently the most popular methods employed for the reduction of TDS in brine water. Capital and operating costs for both these methods are about 0.50/m^3 ($0.08/bbl) for a 19,000 m^3pd (120,000 bwpd) plant [16].

Reverse osmosis has recently been proven in desalinating Fruitland Coal production water. Two RO facilities are located on the Southern Ute Reservation operating under a blanket National Pollutant Discharge Elimination System (NPDES) permit [4] . One of these RO systems is operated by RMI Environmental Service. The facility is skid mounted and suited for oilfield use. A partial list of the components used in the system are: hydrocyclones, ultrafiltration, precipitation, ion exchange, and reverse osmosis. RMI claims a treatment cost of $4.09/$m^3$ ($0.65/bbl) for processing 327 m^3pd (2050 bwpd) from an initial TDS of 3500 ppm to 500 ppm at 75% recovery [27]. According to the Gas Research Institute (GRI), with a decrease in capacity to 27 m^3pd (170 bwpd), the cost of RO skyrockets to $20.13/$m^3$ ($3.20 /bbl). Figure 1 shows cost comparisons for the different desalination processes. The cost data at 27 m^3pd are attributed to a study sponsored by GRI [5].

Only one site was noted as having tested ED for the treatment of Fruitland Coal water. The facility, located near Durango, Colorado, met with limited success. The site had numerous mechanical and operational problems, which led to spills and other complications. GRI, however, suggests that a working ED facility will give results comparable to RO at $24.53/$m^3$ ($3.90/bbl) for a 27 m^3pd operation.

Distillation has yet to be tried in the San Juan Basin in the truest sense. Distillation on a large scale is best suited for desalination of seawater where RO and ED fall short because of the frequent cleaning of membranes. Small scale operations may find distillation competitive due to the simplicity of the facility. GRI found that a 27 m^3pd desalination facility using a natural gas fired multieffect evaporator cost $15.03/$m^3$ ($2.39/bbl). This was their lowest cost per barrel treatment for a 27 m^3pd facility, which included a 20 year amortized capital cost and 10% discount. To compare the cost of a steamer operation to the present study, a facility was designed to recapture the generated water vapor. The economics, at 65% recovery, for a 8 m^3pd (50 bwpd) well included disposal of the waste stream. The results showed a cost of $12.71/$m^3$ ($2.02/bbl), comparable to the findings by GRI.

Ion exchange has not been viewed as a viable method for desalination in the past [1,5,14,16]. When considering the use of ion exchange in the traditional sense, this view is quite understandable; basically, one ion was just exchanged for another. Laboratory results herein show that using an aerated\fluidized hydrogen ion exchange column may effectively reduce the TDS of a 10,000 ppm Fruitland Coal water. The economics of this process appear in line with RO, ED and distillation. A design for a prototype operation applying this concept yields a $12.27/$m^3$ ($1.95/bbl) cost for a 8 m^3pd well.

BACKGROUND

In the 1930's hydrogen ion exchange materials were developed sufficiently for industrial exploitation. These

materials, sulphonated coal, proved quite effective in the dealkalization of water. The alkaline feedwater was passed through these coals, which resulted in the exchange of the alkaline associated cations for the hydrogen ion and the formation of carbon dioxide gas and water as shown in reaction (1) [19,20].

$$HR + NaHCO_3 \rightarrow NaR + H_2O + CO_2\uparrow \quad (1)$$

where: R = the resin phase

In recent years, the application of sulphonated coal has been replaced by manufactured carboxlyic and sulphonic resins. The sulphonic form was used in the present experiments. The carboxylic resin exhibits a higher regeneration efficiency than the sulphonic but has lower exchange rates [14]. The kinetics of the hydrogen form of the sulphonic resin are practically indistinguishable from free hydrogen kinetics since the SAC resin beads typically contain 40 to 60 percent water. in their boundaries. This water may be considered as a continuous extension of the aqueous phase in the flexible polymer system [17,19].

To examine the prospect of applying a strong acid cation exchange (SAC) resin in the desalination of the Fruitland Coal water, Amberlite® IR -120 Plus resin was obtained Rohm and Haas [22]. Most every general water treatment text presents a form of reaction (1) in association with SAC resins. However, the resin has not been used industrially for this purpose in waters containing a high concentration of alkalinity because the reaction produces large quantities of CO_2(g), which blinds the beads and causes slippage. The resulting slippage relates to a substantial decrease in water quality.

The properties of the resin are noted in Table 2. The equilibrium condition of Amberlite® IR -120 Plus with respect to the Na^+ and H^+ may be taken as (John McKnowlty, Technical Manager, Rohm and Haas, 1994):

$$HR + Na^+ \rightarrow NaR + H^+ \quad (2)$$

where: $K_{eq} = \frac{(NaR)(H)}{(HR)(Na)}$

$K_{eq} = 0.301$

Equation (2) can be used to determine the optimum regeneration level for the resin. The economics of a design are optimized by relating the selectivity of the resin in terms of acid concentration to sodium concentration [17]. Resins are frequently used below the maximum cation exchange capacity (CEC) level in view of the disproportional amount of regenerant needed to obtain the higher CEC.

EXPERIMENTAL APPARATUS

The ion exchange column (Figure 2), used to investigate the commercial feasibility of said reaction (1), was constructed to a scale recommended by experts in the ion exchange industry [23]. Sodium bicarbonate was batch mixed in a temporary storage reservoir. This feedstock solution entered the bottom of the column and passed through a length of graded glass beads, which provided support for the resin. Upon passing through the resin, the feed reacted to form carbon dioxide and water. The gas and water rose through the body of the column to a tee located at the top of the column. The tee provided a conduit for the exiting product water while the carbon dioxide gas was pulled through the top of the reactor column by a vacuum pump. In the conduit, the pH was measured prior to the product water entering a sample bottle. Between the top of the reactor and the vacuum pump, two 1.0M NaOH solutions (CO_2(g) traps) were placed in series to intercept the exiting gasses. Specific details of this apparatus are contained in reference 27.

ANALYTICAL METHODS

Special attention was given to volumetric and mass balance for every run. The $NaHCO_3$ was measured in the initial solution and this total inorganic carbon (Ct), equation (3), was accounted for on exit from the column reactor either in the product water or in the NaOH solutions. Mass and volumetric balances were considered imperative to the credibility of the experiments given the simple nature of the analytical methods used. There were discrepancies in both mass and volume in every experiment, but these differences never accounted for more than 5 percent of the total input.

$$[Ct] = [CO_3^{-2}] + [HCO_3^-] + [H_2CO_3^*] \quad (3)$$

As each experiment progressed, the product water was collected at 500 mL intervals. Acid and base titrations were utilized to determine alkalinity (equation 4), aqueous carbon dioxide, and carbonic acid content [28]. The carbonic acid and CO_2(aq) were determined collectively as $H_2CO_3^*$ [21,24]. A 5 mL sample was drawn from each collected bulk volume and released into a 100 mL volume of deionized water. This solution was then titrated with an acid or base to the representative endpoint. These were typically 8.4 and 3.7 respectively. The representative titrated inorganic carbon species (HCO_3^- or $H_2CO_3^*$) was then determined from the equivalents of acid or base added and the other species determined from thier equilibrium relationship (equation 5).

$$[ALK] = 2[CO_3^{-2}] + [HCO_3^-] + [OH^-] - [H^+] \quad (4)$$

$$K_1 = \frac{\gamma[HCO_3^-](H^+)}{[H_2CO_3^*]} \quad (5)$$

where: γ = activity coefficient-Güntelburg approximation [21]

$pK_1 = 6.38$ at 20°C

EXPERIMENTAL RESULTS

All the experiments proceeded in the same general manner. The feedstock solution would reach the ion exchange material where the sodium ion would exchange for the hydrogen cation. The bicarbonate anion then reacted with the hydrogen forming CO_2(g) bubbles and presumably water. Quite likely, a preceding reaction takes place before the formation of water and carbon dioxide gas. This may involve the formation of CO_2(aq) and a hydroxyl ion with the hydrogen ion being used as a catalyst [9,10]. Another approach includes the forming of a hydronium ion that reacts with the bicarbonate ion and decomposes to carbon dioxide and water [12]. In keeping with the spirit of this feasibility study, the discussion will be

limited to a stoichiometric explanation involving reaction (1) with an emphasis on the general mechanics of the system.

Ten laboratory runs are summarily presented with calculations in Table 3 to verify the commercial possibilities of using SAC ion exchange media for reducing both anion and cation concentrations in carbonate waters. The first four experiments were performed under a slight vacuum (0.87 atm). The next run, number 5, had air injected with no vacuum. Laboratory experiments 6 ,7, and 8 were ran with air injection under a slight vacuum. Concluding this series of experiments, numbers 9 and 10 were conducted under the same conditions as run 6 through run 8 only at elevated temperatures.

Because each experiment progressed in a common manner, only one experiment (run 8) is examined in this paper. Of particular importance, is the identification of a progressive trend for $CO_2(g)$ and pH. The pH is important for predicting mixing requirements. The product water carries a lower pH than EPA specifications, thus feed water may be combined with the effluent to reach the desired release pH.

Run number 8 was conducted at a feedstock rate of 0 195 mol/sec (0.1M) at 22° C and 0.94 atm. The trends of the data in experiment 8, shown in Figures 3 and 4, reflect those attributes of the other runs. In Figure 3, the conversion of the bicarbonate to CO_2 reaches the maximum early in the run (pt. A), maintains nearly that level for the life of the resin and then rapidly declines. At point B, the pH reaches a steady state condition for a short time before exhaustion. At the exhaustion of the media (pt. C) , the pH climbs steadily to the 8.3 pH of the bicarbonate solution. The pH climb to and from (pt. C) is chiefly a function of dilution effects rising from the introduction of unreacted bicarbonate solution. Figure 3 shows the pH as determined for each individual sample volume. The initial pH is low due to residual hydrogen ions associated with the resin. Disallowing dilution effects, the pH should look like a step function, with sharp breaks before and after the steady state region.

In determining the change of pH according to volume, a dpH/dVol graph is useful for analysis. Figure 4 depicts the pH as recorded during the experiment. The change of pH is essentially zero during the production of carbon dioxide gas. Therefore, in long term production (a field reactor) the pH would be expected to level off. It was initially considered that the pH change found in the experiments prior to exhaustion of the media was a result of dilution, which in part is correct; however, dilution effects would not fit the pH data in all respects. Alternate mechanisms appear to be in effect such as a change in reaction path [9,12]. It is interesting to observe that on the whole the pH is equal to the $pHCO_3^-$, suggesting an equimolar reaction. Note that at semi-steady state throughput conditions (1600 mL to 2650 mL), the pH is holding between 3.7 and 4.0. At this same volume, $pHCO_3^-$ changes from 4.2 to 3.7, a near mirror image in concentration. This range of pH is represented on a buffer diagram as being an area of minimum buffer intensity. Figure (5) shows this area for a 0.1 M bicarbonate solution corrected for activities. At the minimum buffer intensity, a carbonate solution changes pH readily in the presence of free hydroxyl or hydrogen ions. The pH change in these experiments may be the result of buffer capacity relationships or stochiometrically linked to reaction (1). It will be shown in the following section that if bicarbonate and hydrogen react equimolarly and no further reaction takes place, then the hydrogen concentration is in this 3.0 - 4.0 pH region.

Initially, the experiments were designed to have improved conversion rates in sequential order. The introductory runs, without air, had HCO_3^- conversion rates as high as any other run. In fact, all runs held 100% bicarbonate conversion for the life of the resin. The outstanding difference in the airless runs occurs in the ratio of $CO_2(aq)$ to $CO_2(g)$, which defines the yield of CO_2 (g). A low ratio signifies a larger concentration of $CO_2(g)$, relative to its aqueous counterpart. The ratio of the unaerated experiments averaged 0.40, while the aerated runs averaged half that at 0.20. The results confirm the initial assumption that aeration would increase the efficiency of the process through rapid transport of the carbon dioxide bubbles to the surface. Heat also achieved increased conversion of the bicarbonate ion to carbon dioxide gas [6]. In fact, the last and best run achieved a CO_2 ratio of 0.14 with the added benefit of a substantial increase in CEC/mL resin.

The column identified as CEC/mL resin found in Table (3) is partially a product of the regeneration technique [22] . The resin was not rigorously examined for each run. For the experiments, the resin was renewed by batch mixing the beads in a 10% solution of HCl at two times the quoted 1.9 meq/mL capacity [22]. The resin was then rinsed and the procedure repeated while left to set overnight. Since the resin was regenerated in batches, some comparison may be made in that regard. In run number 1, the enhanced CEC/mL is most likely a product of new resin, even though a cursory attempt to exhaust the resin was made beforehand. Runs 2 - 4 , 5 - 7, and 8 - 10 each shared the same regeneration batch.

Run number 7 exhibited the poorest CEC/mL. The run was made at the mechanical limitations of the reactor column. The flowrate of air and water were 350 mL/min and 2.95 mL/sec respectively, allowing for 70% expansion of the resin. The contact area with the resin appeared to have been reduced enough to show a CEC of 1.18 meq/mL. The beads were probably depleted to a greater degree but this exhaustion must have taken place later in the test where small changes in concentration are difficult to quantify. Run number 2, at 60% expansion, showed no apparent loss in capacity in comparison to runs 3 and 4. Thus it may be assumed, the limit for practical expansion occurs near 70%. All other runs had a bed expansion near 50%.

NUMERICAL MODELLING

Reactor simulations were performed, based on a completely-mixed stirred tank reactor (CSTR) and using currently accepted kinetic equations in an attempt to match data from the experiments to a known reaction [9,10,11]. From the basis of empirically calculated kinetic constants, the decomposition reaction of the bicarbonate ion may be the product of two reactions: the first one being the hydration reaction for aqueous CO_2 (reaction 6) with the second one seeming to be the catalytic reaction (reaction 7).

$$[HCO_3^-]+[H^+]\rightarrow[CO_2]+[H_2O] \qquad (6)$$

$$[HCO_3^-] \xrightarrow{H^+} [CO_2] + [OH^-] \quad (7)$$

In both reactions, the carbon dioxide, under saturated conditions, will go to the gaseous phase. Through application of a simple stoichiometric balance, a model for prediction of CO_2(g) formation and change in pH may be formulated.

The expected concentrations produced in a scaled up column reactor may be predicted with some confidence using the conversions found in run 8. The conversions found here are representative of the other runs. The calculated steady state conversion of HCO_3^- to carbon dioxide is 99.93% (equation 8) with 1 mol of HCO_3^- accounting for 0.88 mol CO_2 (g) and 0.12 mol of CO_2 (aq).

$$HCO_3^- \text{conversion} = \frac{F_{AO} - F_A}{F_{AO}} \quad (8)$$

Substituting the conversions from sample 4 into a modified version of equation (6) gives:

$$(1)[HCO_3^-] + (1)[H^+] \rightarrow (0.88)[CO_{2(g)}] + (0.12)[CO_{2(aq)}] \quad (9)$$

From this equation, the product concentrations may be calculated based on the experimental conversion of the bicarbonate ion. The results, shown graphically in Figure 6, closely reflect the exiting concentrations of all components in the experiment. The calculated effluent pH of 4.2 is similar to run 8's real time steady state pH of 4.0. Based on this, an assumption that HCO_3^- and H^+ react equimolarly and decompose to the same molar concentration appears valid. The concentration of the reactants would be expected to continue at these levels until the resin becomes exhausted. The initial conditions viewed in Figure 6 are calculated considering dilution effects.

The reaction rate (r_A), encountered at steady state for run 8, was calculated as 0.000236 M sec^{-1} (equation 10). The kinetic constant (k_f) is therefore 3.3 sec^{-1} (equation 11). This assumes a first order reaction at steady state in a CSTR with the representative values of: V_R = 820 mL, F_{AO} = 0.195 meq/sec, F_A = 0.000142 meq/sec [8].

$$F_{AO} - F_A = -r_A V_R \quad (10)$$

$$-r_A = k_f C_A \quad (11)$$

The break over to steady state at about 700 mL in Figure 6 corresponds to the change in pH denoted by the dpH/dVol graph (Figure 4) occurring at 850 mL. Again, the change reflected by both these figures is a result of the initial dilution effects.

Given the small amount of time to reach steady state, the reaction may be considered instantaneous from a design standpoint. Experimental kinetic information was calculated for all the runs and is presented in Table 3. It appears that the dominant reaction taking place is exothermic as indicated by the slower k_f values found in the heated runs 9 and 10. The calculated k_f values are near the published value of 18 sec^{-1} for reaction (6) [9,10]. However, this reaction is endothermic which reacts faster with increasing temperature. All ten runs have similar k_f values to an order of magnitude. No explanation is offered for run 5's exaggerated value for k_f. The overall reaction rates suggest that in addition to heat, aeration (runs 6,7,8) may also slightly dampen the reaction speed.

The simple mathematical model presented is based on empirical data. The results indicate that the reaction is fast, where the reaction reaches steady state in less than one space (reactor volume) time. A direct correlation for the calculated kinetic constant in comparison to published rates regarding the decomposition of the bicarbonate anion was not found. The calculated kinetic constants imply that either (1) intermediate reactions are involved, (2) an appropriate reactor volume was not used for calculations, or (3) the reaction is other than first or pseudo-first order. Therefore, in summary, initial designs of the prototype reactor should be based on the average experimental results and practical engineering concepts.

ENGINEERING DESIGN AND ECONOMICS

Under the proposed classification of produced water as a nonexempt waste, desalination facilities may become more prevalent at the wellsite. A desalination facility would typically operate in this manner:

- Production fluids exit the wellhead and flow into a separator,
- Following separation, produced water is processed by desalination equipment,
- Treated water is injected into a shallow aquifer or discharged to surface waters as per a specifications of a NPDES permit
- Saturated brine water is pumped to storage pending transport to a disposal site.

The employment of ion exchange as a desalination process is economically valid for waters where the principal anionic form of the TDS is a carbonate. Other anions are applicable for conversion; however, the wastewater produced may increase significantly. Water production from a Fruitland Coal well is highly variable, ranging from 0 to 800 m^3pd (0 - 5000 bwpd). An example design, presented in the Appendix, outlines an ion exchange process for a well producing 8 m^3pd (50 bwpd). There are several hundred Fruitland Coal wells that produce similar water volumes. The design is based on the averaged results taken from the heated/aerated runs 9 and 10 (Table 3). An iterative calculation procedure was used to obtain a volumetric balance of product water and wastewater [27].

The inlet water quality criteria used for the example design is shown in Table 4. The discharge quality reflects that of an approved NPDES permit from EPA's Region 8 [4]. Table 5 summarizes the overall design. It was calculated that approximately 5.9 m^3pd (37 bwpd) is treated with 2.1 m^3pd (13 bwpd) going to waste storage. Two bicarbonate anion exchange columns, operating alternately, are used to replace a small amount of chloride for bicarbonate. The water then is fed to one of four hydrogen aerated cation exchange columns where the finished product is obtained after pH adjustment.

Economics for the Example Design

The 8 m^3pd example design well, using ion exchange, will generate approximately 2.1 m^3pd of hazardous waste. Under pending EPA rulings, this quantity qualifies the operator as a Large Quantity Generator [15]. As such, the operator may store this waste on site for no more than 3 months. A standard 63.6 m^3 (400 bbl) tank would likely be installed on location to store this waste. The residence time in the tank is then 32 days before waste must be transported off location. If the water was not treated at the well, a truckload may be hauled offsite every 1.6 days. The trucking of this wastewater over large distances on poor roads becomes costly at an average hourly rate of $45. Given a six hour round-trip haul from this particular well to the nearest NMOGCD approved disposal facility, a trucking cost savings of nearly $50,000 would be realized yearly. An additional savings of $21,000/year would be incurred through decreased disposal fees using a current waste acceptance charge of $9.44/$m^3$ ($1.50/bbl). Thus, the operator could feasibly pay out a desalination system of $60,000 in initial invested capital within a year from the total savings incurred.

The economics of the example design operation are separated into three categories: 1) tangible items, 2) intangible items, and 3) operation and maintenance. The tangible items are paid out initially and have installation costs built into the total. The service life of the installation is estimated at 5 years. The nontangible items are those goods or services with no recoverable (salvage value) costs. Again, the economics presume immediate purchase with no amortization.

The facility costs include all valves, piping, sensing devices, ect. needed to operate the system. It does not include monitoring equipment that may be specified by the EPA [4]. The facility estimate is based on building the units entirely in the shop with minor field installation involved. The resin has a 50% contingency built in for loss and damage. Transportation involves the trucking of chemicals to the site at $50/hr and no trucking of wastewater. The disposal cost is inclusive and assumes injection into a nearby Class II disposal well. The O&M figure reflects one person at 2 hours per day.

Tangible Items	
Facility	13600
(6) reactor columns	
(3) holding tanks	
(1) house	
(1) compressor	
necessary plumbing	
contingency	1500
Resin (50% excess)	22850
Total	37950
Intangible Items	
Regenerant	
Acid ($75/ton)	1650
Sodium Bicarbonate ($10/50lbs)	1730
Transportation ($50/hr)	2400
Wastewater Disposal ($1.50/bbl)	7600
Total	13380
O & M (730 hrs/year)	14600

Cost per year based on a 5 year service life: $35,570 or $12.27/$m^3$ ($1.95/bbl).

This cost is realistic and can be used for comparison to other current disposal methods. The initial capital cost does not affect the incremental volume price as predominately as O&M and intangible costs. If the facility costs are increased by 100% (not including resin), the cost per volume increases to only $12.64/$m^3$ ($2.01/bbl). A larger initial investment into high quality products may be rewarded by reduced maintenance while possibly lowering the cost per barrel due to extended life.

SUMMARY AND CONCLUSIONS

Undoubtedly the process discussed in this paper works. Ion exchange, not previously defined for treating Fruitland Coal production water, can be used to treat this water to suitable standards. Concerning this issue, the key points are:

- The process concerning dealkalization of high molar bicarbonate using hydrogen cation exchange media is mechanically feasible.
- The initial economics based on a 8 m^3pd (50 bwpd) facility show the process to be competitive with RO and evaporation.
- Fluidization of the media is critical due to excessive production of carbon dioxide gas.
- The cation exchange reaction presented in this paper appears exothermic. The assumed first order reaction constant (k_f) decreased with increasing temperature.
- Although an increase of temperature within the reactor decreased the fractional conversion of bicarbonate, it increased the yield of CO_2 (g).
- Aeration of the media is helpful in improving the conversion of the bicarbonate ion to CO_2 (g). It appears only to mechanically affect the system as shown by kinetic similarities to the nonaerated experiments.

The experiments were conducted with no real difficulty once modifications to the reactor were made to compensate for the behavior of the process. The most important of these is fluidization and aeration of the resin. Conversions of bicarbonate at 90% and greater can be expected in a scaled up reactor. While the system may be particularly useful in treating Fruitland Coal water, it is economically applicable to the deionization of any groundwater where the primary constituents of the TDS are in a carbonate form.

APPENDIX

Example Design Guidelines

Well Name:	Coal Degas #1
Location :	Sec 24, R10W, T31N, San Juan Co., NM
Production:	Gas-500 mcfpd at 0.63 sg, Water- 50 bwpd at 13,016 mg/L TDS (Table 4)
Effluent:	TDS < 1000 mg/L with Ba^{2+} < 1.0 mg/L, pH 6.5 - 9.0, BTEX (benzene, toluene, ethylene, and xylene) < 0.1 mg/L, Conductivity < 1,200 µmho/cm [4].

Wastewater Discharge Source : Disposal Well #1
Treated Water Discharge Source: Ojo Alamo Injection Well #1

The ion exchange facility includes two anion pre-exchange columns followed by four cation exchange columns with post aeration. Without pre-exchange, the final effluent TDS will be 993 mg/L, mostly as NaCl. This concentration is below the 1000 mg/L effluent limitation. However, this NaCl concentration corresponds to a conductivity of 2,500 µmho/cm, or more than twice the effluent limitation. Essentially, a treated water containing only $NaHCO_3$ as the predominate source of dissolved solids will achieve the limitations imposed by the TDS and conductivity restraints.

Regeneration of the anionic exchange media may be accomplished with one bed volume of water containing 1.25 M $NaHCO_3$, but the solubility product of $NaHCO_3$ is 0.3066 M^2, allowing only a concentration of 0.5534 M to remain in solution. Therefore, 6.8 kg (15 lbs) of sodium bicarbonate per 150 liters of effluent water is required for each regeneration. One bed of rinse water (effluent) after each regeneration is sufficient to prohibit chloride contamination to the main reactor feedstream. For the cation exchange columns, the fluid velocity is constant for 50% expansion of the resin bed. Therefore, the column diameter must be fixed for a given flowrate. Resin volume and expansion dictate the column length. The cations, being significantly sodium, will exchange with the hydrogen ion in this process. Other cations, such as Ca^{2+} and Fe^{2+}, will exceed the sodium exchange potential on the resin. It is assumed that they will only partially be displaced from the resin during regeneration, causing a buildup of these cations over time. However, the exchange of multivalent cations still produces the desired H^+ release.

Based on experimental results, an air flowrate to a cationic exchange column of 70 mL/sec per cm^2 of reactor area is required or approximately 766 Lpm (27 cfm) for the example design. The air flow rate should be optimized in the field to maximize conversion for the given conditions.

Once through the exchange columns, the pH of the treated water must be adjusted to the effluent standards. As the treated water is airstripped post ion exchange, $CO_2(g)$ will evolve and increase the pH and affect the concentration distribution of the carbonates in the system. This pH change is partially calculated through the carbon dioxide buffer equation. The air stripping lowers both the inorganic and organic carbon concentration. To improve the economics, untreated production water is introduced after the air stripping to reach the maximum allowable effluent limitations. This process further raises the pH within the standard. A carbonate buffer equation, while considering the mass balance, is used to predict the amount of produced water to be added [21,27].

NOMENCLATURE

T_R	average reactor temperature (°C)
P_R	average reactor pressure (atm)
V_R	initial reactor volume (mL)
v_o	entering feedstock volumetric flowrate (mL/sec)
v_g	entering air volumetric flowrate (mL/sec)
F_A	exiting molar HCO_3^- flowrate (meq/sec)
F_{A0}	entering molar HCO_3^- flowrate (meq/sec)
X_A	conversion of HCO_3^-
Y_B	yield of $CO_2(g)$ (meq)
Y_C	yield of $H_2CO_3^*$ (meq)
CEC	total ion exchange capacity (meq)
R_l	length of resin (cm)

REFERENCES

1. Cox, D., Decker, A., Stevens, S., 1993: "Analysis of Fruitland Water Production Treatment and Disposal"; Chicago, Ill., Gas Research Institute Topical Report, 69 p.
2. New Mexico Oil and Gas Commission Division, 1991: Oil and Gas Regulations, as amended 3/1/91 in addition to personal correspondence, Santa Fe, NM.
3. New Mexico Water Quality Control Commission, 1986: New Mexico Water Quality Control Commission Regulations, as amended through June 18, 1986, Santa Fe, NM, 70 p.
4. EPA Region 8, 1993: "NPDES Permit issued to Emerald Gas Operating Company" Durango, CO, 40 p.
5. Lawrence, A., Miller, J., Miller, D., Linz, D. (GRI), 1993: "An Evaluation of Produced Water Management Options in the Natural Gas Production Industry"; paper SPE 26004, Proceedings from the SPE/EPA Exploration & Production Environmental Conference 93, San Antonio, TX, p. 581-596.
6. Hikita, H., Konishi, Y., 1984: "Desorption of Carbon Dioxide from Supersaturated Water in an Agitated Vessel"; AIChE J., V.34, p 945-951.
7. Tseng, P.C., et al., 1988: "Carbon Dioxide Adsorption into Promoted Carbonate Solutions"; AIChE J., V.34, p 922-930.
8. Fogler, S., 1992: Elements of Chemical Reactor Engineering: Prentice Hall, Englewood Cliffs, NJ, 550 p.
9. Pocker, Y., Bjorkquist, D., 1977: " Stopped Flow Studies of Carbon Dioxide Hydration and Bicarbonate Dehydration in H_2O and D_2O. Acid-Base Catalysis "; J. Am. Chem. Soc., V. 99, p. 6537-6543.
10. Kern, D., 1960: " The Hydration of Carbon Dioxide"; J. Chem. Educ., V.37, p. 14-23.
11. Roughton, F., 1941: " The Kinetics and Rapid Thermochemistry of Carbonic Acid "; J. Am. Chem. Soc., V.63, p.2930 - 2934.
12. Paneth, P.,O'Leary, M.H., 1985: " Mechanism of the Spontaneous Dehydration of the Bicarbonate Ion"; J. Am. Chem. Soc., V.107, p.7381-7389.
13. Nguyen, M., Ha, T-K, 1984: " A Theoretical Study of the Formation of Carbonic Acid from the Hydration of Carbon Dioxide: A Case of Active Solvent Catalysis"; J. Am. Chem. Soc., V.106, p. 599-602.
14. Ray, J., Engelhardt, F., 1992: Produced Water, Technological/Environmental Issues and Solutions: New York, Plenum Press, 609 p.
15. Wentz, Charles,1989: Hazardous Waste Management: New York , McGraw-Hill, 461 p.
16. Office of Technology Assessment, 1988:Using Desalination Technologies for Water Treatment,. A Background Paper for the Congress of the United States:U.S. GPO, Washington, DC
17. American Water Works Association, 1990: Water Quality and Treatment - Fourth Edition: New York, McGraw-Hill, 1194 p.
18. Fillo, J. et al., 1987:Production Waters Associated with the Production, Processing, Transmission, and Storage of Natural Gas: A Literature Survey: Chicago, Ill., Gas Research Institute, 301 p.
19. Arden , T., 1968: Water Purification by Ion Exchange : New York, Plenum Press, 450 p.
20. Applebaum, S.,1968: Demineralization by Ion Exchange: New York, Academic Press, 350 p.
21. Benefield, L. , Judkins, J. , Weand, B., 1982: Process Chemistry for Water and Wastewater Treatment: Englewood Cliffs, NJ, Prentice Hall, 510 p.
22. Rohm and Haas, 1990: Technical Bulletin - Amberlite® IR 120 Plus: Philadelphia, PA, 15 p.
23. Rohm and Haas, 1990: Rohm and Haas Ion Exchange Resins Laboratory Guide: Philadelphia, PA, 35 p.
24. Snoeyink, V., Jenkins, D., 1980: Water Chemistry, New York, Wiley and Sons, 463 p.
25. Lindberg, M., 1992: Civil Engineering Reference Manual - sixth edition: Belmont, CA, Professional Publications, 500 p.
26. Stone, Bill et al., 1984: Hydrogeologic Rpt. #6: Socorro, NM, New Mexico Bureau of Mines and Mineral Resources, 70 p.
27. Russell, C., 1994: M.S.Thesis; Socorro, NM, New Mexico Tech, 132 p.
28. Hach Co.,1992: Water Analysis Handbook - Second Edition: Loveland CO. 831 p.

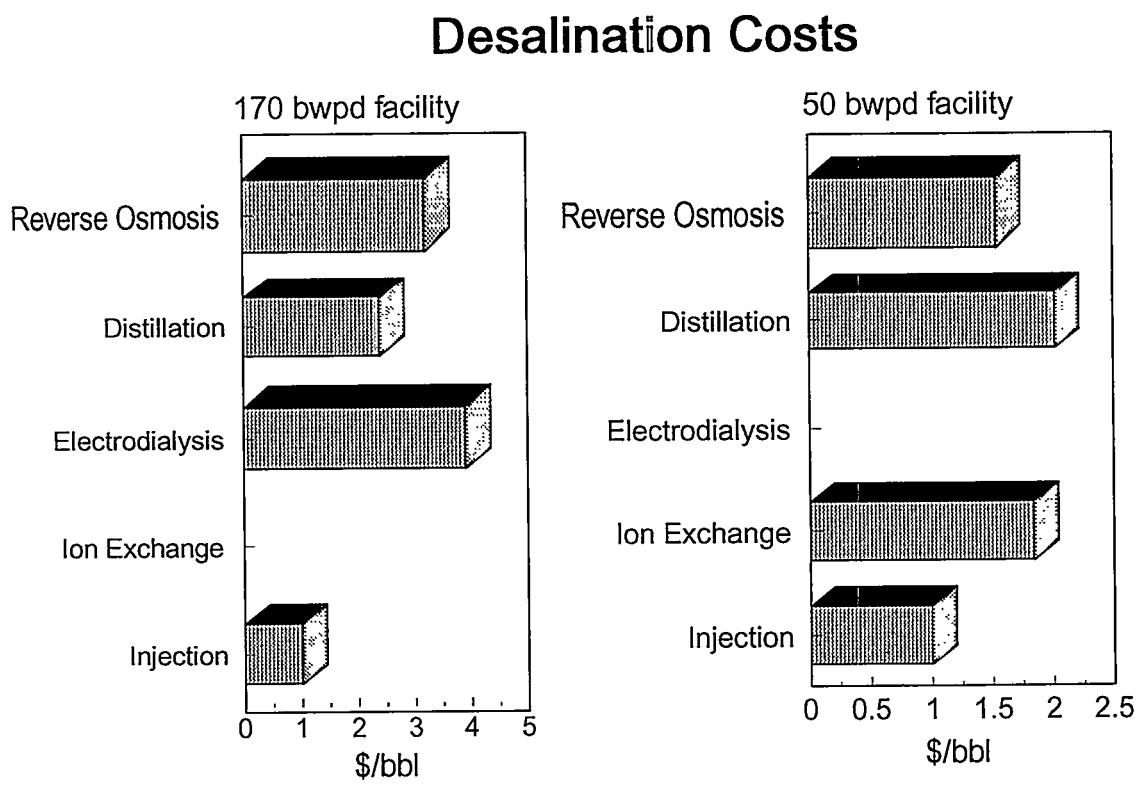


Figure 1. Cost comparison for selected treatment options

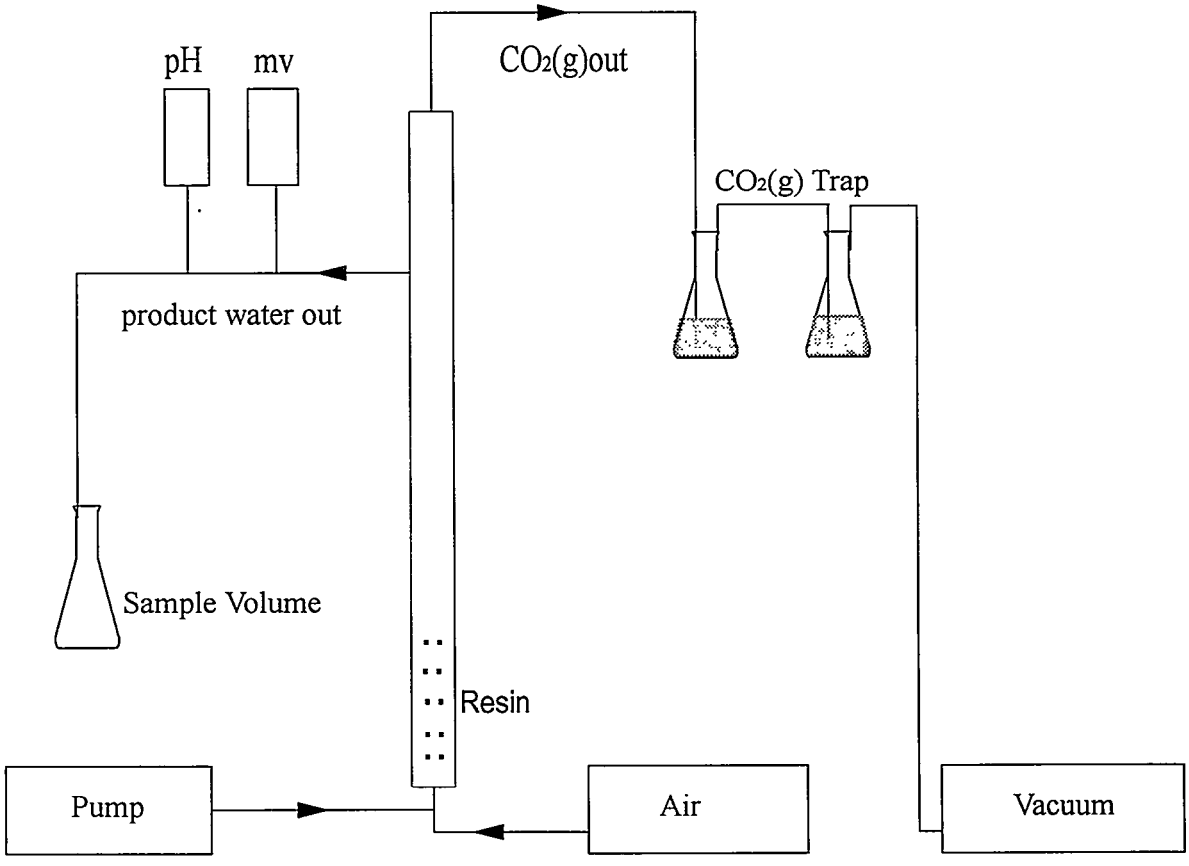


Figure 2. Laboratory ion exchange column apparatus

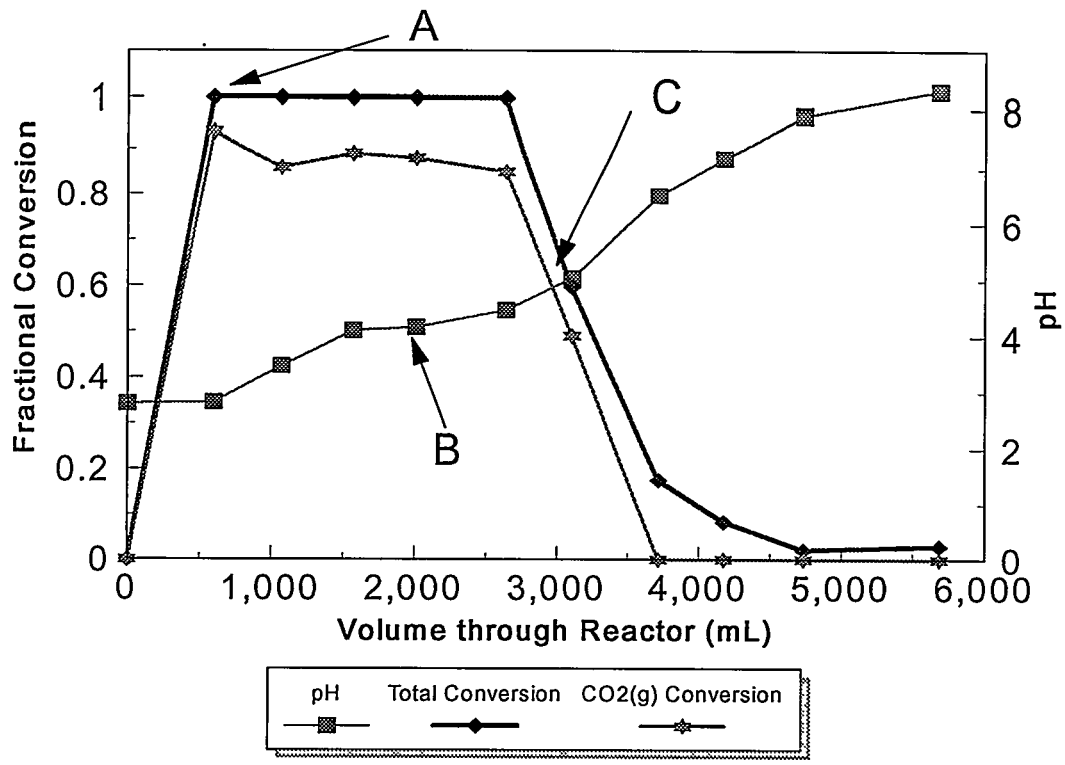


Figure 3. Experimental results for run 8

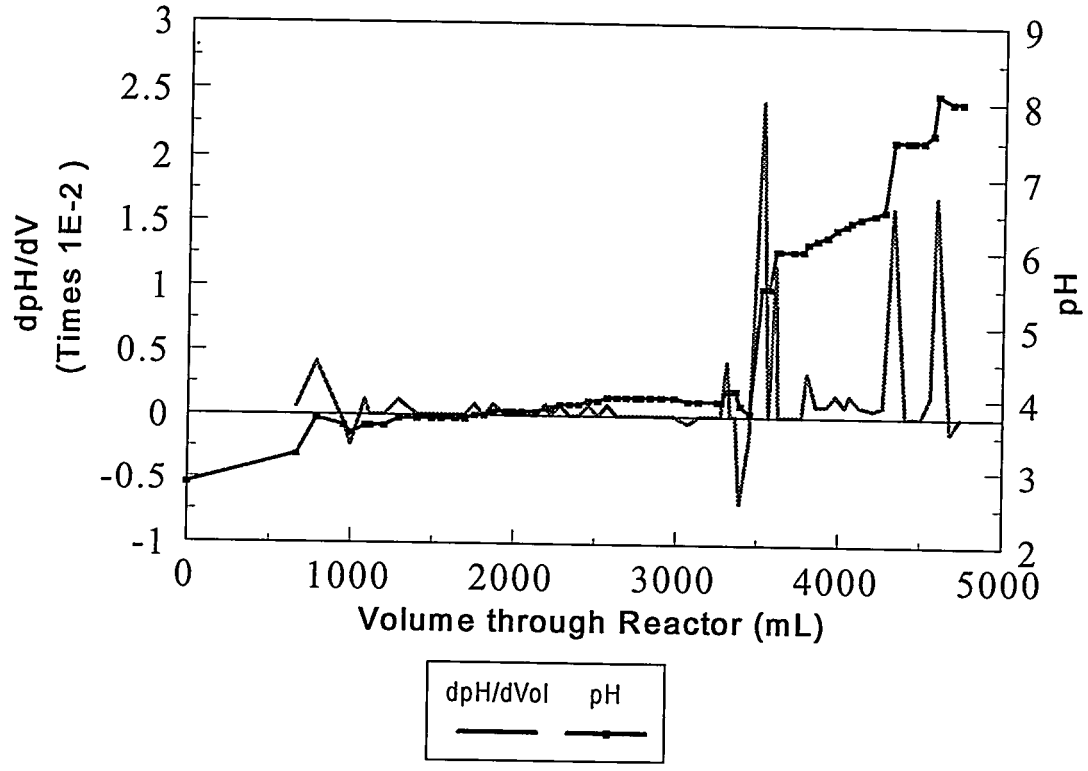


Figure 4. dpH/dVol graph for run 8

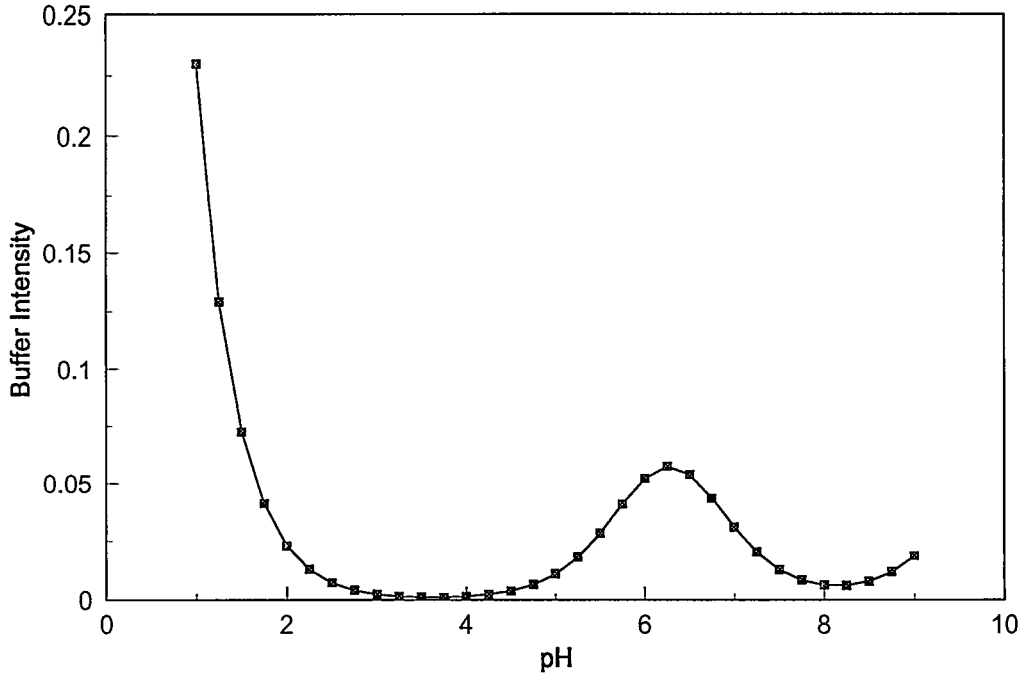


Figure 5. Buffer intensity for a 0.1M carbonate solution

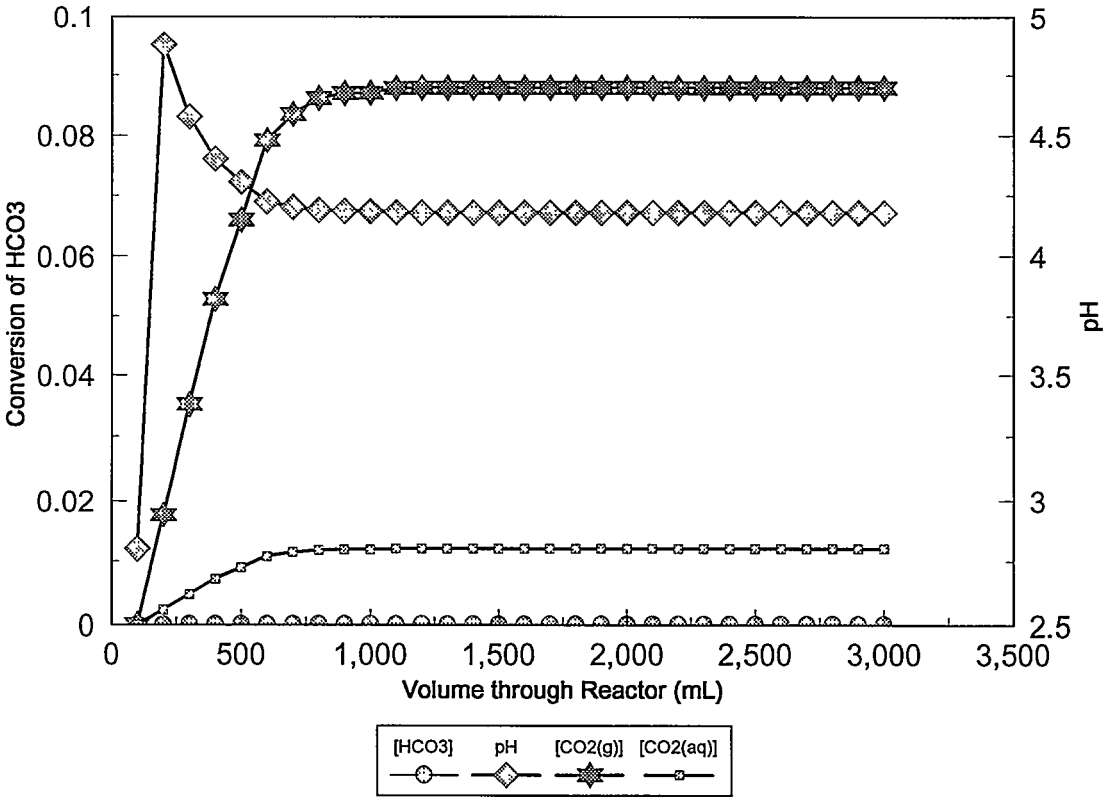


Figure 6. Model of stoichiometric reaction as based data from run 8

Component	mg/L	waste mg/L	Component	mg/L
Aluminum	< 1		Oil and Grease	70.0
Arsenic	0.003	0.0114	Phenols	0.027
Barium	61.9	236.2104	Sulfate	< 20
Cadmium	< 0.005		Benzene	< 0.01
Calcium	29.6	112.9536	Toluene	0.03
Chromium	< 0.01		Ethyl Benzene	< 0.01
Cobalt	< 0.02		Total Xylene	< 0.01
Copper	< 0.25		Alkalinity as $CaCO_3$	14700.0
Iron	4.2	16.0272	pH	8.07
Lead	0.27	1.0303	T. Dissolved Solids	16300
Magnesium	18.4	70.2144	Radium-226	4.3 +/- 1.0
Mercury	< 0.001		Radium-228	8.6 +/- 2.2
Nickel	< 0.03		Strontium - 90	70.7 +/- 1.1
Potassium	48.4	184.6944		
Selenium	< 0.0001	.		
Sodium	5370.0	20491.0		
Strontium	NR			
Vanadium	< 0.1			
Zinc	0.39	1.4882		
Bicarbonate as $CaCO_3$	14700.0	56095.2		
Carbonate as $CaCO_3$	0.0			
Boron	1.6	6.1056		
Chloride	905.0	3453.48		
Fluoride	0.94	3.5870		
Nitrate/Nitrite as N	0.14	0.5342		

Table 1. Chemical characterization of Fruitland Coal well [4]

Parameter	Resin (Hydrogen Cycle)
Water Content	45%
Density (g/L)	768
Effective Size (mm)	0.55
pH	1.0 - 14
Temperature (°C)	0 - 121
Minimum Bed Depth (m)	0.61
Regenerant Conc.	5% - 10% H_2SO_4
Regeneration Rate	4.0 - 6.0
Rinse Flowrate (L/hr/L)	from 4.0 - 12
Rinse Water (L/L)	3.4 - 10.0
Exchange Capacity	~ 1.9

Table 2. Laboratory resin parameters as published by manufacturer [22]

Run No.	T_R	P_R	V_R	v_o	v_g	F_{AO}	F_A	k_f	Y_B	CEC	R_l	CEC/mL
1	22	0.87	1570	2.10	0	0.237	3.15E-05	4.792	147	262	30.1	1.72
2	22	0.87	1380	2.64	0	0.288	3.696E-05	14.906	167	210	30.3	1.37
3	22	0.87	900	1.82	0	0.164	3.458E-05	9.590	157	221	32.8	1.33
4	22	0.98	850	1.89	350	0.125	3.213E-05	8.649	185	256	35.2	1.43
5	22	0.94	850	1.89	0	0.189	5.67E-06	74.116	182	244	35.2	1.37
6	22	0.94	850	1.84	350	0.199	7.176E-05	6.002	208	257	32.1	1.58
7	22	0.94	800	2.95	350	0.295	0.000130	8.379	184	233	39	1.18
8	22	0.94	820	1.95	350	0.195	0.000142	3.256	242	293	34.3	1.69
9	30	0.94	850	1.95	350	0.195	0.000585	0.764	279	318	33.3	1.89
10	38	0.94	850	1.95	350	0.195	0.001047	0.426	263	290	31.6	1.81

Table 3. Summary of laboratory results [27]

Ions	mg/L	meq/L
Sodium	3610	157.0
Calcium	19.73	0.985
Iron	2.80	0.100
Magnesium	12.25	1.008
Potassium	13.26	0.34
Barium	41.25	0.601
Chloride	603.0	17.03
Bicarbonate	8725	143.0
pH	8.2	

Table 4. Fruitland Coal produced water characteristics for example design [27]

Parameter	SAC Columns	SBA Columns
Column ID (cm)	15.24	20.32
Column Length (cm)	2	2
Resin Depth (m)	1	2
Number of Columns	4	2
Column Service Time (hrs)	0.31	15.1
Inlet Produced Water Flowrate (Lpm)	4.17	4.17
% Expansion	50	NA
Air Flowrate (Lpm)	766	NA
Regenerant Concentration	10% H_2SO_4	0.55M $NaHCO_3$
Regenerant Flowrate (Lpm)	6.5	4.3
Resin Exchange Capacity (meq/ml)	0.69	1.0
Rinse Volume (L)	18	65
Average Rinse Flowrate (Lpm)	2.6	17
Pressure Drop (psig)	NA	6
Temperature (°C)	38	38

Table 5. Example design ion exchange column parameters [27]

INTERGAS '95

May 15-19, 1995
The University of Alabama
Tuscaloosa, Alabama USA

9559

The Economics of Converting Coalbed Methane Gas Directly into Liquids

Q. Adams, Earth Resources Technology Services

ABSTRACT

Millions of dollars are being spent on programs to improve technologies for coal liquefaction and gas conversion. Some of the programs include revising and modifying versions of the classical Fisher-Tropsch process developed prior to Word War II. Methane is produced as a by-product of coal gasification. By converting coalbed methane gas into liquids, approximately 60 to 72% of the front end costs for the conversion of coal to gas and gas into liquids can be eliminated.

The Gas Flow Path: Coalbed methane wells usually produce gas though the casing/production tubing annulus. The wells normally produce under minimum back-pressure to optimize gas desorption from the coal and drainage of the water. Once gas reaches the surface, it is normally piped to a two-phase separator, which removes water from the gas. (Alternatively, the gas can be piped directly into the gas gathering system to reduce backpressure on the casinghead.) Then the gas flows through an orifice meter with a 3-pen chart recorder where it is measured. Next, the gas is piped through a field collection line to a gas scrubber, which removes any remaining water before the gas enters the compressor. Finally, the gas exits the compressor, flows through a dehydrator and sales gas meter into the sales gas interstate pipeline.

Thirty-five percent of a synfuels plant output is an odorless and smokeless premium grade diesel Fuel, plus light distillate naphtha used to make jet fuel, paint and special high-density waxes used for industrial lubricants and special resin-wax formulations. Also, by converting methane gas into fuels, waxes, and naphtha, a synfuels plant can provide the owners of natural, coalbed methane gas reserves, landfills and sewer treatment plants with an opportunity to capitalize on previously unprofitable resources.

The recent development in synthetic fuels was motivated by the 1990 Clean Air Act Amendment and not necessarily by economics. Beginning in 1993, urban buses in 39 U.S. Cities with populations over 750,000 or more, must meet a diesel particulate standard of 0.1 gram per brake horsepower/ hour. The standard which applies only to urban transit buses, drops to half that level in 1994. If monitoring data indicates that buses are not meeting the standards, EPA must implement a "low-polluting fuels" program for new buses in large cities. Possible low-polluting fuels include methanol from coalbed methane, and compressed natural and methane gases.

INTRODUCTION

The purpose in developing Synfuel plants for converting coalbed methane gas into transportation fuels is basic economics. Also the products are environmentally friendly synthetic fuels, lubricants and waxes that bring higher prices.

An economical feedstock; Ever since the beginning of recorded history, methane gas or coal gas has been associated with coal mining where the presence of large volumes of methane gas associated with coals, has been common knowledge, particularly to the determent of coal miners, many of whom have lost their lives in underground gas explosions.

Coalbed methane has undergone a transformation from dangerous nuisance to economic energy resource during the past decade, Conservatively estimated at 90 trillion cubic feet of recoverable gas, coalbed methane now represents one-third of proven natural gas reserves in the United States. During 1990, one-third

to one-half of all gas well completions will be coalbed methane wells. By the year 2000, 7,000 coalbed methane gas wells at a cost of $3 Billion is projected, and will supply up to 6% of domestic supply.

Methane production from coal seams is projected to be a highly profitable enterprise in western coal basins such as the San Juan, Raton, and Powder River basins, where thick coal seams at relatively shallow depths provide expected per well gas reserves from 0.4 to 9.0 Billion cubic feet , at finding costs of 8 to 24 cents/mcf. After tax indicators are: internal rate of return 25% to 70%, profit on investment ratios of 3.2 to 14, and payout in 1.8 to 4 years.

Coalbed methane technology is new and long term production profiles and ultimate gas recoveries uncertain. Nevertheless, with careful due diligence, coalbed methane development projects offer a high degree for success.

Coalbed Methane Gas is drilled, dried, compressed, and placed in the interstate pipeline as quality grade, burner tip gas, (1,000 BTU per CF) the same as natural gas. 15% of the U.S. pipeline gas in the U.S. (40% in Alabama) Is methane gas.

Gas futures fluctuates on the commodities market seasonally.

Power and Cogeneration Plants for the past 15 years have been converting to gas, burning both natural and coalbed methane gases. These plants negotiate long term 20 year gas supply contracts with the pipeline or major gas producers resulting in a stabilized gas price rate.

The Resource

1. Drilling into the coalseams and removing the methane gas, vents the coal, and removes any threat of gas explosions.

2. The coal is not mined nor is the surface landscape disturbed. Small 6 - 8 in. diameter holes are drilled into the coal and the gas is removed.

3. The large volume of water processed with the gas from the coals generally is of good quality (5,000 ppm TDS) and can be used for livestock.

(See Table I)

Due to the nature of the feedstock, products do not contain any sulfur or nitrogen and conform to the new EPA Clean Air Act regulations with respect to particulate emissions, sulfur and aromic content. Distillates from this process are finding a premium value in the market .

Environmentally friendly coalbed methane gases used in conjunction with natural gas are the clean burning fuels used for power and cogeneration plants powered by turbine jet engines. The same jet engines are used on jet aircraft.

The basic economics for a coalbed methane gas synfuels plant are substantially enhanced by a low cost feedstock. The economics is best illustrated in the Powder River Basin of northern Wyoming and southeastern Montana.

The Powder River Basin contains unusually thick, low-rank (subbituminous) coals in the Fort Union Formation (Paleocene) and in the overlaying Wasatch Formation (Eocene).

These low-rank coals contain relatively low methane contents compared to bituminous coals (based on measured gas contents), however shallow seams 100 feet or more thick in the basin hold large volumes of gas in place, which can be recovered through low-cost drilling programs utilizing horizontal drilling methods.

Active operators in the area are registering wells at depths from 288 to 218 ft. and also from 440 to 500 ft. Many of these wells are so shallow that they are drilled with conventional water well drilling mobile units. Production rates range from 25 to 500 MCFD (MCFD=1000 c.f. per day). Wells are perforated, and virtually all are stimulated. Table II is an example of the cost to drill and complete a methane gas well.

As stated in the Abstract, the development of synthetic fuels was motivated by the 1990 Clean Air Act. The time for implementing Mobile Source Provisions are as follows:.

1993 - New standards for sulfur content of diesel fuel takes effect, which reduces the maximum sulfur levels by 80%.

1994 - Truck and buses must meet stringent diesel particulate emission standards, equivalent to 5% of the uncontrolled level. All buses in service in cities with populations of 750,000 or more, to be operated on clean alternate fuels.

1996 - Establishes a new program, initially in California and required in 1996, to require the sale of 150,000 ultra-clean vehicles in the state, increasing in 1999 to 300,000 annually.

Clean Fuels, An Overview - What are Clean Fuels?.
The most familiar transportation fuels in this county are gasoline and diesel fuel, but any number of energy sources are capable of powering motor vehicles. These include grain, wood and coal alcohol, electricity natural and methane gases (including coalbed methane) and propane. Some vehicle fuels because of physical or chemical properties, create less pollution than do todays gasoline. These are called "clean fuels".

Synthetic diesel fuels derived from methane gas emits, at a minimum, **18% less particulates, 15% less hydrocarbons, and 14% less carbon monoxide than No. 2 diesel fuel**. Synthetic diesel fuel is the cleanest fuel available, and unlike other alternate fuels, does not require any special equipment or engine alterations.

The Bechtel Group with Amoco Oil Company as the main subcontractor was awarded a $2.5 million contract in 1991 to be completed by the end of 1994. This contract is to assist DOE's PETC in developing a scientific and engineering base for the indirect coal liquefaction technology used in the production of transportation fuels.

The present indirect liquefaction (converting coal to gas and into liquids) technology is being developed as a baseline design study, the PFS model, for a wide range of plant capabilities and operating parameters and will be a research tool for evaluation of future technology advances.

PETC has revised the Bechtel Group contract for modification of Bechtel's baseline design study to include a separate economic analysis for the conversion of natural gas to liquids. This effort was a logical continuation of Bechtel's baseline design study and will provide additional capabilities to the model for future use.

With the appropriate modifications of the current baseline design and computer mode, any hydrocarbon feedstock can be used.

A number of process technologies that convert coal-derived syngas into liquid fuels are also being demonstrated at DOE's Alternate Fuels Development Unit (AFDU), located in LaPorte, Texas.

The MITRE Corp., McLean VA, a DOE consultant is reviewing the development of technologies that can reduce the costs in Bechtel's technoeconomic analysis and analyzing any new Synfuels plant technologies resulting in plant cost and operating reductions including any further cost reductions that may come from capital cost reductions in other plant areas, especially in gasification and oxygen production.

An extensive technoeconomic analysis prepared November, 1991 by the MITRE Corp., McLean, VA developed a Hybrid Plant Coal Liquefaction Concept for a 2,000 barrel per day Synfuels plant, The Great Plains Synfuels plant in Beulah, North Dakota . The report analyzed a number of liquefaction processes and found that the Rentech, Inc. process is rated one of the best economically.

What it does not show is the fact that the Jet Drilling Synfuels plant will eliminate approximately 75% of the front-end cost of direct coal liquefaction.
If we were to deduct from Bechtel's design costs and adjust for modifying the Fisher-Tropsch Synthesis system with Steam Reactors, slurry reactors, and catalyst activity, we could reduce the base cost to approximately $30 million. See Table V, Elements of Costs for converting Methane Gas into Transportation Fuels

Private Industry and many Government agencies have already contributed Millions of dollars in research, and the development of fully operational projects to economically convert coal and natural gas to transportation fuels.

With proper planning and careful technical coordination, the economic savings utilizing Coalbed methane are available.

A Synfuels plant in operation; International Shell Oil's, 12,000 BPD Malaysian synfuels plant is manufacturing synthetic middle distillates from natural gas. The Shell Middle Distillate Synthesis Process (SODS), utilizes a modernized version of the classical Fisher-Tropsch process and is now in operation. Shell International's plant is converting natural gas to high quality gas oil, kerosene and some naphtha via selective hydrocracking.

A Synfuels plant project under consideration; Jet Drilling Corp's 6,000 BPD Synthetic (alternate) fuels, plant with 10 acres greenhouses, in Chautaqua County, Kansas.

The Synfuel plants feedstock requirements to produce 6,000 barrels per day of transportation fuel requires 60,000 MCF per day of methane gas.

DOE's Pittsburgh Energy Technology Center (petc) introduced ERTS to the Syncrude Technology Inc., (STI). STI has developed a new, exciting cobalt catalysis, advanced reactor technology, allowing economics of design relative to previous methods, and other process improvements reducing a Synfuels plant cost by as much as 75%. STI documented their work in a "Proposal for Commercialization of STI's Fisher-Tropsch Process to Convert Natural Gas to Synthetic Crude Oil".

By converting methane gas into clean-burning diesel fuel, wax, and naphtha, a synfuels plant provides owners of coalbed, natural gas reserves, landfills and sewer treatment plants with an opportunity to capitalize on previously unprofitable resources.

Collecting and Measuring Gas: Collecting and measuring gas in a coalbed methane field is similar to the techniques used in a low-pressure oil field. There are similarities in the flow path of the fluids, the production equipment, and the operational problems.

The Gas Flow Path: Coalbed methane wells usually produce gas though the casing/production tubing annulus. The wells normally produce under minimum back-pressure to optimize gas desorption from the coal and drainage of the water. Once gas reaches the surface, it is normally piped to a two-phase separator, which removes water from the gas. (Alternatively, the gas can be piped directly into the gas gathering system to reduce backpressure on the casinghead.) finally, into the sales gas interstate pipeline. Then the gas flows through an orifice meter with a 3-pen chart recorder where it is measured. Next, the gas is piped through a field collection line to a gas scrubber, which removes any remaining water before the gas enters the compressor. Finally, the gas exits the compressor, flows through a dehydrator and sales gas meter, and

The cost of collecting and measuring gas flow from the coalbed methane wells to the sales gas interstate pipeline is an average of 2.66% of the Lease Operating Expenses (LOE). The subcategory "*Miscellaneous Lease Operating Expenses", includes cost of testing well-site meters and discharge water and any expenses not included in other specific subcategories (see Table III).

Description of the typical Fisher-Tropsch Process

FIRST STAGE: Gas Compression and Clean-up: By using pipeline grade coalbed methane gas, this is a major synfuels plant cost reduction item. There will be a little, if any gas clean-up to be done at the synfuels plant.

The laboratory analysis of the methane gas from Jet Drilling's methane gas wells in SE Kansas, shows an average of 96.62% methane, .61% CO2 and no sulfur content. This means that a Synfuels Plant using this coalbed methane gas as feedstock will not require an expensive desulfurization system.

Step One: The pressure of the feedstock gas is increased from atmospheric pressure to 25 psia (170 KPa) and cleaned by passing through charcoal filters, an Alumina bed, and a Permanganate bed. This stage removes chlorides, sulfides and trace elements.

Step Two: Once cleaned the pressure of the feedstock gas is further increased by compressors from 25 psia (170 KPa) to 200 psia (1,380 KPa) and then fed into the Stream Reformer.

SECOND STAGE: Steam Reformer:
Once inside the Steam Reformer, steam is mixed with the feedstock gas. This mixture is then passed over a nickel oxide catalyst which has been heated to 1550° F. (845° C.). This process reforms the mixture into its constituent parts of Hydrogen, carbon, carbon monoxide, carbon dioxide (CO_2) and water vapor.

The resulting gases are then fed into the CO_2 Absorber and Stripper Column.

THIRD STAGE: CO_2 Absorber and Stripper Column:
The CO_2 and water vapor are removed at this point. One of three CO_2 removal systems can be used: amine, Solexol, or membrane.

The solvent containing CO_2 is then sent to the CO_2 Stripper Column at which time CO2 is separated from the solvent.

The CO_2 then can be either discharged of re-introduced- into the feedstock gas at the gas compression inlet.

The remaining gas, a mixture of hydrogen and carbon monoxide called synthesis gas is fed into a slurry type Synthesis Reactor.

FOURTH STAGE: Synthesis Reactor:
The catalyst is suspended in a molten wax slurry which has been heated to approximately 500° F.(260° C.) and pressurized to 200 psia (1380 KPa). The catalyst is iron based with a useful life in excess of 30 days.

Initially the reactor is heated with steam. The synthesis gas bubbles up through the molten wax, comes in contact with the catalyst and produces straight chain hydrocarbons. This process is exothermic.

Long straight chain hydrocarbons collect and are drawn off at this stage in the form of heavy wax. Short straight chain hydrocarbons are fed into the distillation column.

FIFTH STAGE: Distillation Column:
The straight chain hydrocarbons are cooled at various temperatures as they rise up the column. Light wax is drawn off the bottom of the column, diesel fuel is drawn off the intermediate layer and naphtha is drawn off the top.

Need for Synfuels: Around the world a growing concern for people's health and for the well being of our planet is increasing the demand for cleaner-burning fuels. synthetic diesel fuel is the cleanest fuel available. And, unlike other alternate fuels, synthetic diesel fuels does not require special equipment or engine alterations.

Synthetic diesel fuel:

* is free of sulfur and aromatic compounds;
* meets all American Society of Testing and Materials (**ASTM**) specifications;
* exceeds all environmental Protective Agency (EPA) and National Academy of Sciences (**NAS**) proposed changes to diesel fuel;
* emits, at a minimum. 18% less particulates, 15% less hydrocarbons, and 14% less carbonmonoxide that No. 2 diesel fuel.

WAXES:

Waxes produced from Synfuels plants are known as Fisher-Tropsch (F-T) waxes and have the potential to be refined to compete with F-T waxes currently produced in South Africa. They have a very high molecular weight and melting point, and have excellent hardness.

F-T waxes are similar to petroleum hydrocarbon waxes with the exception that they have a larger proportion of higher melting, linear molecules.

The United States alone consumes approximately 25 - 30 million pounds of F-T waxes each year. However, until now, none was produced in the United States. About one-half of the waxes consumed in the U.S. are used in hot melt adhesives, 25 - 30 percent in inks and coatings, mainly as micropulverized materials, and the balance in a large variety of applications such as:

* Candles
* Crayons
* Lipsticks
* Textiles
* Resin-wax polish formulations
* Paste and emulsion polishes for floor, furniture, and automobiles
* Anticorrosion coatings
* Internal lubricants and mold-release agents for plastics.

NAPHTHA

Naphtha produced by the Synfuels process can be used as a feedstock for chemical processing or refined to be used in the following products:

Varnish maker and paints
Type IV mineral spirits
Petroleum ether
Textile spirits and ink oil

CONCLUSION and FUTURE PLANS:

President Clinton and V.P. Gore's Climate Change Action Plans include;

Action #35 Launch Coalbed Methane Outreach Program; Development of outreach materials (technology descriptions, sample RFP's, cost, benefit analysis, financing information), an information clearinghouse, briefing for companies, state, utilities, and others, and demonstration projects.

Action #36 Expand RD&D for Methane Recovery from Coal Mining;

* Lower cost more complete methods for pre-mining recovery of methane from coal seams, such as inert gas flooding;
* Methods for using in-mine de-gasification streams, such as enrichment for pipeline gas and electricity generation;
* Demonstration of the use of fuel cells and other state-of-the-art technologies for waste methane utilization, transferring appropriate practices to the coal industry.

Commercial scale demonstration projects of promising combinations of techniques with industry participation will establish the viability and economics of recovery, expanding the scope of domestic coal seams that can recover methane.

Action #37 Expand RD&D for Methane Recovery from Landfills; This will facilitate design of landfills to maximize generation of methane and recover methane as electricity, fuel or pipeline gas.

For the Fiscal Years of 1994 and 1995 the Administration has obligated approximately $40 million for the above Actions.

Also, there is Section 1332 Clean Coal Technology, and 1608 Environmental Technology of the Energy Policy Act of 1992 (EPACT) describe two technology Transfer Programs for creating jobs and reducing the trade deficit for the United States, through providing financial assistance for projects to improve energy efficiency and reduce environmental emissions including "Greenhouse Gases".

One objective would be to demonstrate a few advanced "showcase" technologies. By DOE having a program to provide financial assistance up to 50% (the cost share could be structured to achieve an acceptable rate of return) of the projected eligible capital and operating costs through cooperative agreements with repayment provisions, the selected "showcase" technologies could be demonstrated for evaluation be potential users.

All of DOE's indirect coal liquefaction for the manufacture of synthetic liquid fuels programs completed or under contract to date start with the processing of coal.

As stated in the Abstract and shown in Table IV, page 15, "**by converting methane gas into liquids, approximately 60 to 72% of the front end costs for the conversion of coal to gas and then the gas into liquids can be eliminated".**

Some of the research targets are;

1. Improving the Synthesis Reactor

2. Development of Improved iron Fisher-Tropsch catalyst presently used.

   a. technology development for iron Fisher-Tropsch catalysts.

3. New and improved catalysts, i.e., Cobalt Fisher-Tropsch catalysts.

We will also analyze;

1. The converting of methane into ethanol or diluted methanol that is now being tested in Arizona as a crop enhanser by the Dept. of Agriculture.

2 Liquid methane, the fuel used in the SR 71, Mach 6 Reconnaissance plane.

3. Methanol used in the fuel-cells for all electric buses, by the Dept. of Transportation.

Some Synfuel Plant Alternates to be considered;

1. A vapor recovery system that will be designed in place of any vented flue gas stacks. The implication of EPA's Clean Air Act requires the removal of hydrocarbon and chemical vapors from emission to the atmosphere.

2. Add an adjoining 25 MW Cogeneration plant producing 34,000 lbs. of process seam/hr., plus 10 Acres of Greenhouses,

3. and oil and gas storage facilities including transportation systems.

4. The Synfuel Plants stage 2 steam reformers require 1,500 to 1,700 Degree F. of process steam. Recommend that the use of Solar Thermal power be reviewed. There were a number of solar thermal installations on chemical plants and refineries in the gulf states from the mid 70's to 80's.

Parabolic trough solar thermal collectors can be used to produce up to 500 Degree F. of the steam heat required. This could save 75% of more of the synfuels plants fuel costs.

Additional Alternatives:

The possibilities of developing an innovative and economical process of bioconversion of coal into clean fuels. The commercialization of molecular biology is the most stunning ethical event in the history of science, and it has happened with astonishing speed.

1. **Ethanol**; Bechtel Group's development of the Indirect Liquefaction Baseline Design Economic analysis for a methane gas to transportation fuels provides us with a baseline that will allow us to compare Bechtel's baseline design to the biological production of **ethanol** from coal synthesis gas.

2. **Alcohol Fuels**; A Virginia BioTech firm has developed a microbial consortia approach to convert coals into methane gas, and in an alternate approach, coals are converted into alcohol fuels such as **ethanol, butanol and propanol**. This novel technology is termed as "MicGAS Process".

One of the most efficient and economical methods to convert COAL to a gas and a gas to a liquid is to do it in the ground, "In-Situ". i.e., ARCTECH, Inc. (a spinoff of the Environmental Science and Technology group of the Atlantic Research Corp.) has developed significant breakthroughs in isolating unique naturally occurring micro-organisms and adapting to coal to accomplish degradation of coals complex molecular structures. In one approach, microbial consortia has been developed to **convert coal into methane gas "In-Situ"** (in place), and in the alternate approach, coal is converted into alcohol fuels such as ethanol, butanol and propanol.

3. **Liquid Fuels**; A bioconversion of coal derived synthetic gas to liquid fuels program, could be the program for the next generation of converting coalbed methane gas to transportation fuels.

4. MIT's **Production of Liquid Fuels and Chemicals.** Conversion of light hydrocarbon gases to metal carbide for the production of liquid fuels and chemicals.

In the petrochemical industry there are no simple answers to the question "What is profitable?", or "What is the best technology". The crux is that one should be knowledgeable in the field to be able to access the technical issues and uncertainties. Furthermore, one should have an astute business sense to match markets, products and technology.

Finally one should be prepared to take well considered ricks - there is a Chinese proverb saying that even the tortoise needs to stick out its neck to make progress! By; Dr. Arie Geertsema, General Manager, Sasol R & D, Republic of South Africa.

Recent events affecting synthetic (alternate) fuels

International Alternate Fuels and Clean Cities Conference - June 28 - July 1, 1994 Hyatt Regency Milwaukee, Wisc.

Renewable Energy in the Americas "94 - June 26 - July 1, 1994, Hyatt Regency Cerromar Beach Puerto Rico.

SUMMARY

The ideal site for a synfuels plant is where you can extract the coalbed methane gas from coal fields that are too far from any Interstate pipeline and process or convert the gas into transportation fuels, waxes and naphtha transporting them by tanker/truck.

ACKNOWLEDGMENTS

Gary Stiegel co-chairperson, Coal Liquefaction and Gas Conversion Contractors Review Conference, September 7-8, 1994 Pittsburgh, PA for extending an invitation to present this paper at the conference and Dennis Lathem, President of the Coalbed methane Assoc. of AL for researching cost and procedure for transmitting coalbed methane gas from the wellhead to the pipeline. Also Dan Thompson, Symposium Chairman, Intergas '95.

References:

1. Synthetic Fuel Capital and Production Costs, Final Draft Report support Data and Analysis provided to alternate fuels supply project. A report prepared for U.S.DOE Aug. 1990 by Chem Systems Inc. Tarrytown, NY.

This Report contains data on: SYNTHETIC FUEL FROM NATURAL GAS (WORLDWIDE) and SYNTHETIC FUEL FROM COAL (U.S.) - Capital Costs and Production Costs on converting;
a. Methanol to Gasoline
b. Natural Gas to Diesel Fuel
c. Natural Gas to Oxidative additives
d. Coal-derived Liquids - Fuels Costs
Gasoline Costs
Diesel Costs
e. comparison of Fuel Costs

2. Technical Report Four: Assessment of Costs and Benefits of Flexible and Alternate Fuel Use in the U.S. Transportation Sector - Vehicle and Fuel Distribution Requirements, Aug. 1991 U.S. DOE this Report contains data on:
* Methanol Fuel Infrastructure Facility Requirements
* Costs for the Methanol Fuel Distribution System
* Natural Gas Infrastructure
* Total Cost Electric and Hybrid Vehicles (1995)

3. Slurry Reactor Design Studies (Final Report Slurry VS. Fixed-Bed Reactors for Fisher-Tropsch and Methanol
by; Bechtel Group, Inc. San Francisco, CA for U.S.DOE, 6/90
Section 6.0 Capital and Operating Cost Comparisons
6.1 Fisher-Tropsch Comparison
6.2 Methanol and Mixed Alcohols

4. Development and Process Evaluation of Improved Fisher-Tropsch Slurry Catalysts - (Final Report) April 1990 prepared for U.S.DOE, Pittsburgh Energy Tech. Ctr. - Economic Evaluation Prepared by; Air Products and Chemicals, Inc. - Allentown, PA
VIII. Task 4. Economic Evaluation
1.2 Synthetic Gas Production
6. Capital Investment

5. Review of Topsoe Methanol Technology by Peter Anderson, Haldoe Topsoe, Inc., Presented -the 1989 World Methanol Conference Houston, TX.

6. The MITRE Corporation, McLean, VA - Hybrid Plant Coal Liquefaction Concept at the Great Plans Synfuels Plant - Report Prepared for Basin Cooperative Services under a U.S.DOE contract, November 1991

7. Viking Systems International Pittsburgh, PA - Design of Slurry Reactor for Indirect Liquefaction Applications Report prepared for U.S. Department of Energy, December 1991

8. Dept. of Chemical Eng., Dept. of Chemistry, Texas A&M and Air Products and Chemical, Inc., - Development and Process Evaluation of Improved Fisher-Tropsch Slurry Catalysis - Final Report prepared for U.S. Department of Energy, PETC, April 1990

9. Sandia National Labs., Albuquerque, NM, - Evaluation of Mixed Alcohol Production Processes and Catalysts - supported at the MITRE Corporation, under a U.S.DOE contract, April 1990

10. Bechtel Group, Inc. San Francisco, CA - Slurry VS. Fixed-Bed Reactors for Fisher-Tropsch and Methanol - Slurry Reactor Design Studies, Final Report prepared for U.S. Department of Energy, June 1990

11. Natural Gas Trends, 1992 - Cambridge Energy Research Associates

12. World Oil Trends, 1992 - Cambridge Energy Research Associates

13. Oil & Gas Federal Income Tax Manual, 1992 - Arthur Anderson & Co.

Some of the papers presented at the Liquefaction Contractor's Review Conference -U.S. DOE/PETC Pittsburgh, PA, Sept., 1993 on - Indirect Liquefaction (F-T) Tech.

1. Technology Demonstration for Cobalt F-T Catalysts
A.H. Singleton, Energy International Corporation

2. The Selective Catalytic Cracking of Fisher-Tropsch Liquids to High Value Transportation Fuels by Amoco Oil Company, Naperville, Ill.

3. Mossbauer Spectroscopy Study of Iron-Based Catalyst Used in Fisher-Tropsch Synthesis - K.R.P.M. Rao, University of Kentucky, CFFLS

4. Opportunities for Reducing Product Costs in Indirect Liquefaction D. Gray, The MITRE Corporation

5. Baseline Design/Economics for Advanced Fisher-Tropsch Technology - Bechtel Group, Inc. San Francisco, CA

6. Technology Development for Iron Fisher-Tropsch Catalysis by 1, B.H. Davis, Center for Applied Energy Research Lexington, KY and 2, University of Kentucky, CAER

TABLE I; an analyses of Methane Gas from shallow Coalbed Wells in the Cherokee Basin

	COAL SEA	RIVERTON	RIVERTON	WIER
	DEPTH (feet)	819 - 822	920	920-932
	ISIP (PSIG)	300	330	315
NITROGEN		1.92	2.64	5.20
CO2		.80	.59	.61
METHANE		97.22	96.62	90.15
ETHANE		.03	.06	2.15
PROPANE		.00	.00	.11
ISOBUTANE		.00	.00	.23
NOR.BUTANE		.00	.01	.03
ISOPENTANE		.00	.00	.03
NOR.PENTANE.00		.01	.06	
HEXANES		.00	.01	.01
GRAVITY		.5699	.5718	.6123
BTU/CF (wet)		962	959	979

TABLE II - SOUTHEAST KANSAS MODEL WELL 1990

Pennsylvanian Weir - Pittsburgh and Riverton Coals @ 600 - 1000 Ft. depth Gas in place and recoverable reserves for a 80 acre unit are as follows:

8' coal x 200 scf/ton x 1,800 tons/acre foot x 80 acres = 230 MMCF in place. x 70% recovery = 161 MMCF recoverable gas

Well Cost:	Land; 80 acres x $10/acre	$	800
	Tangibles		12,500
	Intangibles		18,000
	* Share of facilities		2,500
	TOTAL COST	$	33,800

*Model assumes share of existing conventional gas infrastructure and water injection wells.

Operating cost: $600/month for 12 months, and $400/month thereafter
Production Profile: Initial production @ 50 mcf/d; rising to peak of 100 mcf/d in 6 months; flat for 1 year, declined at 10%/year

1994 Gas Price As high as $ 2.15/mcf

TABLE III - ITEMIZED BREAKDOWN OF LEASE OPERATING EXPENSES

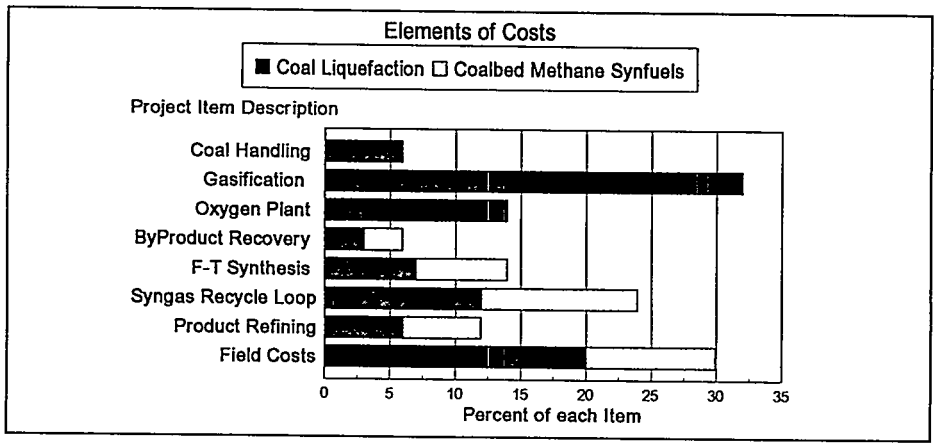
	Expense Item	% of Total LEO / yr
1.	Contract Pumping	5.48
2.	Field supervision	9.76
3.	Chemicals and Treating	2.34
4.	Well Service	8.55
5.	Maint./Repairs/Matl's.	11.22
6.	Trucking and Hauling	1.06
7.	Equipment Rental	5.69
8.	Maint. Leases & Roads	0.22
9.	Misc. Lease Oper. Expenses	2.66
10.	Electric Power	14.55
11.	Field Office	4.51
12.	Company Vehicles	4.10
13.	Production Overhead	29.86
	TOTALS	100.00

TABLE IV: ELEMENTS of COSTS

Bechtel design costs in a indirect coal liquefaction, Baseline Design/Economics for Advanced Fisher-Tropsch Technology. Table IV also shows items omitted or substituted in a Direct Gas Conversion Plant.

	MM $%	%	
Coal Handling	143.3	6	OMIT
Gasification	770.3	32	OMIT
Oxygen Plant	326.8	14	OMIT
Byproduct Recovery	7.1	3	Substitute
Fisher-Tropsch Synthesis	173.7	7	
Syngas Recycle Loop	279.2	12	
Product Refining	152.2	6	
ISBN Field Cost	1912.5	(InSide Battery Limits - ISBN)	
OSBL Field Cost	483.9	(OutSide Battery Limits- OSBL)	
TOTAL Field Cost	**2396.4**	**20**	**OMIT**

Table V: Chart showing substantial saving in costs between a Indirect Coal Liquefaction Plant and a Methane Gas to Transportation Fuels Synfuel Plant.



INTERGAS '95

May 15-19, 1995
The University of Alabama
Tuscaloosa, Alabama USA

9520

Coalbed Methane Resources in the Carboniferous of Nova Scotia: Canada—An Overview and Update

D.J. MacDonald, Department of Natural Resources, Province of Nova Scotia

ABSTRACT

The province of Nova Scotia, situated on the east coast of Canada, has historically derived employment and revenue from a well established coal industry. Some 265 years of mining activity and geological research have generated a wealth of knowledge for the province's three main coal basins.

The province is on the verge of the development of a new energy resource. The success of commercially viable coalbed methane projects in the U.S. has spurred activity in a province which is blessed with substantial coal resources and where 64% of its current energy requirements are met by imports of foreign crude oil. Several initiatives have been undertaken by the province to assess the coalbed methane potential and to facilitate industry's efforts in developing this resource. A Coalbed Methane Policy has been developed which provides for concurrent development of both coal and coalbed methane. Recent Calls for competitive work proposals have resulted in industry acquiring several tracts of land to assess the commercial viability of the resource. A comprehensive coal database and computer models have been developed for three basins which permit the three-dimensional display of virtually any coal attribute or combination thereof. Federal funding was allocated to support investigative studies through the Canada-Nova Scotia Cooperative Agreement on Mineral Development. It is hoped that these assessments will be positive and coalbed methane will become key in meeting the future energy needs of the province.

INTRODUCTION

The purpose of this paper is to present an overview of the coalbed methane activity in Nova Scotia. With no tax incentives and no demonstrated methane production, one might question the potential of this "frontier region".

Past coal mining activities in this region has focused attention on coalbed methane but more as a nuisance and hazard than as a potential resource. The mining of coal has necessitated the removal of the methane through extensive ventilation systems that have liberated the gas to the atmosphere. Efforts by mine owners to capture the gas and use it for fuel to provide heat for the wash house and on-site power generation have been frustrated by the high costs of collecting and handling. More stringent control on the emission of greenhouse gases and environmental credits that can be earned by mitigative techniques, have rekindled an interest in the utilization of the coalbed methane in Nova Scotia.

Three major basins contain more than a hundred seams ranging from less than a metre to almost 15 metres (45 ft) in thickness. The bituminous coals have been long known as "gassy", but their methane treasure is, as yet, undetermined. Preliminary estimates of methane potential for the Cumberland Basin show a range of 56 - 170 x 10^9 m^3 (2 - 6 tcf). More recently there has been interest expressed by the private sector to access and utilize this clean burning fuel and several initiatives have been undertaken. This paper reviews the current status of coalbed methane in Nova Scotia.

GEOLOGIC SETTING

The coal basins in eastern Canada (Figure 1) were formed as part of the Permo-Carboniferous Maritimes Basin complex which includes a series of once-interconnected depocenters (Figure 2). Such depocenters are inferred to have been partially connected, intermontane basins separated by uplands of moderate elevation [1]. The Acadian orogenic event in the mid-late Devonian was responsible for the creation of the large depositional basin which filled with sediments until the late Permian. Sedimentation in the Maritimes Basin was controlled by the presence of a number of large basement fault

blocks and their syndepositional movement [2]. In the eastern part of the eastern Gulf of St. Lawrence sediment fill exceeded 10 km [3]. The basin boundary to the south was, in part, controlled by a transcurrent fault system along a terrane boundary [4]. Adjacent highlands such as the Caledonia, Cobequid, and Antigonish, provided sediment sources for the intervening sub-basins. During the Carboniferous, these local sub-basins became sites of fairly rapid and continuous deposition. Continental redbed clastics and intervening grey beds of the Horton Group of Late Devonian/Earliest Mississippian were localized in very small depositional sites. These gave way to the predominately evaporite sequence which comprises the marine Windsor Group carbonate units. The mainly continental sediments which comprise the "coal measures", developed over much of the Windsor sub-basin areas and marked a period of renewed terrestrial input to the local depocenters. There are eight sub-basins which display significant accumulations of coal; the thickest accumulations occur in the Cumberland, Stellarton, western Cape Breton, and Sydney areas (Figure 2). All of these sub-basins are considered as basins in their own right due to depositional and structural differences. The coal measures span the interval from Tournasian to Namurian, but are thickest in the Wesphalian A to Stephanian strata (middle Pennsylvanian) [4] (Figure 3). The oldest coals are those of the Cumberland Basin which contains the Joggins and Springhill coalfields, and on western Cape Breton Island, the coal fields of Port Hood and St.Rose - Chimney Corner.

The Cumberland Basin contains coals of predominantly mixed fluvial and lacustrine origin producing as many as 95 seams over a stratigraphic interval of 2450 metres (8,040 ft). While only 15 seams are thicker than 1 metre, the basin has an aerial extent of some 2000 km^2 (772 mi^2). Less active basin subsidence, resulting in the establishment of more extensive swamps and mires, allowed the accumulation of much thicker coals of the Pictou Group.

The Stellarton Basin, containing 35 seams of predominantly lacustrine origin, has a smaller aerial extent of only 110 km^2 (42.5 mi^2) . However the typical high volatile A bituminous seams are thicker, in one case attaining an average thickness of 14.2 metres (46.5 ft).

Still later in the latest Westphalian, with very stable conditions, peat forming ecosystems were able to develop over vast areas producing the coals of the mainly offshore Sydney and Gulf of St. Lawrence basins. The Sydney Basin hosts the largest coal resource in eastern Canada. The alluvial and coastal plain coals which have been mined, are part of a basin area that covers some 36,000 km^2 (13,900 mi^2) [5], [6]. The Sydney coalfield, the site of the only current underground coal mining, has seams as thick as 4.3 metres (14.1 ft), with a rank of high volatile to medium volatile A bituminous.

WHAT IS KNOWN AND WHAT NEEDS TO BE DONE

There is a great deal known and understood about the coals of Nova Scotia. Their physical and chemical attributes are well documented. Depositional models have been developed by staff geologists [7][8]. Recent seismic has helped delineate the basins and has given some measure of the likelihood of seam continuity across the basins [9]. Recent attempts to characterize the basic coalbed methane parameters have included underground evaluation of the Harbour seam at Donkin in the Sydney Basin [10], the completion of an exploration program in the Cumberland Basin by Resource Enterprises Inc. (REI), and recent investigative research work sponsored by the Department of Natural Resources [11][12][13][14]. However, much empirical and technical work remains to be done, including (a) hydrologic regime of the basins, (b) structural configuration and control, and (c) formation pressure and (d) coal permeability. Operational techniques and constraints need to be investigated involving such aspects as completion methods, water disposal, and pipeline infrastructure.

EARLY WORK & PRESENT EFFORTS BY INDUSTRY:

Industry Efforts

In the late 1970's and early 1980's an attempt was made by the private sector to characterize the coalbed methane potential of a number of Nova Scotian coals. Algas Resources Ltd. of Calgary, Alberta, Canada drilled 26 holes in an attempt to gather fresh samples for desorption measurements. The provincial department has a number of documents filed by the company, none of which indicate very encouraging results. The program utilized leading edge technology at that time but little was understood about some of the controlling factors. Desorption results showing gas contents in the range of 1.25 cm^3/g - 2.25 cm^3/g (40 to 72 scf/t), in coals with ranks of high volatile A bituminous are difficult to explain [15] [16]. In some cases, drilling locations were found to be too close to old workings, drilling techniques and fluids used were not optimal, desorption canisters were not at formation temperature, and many holes were drilled to depths of less than 150 metres (500 ft). Two wells were brought on production and flowed for a period of some eight years. However daily rates were only 708 m^3 (25 mcf) and local companies could not be lured into any commitments without guarantees of volumes and longevity of supply. As a result the wells were abandoned.

Government Initiatives: Computer Database

With the long history of coal mining activity, there have been more than a 1000 boreholes intersecting more than a 100 seams which have produced a vast data set of physical and chemical parameters. A digital database has been developed over the last nine years and resides with the Geological Survey of Canada at the Institute of Sedimentary and Petroleum Geology in Calgary, Alberta, Canada. Outputs include 100-layer, 3-D computer models which display various coal quality attributes. Limits can also be set to produce customized outputs; for example, a map can be generated which displays cumulative coal thickness with seams of less than 5% ash, greater than 50 metres (150 ft) but less than 1500 metres (4900 ft) in depth, for coals which are 500 metres (1650 ft) away from old workings [17]. Currently lacking in the database is comprehensive data on the gas content of various coals, permeability, pressure, and hydrologic information. As industry releases its data and the provincial government completes its research, this data base will be further enhanced with more detailed coalbed methane parameters.

Government Initiatives: Promotion

The provincial government has recently increased the awareness of the coalbed methane potential of the region by actively promoting the area. Data packages and presentations were prepared and delivered to a considerable number of companies. Calls for Exploration and Production Agreements were issued which resulted in competitive proposals being received. The assignments of rights were made on the basis of the best work program proposed and the financial and technical capability of the company to perform their work obligations. The rights are issued for an appropriate period of time to permit the conduct of the proposed work. Lands which are not evaluated are relinquished to the Crown. Two of the three coal basins have been tendered in this manner, and the third major basin is expected to be offered later this year.

Government Initiatives: Research

The government has sponsored, in whole or part, various investigative and/or research programs to enhance the basic knowledge base. Recent attempts to characterize coalbed methane parameters have included the program at Donkin in the Sydney Basin [10]. Permeability data that were obtained were encouraging. Hydrocarbon and methane generating capabilities of various coals from a number of basins has been investigated using hydrous pyrolysis and surface area determinations [11-14] and [18]. These are attempts to use a predictive approach in identifying seams with the greatest potential for coalbed methane generation.

Government Initiatives: Mineral Development Agreement

There was a dedication of federal funding, under the Canada-Nova Scotia Cooperative Agreement on Mineral Development, to enhance the database for methane explorers in Nova Scotia. Some of the funding was used to support the creation of the coal database as mentioned above, while other funding was used to generate new coalbed methane data as discussed above.

PRESENT STATE OF KNOWLEDGE:

Coal Rank and Type

The onshore basins show a slight variance of coal rank with respect to their location within the Maritimes Basin. The coals of the Joggins-Chignecto coalfields of the Cumberland Basin have a rank of high volatile A bituminous. The slightly younger coals of the Springhill area range from high volatile to medium volatile A bituminous. Maturation is characterized by $>.70$ R_o near the surface at Joggins, to 0.88 R_o at surface near Springhill, and to >1.20 R_o at depth in the central portion of the basin. The coals of the Pictou coalfield range from high volatile A bituminous at surface and medium to low volatile at depth. Coal rank ranges from 0.75 to 1.60 R_o@ 1400 m (4600 ft). The coals of the Sydney coalfield vary considerably, but generally increase in rank to the east and with depth. They are generally classed as high volatile A bituminous but in places reach medium volatile bituminous. Coal rank ranges from 0.70 to 0.80 $R_o$at surface to >1.20 at depth. [5]

Recent investigative work conducted by the department has indicated relationships between coal rank and surface area [11-14][18].

Coal Seam Thickness and Numbers

The depositional history of the Cumberland Basin is given in the evolution of the depositional models as described by Calder [1]. The coals of the 1430 m (4700 ft) thick Joggins Formation are interbedded with a mixed fluvial and lacustrine assemblage whereas those of the overlying 600-800 m (1970 ft - 2625 ft) thick Springhill Mines Formation occur within a fluvial sequence (Figure 4 & 5). Depending upon the correlation of units between the two coal fields there may be upwards of 95 seams which range from $<$ 0.3 - 4.3 metres ($<$ 1 - 14 ft) in thickness [7].

The Stellarton Basin coals are contained within the 2600 m (8530 ft) thick predominantly lacustrine Stellarton Formation of the Wesphalian C to early D age. (Figure 6). There are only some 35 seams but they are typically thicker, reaching 14.2 metres (46 ft). The paleogeographic model displays the interpretation of the thick accumulation of organic debris that accounts for the thick seam development (Figure7).

The Sydney coalfield lies predominantly under the north Atlantic Ocean. Seam thickness varies but ranges at high as 4.3 metres (14 ft) with 13 seams thicker than 1 metre. The seams are were formed in a non-marine alluvial to coastal plain environment, with broad areal distribution [5] (Figure 8).

Coal Macerals, Surface Area & Monolayer Capacity

Much work has been done to describe the typical characteristics of the maceral content of the seams. A number of recent works are available as open file reports that document many seams in detail. Possible links between maceral type/content and monolayer capacity and permeability have been investigated [18]. Maturation maps have been produced.

Reservoir Characterization: Permeability & Pressure

The investigation of the Harbour seam at Donkin in the Sydney Basin saw the drilling of a horizontal hole into a coal face of the Harbour seam which had been exposed for some 5 years prior to the investigative drilling. Gas content measurements taken at successive depths while drilling in the seam, a final in-seam injection test, and a sorption isotherm measurement produced useful data. The gas contents were predictably low showing values of 3.95 cm^3/g close to the face (126 scf/t), with gas content increasing with penetration to a value of 6.99 cm^3/g (224 scf/t) at 65 m (213 ft) into the seam. What was seen as positive was the permeability of 10.8 md derived from the injection testing [10]. Simulation of virgin reservoir pressure suggests that it is equal to the equivalent hydrostatic head [10].

REI, in their exploration efforts in the Cumberland Basin during the fall of 1994 when they drilled four holes for desorption data, attempted to conduct an injection test to provide an indication of the permeability of a 600 m (2000 ft) section of hole. Due to confidentiality provision of their work program, the results are not yet public, however, they will conduct production testing of the coals intersected in this basin during their exploration program slated for the summer of 1995. Slowly, but certainly, new data is being generated to support assumptions about the degree of the cleating and the creation of effective pathways for the movement of the methane.

Gas Content

The Algas work referenced gave inconclusive data. Basic assumptions about coal rank and type predict far greater gas contents that many of those recorded. Other explorers have reviewed much of this earlier data and acknowledged that it is perhaps not representative. As a result, REI and partners have obtained exploration rights and have committed to an exploration program in the Cumberland and Stellarton basins that will provide new data that may discount the earlier Algas results. The first-year work program of 4 wells in the Cumberland Basin has been completed, but results remain confidential. Work planned for the summer of 1995 should produce new data. In the Stellarton Basin the thick coals are expected to produce high gas contents. Coals of the Sydney Basin have historically been considered as gassy coals by the miners. The gas content of the exposed underground coal face at Donkin was low as expected but successive testing showed increasing gas content with increased horizontal penetration. Mine ventilation gas data exists but no definitive desorption data is available other than for the Harbour seam as mentioned.

Unknowns

Several other key factors have yet to be determined. There has not been a hydrologic regime assessment done for any of the basins. The Donkin Project in the Sydney Basin, the Algas production wells in the Stellarton Basin, and the recent production testing of the open hole in the Cumberland Basin have only just begun to provide some insight into this key factor. The structure of the coal basins is generally well documented. New work in the Cumberland Basin has identified two new faults [9]. Less clear is the temporal variation in the stress regime which has affected these basins; in particular the effects of Mesozoic extensional tectonics. Although maceral dependant, cleating has been shown to be well developed in many of the seams that have been examined. Basin maturation studies using vitrinite reflectance and, more recently, fission track techniques suggest the thermal histories of the basins need to be investigated more thoroughly [19]. Basin subsidence, burial depth and timing, sediment induration, and the details of the variance in coal maturation in the vertical and aerial sense are the focus of ongoing investigation. Existing data indicates that the Stellarton Basin may be the most thermally mature of all basins [20], however, complete thermal profiles have not been generated. Deep drill holes are needed for collection of fresh samples for desorption and sorption isotherm

evaluation, and to determine the producibility of the better seams. This work has begun through initiatives of the private sector. Two of the three basins are currently held under agreements with the government to allow exploration and production activities. The next 1-2 years will produce new and more reliable data on the resource potential of the region.

RESOURCE ENDOWMENT

Early estimates of the resource potential of the coal basins of Nova Scotia have produced a wide range of values, largely unsubstantiated. The first figure ever quoted showed possible in-place estimates of 390 x 10^9 m^3 (14 tcf) for the entire Maritimes Basin and relied upon the volumes of only mineable coal [21]. Upon initial assessment of their coalbed methane holdings in the Cumberland Basin, REI estimated that the reserves (in place) might be as high as 168 x 10^3 m^3 (6 tcf) [22]. A recent estimate by the Geologic Survey of Canada, of the same basin, produces a more conservative estimate of some 56 x 10^3 m^3 (2 tcf) [17]. The differences lie in arbitrary cut-offs and assumptions about gas contents of the coals, the true values which are only just coming to light. The Stellarton and the Sydney basins remain essentially untested and resource endowment is uncertain at this time. Production testing will be needed to validate these varying estimates.

CONCLUSIONS

While neither the federal nor provincial government offer similar incentives as the popular Section 29 tax credits in the United States, there are a number of positive aspects of coalbed methane exploration and development in Nova Scotia. There is no complication of ownership by private individuals; the government owns the coalbed methane rights. The government has produced a Coalbed Methane Policy that provides for coincident development of both coal and coalbed methane. Royalties from coalbed methane development will be negotiated, but the emphasis by the government is to encourage the development of this indigenous resource through ensuring that the explorers/developers are rewarded for their risk. The province depends upon foreign imported crude oil to provide some 64% of its energy needs. Locally sourced coal accounts for 27% of the energy mix. The attraction of utilizing indigenous, cleaner burning coalbed methane is obvious. Presently no onshore natural gas development or related infrastructure exists. While this might be viewed as negative, it does point to the uniqueness of such a gas development as there would be no gas-on-gas competition. The next several years will likely see the development of the offshore natural gas fields which would establish pipeline infrastructure through, and adjacent to, the coal basins. Nova Scotia Power Inc., the only power company in the province, is a 50% partner in the coalbed methane rights to the Stellarton Basin and appears to have a ready market for the environmentally friendly, clean burning alternative to coal. Given sufficient reserves, it appears that the timing would be right for the development and utilization of coalbed methane in the province of Nova Scotia.

ACKNOWLEDGEMENTS

The author wishes to acknowledge the technical scrutiny of Dr. John Calder of the Coal Section of the Nova Scotia Department of Natural Resources. In addition the author expresses appreciation to Paul Harvey of the Petroleum Section of the Department of Natural Resources for his usual rigorous editorial comments.

REFERENCES:

1. Calder, J.H., Gibling, M.R., 1994: "The Euramerican Coal Province: controls on Late Palaoezoic peat accumulation", Palaeogeography, Palaeoclimatology, Palaeoecology, 106 (1994): 1-21, Elsevier Science B.V., Amsterdam.

2. Grant, A.C., 1992: "Aspects of seismic character and extent of Upper Carboniferous Coal Measures, Gulf of St. Lawrence and Sydney Basins", Palaeogeography, Palaeoclimatology, Palaeoecology, 106 (1994): 271-285, Elsevier Science B.V., Amsterdam.

3. Howie, R.D., 1988: "Upper Paleozoic evaporites of southeastern Canada", Geol. Surv. Can. Bull., 380, 120pp.

4. Gibling, M.R., Calder, J.H. and Naylor, R.D., 1992: "Carboniferous Coal Basins of Nova Scotia, Field Excursion C-1: Guidebook, Geological Association of Canada and Mineralogical Association of Canada, Joint Annual Meeting 1992, Wolfville, Nova Scotia, Canada".

5. Hacquebard, P.A., 1983: "Geological development and economic evaluation of the Sydney Coal Basin, Nova Scotia, Geological Survey of Canada, Paper 83-1A, p.71- 81.

6. _____ ,1986: "The Gulf of St. Lawerence Carboniferous Basin; the largest coalfield of Eastern Canada", Canadian Institute of Mining Bulletin, v.79, p.67 - 78.

7. Calder, J.H., 1991: "Controls on Westphalian Peat Accumulation: the Springhill Coalfield, Nova Scotia"; unpublished Ph.D. thesis, Dalhousie University, Halifax, Nova Scotia, Canada.

8. Naylor, R.D., Kalkreuth, W., Smith, W.D., and Yeo, G.M., 1989: "Stratigraphy, sedimentology and depositional environments of the coal-bearing Stellarton Formation, Nova Scotia, in Contributions to Canadian Coal Geoscience, Geological Survey of Canada, Paper 89-8, p. 2-13.

9. Bromley, D.S., and Calder, J.H., in press: "Seismic stratigraphy of the Athol Syncline, Cumberland Basin: implications for coal exploration", Geological Survey of Canada Paper.

10. Mavor, M., Pratt, T.J., and Crandlemire, A., 1993: "Assessment of Coalbed Methane Resources at the Donkin Mine Site,Cape Breton, Nova Scotia, Canada", in Proceedings, The 1993 International Coalbed Methane Symposium, Tuscaloosa, Alabama, pp. 471 - 481.

11. Mukhopadhyay, P.K.: "Final report on the organic geochemistry and organic petrography of sandstone, oil shale, and coal samples from three boreholes and opencast pit of the Stellarton Basin, Nova Scotia", Nova Scotia Dept. of Natural Resources Open File Report 95-4

12. Mukhopadhyay, P.K., MacDonald, D.J., Calder, J.H., Hatcher, P.G., 1994: "Geochemical constraints on coalbed methane and C_6^+ hydrocarbon generating capabilities of selected Carboniferous coals for the Stellarton and Cumberland Basins, Nova Scotia, Canada": presentation at the Eighteenth Annual Review of Activities, Mines and Energy Branches, Report 94-2, Nova Scotia Department of Natural Resources, Halifax, Nova Scotia, D. MacDonald, ed.

13. Mukhopadhyay, P.K., Calder, J.H., and Hatcher, P.G., 1993: "Geological and Physiochemical Constraints on Methane and C_6^+ Hydrocarbon Generating Capabilities and Quality of Carboniferous Coals, Cumberland Basin, Nova Scotia, Canada": in Proceedings of the 10th Annual Pittsburgh Coal Conference, Pittsburgh, PA.

14. Mukhopadhyay, P.K., Hatcher, P.G., and Calder, J.H., 1991: "Hydrocarbon generation from deltaic and intermontane fluviodeltaic coal and coaly shale from the Tertiary of Texas and Carboniferous of Nova Scotia (Canada)", in Org. Geochem. Vol 17, NO. 6, pp 765 - 783.

15. Algas Resources Ltd, 1981: "A coalbed methane content evaluation of the Pictou coallfield - Pictou County, Nova Scotia; Nova Scotia Department of Natural Resources, Assessment Report 81-035, 53 pp.

16. Thompson, A.J.P.: "A coalbed methane content evaluation of selected coalfields of Nova Scotia"; Nova Scotia Department on Natural Resources, Assessment Report 81-036, 52 pp.

17. Hughes, J.D., MacNeil, D.J., Evans, C.G., and Irvine, J.A., 1994: "Coalbed Methane Potential of Nova Scotia's Coalfields": in Program and Summaries, Eighteenth Annual Review of Activities, Mines and Energy Branches Report 94-2, Nova Scotia Department of Natural Resources, Halifax, Nova Scotia, p.29.

18. Mukhopadhyay, P.K., 1995, "Evaluation of coalbed methane potential of the Stellarton Basin, Nova Scotia, Canada, based on geological, physical and geochemical parameters"; Nova Scotia Department of Natural Resources Open File Report 94-029.

19. Grist, A.M., Ryan, R.J., and Zentilli, M., 1994: "Timing of Hydrocarbons and Coalbed Methane Generation in the Maritimes Basin: Restrictions from Apatite Fission Track Data", in Program and Summaries, Eighteenth Annual Review of Activities, Mines and Energy Branches Report 94-2, Nova Scotia Department of Natural Resources, Halifax, Nova Scotia, D. MacDonald, ed, p. 66.

20. Naylor, R.D., Calder, J.H., and Ryan, R.J.: "Controls on Formation of Upper Carboniferous Coals in the Intermontane Stellarton and Cumberland Basins of Atlantic Canada", in proceedings of the Canadian Coal and Coalbed Methane Geoscience Forum, Parksville, British Columbia, Feb 2-5, 1992, p. 365-397.

21. Nikols, D. J., 1991: "Resources and Reserves of coalbed methane in Canada:, a paper of the Alberta Geological Survey, Edmonton, Alberta.

22. Sakashita, B.J., 1993, "Exploration for coalbed methane starts up in northwestern Nova Scotia", Oil & Gas Journal, Pennwell.

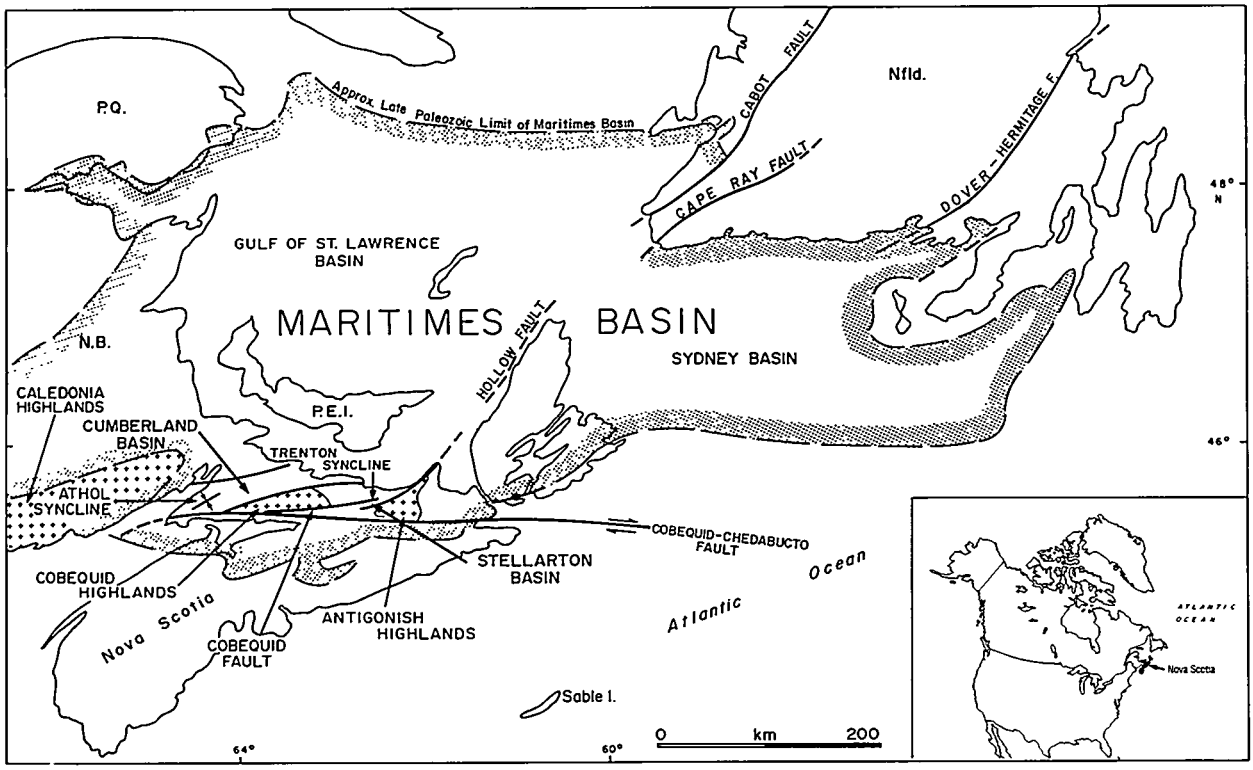


Figure 1 Location of the Maritimes Basin showing major sub-basins; modified from Naylor et al, 1989.

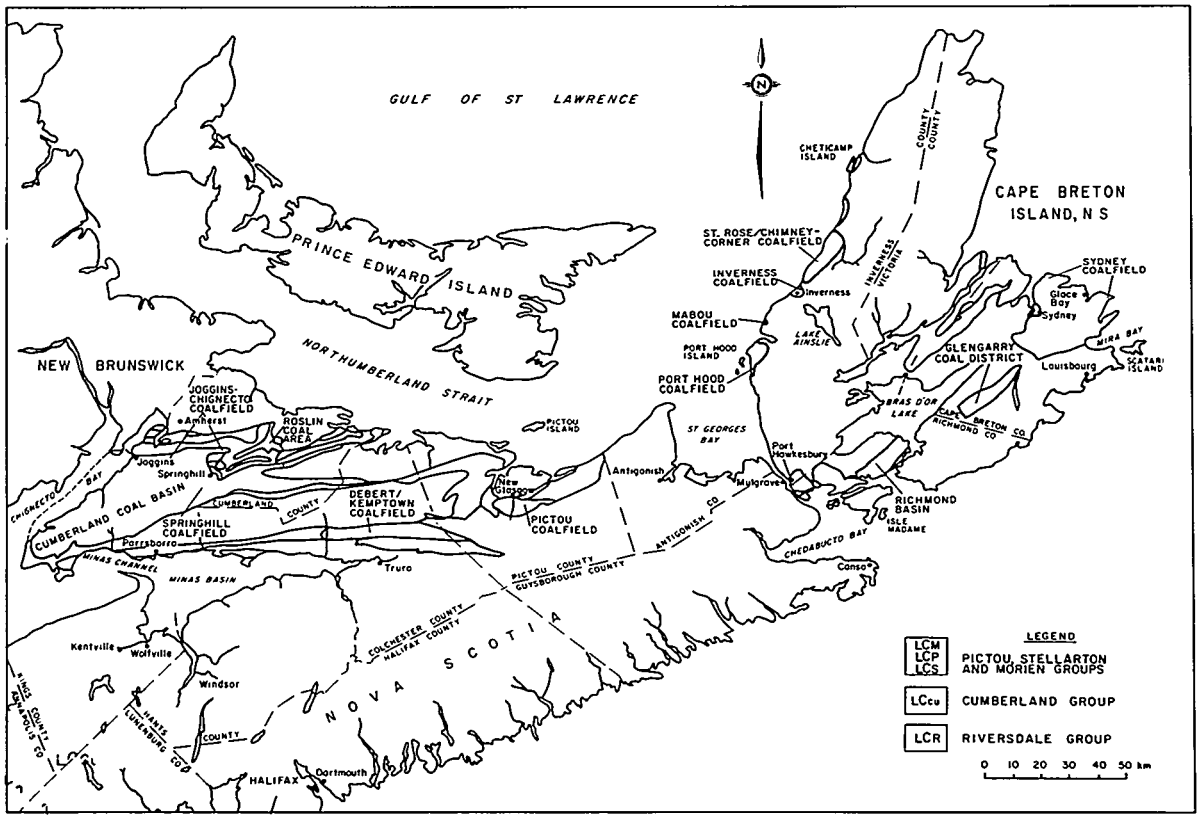


Figure 2 Coalfields of Nova Scotia showing distribution of coal-bearing Groups; after Calder, 1985.

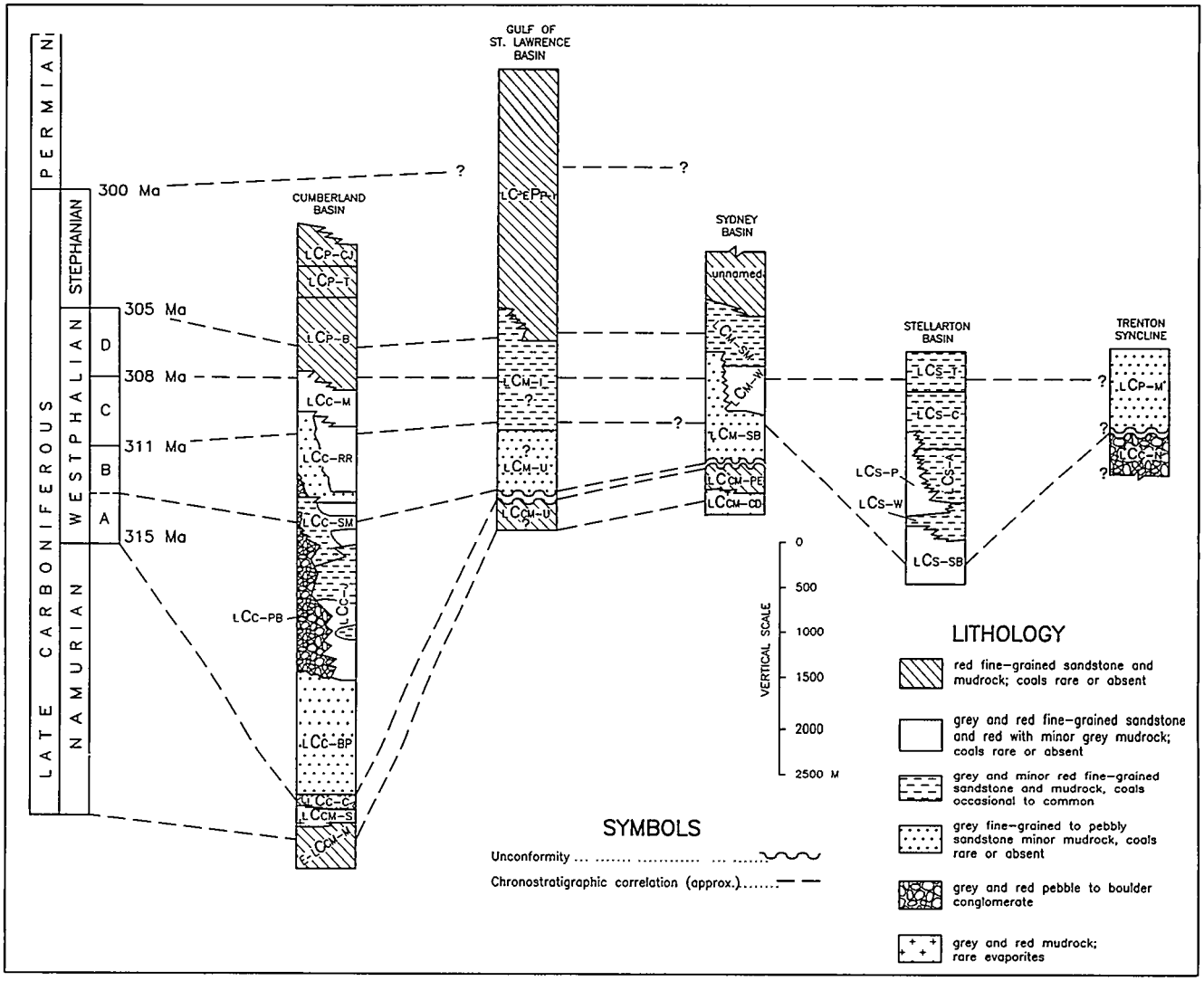


Figure 3 Stratigraphic correlation of the major coal-bearing regions of the Maritimes Basin; modified from Naylor 1985.
(rock units identified by symbol are similarly coded on the geology maps)

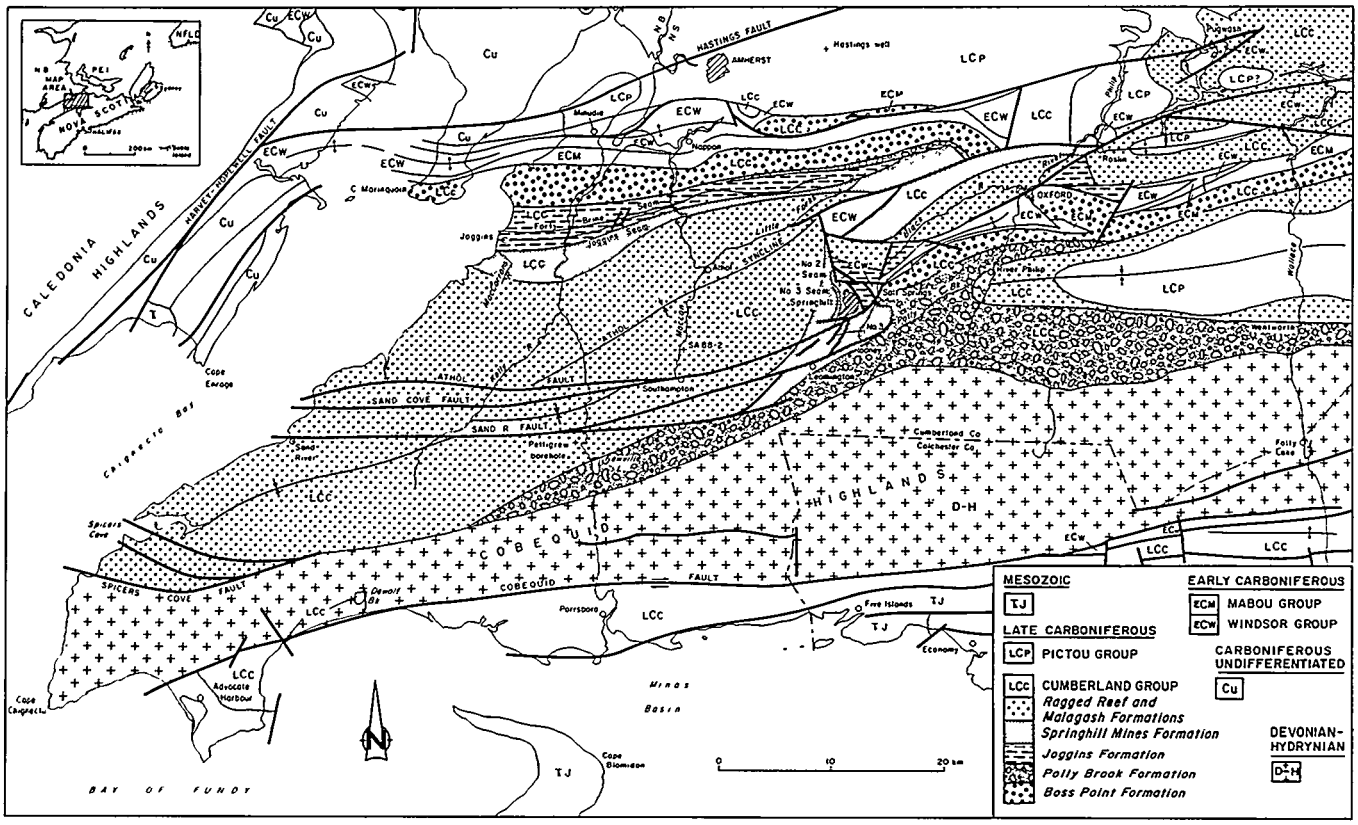


Figure 4 General geology of the western Cumberland Basin; after Calder 1991.

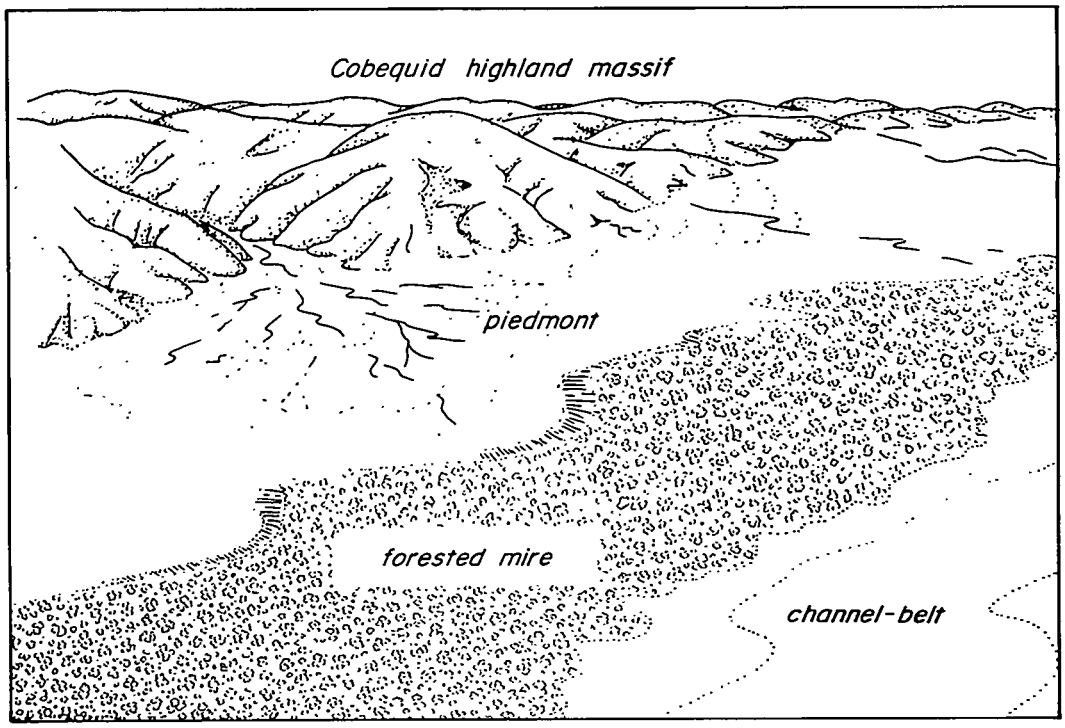


Figure 5 Paleogeographic setting of the Springhill peat-forming ecosystems; after Calder 1993

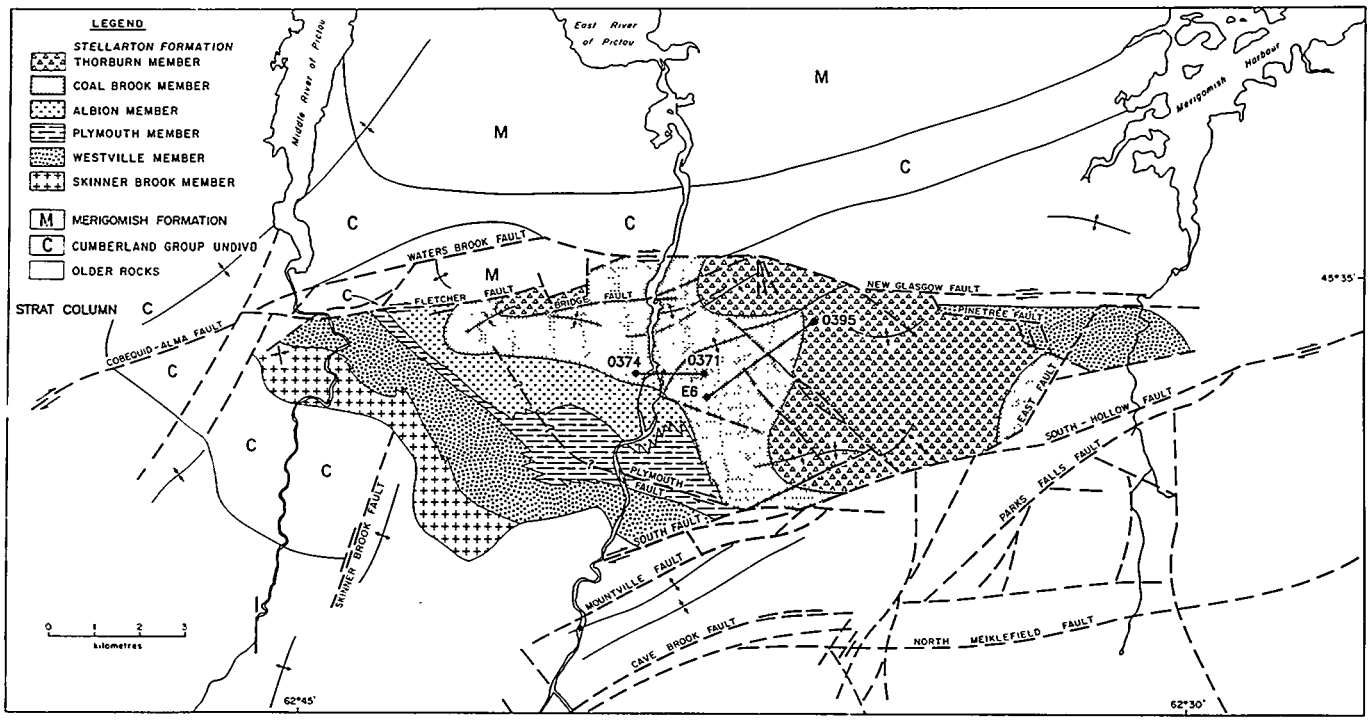


Figure 6 Geological sketch map of the Stellarton Basin; Naylor et al, 1985, after Yeo and Ruixiang (1987).

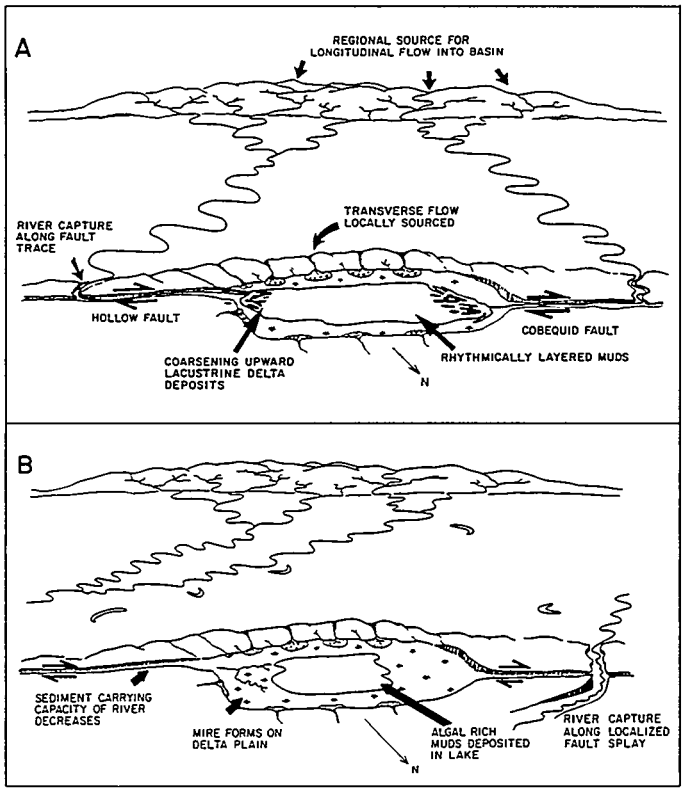


Figure 7

Paleogeographic models of the Stellarton Basin during the deposition of the Thorburn and Coal Brook Members; after Naylor et al, 1992.

A) sediment being supplied to the basin and mouth bar deltas werre building into a central basin lake.

B) sediment supply restricted with mires forming on the abandoned delta plain.

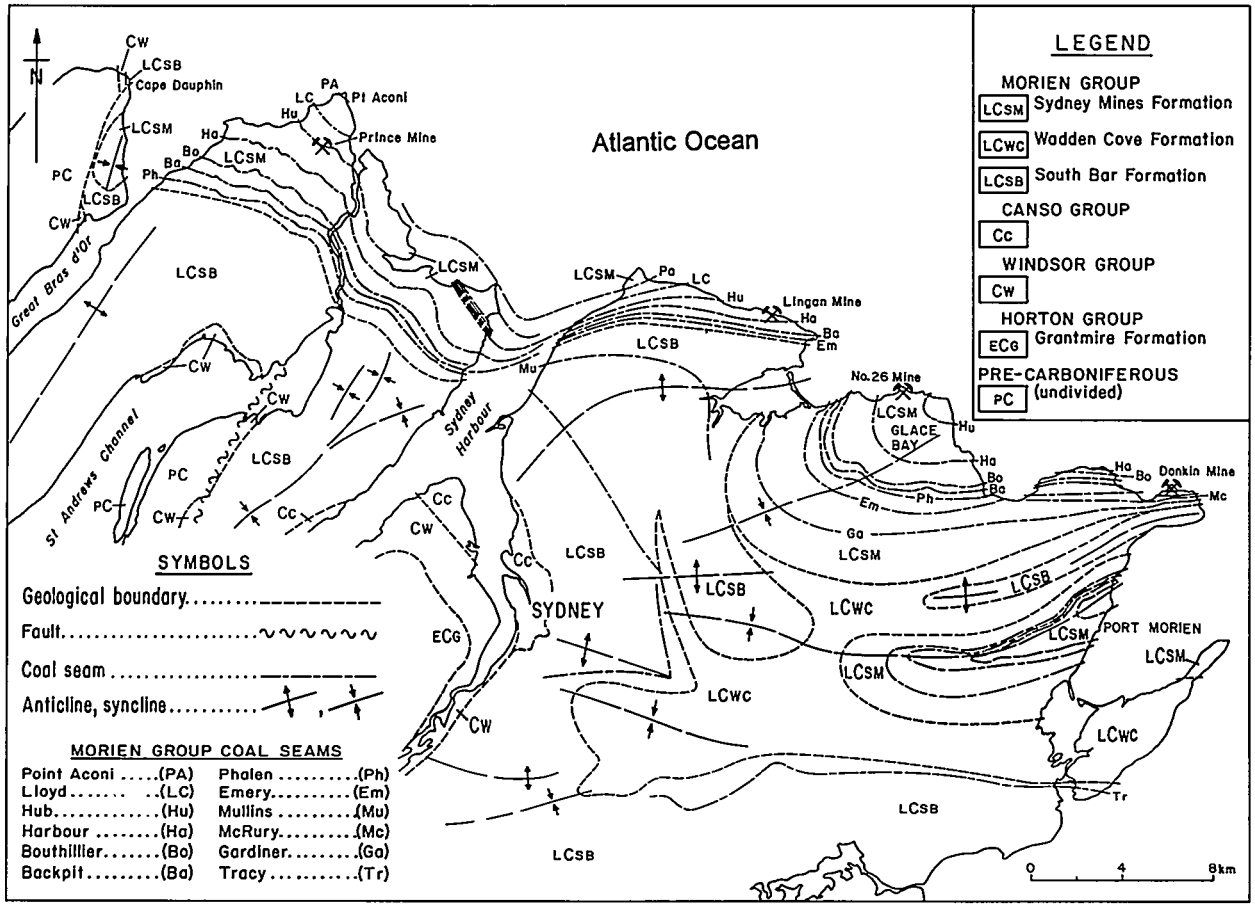


Figure 8 Geological map of the Sydney coalfield; after Calder, 1985.

NOTES



NOTES



NOTES

INTERGAS '95

May 15-19, 1995
The University of Alabama
Tuscaloosa, Alabama USA

9505

Evaluation of Coalbed Methane Potential of the Stellarton Basin, Nova Scotia, Canada, Based on Geological, Physical, and Geochemical Properties

P.K. Mukhopadhyay, Global Geoenergy Research Ltd., Nova Scotia; D.J. MacDonald and J.H. Calder, Nova Scotia Department of Natural Resources

ABSTRACT

The *coalbed methane* potential of selected samples from the Scott, Acadia, Cage, Foord, and McLeod seams (Westphalian B-D in age) from the Stellarton Basin, Nova Scotia, eastern Canada were evaluated by various physical and chemical properties. Influx and fluctuation of water in the ancestral peat mire led to vertically and laterally variable lithotype and maceral composition. Volatile matter (controlled both by inertinite content and depth) type and ash content reflect this unstable setting. A 3-D maturation model of the basin demonstrates that the maturity at the surface varies between 0.75 to 0.85% R_o, increasing to 1.6 to 1.86% R_o at 1250 m depth, although variations exist within different seam profiles.

The CO_2 *surface area* and *monolayer capacity* (77.6 to 266.7 m^2/g and 11.9 to 58.2 cc/g of coal at STP) is dependant on maceral composition, ash content, and maturity. The highest sorption capacity is observed between 0.9 to 1.1% R_{max}, and gradually decreases to values of 1.1-1.4% R_{max} due to an increase in liquid hydrocarbon content. Beyond 1.4% R_{max}, sorption capacity increases due to the cracking of free hydrocarbons to methane. The porosity and permeability data suggest that the mineral matter-rich maceral zones which usually having low permeability, display increased permeability due to the presence of higher concentration of inertinite and vitrinite macerals. The west and northwestern part of the basin show the highest coalbed methane potential; a yield of 10-20 cc of methane per gram of coal at STP is expected.

INTRODUCTION

During the past twenty years, *coalbed methane* studies revitalized coal research in North America. In the San Juan Basin of the United States, more than 15.5 billion m^3 (440 Gcf) of coalbed methane was produced in 1992 alone [1]. Apart from primary and secondary biogenic gases (CH_4, CO_2, and H_2S), methane, carbon dioxide, nitrogen, and C_2+ gases are mainly generated and stored within the coal macromolecule during the catagenetic stage (bituminous and anthracite rank) by either cracking the kerogen part of the coal or cracking free liquid hydrocarbons [1-5].

In contrast to natural gases which remain mostly in a free state and are reservoired in other rocks (sandstone, limestone, etc.), methane and other gases (CO_2, N_2, etc.) are reservoired *within* the coal seam and are usually stored either in a free or in a sorbed phase (mainly in a condensate, near liquid state) within the micro- and macropores of the coal [6]. The direct method of determining the amount of methane in a coalbed is by (a) sorption isotherms in which the equilibrium between the free and sorbed gases is reached by increasing (injecting methane called adsorption) or decreasing (desorption) pressure [7] or (b) by hydrous pyrolysis and quantifying the free gas content [8]. In an indirect method, the methane holding capacity can be measured by correlating the CH_4 adsorption isotherms with the CO_2 and CH_4 monolayer capacities of a coal [9].

As in various coal mines in the world, methane is ubiquitously associated with coal seams in Nova Scotia, having caused serious mine disasters in the Cumberland and Stellarton Basin during the 20th Century. Although coalbed methane assessment in Nova Scotia began in the Stellarton Basin during early 1980's (MacDonald, this volume), it did not evaluate the exact gas content due to inefficient technology at that time. The major work on the evaluation of hydrocarbons in various coal basins in Nova Scotia began only recently [10-12]. Recently, several wells have been drilled in the Cumberland Basin and actual desorption isotherms were carried out to evaluate the potential of coalbed methane (MacDonald, this volume).

The aim of this paper is to evaluate the coalbed methane potential of selected coal seams of the Stellarton Basin and illustrate the relationship among various coal parameters such as rank (maturation), mineral matter and moisture content, coal facies (maceral and minerals), CO_2 surface area and monolayer capacity, amount of liquid hydrocarbons, density, porosity, and permeability. The possible methane holding capacity of those coals was determined indirectly using CO_2 monolayer capacity, maturation and other coal quality parameters.

GEOLOGY

The Stellarton Basin lies in a broad northeast-trending trough located between the Cobequid and Antigonish Highlands and is underlain by Late Carboniferous (late Westphalian B to mid-Westphalian D) strata (Fig. 1). The basin contains 2600m of interbedded red and gray siliciclastics with numerous coal and oil shales which were deposited under predominantly lacustrine conditions [13-16]. The major peat-forming

environment was created mainly in the west and northwest part of the basin during Westphalian B-D. The Stellarton Formation contains four coal-bearing members (Thorburn, Coal Brook, Albion, and Westville) with most of the major, thick coal seams occuring within the Albion and Westville Members (Fig. 2). The Westville Member contains the Acadia (~5 m), Scott (~3 m), and Fourth (~2 m) seams. The Albion Member contains the Foord (~14 m), Cage (~12 m), McGregor (~7 m), Third (~4 m), and New (~ 3 m) seams. The Coal Brook Member contains the thinner McLeod and McBean seams and the Thorburn Member contains the Widow Chisholm, Upper and Lower McKay, Millrace and Captain seams.

SAMPLES

Twenty five samples from five seams (Scott, Acadia, Foord, Cage, and McLeod) were collected from various drillhole and mine locations from various depths. Those samples were used for detailed physical and chemical characterization. Eighteen other samples, collected from other drillholes and depths, were analyzed only for vitrinite reflectance. Six other reflectance data (taken from an earlier report) were also included. Those twenty-five analyzed samples and some other reflectance data were included in Table 1.

ANALYTICAL PROCEDURES

The nomenclature and method for the analysis of lithotype, maceral, vitrinite reflectance, proximate composition, and Rock-Eval pyrolysis were adopted from various earlier work [3, 17-19]. The bulk density of coal represents the bulk volume (V_g) of coal including all of its pore space. The methods for the determination of bulk density, grain density (apparent density, called V_s), and permeability of coal are after ASTM [18]. The total porosity of coal is derived from the following relation:

$$\% \text{ Porosity} = 100 \times (V_g - V_s)/ V_g.$$

The porosity of four coal samples (3-Acadia, 10-Foord, 19-Foord, and 22-McLeod) was also determined microscopically using an earlier method [20].

Carbon dioxide surface area was analyzed in a low pressure volumetric gas adsorption apparatus [9]. Carbon dioxide monolayer capacity was determined by using the following Dubinin-Radushkevich equation [9, 21]:

$$\log V = \log V_o - S \log^2 (P/P_o)$$

where V = volume filled at P/P_o; V_o = total micropore volume; S = constant; P = pressure; P_o = saturation vapour pressure. The surface area was calculated using a value of 17 x 10^{-20} m^2 for the area of the CO_2 molecule [21]. The Hardgrove Grindability Index (HGI) was determined on four samples (3-Acadia, 10-Foord, 19-Foord, 22-McLeod) using the method described in ASTM [18].

RESULTS AND DISCUSSION

Lithotypes

Only two samples (3-Acadia and 23-McLeod) are rich in thick vitrain bands. Other analyzed coal seams are classified into three lithotype assemblages: (a) mixtures of thinly banded vitrain and clarain with some proportions of durain, fusain and dark clarain (example: 25-McLeod); (b) thinly banded coals whose main components are clarain and durain with mixtures of bone, fusain, bright and dull clarain and vitrain (example: 11-Foord); and (c) abundance of bone bands associated with other lithotypes (example: 21-Foord). Some of the coal seams contain thick fusain bands (example: 12-Foord).

Proximate Analysis

Proximate analysis data show that with the exception of samples 9-Cage and 20-Foord, all coal seams have >15% ash content (Table 3). Within those samples, some (example: 17-Foord) have more than 30% ash content; 21-Foord is a shaly coal with 45% ash. In general, most Foord seam samples have higher volatile matter content (17-31% on a dry basis; Table 1). The moisture content (as received) varies between 1.48 (7-Acadia) to 5.43% (9-Cage). Except for two samples, all coals have low sulfur content (0.34 - 0.81 wt. %). The overall ash distribution pattern as revealed in a contour map indicates that the north and northeastern parts of the basin have a lower ash content than the present central area [22]. Based on volatile matter content [18], samples from the Acadia seam (mostly medium volatile bituminous) show higher rank than the Foord seams (mostly high volatile bituminous) (Table 1). Although some variations are depth-related, abundant fusain in most coal samples reduces the effectiveness of volatile matter as a rank parameter in the basin.

Coal Facies and Liquid Hydrocarbon Potential

In comparison to the coals from the Sydney Basin (from unpublished reports of the author) and some western Canadian coals which have >70% vitrinite and low inertinite [9], while the analyzed coals have <70% vitrinite and higher inertinite content (16 to 33%) (Fig. 3A-3F). Some of the samples such as 15-Foord and 25-McLeod have dominant (>30%) telocollinite content (Fig. 3A, 3B, and 3E)), whereas others (17-Foord, 18-Foord) have dominant desmocollinite or corpocollinite content (Fig. 3C and 3D). Vitrinite-rich coal often shows microfractures within the telocollinite bands which can be good conduits for the desorption of methane (Fig. 3A and 3E). In general, the Cage, Foord, and McLeod seams have higher liptinite content (11-22%) (Fig. 3F). In general, low-ash coals have more telocollinite (Fig. 3A and 3E) and high ash coals have more desmocollinite (Fig. 3C). Sample 25-McLeod has anomalously high inertodetrinite (20.2%) (Fig. 3F). The inertinite content in most coals is not related to ash or desmocollinite content. High ash coals generally contain abundant clay minerals (Fig. 3C). Telocollinite-rich McLeod seams have a higher quartz content compared to the Foord seams which possibly increased the porosity and permeability (Fig. 3F). Some samples (example: 17-Foord) contain abundant carbonate (mainly calcite) along with the quartz (Fig. 3B).

Rock-Eval pyrolysis data show that all the Cage and Foord seam samples have anomalously high S_2 (>100 mg HC/g rock) suggesting a higher potential for generating liquid hydrocarbons. The higher liptinite content of those seams may explain this phenomenon. In a T_{max} versus hydrogen index

diagram, some of Foord and Cage seam coal samples lie within the Kerogen Type II and III maturation path [22]. This suggests that those coals have better liquid hydrocarbon potential than typical humic coals [19]. The production index (free liquid hydrocarbons within the coal macromolecule) varies between 0.01 to 0.10 (Table 3). Samples 2-Scott, 6- and 7-Acadia, 20-Foord, 21-Foord have the highest production indices which are mainly related to the higher maturity of those coals. These data suggest in situ generation of liquid hydrocarbons (crude oil) within most coals. The presence of low amounts of free hydrocarbons (S_1) and high hydrocarbon potential (S_2) in some samples indicate less plugging of primary pores and higher methane generating capability in those coals with reflectance values between 0.9 to 1.1% $R_{max.}$.

Maturation

A comparison of three major physical and chemical maturity parameters (*vitrinite reflectance*, T_{max} from Rock-Eval pyrolysis, and volatile matter in dry, mineral-matter-free basis) is documented in Table 1. A plot of mean random versus maximum vitrinite reflectance data showed high correlation coefficients. A similar high correlation coefficient was recognized in the plot of mean random vitrinite reflectance and T_{max}. Using random reflectance data of various samples, a maturation contour map was generated for the basin. A comparison of maturation and depth contours shows that two high maturation inflection points are observed in the central part of the basin (Figs. 4 and 5). The Acadia seam contour lines show an increase in maturity from SW to NE from 0.91% to 1.86% [22].

A 3-D view of maturation was developed using mean random reflectance, co-ordinates and elevation of the wells, and depth of the samples [22]. The data from both the maturation/elevation contour maps and the 3-D view [22] clearly demonstrate the relationship between maturity and depth of the coal seam. It also shows that the southern part of the basin has a higher maturity than the northern and northwestern parts of the basin at the same depth level. The relationship between depth and vitrinite reflectance is also documented from samples collect from the Suncor AP-0355 drillhole (Fig. 6). The upper part of the section and a few samples in the lower part of the drillhole are coal or coaly shale, whereas most samples in the lower part are oil shale. The data on Figure 6 demonstrate that: (a) the increase in reflectance is related to depth and (b) the suppression of vitrinite reflectance in the oil shale samples when compared to coal or coaly shale [23]. The maturation profile of the Acadia seam samples show broad variations in reflectance when plotted against depth (Fig. 7).

Surface Area and Monolayer Capacity

The surface area of a coal measures the accessibility of small molecules (CO_2, CH_4, etc.) to the internal molecular structure of coal [6,7,19]. The surface area is measured by pressurizing the coal with a known amount of CH_4 and CO_2. Higher surface area suggests high sorption capacity of the coal for gases such as methane and carbon dioxide. Surface area is often dependant on pressure, temperature, and moisture content. The surface area and CO_2 adsorption capacity of the analyzed samples varies between 77.6 to 266.7 m^2/g and 4.85 to 29.94 cc/g STP, respectively (Table 3). Most coal samples of McLeod and Foord seams from the northwestern part of the basin (drillholes P6, P21, P28, etc.) have consistently higher surface area, CO_2 adsorption capacity, and CO_2 monolayer capacity (Table 3). Figure 8 shows the relationship between the absolute pressure (mm Hg) and the volume of CO_2 adsorbed in a McLeod seam (25-McLeod). The monolayer capacity of various seams are: Scott = 11.9-20.9; Acadia = 16.9-25.9; Cage = 24.0; Foord = 15.7-32.5; McLeod = 25-58.2 cc/g STP. Both the Foord and Cage seams in drillhole P-47 show higher surface area. It is believed that the dominance of vitrinite (>60%) results in higher surface area in coal, because vitrinite contains mainly micropores (<20A° or 2 nm) compared to inertinite which has mainly mesopores (20-50 nm) and macropores (>50 nm) [7, 25-27]. The relationship between total vitrinite content (dmmf basis) and CO_2 monolayer capacity (MC) of all analyzed samples suggests a broad increase of MC is related to the increase in total vitrinite content in spite of some data scattering (Fig. 9). However, comparing the data from Tables 2 and 3, it is evident that the total amount of inertinite (especially semifusinite and inertodetrinite) plus vitrinite has better correlation to sorption capacity than only total vitrinite content (especially in sample 25-McLeod). This is different from the existing views [9, 28]. From the coal facies analysis, it is evident that the ancestral peat mire of some Foord and McLeod seams evolved more dynamically than a typical rheotrophic mire in a wet swamp situation. This suggests that the maceral combinations of the intermontane, lacustrine deltaic coals may be as important as the total vitrinite content in riverine rheotrophic mire for the enhancement of CO_2 adsorption capacity (possibly CH_4 monolayer capacity) in coal. However, higher vitrinite content (especially telocollinite, gelocollinite and pseudovitrinite) plays a major role in enhancing the sorption capacity of a coal. According to the relationship between R_{max} and CO_2 monolayer capacity (Fig. 10), the highest MC is observed at a coal rank of 0.90-1.10% R_{max} with progressively lower MC realized as the rank increases to 1.4% R_{max}. Beyond 1.4% R_{max}, the CO_2 MC begins to increase again. The lowering of the monolayer capacity between 1.1 to 1.4% R_{max} is possibly due to the corresponding increase in mobile hydrocarbons (formed in situ) which decrease the sorption capacity of coal [24]. The increase of monolayer capacity beyond 1.4%R_{max} is possibly due to the generation of free spaces caused by the cracking of liquid hydrocarbons into methane and other hydrocarbon gases. Mineral matter (especially clay minerals) and liptinite macerals in coal which hold more liquid hydrocarbons definitely decrease the sorption capacity of a coal.

According to early researchers, the monolayer capacity and adsorption capacity of methane is smaller than carbon dioxide [7, 9, 25]. Accordingly, the methane monolayer volume can be extrapolated to give values between 10-20 cc/gm of coal.

Porosity, Permeability, and Density

The porosity of the analyzed coal samples varies from 0.5 to 6.6% (Table 3). The porosity of coal between high

volatile to low volatile bituminous rank generally ranges from 2 to 6% [24]. Accordingly, all analyzed coals have average comparable porosities relative to their rank. Table 3 also shows that the highest grain density in the samples is associated with high maturity (>1.2% R_{max}). The grain density does not correlate with the ash content [22]. The porosity of values of four coal samples determined microscopically (using fluorescence) are 5, 6.5, 3.5, 3.0%, compared to the measured value of 3.9, 5.0, 2.0, 1.7%, respectively. The grain density of the samples, which varies between 1150 to 1630 kg/m^3 (1.15 to 1.63 gm/cm^3), does not show any relationship to the ash content or maturity. HGI values are 58 (3-Acadia), 51 (10-Foord, 19-Foord), and 48 (22-McLeod).

The bireflectance in coal which produces anisotropy, is generally caused by the influence of stress and increasing maturity. In a structurally disturbed area, the bireflectance is higher than in an undisturbed region. The bireflectance of these twenty five coal samples varies from 0.15 to 0.42. The variation of bireflectance in these coals is controlled mainly by the increase in maturity. Stress seems to have little effect on the bireflectance values.

The highest permeability value was observed in 25-McLeod sample which also showed the highest monolayer capacity (Table 3). No correlation was found between total vitrinite content or R_{max} and permeability (Fig. 11). This may indicate that these inertinite- and detrinite-rich coals have different trends compared to overall vitrinite-rich coals in other basins. It is observed that the coal having highest inertodetrinite content shows the highest permeability. This may suggest that mineral matter which usually have low permeabilities may create additional permeable spaces through interconnecting pores due to the presence of higher inertodetrinite and semifusinite where total vitrinite content is less than 70%. Those interconnecting spaces may be formed as a result of variable compaction due to differences in density between mineral matter (>2.0 cm^3/gm), vitrinite (1.3-1.4 cm^3/gm) and inertinite (1.5-1.6 cm^3/gm). A 2-D contour plot of the permeability of various coals suggests that the northeastern part of the basin contains coals with the highest permeabilities.

COALBED METHANE POTENTIAL

Based on the maturity, CO_2 monolayer capacity, and permeability data, the west and northwestern parts of the Stellarton Basin (drillholes P-17, P-22, P-28, and P-47) show the highest coalbed methane potential. The target coals are Acadia, Cage, Foord, and McLeod seams, optimally within a depth of 400 to 500 m. Based on CO_2 adsorption capacity and its relationship with CH_4 adsorption capacity, a production of 10-20 cc of methane per gram of coal at STP should be expected in those coal seams.

ACKNOWLEDGMENTS

This research was funded by the Energy Resources Division of the Nova Scotia Department of Natural Resources. The author acknowledges the help of Kevin Gillis, Lorne McNeil, Rob Naylor, and the drafting section of the Nova Scotia Department of Natural Resources, Stellarton and Halifax, Nova Scotia. The manuscript was critically reviewed by John A. Wade, Atlantic Geoscience Centre, Geological Survey of Canada, Dartmouth, Nova Scotia. The authors acknowledge James Hower of Appled Energy Center, The University of Kentucky, Lexington, Martin Fowler of the Geological Survey of Canada (ISPG), Calgary, Alberta, John Clow of Core Laboratories, Calgary, Alberta, Bruce Hudgins of Hudgtec Consulting Ltd, Halifax, Nova Scotia and Mike Avery, Geological Survey of Canada, Dartmouth, Nova Scotia, for their data.

REFERENCES CITED

1. Scott A.R., Kaiser W.R. and W.B. Ayers,Jr, 1994: "Thermogenic and Secondary Biogenic Gases, Jan Juan Basin, Colorado and New Mexico-Implications for Coalbed Gas Producibility"; American Association of Petroleum Geologists Bulletin, V. 78, No. 8, p. 1186-1209.

2. Hunt J.M., 1979: Petroleum Geochemistry and Geology: W. H. Freeman and Company, New York, 617 p.

3. Tissot B. and Welte, D. H., 1984: Petroleum Formation and Occurrence, 2nd Edition, Springer-Verlag, Berlin, 699 p.

4. Mukhopadhyay P.K., Fowler M.G. and W.G. Dow, eds., 1991: Coal and Terrestrial Organic Matter as a Source Rock for Petroleum: Pergamon Press, Oxford, Organic Geochemistry, V. 17, No. 6, p. 671-918.

5. Law B.E. and D.D. Rice, 1993: Hydrocarbons from Coal: American Association of Petroleum Geologists Studies in Geology 38, Tulas, Oklahoma, 400 p.

6. Yee D., Seidle J.P. and W.B. Hanson, 1993, "Gas Sorption on Coal and Measurement of Gas Content", in. Law, B and Rice, D.D., eds., Hydrocarbons from Coal, American Association of Petroleum Geologists Studies in Geology Series 38, pp. 79-118.

7. Ayers W.B. Jr., Kaiser W.R. and J.R. Levine, 1993, "Coal as Source Rock and Gas Reservoir", Short Course #1 for the Coalbed Methane Symposium, Tuscaloosa, Alabama, p. 1-121.

8. Mukhopadhyay P.K., Calder J.H. and P.G. Hatcher, 1993, "Geological and Physicochemical Constraints on Methane and C_6+ Hydrocarbon Generating Capabilities and Quality of Carboniferous Coals, Cumberland Basin, Nova Scotia, Canada", Proceedings of the 10th Annual International Pittsburgh Coal Conference, Pittsburgh, Pennsylvania, p. 1074-1079.

9. Lamberson M.N. and R.M. Bustin, 1993, "Coalbed Methane Characteristics of Gates Formation Coals, Northern British Columbia: Effect of Maceral Composition", American Association of Petroleum Geologists Bulletin, V. 77, No. 12, p. 2062-2076.

10. Mukhopadhyay P.K., Hatcher P.G. and J.H. Calder, 1991, "Hydrocarbon Generation from Deltaic and Intermontane Fluviodeltaic Coal and Coaly Shale from the Tertiary of Texas and Carboniferous of Nova Scotia", Organic Geochemistry, V.

17, No. 6, p. 765-784.

11. Sakashita B.J., 1993, "Exploration for Coalbed Methane starts up in Northwestern Nova Scotia", Oil & Gas Journal, March 29 Issue, p. 85-86.

12. Grant A.C., 1994, "Aspects of Seismic Character and Extent of Upper Carboniferous Coal Measures, Gulf of St. Lawrence and Sydney Basins": Paleoceanography, Paleoclimatology, Paleoecology, V. 106, p. 271-285.

13. Bell W.A., 1940, "The Pictou Coalfield, Nova Scotia", Geological Survey of Canada Summary Report, 1924, Part C, p. 142-180.

14. Calder J.H., 1978, "Megascopic Petrography and Economic Geology of the Foord Seam Open Pit Mine, Pictou Coalfield, Nova Scotia. Nova Scotia Department of Mines and Energy Open File Report 624, 24 p.

15. Naylor R.D., Kalkreuth W., Smith W.D. and G.M. Yeo, 1989, "Stratigraphy, Sedimentlogy and Depositional Environments of the Coal-bearing Stellarton Formation, Nova Scotia", Geological Survey of Canada Special Paper 89-8, p. 2-13.

16. Gillis K.S., 1991, "Structural Setting and Coal resources of the Stellarton Graben, Nova Scotia", Nova Scotia Department of Mines and Energy Open File Report 91-014, 32p.

17. Stach et al., 1982: Stach's Textbook of Coal Petrology. Gebruder Borntraeger, Berlin, 535 p.

18. American Society for Testing and Materials (ASTM), 1981: Annual Book of Standards, Part. 26., Gaseous Fuels, Coals and Coke, Atmospheric Analysis. Philadelphia, 910 p.

19. Mukhopadhyay P.K. and P. G. Hatcher, 1993: "Composition of Coal", in Law, B and Rice, D.D., eds., Hydrocarbons from Coal, American Association of Petroleum Geologists Studies in Geology Series 38, pp. 79-118.

20. Soeder D.J., 1991, "The Effects of Overburden Stress on Coalbed Methane Production", in Peters, D.C., ed., Geology in Coal Resource Utilization, Techbooks, Washington, D.C. pp. 125-136.

21. Marsh H. 1987, "Adsorption Methods to Study Microporosity in Coals and Carbon - a critique", Carbon, V. 25, p. 49-58.

22. Mukhopadhyay P.K., 1994, "Coalbed Methane Potential of selected Coal Seams from the Stellarton Basin, Nova Scotia based on Maturation, and other Important Physical and Chemical Properties", Nova Scotia Department of Natural resources Open File Report OFR 94-029, 19 p.

23. Mukhopadhyay P.K., 1994, "Vitrinite Reflectance as Maturity Parameter - Applications and Limitations: a Review", in Mukhopadhyay P.K. and Dow W.G. eds., Vitrinite Reflectance as a Maturity Parameter: Applications and Limitations, American Chemical Society Symposium Series 570, Washington D. C., pp. 1-24.

24. Levine J.R., 1991, "The Impact of Oil Formed during Coalification on Generation and Storage of Natural Gas in Coal Bed Reservoir Systems", Proceedings of the 3rd Coalbed Methane Symposium, Tuscaloosa, Alabama, p. 307-315.

25. Gan H.S., Nandi S.P. and P.L. Walker, Jr: "Nature of the Porosity in American Coals", Fuel. V. 51, p.272-277.

26. Thomas J. Jr. and H. H. Damberger, 1976, "Internal Surface Area, Moisture Content, and Porosity in Illinois Coals: Variation with Coal Rank", Illinois State Geological Survey Circular 493, 38p.

27. Harris L.A. and C.S. Yust, 1979, "Ultrafine Structure of Coal Determined by Electron Microscopy. American Chemical Society Division Chemicals preprint paper, V. 24, p. 210-217.

28. Bocking M.A. and C.R. Weber, 1993, "Coalbed Methane in the Sydney Basin-Australia", paper 9304, Proceedings of the 1993 International Coalbed Methane Symposium, The University of Alabama/Tuscaloosa, p. 15-24.

Table 1: Sample location, vitrinite reflectance, T_{max}, volatile matter (VM) and rank (according to VM, dmmf basis)

Borehole/Mine	Sample/seam	Depth(m)	R_o	R_{max}	R_{min}	T_{max}	VM (dmmf)	Rank
Pioneer	1-Scott	10.7-13.7	0.92	0.99	0.84	447	33.4	HVB
P-25	2-Scott	854.7-858.3	1.40	1.50	1.18	472	26.4	MVB
Pioneer	3-Acadia	6.5-8.5	0.91	0.97	0.81	444	24.8	MVB
P-17	4-Acadia	74.3-78.6	0.95	1.01	0.87	446	24.8	MVB
P-18	5-Acadia	251.5-253.7	1.03	1.12	0.91	448	29.1	MVB
P-25	6-Acadia	771.1-774.7	1.34	1.48	1.21	474	20.4	LVB
P-23	7-Acadia	824.6-827.9	1.44	1.59	1.31	476	26.9	MVB
0353	Acadia	640.1-644.3	1.27	1.35	1.06			
0356	Acadia	1254-1262	1.86	2.00	1.54			
0355	Acadia	815-820	1.38	1.51	1.09			
ACC-104A	Acadia	863	1.51	1.62	1.23			
P-44	8-Cage	162-171.7	0.89	0.97	0.83	447	22.6	MVB
P-47	9-Cage	184.4-195.0	0.79	0.84	0.79	439	24.3	MVB
0392	Foord	542-557	1.09					
0397	Foord	619-629	1.11					
WA-14	10-Foord	11.9-17.1	0.86	0.94	0.76	441	36.1	HVB
P-5	11-Foord	99-103	0.87	0.96	0.79	440	35.2	HVB
P-19	12-Foord	22.4-35.1	0.88	0.96	0.80	442	36.5	HVB
P-6	13-Foord	194.1-194.2	0.88	0.94	0.82	442	32.8	HVB
P-21	14-Foord	293.8-299.3	0.94	1.00	0.88	444	33.0	HVB
P-22	15-Foord	320.6-326.1	0.91	0.96	0.85	444	32.6	HVB
P-45	16-Foord	99.2-111.8	0.90	0.96	0.82	444	33.1	HVB
E-10	17-Foord	98.7-109.5	0.90	0.96	0.83	444	47.1	HVB
E-24	18-Foord	21.3-33.7	0.96	1.02	0.87	447	34.6	HVB
P-47	19-Foord	130.9-138.1	0.79	0.85	0.75	436	35.3	HVB
0382	20-Foord	394-409.8	0.97	1.00	0.86	449	33.3	HVB
P-29	21-Foord	497.8-520.8	1.14	1.20	1.01	463	35.1	HVB
P-10	22-McLeod	73.4-75.3	0.80	0.88	0.74	440	33.6	HVB
P-14	23-McLeod	70.6-72.4	0.83	0.90	0.77	443	33.2	HVB
P-15	24-McLeod	196.0-198.1	0.82	0.89	0.76	441	34.3	HVB
P-28	25-McLeod	90.0-91.4	0.81	0.90	0.77	441	32.5	HVB -MVB

Table 2. Group macerals and minerals in volume percent.

Samples	Total Vitrinite 1	2	Total Liptinite 1	2	Total Inertinite 1	2	Total Minerals A	B
1-Scott	50	61	11	13	22	26	17	13
2-Scott	46	53	10	11	32	36	12	12
3-Acadia	58	63	9	9	25	28	8	5.4
4-Acadia	52	61	17	20	16	19	15	10.6
5-Acadia	49	58	15	17	22	25	14	9.7
6-Acadia	70	74	4	4	20	22	6	5.1
7-Acadia	56	65	4	4	26	31	14	7.6
8-Cage	45	49	16	17	31	34	8	8.2
9-Cage	57	60	15	16	23	24	5	4.8
10-Foord	52	61	17	20	16	19	15	11.1
11-Foord	57	66	13	15	16	19	14	10.6
12-Foord	54	61	12	14	22	25	12	12.0
13-Foord	61	64	11	12	22	24	6	7.6
14-Foord	45	51	14	16	30	33	11	10.2
15-Foord	60	62	16	17	20	21	4	6.3
16-Foord	48	52	11	12	33	36	8	7.8
17-Foord	70	81	11	14	4	5	15	12.2
18-Foord	63	64	12	15	21	21	4	6
19-Foord	50	53	22	23	22	24	6	6.9
20-Foord	55	59	12	13	27	28	6	5.2
21-Foord	58	77	6	9	9	14	27*	18.2
22-McLeod	44	56	11	14	23	30	22*	11.6
23-McLeod	59	67	10	12	18	21	13	10.7
24-Mcleod	54	63	9	11	23	26	14	12.6
25-McLeod	49	53	12	13	31	34	8	7.5

1 = Maceral and mineral composition in volume percent; 2 = Maceral composition (in volume percent) in mineral-matter-free basis; mineral matter percent is derived petrographically.
A = Total mineral matter (in volume %) derived from microscopic method; B = mineral matter (in volume %) derived from calibration of ash content [after ASTM, 18].
* = Sample contains more than 10% mineral-bituminous groundmass which was included as minerals.

Table 3: Comparison of the physical properties and ash content (as received basis) of coal

Sample No Well No	Ash (A.R)	Prod.Ind (Rock Eval py)	Porosity (%)	Permeability (mD)	Max. CO_2 Adsorption (cc/g STP)	Grain Density (kg/m^3)	Bulk Density (kg/m^3)	Monolayer Capacity (cc/g STP)	Micropore Surface Area (sq.m./g)
1–Scott Pioneer Mine	32.3	0.01	4.3	0.06	6.77	1510	1449	20.9	95.57
2–Scott (P–25)	30.5	0.09	1.5	0.08	3.54	1470	1444	11.9	54.55
3–Acadia Pioneer Mine	12.3	0.01	3.9	0.02	9.55	1440	1387	25.9	118.18
4–Acadia (P–17)	25.6	0.04	2.4	0.18	12.22	1560	1525	24.9	113.53
5–Acadia (P–18)	24.3	0.05	6.6	0.2	7.82	1440	1344	21.4	97.63
6–Acadia (P–25)	12.7	0.09	2.1	0.26	4.85	1410	1380	17.0	77.6
7–Acadia (P–23)	19.2	0.09	3.1	N.D.	6.09	1630	1578	20.0	91.2
8–Cage (P–45)	20.0	0.04	5.3	0.54	11.71	1400	1330	24.0	109.57
9–Cage (P–47)	10.9	0.04	1.4	0.92	8.24	1390	1367	24.4	111.47
10–Foord (WA–14)	27.5	0.01	5.0	0.61	8.08	1440	1365	21.4	97.90
11–Foord (P–5)	26.3	0.02	1.4	0.78	7.88	1520	1501	21.0	95.76
12–Foord (P–19)	29.9	0.02	1.1	0.09	7.10	1450	1437	20.0	90.87
13–Foord (P–6)	18.8	0.02	1.2	0.03	15.88	1540	1525	32.5	148.42
14–Foord (P–21)	26.5	0.04	2.0	0.2	14.82	1450	1421	29.7	135.57
15–Foord (P–22)	15.5	0.03	4.4	0.12	15.57	1500	1429	30.3	138.42
16–Foord (P–45)	19.3	0.05	2.4	0.25	5.67	1600	1560	17.8	82.20
17–Foord (E–10)	30.7	0.06	6.6	0.07	9.33	1350	1261	19.7	90.03
18–Foord (E–24)	15.0	0.05	2.5	0.03	4.80	1440	1405	15.5	70.94
19–Foord (P–47)	16.8	0.04	2.0	0.02	15.48	1420	1395	30.9	141.07
20–Foord (0382)	12.8	0.08	4.2	0.89	6.23	1400	1346	18.2	82.94
21–Foord (P–29)	45.9	0.10	0.5	0.68	7.46	1160	1410	15.9	72.52
22–McLeod (P–10)	27.7	0.01	1.7	0.04	13.10	1440	1419	25.1	114.99
23–McLeod (P–14)	25.8	0.01	6.6	0.35	11.50	1420	1326	35.8	163.72
24–McLeod (P–15)	30.7	0.06	1.7	0.09	5.26	1450	1423	25.0	114.19
25–McLeod (P–28)	18.1	0.02	5.5	1.01	29.94	1540	1454	58.2	266.07

A.R. = as received basis; Prod. Ind. = production index (S_1/S_1+S_2) from Rock–Eval pyrolysis

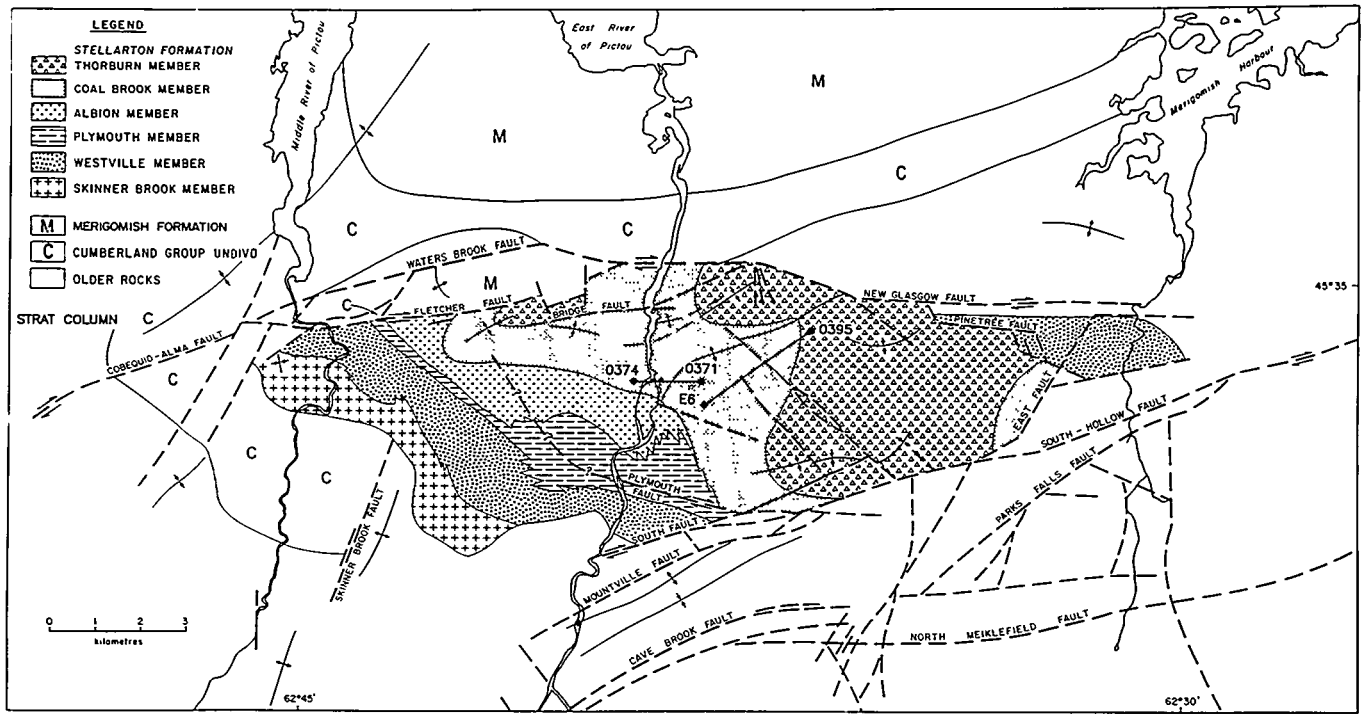


Figure 1. General geology of the Stellarton Basin (Pictou Coalfield) [after Naylor et al., 15].

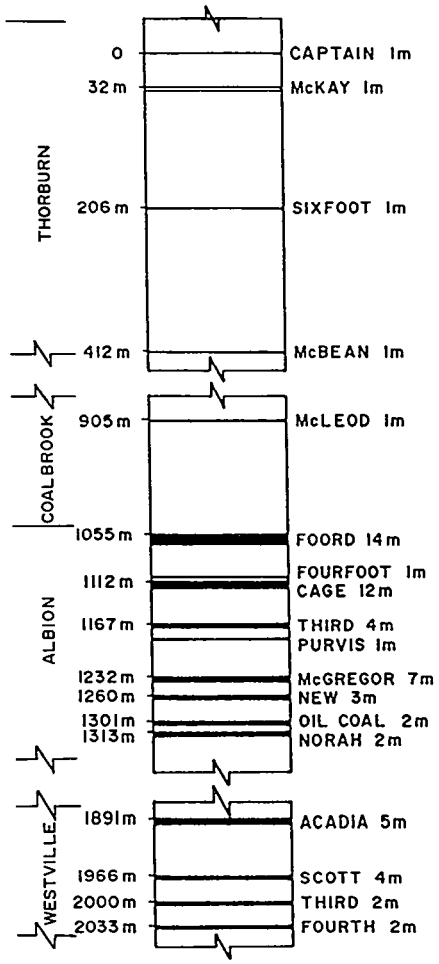


Figure 2. Stratigraphy and thickness of various coal seams.

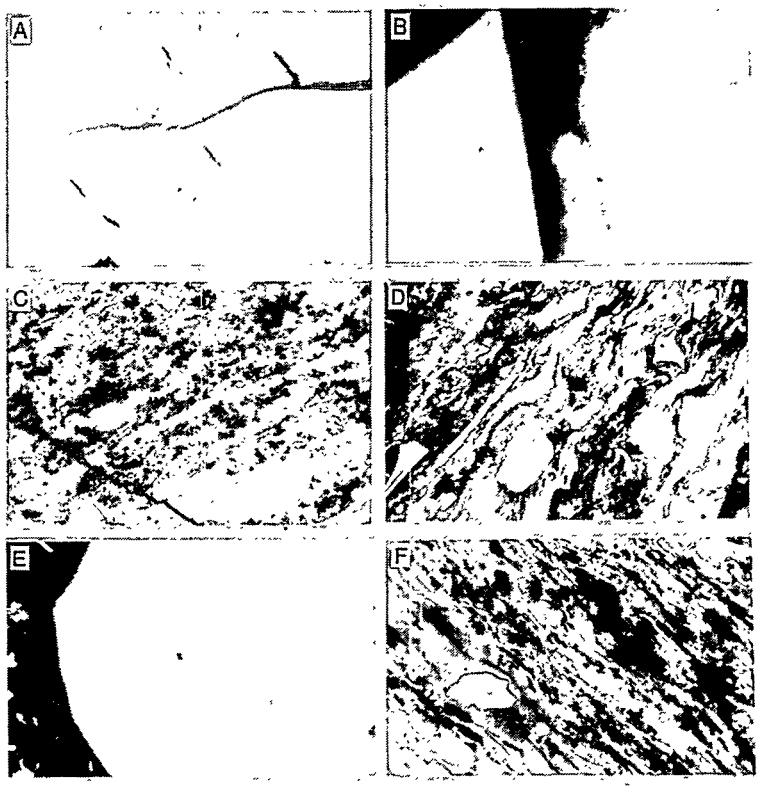


Figure 3. Photomicrographs of various macerals taken under incident white light using oil immersion objective. X 450.
(A) 15-Foord. Telocollinite with micro-fracture, (B) 15-Foord. Telocollinite and carbonate (calcite) grains, (C) 17-Foord. Vitrodetrinite and desmocollinite with quartz grains (D) 17-Foord. Corpocollinite, gelocollinite, cutinite, bituminite, inertodetrinite, and quartz grains, (E) 25-McLeod. Telocollinite forming pseudovitrinite, (F) 25-Mcleod. Inertodetrinite and desmocollinite with liptinite macerals and quartz grains.

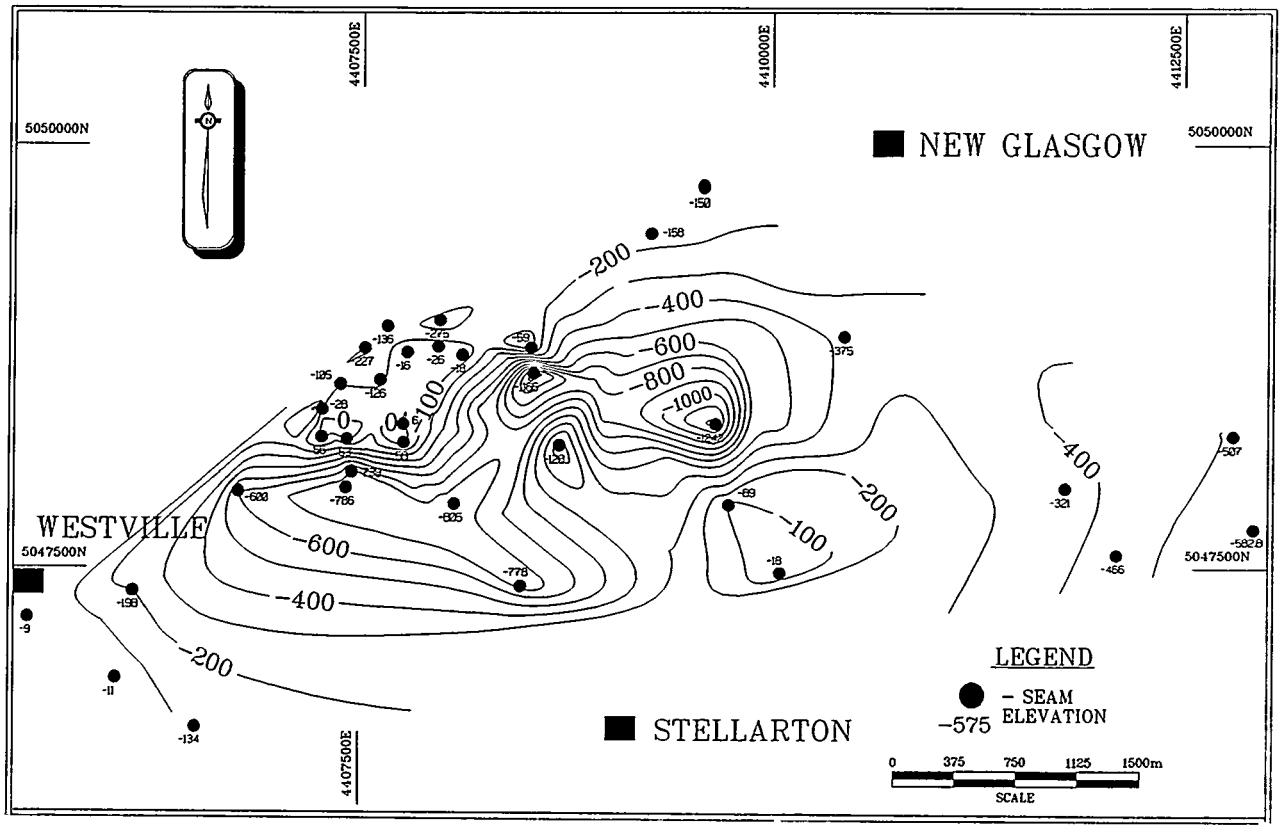


Figure 4. Elevation contours of all samples from five seams.

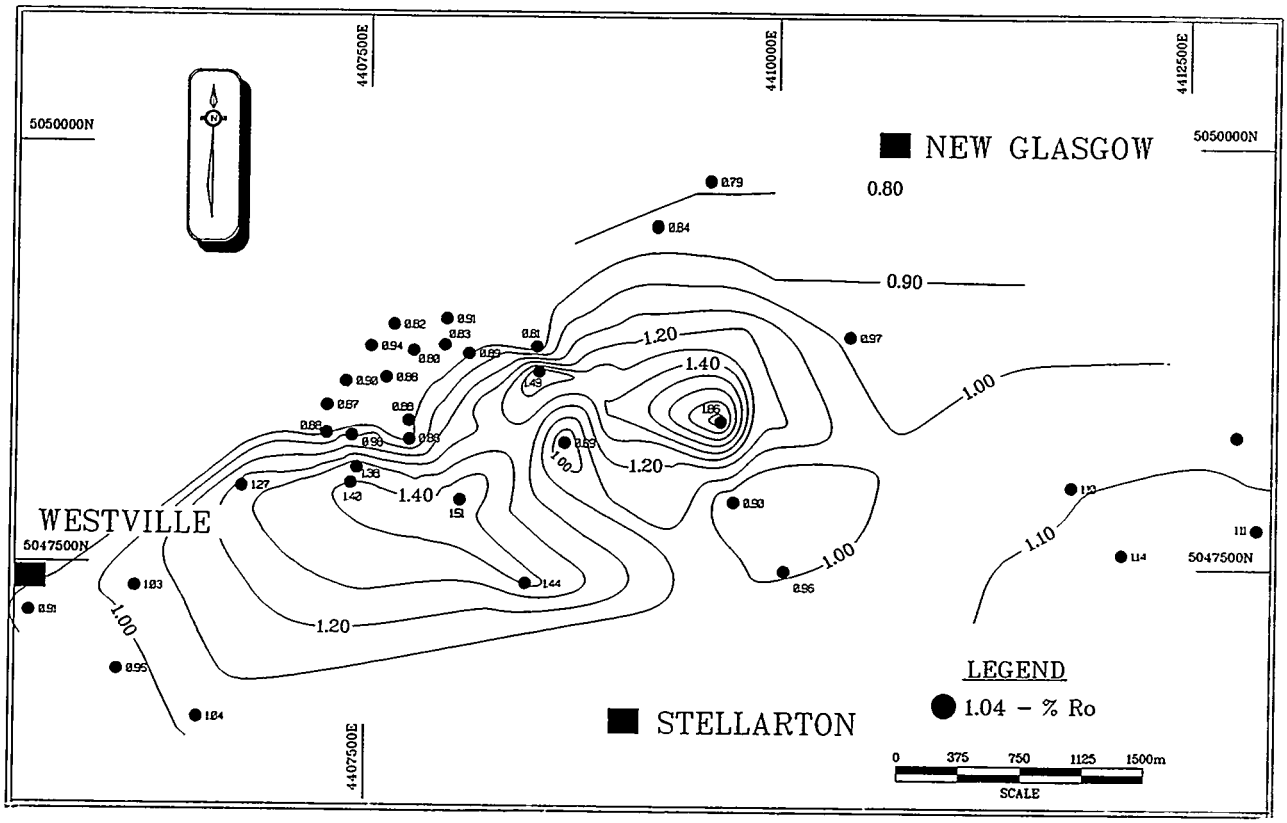


Figure 5. Maturation contour lines derived from all data on vitrinite reflectance from five seams (Scott, Acadia, Cage, Foord, McLeod).

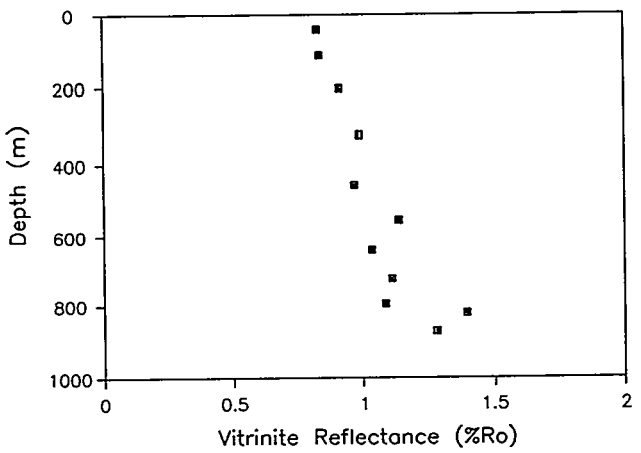


Figure 6. Vitrinite reflectance versus depth (m) of the analyzed samples from the drillhole Suncor AP-0355.

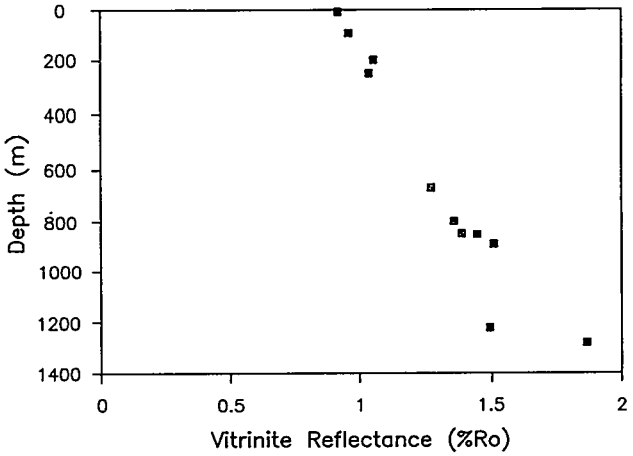


Figure 7. Vitrinite reflectance versus depth (m) of all analyzed samples from the Acadia seam.

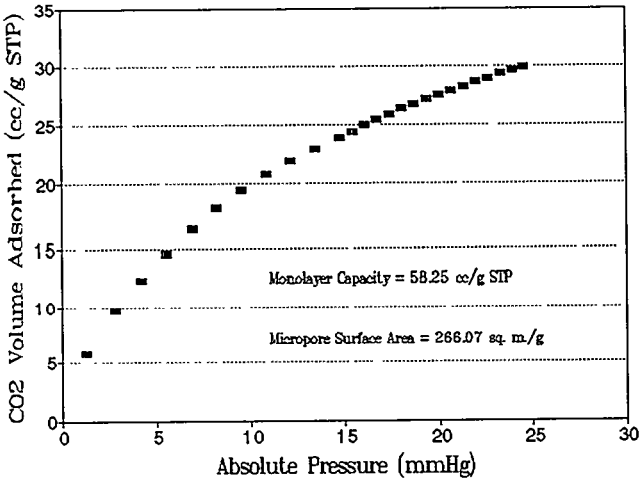


Figure 8. The plot of total volume of CO_2 adsorbed and the injected pressure (in mm Hg).

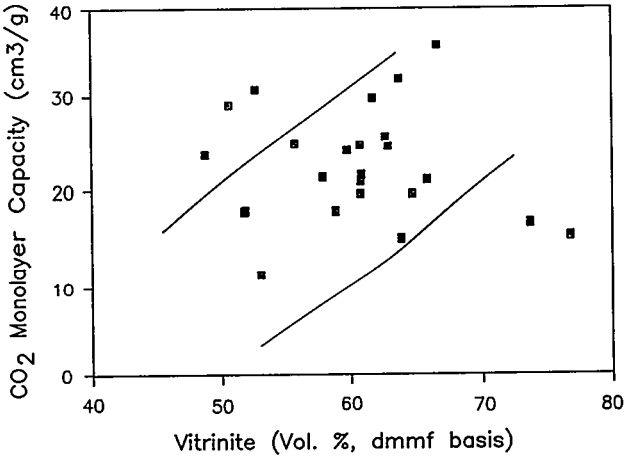


Figure 9. The relationship between CO_2 monolayer capacity or volume (cm^3/gm) with volume percent of vitrinite.

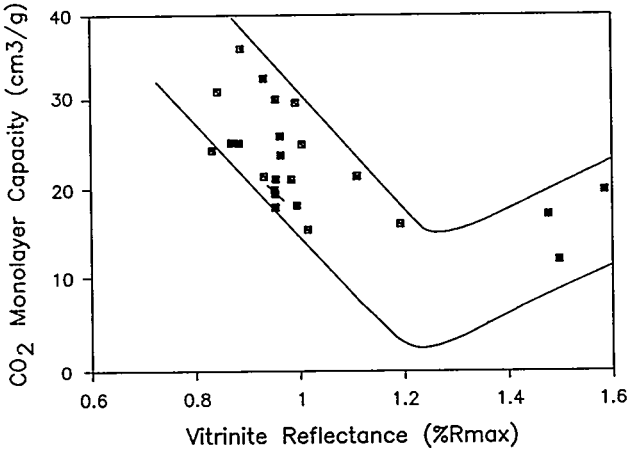


Figure 10. The relationship between CO_2 monolayer capacity (cm^3/gm) and percent mean maximum vitrinite reflectance.

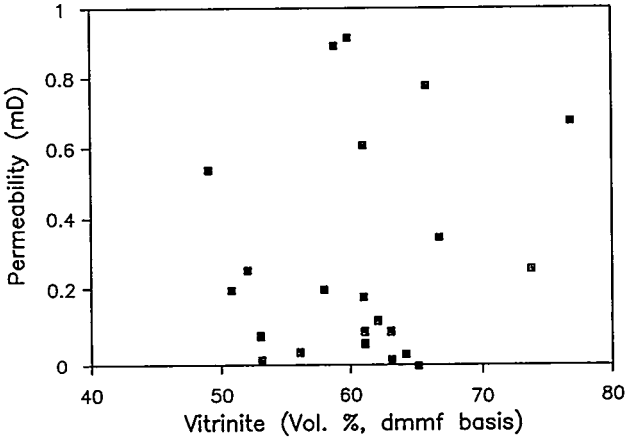


Figure 11. The relationship between permeability (mD) and volume percent of total vitrinite (dmmf).

INTERGAS '95

May 15-19, 1995
The University of Alabama
Tuscaloosa, Alabama USA

9506

The Status of Coalbed Methane Research and Development in Australia

J.R. Enever, CSIRO Australia

ABSTRACT

Some of the technical issues facing the fledgling coalbed methane industry in Australia are discussed, and a description given of the status of CSIRO's research into various areas under the broad headings of:

- exploration,
- reservoir simulation,
- stimulation technology.

In relation to exploration, emphasis is focused on issues related to targeting and on the application of innovative well testing technology. In the area of reservoir simulation, the use of quasi porous flow and discrete fracture flow models is discussed. With regard to stimulation technology, a summary is given of CSIRO's research in support of hydraulic fracturing and cavity completion as well as a discussion around the prospects of enhancing permeability by removal of secondary mineralisation. The approaches being used to ensure the uptake of R&D results by the industry are summarised.

1 INTRODUCTION

Exploration for coalbed methane has been progressing vigorously in Australia for the past five years or so. In a few cases exploration has led to small scale production trials. While extrapolation of experience gained from the USA coalbed methane industry is still a major feature of the emerging Australian industry, a number of unique aspects of Australian coal basins have been recognised, giving rise to a significant locally based R&D program.

Coalbed methane research in Australia is focusing on three streams:

- development of strategies for targeting areas of higher gas content and permeability during exploration programs, including the development and application of innovative exploration techniques;

  In this stream emphasis is focusing primarily on the development of an understanding of the relationship between coal seam permeability/gas content and the geological environment. A number of investigation techniques are being applied innovatively to provide data of importance to the development of this understanding. Considerable effort has been devoted to the development and application of well testing techniques aimed specifically at the needs of coalbed methane exploration in the Australian context.

- development of reservoir models to describe coal seams and the incorporation of developments into refinement of reservoir simulators;

  In this stream emphasis is focusing on the development of conceptual models to describe the reservoir characteristics of Australian coal seams, and the incorporation of such understanding, as it is reached, into improved reservoir simulators. Particular attention is being devoted to the integration of pseudo porous flow models and discrete fracture flow models.

- support for the introduction of generic stimulation technologies into Australian coal basin environments, and the development of stimulation techniques tailored to problems perceived to be of particular concern in Australia;

  In this stream emphasis is focusing on two parallel approaches. The first involves research into the mechanisms underlying generic technologies, specifically hydraulic fracturing and cavity completion. The second approach is centring predominantly around the enhancement of permeability by the leaching of secondary mineralisation.

This paper discusses the current status of activities in these three streams based on CSIRO's activities. A discussion of the steps being taken to ensure integration of research into operations is included.

2 EXPLORATION

2.1 Permeability

Early attempts at coalbed methane development in Australia have led to the widely held view that the coals of the major eastern states coal basins (Fig. 1) generally suffer low to extremely low permeability (well testing often producing permeabilities less than 100 microdarcy and generally less than 1 millidarcy). This has led to investment of effort into the development of strategies for targeting areas of relatively higher coal seam permeability. Three specific ideas have been pursued with respect to this issue:

- the relationship between coal seam permeability and the intensity of coal seam fracturing, based on the premise that coal permeability is primarily governed by fracture flow;
- the influence of the in-situ stress field in the coal and adjacent rock units on coal seam permeability;
- the impact of secondary mineralisation deposited in the fracture systems in the coal on permeability.

Figure 2 is a summary of data collected during a major exploration activity in the Bowen Basin of central Queensland

during which comprehensive information was collected on the intensity and nature of coal seam fracturing based on a core logging program. Coal seam permeability and the in-situ stress in coal seams and adjacent rock were measured during the exploration program by injection/decay testing and hydraulic fracture stress measurement respectively [1].

Figure 2 indicates a sensitivity of coal seam permeability to the intensity of coal seam fracturing, for fractures free of secondary mineralisation. While this might be considered intuitively logical, less obvious is the apparent greater sensitivity of permeability to the magnitude of the minimum in-situ stress component in the coal. An implication of this is that coal seams might be considered as stress dependent quasi uniform reservoirs, at least for the purposes of conducting initial studies of prospectivity. This is consistent with the approach taken in most reservoir simulation studies.

Figure 2 assumes that fractures containing secondary mineralisation do not contribute anything to net coal seam permeability. This assumption has been confirmed during laboratory testing of coal samples [2]. The significance of secondary mineralisation in relation to the potential permeability of coal has been studied during investigation of the prospects for leaching as a stimulation technique (see below). In terms of an exploration strategy, selection of areas relatively free of secondary mineralisation should generally result in a higher open coal fracture intensity, and therefore relatively higher permeability. Likewise, targeting of areas of relatively low stress should generally result in highest coal seam permeability.

Figure 3 is an alternate presentation of the data in Figure 2, emphasising the relationship between permeability and the minimum total stress existing in coal seams. Figures 4 (a&b) are summaries of data from two sites in the Sydney Basin, further emphasising the relationship between permeability and in-situ coal stress. In these cases, effective stress (minimum total stress−reservoir pressure) was found to produce the most systematic relationship between stress and permeability. These examples were drawn from sites exhibiting relatively low coal and associated rock stress magnitude (Fig. 5), and correspondingly high coal seam permeability. Experience suggests that rock stress magnitude broadly reflects coal seam permeability [3]. Relatively high horizontal rock stress magnitude has been found to be associated with extremely low coal permeability in many exploration holes drilled in the Sydney and Bowen Basins to date.

Based on this evidence, emphasis in targeting logically should centre on location of geological environments conducive to low stress field magnitude. One tool that is proving useful in this regard is numerical stress analysis. Figure 6 summarises the results of a simple two-dimensional model of the formation of a synclinal structure produced by downward warping of the sediments as would occur during the generation of a graben structure. The results of this sort of analysis, in conjunction with in-situ stress measurement, are helping in the identification of low stress regions as potential targets.

In relation to the impact of secondary mineralisation, examination of the extensive database of information available with respect to coal ash content and its physical/chemical characteristics from programs undertaken for coal resource assessment is proving useful [4]. Compilation of this information for the Sydney Basin is helping with identification of areas of relatively lower mineral content as well as the potential amenability of the mineralisation to chemical leaching.

2.2 Gas Content

Measurement of gas content, and associated gas composition and storage capacity, has been based on conventional, well documented procedures, generally as used in the USA. Considerable data has been accumulated on some of the factors controlling gas storage capacity and the desorption process [5], and on the parameters influencing gas composition. One very important issue that has arisen in relation to relative gas saturation (gas content at reservoir pressure as a fraction of corresponding gas storage capacity at same pressure) is the possibility of higher coal seam permeability correlating with relatively under-saturated coal seams. The notion of higher coal seam permeability providing a path for escape of gas is obvious, if not necessarily well founded, and potentially could have a negative impact on assessment of prospectivity.

Figure 7 is a compilation of data from two sources, clearly indicating the lack of correlation between permeability and relative gas saturation for a range of Australian coal seams. The causes of under-saturation in Australian coal basins are not well understood. Investigations are continuing into the impact of geological and hydrological history on current-day gas contents [6].

2.3 Well Testing

The development of a reliable procedure for the conduct and analysis of well tests in Australia's generally low permeability coal seams has absorbed a lot of energy and raised a deal of conjecture during recent years. Injection/decay tests have generally been favoured to avoid the possibility of multiphase flow complicating the test procedure and/or analysis. For first pass purposes, such as the initial grading of development targets, this has proved reasonably satisfactory. For more detailed assessment of production potential, however, results taken directly from such well tests have often been hard to reconcile with subsequent trial production histories. In recognition of this issue, CSIRO has developed a wireline based, multi-phase production testing capability specifically geared to the needs of coalbed methane exploration in Australia, where slim-hole wireline diamond drilling is heavily favoured.

In essence, the facility allows for the conduct of short-term production of water and gas within the framework of exploration in slim holes [7]. The straddle configuration of the tool allows for individual seams to be tested as they are exposed with negligible wellbore storage effect. This reduces the period of testing required to produce the necessary data from several weeks when conducting full scale production trials, to hours or days, depending on coal seam permeability. The tool's compressed air driven pump allows constant rate production of fluids to the surface through successive phases of single phase water production, mixed phase water/gas production to continuous gas production. Water and gas are separated at the surface and the respective flow rates measured. The down-hole pressure within the test interval is monitored throughout the process.

The wireline handling system is designed to take advantage of the benefits offered by the wireline diamond drilling environment. As a coal seam is exposed by drilling, the core barrel can be removed on a wireline and the testing tool located in its place. This allows for rapid testing after exposure of a seam, if desired, within a safe working environment. Only the bottom straddle isolating the seam to be tested protrudes from the drill rod string. Figures 8 and 9 show the wireline handling system.

Figures 10(a&b) represent a typical set of data produced by the system. The pressure drawdown recorded by the down hole pressure monitoring systems show distinct phases of:

- single phase water flow allowing for determination of absolute permeability by conventional well test analysis;

- onset of gas desorption influencing the shape of the drawdown curve and allowing for identification of critical desorption pressure;
- multiphase flow allowing for back analysis of relative permeability curves by use of a reservoir simulator;
- sustained gas flow.

Application of this technology offers the prospect of short-circuiting some of the problems associated with conventional testing procedures, at a cost and with a culture consistent with Australian coalbed methane exploration activities.

3 RESERVOIR SIMULATION

The need for a reliable reservoir simulation capacity to facilitate evaluation of the prospectivity of alternate sites and/or the likely effectiveness of alternate production strategies has been recognised in Australia as elsewhere. CSIRO and the University of New South Wales have joined together to undertake development and promote usage of SIMED II [8]. SIMED II is an implicit finite-difference code developed to describe simultaneous gas and water flow in coal. SIMED II differs from most other coalbed methane simulators in that it can model the adsorption and desorption of mixed gases (CH_4, CO_2, N_2), making it particularly powerful for studies of processes such as gas stripping [10].

SIMED II has been used to conduct studies of competing stimulation technologies and to carry out matching of production histories. A more recent development has been the application of fully linked stress-fluid flow numerical models [9] to simulate specific fracture fluid flow in a coal seam with a discrete fracture system at various scales. This approach to reservoir simulation has proved very useful when studying the detailed processes associated with stimulation technologies such as cavity completion, as well as the analysis of well test results. Figures 11 (a & b) summarise the results from one such study, illustrating the mechanistic realism offered by this style of modelling. Efforts are currently underway to integrate specific fracture controlled performance, as illustrated above, with pseudo porous flow/diffusion based performance as engendered in more conventional coalbed methane simulators such as SIMED II.

4 STIMULATION TECHNOLOGIES

4.1 Hydraulic Fracturing and Cavity Completion

Primary concern in regard to these technologies has been with providing R&D support for their introduction into Australian practice. In both cases effort has concentrated on studies of the mechanisms underlying the techniques, with a view to helping the transport of the technologies from U.S. to Australian coal basin conditions. In both instances this is being achieved through an integrated laboratory and field program.

In regard to hydraulic fracturing, major effort has centred on a field program involving a series of medium scale fracture treatments placed, from the surface, ahead of coal mining activities, and subsequent "mine-backs" to examine the detailed geometry and related characteristics of the fractures produced. This has involved the development of an experimental scale fracturing system (Figs. 12(a&b)) capable of allowing the conduct of substantial fracture treatments (typically 15-20,000 litres of fluid and 2,000 kg of proppant) at a cost and in a style consistent with R&D activities. The system has been designed with an eye to maximum flexibility and with a comprehensive instrumentation capability. Functionally, the system is essentially a scaled down version of a commercial fracturing operation.

To date six experimental fractures have been conducted with the system [11], and subsequently mined back, at depths to around 300 metres and in a range of coal seam types. In each case, the site has been carefully characterised prior to fracturing by conducting well tests, stress measurements in coal and rock and measuring mechanical properties. The program to date has demonstrated the prospects for the generation of predominantly vertical, well propped fractures, generally contained within the seam, for a range of in-situ stress conditions and coal types (Fig. 13). While more work is planned, the effort so far has provided some confidence that hydraulic fracturing can be used successfully in Australian coal basins as a base level stimulation technology.

Among the detailed observations made with regard to fracture geometry from the program, one of the more interesting has been the revelation of marked asymmetric fracture propping [12] with substantially greater extent of propping down-dip compared to the corresponding up-dip wings of the fractures. Asymmetric propping has been noted at relatively gentle dips (less than 10°). Gravity currents [12] have been examined as a possible mechanism for this asymmetry, and appear to offer a reasonable explanation. Figures 14(a, b & c) are representative of the results of a laboratory investigation into the effect of dip on proppant distribution. Present activity is concentrating on incorporation of the findings of the experimental program into numerical fracture design codes.

In the case of cavity completion, a vigorous R&D effort has been mounted over the past three years to underpin the trial of this technology in Australia. Two full scale field trials, complete with comprehensive site characterisation and performance monitoring, have been undertaken in this period. These trials have produced a database of information that is being used to investigate the mechanisms critical to the success of stimulation by transient fluid injection/pressure surging.

Laboratory investigations with regard to cavity completion are focusing on two main themes:

- prediction of the proneness of various coals to cavity formation. To this end a procedure has been developed [13] to allow cavitation experiments to be conducted on coal cores under approximate reservoir conditions (Figure 15). The cell allows variation of the controllable field parameters (injection fluid pressure, duration of injection and rate of depressurisation) to establish the critical combination of parameters for a given coal type that will produce cavitation or, in some cases, to establish whether cavitation can be accomplished. Figure 16 is typical of the cavitations produced in the cell.
- elaboration of the mechanisms accompanying air injection/pressure surging. In this instance a series of tests have been conducted on large coal blocks (.4m x .4m x .4m) under polyaxial stress states to study both the process of cavity formation in a stress field representative of a field condition, and the impact of fluid injection on the far field deformation, coal permeability and pore pressure distribution [14]. To this end, coal blocks have been intensively instrumented with deformation and pore pressure measuring devices and then loaded in a polyaxial test frame prior to conduct of cavity completion simulations. The experimental arrangement is shown in Figure 17. Results of this work are presently being analysed and will be published in the near future. Figure 18 illustrates the style of failure produced during these tests, in this case in an artificial sand/plaster block.

4.2 Leaching of Secondary Mineralisation

The potential impact of secondary mineralisation on coal seam permeability has been discussed above. The prospect of enhancing permeability by removing all or some of the

mineralisation through chemical leaching, or some other process, is an obvious concept. Investigations to date have concentrated on the nature and physical occurrence of secondary mineralisation in coals of the Sydney and Bowen Basins. Coupled with this have been studies of the chemistry associated with removal of such secondary mineralisation by leaching. Figures 19 and 20 are typical of the distribution of secondary mineralisation in Australian coals [15].

Figure 21 represents a typical set of data obtained during a series of tests designed to examine the impact on coal sample permeability of removal of secondary mineralisation by leaching at atmospheric conditions. Laboratory permeability tests were conducted on core samples, at a range of external isotropic stress conditions, before and after removal of the mineralisation. Figure 21 suggests the potential for enhancement of permeability by at least the same amount through removal of mineralisation as the sensitivity of permeability to stress over the range of stress investigated. While encouraging, these results need to be viewed cautiously, given the complexity likely to be associated with leaching at reservoir conditions and the critical importance of cost effectiveness (measured by the cost of acquisition and injection of reagent against the present value of the additional gas produced).

Future plans in this area centre on evaluation of the prospects for the development of a commercial process, involving laboratory studies of the kinematics of leaching at reservoir conditions. One tool that is proving powerful with regard to the study of leaching kinematics is an X-ray CT scanner [16] allowing visualisation of the flow paths formed by progressive removal of mineralisation (Figs. 22 (a & b)).

5 ASSIMILATION OF R&D

A major concern in Australia, as elsewhere, is the assimilation of R&D outcomes into on-going practice. In Australia, this is being achieved through a number of parallel strategies. In the exploration context, development and deployment of ideas is being expedited by direct involvement of researchers in the exploration activities of commercial operators. To supplement this, technologies that are proving useful are being made available for routine application through commercial service providers. In the area of reservoir simulation, commercialisation is being achieved through provision of the simulator on a commercial basis, coupled with active collaboration between the researchers and commercial operators. In the case of cavity completion, investigations are being conducted in conjunction with a major operator to ensure that findings are taken up directly. In the case of hydraulic fracturing, the results are being incorporated into a commercially available fracture design model. In the case of the potential for leaching of secondary mineralisation as a stimulation technique for low permeability coals, a technology development joint venture between the research organisation and an operator has been chosen as the most appropriate vehicle to ensure a suitable commercial outcome.

6 ACKNOWLEDGEMENTS

The author would like to sincerely thank his colleagues for their efforts in the various areas of research reported and for their cooperation in the preparation of the manuscript. The support of CSIRO's various collaborators is gratefully acknowledged. particularly:

MIM Holdings
MGCRA
Pacific Power

7 REFERENCES

1. Enever, J.R., Pattison, C.I., McWatters, R.H. and Clark, I.H., 1994: "The Relationship between In-Situ Stress and Reservoir Permeability as a Component in Developing an Exploration Strategy for Coalbed Methane in Australia". Proc. Eurock '94, SPE/ISRM Conf. on Rock Mechanics in Pet. Engg., Delft, The Netherlands (SPE Paper 28048), pp.163-174.
2. Gamson, P.G., 1994: Personal communication
3. Enever, J.R., Bocking, M.A. and Clark, I.H. 1994: The Application of In-Situ Stress Measurement and Numerical Stress Analysis to Coalbed Methane Exploration in Australia. Proc. SPE Asia Pacific Oil & Gas Conf., Melbourne, Aust. (SPE Paper 28780), pp.373-381.
4. Shields, A. 1994: Personal communication
5. Levy, J.L., Day, S.J. and Killingley, J.S. 1995: "Methane Adsorption on Coals of the Bowen Basin, Queensland", Proc. Intergas '95, Tuscaloosa, USA, May 1995.
6. Clare, R. and White, J. 1994: Personal communication
7. Koenig, R.A., Dean, A. and Lupton, G. 1992: Development and initial trials of a new multiphase well testing tool for coalbed methane evaluation. Proc. Symp. on Coalbed Methane Research and Development in Australia, Vol.2, eds. B.B. Beamish and P.D. Gamson, Townsville, Aust., pp.97-106.
8. Stevenson, M.D., Pinczewski, W.V., Meaney, K. and Paterson, L. 1994: "Coal Seam Reservoir Simulation". APEA Jnl. 1994, pp.114-120.
9. Choi, S. and Wold, M.B. 1994: "Simulation of Fluid Flow in Coal Using a Discrete Fracture Network Model", Proc. SPE Asia Pacific Oil & Gas Conf., Melbourne, Aust. (SPE Paper 28781), pp.383-393.
10. Levy, J., Day, S. and Hoar, I. 1994: Personal communication
11. Enever, J.R., Jeffrey, R.G. and Vlahovic, W. 1995: "Hydraulic Fracture Development in Australian Coal Seams". Proc. Intl. Symp. on Management and Control of High Gas Emissions and Outbursts in Underground Coal Mines, Wollongong, Aust.
12. Jeffrey, R.G. 1994: "Asymmetrically Propped Hydraulic Fractures", Proc. Eurock '94, SPE/ISRM Conf. on Rock Mechanics in Pet. Engg., Delft, The Netherlands (SPE Paper 28079), pp.425-434.
13. Paterson, L. and Wold, M.B. 1995: "Implications from Cavity Completion Research on the Prediction and Prevention of Outbursts", Proc. Intl. Symp. on Management and Control of High Gas Emissions and Outbursts in Underground Coal Mines, Wollongong, Aust.
14. Wu, B. 1995: Personal communication
15. Gamson, P. G. 1994: "Secondary Mineralisation in Coals and its Effect on Methane Recovery: An Australian Perspective", World Coal, Coalbed Methane Review, December 1994, pp.xiii-xvi.
16. Hennig, A. and Meaney, K. 1995: Personal communication

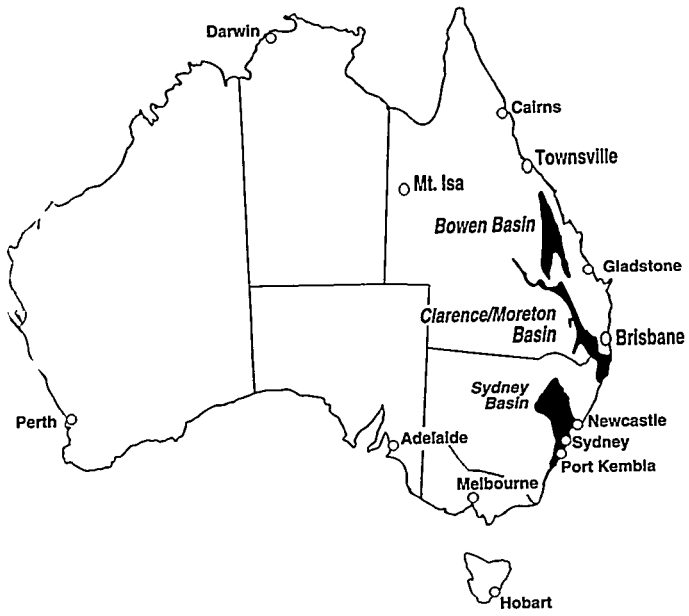


Figure 1: Major eastern coal basins with significant coalbed methane potential

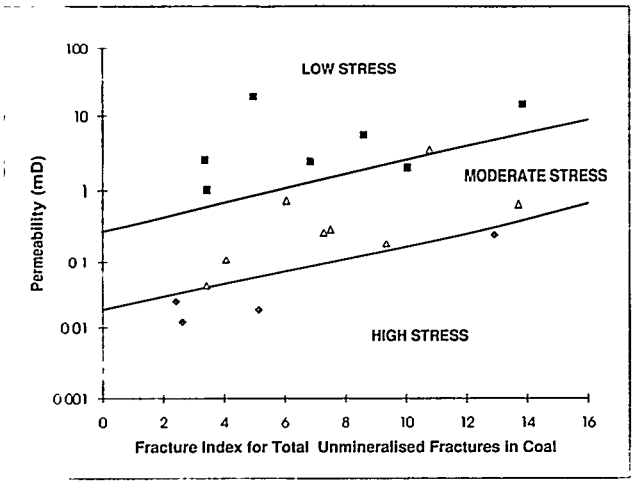


Figure 2: Relationship between coal seam permeabililty measured by well testing and corresponding intensity of coal seam fracturing (measured by fracture index = function of fracture spacing and extent) for fractures without secondary mineral infilling, from an exploration program in the Bowen Basin

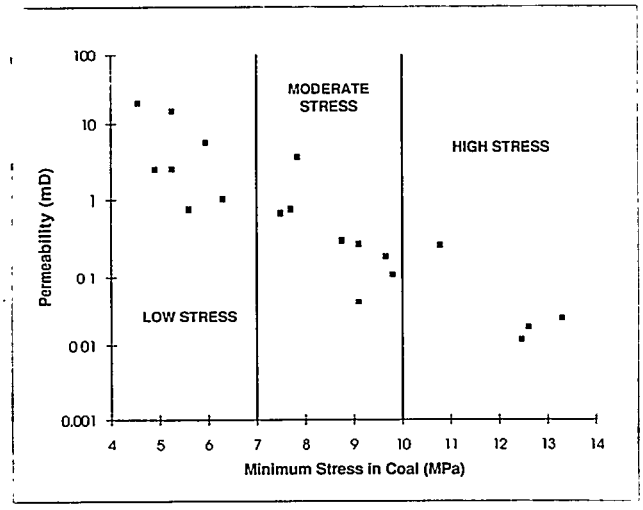
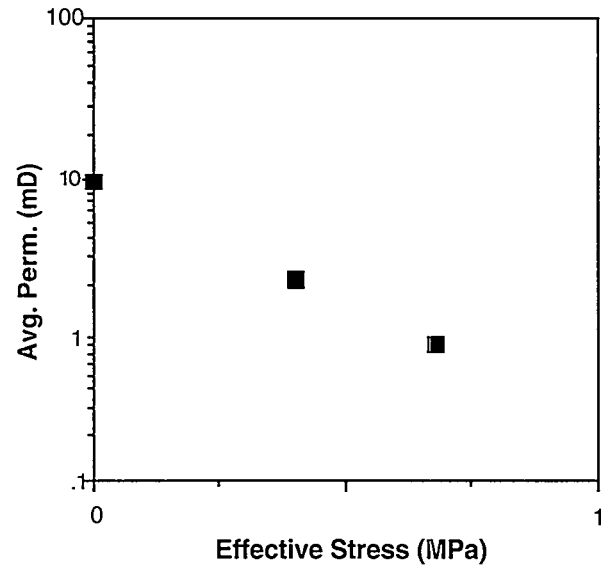


Figure 3: Relationship between coal seam permeability and corresponding minimum total stress in coal seam for data in Figure 2



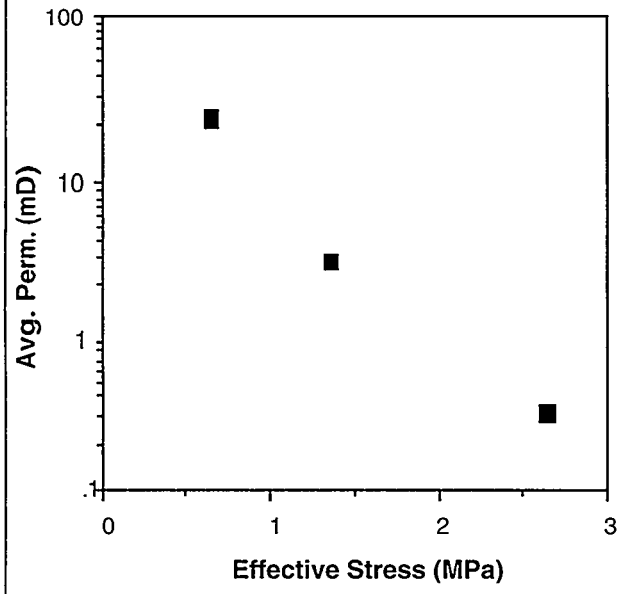


Figure 4 (a & b): Relationship between coal seam permeability measured by well testing and corresponding effective stress for two sites in the Sydney Basin

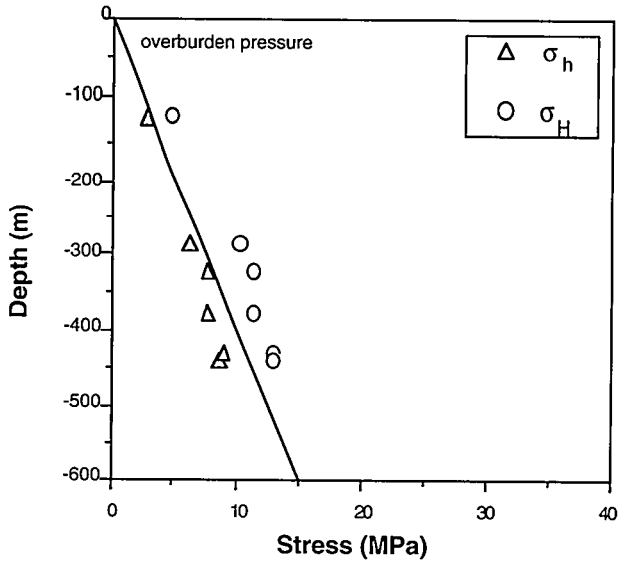


Figure 5: Profile of horizontal secondary principal stresses in rock units at a site reflecting low rock and coal stresses and correspondingly high coal seam permeability

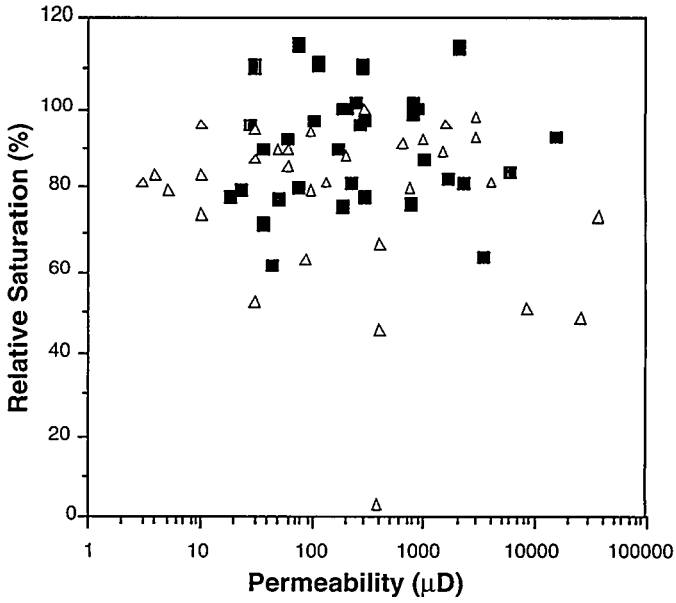


Figure 7: Relationship between relative gas saturation and corresponding coal seam permeability for two sets of data

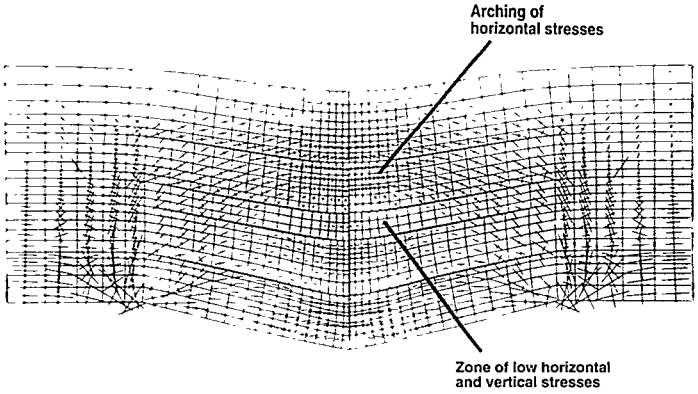


Figure 6: Modified stress field resulting from formation of a synclinal structure by downwarping. Model allows slippage between layers resulting in redistribution of stress field as indicated



Figure 8: Wireline cable (incorporating pneumatic packer inflation hose, compressed air supply and exhaust lines for pump, delivery conduit and instrumentation cables) allowing multi-phase well testing to 700 m.

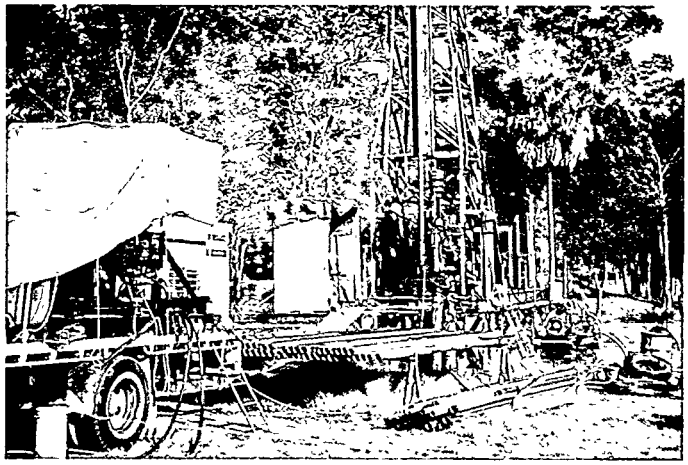
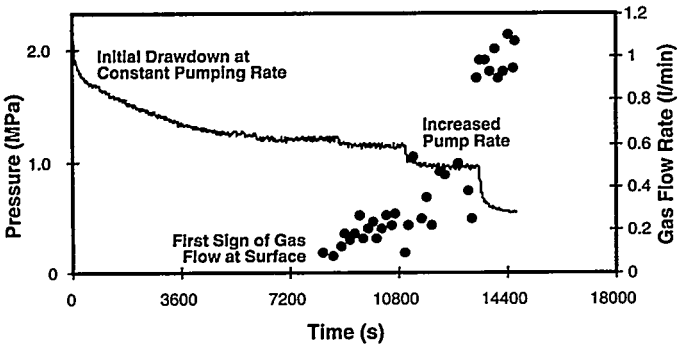


Figure 9: General arrangement of truck mounted testing equipment and drill rig in a typical Australian exploration context



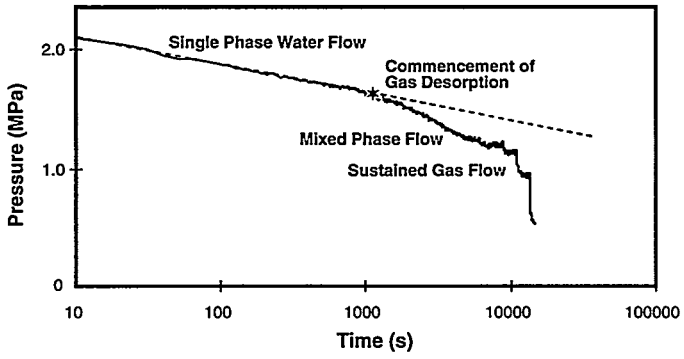
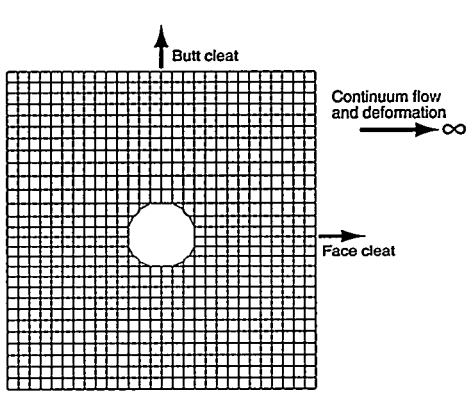


Figure 10 (a & b): Typical results obtained from multi-phase well testing



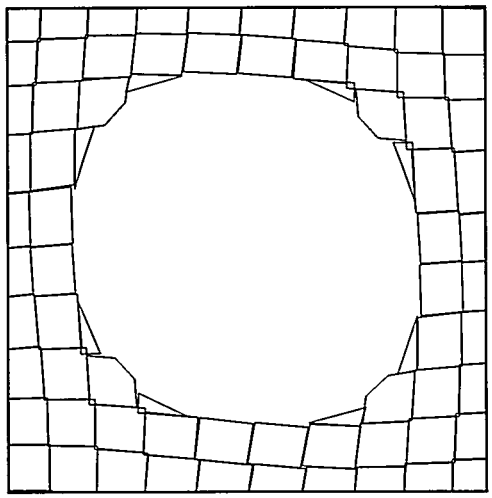


Figure 11 (a & b): Illustration of results obtainable from coupled stress-fluid flow modelling of a coal seam with a well defined cleat system. Deformations and consequent changes to coal permeability resulting from water injection are apparent.



Figure 12(a & b): CSIRO's experimental scale hydraulic fracturing system showing pumps, blenders, tanks etc.



Figure 13: Hydraulic fracture exposed in coal floor plys after mineback of fracture treatment undertaken by CSIRO

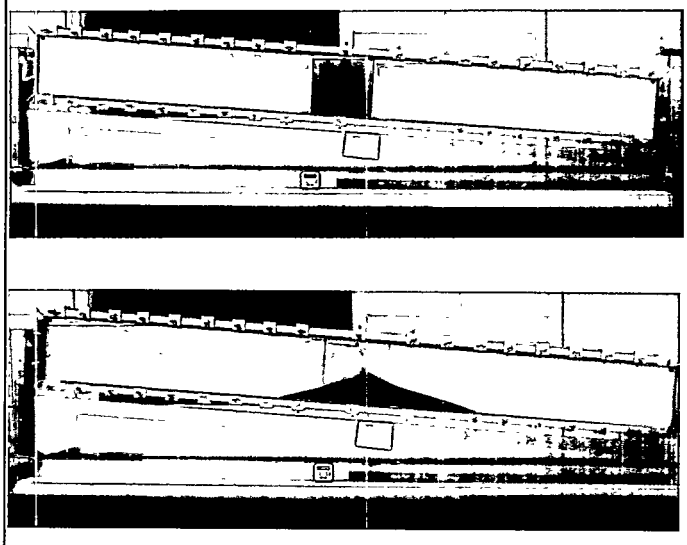


Figure 14 (a , b & c): Laboratory results indicating progressive development of gravity currents in a simulated dipping hydraulic fracture

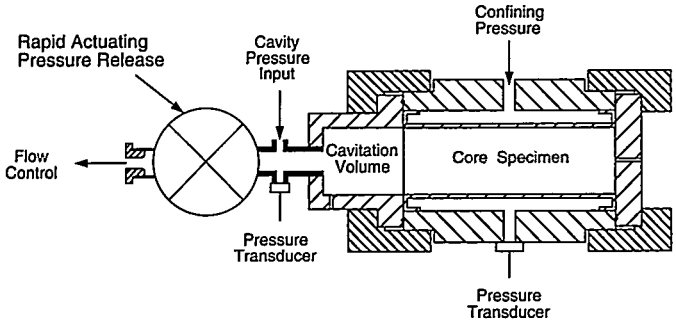


Figure 15: Test cell used to investigate proneness of coal cores to cavitation

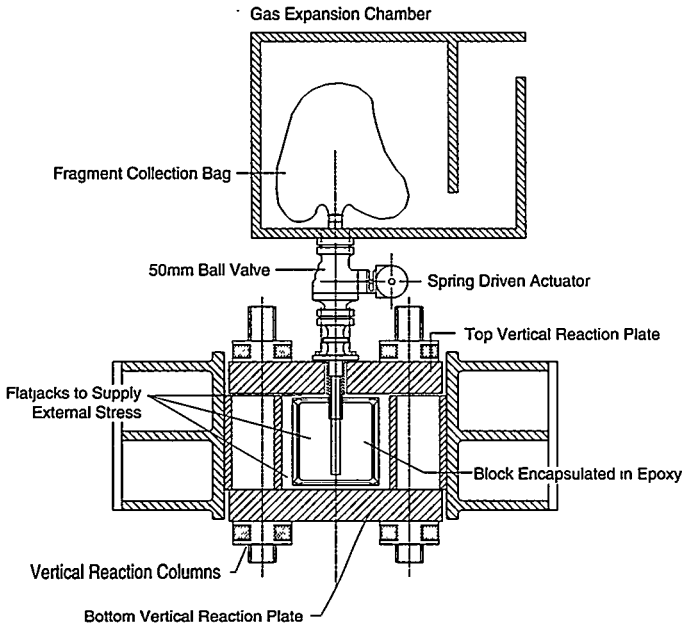


Figure 17: Experimental arrangement for investigation of cavity completion in coal blocks

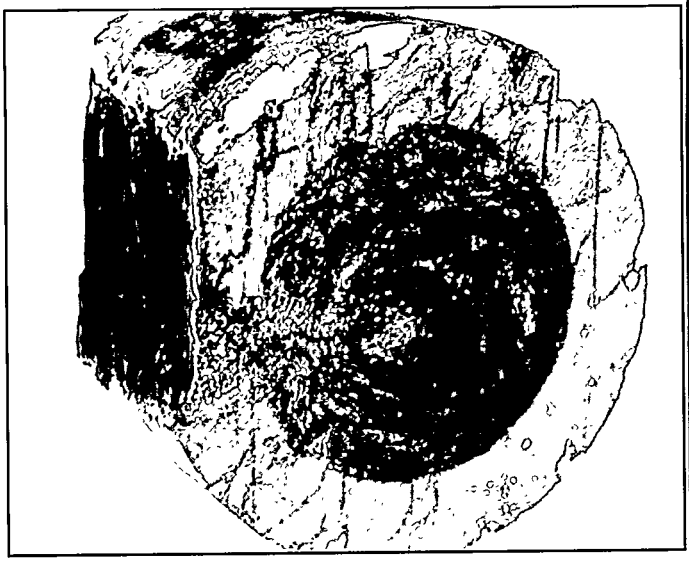


Figure 16: Typical cavity produced in coal core during experiment in cavitation cell



Figure 18: Failure style induced in sand/plaster block by cavitation

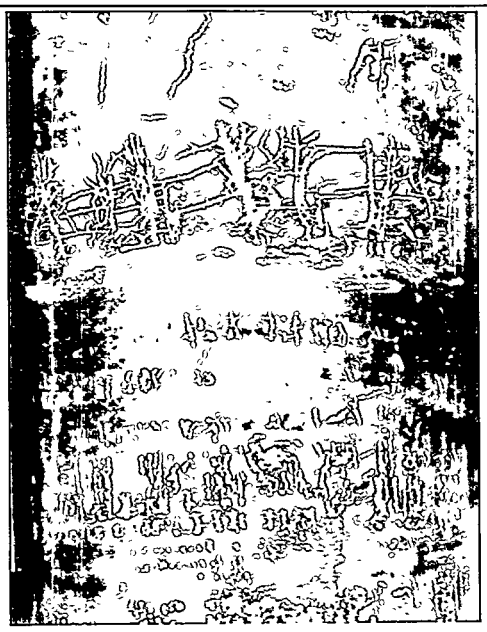


Figure 19: Typical distribution of secondary mineralisation in Australian coals

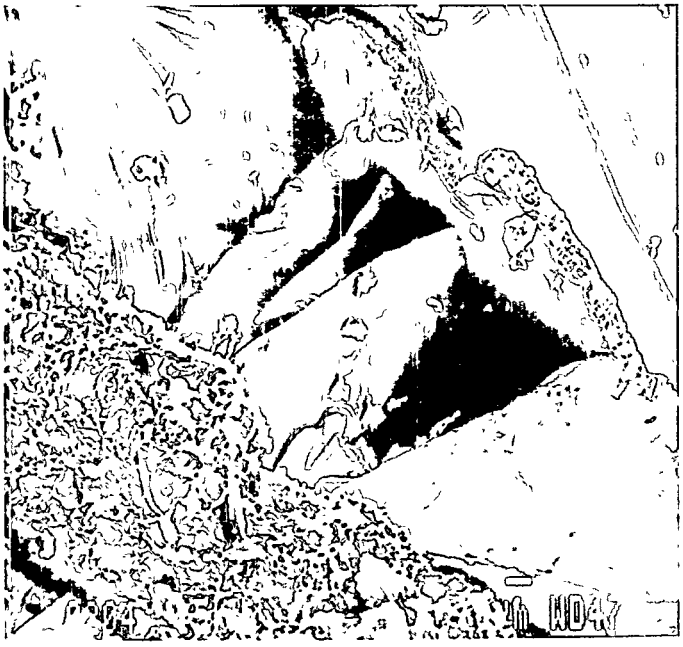


Figure 20: SEM image showing secondary mineralisation tightly infilling fracture in coal

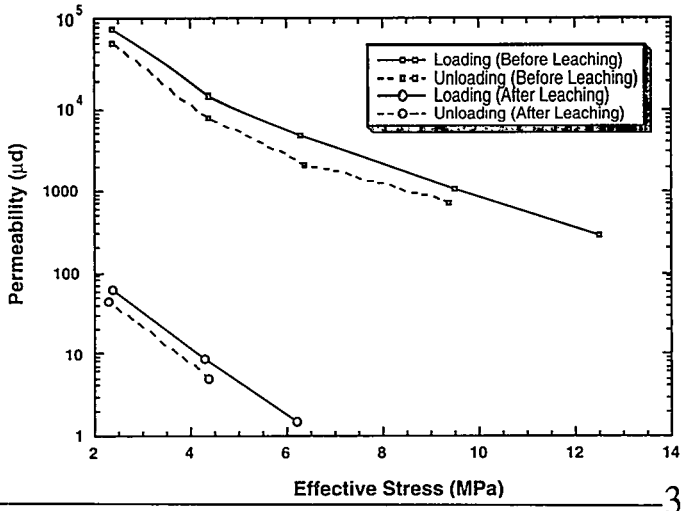
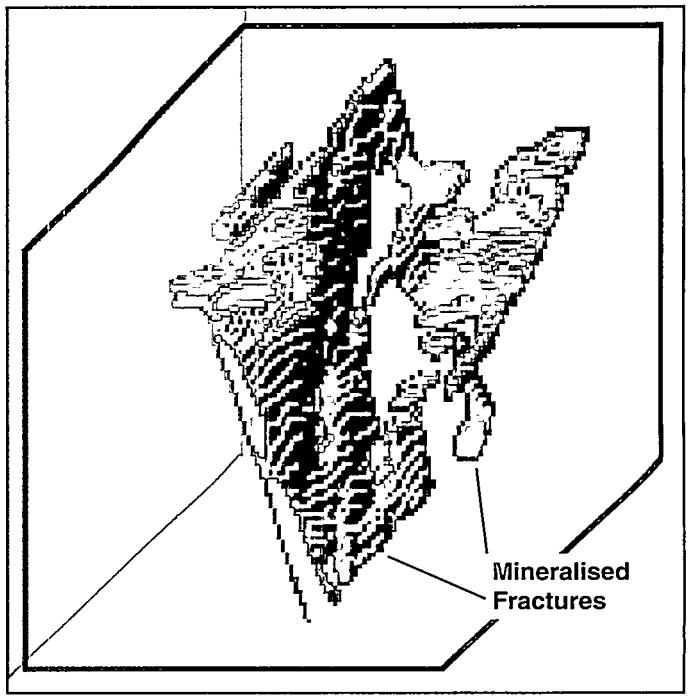


Figure 21: Results of laboratory permeability tests on coal core showing relative impact on permeability of stress and removal of mineralisation by leaching



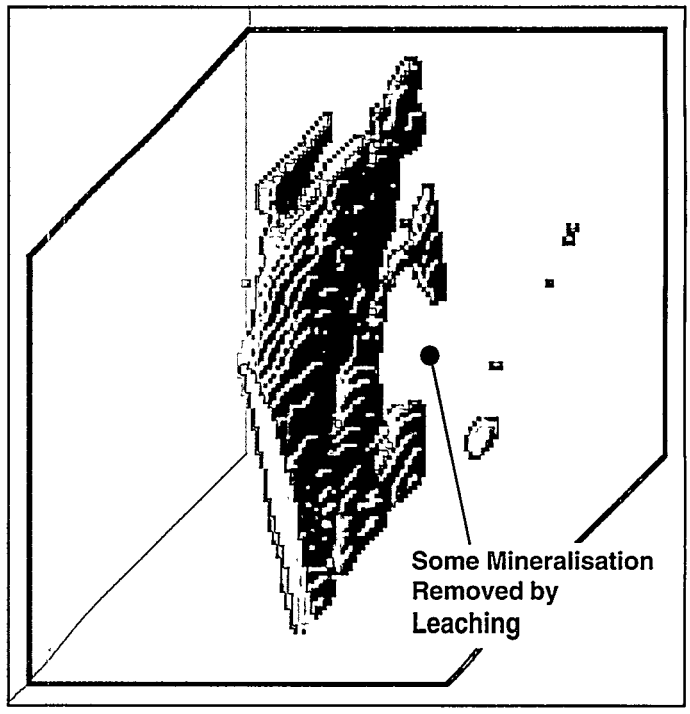


Figure 22(a & b): X-ray CT scanning images of coal cores showing impact of leaching on distribution of mineralisation

INTERGAS '95

May 15-19, 1995
The University of Alabama
Tuscaloosa, Alabama USA

9531

Coalbed Methane Development in the Galilee Basin of Central Queensland, Australia

M.R. Herrington, ENRON Exploration Australia Pty Ltd; and M. Zebrowitz, Advanced Resources International, Inc.

ABSTRACT

The Galilee Basin in central Queensland, Australia was selected as the optimum basin for a commercial coalbed methane project in Australia by Enron Exploration Australia Pty Ltd (EEAPL) in 1992. The entire eastern portion of the basin believed to have coalbed methane potential, approximately 48,000 km^2 (18,500 mi^2), is held by EEAPL. During 1993 exploratory drilling was conducted with slim-hole equipment allowing for an extensive collection of detailed reservoir data. Well sites were selected after performing an extensive study of lateral and vertical coal continuity and thickness, modelling lateral and vertical thermal maturity, and implementing a state-of-the-art fracture detection program for locating fracture permeability. On-site evaluation methods included desorption at reservoir temperature, and on-site final gas content measurements utilized crushing with a modified ring mill. Drill stem tests (DST's) were performed with slim-hole straddle packer tools. Pressure transient analysis was performed on-site to determine both the mechanical integrity of the test and estimate reservoir permeability, pressure, and skin. Based on the test results, an estimate of the productive capacity of the core wells drilled in the Galilee Basin was determined using measured and inferred reservoir parameters. Typical well profiles were developed using results from the geologic and well testing analyses.

INTRODUCTION

During the past few years, coalbed methane recovery (CMR) has evolved from a poorly understood unconventional gas resource to a significant contributor of gas production and reserves. During 1993 there was a total of 21 MMm^3 (730 Bcf) of coalbed methane produced from United States coal basins which accounted for 3 percent of the total US domestic natural gas production. This represents 340 MMm^3 (12 Tcf) of booked coalbed methane reserves or 5% of total US gas reserves.

Recognizing that similar coalbed methane reserves should be present in coal bearing basins outside the United States, Enron Exploration formed a team of geologists and engineers who had specialized CMR experience in the United States to aggressively pursue coalbed methane opportunities on a global basis. As part of that effort, all coal basins in Australia were evaluated and compared to determine the most favourable basin for a near term commercial CMR program. From the standpoint of size, coal thickness, gas-in-place, permeability, and proximity to large undedicated gas markets, the Galilee Basin in central Queensland was selected as the optimum basin for a commercial CMR project. The entire eastern portion of the basin believed to have CMR potential approximately 48,000 km^2 (18,500 mi^2), was applied for and awarded to Enron Exploration Australia Pty Ltd (EEAPL) in November 1992 as Authority to Prospect (ATP) 529P, Figure 1.

Well sites were selected after performing an extensive study of lateral and vertical coal continuity and thickness, modelling lateral and vertical thermal maturity, and implementing a state-of-the-art fracture detection program for locating fracture permeability, Figure 2. The geological evaluation involved the interpretation and integration of 40,000 km^2 (15,500 mi^2) of space borne imagery, 10,000 line kilometers (6,200 line miles) of seismic data, aeromagnetic and gravity surveys, a large vitrinite reflectance database, a network of stratigraphic cross sections, and a series of isopach maps. The Galilee Basin consists of two structural regions, the Koburra Trough and the Maneroo Platform ramp. Two exploratory wells were dedicated to each region with a single well straddling both regions. Exploratory drilling was conducted with slim-hole equipment allowing for an extensive collection of detailed reservoir data. During the 1993 drilling program, 7.1 km (4.4 mi) of hole were drilled recovering 1.5 km (0.9 mi) of core and 88 gas content samples. Thirty-four permeability tests were

performed, Table 1.

During the 1993 exploration program, the Crossmore and Rodney Creek Anticlines were identified as potential significant gas discoveries. Reservoir properties at the Crossmore area include: 24 m (79 ft) of fully gas charged coal, permeability measurements averaging 52 md, and an estimated 17 Bm^3 (600 Bcf) gas-in-place. The Rodney Creek area is underlain by 30-35 m (98-115 ft) of fully gas charged coal, permeability measurements averaging 13 md, and an estimated 23 Bm^3 (800 Bcf) gas-in-place. There is an additional estimated 11 Tcf gas-in-place immediately offsetting and surrounding the Rodney Creek and Crossmore areas.

Utilizing the extensive reservoir data set and developing the two structures on 640 acre spacing, a reservoir simulation study was conducted to forecast gas rates and cumulative gas recovery. Two production wells will be drilled in early 1995 to establish baseline gas production rates.

GEOLOGICAL FRAMEWORK OF THE GALILEE BASIN

Overview

The coalbed methane potential of all known Australian coal basins were evaluated to identify the areas having optimal conditions for economic gas recovery to meet (long term) energy requirements. The Bowen, Surat, Galilee, Cooper, Sydney and Gunnedah basins, among others, were compared with respect to the critical parameters of coal permeability and gas-in-place. The tectonic conditions necessary for high permeability, highly flexured zones constrained within a low stress environment at reasonable burial depth (i.e. a low vertical stress component), were present only in the Galilee Basin. In addition, a period of extensive coal formation that subsequently reached adequate thermal maturity for gas generation and retention resulted in thick gas bearing coals within the Galilee Basin.

The Galilee is a relatively large and under-explored basin, however a significant amount of data is available. 21,000 kilometers of seismic data and numerous wells penetrating the Permian Coal section provide essential information for delineating thick, fractured coal sections. This information to some degree was missing or inadequate in other coal basins. Moreover, the areas not covered by magnetic, gravity, seismic or well data were evaluated and tied by remote sensing techniques. The geologic conditions necessary for the development of thick, permeable and gas bearing coal may be more favourable in the Galilee Basin than any other Australian coal basin. The geologic and geophysical tools necessary to study these critical reservoir characteristics are already available to a large degree in the Galilee Basin.

All portions of the Galilee Basin thought to have potential for CMR development were identified and an Authority to Prospect (ATP) was applied for. Subsequent exploratory drilling has confirmed the regional models of extensive, permeable, thick, gas bearing coal sections. The detailed geologic/geophysical/remote sensing work performed to locate exploration wells is explained in the following section.

Basin Setting and Structure

EEAPL's ATP 529P, one of the largest ATP's in Australia, covers 48,000 km^2 (18,500 mi^2) of the northeastern section of the Galilee Basin. It encompasses rocks of Late Carboniferous to Triassic age. Its margins are marked by disconformable and unconformable contacts with the underlying strata. To the east it is bounded by Devonian/Carboniferous rocks of the Drummond Basin and to the north by Early Palaeozoic sediments, volcanics, metasediments and the Lolworth-Ravenswood Block granite. Subcropping high grade metamorphics and granitic rocks of the Mount Isa Inlier mark the western and northwestern edges, while Late Precambrian to Early Ordovician granites and metasediments of the Maneroo Platform define both the south central limit and the limit between the northeastern and southwestern areas of the basin [1].

Within ATP 529P, the Galilee Basin sequence is underlain by Drummond Basin sediments in the east and older metamorphic, volcanic and crystalline rocks, possibly belonging to the Mount Isa Inlier, to the west, Figure 3 [2]. Sedimentary rocks of Early Jurassic to Late Cretaceous age belonging to the Eromanga Basin overlie the Galilee Basin throughout most of the ATP. These conceal the Galilee Basin over most of the region except in the east where the Permian and Triassic successions outcrop. The Maneroo Platform defines the southwestern boundary of coal deposition within the ATP.

During the Late Triassic, an east-west compressional event gave rise to uplift with subsequent partial erosion of the Triassic formations over and adjacent to the Maneroo Platform. This episode was followed in the Early Jurassic by the onset of deposition of the Eromanga Basin succession.

Coal Geology

The Aramac Coal Measures are preserved over a relatively small area of the eastern Galilee Basin. It is known that they contain up to 20 percent coal over intervals of up to 270 m (890 ft). The Bandanna Formation/Colinlea Sandstone (Betts Creek Beds) is present over a large part of the basin. Three areas of particularly marked coal deposition have been identified: the Koburra Trough, the area northeast of the Maneroo Platform, and the Lovelle Depression. Outside these areas of maximum development, the total coal isopach thins. It appears that this thinning is depositional to the north and west and erosional to the south and east. Individual coal seams vary in thickness from 1.5 to 9 m (5 to 30 ft), Figure 4.

In terms of depositional environment the geological setting of the Aramac Coal Measures suggests a swamp dominated fluvial system, probably in a periglacial tundra type environment. In contrast, the Bandanna Formation/Colinlea Sandstone (Betts Creek Beds) coals were laid down in what is interpreted as a large prograding delta or alluvial system that gave rise to extensive coal deposition over a large area. Temperate climatic conditions appear to have prevailed during this period.

Thermal Maturity

Thermal modelling based on Sweeney and Burnham's (1990) method has been carried out by several authors on data from selected wells that intersected both the Eromanga and Galilee Basins [3,4]. These studies suggest two main thermal events, one during the Triassic which peaked 225 million years ago and the other during the Tertiary between 70 and 90 million years ago. The Triassic event only affected certain areas; however, the Tertiary event was much more widespread, affecting most of the Galilee Basin.

Present day geothermal gradients are generally close to average for this type of sedimentary basin, with values in the 0.3 - 0.35 °C/100 m (1.14-1.17 °F/100 ft) range. Some areas over the Maneroo Platform and Lovelle Depression have present day gradients that may be sufficient to explain the observed maturities.

Vitrinite reflectance data were obtained from deep exploration wells and contouring on a regional scale [6]. The vitrinite reflectance (Vro) values for the top of the Betts Creek Beds vary from 0.55 to 0.75 percent. Two areas of relatively high thermal maturity exist within this ATP. They occur in the Koburra Trough and east of the Maneroo Platform.

EXPLORATION ACTIVITIES AND RESULTS

Regional Exploration and Wellsite Selection

Virtually all 48,000 km^2 (9.6 million acres) of the permit is underlain by Permian coals at reasonable drilling depths, thereby making the entire permit prospective for CMR. In terms of size, the permit is over three times larger than the entire San Juan Basin. Using all available geological and geophysical data, a comprehensive exploration approach was adapted to locate the areas that would be underlain with a highly fractured, gassy, thick coal section. The fracture detection program centered on a fracture kinetics model whereby open fractures are most likely to form from the draping and warping of sediments over basement features. This model was developed as an analog to the broad platform of continuous permeability present in the San Juan Basin coalbed methane production "Fairway".

The primary basis for wellsite selection was the interpretation and integration of 40,000 km^2 (15,500 mi^2) of landsat thematic mapper imagery, aeromagnetic and gravity coverage, and approximately 10,000 line kilometers (6,200 line miles) of seismic data used to detect subtle basement features with fracture related permeability. Time structure maps have been used to identify the structural fabric of the basement. A network of cross sections using all well control points were constructed to correlate and establish the thickness of the Permian coal section and individual coal seams. Essentially all coal development occurs in a 150 m (490 ft) thick section of Upper and Lower Permian coals referred to as the Bandanna/Colinlea (Betts Creek Beds) and Aramac Coal Measures.

As no gas content measurements had ever been taken in the Galilee Basin, vertical and lateral thermal maturity modelling was conducted to locate regions of maximum gas generation and retention.

Vitrinite reflectance data was compiled from company reports submitted to the Queensland Department of Minerals and Energy (DME) for all wells drilled in the eastern half of the Galilee Basin. The vitrinite data set was augmented by a DME regional assessment of the hydrocarbon potential of the Galilee Basin and the overlying Eromanga Basin [5]. The region of maximum vitrinite reflectance and reflectance gradient, and thereby the inferred highest gas content, overlaps the Maneroo Platform. The symmetry of the iso-reflectance contours which parallel the Maneroo Platform and the relatively thin

veneer of sediments over the platform suggest that higher maturity and gradients are related to heat flow from basement rocks.

Vitrinite reflectance of Permian coals on the margin of the Maneroo Platform are in excess of 0.70 V_{ro}, a rank adequate for gas generation and corresponding gas content retention, Figure 5. A second vitrinite reflectance anomaly and inferred region of gas generation overlies the Koburra Trough. This trend is less well-defined but is thought to have developed because of a greater depth of burial during Permian times.

A regional exploratory drilling program was designed to assess the viability of multiple exploration targets. Two exploratory wells were dedicated to establishing gas content of the Betts Creek Beds/Bandanna/Colinlea coal sequence in the northern and southern parts of the Koburra Trough. A third well was located southwest of the Koburra Trough to test coal gas contents in an area of low coal thermal maturity. Although all three wells in the Koburra Trough and nearby region were designed to test coal gas contents, each location was also sited to locate subsurface fracture permeability.

The area offsetting the northeast perimeter of the Maneroo Platform contains the thickest and most thermally mature coals within the ATP. Two wells were located to test the coalbed methane production potential on two separate but parallel anticlines. An additional well was added to the program to confirm and delineate the apparent discovery.

Exploration Drilling Program

Accurate evaluation of a coalbed methane prospect requires a comprehensive collection of core data and reservoir testing. Continuous slim-hole coring and testing provides the most comprehensive data set for a minimum amount of time and expense [6]. All exploration wells were drilled with slim-hole equipment from June to December 1993. The coring program was carried out using the most advanced techniques of on-site gas desorption and pressure transient analysis. On-site evaluation methods included desorption at reservoir temperature, and on-site final gas content measurements utilized crushing with a modified ring mill. Drill stem tests (DST's) were performed with slim-hole straddle packer tools. Pressure data was measured with a quartz memory gauge. Pressure transient analysis was performed on-site to determine both the mechanical integrity of the test and estimate reservoir permeability, pressure, and skin. A satellite link from each wellsite to office support staff allowed real time data transfer for data reduction interpretation and test modifications. In addition to the DST's, mini-fracs were conducted utilizing the straddle packer system.

Gas contents were determined to estimate the in-place gas resource of ATP 529P. The standard US Bureau of Mines direct-method was used to calculate the gas content. Eighty-eight gas content measurements were performed during the six well program. The average ash free gas content per well was estimated to be 2.6 sm^3/ton (90 scft/ton); when corrected for an average ash content of 14% per sample. However, for the Rodney Creek/Crossmore development area, the ash-free gas content of the coals is higher; estimated to be 4 sm^3/ton (140 scft/ton) and more importantly the coals are fully saturated.

The Galilee Basin coals are lower in rank and have a corresponding lower storage capacity than higher rank coals. The lower rank coals have a more favorable gas release mechanism for coalbed methane production due to differences in desorption pressures as observed on adsorption isotherms, Figure 6. The Galilee Basin gas contents on first observation may appear low when compared to the San Juan Basin where the coal is of a medium to high rank. While it is true that the gas content in low rank coals may be lower than those found in higher rank coals, this characteristic is related to the coal storage capacity, not to the commercial potential. Lower rank coals physically store less gas within the coal matrix and this characteristic should not be confused with a low absolute value for gas content. Coalbed methane reservoirs may contain several times the gas of similarly pressured conventional reservoirs; lower rank coals simply have a lower multiplier (2 times as much compared with 4 to 5 times as much for higher ranked coals).

More than thirty DST's were performed to estimate the in-situ characteristics of the reservoir. An average of 15 m (50 ft) of coal was tested on each well. Permeabilities ranged from less than 1 md to more than 200 md within the coal groups. Most of the well tests revealed slight overpressuring and had high skin factors which are normally associated with natural fractures.

PRODUCTION ESTIMATES

Based on the test results, an estimate of the productive capacity of the core wells drilled in the Galilee Basin can be determined using measured and inferred reservoir parameters. Twenty-year gas and water production simulations were performed using COMET-3D, a widely used proprietary coalbed

methane reservoir simulator. COMET-3D is a fully implicit, three-dimensional, finite-difference reservoir simulator specifically designed for modeling the flow of gas and water in coal seams. This model includes gas desorption and diffusion processes which are essential for modelling gas production from coalbeds.

A typical well profile was developed using results from the geologic and well testing analyses. Model input parameters for a base case reservoir simulation are summarized in Table 2.

In the simulation study, the Crossmore and Rodney Creek areas were developed with 160 wells leading to 23 Bm^3 (800 Bcf) of recoverable gas. The Crossmore wells peak at 85 to 140 Mm^3/d (3 to 5 MMcf/d) and decline rapidly, Figure 7. The Rodney Creek wells peak at 35 Mm^3/d (1 MMcf/d) and decline slowly, Figure 8. The exact well production rates depend on their location with respect to structure and confinement. The wells in each area are developed on 260 hectares (640 acres) and contain an average 140 MMm^3 (5 Bcf) of recoverable gas on a per well basis.

The reservoir properties used in the simulation are discussed below:

- ***Crossmore.*** A three zone model was used to represent the three distinct permeabilities measured in the well tests, as follows:

  Zone 1: 5.2 m (17 ft) of 229 md coal
  Zone 2: 4.0 m (13 ft) of 14 md coal
  Zone 3: 13.1 m (43 ft) of 2 md coal

  The 22.3 net meters (73 net feet) of coal contain an average of 3.7 sm^3/ton (129 scft/ton). This equals 323 MMm^3 (11.4 Bcf) of gas per square mile. At 142 MMm^3 (5 Bcf) per well, recovery efficiency is 44 percent of the gas-in-place.

- ***Rodney Creek.*** A two zone model was used to represent the two permeability intervals measured in the well tests, as follows:

  Zone 1: 9.8 m (32 ft) of 16 md coal
  Zone 2: 10.7 m (35 ft) of 2 md coal

  The 20.5 net meters (67 net feet) of coal contain an average of 4.3 sm^3/ton (150 scf/ton). This equals 340 MMm^3 (12 Bcf) of gas per square mile. At 142 MMm^3 (5 Bcf) per well, recovery efficiency is 41 percent of the gas-in-place.

The forecasted gas production rates presented in this section serve as one of the primary input parameters for the economic analysis. Ultimately, drilling, completing, and producing the fields is the only certain method of establishing the gas production rates. Therefore, production testing is the primary focus for the 1995 program.

CONCLUSIONS

1. All of the six exploration wells encountered thick, permeable (1 well not tested for permeability), and gas bearing coal sections.

2. Although test results are encouraging, production wells will be required to confirm gas production potential.

3. Lateral and vertical homogeneity of permeability is uncertain and will require additional test wells.

4. The slim hole technologies and strategy successfully developed under the 1993 Galilee Basin program can be applied to other remote, frontier basins at substantial cost savings when compared to conventional drilling and testing.

5. Reservoirs are at or above hydrostatic pressure and reservoir properties are favorable for gas production.

REFERENCES

1. Jackson, K.S., Horvath, Z., and Hawkins, P.J., "An Assessment of the Petroleum Prospects for the Galilee Basin, Queensland," The APEA Journal 21, 1981.

2. Gray, A.R.G., and Swarbrick, C.F.J., "Nomenclature of Late Palaeozoic Strata in the Northeastern Galilee Basin," Queensland Government Mining Journal, 76, 1975.

3. Sweeney, J.J. and Burnham, A.K., "Evaluation of a Simple Model of Vitrinite Reflectance Based on Chemical Kinetics," AAPG Bulletin, 74, 1990.

4. Hawkins, P.J. and Green, P.M., "Exploration Results, Hydrocarbon Potential, and Future Strategies for the Northern Galilee Basin," The APEA Journal, presented at the 1993 APEA Conference, Gold Coast, Australia, March 28-31, 1993.

5. Scott, S.G. and Hawkins, P.J., "Coal Geology of the Northern Galilee Basin and its Implication for Coalseam Methane Investigations," presented at the 1992 Symposium on Coalbed Methane Research and Development in Australia, Townsville, Australia, November 1992.

6. Reeves, S.R., Boyer, C.M., and Herrington, M.R., "Designing Practical Reservoir Evaluation Programs for Frontier International Coalbed Methane Plays," paper 9363, presented at the 1993 International Coalbed Methane Symposium, Tuscaloosa, Alabama, May 17-21, 1993.

TABLE 1. 1993 FORMATION EVALUATION SUMMARY

Description & No. of Tests per Well	Fleetwood #1	Rodney Creek #1	Crossmore #1	Splitters Creek #1	Aberfoyle #1A	Rodney Creek #2
Permeability (In situ)	2	6	5	0	5	13
Gas Content (Crushed)	5	12	5	14	13	22
Gas Content (Canister)	16	4	1	1	4	0
Adsorption Isotherms	2	2	2	1	2	2
Coal Microstructure	4	4	4	4	4	4
SEM (Sandstone)	3	3	3	--	4	4
Maceral (Coal)	4	4	4	4	4	4
Vitrinite Reflectance	4	4	4	2	4	4
Proximate Analysis	16	16	6	4	14	22
Ultimate Analysis	4	4	4	2	4	4
Water Analysis	1	5	5	N/A	6	16
Gas Analysis	2	4	1	N/A	2	0
Depth (m)	1,237	1,166	1,061	1,004	1,497	1,118
Core Recovery (m)	280	278	236	148	242	246

TABLE 2.

RESERVOIR PROPERTIES USED FOR SIMULATION OF WELL PERFORMANCE

Reservoir Property	Crossmore			Rodney Creek	
	Zone 1	Zone 2	Zone 3	Zone 1	Zone 2
Mid-Point Depth of Coal, meters (feet)	917-1009 (3007-3309)	936-1028 (3071-3374)	1037-1129 (3401-3704)	920-1011 (3018-3318)	989-1081 (3246-3546)
Coal Thickness, meters (feet)	5.2 (17)	4.0 (13)	13.1 (43)	10.7 (35)	9.8 (32)
Average Initial Reservoir Pressure, MPa (psia)	10.2 (1479)	10.4 (1508)	11.4 (1655)	10.3 (1491)	11.0 (1592)
Cleat Porosity, %	2	2	2	2	2
Initial Water Saturation, %	100	100	100	100	100
Absolute Cleat Permeability, md	229	14	2	229	2
In Situ Langmuir Volume, sm^3/ton (scf/ton)	5.4 (188)	5.4 (188)	5.4 (188)	10.4 (363)	10 4 (363)
Langmuir Pressure, MPa (psia)	5.0 (721)	5.0 (721)	5.0 (721)	15.1 (2189)	15.1 (2189)
Average Desorption Pressure, MPa (psia)	10.2 (1479)	10.4 (1508)	11 4 (1655)	10.3 (1491)	11 0 (1592)
Average In Situ Gas Content, sm^3/ton (scf/ton)	3 6 (126)	3.6 (127)	3 7 (131)	4 2 (147)	4.4 (153)

FIGURE 1. GALILEE BASIN PERMIT LOCATION

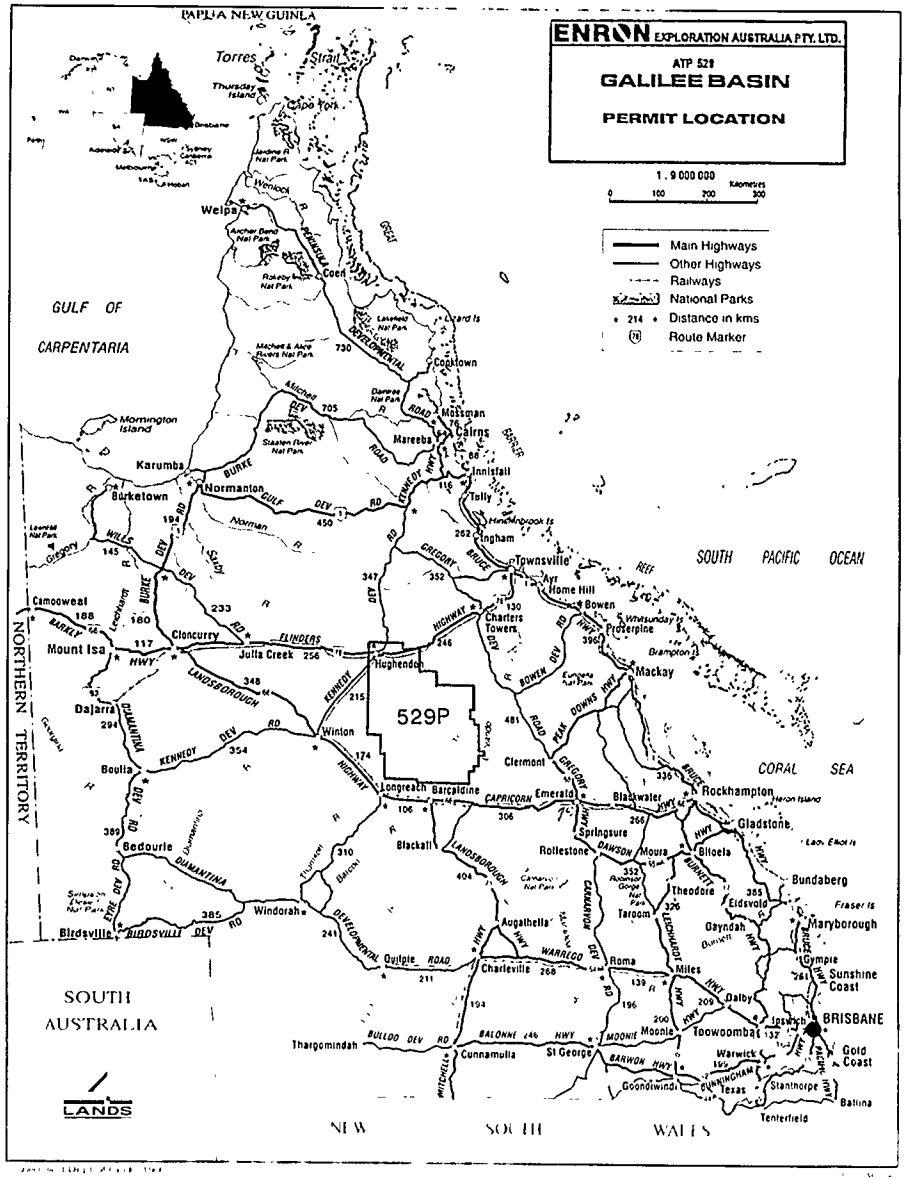


FIGURE 2. GALILEE BASIN BASE MAP

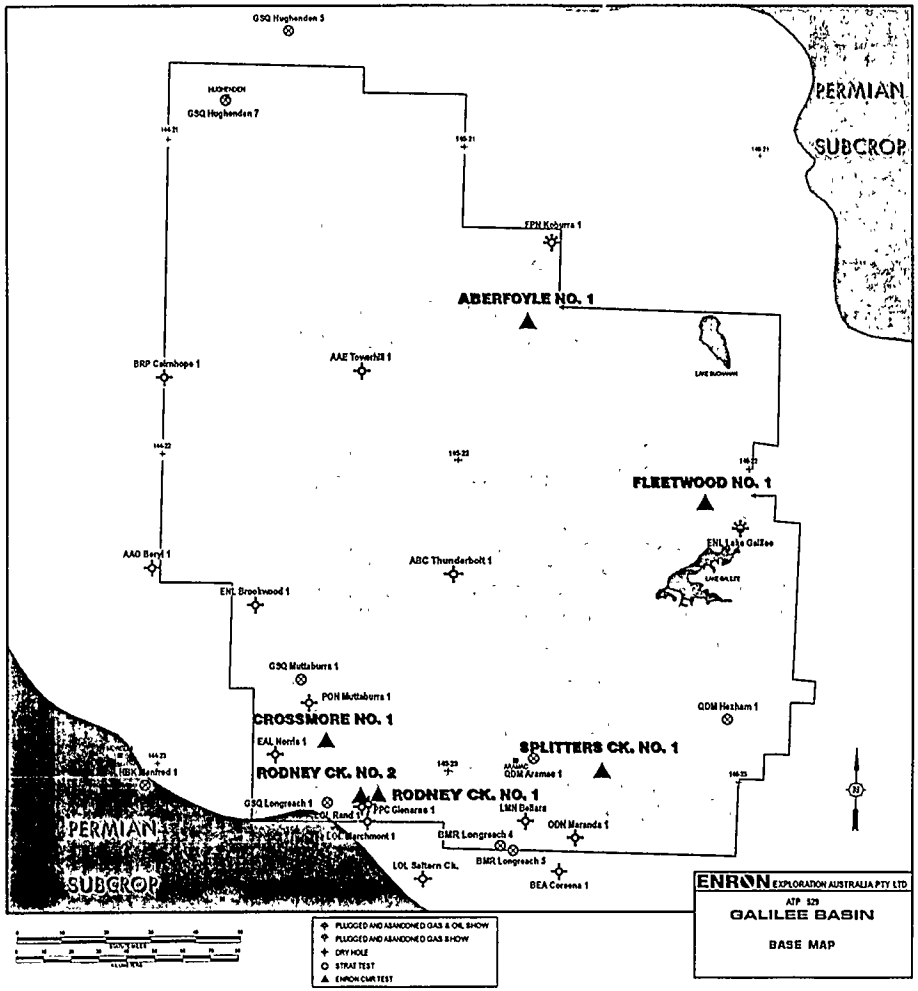
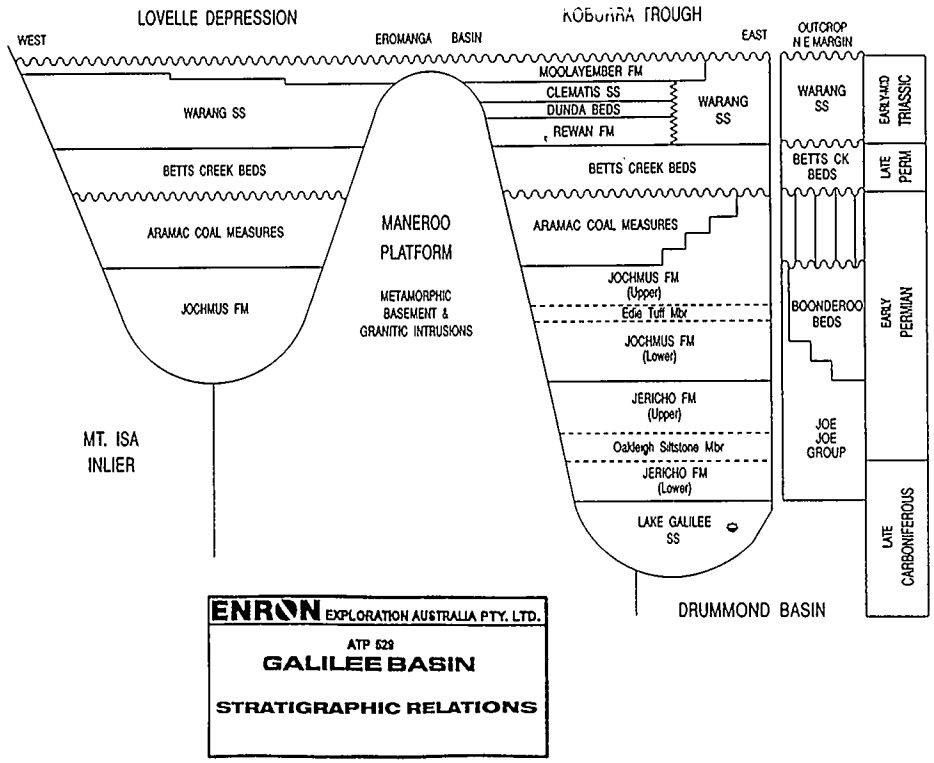


FIGURE 3. GALILEE BASIN STRATIGRAPHIC RELATIONS



(AFTER GRAY AND SWARBRICK, 1975)

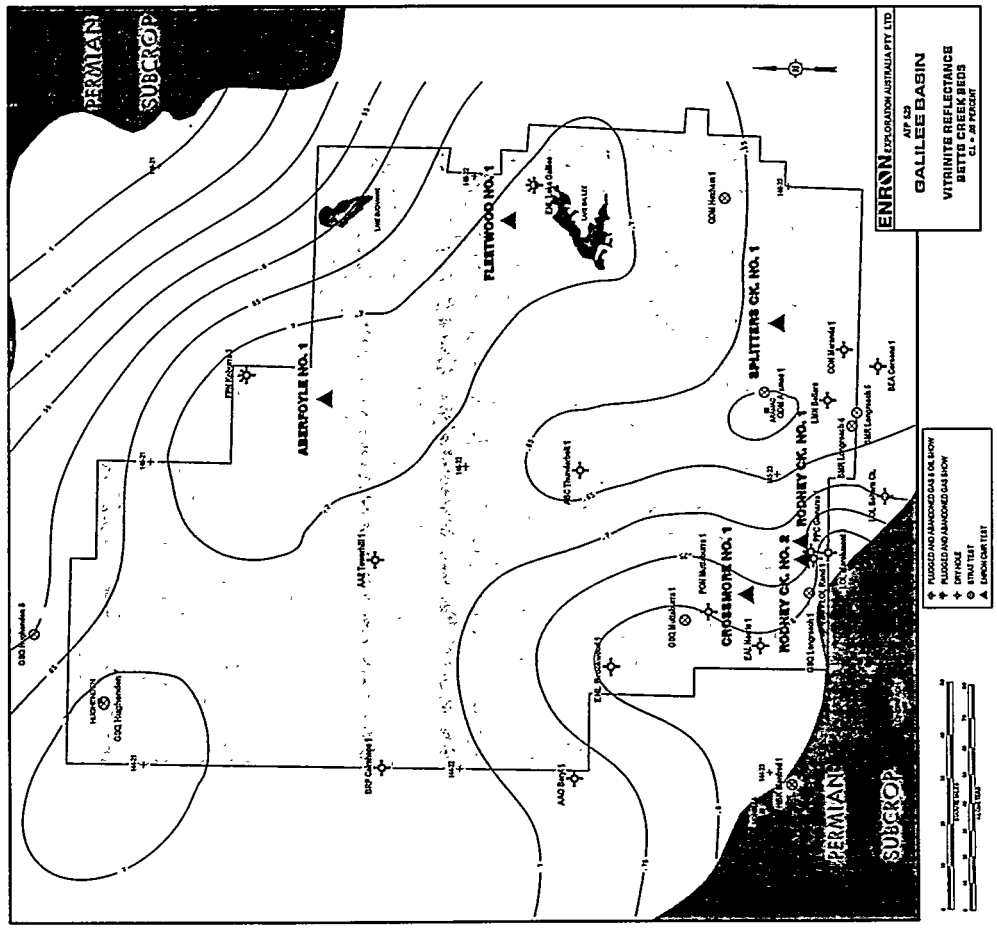


FIGURE 5. GALILEE BASIN VITRINITE REFLECTANCE

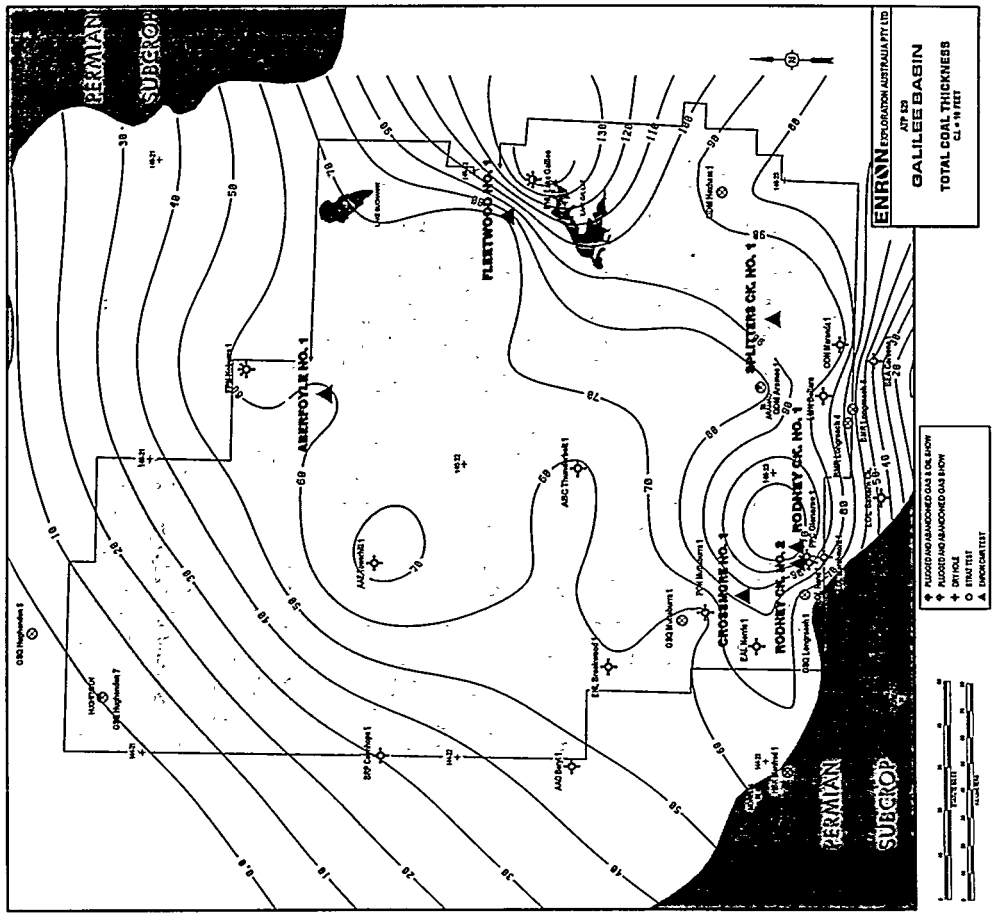


FIGURE 4. GALILEE BASIN TOTAL COAL THICKNESS

FIGURE 6. ADSORPTION ISOTHERM COMPARISONS

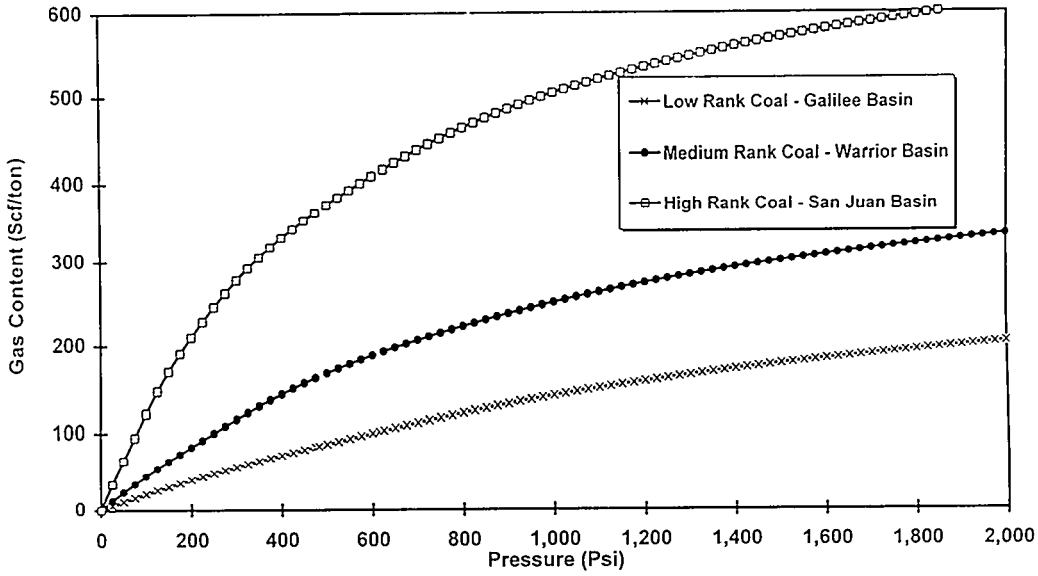


FIGURE 7. SIMULATED CROSSMORE GAS PRODUCTION

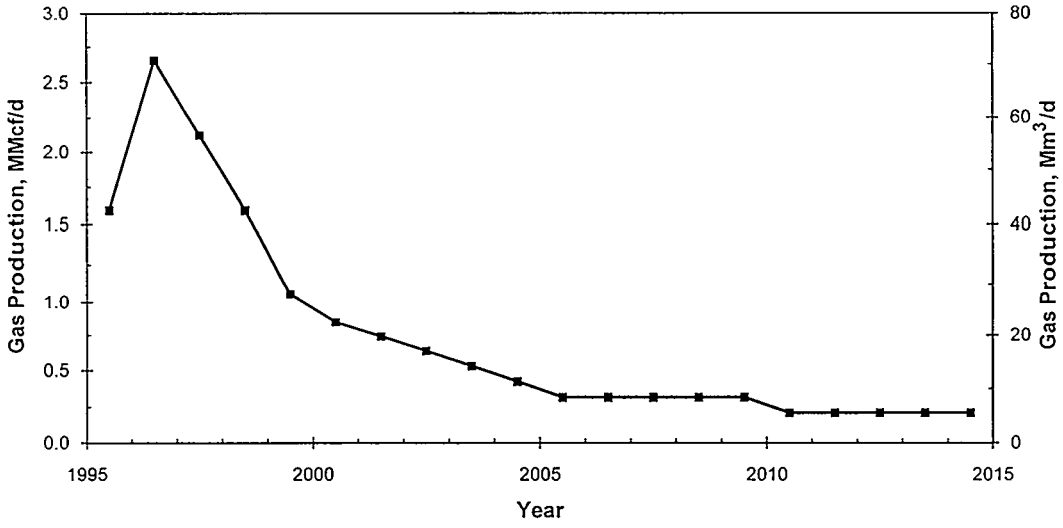
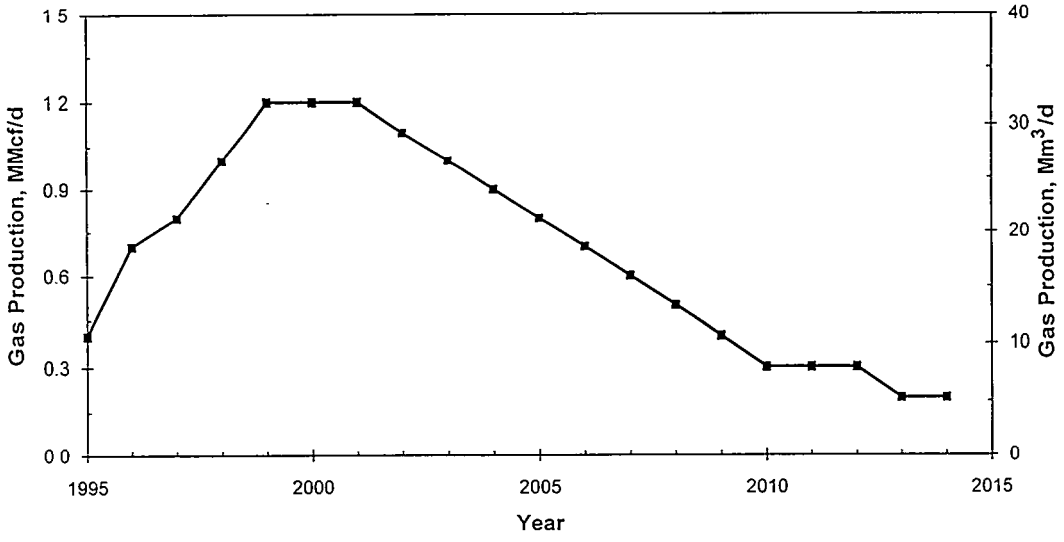


FIGURE 8. SIMULATED RODNEY CREEK GAS PRODUCTION



INTERGAS '95

May 15-19, 1995
The University of Alabama
Tuscaloosa, Alabama USA

9534

Coalbed Methane of the Damodar Valley Coal Fields—Bihar and West Bengal, India

J.L. Cooper, Amoco India Petroleum Company; and P. Kumar, Central Mine Planning and Design Institute, Ranchi, Bihar

Abstract

India has numerous coalfields with potential for Coalbed Methane (CBM) development. The Damodar Valley coalfields provide a favorable combination of coal thickness, rank and burial depth. The coals are Permian age of the Gondwana sequence. The major coal seams are within the Barakar and the Raniganj Formations, with some areas having over 100 meters of net coal. The coal belt has separate coal basins elongated east/west along the Damodar River. The structural and depositional settings vary significantly among these basin. The coalfields were deposited in narrow basins and the coal seams have been mined extensively. This may inhibit potential areas for CBM development although several worldwide coal provinces are demonstrating a positive coexistence between mining operations and CBM development.

The major challenges facing any CBM project are both technical and commercial. The technical challenges are dominantly gas content and permeability of the coals. Two main commercial aspects are gas market and gas pipeline infrastructure. In the Damodar Valley, there currently are no gas markets, a market may develop when gas production is established. The region does not have a pipeline infrastructure and the closest connection to an existing pipeline is 500 kilometers to the west.

Gas in place (GIP) calculations require coal thickness, area, and gas content. Thickness and area are well documented, but gas content is unknown for these coals. Gas content assumptions can be made from isotherms, coal rank, and maceral information. Assuming saturated coal seams, conservative GIP estimates range from 400 to 700 billion cubic meters (15 to 25 TCF). This estimate is limited to the undeveloped areas, and thickness of 30 to 100 meters of net coal. Direct gas content measurements are required to determine the actual gas content. Recoverable reserves are controlled by permeability, gas saturation, structural and stratigraphic variables. This resource potential makes the Damodar Valley area an excellent CBM exploration target.

Introduction

Successful Coalbed Methane (CBM) production in the United States has encouraged companies to explore for CBM worldwide. U.S. CBM production will exceeded 57 million cubic meters per day (2 BCF) in 1994. The San Juan basin in Colorado / New Mexico and the Black Warrior basin in Alabama are the two largest producers. These basins serve as exploration models for CBM exploration worldwide and set the criteria for minimum coal thickness, coal rank, and reservoir burial depth.

India is among the top 10 countries in coal resources. The estimated coal reserves are 160 billion metric tons. Significant coal resources occur in the Permian (Lower Gondwana). The Permian coals are extensively developed in the eastern part of India (Figure 1). The thickest bituminous coals are the Raniganj and Barakar Formation coals (Figure 2) in the Damodar Valley area of Bihar and West Bengal. The four largest Damodar coalfields (Raniganj, Jharia, Bokaro and North Karanpura; Figure 3) have similar coal rank and burial depth. The major difference between the Damodar Valley coal seams and those of the San Juan and Black Warrior basins are the thickness and area. The Damodar Basin coals are significantly thicker than either the San Juan or Black Warrior Basin coals but are confined to a much smaller area (Figure 3). The maximum burial depth is about 2,000 meters. Based on thickness, burial depth, and rank, the authors believe that the Damodar area has the greatest CBM potential of any area in India.

Geologic Setting

The geology of the Damodar Valley is described in detail in Singh, (1987), and Rao, (1987). The Gondwana sediments of the Damodar Valley extend in an east - west

linear belt from Durgapur in West Bengal westward through southern Bihar. The sediments indicate a variety of depositional settings caused by the dynamic nature of the basinal areas. The coal bearing section is limited to the Permian age sediments, which consist of the Talchir, Karharbari, Barakar, Barren Measures and Raniganj Formations (Figure 2). The Barakar and Ranijanj Formations contain the significant coal measures. The Barakar Formation ranges from 300 to over 1250 meters in the area, with the Raniganj Formation attaining a maximum thickness of about 800 meters. The Permian deposition was followed the Triassic Panchet and Mahadeva. These sediments were later intruded by Lower Cretaceous intrusives.

The coal measures in Raniganj, Jharia and Bokaro have been extensively intruded by these Lower Cretaceous dikes and sills (Rao,1987). The dikes are significant since they act as permeability barriers effecting exploration and development plans. The Gondwana coals were deposited in an environment totally different from the Carboniferous and Cretaceous coals that have been exploited for CBM in the United States. The basal Talchir Formation contains glacial and periglacial sediments (Singh, 1987). These coals formed at high latitudes and probably had a higher variation in wet and dry periods. This led to a fluctuating environment which is represented by high inertinite and ash content. Modern analogs are the peat swamps in Canada.

Coalbed Methane Potential

Coal thickness, area, and gas content are required to determine the gas in place (GIP) calculation for coal reservoirs. The area and coal thickness are relatively well known for these coal fields. However, the gas content for the coals is unknown. Assumptions on ideal gas content can be made from coal isotherms or estimated from coal rank, reservoir depth and maceral content. The coal thickness in these coal fields range from 50 to over 300 feet (Figure 4).

Several samples have been analyzed for maturity, coal quality, maceral content and sorption (Figures 5 and 6). Coal rank varies from high volatile bituminous C to medium volatile bituminous. the rank is highest at Jharia and East Bokaro and decreases both to the east and west. The is some influence around the sills and dikes but the affect is limited to the immediate area around the intrusives. Although coal quality varies greatly, the coals can be generally be classified as high ash coals ranging from 10 to 40 percent. Maceral content varies dramatically from vitrinite rich to inertinite rich and the variation occurs both laterally and vertically. Figure 5 and 6 show the adverse affect that inertinite has on gas adsorption. Figure 5 shows the isotherm for a medium vol. coal with 43% inertinite content with 15% mineral matter. The absolute sorption value is 750 SCF/T on a dry mineral matter free basis. Figure 6 is from a lower rank (high vol. A) coal with 77% vitrinite and 23.5% mineral matter, this sample shows an absolute sorption value of 1333 SCF/T. Obviously the variation in rank, ash and maceral content will have a significant effect on the CBM resources.

The Damodar Valley coal fields have been extensively mined and the resource potential will initially be restricted to the unmined areas of the coalfields, with the exception of North Karanpura. Based on the rank, thickness, quality and sorption isotherm data the CBM gas in place potential (GIP) of the unmined portions of these coal fields could range from 10 to 24 TCF, assuming a 50% recovery rate recoverable reserves could range from 5 to 12 TCF. Other sources have estimated the GIP potential for the entire Damodar Valley area (including the four fields mentioned) from 60 to over 144 TCF. These estimates provide a rough guess potential for gas in place, but direct measurements are necessary for accurate GIP used for economic evaluation. Currently there a very few desorption measurements, and since these are narrow basins the risk of under-saturation is considerable. An additional complication is gas quality. Currently the gas quality is unknown, carbon dioxide, nitrogen or other inert gases impurities in the methane can make it noncommercial.

There is mixed evidence on gas saturation. The Ahlambad mine, in Jharia, is a moderate depth mine which has experienced some methane emission into the mine works. However, in-mine degassification attempts have not produced significant sustained gas flow, indicating potentially low gas content or low permeability. The positive indications on gas presence are from the gas shows in coal exploration boreholes and gas seeps in the nalas and rivers which flow over the coal outcrops. There is a documented example of a gas flare from an abandoned coal exploration corehole in the Raniganj field near the Salma Dike. In summary the data concerning gas presence and gas content is conflicting. The gas content question will not be resolved until careful direct measurements are made from adequately retrieved fresh cores.

Conclusions

The Damodar Valley coal fields offer international scale CBM potential. A staged exploration approach is required to establish gas content, permeability, and eventually commercial viability. If coalbed methane from the Damodar Valley is successful, it will open up exploration on higher risk CBM plays in other coal bearing areas within India. With India's acute need for indigenous energy, coalbed methane offers a very viable alternative. Additionally, coalbed methane production could allow future economic growth in this area at reduced risk to the environment.

REFERENCES

Rao, P.V., 1987, "Coalfields of Bihar", Geologic Survey of India Bulletin, Series A, No. 45, Vol. 4, p. 1-8, 8-61, 201-246.

Singh, R.M., Editor,1987, "Proceedings of the National Seminar on Coal Resources of India", p. 1-13, 121-137, 341-358.

Verma, R.P. et al, 1989, "Compendium on Updated and Revised Geology of Jharia Coalfield", p. 1-12.

Figures

Figure 1 Coal Fields of India
Figure 2 Damodar Valley Stratigraphic Section
Figure 3 Damodar Valley Coalfields
Figure 4 Coal Sections, N. Karanpura, E. Bokaro, & Jharia
Figure 5 Langmuir Isotherm Jharia Coal Field
Figure 6 Langmuir Isotherm Jharia Coal

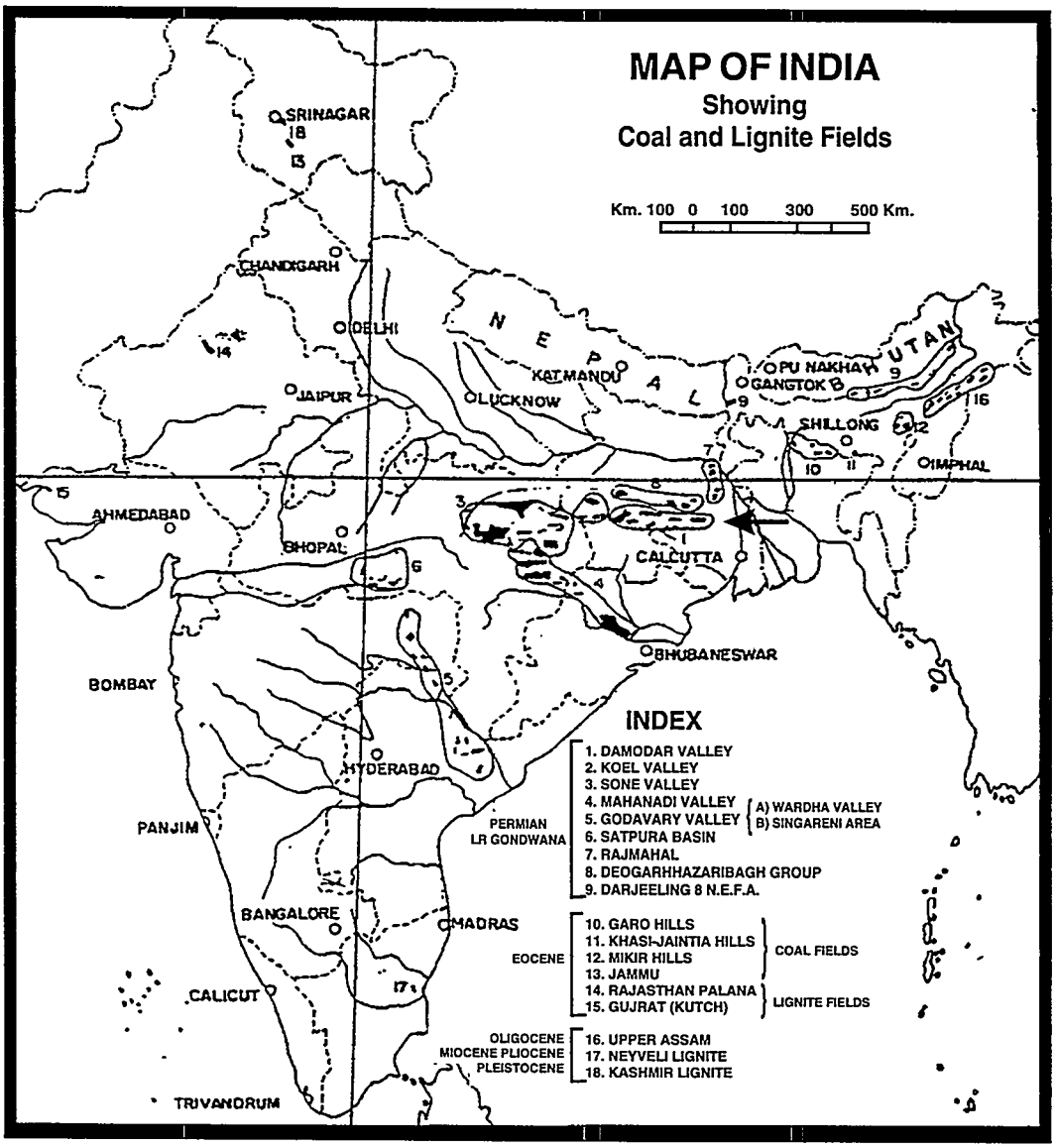

MAP OF INDIA
Showing
Coal and Lignite Fields
Km. 100 0 100 300 500 Km.
SRINAGAR
CHANDIGARH
DELHI
JAIPUR
LUCKNOW
KATMANDU
NEPAL
BHUTAN
PU NAKHAH
GANGTOK
SHILLONG
IMPHAL
AHMEDABAD
BHOPAL
CALCUTTA
BHUBANESWAR
BOMBAY
HYDERABAD
PANJIM
BANGALORE
MADRAS
CALICUT
TRIVANDRUM
INDEX
1. DAMODAR VALLEY
2. KOEL VALLEY
3. SONE VALLEY
4. MAHANADI VALLEY
5. GODAVARY VALLEY
A) WARDHA VALLEY
B) SINGARENI AREA
6. SATPURA BASIN
7. RAJMAHAL
8. DEOGARHHAZARIBAGH GROUP
9. DARJEELING 8 N.E.F.A.
PERMIAN
LR GONDWANA
EOCENE
10. GARO HILLS
11. KHASI-JAINTIA HILLS
12. MIKIR HILLS
13. JAMMU
COAL FIELDS
14. RAJASTHAN PALANA
15. GUJRAT (KUTCH)
LIGNITE FIELDS
OLIGOCENE
MIOCENE PLIOCENE
PLEISTOCENE
16. UPPER ASSAM
17. NEYVELI LIGNITE
18. KASHMIR LIGNITE

Figure 1

INDIA - GONDWANA SYSTEM STRATIGRAPHY

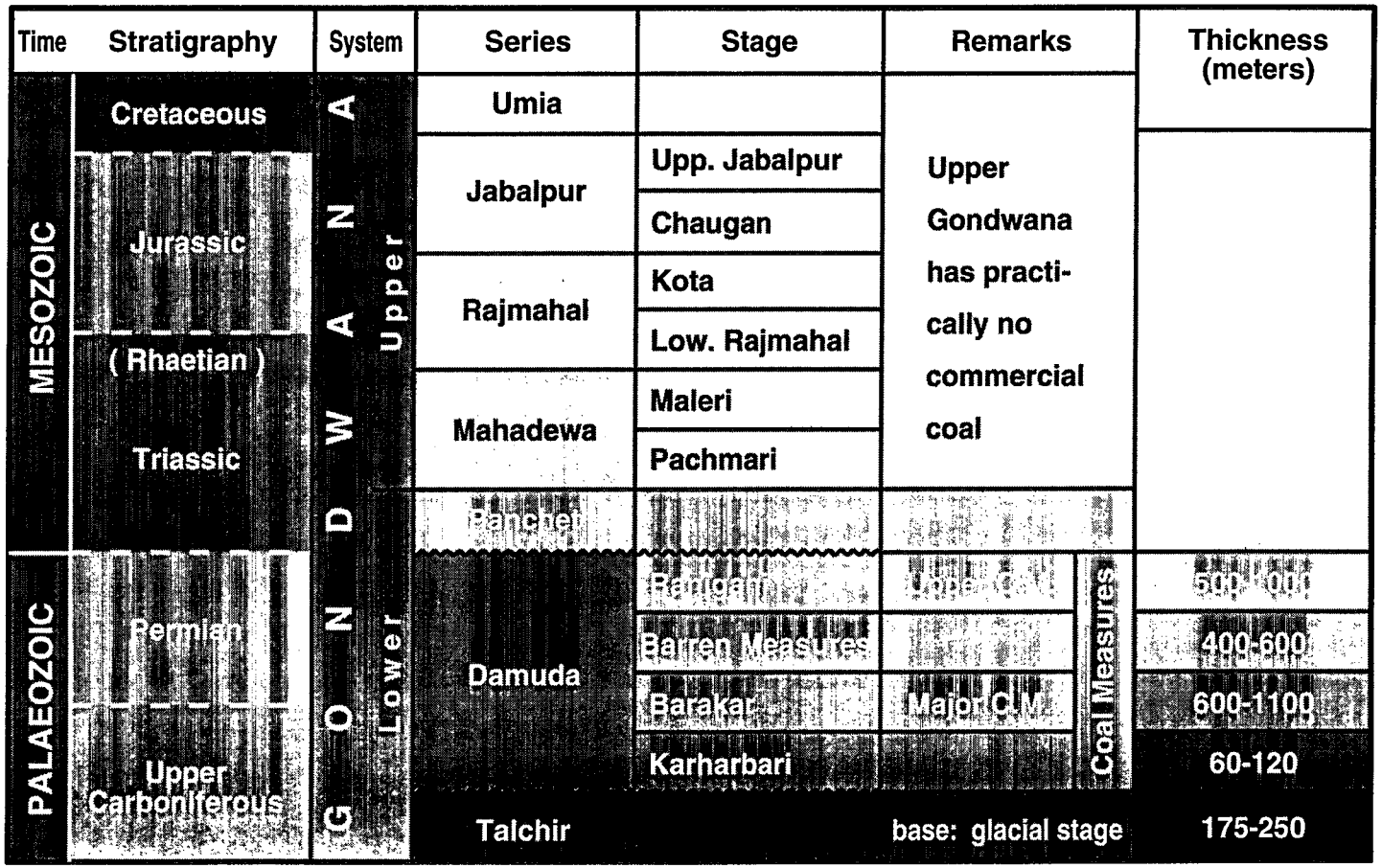


Figure 2

From: Petroconsultants Coal Worldwide

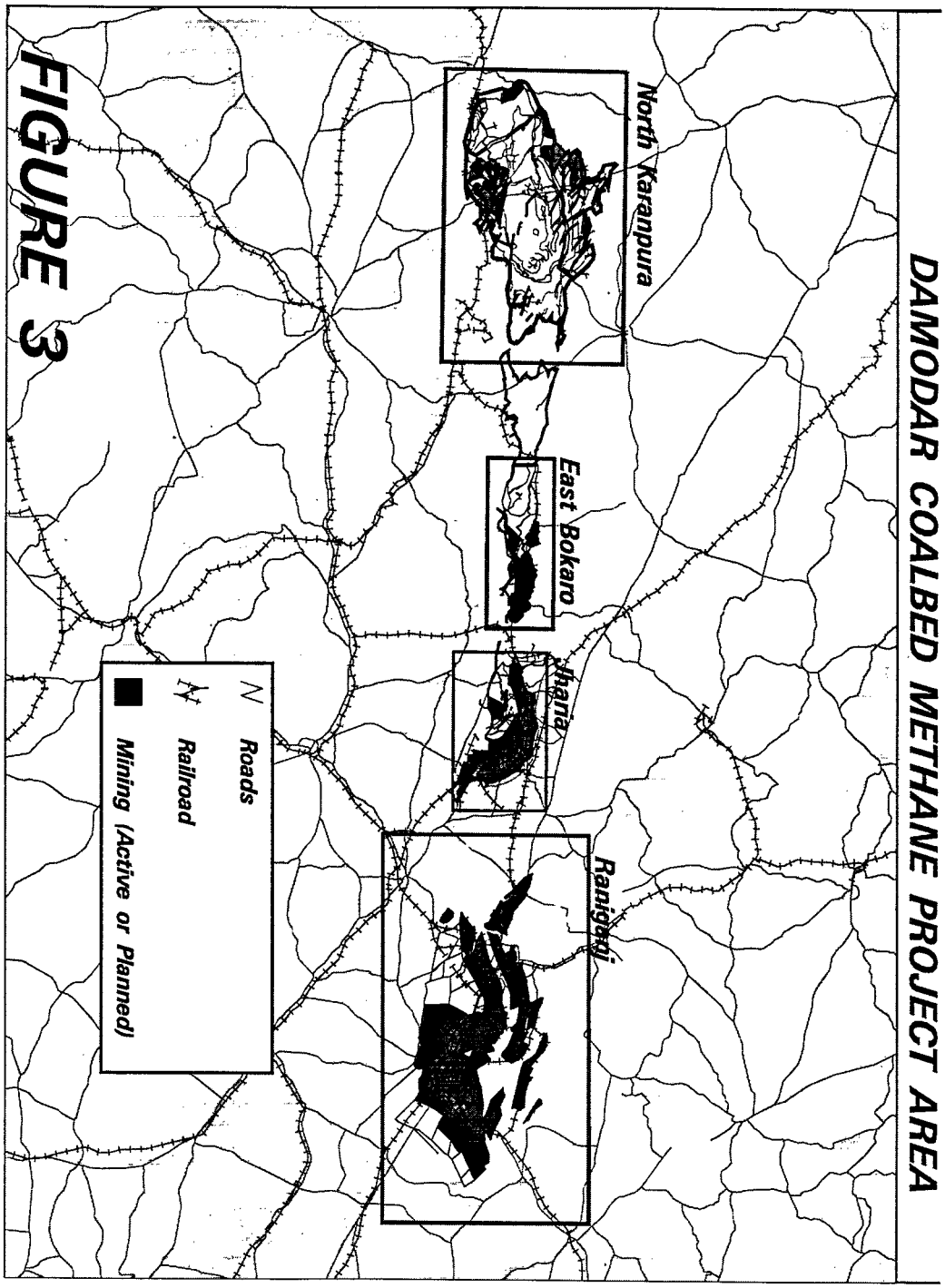

DAMODAR COALBED METHANE PROJECT AREA
North Karanpura
East Bokaro
Jharia
Raniganj
Roads
Railroad
Mining (Active or Planned)

FIGURE 3

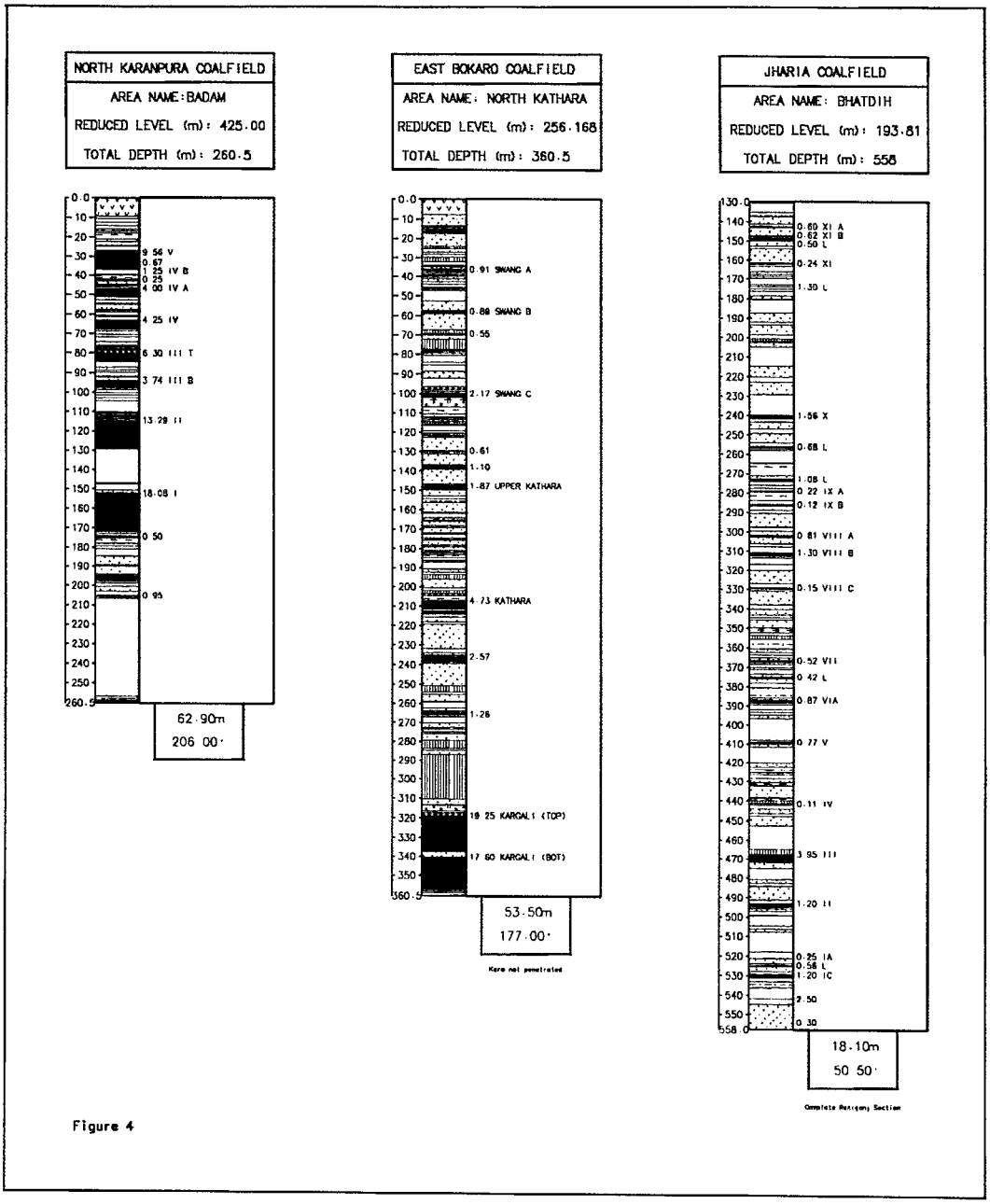

NORTH KARANPURA COALFIELD
AREA NAME:BADAM
REDUCED LEVEL (m): 425.00
TOTAL DEPTH (m): 260.5
9.56 V
0.67
1.25 IV B
0.25
4.00 IV A
4.25 IV
6.30 III T
3.74 III B
13.29 II
18.08 I
0.50
0.95
62.90m
206.00'
EAST BOKARO COALFIELD
AREA NAME: NORTH KATHARA
REDUCED LEVEL (m): 256.168
TOTAL DEPTH (m): 360.5
0.91 SWANG A
0.88 SWANG B
0.55
2.17 SWANG C
0.61
1.10
1.87 UPPER KATHARA
4.73 KATHARA
2.57
1.28
18.25 KARGALI (TOP)
17.60 KARGALI (BOT)
53.50m
177.00'
Core not penetrated
JHARIA COALFIELD
AREA NAME: BHATDIH
REDUCED LEVEL (m): 193.81
TOTAL DEPTH (m): 558
0.60 XI A
0.62 XI B
0.50 L
0.24 XI
1.30 L
1.56 X
0.68 L
1.08 L
0.22 IX A
0.12 IX B
0.81 VIII A
1.30 VIII B
0.15 VIII C
0.52 VII
0.42 L
0.87 VIA
0.77 V
0.11 IV
3.95 III
1.20 II
0.25 IA
0.56 L
1.20 IC
2.50
0.30
18.10m
50.50'
Complete Raniganj Section

Figure 4

Langmuir Isotherm - Jharia Coalfield

Langmuir Isotherm			Amoco Production Research - Reservoir Technologies - Coalbed Methane	
	Mineral Matter (dry)			
	14.82%			
b	VM	VM		
1/psi	SCF/ton	SCF/ton	Experimental Data	
0.001805	638.48	749.57	Absolute Sorption	
P	V	V	P	VTRUE
psia	SCF/ton	SCF/ton	psia	SCF/ton
0.00	0.00	0.00	0.00	0.00
100.00	97.63	114.61	64.40	66.95
200.00	169.36	198.82	130.05	122.72
300.00	224.29	263.31	378.10	273.95
400.00	267.71	314.28	816.60	368.30
500.00	302.88	355.58	1293.35	417.17
600.00	331.97	389.72	1631.30	503.58
700.00	356.41	418.42	0.00	0.00
800.00	377.24	442.87	0.00	0.00
900.00	395.21	463.97	0.00	0.00
1000.00	410.86	482.35		
1100.00	424.62	498.50		
1200.00	436.82	512.82		
1300.00	447.69	525.59		
1400.00	457.46	537.05		
1500.00	466.27	547.39		
1600.00	474.27	556.78		
1700.00	481.55	565.33		
1800.00	488.22	573.16		
1900.00	494.34	580.35		
2000.00	499.98	586.97		
Instructions				
Enter sample description information				
Enter additional measurement data				
Enter values for VM & b				
Enter value for mineral matter (dry)				
Enter experimental sorption P & V (absolute)				

Sample Description			Additional Measurement Data				
Country:	India		Moist: As Rec.	1.35%	mass	X-Ray Diffrac	volume
Basin:	Damodar		Eq Moist:	3.49%	mass	Coal:	
State:	Bihar		He Density:	1.5	g/cc	Silicia:	
Well/API No.	97-357-99800-18		ASTM Rank:	MvBit			
Formation:	Barakar		Vol Mat:	26.49	dmmf		
Seam:	XV		Heat Value:	14868	BTU/bm mmmf		
Depth:	Amlabad Mine		Min Mat:	14.82%	dry mass		
Sample ID:	IND 7		Pure Coal:	85.18%	dry mass		
Notes:			Vit Reflect:	1.08			
			Vitrinite:	57	volume		
Moist:		mass	Inertinite:	42.6	volume		
Temp:	115	F	Liptinite:	0.4	volume		

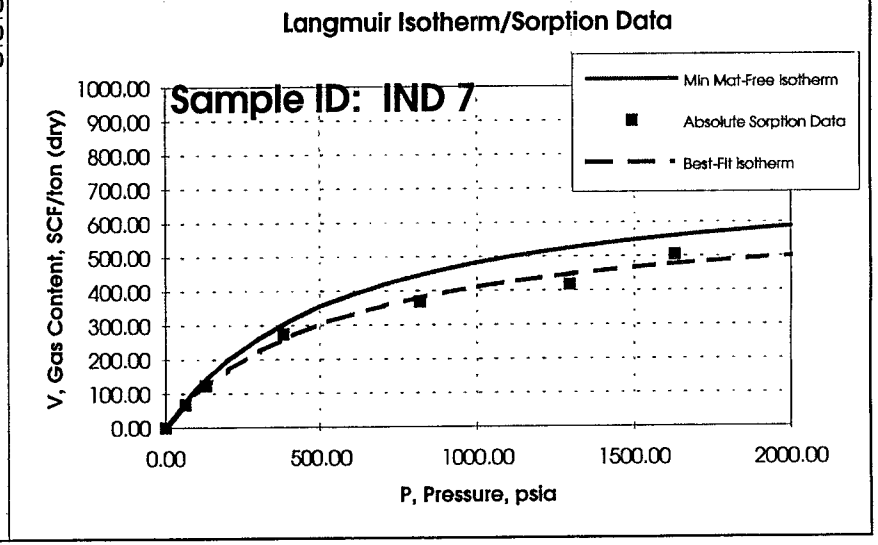


Figure 5

Langmuir Isotherm - Jharia Coalfield

Langmuir Isotherm			*Amoco Production Research - Reservoir Technologies - Coalbed Methane*										
	Mineral Matter (dry)				Sample Description			Additional Measurement Data					
	23.51%				Country:	India		Moist: As Rec.	1.42%	mass	X-Ray Diffrac	volume	
b	VM	VM			Basin:	Damodar		Eq Moist:	3.00%	mass	Coal:		
1/psi	SCF/ton	SCF/ton	Experimental Data		State:	Bihar		He Density:	1.47	g/cc	Silicia:		
0.000851	1019.655	1333.06	Absolute Sorption		Well/API No.	97-357-99800-20		ASTM Rank:	HvBitA				
P	V	V	P	V	Formation:	Barakar		Vol Mat:	36.85	dmmf			
psia	SCF/ton	SCF/ton	psia	SCF/ton	Seam:	Jarangdil		Heat Value:	14603	BTU/lbm mmmf			
0.00	0.00	0.00	0.00	0.00	Depth:	Jarangdih Mine		Min Mat:	23.51%	dry mass			
100.00	79.93	104.50	280.05	204.53	Sample ID:	IND 9		Pure Coal:	76.49%	dry mass			
200.00	148.24	193.81	600.35	336.42	Notes:			Vit Reflect:	0.83	volume			
300.00	207.30	271.01	910.05	432.60				Vitrinite:	76.9	volume			
400.00	258.85	338.41	1202.65	516.83	Moist:	9.10%	mass	Inertinite:	20.6	volume			
500.00	304.26	397.77	1501.40	580.06	Temp:	115	F	Liptinite:	2.5	volume			
600.00	344.55	450.44	0.00	0.00									
700.00	380.54	497.50	0.00	0.00									
800.00	412.89	539.79	0.00	0.00									
900.00	442.12	578.01	0.00	0.00									
1000.00	468.67	612.72											
1100.00	492.88	644.37											
1200.00	515.05	673.36											
1300.00	535.43	700.01											
1400.00	554.23	724.58											
1500.00	571.63	747.33											
1600.00	587.77	768.43											
1700.00	602.79	788.06											
1800.00	616.80	806.38											
1900.00	629.90	823.50											
2000.00	642.17	839.55											
Instructions													
Enter sample description information													
Enter additional measurement data													
Enter values for VM & b													
Enter value for mineral matter (dry)													
Enter experimental sorption P & V (absolute)													

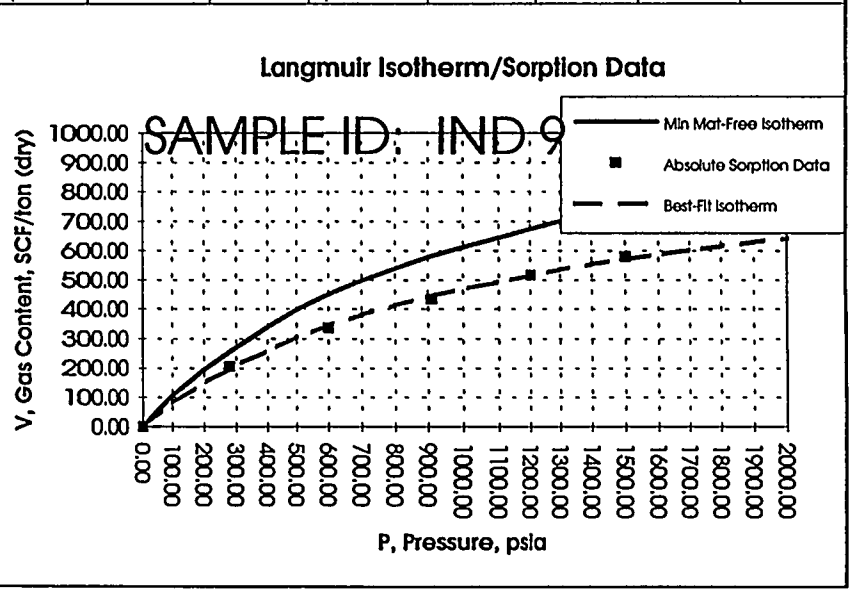


Figure 6



NOTES

INTERGAS '95

May 15-19, 1995
The University of Alabama
Tuscaloosa, Alabama USA

9522

Opportunities for the Development and Utilization of Coalbed Methane in Three Coal Basins in Russia and Ukraine

J.S. Marshall, R.C. Pilcher and C.J. Bibler,
Raven Ridge Resources, Incorporated

ABSTRACT

Increased utilization of coalbed methane in Russia and Ukraine would help meet environmental goals as well as increase mine productivity, efficiency, profitability, and safety. Natural gas dominates the fuel mix of these countries. While coal remains a prominent fuel source, production has been steadily decreasing, falling 31% since 1986. Conventional oil production peaked in 1987-1988 with current production at only 69% of peak. Natural gas production has remained relatively steady, with only a slight decline; comprising 46% of the fuel mix in Russia and 42% in Ukraine. Russia produced 640 billion cubic meters of natural gas in 1992, exporting 186 billion cubic meters, while Ukraine imported 90 billion cubic meters in 1992, mostly from Russia. Increased consideration is being given to environmental problems as a result of continued mining and use of coal. Consequently, there is a desire to decrease dependency on low grade coal and utilize more natural gas. The coal mining regions of Russia and Ukraine liberate almost 4.5 billion cubic meters of methane annually, of which only 3.9% is being utilized. Development of coalbed methane resources will help these nations achieve economic objectives while making a significant contribution to improving the environment on both a regional and global level.

INTRODUCTION

This paper is a synopsis of a report written for the U.S. EPA entitled "Reducing Methane Emissions from Coal Mines in Russia and Ukraine: The Potential for Coalbed Methane Development", which is part of an ongoing U.S. EPA program being conducted in Russia and Ukraine to reduce methane emissions while increasing its utilization [1].

The Commonwealth of Independent States (CIS) is the third largest producer of coal in the world behind China and the United States. In 1990, an estimated 7.2 to 10.7 billion cubic meters (4.8 to 7.2 teragrams) of methane were emitted to the atmosphere from coal mining operations in the CIS, which represented about 20 percent of world coal mine methane emissions [2]. Between 80 and 90 percent of these emissions were liberated by underground mining operations, which are primarily located in the republics of Ukraine, Russia and Kazakhstan.

ENERGY CONSUMPTION AND PRODUCTION

Natural gas dominates the fuel mix of the CIS. It comprised 45 percent of the energy consumed in 1992, followed by oil at 27 percent and coal at 18 percent. Hard coal accounted for 88 percent of the coal consumed in 1992, and lignite (including brown coal) 12 percent.

The fuel mix for the republics of Russia and Ukraine are quite similar to the overall fuel mix of the CIS, which is to be expected because these republics are the Commonwealth's largest economic units. In Russia, natural gas accounted for 46 percent of total energy consumption in 1992, with oil accounting for 27 percent [3]. Coal comprised only 18 percent of the fuel mix; hard coal accounted for about 83 percent of the total energy derived from coal, and the remainder was from lignite. Likewise, in Ukraine natural gas dominated the fuel mix in 1992, accounting for 42 percent of total energy consumption. Oil represented 19 percent, and coal accounted for 29 percent, with hard coal accounting for more than 98 percent of all energy derived from coal [4].

Although natural gas dominates the fuel mix of both Russia and Ukraine, the two republics differ greatly in natural gas production. Russia produced 640 billion cubic meters in 1992, more than 30 percent of which was exported to other republics and European countries. Ukraine, in contrast, produced only 21 billion cubic meters of natural gas in 1991, which satisfied less than 19 percent of its natural gas demand, and it was forced to import an additional 90 billion cubic meters of natural gas to meet its energy needs.

The CIS is currently the world's third largest coal producer, after the People's Republic of China and the United States. Coal production in the USSR peaked in 1988, with total production of almost 600 million tons. Since then, however, hard coal production has declined significantly, primarily as a result of labor disruptions, chronic equipment shortages, and difficult mining conditions. Lower coal production has resulted in coal shortages in many parts of the CIS, which have led to lower output in other industries [5].

NATURAL GAS: THE DOMINANT FUEL

The CIS is the largest producer, transporter, consumer, and exporter of natural gas in the world, producing almost 40 percent more gas than the next largest producer, the United States. The CIS produced more than 778 billion cubic meters of natural gas in 1992, which represented a decline of 4 percent from the previous year. This is relatively stable compared to the large decline in oil production. Natural gas production decreased between 1991 and 1992 in every republic except Kazakhstan (up 11 percent).

Natural gas is an extremely important fuel in the CIS. Gas consumption increased over 75 percent in the 1980's [6], and it provided about 45 percent of primary energy consumed in the CIS in 1992. However, natural gas consumption decreased by 4 percent between 1991 and 1992, due to plunging economic output and rising prices (especially outside of Russia).

Coalbed methane can also be a significant gas resource that may be beneficial to develop in its own right. While various countries have long used this resource on a small scale, primarily for on-site needs at mines, it has been only within the past decade that coalbed methane has gained widespread recognition as a viable alternative to conventional fuels. Mining industry and government officials in Russia and Ukraine have stated their desire to recover and utilize more coalbed methane, but funding and technology transfer are needed in order for these countries to implement new coalbed methane resource development projects.

There are four coal basins in Russia and Ukraine where hard coal is mined and which have the potential for coalbed methane development (Figure 1). They are:

- The Donetsk Basin (Donbass): located in southeastern Ukraine and western Russia;
- The Kuznetsk Basin (Kuzbass) located in western Siberia;
- The L'vov-Volyn Basin: located in western Ukraine, is the southeastern extension of the Lublin Basin in Poland;
- The Pechora Basin: located in northern Russia, almost entirely above the Arctic Circle.

This paper will focus on the Donetsk, Kuznetsk, and L'vov-Volyn basins (the Pechora basin has not yet been evaluated).

Of the three basins, the Donetsk and Kuznetsk appear to have the largest near-term potential for coalbed methane development. Both of these regions are heavily industrialized and would have many opportunities for coalbed methane utilization. The L'vov-Volyn region is predominantly agricultural, and it is likely that coalbed methane use would primarily be limited to the mines.

Characteristics of each basin are summarized in Table 1 and a more detailed description of each basin is provided below.

The Donetsk Basin

As shown in Figure 2, the northwestern portion of the Donetsk Coal Basin is in Ukraine, while the southeastern portion is in Russia. Coal mining began in the basin in 1723, and as of 1991 there were 24 coal production associations operating 308 underground mines [12]. The Carboniferous deposits contain over three hundred seams, of which one hundred seams are considered workable. Seams vary in thickness from 0.45 to 2.5 meters, averaging 0.9 meters, and dip from horizontal to greater than 35°. Coal mines in the Donetsk are extremely deep. Over 40 percent of the mines have workings deeper than 700 meters, and one-third have workings deeper than 1000 meters [13].

Methane Liberation

Coal mines in the Donetsk Basin are some of the gassiest in the world. Of the basin's 25 coal production associations, 19 contain mines that liberated methane in 1991. Nearly 3.4 billion cubic meters of methane were liberated, with 16 percent, or 539 billion cubic meters captured by methane drainage systems in 100 mines. Only 170 million cubic meters of this methane were used (exclusively in boilers at the mines), thus 3.2 billion cubic meters were emitted to the atmosphere. Methane used by the mines represents 32 percent of the total drained methane, and only 5 percent of the total methane liberated.

These data suggest that there are good opportunities for increased methane drainage and utilization at Donetsk Basin mines. For example, Pochenkova, a typical mine in the Makeevugol coal production association, drained only 20 percent of the methane it liberated in 1991, and used only about half of the methane it drained.

The L'vov-Volyn Basin

The L'vov-Volyn Coal Basin, located in western Ukraine (Figure 3), is the southeastern extension of the Lublin Coal Basin in Poland. Coal mining began in 1954 and there is currently one coal production association, Ukrzapadugol, operating 17 mines. The average seam thickness is 0.95 m and the depth of mining ranges from 300 to 600 m [14].

Methane Liberation

The twelve mines in the southern part of the basin, together with one in the northern part, emitted 153 million cubic meters of methane in 1991. This amount represents only 5 percent of total coal mining methane emissions from Ukraine. Although four of the mines have methane drainage systems, only 6 percent of all methane liberated is captured by those drainage systems, and none is utilized.

Potentially significant project opportunities exist at several mines. No. 10 Velikomostovsk, for example, produced more than 1 million tons of coal in 1991, and emitted 28 million cubic meters of methane to the atmosphere. Of this, nearly 3 million cubic meters (approximately 10 percent) were medium-quality gas recovered by mine drainage systems, and the remaining 25 million cubic meters were released in mine ventilation air. The No. 4 Velikomostovksk produced 792.8 thousand tons of coal, and emitted nearly 12 million cubic meters of methane to the atmosphere. Of this, approximately 4 million cubic meters (35 percent) were medium-quality gas recovered by drainage systems.

The Kuznetsk Basin

The Kuznetsk Coal Basin, also known as the Kuzbass, is the second largest coal basin in the CIS and is located in western Siberia. Coal mining began in the mid-nineteenth century as the Trans-Siberian railway was being developed. Kemerovo, located in the northern end of the basin, and Novokuznetsk in the south are important industrial centers. The basin contains 25 geological-commercial regions, 10 of which do not have active mines. As of 1991, the basin contained 71 mines operated by 6 coal production associations (Figure 4). More than 100 seams, with an average thickness of 2.5 m., are being mined. The thickness of the overburden of the seams mined underground ranges from 300 to 800 m [15].

Methane Liberation

In 1951, the Kuznetsk Coal Basin became the first area to utilize methane drainage systems in underground mining in the USSR. All of the active underground mines are gassy, liberating more than 1.2 billion cubic meters in 1991. In spite of highly gassy conditions, only 211.9 million cubic meters (17 percent) of this gas were removed by drainage systems in 32 mines. All of this gas was then emitted to the atmosphere, as none was utilized.

COALBED METHANE RESOURCE ESTIMATES

These estimates of associated coalbed methane resources were based on data which was provided by the Skochinsky Mining Institute in Lyubertsy, Russia, and by mining enterprises and research institutes that have collected data for purposes of producing coal and maintaining mine safety.

These estimates should be considered preliminary, but mining experience in Russia and Ukraine and available data indicate that the coalbed methane resource is large. It is clear that more detailed data collection activities are warranted to better assess the resource and identify the most promising production locations.

Preliminary estimates suggest that the coalbed methane resources associated with balance reserves of coal contained in mines of the Donetsk, Kuznetsk, and L'vov-Volyn Coal Basins are substantial, ranging from 627 billion to 1.1 trillion cubic meters. Additional methane resources are present in non-balance coal reserves and in areas beyond the boundaries of the coal production associations and their associated mines. According to data from the former USSR Academy of Sciences [16] and the Eastern Mine Safety Research Institute [17], the total estimated coalbed methane resource contained in just the coal seams of the three basins is greater than 7.8 trillion cubic meters. Additional methane resources are contained in the partings and strata surrounding the coal seams. It is estimated by the above mentioned institutions that the total coalbed methane resource contained in the three basins is more than 52.1 trillion cubic meters.

To fully evaluate the coalbed methane development potential of each coal basin, it will be necessary to estimate coalbed methane resources and assess what percentage is recoverable using available technologies. This effort will require detailed information on the coal reserves, including geologic and reservoir characteristics, which would be generated by a carefully designed exploration program.

Such information is not currently available for the coal reserves of the Donetsk, Kuznetsk and L'vov-Volyn basins. Thus, in this paper the coalbed methane resources associated with the balance coal reserves of these basins have been estimated based on available data using two approaches. To reflect the uncertainties associated with preparing such estimates where data are limited, the coalbed methane resource estimates are presented as ranges. For the low end of the range, estimates were based on the measured methane contents of coal reserves in each basin. The high-end estimates were developed using specific emissions (i.e., the amount of methane liberated per ton of coal mined). These methods, and the uncertainties associated with them, are discussed briefly below.

Coalbed Methane Resources of the Donetsk Basin

The coalbed methane resources associated with the balance coal reserves of all mines in Donetsk coal basin are estimated to range from 430 to 790 billion cubic meters. Of these resources, an estimated 140 to 280 billion cubic meters of methane are associated with the coal contained in active mining areas and 109 to 210 billion cubic meters are associated with the basin's industrial coal reserves (i.e., those scheduled for mining).

Additional methane resources are associated with non-balance reserves of coal, as well as with coal resources located beyond the boundaries of the coal production associations. According to the former USSR Academy of Sciences [16] the total estimated methane resources in the coal seams in the Donetsk basin are 1.2 trillion cubic meters, and the total estimated methane resources contained in the basin (including the coal seams, partings, and surrounding strata) are 25.4 trillion cubic meters. If these estimates are accurate, the coalbed methane resources contained in the coals account for less than five percent of the total methane resources, indicating that there are potentially numerous other types of prospective gas reservoirs within the basin including conventional stratigraphic and structural traps. The methane resources in coal and other strata could be produced if a program of pre-mining drainage or stand-alone development is initiated.

Coalbed Methane Resources of the L'vov-Volyn Basin

The coalbed methane resources associated with the balance coal reserves of all mines in the L'vov-Volyn coal basin are estimated to range from 1.0 billion to 3.3 billion cubic meters. Since coal resource data for all mines and for industrial reserves were not available, methane resource estimates could not be calculated for these categories.

Additional methane resources are associated with non-balance reserves of coal, as well as with coal resources located beyond the boundaries of the mines ("reserve regions"). Based on average gas contents calculated from data supplied by the Skochinsky Mining Institute [12, 18], and coal reserve data contained in Struev et al [19], it is estimated that these additional methane resources may amount to 1.9 billion cubic meters of methane.

Coalbed Methane Resources of the Kuznetsk Basin

The coalbed methane resources associated with balance coal reserves of all mines in the Kuznetsk coal basin are estimated to range from 194 to 342 billion cubic meters. Of these resources, an estimated 119 to 204 billion cubic meters of methane are associated with the coal contained in active mining areas and 69 to 120 billion cubic meters are associated with the basin's industrial coal reserves (i.e., those scheduled for mining).

Additional methane resources are associated with non-balance reserves of coal, as well as with coal resources located beyond the boundaries of the coal production associations. According to the Eastern Mine Safety Research Institute, the total estimated methane resources contained in coal seams of the Kuznetsk Basin are 6.6 trillion cubic meters, and the total estimated methane resources contained in the basin (including the coal seams, partings, and surrounding strata) are 26.7 trillion cubic meters. If these estimates are accurate, the coalbed methane resources contained in the coals of the basin account for less than 25 percent of the basin's total methane resources.

COALBED METHANE RECOVERY

Many opportunities for increased recovery of coalbed methane exist in Russia and Ukraine. Nearly 4.5 billion cubic meters of methane were liberated from coal mining activities in the Donetsk, Kuznetsk, and L'vov-Volyn coal basins in 1991 (Table 1). Of the 396 mines currently operating in these three basins, 136 mines, or 34 percent, had methane drainage systems in 1991. Drainage systems at these mines recovered 740.7 billion cubic meters, or 17 percent, of the methane liberated by mining, but only 170 million cubic meters (3.8 percent of total liberated) were utilized, resulting in methane emissions of over 4.3 billion cubic meters. Methane that is currently being drained but then vented to the atmosphere could now be used rather than wasted, and significantly more gas could be available for utilization with an integrated approach to methane recovery in conjunction with mining operations.

Reduction of the methane concentration in mine ventilation air for safety reasons is a prime concern in gassy coal mines throughout the world. This can be accomplished by increasing ventilation, or by decreasing the amount of gas liberated into the mine workings from the coals. Increased ventilation can be achieved by increasing the size of the fans or adding additional ventilation shafts. As the amount of methane liberated per ton of coal mined increases, the capacity of the ventilation system must also increase. Experience elsewhere has shown that there are economic limits to the amount of methane that can be removed by ventilation systems alone, and there are no economic benefits to simply venting methane to the atmosphere. Expanded methane drainage can be a profitable means of reducing the methane concentration in ventilation air, in that ventilation requirements are reduced, coal can be more rapidly extracted, and that gas recovered by drainage is often of saleable quality.

Methane Drainage Methods

There are several techniques for recovering methane in conjunction with coal mining. The optimal choice among these methods depends on site specific conditions, including:

- the thickness and depth of the targeted seam;
- the amount of methane contained in the coals;
- the number of mined seams;
- the efficiency of the ventilation system.

Detailed descriptions of the principal methane recovery techniques used in each coal basin are presented below.

The Kuznetsk Basin: Of the 71 mines in the Kuznetsk Coal Basin, 32 have methane drainage systems. The principal systems of drainage include the use of small diameter boreholes drilled from the surface into the coal seam targeted for mining, and large diameter boreholes drilled from the surface into the roadway located behind the retreating longwall. The small diameter boreholes drilled into the coal in advance of mining provide dual service by pre-draining methane and then being converted into gob wells after mining has passed. Portable pumping stations on the surface are connected to these wells to insure the evacuation of the gas from the gob, and can be moved to other wells as mining progresses. The large diameter boreholes are fitted with a manifold and fan system to remove the gas that is being produced in the gob areas. This methane is vented to the surface, which keeps it from migrating back into the active working face area.

In many active mines of the Kuznetsk Basin, underground drainage methods have been insufficient to drain the quantities of methane needed to meet safe mining standards. This is due to a pressure differential in the mines caused by the conventional ventilation systems and booster auxiliary fans. In many mines, these systems prevent efficient flow of methane into in-mine drainage systems, which cannot create a sufficient vacuum.

Donetsk and L'vov-Volyn Basins: Of the 269 mines in the Donetsk Coal Basin, 100 have methane drainage systems; four of the 17 mines in the L'vov-Volyn Coal Basin drain methane. Because of the depth of mining, underground drainage is the preferred methane recovery technique used in both basins. The two most widely used methods are cross-measure boreholes drilled from the roadways into surrounding strata and boreholes drilled from the roadways into gob areas. Underground booster pumping stations are often used to drain the methane from the boreholes. The methane is either discharged into the ventilation system away from the active mining areas, or pumped to a central vertical well and piped to the surface via surface vacuum pumps.

Options for Increased Recovery

As indicated by the discussion above, a variety of methane recovery methods are used in Russia and Ukraine, but many mines confront technical difficulties in their application. In addition, in many cases, necessary investment capital is not available to support the development of a fully integrated system of methane recovery. Methane recovery could be significantly improved in Russia and Ukraine through a variety of measures applied in the near term or over longer periods.

In the near term, basic technical improvements could increase the quality and quantity of gas recovered. Such improvements could include:

- gas quality monitoring to prevent large fluctuations in methane concentration;
- repair of leaks in the in-mine and surface gas gathering systems;
- modified drilling and completion techniques, including hydraulic fracturing, for both in-mine and surface drainage wells. This could also include changing the type of material used to cement stand pipes in place and better positioning of drainage wells.

In the longer term, an integrated approach to mine drainage could maximize the recovery of methane and improve mine profitability and safety. This approach could include recovery of methane before, during, and after mining, both from the surface and within the mine..

COALBED METHANE UTILIZATION

The best utilization options for methane from coal mines will vary from region to region, depending on the quality and quantity of the gas and local energy markets. In the Donbass and the L'vov-Volyn Basin, coalbed methane could be used as an alternative to natural gas. Ukraine is a net importer of natural gas so any replacement of natural gas with coalbed methane would reduce its dependence on imports. In the Kuznetsk Basin, high-quality coal is exported out of the region while low-quality coal is consumed locally in the domestic and industrial sectors. Thus, in this region coalbed methane use could replace this low-quality coal consumption, which would improve local air quality. The principal utilization options are discussed in more detail below.

Direct Utilization Options

The Donetsk and Kuznetsk Basins are both heavily industrialized regions, and coal is used extensively for steam and electrical generation. The largest consumers of energy in these regions are machine factories, petrochemical plants, metallurgical factories, and of course the coal industry. The mining, power, and industrial complexes which dominate both regions were originally developed with an emphasis on large-scale production, often at the expense of efficiency, profitability, and the environment. The sheer size of these complexes makes the task of addressing economic, social, and environmental reforms very difficult.

Coalbed methane utilization would clearly benefit these regions by helping them meet increasing energy needs with a less polluting, local energy source. Like conventional natural gas, coalbed methane is an environmentally acceptable fuel because when burned, it emits virtually no pollutants such as sulfur dioxide or particulates, and it emits much less carbon dioxide than coal and oil. Some fuels that coalbed methane

could replace are brown coal, low-quality hard coal, and coke oven gas. Specific uses will be dependent on the conditions in the vicinity of the mines, but could include:

- on-site coal drying;
- on-site heating of water and air;
- heating or refrigeration of ventilation air;

Utilization options in other local industries include, but are not limited to:

- displacement of brown coal and low-quality hard coal,
- displacement of coke-oven gas, and
- displacement of imported natural gas, primarily in Ukraine.

Power Generation Options

Currently, there are only 17 mines in the Donetsk Basin that utilize coalbed methane, and all of them use it in boilers at the mine site. No mines in the L'vov-Volyn or Kuznetsk regions utilize coalbed methane. Opportunities exist for the generation of electricity and steam at mine power plants; electrical power is used at all coal mines and thermal heat is supplied to the surrounding communities for district heating. Currently, these mines generate the majority of their electricity and steam from coal. Coalbed methane could displace the burning of coal which pollutes, and, in regions such as the Donetsk Basin, is in increasingly short supply. Several power generation options are:

- converting boilers to intermittent use of gas,
- gas turbines,
- internal combustion engines, and
- cofiring with natural gas.

SUMMARY AND RECOMMENDATIONS

Development of coalbed methane as an integral part of the energy economies of Russia and Ukraine will require developing and implementing comprehensive programs for resource development and utilization. Such programs would recognize the importance of developing coalbed methane in concert with coal extraction. As has been described in previous chapters, economic benefits to coal mining are enhanced when methane drainage and use are improved. Many opportunities for the near-term use of coalbed methane exist. The most likely candidates for near-term increases in coalbed methane development are projects that will directly impact the economics of the mining industry and improve the safety and health of miners and the surrounding community. Furthermore, regional economic benefits, such as jobs and an increased domestic energy base, will occur as coalbed methane recovery and use increases. As has been stated previously, coalbed methane is most valuable when used locally by the mine from which the coalbed methane is being recovered or in nearby allied industries. Value of the methane as a substitute for other fuels is increased when enrichment, drying, and compression of the gas are not required. Of course, if large amounts of imported conventional natural gas are consumed, preparation required for upgrading coalbed methane for injection into pipelines may be a viable economic option.

There is a keen interest in coalbed methane development in both Russia and Ukraine. Agencies such as the Ministry of Fuel and Energy of Russia and the State Coal Committee of Ukraine, numerous coal industry research institutes, as well as several of the coal production associations of the L'vov-Volyn, Donetsk, and Kuznetsk basins are all actively investigating opportunities to expand methane recovery and use. Based on the results of this study, it is clear that the development and utilization of coalbed methane in Russia and Ukraine, and specifically the three study regions, should be further investigated. Mechanisms for encouraging or facilitating coalbed methane use should be evaluated, appropriate policies and incentives should be developed, and development and utilization of coalbed methane should be a priority in the energy sector restructuring programs of the two republics.

Foreign governments and international agencies, as well as foreign companies, can assist Russia and Ukraine with this process by providing financial and technical assistance for coalbed methane projects. Follow-up efforts to this report should be designed to inform, educate, and train the appropriate technical experts and government personnel regarding the potential role for coalbed methane development. Subsequent studies should evaluate the feasibility of coalbed methane development and utilization at specific sites, ultimately leading to the implementation of demonstration projects and/or commercial coalbed methane projects.

REFERENCES

1. Marshall, J.S., R.C. Pilcher, C.J. Bibler and D.W. Kruger, 1994, Assessment of the Potential for Economic Development and Utilization of Coalbed Methane In Russia and Ukraine: U. S. EPA, Washington, D.C., 68 p.

2. EPA, 1993, International Methane Emissions Estimates: 1990: Office of Policy, Planning & Evaluation, in preparation.

3. DOE, EIA, 1994, International Energy Annual 1992, Washington, D.C.

4. PlanEcon, Inc., 1993a, PlanEcon Energy Outlook for the Former Soviet Republics, Washington, D.C., June 1993.

5. International Monetary Fund (IMF), 1992, Economic Review: The economy of the former U.S.S.R. in 1991: International Monetary Fund, Washington, D.C. April 1992, 103 p.

6. DOE, EIA, 1992, International Energy Annual 1990, Washington, D.C., 187 p.

7. PlanEcon, Inc., 1992b, PlanEcon Energy Report, Washington, D.C., vol.2, no. 2, 92 p.

8. Foreign Broadcast Information Service (FBIS), 1992a, Fact sheet on Russia's coal sector, FBIS-USR-92, 28 September 1992.

9. Foreign Broadcast Information Service (FBIS), 1992b, Coal production potential examined FBIS-USR-92-150, 23 November 1992, p. 71-73.

10. PlanEcon, Inc., 1993c, PlanEcon Energy Report, Washington, D.C., vol. 3, no. 4, 44 p.

11. Sagers, M.J., 1993, The energy industries of the former USSR: A mid-year survey: Post-Soviet Geography, v. 34, p. 341-418.

12. Skochinsky Mining Institute, 1993, Data tables received during visit to Skochinsky Mining Institute in Lyubertsy, Russia, March 1993.

13. Foreign Broadcast Information Service (FBIS), 1992c, Data on safety conditions in mining sector/Ukraine, FBIS-USR-92-085, 8 July 1992, p. 94.

14. Kozlovsky, E., ed., 1987, Gornaya Encyclopedia: Sovietskaya Encyclopedia, Moscow, vol. 3.

15. Airuni, A.T., 1991, Sposoby bor'by s vydeleniem metana na ugol'nykh shakhtakh: published by TsNIElugol, Moscow, 64 p.

16. USSR Academy of Sciences, 1990, Gazobil'nost' kamenougol 'nykh shakht SSSR: Kompleksnoe osvoenie gazonosnykh ugol'nykh mestorozhdenii, Moscow: Nauka, p. 39-3.

17. Eastern Mine Safety Research Institute, 1992, Data sheet given to J.S. Marshall and R.C. Pilcher during meeting in Kemerovo, Russia, 13 April, 1992.

18. Skochinsky Mining Institute, 1991b, Prognoznyi katalog shakhtoplastov Podmoskovnogo, Lvovsko-Volynskogo, i Dneprskogo Ugolnykh Basseinov s kharakteristikoi gorno-geologicheskikh i gornotekhnicheskikh faktorov na 1995 i 2000: published by The Skochinsky Mining Institute, Moscow, 38 p.

19. Struev, M.I., V.I. Isakov, V.B. Shpakova, et al, 1984, L'vovsko-Volynskii kamennouogol'nyi bassein, Geologo-promyshlennyi ocherk: published by Naukova Dumka, Kiev, Ukraine, 270 p.

20. Silinnii, V.I., 1992, Map given to J.S. Marshall and R.C.Pilcher during meeting at Ukrainian Volynsk Geological Exploration Expedition, Vladimir-Volynsk, Ukraine, 4 April 1992.

21. Zabourdyaev, V., 1992, Data tables received during visit to Skochinsky Mining Institute in Lyubertsy, Russia, April 1992.

22. Kozlovsky, E., ed., 1986, Gornaya Encyclopedia: Sovietskaya Encyclopedia, Moscow, vol. 2.

TABLE 1. SUMMARY OF SELECTED COAL BASIN CHARACTERISTICS (1991 DATA EXCEPT WHERE OTHERWISE NOTED)

CHARACTERISTIC	DONETSK COAL BASIN	L'VOV-VOLYN COAL BASIN	KUZNETSK COAL BASIN	TOTAL
GENERAL CHARACTERISTICS				
Basin Area (thousand square kilometers)	60	3.2	26.7	89.9
Total Documented Coal Reserves (Billion Tons)	140.8	2.1	637.0	779.9
Coal Production, (Million Tons)	150.4	9.5	58.9	218.8
Average Methane Content (m^3/T)	14.7	6.9	11.9	
MINE DATA				
Number of Mines	308	17	71	396
Number of Mines That Emit Methane	211*	13	71	295
Number of Mines That Drain Methane	100	4	32	136
Number of Mines That Utilize Methane	17	0	0	17
METHANE LIBERATION DATA				
Total Methane Liberated (Mm^3)	3,390.4	153.0	942.3	4,485.7
Methane Liberated From Mines With Drainage Systems (Mm^3)	2,452.4	63.8	992.6	3,508.8
Methane Captured by Drainage Systems (Mm^3)	538.9	6.3	243.5	788.7
Methane Utilized (Mm^3)	170.2	0	0	170.2
Specific Emissions (m^3 methane/ton of coal mined)	22.5	12.8	21.0	

Sources: [12, 14, 21, 22]
*1990 Data

TABLE 2. SUMMARY OF ESTIMATED METHANE RESOURCES ASSOCIATED WITH BALANCE RESERVES OF COAL IN THE DONETSK, L'VOV-VOLYN, AND KUZNETSK COAL BASINS

	ESTIMATED METHANE RESOURCES (BILLION m^3) ASSOCIATED WITH BALANCE RESERVES OF COAL, CALCULATED ACCORDING TO:		
COAL BASIN	ALL MINES	ACTIVE MINES	INDUSTRIAL RESERVES
DONETSK	433-788	144-279	109-209
L'VOV-VOLYN	Not Available	1-3	Not Available
KUZNETSK	194-342	119-204	69-120
TOTAL	627-1131	264-486	178-329

FIGURE 1 MAJOR COAL BASINS OF THE FORMER SOVIET UNION

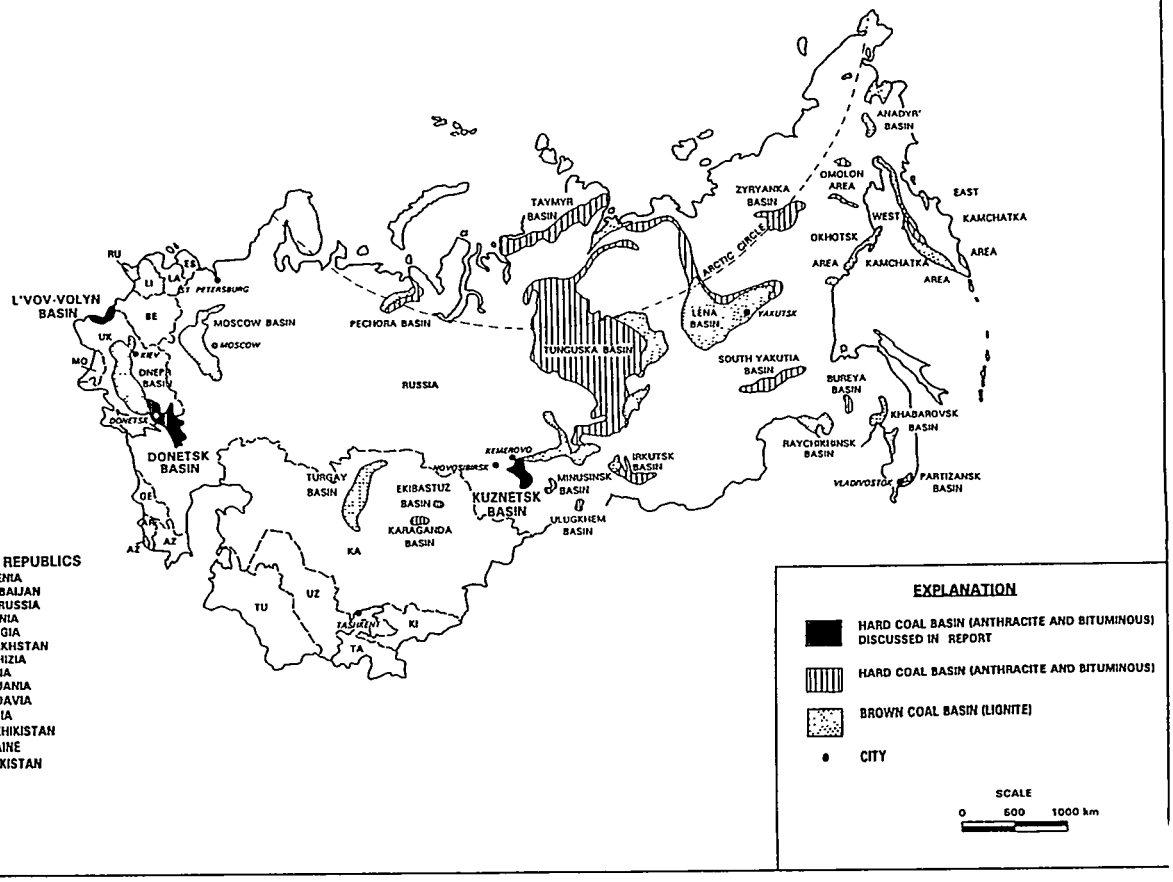


FIGURE 2 LOCATION OF PRODUCTION ASSOCIATIONS IN THE DONETSK COAL BASIN, UKRAINE AND RUSSIA

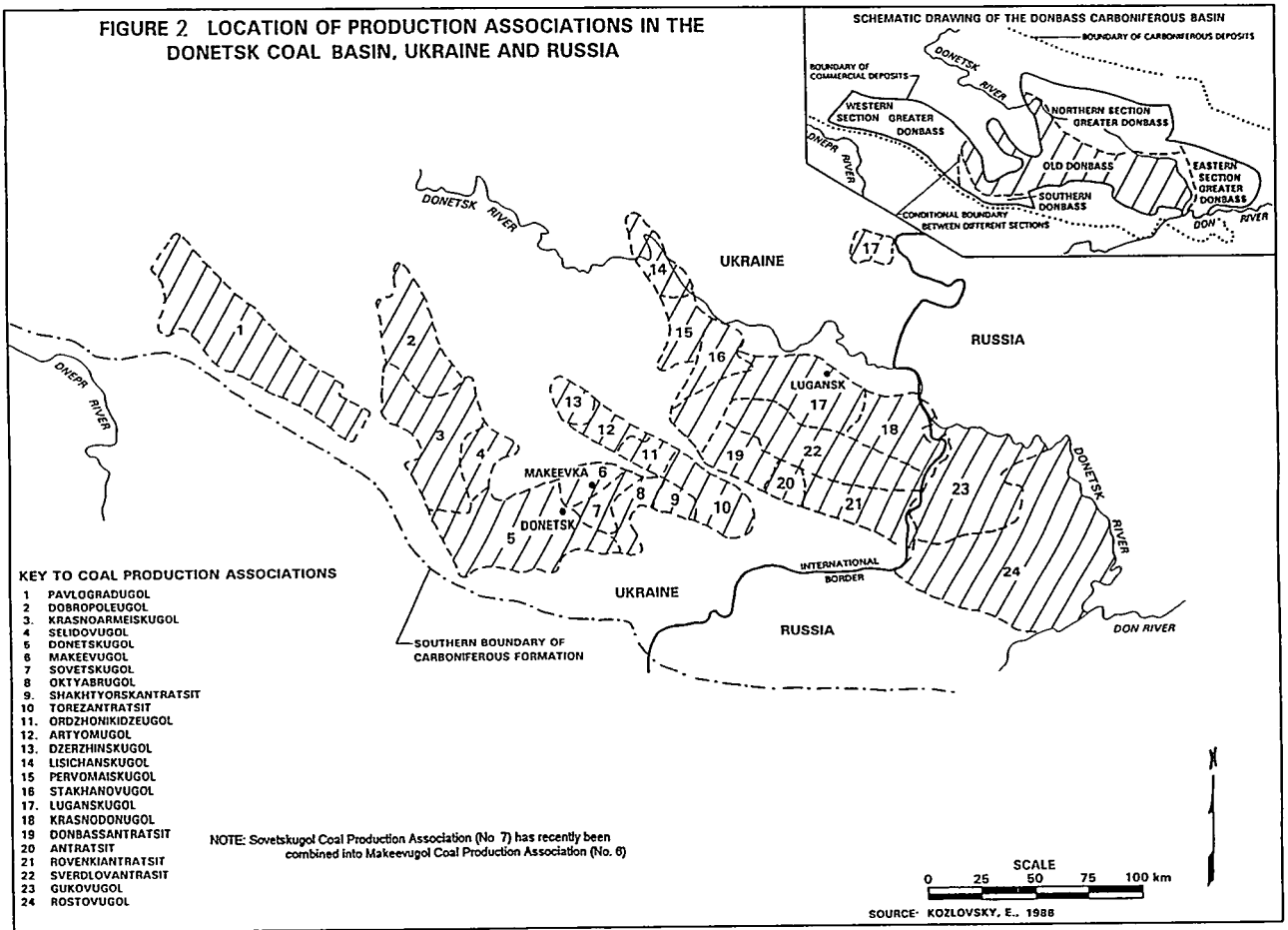


FIGURE 3 . L'VOV-VOLYN COAL BASIN, UKRAINE

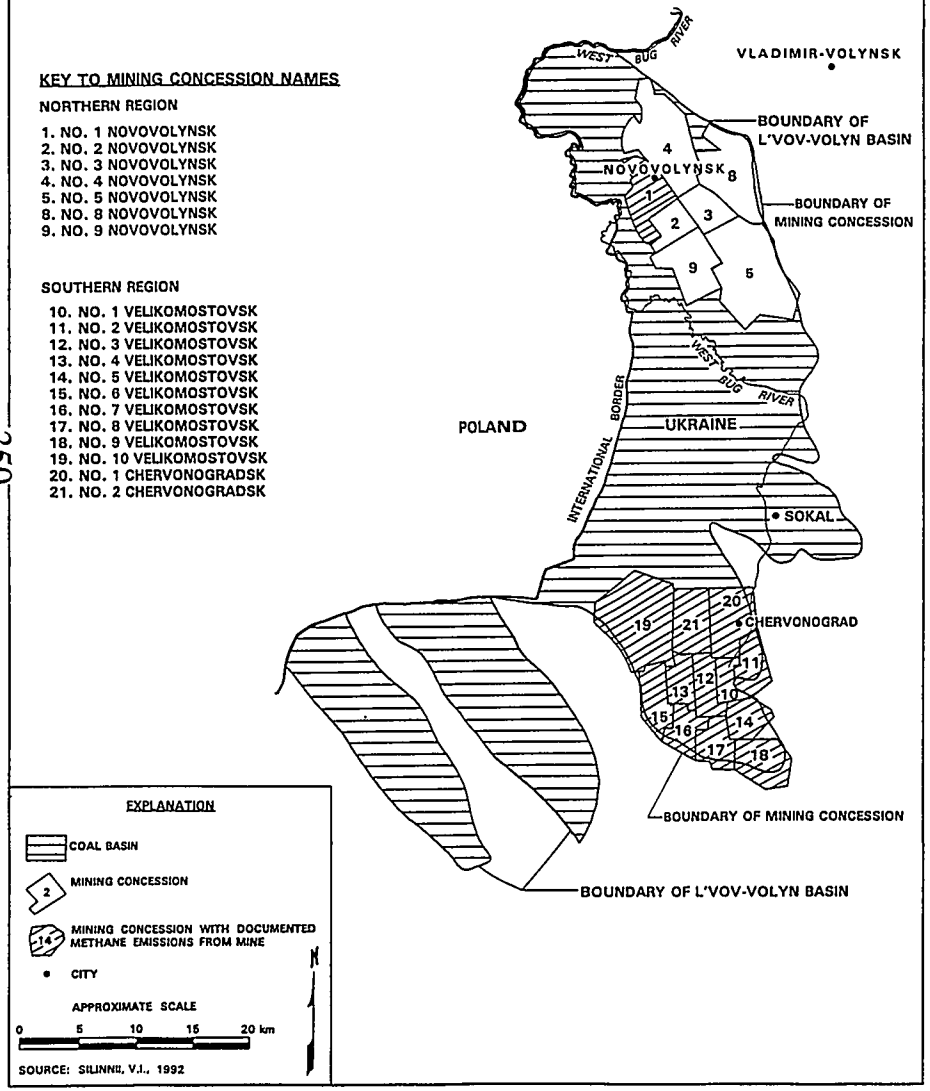
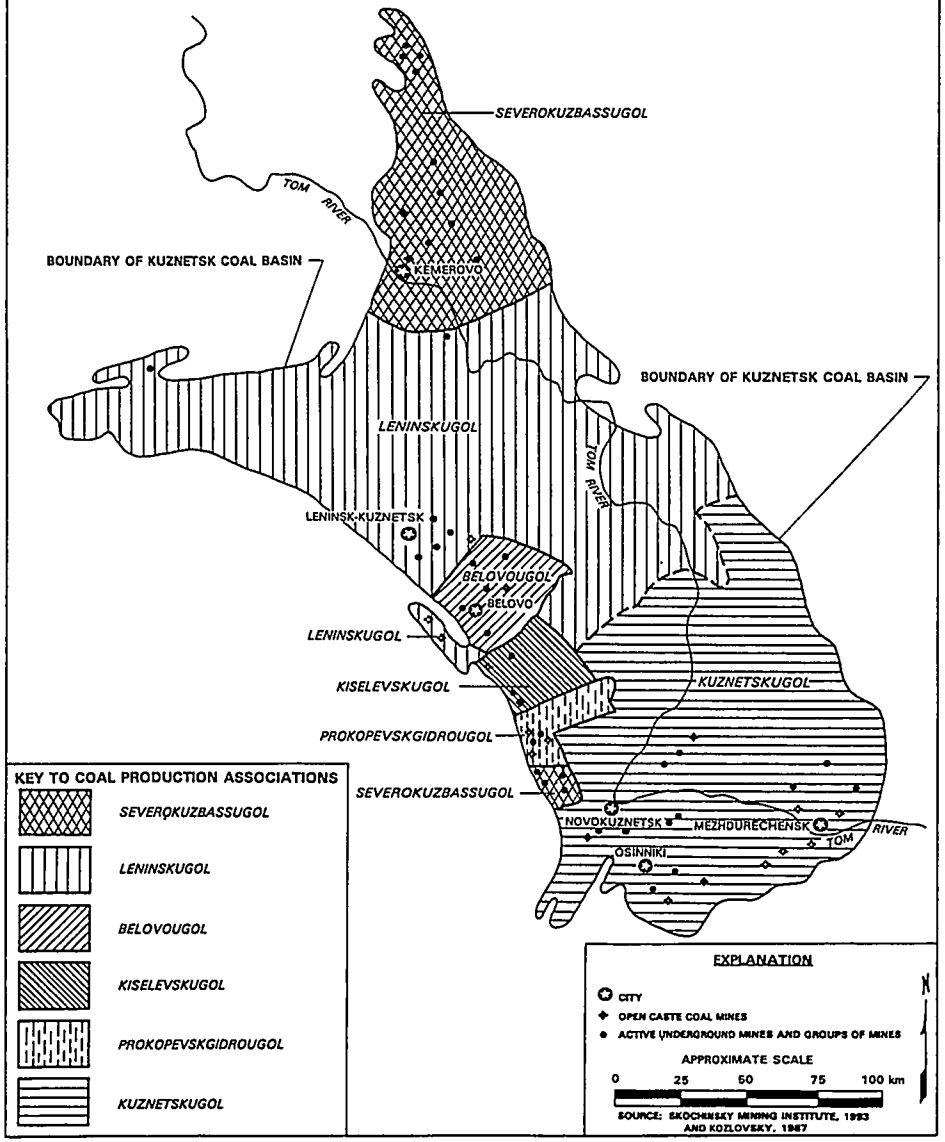


FIGURE 4 LOCATION OF COAL PRODUCTION ASSOCIATIONS IN THE KUZNETSK COAL BASIN IN RUSSIA





NOTES

INTERGAS '95

May 15-19, 1995
The University of Alabama
Tuscaloosa, Alabama USA

9557

Coalbed Methane Recovery in the Czech Republic

G. Takla, J. Bezdek and Z. Vavrusak, Underground Exploration and Mine Safety, Inc., The Czech Republic

ABSTRACT

The most important hard coal basin in the Czech Republic is the Ostrava - Karviná Coal Basin (OKR). This basin extends over an area of 1600 km^2 (400,000 acres). The Carboniferous basin fill contains 255 seams, ranging from high volatile bituminous coal to anthracite. The net coal thickness amounts to 150 m (492 ft). The coal has a methane content between 4.4 to 20 m^3/t (141-640 cuft/t).

In the OKR, about 120 million cubic meters per year (about 4.24 Bcf/y) of methane are produced by gas drainage plants from a number of collieries. The methane is used in local industries. Several measures were taken to increase the methane extraction in active mines and in areas of shut down collieries. Additionally, pilot projects for coalbed methane production have been started in virgin coal bearing areas with no previous coal production. The authors' company is progressing with such a pilot project, with the first CBM well completed recently. Results up to date are encouraging. All these activities are designed to increase the safety in mines, to reduce methane emissions to the atmosphere, and to develop new sources of energy.

INTRODUCTION

The hard coal reserves in the Czech Republic are found in one major and three minor coal mining districts areas : Ostrava - Karviná, East Bohemia, Kladno and in West Bohemia (Fig. 1).

The Ostrava - Karviná Coal Basin (OKR) contains the most significant of the coal deposits. It covers an area of about 1600 square kilometers (about 0.4 million acres). This corresponds to about 25% of the Upper Silesian Coal Basin, which straddles the Polish/Czech border. Within that area about 335 km^2 (83 000 acres) belong to mining claims of individual collieries. Hard coal production in the OKR represents more than 95% of the total hard coal production in the Czech Republic. More than 99.8 % of methane emissions from mines in the Czech Republic are related to mining operations in the OKR.

Coal in OKR is extracted by two mining companies, namely by OKD Inc., Ostrava, and by CMD Inc., Kladno. The authors' company, DPB Inc., Paskov, is a subsidiary of OKD Inc.

THE OSTRAVA-KARVINÁ COAL BASIN : BRIEF GEOLOGIC DESCRIPTION

Coal bearing sediments of the OKR range in age from Namurian A to Westphalian A. The OKR contains two different Carboniferous formations:

The Ostrava Formation was laid down under coastal plain conditions, with marine transgressions and regressions. It consists of four members. The coal seams of the Ostrava Formation are characterized by a relatively high dispersion of the volatile matter values.

The Karviná Formation was formed after a short hiatus under entirely continental conditions. This resulted in a substantially greater coal seam thickness, with less dispersion in coal rank values. The formation is divided into three members.

Both formations contain productive layers with a total of 255 coal seams, 120 of which are considered as workable. The total net coal thickness is appoximately 150 meters (492 feet).

The Ostrava Formation contains 168 coal seams with an average coal thickness of 0.73 m (2.4 ft), and the Karviná Formation 87 coal seams with an average coal thickness of 1.2 m (3.94 ft).

The coal bearing Carboniferous formations are overlain by Miocene clays in the northern part of the OKR, and by hard rocks of the Silesian and Upper Silesian nappes in the southeastern part. The overburden thickness varies between 220 and 1000 meters (722-3280 ft).

In the OKR coals ranging from hight volatil bituminous coal rank to anthracite are exploited. As an average, OKR coal contains 0.6% of sulphur, 15% of ash, 3.5% of moisture, and 23% of volatile matter. The average heating value is 25.5 MJ/Kg (corresponding to 10,965 Btu/lb). Approximately 73% of the coal is of coking grade.

The structural style of the OKR changes across the Orlová - Michálkovice folded and faulted zone. The structural differences between the two sides of the tectonic feature are also expressed in the hydrogeology of these areas. Furthermore, this tectonic boundary separates two areas with different rates of gas emanations in coal mining operations. Coal mines in the western area tend to release higher amounts of gas during mining, combined with a higher water production, compared to the ones on the eastern side of the tectonic feature.

According to the present state of knowledge, and also in comparison to the Polish part of the Upper Silesian coal basin, the coal of the OKR contains an average of 4.4 to 20 cubic meters of methane per metric ton of coal (equivalent to 141-640 cuft/t according to U.S. standard), (Fig. 2).

The coal layers in the OKR are generally considered as dry. The primary source of water in the coal mines is the Miocene detritic layer, a sandstone aquifer overlying the Carboniferous. The water in the mines is highly saline, with a high amount of dissolved chlorides and sulphates.

HISTORY OF MINE GAS DRAINAGE IN THE OSTRAVA - KARVINÁ BASIN

Coal mining in the OKR started about 200 years ago. In the course of industrial mining development, difficulties were experienced from the high methane content of the coal. Since the middle of last century, a total of 68 gas explosions was recorded from the mines operated, with many miners killed and severe economic losses. At the beginning of this century, total coal production per year in the OKR exceeded five million tons. The oldest recording of the quantity of methane drained by mine ventilation is known from the year 1910. In the course of this year the coal production increased to 7.67 million metric tons (8.45 million short tons) per year, accompanied by a release of methane averaging 589,000 cubic meters per day (20.8 million cubic feet per day). From the years 1905-1908, first methane outbursts became known from exploration drilling in coal beds of new coal fields south of the mining areas in operation at the time. Historical data on coal production and total methane released in the OKR are summarized in Table 1.

In the course of the advance of mine mechanization and increase of coal mining intensity, it became necessary to introduce a system of methane drainage in the mines, for safety reasons. Following the experience in other European coal mine districts, a system was designed to insulate and drain part of the methane liberated during coal mining.

At the surface of each colliery, a methane drainage plant was erected, equipped with vacuum pumps. The methane is drawn into these plants by means of pipes, connecting the surface facilities with the sites of underground operations. In the vicinity of mine workings and into the hanging-wall of gas bearing coal, boreholes were drilled to drain the gas from the mines. In some longwalls, applying this method, it is possible to reduce the amount of methane released into the atmosphere by up to 50 % or more. During the 30 years of operation of mine methane drainage, an efficiency of about 30 % of all the methane released was reached. This means that about 30 % of the total amount of methane released from mining operations in the whole mining district is collected and drawn into the methane drainage plants.

There must be kept in mind that due to leakages in rock strata, imperfections in the conductor casing strings of boreholes etc., some dilution of the mine gas occurs. Considering the fact that the whole system works below atmospheric pressure, some air may be sucked in, so that the final methane concentration becomes reduced to about 50-55 %.

It should also be kept in mind that this system was designed for mine safety in the first place, and that in the first period of operation all drained gas was vented into the atmosphere. But within a short period of time, after further development of the mine gas drainage network, ways if using this source of energy were investigated. In most mines heating plants were modified in such a way to enable them to use mine gas for heating and for the production of hot water. For the remaining amount of mine gas, which reached up to 200 million cubic meters per year (7 Bcf/y), gas pipelines were laid, in collaboration with regional gas utilities. Also, the use of methane in local industry was established, mainly in metallurgical plants and power stations.

OVERWIEV OF THE PRESENT STATE

At present, the mine gas drainage system in the OKR consists of 21 individual mine gas drainage plants with a total of 115 vacuum pumps installed. An extensive underground pipeline network connects about 5000 mine gas sources, mainly mine boreholes to this system. In addition to these boreholes, abandoned mine and "old-man" workings are connected to the system as well, separated from active mine workings by seals. From individual mine gas drainage plants, pipelines feed into the main pipeline system of the local gas utility. The gas mixture collected is then delivered to consumers in local industry, mainly heating plants and steelworks. The gas delivered consists of a mixture of methane with air, with a methane content of about 50-55 %. The equipment burning that gas has to be designed in a way to take this fact into account. The modification means that it cannot be used for a different type of gas. The typical gas mixture consists of 50-55 % of methane , 2-4 % of carbon dioxide, 1-3 % of oxygen, and 47-38 % of nitrogen. The heating value of such gas is about 19-20 Megajoule per cubic meter (510-537 Btu/cuft).

The present gas pipeline network forms a system of about 60 km (37.5 miles) total length. In view of the very low operating pressure, the diameter of the pipe used is relatively large : 200 up to 500 mm (7.8 - 19.7 in). This is due to the technical characteristics of the vacuum pumps used, which produce a pressure of only 45-50 kPa (6.5 - 7.25 psi) on the delivery side. Fig 3 shows a schematic drawing of the gas pipeline system and mine gas drainage plants.

Since the start of mine gas drainage in the OKR, a problem of venting surplus gas into the atmosphere existed. The problem is related to the requirement for operating the gas pumping plants continuously for the sake of the safety of the collieries and also to handle irregularities in consumption and deliveries. Such irregularities may occur for many technological and administrative reasons, ranging from breaks or reductions in consumption due to holidays, spersonells shifts, maintenance and repair of equipment, etc. Also, consumption increases within the collieries themselves during the winter month, or insufficient mine gas is available in the summer, leading to irregular and often insufficient deliveries to other industrial consumers.

In addition to these problems we also have to mention those related to interruptions of gas deliveries due to increases in dangerous concentrations of gas mixtures pumped from the mines, or to a reduction of the combustible mine gas content below the level allowed, limiting its use.

The surplus gas vented into the atmosphere amounts to about 10 % of the total mine gas produced by drainage systems of individual mines. Venting not only causes economical losses of gas that could potentially be used commercially, but it also raises environmental concerns by increasing total methane emissions into the atmosphere. In 1993, the volume vented into the atmosphere amounted to more than 12.6 million cubic meters (445 MMcf) of net methane. Table 2 gives an overview on the methane production from mine gas drainage plants and on the consumption of gas within the mines themselves or in the regional industry.

To increase the proportion of the gas made available to consumption and to avoid having to vent gas into the atmosphere, our company, DPB, installed a new collecting gas pipeline of more than 32 km (about 20 miles) length. This pipeline allowed to deliver a large amount of gas from the mine gas drainage plants to new customer, a large metallurgical enterprise named "Nová Hut" in Ostrava. In this case, the mine drainage gas replaces coke oven gas, which was used as long it was available before the coke production fell off. The technological use of mine drainage gas in the "Nová Hut" plant allows a continuous supply and consumption of this gas without any negative effects related to the quality of the gas mixture or irregularities in the supply of gas. Contracted volumes amount to 30-40 million cubic meters (1.06 - 1.41 Bcf) per year. These figures are based on a recalculated net content of 92 % of methane of the gas delivered. This contract allows to use all the gas produced in the mines for consumption and thus to avoid any undesirable further venting of surplus mine gas into the atmosphere for the future. The gas pipeline was put into operation on May 1, 1994.

Due to the recent reduction in the intensity of coal mining and improvements in the efficiency of mine ventilation systems, the importance of mine gas drainage for the safety of mine operations is gradually decreasing. In view of this development, DPB has worked out new methods for collecting methane from active mines.

Based on a detailed study of geological data, new locations and rock sequences were explored, where methane could have accumulated in greater quantities. At such locations specially designed mine boreholes are drilled, leading to increases in total coalbed methane production. Locations favourable for methane production could be found in the upper part of mine claims, in weathered Carboniferous strata, in faulted intervals, and also in areas with unconsolidated rocks covering coal mine areas. According to results of first tests, a development of such opportunities could considerably increase mine gas production from gas drainage plants in active mines. In the mine CSM in Stonava for example, four mine boreholes of up to 150 m (492 ft) depths were drilled into beds close to the top of the Carboniferous. After a few months of operation, production of methane from these holes rose to up to 12,000 cubic meters per day (424 Mcf/d).

In addition to conventional gas drainage in coal mines, DPB has also been involved in two fundamental development programs for exploration, production and utilization of coalbed methane from
- abandoned coal mines, and
- virgin coal seams.

These programs are based on the study "Assessment of the Potencial for Economic Development and Utilization of Coalbed Methane in Czechoslovakia" (mainly in the OKR), worked out by the U.S.Environmental Protection Agency (EPA), Global Change Division. This study recommended an integrated approach to CBM recovery in the OKR.

GAS RECOVERY FROM ABANDONED COAL MINES

Due to the political and social changes in the Czech Republic, which started in 1989/1990, coal production decreased as the coal industry was restructured and unprofitable coal mines were closed down. In the Ostrava part of the mining district of the OKR, four collieries were shut down. Mine claims of these collieries cover an area of more than 100 square kilometers (more than 24,700 acres) extending partly over very densely populated quarters of Ostrava town. After abandoning operations, the collieries were liquidated and hoisting and outlet shafts filled up in steps. Operations had continued for more than 200 years, before the ventilation systems, that diluted and vented the mine gases, were shut down. The water level in the mines would raise as predicted,

along with a gradual flooding of the mine workings to the level expected. During this stage some mine gas may leak out to the surface and out of control via old mine shafts and other potential leaks in their vicinity, and also via natural migration channels, such as fissures and tectonic faults. A risk of explosion or fire would occur, with such gas possibly finding its way into basements of buildings or industrial plants, combined with the risk of deteriorating the quality of the air by releasing methane into the atmosphere.

At three former mine sites, mine gas drainage systems and plants had been in operation at the surface before the decision to close the mines was taken. The authors'company, DPB Inc., prepared a study, showing the necessity to maintain mine gas drainage from shut-down mines even after the termination of mining in the OKR. This was the reason why the company bought the surface equipment of complex mine gas drainage plants of two mines before their closure. DPB are now converting this equipment for using it in a new function, namely for the permanent extraction of mine gas from closed down mine workings after the termination of coal mining in the area. Before the mine shafts were filled up, boreholes were drilled at mine locations noted for their maximum presence of methane. These borcholes were connected to an existing pipeline. Precautions had do be taken to avoid damage of the mine gas pipeline while the mine shafts were filled up. Some of the abandoned shafts were selected to adapt them as gas production shafts, by filling in their upper section only and leaving the bottom parts open and connected to former mine working levels, so that those could act as a reservoir for mine gas. In the upper filled up part of such shafts, pipes had to be installed so that the mine gas collected could be pumped into the mine gas drainage plant.

DPB Inc. believes that mine gas of a quality sufficient for industrial use can be pumped out from closed down mines of the Ostrava mining district. The methane content of the gas mixture produced varies from 40 to 80 %, but an increase in methane content can be expected once the filling up of the abandoned shafts is completed. A similar situation as in the case described above incited DPB in 1992/93 to put their first two surface gob wells in operation in an area of abandoned coal mines, with the purpose to verify

- the possibility of recovering gas from abandoned coal mines,
- the technical and technological requirements for drilling, completing and testing such boreholes, and
- the possibility of commercial use of this gas.

When selecting locations for gob wells, a number of geological, production, technical and organisational criteria have to be taken into account as listed in the following.

Geological and Production Criteria

- History match of gas emissions in comparison to similar observed during active coal production in selected areas.
- The chances for the presence of gas accumulations in the uppermost part of the Carboniferous sequence.
- The chances for the presence of gas that accumuled in abandoned mine workings situated in the top part of the Carboniferous formation.
- The chances for natural sealing of selected Carboniferous intervals by impermeable Miocene clays and marls.
- The chances for the presence of a large accumulation and of drainage areas in gobs for gas that was liberated while mining at deeper parts of the mines.

Technical and Organizational Criteria

- The possibility to seal off abandoned sections of coal mines from active ones by installing barriers.
- The possibility of regular inspections at the barriers to keep gas leakage under control.
- A gob gas production borchole should connect to as many gob zones as possible to take advantage of the size and drainage area of a gob gas accumulation.
- There should be adequate surface area available for the drill site.
- The technology selected for drilling into the gob zones should take into account the risk of total loss of drilling fluids.
- The possibility of connecting gob wells to existing gas drainage plants or to a gas pipeline of a local user.

The gob wells drilled were located in abandoned mine workings of Vrbice and Rychvald in the Ostrava part of the OKR, where active mining was discontinued already in the fifties.

When designing gob wells, we required that the drilling technique applied should address at least the following problems :

- Total loss of drilling fluids into the gob zones.
- Caving and deteriorating borehole stability while drilling through gob zones.
- Risk of contamination of gob zones by drilling fluids.
- Compaction of gobs that could reduce gas drainage.
- Risk of brine flowing into the borehole.
- Low methane concentration caused by long-term dilution of formation gas by mine ventilation.
- Lack of well testing methods and proper equipment available at the time.

Design and technical performance of gob wells should fulfill the following requirements :

- Low drilling and completion costs in comparison to conventional gas wells, to ensure profitablility despite relatively low production rates.
- Prevention of contamination of gob zones by drilling fluids.
- Maintenance of safety standards in drilling and production in accordance to regulations issued by the Czech Bureau of Mines.

Both gob wells were drilled in 1992/93 without coring. The design of gob well V-3 is shown on Fig. 4.

Testing of Surface Gob Wells

Testing of gob wells is expected to yield fundamental information on production pressure, volume of gas production and methane concentration, to allow estimates of profitability and to provide a basis for planning to tie in the wells into the production system of gas drainage plants already existing.

Compared to conventional gas wells, gob wells are characterized by very low wellhead pressures. The wellhead pressure of our two gob wells varied between 101.21 - 101.62 kPa (14.68 - 14.74 psi), depending on barometric pressure. The technique of well testing was therefore modified in such a way to take this peculiarity into account. A mobile vacuum pump was constructed by modifying a conventional vacuum pump so as to create the underpressure required to stimulate the flow of gas from the gob zones. The vacuum unit consisted of a vacuum pump, a measuring line allowing gas sampling, and an electric motor. The results of a short-term production test at the V-3 gob well are given in Fig. 5.

After completion of evaluating the results of the short-term production tests, a flow line was laid between the boreholes and existing gas drainage plants. Fig. 6 displays the characteristics of the gas production from the V-3 well during its first year of operation.

Both pilot gob wells of DPB Inc. demonstrated the feasibility of gob gas extraction from abandoned coal mines.

COALBED METHANE DEVELOPMENT IN VIRGIN COAL SEAMS

CBM development in virgin coal seams in the Czech Republic dates back to early 1992. This development was encouraged for several reasons :

- The occurrence of methane in active mines of the OKR.
- The high density of previous exploration throughout the OKR region, including exploration wells, evaluations and assessments of coal reserves, studies of coal deposits, etc.
- The government policy for the diversification of gas resources.
- The interest of the Czech Government and of private companies regarding the exploration and production of coalbed methane.

According to the Mining Law, the area of virgin coal seams was devided among four CBM concessionaires :

- Důlní průzkum a bezpečnost Paskov, a.s. (DPB, Inc.)
- Energie Kladno, a.s.
- Geologický průzkum Ostrava, a.s. (GPO, Inc.)
- Unigeo Ostrava, a.s.

A permit to explor for CBM was granted to all four companies. According to the Mining Law, the companies may expect to obtain a production concession in the case of successful results.

According to the energy resource policy of the Czech Government, CBM exploration is financially supported by the Ministry of Economy. Until the end of 1994, nine CBM wells were drilled. Two of the wells were fractured, with promising results for future production. Six new wells are expected to be drilled in 1995.

DPB, Inc.'s Project for Coalbed Methane Development

DPB, Inc. owns a concession for CBM exploration in ten prospection areas, covering a total of 240 square kilometers (59,304 ac) of virgin coal fields that contain 4.1 billion metric tonnes (4.5 billion short tons) of hard coal reserves. These areas are characterized by a high density of exploration wells, drilled for coal, gas and water prospection on a spacing of some 1.5 km (just under a 640 acre spacing). Several geological evaluations and studies were carried out to assess the importance of the coal reserves and to work out a documentation on the coal reserves. Accordingly, the coal deposits of these areas are well documented, with very good geological information about each of the prospection areas. However, the occurrence of methane in virgin coal seams is not well documented so far. For most of the prospection areas, data on gas content of the coal are either not available at all, or very incomplete at best. For this reason, a CBM exploration campaign with a chance of success would first have to identify the most favourable areas and coal seams by drilling pilot wells.

The CBM pilot project proposed by DPB, Inc., comprises six pilot test wells in the most promising exploration areas, which are named as follows :

- Dětmarovice - Petrovice
- Václavovice
- Příbor - západ
- Trojanovice - Frenštát.

Each of the wells will be cored in the Carboniferous interval to obtain first of all information on the gas content in the rock sequence. Core samples of the coal will be subjected to standard canister desorption tests (according to the Standard of the U.S.Bureau of Mines). Simultaneously, coals and rocks surrounding the coal sampling points will be tested to obtain information required for the design and evaluation of hydraulic frac jobs on the coal.

Work on the CBM project and exploration is carried in cooperation with U.S.experts, enabling to bridge any gaps in technical information and know-how.

Drilling, coring and completion will be assigned to local contractors, such as Moravské naftové doly Hodonín, a.s., and GPO, Inc. Special services, including hydraulic frac jobs, are contracted to a local service company, Karotáž a cementace Hodonín, a.s.

DPB´s pilot project is mainly financed by DPB itself, with contributions by the Government. But there is no doubt that foreign capital participation and foreign technical help will be required in the production phase.

The first pilot well was completed in the area of Dětmarovice. At the time of writing, at the end of 1994, core samples were subjected to laboratory tests and evaluation. Sections of three coal seams were selected for hydraulic frac treatment. The authors hope to be able to present the results at the Intergas ´95 Symposium.

Additional three pilot wells are planned for spudding in 1995 in the prospection areas of Václavovice, Příbram - západ, and Frenštát.

SUMMARY

In the present paper the authors tried to present information on some methods of coal gas processing and utilization in the largest hard coal basin of the Czech Republic., i.e. in the Ostrava - Karviná Mining District. Improvements in the methods of mine gas drainage, increased recovery of methane from shut down mines, and new coalbed methane production from coal fields of the region could contribute to the world-wide aim at improving the use of clean energy sources and reducing the emission of methane into the atmosphere.

Tab. 1 COAL PRODUCTION AND METHANE EXHALATION IN OKR

YEAR	COAL PRODUCTION (mio.t/year)	METHANE CONTENT IN OUTLET SHAFTS (thousands m^3 /day)	METHANE QUANTITY DRAINED (thousands m^3 /day)	TOTAL METHANE RECOVERY (thousands m^3 /day)
1910	7,67	589	-	589
1920	7,59	856	-	856
1930	10,67	873	-	863
1940	16,25	869	-	869
1950	13,72	910	-	910
1960	20,87	957	32,9	989,9
1970	23,86	1526,4	553,7	2080,1
1980	24,69	1381,4	568,3	1949,7
1990	20,06	999,6	379,7	1379,3
1993	16,39	677	297,9	974,9

Tab. 2 METHANE PRODUCTION FROM MINE GAS DRAINAGE AND ITS UTILIZATION (in thousands m^3 /year)

YEAR	TOTAL PRODUCTION	OWN UTILIZATION	DELIVERIES TO CONSUMERS	VENTED
1958	4300	-	2100	2200
1960	14300	-	12100	2200
1965	76233	542	61966	13725
1970	239713	41617	127907	70189
1975	235700	61158	168970	5571
1980	225028	69843	136533	18652
1985	207459	64230	120261	22969
1990	150395	65023	69085	16287
1993	117939	56544	48708	12688

Figure 1. HARD COAL DEPOSITS IN THE CZECH REPUBLIC

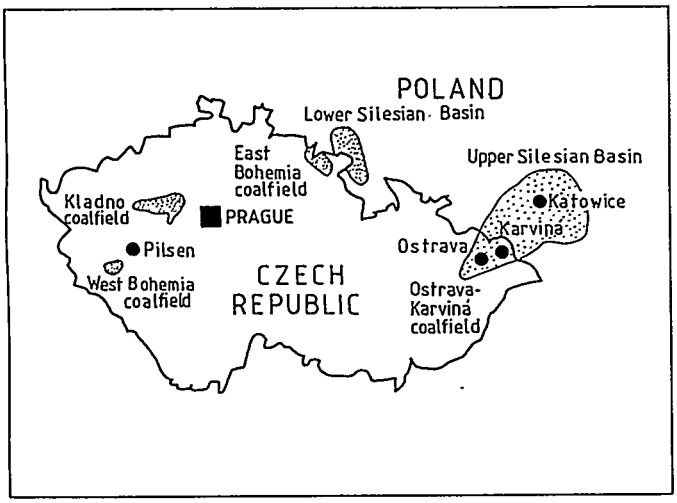


Figure 2. CONTOUR MAP OF METHANE LIBERATED DURING MINING - UPPER SILESIAN COAL BASIN, OKR - CZECH REPUBLIC (SOURCE US EPA 1992)

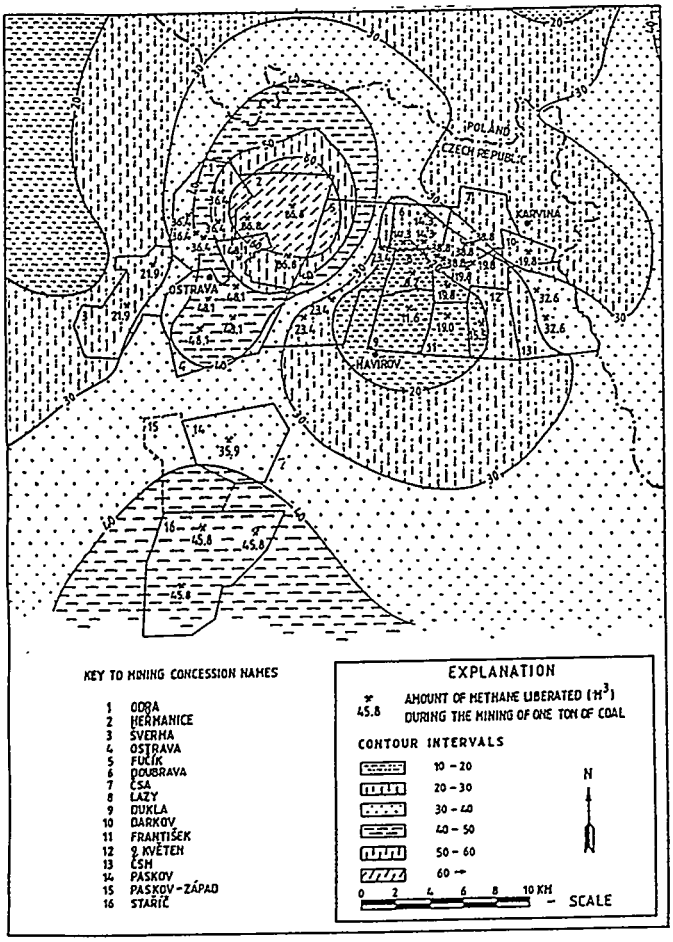


Figure 3. SCHEMATIC DRAWING OF PIPELINE SYSTEM AND MINE GAS DRAINAGE PLANTS IN OKR - CZECH REPUBLIC

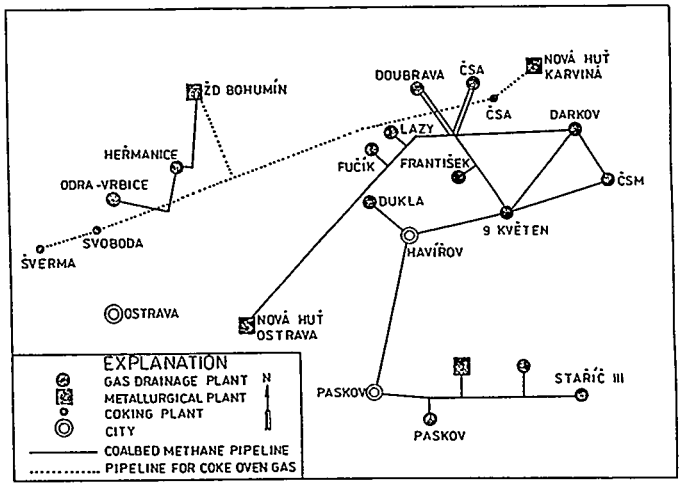


Figure 4. DESIGN OF V-3 SURFACE GOB WELL

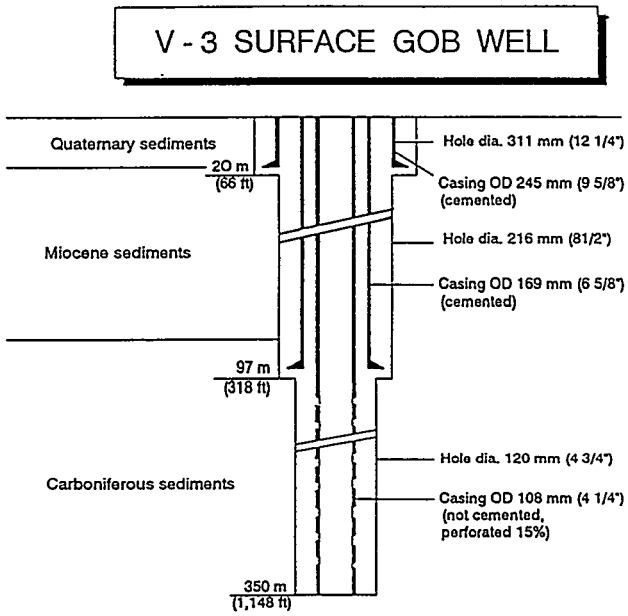


Figure 5. SHORT-TERM PRODUCTION TEST OF THE V-3 GOB WELL

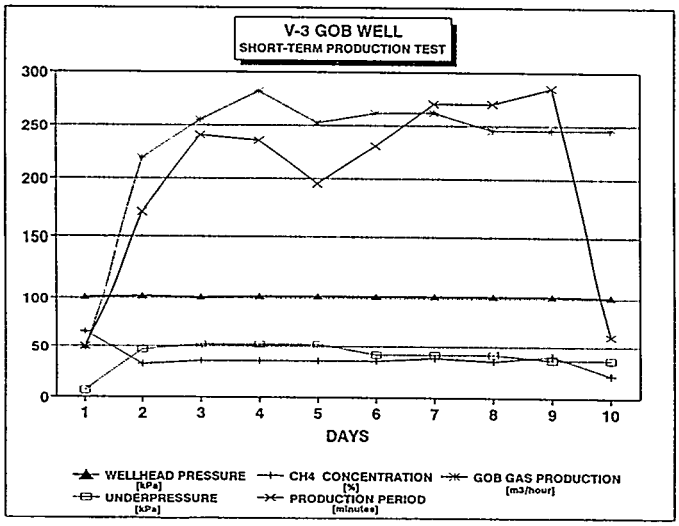


Figure 6. GAS PRODUCTION OF THE V-3 GOB WELL DURING FIRST YEAR OF PRODUCTION

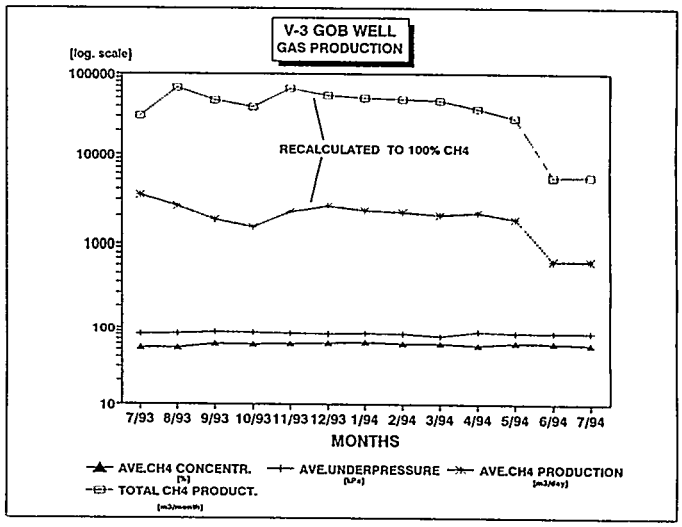
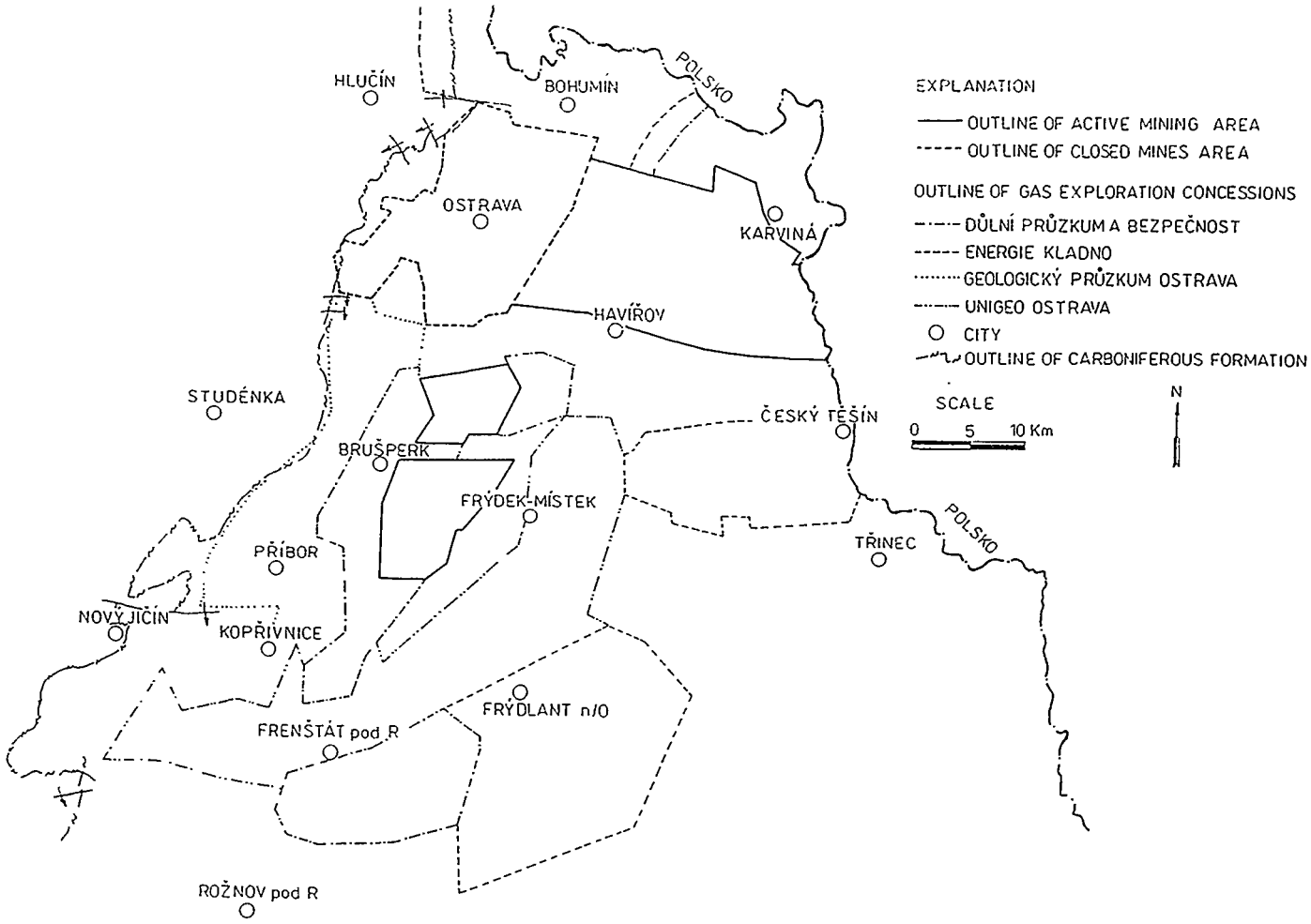


Figure 7. OUTLINE OF MINING AREAS AND GAS EXPLORATION CONCESSIONS IN OKR - CZECH REPUBLIC



INTERGAS '95

May 15-19, 1995
The University of Alabama
Tuscaloosa, Alabama USA

9562

The Resource and Exploration of Coalbed Methane in China

Su Xiaopeng, Natural Gas Laboratory, China National Petroleum Corporation, People's Republic of China

ABSTRACT

China is one of the countries with a huge coal resource in the world, and one of the four countries with the richest coalbed methane resource. By estimation, China has a total coalbed methane resource of 30-35 trillion m^3 (approx. 1000-1200 Tcf). The coalbed methane resource in these four countries including Russia, China, America and Canada, account for 90% of the total coalbed methane resource in the whole world. Most of the coalbed methane in China concentrates in the eastern part which has a dense population and relatively advanced industry. The coal is characterized by great thickness, high gas content and shallow burial. It is very favorable to the exploration and development of coalbed methane.

CHINA OWNS RICH COALBED METHANE RESOURCES

China has rich coal reserves, and coal is widely distributed across the central and eastern parts, from Harbin-Xilin in the north, to Shanghai-Kunming in the south, as well as in Xinjiang Uyge Autonomous Region. China has about 60 coal-bearing regions (Fig. 1), and the estimated total coal reserve is about 5 trillion tons, ranking among the top countries in the world. In the view of age, there are 6 coal-forming periods, including Carboniferous, Permian, Triassic, Jurassic, Cretaceous and Tertiary. The Carboniferous-Permian, Late Permian and Jurassic are the most important.

The Carboniferous-Permian is the most important, coal-bearing period, with coal widely distributed in Shandong, Henan, Hebei, and Shanxi provinces. Both the Taiyuan and the Shanxi formations developed coal beds. The coal in Taiyuan formation is massive and thick, up to 10-30m, with a maximum of 80m. Shanxi formation contains three to seven coal layers, commonly thicker than 10m. The maceral of these coals is dominated by vitrinite with locally intercalating exinite sublayer, such as in Suqiao area of Jizhong Depression. The coal is not only able to generate gas, but also able to produce oil. The coal is in the range of gas coal to anthracite. The coal in Longtan formation is typical of late Permian coal. It is very important in Southern China and is widely distributed in all the 12 provinces in the southern China. There are up to 20-40 coal layers and the minable thickness is 0.5-43m. The maceral is dominated by vitrinite, but in the region along Jiangxi-Hunan, Guizhou and Kunming, there is more exinite.

Early-middle Jurassic was a very important coal-forming period in China with coals spread almost across the whole country. However, the accumulative scale and coal development are strongly variable. The coal development is better in the north of Kunlun-Qinning mountain than in the south. Some coal basins cover several hundred thousand km^2. The inertinite content is high, generally 25-40%, with an exception of Northeast China where it is less than 10%. The coal is commonly metamorphosed slightly, and is dominated by flame coal and gas coal. The thickness is highly variable, from 1-160m. Southern Anhui province and Turfan-Hami region have the thickest coal beds. In the view of coal metamorphism, 35% of the coal resource in China is meso-peranthracite. By estimation, China has a total coalbed methane resource of 30-35 trillion m^3 (approx. 1000-1200 Tcf). Seven basins have the resource of more than 1 trillion m^3 (approx. 35 Tcf), including Ordos, Qinshui, North Huabei, South Huabei, Turfan-Hami and Junger basins and Yunnan-Guangxi-Guizhou region (Fig. 1).

THE ACCUMULATIVE CONDITION OF COALBED METHANE IN CHINA

The study of coalbed methane accumulative condition is the key of coalbed methane exploration because we may not produce gas everywhere coal is developed. The study can help us to carry out the comprehensive assessment,

choose the best place to drill and improve the exploration efficiency. Integrating the research achievements from different research institutes and the practical experiences from the coal industry, we conclude the coalbed methane accumulation is controlled by the following 12 factors.

1. Coal Rank

Because coalbed methane is mainly absorbed in the inner surface of coal matrix, there are almost no large-scale secondary migration and accumulation processes. Therefore, gas accumulation depends on the amount of gas which generated from coal and, in turn, the gas amount depends on the coal rank. According to the pyrolysis, as the coal rank becomes higher (Fig. 2), we can see the gas-generating rate increases linearly as the vitrinite reflectance increases, until anthracite is formed. From Fig. 3, gas-generating rate increases quickly from coking coal to anthracite, with the biggest increase during lean coal.

From China's coal industry, it is known that the gas (coalbed methane) content increases with the coal rank. According to the statistics from 60 coal mines, most of China's high-gas mines are found in the high-ranked lean coal and anthracite areas.

At Yangquan coal mine, which produces anthracite by surface drilling gas, is withdrawn from the coalbed and the gas is withdrawn from the coalbed and the highest single well daily production is more than 10 thousand m^3 (approx. 350 MCFD).

2. Material Composition of Coal Rock

First, the coalbed methane content is related to the coal maceral. By stimulation experiment, liptinite has the higher gas-generating capability, vitrinite and inertinite have lower capability. The former is 2.5-3 times higher than the later two.

Secondly, the gas absorptive capacity is different for different maceral coal. If the coal rank is higher than flat coal, the capacity of vitrinite is much higher than fusinite.

Third, ash content has strong influence on the coalbed methane content. The lower the ash content, the higher the gas content. According to the statistics from 20 coal mines, all of them produce low-ash coal.

3. Coal Bed Thickness

Coal is the material base of coalbed methane and the thicker the coal bed, the larger the gas amount. In the areas with multiple coal beds, the thicker coal beds usually have higher gas contents. Gas surge mainly happens near thick coalbeds, such as in Southern Anhui province, Northern Anhui province and Tianfu mining area in Sichuan province (Fig. 4).

4. Coal Bed Ratio

Coal bed ratio means the percentage of total coal bed thickness and the total coal measure strata thickness. Because coalbed methane is mainly absorbed in the inner surface of coal bed, so the thicker the coal bed, the higher the coal bed ratio, so is the relative gas content.

5. Seam Top and Seam Floor

The sealing capability and thickness of the seam top and seam floor play a controlling role in the accumulation of coalbed gas. Generally speaking, mudstone is better than sandstone. For example, in Fushun coal mine of Liaoning province, the seam top is shale and mudstone, so the gas outflow rate is 9-21 m^3/t (318-741 $ft^3/t/d$). However, in Jingxi coal mine, the seam top and floor are sandstone, the gas outflow rate is only 1-3 $m^3/t/d$ (35-105 $ft^3/t/d$). The drilling data from Nantong coal mine in Sichuan province have demonstrated that the gas content in the coal bed is low in the places where the seam top and floor contain more gas, and vice versa.

6. Geological Structure

The accumulation of coalbed methane is closely related to geological structure. Generally speaking, gas is more concentrated in the active structural area and in the linement structure area, as well as in the adjacent area of faults, because of the well-developed fractures. According to the statistics from 10 Chinese coal mines, the gas enriched area is mainly in arc-shaped folds, two flanks of fault, arch, nosal structure, anticlinal axis and the updip end of syncline.

However, fault and structure also have negative effects on gas accumulation. In certain circumstances, both fault and structure may destroy gas accumulation, i.e., when structure is heavily reformed or faults destroy the completeness of the coal bed and cut through surface, the methane may escape and gas content decrease, such as in the east flank of Taihang mountain, west Shangdong province, Putian area of Shanxi province and Nantong area of Sichuan province. Therefore, the best area to drill is one which has active structure, but the structural activity is not too strong to destroy the strata.

7. Underground Water

Underground water also has dual effect on the gas accumulation. If the subsurface fracture is well-developed, and extends to surface, the underground water may be very active and a large amount of water could flow through, resulting in low gas content in the coal bed. The more the volume of flow, the smaller the coalbed methane content, such as in Wantong and Shaoyang regions. But if the coal bed is isolated from the surrounding strata, withdrawal of a large amount of water is favorable to the expelling of coal bed methane, because of the well-developed fracture. Therefore, high yield wells can be expected.

8. Burial Depth

Coal bed methane content generally increases with the burial depth of coal bed until a certain depth, below which the gas content can not increase anymore. For example, in Jixi coal mine (Fig. 5), where develops flame coal and gas coal. Coal bed methane content increases significantly with the burial depth above 600m, but increases only slightly between 600-800m and does not increase below 900m.

Coalbed methane content change is consistent with the gas pressure, both of which are directly proportional to the burial depth. The reasons include: (1) the coal may be more deeply metamorphosed with burial depth increase; (2) the coal has a certain absorptive methane gas; (3) the temperature increases as the depth increases resulting in more free methane in the coal bed. Therefore, coalbed methane content can not always increase as the burial depth increases. But it is important to note this does not mean there is no gas in the deep formation, but the gas content will not increase more.

When a coal bed has undergone regional metamorphism (plutonism), for example, the Taiyuan formation coal in a coal mine of Huabei region, the metamorphism shows a ring-shaped distribution pattern. This is similar to the original outline of the sedimentary basin and is consistent with the coal measure strata thickness change. In the central basin, coal measure strata is very thick and deeply buried, the coal is highly metamorphosed; but in the basin margin, coal measure strata is thin and shallow, the coal is slightly metamorphosed (Fig. 6). Therefore, the coalbed methane content is variable.

9. Unconformity

During the geological history, coal measure strata may occasionally be uplifted to surface and exposed to air and underground water leaching and weathering, resulting in gas weathering zone with a vertical depth of 50-200m. Coalbed methane could escape from the coal bed, and the gas content and pressure decrease from deep to shallow section. This can be seen clearly from Zadu coal mine of Hunan province (Fig. 7). Therefore, when we evaluate a region, we must study the weathering zone, so as to improve the exploration and development efficiencies.

Meanwhile, if the coal bed is close to outcrop, the gas content will be very low, but when the coal bed is far away from outcrop, and is deeply buried, the gas content will be high. For example, in Fushui coal mine, the methane content of the coal near the outcrop is less than $10m^3/t$ ($350\ ft^3/t$), but in the places far away from the outcrop, the methane content is up to $20\text{-}30m^3/t$ ($700\text{->}1000\ ft^3/t$). Therefore, exploratory well should be located in the area away from the outcrop.

10. Porosity Structure and Air Permeability of Coal Beds

The air permeability of coal is the movability of gas through coal body, and thereby controls the possibility of gas withdrawal. However, the air permeability depends on the porosity structure of coal and according to the study by Xi'an Branch of Chinese Coal Academy, micropores have high displacement pressures, but macro pores have low displacement pressures.

11. Igneous Rock

When a coal bed is intruded by igneous rock, the rank of the coal will be higher because of contact metamorphism. For example, in Suqiao-Wenan region, the burial depth of coal is in the range of 4000-5000m and R_0<1%, but in the places where have intrusive rocks, the R_0 of coal in the same depth increases to 1.2-2/3% (Fig. 8).

In Ganxing coal field of Hebei province, taking Wu'an coal mine as the center, the metamorphism of the coal shows a ring-shaped distribution. From the center, meager coal, lean coal, coking coal and gas coal are distributed. The gas coal ring is about 50 km away from the igneous rock in the center (Fig. 9).

However, it is important to note that igneous rock can also have a negative effect on coalbed methane accumulation. In Wu'an coal mine, anthracite locally becomes natural coke because of strong magmatism.

12. Geological Age's Effect on Metamorphism of Coal

The younger the coal, the slighter the metamorphism, because the older coal has undergone metamorphism for a longer time. In northern Hebei province, the coal is Jurassic-Cretaceous, so the metamorphism of the coal is low (flame coal-gas coal), but in the central and southern province, coal is older (Carboniferous and Permian), and the coal has higher metamorphism (fat coal-anthracite).

From vitrinite reflectance values of main coal-bearing formations in China, we also observe that the older the coal, the higher the Ro, so the higher the metamorphism of coal (Fig. 10).

So when we evaluate drilling targets, we should choose older formations first.

BRIEF INTRODUCTION TO THE COAL LANDS IN DACHENG ARCH IN JIZHONG DEPRESSION (CENTRAL PART OF HEBEI PROVINCE)

There are a large number of coal lands in China, which are very abundant in coalbed methane resources. We take the coal lands in Dacheng Arch in Jizhong Depression as an example to describe the geological conditions of coal bed series.

Three relict basins of the Carboniferous and the Permian existed in Jizhong Depression, that is, the northeast part of Jizhong Depression, Fucheng syncline and Shenxian-Shulu area. The northeast part of Jizhong Depression covers an area of 5000 km^2. Dachang Arch is located in the northeast part of Jizhong Depression (Fig. 11), which is within Tianijin City and Hebei province with an area of 2500 km^2. Coal bearing strata of the Carboniferous and the Permian have been encountered in 14 wells drilled.

1. Development History

During Early Paleozoic to the middle of the upper Proterozoic, the platform was developed and carbonate rock with a thickness of several thousands meters was deposited. Up to the early stage of the late Paleozoic, the platform was exposed to surface and then had undergone weathering and erosion for a period of about 100 million years.

Starting from the Middle Carboniferous, the platform subsided, resulting in extensively alternating deposits of marine and terrestrial facies of the Carboniferous. Coal-bearing strata were deposited in this hot and humid environment. The Upper and Lower Shihezi Formation was the continental sediments under the severe dry interior basin. After holding the sediments of the Carboniferous and Permian, the North China Platform rose again and underwent a serious erosion, forming several relict coal-bearing basins on various scales.

2. Stratigraphic Characteristics

It can be described as follows from the Lower part to upper part (Fig. 12). Paleozoic Ordovician (o): The Middle to Lower Ordovician are grey limestone and dolomite with a thickness of 750-850m, which are the main hydrocarbon producing zones in the area. The Upper Ordovician through the lower Carboniferous are absent from the area.

Paleozoic:

Middle Carboniferous: Benxi Formation (C2b) with a thickness of about 0-30m is the major cap rock in the area, which is composed of bauxite at the bottom and bauxite interbedded with 1-4 layers of limestone in the upper part.

Upper Carboniferous: Taiyuan Formation (C3t) with a thickness of about 1-150m is a set of coal-bearing strata, containing 3-10 coal beds. The lithologic profile consists of dark grey mudstone, intercalated with limestone.

Lower Permian: Shanxi Formation (P1s) with a thickness of about 0-140m is a set of grey laminated sandstone and shale, containing 2 to 8 coal beds.

Lower Shihezi Formation (P1%) with a thickness of about 0-240m is a set of grey laminated sandstone and shale.

Upper Permian: Upper Shihezi Formation (P2S) with a thickness of 0-300m consists of the lower part sandstone and the upper part mudstone. The lower part sandstone with a thickness of 200m is the main gas producting zone in the adiacent area. The grey and purplish red mudstone in the upper part is a local cap rock.

Shiqianfeng Formation (P2sh) with a thickness of 0-150m consists of purple shaly sandstone sediments.

Mesozoic:

The Triassic (T) is a set of greyish green and greyish brown mudstone intercalated with sandstone, with a thickness of 0-659m.

The Jurassic (J) is a set of continental coal bearing sediments with a coal bed thickness up to 7-80m.

The Cretaceous (K) consists of grey mudstone intercalcated with sandstone, with a thickness of 0-400m.

Cenozoic:

The Paleogene (E) is absent from the area.

The Neogene (N) is a purplish red and light grey sandstone and mudstone, with a thickness of 550-1050m.

The Quaternary (QP) is a set of yellow sandy clay with a thickness of 200-400m.

In summary, there are primarily three sets of source-reservoir-cap rock assemblages in the Carboniferous to the Permian in the area with a total sediment thickness of 1000m.

The first assemblage is that the Ordovician acts as a reservoir and the bauxitic mudstone at the bottom of the Carboniferous acts as a cap rock. The known examples are Suqiao gas field in Huabei and Ordos gas field.

The second one is that the Taiyuan and Shanxi Formations of the Carboniferous constitute the self source-reservoir-cap rocks assemblage. A coalbed methane reservoir with a thickness of 10-30m existed in the assemblage.

The final one is the lower part of source rock and the upper part of reservoir rock in the Carboniferous to the Permian. The known one is Suqiao gas field.

3. Geological Configuration

The area is primarily characterized by a monoclinal structure with uplifting in the east. The anticlinal structure only occurred on the top in the south part (Fig.13).

4. Coal Bed Characteristics

The coal beds in the Carboniferous to the Permian are widespread in the area. The coal bed is 7-33.5m thick with a single bed thickness of 1-4.8m. The coal rank primarily belongs to fat coal. The absorbed value measured by Milaner isothermal adsorbability curves is in good correlation with the average value in San Juan and Black Warrior Basins in the U.S.A. The methane content in coal beds is9-15m^3/T. A great amount of methane resources occurs in the coal beds.

In addition, the coal beds of the Jurassic in the northwest part of the area are 7-80m thick, which is a potential target of methane exploration.

In summary, Dacheng Arch is close by Beijing and Tianjin and has transport facilities. Dacheng Arch is a favorable region for the accumulation of coalbed methane, with the features of shallow buried depth, thick coal beds, large area, high methane content and large resources. It is a favourable area for the exploration of coal bed gas.

EXPLORATION STATUS OF COAL BED METHANE IN CHINA

Although China has just begun the exploration for coal bed methane, it has paid close attention to this new resource exploration area. Now, China has organized several special scientific research departments working on coalbed methane exploration such as Langfang Branch of Scientific Research Institute of Petroleum Exploration and Development of China and Xi'an Branch of Chinese Academy of Science. We have set up a modern Laboratory equipped with a complete set of equipment and are conducting research projects. China National Petroleum Corporation (Huabei Oifield, Liaohe Oilfield and Dianqiangui Oilfield), ministry of Geology and Mineral Resources (Huabi and Tianjin Departments) and Ministry of Coal Industry (Kailuan Coal Mine, Coal Geology Bureau of Inner Mongolia, Coal Gas Company of Shenyan) are all engaged in the exploration of coal bed gas. Coal Gas company of Shenyang and Kailuan Coal Mine are cooperating with ICF and ARI companies of America to explore and develop coal bed gas, which is supported by the related Departments of the United Nations. Amoco and South Korea also have intentions to cooperate with the related units to develop coal bed gas. Huabei Petroleum Geology Bureau has made drilling operation for coal bed gas. They have drilled one well in Huainan of Anhui Province, three wells in Anyang of Henan Province and one well in Luilin of Shanxi Province. Shenyang Coal Gas Company has drilled five wells in Hongyang coal field. Two wells have been drilled in Kailuan coal mine. Huabei oilfield has drilled one well in Dacheng Arch in Hebei Province, one well in Paishui Basin in Shanxi Province. Liaohe oilfield has drilled one well in Liaoning Province. Good gas shows have been observed in all of those 15 wells. Some wells

have produced gas after fracturing operation. Coal gas has been produced in the north part area of Shenyang. Yangquan coal mine of Shaixi have been using coal gas as a fuel for a long time. A total of ten thousand families in the vicinity of the coal mine have used the coal gas since 1984.

In order to speed up the exploration and development of coal bed methane, China National Petroleum Corporation has selected four exploration and development bases for coal bed methane in Huabei, Hubei and Jianxi. It is expected to obtain a good result in those projects.

SUMMARY

China has great potential for future coal bed methane exploration.

China is very abundant in coal bed methane resources with total resources of 30-35 trillion m^3 (about 1000–1200 tcf). This is a considerable amount of the world's known coalbed methane resource.

The coal bed methane bearing regions are primarily distributed in the densely populated and industrialized area in the east part of China such as Beijing, Tianjin, Shanghai, Shenyang, Haerbin, Taiyuan, Xi'an, Chongqing and Kunming. Most of the coalbed methane bearing regions are close by the coastal areas which are located right next to Japan, Korea, Taiwan of China, Hongkong and countries of Southeast Asia. Thus, it is very advantageous to the transportation of methane gas to the other regions or countries.

There are favourable geological conditions for the coal bed methane in China. The degree of coalification generally ranges from the middle rank to the high rank, that is fat coal to anthracite with low to middle volatility. Methane content per ton of coal generally ranges from 9 to 15 m^3/t with a maximum value up to 30 to 40 m^3/t. The methane bearing coal bed is moderately buried in a depth of 500 to 1000m. Many methane bearing coal beds are undeveloped except for the coal mines where methane gas is required to be swabbed.

The Chinese petroleum industry has the operating experience and technologic knowhow to do the drilling and fracturing operations required in methane exploration and development. China is acquiring first class technology and equipment and the Ministry of Geology and Mineral Resources together with the Ministry of Coal Industry have a strong capability to do research and exploration work on methane gas. At present, China is being more open to the world and has developed good cooperative relationships with the foreign companies. We believe that this kind kind of cooperation will be further developed in the future.

The economic efficiency for the exploration and development of methane gas will be extremely high. Based on the estimation by our related departments, all the capital outlay for the exploration and development of coalbed methane will be recovered in two or three years. This has an important significance to the improvement of our country's energy reserves, turning bane into boon and improving our environment.

In conclusion, China has a great prospect for the exploration and development of coalbed methane. The key point is that we shall conduct more effective exploration and development work.

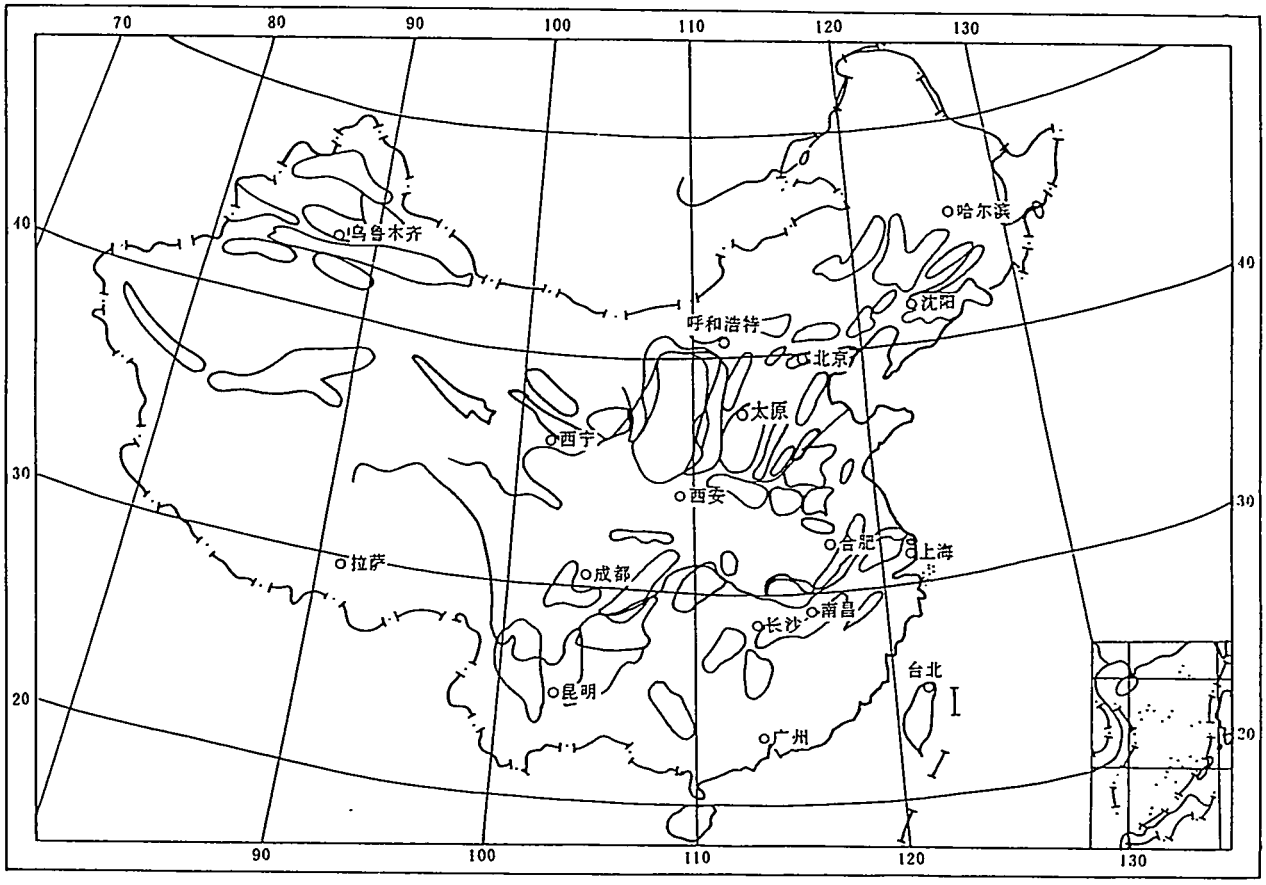


Fig. 1 The coalbed methane resource distribution in China

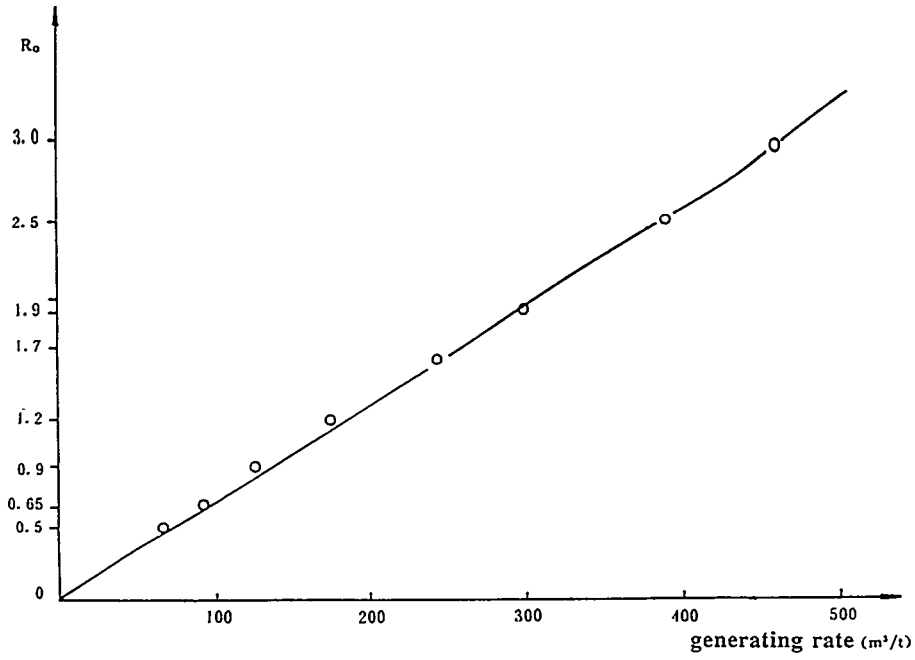


Fig. 2 Methane generation of coal during thermal evaluation

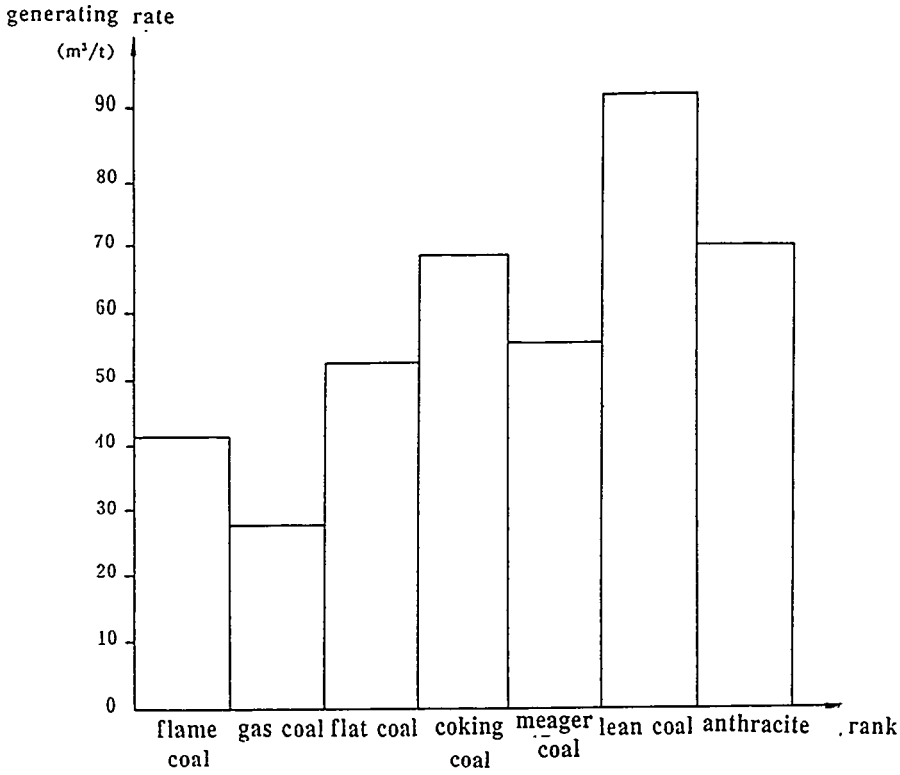


Fig. 3 The maximum generating amount histogram for each coal rank

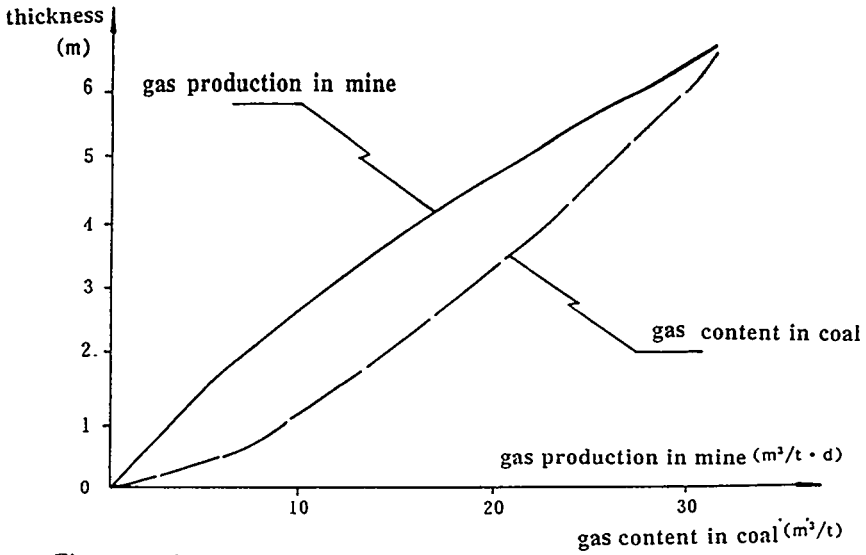


Fig. 4 A diagram of coalbed methane content vs. gas production in mine and gas content in coal in Southern Anhui province

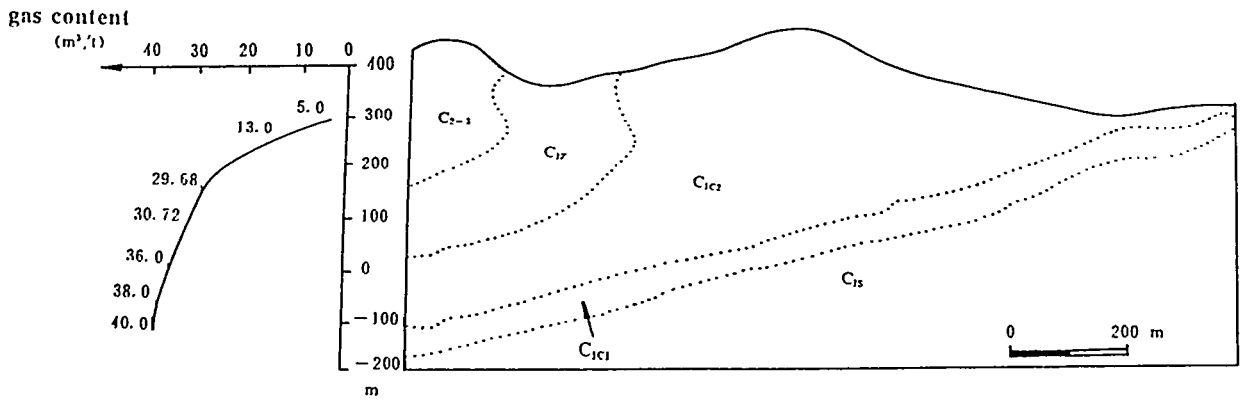


Fig. 7 A diagram of gas content vs. burial depth in Zhadu coal mine of Hunan province

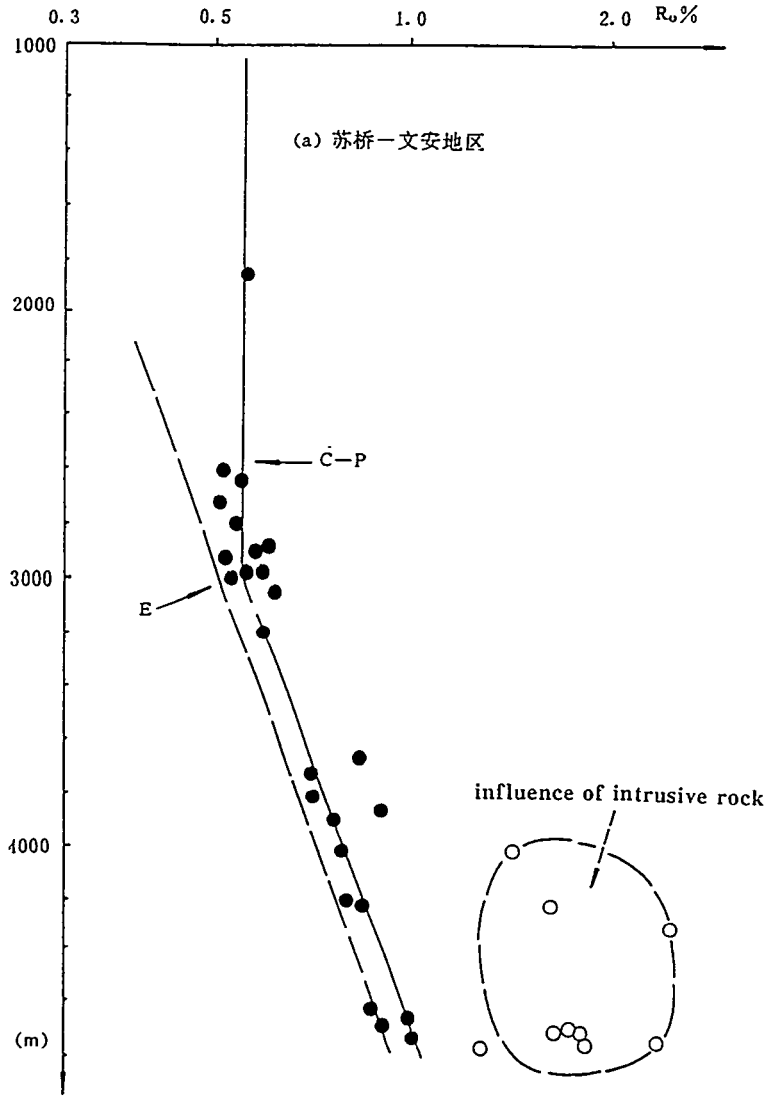


Fig. 8 Ro variation with burial depth in Suqiao—Wen'an area

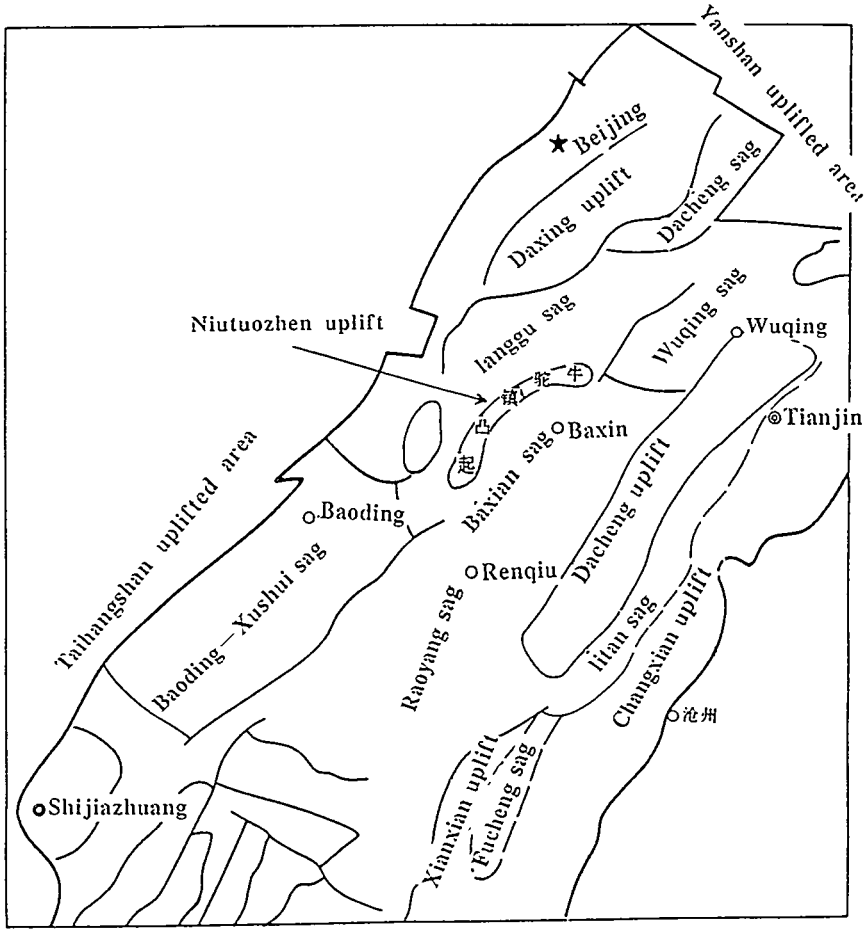


Fig. 11 Tectonic location of Dacheng uplift in Jizhong Depression

1 : 500000

INTERGAS '95

May 15-19, 1995
The University of Alabama
Tuscaloosa, Alabama USA

9525

Quantitative Evaluation of Coal Seam Gas Content Estimate Accuracy

M.J. Mavor, Tesseract Corporation; T.J. Pratt, Geologic Consultant; and C.R. Nelson, Gas Research Institute

Abstract

The proper measurement and analysis of gas desorption data from freshly cut coal samples is crucial for reliably predicting the gas production performance and reserve potential of coal seam gas reservoirs. The technical literature offers many procedures for evaluating the total sorbed gas content of coal samples. This paper critically evaluates the accuracy and comparability of gas content estimates for freshly cut San Juan Basin Fruitland Formation and Piceance Basin Cameo coal samples obtained using commonly practiced analysis procedures. Benchmark (or "ground truth") gas content values were assembled from pressure core and sorption isotherm data for comparison against gas content estimates obtained from conventional whole core, sidewall core, and drill cutting samples. Lost gas content estimate accuracy determined by the Direct (U.S. Bureau of Mines) Method,[1,2,3,4] the Smith & Williams Method,[5,6] and the Amoco Method[7,8] was evaluated and compared. Assessments were also made of the sources and magnitudes of sampling and procedural method errors on the accuracy of the gas content estimates. The choices of sample type, gas desorption temperature conditions, and lost gas analysis method significantly affected the accuracy of the gas content values. The Direct Method analysis of conventional whole core, reservoir temperature gas desorption data provided the most accurate gas content values. Using ambient temperature gas desorption conditions rather than reservoir temperature conditions was the greatest source of error in gas content estimates.

Introduction

Coal seam gas reservoirs hold a significant portion, approximately 14 percent (135 Tcf), of U.S. natural gas reserves and currently account for approximately 4 percent (800 Bcf) of annual, domestic gas production.[9] This new gas resource still holds a significant, untapped gas deliverability potential. In the years to come, production from this new gas play will be critical to providing adequate gas supplies at reasonable prices.

The gas deliverability from coal seam reservoirs depends upon the amount of gas-in-place and the coal's gas sorption storage and production mechanisms.[9] There are no standard, petroleum industry procedures for performing gas content analysis of coal seam reservoirs. Current methods used for determining coal seam reservoir gas content values require that coal samples be obtained at the time of drilling exploration or development wells. The freshly cut coal samples are used in gas desorption experiments that are started on location as soon as possible after sample collection. The need for on-site gas desorption experiments results from two limitations of available technology.

First, at the present time, accurate coal seam gas content estimates cannot be obtained from wireline log data without calibration by core derived sorbed gas content data. This limitation occurs since the presence of gas has little affect upon the bulk properties of the coal. For example, an in-situ methane content of 400 scf/ton increases the density of a pure coal sample of density equal to 1.25 g/cm^3 by 0.010 g/cm^3 or 0.8%.

Second, the total gas content cannot be directly measured. Three separate procedures are required to obtain total gas content estimates. These three procedures are: 1. measurement of the volume of gas desorbed from the sample, 2. estimation of the volume of gas lost from the sample and, 3. measurement of the residual gas content remaining in the sample at the end of desorption. Some gas desorbs and is lost during the sample recovery process unless pressure coring equipment is used, and some gas does not readily desorb at ambient temperature and pressure conditions. The lost gas volume is estimated by measuring gas emission volume data as a function of time and then extrapolating these data to the point at which gas desorption began. The undesorbed or residual gas content value is determined by crushing the sample at the conclusion of the desorption experiment. Thus, the evaluation of the total sorbed gas content of coal samples requires summation of the three components: the lost gas, desorbed gas, and residual gas volume. The gas volume values are converted to gas content values by dividing by the sample mass.

The methods used to collect gas desorption samples, conduct gas desorption tests, and analyze gas desorption data (i.e., estimate the lost gas volume) affect the estimated total sorbed gas content value.[10] The majority of the total gas content estimate error is due to errors in the lost gas content estimate.[10,11] Three procedures are available for estimating the lost gas content. These are:

- Direct (U.S. Bureau of Mines) Method[1,2,3,4]
- Smith and Williams Method[5,6]
- Amoco Method[7,8]

Improvement of formation evaluation technology for coal gas reservoirs was a major goal of the Western Cretaceous Coal Seam Project of the Gas Research Institute (GRI).[9] One aspect of the research was to collect data sets that included core, wireline log and welltest data from cooperative research wells. A high quality set of gas desorption data was available in conjunction with other estimates of reservoir properties such as gross thickness, pressure, and temperature at nine well locations that are summarized in Table 1. A thorough study of these data was performed to evaluate the accuracy of gas content estimates.

This paper summarizes the results of the data evaluations that were published in References 10 and 11 and summarized in Reference 12. The data for individual desorption experiments can be obtained from the Gas Research Institute.[13]

Benchmark Gas Content Estimates

Estimates of benchmark (or "ground truth") gas content values for each well were required to compare the accuracy of total gas content estimates obtained by various analysis techniques and from various sample types. Ideally, the benchmark values should be obtained from pressure core samples. Pressure coring equipment seals rock samples down hole preventing the loss of gas and other fluids prior to desorption of the entire core barrel. As a result, the total gas content can be measured without need to estimate the lost gas content.

Two pressure core samples were collected during the GRI Western Cretaceous Coal Seam Project. The pressure and Direct Method conventional core gas content estimates were within 7.2% for the Slant Hole Completion Test #1 well and 5.8% for the Southern Ute - Mobil 36-1 well.[10] In view of the errors involved in both the pressure core and conventional core desorption experiments, this agreement was within an acceptable range for comparison of estimate accuracy. Since both the pressure core and conventional core gas content estimates were performed at ambient temperature rather than reservoir temperature conditions, both estimates may have been low.

For the other seven wells, methane and methane-carbon dioxide sorption isotherm data were used as the basis for determining the benchmark gas content values.[10] This benchmarking procedure could be used since the reservoirs were gas saturated with the in-situ gas content being equal to the gas storage capacity at the reservoir pressure, temperature, and coal equilibrium moisture content conditions. Gas saturated reservoir conditions existed since the wells produced gas immediately upon production.

The benchmark dry, ash-free, total gas content estimates are listed in Table 2. In addition, total gas content estimates obtained by each of the three lost gas estimate procedures for each available sample type are included. The values listed in this table are greater than the in-situ values due to correction for dilution by non-coal components to a dry, ash-free basis. The benchmark gas content estimates at in-situ conditions along with the average ash and moisture contents of the reservoirs are summarized in Table 3.

The use of a dry, ash-free, basis was to remove differences caused by coal composition variation. The relationship between gas content on an in-situ basis and on a dry, ash-free, basis is as follows.

$$G_c = G_{caf}\left[1-\left(a+w_c\right)\right] \quad \text{..... (1)}$$

The terms and units for all relationships included in this paper are listed in the Nomenclature Section. The methods of obtaining the isotherm benchmark and other gas content estimates will be discussed throughout the remainder of this paper.

Multicomponent Sorption Isotherm Benchmark Values

Single component methane and carbon dioxide isotherm data were measured using previously described procedures.[14] Multicomponent isotherm relationships were computed from single component data through the use of extended Langmuir isotherm theory[15] based upon either produced or desorbed gas composition.

All methane isotherm storage capacity estimates were less than the total gas content estimates obtained with the Direct Method when desorption was performed at reservoir temperature. These data comparisons are illustrated in Figure 1. The discrepancy was caused by sorbed gas compositions that included significant concentrations of carbon dioxide.

As an example of the importance of including carbon dioxide in isotherm benchmark values, consider the Southern Ute 5-7 case. The dry, ash-free, gas content was estimated, by desorption of core samples at reservoir temperature, to be 518.9 ± 30.7 scf/ton. A methane isotherm was measured and resulted in a methane storage capacity estimate of 340 scf/ton on a dry, ash-free, basis at the reservoir temperature of 108°F, pressure of 620 psia, and equilibrium moisture content of 1.91%. The gas composition of two canister desorption samples was measured during the gas desorption process. The compositional analysis data indicated that the desorbed gas contained between 30% and 40% carbon dioxide with the vast majority of the remainder being methane. A carbon dioxide isotherm was measured in addition to the methane isotherm. The methane and carbon-dioxide Langmuir pressures were 362.2 and 238.5 psia, respectively. The dry, ash-free, Langmuir methane and carbon dioxide storage capacities were 538.7 and 1,019.0 scf/ton, respectively. Computation of the storage capacity for a binary gas mixture containing 38% carbon dioxide resulted in a storage capacity estimate that was within 1 scf/ton of the gas content value estimated using the volumetric gas desorption data.

The multicomponent isotherm was an acceptable benchmark for the coal samples collected from the Southern Ute 5-7 well. Similar extended Langmuir isotherm estimates of the storage capacity of samples collected from the other wells were also acceptable benchmark values. Methane isotherm data provided the benchmark values for reservoir gases with low carbon dioxide content.

A second source of error in isotherm storage capacity estimates was due to fitting measured points with the Langmuir isotherm relationship.[16] Estimates of error due to this source were obtained by computing the 95% confidence intervals by linear regression. The range in the isotherm gas content estimates listed in Tables 2 and 3 was computed from the 95% statistical significance levels at the specified reservoir conditions. Earlier publications discuss the Langmuir isotherm errors in more detail.[10,12]

Review of Gas Content Estimate Procedures

The general procedures used to perform the gas desorption experiments discussed in this paper are summarized below. Some steps were not applied to samples from the earliest studied wells. Additional details on each step are given in References 10 and 11.

1. The coal core was cut into one foot long sections.
2. The cut core was placed into tightly fitting plastic sleeves.
3. The sleeved core was placed into desorption canisters of known weight.
4. The filled canisters were weighed.
5. The filled canisters were placed in water baths regulated at reservoir temperature.
6. The desorbed gas volume was measured as a function of time and ambient pressure and temperature conditions.
7. Gas samples were periodically collected for composition analysis.
8. The experiments were terminated when desorption volumes were negligible.
9. Extraneous material was separated from the coal which was then air-dried.
10. The coal sample was weighed.
11. The residual gas content was determined.
12. Measured gas volumes were corrected to standard temperature and pressure conditions.
13. The measured volumes were corrected for the expansion or contraction of gases trapped in the canister void space.
14. The lost gas content was estimated.
15. Ash and moisture analyses were performed on representative samples from each canister.

The lost gas content estimates are based upon a solution to a partial differential equation (PDE) describing constant temperature diffusion from a sphere originally at uniform concentration. The Direct Method[1,2,3,4] lost gas estimate procedure is based upon a simplification to the PDE solution that suggests that the measured gas content is a function of the square root of time since the start of desorption. The early time data is extrapolated to time zero to obtain an estimate of g_L. The slope of the graph is used to obtain an estimate of the diffusivity, D/r^2. Diffusivity is generally not separated into the individual components due to difficulty in determining an average diffusion distance for a sample.

Smith and Williams developed a lost gas volume estimation method for use with drill cutting coal samples which attempted to accounted for the pressure change that samples undergo prior to sealing in desorption canisters.[5,6] The Smith and Williams lost gas estimate method uses a graph that relates a volume correction factor to a lost time ratio and a surface time ratio. The measured gas content is multiplied by the correction factor to determine the total gas content exclusive of residual gas. The lost gas volume is the difference between the calculated total and measured gas contents. A significant limitation of the Smith & Williams Method is the inability to compute the lost gas volume until the conclusion of the gas desorption experiment.

Amoco[7,8] developed a lost gas volume estimate methodology based upon the same PDE solution as used for the Direct Method. A non-linear regression technique was used to determine the three unknowns, g_i', g_L, and D/r^2.

Additional details on the Direct Method, Smith & Williams Method, and Amoco Method lost gas content analysis procedures are given in References 10 and 11.

Single Sample Total Gas Content Estimate Errors

Procedures used to perform the desorption experiments can introduce significant error into the estimates of the measured and lost gas contents. The primary error sources are as follows.

- Desorption at non-reservoir temperature conditions.
- Desorption volume measurement error.
- Failure to correct measured gas volume to standard conditions.
- Failure to account for canister free gas volume (head space) changes.
- Sample weight measurement error.
- Failure to determine residual gas content.

San Juan Basin Fruitland Formation coal core samples undergo significant temperature variations upon extraction from the reservoir. The reservoir temperature varies from approximately 90°F near the western outcrop of the basin to 125°F in the interior of the basin due to depth variation. Ambient temperature on the surface can vary from as low as -10°F during winter nights to 95°F during summer days. The surface temperature variation causes dramatic differences in the coring fluid circulation temperature. During the winter, the temperature of the coring fluid upon entering the well can be as low as 35°F with a temperature upon returning to the surface of 45°F.

The use of non-reservoir temperature conditions during collection of gas desorption data affected the estimate of the lost gas content and the measured desorption volume. As an example, Figure 2 illustrates the early time desorption data measured on five intermediate zone Fruitland Formation coal samples from the Southern Ute 5-7 well. Three of the gas desorption experiments were performed by reheating the desorption canisters containing the coal samples to reservoir temperature conditions using a water bath. The other two gas desorption experiments were conducted by maintaining the canisters containing the coal samples at ambient surface temperature conditions. The rate of gas desorption (the slope of the lines) and the measured gas content were significantly greater for the gas desorption experiments conducted at reservoir temperature.

Approximately the same length of time was required to return samples to reservoir temperature as the length

of time between drilling the sample and placing the sample in a heated water bath. This observation was based upon field and laboratory measurements. We have referred to this time as the "temperature recovery time." Gas content values obtained using the Direct Method lost gas analysis procedure were more accurate (in closer agreement with the benchmark total gas content) when applied to the data collected after the temperature recovery time interval. All Direct Method estimates of the total gas content listed in this paper were obtained by basing the lost gas content estimate upon backwards extrapolation to time zero of data measured immediately after the temperature recovery time interval. Time zero for core samples was the time when the wellbore pressure due to the hydrostatic head of the drilling fluid was equal to the reservoir pressure. Time zero for drill cutting samples was the time at which the sample was drilled.

The results for the Southern Ute 5-7 intermediate zone Fruitland Formation coal samples indicated that the total dry, ash-free, gas content estimate was 30.3% less for the ambient temperature experiments than for the reservoir temperature experiments. The cause of the difference was due to differences in both the measured and lost gas content estimates. The ambient temperature experiment dry, ash-free, measured gas content averaged 20% less than those obtained at reservoir temperature. The estimates of the lost gas fraction were 45.6% less for the ambient temperature experiments. The reservoir temperature average diffusivity value was a factor of 2.9 greater than the ambient temperature diffusivity value estimate.

For the Southern Ute 5-7 basal zone Fruitland Formation coal samples, the ambient temperature data indicated that the dry, ash-free, gas content estimates averaged 33.2% less than the reservoir temperature results. The measured and lost gas contents for the ambient temperature experiments were 25.5% and 61.4% less than the reservoir temperature results. For these basal Fruitland Formation coal samples, the diffusivity value estimated from the reservoir temperature gas desorption data was a factor of 4.1 greater than that obtained for the ambient temperature gas desorption data.

The cause of the lower lost gas and diffusivity estimates is easily observed in Figure 2. The gas desorption rate at ambient temperature conditions was much less than the rate at reservoir temperature conditions. The lost gas content estimate for the ambient temperature data was obtained by linear regression of the data collected immediately after the start of measurements. The data measured after the temperature recovery time interval was used for the reservoir temperature regression. Due to the significant difference in slope, the extrapolated lost gas content was much more negative (greater absolute value and greater lost gas content) for the reservoir temperature data than for the ambient temperature data.

Sevenster[17] reported that the diffusion coefficients of methane and water vapor through coal samples were exponentially dependent upon absolute temperature. Nandi and Walker[18,19] confirmed this observation and presented a relationship for the temperature dependence of the diffusivity that illustrated the exponential relationship. In Nandi and Walker's experiments, an increase of temperature from 32 to 122°F increased the diffusivity of a high volatile A bituminous coal by factor of 5.8. The reported increase in the diffusivity as a function of temperature is in line with that observed for the high volatile A bituminous Southern Ute 5-7 samples.

The errors cased by other procedural methods to determine the measured gas content were investigated as part of this study. The details for the error analyses are included in Reference 11. Table 4 summarizes the error estimates.

Procedural error affected the lost gas content estimates also. Figure 3 summarizes the magnitude of the procedural errors for each of the three lost gas analysis methods. The vertically descending order in this figure is Direct, Smith & Williams, and Amoco for each error source.

Multiple Sample Total Gas Content Estimates

The estimates of the total gas content listed in Tables 2 and 3 were determined by statistical analysis of gas content estimates obtained by desorption of multiple samples. The multiple sample regression analysis is illustrated by Figure 4. Analysis of the accuracy of the relationship between total gas content and non-coal content was based upon linear regression of the following relationship.

$$G_c = G_{caf} + \beta_1(a + w_c) \quad \text{..... (2)}$$

The intercept at an ash plus moisture content of zero was equal to the dry, ash-free, total gas content estimate for the reservoir(s) of interest. The estimate of the error of the intercept was determined by the 95% statistical confidence interval estimates represented by the dashed lines in Figure 4.

The errors that caused the statistical variation in the individual data points were due to the following primary sources.

- Selection of unrepresentative samples
- Selection of unrepresentative sample splits for proximate analyses
- Proximate analysis error
- Selection of insufficient number of samples

The selection of unrepresentative samples may occur due to poor sample recovery. In this situation, only a portion of the cored sample is retained within the sample collection equipment. As an example, when coring a highly fractured coal seam, the intervals of greatest fracturing may be washed from the sample due to circulation of the coring fluid. As a result, samples from the less fractured intervals of the reservoir are collected. This condition was observed occasionally by the authors when using conventional coring equipment and was more common when using side wall coring equipment.

A second cause of unrepresentative samples results when samples are not selected from all portions of the reservoirs. Ideally, samples with a wide range of coal lithotypes and non-coal fractions are desired so that all portions of the reservoir are sampled and evaluated. In addition, accurate statistical evaluation of the data requires that numerous samples be collected with a wide range of non-coal fractions. The number of samples that

is required can be quantified and the variation in non-coal fractions required was discussed in References 11 and 12.

The use of confidence interval estimates for the parameters G_{caf} and β_1 allowed computation of the accuracy of the dry, ash-free, total gas content estimate and the proximate analysis derived estimates of the ash and moisture content. The intercept illustrated in Figure 5 is 518.7±30.7 scf/ton and the slope is -539.8±80.1 scf/ton. There is a 95% probability that the pure coal gas content was within 30.7 scf/ton of the intercept assuming that the individual experiment results were correct. The error in the non-coal content estimate can be estimated from the slope. The ratio of the error of the slope to the absolute value of the slope is 0.148. Therefore, the error in the non-coal content is on the order of 15%.

The estimate of the error based upon the regression analysis was believed to be a maximum error as the errors in the non-coal fraction estimates were dependent upon the errors in the gas content estimates and vice versa. This error was primarily caused by selection of a sample split that was not representative of the entire sample rather than errors in the proximate analysis procedure. The ASTM procedure specifies that the precision of the moisture content analysis is 0.2% and the precision of the ash content analysis is 0.3%.[20] Proximate analyses were also performed on duplicate samples to confirm the precision.

Unrepresentative proximate analysis samples may have resulted since the entire sample was not crushed prior to selecting sample splits. In many cases, the core samples were split in half longitudinally. One half of the core sample was crushed while the other half was preserved for other measurements. Inhomogeneity of the sample may have caused the proximate analysis measurements to be different than had the entire sample been crushed.

Table 5 summarizes the maximum errors in the non-coal fraction for four of the Direct Method analyses of core gas content included in the data base. Data sets with less than ten core samples were eliminated from this table due to lack of statistical significance. The apparent errors ranged from 14.8 to 27.8% for the first three wells in the table. These estimates of the range of maximum error were believed to be reasonable. The excessive maximum error of 67% for the Southern Ute - Mobil 36-1 well was also believed to be correct. The greater error was likely due to relatively poor sample split selection and handling procedures.

Comparison of Gas Content Estimates

Comparisons were made of the dry, ash-free, total gas content estimates obtained with each lost gas technique. These results are compared in Table 2 and in Figure 5. The Amoco Method resulted in greater estimates than the Direct Method and the Smith & Williams Method resulted in lesser estimates. The data presented in papers by Smith and Williams[21,22] and Yee et al.[8], show the same trends as illustrated in Figure 5. However, the data presented in References 8, 21, and 22 cannot be used to assess which lost gas analysis method gives the more accurate result. The benchmark gas content data presented in this paper (see Table 3) provide a means to resolve this outstanding question. As shown in Figure 5, the benchmark gas content data indicate that the Direct Method lost gas analysis procedure provides the most accurate gas content value estimates.

The Smith & Williams Method[5,6] was developed for use with coal drill cuttings. Based upon the results shown in Figure 5, this lost gas volume estimation method does not appear to be applicable for analysis of conventional whole core gas desorption data.

Table 2 and Figure 6 contrast the Direct Method, conventional whole core gas content estimates with those obtained from side wall core and drill cutting samples. The side wall core derived gas content estimates were -22% for GRI #2 and +25% for Southern Ute - Mobil 36-1 of the Direct Method conventional whole core gas content estimates.

In general, gas desorption data obtained from drill cuttings cannot be used to quantify the total sorbed gas content of coal seam reservoirs. The estimates of total gas content obtained by desorption of drill cutting samples were less than those obtained by desorption of conventional whole core samples. This finding is comparable to results obtained by others as discussed in Reference 8. The gas content estimate obtained for the FC Federal #12 Fruitland Formation coal drill cuttings data appears to contradict this general trend as the drill cutting sample total gas content estimate was 106.7%± 36.6% of the core sample estimate. The apparent discrepancy was caused by statistical uncertainty exemplified by the wide error range of the pure coal gas content estimate. The wide error range was caused by inconsistency in the total gas content as a function of the non-coal content relationship. The inconsistency was caused by inclusion of rock debris of differing densities with the coal sample. As a result, the proximate analysis derived estimates of the ash content were not representative of the ash content of the coal. Because of inclusion of extraneous material, drill cutting gas content data often cannot be accurately evaluated for pure coal gas content estimates. This error was investigated further in Reference 11.

Conclusions

The major conclusions that resulted during this study are as follows.

There was satisfactory agreement (5.8 to 7.2%) between pressure core and conventional core gas content estimates if gas desorption was performed at similar temperatures.

Gas content estimates obtained from reservoir temperature gas desorption data were in agreement with benchmark values when lost gas content estimates were obtained with the Direct Method analysis procedure. The agreement ranged from 103.1%±6.1% to 119.7%±12.8% of the benchmark value when sufficient distribution of sample ash content was present.

The Smith & Williams Method resulted in total dry, ash-free, gas content estimates that averaged 27.3% less than the values obtained with the Direct Method. The Amoco Method resulted in total dry, ash-free, gas content estimates that averaged 20.6% greater than those obtained with the Direct Method. The differences were due to differences in the estimates of the lost gas content.

The greatest cause of error in the total gas content estimates was due to conducting gas desorption experiments at ambient temperature conditions rather than at reservoir temperature conditions. The use of ambient temperature conditions resulted in estimates of the Direct Method dry, ash-free, gas content that were lower by 33% to 30% than the results obtained from reservoir temperature gas desorption.

The use of ambient temperature conditions caused the greatest error in the estimates of the diffusivity of the coal samples. Direct Method ambient temperature (approximately 70°F) diffusivity estimates were 2.9 to 4.5 times less than the estimates obtained at 108°F. The effect of temperature upon the diffusivity estimates was in line with that reported in the literature.

An insufficient number of drill cutting gas desorption data sets were available to derive statistically significant conclusions concerning the source of the error resulting from using this sample type. In two cases, the drill cutting, Direct Method, dry, ash-free, gas content estimates were 74% to 75% of the benchmark gas content value. Lower gas content estimates from drill cutting samples relative to those obtained from conventional core samples is the most common result.

Two side-wall core desorption data sets were available in the data base. One set resulted in an Direct Method estimate of the dry, ash-free, gas content that was 77.5%±13.0% of the benchmark gas content. The second set resulted in an estimate that was 132.2%± 27.8% of the benchmark value. The cause of the difference was not resolved but did not appear to be caused by measurement errors or significantly different lost gas times.

Gas storage capacity estimates based upon pure methane sorption isotherm data were found to be lower than the gas content estimates when sorbed gas compositions included substantial amounts of carbon dioxide.

Uncertainty in the gas content estimates was caused by errors in individual desorption experiment results and by errors in the proximate analysis of the samples caused by selection of unrepresentative proximate analysis samples. Unrepresentative proximate analysis samples caused an error in the non-coal fraction estimates that was between ±14% and ±67% the correct value.

Acknowledgments

The efforts reported upon in this paper were made possible by funding from the Gas Research Institute under contracts 5088-214-1657 and 5092-260-2648. Contributors to collection of the data included R.N. Britton, J.C. Close, R. Copenhafer, T. Erwin, T.L. Logan, and R.M. Marshall. The assistance of cooperative operators listed in Table 1 is greatly appreciated.

Nomenclature

a	ash content, fraction
D	diffusion coefficient, cm^2/sec
G_c	sample total gas content, scf/ton
G_{caf}	sample dry, ash-free, total gas content, scf/ton
w_c	moisture content, fraction
β_1	slope of the gas content-non coal content relationship, scf/ton

References

1. Bertard, C., Bruyet, B., and Gunther, J.: "Determination of Desorbable Gas Concentration of Coal (Direct Method)," Int. J. Rock Mech. Min. Sci., **7** (1970) pp. 43-65.

2. Diamond, W.P. and Levine, J.R.: "Direct Method Determination of the Gas Content of Coal: Procedures and Results," Report of Investigations 8515, United States Department of the Interior, Bureau of Mines, Washington, D.C. (1981).

3. Kissell, F.N., McCulloch, C.M., and Elder, C.H.: "The Direct Method of Determining Methane Content of Coalbeds for Ventilation Design," Report of Investigations 7767, United States Department of the Interior, Bureau of Mines, Washington, D.C. (1973).

4. Ulery, J.P., Hyman, D.M.: "The Modified Direct Method of Gas Content Determination: Applications and Results," Paper 9163, Proceedings of the 1993 International Coalbed Methane Symposium, The University of Alabama / Tuscaloosa (May, 1993) pp. 489-500.

5. Smith, D.M. and Williams, F.L.: "A New Technique for Determining the Methane Content of Coal," Proceedings of the 16th Intersociety Energy Conservation Engineering Conference, Atlanta, Georgia, (1981) pp. 1,167-1,272.

6. Smith, D.M., Methane Diffusion and Desorption in Coal, Dissertation Submitted in Partial Fulfillment of the Requirements for the Degree of Doctor of Philosophy in Chemical Engineering, The University of New Mexico, Albuquerque, New Mexico (May, 1982).

7. Metcalfe, R.S., Yee, D., Seidle, J., and Puri, R.: "Review of Research Efforts in Coalbed Methane Recovery," Paper SPE 23025 presented at the SPE Asia-Pacific Conference held in Perth, Western Australia, (November 4-7, 1991).

8. Yee, D., Seidle, J.P., and Hanson, W.B.: "Gas Sorption on Coal and Measurement of Gas Content," Hydrocarbons from Coal, Chapter 9, American Association of Petroleum Geologists, Tulsa, OK (1993) pp. 203-218.

9. Schraufnagel, R.A., Hill, D.G., and McBane, R.A.: "Coalbed Methane - A Decade of Success," Paper SPE 28581 presented at the 69th Annual Technical Conference and Exhibition of the Society of Petroleum Engineers, New Orleans, Louisiana, (Sept., 25-28, 1994).

10. Mavor, M.J., Pratt, T.J., and Britton, R.N.: Improved Methodology for Determining Total Gas Content, Volume I. Desorption Data Summary, Gas Research Institute Report No. GRI-93/0410, Chicago, Illinois (May, 1994).

11. Mavor, M.J. and Pratt, T.J.: Improved Methodology for Determining Total Gas Content, Volume II. Comparative Evaluation of the Accuracy of Gas in Place Estimates, Gas Research Institute Report No. GRI-94/0429, Chicago, Illinois (Dec., 1994).

12. Mavor, M.J., Pratt, T.J., and Nelson, C.R.: "Quantitative Evaluation of Coal Seam Gas Content Estimate Accuracy," Paper SPE 29577 presented at the 1995 Joint Rocky Mountain Regional / Low-Permeability Reservoirs Symposium, Denver, Colorado, (March 20-22, 1995).

13. Mavor, M.J., and Pratt, T.J.: *CoreGas*™ Database, © 1994 Gas Research Institute.

14. Mavor, M.J., Owen, L.B., and Pratt, T.J.: "Measurement and Evaluation of Coal Sorption Isotherm Data," Paper SPE 20728 presented at the 65th Annual Technical Conference of the Society of Petroleum Engineers, New Orleans, Louisiana, (Sept. 23-26, 1990).

15. Arri, L.E., Yee, D., Morgan, W.D., and Jeansonne, M.W.: "Modeling Coalbed Methane Production with Binary Gas Sorption," Paper SPE 24363 presented at the SPE Rocky Mountain Regional Meeting, Casper, Wyoming, (May 19-21, 1992).

16. Langmuir, I.: "Adsorption of Gases on Glass, Mica, and Platinum," J. Am. Chem. Soc. **40** (1918) p. 1,361.

17. Sevenster, P.G.: "Diffusion of Gases Through Coal," Fuel, **38** (1959) pp. 403-418.

18. Nandi, S.P. and Walker, P.L.: "Activated Diffusion of Methane in Coal," Fuel, **49** (1970) pp. 309-323.

19. Nandi, S.P. and Walker, P.L., Jr.: "Activated Diffusion of Methane from Coals at Elevated Pressures," Fuel, **54** (1975) pp. 81-86.

20. 1993 Annual Book of ASTM Standards, Volume 5.05 Gaseous Fuels; Coal and Coke, American Society for Testing and Materials, Philadelphia, PA (1993).

21. Smith, D.M. and Williams, F.L.: "Diffusion Models for Gas Production From Coals. Application to Methane Content Determination," Fuel, **63** (1984) pp. 251-255.

22. Smith, D.M. and Williams, F.L.: "Direct Method of Determining the Methane Content of Coal-A Modification," Fuel, **63** (1984) pp. 425-427.

Table 1. **Well Location Detail.**

Well Name	Operator	State	County	Section	Township	Range
Southern Ute 5-7	Amax Oil & Gas, Inc.	Colorado	La Plata	7	32 N	11 W
South Shale Ridge #11-15	Conquest Oil Company	Colorado	Mesa	15	8 S	98 W
GRI Observation Well #2	Amoco Production Co.	Colorado	La Plata	17	32 N	10 W
GRI Observation Well #1	Amoco Production Co.	Colorado	La Plata	17	32 N	10 W
S. Ute Tribal I PLA 9 #2	Amoco Production Co.	Colorado	La Plata	17	32 N	10 W
Valencia Canyon 32-1	Emerald Gas Oper. Co.	Colorado	La Plata	32	33 N	11 W
FC Federal #12	Mesa Limited Partnership	New Mexico	Rio Arriba	33	26 N	7 W
Slant Hole Completion Test #1	CER Corporation	Colorado	Garfield	34	6 S	94 W
Southern Ute - Mobil 36-1	McKenzie Methane Co.	Colorado	La Plata	36	34 N	10 W

Table 2. (see page 8).

Table 3. **Summary of Benchmark Gas Content Estimates at In-Situ Conditions.**

Well	Pressure	Temp-erature	Coal Rank	Ash Content	Moisture Content	In-Situ Gas Content
	psia	°F	-	%	%	scf/ton
Southern Ute 5-7	620	108	high volatile A bit.	21.0	1.93	388 ± 18
South Shale Ridge #11-15	1,480	118	high volatile A bit.	10.6	1.65	328 ± 12
COAL Site	1,550	120	high volatile A bit.	29.9	0.89	632
Valencia Canyon 32-1	913	100	high volatile A bit.	28.9	1.74	432 ± 10
FC Federal #12	890	96	high volatile B bit.	27.5	3.54	176 ± 5
Slant Hole Completion Test #1	5,200	205	low volatile bit.	8.3	0.09	768
Southern Ute - Mobil 36-1	1,366	125	medium volatile bit.	30.4	0.37	416

Table 4. **Summary of Desorption Experiment Procedural Errors.**

Description	Error
Desorption volume measurement error	±0.8%
Failure to correct to standard pressure	+17.6%
Failure to correct to standard temperature	+1.9%
Failure to correct for head space variations	-1.0 to +0.3%
Sample weight measurement error	±0.05 to 0.1%
Lack of residual gas content estimates	-7 to 0%

Table 5. **Summary of Core Direct Method Maximum Estimates of the Non-Coal Fraction Error**

Well	Number of Points	Maximum Non-Coal Fraction Error
		%
Southern Ute 5-7	26	14.8
South Shale Ridge #11-15	21	27.8
FC Federal #12	13	24.2
Southern Ute - Mobil 36-1	16	66.9

Table 2. Comparison of Dry, Ash-free, Gas Content, Pressure Core, and Isotherm Analyses.

Well	Sample and Analysis Type (Benchmark values are shaded and italicized).	Total Gas Content or Storage Capacity scf/ton	Relative Gas Content or Storage Capacity* %
Southern Ute 5-7	Binary 65% Methane - 35% Carbon Dioxide Isotherm 5 (620 psia)	472±37	93.8±7.4
	Carbon Dioxide Isotherm 4 (620 psia)	736±41	146.3±8.2
	65% CH_4 - 35% CO_2 Extended Langmuir Isotherm (620 psia)	***503±23***	***100±4.6***
	Methane Isotherm 2 (620 psia)	340±29	67.6±5.8
	Core Direct Method Gas-Coal Content	518.7±30.7	103.1±6.1
	Core S & W Method Gas-Coal Content	406.8±103.2	80.9±6.1
	Core Amoco Method Gas-Coal Content	594.8±30.9	118.3±6.1
South Shale Ridge #11-15	***Methane Isotherm 2 (1,480 psia)***	***374±14***	***100.0±3.7***
	Core Direct Method Gas-Coal Content	449.9±100.4	120.3±26.8
	Core S & W Method Gas-Coal Content	125.2±162.6	33.5±43.5
	Core Amoco Method Gas-Coal Content	497.2±117.5	132.9±31.4
COAL Site			
GRI Observation Well #2	Core Direct Method Gas-Coal Content	908.8±199.4	99.5±21.8
	Core S & W Method Gas-Coal Content	789.6±185.4	86.5±20.3
	Core Amoco Method Gas-Coal Content	1063.5±268.4	116.5±29.4
	Side Wall Core Direct Method Gas-Coal Content	707.3±118.8	77.5±13.0
	Side Wall Core S & W Method Gas-Coal Content	754.6±170.8	82.7±18.7
	Side Wall Core Amoco Method Gas-Coal Content	641.1±106.0	70.2±11.6
GRI Observation Well #1	Methane Isotherm 2 (1,550 psia)	804±14	88.1±1.5
	Oxidation Corrected Carbon Dioxide Isotherm (1,550 psia)	1,057	115.8
	87% CH_4 - 13% CO_2 Extended Langmuir Isotherm (1,550 psia)	***913***	***100***
	Core Direct Method Gas-Coal Content	910.7±902.0	99.7±98.8
	Core S & W Method Gas-Coal Content	498.5±383.0	54.6±41.9
	Core Amoco Method Gas-Coal Content	961.8±1093.8	105.3±119.8
S. Ute Tribal I PLA 9 #2	Drill Cuttings Direct Method Gas-Coal Content	677.8±121.2	74.2±13.3
	Drill Cuttings S & W Method Gas-Coal Content	609.8±427.6	66.8±46.8
	Drill Cuttings Amoco Method Gas-Coal Content	745.1±482.7	81.6±52.9
Valencia Canyon 32-1	Int. Zone Methane Isotherm 1 (956 psia)	454±11	72.9±1.8
	Basal Zone Methane Isotherm 3 (913 psia)	487±38	78.2±6.1
	Basal Zone Carbon Dioxide Isotherm 4 (913 psia)	929±17	149.1±2.7
	72% CH_4-28% CO_2 Basal Extended Langmuir Isotherm (913 psia)	***623±15***	***100.0±2.4***
	Core Direct Method Gas-Coal Content	679.1±79.1	109.0±12.7
	Core S & W Method Gas-Coal Content	678.3±161.6	108.9±25.9
	Core Amoco Method Gas-Coal Content	941.1±155.1	151.1±24.9
FC Federal #12	***Methane Isotherm 1 (890 psia)***	***225±7***	***100.0±3.1***
	Core Direct Method Gas-Coal Content	269.3±28.9	119.7±12.8
	Core S & W Method Gas-Coal Content	257.4±24.5	114.4±10.9
	Core Amoco Method Gas-Coal Content	492.2±98.6	218.8±43.8
	Cuttings Direct Method Gas-Coal Content	287.2±283.0	127.6±125.8
	Cuttings S & W Method Gas-Coal Content	259.8±287.4	115.5±127.7
	Cuttings Amoco Method Gas-Coal Content	148.4±624.6	66.0±277.6
Slant Hole Completion Test #1	***Pressure Core (5,200 psia)***	***838***	***100.0***
	Methane Isotherm 2 (5,200 psia)	880.0±32	105.0±3.8
	Core Direct Method Gas-Coal Content	778.0	92.8
	Core S & W Method Gas-Coal Content	500.2	59.7
	Core Amoco Method Gas-Coal Content	582.4	69.5
Southern Ute Mobil 36-1	***Pressure Core (1,366 psia)***	***601.5***	***100.0***
	Methane Isotherm 4 (1,366 psia)	549±20	91.3±3.3
	Core Direct Method Gas-Coal Content	636.5±153.7	105.8±25.6
	Core S & W Method Gas-Coal Content	475.6±111.2	79.1±18.5
	Core Amoco Method Gas-Coal Content	677.5±179.3	112.6±29.8
	Drill Cuttings Direct Method Gas-Coal Content	449.3	74.7
	Drill Cuttings S & W Method Gas-Coal Content	430.8	71.6
	Drill Cuttings Amoco Method Gas-Coal Content	464.1	77.2
	Side Wall Core Direct Method Gas-Coal Content	795.0±167.3	132.2±27.8
	Side Wall Core S & W Method Gas-Coal Content	735.4±199.3	122.3±33.1
	Side Wall Core Amoco Method Gas-Coal Content	1,240.0±472.0	206.2±78.5

* The basis of this ratio is the benchmark gas content estimate.

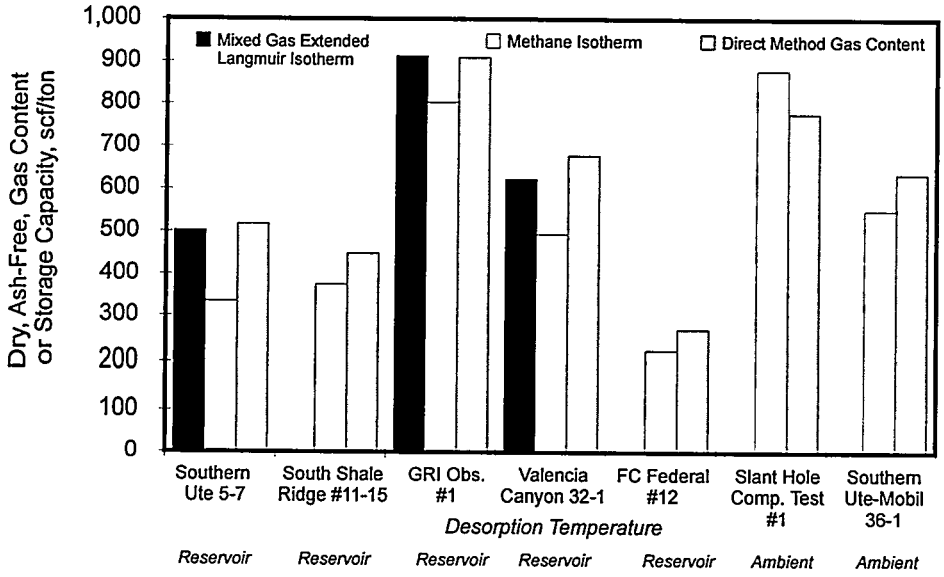


Figure 1. Comparison of Direct Method Dry, Ash-Free, Gas Content and Storage Capacity.

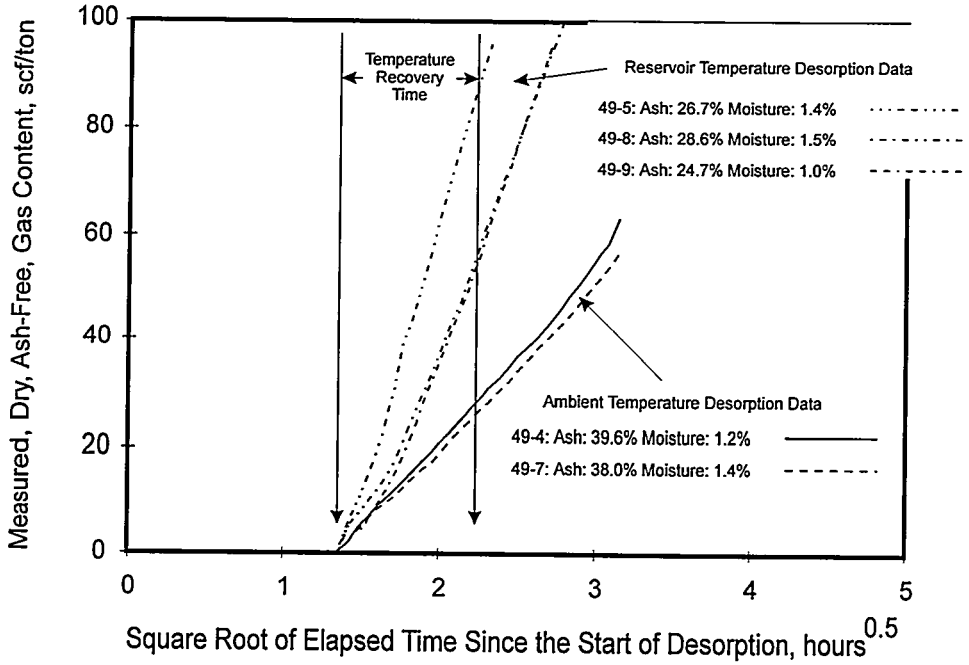


Figure 2. Southern Ute 5-7, Comparison of Intermediate Zone Initial Desorption Data.

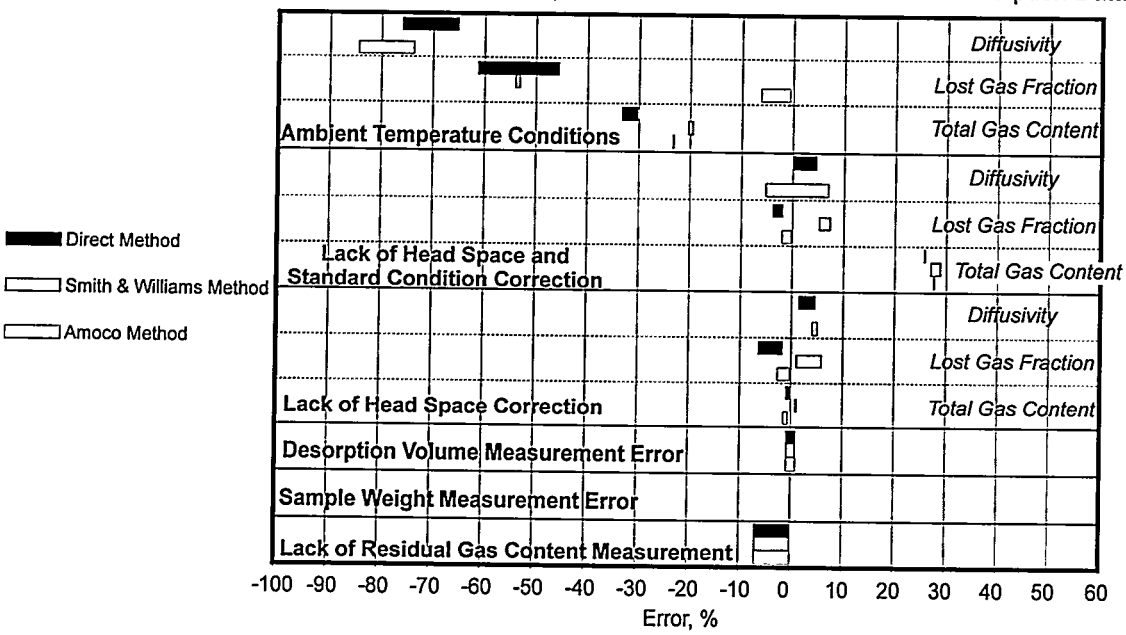


Figure 3. Comparison of Gas Content Analysis Errors.

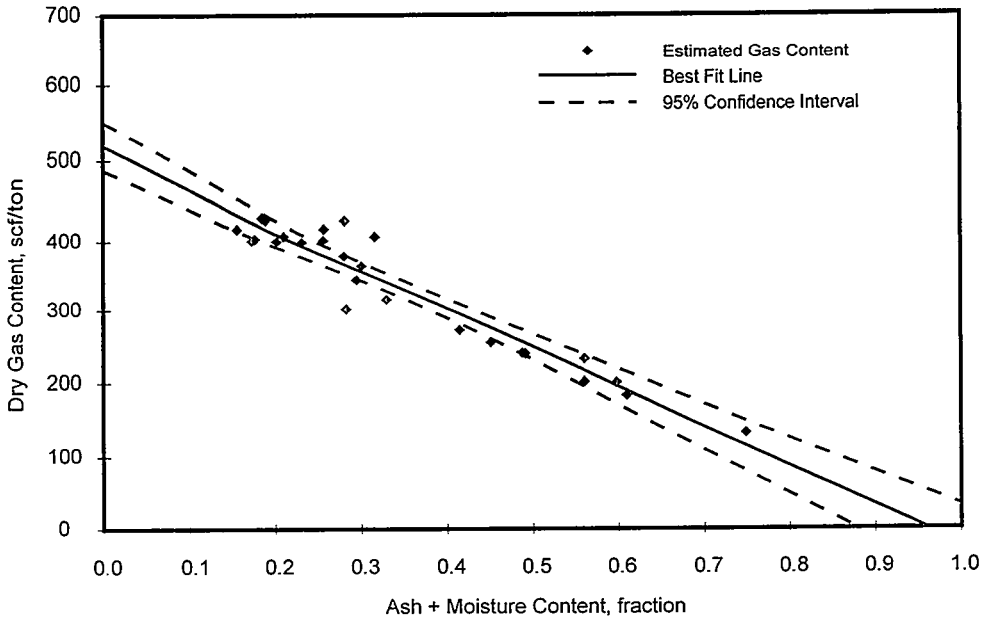


Figure 4.
Southern Ute 5-7, Relationship Between Direct Method Core Total Gas Content and Non-Coal Content.

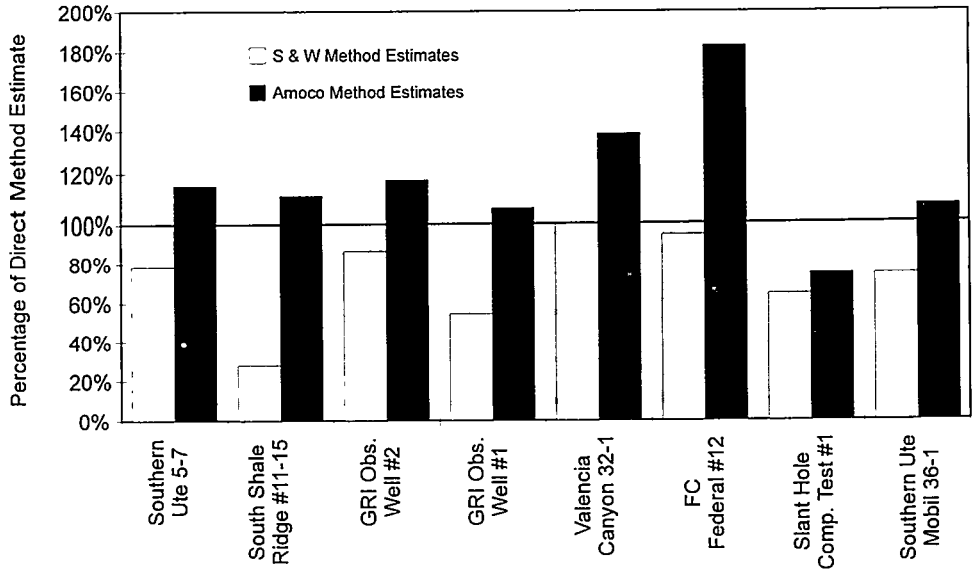


Figure 5. Comparison of Core Sample Dry, Ash-Free Gas Content Estimates for Each Lost Gas Analysis Method.

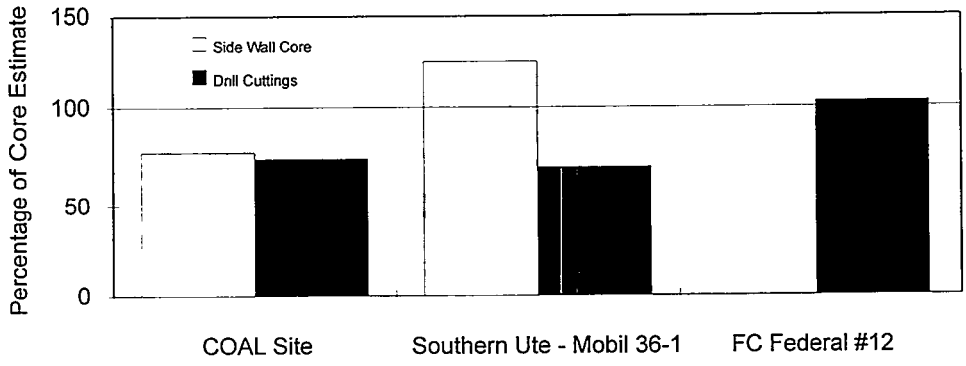


Figure 6. Comparison of Direct Method Side Wall Core and Drill Cutting Gas Content with Conventional Core Gas Content Estimates.

INTERGAS '95

May 15-19, 1995
The University of Alabama
Tuscaloosa, Alabama USA

9523

Analysis of Sorption and Thermodynamic Data and a Discussion of an Empirical Model for Sorbed Gases in Coal

J.C. Huddleston, J.S. Marshall and R.C. Pilcher, Raven Ridge Resources, Incorporated

ABSTRACT

Langmuir developed a theory of monolayer adsorption that has been widely accepted as the basis for modeling adsorption of methane on coal. Recent theoretical investigations and empirical evidence suggest that the Langmuir model may not be the best model for sorption of gases on all coals under all conditions. The in situ pressure and temperature regime found in most prospective coalbed methane reservoirs exceeds supercritical conditions for methane. This implies that the methane residing in the reservoir has characteristics of both a liquid and a gas. Therefore, the Real Gas Law may not accurately predict the behavior of methane at high reservoir pressures and temperatures.

Potential theory may be used to predict the existence of a fluid density gradient in the pore structure of coals. This model is used to explain the short comings of using simple mathematical forms such as the Langmuir model to characterize the behavior of gases at reservoir conditions. In an attempt to quantify the state of sorbed gases in coals at high pressures and temperatures that exist in economically significant reservoirs, gas capacity and surface area measurement tests, and micropore analysis have been performed on several coals and activated charcoal at various sizes classes ranging from <80 to one mesh.

The results of these investigations allow for a more accurate mathematical representation of, as well as a better understanding of the behavior of gassy coals under actual reservoir conditions, through the use of empirical modeling techniques.

INTRODUCTION

Langmuir adsorption theory has been widely accepted as the best model for gas adsorption on coals. The theory was developed in 1916 to describe the behavior of gas adsorption on various surface types. The Langmuir model states that a single layer of molecules may adhere to the substrate surface, thus adsorptive capacity would be limited to the total number of molecules that are required to cover the solid surface with one layer of molecules. In 1938, Brunauer, Emmett and Teller, developed the BET isotherm, an adsorption model that allowed for multi-layer adsorption. The empirical and thermodynamic support for both of these models requires that sorbates exist at very low pressures and temperatures. In a discussion of adsorption models such as BET and Langmuir, methane adsorption data presented by Brunauer [1] were collected at pressures below 1 atm (14.73 psia) and temperatures below the critical temperature for methane -116.7 °F (-116.7 °C).

Reservoir conditions for economic extraction of coalbed methane generally range from pressures of 1000 to 2000 psia and temperatures of 80 °F to 125 °F. The Langmuir isotherm empirically may fit adsorption data up to about 600 psia, but often fails over wide pressure ranges, especially above 1500 psia. The BET form presents a better empirical fit to most data that ranges from 0 to 2000 psia, but both models fail to fully explain the sorption process at these high pressures and temperatures. The inadequacy of these models results from the fact that mono-layer and multi-layer physical adsorption capacities have been greatly exceeded at such high pressures [2,3].

Potential theory, as developed by Polanyi and Dubinin, attempts to explain the adsorption mechanism by assigning the sorbate a quantifiable adsorption potential varying as a function of distance from the substrate surface. In other words, under reservoir conditions a density gradient develops and the density of the sorbate increases as distance to the substrate surface decreases. Equipotential surfaces could then be drawn at given distances from the surface to model the state of the sorbate. In 1991, Collins developed a Langmuir based, large pore adsorption model that resembles potential theory models. They state that, under reservoir conditions the density of the sorbate can exceed that of the liquid phase for most gases. The resulting density gradient is referred to as "phase layering" where phase boundaries are defined by equipotential surfaces. The surface layer is defined by a finite number of sites and a corresponding finite volume just as a mono-layer is described by the Langmuir model. The use of the Langmuir model to describe gas capacity may be inadequate because it does not account for the formation of multi-layers in the sorbed phase or the existence of a phase gradient over the sorbed layer.

Phase layering is used here to describe, not only a density gradient, but also the possible existence of definite phase boundaries that are described by equipotential surfaces. The model described by Collins applies only to large pores (>30 angstroms in diameter), but it is believed that the same type of density gradient (and phase layering) may occur within smaller pore spaces as well. Further, it is proposed that a density gradient is steeper in a micropore than in a macropore, which results in an increased relative gas capacity for micropores. The results from adsorption isotherms, surface area measurements, and micropore analysis for substrates of varying structure, demonstrate how pore size influences gas capacity. Low pressure CO_2 adsorption experiments were performed on the substrates to

determine their relative pore surface area and pore volume. Calorimetry experiments were performed to further demonstrate the existence of phase layering of methane in micropores.

EXPERIMENTAL PROCEDURE

Substrate Description and Adsorption Test Preparation

Four substrates were chosen for sorption experimentation. Two vitrinitic coals (#1 and #2) were chosen and sampled from high pressure and temperature reservoirs (1960 psia and 125 °F) because of there homogeneous composition. Coal #3 is a non-homogeneous banded coal, with alternating thin layers of vitrain and thicker layers of durain. The fourth substrate, activated charcoal, served as a compositional control. Sorption data is not presented for coal #3, however, surface area measurements are presented. Coals #1 and #2 are approximately one cubic inch in size, cut from the middle of a four inch diameter core. Coal #3 was cut as a one inch length of a two inch diameter core. The activated charcoal was supplied in 6 x 8 mesh pellet form, thus limiting the maximum sample size for this substrate. Activated charcoal is extremely porous and permeable. The total measured surface changes by about 2.5 ten thousandths of a percent between one inch and 6 x 8 mesh particles. For this reason, the surface areas between 6 x 8 mesh and one cubic inch or two inch diameter particles are not considered to be significantly different, thus allowing comparison of adsorption data for all four of the above substrates.

The temperature for the experimental isotherms was chosen to be 125 °F (51.8 °C) to match the reservoir temperature of the coal samples that were tested, and because previous isotherm data on the coal samples was collected at this temperature. Before testing, the activated charcoal and coal #3 were saturated with distilled water and allowed to come to equilibrium moisture with a saturated solution of potassium sulfate in accordance with ASTM procedure D 1412 Section 8. Coal #1 and #2 were saturated with water from the reservoir rather than distilled water and allowed to come to equilibrium in the same manner. A second 6 x 8 mesh activated charcoal sample, dried at 392 °F (200 °C) for 8 hours, was also tested to determine gas capacity.

Several different size classes of these three substrates were tested to determine the effects of structure on gas capacity. Each of the samples were progressively ground to 20 x 32, 60 x 80, then <80 mesh sizes. Adsorption tests were performed on each of the size classes including the unground, one inch cubed, and 6 x 8 mesh samples to demonstrate how particle size affects the gas capacity and other important measured parameters of a porous carbon substrate. Some past workers have suggested preparing adsorption samples by grinding to minus 60 mesh [4]. Some experimental data has suggested that this conclusion may not be warranted, therefore a comprehensive test was designed to demonstrate the variation in gas capacity with change in particle size.

Experimental Isotherms and Curve Fitting Procedures

The Real Gas Law is useful in determining the apparent amount that is sorbed in the coal. The number of molecules that are considered sorbed to the surface of the substrate is determined by calculating the change in the number of molecules in the gas or fluid phase using the Real Gas Law:

$$n = pV(f_{pV})^2/(RT) \quad (1)$$

where f_{pV} is the supercompressibility factor as calculated from the equilibrium pressure and temperature using the American Gas Association (AGA) Gas Orifice Flow program [5]. Corrections as suggested by Yee, et al. [6] have also been made for changes in free volume of the canister resulting from occupation by the sorbed phase.

$$V_{absolute} = V_{Gibbs}/(1 - \rho_{free}/\rho_{sorbed}) \quad (2)$$

where ρ_{sorbed} is the density of the sorbed phase, ρ_{free} is the density of the gas or fluid phase and V_{Gibbs} is the gas content at standard temperature and pressure as calculated from the measured equilibrium pressure and temperature. Yee et al. also suggests using the Van der Waals volume correction term (b), to calculate the density of the sorbed phase at temperatures above the critical temperature (-82.6 °C for methane). This results in a sorbed phase density of 0.375 g/cc for methane. The density of the free gas phase is calculated from the measured pressure and temperature using the AGA Gas Orifice Flow program. It should be noted that no correction has been made for density changes in the fluid phase due to surface attractions, as the authors are not aware of a convenient method to make this correction.

To calculate the experimental amount of methane sorbed by the substrate at a given pressure, the number of moles of methane contained by the system at the end of a test is subtracted from the number of moles contained by the system at the beginning of the test. The amount of methane in the system at the beginning of a test is equal to the number of moles of fluid in the sample vessel (at equilibrium from the previous test) plus the number of moles of gas in a reference vessel. The reference vessel is at a calculated higher pressure to achieve a desired beginning pressure on the sample when the vessels are opened to each-other. The test begins when the sample vessel is opened to the reference vessel. The final amount of methane contained by the system is determined when the number of moles in the system, as calculated by the Real Gas equation (1), has stabilized for more than one hour within +/-1.0 x 10^{-5} moles. This test procedure is repeated seven times at equal pressure increases of approximately 300 psia each to achieve a maximum pressure of approximately 2100 psia. The volume correction given by equation (2) was applied to each equilibrium test point.

Because at high pressures and temperatures, the Langmuir model is merely an empirical fit to adsorption data, and because the data does not always meet the requirements of the Langmuir model over a wide range of pressures, other statistical fits have been employed with good results. The authors have observed that most isotherm data below 2500 psia are best fit by third order polynomials. This type of empirical fit closely replicates the graphical form of multi-layer and/or phase-layer models such as BET or Polanyi type. Figure 1 graphically compares a model BET equation with a third-order polynomial regression curve. The polynomial regression is a best fit through the labeled points which were calculated from the BET equation. The close fit of the two equations is both visually and statistically apparent, as the level of confidence is greater than 99% for the regression fit.

Surface Area Measurements

In order to understand how the structure of the coals changes with particle size, the surface area of each size fraction was measured. This was accomplished by adsorbing CO_2 to the samples and calculating the total surface area using the BET isotherm as described by Mahajan [7], at pressures between 4 and 30 psia and at a

temperature of 77° F (25° C). Micropore analysis was performed by applying the Dubinin-Radushkovich equation as outlined by Adamson [8] and Mahajan to the CO_2 adsorption data. Determination of the micropore surface area from volumetric data requires some knowledge of the geometry and size distribution of the micropore structures. The micropore surface values that appear in Table 1 and figure 2 are based on a slit geometry and a pore width of 20 angstroms.

Calorimetry Testing

The calorimetric apparatus used to measure desorption energies is similar in construction and configuration to a high pressure adsorption apparatus. Desorption energies were calculated by subtracting the amount of thermal energy that was lost to the surroundings from the amount of energy required to maintain a constant temperature in the adsorption vessel. A plot of heats of desorption for dry activated charcoal, measured isothermally at pressures up to 2050 psia, appears in figure 3. The heats of desorption vary widely and are as much as two orders of magnitude above values that are commonly predicted by Langmuir theory. Further, the graph displays two important features. The first is the high change in enthalpy on both sides of the critical pressure, accompanied by a trough at the critical pressure (640 psia). The second feature is the rhythmic steady rise and sharp drop in desorption energies as pressure decreases. These rhythmic fluctuations continue from the maximum pressure of 2050 psia down to the critical pressure trough. Even though supercritical fluid behavior is poorly understood, the trough at critical pressure is significant because it clearly marks the transition from dense gas to supercritical fluid.

DISCUSSION OF RESULTS

Adsorption Modeling

From the methane adsorption isotherms for coals #1 and #2 and the activated charcoal (fig. 4 through 6), two characteristics are immediately apparent. The most obvious is that particle size appears to affect the gas capacity of each sample. All samples show the same trend; an increase in gas capacity as the particle size decreases, reaching a maximum for the 60 x 80 mesh sample, then dramatically decreasing in capacity for the <80 mesh sample. This relationship is presented graphically in three dimensions in figure 7. Water content and sample density may also be affected by grinding (Table 2). Secondly, none of the isotherms are described well with a Langmuir form over the wide pressure range that is plotted. In fact, most equations describing the data appear to have a relatively complex form.

The isotherm data for the coal core samples is graphed in figures 8 and 9. These data have been fit with a third-order polynomial. The calculated Langmuir form for the first three points is also presented. Utilizing the total surface area measurements from the CO_2 experiments, the maximum number of adsorption sites available in a mono-layer were calculated, and a theoretical methane Langmuir isotherm derived. This "true" Langmuir isotherm appears along the pressure axis in each graph. It is apparent that the adsorbed mono-layer is a tiny, almost insignificant, portion of the total sorbed gas content when the coal exists at reservoir conditions. The empirical Langmuir isotherm that is fit to the adsorption data is clearly not equivalent to the calculated "true" mono-layer Langmuir form. Therefore the empirical fit must correspond to a multi-layer component or pore filling [2,7,8].

The deviation of the third-order curve from the empirical Langmuir fit at about 900 psia suggests that there is more than one component to the sorbed gas. As discussed earlier, Collins propose an adsorption model that is based in Langmuir theory, but allows for a density gradient and consequently liquid and "dense gas" phases over the sorbed layer. Such a marriage between physical adsorption models and potential theory could help explain the complex character of sorption data for gases in coals at elevated pressures.

The model that Collins developed is limited to large pores (>30 angstrom radius), and its application is rather cumbersome because it requires a thorough knowledge of the geometry and distribution of the substrate pore spaces and the ability to calculate substrate and sorbate dependent potential energy parameters. However, this theoretical approach permits justification for empirical models that exceed the simplicity of the Langmuir model. As pressure increases, it is not uncommon for multi-layer formation, condensation, and density gradients to result in multi-component isotherms. Additional factors affecting sorption capacity include: pressure dependent permeability, water content, and gas composition. Figures 10 and 11 shows the isotherm data for the core and 60 x 80 mesh samples for two of the coals plotted with Langmuir type isotherms through the first three points followed by third-order fits through the remaining points. The Langmuir form for the lower pressure data points may correspond to the formation of a thick sorbed layer, or to the filling of a particular size fraction of pores. The deviation from the Langmuir model near 900 psia results from the effect of pressure dependent components such as permeability, condensation, and gas composition.

A similar correlation between mesh size and gas capacity exists for the charcoal as does for the coals. The isotherm forms are decidedly concave-up. This is due to the fact that the initial equilibrium moisture content of the samples was between 30 and 40 percent (Table 2). As the pressure is increased, it is thought that water is displaced and gas capacity correspondingly increased. The suppression of gas capacity at lower pressures results in the concave-up form. Figure 12 compares the adsorption isotherm for "dry" 6 x 8 mesh activated charcoal to those of the water saturated samples. Even though it clearly does not fit the Langmuir model, the form of the isotherm for the "dry" activated charcoal is relatively simple. This simplicity may be the result of a limited number of possible components. The substrate is homogeneous and the structure is relatively regular.

Micropore Distribution And Gas Capacity

The results of the CO_2 adsorption experiments show that as particle size of the sample decreases to 20 x 32 and 60 x 80 mesh size, the micropore surface area (and corresponding micropore volume) increases (fig. 2). But when the mesh size is decreased to <80, the micropore surface area of the sample decreases. The effect of particle size on gas capacity at 300 psia and 1000 psia is presented in figure 13 for comparison with the change in micropore surface area in figure 2. The trend for the change in gas capacity with particle size follows that for the change in micropore surface area with particle size. It could be argued that decreasing the mesh size increases the effective permeability, increasing the accessibility of the micropores. If it is assumed that the principal adsorbent surface is contained by the micropores, then the decrease in methane capacity for the <80 mesh coal sample is explained by the fact that the particle size is approaching that of the micropores and that the micropore structures are being destroyed.

Calorimetry And Fluid Density

The desorption energies measured by the calorimeter are stated in kilojoules per mole. These values quantify the energy needed to desorb the gas in terms of the number of moles of gas that were adsorbed to the amount of energy that was needed for the sorption process. Figure 14 demonstrates how the number of molecules that exist over the sorbed phase increases in proportion to the density of the gas or fluid phase. For any given pressure at "A", a model based on the Real Gas Law calculates the number of molecules in the system by assuming that the gas or fluid density at "A" is equal to the density at "B". When considering a fluid density that increases near the substrate surface, the amount of gas or fluid phase sorbate would be under calculated by any equation of state that does not account for a density gradient, and concomitant increase in the number of molecules sorbed. The desorption energies obtained by the calorimetry measurements are high, even by chemi-sorption standards. The number of molecules involved in the sorption process is under calculated by the Real Gas Law and amount of energy per mole of gas sorbed is overestimated. The resultant calculated desorption energies are inflated; but, they are proportional to the actual desorption energies. Therefore, the desorption energy measurements have qualitative significance in that the shape of the desorption energy graph (fig 3) is representative of the pattern of energy flux that takes place during adsorption/desorption. With this in mind, the high desorption energies that were measured reflect the movement of an equipotential phase boundary toward the substrate surface, and the peaks on the graph would represent the formation of potential energy surfaces coincident with these phase boundaries.

CONCLUSIONS

Three categories of data have been collected and analyzed. These include isothermally determined gas capacities of the four substrates, surface and relative pore volume measurements of the four substrates, and calorimetrically measured desorption energies for activated charcoal. Regardless of the phase or mechanism of adsorption of methane on coal, it is obvious from the surface plots of mesh size and pressure against gas capacity that particle size affects the gas capacity of a coal. Intuitively, one might predict that, because the surface area of the particles is increasing as the mesh size decreases, that the gas capacity would also increase. This relationship appears to be true for relatively large particles, but as mesh size of the particles continues to decrease, the gas capacity also begins to decrease. The nature of the mechanism for such a relation between particle size and gas capacity is not readily apparent. However, if the gas capacity of the coal is controlled by the availability and accessibility of micropores, then the relationship between gas capacity and mesh size is easily explained.

It has been shown that for the substrates that were tested, gas capacity is affected by pore size distribution, which is affected by particle size. Changing the particle size of the adsorption sample will change the measured gas capacity. All of the data presented supports the existence of density gradients or phase-layering in micropore spaces. Measurement of the density and the amount of a fluid that is involved in the sorption process is not possible by conventional methods. Potential theory predicts such problems in measuring sorbed gasses, but offers no solutions, beyond a better understanding of the sorption process. However, armed with this better understanding, empirical models can be used to better describe the sorption process, and would be more useful in predicting the behavior of gas in the reservoir. Moreover, modeling by empirical methods allows the model to most accurately fit the data, rather than forcing the data to fit a simple mathematical form.

REFERENCES

1. Brunauer, S., 1945, The Adsorption of Gases and Vapors; Volume I, Princeton University Press, Princeton, 497 p.

2. Collins, R. E., 1991, New Theory for gas Adsorption and Transport in Coal, Proceedings of the 1991 Coalbed Methane Symposium, May 13-16, 1991, 7 p.

3. Tan, Z. and K. E. Gubbins, 1990, Adsorption in Carbon Micropores at Supercritical Temperatures, Journal of Physical Chemistry, v. 94, no. 15, p. 6061-9.

4. Mavor, M. J., L. B. Owen and T. J. Pratt, 1990, Measurement and Evaluation of Coal Sorption Isotherm Data, Society of Petroleum Engineers 65th Annual Technical Conference Paper 20728, 14 p.

5. American Gas Association Gas Orifice Flow Program, Starling Associates, Inc., 1993.

6. Yee, D, J. P. Seidle and W. B. Hanson, 1994, Gas Sorption on Coal and Measurement of Gas Content, AAPG Studies in Geology #38: Hydrocarbons from Coal, p. 203-218.

7. Mahajan, O. P., 1982, Coal Porosity, *in* Coal Structure, R A. Meyers ed., p. 51-86.

8. Adamson, A. W., Physical Chemistry of Surfaces; 5th ed., John Wiley and Sons, New York, 1990

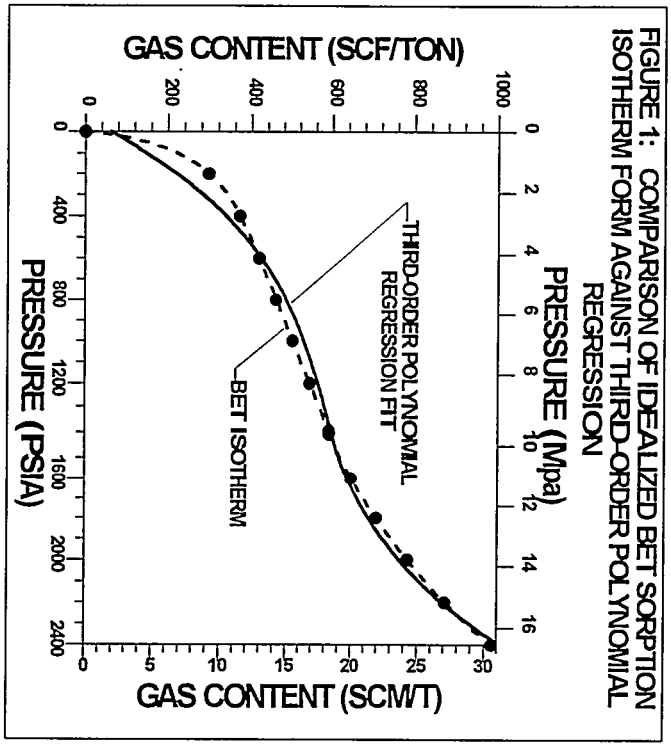


FIGURE 1: COMPARISON OF IDEALIZED BET SORPTION ISOTHERM FORM AGAINST THIRD-ORDER POLYNOMIAL REGRESSION

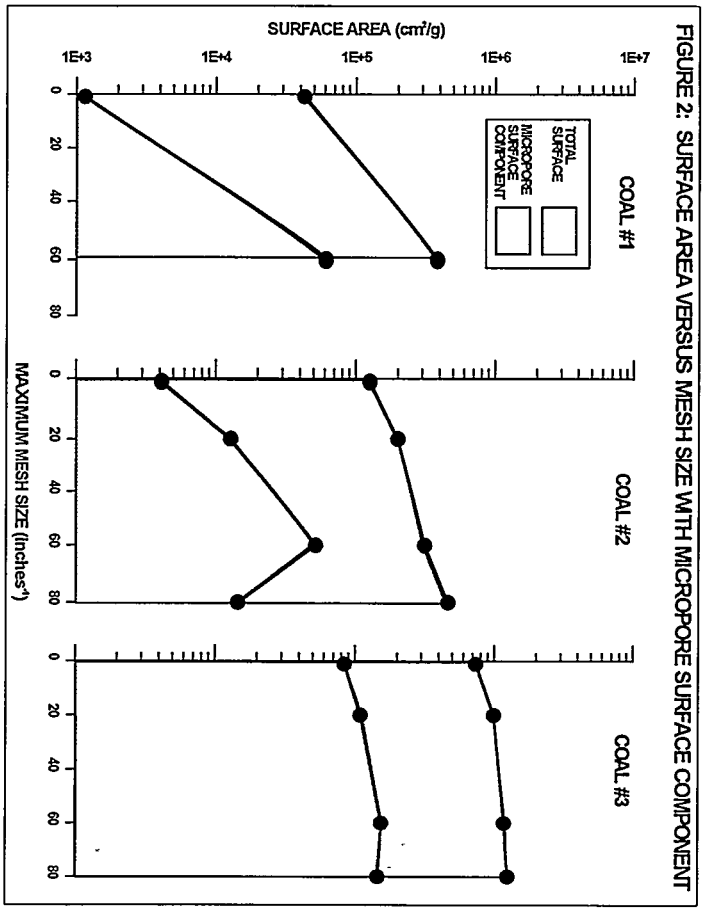


FIGURE 2: SURFACE AREA VERSUS MESH SIZE WITH MICROPORE SURFACE COMPONENT

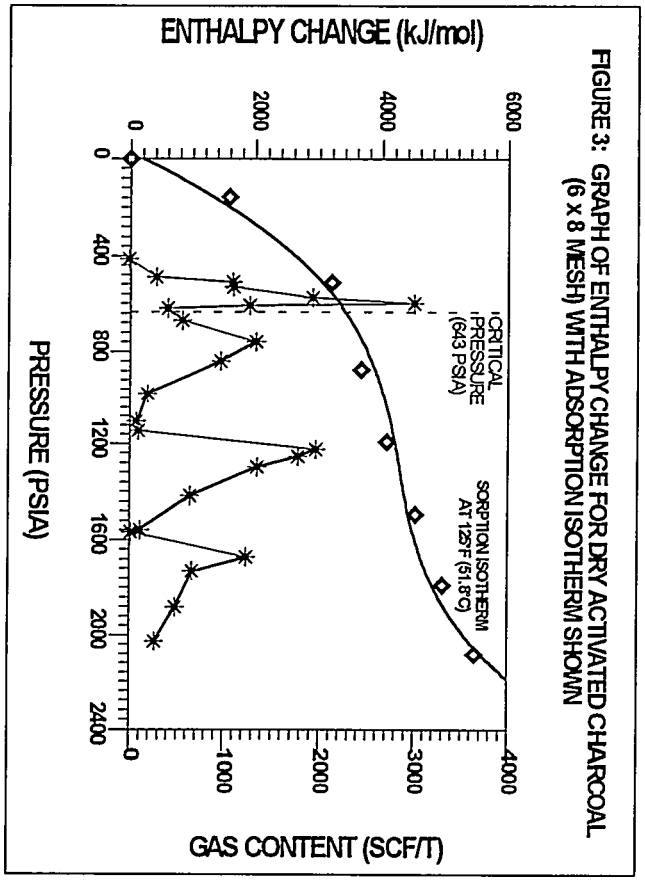


FIGURE 3: GRAPH OF ENTHALPY CHANGE FOR DRY ACTIVATED CHARCOAL (6 x 8 MESH) WITH ADSORPTION ISOTHERM SHOWN

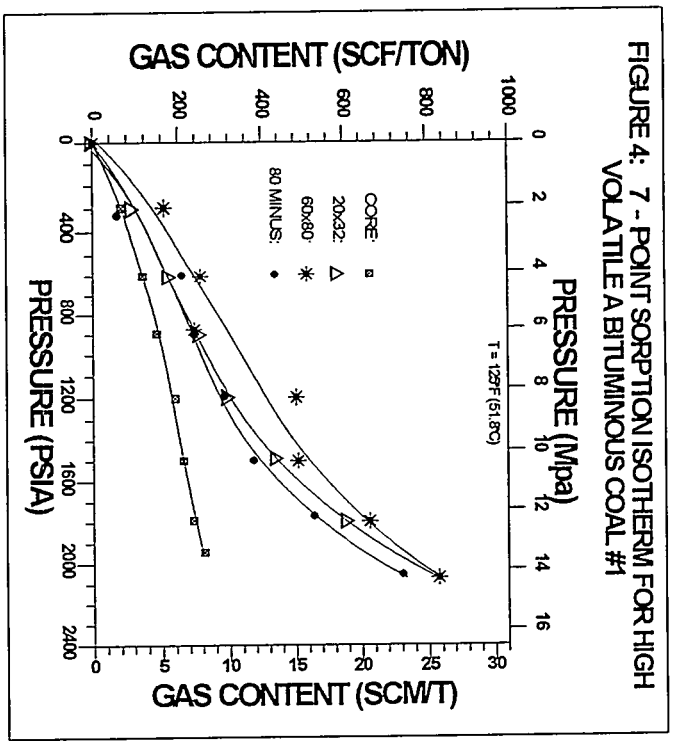


FIGURE 4: 7 - POINT SORPTION ISOTHERM FOR HIGH VOLATILE A BITUMINOUS COAL #1

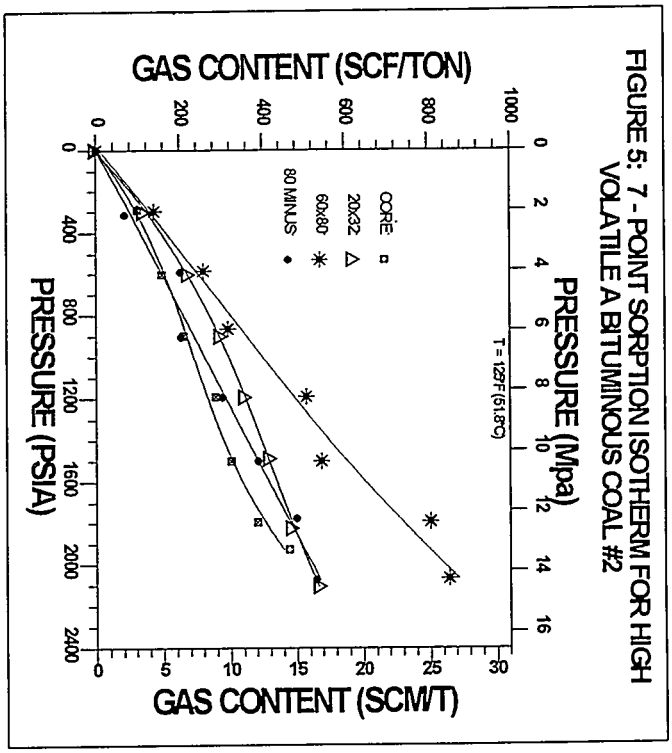


FIGURE 5: 7 - POINT SORPTION ISOTHERM FOR HIGH VOLATILE A BITUMINOUS COAL #2

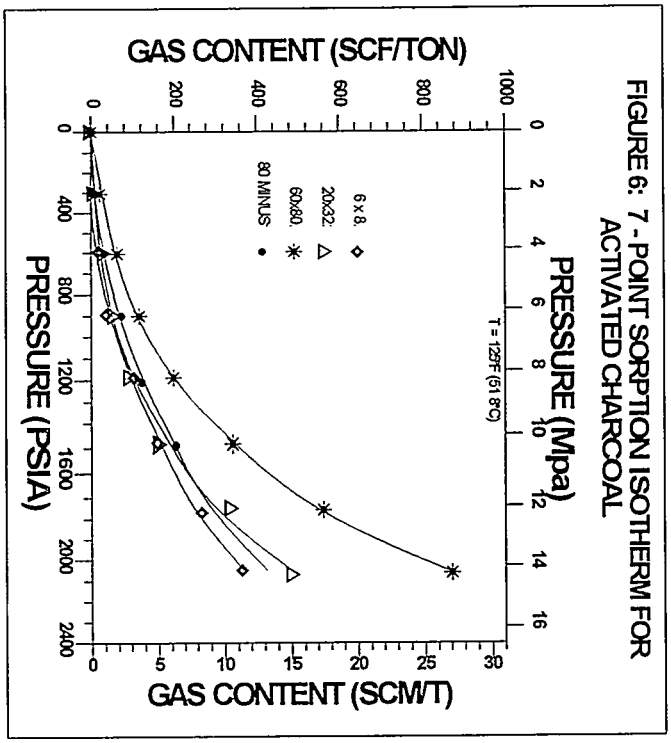


FIGURE 6: 7 - POINT SORPTION ISOTHERM FOR ACTIVATED CHARCOAL

FIGURE 7: SURFACE PLOTS OF GAS CONTENT AND PRESSURE VERSUS MESH SIZE

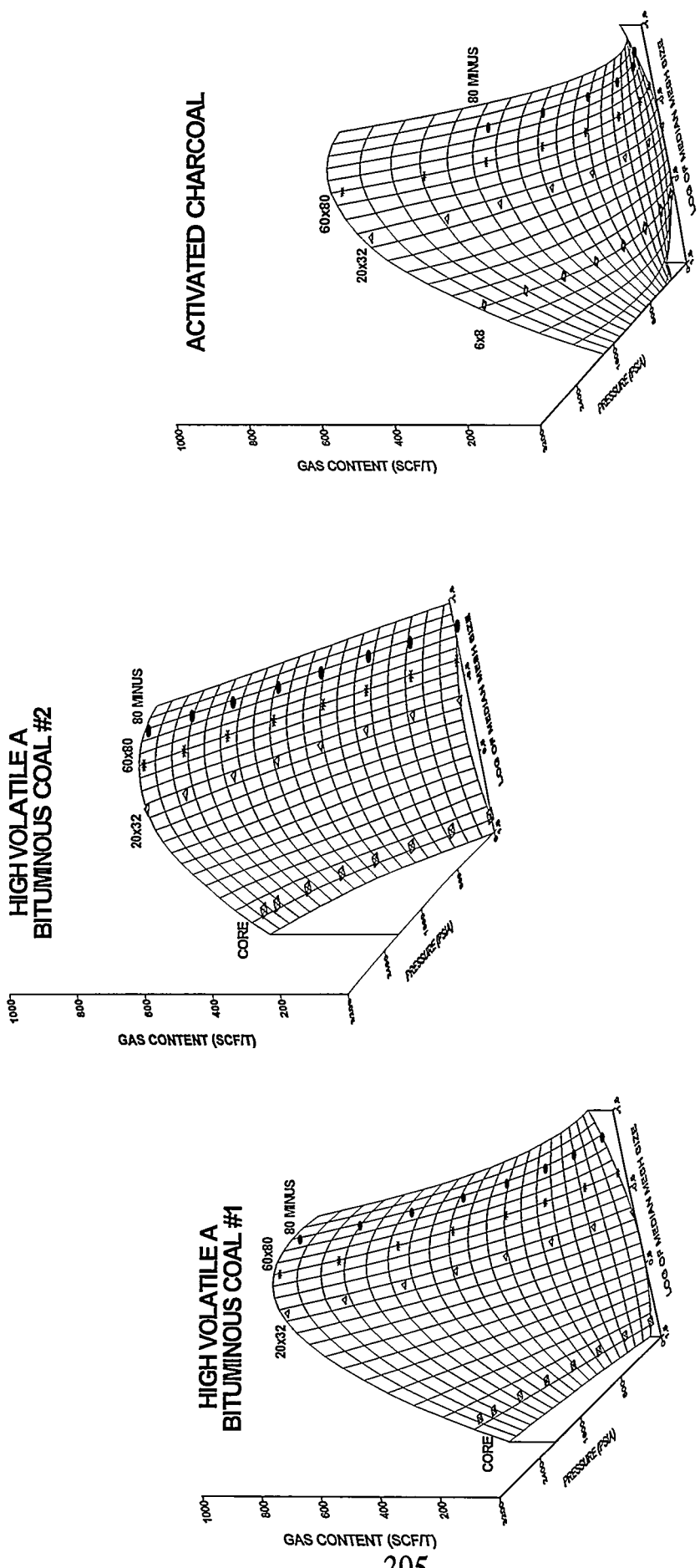


FIGURE 8: SORPTION ISOTHERM MODELS FOR HIGH VOLATILE A BITUMINOUS COAL #1 (CORE)

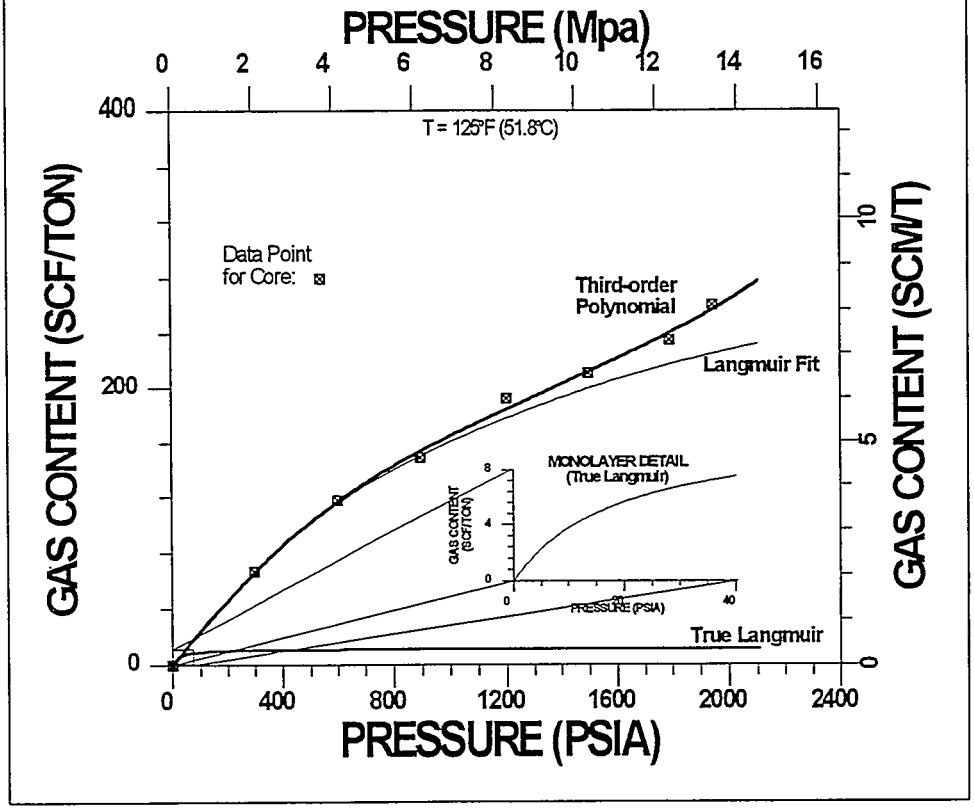
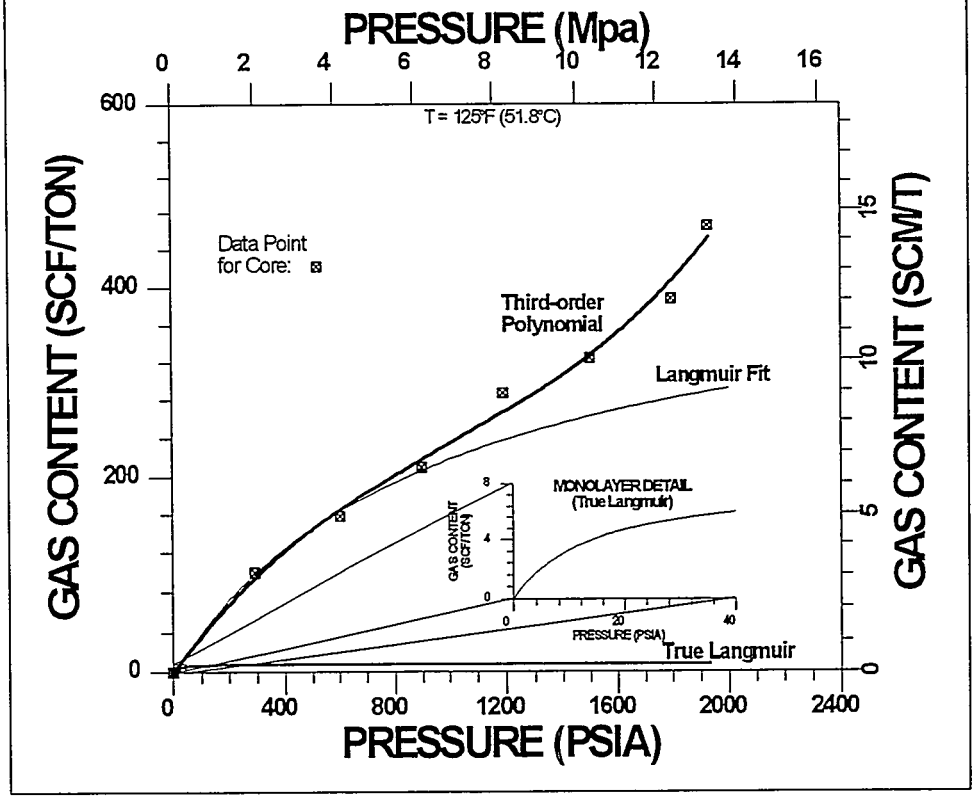


FIGURE 9: SORPTION ISOTHERM MODELS FOR HIGH VOLATILE A BITUMINOUS COAL #2 (CORE)



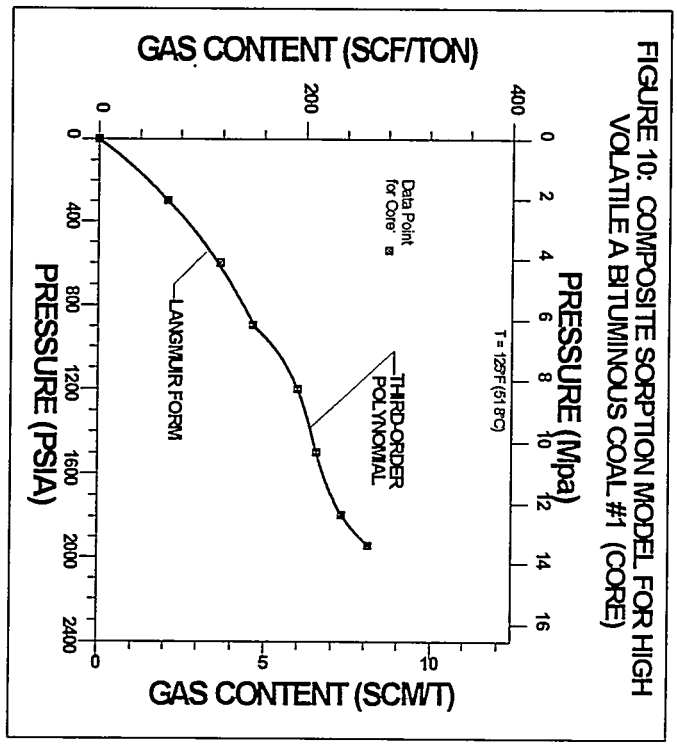


FIGURE 10: COMPOSITE SORPTION MODEL FOR HIGH VOLATILE A BITUMINOUS COAL #1 (CORE)

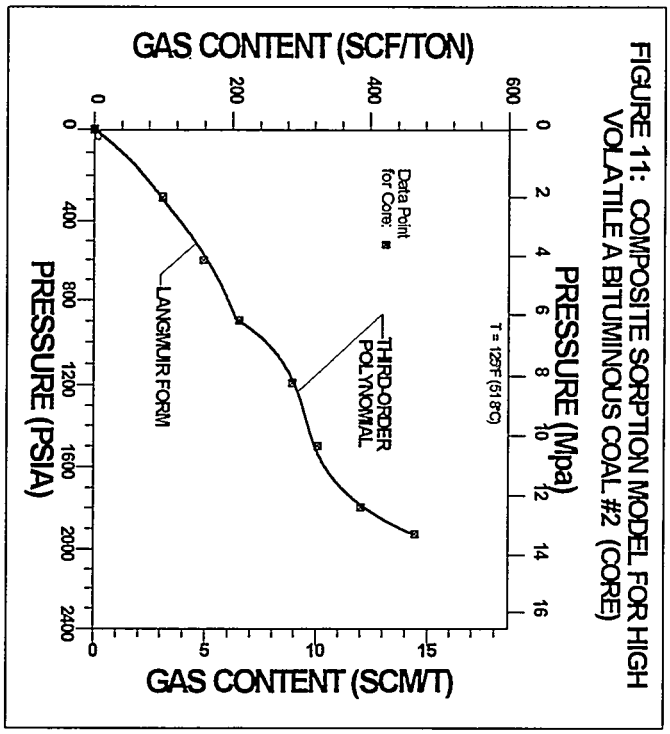


FIGURE 11: COMPOSITE SORPTION MODEL FOR HIGH VOLATILE A BITUMINOUS COAL #2 (CORE)

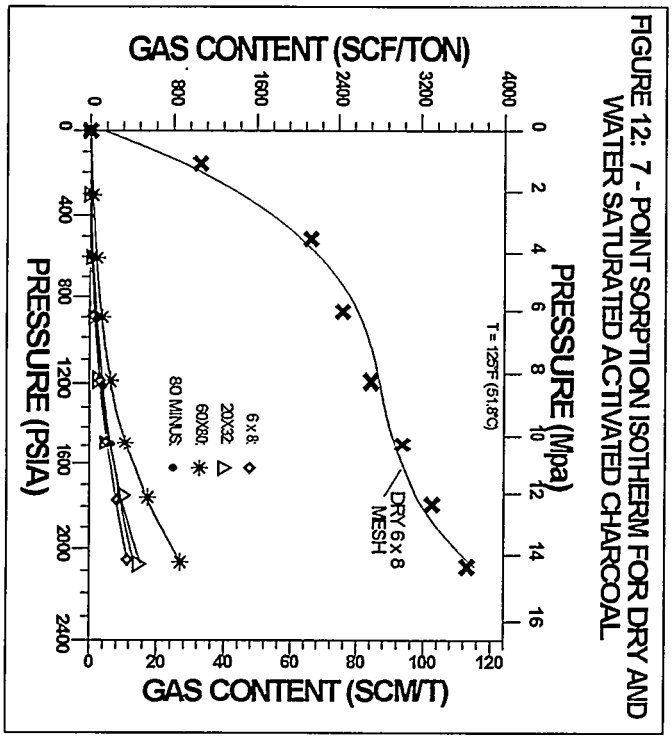


FIGURE 12: 7 - POINT SORPTION ISOTHERM FOR DRY AND WATER SATURATED ACTIVATED CHARCOAL

FIGURE 13: GAS CONTENT VERSUS MESH SIZE AT 300 PSIA AND 1000 PSIA

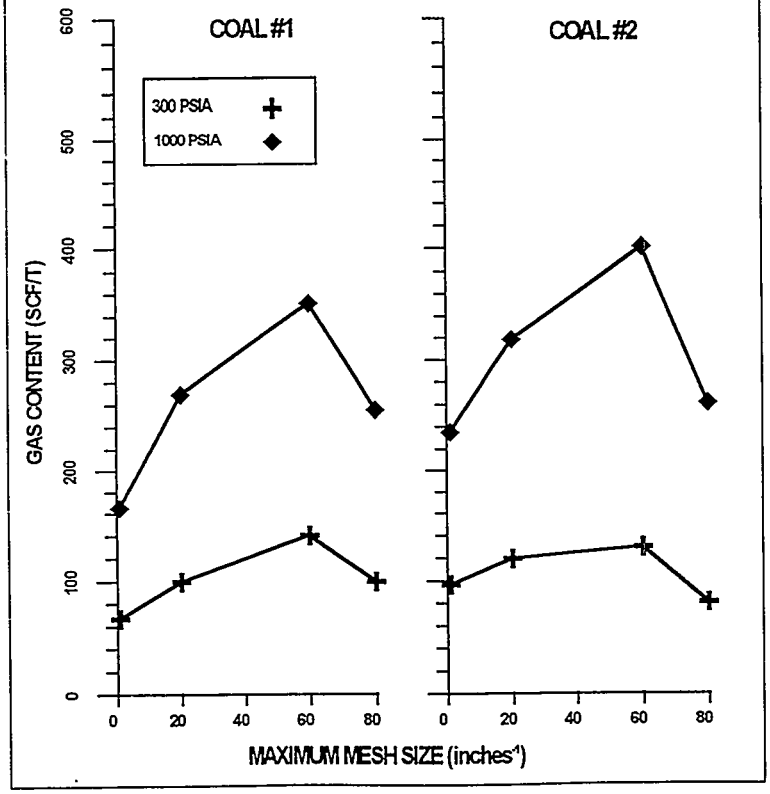


FIGURE 14: COMPARISON OF FLUID DENSITY MODELS

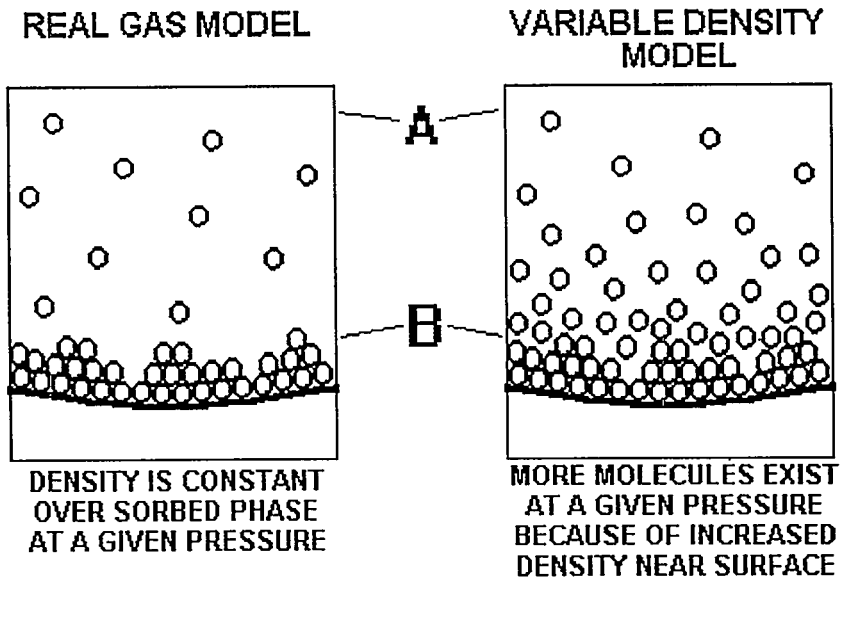


TABLE 1: DATA FOR TOTAL SURFACE AND MICROPORE SURFACE AREA				
TOTAL SURFACE AREA (cm^2/g)				
	COAL #1	COAL #2	COAL #3	A/C*
CORE	4.23E+04	1.26E+05	7.37E+05	-
6 X 8	-	-	-	7.76E+07
20 X 32	-	2.01E+05	9.91E+05	-
60 X 80	3.78E+05	3.15E+05	1.19E+06	-
<80	-	4.64E+05	1.25E+06	-
MICROPORE SURFACE AREA (cm^2/g)**				
	COAL #1	COAL #2	COAL #3	A/C*
CORE	1.06E+03	4.15E+03	8.45E+04	-
6 X 8	-	-	-	8.85E+04
20 X 32	-	1.28E+04	1.10E+05	-
60 X 80	6.08E+04	5.22E+04	1.56E+05	-
<80	-	1.46E+04	1.47E+05	-

* ACTIVATED CHARCOAL

** BASED ON SLIT GEOMETRY AND A PORE WIDTH OF 20 ANGSTROMS

TABLE 2: GAS CAPACITY, WATER CONTENT AND DENSITY FOR ADSORPTION SAMPLES			
PARTICLE SIZE	METHANE CAPACITY @ 300 psia (SCF/T)	MOISTURE CONTENT (% by mass)	HELIUM DENSITY (g/cc)
BITUMINUS COAL #1			
CORE	67.0	0.8%	1.82
20X32 MESH	99.6	6.0%	1.84
60X80 MESH	140.1	2.1%	1.87
<80 MESH	99.6	33.3%	1.75
BITUMINUS COAL #2			
CORE	96.6	0.2%	1.50
20X32 MESH	119.1	4.7%	1.79
60X80 MESH	129.6	2.9%	2.05
<80 MESH	80.7	28.7%	2.08
ACTIVATED CHARCOAL			
6X8 MESH	0.0	38.8%	3.26
20X32 MESH	8.9	29.6%	3.81
60X80 MESH	26.1	32.0%	4.43
<80 MESH	8.5	33.6%	2.98



NOTES

INTERGAS '95

May 15-19, 1995
The University of Alabama
Tuscaloosa, Alabama USA

9503

Methane Adsorption on Coals of the Bowen Basin, Queensland, Australia

J. Killingley, J. Levy and S. Day, CSIRO Australia

ABSTRACT

To help in assessing coalbed methane resources, methane adsorption capacities of Permian coals from the Bowen Basin of Queensland, Australia, have been investigated and related to other coal properties. Maximum methane capacities on moisture-equilibrated coals, normalised to a pressure of 5 MPa and 30°C, showed a continuously increasing (and reasonably linear) trend with increasing rank (corresponding to 60 - 92% fixed carbon and 80 - 92% total carbon). Such a linear trend was not observed for methane adsorption calculated on a dry basis. Methane adsorption capacity decreased as a function of increasing temperature by about 0.12 mL methane/g coal/°C. Methane capacity also decreased as moisture content increased: a reduction of about 4.2 mL/g coal for 1% increase in moisture content. Coal surface area (CO_2, Dubinin-Radushkevich) showed reasonable agreement with methane capacity although not precise enough to provide a reliable estimate of capacity. Langmuir adsorption isotherms for nitrogen and carbon dioxide on Bowen Basin coals were compared with the corresponding methane isotherms, and showed that, with a knowledge of the methane isotherm alone, nitrogen and carbon dioxide isotherms could be reliably constructed. Volumetric and gravimetric methane isotherms, measured on the same coal, were identical, confirming the accuracy of the procedures and calculations used.

INTRODUCTION

A renewal of interest in the coalbed methane potential of coal deposits along the Australian eastern seaboard has led to some recent intensive studies of Permian coals of the Bowen Basin of Queensland. In association with these studies, we are investigating the relationships between the methane adsorption capacities of Bowen coals and their characteristic properties. Information of this type should help in assessing the gas holding potential of these coals, given a knowledge of their specific dispositions such as seam temperature, seam pressure, moisture content and carbon content.

For United States coals various relationships between adsorbed methane and corresponding coal properties have been reported [1,2,3] and, in the present study, we compare some of the US relationships with those observed for Bowen coals.

EXPERIMENTAL

Coal Samples

Permian coal samples were from cores of about thirty separate drill holes across the Bowen Basin. Individual drill holes intersected up to eight coal seams, which were sampled for methane adsorption isotherms and other analyses. Seam depths ranged from about 200m to about 1km.

Methods

Volumetric Adsorption Isotherms. Volumetric gas isotherms were generally measured on moisture-equilibrated crushed coal samples using a method which involved automated high pressure volumetric equipment and calculations based on real gas laws [4]. The experimental system is based on that described by Mavor et al.[5].

Gravimetric Adsorption Isotherms. High pressure Sartorius microbalances were used to measure gravimetric isotherms on dry coal. These balances measure weight change on small samples (up to 100mg) at pressures up to 16MPa. The basic technique has been described previouly [6].

Proximate Analyses. Thermogravimetric proximate analyses for moisture, ash and fixed carbon were made on sub-samples of the crushed coal that was used in the isotherm measurements. Analyses were made on a Stanton Redcroft thermogravimetric balance using a technique that correlates well with ASTM Standards (D3172-73, re-approved 1984, and D5142-90): moisture and volatiles were determined by heating samples in flowing dry nitrogen and measuring weight loss at 170 and 940°C, respectively. Ash content was determined by subsequent combustion of the sample residue in flowing air. Fixed carbon was calculated by subtracting the moisture, ash and volatile percentages from 100%.

Coal Moistures. To investigate the effect of moisture on methane adsorption capacity, a crushed coal sample was fully wetted and then sequentially dried, first in air and then under vacuum, to progressively lower its moisture content to obtain a range from about 4% to 0% moisture.

Surface Area Measurements. Coal surface areas were determined using a Micromeritics ASAP 2400 Surface Area Analyser: an automatic instrument which operates on the

principle of gas adsorption. This instrument is usually operated using nitrogen as the adsorbate gas with the sample maintained at liquid nitrogen temperature but for the coal samples we used carbon dioxide as the adsorbate and measurements were taken at a temperature of 0°C.

Approximately one gram of sample was used for each surface area determination and was de-gassed at 50°C overnight before starting the analysis. Isotherm data were collected on each sample for a CO_2 pressure (P) range of approximately 6.0kPa to 120kPa, equivalent to a relative pressure (P/P_o) range of 0.002 to 0.034 (since the saturated vapour pressure, P_o, of CO_2 at 0°C is 3.4853MPa). Surface areas of the coals were calculated using the Dubinin-Radushkevich equation:

$$\log W = \log W_o - D\log^2(P_o/P) \quad (1)$$

where W = volume of adsorbate (mol/g) in porosity at relative pressure P/P_o, W_o = total micropore volume (mol/g) and D = a constant at constant temperature. A plot of logW versus $\log^2(P_o/P)$ yields a straight line with the intercept equal to $\log W_o$. Surface area (S) was then calculated as:

$$S = W_o NA \quad (2)$$

where N = Avagadro's number and A = the cross sectional area of the adsorbate (0.253 nm^2 for CO_2).

Total Carbon Analyses. Coal samples were analysed for total carbon content using an Australian Standard method (AS 1038.6.1) in which the coal is combusted at 1350°C and the amount of CO_2 evolved is determined gravimetrically.

RESULTS

Effect of Temperature on Methane Adsorption Capacity

Over the temperature range studied (20 to 65 °C) on moisture equilibrated Bowen coal there was a linear decrease in methane adsorption capacity with increase in temperature (Figure 1). The average decrease in capacity was 0.12 mL/g for each degree centigrade rise in temperature. This is similar to that reported previously [7] for several Australian coals.

Effect of Moisture on Methane Adsorption Capacity

As coal moisture contents increased, over a range from 0.9 to 3.7% H_2O, the methane adsorption capacity decreased in a linear fashion: at a rate of about 4.2 mL/g for each percent increase in moisture content (Figure 2). This dependence of methane capacity on moisture content may be expressed as:

$$V_d = V_m (1+0.39m) \quad (3)$$

where V_d and V_m are methane capacities for dry and moist coal, respectively, and m is the coal moisture content.

This is similar to the relationship described by Ettinger [8] where a multiplier of 0.31 was reported, in place of our 0.39. Joubert et al.[1], in a study of US coals, reported a multiplier of 0.23 for coals with about the same range of moisture contents as ours. They reported a critical value of moisture content which was coal-dependent and above which there was no further reduction in methane adsorption capacity. This is, apparently, the adsorbed water saturation value of the coal.

Coal Surface Areas

The amount of methane adsorbed on coal must be directly related to the coal's surface area, which is mainly the area of the micropores (less than 2nm in width). It was of interest, therefore, to relate the surface areas of the Bowen coals to their methane adsorption capacities to establish whether surface area measurements (using automated equipment) could be used as a rapid method of estimating total methane holding capacity of such coal samples.

Surface area measurements at very low temperatures (using nitrogen or argon, for example) are affected by activated diffusion limitations and also by some decrease in the micropore size [9]. Therefore, the use of carbon dioxide as the adsorbate at 0°C, and the Dubinin-Radushkevich treatment, provides more realistic surface area values. Although the accuracy of surface area determinations on porous materials is the subject of debate, by using this method it is possible to obtain good relative values.

Results of Dubinin-Radushkevich surface area measurements - on a dry ash-free basis (daf) - for the Bowen coals showed a reasonable correlation with methane adsorption on moisture equilibrated coals, as indicated by their Langmuir Volumes (Figure 3, solid black data points). These volumes, which had been measured at seam temperatures, were normalised to 30°C using the relationship described above. The Langmuir Volume is the constant (V_L) in the Langmuir equation:

$$V = V_L * P/(P_L+P) \quad (4)$$

where V is the volume of gas adsorbed at constant temperature (normalised to STP) per gram of coal; P is the absolute gas pressure and P_L is a second constant (the Langmuir Pressure). The Langmuir equation adequately represents the adsorption of methane on coal for pressures typical of coalbed methane operations and is based on monolayer coverage being complete at infinite pressure. The Langmuir Volume, therefore, is the volume of gas which is calculated, by Langmuir theory, to be adsorbed at infinite pressure. However, at very high pressures the simple Langmuir model of adsorption would not apply and the amount of gas adsorbed would be quite different.

To compare the surface areas with methane adsorption on a dry-basis the measured surface-area/adsorption data were treated in two separate ways:

1. Using the relationship which related methane capacity to moisture content, described above, the Langmuir Volumes at 30°C (Figure 3, solid black data points) were converted to Langmuir Volumes on a dry-basis (Figure 3, solid gray data points).
2. Assuming a molecular area of 0.106 nm^2 [9] for water adsorbed on the coal we calculated that 1% moisture would be equivalent to the monolayer water coverage of an area of 35.4m^2 on hydrophilic coal surfaces. On this basis, the surface area occupied by water on each coal

sample (based on its equilibrium water content) was calculated and subtracted from the corresponding, measured, surface area. The resultant area was then expected to correspond to the area, in each case, actually occupied by methane at 30°C. These values are shown as open data points in Figure 3.

The data sets, produced by two quite different assumptions, show reasonable coherence; the combined data plot was found to have a correlation coefficient (r^2) of 0.80. The slope of the line was 0.16. This means that, for example, a coal surface area of 100m^2/g corresponds to a methane Langmuir Volume of 16mL/g on a dry-basis but with a relative error of about 20%.

The scatter in the data points of the reduced data may be due, in part, to some of the equilibrium moisture being associated with the inorganic matter, and not adsorbed on the coal micropore surfaces in place of methane.

It appears that the error in the methane capacity/surface area relationship is sufficient to rule out surface area measurement as a fast and accurate estimate of the coal's potential to hold methane. However, it is a useful method for screening a large number of samples before selection for more detailed isotherm evaluations.

Methane Adsorption: Relationship to Fixed Carbon Content

Methane capacities, obtained from the methane adsorption isotherms measured on the Bowen coals, were compared with the fixed carbon values of the coals. In Figure 4 the methane capacities at 5 MPa (measured at seam temperature on moisture-equilibrated coals and corrected to 30°C) are plotted against fixed carbon content (daf) which is a general indicator of the coal rank. There is a continuous increase in methane capacity with fixed carbon from 60 to 90% carbon, such that a 10% increase in fixed carbon content, for example, would be expected to increase the methane capacity by about 3mL/g (at 5MPa and 30°C).

A large set of methane adsorption data for US coals has been reported [2] where measurements were made on dry coals. To enable a comparison to be made between these coals and Bowen coals it was necessary to convert our moisture-equilibrated coal data to a dry coal basis and we did this by using equation (3), above, and the measured equilibration moisture values. These moisture values are plotted versus fixed carbon (Figure 5) and show a broad minimum at around 80% fixed carbon, consistent with previous observations [12] on other coals.

The resultant set of data for dry Bowen coal is plotted in Figure 4, represented by open symbols. There is a much wider scatter in the dry-basis data, reflecting the combined variation of the moist-basis data and the coal moisture content. The difference in the methane capacity between dry and moist methane capacities is related to adsorption sites which are preferentially occupied by water, rather than methane. It is noteworthy that, for a given fixed carbon, the amount of methane potentially adsorbed on the dry-basis is much more variable than on a moist-basis. This implies that there is a variable range of hydrophilic sites (which preferentially host water molecules) but a more constant number of sites which are occupied by methane. These "methane-preferred" sites are probably less hydrophilic and/or less accessible to water molecules.

We adjusted the methane adsorption data for US coals [2] to a 30°C basis and plotted them against fixed carbon content (Figure 6, square symbols) for comparison with the Bowen coal data (shown in Figure 6 as the envelope of data from Figure 4). The scatter in the US data is similar to that for the Bowen data for about the same number of samples. However, on a dry-basis, where the fixed carbon ranges overlap, the Bowen coals have the potential to hold about 50% more methane, on average, than the US coals that are represented here.

While it is somewhat speculative to draw conclusions from data with such scatter, the combined data sets, adjusted to about the same average level, would indicate a broad minimum at a fixed carbon value of about 70%. This observation is consistent with a coalification "jump" at this point [10], corresponding to a marked reduction in oxygen content, an increase in methane release during coalification and the approximate end of oil generation.

The dry-basis adsorption data are obviously limited in terms of practical assessments of the methane-holding potential of coal seams (which are usually water saturated) and the results from the measurements of gas adsorption on water-saturated coal are more useful. This has been implied previously [11,12].

Methane Adsorption: Relationship to Total Carbon Content

Plots similar to those presented for coal fixed carbon contents, above, were made for coal total carbon content: firstly, for methane adsorption versus total carbon, a comparison was made between moist coal and dry coal and, secondly, a comparison was made between Bowen and US coal data. Total carbon contents ranged between 82 and 92% (daf).

Methane adsorbed at 5MPa and 30°C on moist coal (Figure 7, solid data points) showed a reasonably linear relationship of increasing methane adsorption with total carbon content, such that a 10% increase in total carbon was associated with about 8 mL/g increase in methane adsorption capacity.

The methane adsorption capacity, calculated on a dry-basis (from the moist coal data and the equilibrium moisture content) showed a sharp increase above 90% total carbon (Figure 7, open circle data points) but, for practical purposes (and as pointed out for the fixed carbon data), the moisture equilibrated data are likely to be more useful for assessing coalbed methane potential than dry adsorption data. For example, no sharp increase in capacity would be expected above a total carbon content of 90% for in-seam conditions.

A comparison was made between the Bowen dry-basis methane adsorption data versus total carbon (daf) and corresponding US coal data (Figure 8). For US coals, a minimum in methane adsorption (on a dry-basis) at around 85% total carbon has been suggested previously [2] and this also appears to be the case for the Bowen coals, although the

scatter, and lack of low total carbon data points, make this uncertain.

The surface area data, when plotted against total carbon (Figure 9), produced a profile similar to that of the dry-basis methane adsorption data and was also similar to a surface area versus total carbon profile reported for US coals [3] that showed a sharp increase in surface area above 90% carbon. However, our data suggest a minimum surface area between 85 and 90% total carbon, which contrasts with the shallow minimum at around 80% total carbon for the US data.

Adsorption of Nitrogen and Carbon Dioxide Relative to Methane Adsorption

Carbon dioxide or nitrogen can be injected into coal seams to improve methane recovery and, to model such processes, it is necessary to have knowledge of their adsorption isotherms for the specific coal under study.

Methane, nitrogen and carbon dioxide isotherms were measured on a selection of moisture-equilibrated Bowen coals (with fixed carbon contents in the range 65 to 82%). The isotherms showed that the amount of nitrogen adsorbed on these coals was about half that of methane which, in turn, was about half that of carbon dioxide. Nitrogen and carbon dioxide have similar kinetic diameters (0.36 and 0.33nm, respectively), and so the difference in their adsorption behaviour must be largely due to the polar nature of carbon dioxide, which (unlike nitrogen) allows it to adsorb on certain sites in place of water.

Langmuir Volumes and Pressures for nitrogen and carbon dioxide were plotted against the corresponding methane Langmuir constants in Figures 10 and 11. The Langmuir Volumes showed good linear relationships over the range considered (Figure 10), as did the Langmuir Pressures (Figure 11).

The carbon dioxide and nitrogen lines (Figure 10) are parallel, showing that, as the methane adsorption capacity of the coals increase, the carbon dioxide and nitrogen adsorption capacities increase at the same rate. By contrast, as the methane Langmuir Pressure increases (Figure11) the rate of change of the nitrogen Langmuir Pressure is greater than that of carbon dioxide. An increase in Langmuir Pressure can be interpreted as a change in the nature of adsorption bonding; a trend to bonding of increased physical character, with lower heat of adsorption.

The significance of the relationships presented in Figures 10 and 11 is that for coals of this type, at least, it is possible to construct nitrogen and carbon dioxide isotherms from a knowledge of the corresponding methane isotherm for the coal seam under study. We do not know how general these relationships are for other coals and this may be an appropriate area for future study.

Volumetric and Gravimetric Isotherms Compared

Accurate methane on coal adsorption isotherms are essential to proper coalbed methane evaluations. To obtain accurate isotherms it is essential to pay close attention to experimental assumptions and equipment variables. Because there is no standard reference coal sample with measured isotherms, we considered it important to verify the accuracy of our volumetric method of measuring isotherms by carrying out measurements on the same sample using a gravimetric method.

The gravimetric method which we used, using a high pressure microbalance, is not suitable for moist coal samples. We therefore used a coal which had been thoroughly dried by heating at 50°C under vacuum for 48 hours and then evacuated overnight after being loaded into either the gravimetric or volumetric equipment. Measurements were made at 30°C, from 0 to 10 MPa.

Two gravimetric isotherms were run on the microbalance on separate 100mg samples which were taken from about 80g of the crushed dried coal before it was loaded into the volumetric apparatus.

The resulting isotherms (Figure 12) from the gravimetric measurements (cross and open circle symbols in the figure) show very good reproducibility and are also in very good agreement with the volumetric isotherm (solid data points in Figure 12). Methane adsorption values at 5 MPa were 20.3 and 20.5mL/g for the gravimetric method, compared with 19.95mL/g for the volumetric method. Langmuir Volumes were 27.9 and 28.2mL/g for the gravimetric method and 26.8 for the volumetric method. The fact that the measurements made on 100mg samples were reproducible and accurate implies that the coal sample selected for the comparison was very homogeneous.

One of the uncertain assumptions in isotherm calculations is the density of the adsorbed phase. We, like other workers [13], assume a density for adsorbed methane of 0.42mL/g: the density of methane liquid at its boiling point. This density is used in the calculations of available void space for gas in the volumetric equipment and it is also used for buoyancy corrections in the gravimetric measurements. Agreement between the volumetric and the gravimetric procedures indicates that the assumed density is reasonable, although we plan to carry out further work to verify this.

CONCLUSIONS

- We measured the reduction in methane adsorption capacity of Bowen Basin coals as temperature and moisture content increased. An increase of 1°C in temperature was associated with a reduction in methane capacity of 0.12 mL/g of coal, on a dry, ash-free, basis. For an increase in coal moisture content of 1% there was a corresponding reduction in methane capacity of about 4.2 mL/g of coal.
- Surface area measurements (CO_2, Dubinin-Radushkevich) on Bowen Basin coals showed good agreement with methane capacities and, although not precise enough to substitute for methane adsorption measurements, we consider them useful for rapid initial screening of coal samples to indicate potential gas capacities.
- Methane adsorption capacities were related both to fixed carbon and total carbon contents. In both cases, as the carbon contents increased the methane capacity for

moisture-equilibrated coals increased in a reasonably linear fashion. This, however, was not the case for methane adsorption calculated on a dry basis, where the data were more scattered and there was a sharp increase in methane capacity for high rank coals (above 88% fixed carbon or 90% total carbon). Variations in methane capacity of dry coals related to carbon content are of limited practical use and the corresponding relationships for moisture-equilibrated coals are to be preferred for most coalbed methane estimates.

- Methane, carbon dioxide, and nitrogen isotherms were measured on a set of Bowen Basin coals. Linear relationships between their respective Langmuir constants showed that carbon dioxide and nitrogen isotherms can be reliably constructed for these coals, given a knowledge of the corresponding methane isotherm.
- A comparison of methane adsorption isotherms determined by both gravimetric and volumetric methods confirmed the accuracy of the methods and indicated that assumptions used in their respective calculations are valid.
- Results on Bowen Basin coals showed values and trends generally consistent with those reported for US coals.

ACKNOWLEDGMENTS

We are grateful to Mount Isa Mines Holding Ltd. and to Mitsubishi Gas Chemical Resources Australia Pty. Ltd. for permission to publish gas adsorption data and surface area data that had been produced on their behalf in our laboratories. We are also grateful to Ken Riley for the total carbon analyses and to Adam Berkovich and Michael Tadros for assistance in the laboratory work.

REFERENCES

1. Joubert, J.I., Grein, C.T., and Bienstock, D., 1974: "Effect of Moisture on the Methane Capacity of American Coals"; Fuel, V. 53, p. 186-191.
2. Schwarzer, R.R., and Byrer, C.W., 1983: "Variations in the Quantity of Methane Adsorbed by Selected Coals as a Function of Coal Petrology and Coal Chemistry"; Final Draft Report, U.S. Department of Energy Contract No. De-AC21-80MC14219.
3. Gan, H., Nandi, S.P., and Walker, P.L.Jr., 1972: "Nature of the Porosity of American Coals"; Fuel, V.51, p.272-277.
4. Levy, J.H., Killingley, J.S., Day, S.J., and Liepa, I., 1992: "Measurement of Coalbed Methane Isotherms for Some Australian Coals", Proceedings of the Symposium on Coalbed Methane Research and Development in Australia, Townsville, Queensland, Australia, V.4, p.1-8
5. Mavor, M.J., Owen, L.B. and Pratt, T.J., 1990: "Measurement and Evaluation of Coal Sorption Data", Paper SPE 20728, Proceedings of the 1990 SPE Annual Technical Conference and Exhibition, New Orleans, Louisiana, USA, p.1-14.
6. Killingley, J.S., Low, G., Pandolfo, A.G., Hoare, I., Amini Amoli, M., and Chaffee, A.L., 1991: "Advanced Methods for Natural Gas Storage", End of Grant Report on NERDDP Project 1359, CSIRO Division of Coal and Energy Technology, Sydney, Australia.
7. Bartosiewicz, H. and Hargraves, A.J., 1984: "Gas Properties of Australian Coals", Bull. Proc. Australas. Inst. Min. Metall., V.290, No.1, p. 71-77.
8. Ettinger, I., Lidin, I.L., Dmitriev, A.M., and Shaupakhina, E.S.,1958:"Systematic Handbook for the Determination of the Methane Content of Coal Seams from the Seam Pressure of the Gas and the Methane Capacity of the Coal", Institute of Mining, Academy of Sciences, USSR, US Bureau of Mines Translation No. 1505, NCB Translation A1606SEH.
9. Walker, P.L., Jr., 1981: "Microporosity in Coal: Its Characterization and its Implication for Coal Utilization", Phil. Trans. R. Soc. Lond. A 300, p. 65-81.
10. Stach, E., Mackowsky, M., Teichmuller, M., Taylor, G.H., Chandra, D., and Teichmuller, R., eds., 1982: Stach's Textbook on Coal Petrology, 3rd edn., Gebruder Borntraeger, Berlin.
11. Levine, J.R., 1992: " Oversimplifications Can Lead to Faulty Coalbed Gas Reservoir Analysis"; Oil and Gas Journal, Nov. 23 1992 , p.63-69.
12. Levine, J.R., 1993: "Coalification: The Evolution of Coal as Source Rock and Reservoir Rock for Oil and Gas", in Hydrocarbons from Coal, eds Law, B.E and Rice, D.D., AAPG Studies in Geology #38, Tulsa, Okalahoma USA, 400p.
13. Stevenson, M.D., Pinczewski, W.V., Somers, M.L. and Bagio, S.E., 1991: "Adsorption/Desorption of Multicomponent Gas Mixtures on Coal at In-Seam Conditions", paper SPE 23026, Proceedings of the 1991 SPE Asia-Pacific Conference, Perth, Western Australia, p.1-14.

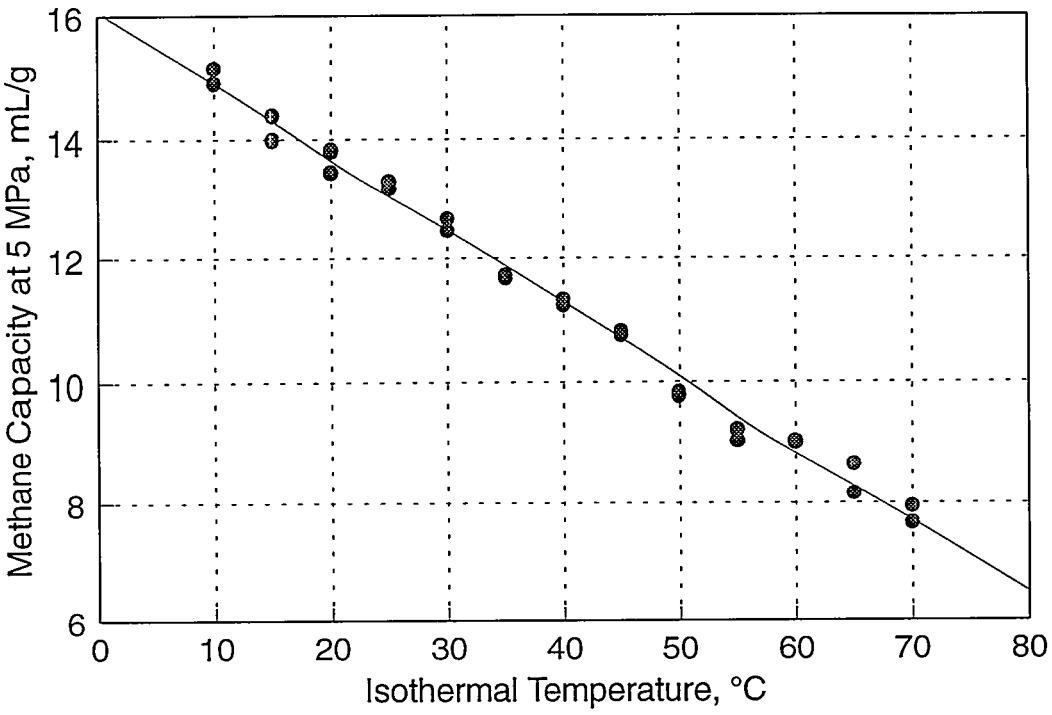


Figure 1. Effect of temperature on methane adsorption capacity (at 5 MPa).

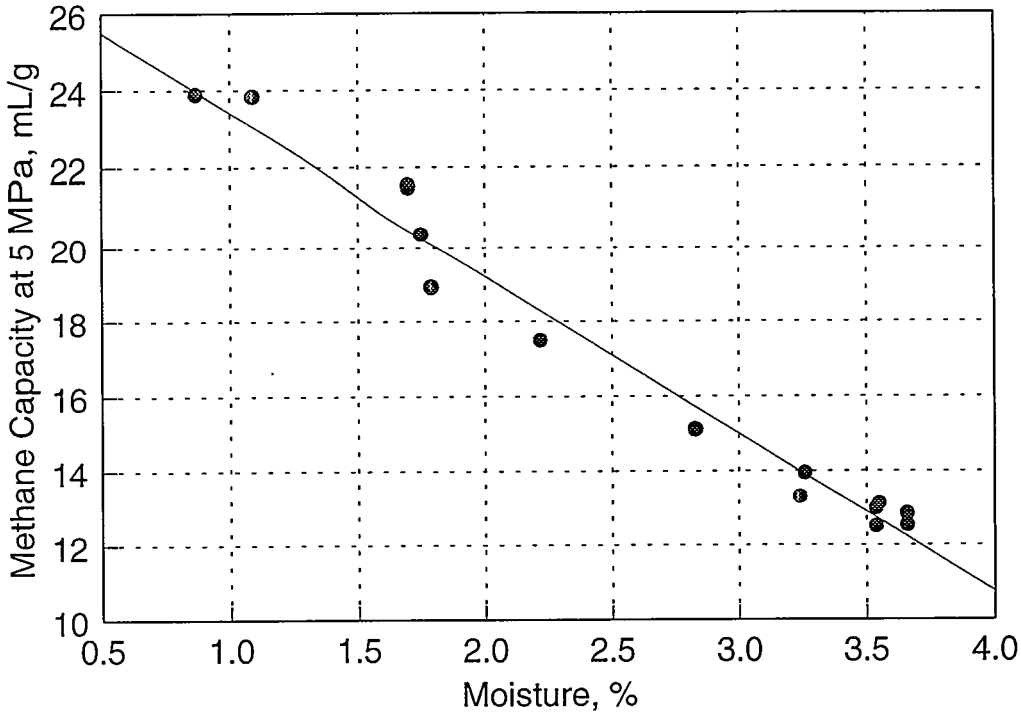


Figure 2. Effect of moisture on methane adsorption capacity (at 5 MPa).

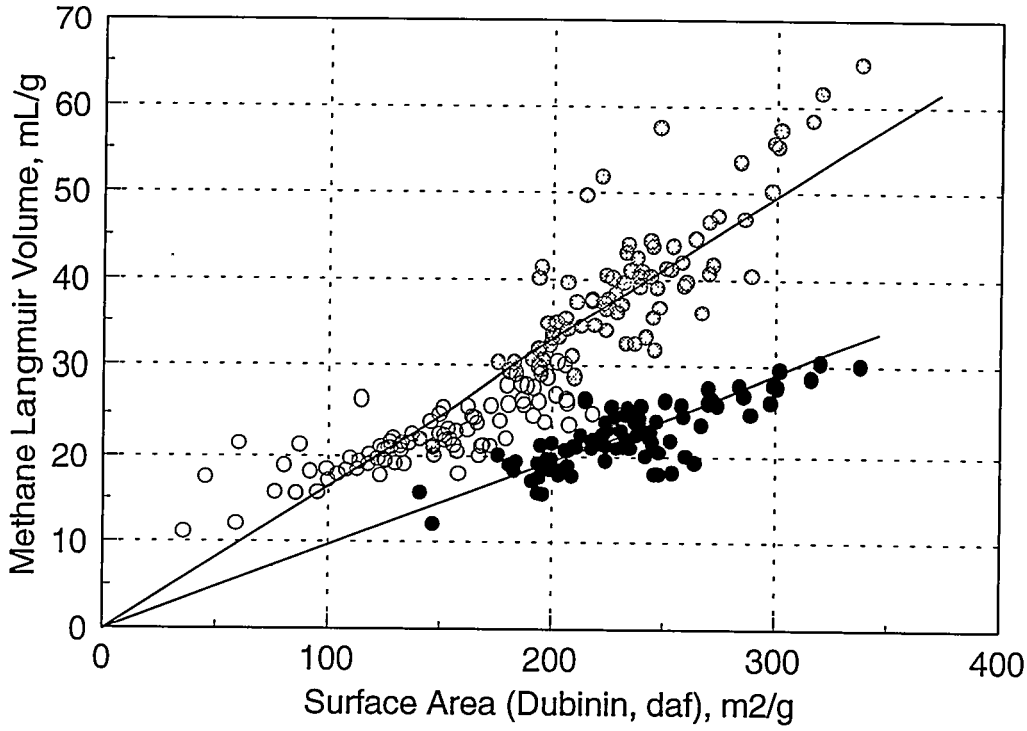


Figure 3. Relationship between total methane adsorption capacity and coal surface area for Bowen Basin coals. (Solid black data points correspond to methane capacity of moist coal. Grey data points and open data points correspond to calculated capacity of dry coal.)

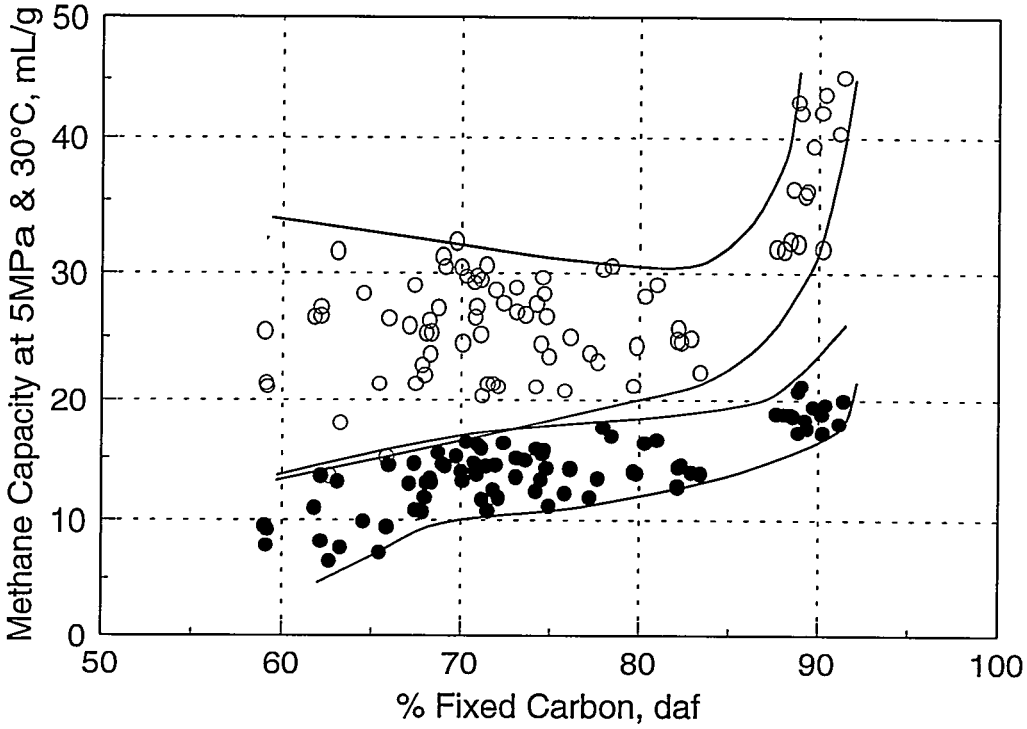


Figure 4. Relationship between methane capacity and fixed carbon for Bowen Basin coals. (Solid data points correspond to methane capacity of moist coal. Open data points correspond to calculated capacity of dry coal.)

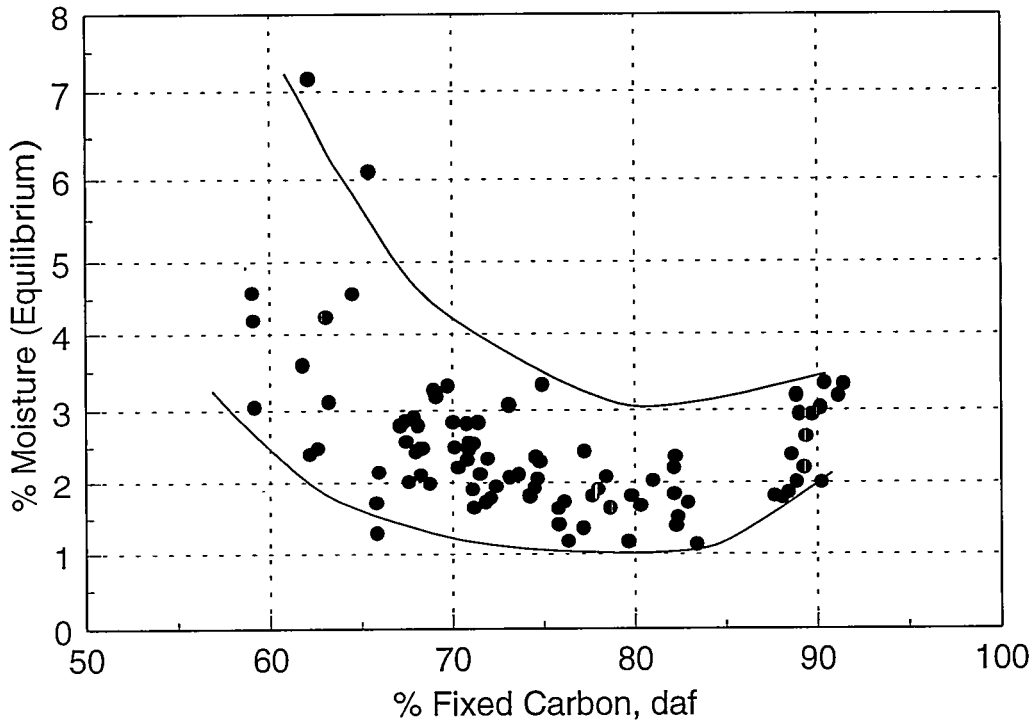


Figure 5. Relationship between equilibrium moisture content and fixed carbon for Bowen Basin coals.

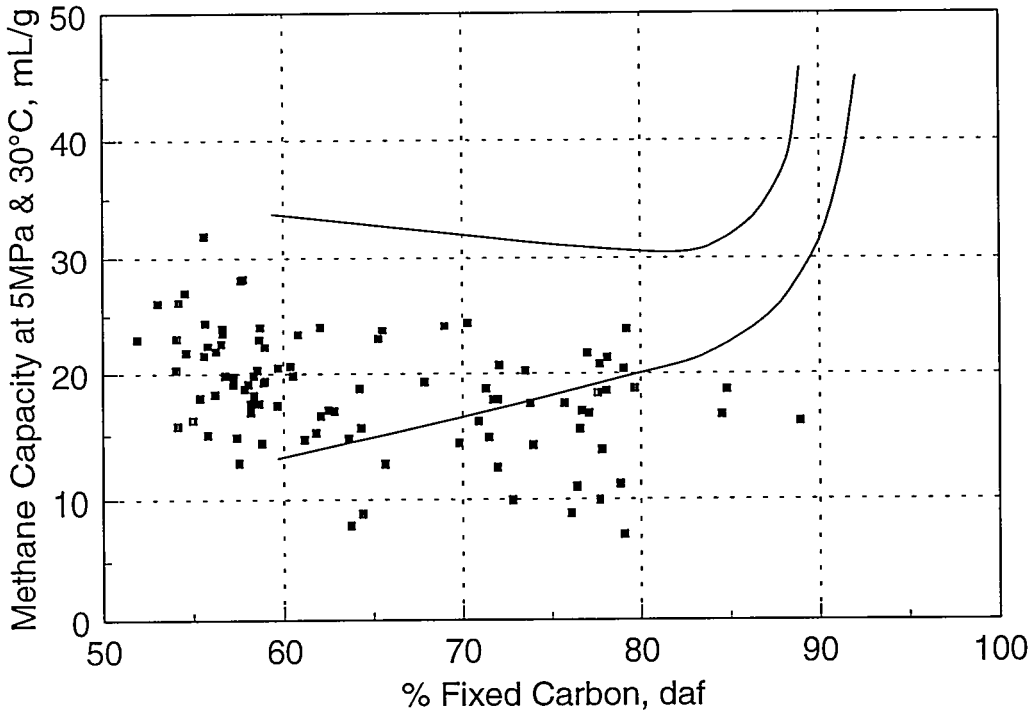


Figure 6. Relationship between methane capacity and fixed carbon for Bowen Basin coals (envelope indicates area of data points) and for United States coals (square data points, after Schwarzer and Byrer [2]).

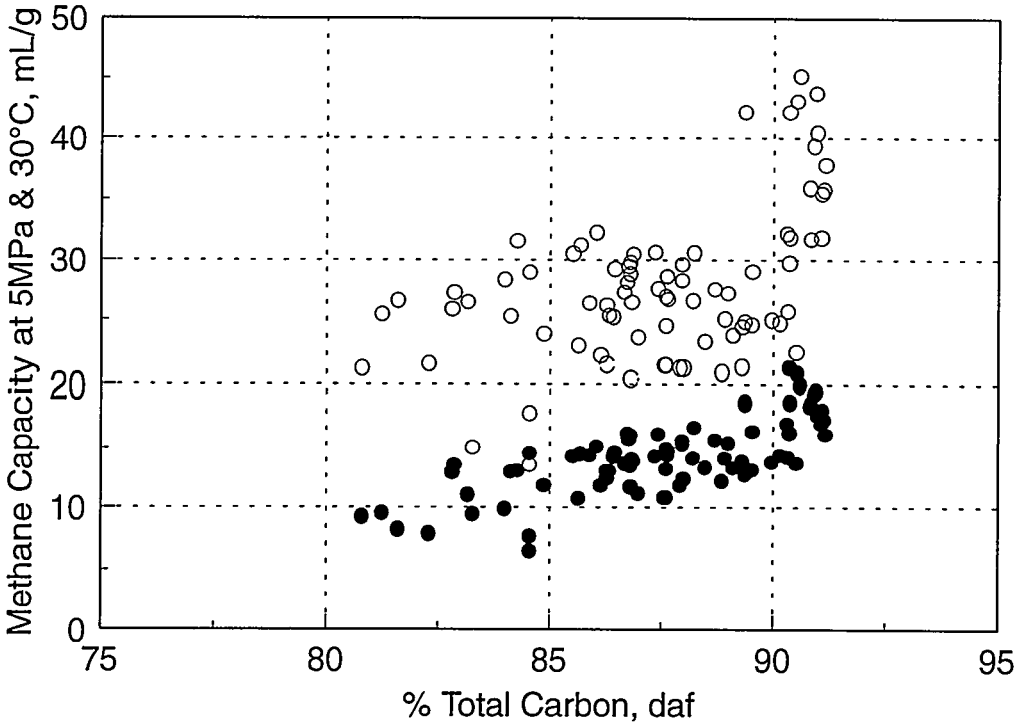


Figure 7. Relationship between methane capacity and total carbon for Bowen Basin coals. (Solid data points correspond to methane capacity of moist coal. Open data points correspond to calculated capacity of dry coal.)

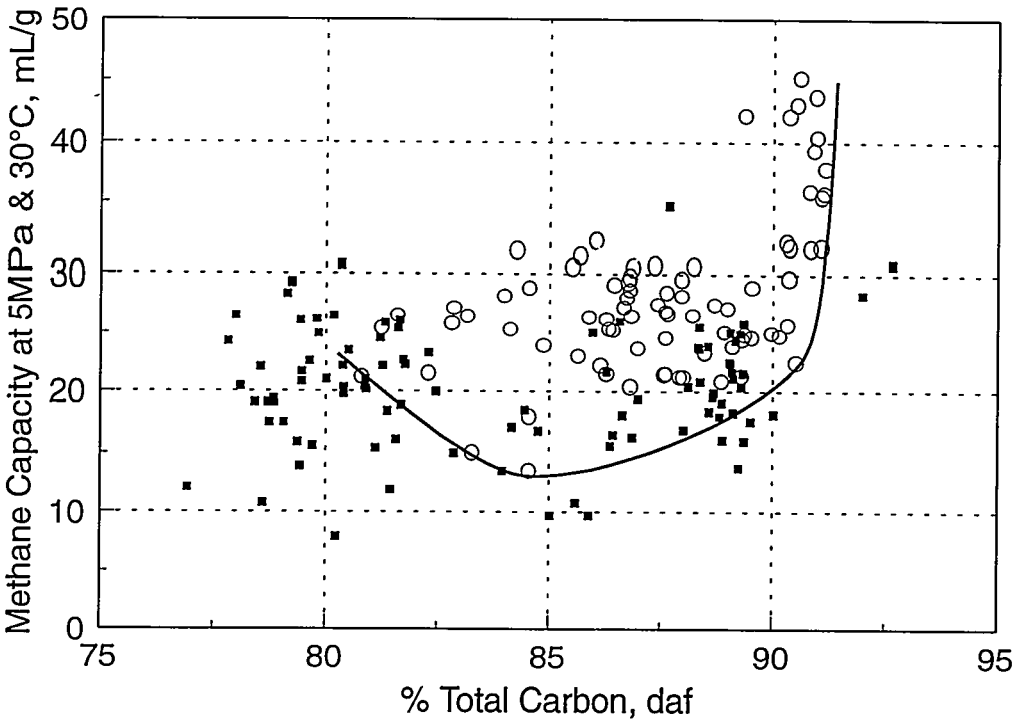


Figure 8. Relationship between methane capacity and total carbon for Bowen Basin coals (open circle data points) and for United States coals (square data points, after Schwarzer and Byrer [2]).

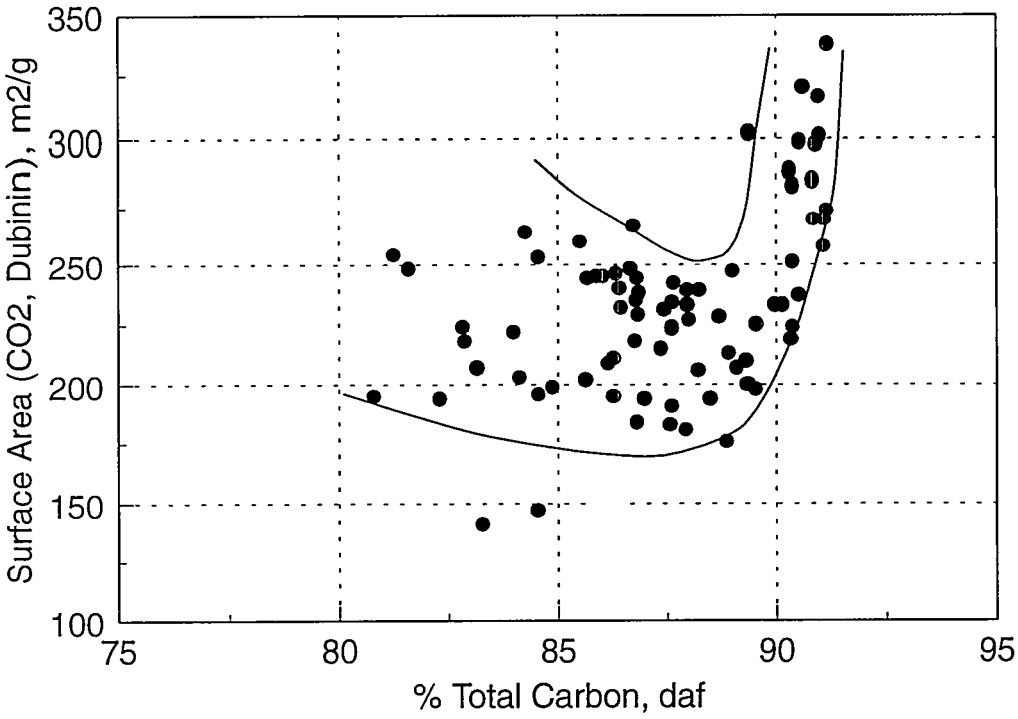


Figure 9. Relationship between coal surface area and total carbon for Bowen Basin coals.

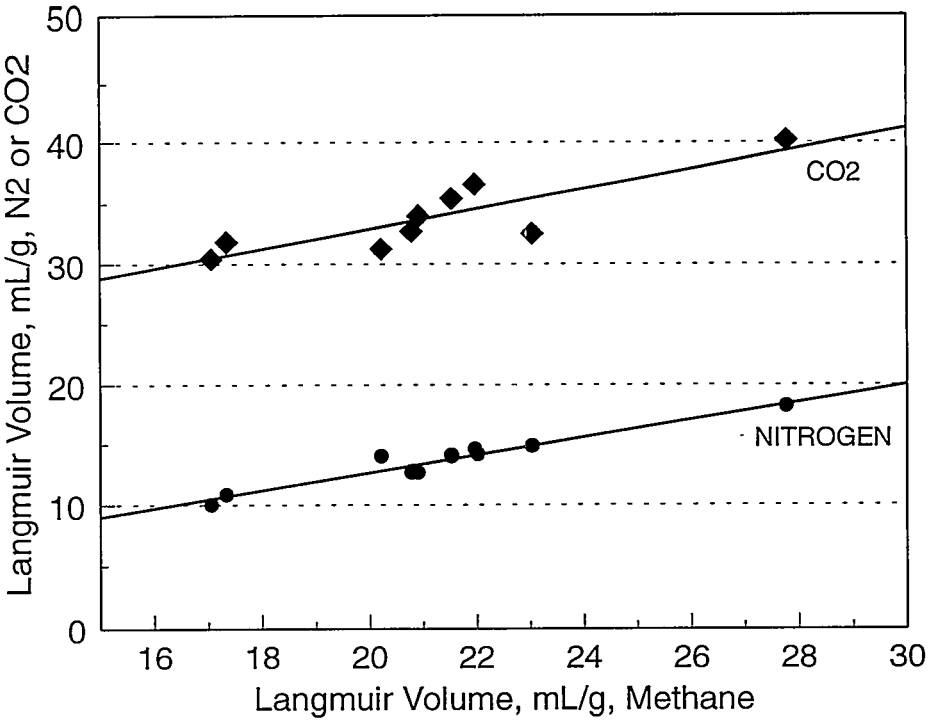


Figure 10. Relationship of nitrogen and carbon dioxide Langmuir Volumes to corresponding methane Langmuir Volumes for Bowen Basin coals.

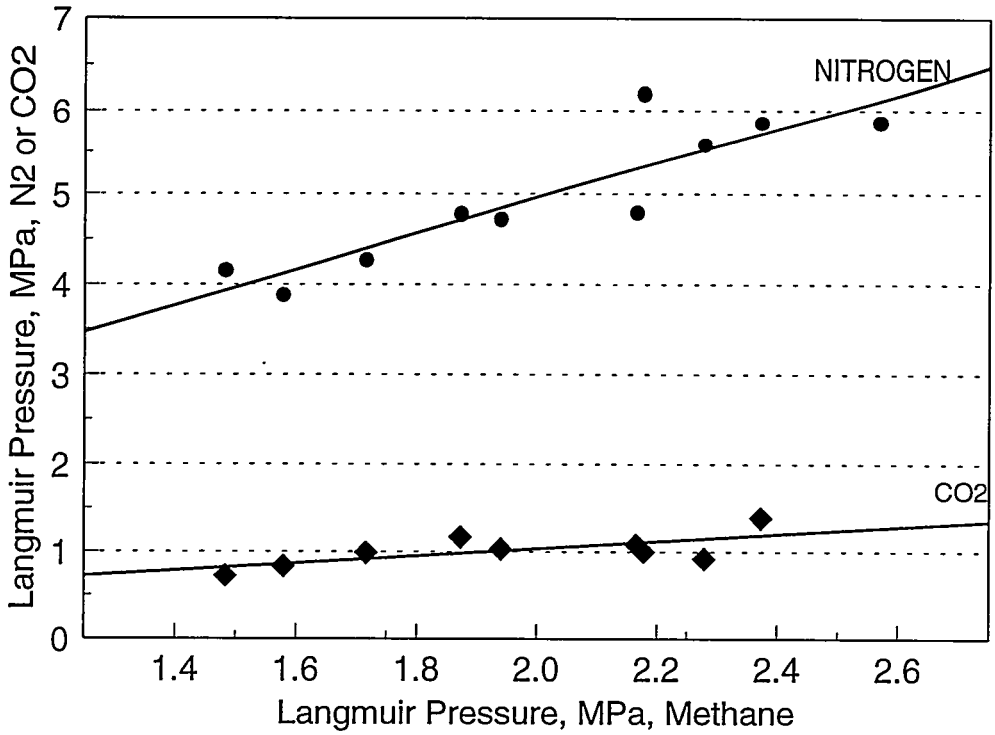


Figure 11. Relationship of nitrogen and carbon dioxide Langmuir Pressures to corresponding methane Langmuir Pressures for Bowen Basin coals.

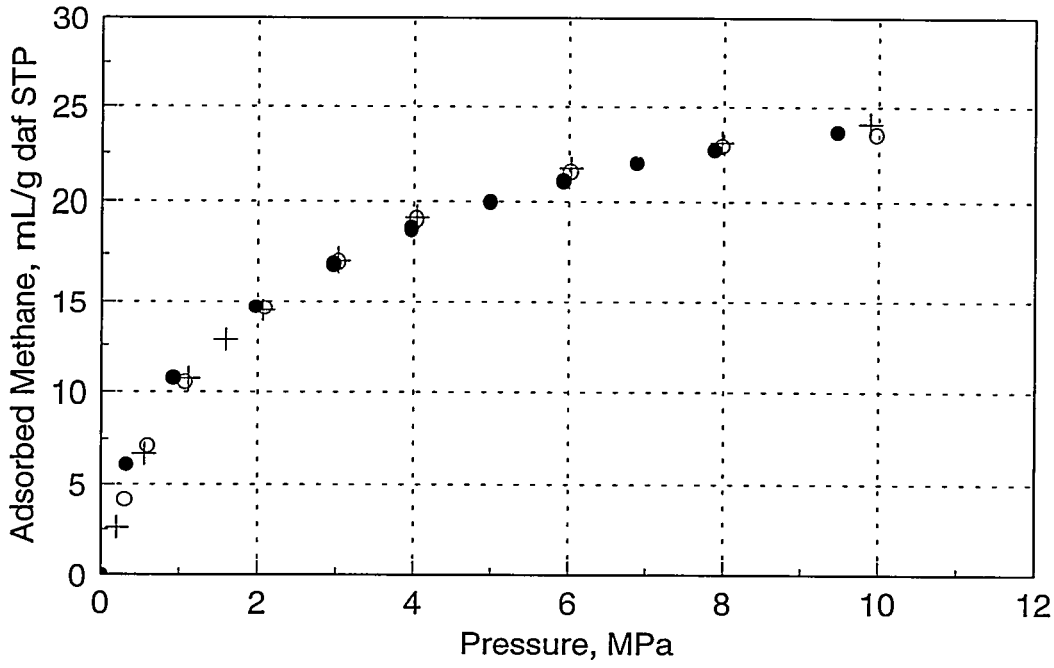


Figure 12. Comparison of methane adsorption isotherms determined by a volumetric technique (solid circle data points) and by a gravimetric technique (cross and open circle data points).



NOTES

INTERGAS '95

May 15-19, 1995
The University of Alabama
Tuscaloosa, Alabama USA

9528

Numerical Modelling and Verification of Stress and Pore Pressure Dependent Dynamic Permeability Behaviour of Coal Seams Around Wellbores

S. Durucan, T.S. Daltaban, J.Q. Shi and J.M. Wang, Imperial College of Science, Technology and Medicine, Royal School of Mines, England

ABSTRACT

Accurate characterisation of the dynamic nature of permeability both near to and away from the wellbore becomes increasingly important as coalbed methane wells are stimulated and during later stages of production where there is a significant decline in the reservoir pressure. Previous research has shown that coal permeability is highly stress dependent. The coal matrix exhibits an elasto-plastic behaviour under varying magnitudes of gas pressure and there is a significant degree of hysterisis effect due to stress/pressure history. It has been shown that permeability of fractured coal can be up to two to three orders higher than that of intact coal. Experimental work by the authors has established relationships for coal permeability as a function of effective stress and matrix/cleat compressibility for both intact and fractured coals. A finite element model was developed to characterise the near wellbore dynamic stress behaviour in coal seams yielding profiles of dynamic stress, pore pressure and permeability around a wellbore. The dynamic changes in far field permeabilities are also accounted for as function of effective stress. This model was coupled with a dual-medium finite difference coalbed methane simulator so that full field flow simulation can be performed by updating the permeabilities continuously.

INTRODUCTION

General field observations and experimental results on coal permeability suggest a decrease in absolute permeability of coal with increasing effective stress (decreasing pore pressure). Methane recovery from coalbeds is almost always associated with significant pressure depletion. It has been reported that coal permeability may decrease by up to two or three orders of magnitude when coal samples are stressed [1,2]. On the other hand, the permeability of coal, which has experienced material failure, will be greatly enhanced [3,4]. Therefore, stress and pore pressure dependent ***dynamic permeability*** option [4], which updates the permeability distribution in the reservoir continuously, was implemented in the coalbed methane model developed at Imperial College.

When a well is drilled through a coal seam of interest, the *in situ* stress state in the near-wellbore region of the coal seam will be disturbed and stresses are redistributed. The radial stress is relieved with the load being transferred into a higher tangential stress. The extent of stress disturbance zone will depend on the *in situ* stress state, the elastic properties of coal and the depth of coal seam concerned. Generally, the width of this zone is no more than several times the well radius. Beyond this zone the stress state remains unchanged.

In most deep coal seam applications the maximum shear stress at the wellbore would exceed the shear strength of coal causing material failure and forming a plastic zone around the wellbore. Since the load bearing capacity of this plastic zone is lower the extra load is transferred outwards until stress equilibrium is reached in the structure. The extent of this plastic zone is largely determined by the post-failure strength of coal.

Thus with the drilling of a well, a zone of heterogeneous permeability is created in the near-wellbore region: a plastic zone of high permeability in the vicinity of the wellbore, surrounded by an elastic zone of varying permeability. When production starts, the pore pressure distribution and the stress state of the formation will change as the reservoir pressure is depleted. Accordingly the permeability within the heterogeneous zone will also vary with time. In field operations, of course, other factors such as damage by drilling mud, well stimulation and completion will also affect the formation permeability in the near-wellbore region. In this paper, only the permeability changes resulting from changes in pore pressures and stress state are considered.

A numerical study on the impact of reservoir pressure/effective stress dependent permeability has been reported by Puri and Seidle [5]. Using an experimental stress-permeability relationship, the authors demonstrated that the effect of reservoir pressure depletion on coal seam permeability is similar to that of a constantly deteriorating wellbore skin. In other words, the gas and water production curves obtained from the simulation with reservoir pressure-dependent permeability could be matched, with satisfactory accuracy, by adding a

positive skin factor to the simulation where the permeability is kept constant. In the far field away from the wellbore, the *in situ* stress acting on the reservoir remains largely unchanged during production and the decline in permeability may be considered entirely due to pressure depletion in the reservoir. In the near-wellbore region, however, the total stress as well as the pore pressure change with time. To characterise the dynamic behaviour of permeability in this region, a wellbore mechanics and flow model taking into account the interaction between the fluid flow and porous medium deformation was developed. This model has been coupled with a dual-medium finite difference coalbed methane simulator so that full field flow simulation can be performed by updating the spatial permeabilities continuously.

STRESS PERMEABILITY RELATIONSHIPS

Intact Coal Behaviour

The effects of stress on coal permeability have been studied by a number of researchers [1,5,6,7,8,9]. The exponential decline of permeability with increasing net confining pressure have been confirmed by a majority of these studies. Based on his results of a number of permeability test carried out on seven different coals, Durucan [8] established an empirical stress-permeability relationship as follows:

$$k = k_0(1.12 - 0.03\sigma_3)\, e^{[-(1.12-0.03\sigma_3)\, c\sigma_3]} \qquad (1)$$

where σ_3 is the net confining pressure and, c and k_0 are constants. Constant c represents the combined compressibility of coal matrix and cleat and should be determined individually for each coal seam. It ranges from 0.4 to 0.7 for the seven coals initially tested [8]. The effect of c on the permeability behaviour of can be seen in Figure 1. The permeability of coal with a relatively high c experiences a larger decrease in permeability as the coal is stressed. Constant k_0 defines the base permeability at $\sigma_3 = 0$. Therefore, the value of k_0 for a particular coal seam would depend solely upon its stress history.

Two other examples of empirical stress permeability correlations suggested by other researchers are as follows:

Somerton *et al* [1]:

$$k = k_0\left[e^{\left(-3x10^3\sigma k_0^{-0.1}\right)} + 2x10^{-4}\sigma^{1/3}k_0^{\,1/3}\right] \qquad (2)$$

Puri and Seidle [5]:

$$k = k_0 e^{\left[1.69\left(\frac{p}{p_0}-1\right)\right]} \qquad (3)$$

Figure 2 illustrates the comparison between the three empirical relationships described above. The reduction in coal permeability in all three cases is due to pressure depletion in an example reservoir, the physical properties of which are assumed to be the same for the three cases concerned.

Employing pore compressibility as the primary parameter, McKee *et al* [9] developed a theoretical relationship between coal permeability and effective stress under hydrostatic stress conditions. Permeability is shown to decrease exponentially with increasing effective stress:

$$k = k_0 e^{-3c(\sigma-\sigma_0)} \qquad (4)$$

where k_0 is the permeability at σ_0 and c is the average pore compressibility over the stress range concerned.

Pore compressibility data of coal is scarce in the literature. In general, pore compressibility is a function of stress. Somerton *et al* [1] measured bulk and pore compressibility of one coal sample under hydrostatic stress conditions and found that the stress-pore compressibility curve was highly non-linear: the pore compressibility declined sharply initially then gradually as the stress was increased. The large decrease at lower stresses is a reflection of major fracture closure and the moderate decrease at higher stresses is due to partial closure of finer fractures and pores.

Post-Failure Behaviour of Coal

Coal under triaxial compression would fail once its ultimate strength is reached and this would result in a significant change in its mechanical strength (residual strength) and elasto-plastic behaviour. Data on the post-failure permeability behaviour of coal under triaxial stress conditions is very sparse in the literature. Permeability data on post-failure behaviour of three British coals have recently been reported [3,4]. The following empirical expression was found to describe the measured permeability data best:

$$\ln k = A - B \ln \sigma_3 \qquad (5)$$

where σ_3 is the net confining stress, and k is the permeability. A and B are empirical constants.

Equations (1) and (5) were used in describing the intact and post-failure stress-permeability behaviour of coal in the numerical simulations discussed below.

COUPLED WELLBORE-FAR FIELD FLOW MODEL

Wellbore Model

The finite element model developed enables the study of the interaction between fluid flow and stress field around a wellbore. This model has been coupled with the coalbed methane simulator, **METSIM** [4]. In this paper, the current state of the model is described and the results of numerical validation tests are presented.

Governing Equations. The phenomena of fluid flow and solid deformation in a porous medium can be described by a set of coupled partial differential equations. Their solutions give rise to the fluid or pore pressure distribution and displacement in the medium. Consider a volume of an elastic porous medium filled with a homogeneous fluid. The distribution of total stress within this volume can be shown to satisfy the equilibrium equation:

$$\frac{\partial \tau_{ij}}{\partial x_j} + F_i = 0 \qquad j = 1, 2, 3 \qquad (6)$$

where τ_{ij} is the total stress on the medium and F_i is the body force per unit volume of the medium. The total stress τ_{ij} can be expressed as:

$$\tau_{ij} = \sigma_{ij} - \alpha p \qquad (7)$$

where σ_{ij} is referred to as the "effective" stress acting on the solid skeleton, p is the fluid pressure, and α is a physical constant, which may be interpreted as the "ratio of the fluid volume squeezed out to the volume change of the porous medium if the latter is compressed while allowing the fluid to escape" [10]. For a saturated porous medium, α approaches unity.

Substituting Equation (6) into (7) and, assuming that the porous medium is isotropic, the governing equations for the solid matrix displacement can be derived:

$$G\frac{\partial^2 u_i}{\partial x_j \partial x_j} + (\lambda + G)\frac{\partial^2 u_j}{\partial x_i \partial x_j} - \alpha\frac{\partial p}{\partial x_i} = -F_i - \frac{\partial \sigma_{ij}^0}{\partial x_j} \qquad (8)$$

where u_i denotes the incremental displacement vector of the solid skeleton and G and λ are Lame's constants.

A mathematical description of fluid flow in a compacting medium can be obtained by combining Darcy's law with the mass conservation equations of the fluid and solid. The final governing equation for fluid flow can be written as:

$$\frac{1}{\rho_f}\frac{\partial}{\partial x_i}\left[\rho_f \frac{k_i}{\mu}\left(\frac{\partial p}{\partial x_i}\right)\right] - \left[\phi\beta + (1-\phi)C_s\right]\frac{\partial p}{\partial t} - \frac{\partial}{\partial t}\left(\frac{\partial u_i}{\partial x_i}\right) = 0 \qquad (9)$$

where β and C_s are the compressibility of fluid and solid grains, respectively. The detailed derivation of Equations (8) and (9) and their finite element approximations are given by Huyakorn and Pinder [11].

Solution Procedure. The flow and displacement equations are fully coupled. The pressure field is coupled into the displacement equation via the Biot effective stress, which in turn is influenced by stress-dependent permeability as well as the incremental changes in solid. In the model, a sequential iterative solution procedure is adopted. At each time step, first the pressure equation is solved and the pressures are updated. The resulting pressure values are then used in the displacement equation to solve for the displacements, from which incremental strains are derived. The incremental stresses are calculated using a linear elastic stress-strain relationship.

Before the stresses can be updated, the stress state at all the integral sampling points within the domain is checked against the Mohr-Coulomb failure criterion for shear failure and the tensile strength for tensile failure. It is known from trial axial experiments that coal measures rocks generally exhibit elasto-plastic behaviour with reduced residual strength after failure. When shear failure is detected at a sample point, the local material assumes a plastic behaviour and the elasticity matrix is replaced by an appropriate elasto-plasticity matrix and the stresses are updated accordingly. The permeabilities corresponding to the updated stresses are then calculated using Equations (1) and (5) for intact and failed coal, respectively. The pressure equation is solved again with the updated values of permeability, followed by the solution of the displacement equation. This iteration process is repeated until convergence is reached for both the flow and displacement equations.

Model Validation. Assuming that flow in the near-wellbore region is in a steady state, Risnes *et al* [12] obtained a set of analytical solutions for total stresses around a vertical cylindrical wellbore at plain strain conditions. An isotropic and homogeneous formation which exhibits elasto-plastic material behaviour was assumed. The steady state radial flow was driven by a constant pressure differential across the near-wellbore region. The solution was obtained by completely decoupling the pressure equation from the displacement field and therefore it can be solved independent of the displacement equation. The displacement equation is still coupled with the pressure filed via the Biot's effective stress and can be solved when the pressure distribution is known.

The finite element model developed by the authors was validated against the analytical solutions. The reservoir characteristics and the mechanical properties of a UK coal seam which was used in the numerical experiments reported in this paper are given in Table 1.

The finite element mesh used consists of 25 isoparametric elements. The mesh is finer at the wellbore and gets progressively coarser towards the outer boundary in a logarithmic scale. The bottom and top boundaries were restrained vertically to represent the plain strain condition. The predicted effective radial and tangential stresses are shown in Figure 3 together with the analytical solutions. All stresses referred to in the text are effective stresses unless otherwise specified. The stresses obtained from the numerical model have shown an excellent agreement with the stresses in the analytical model.

To appreciate the effect of fluid flow on stress distribution around the wellbore, the radial and tangential stresses prior to the initiation of flow are also plotted in Figure 3. It can be seen that the magnitudes of both the radial and tangential stresses have increased in the presence of a steady state flow. This increase in the stress magnitude is required to balance the radial force

exerted by the pressure gradient. An extension of the plastic zone is also observed. Figure 4 compares the permeability distribution in the wellbore region for the stages before and after the production starts.

Model Coupling Procedure. The above analyses indicate that, for a given formation, the permeability around the wellbore would vary with time during production, depending on the changes in the stress state and pore pressure in the near-wellbore region. These dynamic changes in permeability, however, is not considered in any of the conventional coalbed methane simulators. An attempt was made to couple the finite element wellbore model with the in-house coalbed methane simulator, **METSIM** in order to study the effect of dynamic permeability changes on flow into the well. Hence the near-wellbore stress/pore pressure changes can be fully accounted for in characterising the flow in the area.

Moving sufficiently away from the wellbore, the stress-dependent changes in permeability are almost entirely caused by pressure depletion of the reservoir. The dynamic changes in far field permeability are accounted for in **METSIM** as function of effective stress based on Equation (1).

In reservoir simulators, the well flow rate, bottom-hole pressure and average well-block pressure are normally related through a pseudo-steady state equation assuming a constant permeability. The following Peaceman Equation [13] is widely used:

$$Q_l = CCF \frac{k_{rl}}{\mu_l B_l}(p_{wf} - p_l) \qquad (10)$$

where subscript l denotes water or gas phase and the completion connection factor *CCF* is given by:

$$CCF = \frac{2\pi kh}{\ln(\frac{r_{eq}}{r_w}) + S} \qquad (11)$$

where k and r_{eq} are the equivalent absolute permeability and equivalent well-block radius, respectively.

The essence of coupling the wellbore model described above with **METSIM** is to provide an updated absolute permeability for the well flow calculations, taking into account the continuous changes in stress state and pressure distribution both in the well-block and in the reservoir. A schematic representation of the concept is illustrated in Figure 5. In the model, the permeability is updated at the end of each time step using the output of the wellbore model. The solution procedure is described below.

Since the flow into the well is assumed to be in a pseudo-steady state, the flow calculation in the wellbore model may be simplified. The gas/water flow rate through the *i*th element (between radii r_i and r_{i+1} and pressure p_i and p_{i+1} as shown in Figure 5) may be written as:

$$Q_{l(i)} = \frac{2\pi k_{rl} k_i (p_{l(i+1)} - p_{l(i)})}{\mu_{l(i)} B_{l(i)} \ln \frac{r_{i+1}}{r_i}} \qquad (12)$$

where k_i is the absolute permeability for the *i*th element. At the steady state, $Q_{l(i)} = Q_l$ (rate is independent of time). Combining Equations (10) and (12) and introducing the boundary conditions, i.e., p_{wf} at the wellbore and p_l at r_{eq}, the pressure distribution for each phase can be obtained. When the pressure values for both the gas and water phases are available, the mean pressure distribution is calculated and substituted into the displacement equation to solve for displacements. The absolute permeability for each element is then calculated as described above.

The overall permeability (k_o) for the near-wellbore region as a whole can be determined from:

$$\frac{\ln \frac{r_{eq}}{r_w}}{k_o} = \frac{\ln \frac{r_2}{r_w}}{k_1} + \cdots + \frac{\ln \frac{r_{eq}}{r_n}}{k_n} \qquad (13)$$

where n is the number of elements and k_1, .., k_n are the absolute permeability for each individual element. The resulting effective permeability is used to determine the source term for full-field finite difference simulation. This in turn leads to the solution for the well block pressure value. In this way, the cycle is complete and the subsequent permeabilities can be updated.

Numerical Results and Discussions

Numerical simulations were performed for three different test cases: Case 1, the base case with constant permeability throughout the reservoir; Case 2, where the dynamic permeability concept is implemented in the near wellbore region only; and Case 3, with dynamic permeability implementation in the far field as well as in the wellbore block. A 11x11x1 grid was used for the simulation of the reservoir. The region bounded by the wellbore radius and the equivalent radius for the well-block was subdivided into 25 isoparametric elements in the wellbore model.

Figures 6 and 7 show gas and water production rates, respectively, from a single well situated in the centre of the 40 acre drainage area. Comparing the gas production curves obtained for Cases 1 and 2, a reduction of around 25% in gas production is observed in the first 4 years for the case where the dynamic permeability concept is applied to the near-wellbore region. The two production curves gradually converge in the later stages of production as the reservoir depletes comparatively slower in Case 2 to partially compensate for lower permeabilities. In Case 3, the gas production rate is further reduced when the reservoir-wide permeability decreases through far field dynamic permeability implementation as the reservoir is depleted.

The initial steep decline in the water production curves in Figure 7 again is because of the draining of the

existing free gas. The impact of dynamic permeability modelling on water production appears less marked than that on the gas rates. The three production curves practically merge into one after 2000 days.

Figure 8 illustrates the progressive changes in spatial distribution of reservoir permeability during production. After production for ten years, the permeability is reduced to less than half of its initial value.

Puri and Seidle [5] have shown in their simulation studies that reservoir pressure-dependent permeability could be accounted for by introducing a positive skin factor. In a similar approach, numerical simulations were carried out to "history match" the production curves in Cases 2 and 3 above. Skin factors of 3 and 5 were used in Case 1 and the results obtained are compared with the results of Cases 2 and 3 (Figures 9 - 12). As shown in the figures, the gas and water production curves in Case 2 (dynamic permeability in the well-block only) were reasonably matched by using a skin factor of 3. In Case 3, where dynamic permeability concept is implemented in both the near-wellbore region and in the far field, however, the use of a skin factor did not lead to a satisfactory match (Figures 11 and 12). This confirms that the skin factor can only be associated with the wellbore and that the effective stress dependent permeability changes in the far field can not be accounted for by adjusting the skin factor alone.

CONCLUSIONS

The characterisation of the dynamic nature of permeability both near to and away from the wellbore was achieved by coupling a finite element wellbore stress-permeability model with a dual-medium finite difference coalbed methane simulator. During simulation runs, coal seam permeabilities in different sectors of the reservoir were updated, continuously, through the implementation of the dynamic permeability concept in the coupled model. Gas and water production rates observed in the numerical experiments using a UK coal seam reservoir suggest that:

- The permeability in the near-wellbore region is highly heterogeneous. In the shear failure zone immediate to the wellbore, the permeability is enhanced due to the opening of new flow channels; the permeability in the adjacent stressed zone is reduced, resulting in a reduced overall permeability.
- The implementation of the dynamic permeability concept in the near-wellbore region and in the reservoir results in a significant reduction in gas production rates. The reduction observed in water production was less marked.
- The stresses and pore pressure-dependent permeability in the near-wellbore region could be accounted for by introducing an appropriate wellbore skin factor. However, the production curves for the coupled case could not be matched by adjusting the skin factors alone.

NOMENCLATURE

A, B	Empirical constants
B	Formation volume factor
CCF	Connection completion factor
C_s	Compressibility of solid grain
c	Empirical coal matrix/cleat compressibility
F	Body force per unit volume
G, λ	Lame's constants
h	Thickness of production formation
k, k_0 /k_0	Absolute permeability, initial / overall
k_r	Relative permeability
p, p_e, /p_w	Pore pressure, at block boundary / wellbore
Q	Volumetric flow rate
S	Skin factor
r_w/r_e, r_{eq}	Radius at wellbore / block boundary, equivalent well-block radius
u	(Incremental) displacement
α	Biot's effective stress constant
β	Compressibility of pore fluid
ρ_ϕ	Fluid density
μ	Fluid viscosity
ϕ	Porosity
σ_0/σ	Initial / effective stress
σ_r/σ_θ	Radial / tangential stress
τ	Total stress

CONVERSION FACTORS

μm^2	x 1013.3	= md
m	x 3.281	= ft
m^3	x 35.32	= ft^3
	x 6.29	= bbl
MPa	x 145.1	= psi

ACKNOWLEDGEMENTS

The authors wish to thank the Engineering and Physical Sciences Research Council (EPSRC) and the Department of Trade and Industry (DTI) for their support of the coalbed methane research at Imperial College. Special thanks also to Evergreen Resources UK Limited for providing field data and industrial support to the work reported in this paper.

REFERENCES

1. Somerton W., Söylemezoglu I. and R. Dudley, 1975: "Effect of Stress of Permeability of Coal"; Int. J. Rock Mech. Min. Sci. and Geomech. Abstr., V.2, No.5, p.129-145.
2. Durucan S. and J. Edwards, 1986: "The Effects of Stress and Fracturing on Permeability of Coal"; Mining Science and Technology, V.3, p.205-216.
3. Durucan S., Creedy D.P. and J.S. Edwards, 1992: "Geological and Geotechnical Factors Controlling the Occurrence and Flow of Methane in Coal Seams", Proceedings of the Symposium on Coalbed Methane Research and Development in Australia, Townsville, Queensland, V.2, p.33-49.

4. Durucan S., Daltaban T.S., Shi, J.Q. and L. Foley, 1993: "Permeability Characterisation for Modelling Methane Flow in Coal Seams", Proceedings of the 1993 Coalbed Methane Symposium, Birmingham, Alabama, p.453-460.

5. Puri R. and J.P. Seidle, 1992: "Measurement of Stress-Dependent Permeability in Coal and its Influence on Coalbed Methane Production"; In Situ, V.16, No.3, p.183-202.

6. Patching T.H. 1965: "Variations in Permeability of Coal"; Proceedings of the 3rd Rock Mech. Symp., University of Toronto, p.185-199.

7. Dabbous M.K., Reznik, A.A. and P.F. Fulton, 1974: "The Permeability of Coal to Gas and Water"; Trans. AIME, Petroleum Branch, V.257, p.563-572.

8. Durucan S., 1981: An Investigation into the Stress-Permeability Relationship of Coals and Flow Patterns around Working Longwall Faces: PhD Thesis, University of Nottingham, 301p.

9. McKee C.R., Bumb A.C. and R.A. Koenig, 1987: "Stress-Dependent Permeability and Porosity of Coal", Proceedings of the 1987 Coalbed Methane Symposium, Tuscaloosa, Alabama, p.183-193.

10. Biot, M.A., 1941: "General Theory of Three-Dimensional Consolidation"; J. Appl. Phys. V.12, p.155-164.

11. Huyakorn, P. S. and G.F. Pinder, 1983: Computational Methods in Subsurface Flow: Academic Press.

12. Risnes R., Bratli R.K. and P. Horsrud, 1982: "Sand Stresses Around a Wellbore"; SPE Journal, Dec., p.883-898.

13. Peaceman, D.W., 1977: "Interpretation of Well-Block Pressure in Numerical Reservoir Simulation", paper SPE 6893, Proceedings of the 52nd Annual Fall Technical Conference and Exhibition, Denver.

Table 1. Coalbed reservoir characteristics and mechanical properties used in the numerical experiments.

Coal seam depth, m	500	(1640 ft)
Wellbore radius, m	0.09	(0.3 ft)
Initial water saturation	0.80	
In situ hydrostatic stress, MPa	12.2	(1775 psi)
In situ pore pressure, MPa	4.5	(650 psi)
Bottom-hole pressure, MPa	0.34	(50 psi)
In situ permeability, μm^2	0.003	(3 md)
Constant alpha	1.0	
Porosity	0.01	
Matrix/cleat compressibility factor	0.5	
Young's modulus, MPa	3200	(22.1 psi)
Poisson's ratio	0.31	
Material cohesion, MPa	1.1	(0.0076 psi)
Internal frictional angle, °	20	

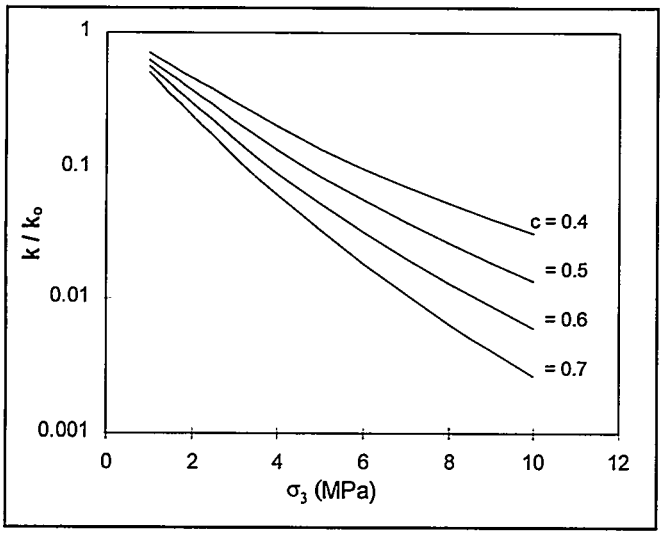


Figure 1. The effect of matrix/cleat compressibility (c) on coal permeability.

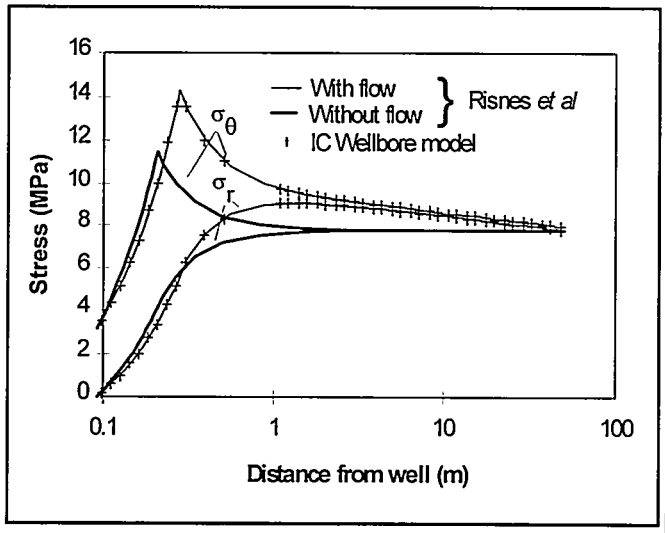


Figure 3. Wellbore model validation results.

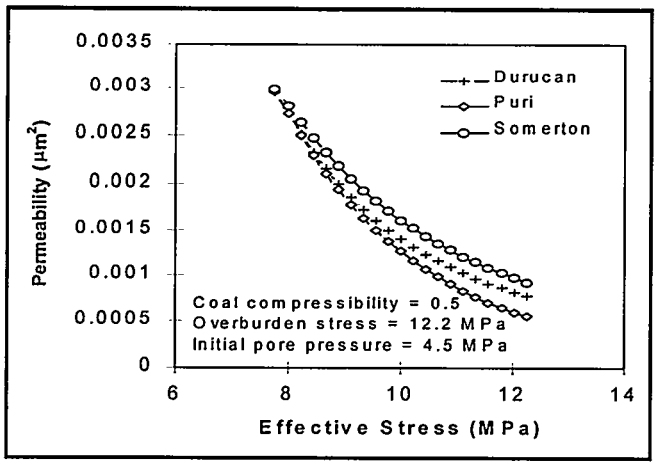


Figure 2. Stress-permeability relationships for coal.

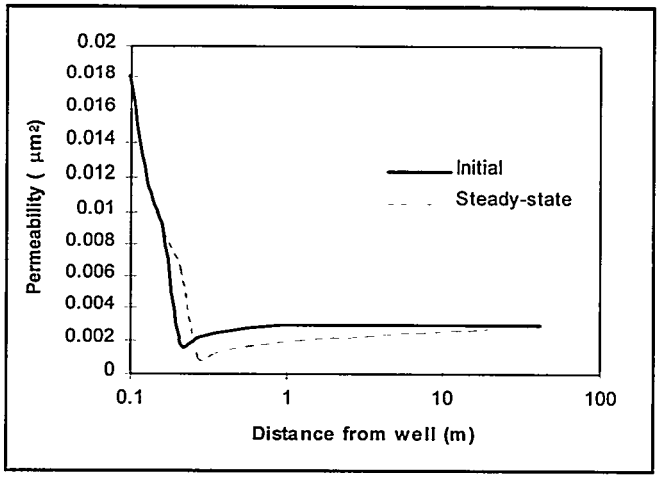


Figure 4. Permeability distribution in the wellbore region.

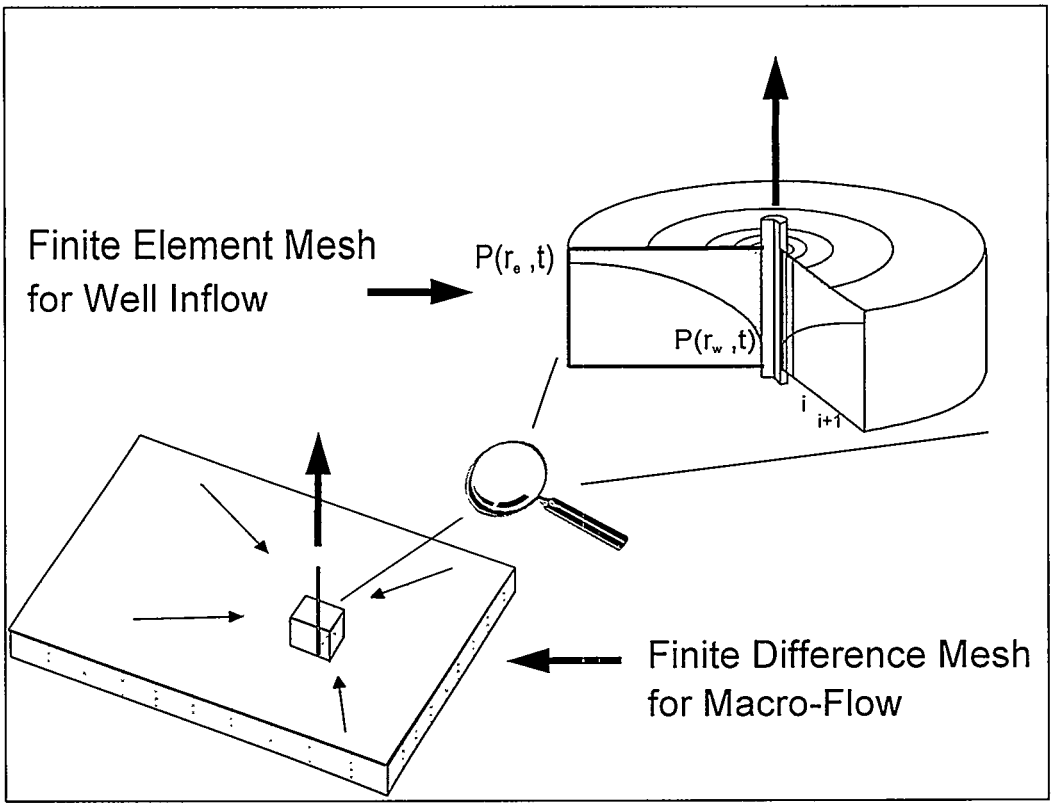


Figure 5. Illustration of the application of dynamic permeability concept in coalbed methane flow simulation.

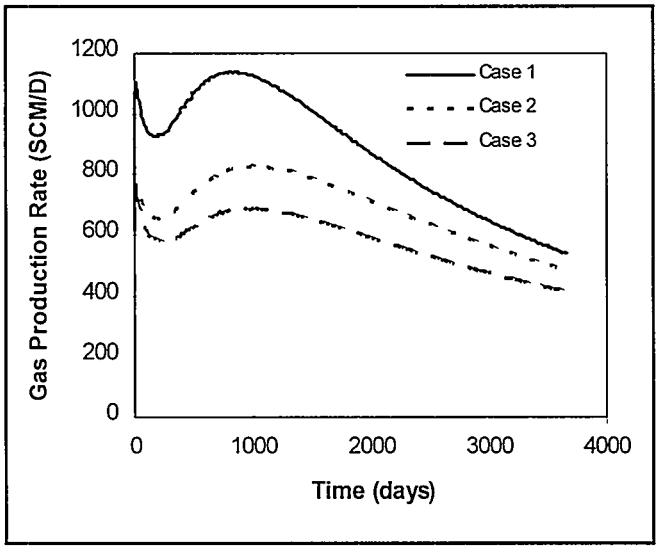


Figure 6. Gas production rates obtained from the test cases.

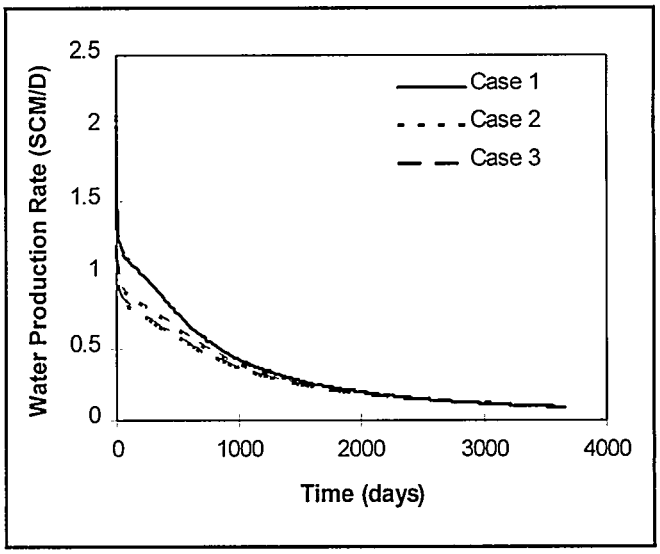


Figure 7. Water production rates obtained from the test cases.

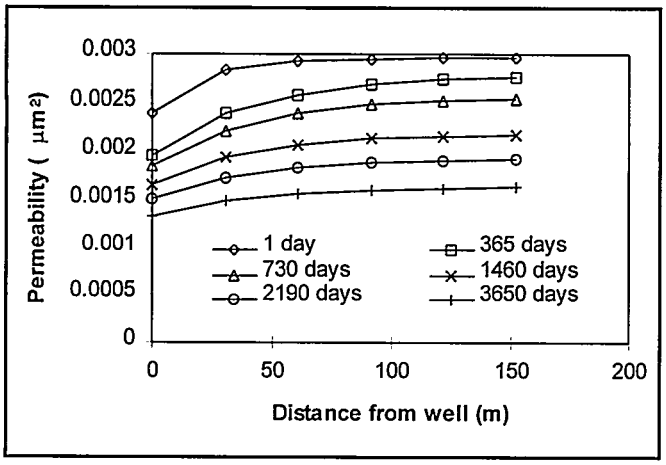


Figure 8. Far field permeability distribution in a producing coalbed methane reservoir.

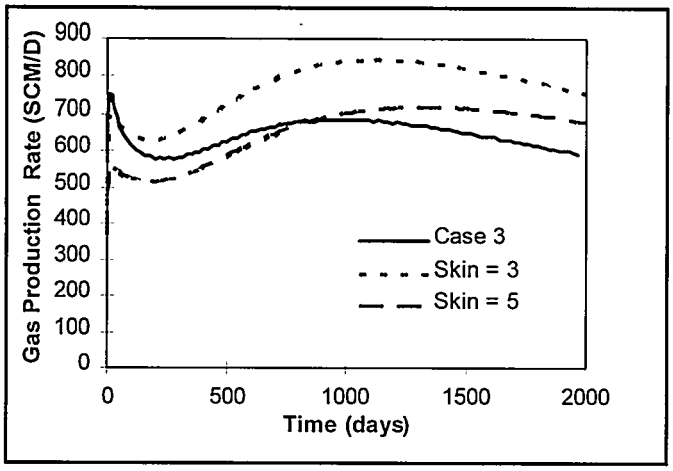


Figure 11. The comparison of predicted gas production rates using the coupled wellbore/reservoir model and the constant permeability model with skin factors.

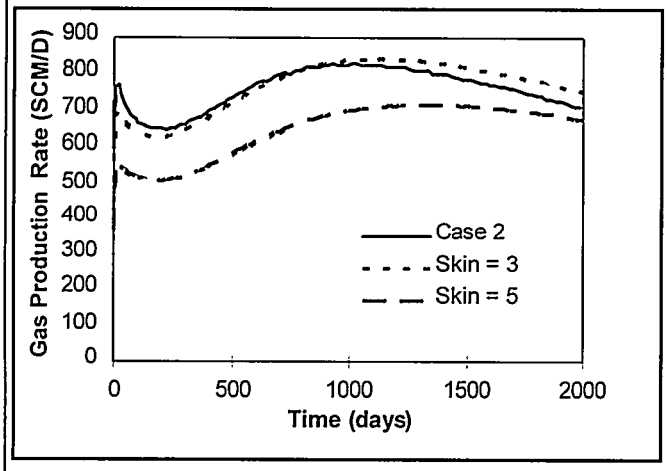


Figure 9. The comparison of predicted gas production rates using the wellbore model and the constant permeability model with skin factors.

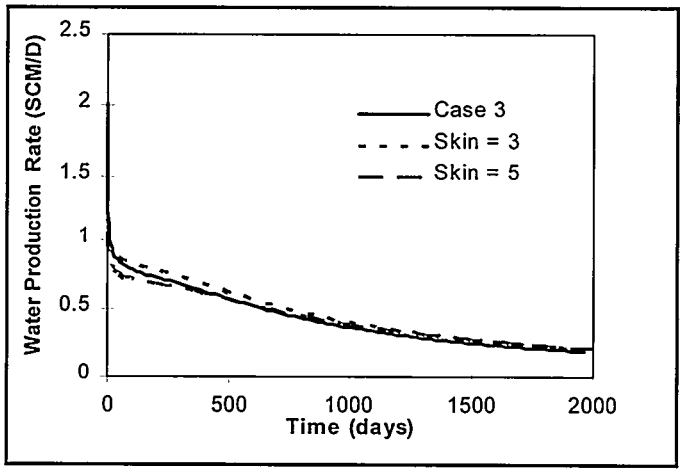


Figure 12. The comparison of predicted water production rates using the coupled wellbore/reservoir model and the constant permeability model with skin factors.

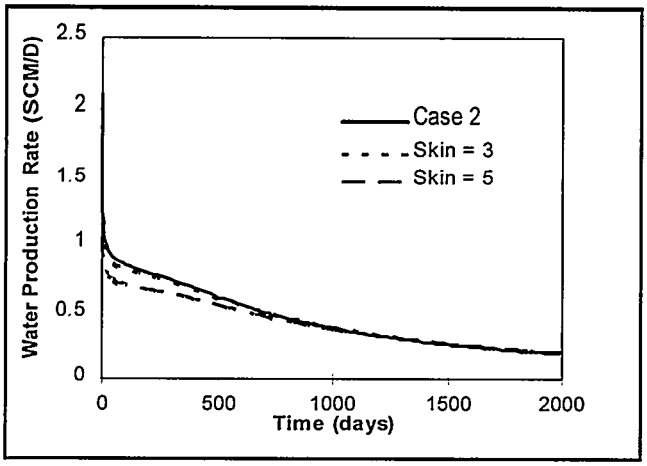


Figure 10. The comparison of predicted water production rates using the wellbore model and the constant permeability model with skin factors.



NOTES

INTERGAS '95

May 15-19, 1995
The University of Alabama
Tuscaloosa, Alabama USA

9509

Limitations and Benefits of Microbially Enhanced Coalbed Methane

A.R. Scott, Bureau of Economic Geology, The University of Texas at Austin

ABSTRACT

Microbially enhanced coalbed methane (MECoM) imitates and enhances the natural process of secondary biogenic gas generation in coal beds that occurs in coal basins worldwide. MECoM involves the introduction of anaerobic bacterial consortia, consisting of hydrolyzers, acetogens and methanogens, and/or nutrients into coalbed methane wells. Coalbed methane production may increase through generation of additional methane, removal of pore-plugging coal waxes, and permeability enhancement as cleat-aperture width is enlarged during biogasification. The amount of coal gas potentially generated by MECoM is large. If only one-hundredth of one percent (1/10,000) of U.S. (lower 48) coal resources were converted into methane using MECoM, gas resources would increase by 23 Tcf, or approximately 16% of current lower 48 nonassociated reserves. However, coal surface area and biogasification reaction rates in the subsurface may potentially limit gas generation, indicating that permeability enhancement may be the most significant benefit of MECoM. Additional research, including microbial sampling of deeply buried bituminous coals to identify genetically unique consortia, is required to fully evaluate MECoM and to determine if the process will improve coalbed methane producibility. If economically feasible, MECoM can generate methane in coal beds that currently have limited coalbed methane potential, and thereby, provide cheap, environmentally clean energy for many parts of the world.

INTRODUCTION

"Combustible air" has been known since ancient times, but widespread interest and the scientific foundation for the study of biological gas started in 1776 with the experiments of Alessandro Volta, who collected "combustible air" by poking his cane in the bottom of marshy sediments [1]. Although the association of combustible gas with water was initially discovered by Volta, the microbiological origin of the gas was not discovered until nearly a century later, and the recognition of methanogens as a genetically separate group of bacteria (Archaeobacteria) until the late 1970's [2, 3]. Since the simple experiments of Volta, methanogenic bacteria have been found in a wide variety of anaerobic environments ranging from acidic bogs to deep ocean sediments, from freshwater environments to hypersaline lakes, and from tundra to hot thermal vents [4-6]. More recently, anaerobic bacterial consortia were recovered from sidewall cores taken from overpressured (0.51 to 0.56 psi/ft; 11.5 to 12.6 kPa/m) rocks at depths ranging from 8,700 to 9,180 ft (2,650 to 2,798 m) at temperatures between 149 and 167°F (65 and 75°C) [7] suggesting that bacteria are probably more common in sedimentary basins than previously recognized.

Research on Microbially Enhanced Oil Recovery (MEOR) in the late 1940's indicated that anaerobic sulfate-reducing bacteria indigenous to oil reservoirs could displace oil under the appropriate conditions [8]. Most MEOR processes involve the injection of carbohydrates and nutrients into wells to stimulate naturally occurring or introduced organisms [9]. Enhanced oil recovery is achieved when carbon dioxide and other gases evolved during fermentation repressurize the reservoir and dissolve into the oil, thus decreasing oil viscosity, whereas surfactants produced during microbial growth lower the interfacial tension between oil and water [8].

The acronym for Microbially Enhanced Coalbed Methane, MECoM, is derived from Microbially Enhanced Oil Recovery (MEOR) and applies to the processes by which enhanced coalbed methane recovery is achieved through the introduction of bacterial consortia and nutrients into coal beds. Improved coalbed methane productivity may be accomplished through the generation of additional methane, removal of pore-plugging coalbed waxes and paraffins, and an increase in permeability as coal is removed from cleat surfaces. The objectives of this paper are to briefly review previous work on coal biogasification and microbial processes and to describe benefits and possible limitations of MECoM.

COAL BIOGASIFICATION

A wide range of organisms have shown the ability to promote coal solubilization since the ability of fungi to degrade coal solids was first recognized in the early 1980's [10]. Much of the earlier research focused on using bacteria for the precombustion removal of organic and inorganic

sulfur from coal [11], whereas subsequent research included the biological conversion of coal into methane [12–16]. Nearly all previous studies on coal biogasification have focused on using bacterial consortia to convert coal into methane, carbon dioxide, and other organic molecules in surface bioreactors. A two-stage process has been proposed [12] in which pulverized coal is first solubilized and transferred to a bioreactor, where the coal is converted into smaller organic compounds by bacterial consortia. These organic precursors are then transferred to a second bioreactor containing methanogens. Conversion of lignite by bacterial consortia resulted in a direct conversion efficiency of coal carbon to methane ranging from 35 to 50% [12]. Preliminary cost estimates for methane production from bioreactors ranges from $2.69 to $9.78 per Mcf [15].

Lignites and/or subbituminous coals are used as substrates in nearly all coal biogasification experiments, whereas Paleozoic-age bituminous coals are used less frequently. Most bituminous coals are assumed to be recalcitrant to biodegradation [12] because microbial activity generally decreases with decreasing oxygen content (fig. 1); very little, if any, biogasification research has been performed on hydrogen-rich Cretaceous and Tertiary bituminous coals. One bituminous coal in figure 1 has the same biosolubility as lower-rank, higher-oxygen content coals, suggesting that bacterial degradation of higher-rank coals is possible. Microbial consortia capable of generating methane from coal have been isolated from a Paleozoic-age bituminous coal in an abandoned mine [17], providing additional evidence that bituminous coals can be metabolized.

The presence of viable organisms in naturally occurring coal samples has been debated [18, 19], even though microorganisms from coal-associated sources such as coal outcrops, coal slurry pits, and run-offs from coal piles [12, 20, 21] have been isolated. Hydrogeologic, gas compositional, and isotopic data from coalbed methane wells in the Upper Cretaceous Fruitland Formation in the San Juan Basin [22–24] show that microbial activity in bituminous coals occurs naturally and is probably more widespread than previously thought.

METHANOGENESIS

Microbial degradation of organic compounds often requires the metabolic interaction of microbial consortia where individual bacterial species feed off the products of another species. Three functionally different trophic groups of bacteria (fig. 2) are required to convert organic matter to methane [4, 25, 26]: (1) hydrolytic fermentative bacteria, (2) syntrophic acetogenic bacteria, and (3) methanogenic bacteria.

Fermentative bacteria initially hydrolyze complex organic compounds to acetate, longer-chained fatty acids, carbon dioxide, hydrogen, NH_4^+, and HS^-. These bacteria are mostly obligate anaerobes, although facultative anaerobes may be present as well. Syntrophic, hydrogen-producing (proton-reducing) acetogenic bacteria reduce intermediary metabolites into acetate, carbon dioxide, and hydrogen. Hydrogen-utilizing acetogenic bacteria demethoxylate low-molecular-weight ligneous compounds and ferment some hydroxylated aromatic compounds [25]. Methanogenic bacteria are dependent on hydrogen produced by the other bacteria to reduce carbon dioxide (or bicarbonate) to methane. The hydrogen partial pressure in methanogenic environments is low, ranging between 10^{-5} and 10^{-4} atm (1 and 10 Pa) [27] because of the great capacity methanogens have for utilizing hydrogen. If the methanogenic populations become stressed, hydrogen activity increases, making reactions thermodynamically unfavorable for the degradation of organic compounds by hydrogen-producing acetogens [25]. Therefore, syntrophic interspecies hydrogen transfer regulates metabolic efficiency and growth yield of acetogenic and methanogenic bacteria.

Aerobic bacteria are capable of metabolizing a wide variety of organic substrates. One species of *Pseudomonas* was shown to grow on at least 127 different organic molecules and possibly more; the researchers ran out of ideas as to what organic compounds to feed it [28]. Methanogens, however, are generally limited to hydrogen, carbon dioxide, and simple organic compounds, including formate, carbon monoxide, methanol, acetate, methylated amines, short-chained alcohols, and methyl mercaptan [4, 6], most of which contain only one carbon atom. Nearly all methanogens are highly specialized and can use only one or two substrates as food sources, again stressing the importance of other bacteria in providing suitable organic compounds for methanogenesis.

Carbonate reduction and acetate fermentation are the metabolic pathways for methane generation in natural environments (fig. 2). Carbonate reduction occurs primarily, but is not restricted to, marine waters containing sulfate, whereas acetate fermentation is the dominant process by which methane is produced in fresh water [29]. Carbon dioxide is not necessarily consumed during carbonate reduction if multiple bacterial species are participating. Carbon dioxide/bicarbonate are used in intermediary steps such that the net chemical reaction involving two or more bacterial species may result in a net gain of carbon dioxide (bicarbonate ions) rather than the removal of carbon dioxide from the system [6]. Acetate fermentation, which involves the reduction of acetate by methanogenic bacteria, is not comparable to the generation of acetate by acetogenic bacteria discussed previously. Unlike carbonate reduction, the hydrogen in methane generated through acetate fermentation is derived primarily from the methyl group, and only 25% of the hydrogen is obtained from the formation water [29]. The reduction of a methyl group to methane is coupled with the oxidation of the carbonyl group to carbon dioxide during acetate fermentation.

MICROBIALLY ENHANCED COALBED METHANE

Primary biogenic methane that is generated shortly after deposition during early coalification stages is probably not retained by peat in large quantities because of low pressures and the high moisture content of peat. Secondary biogenic gases are generated after burial, coalification, and subsequent uplift and erosion along basin margins [30, 31].

Data from the San Juan Basin in Colorado and New Mexico provide the best evidence of secondary biogenic gas generation. Overpressure in the northern part of the basin is artesian in origin and probably developed during the middle Pliocene [22]; a carbon-14 age date of 31,176 yr [32] is additional evidence of geologically young formation waters. Methane, carbon dioxide, and bicarbonate isotopic values, abrupt change in coal gas chemistry, and the "biodegraded" n-alkane pattern of some coal extract samples in the northern San Juan Basin, when coupled with evidence of meteoric recharge, suggest that secondary biogenic gas generation occurred when bacteria were introduced into permeable coal beds during meteoric recharge [22, 23, 31].

MECoM imitates and enhances the natural processes of secondary biogenic gas generation through the introduction of nutrients and trace elements and/or anaerobic bacterial consortia into coalbed methane wells to stimulate coalbed methane production. Anaerobic bacterial consortia can probably be collected from produced formation waters and/or fresh sidewall and whole core samples; pressurized cores present the best opportunity to collect viable consortia. Although methanogens will not grow or generate methane in the presence of even trace quantities of oxygen, they can remain viable in the presence of oxygen up to 24 hours by forming multicellular lumps [33]. Anoxic/reducing microenvironments in an oxygenated system can potentially extend bacteria viability. Therefore, the oxygen tolerance of methanogenic bacteria improves the probability of recovering methanogenic bacteria from the subsurface.

The relatively short doubling times for bacterial growth, coupled with genetic enhancement through natural selection, suggest that bacteria in coal beds will genetically evolve over a relatively short timespan to more efficiently metabolize coal. Furthermore, bacterial consortia isolated from different basins, or possibly individual coal beds, are probably unique genetically because of subtle differences in environmental conditions and coal substrates. Once collected, these bacteria can be grown in laboratory cultures to evaluate and determine factors enhancing and/or limiting the conversion of coal into methane. With the progressive development of genetic engineering technology, biologists are now capable of genetically engineering microorganisms to have abilities beyond their "normal" abilities [34]. Special bacterial consortia adapted over time in the laboratory to efficiently metabolize coal and/or genetically engineered bacteria, along with appropriate nutrients when injected into coal beds, may enhance coalbed methane production. However, there remain many unknowns about the technical aspects of microbially processing coal in the subsurface and about the economic feasibility of the technology.

Possible Benefits of Microbially Enhanced Coalbed Methane

Increased Reserves. The amount of biogenic gas potentially generated from coal using MECoM is huge. If 1% (weight) of coal is converted into methane using bacterial consortia, gas content would increase by 488 scf/ton (15.2 cm^3/g). For a 32.8-ft (10-m) thick ash-free coal bed having a density of 1,659 tons/acre-ft (1.22 g/cc) and covering 10 acres (40,468 m^2), more than 265,000 Mcf of methane would be produced. At $2.00/Mcf this comes to more than $530,000. If only one-hundredth of 1% (1/10,000) of U.S. coal resources were converted into methane using MECoM, gas resources would increase by 23 Tcf [35] or approximately 16% of current nonassociated reserves. Therefore, MECoM potentially may have a significant impact on U.S. gas reserves. MECoM can also be used to generate methane in coal beds that currently have limited coalbed methane potential and thereby provide cheap, environmentally clean energy for many parts of the world.

Increased Permeability. The quantity of gases generated during MECoM will ultimately depend on bacterial access to the coal and the surface area of coal exposed to the bacteria. Permeability in coal beds is restricted to an interconnected natural fracture (cleat) system because the coal matrix is essentially impermeable. Face cleats develop first, are more continuous, and usually have the higher permeability, depending on in situ stress orientation. Butt cleats abut the face cleats and are less continuous, resulting in lower permeability. Face cleat spacing is highly variable, ranging from less than 0.05 cleats/inch (0.02 cleats/cm) in lignites (W.R. Kaiser, personal com., 1994) to more than 100 cleats/inch (40 cleats/cm) in vitrain bands [36]. Cleat spacing is highly variable and depends on maceral type and ash content, although cleat spacing generally increases with increasing coal rank through the high-volatile bituminous coals [37].

Fracture permeability in coal beds ranges from microdarcys to darcys. Direct permeability measurements on coal are difficult or impossible to obtain, but indirect measurements using drill-stem tests and/or production modeling suggest that permeability is generally between 1 and 100 md. Cleat aperture width is believed to range between 0.1 and 100 microns on the basis of an analogy with fracture aperture width in conventional reservoirs [38]. The relation among fracture (or cleat) spacing, permeability, and fracture aperture width in carbonate rocks is discussed by Lucia [39]. The equation relating these three variables can be used to estimate cleat aperture width in the subsurface because both fractured carbonate and coal reservoirs are characterized by a fracture network separated by an impermeable matrix. The relation among cleat spacing, permeability, and cleat aperture width is shown in figure 3.

Assuming a cleat spacing of 10 cleats/inch (3.9 cleats/cm) and permeabilities between 1 and 100 md, cleat aperture wide in the subsurface probably ranges between 3 and 15 microns (fig. 3). If the permeability range (1 to 100 md) remains the same but cleat spacing is decreased to 1 cleat/inch (0.4 cleats/cm), cleat aperture width would range between 7 and 30 microns. These estimated ranges of cleat aperture width are well within the size range of many bacteria (1 to 3 microns in diameter) and much larger than ultramicrobacteria, which have diameters of <0.3 microns [6, 40]. Therefore, the smallness of bacteria indicates that bacteria can be injected into low-permeability coal reservoirs and be expected to access the coal through a cleat aperture <1 micron wide.

In addition to generating additional methane, MECoM may increase coalbed methane production by increasing permeability. Because bacteria are capable of accessing the coal only through the cleat system, cleat aperture width will increase as the bacteria convert coal into methane (fig. 4). For example, coal having a cleat spacing of 6 cleats per inch (2.4 cleats/cm) and a cleat aperture width of 2 microns has an estimated permeability of 0.16 md (fig. 3). If bacteria remove 2 microns from each side of the cleat, the cleat aperture width increases to 6 microns and the permeability to 4.31 md (figs. 3 and 4). Because permeability increases with the cube of cleat aperture width, permeability enhancement is more pronounced in low-permeability reservoirs having narrow cleat apertures than in higher-permeability reservoirs if the same volume of coal is removed in each reservoir (fig. 5). For example, if the cleat width in a 1-md reservoir is increased by 1 micron, permeability will double, whereas a 1-micron increase in cleat aperture width in a 1,000-md reservoir will have negligible effect on permeability (fig. 5).

Well Remediation. Chemically wet gases, condensate, and waxes are generated from hydrogen-rich coals during coalification and are produced from coalbed methane wells. These organic compounds can be metabolized by bacteria and may represent an important food source in bituminous coals. Significant quantities of these compounds can be generated from high-volatile hydrogen-rich coals. Excessive wax production in parts of the San Juan Basin has resulted in some coalbed methane wells being temporarily shut-in. Coal is a complex organic substance, and organic solvents injected into coalbed methane wells to remove coal wax have lowered permeability and damaged the reservoir rather than enhancing producibility. Coal gases and organic compounds are readily sorbed onto the coal surface and may result in a decrease in relative permeability [41], coal swelling, and/or decrease sorption capacity depending on the organic solvent and coal properties.

Waxes from coalbed methane wells in the San Juan Basin are composed predominantly of long-chained n-alkanes [42], suggesting that they may be susceptible to biodegradation. Although the lighter-weight n-alkanes ($<C_{20}$) are preferentially removed first during biodegradation, heavier-weight n-alkanes (C_{15} to C_{35}) are biodegraded before branched alkanes [43, 44]. Bacteria capable of metabolizing pore-occluding n-alkanes and waxes in coal beds to generate biogenic methane may also modify the coal surface structure to increase methane adsorptive capacity and total gas content. When bacteria metabolize and remove wet gases, n-alkanes, and other pore-plugging organic compounds on the coal surface during biogasification, the methane generated during MECoM may be readily sorbed onto the sorption sites previously occupied by the pore-plugging organic compounds. In a sense, bacteria can be thought of as nature's soxhlet extractor for coal beds because they are capable of removing soluble organic compounds from the coal. Unlike organic solvents, bacterial consortia may remove organic compounds without damaging the reservoir.

Possible Limitations of Microbially Enhanced Coalbed Methane

Biodegradation of Organic Compounds. Methanogenic bacteria are just one component of complex trophic consortia (consortia having specific nutritional levels) required to convert coal into methane under anaerobic conditions. Much research has been performed on the aerobic degradation of hydrocarbons in oil reservoirs and organic compounds during bioremediation [43–45]. Anaerobic degradation of hydrocarbons and organic compounds occurs naturally, and biodegradation of many oils in deeper reservoirs probably occurred under anaerobic conditions rather than aerobic; even methane oxidation occurs under aerobic and anaerobic conditions [46–48].

Most oil samples are composed predominantly of organic compounds that are relatively easily biodegradable, whereas coals are composed of an interconnected network of hydroaromatic and cycloalkanes, which are less easily biodegradable. The resistance of lignin and lignocellulose to biodegradation in anoxic environments results in the accumulation of peat and eventually coal upon maturation. However, recent studies indicate that lignin, lignocellulose, and other complex organic compounds thought to be representative of the coal structure can be biodegraded under anaerobic conditions [49–52]. Therefore, the complexity and nature of the coal structure should not be used to dismiss the possibility of MECoM to improve coalbed methane producibility. However, if waste products toxic to bacteria, generated during coal biogasification, are not removed from the system, MECoM recovery could be reduced or inhibited.

Temperature. Methanogenic bacteria are found at temperatures ranging from 36° to 230°F (2° to 110° C) [4, 6, 53, 54], but the optimum temperature range for biogenic gas generation is 95 to 113°F (35 to 45°C) [55]. Muralidharan and others [56] suggested that higher microbial reaction rates may be achieved at higher temperatures. How long the bacteria present at the time of deposition can survive during burial and thermal maturation remains unknown at this time. At very high temperatures and/or in the absence of food sources or without appropriate nutrients over extended periods of time, bacteria will probably not survive. However, bacteria may remain viable, though dormant during burial, and when environmental conditions become more favorable during uplift and erosion, growth is reinitiated [57]. Therefore, the full effects of temperature on in situ biogasification of coal remain uncertain but are an important consideration for MECoM.

Cleat Surface Area. Another important factor affecting MECoM is the surface area available for bioconversion of coal into methane. A large coal surface area available for coal biogasification will result in higher methane yields during MECoM. Therefore, an evaluation of the total surface area based on cleat spacing can be used to estimate the amount of gas generated during MECoM. A bituminous ash-free coal having a density of 1.22 g/cc (1,659 tons/acre-ft)

will occupy a volume of 26.26 ft^3 (0.744 m^3) equivalent to a cube 35.67 inches (0.906 m) per side. Therefore, each face cleat in a ton of coal will have a surface area equal to 17.67 ft^2 (1.641 m^2), and the total cleat surface area per ton of coal will increase linearly with decreasing cleat spacing (fig. 6). A 32.8-ft (10-m) thick ash-free bituminous coal covering 10 acres (40,468 m^2) will contain 544,226 tons (493,714 t) of coal. Assuming a cleat spacing of 6 cleats/inch (2.4 cleats/cm), the total face cleat surface area would be 2.06×10^9 ft^2 (1.91×10^8 m^2), whereas a cleat spacing of 10 cleats/inch (3.9 cleats/cm) would have a total face cleat surface area of 3.43×10^9 ft^2 (3.18×10^8 m^2). If the cleat aperture width of the butt cleats is large enough for bacterial access, then the total cleat surface areas calculated above would be doubled, assuming similar cleat spacing.

The amount of gas generated during MECoM is proportional to the surface area and the amount of coal removed from either side of the cleat during biogasification. A previous example demonstrated that permeability in a bituminous coal having a cleat spacing of 6 cleats/inch (2.4 cleats/cm) and an initial cleat aperture of 2 microns would increase to 4.31 md if bacteria remove 2 microns from either side of the cleat (4 microns total). The amount of methane generated during MECoM can be estimated using cleat surface area and the volume of coal converted into methane.

One ton of ash-free bituminous coal occupies a volume of 26.25 ft^3 (0.744 m^3), equivalent to a cube 35.67 inches (90.60 cm) on a side. Therefore, a total of 214 cleats are in 1 ton of coal and the total surface area is 351 m^2 (fig. 6). Assuming 2 microns of coal is removed from both sides of each cleat, the total volume of coal is 7.026×10^{-4} m^3 (42.9 in^3), or 0.095 percent of the total weight of the coal. The total yield for a 1 wt. % conversion of coal into methane is estimated to be 488 scf/ton (15.3 cm^3/g), indicating that the total methane generation from 0.095% conversion is between 46 and 92 scf/ton (1.4 and 2.9 cm^3/g) (table 1). The conversion of 10 microns per cleat of coal into methane in a coal with a cleat spacing of 10 cleats/inch (3.9 cleats/cm) would yield between 192 and 384 scf/ton (6.0 and 12.0 cm^3/g). However, the preceding examples assume that bioconversion of coal generates only methane and no other gases. Therefore, the actual amount of methane generated per ton of coal during MECoM could be significantly less than the amount indicated in table 1.

Reaction Rates. Another major factor affecting MECoM economics is the rate at which bacterial consortia will convert coal into methane. If the conversion rate is too slow, the process will be uneconomic regardless of the quantity of gas generated or how much permeability is increased. Unfortunately, insufficient data are available to fully evaluate laboratory reaction rates in the context of the subsurface environment and to extrapolate those reaction rates now.

Laboratory experiments on the direct conversion of lignite by a bacterial consortia resulted in a direct conversion efficiency of coal carbon into methane ranging from 35 to 50% and found that methane generation began soon after the coals were inoculated with bacteria and increase steadily for 2 to 3 weeks [12]. One experiment using bacterial consortia specially adapted to converting coal into methane achieved a peak methane generation rate of 30.5 cm^3/g of coal/day (978 scf/ton/day) after only 7 days; methane production subsequently declined after 21 days [13]. However, coal biogasification experiments are performed on crushed coal samples having a large net surface area and, therefore, much higher reaction rates. Additionally, laboratory experiments are performed under controlled conditions, whereas bacterial consortia utilized in MECoM would have to perform under more adverse conditions.

If the laboratory reaction rates discussed above are reduced by three orders of magnitude in the subsurface to 0.98 scf/ton/day (0.03 cm^3/g of coal/day), the additional gas generated by MECoM could be significant in a large volume of coal. For example, a 32.8 ft (10 m) coal covering an area of 10 acres (40,468 m^2) with a total coal tonnage of 544,226 tons (493,714 t) of coal would produce an additional 533 Mcf/d for a total of 195 MMcf in 1 year from the face cleat surfaces only; at $2.00/Mcf, this comes to an additional $390,000. However, additional bacteria and/or nutrients would probably have to be reinjected periodically to maintain high gas generation rates. Therefore, bacterial consortia would probably not generate gas at high rates consistently over long periods of time without reinoculation, particularly if toxic waste products accumulate.

Bacteria are capable of generating large quantities of methane in relatively short time periods under natural conditions, sometimes with dramatic results. During construction of the Buckman Bridge outside of Jacksonville, Florida, water from the St. Johns River was used to fill hollow bridge pilings [58]. The prestressed 2 × 2 ft (61 × 61 cm) concrete pilings with cardboard-lined hollow centers supported piers of the 3.1 mi (5 km) bridge. Anaerobic bacteria, derived from raw sewage dumped in the St. Johns River, metabolized the cardboard liners and generated enough methane to rupture the reinforced concrete pilings and destabilize part of the bridge [58]. Divers later found cracks ranging in size from hairline to 10 inches (25.4 cm) wide in 32 pilings; the remaining pilings were vented to prevent additional explosions. Although laboratory data and unusual events such as the Buckman Bridge suggest that coal biogasification rates may be adequate for MECoM, additional research using bacterial consortia derived from bituminous coals and/or consortia genetically adapted to bituminous coals is required to fully evaluate the economic feasibility of MECoM.

MECoM SUMMARY

MECoM may improve coalbed methane production through the generation of additional methane, removal of pore-plugging coal waxes, and/or permeability enhancement as cleat aperture width is enlarged during biogasification. Removal of coal waxes and enlargement of cleat apertures as bacteria convert coal into methane will generate additional methane and increase permeability. Preliminary calculations suggest that permeability enhancement will be more pronounced in

low-permeability coal reservoirs than in high-permeability ones and may prove to be the greatest benefit of MECoM.

The genetic development or discovery of bacteria consortia capable of efficiently converting coal into methane, available coal surface area, and biogasification reaction rates are factors that will impact MECoM development. Previous studies, using genetically adapted bacterial cultures, indicate that 35 to 50% of the coal can be converted to methane in the laboratory, which is equivalent to 17,080 to 24,000 scf/ton (534 to 763 cm^3/g). However, calculations of coal surface area available for biogasification based on cleat spacing indicate that the quantity of methane generated in the subsurface will probably be substantially less. Insufficient data currently exist to extrapolate laboratory biogasification reaction rates to the subsurface, but the results of these previous studies are encouraging.

Research including microbial sampling of deeply buried bituminous coals is required to fully evaluate MECoM and to determine if the process will improve coalbed methane producibility and recovery. In addition to microbiological considerations, a detailed understanding of hydrogeologic factors affecting coalbed methane producibility is critical for the successful implementation of MECoM. Coalbed methane producibility is determined by the complex interplay of coal distribution, coal rank, gas content, permeability, ground-water flow, and depositional and structural setting [59], which may vary from one part of a basin (or subbasin) to another.

CONCLUSIONS

(1) MECoM imitates and enhances the natural process of secondary biogenic gas generation in coal beds that occur in basins worldwide through the introduction of anaerobic bacterial consortia into coalbed methane wells.

(2) If only one-hundredth of 1% (1/10,000) of U.S. (lower 48) coal resources were converted into methane using MECoM, gas resources would increase by 23 Tcf, or approximately 16% of current lower 48 nonassociated reserves.

(3) MECoM benefits include the generation of additional coal gas, removal of pore-plugging waxes, and permeability enhancement as cleat aperture widths are increased during biogasification.

(4) Limitations of MECoM include the total cleat surface area (which is a function of cleat spacing) accessible to bacteria in the subsurface, biogasification reaction rates, very-high temperatures (>230°F; 110°C), and the possible generation and/or removal of toxic waste products associated with microbial activity.

(5) Permeability enhancement during MECoM may prove to be more beneficial to coalbed methane producibility than additional gas generation. Permeability enhancement would be more important in low-permeability coal reservoirs than in higher-permeability reservoirs.

(6) A detailed understanding of hydrogeologic factors affecting coalbed methane producibility in addition to microbiological considerations is critical for the successful implementation of MECoM.

ACKNOWLEDGMENTS

The concepts discussed evolved from coalbed methane research funded by the Gas Research Institute under contract numbers 5087-214-1544 and 5091-214-2261. Critical reviews of the manuscript by W. R. Kaiser, Ronald G. McMurry, Muhammad Razi, and Tucker F. Hentz improved the manuscript. Word processing was by Susan Lloyd and layout was by Jamie H. Coggin. Editing was by Amanda R. Masterson. Drafting was provided by the cartographic staff of the Bureau of Economic Geology under the direction of R. L. Dillon. This publication was authorized by the Director, Bureau of Economic Geology, The University of Texas at Austin.

REFERENCES CITED

1. Wolfe, R. S., 1993, "An historical overview of methanogenesis": *in* Ferry, J. G., ed., *Methanogenesis*: New York, Chapman & Hall, p. 1–32.
2. Fox, G. E., Magrum, M. W., Balch, W. E., Wolfe, R. S., and Woese, C. R., 1977, "Classification of methanogenic bacteria by ^{16}S ribosomal RNA characterization": Proceedings of the National Academy of Science, USA, v. 74, p. 4537–4541.
3. Woese, C. R., and Fox, G. E., 1977, "Phylogenetic structure of the prokaryotic domain: the primary kingdoms": Proceedings of the National Academy of Science, USA, v. 74, p. 5088–5090.
4. Winfrey, M. R., 1984, "Microbial production of methane": *in* Atlas, R. M., ed., *Petroleum Microbiology*: New York, Macmillan, Ch. 5, p. 153–220.
5. Goodwin, S., and Zeikus, J. G., 1987, "Ecophysiological adaptations of anaerobic bacteria to low pH: analysis of anaerobic degradation in acidic peat bog sediments": Applied Environmental Microbiology, v. 53, p. 57–64.
6. Zinder, S. H., 1993, "Physiological ecology of methanogens": *in* Ferry, J. G., ed., *Methanogenesis*: New York, Chapman & Hall, p. 128–206.
7. Balkwill, D., and others, 1994, "DOE seeks origin of deep subsurface bacteria": Transactions, American Geophysical Union, v. 75, no. 34, p. 385,395–385,396.
8. Jack, T. R., 1983, "Enhanced oil recovery by microbial action": *in* Yen, T. F., Kawahara, F. K., and Hertzberg, R., eds., *Chemical and geochemical aspects of fossil energy extraction*: Ann Arbor, Ann Arbor Science, 266 p.
9. Sperl, P. L., and Sperl, G. T., 1993, "New microorganisms and processes for MEOR": final report prepared for the U.S. Department of Energy, DOE/BC/14663-11, 46 p.
10. Cohen, M. S., and Gabriele, P. D., 1982, "Degradation of coal by the fungi *Polyporus versicolor* and *Poria monticoloa*": Applied Environmental Microbiology, v. 44, p. 23–27.
11. Olson, G. J., Brickman, F. E., and Iverson, W. P., 1986, "Processing of coal with microorganisms": final report prepared for the Electric Power Research Institute, EPRI AP-4472, variously paginated.
12. ARCTECH, Inc., 1990, "Biological gasification of coals": final report prepared for the Department of Energy under contract number DE-AC21-87MC23285: DOE/MC/23285-2878 (DE90015337), 130 p.

13. ARCTECH, Inc., 1993, "Biogasification of low-rank coals": final report prepared for the Electric Power Research Institute, EPRI TR-101572, variously paginated.
14. Barik, S., Isbister, J., Hawley, B., Forgacs, T., and Reed, L., 1988, "Microbial conversion of coals to clean fuel forms": *in* Preprints of Papers Presented at the 196th American Chemical Society National Meeting, September 25–30, 1988, v. 33, no. 4, p. 548–553.
15. Barik, S., Isbister, R., and Berrill, P., 1991a, "Coal biogasification research and process development": *in* Proceedings, Second International Symposium on the Biological Processing of Coal: Palo Alto, CA, Electric Power Research Institute, EPRI GS-7482, p. 6-23 to 6-38.
16. Barik, S., Tiemans, K., and Isbister, J., 1991b, "Investigations of metabolites and optimization of bacterial culture for coal biogasification": final report prepared for the Gas Research Institute, under contract number 5088-221-1756 (GRI-91/0051), 67 p.
17. Volkwein, J., 1990, "Preliminary evidence microbial gasification of Pittsburgh seam coal": *in* Proceedings, First International Symposium on the Biological Processing of Coal: Palo Alto, CA, Electric Power Research Institute, EPRI GS-6970, p. P-37 to P-43.
18. Vorres, K. S., 1990, "The Argonne premium coal sample program": Energy & Fuels, 1990, v. 4, p. 420–426.
19. Polman, K. J., Breckenridge, C. R., and Delezene-Briggs, K. M., 1993, "Microbiological analysis of Argonne Premium coal samples": Energy and Fuels, v. 7, p. 380–383.
20. Roberts, M. A., and Crawford, D. L., 1991, "Peroxidase and esterase production by coal depolymerizing Pseudodmonas strain DLC-62": *in* Proceedings, Second International Symposium on the Biological Processing of Coal: Palo Alto, CA, Electric Power Research Institute, EPRI GS-6970, p. 4-5 to 4-22.
21. Scott, C. D., Faison, B. D., Woodward, C. A., and Brunson, R. R., 1991a, "Anaerobic solubilization of coal by microorganisms and isolated enzymes": *in* Proceedings, Second International Symposium on the Biological Processing of Coal: Palo Alto, CA, Electric Power Research Institute, EPRI GS-7482, p. 4-29 to 4-46.
22. Kaiser, W. R., Swartz, T. E., and Hawkins, G. J., 1991, "Hydrology of the Fruitland Formation, San Juan Basin": *in* Ayers, W. B., Jr., and others, Geologic controls on the producibility of coalbed methane, Fruitland Formation, San Juan Basin: Gas Research Institute Topical Report GRI-91/0072, p. 195–241.
23. Scott, A. R., and Kaiser, W. R., 1991, "Relation between basin hydrology and Fruitland gas composition, San Juan Basin, Colorado and New Mexico": Quarterly Review of Methane from Coal Seams Technology, v. 9, no. 1, p. 10–18.
24. Scott, A. R., Kaiser, W. R., and Ayers, W. B., Jr., 1991b, "Composition, distribution and origin of Fruitland and Pictured Cliffs Sandstone Gases, San Juan Basin, Colorado and New Mexico": *in* Schwochow, S., ed., Coalbed methane of western North America: Rocky Mountain Association of Geologists Guidebook, p. 93–108.
25. McInerney, M. J., and Beaty, P. S., "Anaerobic community structure from a nonequilibrium thermodynamic perspective": Canadian Journal of Microbiology, v. 34, p. 487–493.
26. Thiele, J. H., Chartrain, M., and Zeikus, J. G., 1988, "Control of interspecies electron flow during anaerobic digestion: role of floc formation in syntrophic methanogenesis": Applied and Environmental Microbiology, v. 54, no. 1, p. 10–19.
27. Thauer, R. K., 1990, "Energy metabolism of methanogenic bacteria": Biochimica et Biophysica Acta, v. 1018, p. 256–259.
28. Chapelle, F. H., 1993, *Ground-water microbiology and geochemistry:* New York, John Wiley & Sons, 424 p.
29. Whiticar, M. J., Faber, E., and Schoell, M., 1986, "Biogenic methane formation in marine and freshwater environments: CO_2 reduction vs. acetate fermentation-isotopic evidence": Geochimica et Cosmochimica Acta, v. 50, p. 693–709.
30. Scott, A. R., 1993, "Composition and origin of coalbed gases from selected basins in the United States": Proceedings, 1993 International Coalbed Methane Symposium, v. I, p. 207–216.
31. Scott, A. R., Kaiser, W. R., and Ayers, W. B., Jr., 1994, "Thermogenic and secondary biogenic gases, San Juan Basin, Colorado and New Mexico—implications for coalbed gas producibility": American Association of Petroleum Geologists Bulletin, v. 78, no. 8, p. 1186–1209.
32. Mavor, M. J., Close, J. C., and Pratt, T. J., 1991, "Western Cretaceous coal seam project summary of the Completion Optimization and Assessment Laboratory (COAL) site": Gas Research Institute Topical Report, GRI 91/0377, variously paginated.
33. Kiener, A., and Leisinger, T., 1983, "Oxygen sensitivity of methanogenic bacteria": Systematic and Applied Microbiology, v. 4, p. 305–312.
34. Bayer, P. E., 1991, "Gene transfer in the environment and coal bioprocessing with genetically engineered microorganisms": Proceedings, Second International Symposium on the Biological Processing of Coal: Palo Alto, CA, Electric Power Research Institute, EPRI GS-7482, p. 2-17 to 2-32.
35. Scott, A. R., and Kaiser, W. R., in press, "Microbially enhanced coalbed methane: limitations and possible benefits" (abs.): American Association of Petroleum Geologists Program, v. 4.
37. Law, B. E., 1993, "The relation between coal rank and cleat spacing: implications for the prediction of permeability in coal": Proceedings, 1993 International Coalbed Methane Symposium, v. I, p. 435–442.
38. Close, J. C., 1993, "Natural fractures in coal": *in* Law, B. E., and Rice, D. D., eds., Hydrocarbons from coal: American Association of Petroleum Geologists Studies in Geology no. 38, p. 119–132.
39. Lucia, F. J., 1983, "Petrophysical parameters estimated from visual descriptions of carbonate rocks: a field classification of carbonate pore space": Journal of Petroleum Technology, March, p. 629–637.
40. Torella, F., and Morita, R. Y., 1981, "Microcultural study of bacterial size changes and microcolony and ultramicrocolony formation by heterotrophic bacteria in seawater": Applied and Environmental Microbiology, Feb., p. 518–527.
41. Penny, G., S., and Conway, M. W., 1993, "Coordinated studies in support of hydraulic fracturing of coalbed

methane": Gas Research Institute Annual Report, GRI 93/0125, variously paginated.
42. Vorkink, W. P., and Lee, M. L., 1993, "Appraisal of heavy hydrocarbons in coal seam gas reservoirs": Gas Research Institute Annual Report, GRI 92/0501, 31 p.
43. Hunt, J. M., 1979, *Petroleum geochemistry and geology:* San Francisco, W. H. Freeman, 617 p.
44. Connan, Jacques, 1984, "Biodegradation of crude oils in reservoirs": *in* Advances in Organic Geochemistry, 1984, v. 1, p. 300–335.
45. Rittman, B. E., Valocchi, A. J., Seagren, E., Ray, C., Wrenn, B., and Gallagher, J. R., 1992, "A critical review of bioremediation": topical report prepared for the Gas Research Institute, (GRI-92/0322), 152 p.
46. Zhender, A. J. B., and Brock, T. D., 1980, "Anaerobic methane oxidation: occurrence and ecology": Applied and Environmental Microbiology, v. 39, p. 194–204.
47. Coleman, D. D., Risatti, J. B., and Schoell, M., 1981, "Fractionation of carbon and hydrogen isotopes by methane oxidizing bacteria": Geochimica et Cosmochimica Acta, v. 45, p. 1033–1037.
48. Whiticar, M. J., and Faber, E., 1986, "Methane oxidation in sediment and water column environments—isotopic evidence": Advances in Organic Geochemistry 1985, v. 10, p. 759–768.
49. Colberg, P. J., and Young., L. Y., 1985, "Aromatic and volatile acid intermediates observed during anaerobic metabolism of lignin-derived oligomers": Applied and Environmental Microbiology, Feb., p. 350–358.
50. Benner, R., Maccubbin, A. E., and Hodson, R. E., 1984, "Anaerobic biodegradation of the lignin and polysaccharide components of lignocellulose and synthetic lignin by sediment microflora": Applied and Environmental Microbiology, May, p. 998–1004.
51. Crawford, D. L., Gupta, R. K., Deobald, L. A., and Roberts, D. J., 1990, "Biotransformations of coal and coal substructure model compounds by bacteria under aerobic and anaerobic conditions": *in* Proceedings, First International Symposium on the Biological Processing of Coal: Palo Alto, CA, Electric Power Research Institute, EPRI GS-6970, p. 4-29 to 4-43.
52. Davison, B. H., Nicklaus, D. M., Misra, A., Lewis, S. N., and Faison, B. D., 1990, "Utilization of microbially solubilized coal": Applied Biochemistry and Biotechnology, v. 24/25, p. 447–456.
53. Stettler, K. O., 1986, "Diversity of extremely thermophilic Archaebacteria": *in* Brock, T. D., ed., *Thermophiles: general, molecular, and applied microbiology*: New York, John Wiley & Sons.
54. Kelley, R. M., and Deming, J. W., 1988, "Extremely thermophilic Archaebacteria: biological and engineering consideration": Biotechnological Progress, v. 4, p. 47–62.
55. Zeikus, J. G., and Winfrey, M. R., 1976, "Temperature limitations of methanogenesis in aquatic sediments": Applied and Environmental Microbiology, v. 31, p. 99–107.
56. Muralidharan, V., Hirsh, I. S., Peeples, T. L., and Kelley, R. M., 1991, "Mixed cultures of high temperature bacteria: Prospects for bioprocessing of fossil fuels": *in* Proceedings, Second International Symposium on the Biological Processing of Coal: Palo Alto, CA, Electric Power Research Institute, EPRI GS-7482, p. 6-51 to 6-67.
57. Clayton, J. L., 1992, "Role of microbial processes in petroleum systems": *in* The petroleum system—status of research and methods: U.S. Geological Survey Bulletin 2007, p. 16–19.
58. Dunker, K. F., and Rabat, B. G., 1993, "Why America's bridges are crumbling": Scientific American, March, p. 68.
59. Kaiser, W. R., Hamilton, D. S., Scott, A. R., Tyler Roger, and Finley, R. J., 1994, "Geologic and hydrologic controls on the producibility of coalbed methane": Journal of the Geological Society of London, v. 151, p. 417–420.
60. Quigley, D. R., Ward, B., Crawford, D. L., Hatcher, H. J., and Dugan, P. R., 1989, "Evidence that microbially produced alkaline materials are involved in coal biosolubilization": Applied Biochemistry and Biotechnology, v. 20/21, p. 753–763.
61. Scott, A. R., Zhou, Naijiang, and Levine, J. R., in press, "An improved approach to estimating coal and coal gas resources: example from the Sand Wash Basin": American Association of Petroleum Geologists Bulletin.

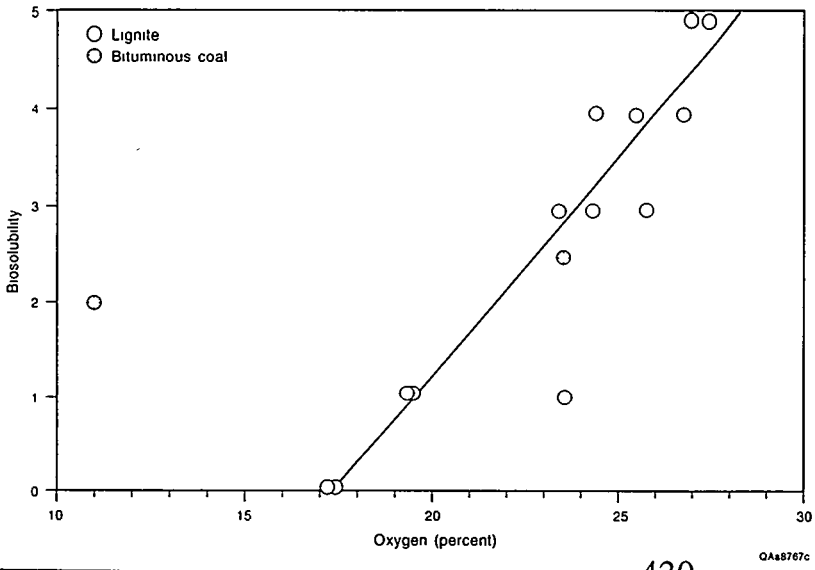


Figure 1. Relation between biosolubility and rank. Biosolubility is ranked from minimum (0) to maximum (5) based on the discoloration of the aqueous medium during culture period. Biosolubility generally decreases with decreasing oxygen content (rank) although some higher-rank coals have higher biosolubility, suggesting that bituminous coals can be metabolized. Modified from [60].

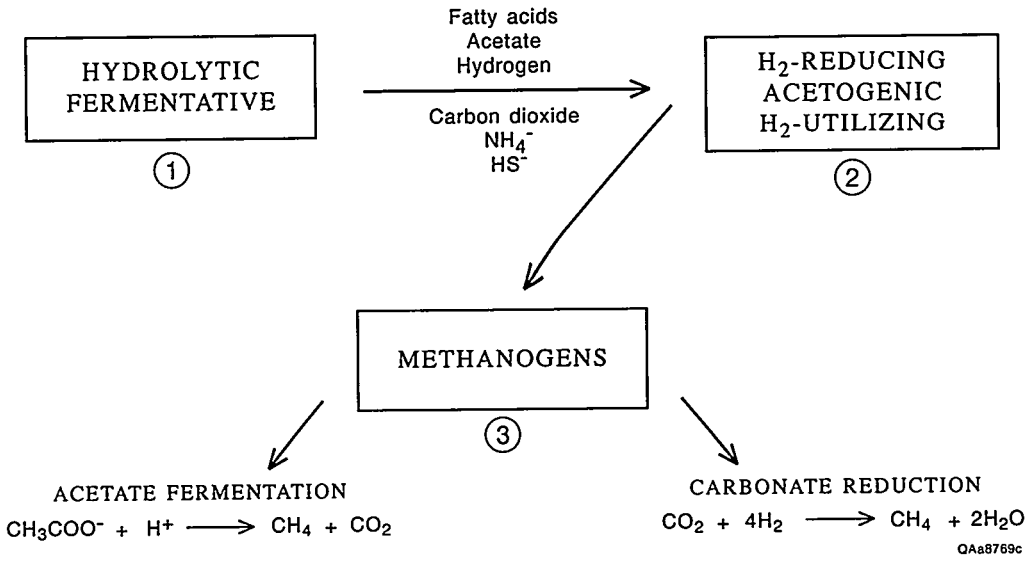


Figure 2. Generalized flow diagram for the anaerobic decomposition of organic matter and generation of methane. Modified from [4].

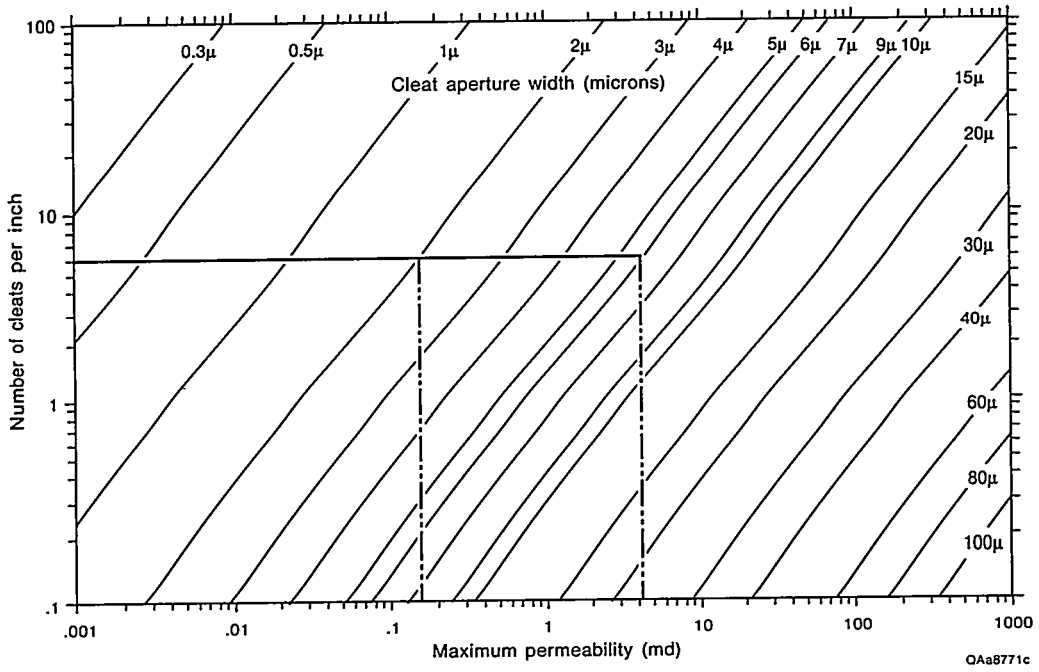


Figure 3. Relation among face cleat spacing, permeability, and face cleat aperture width based on the equations in [39]. Cleat tortuosity will decrease fluid permeability, suggesting that cleat aperture widths in the subsurface may be larger than indicated on the figure.

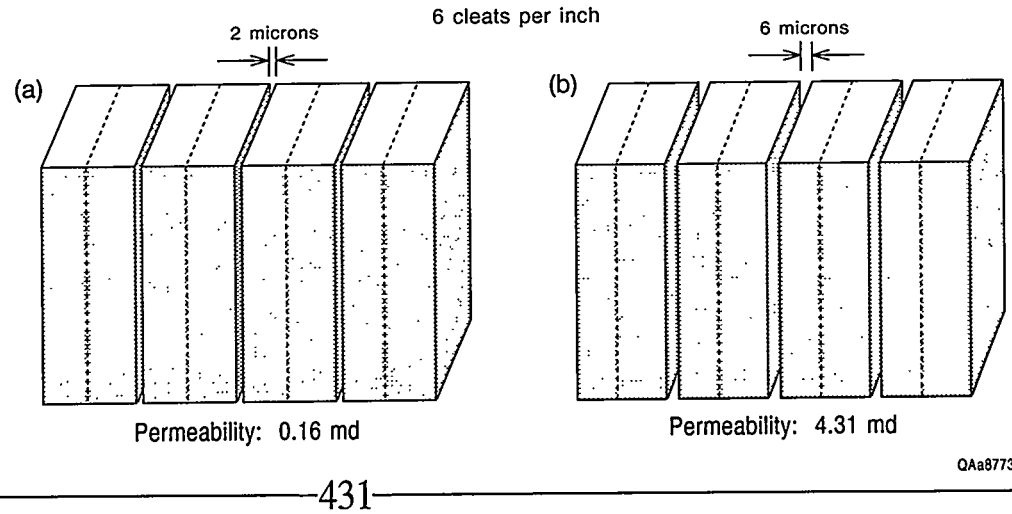


Figure 4. Changes in face cleat aperture width during MECoM. Removal of coal from cleat surfaces during MECoM will increase cleat aperture width, resulting in permeability enhancement.

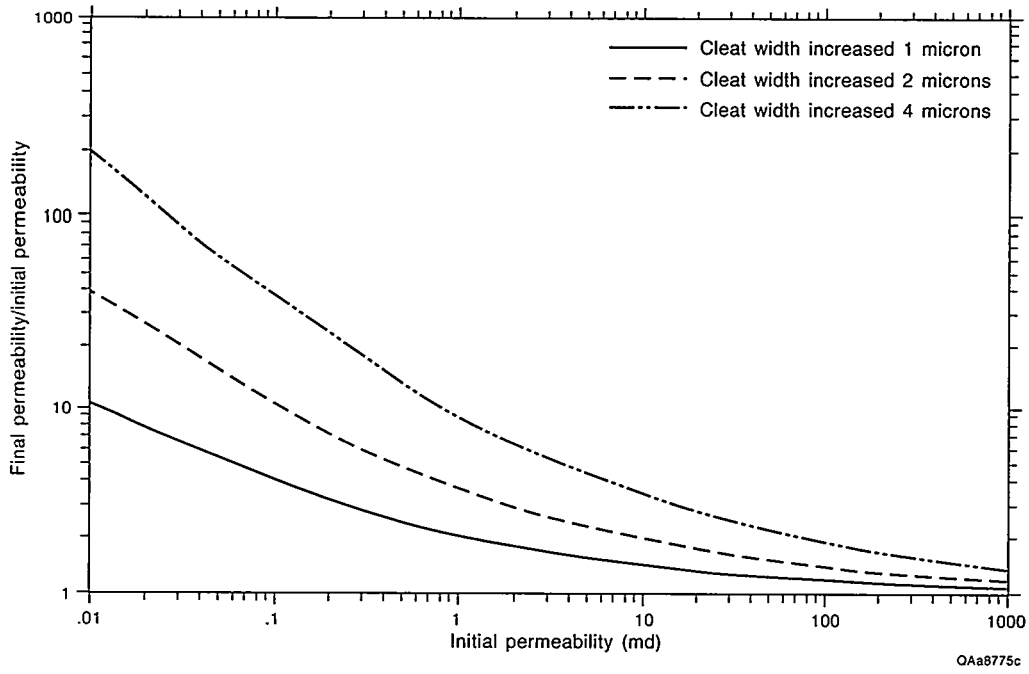


Figure 5. Potential permeability enhancement during MECoM assuming 6 cleats/inch. Permeability enhancement may be more important to coalbed methane producibility than the total amount of methane produced. The ratio of final permeability (after MECoM) to initial permeability (before MECoM) is much greater in low-permeability coal reservoirs (permeability <1 md).

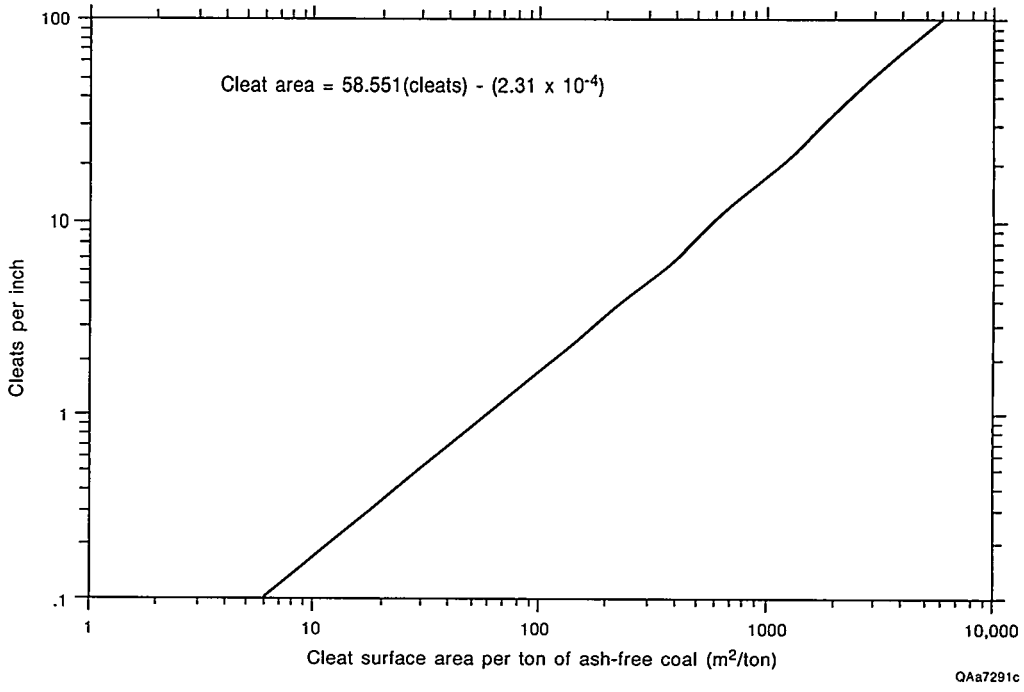


Figure 6. Relation between cleat spacing and cleat surface area per ton of ash-free bituminous coal. Face cleat and butt cleat spacing may differ slightly, and the total butt cleat surface area may be partially inaccessible to bacteria. Equations in [61] can be used to correct cleat surface area (coal volume) for weight percent ash.

Table 1. Estimated quantities of methane generated during MECoM. Calculations assume that methane is the only gas generated during biogasification. Other assumptions are discussed in text.

Available surface area	scf/ton[b]	scf/ton/cleat/micron[c]
Face cleat only	46.13	1.92216
Face cleat and partial butt cleat[a]	69.19	2.88325
Face and butt cleat	92.26	3.84433

[a] assumes butt cleats are partially accessible to bacteria, therefore having only half the surface area of the face cleat.

[b] estimate based on 6 cleats/inch and 4 microns of coal/cleat converted into methane.

[c] "micron" refers to how many microns of coal in each cleat are converted into methane in the example above: (1.92216)(4 microns)(6 cleats) = 46.128 scf/ton.

INTERGAS '95

May 15-19, 1995
The University of Alabama
Tuscaloosa, Alabama USA

9529

On the Type of Generation and Storage of Coalbed Methane Reservoir

Zhang Xinmin and Zhong Lingwen, Central Coal Mining Research Institute, Xian Branch, People's Republic of China

ABSTRACT

Coalbed methane is a sort of natural gas , for which the coal acts both as the source rock and as the reservoir. Approximately 90 percent of the coalbed methane is stored in adsorbed state in coal seams.

By studing deeply the characteristics of generation and storage of gas in coal, this paper has developed a new concept, i.e., the types of generation-storage of coalbed methane reservoir. According to the amount of methane generated and storage capacity of coal,the coal is divided into following four types in coalification sequence: 1) Less generation and middling storage type, which includes long-flame coal and gas coal, the amount of methane generated is small while the storage capacity is medium; 2) Much generation and low storage type, the coal rank of which is fat coal, coking coal and lean coal, the methane generating ability is high, but the storage capacity is lower; 3) Much generation and high storage type, which includes meagre coal, anthracite-3 and anthracite-2, the methane generating ability and storage capacity both are high; 4) Metamict generation and little storage type, this type includes only anthracite-1, the methane splits apart into carbon and hydrogen, and the coal has basically no adsorbability. Each type of coal generates defferent quantities of methane, has different capacity of adsorption, different porosity and/or fracture. All of this variety was created by physical-chemical properties changes of coal in coalification process.

This concenpt and dividing programme can be used for calculation of gas content and degasification of coalbed methane, thus can serve the purpose of coalbed methane resouece development and geology of mine gas.

INTRODUCTION

Coal is of interest to the geologist work in natural gas merely as one kind of source rock, and have been studied widely. By contrast, it had not been attached importance to the properties of coal which acts as unconventional gas reservoir.

For conventional gas reservoir rock, such as sandstone, it can be classified according to the porosity and permeability[1]. However, coalbed methane is a type of unconventional natural gas, the coal acts both as the source rock and as the reservoir rock. In general, the porosity and permeability of coal seam are low and vary significantly during production,thus the capacity of generation and storage of methane are the principal properties of coalbed methane reservoir. From the capacity of gas generation, property of gas storage, split phenomenon of methane and so on, this paper will discuss the gas-bearing characteristics of coal seam, establish and set forward the concept of type of generation-storage of coalbed methane reservoir. These can provide a theory foundation for coalbed methane development and disaster prevention of mine gas.

GAS-BEARING CHARACTERISTICS OF COAL SEAMS

Gas Component

The natural gas in coal seams is methane predominantly with minor amounts of heavier hydrocarbons and other gases. Analyses of coalbed gas samples obtained from desorption tests are shown in Table 1. The gases from various ranks of coal, except super-anthracite, are usually 94 to 97 percent methane. Heavier hydrocarbons are also

associated with coalbed reservoirs, but in general amount to 1 to 5 percent. The non-hydrocarbon gases, including CO2, N2, and so on, are usually less than 5 percent. The gases which were found in super-anthracite are predominantly non-hydrocarbon gases, and the methane is less than 50 percent and without heavier hydrocarbon.

State of Gas Storage

Methane in coalbed is storaged in three states, i.e., adsorbed on internal surface of micropores, filled in fractures and cleats as free gas, and dissolved in ground water in coalbed. The adsorbed methane can be represented by Langmuir equation, the free methane follows the real gas equation and has some pressure, and the amount of dissolved methane is controlled by pressure, temperature and salinity of water. Generally speaking, the methane generated during coalification was adsorbed at first, then liberated as free gas and dissolved in water. Under certain pressure and temperature, these three states of methane are in the unified dynamic equilibrium system.

Because coal has low porosity and is mainly microporous, the majority of methane is present as adsorbed gas, and the amount of free gas is a litter. Since dissolvability of methane in water is low and the moisture of coal is very low, therefore, the dissolved methane in coal is insignificant and constitutes only 1 percent of total gas content[2].

Capacity of Gas Storage

Coal is a porous medium, and the pores are mainly micropore. For adsorbing of methane, the most effective radii of pores range from 15 Å to 1.000 Å. From the mercury injection test, it is indicated that 60 to 80 percent of the total porosity were constituted by pores of radii from 18 Å to 500 Å, and the percentage would be much higher if pores of radii from 500 Å to 1,000 Å were added [2]. These have made coal have very large internal surface area, and methane molecules can tightly pack on the internal surface as a monomolecular layer. Therefore, significant quantities of methane are held in coal seams. Gas contents of 10 ~ 30 cm^3/g (daf) have been measured for low volatile bituminous coal and anthracite in China. Thus, coal seam is a sort of reservoir rocks with greater potentiality and can hold two to three times as much gas in place as the same volume of a conventional sand reservoir [3].

THE TYPE OF GENERATION-STORAGE OF COALBED METHANE RESERVOIR

The methane which retained presently in coal seams is the rest of hydrocarbon gases that generated from organic matter during coalification and have migrated out of coal bed. This feature of gas reservoir results in that gas-bearing potentialities of a seam is controlled not only by the capacity (adsorbability and pores), but also by methane volume generated by coal itself. For a given seam, under favourable external conditions (mainly referred to confining condition), it could contained some amount of methane only in the case that sufficiency of methane must be generated by coal itself. If gas generating volume is lower than that, the volume of gas storage of coal could be considered as not full of. Only when gas generating volume is greater than storage capacity of coal, methane could fill pores of coal and migrate outward in free state. And only in this case, coal would become the source rock of conventional gas substantially. Moreover, methane can change itself on certain conditions. All of these are quite different from conventional gas reservoir rocks such as sandstone and limestone.

Generation and Existence of Coalbed Methane

A great attention has been payed to the mechanism and scale of hydrocarbon generated from coal. In 1980's many thermal simulation experiments were counducted using peat and lignite in China.The results of some experiments are summarized in Table 2. Based on these studies and in combination with the process of coalification, the generation and existence of coalbed methane can be divided into three stages.

Stage of Biodegradation It refers to the stage from peat to lignite ($R^0max < 0.5\%$). Under biochemical degradation of bacteria and oxygen, organic matters were converted, and generated certain amount of CO2, H2O, CH4 and so on. Biogenic hydrocarbon gas is consisted primarily of methane, contained not or very little heavier hydrocarbon. Such gas is dry and was known as biogas. Generally, a small amount of gas was generated in this stage. In addition, lignite was buried in shallow depth and very permeable, so the gas would be preserved poorly.

Thermogenic Stage This stage is lasted from long-flame coal to anthracite-3 ($0.5\% < R^0max < 4.0\%$). Under thermal degradation, a large amount of hydrocarbon compounds was generated,and methane was the main component of hydrocarbon gases. The quantity of methane

generated in the early stage is smaller.In the median stage the large volume of methane was produced. It is the major methane-generating period and characterized by the coexistence of oil and gases. The hydrocarbon gases are wet gas. In the late stage, the potentiality that methane was generated directly from organic matter of coal decreased significantly, but oil and heavier hydrocarbon gas generated previously were splitted and decomposed under high temperature, resulting in methane generation.

Metamict Stage After anthracite-2 (R^0max > 4.0%) the organic metter does not generate any gas basically. Wang and Yang's work (citied from Bao Ci [4]) on thermal simulation test using sapropelic kerogen indicated that there was nearly no heavier hydrocarbon in pyrolysis products when the temperature attained 600°C (R^0max = 4.08%), and the main components of gases were methane and hydrogen. At 800°C (R^0max =5.32%), methane begun to be disintegrated into carbon and hydrogen. At 1,200°C (R^0max =6.45%), methane disappeared and the final products were residual carbon and hydrogen.We considered that the phenomena of methane disintegration and disappearance described above could also appear in humic kerogen if the condition is similar. In other words, coalbed methane begun to be splited in the anthracite-2 stage, and anthracite-1 (R^0max > 6.0%, super-anthracite) could be considered as the period in which coalbed methane would disappear.

The Adsorption Capacity of Coal

As above-mentioned, methane in coalbed reservior is presented mainly in adsorption state, therefore, the maximum adsorption volume, i.e. the Langmuir sorption constant, represents quantitatively the capacity of gas storage in coal.

In order to study the variation regularity of adsorbability of coal, we conducted adsorption isotherm experiments using many coal samples from various ages and coal fields throughout China, and measured the maximum adsorption volume. The adsorption data of 65 samples were plotted in Figure 1. From this figure, it can be seen that the maximum adsorption volume of coal ranges from 0 to 41.14 cm^3/g (daf) and is closely related to metamorphic grade of coal (i. e. coal rank). Figure 1 also indicates that the maximum adsorption volume of coal is not simply in direct proportion to coal rank, as traditionally thought, but in a pattern of a complex curve. From long-flame coal to fat coal (R^0max = 0.5%–1.2%), the maximum adsorption volume of coal decreases with rank, and with the lowest in fat coal. From fat coal to anthracite-2 (1.2% < R^0max <4.0%) the maximum adsorption volume increases with coal rank, and reaches the highest in anthracite-2. But afterwards, it decreases sharply with coal rank until almost no adsorbability in anthracite-1. The turning points of the curve are roughly the same as points of "coalification jump". It indicates that the variation of coal adsorbability are caused by coalification which evolved serial changes of physical and chemical properties of coal.

Classification of Coalbed Methane Reservoir

In the preceding discuss, it was found that, apart from coal petrography and coal quality, the decisive factor influencing coalbed methane generation and storage was coalification degree (i. e. coal rank). The mining and coalbed methane production practices also indicated that both gas discharge in mines and reservoir properties of coal, such as gas content, porosity and pemeability of seam, are closely related with coal rank. All of these have made it possible that coalbed reservoirs were classified into various types in the sequence of coalification according to gas generation and storage capacity.

At first, according to the comparison between gas-generating amount and adsorption constant value "a", and the phenomena of disintegration and disappearance of methane, coalbed reservoirs were devided into three categories, i. e., less generation capacity, much generation capacity and metamict generation. In coal ranks before gas coal, the amount of methane generated was smaller than the adsorption constant "a". In this stage, the amount of methane generated controlled significantly methane content in coal bed. In coal ranks after fat coal, the amount of methane generated was larger than the maximum adsorption volume, and coalbed methane content was not related with gas-generating amount but depended on the adsorption capacity of coal (compare Tab.2 and Fig.1). In the rank of anthracite-1, primary methane was splitted and disappeared. Then, according to the change tendency of maximum adsorption volume and existing classification of coal ranks, the storage capacity was subdivided into four classes, i. e. high, medium, low and little. Finally, combining the categories of gas-generating amount with classes of adsorption capacity, the coalbed reservoirs were divided into four types of generation and storage capacity: 1) less generation and middling storage type, 2) much generation and low storage type, 3) much generation and high storage type, and 4) metamict generation and little storage type. The primary characteristics of each type are summarized in Table 3.

The column of maximum adsorption volume in Table 3 represents an average of adsorption constants for each coal rank, these adsorption constants were measured in our experiments of adsorption isotherm.

SUMMARY

1. From above discussion, it can be seen that different types of coalbed methane reservoirs are differential in methane-generating and adsorpting capacity and have different porosity and/or fracture characteristics, these resulted in differences at methane content, primary permeability, which led in turn to different degree of difficulty for gas drainage. All of these differences were caused by physico-chemical changes of organic matter during coalification. This concept and programme of classification reveals the primary properties of coalbed methane reservoir.Therefor, it can serve coalbed methane resources assessment and mining safety, representing great theoretical and practical importance. In addition, petrographic composition and changes of coal quality, and even local structure, will have influence more or less on the gas generating capacity, adsorption properties, porosity and/or fracture characteristics, making the situations said above become more complex. Therefore, when using this classification in practices, it must combine with geological and structural conditions as well as properties of coalbed itself, and conduct detailed analgses.

2. The methane content is a critical parameter for coalbed methane resource assessment and mine gas prediction. In general, data of measured coalbed methane content are limited, it is required to determine coalbed methane content using indirect methods, such as by analogy and/or calculation, especially for prediction of methane content in deep seams. For coal of less generation and middling storage type, the methane content is mainly controlled by gas-generated amount. Therefor, in the absence of measured gas pressure data, it cound determine methane content of this type coal only by analoge. For metamict generation and little storage type (i.e. anthracite-1), the determination of methane content is also only by analogy. But for coals both much generation and low storage type as well as much generation and high storage type, the methane content principally depends upon adsorption capacity, and increases with metamorphic digree of coal. Based on the experimental data, we took the averages of measured porosities and adsorption constants of each rank of coal to represent the storage properties of this coal rank, then substituted the averages into the corresponding formulas to calculate the methane content [2]. The methane contents of seams at depth more than 1000m shown in Table 4 were predicted using above methods.

3. Different type has different characteristics in production of coalbed methane, respectively.

· less generation and middling storage type: The porosity is great, permeability of coal bed is good. But the methane content is smaller because gas generation amount is less.

· Much generation and low storage type: The porosity is very low, but natural fractures (cleats) are developed very well, so the permeability of coal seam is higher, and the methane content is bigger. In addition, the brittleness of coal is higher, so coal seam will be fractured easily. Therefore, it can be expected to obtain higher production rate from this type of coal seams.

· Much generation and high storage type: The methane content is very high, but the permeability is very low. The brittleness of coal is low and the hardness is higher, so coal seam will be stimulated difficultly. Therefore, this type is unfavourable for coalbed methane production.

· Metamict generation and little storage type: The methane content is smallness, so there have no trouble from coalbed methane in those mines which are mineing the anthracite-1. So anthracite-1 rank coal seams not belong to the category of coalbed methane reserovir.

ACKNOWLEDGEMENTS

The authors extend thanks to our associates' helps in collection of coal samples and for tests, they are Zhang Suian, Zhu Zhaoying, Li Jin and Lu Zhifa.

REFERENCES

1. Dai Jinxing, Pei Xigu and Qi Houfa, 1992: Natural Gas Geology In China Vol.1,Beijing, The Petroleum Industry Press, p. 206-208 (in Chinese).

2. Zhang Xinming et al., 1991: Coalbed Methane In China, Xi'an, Shaanxi Science and Technology Publishing House (in Chinese).

3. Kuuskraa, V.A. and Brandenburg, C. F., 1989: "Coalbed Methane Sparks a New Energy Industry", Oil and Gas Journal, Oct., 1989, p. 49-56.

4. Bao Ci, 1989: Natural Gas Geology , Beijing, Science Press, p.30-41 (in Chinese).

Table 1 The Composition of Natural Gas in Coal Bed

Samplas Place	Coal Age and Name	Depth (m)	Gas Composition (Volume per cent)				Coal Kind
			CH_4	C^{+2}	CO_2	N_2	
Hongyang, Liaoning	C-P, 12# Coal seam	800	95.09	—	3.01	1.90	Meager Coal
Ducun, Suzhou	P_2	514	97.65	0.34	1.44	0.57	Gas Coal
Fengcheng, Jiangxi	P_2, B_4 Coal seam	1148	94.42	1.51	0.66	3.41	Coking Coal
Tianfu, Sichuan	P_2	780	89.12	8.75	0.64	1.54	Coking Coal
Nantong, Sichuan	P_2, 4# Coal seam	766	96.72	0.94	0.60	1.74	Meager Coal
Jixi, Heilongjiang	J_3-K_1, 7# Coal seam	945	91.54	4.95	2.12	1.39	Fat Coal
Xinshui, Shanxi	C_3	505	97.36	—	0.58	0.91	Anthracite
Anfu, Jiangxi	P_2	617	48.36	—	4.52	47.12	Super-anthracite

Table 2 Gas-generated Amount by Thermo-Simulation of Some coal Samples from China

Tester	Gas-generated Amount From coal(m^3/ton)	Un-metamorphic stage	Low Metamorphic Stage		Medium Metamorphic stage			High Metamorphic stage	
		Lignite	Long-flame coal	Gas coal	Fat coal	Coking coal	Lean coal	Meagre coal	Anthracite
Xi'an Branch, Central Coal, Mining Research Institute (1987)*	Apparent Gas-generated Amount		3~25	10~54	27~102	55~170	108~246	134~333	268~393
	Gas-generated Amount	38~68	41~93	48~122	65~170	93~238	146~314	172~401	306~461
Petroleum Development Research Institute (1985)*	Apparent Gas-generated Amount		4~31	7~58	26~108	48~176	86~230	114~321	168~390
	Gas-generated Amount	38~68	42~69	45~126	64~176	86~244	124~298	152~389	206~458
Petroleum Geology Research Institute, MOGMR (1985, Lignite, From Shunan)	Apparent Gas-generated Amount								
	Gas-generated Amount	0.55	1.06	4.25	24.32	55.9	94.77	127.72	221.13
Xu Yong Chang et al. (1986, Lignite From Xin jiang)	Apparent Gas-generated Amount		2.49	22.92	53.04	113.57		183.34	325.23
	Gas-generated Amount	1.61	4.10	24.53	54.65	115.18		184.95	326.84

* — Synthesized Data.

Table 3 The Classification of Coalbed Mechane Reservoir and Their Characters

Type	Metamorphic grade of stage	Coal Rank		Code (in C.P.A.)	Refl. R^0_{max}(%)	Generation and Existence of Meth: Stage	Generation and Existence of Meth: Features	Maximum Sorption Volum (cm^3/g)	Description	Examples
	Un-metamophic stage	Lignite	Lignite	HM	< 0.5	Biodegradation	Biogas	0 10 20 30 40	Biogas, poorly preserved	
Less Generation and Midding Storage	Low metamorphic stage	Bituminous coal	Long-flame Coal	CY	0.50~0.65	Thermogenic	Gas generated amount is smaller		Amount of generated gas is smaller than maximum sorption, volum, great porosity, good permeability.	Fushun, Baotou
			Gas Coal	QM	0.65~0.90					
Much Generation and Low Storage	Medium Metamorphic Stage		Fat Coal	FM	0.90~1.20		Gas generated amount is Large		Amount of generated gas is bigger than maximum sorption volum, very low porosity, cleats developed very well, high permeability, high brittleness.	Fencheng Nantong, Fengfeng
			Coking Coal	JM	1.20~1.70					
			Lean Coal	SM	1.70~1.90					
Much Generation and High Storage	High Metamorphic Stage		Meagre Coal	PM	1.90~2.50				Amount of generated gas is bigger than maximum sorption volum, lower porosity, cleats undeveloped, poor permeability, low brittleness, high hardness.	Yangquan, Songzhao, Jincheng
		Anthracite	Anthracite-3	WY_3	2.50~4.00					
			Anthracite-2	WY_2	4.00~6.00		Disintegration			
Metamict Generation and Little Storage	Super-metamorphic Stage	Supper-anthracite	Anthracite-1	WY_1	6.45 >6.00	Metamict	Disappearance		CH_4 disintegrate into C and H_2, basically non-adsorption, very low porosity, low gas mines, not reservoir rock.	Mentougou

C. P. A. is abbreviated from the Chinese Phonetic Alphabet.

Table 4 Predicted methane content of different rank coal (at depth of more than 1,000 m)

Coal rank	R^0_{max} (%)	Mtehane content ($cm^3/g \cdot daf$)	Notes
Long-flame coal	0.50 ~ 0.65	5 ~ 6	Infered from southern field of Junggar basin
Gas Coal	0.65 ~ 0.90	7 ~ 8	By analogy with Jixi Coal field
Fat Coal	0.90 ~ 1.20	14.20	Calculated
Coking Coal	1.20 ~ 1.70	14.89	Calculated
Lean Coal	1.70 ~ 1.90	17.35	Calculated
Meagre Coal	1.90 ~ 2.50	19.62	Calculated
Anthracite - 3	2.50 ~ 4.00	26.19	Calculated
Anthracite - 2	4.00 ~ 6.00	25 ~ 30	Estimated
Anthracite - 1	> 6.00	2 ~ 3	By analogy with Anfu mine area, Jiangxi. and Donbass basin, Russia.

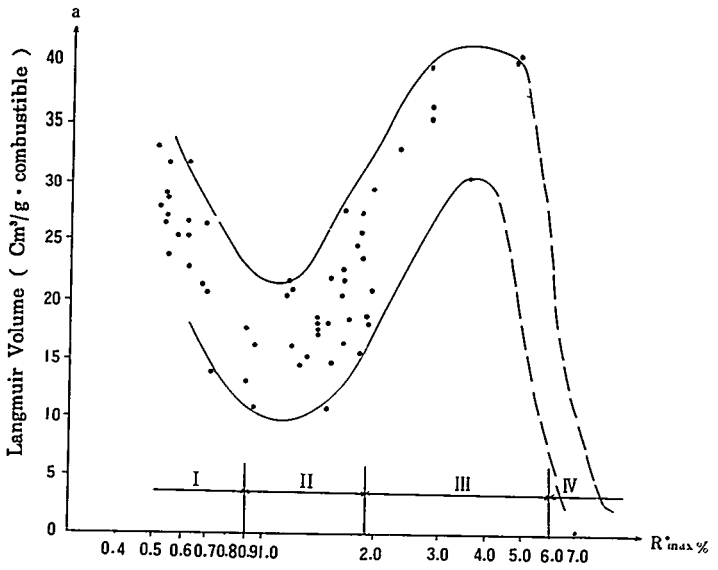


Figure 1 The relationship between Langmuir Volume and R^o_{max}



NOTES

INTERGAS '95

May 15-19, 1995
The University of Alabama
Tuscaloosa, Alabama USA

9507

Methane Seeps in the San Juan Basin: Potential Pathways

S.A. Marinello and J.C. Quinn, Colorado School of Mines

ABSTRACT

The presence and release of methane from shallow aquifers is a matter of considerable concern in close proximity to oil and gas development particularly in the San Juan Basin. Considerable consternation has been expressed in public meetings, reported in the media and argued in the legal system regarding safety and health aspects and the source of the "contaminant" methane. At issue are the probable mechanisms and pathways by which it may have migrated to specific locations. Proximate to gas activities it has been easy for some to draw the conclusion that shallow aquifers are being contaminated during development. The loss of well integrity is often the stated or perceived culprit, despite the fact that potential sources and pathways existed before development began, as did gas shows which factored into exploration efforts. That engineering studies fail to support specific cases is deemed irrelevant, particularly if poor science can be held up supporting a presupposed conclusion drawn in spite of existing data and alternative scenarios. Microbial activity can generate gas from carbonaceous materials in aquifers, such as coal or shale stringers, particularly when active aquifer recharge provides necessary supplemental nutrients as in the San Juan Basin. The general hydrologic flow through the Fruitland/Kirtland aquifer(s) is also known to encounter a permeability barrier in the mid-basin causing upward flow into a highly stressed/increased permeability region, one of the primary areas where seepage is observed at the surface. Desorption and/or release of methane can take place with fluid pressure reduction concurrent with upward flow, increased by aquifer withdrawal reducing the hydraulic head.

INTRODUCTION

An all too frequent occurrence in areas overlying natural gas reservoirs is the presence of methane gas shows in freshwater aquifers tapped for domestic, livestock, and agricultural uses. If a reservoir zone below the aquifer or the aquifer zone itself is being developed for natural gas production, a strong suspicion often arises that the development activity is causing, or at least exacerbating, the presence of the methane in the groundwater.

Regardless of the technical aspects of such situations, the issues are often argued from an emotional stance, often fanned by external sources with their own agendas, rather than with a logical examination of the known and/or discernible scientific and historical facts. This paper addresses such a situation in the San Juan Basin of Colorado and New Mexico where such occurrences have sparked significant debate. There has been considerable analysis by parties on both sides of the issue and arguments have been presented that often appear to discount evidence establishing conclusions or possible interpretations counter to those being argued.

We attempt to provide background on some of the technical aspects of these issues and to provide some analogous information from another sedimentary basin, the Denver-Julesberg Basin, where methane seeps have been determined to have reached productive water wells and/or the surface. The actual area of concern remains, of course, the San Juan Basin, particularly in the Pine River Outcrop region where there are active attempts to deal with methane seepage and to determine the actual cause and effect relationships that might exist.

BACKGROUND

There are many variations in the structure of geologic basins where coal and natural gas are found. Some areas are fairly consistent in geological structure with large regional barriers between aquifers while others are more geologically complex, having more unknowns and lacking definable permeability barriers. Some geologically complex western basins are highly fractured with a long history of hydrocarbon seeps leading to the presence of gas in stratigraphically higher aquifers and/or shows at the surface. Other basins have few fractures and definitive permeability barriers and have few documented seeps. Seepage from hydrocarbon containing formations is also not the only documented source of methane gas in aquifers. Methane may be formed by microbially enhanced and/or chemical decomposition of carbonaceous constituents in shales, sandstones, and coal stringers within an aquifer. The necessary carbon can also be introduced by the meteoric waters providing recharge to the aquifer and can come from natural sources or those generated by man, such as agricultural or feedlot drainage. In addition, there can also be generation of methane in other "wet" formations below the aquifer contributing to the methane found in the main aquifer body after gravity driven vertical migration as would be the case with migration from hydrocarbon-bearing formations at greater depth.

Liquid hydrocarbons and natural gas are both formed almost entirely through the decomposition of organic material. As mentioned previously, when this decomposition occurs in a deeply buried formation, the hydrocarbons can migrate upward, driven by a gravity differential, from the stratigraphic member where they were formed until an impermeable barrier halts their movement. When coal is the source deposit, however, we have a notable exception to such a migration scenario. Methane gas formed in intermediate ranks of coal adsorbs onto the coal matrix surfaces. Due to the fact that coal has a very high surface area to volume ratio, a significant trapped resource can exist when the surface area is completely covered. Therefore, coal can be

considered both the source rock and the reservoir. Particularly important in the following discussions is that this explains how coal can be a reservoir without an impermeable upper barrier (caprock) as is usually the case for a hydrocarbon reservoir.

Organic decomposition that results in the production of methane, or other hydrocarbons, is of two types: biogenic and thermogenic. Biogenic gas is that generated through microbial action,[2,5,6,12] while thermogenic gas generation is through the combination of heat and pressure exerted on the source organic materials over long time periods.[2,6,12] These two processes create gases with different chemical and molecular structures and therefore provide a method for identification of the origin of the gas. However, there exists an overlap region of the identifying characteristics which can cloud the exactitude of identification. In general, lower rank coals produce biogenic coal and higher rank coals produce thermogenically. Because depth of burial and meteoric water influx override and/or supplement other factors in gas generation, biogenic gases can be present in any coal rank.[12] In fact, surface prospecting for gas has been shown to be deficient in many cases due to the presence of biogenic gases of recent, non-petroleum origin emanating from shallow sediments and soils in the region being evaluated. Methane derived from oil or thermal gas will likely be overwhelmed by the biogenic components existing in the retrieved sample. In order to identify any thermally generated methane, carbon isotope determinations, as discussed shortly, are the only means of analysis available.

There are three methods for identifying a particular produced gas origin. The three methods are: *wetness*, the relationship of methane molecules to heavier hydrocarbons (C_1/C_1–C_5); *isotopic composition*, where methane $\partial^{13}C_1$ values are measured, which range from –90‰ to –16.8‰ and carbon dioxide values range from –26.6‰ to +18.6‰; and the *chemical mixture* of major non–hydrocarbon constituents.[12]

Gas wetness, or dryness, is usually gauged as follows:[7]

Dryness	C_1/C_1–C_5
Very Dry	>0.99
Dry	0.94–0.99
Wet	0.86–0.94
Very Wet	<0.86

Thermogenic gas becomes chemically drier with increasing maturity while the dryness of biogenic gas depends upon associated chemicals. In the northern overpressured region of the San Juan Basin, the gas is dry to very dry and was initially identified as purely thermogenic.[1,6,7,8] Biogenic gas generated by carbonate reduction and/or acetate dissimilation can, however, produce both chemically very dry gas and isotopically heavy bicarbonate. Likewise, bacterial alteration of chemically wet gas can remove nearly all of the heavier gas components.[7] There has been sufficient chemical evidence gathered and analyzed in that northern overpressured region to convince several researchers that Fruitland methane is at least partly of biogenic origin.[6,7,8]

The isotopic carbon composition of a gas is the primary method used to identify biogenic or thermogenic origins. It is typically measured in *permils*, which are parts per thousand, denoted by ‰. The difference between a standard and a sample, the ∂ (delta) value, is calculated by:

$$\delta^{13}C = \left[\frac{(^{13}C/^{12}C)\text{sample}}{(^{13}C/^{12}C)\text{standard}} - 1\right] X\ 1000$$

Measured values of $\partial^{13}C_1$ for methane range from –90‰ to –16.8‰ and for carbon dioxide values range from –26.6‰ to +18.6‰. Initially it was believed that thermogenically generated gas had a signature in the range from –16.8‰ to –55.0‰ while gas in the –55.0‰ to –90.0‰ was of biogenic origin.[12] More recent investigations have shown that biogenic gas can exhibit a signature ranging from –40.0‰ to –90.0‰, which means that an overlap region exists between –40.0‰ to –55.0‰, where the gas may be biogenic, thermogenic, or a combination of the two.[6,7,8] Methane $\partial^{13}C_1$ values of gas decrease with increasing thermal maturity. In the San Juan Basin, Fruitland methane $\partial^{13}C_1$ values remain relatively constant between –41.0‰ to –43.9‰, across the basin extant, despite the fact that vitrinite reflectance values, another indicator of thermal maturity, increase from 0.5 to 1.5 percent. These reflectance values indicate variance in thermal maturity unless the process of thermogenic gas generation from coal differs from that of other sources, a situation that does not seem apparent or likely. From the relatively constant $\partial^{13}C_1$ values observed, it can then be inferred that the gases in that region are at least partially biogenic.[6,7,8]

The primary determinators of hydrocarbon gas composition are coal rank and maceral composition, depth and temperature, basin hydrodynamics, and, most importantly, the abundance of hydrogen–rich organic material. Thermogenic gas production will not yield substantial quantities at temperatures below approximately 212°F (100°C).[2] These conditions are met in the Fruitland Formation of the San Juan Basin and in other regions exhibiting similar gas migration occurrences, such as the Fox Hills Aquifer in the Denver Basin.

The relationship between coalbed depth and gas composition is stronger than the relationship between composition and coal rank. Biogenic gas is formed during two different stages of coalbed development. Early stage gases form quickly during the early burial history of low ranked coals. As the coal undergoes transformation from peat to the rank of subbituminous, these early stage gases form. If rapid sedimentation occurs some of this gas may be trapped, but it usually diffuses before larger scale hydrocarbon development begins.[12] Late stage biogenic gases, formed in conjunction with shallow depth and low temperature anoxic conditions, are generated if the aquifer groundwater provides a favorable nutrient environment the microbial activity.[12] Biogenic gas may be generated by coal of any rank at shallow depths and low temperatures when the coal has associated groundwater flow supplying the nutrients necessary to support microbial activity, as exists in the Fruitland formation.[12] Shallow coals also tend to contain isotopically lighter methane relative to deeper coal beds. This is interpreted as the result of original gas being altered by secondary processes, such as microbial degradation and oxidation of wet gas components, along with mixing of older gases with younger biogenic gas.[13]

METHANE DESORPTION

The production or mobilization of methane from coal seams is a complex process and several interrelated mechanisms occur.[15] The coal seam is a dual porosity medium consisting of a solid matrix, containing micropores and a natural fracture system, known as cleats. Prior to production, gas saturated water occupies the cleats, while the bulk of the gas remains adsorbed to the walls of the matrix micropores. As water moves through the coalbed the entrained gas moves with it. Newly introduced water, moving along the hydrologic gradient, becomes saturated as it contacts the coal and gas desorbs due to the concentration gradient.

The coal itself is said to be saturated with methane when all surfaces have methane adsorbed to them. The degree of saturation varies with pressure and, within limits, higher pressure allows more saturation and lowering the pressure desorbs gas to the new lower saturation limit. If the coal is generating methane at a given time, a pressure increase will result which will allow additional adsorption storage. When an operator drills a well into a coal seam and water production ensues, or when the water column in hydrologic contact with the coalbed has a lowered water level, the reservoir pressure, that pressure holding the adsorbed methane in place on the coal matrix surface, will be reduced and gas will begin to desorb from the micropore walls. A concentration and pressure differential results between the gas in the matrix and in the cleats. The gas then diffuses through the pores into the cleat system and into the water. It will then move with the water as it flows and/or will move upward due to the gravity gradient.[15] If there is enough methane to be released by this depressuring, economic gas production may be sustained. In the case of a lowered aquifer pressure (head), the methane may find its way along fractures or bed boundaries until it contacts an impermeable barrier and is trapped or it may reach the surface by percolating upward through naturally permeable strata, along natural fissures, or through wellbores drilled into the aquifer.

DENVER JULESBERG BASIN

The Denver-Julesberg Basin is located in northeastern Colorado and is a major producer of both natural gas and liquid hydrocarbons. The geologic formations are consistent over most of the basin and extensive drilling and logging have provided the data for regional mapping. The Fox Hills Aquifer, more correctly termed the Laramie–Fox Hills aquifer, is the lowest of four bed rock aquifers in the Denver Basin. It consists of the cretaceous Fox Hills Sandstone, the lower part of the overlying cretaceous Laramie Formation and in some places the upper 100 to 200 feet of the underlying Pierre Shale. The Fox Hills Sandstone is predominantly sandstone with some siltstone and a few shale beds. The lower part of the Laramie Formation is sandstone, interbedded with some siltstone and shale. The included portions of the Pierre Shale are layers of coarse grained shale. The overall thickness of the aquifer is from 200 to 300 feet. The upper confining unit is the upper portion of the Laramie Formation which is 400 to 500 feet of mostly shale, interbedded with coal and some siltstone and sandstone. The lower confining unit, all or the bulk of the Pierre Shale in a given area, is a tight marine shale exceeding 5,000 feet in thickness. The Laramie–Fox Hills is considered a confined aquifer due to the very low permeabilities of the upper and lower confining units.[12]

In investigating the occurrence and origin of methane–rich gas in the Southern part of Weld County, Colorado, carbon isotope ratios were chosen as the best method to determine the origin of the gas. In this area the Laramie–Fox Hills aquifer is present at depths of about 500 feet (150 m) or less with the tight sandstone reservoir of the Wattenberg Field located at depths of 7500 feet to 8500 feet (2300 m to 2600 m). Gas formed at or below this depth which migrates upward to the sandstone will be thermogenic due to depth. Gas formed stratigraphically higher in the aquifer will be biogenic due to the shallow depth of burial and the microbial action associated with groundwater recharge. Gas samples tested from three producing gas wells confirmed that the reservoir gas is thermogenic, with $\partial^{13}C_1$ values ranging from –43.1‰ to –43.5‰. Methane samples from the water wells in the area showed values ranging from –72.8‰ to –73.5‰. This isotopic difference clearly differentiates the origins of free gas and led the authors of the study to conclude that the methane in the aquifer is biogenerated in the aquifer environment by decomposition of organic matter deposited in the matrix.[2,11]

Drillers sinking wells for deep gas and oil in the basin are very aware that safety precautions have to be taken when drilling through some of the aquifer bodies due to the possibility of significant methane levels. The methane encountered is probably from both desorbed gas, as the aquifer pressure is drawn down with increased use, and by more recent biogenically generated methane. In analyzing another surface seep at La Salle, Colorado, however, the gas was determined to be thermogenic, originating from the hydrocarbon bearing formations thousands of feet below. It was believed that deep abandoned water wells located nearby provided the pressure differential and the travel conduit for gas migration.[2] These investigations and others in this area are relatively straightforward because of the regional consistency of the formations, the confined configuration of the aquifer form above and below, and the distinct difference in isotopic signatures of the gases encountered. That is not necessarily the case in the San Juan Basin.

SAN JUAN BASIN

Located primarily in northwestern New Mexico with the northern tip of the basin in southwest Colorado, this area has been the site of significant coalbed development since the late 1980's. Several water wells in the northern part of the basin, where most of gas production and development has been located, have been shown to be contaminated with methane gas. Some residents of La Plata County, Colorado, have filed a lawsuit seeking to assign the blame to the oil companies, while the oil companies and the BLM have claimed natural seeps could, and most likely are, the culprit.[14] The major point of contention is whether the methane in the water wells is there as a result of poor well design, completion, and maintenance by the oil companies or through natural migration of the methane from the basin or by methane which is generated within the specific aquifer itself. Resource company studies indicate the well integrity is being maintained and raise questions as to whether the gas "contaminating" the aquifers is coming from the dominant producing horizon, the Fruitland Coal.

In the cretaceous and younger portion of the basin, every formation except the Mancos Shale and the Lewis Shale is defined as an aquifer and contains water wells for domestic and/or stock use.[10] Regional groundwater flow is recharged in high outcrop areas and flows toward lower areas of the basin (Figure 4). Along the northern and northeastern portion of the basin the recharge occurs in Colorado, some of which comes from San Juan Mountains snowmelt. Primary flow is through the formation from the higher meteoric water recharge area to the lower discharge areas in the South. Inter-aquifer leakage is part of the groundwater flow system and is primarily driven by pressure differentials.

In general the rate of inter-aquifer leakage is low. Exceptions include highly fractured areas, fault zones, and those regions along igneous intrusions.[1,10] The aforementioned shale beds, along with the Pictured Cliffs Sandstone and the Kirtland Shale/Fruitland Coal are considered the confining beds for the aquifers. The Pictured Cliffs Sandstone is also considered a tight aquifer and supplies water for a few stock wells. The Kirtland Shale and the Fruitland Formation are considered to be one aquifer because their hydrologic characteristics are so similar. All of the formations above the Kirtland Shale are much more permeable and the region is devoid of any blanket confining formation.[1,10] The Kirtland/Fruitland aquifer is currently used for a few stock wells but is believed in at least one study to have the highest hydraulic potential of any aquifer within the system.[1] This potential exists only in the north and central portions of the basin and coincide with the high

pressured area of the Fruitland Formation. It is critically important to note that the Fruitland formation is divided into overpressured and underpressured zones. The presence of an impermeable barrier or permeability discontinuity within the Fruitland is therefore strongly inferred.[5,8] This barrier interrupts the flow of the Fruitland water from the high areas of recharge to the lower elevation discharge zones at the Southern Outcrop and, with tight sandstone located below, forces the water to flow upward into the aquifers above (Figure 3).[1,8] Fruitland formation waters discharge into the tertiary sandstones and into five perennial rivers that cross the formation outcrop.[1,3]

When coalbeds generate methane, only part of the gas is adsorbed onto the coal. the rest is released into the cleat system. If a relatively impervious cap rock exists, a pressurized free gas reservoir forms. If a migration route exists, the gas will move stratigraphically upwards to another trap or to the atmosphere.[4] When water flows through the Fruitland Formation it provides an avenue for dissolved solution gas and free gas to flow upward. The Kirtland Shale also contains coal in its lower portions and carbonaceous shale throughout. The Ojo Alamo is partly shale and the Nacimiento and San Jose Formations are partially carbonaceous mudstone.[10] Most shale and all carbonaceous material (when in an environment of aquifer flow including meteoric water recharge have the capability to generate methane. Drilling logs have recorded gas shows in the Animas, Nacimiento, Ojo Alamo, and Kirtland Formations. Gas producing wells have been completed in the Kirtland , Animas, and Nacimiento formations.[2,9] With this evidence it is well established that gas permeates all of the formations above Pictured Cliffs formation. A USGS unconventional reservoir study by the Branch of Petroleum Geology classified the San Juan Basin as a *continuous gas area* where any well drilled will encounter natural gas to some degree. The only question is whether commercial quantities will be found.

Despite the preponderance of evidence contradicting such a conclusion, a recent United States Geological Survey report stated that incompetent gas wellbores were the only probable path by which gas can migrate to the surface.[2] This statement has been hotly disputed by the industry, by other groups within the USGS and by the authors of this paper. With the known presence of basin wide fractures, the existence of a mechanism for aquifer recharge and mobilization into the regions of recorded seeps, the carbon isotopic signature data from other researchers, the history of seeps in the basin and the lack of a true cap rock, it would appear that such conclusions are extremely tenuous and premature, at best. The fact that a well might be a conduit as suggested is unproved, but not impossible.

The fact is that other evidence, some even addressed in a cursory manner, and discarded, in the USGS report, suggest mechanisms that are more likely to be the mechanism of contamination, particularly considering historical evidence of methane seeps in the area of concern. This historic data has not, unfortunately, been as well documented as it should have been over the years of Basin exploration and development. However, legal depositions have been gathered, on behalf of the operators and landowners, by attorneys in the Durango area that point strongly to the existence of the same type of seeps and "contamination" before development took place.

The major recharge of the valley fill alluvium is from irrigation water. Human activities, such as fertilization of agricultural lands, could cause an increase in microbial methane generation by the addition of higher nutrient concentrations. This would tend to show up in analyses, indicated by an increased younger and non-thermogenic gas signature component. In an area where methane releases toward the atmosphere there will be a large active population of methane consuming microbes in the vadose zone and the upper reaches of the water table.[16] These microbial populations will form a barrier to upward migration of methane, preventing release into the atmosphere. Shallow soil sampling in areas above such a barrier will result in a "no methane seepage" conclusion. Only areas with a large volume flow would penetrate to the surface unless something caused the demise of the indigenous microbe population. The application of pesticides washed down through the vadose zone could easily cause the death of the insulating barrier of microbes and a resultant detectable seep, providing another potential cause of such occurrences. Despite the obvious incompatibility of these two arguments, either is possible under a given set of conditions.

In the region of greatest concern, or at least that generating the most discourse, methane has been found in an increasing number of water wells. This Pine River Fruitland Outcrop region is located at the Northern Outcrop where aquifer recharge occurs, as shown in Figure 3. Meteoric recharge of the aquifer takes place through the Pine River drainage system at the north end of the Basin. Bacteria carried by these waters are believed to metabolize the wet gas components and existing n-alkanes to produce secondary biogenic gases as the water flows down structure towards the south. The isotopic signatures of gases sampled from water and coal gas wells in the Pine River region indicate a higher biogenic component than do gases from further south and deeper in the basin. The coal gas wells have a stronger biogenic signature (from roughly -49.8‰ to -45.6‰) than the more southern coal gas wells (approximately -43‰). All but one of these wells have isotopic signatures below the -47‰ mark. The water wells have an even stronger biogenic signature than the northern coal gas wells, ranging from -56.85‰ to -47.12‰, with the majority having values below -50‰. In this region, the sands are highly permeable, exceeding one darcy to a depth of over a mile. This accounts for the recharge capability of the region. It is also through this highly permeable portion of the basin structure that the major gas seepage of concern is taking place.

Additionally, at a mid point in the basin, a permeability barrier exists structurally which causes the waters to be diverted upward, charging the Kirtland Shale and moving through fractures into formations further up-structure, and potentially through to the surface or into water well boreholes. This area of the basin exhibits highly fractured characteristics and the permeability in the upper zones is high compared with formations located structurally below in the basin. This is the second area of major gas seepage concerns, located near Aztec, New Mexico in the region of Kiffin Canyon. Kiffin Canyon is an area where perennial spring-fed water flows through a canyon at a higher elevation than the San Juan River Valley below. The canyon is heavily populated with gas wells and indications of fractures intersecting the surface. There is an extended region of gas seeps following the canyon floor with significant variance in volume at any given location over time. The State of New Mexico has required competence testing of all wells in the area with no evidence of leakage found. It is believed that these seeps were in existence before development occurred, although there are some who dispute that fact.

The amount of gas released and/or migrating upward with mobile water is directly dependent on the hydraulic head exerting pressure on the formations and fluids below. Just as the dewatering of coal seams causes the release of adsorbed methane due to an induced pressure differential, the reduction of hydraulic head, which is pressure, on the aquifers nearer the surface will cause more gas to be released from solution in the aquifer waters and will allow an increase in migration of waters originating deeper in the structure. Considering the fractured matrix existing in the area and the evidence of probable biogenic gas generation at shallow and deeper depths, the likelihood of increased gas release from shallow aquifers and increased deep waters migration is significant with increased utilization of the water resource for surface uses. It should be noted that the depressurization of a finite wellbore area to allow produced gas

flow will not necessarily result in increased vertical migration away from the wellbore. That action takes place because of a reduction in the hydraulic head above the producing formation. The two situations are not necessarily interrelated.

There is an ongoing study and a "repressurization" effort going on as a result of the Pine River Fruitland Coal Outcrop Investigative Team. This effort focuses on repressuring the coal seams in order to reduce desorption and to attempt to force the equilibrium sorption levels in the other direction, increasing the methane levels in the coals. The results of this effort are being viewed with great interest. Again, repressuring of the aquifers collectively providing the hydraulic head in a given area would inhibit vertical migration and/or release of water and gas. However, repressurization of the productive aquifer zone below has the potential to increase the pressure differential between deep and shallow zones and thereby increasing vertical gas migration. Additionally, increased untreated water flow may accelerate biogenic gas formation, or at least its migration deeper into the basin.

SUMMARY

1. There is no true blanket cap rock above the Fruitland Formation and the Pictured Cliffs Sandstone in the San Juan Basin system. This would allow gas released from the associated aquifer to migrate upwards along permeability streaks, fissures, or through natural percolation through the strata due to the gravity differential. There is ample evidence that a constant natural flow of water rises from the Fruitland/Kirtland Aquifer into the uncapped Tertiary formations above. This water will be methane saturated from residence within the Fruitland/Kirtland Aquifer.

2. Biogenic methane could be generated in any of the formations above the Fruitland Formation due to the carbon content in carbonaceous deposits therein and the influx of meteoric waters from the Northern Outcrop recharge zone. It could then migrate upwards further south due to the absence of any blanketing cap rock. The burial depth is shallow enough to support biogenic generation.

3. Continuous upward flow into the vadose zone of methane generated below can cause microbial populations to form a natural barrier between methane seepage and the surface. Soil testing in the vadose zone would not then show methane contamination.

4. There is an abundance of information to support the contention that the gas releases in the San Juan are predominantly from natural sources and do not require any human activity for them to occur. There has been a (poorly) documented history of gas seeps in the basin and, in fact, this was one of the reasons for initial exploration. There is conflicting documentation as to the sources of the methane, but most of what is presented to support the contention that the gas seeps are due to reservoir development activity are fairly easily argued against and appear possibly premeditated in their conclusions.

5. Human activity other than oil and gas operations could be the cause of some methane release. Drawdown of the aquifer head can cause desorption and a pressure differential driven migration of methane. The major recharge to the groundwater is from irrigation drainage. Irrigation waters can provide nutrients necessary to enhance biogenic methane generation, or they can contain substances harmful to methane consuming microbes that might have been a stable barrier to methane migration.

CONCLUSIONS

Research into the cause(s) of methane presence in surface aquifers is far from sufficient for finger pointing. A primary need is to develop a better historical record of seeps in the area and to try to correlate them with known hydrologic flows within the basin. The presence and impact of both major and minor permeability barriers or discontinuities in the basin sediments must be defined, as well as the hydraulic pressure differentials that exist and are being altered by production through wellbores and surface use of aquifer waters. When this is accomplished, a better understanding of the parameters affecting gas migration and release in local areas and basin-wide will be realized.

ACKNOWLEDGEMENTS

This research was supported by the United States Environmental Protection Agency's Oil & Gas Division of the Office of Solid Waste through Grant #X-820444-01-0, made through the Petroleum Engineering Department at the Colorado School of Mines.

REFERENCES

1. McCord, J. P.: Hydrogeology of a Fruitland Formation Aquifer, San Juan Basin – New Mexico and Colorado, with Emphasis on Using Temperature Distribution Data to Estimate Lateral Groundwater Velocity, Master of Science Thesis, New Mexico Institute of Mining and Technology, 1988.

2. Chafin, D. T.: "Sources and Migration Pathways of Natural Gas in Near– Surface Ground Water Beneath the Animas River Valley, Colorado and New Mexico," Water–Resources Investigations Report 94–4006, U.S. Geological Survey with the Cooperation of Colorado Oil and Gas Conversation Commission, La Plata County, and the Southern Ute Tribal Council, 1994.

3. Oldaker, P. R.: "Hydrogeology of the Fruitland Formation, San Juan Basin, Colorado and New Mexico," Coalbed Methane of Western North America, Rocky Mountain Association of Geologists Fall Conference, Glenwood Springs, Colorado, September 17–20, 1991.

4. Century, J. R.: "Structural Controls on Coalbed Methane in the San Juan and Western Canada Sedimentary Basins," Coalbed Methane of Western North America, Rocky Mountain Association of Geologists Fall Conference, Glenwood Springs, Colorado, September 17–20, 1991.

5. Kaiser, W. R.: "Abnormal Pressure in Coal Basins of the Western United States," paper 9333, presented at the International Coalbed Methane Symposium, Birmingham, Alabama, May 17–21, 1993.

6. Scott, A. R.: "Composition and Origin of Coalbed Gases from Selected Basins in the United States," paper 9370, presented at the International Coalbed Methane Symposium, Birmingham, Alabama, May 17–21, 1993.

7. Scott, A. R., Kaiser, W. R., Ayers, W. B.: "Composition, Distribution, and Origin of Fruitland Formation and Pictured Cliffs Sandstone Gases, San Juan Basin, Colorado and New Mexico," Coalbed Methane of Western North America, Rocky Mountain Association of Geologists Fall Conference, Glenwood Springs, Colorado, September 17–20, 1991.

8. Scott, A. R., Kaiser, W. R.: "Relation Between Basin Hydrology and Fruitland Gas Composition, San Juan Basin, Colorado and New Mexico," Quarterly Review of Methane from Coal Seams Technology, Gas Research Institute, November 1991.

9. Bureau of Land Management Report: "Bradenhead Testing and Groundwater Protection Program Overview and 1992 Test Results," Bureau of Land Management San Juan Resource, April 28, 1993.

10. Stone, W. J., Lyford, F. P., Frenzel, P. F., Mizell, N. H., Padgett, E. T.: "Hydrogeology and Water Resources of San Juan Basin, New Mexico," New Mexico Bureau of Mines & Mineral Resources Report with United States Geological Survey and the Water Resources Division of New Mexico Natural Resources Department, 1983.

11. Rice, D. D., Threlkeld, C. N.: "Occurrence and Origin of Natural Gas in Ground Water, Southern Weld County, Colorado," United States Geological Survey Open File Report 82–496, 1982.

12. Rice, D. D., 1993: "Controls of Coalbed Gas Composition," paper 9394 Presented at the International Coalbed Methane Symposium, Birmingham, Alabama, May 17–21, 1993.

13. Banta, E. R.: "Hydrologic Effects of Pumpage from the Denver Basin Bedrock Aquifers of Northern El Paso County, Colorado," United States Geological Survey, Water–Resources Investigations Report 88–4033, with the City of Colorado Springs, 1989.

14. Wright, K.: "Fouled Water Leads to Court: High Country News," April 19, 1993.

15. Gray, I.: "Reservoir Engineering in Coal Seams: Part 1 – The Physical Process of Gas Storage and Movement in Coal Seams," SPE Reservoir Engineering, February 1987.

16. Waples, D. W.: Geochemistry in Petroleum Exploration, IHRDC, Boston, MA, 1985.

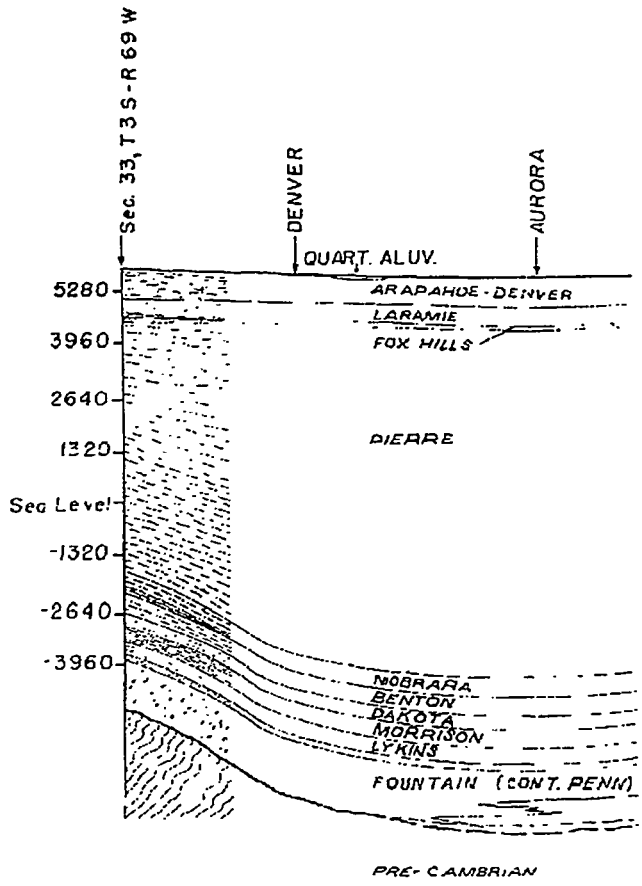


Figure 1. East-West cross-section of the Denver Basin through the City of Denver, File Map, CSM Library

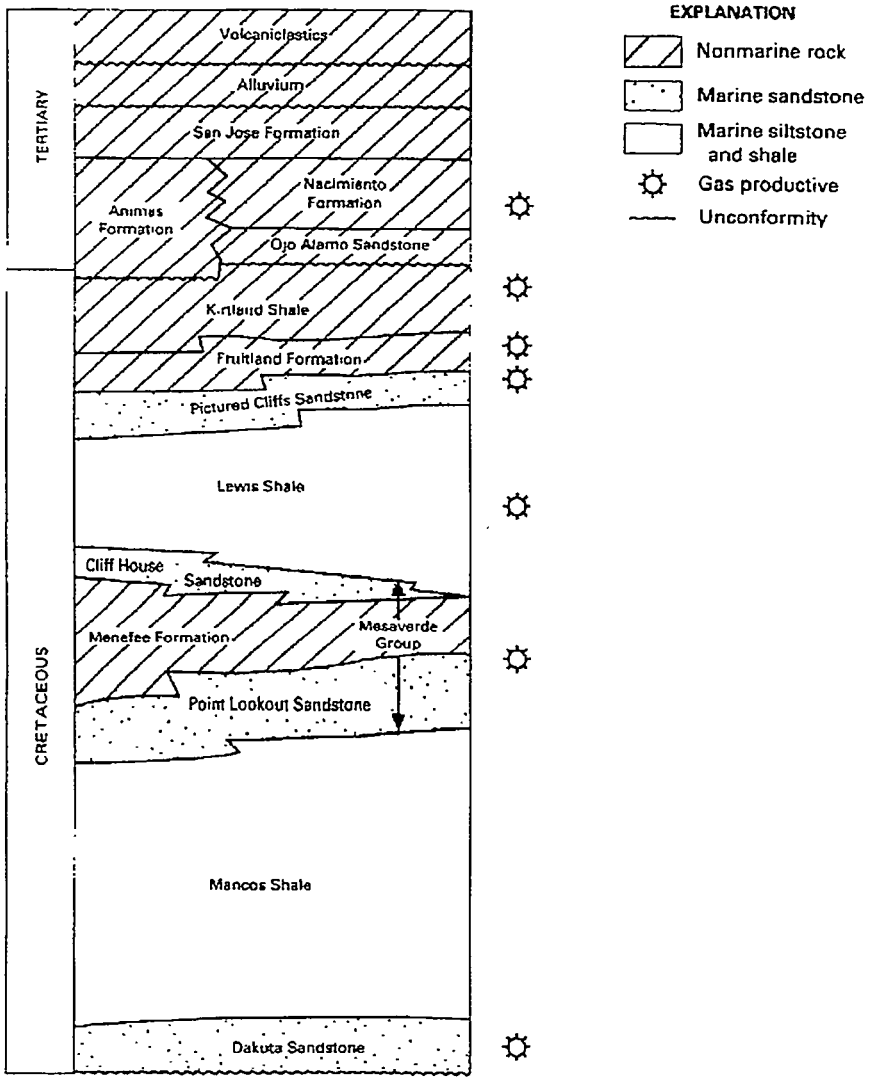


Figure 2. Sedimentary cross-section beneath the Animas River Valley, Colorado and New Mexico, modified from Chafin[2]

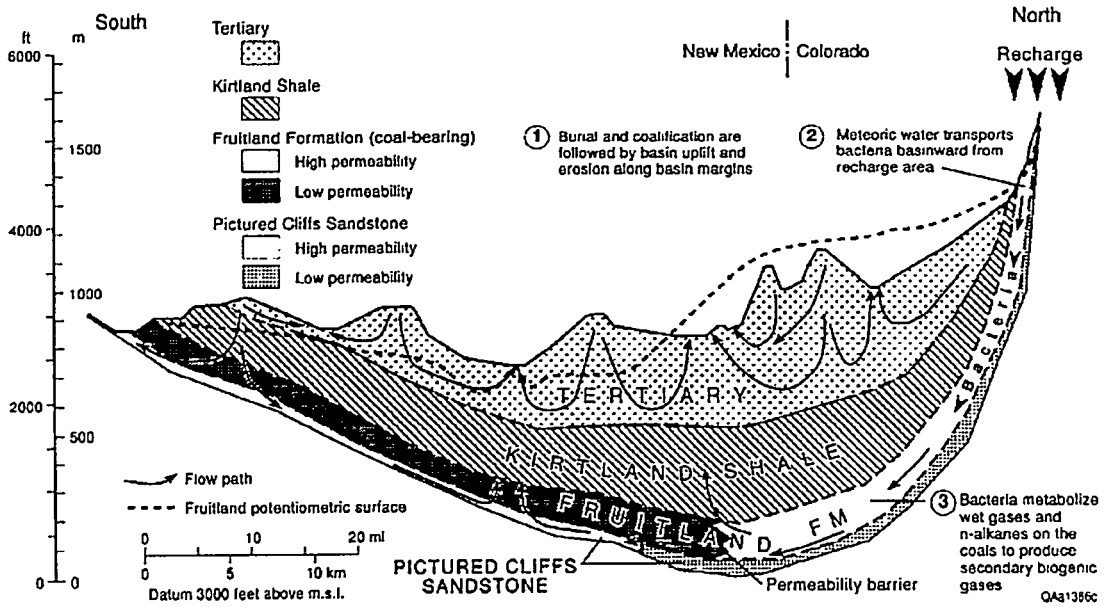


Figure 3. Schematic cross-section showing groundwater flow and generation of secondary biogenic gases in the San Juan Basin.[6]

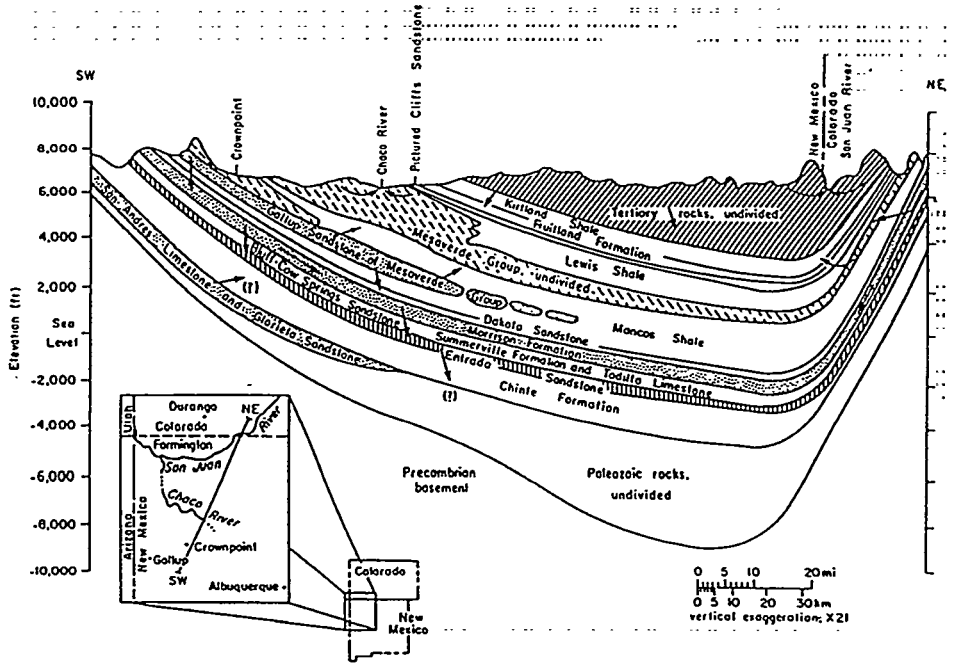


Figure 4. Generalized hydrogeologic cross-section of the San Juan Basin showing major aquifers and directions of flow.[10]



NOTES

INTERGAS '95

May 15-19, 1995
The University of Alabama
Tuscaloosa, Alabama USA

9535

Secondary Mineralisation and Its Effect on Coal Permeability

P.J. Tarabbia, J.K. Warren, West Australia Centre for Petroleum Exploration, Curtin University; and P.D. Gamson, CSIRO Australia

ABSTRACT

Secondary mineralisation infilling cleat and fracture systems of Australian Hunter Valley Coalfield coals is believed to be a major impediment to permeability and therefore the successful recovery of coalseam methane. Given this problem, a program of research was initiated to understand the nature, distribution and diagenetic sequence of secondary mineralisation in coals and the effect of mineralisation on permeability. Epigenetic Fe-Mg-Ca carbonates, Sr-Ba-Ca carbonates, dawsonite, quartz, pyrite and kaolinite were identified as the major diagenetic cements. This assemblage of minerals precipitated in cleats and fractures as a function of the depletion of anions within an evolving fluid in a closed hydrological system. Other localised sources of secondary minerals from open hydrological systems include: anions imported into the sequence by active mass transport, or devolatilisation of plutonic intrusions. Knowledge of diagenetic cement emplacement specific to the coals of the Hunter Valley will allow targeting of coals with either 1) lesser amounts of mineralisation or 2) mineral fills suitable for stimulation such as acid leaching.

INTRODUCTION

This paper contains results from an ongoing study of pervasive secondary mineralisation within Permian coals from the Hunter Valley Coalfield (HVC).

The HVC (approximately 2100 square kilometres) is one of Australia's largest coal producing districts with "in-situ" coal reserves exceeding 22.6 billion (10^9) tonnes [1]. The area includes potential coalseam methane production reserves of a trillion cubic feet.

The HVC (Figure 1), on the north-eastern periphery of the Sydney Basin is bound to the north-east by the Hunter Thrust, a large reverse fault thrusting Carboniferous rocks south and east over Permian sediments of the HVC. Migration of the thrust front into the coalfield is responsible for propagated splay faults and folding en echelon proximal coal strata with their axes parallel to the thrust. Faulting and folding imposed by the thrust were generated by the southward and westward compression of the Sydney Basin by the rocks of the New England Orogen in a NNW-SSE dextral shear couple [2]. Thrusting ceased in the Triassic. The HVC is bounded to the south-west by a scarp of Triassic sediments and separated from coalfields to the west by the Lochinvar Anticline.

The HVC is dominated by rocks of Permo-Triassic age deposited in an island arc retroarc basin setting [3]. Sedimentation was eustatically and tectonically controlled [4]. Permian sediments in the HVC were sourced mainly from the NNE off the Hunter Thrust. Coal seam development, interbedded with these transported sediments constitute a large portion of the sequences deposited within the HVC. The coal measures contain abundant tuff horizons supplied from an eastern source [5].

The coal measures have undergone compaction and burial, with subsequent uplift, resulting in the exposure of some bituminous rank coals at the surface in the HVC. Fractures and cleats within the coals of the HVC are the result of burial and uplift processes in the region. The HVC coals have also been intruded by Jurassic and Tertiary igneous bodies (Figure 1). Some of these intrusions caused minor folding which increased fractures within the coals.

Given that cleat and fractures within the HVC are considered the primary permeability pathway for methane transport, it is important that the distribution of secondary mineralisation within the cleat and fractures is understood. Understanding mineral emplacement will allow prediction of possible mineralisation occurences elsewhere in the Hunter Valley Coalfield. This will allow the targeting of seams with lesser amounts of mineralisation and/or selection of seams suitable for leaching stimulation.

METHODOLOGY

Sampling concentrated on rare Diamond Drill Hole (DDH) coal core within the Whybrow and Redbank Creek seams of the Jerrys Plains Subgroup (Figure 2). Five wells were sampled from the HVC (Figure 1). Table 1 displays the total distribution of samples studied as well as depth, seam name, vitrinite reflectance and cement identified. Depths of the samples collected varied from 184-554 metres with vitrinite reflectance (R_O max) of the coals ranging from 0.577 to 0.71.

Scanning Electron Microscopy (SEM)

Core samples were carefully broken by hand to expose fresh internal mineralised cleats/fractures. Small oriented portions of coal exhibiting in-situ mineralisation were then fixed to SEM stubs with araldite. The stub samples were then coated with carbon and studied using a Phillip's 505 SEM. Scanning electron microscope mineral identification was obtained using an energy dispersive (EDAX) system in combination with visual analysis of crystal morphology. The separation of ferroan dolomite and ankerite was made using relative peak height of the Fe spectrum on the EDAX system. Backscatter electron viewing of the samples was used during the identification process to help differentiate mineral phases.

X-ray diffraction (XRD)

For qualitative XRD determination the minerals in the cleats were separated from the coal using a fine pair of tweezers. They were then ground and mixed with acetone to produce a paste and then transferred to a glass slide. Sample analysis was done on a Phillips PW1700 automatic diffractometer using a Cu tube.

SECONDARY MINERALISATION

The mineralisation studied in the sampled cleats and fractures is typically authigenic. Minerals infilling the cleat/fracture system include Fe-Mg-Ca carbonates, Sr-Ba-Ca carbonates, dawsonite ($NaAl[CO_3][OH]_2$), kaolinite, quartz and pyrite.

Typically the Fe-Mg-Ca carbonates comprise 6 mineral species; siderite, ankerite, ferroan dolomite, dolomite, ferroan calcite and calcite. These carbonate cements display typical morphologies, namely, calcite "nail-head spar", scalenohedral "dog-tooth spar", and dolomite rhombohedra. These carbonates differ morphologically from the second group of carbonates, the Sr-Ba-Ca carbonate group, which comprise strontianite [$Sr\ CO_3$], witherite [$Ba\ CO_3$] and alstonite [$CaBa\ (CO_3)2$] [6]. Typically strontianite displays a unique spear-shaped morphology. In contrast witherite and Alstonite could not be identified morphologically and could only be identified using EDAX. Dawsonite is typically a fibrous to acicular diagenetic cement. Within the cleats, matting of the dawsonite crystal fibres is stronger or denser in the flow direction of the pore fluid, while acicular and splayed forms grow into voids previously devoid of mineralisation [6]. Druse quartz and pyrite are present as authigenic cements.

Emplacement of mineralisation

Given that the minerals infilling coal cleats/fractures is pervasive in the coals studied, it is important that their emplacement is understood in order to assess their possible distribution within other coal seams of the HVC.

During the emplacement of mineralisation, factors such as the amount of original void space available, pressure and temperature conditions, and the fluid chemistry interaction with the coal all influence the final product. Using a combination coal core logging and the use of SEM with EDAX and XRD, four stages of fracture/cleat evolution and mineral emplacement are recognised (Figure 3):

A) Early horizontal to sub-horizontal fractures form in susceptible intervals. These horizontal fractures are possibly produced by Fe-fixing bacteria, precipitating Fe carbonates on boundaries between the bright and dull coal. Early development of vertical fractures and cleats is the result of hydrofracturing from overpressure building in the seams (Figure 3). As fluid pressure in the seam exceeds the lithostatic pressure, fractures propagate vertically within bright or vitrinite-rich coals. These openings fill with mineralised fluid derived from the coal measures. During this early phase Fe-Mg-Ca carbonates are precipitated upon pressure relaxation within the seam. It is likely that carbonate formation would have been assisted by desorption of CO_2 from the coal. Typically mineralisation within hydrofractured cleats and fractures display no characteristic crystal morphologies. Mineralisation forms as a cast of the coal maceral banding.

B) Sequences of over-pressuring and subsequent fracturing in the coals allows fluids, still derived from the coal measures, to infiltrate. Fluids flow in earlier formed fractures and cleats which have re-opened and along newly formed fractures. As pressure falls after each phase of fracturing, precipitation of carbonates occurred. Typically there was an earlier phase comprising Fe-Mg-Ca carbonates which was followed by a later phase Sr-Ba-Ca carbonate cementation. Consequently, mineralisation within fractures and cleats display multiple precipitation events and good crystal morphology. Characteristically the dull or inertinite-rich coal still does not allow the propagation of fractures as it disperses the energy.

C) Uplift of the basin occurs. Fractures and cleats now develop as tectonic re-adjustment, not overpressuring, resulting in the warping of the coal measures. Changes in temperature, pressure and fluid chemistry now favour dawsonite development within fractures and cleats. Dawsonite either occupies late butt cleat development if it is present or cleat inter-mineralised void space that was previously devoid of mineralisation.

D) Development of large-late stage vertical fractures crosscutting previously developed fracture and cleats, possibly produced by igneous intrusions, are filled with Fe-Mg-Ca carbonates. Sr-Ba-Ca group carbonates are not observed in these fractures. Druse quartz and kaolinite are the last cements observed in the cleat and fractures.

A diagenetic sequence of the events is shown in Figure 4. Secondary mineralisation observed in HVC coals may have occurred under an open or closed hydrological system within the region.

Source of Mineralising Fluids

In a discussion of open vs closed hydrological systems for the source of mineralising fluids, it is important to examine the entire sedimentary sequence for evidence of fluid migration.

The lithiclastic sandstones within the sequence may have acted as early aquifers, allowing fluid migration of the compacting coals as they underwent coalification. The sandstones are now tightly cemented by Fe-Mg-Ca

carbonates, the first cements observed in the coals and it is proposed that the sandstones were cemented pre-fracture development in the coals. It is a well known fact that claystones or siltstones form excellent seal rocks. The coal measure sequences in the HVC are bounded by these rocks. The diagenetic sequence is also quite uniform throughout the basin with no dissolution of cements observed. Hence the process of a precipitate continuum in a hydrologically closed system within the coal sequence may explain the evolution of cements observed (Figure 5).

Under this system, minerals of the Fe-Mg-Ca group would have precipitated first as they are the first cements observed in the cleats and fractures. With the eventual depletion of these anions, the precipitation of the next group of minerals identified, namely the Sr-Ba-Ca carbonates would have occurred. As these anions were removed from the waters of the coal measures, the remaining anions would include Na, Al, K and Si. The last minerals to precipitate from the evolving pore fluid would contain these anions, resulting in the formation of dawsonite, kaolinite and quartz.

The Hunter Valley is however, too structurally and tectonically complicated for a closed system model to have operated on its own. Local pockets of mineralisation may be influenced by particular models described in Figure 6. It is believed that the bulk of the minerals were precipitated in a closed system. The resolution of open vs closed hydrological systems will be better resolved by laser ablation isotope studies of the cements that are currently under way.

IMPLICATIONS

This study has shown that for two coal seams in the Hunter Valley Coalfield, minerals commonly fill cleats and fractures. Typically these minerals tightly infill the coals and are thought to be the primary reason for the low permeability of the cleats. The diagenetic sequence of events presented for these coals suggest that local geological and hydrological factors were primary factors allowing the emplacement of various minerals, in particular carbonates. These studies of the cleat and fracture mineralogy have the potential of being able to predict and target environments with either: 1) lesser amounts of mineralisation or 2) zones suitable for leaching.

ACKNOWLEDGMENTS

The research presented in this contribution was prepared for publication while the senior author was the recipient of a fellowship from the CSIRO Division of Petroleum Resources, Glen Waverley, Victoria, Australia, and their financial support is gratefully acknowledged.

REFERENCES

1. Sniffen N., Sayers P. and Beckett J., 1987: New South Wales Coal Resources and Reserves,1986: North Sydney, New South Wales Department of Mineral Resources Publication, 136p.

2. Harrington H.J. and Korsch R.J., 1979: "Structural History and tectonics of the New England Orogen", *In* Denham D. ed.- Crust and Upper Mantle of southeast Australia,Sydney, Bureau of Mineral Resources Record 1979/2 (unpubl.).

3. Jones B.G., 1983: "Illawarra Coal Measures, Sydney Basin, NSW"; *In* Williams B.P.J. and Moore P.S. ed.- Fluvial Sedimentology Workshop, Australian Sedimentologists Specialists Group, Adelaide, South Australia, p.366-375.

4. Scheibner E., 1976: Explanatory notes on the Tectonic Map of New South Wales, scale 1:1 000 000: New South Wales Geological Survey, 283p.

5. Brownlow J.W., 1987: "The New England Connection", Proceedings of the 21st Symposium on the Advances in the Study of the Sydney Basin, University of Newcastle, New South Wales, p.179-183.

6. Tarabbia P.J., 1994: "Authigenic Sr-Ba-Ca carbonate minerals in coals of the Hunter Valley, New South Wales"; Australian Journal of Earth Sciences, 41, p.617-620.

Table 1 Cements present in cleats/fractures within coal samples of the Hunter Valley Coalfield.

Depth (m)	Sample	Seam	Ro max	Alst	Ank	Cal	Daw	Dol	F Cal	F Dol	Sid	Stro	Wit	K	Qtz	Py
184.00	WY1-3	Whybrow seam	0.702		x			x				x		x	x	
190.35	WK8-3	Whybrow seam	0.679					x						x	x	
190.80	WK8-5	Whybrow seam						x		x	x			x		
191.41	WK8-6	Whybrow seam								x	x			x		
192.33	WK8-7	Whybrow seam	0.624					x						x		
193.55	WK8-9	Whybrow seam						x				x		x	x	
238.51	WK8-14	Whybrow seam	0.71		x		x		x	x		x				
238.90	JP11-2	Whybrow seam										x		x		
240.79	WK8-16	Redbank Ck seam								x		x	x			
241.10	WK8-17	Redbank Ck seam	0.667	x		x	x			x		x	x	x		x
242.01	WK8-18	Redbank Ck seam					x			x				x		
243.84	WK8-21	Redbank Ck seam			x	x	x			x	x			x		
247.10	JP11-3	Redbank Ck seam									x			x		
247.44	JP11-4	Redbank Ck seam								x		x		x		
247.45	JP11-5	Redbank Ck seam	0.631									x		x		
247.46	JP11-6	Redbank Ck seam										x	x	x		
248.56	WK8-25B	Redbank Ck seam			x		x			x		x	x	x		
248.72	WK8-25C	Redbank Ck seam		x			x			x		x	x	x		
249.00	WY1-13	Redbank Ck seam			x		x	x	x	x	x	x	x	x		
354.63	DC9-2	Redbank Ck seam		x			x					x		x		
356.01	DC9-3	Redbank Ck seam			x									x		
357.23	DC9-4	Redbank Ck seam		x	x						x			x	x	
547.20	WY2-2	Redbank Ck seam	0.577					x		x				x		
554.80	WY2-5	Redbank Ck seam	0.62			x		x		x		x	x	x		

Alst=Alstonite; Ank=Ankerite; Cal=Calcite; Daw=Dawsonite; Dol= Dolomite; F Cal=Ferroan Calcite; F Dol=Ferroan Dolomite; Sid=Siderite; Stro=Strontianite; Wit=Witherite; K=Kaolinite; Qtz=Quartz; Py=Pyrite.

Sample name made up of well and coal sample eg WK8-21=Warkworth DDH8-coal sample 21

X represents cement identified within cleat/fractures.

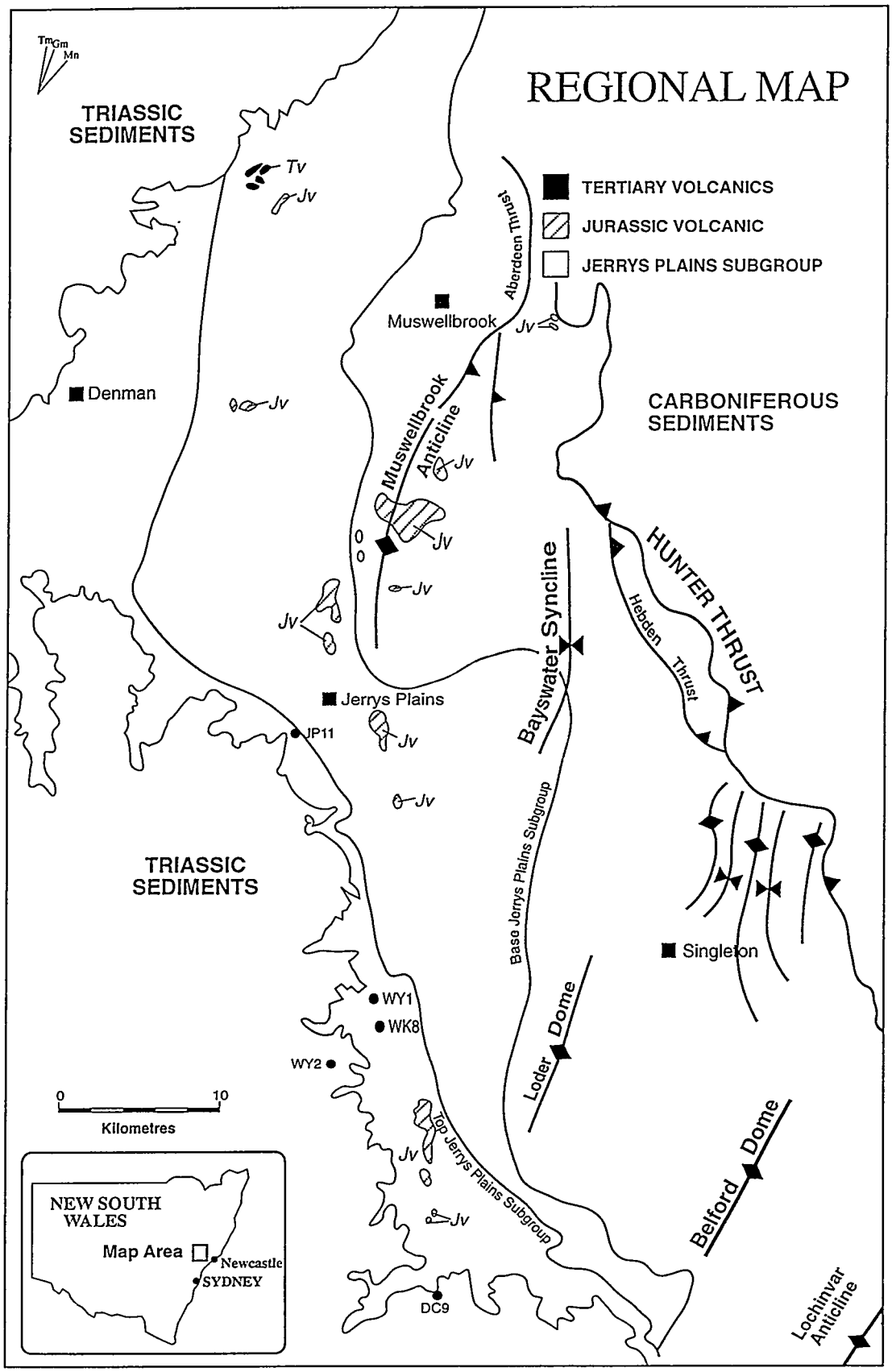


Figure 1 - Regional map displaying the outcrop of the Jerrys Plains subgroup in the Hunter Valley Coalfield, the surface exposure of igneous intrusions, several structural features and the well locations.
Note: The coal measures dip to the SW beneath the Triassic sediments. JP11=Jerrys Plains DDH11; WY1=Whybrow DDH1; WY2=Whybrow DDH2; WK8=Warkworth DDH8; DC9=Doyles Creek DDH9.

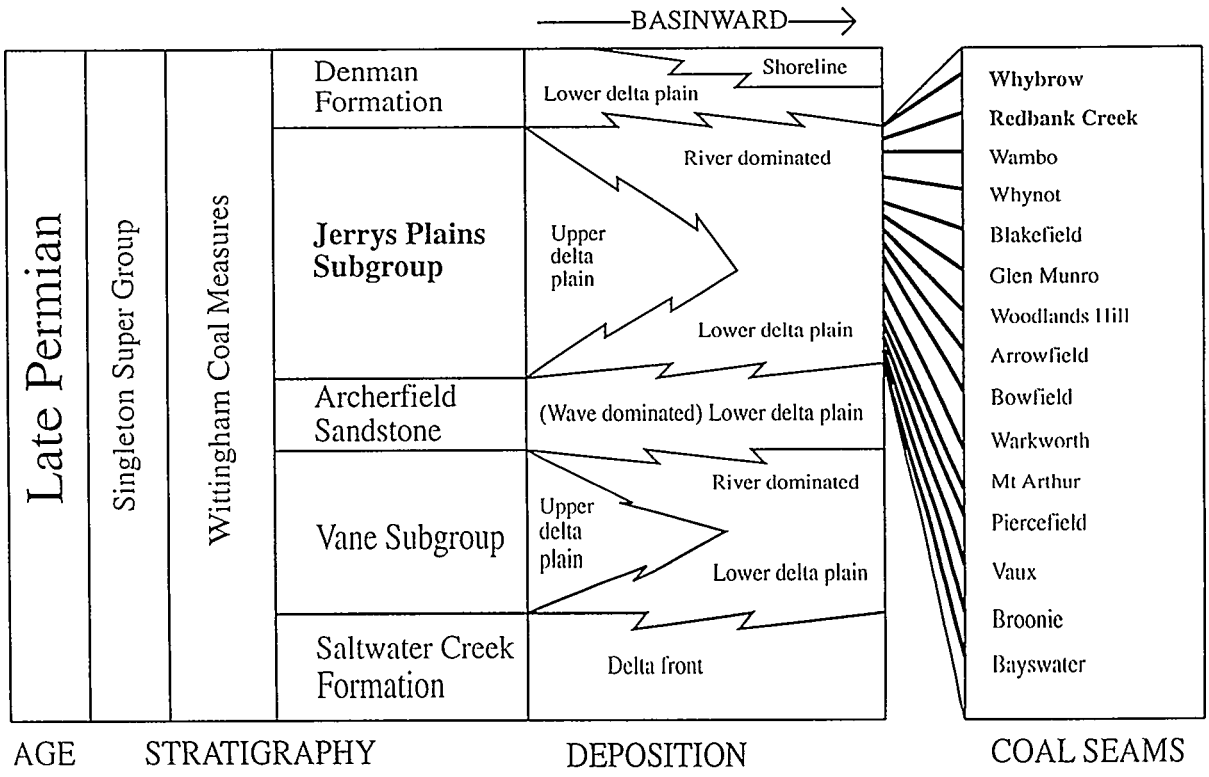


Figure 2 - Stratigraphy, depositional environments and coal seams of the Hunter Valley Coalfield.

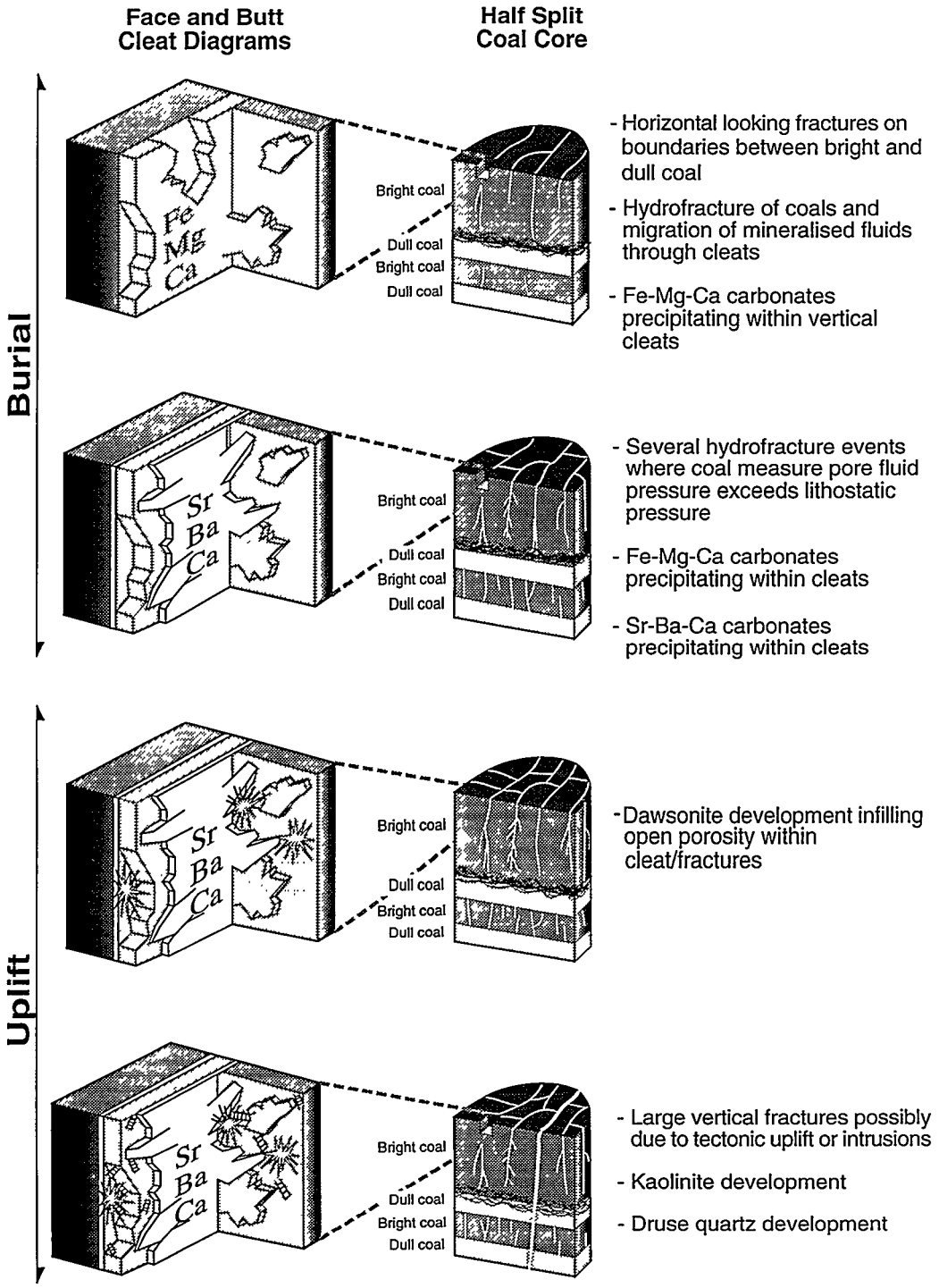


Figure 3 - Fracture/cleat evolution stages observed in coals of the Hunter Valley Coalfield. Note: Core diagrams are based on visual observations.

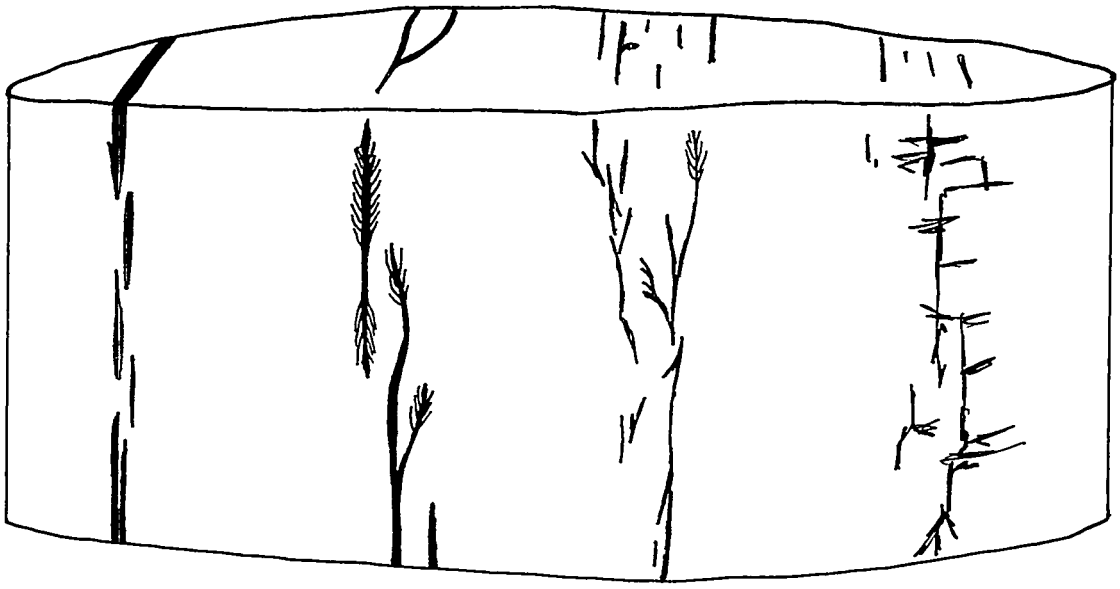


Figure 4 - Diagrammatic representation of observed hydrofracture of coal core. Note: Fine hair-like branching of fractures and en-echelon development.

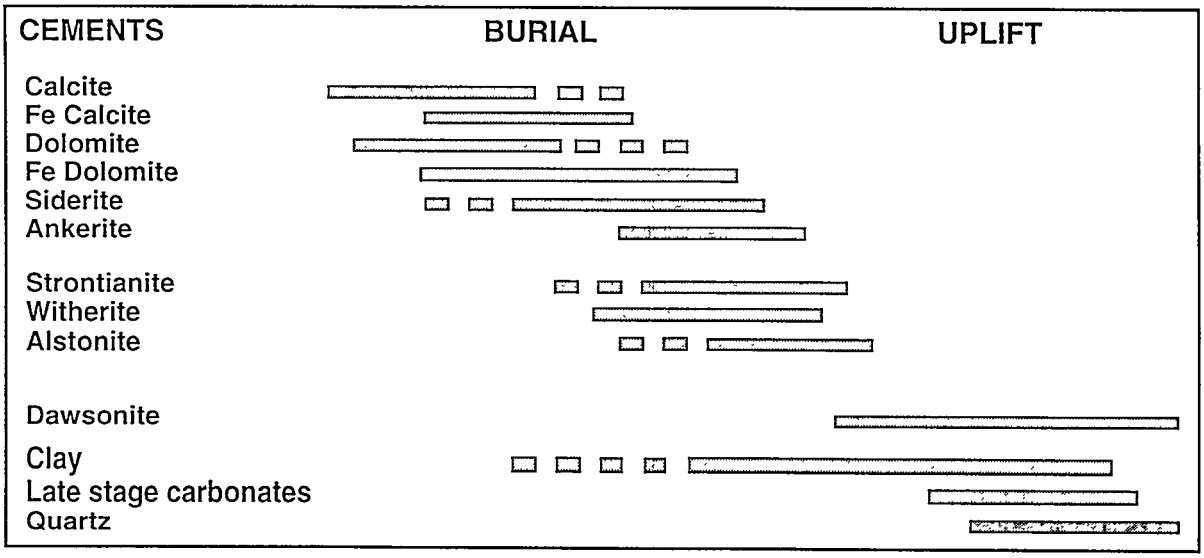


Figure 5 - Diagenetic profile of mineralisation found in cleats and fractures of Hunter Valley Coalfield coals.

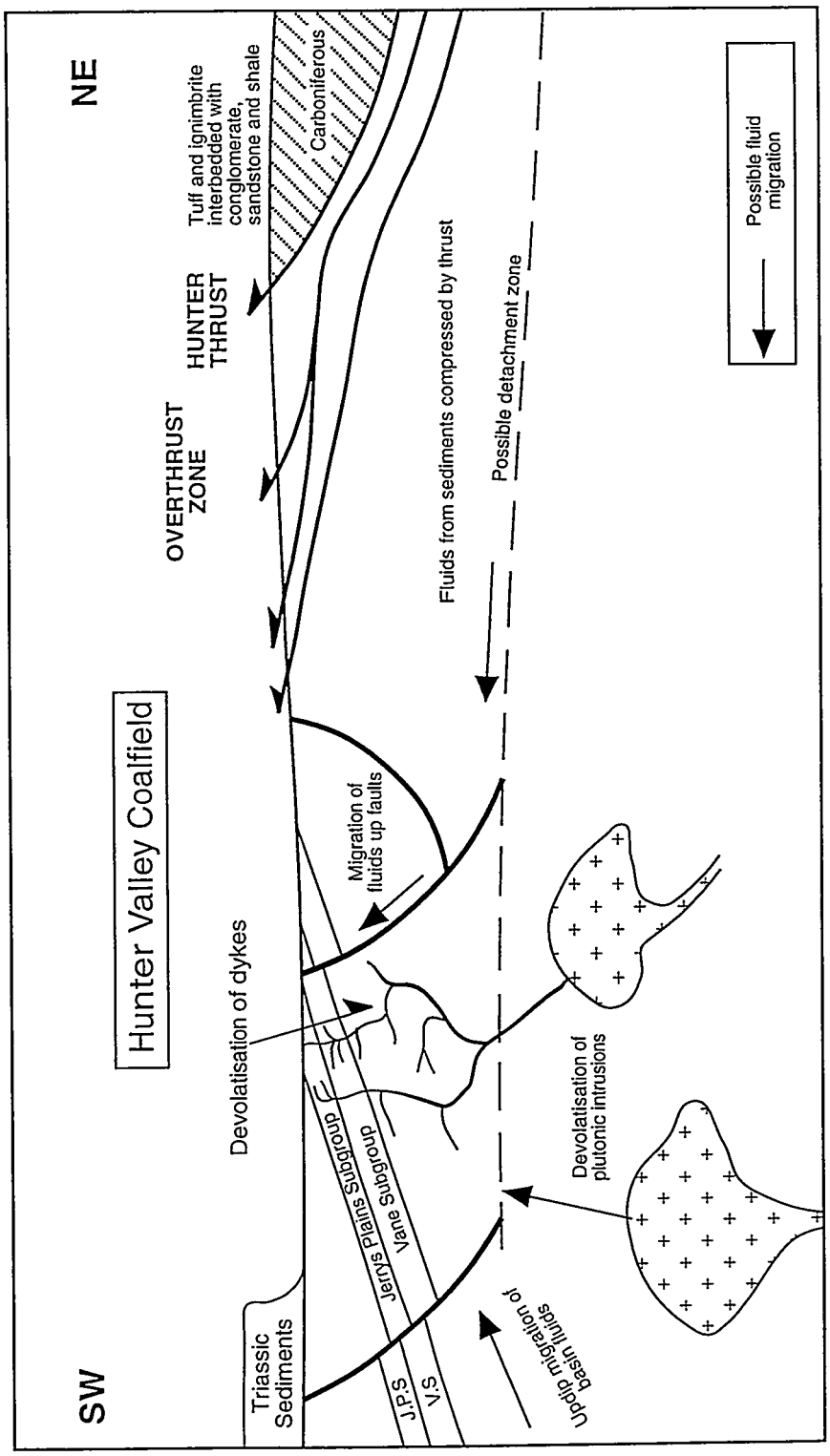


Figure 6 - Schematic section perpendicular to the Hunter Thrust of the Hunter Valley Coalfield showing possible mechanisms for fluid source and migration.



NOTES

INTERGAS '95

May 15-19, 1995
The University of Alabama
Tuscaloosa, Alabama USA

9564

Structurally Controlled and Aligned Tight Gas Reservoir Compartmentalization in the San Juan and Piceance Basins

A.D. Decker, V.A. Kuuskraa and A.L. Klawitter,
Advanced Resources International, Inc.

ABSTRACT

Recurrent basement faulting is the primary controlling mechanism for aligning and compartmentalizing upper Cretaceous aged tight gas reservoirs of the San Juan and Piceance Basins. Northwest trending structural lineaments that formed in conjunction with the Uncompahgre Highlands have profoundly influenced sedimentation trends and created boundaries for gas migration; sealing and compartmentalizing sedimentary packages in both basins. Fractures which formed over the structural lineaments provide permeability pathways which allowing gas recovery from otherwise tight gas reservoirs. Structural alignments and associated reservoir compartments have been accurately targeted by integrating advanced remote sensing imagery, high resolution aeromagnetics, seismic interpretation, stratigraphic mapping and dynamic structural modelling. This unifying methodology is a powerful tool for exploration geologists and is also a systematic approach to tight gas resource assessment in frontier basins.

INTRODUCTION

Tight gas reservoir performance is controlled by fracture permeability, reservoir pressure, gas saturation and reservoir distribution. Within the Rocky Mountain Basins these critical reservoir properties are formed and compartmentalized by recurrent basement faulting. This paper presents examples of structurally aligned sedimentary (reservoir) packages that have been identified in the San Juan and Piceance basins. Structural lineaments act as barriers to hydrocarbon and water migration thereby forming compartments of abnormally pressured gas accumulations. Fractures which form over the structural lineaments provide permeability pathways allowing gas recovery from otherwise tight reservoirs. Mapping these first and second order structural elements provided the explorer a powerful tool for partitioning a basin by reservoir properties. Moreover, accurate prediction of reservoir characteristics in advance of drilling enables the producer to select drilling sites and optimize completion strategies thus maximizing gas production and reducing the cost of producing gas.

Beyond the benefits of this methodology to operators, a similar approach can be used for larger scale resource studies to asses and economically grade the vast continuous type deposits (tight sands, gas shale and coalbed methane).

The San Juan and Piceance Basins have been extensively exploited for tight gas sand and coalbed methane production. Numerous wells producing from tight gas reservoirs provide excellent information on permeability anisotropy. Both basins are undergoing comprehensive integrated geologic evaluation relying on advanced methods of remote sensing imagery, high resolution aeromagnetics, stratigraphic mapping, seismic interpretation and dynamic structural modeling to establish the origin of the geologic systems controlling gas production. Three additional papers, presented at this symposium, one by Klawitter on the San Juan Basin and two by Hoak on the Piceance Basin, detail the results of the integrated exploration approach. This paper builds on the geologic work of Klawitter and Hoak to establish the application of integrated exploration for basin partitioning.

Dynamic Tectonic Modeling of the San Juan and Piceance Basins

The western Cretaceous basins formed as part of a larger foreland basin. Similarities or differences in these basins can be best understood by establishing the tectonic framework that caused the basins to become stratigraphically and structurally distinct. The inseparable linkage between tectonics and sedimentation is the foundation for all interpretations.

The NW-trending Uncompahgre Precambrian Highlands is a prominent boundary separating the San Juan and Piceance Basins (figure 1). This NW anisotropy trend was multiply reactivated during Precambrian, Paleozoic and Tertiary orogenies. Although surface mapping has located the core structure and overall dimensions of this NW basement block, recent geologic evaluation has established corresponding NW structural domains that extend to the interior of the San Juan and Piceance Basins. Structural lineaments NW1, NW2, NW3, NW4, and NW5 that formed in conjunction with the Uncompahgre Highlands have profoundly influenced sedimentation trends and created boundaries for hydrocarbon migration by sealing and compartmentalizing these sedimentary packages. Horst and graben development during the Paleozoic orogeny caused regional NW-trending truncations of Paleozoic sections within up thrown blocks of the core structure and basin interiors. Reactivation and structural inversion during Cretaceous sedimentation formed a NW-trending embayment separating the San Juan and Piceance basins. Northwest trending strand plain deposits of the Pictured Cliffs sandstone

and the Rollins sandstone formed simultaneously on both sides of the embayment. Deposition of the two strandline deposits and coals forming behind the strandlines marked the simultaneous development of structurally aligned reservoir compartments in two adjacent basins.

Stratigraphically Aligned Hingeline Deposits

A comparison of late Campanian regressive deposits in the Piceance Basin to those found in the San Juan Basin to the south reveals stratigraphic, depositional, and paleogeographic similarities. Most importantly, each of these important coal-bearing intervals have in common a relationship to a structural hingeline. The late Campanian Pictured Cliffs shoreline sandstones in the San Juan Basin are believed to be time equivalent to the Rollins/Trout Creek sandstones in the Piceance Basin through age relationships determined by ammoniate zonations of the regressive wedges that bracket the sandstones (Newman, 1982). Newman (1982) also postulates that sediments from the Piceance Delta (Collins, 1970, 1976) were swept to the southeast by longshore currents and deposited as linear barrier sheet sands of the Pictured Cliffs. The progradational Pictured Cliffs-Fruitland coals succession in the San Juan Basin is therefore equivalent to the Rollins/Trout Creek-Cameo coals succession in the Piceance Basin. Franczyk and others (1992) have also interpreted a continuous shoreline and related paleogeographic setting between the Piceance and northern San Juan Basins during late Campanian time.

Gross interval thickening, maximum thickness of net coal, and the identification of transgressive events and their relationship to the hingeline (NW2) in the San Juan Basin are also observed in the Piceance Basin. The upper Cretaceous interval in the San Juan Basin thickens markedly northeast of the hingeline, and the regressive marine Pictured Cliffs sandstones pinch out near the structural hingeline that separates the northeast-dipping monocline of the southern half of the basin from the low-relief basin floor (fig 2). In addition, the greatest net-coal thickness of the Fruitland coals occurs in the north-central part of the basin, parallel to this southern hingeline (Ayers and others, 1991).

Stratigraphic studies of the Upper Cretaceous Mesaverde Group in the southern Piceance Basin have suggested the presence of a northwest-southeast trending hingeline (NW4). The identification and interpretation of the hingeline is supported by the following observations: 1) gross interval isopach mapping indicates an increased rate of sediment thickening east of the NW4 hingeline; 2) net thickness of the Cameo coals and gross thickness of the Williams Fork interval increases significantly east of the hingeline; 3) at least three marine sequences are present in the lower part of the Williams Fork and reach their landward limits near the approximate hingeline position; and, 4) similar relationships are observed in the northern San Juan basin, located approximately 60 mi (96 km) to the south. Reservoir properties that evolved in the hingeline sedimentary packages will be discussed within the context of the individual basins.

Hingeline Development and Reservoir Compartmentalization in the San Juan and Piceance Basins

The San Juan Basin hingeline is a northwest trending structural lineament extending an estimated 70 miles long, transecting the northern basin roughly overlying and parallelling the basin structural axis. The hingeline was first inferred by Stevenson (1983) due to sudden thickening in Paleozoic section near the northwest basin margin along an interpreted basement alignment. The northwest stratigraphic alignment in the Pictured Cliffs barrier-strand plain system and pulsatory oscillation of the shoreline led Ayers (1991) to conclude that a structural hingeline existed at Cretaceous time to accommodate the stratigraphic thickening. More recently, Klawitter (this publication) identified the structural hingeline, NW2, and its associated fractures using the integration of remote imagery, gravity, seismic, stratigraphic and structural studies.

The hingeline has compartmentalized basin wide coal reservoir properties and is responsible for the favorable coal reservoir properties that have led to the prolific coalbed methane production "fairway" that overlies and parallels the hingeline (figure 3). The economically favorable implications of structurally aligned production "fairways" involving tight gas reservoirs give incentive for establishing an exploration rationale so that similar reservoir trends can be identified and exploited.

Pronounced geometry of the strong NW elongate production trend suggests structural involvement. As in most western basins, structural activity causes changes in depositional systems. The close correlation of the San Juan basin hingeline (figure 4) to total Fruitland coal thickness supports syndepositional subsidence. The NW elongate high pressure cell parallelling and immediately to the north of the hingeline (figure 5) is a remnant from gas generation in a gas centered basin. The hingeline traps southward gas migration thus creating conditions for overpressuring. South of the hingeline, Fruitland coals and Pictured Cliffs sandstones are fully gas saturated and underpressured. North of the overpressured cell, slight overpressuring has been interpreted (Kaiser, 1991) to be due to artesian conditions from an elevated outcrop. Immediately north of the hinge and directly overlapping the production fairway is a high density cluster of surfical linear features interpreted from satellite imagery (figure 6). The combination of high fracture permeability, overpressuring, thick coals and high gas saturation account for the origin of the prolific production fairway. In turn, the origins and presence of this fairway have been accurately identified by integrating remotely sensed data, stratigraphic mapping and dynamic tectonic modelling.

The integrated exploration approach used in the San Juan Basin provides a useful analog for identifying commercial reservoir compartments in other basins. The Piceance Basin will serve as the demonstration site for further verification and development of this integrated exploration approach.

Multiple Source Data Interpretation for Structural Analysis of the Piceance Basin

When compared to the San Juan Basin, the Piceance Basin has undergone a more complex tectonic history and is

sparsely drilled. A rigorous approach to structural analysis has been undertaken to successfully determine basement features under these challenging conditions. To provide a foundation for structural interpretation, a high resolution aeromagnetic survey was acquired and processed over the southern basin. To minimize interpretation subjectivity and establish credibility of interpreted features, basement features were also interpreted utilizing 400 line miles of seismic surveys, and utilizing Landsat Thematic Mapper (TM) and Side Looking Airborne Radar (SLAR) imagery for the basin and surrounding areas.

Spatially detailed aeromagnetic maps were used to interpret zones of basement structure. Basement structures, some verified by seismic profiles, corresponded to steep magnetic gradients and linear trending contours. Utilizing this technique, first order and second order basement features have been located on the reduced-to-pole total field magnetic intensity contour map (figure 7). The most prominent features include an interpreted paleobasement high in the east central portion of the basin flanked on the east and west by northwest trending faults NW3 and NW4 and on the north and south by EW3 and EW2 respectively interpreted as east - west trending faults. Seismic coverage (figure 8) has confirmed the basement high which has caused truncation of the Paleozoic section. At basement level, structural lineament NW4 is formed by low angle thrust faults that typically terminate within the Mancos shale. Mild warping and draping of the sediments occurs along the fault termination boundaries.

Coincident features to the identified first and second order northwest lineaments have been mapped through linear feature analysis of TM imagery. These lineaments are a composite of individual linear features as interpreted from Landsat Thematic Mapper imagery. Northwest-trending linear features were contoured with respect to frequency of occurrence. Imagery lineaments are defined as zones of aligned and concentrated linear features, which are linear elements interpreted directly from imagery. Figure 9 presents lineaments interpreted from NW-trending linear features in the southern portion of the basin. Note on figure 9 the close correlation of lineaments as interpreted from imagery to basement faults as interpreted from aeromagnetics. This close correlation and further calibration from seismic lines establishes interpreted NW lineament features as significant structural lineaments. Surface analysis of the E-W trending features is in progress. Preliminary interpretation of E-W structural elements suggests lateral movement along fault zones. Stratigraphic interpretation indicates the NW4 structural element acted as a basin hingeline during Cretaceous deposition.

Hingeline Development in the Piceance Basin

Gross interval isopach maps were prepared for three discrete genetic sequences as well as several major intervals in the Upper Cretaceous section figure . These maps include isopachs of the late Campanian Corcoran, Cozzette, and Rollins genetic sequences; the coal-bearing interval between the top of the Cameo Coal group and the Rollins sandstone (figure 10); and other gross interval isopach maps such as the top of Cretaceous to base of the Rollins sequence, included as figure 11. As each of these preliminary maps illustrates, a gradual rate of interval thickening occurs from the position of the hingeline eastward to the limit of subsurface control.

Net thickness of Upper Cretaceous (Williams Fork Fm.) coals reaches a maximum in an area parallel to and east of the hingeline (figure 12). The fact that coal thickness is greatest in the eastern part of the basin also implies that a significant amount of accommodation space was available for the deposition of sediments and the compaction of organics necessary to produce the thick coal seams and total net coal that is found in this part of the basin. In addition, a stratigraphically higher coal-bearing interval in the Williams Fork Formation (the Coal Ridge coal group) is present only in the area of the basin east of the hinge line. The Coal Ridge coals are associated with what was perhaps one of the final marine transgressions in the late Campanian.

At least three late Campanian marine sequences have been identified along the eastern margin of the Piceance basin overlying the nonmarine coastal plain/lower delta plain facies of the early Williams Fork Formation. Marine sandstones within this section have been termed the middle and upper sandstones (Collins, 1970). As these regressive sequences shoal upward into lower delta plain and coastal plain facies, coal beds of the Coal Ridge group were formed. Correlation of the marine sequences westward into their nonmarine equivalents is difficult. Interestingly, the general position of the transition from marine to nonmarine facies (and the pinching out of the Coal Ridge coals) in these sequences occurs near the hingeline (figure 13). Again, this suggests differential subsidence and/or increasing accommodation space in the eastern portion of the basin. This results in a relative rise of sea level with marine incursions reaching a landward limit at approximately the same position as the hingeline.

Structurally Aligned Reservoir Compartmentalization

The best production from the Cameo coals and overlying tight gas sands of the Piceance Basin has been established in the Rulison, Parachute and Grand Valley Fields. Iso-production contouring of these three fields has been performed separately on the coal and tight gas sand as part of an effort to determine geologic controls on gas production. The strong NW trend of the production contouring from both intervals implies a common event causing permeability anisotropy. The close proximity and alignment of northwest trending basement faults (figure 14) to the production anisotropy is interpreted as being fracture controlled. Fractures have been generated by basement faults causing the northwest aligned production trend. A region of high stress occurring within close proximity to the structural lineament causes closure of the fracture system and results in a no-flow boundary. Gas migrating southward out of the gas-centered basin became trapped along the no flow boundary causing an overpressuring along the northwest flanks of the basin hingeline NW4 (figure 15). Southwest of the hingeline, the Cretaceous reservoirs are gas saturated and underpressured because the hingeline has isolated water recharge from the Northeastern basin elevated outcrop from the southwestern basin. High fracture permeability and overpressuring conditions are responsible for the better reservoir performance observed at Rulison field when compared to other fields producing from Cameo coals and overlying tight gas sands. Since the favorable reservoir properties at the Rulison Field are associated with the basin hingeline, similar reservoir compartments are likely to exist northwest and southeast of the Rulison field along the basin

hingeline. A graphic summary of partitions in the two basins (figure 16 and 17) demonstrate the remarkable parallel reservoir properties development between the two.

Use of Basin Partitioning Methods for Reconnaissance Exploration and National Resource Studies of Continuous Deposits

Recent national level natural gas resource assessments, such as by the National Petroleum Council and the U.S. Geological Survey, show that "continuously deposited reservoirs", such as tight sands, gas shales, and coalbed methane, represent the largest undeveloped source of natural gas in the U.S. Recent presentations at the GRI sponsored Global Gas Resource Workshop indicates that this finding may be true not just for the U.S. but for the gas basins of the world.

While it has been possible to reasonably establish the volume of gas in place, no easy to use, reliable methods have been set forth for categorizing or grading these deposits into high, medium and low quality and thus establishing their economic viability. The coalbed methane portion of the recent USGS National Assessment took a step toward this goal by using detailed reservoir data supported by extensive reservoir simulation, using COMETPC 3-D. This simulation-based approach provided a strong foundation for defining the probable reserves in already partially drilled and defined basins. However, no comparably reliable methodology exists for frontier or lightly explored continuous type basins.

With modification appropriate to the scope and regional nature of the effort, the integrated exploration approach set forth in this paper would enable an exploration geologist or a resource assessor to partition a frontier-type, continuously deposited basin. The use of basin partitioning with reservoir simulation to establish distinct basin area of high gas flow and per well reserves would provide a solid foundation for determining the economics of frontier tight gas, gas shale and coalbed methane basins.

CONCLUSIONS

Structurally aligned reservoir compartments represent some of the most prolific gas reservoirs in the San Juan and Piceance Basins. Accurate targeting of structural corridors and associated reservoir compartments is possible through the utilization and integration of advanced methods of remote sensing imagery, high resolution aeromagnetics, stratigraphic mapping, seismic interpretation and dynamic structural modeling. Utilization of this method is likely to yield additional gas discoveries in the San Juan and Piceance Basins. The analogs developed in these basins will serve as a valuable template for evaluation and exploration of other western basins and conducting improved resource studies of continuous type deposits.

ACKNOWLEDGMENTS

The authors would like to acknowledge financial support for this paper from the U.S. Department of Energy, Morgantown Energy Technology Center, SBIR Phase II grant DE-FG03-93ER81502. We also thank Patricia Martinez-Valdez for manuscript preparation, Barry Perow and David Devitt for graphics, and Owen Fitzsimmons for geologic assistance and Lee Jirik for stratigraphic interpretations.

REFERENCES

1. Ayers, W.B., et al, 1991: "Geologic and Hydrologic Controls on the Occurrence and Producibility of Coalbed Methane, Fruitland Formation, San Juan Basin," The Univ. of Texas at Austin, Bur. of Eco. Geol., Topical Report prepared for GRI under contract 5087-214-1544.

2. Collins, B. A., 1976, Coal deposits of the Carbondale, Grand Hogback, and southern Danforth Hills coal fields, eastern Piceance Basin, Colorado: Colorado School of Mines Quarterly, V. 71, no.1, 137 p.

3. Collins, B. A., 1970, Geology of the coal-bearing Mesaverde Formation (Cretaceous), Coal Basin area, Pitkin County, Colorado: Colorado School of Mines Masters thesis, 116 p.

4. Franczyk, K. J., Fouch, T. D., Johnson, R. C., Molenaar, C. M., and Cobban, W. A., 1992, Cretaceous and Tertiary paleogeographic reconstructions for the Uinta-Piceance Basin study area, Colorado and Utah: U. S. Geological Survey Bulletin 1787-Q, 37 p.

5. Kaiser, W.R., Swartz, T.E., and G.J. Hawkins, 1991: "Hydrology of the Fruitland Formation, San Juan Basin," *in*: Ayers, W.B., et al., Geol. and Hydro. Controls on the Occurrence and Producibility of Coalbed Methane, Fruitland Formation, San Juan Basin, The Univ. of Tex. at Austin, Bur. of Eco. Geol., Topical Rpt. prepared for GRI under contract 5087-214-1544, pp. 195-241.

6. McFall, K.S., Wicks, D.E., Kuuskraa, V.A., and Sedwick, K.B., 1986, A Geologic Assessment of Natural Gas From Coal Seams in the Piceance Basin, Colorado, Topical Report GRI 8710060, 76 p.

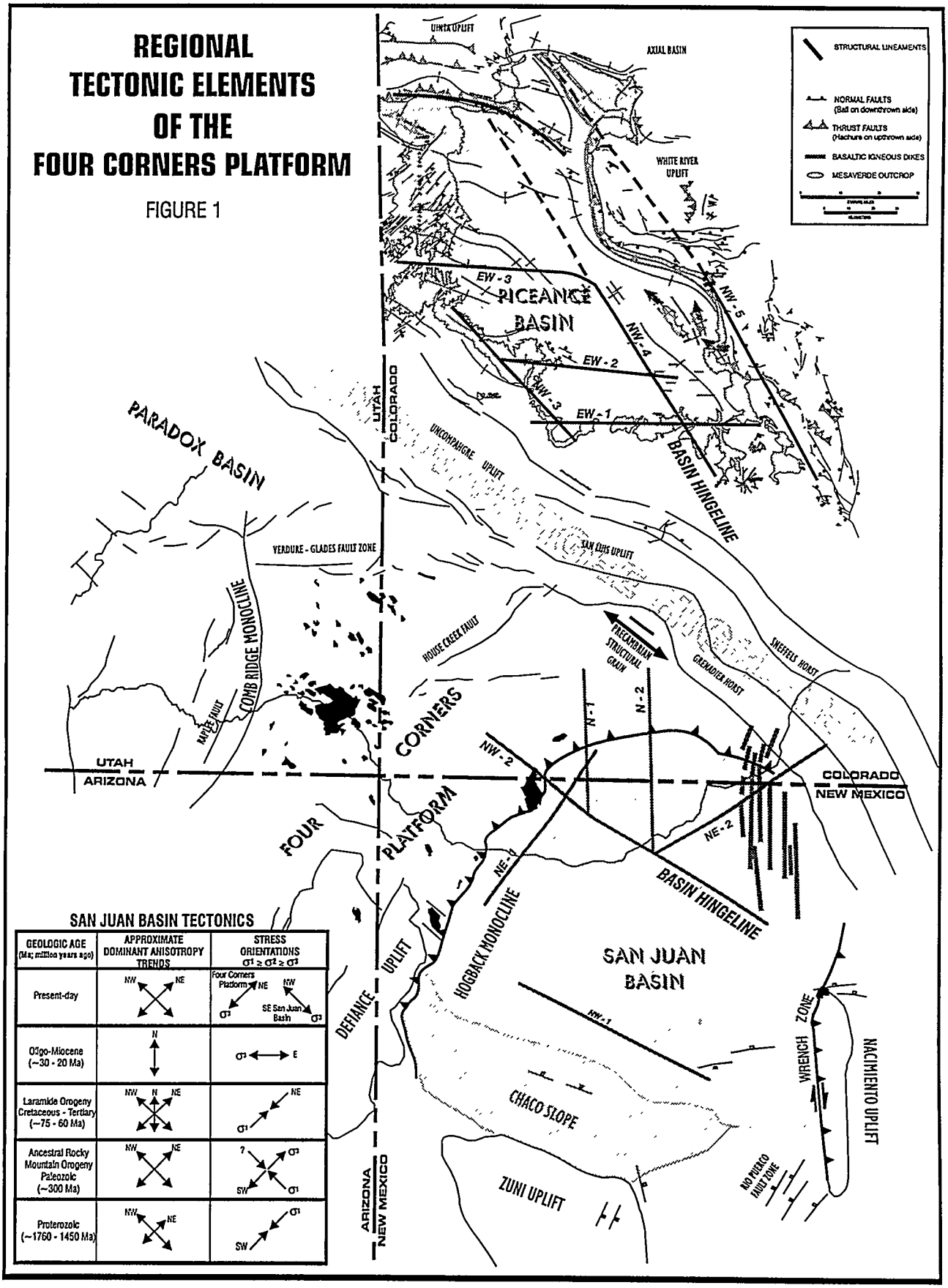
7. Newman, K. R., 1982, Stratigraphic framework of upper Cretaceous (Campanian) coal in western Colorado: Grand Junction Geological Society, 1982 Field Trip, p. 61-64.

8. Reinecke, K.M., Rice, D.D and Johnson, R.C., 1991, Characteristics and Development of Fluvial Sandstone and Coalbed Reservoirs of Upper Cretaceous Mesaverde Group, Grand Valley, Colorado, In: *Coalbed Methane*, Rocky Mountain Association of Geologists Publication, 209-225.

9. Stevenson, G.M., 1983: "Paleozoic Rocks of the San Juan Basin: An Exploration Frontier," *in*: Four Corners Geol. Soc. pub., Oil and Gas Fields of the Four Corners Area, 780-788.

REGIONAL TECTONIC ELEMENTS OF THE FOUR CORNERS PLATFORM

FIGURE 1

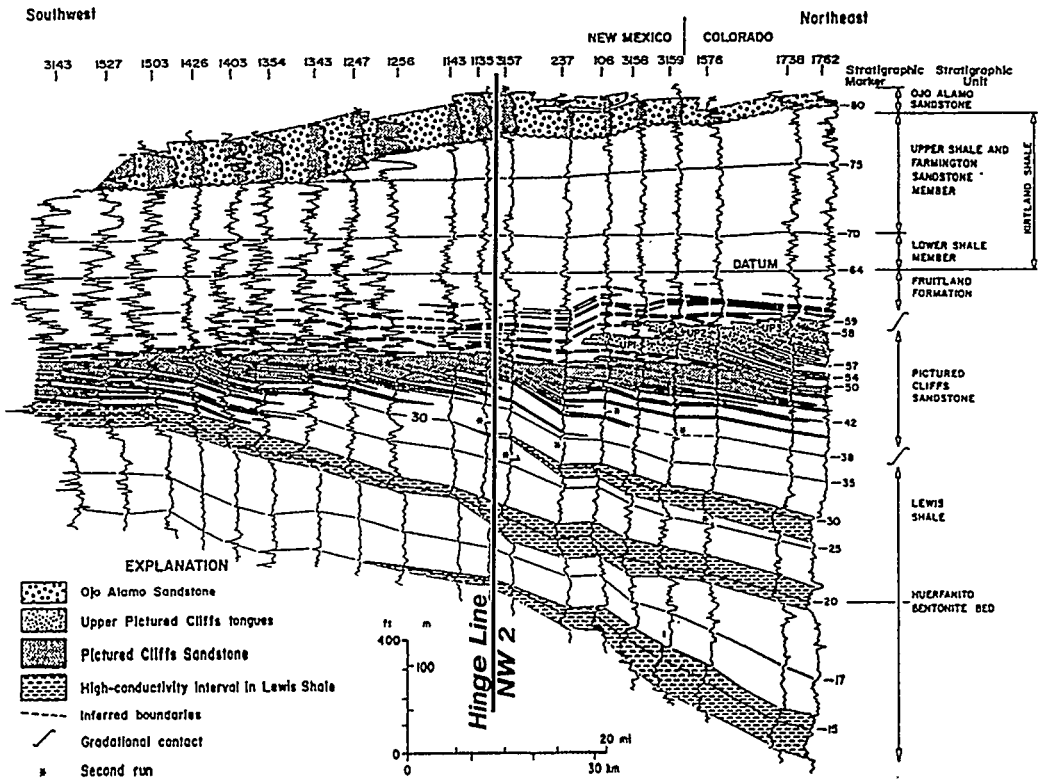


SAN JUAN BASIN TECTONICS

GEOLOGIC AGE (Ma; million years ago)	APPROXIMATE DOMINANT ANISOTROPY TRENDS	STRESS ORIENTATIONS $\sigma^1 \geq \sigma^2 \geq \sigma^3$
Present-day	NW, NE	Four Corners Platform: NE, NW; SE San Juan Basin: σ^3, σ^3
Oligo-Miocene (~30 - 20 Ma)	N	σ^3 ↔ E
Laramide Orogeny Cretaceous - Tertiary (~75 - 60 Ma)	NW, N, NE	NE, σ^1
Ancestral Rocky Mountain Orogeny Paleozoic (~300 Ma)	NW, NE	?, σ^3, SW, σ^1
Proterozoic (~1760 - 1450 Ma)	NW, NE	σ^3, SW

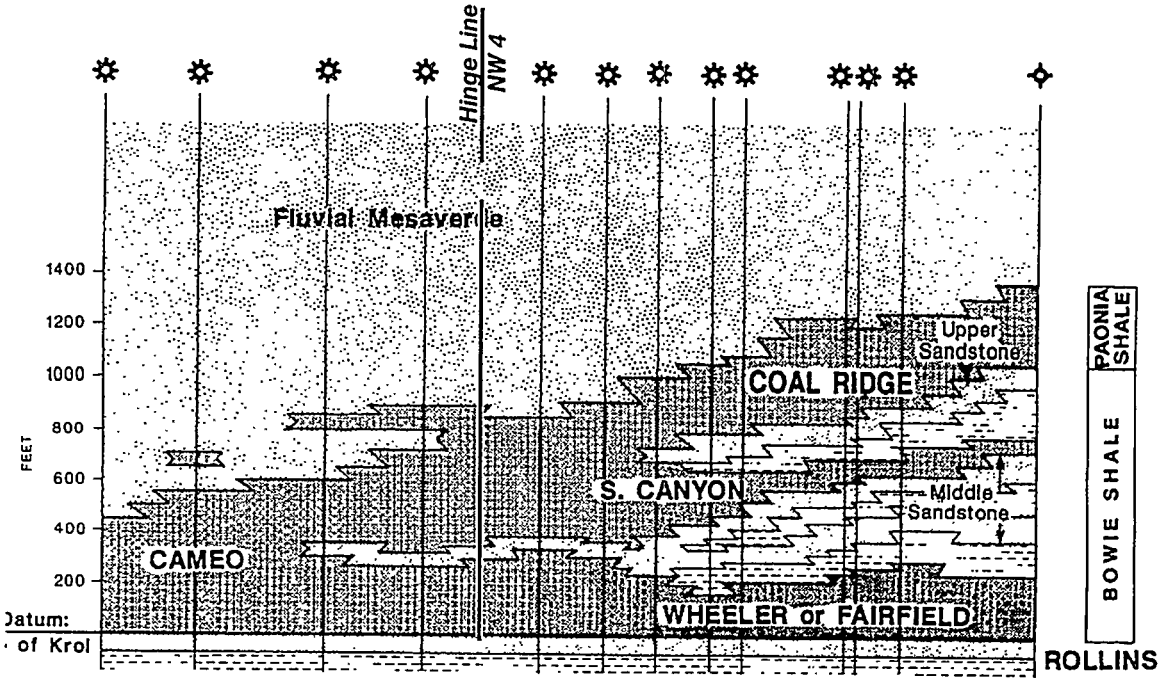
FIGURE 2

SAN JUAN BASIN



Modified from Ayers and Others, 1990

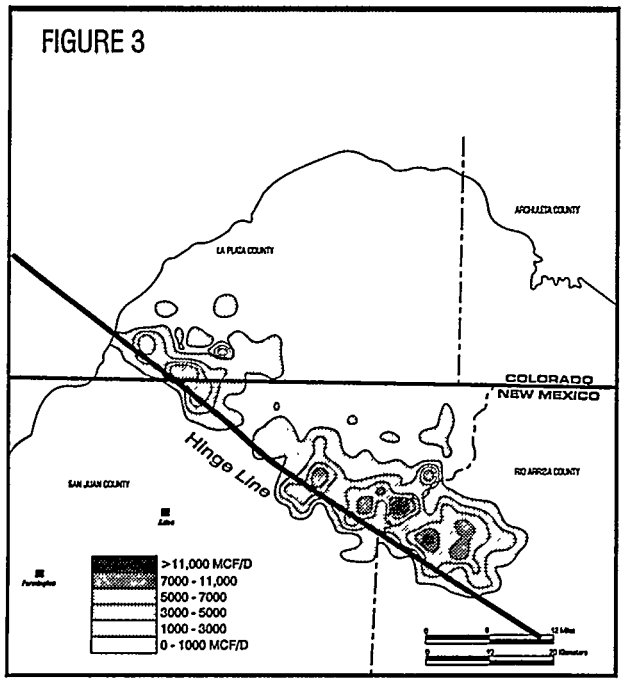
PICEANCE BASIN



Modified from Reinecke and Others, 1991

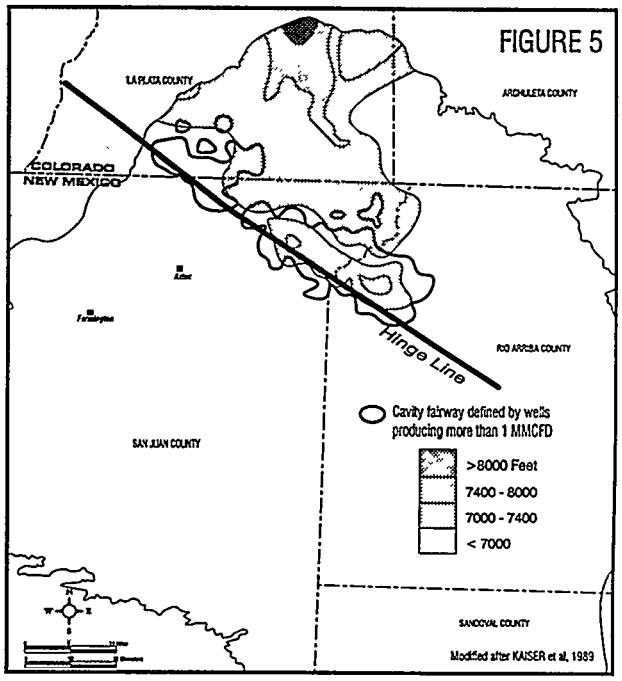
AVERAGE DAILY GAS PRODUCTION FROM FRUITLAND COALS IN CAVITATION FAIRWAY

FIGURE 3



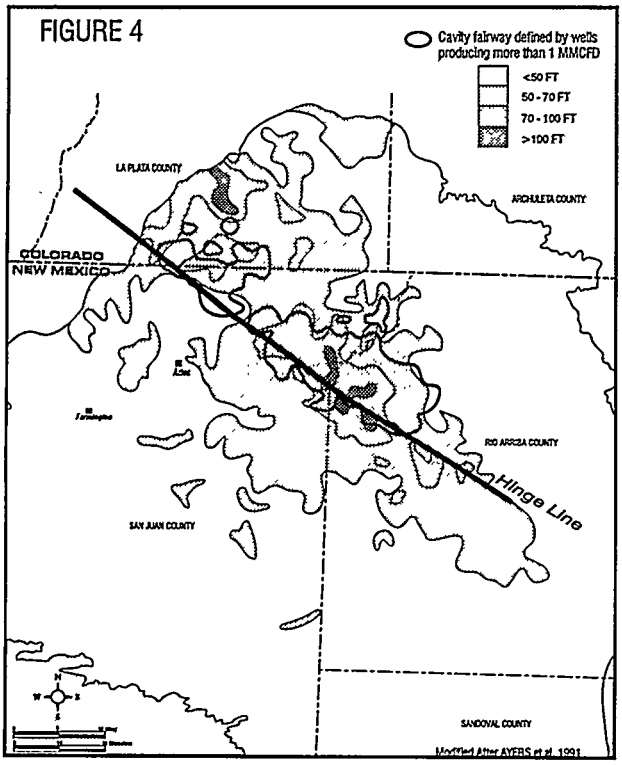
POTENTIOMETRIC SURFACE OF THE FRUITLAND COALS

FIGURE 5



NET COAL THICKNESS OF FRUITLAND FORMATION

FIGURE 4



LINEAR FEATURE ANALYSIS NW-TRENDING LINEAR FEATURES COMBINED FREQUENCY GRIDS

FIGURE 6

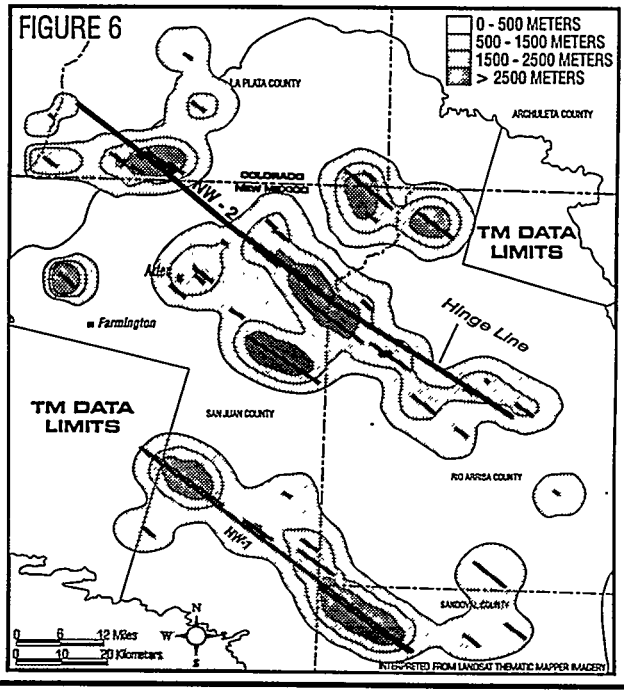
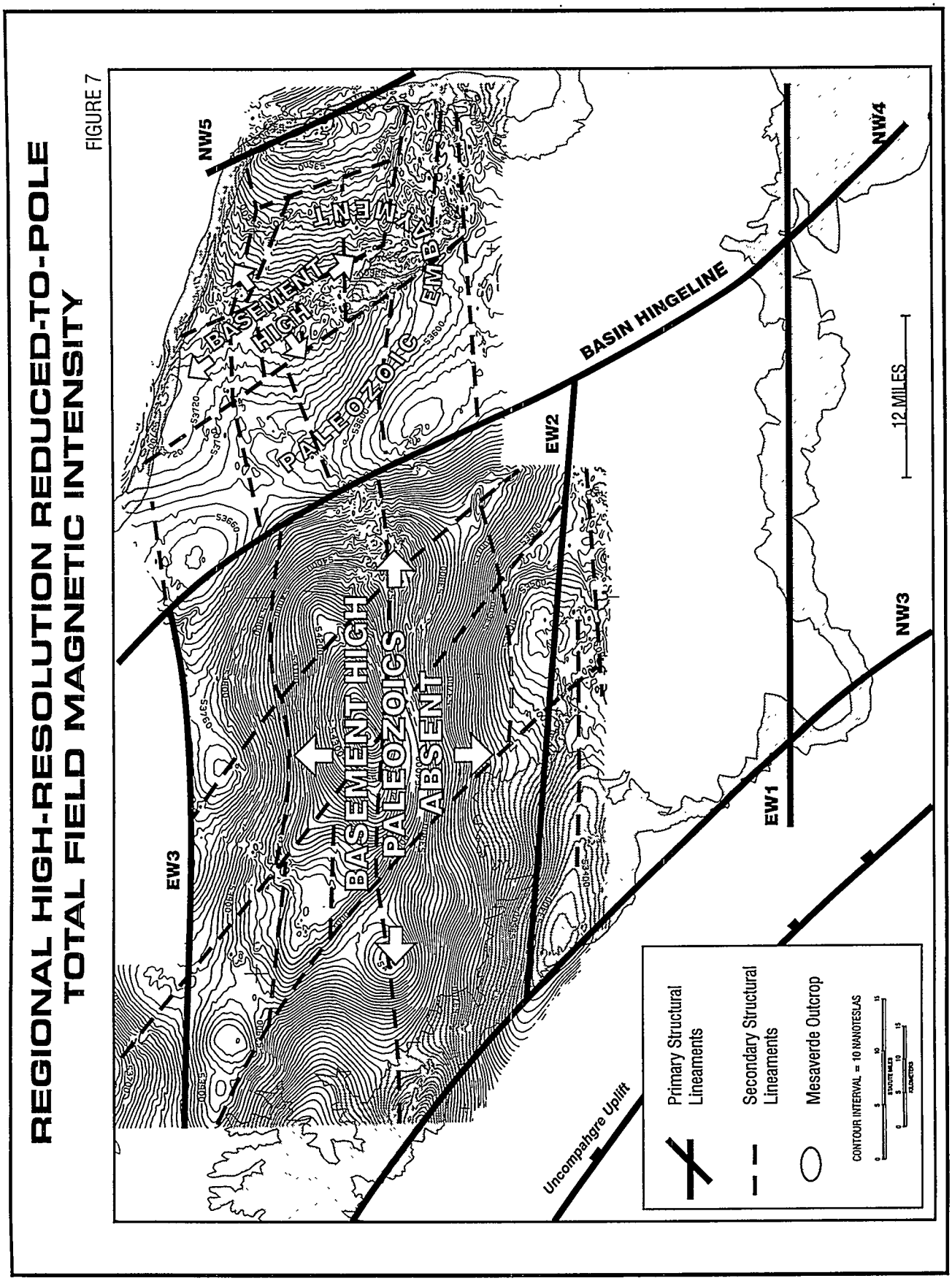
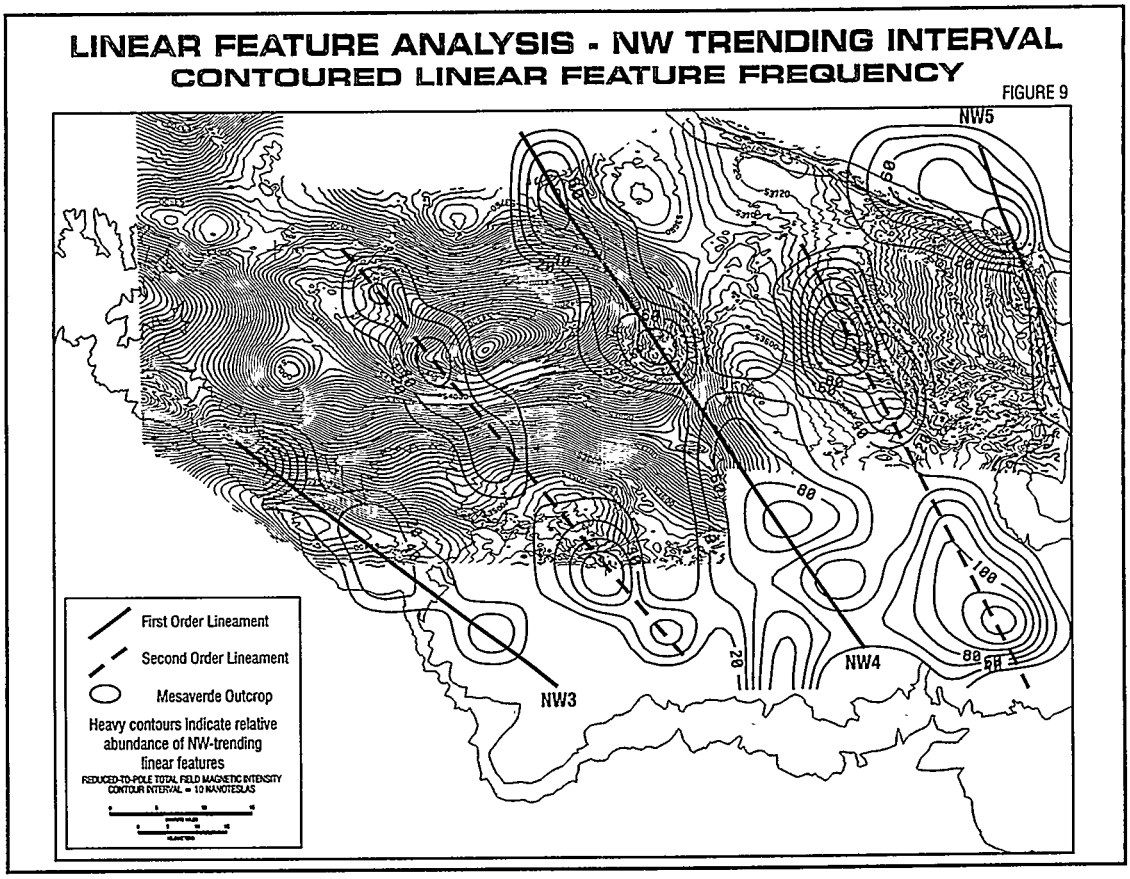


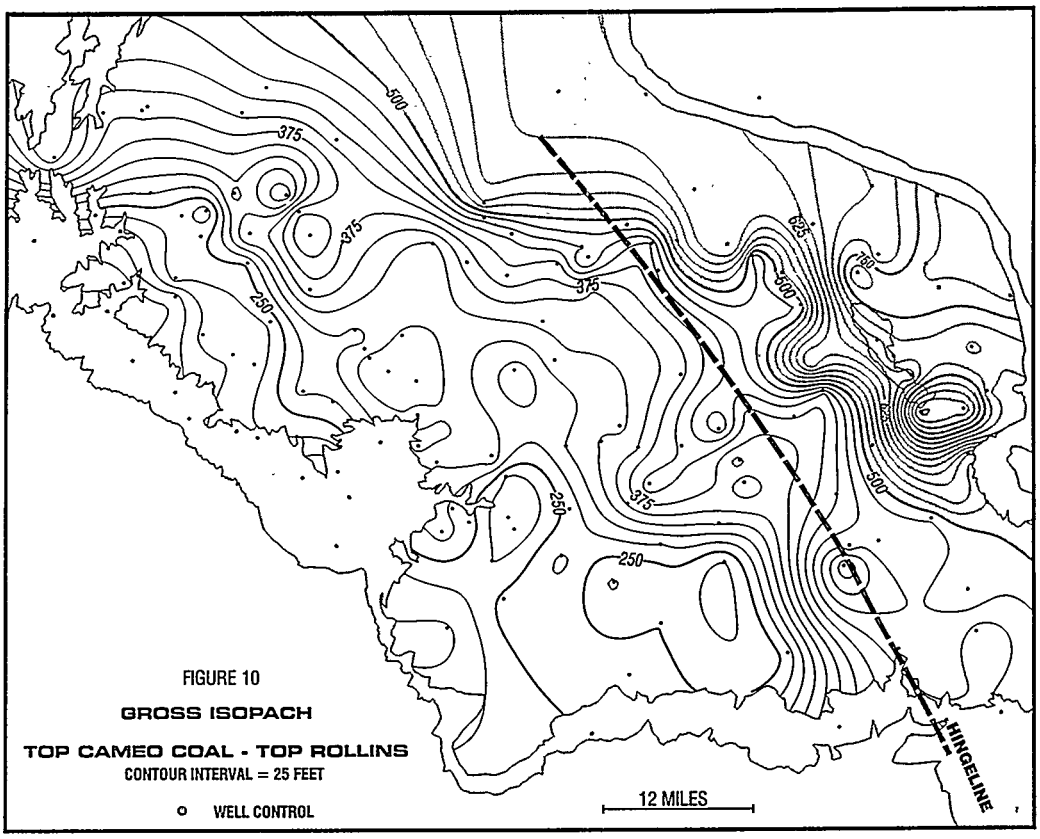
FIGURE 7


REGIONAL HIGH-RESOLUTION REDUCED-TO-POLE
TOTAL FIELD MAGNETIC INTENSITY
NW5
NW4
NW3
EW3
EW2
EW1
BASIN HINGELINE
BASEMENT HIGH
PALEOZOIC EMBAYMENT
BASEMENT HIGH
PALEOZOICS ABSENT
Uncompahgre Uplift
12 MILES
Primary Structural Lineaments
Secondary Structural Lineaments
Mesaverde Outcrop
CONTOUR INTERVAL = 10 NANOTESLAS

BASEMENT FAULTS INTERPRETED FROM SEISMIC
SEISMIC COVERAGE
12 MILES
STRUCTURE ON TOP OF ROLLINS SANDSTONE
(ILES FORMATION)
CONTOUR INTERVAL = 1000 FEET
THRUST FAULT
NORMAL FAULT
(ball on downthrown side)
FROM SEISMIC
MESAVERDE OUTCROP

FIGURE 8


LINEAR FEATURE ANALYSIS - NW TRENDING INTERVAL
CONTOURED LINEAR FEATURE FREQUENCY
FIGURE 9
NW5
NW4
NW3
First Order Lineament
Second Order Lineament
Mesaverde Outcrop
Heavy contours indicate relative abundance of NW-trending linear features
REDUCED-TO-POLE TOTAL FIELD MAGNETIC INTENSITY
CONTOUR INTERVAL = 10 NANOTESLAS


FIGURE 10
GROSS ISOPACH
TOP CAMEO COAL - TOP ROLLINS
CONTOUR INTERVAL = 25 FEET
WELL CONTROL
12 MILES
HINGELINE

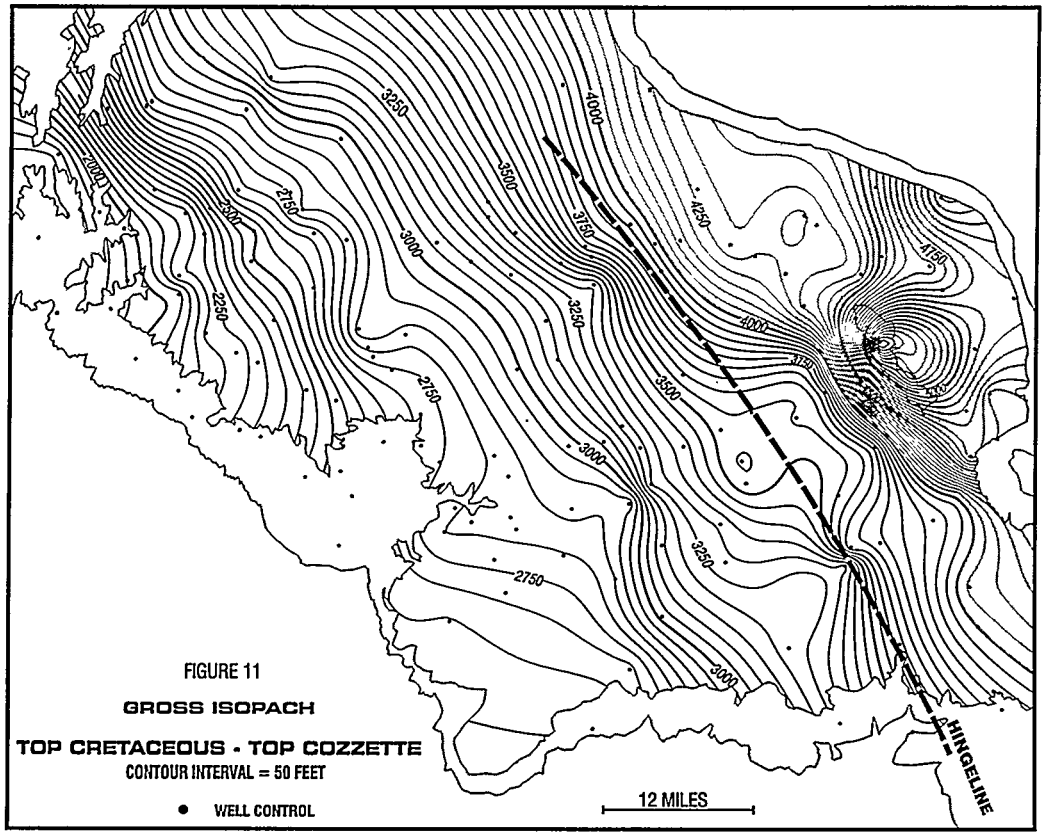


FIGURE 11

GROSS ISOPACH

TOP CRETACEOUS - TOP COZZETTE

CONTOUR INTERVAL = 50 FEET

TOTAL COAL ISOCHORE - WILLIAMS FORK FORMATION

FIGURE 12

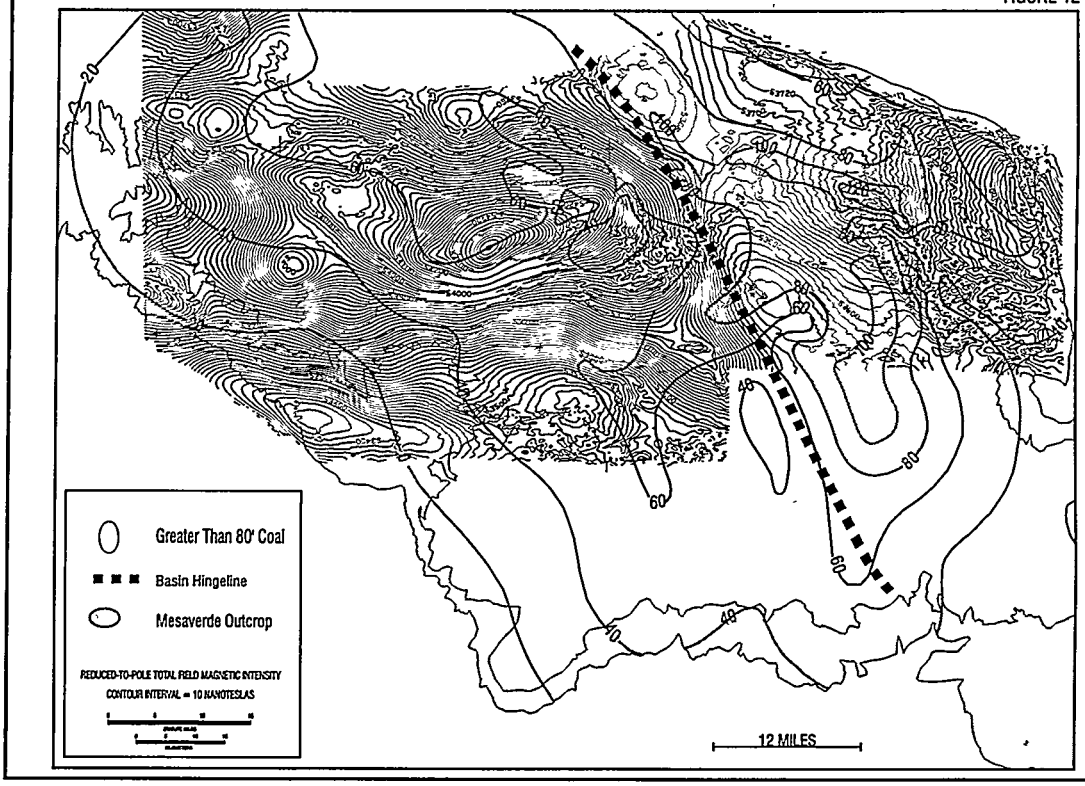


FIGURE 13

TOTAL COAL ISOCHORE - COAL RIDGE GROUP

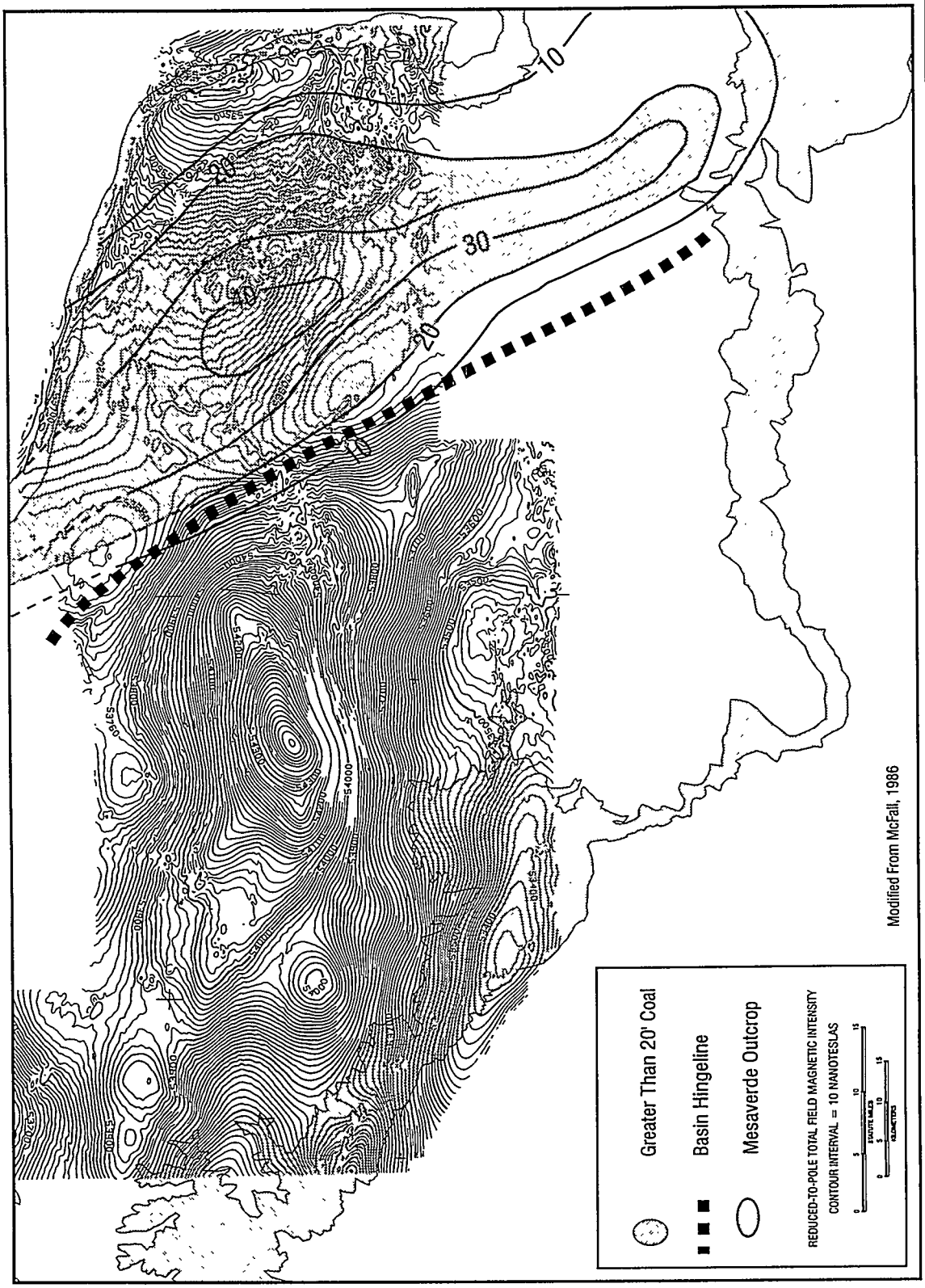
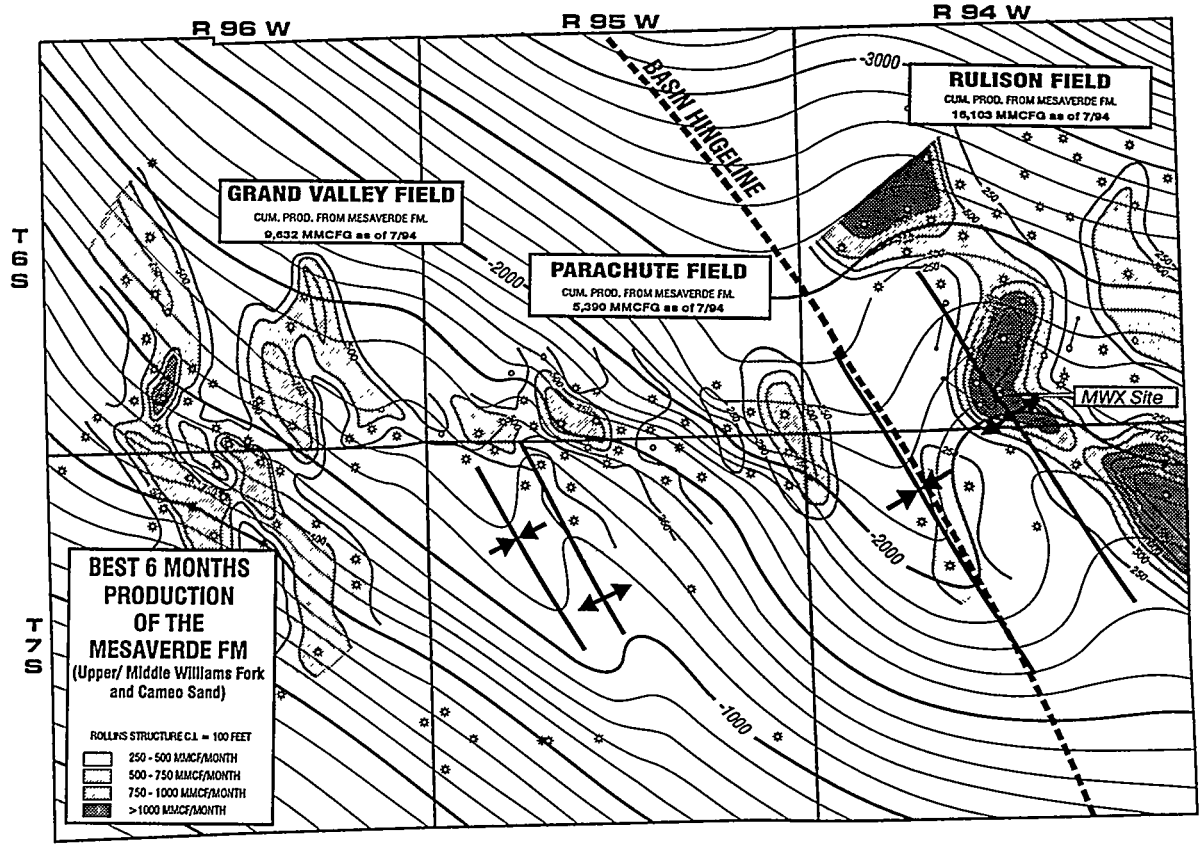
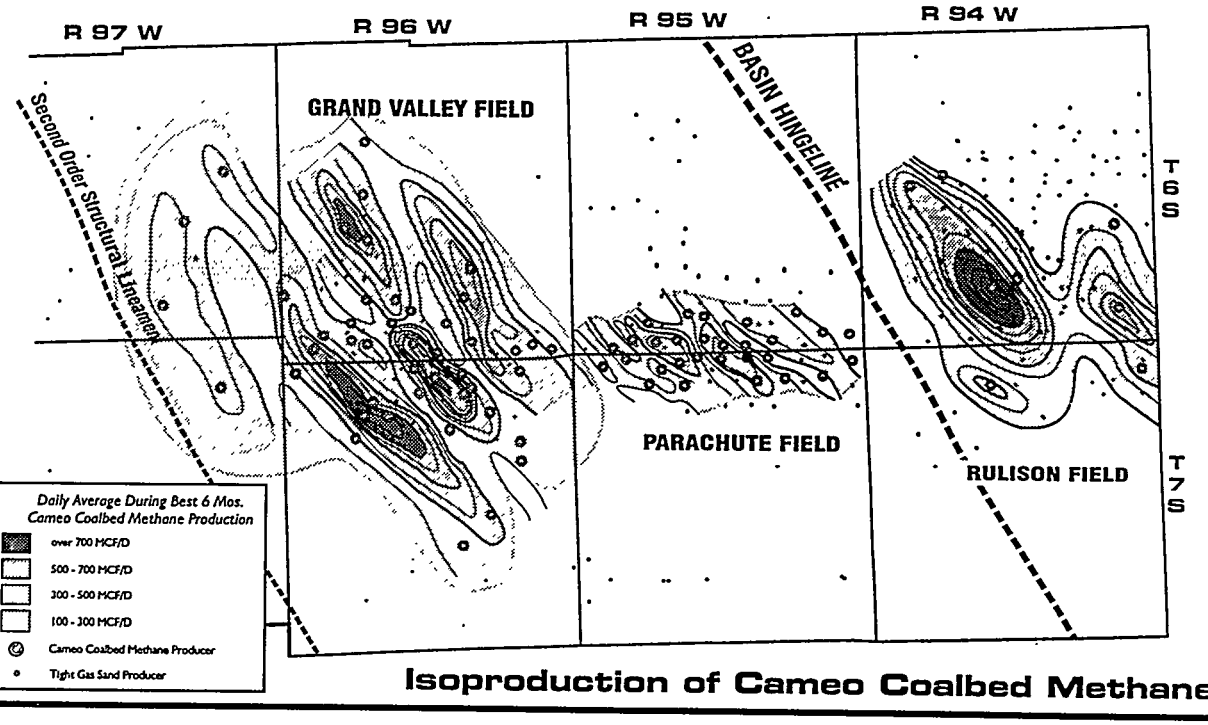


FIGURE 14

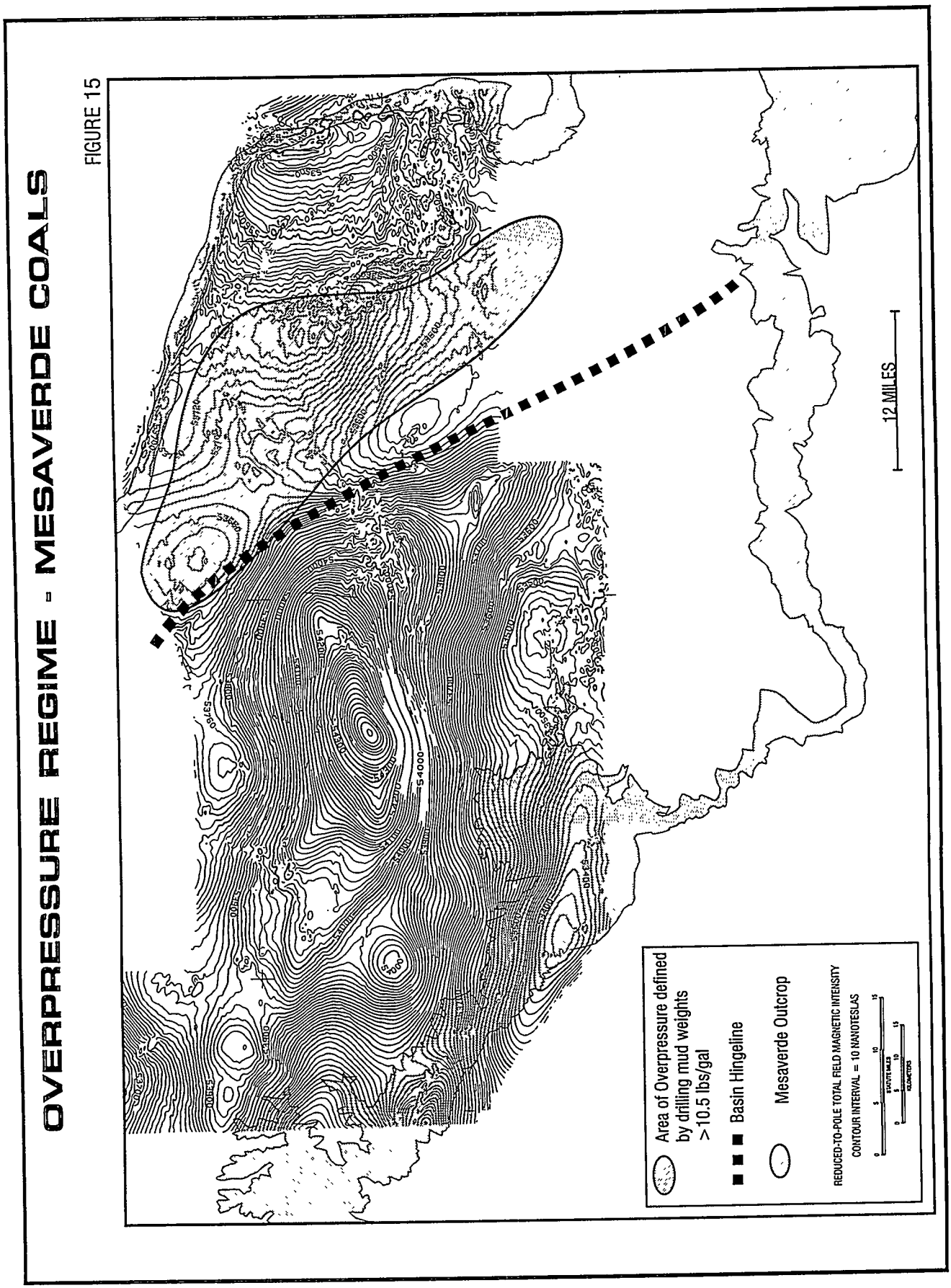
RELATIONSHIP BETWEEN STRUCTURE AND PRODUCTION
Grand Valley, Parachute and Rulison Fields, Piceance Basin





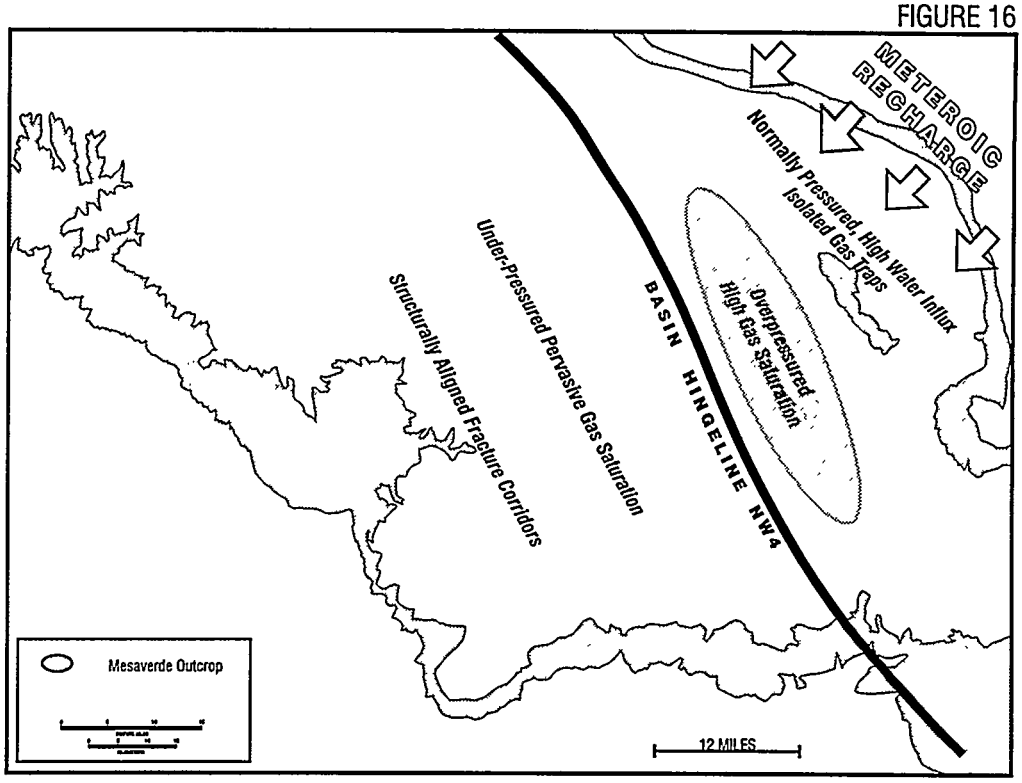
Isoproduction of Cameo Coalbed Methane

FIGURE 15


OVERPRESSURE REGIME - MESAVERDE COALS
Area of Overpressure defined by drilling mud weights >10.5 lbs/gal
Basin Hingeline
Mesaverde Outcrop
REDUCED-TO-POLE TOTAL FIELD MAGNETIC INTENSITY
CONTOUR INTERVAL = 10 NANOTESLAS
12 MILES

SOUTHERN PICEANCE BASIN PARTITIONS

FIGURE 16



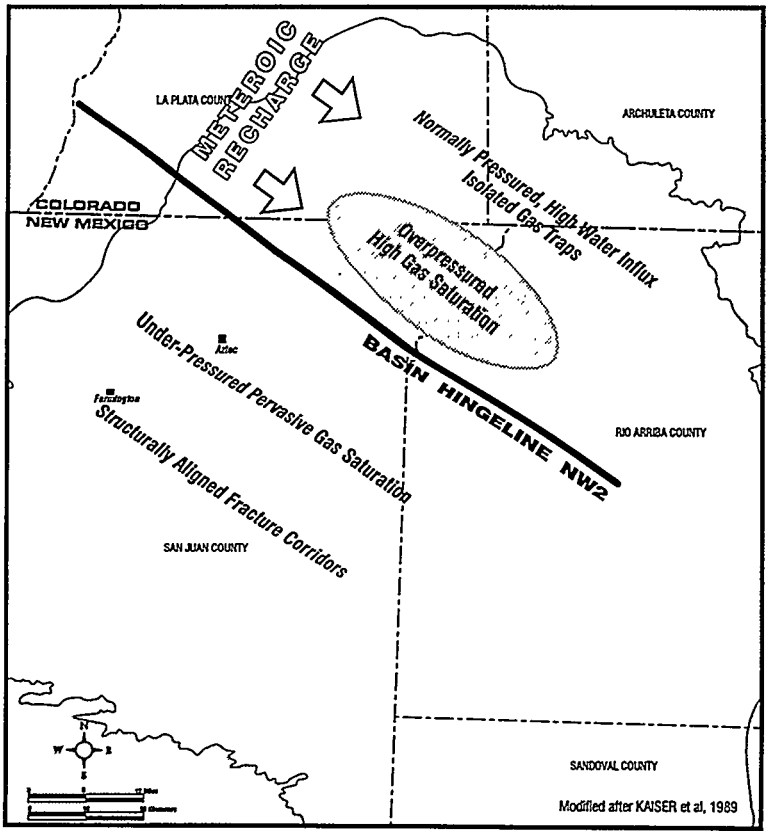


FIGURE 17

SAN JUAN BASIN PARTITIONS



NOTES

INTERGAS '95

May 15-19, 1995
The University of Alabama
Tuscaloosa, Alabama USA

9511

A Comprehensive Assessment of the Potential to Reduce Methane Emissions from U.S. Coal Mines

K. Schultz, Coalbed Methane Outreach Program,
U.S. Environmental Protection Agency

ABSTRACT

The EPA's Coalbed Methane Outreach Program has identified through its outreach and studies the best prospects for reducing methane emissions from U.S. coal mines. This paper reports the findings of three major program initiatives: (1) EPA's report, *Identifying Opportunities for Methane Recovery at U.S. Coal Mines*, that includes the key criteria needed to identify the most promising mines for methane reduction projects and profiles the most promising of U.S. mines; (2) an evaluation of the best local-use alternatives to pipeline injection and how coal mines, local authorities, and local businesses may partner to secure project financing; and, (3) opportunities for electric utilities to participate in coal mine methane recovery as a part of their voluntary greenhouse gas emissions goals.

INTRODUCTION

The U.S. EPA's Coalbed Methane Outreach Program (CMOP) is one of the U.S. Government's 50 *Climate Change Action Plan* programs [1]. *Action Plan* programs aim to fulfill our international agreement to stabilize greenhouse gas emissions in the year 2000 at their 1990 levels. CMOP will meet its goal of capturing an additional twenty billion cubic feet of methane in 2000 if it can successfully encourage new mine methane projects at between ten and fifteen mines. To achieve this goal the program publicizes opportunities to reduce methane emissions at U.S. coal mines using available technologies. It also tackles the various barriers to project development, such as ambiguity of resource ownership, lack of apparent sources of capital, and imperfect markets for coal mine methane.

The prospects look bright for methane recovery at the gassiest of our nation's coal mines. This paper reports the findings of recent CMOP assessments and outreach to determine which mines and end-uses promise the best opportunities for mine gas project development. It focuses on three major program initiatives: an assessment of opportunities at the gassiest of coal mines, market and technical assessments in some important mining regions, and outreach to electric utilities that are searching for projects that reduce greenhouse gas emissions. By examining the potential of these three initiatives to catalyze projects, the paper provides a comprehensive overview of the prospects for coal mine methane recovery in the United States.

THE BEST MINES FOR COALBED METHANE RECOVERY

In September 1994 the Coalbed Methane Program released a new report, *Identifying Opportunities for Methane Recovery at U.S. Coal Mines: Draft Profiles of Selected Gassy Underground Coal Mines* [2]. These profiles present the key information needed to begin considering which coal mines are the best prospects for methane recovery projects. A brief analysis of the different mines shows that some mines are clearly better candidates than others for particular projects.

For instance, the report identifies twenty-three mines that in 1990 had mine degasification programs but no methane use program. It also estimates their 1990 degasification system emissions. Methane recovery projects using today's technologies will most likely use methane recovered from mine degasification systems rather than the very dilute methane emitted by mine ventilation shafts. In addition, many of the most profitable projects will likely be developed at those U.S. mines with degasification systems already in place. These mines do not require as much capital as other mines to develop methane use projects since they already have a recovery system in place. If they produce high quality gas, the incremental costs of gathering, compressing, and moving this gas to the nearest natural gas pipeline are all that remains. As Table 1 indicates, in 1990 U.S. mines released to the atmosphere from their degasification systems approximately 60 million cubic feet of methane each day (twenty-two Bcf per year). Over a dozen mines released at least two million cubic feet per day, (.73 Bcf per year) and the report estimates nineteen mines released more than one mmcfd (.37 Bcf per year) of medium to high quality gas.

The profiles also contain data on coal production levels, coal sulfur content, mine life expectancy, coal sales information and summaries of recent mine news, which may give an indication of a mine's future business prospects. Further, the profiles include the carbon dioxide equivalent of a mine's recoverable methane that is released to the atmosphere each year (based on the comparative global warming potential of methane), which is helpful for those companies interested in reducing greenhouse gas emissions. Finally, the profiles present site-specific information on the conditions that affect the potential for particular types of methane use projects, such as distances to the nearest natural gas transmission lines , the name of the electricity supplier and a mine's estimated electricity demand. All told, these profiles contain the essential facts any company or agency needs to begin evaluating mines for methane projects.

Carrying this mine-specific analysis further, the Coalbed Methane Outreach Program recently developed detailed economic assessments of several mine-specific projects. These assessments give potential investors a clearer idea of how profitable mine methane projects may be [3]. The assessments examine pipeline and power generation options under a number of different project and wellhead gas price scenarios. They show that at many mines attractive returns on a mine methane investment are possible even with the most conservative of assumptions. Together, the profiles and economic assessments point the way towards a number of creative projects.

ALTERNATIVE MARKETS FOR COALBED METHANE

Some mines, even those with degasification systems, may not be able to profitably sell their methane to a natural gas transmission company. The nearest transmission line may be prohibitively far from the mine. The quality or quantity of gas may be too low to justify the costs of gas cleaning or pipeline construction. Or the transmission company may not want to purchase the gas. In fact, for any number of reasons, a coal mine might conclude that a particular pipeline project would not be the ideal investment. In such situations, coal mines may find alternative uses and markets for their methane much more desirable.

The Coalbed Methane Outreach Program is currently working with several coal companies to identify profitable alternative mine methane uses. Usually these alternative uses are site-specific. What may work at one mine in one area, with its region's industries and energy demands, may be unwise at another mine. In general, however, there are three different types of alternative uses for medium and high quality methane: (1) direct on-site industrial uses, such as coal drying, (2) on- or off-site power generation, or (3) off-site industrial or commercial uses, such as building heating.

Coal mines might discover that they can use their methane on-site and increase coal production while lowering fuel costs. Nearly all large underground coal mines have preparation plants located nearby. Mines have traditionally used their own coal to fuel these plants. While no U.S. coal mines currently use recovered methane to fuel a preparation plant, several Polish mines successfully have. The CMOP is developing an economic and technical study to evaluate this option, which might be an attractive way for a coal mine to use a waste fuel (its methane) and sell more of the coal it now burns up in the prep plant.

Given the large energy requirements of coal mines, they may realize significant cost savings by generating power from recovered methane. Nearly every piece of equipment in an underground mine operates on electricity, including mining machines, conveyor belts, ventilation fans, and elevators. A mine's electricity bill can exceed several million dollars a year. Even with these significant electricity demands, however, large and gassy mines may be able to generate power in excess of on-site demand. In such cases, a mine may profit from selling power to a nearby utility. Under some circumstances, a mine might arrange to sell electricity to a utility, but continue to purchase electricity from the utility for its own on-site uses. The Coalbed Methane Outreach Program is evaluating power markets and working with utilities to involve them where possible in mine methane power generation projects.

Selling recovered methane to a nearby industrial or institutional facility may also be a promising option, especially for mines emitting significant quantities of medium quality gas, which requires cleaning to make pipeline quality. An ideal gas customer would be close to the methane source and have continuous demand for fuel. Both medium- and high-quality mine methane could fuel a cogeneration system, fire boilers or chillers, or provide space heating.

Difficulties in financing an otherwise economically-sound coal mine methane recovery venture can obstruct project development. To address this barrier, the Coalbed Methane Outreach Program has prepared finance opportunity guides describing Pennsylvania, West Virginia and federal programs that could provide financial and technical assistance [4, 5, 6]. Interested parties that may benefit from assistance programs include coal companies that own gassy mines, local governments interested in promoting local development, industries that could use recovered methane as a source of fuel, natural gas companies and electric utilities.

Since coal companies, local governments, and local or regional businesses all can gain from a coal mine methane project, they may consider jointly developing projects. Many financing opportunities require or encourage such partnerships. For instance, a local government may wish to partner with a coal

company as a means of obtaining an inexpensive local fuel source for businesses in an industrial park or municipal buildings. A local government could apply for infrastructure, energy, or economic development assistance and benefit from improved infrastructure and a stronger tax base. By partnering, the coal mine would have overcome the financing barriers to starting a project, and would have a solid consumer for its formerly wasted methane. The fuel users would enjoy improved infrastructure and lower heating costs. In addition, the methane heating project would directly provide jobs, and by lowering an industrial park's operating costs, make the operation more competitive, indirectly creating additional jobs.

A Coalbed Methane Outreach Program study, *The Environmental and Economic Benefits of Coalbed Methane Development in the Appalachian Region,* demonstrates why a number of state and federal programs may wish to finance coal mine methane projects [7]. Using conservative assumptions, the study found that over 6,000 jobs could be created by 2010 with the profitable recovery of coal mine methane in the Appalachian Region. The study estimated that state revenues would be around twenty million dollars. [See Tables 2 and 3.] The environmental benefits would also be significant. Profitable projects in the Appalachian Region would reduce U.S. methane emissions from coal mining by ten to twenty percent, representing the amount of CO_2 emitted by one to two million cars.

OPPORTUNITIES FOR ELECTRIC UTILITIES TO SUPPORT COAL MINE METHANE PROJECTS

Electric utilities that project increasing emissions of greenhouse gases may be especially interested in participating in coal mine methane recovery projects to offset their emissions. Many have joined DOE's Climate Challenge program, which encourages utilities to voluntarily reduce their greenhouse gas emissions. Mine and project specific economic analyses recently developed by the Coalbed Methane Outreach Program show that a number of mine methane projects may be both cost-effective and generate revenues for utilities seeking projects.

Further, as Table 1 indicates, reducing methane emissions from any of a number of coal mines could be a very effective strategy to reduce greenhouse gases. Even relatively large utilities could find from 25 to over 100 percent of their 1990 to 2000 emissions increase could be offset with one large coal mine methane project. Mine methane projects are likely to be one of the least costly emissions reduction investments, and have the added advantage of being easily verified and relatively simple to execute.

Utilities may discover flaring coal mine gas is a low-cost means of obtaining very significant greenhouse gas emission reductions. A draft CMOP report, *A Technical and Economic Assessment of the Potential to Flare Methane Emissions from Coal Mines* suggests that the flaring of mine methane gas may be a safe, inexpensive investment [8]. Even with the most conservative of safety features added to a system, it estimates that at many mines flaring would cost around or under one dollar per ton of carbon dioxide equivalent emissions reduced. This compares favorably to the costs of other mitigation options, such as forestry projects. Average domestic forestry project costs are estimated to be over two dollars per ton of carbon dioxide sequestered [8]. Utilities could acquire very significant reductions from one coal mine methane flaring project at an extremely competitive price.

Coal companies and utilities are free to develop any sort of methane reduction project. In fact, the unique relationships that many utilities have with coal companies provides opportunities for some interesting and mutually beneficial agreements:

- "Green Coal" deals -- coal companies may find that marketing methane reductions with coal purchases will make their coal more competitive or the terms of contracts more favorable.
- SO_2 - CO_2 Swap – utilities seeking sulfur dioxide pollution allowances may wish to invest in a revenue-generating coal mine methane project, achieve emission reductions above its Climate Challenge goal, and trade these reductions to a utility with excess SO_2 allowances and significant projected growth in its greenhouse gas emissions as Niagara Mohawk and Arizona Public Service did [9]. Coal companies could also participate in an emissions swap.
- Smaller utilities or utilities with modest emissions reduction goals or diversified reduction strategies may wish to invest in a multi-utility project and share the profits and emission reductions. The joint venture could request proposals from coal mines and invest in the most competitive.
- Coal companies could develop a methane recovery project and market the emission reductions for cash. This scheme presents the least degree of risk for a utility and may bring the highest returns for a coal company.
- Utilities and coal companies could be joint investors in a project. The emissions reductions could be transferred completely to the utility, the coal company in return could take a greater share of the profit or negotiate better terms for a coal sale.

Coal companies and utilities could develop any of a number of alternative schemes.

CONCLUSION AND A LOOK AT FUTURE CMOP ACTIVITIES

The prospects for coal companies and their partners to develop profitable mine methane projects are great. The Coalbed Methane Outreach Program has prepared reports and economic assessments that will help potential investors identify the best projects to meet their varying objectives. Coal mine methane use projects can serve a number of mutually-supporting ends, including mine safety, increased coal production, lower energy costs while using more of America's energy resources, and greenhouse gas emission reductions. The Program will continue to provide information, analysis, and forums for discussion that will lower the threshold to profitable recovery and use, ultimately benefitting the U.S. economy and the global environment.

NOMENCLATURE

Bcf	=	billion cubic feet
CMOP	=	Coalbed Methane Outreach Program
DOE	=	U.S. Department of Energy
EPA	=	U.S. Environmental Protection Agency
mmcfd	=	million cubic feet per day
mm Tons/Year	=	million metric tons per year

REFERENCES

1. Clinton W.J. and A. Gore, eds., 1993: The Climate Change Action Plan: 50 p.
2. EPA (1994a): Identifying Opportunities for Methane Recovery at U.S. Coal Mines: Draft Profiles of Selected Gassy Underground Coal Mines: U.S. Environmental Protection Agency/Office of Air and Radiation, EPA-430-R-94-012.
3. EPA (1995a): Economic Assessment of the Potential for the Cost-Effective Recovery and Utilization of Methane at Ten Gassy Underground Mines in the U.S.: U.S. Environmental Protection Agency/Office of Air and Radiation (in preparation).
4. EPA (1995b): Financing Opportunities for Coal Mine Methane Projects: A Guide for Pennsylvania: U.S. Environmental Protection Agency/Office of Air and Radiation (in preparation).
5. EPA (1995c): Financing Opportunities for Coal Mine Methane Projects: A Guide for West Virginia: U.S. Environmental Protection Agency/Office of Air and Radiation (in preparation).
6. EPA (1995d): Financing Opportunities for Coal Mine Methane Projects: A Guide for Federal Programs: U.S. Environmental Protection Agency/Office of Air and Radiation (in preparation).
7. EPA (1994b): The Environmental and Economic Benefits of Coalbed Methane Development in the Appalachian Region: U.S. Environmental Protection Agency/Office of Air and Radiation, EPA-430-R-94-007, 30 p.
8. EPA (1995e): A Technical and Economic Assessment of the Potential to Flare Methane Emissions from Coal Mines: U.S. Environmental Protection Agency/Office of Air and Radiation (in preparation).
9. EPA (1994c): "Did You Hear? APS and Niagara Mohawk Swap SO2 Allowances for CO2 Credits" Coalbed Methane EXTRA, V. 1, No. 1, p. 1, U.S. Environmental Protection Agency/Office of Air and Radiation, EPA-430-N-94-019.

TABLES

Table 1: Estimated 1990 Degasification Emissions and CO_2 Equivalent from U.S. Mines with Degasification Systems

Mine Name	Degasification Emissions (mmcfd)	CO2 Equivalent (mm Tons/Year)
Gary No. 50	7.8	1.27
VP No. 1	7.5	0.96
Federal No. 2	5.7	0.92
Blacksville No. 2	5.0	0.81
Humphrey No. 7	3.4	0.55
Golden Eagle	3.3	0.53
Cumberland	3.1	0.51
Dutch Creek M & B	3.1	0.51
Loveridge No. 22	2.7	0.45
Blacksville No. 1	2.6	0.43
Bailey	2.6	0.42
Arkwright No. 1	2.1	0.34
Osage No. 3	2.0	0.33
Cambria No. 33	1.8	0.30
Emerald No. 1	1.7	0.27
Amonate No. 31	1.2	0.19
Robinson Run No. 95	1.1	0.18
Old Ben No. 25	1.0	0.17
Old Ben No. 26	1.0	0.16
Deserado	0.8	0.13
Wheatcroft No. 9	0.3	0.05
Eagle No. 5 & 6	0.1	0.01
Enlow Fork	0.1	0.02
TOTAL	**60.0**	**9.51**

Table 2. Estimated Employment Associated with Coalbed Methane Production in the Appalachian Region

	Low Scenario		High Scenario	
State	2000	2010	2000	2010
Ohio	150	645	185	720
Pennsylvania	400	1865	525	2295
Virginia	255	365	370	435
West Virginia	1200	3545	1700	4315
TOTAL	**2000**	**6420**	**2780**	**7765**

Table 3. Estimated State Revenues Associated with Appalachian Region Coalbed Methane Production (in millions of $1990)

	Low Scenario		High Scenario	
State	2000	2010	2000	2010
Ohio	0.1	0.6	0.2	0.8
Pennsylvania	NA	NA	NA	NA
Virginia	0.4	1.1	0.7	1.4
West Virginia	3.3	17.4	5.5	22.5
TOTAL	**3.8**	**19.1**	**6.4**	**24.6**

INTERGAS '95

May 15-19, 1995
The University of Alabama
Tuscaloosa, Alabama USA

9551

Development and Utilization Strategies for Recovery and Utilization of Coal Mine Methane

C.W. Byrer, A.W. Layne and H.D. Guthrie, U.S. Department of Energy, Morgantown Energy Technology Center

ABSTRACT

The U.S. Department of Energy (DOE), at its Morgantown Energy Technology Center, has been involved in natural gas research since the 1970's. DOE has assessed the potential of gas in coals throughout the U.S. and promoted research and development for recovery and use of methane found in minable and unminable coalbeds. DOE efforts have focused on the use of coal mine methane for regional economic gas self-sufficiency, energy parks, self-help initiatives, and small-power generation. This paper focuses on DOE's past and present efforts to more effectively and efficiently recover and use this valuable domestic energy source.

The Climate Change Action Plan (CCAP) [1] lists a series of 50 voluntary initiatives designed to reduce greenhouse gas emissions, such as methane from mining operations, to their 1990 levels. Action No. 36 of the CCAP expands the DOE research, development, and demonstration (RD&D) efforts to broaden the range of cost-effective technologies and practices for recovering methane associated with coal mining operations.

The major thrust of Action No. 36 is to reduce methane emissions associated with coal mining operations from target year 2000 levels by 1.5 MMT of carbon equivalent. DOE/FE proposes to implement a near-term effort compatible with existing RD&D programs to meet the Administration's goal and the Energy Policy Act of 1992 concerning coal seam gas emissions from coal mining.

Crosscutting activities in the DOE Natural Gas Program supply and utilization sectors will address RD&D to reduce methane emissions released from various mining operations, focusing on recovery and end use technology systems to effectively drain, capture, and utilize the emitted gas. Pilot projects with industry partners will develop and test the most effective methods and technology systems for economic recovery and utilization of coal mine gas emissions in regions where industry considers efforts to be presently non-economic.

These existing RD&D programs focus on near-term gas recovery and gathering systems, gas upgrading, and power generation. Methods include lower cost, higher recovery drilling methods for pre-mining and post-mining recovery for pipeline injection and electricity generation. The RD&D effort also evaluates and demonstrates the use of fuel cells, gas turbines, and other state-of-the-art technologies for waste methane utilization, transferring appropriate practices to the gas, coal, and power industries.

INTRODUCTION

The Appalachian Coal Basin extending from Pennsylvania to Alabama has tremendous potential for developing natural gas from shallow multiple gas-bearing strata, such as shallow coalbeds (Figure 1).

The region is composed of portions of eight states: Pennsylvania, West Virginia, Ohio, Kentucky, Maryland, Virginia, Tennessee, and Alabama. Most of these states have not developed the remaining shallow gas sources, particularly associated with coalbeds. West Virginia and Pennsylvania, for example, have long been energy producing states with very large coal and natural gas reserves. The states are situated in the heart of this region and are representative of the potential existing in the other Appalachian coal and gas-bearing states. The states of Virginia and Alabama have already been involved in producing coalbed gas.

Estimates by the U.S. Geological Survey, for example, show that West Virginia has a 300-year supply of coal and nearly 200 years of natural gas. Data compiled by the U.S. Energy Information Administration shows the annual coal production for West Virginia at 170 million tons and gas production is about 170 billion cubic feet (Bcf) of gas per year [2]. West Virginia is the only eastern state which produces enough natural gas to meet its needs and then export (out-of-state) 76 Bcf of gas to nearby gas markets [3]. Other states in the Appalachian basin could become greater gas producers and even exporters of gas if shallow gas resources are considered (Figure 2).

Tremendous volumes of natural gas are found in the shallow unmined strata of Appalachian coals. Coal is an energy resource with "dual-fuel" capability: the solid coal and the gaseous fuel within the coal matrix - methane or natural gas. Coal

mine methane or "coal damp" has long been considered a nemesis by the coal industry (Figure 3). During the 1980's coalbed methane became recognized as a valuable domestic energy resource. Methane is found in various types of coal in 37 states. DOE and the Gas Research Institute have estimated the coalbed methane resource for the U.S. at 400 trillion cubic feet of gas-in-place. West Virginia, alone, has over 40 trillion cubic feet of methane in its numerous coalbeds.

The U.S. DOE, at its Morgantown Energy Technology Center, has been involved in natural gas research since the 1970's. Research efforts have been focused to enhance development of "nonconventional gas resources" from Devonian shale, coalbeds, tight sands, hydrates, deep sedimentary basins, geopressurized aquifers, and complex, mature reservoirs.

The U.S. DOE has assessed the potential of gas in coals throughout the U.S. and promoted research and development for the recovery and use of methane found in minable and unminable coalbeds. DOE efforts have focused on the use of coal mine methane for regional economic gas self-sufficiency, energy parks, self-help initiatives, co-generation, and small-power generation potential.

The northern and central Appalachian region has been of keen interest to DOE because of the large gas resource in the various coal mines and because of its proximity to the eastern gas market, presently one of the largest gas markets in the U.S. In cooperation with the EPA, DOE is currently focusing on these two regions for implementation of the CCAP initiative of the Clinton Administration.

Climate Change Action Plan

The initiative set forth by the Clinton Administration in the CCAP is to reduce greenhouse gas emissions to 1990 levels by the year 2000. Methane emissions from coal mining operations have been one of the sources targeted for reduction during this period. The current rate of emissions from (Figure 4) coal mining operations is estimated at 300 Bcf per year, and these emissions are projected to increase by 39 to 50 percent in 2010.

The President's pledge to reduce greenhouse gases currently escaping into the atmosphere will place continued pressure on the coal industry to recover and utilize methane associated with coal mining operations. The remedial options for reducing methane emissions could be handled either by regulation or by development of relevant methane capture and recovery technologies. However, the development of these technologies affords an enhanced solution which reduces methane emissions, recovers a previously wasted energy resource, and enhances the mining of coal.

Each coal basin has different geologic settings with eastern U.S. minable coals having region-specific problems when various mining technologies affect the target coal and associated gas-bearing strata. Most of the underground mining operations in the U.S. are in these eastern basins with methane emissions associated with each mine. Because of required safety considerations during mining, venting methane has been standard mining practice for decades. Development of more effective technologies are required to capture and upgrade gas from minable coals and nearby gas-bearing strata.

Under the CCAP, pilot projects with industry partners are planned by DOE to develop and test the most effective methods and technology systems for economic recovery and utilization of mine gas emissions in regions where industry considers efforts to be presently non-economic. By 1995, demonstration efforts could be initiated to develop an optimal well placement and completion methane recovery system for minable coal seams. Simultaneously, pilot projects could demonstrate utilization options for power generation, heating source for coal drying, and/or an alternate fuel for transportation.

Coal Mine Methane Resources

One of the areas in which DOE has been actively involved is the enhancement of mine safety with reductions in methane in minable coals. Degasification of coalbeds prior to mining with various vertical and in-mine horizontal drilling has been part of the program effort to capture and use methane associated with mining operations in the U.S.

Since 1987, DOE has been assessing the potential for retrieving coalbed gas from vertical degasification wells above active longwall panels. The theme of DOE's research effort in this area has unofficially been "Mine Safety at a Profit," effectively and efficiently reducing methane levels within the mine in order to reduce "down time" of coal production and enhance mine safety while selling the gas for additional profit to the mine operator.

West Virginia, Pennsylvania, Alabama, and Virginia lead the country in longwall mining systems and have tremendous potential for developing the mine gas presently vented to the atmosphere [4] (Figure 5). Geologic strata above minable coals usually include gassy coals, sands, and shales representing a large multiple-strata reservoir of natural gas. The DOE has been involved in supporting efforts to produce shallow gassy coals and shallow historical gas sands from single multiple completion wells [5].

During longwall mining operations, rock strata above the minable coalseam fracture and collapse into the mined-out cavity (Figure 6). The zone in which the overlying rock breaks and fractures is referred to as the "gob." As a result of the large increase in permeability with subsidence of the roof rock in the mined-out area, methane gas is released from overlying coal seams and other gas-bearing formations and flows into the gob area. The release of large volumes of methane pose serious ventilation problems in longwall mines, and effective removal of the gas from the mine becomes a primary safety concern.

Vertical wells are drilled and completed prior to actual longwall mining operations. These wells are usually completed to a depth above the

minable coal with the bottom sections of casing slotted to allow methane to flow into the wellbore (Figure 7).

Utilization of Coal Mine Methane

Often methane emissions released during the mining process are contaminated with gases other than methane. If the gas is to comply with pipeline quality standards and be transported to an end-use site, these contaminated gases need to be removed from the methane stream. Alternatively, these low-quality gases may be used as an energy source for on-site mine power generation. Efforts to demonstrate existing or new gas technology systems could lead to upgrading mine emissions to pipeline quality or to new methods for utilizing these gases as a mine-power source (Figure 8).

Coal Mine Methane Pipeline Injection

Under the Climate Change Action initiative, coal mine gases may be upgraded or gathered, and injected into a natural gas pipeline. Based on past experience in the Appalachian Basin, tremendous potential exists for capture of coal mine emissions and injection into natural gas pipelines.

Jim Walter Resources, a large mining operator in Alabama, has been selling coalbed methane from its longwall mining operations for nearly 10 years. The company produces over 40 million cubic feet per day of pipeline quality gas from its longwall mine degasification system. About 4 million cubic feet of gas per day can be attributed to in-mine horizontal boreholes. The balance of the gas is collected by over 85 active gob-gas recovery wells that have produced over 50 Bcf of coalbed methane for pipeline utility use [6].

In 1992 a 40-mile pipeline located in Virginia was completed by two of the larger coal operators in Appalachia for the purpose of capturing and selling their mine gas to a pipeline utility. Some of these longwall mining gob wells have been reported to produce several million cubic feet of pipeline-quality methane a day [7].

The CCAP, Action 36 will build on this experience and effort gained in the Southern and Central Appalachian basins to further reduce coal mine methane emissions in the United States.

Power Generation with Mine Gases

Prior DOE field pilot projects have demonstrated the use of internal combustion engines and gas turbine systems for limited on-site mine gas utilization. Other nations are currently utilizing gas turbines to generate power for on-site mine use. These efforts are a larger scale than any previous demonstrations at U.S. coal mines. Currently and historically, DOE/FE has successfully demonstrated advanced power systems with alternate fuel sources such as low quality gas and synthetic gas from coal.

Over the next decade, there will be an increase in demand for clean, efficient sources of electrical power generation. Utilizing mine gases as an additional source of fuel for advanced gas turbines and fuel cells could satisfy this increase, or provide coal mines with an ample power source.

The phosphoric acid fuel cell has produced energy conversion efficiencies that range from 50 to 60 percent, and respond smoothly to cold starts within hours. For remotely located areas, fuel cells offset the costs of right-of-way access and transmission and distribution lines. The fuel cell is inherently modular and can be configured in a wide range of electricity outputs. The primary fuel source is hydrogen, which can be obtained from natural gas, coal-gas, methanol, and other fuels containing hydrocarbons (coal mine methane). Gas turbines offer similar characteristics as the fuel cell in efficiency, low emissions, and modularity. The energy conversion for the gas turbine has been demonstrated on medium quality coalbed methane. Both technologies could enhance the current coalbed methane utilization program through demonstrations of integrated mine gas power generation systems.

Novel Technology Using Coal Mine Methane

Along with the approaches listed above for developing and using coal mine methane resources, the U.S. DOE has been sponsoring the development of a novel technology for improving disposal options of produced waters from coalbeds and gas sands. This effort is being developed by Aquatech Services in conjunction with Lawrence Livermore National Laboratory and the College of West Virginia. This evolving technology consists of a submerged evaporator in conjunction with reverse osmosis for disposal and/or usage of produced brine waters [8]. Presently, this technology is being tested at a large coal mine in Upper Silesia, Poland. A successful field demonstration of this evolving technology could give coal and gas industries an economic option in treating or disposing of produced waters rather than the re-injection wells approach. It also reduces a potent greenhouse gas by using the methane as a fuel source for the technology (Figure 9).

Benefits to the Appalachian and Other Coal Regions

With more and more emphasis on environmental concerns for improved air and water quality, particularly in reducing greenhouse gas emissions, DOE's efforts toward demonstrating applicable and evolving technologies for using coal mine methane supports the initiatives under the CCAP.

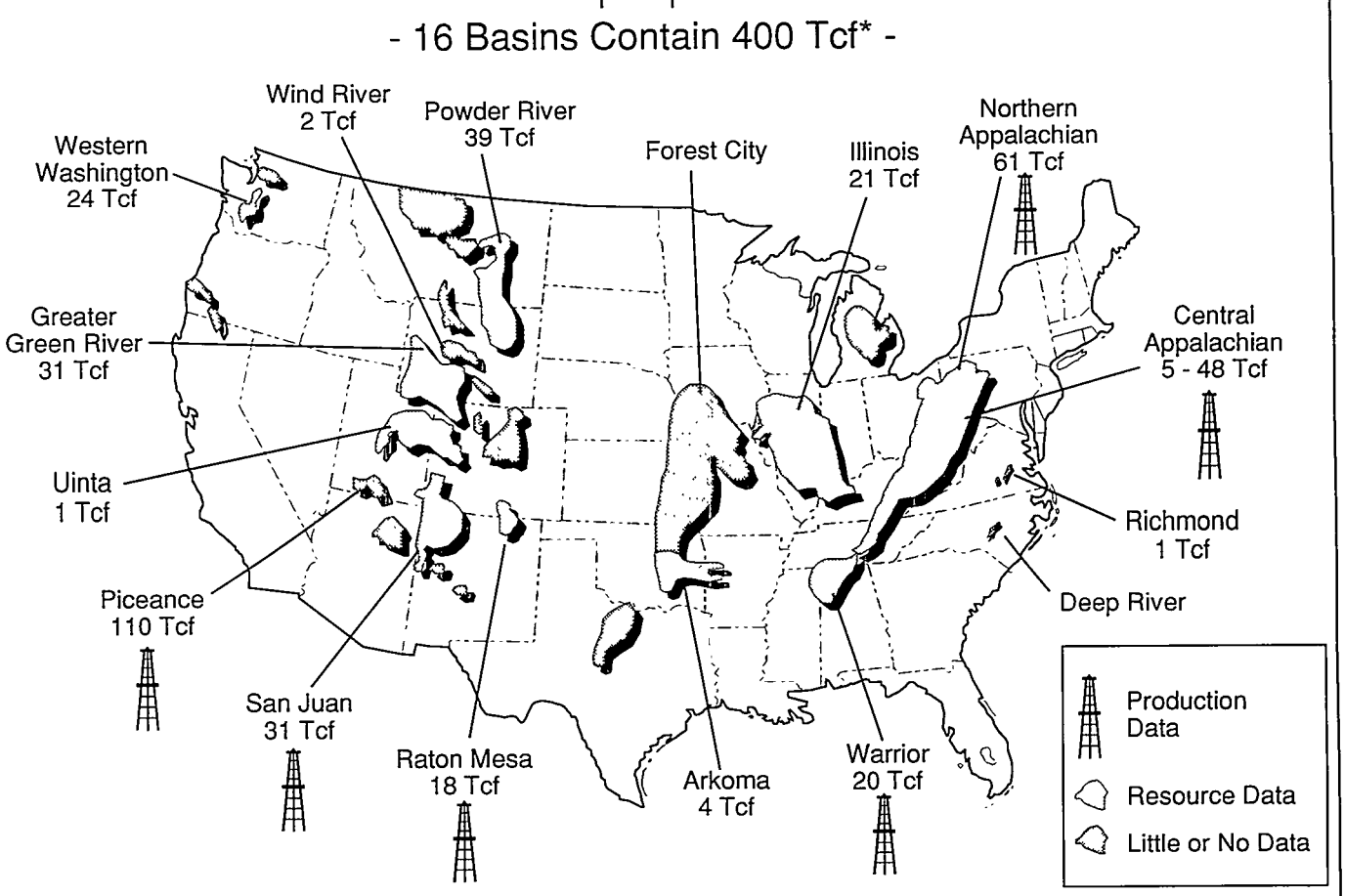
The successful commercial efforts described herein involve shallow, multiple gas-strata of coals, sands, and shales. The potential for northern Appalachia to develop gas from these multiple strata involving coalbeds is great. The shallow-gas strata represent a large energy resource in Appalachia which could be very beneficial to the coal companies, natural gas and electric power utilities, local municipalities, institutions, and the industrial sector.

Similar coal basins in the U.S. and in other coal-bearing countries are potential sites for further demonstration of the approaches discussed herein. Coal mine gas in Appalachia is

an abundant, shallow source of natural gas which could supply cheaper energy for local industrial (or energy) parks or maintaining and attracting industry. The technology developed or applied for domestic coal mine methane utilization holds both regional and global market potential.

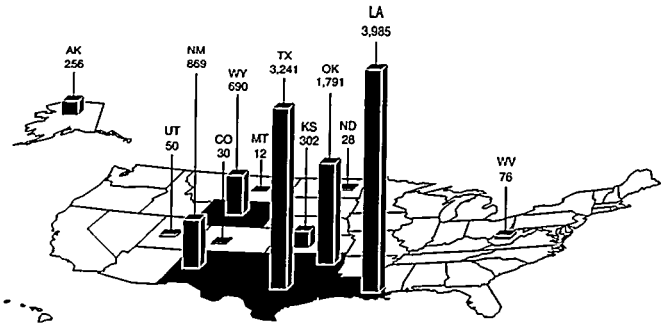
REFERENCES

1. The Climate Change Action Plan: Technical Supplement, U.S. DOE, March 1994.
2. Annual Outlook for Oil and Gas 1993, Energy Information Administration, U.S. DOE, Washington, DC.
3. Natural Gas Trends, North America, 1992, Arthur Anderson/Cambridge Energy Research Associates, Houston, Texas and Cambridge, Massachusetts.
4. Longwall Census, COAL, February 1994.
5. A Novel Geotechnical/Geostatistical Approach for Exploration and Production of Natural Gas from Multiple Geologic Strata, Topical Report, May 1991, BDM Engineering Services Company, Morgantown, West Virginia.
6. Underground Developments in Methane Recovery, COAL, December 1990, pp. 55-59.
7. Past Reflections - Future Perspectives, 1994 Spring Session, Pittsburgh Coal Mine Methane Forum, Pittsburgh, Pennsylvania.
8. Process for Coal Mine Brine Disposal, The American Oil & Gas Reporter, September, 1992.



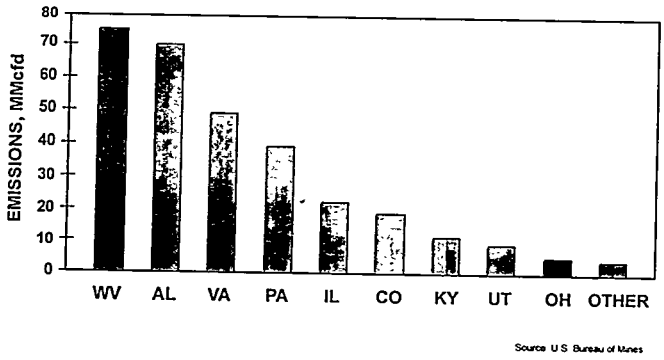
* This represents 8 Eastern Coal Basins and 8 Western Coal Basins.

Figure 1. Coalbed methane production and resource data in U.S. basins.



Source Natural Gas Trends, 1992

Figure 2. West Virginia is the only eastern state with net marketed production (Bcf).



Source U S Bureau of Mines

Figure 4. Distribution of 1988 gas emissions from U.S. coal mines.

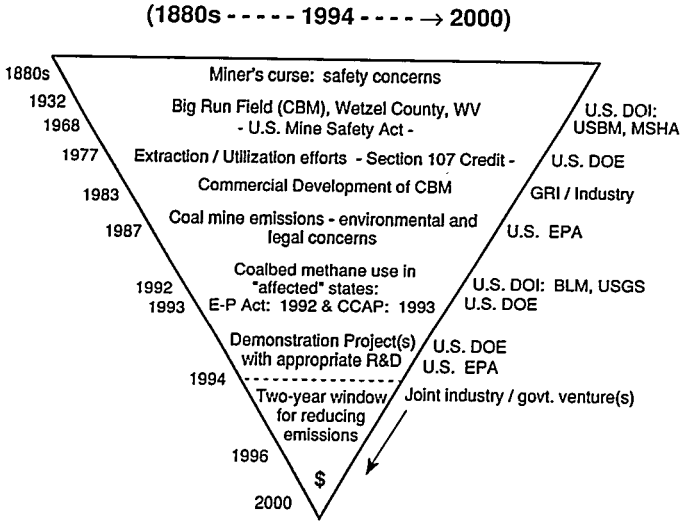


Figure 3. Chronology of coalbed methane development.

Mining Companies	No. of Longwalls
Consolidated Coal	24
Jim Walter Resources	7
Peabody Coal	6
Cyprus Amax	6
Zeigler	5
U.S. Steel Mining	4
BethEnergy Mines	3
American Electric Power	3
Coastal States Energy	3
Energy West	2
Kerr-McGee Coal	2
Mapco	2
Pittsburgh & Midway	2
Westmoreland	2
Total	71

Reference Coal, February 1994

Figure 5. Longwall mining technology in the U.S. Top 14 longwall mining companies (1994).

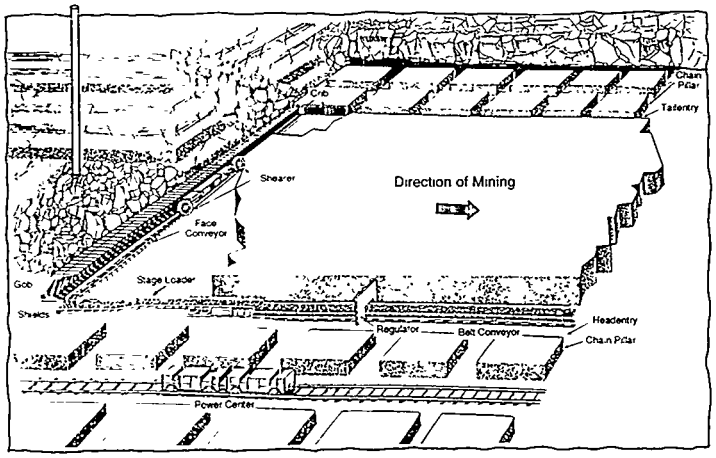


Figure 6.

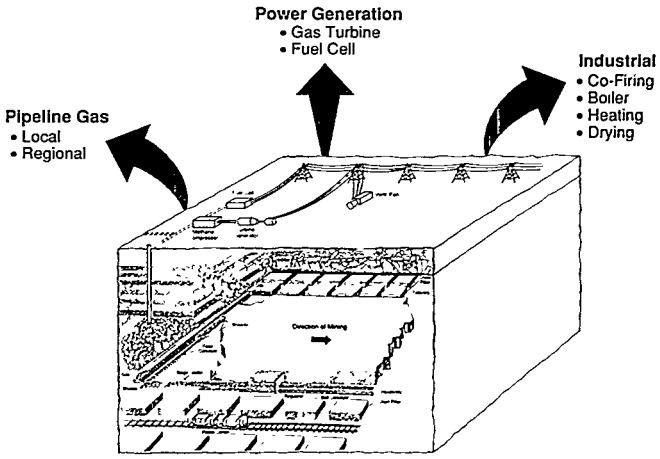


Figure 8. Coal mine gas utilization options.

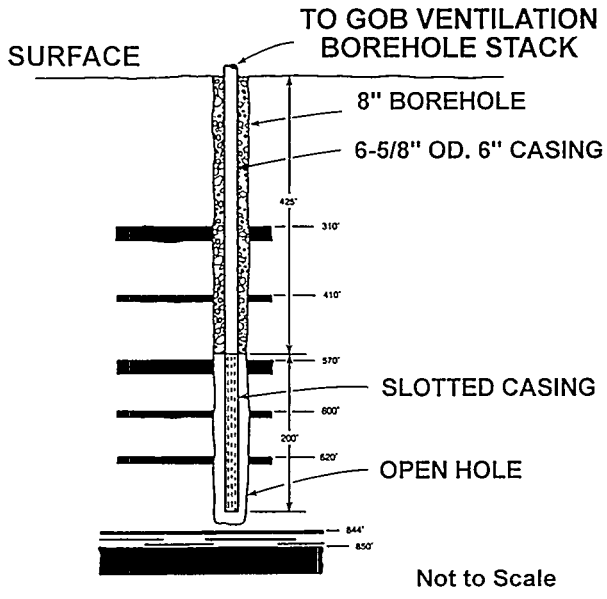


Figure 7. Completed gob gas ventilation borehole.

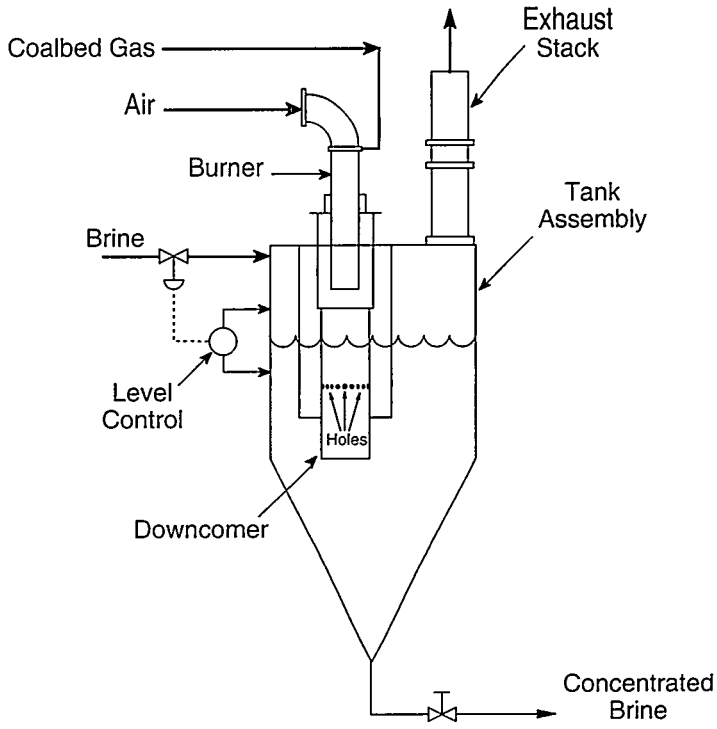


Figure 9. Aquatech Services' submerged combustion evaporator for brine evaporation process using coalbed gas production.

INTERGAS '95

May 15-19, 1995
The University of Alabama
Tuscaloosa, Alabama USA

9513

Recent Federal Initiatives to Promote Unconventional Gas: High Octane Delivery or Just Hot Air?

M.T. Griff, Berkowitz, Lefkovits, Isom & Kushner

ABSTRACT

This paper provides an overview of recent initiatives of the United States which promote greater use of natural gas and unconventional gas as one part of this nation's larger response to the global warming threat. Measurable increases in greenhouse gas concentrations since the beginning of the industrial revolution have led to the belief in the existence of a global warming problem. The international community has responded to the global warming threat with the United Nations Framework Convention on Climate Change which is directed toward the stabilization of greenhouse gases in the atmosphere. The Climate Change Action Plan is the Clinton Administration's detailed response to the global warming threat. It is designed to return United States emissions of greenhouse gases to their 1990 levels by the year 2000. The Action Plan targets all greenhouse gases and emphasizes energy efficiency. Significant regulatory reformation designed to increase the efficiency of the natural gas industry has already occurred and will be continued. Recovery of methane emissions from landfills will be encouraged through identification of suitable sites and use of existing technology and development of new technology. Recovery of methane from coal mining operations will be promoted by targeting 50 of the gassiest mines in the United States. Even if the Action Plan is fully implemented, legitimate questions arise as to whether its goals will be achieved as a result of funding shortfalls.

INTRODUCTION

This paper presents an overview of recent initiatives of the United States to promote the use of natural gas and unconventional gas that are a direct outgrowth of the perceived global warming threat. "Unconventional gas" as used in this paper denotes methane from landfill sites and coal mining operations.

The global warming threat, the object of much skepticism, has at its root verifiable measured increases in atmospheric concentrations of certain greenhouse gases. The first part of the paper provides a general review of the bases for the belief there is a global warming risk and discusses the adverse consequences that some are predicting may result.

Despite the uncertainties associated with global warming, in 1992 the international community negotiated the United Nations Framework Convention on Climate Change (Framework Convention) in which a plan for international action to address this threat has been developed [1]. In the second part of the paper, the Framework Convention is discussed, highlighting key provisions of the agreement.

In response to the Framework Convention, the United States developed the Climate Change Action Plan (Action Plan) which is designed to be its blueprint for responding to the global warming threat. The third part of the paper summarizes key features of the Action Plan and focuses on its specific initiatives which are directed toward achieving enhanced natural gas use and methane recovery.

The last part of the paper briefly addresses what the future may hold for achieving the goals of the Action Plan.

A LOT OF HOT AIR- THE GLOBAL WARMING PROBLEM

On an annual basis, human activity adds approximately six billion tons of carbon into the atmosphere chiefly from the burning of fossil fuels.

This amount represents more than a ton for every human being on the planet.

Scientists have estimated that if current human activities leading to the increasing atmospheric concentrations of certain emissions go unchecked, the earth will warm in the range of approximately 2 to 5 degrees Centigrade (3.6 to 9 degrees Fahrenheit) by the end of the next century [2]. Although skepticism abounds with respect to the consequences of these underlying atmospheric increases, some have predicted such a temperature rise could lead to devastating effects on the human environment and the global ecosystem, such as the loss of forests and wetlands, shifts in agricultural zones, impaired water resources, hurricanes, storm surges and flooding of low-lying coastal regions and islands.

This global warming is predicted to result from increases in certain atmospheric gases as the direct result of human activity in combination with the naturally occurring phenomenon known as the "greenhouse effect." The greenhouse effect is the process by which certain trace gases in the atmosphere allow visible light from the sun to pass through the atmosphere but trap the infrared wavelengths radiated back by the earth reradiating them as heat and thereby raising the earth's temperature. In the absence of the naturally occurring greenhouse effect, the earth would be 33° Celsius (60° Fahrenheit) colder.

The most important naturally occurring greenhouse gas is water vapor. Other greenhouse gases which also occur naturally, but which are increasing as a result of "anthropogenic" (human induced) activity, include carbon dioxide (CO_2), methane, nitrous oxide, and ozone.

Principally as a result of industrialization and population growth, the atmospheric concentration of greenhouse gases has increased dramatically. While most of these increases are attributable to the burning of fossil fuels, deforestation is also believed to have resulted in a substantial increase in the amount of CO_2 in the atmosphere. Since the beginning of the industrial revolution, scientists have calculated the atmospheric concentration of CO_2, which accounts for more than 50% of the predicted warming, has increased by 25% and continues to increase at a rate of approximately 0.5% per year. While the impacts of methane are less well understood, its concentrations have doubled over the same period and are increasing at a rate of approximately 0.9% per year. Significantly, methane is estimated to be between 11 and 22 times more effective at trapping heat in the atmosphere than CO_2 [2].

These increased greenhouse gas concentrations have outpaced their removal by so-called "sinks." Sinks occur naturally and during pre-industrial times kept atmospheric concentrations at relatively constant levels. Carbon sinks include plants and trees which absorb CO_2 through photosynthesis and oceans which take up carbon at the surface and store it within the ocean. Other greenhouse gases are removed from the atmosphere largely through atmospheric reactions.

Most climate scientists view the increases in greenhouse gases as leading to an anthropogenic greenhouse effect, although the rate, magnitude, timing and impacts are highly uncertain. The imprecision in determining the likely effects of increasing greenhouse gas emissions is due largely to the fact that predictions of global warming are based primarily on computer models of the atmosphere. These, however, have not yet been confirmed by available temperature records. Further uncertainty results from the predicted secondary effects of global warming, such as the increased cloud cover that may occur, and whether these secondary effects will enhance or offset global warming.

THINGS HEAT UP- THE INTERNATIONAL RESPONSE

There are two general policy responses that are available to meet the threat of global warming. These are abatement and adaptation. Adaptation involves a responsive course of action to the adverse effects of global warming, such as through greater reliance on air conditioning or building or improving sea walls to avoid coastal flooding. Abatement involves reducing greenhouse gas emissions and enhancing sinks.

Notwithstanding the uncertainties associated with the possible effects of the increases in greenhouse gas concentrations, the international community has taken significant steps to prevent global warming. These have generally focused on wealthier, industrialized countries assuming the lead on efforts to abate greenhouse gases, chiefly CO_2, and to a lesser extent, methane and nitrous oxide [3].

As might be expected, practical and political considerations have shaped the debate on and the international response to the threat of global warming. On the one hand, as a general rule only industrialized countries have sufficient resources to dedicate to the problem of global warming. There is some rough equity in this, however, since industrialized nations are responsible for approximately 75% of the CO_2 emissions occurring worldwide and their contributions to greenhouse gases emissions are generally higher on

a per capita basis. Indeed, it has been calculated that the United States is responsible for about one-quarter of the worldwide total. On the other hand, developing countries, with 80% of the world's population, account for only 25% of the total global CO_2 emissions (although these emissions are predicted to increase significantly in the near term as development accelerates in these countries). Even if developing countries have the resources to direct to abating greenhouse gas emissions, generally these countries resist efforts to do so. They view such actions as compromising their future development so as to meet a problem created by the industrialized countries in the first instance [3].

By the late 1980s, the international community was sufficiently convinced that increasing greenhouse gas concentrations necessitated a coordinated response. The Framework Convention which was opened for signature at the 1992 Earth Summit in Rio de Janeiro, Brazil, is the world's formal reaction to the global warming threat. In rapid fashion, especially for an international treaty of this sort, the Framework Convention entered into force in March 1994, just 20 months from its opening signature. As of February 1995, 120 nations had become signatories to the Framework Convention.

The Framework Convention has been viewed both as a success and a failure for what it includes and omits. To those who view it favorably, it is more comprehensive and substantive than previous "framework" conventions, such as the Vienna Convention for the Protection of the Ozone Layer [4] which served as its original model. Its critics correctly point out, however, that it contains no binding commitments for the reduction of greenhouse gases.

The Framework Convention, has as its ultimate objective the:

> stabilization of greenhouse gas concentrations in the atmosphere at a level that would prevent dangerous anthropogenic interference with the climate system . . . within a time frame sufficient to allow ecosystems to adapt naturally to climate change, to ensure that food production is not threatened, and to enable economic development to proceed in a sustainable manner.

Framework Convention, Article 2.

However laudatory the purpose of the Framework Convention may be, the United States prevailed in pressing for the exclusion from it of any textual references to legally binding targets and timetables to reduce anthropogenic emissions of greenhouse gases. Nevertheless, while the Framework Convention includes no obligations in this regard, each of the Annex I parties (i.e., developed countries and countries with economies in transition) is committed to:

> adopt national policies and take corresponding measures on the mitigation of climate change, by limiting its anthropogenic emissions of greenhouse gases and protecting and enhancing its greenhouse gas sinks and reservoirs. These policies and measures will demonstrate that developed countries are taking the lead in modifying longer-term trends in anthropogenic emissions consistent with the objective of the Convention, recognizing that the return by the end of the present decade to earlier levels of anthropogenic emissions of carbon dioxide and other greenhouse gases not controlled by the Montreal Protocol [designed to protect the earth's ozone layer] would contribute to such modification.

Framework Convention, Article 4, Paragraph 2(a). The Framework Convention is silent with respect to emissions beyond the year 2000.

The Framework Convention calls upon countries to develop greenhouse gas inventories, formulate national strategies and cooperate in scientific research but contains no sanctions for non-compliance. So as to provide guidance, the Framework Convention establishes a set of non-binding standards by which to measure performance. Progress is to be reported annually to the United Nations. Significantly, however, the Framework Convention omits any obligation on the part of industrialized countries to pay for the costs of responsive actions, although it incorporates the principle that they will provide financial and technical assistance to developing countries to assist them in meeting their reporting requirements. Article 4.2 is likely to assume greater importance over time because it permits industrialized countries to implement their policies jointly with other countries. This provision is viewed as the basis for a global trading and marketing of emissions permits. Perhaps most importantly, the Framework Convention contains procedures by which it is to be reviewed and strengthened as better information becomes available over time.

THE GOVERNMENT STEPS ON THE GAS- THE UNITED STATES RESPONSE

In connection with the United States' becoming a signatory party to the Framework Convention, on April 21, 1993, Earth Day, President Clinton committed the United States to reduce the nation's emissions of greenhouse gases. In accordance with the President's directive, the Clinton administration released the Action Plan on October 19, 1993. The Action Plan is designed to return United States net emissions of greenhouse gases (emissions minus net sinks) to their 1990 levels by the year 2000. The Action Plan acknowledges, however, it is "unlikely to stabilize emissions at 1990 levels in the longer term" [5].

The Action Plan is intended to limit greenhouse gas emissions while simultaneously continuing to guide the nation's economy toward environmentally sound economic growth into the next century. In targeting all greenhouse gases and all sections of the economy through a portfolio approach of nearly fifty different actions, the Action Plan is unquestionably comprehensive. It builds on existing technologies, programs and voluntary efforts. The Action Plan calls for joint implementation pilot projects, but does not count any emission reductions from these projects toward achieving the national target.

Under the Action Plan, energy efficiency is considered crucial, because fossil fuel consumption by homes, offices and factories is responsible for more than 85% of United States greenhouse gases. One half the Action Plan's projected emissions reductions are from measures to restrain demand for energy in each sector of the economy, such as by strengthening residential building codes and encouraging development of super-efficient appliances and industrial equipment. Transportation, which accounts for 27% of all greenhouse gases, is targeted for 7.5% of the Action Plan's overall emission reductions, through such measures as promoting telecommuting and requiring fuel economy labels on tires [5].

Interestingly, while the Action Plan stresses energy efficiency, emissions of CO_2 are expected to increase as methane reductions are targeted first in reducing net carbon emissions. The balance of reductions are to come from measures to encourage use of non-carbon renewable fuels and natural gas and to protect sinks.

Natural Gas Initiatives

Initiatives taken at the federal level, many of which predate the Action Plan, have resulted in tremendous changes in the United States energy industry. For example, various undertakings by the Federal Energy Regulatory Commission (FERC), particularly its recent steps to restructure the natural gas pipeline industry under Order No. 636 [6], have created a streamlined regulatory environment. It is widely believed these efforts will lead to far more efficient deliveries of natural gas over interstate pipelines and, therefore, increased natural gas use. New requirements under the Energy Policy Act of 1992 and the Clean Air Act are also expected to give a further boost to greater use of cleaner fuels such as natural gas. The Action Plan builds on these regulatory and statutory developments in furtherance of reducing the amount of carbon emitted from energy products and use.

In fossil fuels, the amount of carbon per unit of energy varies significantly by fuel type. For example, coal has the highest amount, while petroleum has about 20% less and natural gas about 45% less. Because natural gas is both abundant as a domestic fuel source and significantly cleaner than either coal or oil, the Action Plan seeks to increase natural gas usage over these other fuels.

Action No. 23, involving the FERC, states that the FERC should continue with its efforts to reform its regulations so as to improve competition and service in the natural gas industry. In the near future, the FERC is expected to refine Order No. 636, particularly with respect to stimulating secondary transportation markets. In addition, the FERC will likely streamline its certificate and ratemaking rules. The Department of Energy (DOE) estimates these FERC initiatives could result in an additional 0.37 trillion cubic feet of gas use by the year 2000.

Under Action No. 24, the Administration has committed to encourage aggressively the seasonal use of natural gas in existing utility and industry coal- and oil-fired generator plants as a strategy to reduce nitrogen oxide emissions (reductions in CO_2 will be a secondary benefit). Under authority of Title I of the Clean Air Act, the Environmental Protection Agency (EPA) is expected to devise strategies that will help states meet air quality goals through flexible fuel-switching approaches.

Methane Initiatives

Thirty percent of the Action Plan's projected reductions comes from steps to lower emissions of other greenhouse gases. The reduction of methane is believed to be a desirable means of reducing greenhouse gases. This derives from the special

characteristics unique to methane. As noted above, methane is between 11 and 22 times more effective than CO_2 in trapping heat in the atmosphere. However, methane has a relatively short atmospheric lifetime. The combination of these factors leads scientists to believe that the stabilization of methane emissions will have essentially the same effect on limiting future global warming as stabilizing CO_2 emissions at 1990 levels [7]. Especially important in this regard and in contrast to other greenhouse gases, is the fact that a few large facilities account for a great portion of total United States methane emissions. By applying emission reduction strategies to these limited number of methane sources, a substantial decrease can be achieved in the quantity of emitted methane. In many instances, current technologies exist and can be implemented at low cost or even at a profit to recover methane that would otherwise be emitted into the atmosphere. The EPA estimates that currently available technology makes it feasible to reduce methane emissions from anthropogenic sources by about 50%, although economically justified options reduces this recovery percentage to between 20-30% [7].

Landfill gas is the largest source of methane emissions in the United States. In 1990, about 37% of total United States methane emissions were determined to have originated from landfill sources. About 90-95% of total landfill emissions were attributable to emissions from municipal solid waste landfills which received over 70% of the total solid waste generated in the United States in 1990. Industrial landfills accounted for the rest [7].

Methane from landfills can be used to fire boilers but is most commonly used for electric generation. The EPA has estimated that at a price of $.04 per kWh, about 15-25% of emissions from 60 landfills could profitably be recovered as an energy source. Increases in electrical costs creates the potential for recovery of significant additional amounts of methane. For example, at $0.05 per kWh, 60-80% of emissions could be recovered [7].

Action Nos. 33, 34 and 37 are directed towards reducing landfill gas emissions and increasing methane recovery from landfills. Action No. 33 sets forth steps to reduce emissions of volatile organic compounds in landfills. In Action No. 34, the EPA is expected to identify and work with suitable landfill sites to overcome any critical barriers that may otherwise prevent the capture of methane. Action No. 37 expands DOE programs in the research, development and demonstration areas for technologies to recover landfill methane. The Administration has proposed to obligate $6.4 million and $9 million through the year 2000 for the activities outlined in Actions 34 and 37, respectively.

Coal mining and related activities such as coal processing, transportation and consumption are the third largest source of methane emissions in the United States (following emissions from domesticated livestock). Estimates for 1990 place coal mining emissions as contributing approximately 16% of total United States methane emissions [7].

Methane is trapped within coal seams and its surrounding rock strata. During the mining of coal, methane is released into the atmosphere. The quantity of methane released from coal mining depends mainly upon the type of coal being mined and its depth. As a general rule, deeper mines emit more methane. Methane from surface mines is emitted directly into the atmosphere as the rock strata surrounding the coal seams are removed. However, between 70-80% of coal related methane emissions is associated with underground mining operations. Significantly, the preponderance of these emissions, between 20-45%, is released into the atmosphere as a result of the degasification systems used at gassier mines.

Currently, recovered methane can be sold for power generation and for consumption by natural gas pipeline customers. The EPA estimates it is technologically feasible to recover and use about 60% of the methane in all large and gassy mines (mines with production in excess of 0.5 million tons per year with methane per ton in excess of 500 cubic feet per ton). At this time, methane recovery is not considered technologically feasible at surface mines or at small, less gassy underground coal mines. As might be expected, gas and electric prices make the economic recovery of methane recovery highly variable. Currently, about 10 domestic mines profitably recover and utilize methane from coal mines. The EPA estimates that wellhead gas prices at $2.25 per Mcf could double the number of mines that would be able to recover methane profitably [7]. However, other constraints exist which affect methane recovery from mines. These include the ambiguities of ownership of the methane (uncertainties as to which parties may claim ownership of the methane creates a disincentive to invest in these projects), quality of the gas recovered (impurities and low heat content impair the marketability of methane), as well as location and access to the pipeline transportation grid (high transportation costs can make the methane uneconomical and prevent its entering the market). The Energy Policy Act of 1992 is expected to reduce some of the ownership issues by requiring states to implement mechanisms to address ownership issues.

The FERC's regulatory initiatives should improve the marketability of competitively priced methane.

Actions 35 and 36 are the Administration's proposals under the Action Plan to encourage the productive use of methane captured from coal mining operations. Action No. 35, the Coalbed Methane Outreach Program, is designed to create an awareness of the potential for cost-effective emissions reductions with key coal companies and state agencies. It is built on existing activities of the EPA and includes identifying and eliminating project barriers, development of outreach materials on successful projects and available technologies, operation of an information clearinghouse, briefings for companies, states, utilities and others and demonstration projects. The program seeks to target approximately 50 of the gassiest mines in the United States. The Administration projects to eliminate annual methane emissions by 2.2 MMT carbon equivalent by the year 2000.

Action No. 36 is intended to expand research, design and development of cost effective technologies and practices for recovering methane associated with mining. Projects are to be co-funded by the DOE and industry on a 50% cost sharing basis. Under this action, the Administration hopes to devise lower cost methods for pre-mining recovery of methane from coal seams and methods for using in-mine degasification streams, such as enrichment for pipeline gas and electricity generation.

HIGH OCTANE DELIVERY OR JUST HOT AIR?- CONCLUSION

According to the Climate Action Report (Report) which the United States submitted in the Fall of 1994 and which is the first United States communication under the Framework Convention, the Action Plan's broad comprehensive approach "lessens the risk that poor performance in one section will jeopardize the [Action] Plan as a whole [8]." The Report highlights that under the "Green Lights" program, which was launched three years ago by the EPA to offer technical support to businesses considering upgrading their lighting system, "over 1,500 organizations have committed to a national effort to improve the efficiency of their lighting systems," and under the Climate Challenge, "more than 750 utilities, representing over 80 percent of U. S. electric utility generation capacity, . . . will inventory current emissions and commit to undertake and to report on actions to reduce greenhouse gases [8]."

Notwithstanding these positive advances, even if fully implemented, legitimate questions arise as to whether the Action Plan's goal of returning greenhouse gas reductions to 1990 levels by the year 2000 can be achieved. Since the Action Plan was unveiled, the economic growth of the United States has exceeded earlier forecasts of less than 2.5 percent. At the same time, the Action Plan assumed higher oil prices in its emission projections than appear likely to occur. Moreover, it appears that full implementation of the Action Plan is unlikely, since public spending is already falling short of the original targets.

Even though the Action Plan was presented as a "win-win" program, in fiscal 1995, the Action Plan received only $232 million, significantly less than the $344 million sought by President Clinton. Significantly, the DOE, an important agency involved in effectuating the Action Plan, received just over half its hoped-for $208 million. Without such funding, the Action Plan's emission reduction goals are threatened because nearly two-thirds of the reductions depend on voluntary public/private partnerships. Indeed, in previous testimony before Congress, DOE Secretary O'Leary testified that a shortfall of this magnitude would "cripple" the Action Plan and cause greenhouse gas emissions to "rise dramatically." It is also unlikely that full funding of the Action Plan will occur in the near future. The current Congress is less sympathetic to environmental and international environmental issues, and has even threatened to cut funding from programs already appropriated. Given this change in the political landscape, the Administration appears less enthusiastic about placing the Action Plan at the top of its agenda.

Even though the primary goal of the Action Plan may not be achieved, increased usage of natural gas and unconventional gas may still be possible. In reality, the FERC's initiatives to improve the efficiency of natural gas markets depend little on the Action Plan. The FERC continues to enjoy general support from Congress in its steps to achieve regulatory reform. The effects of funding shortfalls on the actions which are designed to spur recovery of methane from landfills and mining operations is less clear, however, particularly since success in these areas depends in many respects on public/private partnerships. Nevertheless, any setbacks to these programs from a lack of federal funding could be offset by relatively slight increases in the prices of electricity and natural gas.

REFERENCES CITED

1. United Nations Framework Convention on Climate Change, opened for signature June

1992, entered into force March 21, 1994, 31 I.L.M. 849.

2. Intergovernmental Panel on Climate Change (IPCC), 1992, Climate Change 1992: The IPCC Scientific Assessment: Cambridge (U.K.), Cambridge University Press.

3. Bodansky, D., 1993: "The United Nations Framework Convention on Climate Change: A Commentary," The Yale Journal of International Law, v. 18, No. 2, p. 451-558.

4. Vienna Convention for the Protection of the Ozone Layer, adopted and opened for signature March 22, 1985, entered into force September 22, 1988, 26 I.L.M. 1529.

5. The Climate Change Action Plan, 1993, Washington, D.C., DOE/PO-0011-2.

6. Pipeline Service Obligations and Revisions to Regulations Governing Self-Implementing Transportation; and Regulation of Natural Gas Pipelines After Partial Wellhead Decontrol, 57 Fed. Reg. 13,267 (April 16, 1992) (Order No. 636), order on reh'g, Order No. 636-A, 57 Fed. Reg. 36,128 (August 12, 1992) (Order No. 636-A), order on reh'g, Order No. 636-B, 57 Fed. Reg. 57,911 (December 8, 1992) (Order No. 636-B), (Order Nos. 636, 636-A and 636-B hereafter referred to together as "Order No. 636"). The FERC's main objective under Order No. 636 was to effectuate the "unbundling," or separation, of pipeline sales services from transportation services and, in effect, to permit customers to purchase and use only those discreet pipeline services they desire and need.

7. USEPA, Hogan K.B., ed., 1993: Opportunities to Reduce Anthropogenic Methane Emissions in the United States, Washington, D.C., USEPA Office of Air and Radiation, EPA 430-R-93-012.

8. Submission of the United States of America Under the United Nations Framework Convention on Climate Change, 1994: Climate Action Report: Washington D.C.

NOTES

INTERGAS '95

May 15-19, 1995
The University of Alabama
Tuscaloosa, Alabama USA

9540

Energy and Environmental Policy Options to Promote Coalbed Methane Recovery

J.L. Lewin, Widener University School of Law

ABSTRACT

This paper analyzes policy options to promote recovery of coalbed methane (CBM) in furtherance of U.S. energy and environmental policy. Recent studies of methane emissions from U.S. mines demonstrate that policy options should focus on promoting methane recovery at fewer than 100 large gassy mines which account for the majority of U.S. methane emissions from mining. Policy options include direct command-and-control regulation and indirect economic incentives. The variability of mine-specific factors makes it difficult to employ the two traditional forms of command-and-control regulation: "technology standards" that mandate use of particular recovery techniques or "performance standards" that establish ceilings on emissions. Direct regulation may be appropriate, however, to prohibit venting of methane from degas systems whenever flaring would be a safe alternative. Economic incentives, especially emission fees or subsidies, are more feasible and could be effective, but each of these policy instruments is likely to have adverse secondary consequences. A subsidy for CBM recovery funded by methane emission fees would generate the best incentives while minimizing the impact on the coal industry and other adverse secondary consequences.

INTRODUCTION

This paper analyzes policy options to promote recovery of CBM in furtherance of U.S. energy and environmental policy. The term "recovery" refers to any capture of CBM that does not result in venting of the gas into the atmosphere. Recovery thus includes capture for current or future use of the gas as a fuel or as a chemical feedstock, as well flaring of the gas on-site.

My previous works have focused on the barriers to recovery of CBM posed by uncertainty about its ownership [1,2,3]. Ownership rules are being clarified through litigation [3,4,5,6], and recent federal [7] and state [8] forced pooling laws should help overcome the problem of legal uncertainty by allowing claimants to undertake CBM recovery projects despite the existence of competing ownership claims so long as a share of the profits is held in escrow pending resolution of disputes [3].

As legal barriers are being surmounted, the primary impediment to CBM recovery now appears to be the doubtful viability of project economics in light of the loss of the Section 29 tax credit and the continued softness of gas prices. As a result, CBM often is vented at mines where recovery would be feasible, thereby wasting a valuable energy resource and contributing to the problem of global warming. The first part of the paper provides a general perspective on the role of CBM in U.S. energy and environmental policy.

Crucial to formulating energy and environmental policy is information about current and projected methane emissions from mining and about the prospects for recovery. The second part of the paper examines aggregate data on methane emissions from mining and on the percentage that feasibly might be recovered and utilized.

In addition to aggregate data, policy planners need to know more about the attributes of the mines at which recovery projects are most likely to be feasible. The third part of the paper analyzes a recent EPA study of methane emissions at selected gassy mines [9]. This study demonstrates that policy options should focus on promoting methane recovery at a relatively small number of large gassy mines which account for the majority of U.S. methane emissions from mining.

The fourth part of the paper explains the economic justification for government regulatory policy to encourage private sector CBM recovery projects, and it briefly describes the various policy instruments available to the government. Policy options include direct command-and-control regulation and indirect economic incentives.

The fifth part of the paper evaluates two traditional forms of command-and-control regulations: "technology standards" that mandate use of particular recovery techniques, and "performance standards" that establish ceilings on emissions. Because the feasibility of CBM recovery depends on a host of mine-specific factors, the analysis of regulatory options suggests that neither technology standards nor performance standards are appropriate policy options. Direct regulation might be appropriate, however, with respect to degasification (degas) systems. If a technology existed for safe flaring of unutilized methane from degas wells, regulations could mandate the use of flaring technology or ban the emission of methane from these wells.

The sixth part of the paper evaluates programs that employ economic incentives, which include tradeable emissions rights, emission fees, subsidies or tax credits, and deposit-refund systems. Economic incentives, especially emission fees or subsidies, are more feasible than direct regulation and could be effective in promoting CBM recovery, but each of these policy instruments is likely to have adverse secondary consequences. Emission fees would be costly to the coal industry, while a subsidy would be costly to taxpayers and would distort the price of coal relative to fuels that generated lower levels of greenhouse gas emissions. A subsidy for CBM recovery funded by methane emission fees would generate the best incentives while minimizing the impact on the coal industry and other adverse secondary consequences.

CBM AND U.S. ENERGY AND ENVIRONMENTAL POLICY

CBM and Energy Policy

Despite the end of the Cold War and the persistence of relatively low prices for oil and gas, development of domestic energy reserves remains a central element of American energy policy. Among the various possible sources of additional energy supply, both conventional and unconventional, CBM is unique in the degree to which immediate action must be taken to develop the resource. Whereas most energy resources can be held in reserve and developed at a later date, the failure to recover CBM in conjunction with current underground mining operations in the U.S. results in permanent dissipation of roughly 3.4 Tg of methane each year, one-third to one-half of which might be recovered using existing technology [10,11]. To the extent we recover CBM in conjunction with mining, we can postpone the depletion of an equivalent amount of our nonrenewable fossil fuel reserves.

CBM and Environmental Policy.

In signing the United Nations Framework Convention on Climate Change, the U.S. committed itself to the goal of stabilizing atmospheric greenhouse gas concentrations. President Clinton's Climate Action Plan seeks to stabilize greenhouse gas emissions at 1990 levels by the year 2000. While debate continues among scientists about the imminence of the threat of global warming, the conservative decision to stabilize greenhouse gas emissions has become a central focus of American and international environmental policy.

CBM has the potential to make a significant contribution to greenhouse policy for several related reasons. First, methane is a potent greenhouse gas, with an impact 22 times as great as carbon dioxide per ton emitted, and it also has a far shorter atmospheric lifetime [10]. Thus, even though methane is responsible for only 15-20% of radiative forcing from all greenhouse gases, stabilization of methane concentrations at 1990 levels would have roughly the same effect on global warming as would stabilizing carbon dioxide levels at 1990 levels [10]. Second, commercially feasible technology already exists for the recovery of CBM, assuring that substantial emissions reductions can be achieved relatively quickly, without the delay and uncertainty that will attend the development of new technologies in other fields [10,11]. Third, CBM recovery is an attractive target of a "no-regrets" strategy in that recovery has already proven to be cost-justified in several major projects, and a relatively modest investment of effort and resources by the government could be leveraged into substantial emissions reductions through a small but significant improvement in project economics at other mines [10].

While American greenhouse policy continues to focus on the reduction of carbon dioxide emissions by utilities, it appears that utilities may be able to receive credit for recovery of CBM as an offset against limits that eventually may be set on their carbon dioxide emissions. Under Section 1605(b) of the Energy Policy Act of 1992, mine operators are encouraged to voluntarily report their recovery of CBM in conjunction with mining so that they may receive credit in future years for their current success in reducing methane emissions from mining. Draft Guidelines for the implementation of Section 1605(b) were published in the fall of 1994 [12], followed by a proposed form on which to report reductions of greenhouse gas emissions [13]. Thus, the reporting program already may be in effect by the time this paper is presented. The willingness of utilities to purchase offset credits for CBM recovery could help overcome the traditional reluctance on the part of coal owners and operators to invest in the development of what they have previously perceived as a competing resource.

METHANE EMISSIONS FROM MINING AND THE POTENTIAL FOR RECOVERY

In order to assess the prospects for governmental efforts to reduce CBM emissions, it is essential to have a basic understanding of the quantity of emissions involved and of the extent to which they might be recovered.

Global Emissions of Methane

According to the Intergovernmental Panel on Climate Change (IPCC), global methane emissions from all sources totaled slightly over 500 Tg (1 Tg = 52.6 Bcf of methane), of which approximately 350-360 Tg or 70% came from anthropogenic (human) sources [14,15]. Global emissions from coal mining totaled roughly 40 Tg (25-47 Tg), representing nearly 8% of all emissions and more than 10% of all emissions from human sources [15]. Estimates of methane emissions made by the International Energy Agency (IEA) are similar to but somewhat lower than those of IPCC. IEA estimates that global methane emissions in 1990 were 425-675 Tg, of which anthropogenic sources accounted for only 40%, and that methane emissions from mining totaled roughly 24 Tg [16].

The U.S. Environmental Protection Agency (EPA) has accepted the IPCC estimates, including the 40 Tg (25-50 Tg) estimate for global methane emissions from coal mining [10]. EPA's own estimate of global methane emissions from coal mining in 1990 is 24.4-39.6 Tg [17], which is lower than that of the IPCC and closer to that of the IEA. Based on current recovery methods, EPA estimates it would be technically feasible to reduce these mining-related methane emissions by 40% or 11.6 Tg; economically viable reductions may be up to 7.0 Tg in the near term and up to 11.0 Tg in the long term [17]. Since stabilization of global methane emissions would require a reduction of approximately 30 to 40 Tg per year [10,17], a substantial reduction in methane emissions from mining could make a major contribution to stabilization of global methane emissions.

Methane Emissions from U.S. Mines

EPA estimated total methane emissions from U.S. mines in 1988 at 3.3-5.2 Tg: 2.6-3.7 Tg from ventilation and degas systems in underground mines; 0.5-0.8 Tg from post-mining emissions released during transportation, storage, and handling of the coal prior to combustion; and 0.2-0.7 Tg from surface mines [18]. Extrapolating from these data to reflect an 8% increase in coal production between 1988 and 1990, EPA estimated 1990 emissions from mining at 3.6-5.7 Tg, of which 2.8-4.1 Tg came from underground mines. The IEA estimates of 1990 methane emissions from U.S. mines are slightly lower than those of EPA, totaling 3.3 Tg: 3.0 Tg from underground mines; 0.25 Tg from post-mining activities; and less than 0.1 Tg from surface mines [16].

Methane recovery efforts have focused on underground mines, which account for roughly 75% (EPA) to 90% (IEA) of methane emissions from U.S. mines. Methane emissions from underground mines come primarily from two sources: the regular ventilation systems required in all underground mines and the special degas systems employed in some gassy mines, especially in conjunction with longwall mining.

Excellent data exist on methane emissions from mine ventilation systems. This information is regularly collected by the U.S. Mine Safety and Health Administration (MSHA), and since 1973 the U.S. Bureau of Mines (BOM) has published compilations of data on methane emissions from mine ventilation systems on a fairly regular basis [19,20,21,22,23,24]. In 1988, the latest year for which published data are available, 487 underground mines with detectable emissions produced a total

of 2.0 Tg (294.9 MMcf/d = 107.6 Bcf/yr) of methane through their ventilation systems [24]. EPA estimated that another 1,400 mines with non-detectable methane emissions contributed an additional 30 MMcm (1 Bcf), so that the total of all methane emissions from ventilation systems in 1988 was 2.1 Tg [18].

The estimates of methane emissions from degas systems are less accurate, because data on degas emissions are not regularly compiled. In an initial evaluation of methane emissions from mining prepared for EPA in 1990, ICF Resources estimated that gob wells associated with longwall mining emitted 1.5 Tg of methane in 1987. This estimate was based on the number and size of operating longwall systems and published data on gob well production; it did not include in-mine horizontal or cross-measure boreholes [25]. In a subsequent survey, EPA included both in-mine boreholes and gob wells in an estimate of methane emissions from degas systems at 35 mines that were known to have such systems. Based on discussions with industry personnel, EPA assumed that a typical mine would recover between 40 and 65 percent of total emissions in its degas system, and it estimated that in 1988 the methane emissions from the degas systems of these 35 mines (not including amounts recovered and utilized) was 0.5-1.6 Tg [18]. Using similar information, the IEA estimated that methane emissions from degas systems in U.S. mines totaled roughly 0.5-1.8 Tg in 1990 [16].

In a more recent analysis of 1990 data for 34 mines known to have degas systems, EPA assumed that degas systems accounted for only 35% of total emissions, and the total degas emissions for these mines were estimated to be 1.1 Tg (153.1 MMcf/d = 55.9 Bcf/yr), of which .3 Tg (40 MMcf/d = 14.6 Bcf/yr) was utilized and the remaining .8 Tg was released into the atmosphere [9].

It is not clear whether EPA's 1994 survey successfully identified all operating mines that employ degas systems. EPA's analysis of 84 mines included 59 longwall mines, of which 32 had degas systems. While several of these mines had more than one longwall system, the EPA survey accounts for only 68 of the 95 longwall systems listed in the February 1990 longwall census [26], and only 69 of the 96 longwall systems listed in the February 1991 longwall census [27], so that it fails to account for 27 longwall systems that were known to be operating in 1990. It seems likely that several of these longwall mines would have employed some form of degas system in addition to the regular ventilation system. Indeed, the ICF estimates for 1987 had assumed that every longwall operation would employ three gob wells per panel [25]. Although several of the longwall systems omitted from the EPA survey had relatively low emissions from the ventilation systems, it would be surprising if none of these mines had degas systems, suggesting that the EPA list may be incomplete.

Finally, existing estimates of emissions from ventilation and degas systems do not reflect the substantial quantities of methane released from underground coal seams in conjunction with mining that may enter the atmosphere without passing through ventilation or degas systems. Subsidence associated with longwall mining often produces fractures that extend upward to the surface, facilitating release of methane from any coals lying above the primary seam. For example, a film shown at a recent coalbed methane forum depicted methane bubbling up through a pond or creek above a longwall mine. In addition, substantial quantities of methane undoubtedly escape from inactive and abandoned mines. Although these mines are sealed, abandoned mines have been known to produce significant quantities of gas [18]. No estimates yet exist for methane emissions from underground mines that bypass the ventilation and degas systems. To the extent that methane recovery projects might capture some of this gas, it would be useful to have better estimates of the amount of CBM that reaches the atmosphere without passing through ventilation or degas systems.

METHANE RECOVERY IS MOST FEASIBLE AT A FEW LARGE AND EXCEPTIONALLY GASSY MINES

Although the estimates of methane emissions from mining may be incomplete, they do provide an adequate background for an assessment of the policy options available for encouraging recovery of CBM. In general, they demonstrate that methane recovery is most feasible at a relative small number of very large and exceptionally gassy mines, mines that produce more than 0.5 million tons of coal per year and have methane emissions in excess of 28.32 Mcm/d (1.0 MMcf/d)

While there are nearly 2,000 underground mines in the U.S., methane recovery is most likely to be economically feasible at fewer than 100 of the largest and gassiest underground mines. Roughly 1,400 underground mines had methane levels in their ventilation systems that were too low to detect, and EPA estimates that the methane from these mines collectively amounted to only 1% of measured methane emissions [18]. Moreover, of the 487 mines with measurable ventilation system emissions in 1988, the 294 with emissions of less than 2.832 Mcm/d (0.1 MMcf/d) produced only about 1% of the total. Thus, 98% of the estimated emissions from underground mines, and 99% of the measured emissions, came from the 193 gassy mines with emissions in excess of 2.832 Mcm/d (0.1 MMcf/d) [18,24]. Finally, over 85% of the measured emissions came from an even smaller group of exceptionally gassy mines, with emissions in excess of 28.32 Mcm/d (1.0 MMcf/d).

The percentage of emissions from the exceptionally gassy mines, with emissions in excess of 28.32 Mcm/d (1.0 MMcf/d), has increased substantially since 1980. This change is attributable to a combination of factors including the opening of large new mines in deeper, gassier coalbeds, the advent of high-extraction mining systems (particularly longwall systems), and the expansion of the dimensions of longwall panels [23,24] While the emissions from exceptionally gassy mines represented roughly 80% of measured emissions from ventilation systems between 1972 and 1980, in 1985 the 69 mines in this category accounted for 87% of all ventilation emissions [23], and in 1988 the 65 mines in this category accounted for roughly 88% of all ventilation emissions [24].

Moreover, these exceptionally gassy mines are also the ones most likely to employ degas systems. EPA recently compiled data on "selected gassy mines" that already have successful methane recovery projects (n=10) or that may be candidates for future methane recovery projects (n=74) [9]. The 84 gassy mines in the EPA study included 34 mines that were known to have degas systems. EPA's Table 13 listed these 84 mines in terms of their daily ventilation emissions. Of the 36 mines that had ventilation emissions in excess of 56.64 Mcm/d (2.0 MMcf/d), 27 had active degas systems in operation. Moreover all 21 mines with ventilation emissions in excess of 127.44 Mcm/d (4.5 MMcf/d) also had active degas systems. Indeed, the five mines with the highest ventilation system emissions were the mines in the Black Warrior Basin that already were utilizing the methane captured in their degas systems. (Oak Grove and Blue Creek Nos. 3, 4, 5, and 7) The other mine that was then utilizing methane from its degas system (Soldier Canyon) was ranked 21st in ventilation emissions. Four Virginia mines that subsequently went on-line with recovery of methane from degas systems were ranked 6th (VP No. 5), 8th (VP No. 6), 11th (Buchanan No. 1) and 12th (VP No. 3) in ventilation emissions in 1990.

The total methane emissions (ventilation plus degas) from the mines in the EPA survey are analyzed in Table 1. These 84 mines emitted 2.99 Tg of methane in 1990, of which only .28 Tg was utilized, so they account for 75-80% of all methane

emissions from underground U.S. mines that year. Moreover, the bulk of methane emissions came from a smaller subset of this group. The 57 exceptionally gassy mines in the survey, with daily emissions in excess of 28.32 Mcm/d (1.0 MMcf/d), had total emissions of 2.90 Tg. Narrowing the field even further, the 40 gassiest mines, with emissions in excess of 56.64 Mcm/d (2.0 MMcf/d), had total emissions of 2.75 Tg. Finally, the 13 gassiest mines, having emissions in excess of 283.2 Mcm/d (10 MMcf/d), alone accounted for 1.84 Tg, and the unrecovered emissions from these mines represented nearly half of all emissions from U.S. underground mines. The foregoing analysis demonstrates that the vast bulk of methane emissions in the United States come from a relatively small number of exceptionally gassy mines, many of which are prime candidates for methane recovery projects. Indeed, the ten mines in the EPA survey that currently utilize methane from degas systems were ranked 1st through 9th and 16th in total methane emissions in 1990 [9].

In addition to having high levels of methane emissions, the mines which are the best candidates for methane recovery are those that already employ degas systems to remove methane from the mine. Of the 74 candidate mines in the EPA survey, 24 already had degas systems in operation [9]. As EPA noted in the executive summary to its analysis:

> The mines that already use degasification systems may be especially good candidates for the development of cost-effective methane recovery projects because the cost of drilling and installing these systems would not be an additional cost associated with the project [9].

Similarly, the IEA emphasized that CBM recovery was most likely to be commercially feasible at large gassy mines with existing degas systems:

> These projects typically require mining operations with high volumes of high quality gas, where degasification is necessary for the safe operation of the mine. Thus, coal production costs associated with coalbed methane recovery through degasification can be considered sunk and the economics for utilization can be evaluated on an incremental basis [16].

Thus, when evaluating alternative regulatory strategies to promote CBM recovery, it is important to bear in mind that the primary target of all such efforts should be a relatively small number of exceptionally gassy mines, many of which already employ degas systems in the interest of mine safety and efficiency.

POLICY OPTIONS TO CORRECT MARKET FAILURE AND PROMOTE CBM RECOVERY

A vast body of recent theoretical work on environmental economics has been implemented and refined during the past 25 years of serious environmental regulation [28,29]. Much of this work is incorporated in a 1989 U.S. Department of Energy (DOE) Report to Congress entitled A Compendium of Options for Government Policy to Encourage Private Sector Responses to Potential Climate Change [30].

The need for government action to address potential climate change is premised on the existence of "market failure," the inability of market prices to reflect the true costs of commodities because some portion of those costs is imposed on third parties and not taken into account by the producers and purchasers of those commodities. As explained in the DOE Compendium:

> The need for government policy may arise if free-market decisions under current regulations and market rules are leading to what many people in the scientific and policy communities consider excessive greenhouse gas emissions. As with particulates from smokestacks or large manufacturing plants or the pollution from private cars, the social cost of greenhouse gas emissions from private sector activities may not be included adequately in the profit-loss calculations of their operators, who even may be unaware of the potential effects of their actions. Therefore, current private sector activities may produce an acceptable amount of greenhouse gas from the viewpoint of their operators, but, possibly, excessive amounts from the viewpoint of society. The costs of global warming and other side effects of increased greenhouse gases in the atmosphere are neglected when such market failures exist [30].

Global warming represents a classic example of market failure arising from the inability of the price system to force current actors to "internalize" or bear the costs of their actions. Until the past few years, those who emitted greenhouse gases such as methane and carbon dioxide were not even aware that their actions were potentially harmful, and even today the extent of the potential damage from global warming is difficult to estimate [31,32]. Those damages, if and when they occur, will be inflicted on people who live in different nations or even on different continents from those who emitted the gases, and most of the impact will be upon people who have not yet been born.

As applied to CBM, market failure exists because the production of coal necessarily releases vast quantities of methane, which contributes to long-term damages from global warming that are not reflected in the price of coal. The price of coal reflects the costs of capital, labor, and energy used to mine, process and transport it, but the price does not include the cost of environmental damages, which are "external" to the business decisions of coal producers and their customers.

The DOE Compendium described and analyzed a variety of "policy instruments" that government might employ to correct the market failure arising from the inability of the market to internalize the long-term costs of global warming into current prices for coal and other commodities. These instruments fall within two general categories: regulation and fiscal incentives.

COMMAND-AND-CONTROL REGULATION

DOE defined regulation as "legislation or rules, supported by sanctions and having the force of law, that are designed to limit the discretion that may be exercised by public and private decision makers [30]." Most environmental regulations are enforced by a specialized regulatory agency, such as EPA or equivalent state agencies, and they often require that regulated entities have a license or permit for their operations.

Regulations can take two basic forms: (1) technology or input standards, and (2) performance or output standards. Mandatory technology or input standards specify the process or method that must be employed, such as a requirement that utilities burn low sulfur coal or employ scrubbers to remove sulfur dioxide on all coal-fired plants. Performance standards specify the output that must be achieved, such as a limit on the daily emissions of sulfur dioxide. Regulations differ in the degree of specificity and in the degree of discretion left to the administrative agency. In some cases, precise technology or performance standards are incorporated in the statute or the regulations, while in other cases the agency has discretion to establish standards on a case-by-case basis in accordance with a general qualitative directive to use the best available

technology or achieve the lowest feasible level of emissions. Economists and legal scholars have raised a variety of theoretical and practical objections to command-and-control regulation, primarily that it tends to ignore differences among plants and industries in the cost of reducing pollution and that it fails to create incentives for firms to reduce pollution below the mandated levels [28,29,30,33,34].

Technology Controls

Mandatory technology controls are likely to play at most a limited role in any regulation of CBM emissions. Several different technologies exist for the capture of CBM in advance of or in conjunction with mining operations: pre-mining degasification through vertical boreholes, in-mine drainage through long-hole, short-hole or cross-measure boreholes, and post-mining recovery from gob wells [1,2,3,10,18,25]. Having determined when and how to capture the methane, the operator must then decide whether to burn it in on-site generators or process and transmit it into gas pipelines. These technologies for capture and utilization of CBM may be employed in a variety of combinations. Most importantly, the appropriate mix of technologies depends on a large number of mine-specific factors that are likely to vary from basin to basin and even among the mines in a particular basin [35]. Important variables in selecting the appropriate method of CBM recovery, if any, include mine conditions and mining method; the geologic and reservoir characteristics of the coal basin, such as the depth, rank and gas content of the primary seam, the geology of the overburden, the thickness and gas content of secondary seams in the overburden, and hydrologic conditions; proximity to old mine workings; surface topography; potential gas quality; proximity to gas transmission lines; and other use options.

It would be impossible to draft a statute or regulation that could incorporate all of these factors. Nor would it be feasible for a regulatory agency to license mine operations on a case-by-case basis under some broad standard that required use of the best available technology. Selection of the appropriate mix of technologies for capture and utilization of CBM involves a subtle balancing of technical and economic factors that must necessarily be undertaken by each mine operator based on its own financial status and other related operations. It is inconceivable that a regulatory agency could acquire the requisite information and expertise, and even if it were able to do so, it would be inappropriate for the regulators to second-guess the mine operators in the exercise of their business judgment.

There is one type of mandatory technology standard that might eventually be employed, however, to limit methane emissions from the degas systems of coal mines. Because methane is a much more potent greenhouse gas than carbon dioxide, the impact of CBM emissions could be substantially lessened if the gas were flared instead of vented [9]. While flaring the gas would waste its value as a potential source of energy, flaring is far preferable to venting from an environmental perspective. Today, nearly one-third of methane emissions from U.S. underground mines escape by way of the degas systems at fewer than 50 mines, and the mandatory flaring of degas emissions at these mines could reduce methane emissions by roughly 1 Tg.

Unfortunately, there exists a concern that flaring of methane above ground could increase the risk of fire or explosion in the mines below, and it is not certain whether there yet exists a proven technology for the safe flaring of methane above active coal mines [9]. Apparently, the fear is that a fluctuation in CBM emissions could create negative pressure in the degas well and enable the flame to propagate down the hole and into an area with methane concentrations in the explosive range of 5% to 15%. Even if the technology for safe flaring of degas wells does not yet exist, there is no obvious impediment to its rapid development. The government ought to consider funding research to develop safe technology for safe flaring of methane above active coal mines. Once this technology becomes available, the government could reasonably mandate its use at mines that were not utilizing the gas produced by their degas systems.

Performance Standards

Mandatory performance standards are also likely to play a modest role in government efforts to reduce methane emissions from coal mines. The simplest form of performance standard is a ban or prohibition of activities that produce undesired social effects. Bans are relatively inexpensive to administer, but they are most appropriate for activities with no positive social value, such as improper disposal of toxic waste [30]. Coal mining is a socially beneficial activity, however, and it is impossible to mine coal without releasing methane, so a total ban on methane emissions from mining is inconceivable.

The more usual form of performance standard is not a ban on emissions but a quantitative limit on the amount of emissions or a specification of the percentage that must be captured. Ordinarily, performance standards are preferable to technology standards in that they leave more flexibility to the regulated firms, which then have the incentive to control emissions at the lowest possible cost.

With CBM, however, quantitative performance standards would be even less appropriate than mandatory technology standards. The level of methane emissions from most coal mines is not really within the control of the mine operator. Only at a relatively small number of large and gassy mines can the operators be expected to undertake methane recovery projects, and even at these mines it would be impossible to predict with any accuracy either the percentage of methane that would be captured or the amount of residual methane emissions from the ventilation system. While the regulators might be able to identify the mines at which CBM recovery would be feasible, and they could conceivably determine an appropriate mix of degasification and utilization technologies, it is not even theoretically possible for them to specify a required percentage of capture or an allowable level of residual methane emissions.

In order to specify a required percentage of capture or an allowable level of residual emissions, the regulators would need a baseline of emissions in the absence of capture, but this data does not exist because of the inherent variability of methane emissions. Unlike most industrial plants which continue their operations at a fixed location with a fixed plant before and after the adoption of a new control technology, so that most of the potential variables can be kept constant, coal mine operations continually change their locations and alter a variety of mine-specific variables as they advance through the coal seam, causing the level of emissions to vary from day to day and from month to month, wholly apart from any CBM recovery project. Thus, coal mine operations are inherently unsuited to the imposition of performance standards phrased in terms of the percentage of recovery or the maximum allowable level of residual emissions.

Performance standards would be feasible for CBM only with respect to degas systems, and only if the technology existed for safe flaring of the gas. Instead of mandating the use of flaring technology on degas systems, a regulatory program could prohibit the emission of substantial quantities of methane from degas systems, allowing individual mine operators to determine for themselves whether to recover the gas or flare it.

MARKET-BASED FISCAL INCENTIVES

Unlike regulations, which directly limit the discretion of the regulated firms, market-based fiscal incentives operate indirectly by changing the effective prices of the activities in question [28,29,30]. Important fiscal instruments include tradeable emission rights, emission fees, subsidies, and deposit-refund systems.

Tradeable Emission Rights

Tradeable emission rights begin with a government determination of the total overall amount or rate of emissions it will allow an industry to generate. This total amount is allocated among the firms in the industry, usually in conjunction with a permit system, so that each firm receives the right to emit a certain number of units. After the initial allocation, the firms can exchange these units, and a market develops for emission rights in which the price of a unit of emissions roughly equals the marginal cost of further emission reductions. Firms that can reduce their emissions more cheaply will have excess emission rights available to sell, while firms that have high costs of emission reduction will find it less expensive to purchase excess emission rights from others. For example, as a result of limits on sulfur dioxide emissions in the 1990 amendments to the Clean Air Act, a market in sulfur dioxide emissions credits now exists on the Chicago Board of Trade [29]. Tradeable emission rights represent an improvement over existing permit systems that set non-tradeable performance standards for each firm, because they give each firm an incentive to reduce emissions below the level of its initial allocation, while allowing other firms to purchase additional emissions credits instead of engaging in inefficient efforts at emission reduction [28,29,30,33,34,36,37].

Despite its theoretical advantages, a program of tradeable emission rights would not be feasible for CBM. A program of tradeable emission rights can only function in conjunction with a regulatory program that employs performance standards to compel each firm to monitor its emissions and keep them below specified limits. The requisite program of performance standards is not feasible for CBM because of the unpredictability and variability of methane emissions for each mine, so it would be virtually impossible to establish a program of tradeable emission rights for CBM.

Although a system for tradeable emission rights in CBM would not be feasible, credits for recovery of CBM might be exchangeable within a system of tradeable emission rights in carbon dioxide. Section 1605(b) of the Energy Policy Act of 1992 includes CBM within a program for the voluntary reporting of greenhouse gas emissions reductions, and the purpose of this program is to document these reductions so that they might be counted in future federal or international greenhouse gas reduction programs, which could include a system of tradeable emission rights applicable to carbon dioxide or other greenhouse gases.

The rationale for including CBM reductions within such a program is unclear. The primary justification for the voluntary reporting program is to provide utilities and other major sources of carbon dioxide emissions with the assurance that they will not be penalized for current voluntary efforts to reduce their emissions in the event that future greenhouse gas reduction programs were to mandate percentage reductions from a baseline established at some later date. If a future greenhouse gas reduction program were to set limits on methane emissions from mining, then offset credits for earlier CBM recovery projects certainly would be warranted. But if, as is more likely, the future greenhouse gas reduction program did not set limits on CBM emissions, then it would not seem appropriate for current CBM recovery projects to yield offset credits in that program.

The only other possible justification for granting offset credits for CBM recovery achieved prior to the implementation of a future greenhouse gas reduction program would be if the promise of such future credits were a decisive factor in the current decision to undertake a CBM recovery project. That is, it would have to be true that industry executives who were evaluating the profitability of proposed CBM recovery projects would attribute a substantial dollar value to the possibility that these emissions reductions eventually would be exchangeable within a market for greenhouse gas emission permits.

Based on anecdotal evidence, it appears that the impact of Section 1605(b) on current CBM projects is indirect at best. There is little evidence that the coal producers who are contemplating current CBM projects are giving substantial weight to the prospect of future credits for methane emission reductions. While members of the utility industry are engaged in serious efforts to reduce greenhouse gas emissions voluntarily in order to forestall regulatory activity, and utilities understand that offset credits for CBM recovery projects may be among the most cost-effective means of achieving their emissions reduction targets [38], it is nevertheless uncertain whether this utility industry interest will translate into current CBM recovery projects that would not otherwise have been undertaken. For example, one recent study that emphasized the potential value of CBM offset credits did not contemplate any current investment in CBM recovery projects:

> AEP's cost for the coalbed methane offsets was set at zero, as recovery is already cost-effective for mine operators and it is assumed that these credits might be included as part of coal sales terms in order to maintain sales [38].

If this response is typical, then the prospect of future offset credits for CBM recovery under Section 1605(b) may have little or no impact on current CBM recovery projects. To the extent that coal operators are currently recovering and utilizing CBM based on its profitability under current market conditions, they do not need the added incentive provided by Section 1605(b). If these operators eventually were to receive tradeable offset credits for current CBM emissions reductions, the proceeds from the sale of these credits would be a pure windfall to these firms.

Emission Fees

Emission fees are quite popular with theoretical economists, and they have certain advantages over direct regulation. An emission fee can be applied fairly and uniformly to all sources of a particular greenhouse gas, leaving it to the sources themselves to determine whether it is more efficient to pay the fee or engage in emissions reduction. Emission fees thus substitute market incentives for rigid uniform performance standards [28,29,30,33,34,36].

Emission fees can be employed as a substitute for direct regulation if the level of the fees can be set so as to induce the same total amount of emissions reduction as would have been accomplished through technology or performance standards, but at lower overall cost. Instead of requiring all firms to employ a particular technology or achieve the mandated level of emissions reduction, regardless of the cost to the firm, an emission fee creates an incentive for firms to reduce their emissions only if they can do so at low cost (i.e., at a unit cost below the unit cost of the emission fee). Firms that faced higher costs of emissions reduction would have the option of paying the emission fee in lieu of spending larger sums on emission reduction.

When used as a substitute for direct regulation, emission fees can succeed only if the regulators have good information about the emission control costs of the regulated firms. If the fees were set too low, they would fail to induce any substantial

change in behavior and would simply function as an excise tax, but with far higher costs of administration. If the fees were set too high, they could induce too much emissions reduction and distort the market price of the firms' output. Thus, emission fees are not well-suited to the goal of achieving a particular level of emissions or emissions reduction. (Indeed, if the ultimate goal were to achieve a certain level of emissions or emissions reduction, the best instrument would be a program of tradeable emissions rights rather than a program of emission fees. Such a program would have far more assurance of success because it would establishing the ceiling directly and then employ tradeable emissions rights to allocate production efficiently.)

The discussion in the preceding two paragraphs is largely academic, however, for neither technology nor performance standards are feasible for CBM. Thus, a CBM emissions fee cannot be justified as a more efficient alternative to direct regulation.

The principal justification for emission fees is not as a substitute for direct regulation but as a means of correcting market failure by forcing firms to "internalize" or take into account the damages they inflict on the environment. By setting an emission fee at a level equal to the environmental damage caused by the emissions, the cost of environmental damage becomes a production cost to the firm, and the price of the product reflects the full cost of its production.

An emission fee can only internalize the cost of environmental damage if the extent of that damage can be estimated with some degree of accuracy on a per unit basis. Moreover, for purposes of cost internalization, one must know more than just the total amount of environmental damage and the total quantity of emissions, for the amount of damage per unit of emissions may not be a linear function. With many pollutants there are "threshold effects" so that no damages are inflicted until a certain minimum concentration is reached, and the extent of damage beyond that point may increase exponentially rather than in a linear fashion with additional levels of pollution.

For global warming, only very rough estimates exist of the total cost or damage from a doubling of carbon dioxide levels [31], and no estimates have been made of the marginal cost to society per Tg of carbon dioxide or methane. Indeed, the comprehensive Pace University study of the environmental costs associated with the production of electricity concluded that it was virtually impossible to develop a damage-based estimate of the costs of global warming [32].

While we cannot estimate the environmental cost or damage from methane emissions, we may be able to determine the value to society from a reduction in methane emissions. We have made a commitment to reduce and stabilize greenhouse gas emissions at 1990 levels, and once that ultimate goal is accepted, the aim of greenhouse policy should be to achieve that goal at the lowest possible cost. A variety of technical options exist for reducing the emissions of carbon dioxide, methane and other greenhouse gases, and these options can be evaluated in terms of their comparative cost of achieving the same reduction in global warming potential. *In assessing its contribution to greenhouse policy, the social value of recovering a given quantity of methane would be the savings to society from not having to bear the cost of obtaining an equivalent quantity of greenhouse gas emissions reduction in some other fashion.*

The Pace University analysis of the environmental costs of electricity adopted this "avoided control cost" approach to estimating the cost of global warming from utility emissions of carbon dioxide [32]. The authors concluded that "[t]he external environmental cost of global warming should represent the cost of the marginal measures necessary to slow climate change to an acceptable rate." The Pace study focused on the sequestering of carbon in trees, which employed a proven and well-known technology that was amenable to a concrete cost analysis. The Pace study surveyed various projects that could directly or indirectly contribute to slowing the rate of deforestation or expanding reforestation efforts, and it critically assessed existing estimates of tree planting or reforestation costs in a large number of published studies. It found cost estimates ranging from $1 to $200 per ton of carbon, and it seemed to approve of estimates ranging from $20 to $120 per ton. In particular, it reported that the California Energy Commission adopted a $54 per ton of carbon as the appropriate marginal cost. The Pace study did not select any particular value but instead cautioned that "any estimate ... must be adopted conservatively; that is, any error should be in favor of higher costs to reflect the risk of currently unforeseen catastrophe."

EPA has endorsed the avoided control cost approach to estimating the value of methane emissions reductions in relation to the value of carbon sequestration through reforestation. In a recent report, EPA translated the value of carbon emissions reductions into the value of methane recovery from mining through a formula reflecting the relative molecular weights of carbon dioxide and methane and the fact that methane is 22 times as potent a greenhouse gas as carbon dioxide [10]. Without endorsing any particular measure, EPA suggested a range of possible values per ton of carbon emissions avoided: $5, $20 and $100, which translate into possible values of $.57, $2.30 and $11.50 per Mcf of methane recovered [10]. (Although EPA derived these values to determine possible subsidies for methane recovery, they also can be used to determine appropriate methane emission fees.)

In the remainder of this paper, the analysis employs a value of $5 per ton of carbon emissions avoided, which is equivalent to a fee of $.57 per Mcf of methane. The $5 value probably understates the cost of carbon sequestration, but it is consistent with EPA's estimates and thus makes it possible to employ those estimates in the analysis of alternative policy options.

It is significant that a value of $10 per ton of carbon yields a value of $1.15 per Mcf of methane, which exceeds the value of the former tax credit under Section 29. Even a methane emission fee of $.57 per Mcf may suffice to induce substantial investment in methane recovery at the mines identified by EPA as the prime candidates for such projects.

Once an appropriate methane emission fee has been established, the next task is to determine the scope of the program and decide how the fee should be assessed. Should the fee be collected from all coal mines, including surface mines, or only from underground mines? If limited to underground mines, should the fee be collected from all such mines, or only those with detectable emissions, or only the large gassy mines at which recovery is most likely to be feasible? The decision about the scope of the program is inextricably intertwined with the decision about whether to base the emission fee on actual measured emissions, on engineering estimates for each mine, or on general averages. All of these decisions depend, in turn, on the underlying purpose of the fee system, as well as considerations of administrative cost, allocative efficiency, distributional equity and political feasibility [30].

The scope of a methane emission fee program should primarily depend on the policy goal sought to be advanced. If the purpose of the fee were to internalize the projected damages from climate change, then it would be important to impose the fee on emissions from all mines. For example, surface mining generates relatively low levels of methane emissions on a per-mine basis, but surface mines collectively account for 60% of all coal production and roughly 5% to 15% of all mine-related methane emissions, so they ought to be included if the purpose of the program were to internalize methane emissions costs. On

the other hand, if the purpose of the fee were to encourage methane recovery projects, then it should suffice to impose the fee only on mines that were large enough and gassy enough to undertake recovery projects, which could be a group of fewer than 200 mines with ventilation emissions in excess of 2.832 Mcm/d (0.1 MMcf/d) or perhaps fewer than 100 mines with emissions in excess of 28.32 Mcm/d (1.0 MMcf/d). The EPA survey suggested that the prime candidates for methane recovery were fewer than 100 large gassy mines, with annual coal production in excess of .5 million tons, emissions in excess of 2.832 cm (100 cf) per ton of coal, and total emissions in excess of 14.16 Mcm/d (500 Mcf/d) [9].

The administrative cost of the program would depend on the number of mines involved and the method of assessment. Ideally, an emission fee should be based on actual emissions as measured by a continuously operated monitoring device. The cost of continuous monitoring probably would be justified only for degas systems, which emit large quantities of methane from a relatively small number of openings. For emissions from ventilation systems, MSHA already engages in periodic monitoring of all underground mines on a quarterly basis, with a margin of error of approximately 20% [10]. If precise damage internalization were the goal, it might be worth the added cost of more frequent monitoring. But since precise damage estimates do not exist, and the primary purpose of the fee is to encourage methane recovery, a fee based on periodic monitoring should be sufficiently accurate to generate appropriate incentives for recovery. The assessment of a methane emission fee for underground mines based on MSHA's periodic monitoring would not entail significant additional cost. Thus, the decision whether to impose the fee only on the 200 gassiest mines or to extend the program to all mines with measurable methane emissions would not involve a substantial difference in administrative cost.

If the program were extended to roughly 1,400 mines without measurable methane emissions, three alternative methods could be used to assess the fee: (1) develop more sophisticated monitoring devices; (2) compute the fee using engineering estimates for each mine based on core samples of the target coal and other seams from which methane might be released; or (3) compute the fee using basin-wide or national averages of methane emissions per ton of coal mined. Development of new monitoring technology could be quite costly, and its periodic use at each of these mines could substantially increase the administrative cost of the program. Likewise, the development of mine-by-mine engineering estimates would involve substantial costs of core drilling and computer modeling. Because these non-gassy mines produce less than 1% of all ventilation system emissions, the marginal improvement in accuracy from monitoring or engineering estimates would not seem to justify the added cost. The emission fees for these non-gassy underground mines should be based on basin-wide or national averages, which would involve little additional administrative cost.

For surface mines, which release methane directly into the atmosphere, monitoring is not even theoretically possible. As with non-gassy underground mines, the cost of developing mine-by-mine engineering estimates for these mines would seem to outweigh any possible gains in accuracy relative to the use of basin-wide or national averages of methane emissions per ton of coal mined.

Considerations of allocative efficiency would support the inclusion of all coal mines within any methane emission fee program. Limiting the program to underground mines would lead to allocative inefficiency through distortion of market prices. Imposition of the fee on underground mines would raise the price of coal from those mines relative to coal from surface mines, leading to reduced coal production from underground mines and increased production from surface mines. Insofar as surface mining also generates substantial external costs that are not fully internalized by existing federal and state regulations, the increase in production from surface mines would increase the level of environmental damage from surface mining. Under this scenario, a methane emission fee that was imposed to protect against the uncertain long run climate change damage caused by underground mines could exacerbate the more certain and immediate damage caused by surface mines, which would not seem to be an environmentally optimal result.

Even if the primary justification for a methane emission fee were the incentive it created for reduction of emissions from large gassy mines, the imposition of the fee on emissions from other mines would have the secondary benefit of internalizing the cost of methane emissions from mining on all mines in proportion to their level of methane emissions. The fact that a methane emission fee would increase the cost of coal and lead to a decrease in coal sales would not be viewed by economists as a cost of the program. To the contrary, economists would say that such a program corrected a market failure by forcing mine operators to include the environmental costs of methane emissions as part of the true cost of coal production.

Considerations of distributional equity also seem to support broad imposition of a methane emission fee. Focusing the fee on large underground mines would seem unfair insofar as these mines would be singled out to bear more than their fair share of the cost of methane emissions from mining, while smaller mines would escape all responsibility for their contribution to the problem. While the large gassy mines generally are owned by large diversified corporations that probably would be capable of absorbing these costs, a methane emission fee that caused a reduction in demand for coal from these mines would have adverse secondary consequences for their employees, suppliers and other associated businesses.

Political considerations may be the determinative factor in establishing the scope of a methane emissions fee. It is not altogether clear, however, whether political considerations favor a broad-based methane emission fee on all mines or a narrower fee only for emissions from large underground mines. While the large gassy mines are concentrated in a few states (especially Alabama, Colorado, Illinois, Kentucky, Pennsylvania, Virginia and West Virginia), they also have a larger number of employees, and they may function as a more organized and cohesive group than the diverse group of firms engaged in surface mining and smaller-scale underground mining. It is hard to predict which group would have more power in the political process.

The primary drawback to the imposition of a methane emission fee would be the adverse consequences for the coal industry and ultimately for consumers from an increase in the price of coal. EPA estimated that in the year 2000, U.S. coal mines would produce 1,095 million tons of coal: 404 million tons from underground mines and 691 million tons from surface mines; that these mines would generate 5.4 Tg of methane emissions: 4.2 Tg from underground mines, .7 Tg from surface mines, and .5 Tg from post-mining activities; that 1.7 Tg of these emissions would be captured in the absence of a subsidy and that 1.9 Tg would be captured with a subsidy (or emission fee) of $.57 per Mcf [18]. (The figures used here include .3 Tg of methane that EPA omitted from its analysis because it was already being recovered in 1990.)

Based on these EPA estimates, an emission fee of $.57 per Mcf methane or roughly $30 million per Tg would result in fees totalling $90 million, of which $69 million would be collected from underground mines, at an average cost of $.17 per ton of coal, and $21 million would be collected from surface mines, at an average cost of $.03 per ton of coal. (If the fees for underground mines were adjusted to reflect the .5 Tg of post-

mining emissions, the total amount of fees collected from these mines would be $15 million higher, and the cost per ton of underground coal would be $.04 higher.)

Subsidies or Tax Credits

If the sole goal of the regulatory program were to encourage recovery of CBM, this goal also could be accomplished through a subsidy or tax credit for CBM recovery. The Section 29 tax credit for unconventional gas was crucial to the economic feasibility of many CBM recovery projects on which drilling was completed prior to the end of 1992, and an equivalent tax credit or subsidy could provide the profit margin necessary to spur investment in CBM recovery at the 60 to 75 large gassy mines that have been identified as the primary candidates for such projects.

In a recent report, EPA evaluated the potential impact of a subsidy for CBM recovery based on the social value of the equivalent reduction in carbon emissions [10]. If the subsidy were $.57 per Mcf (based on a value of $5 per ton of carbon), an additional .2 Tg of methane would be recovered each year from the year 2000 to 2010. With a subsidy of $2.30 per Mcf ($20 per ton of carbon), the incremental reduction would be .4 Tg each year. Finally, with a subsidy of $11.50 per Mcf ($100 per ton of carbon), "all technologically feasible emissions reductions could be achieved," yielding an incremental reduction of .6 Tg above the level that would obtain in the absence of a subsidy.

Under a subsidy program, tax credits should be given for either utilization or flaring of the gas, because the environmental gains from flaring are nearly as great as those from utilization. A somewhat higher subsidy should be paid for utilization than for flaring, however, to reflect the greater social benefit from utilization of the gas. According to EPA, reducing methane emissions by using the gas for energy purposes is worth about 21 times more than reducing an equivalent amount of carbon dioxide emissions, whereas flaring is worth only 19 times more than reducing an equivalent amount of carbon dioxide emissions; the difference apparently reflects incomplete combustion during burning [9]. This difference alone warrants a 10% differential between the subsidies for recovery and for flaring. Moreover, recovery and use of the gas contributes to energy policy as well as environmental policy, reducing the need to burn other fossil fuels. When this benefit is taken into account, the differential between the subsidies for recovery and flaring of the gas should be even greater.

The positive incentives of a tax credit or subsidy would be far more attractive to the coal industry than the negative incentives of a methane emission fee. A tax credit also would be far less costly to administer than an emission fee program, because only those mines that actively engaged in recovery would interact with the regulators.

The primary drawback to a methane recovery subsidy would be its cost to the taxpayers. Even a relatively small subsidy could be quite costly if it were available to all coal operators who recovered CBM and not just to the incremental producers whose investment decisions were influenced by the subsidy. *Based on the EPA's projections for the year 2000, a subsidy of $.57 per Mcf ($30 million per Tg) would increase the level of profitable methane recovery by .2 Tg, from 1.7 Tg to 1.9 Tg, but this subsidy would cost the taxpayers a total of $57 million.* Moreover, the bulk of this subsidy would go to producers who would have recovered the gas even without the subsidy, so the marginal cost of generating the additional .2 Tg reduction would be roughly $5.41 per Mcf, more than nine times the nominal amount of the subsidy.

In addition to its cost, a subsidy for methane recovery is objectionable on efficiency grounds insofar as it would exacerbate the misallocation of resources resulting from the failure to internalize the costs of methane emissions. Because the costs of global warming attributable to methane emissions are not internalized, the price of coal is already too low, and production is too high. A subsidy to the coal industry that encouraged investment in methane recovery would necessarily increase the profitability of that industry, causing resources to shift into coal production and away from other energy sources that generate lower levels of methane and carbon dioxide per Btu. Thus, the incremental reduction in methane emissions attributable to subsidy-induced investment in methane recovery projects could be offset by increased levels of methane and carbon dioxide emissions attributable to subsidy-induced increases in coal production relative to other fuels [28].

The Deposit-Refund System

The deposit-refund system first received comprehensive theoretical treatment in the 1980s [39], and it is now considered one of the standard fiscal instruments for environmental policy [28,29,30,36]. Many Americans are familiar with the deposit-refund system that several states have established for disposable beverage containers. In these deposit-refund systems, the consumer pays a deposit upon purchase of the container and receives a return of the deposit if the container is returned. By collecting the deposit at the time of manufacture or purchase, a deposit-refund system eliminates the cost and difficulty of monitoring improper disposal. A number of European nations employ deposit-refund systems for waste lubrication oil, automobile hulks, and car batteries [36,39].

Deposit-refund systems achieve two related but distinct goals. First, insofar as the deposit approximates the social cost of improper disposal, parties are forced to internalize the full social cost of the product. Second, the possibility of receiving a refund gives parties an incentive to dispose of the product in an appropriate manner.

Deposit-refund systems are superior to both fees and subsidies in that they can be essentially revenue neutral: if all of the product is returned, the system imposes little net cost on either the regulated parties or the taxpayers. Even if some percentage of the product is not returned, the net cost to the parties is far less than the original amount of the deposit. A deposit-refund system produces far less economic distortion than systems of emission fees or subsidies alone. Unlike a subsidy, the parties in a deposit-refund system get no net benefit, so there is no increase in demand for the activity. In comparison to an emission fee, a deposit-refund system results in far lower net cost to the parties, so there is less impact on the price of the regulated activity relative to possible substitutes and thus fewer adverse secondary consequences.

As applied to CBM, a deposit-refund system would require that coal operators pay a "deposit" based on the potential methane emissions from their mines at the time the coal was extracted and then obtain a "refund" upon proof that the methane had been utilized or flared. (As with a subsidy program, the refund for flaring should be less than the refund for recovery and utilization.)

There are two reasons why a deposit-refund system is not well-suited to CBM. First, a deposit-refund system is most appropriate where the amount of emissions is more easily predicted than monitored, whereas with CBM the periodic monitoring of methane emissions that already takes place is probably more accurate than any possible pre-mining emissions estimates. Second, even the most successful CBM utilization projects are likely to achieve no more than 50-65% recovery, so a deposit-refund system would impose a substantial cost on the industry as a whole.

The impact of a pure deposit-refund system for CBM would be virtually identical to that of a system of methane emission fees, except that it would be less accurate and less efficient to the extent that deposits were based on estimated rather than actual emissions. For comparison, consider a system in which deposits and refunds were based on a value of $.57 per Mcf of methane emissions. If the deposits were assessed on the basis of nationwide averages of methane emissions per ton of coal, the earlier analysis of a methane emissions fee demonstrated that the deposits would amount to $.17 per ton of coal from underground mines (if post-mining emissions were excluded) and $.03 per ton of coal from surface mines. Mines that did not engage in recovery would pay this deposit on all estimated emissions and would receive no refunds, so the impact would be identical to a methane emission fee. Underground mines that engaged in recovery would pay the deposit on all estimated emissions, both recovered and unrecovered, and would receive a refund for the methane recovered, so the net impact would be the equivalent to a fee on all unrecovered methane emissions.

The primary difference between a deposit-refund system as just described and a methane emission fee is that the deposits in this system would be based on a nationwide average rather than on actual emissions. In comparison to a program involving fees based on actual emissions, a deposit-refund system based on nationwide averages would impose a disproportionately high fee on non-gassy mines and a disproportionately low fee on gassy mines. A deposit-refund system based on average emissions data would thus raise the profitability of gassy mines relative to non-gassy mines, sending precisely the wrong price signals to producers and consumers. This problem could be overcome if the deposits were assessed on a mine-by-mine basis, using data on actual emissions or mine-specific engineering estimates, but a deposit-refund system based on mine-by-mine emissions would be identical in all respects to a program of methane emission fees.

A Subsidy Funded by an Emission Fee

The above discussion of methane emission fees, subsidies and deposit-refund systems demonstrates that each approach has certain disadvantages. A methane emission fee would impose substantial costs on the coal industry, and, if limited to underground mines, it would distort resource allocation by shifting production to surface mines. A deposit-refund system would be functionally equivalent to a methane emission fee, and to the extent that deposits were assessed on the basis of nationwide averages it might produce even worse distortions in relative prices by shifting production to gassier mines. A subsidy for methane recovery would impose substantial costs on the taxpayers, and it would distort resource allocation by shifting production toward coal and away from other fuels that generate lower levels of greenhouse gas emissions.

Most of these problems could be avoided in a subsidy program for methane recovery that was funded by methane emission fees. The subsidy would create appropriate incentives for methane recovery, while the use of an emission fee for funding would render the program essentially revenue neutral, thereby eliminating any cost to taxpayers and minimizing the price distortion that otherwise would be engendered by subsidies or emission fees alone.

Consider, for example, the possibility of using a methane emission fee of $.57 per Mcf to fund a methane recovery subsidy of $.57 per Mcf. In such a program, mines that recovered more than 50% of their potential methane emissions would receive more in subsidies than they paid in emission fees. The earlier analysis of a subsidy program, based on EPA's projections, concluded that a subsidy of $.57 per Mcf would cost $30 million per Tg of methane recovered and would yield a total recovery of 1.9 Tg of methane in the year 2000 at a total cost of $57 million. The earlier analysis of an emission fee program concluded that a $.57 per Mcf emission fee would generate revenues of $69 million from underground mines and $21 million from surface mines. In a program of subsidies funded by emission fees, the net cost to underground mines would be $12 million, or $.03 per ton of coal from underground mines, and the net cost to surface mines would be $21 million, or $.03 per ton of coal from surface mines.

A program of subsidies funded by emission fees could be fine-tuned to satisfy a variety of subsidiary concerns. For example, the scope of the program could be narrowed by limiting it to underground mines, or to underground mines with detectable emissions, or even to underground mines with emissions above a minimum threshold. Also, the emission fee could be adjusted downward so that the program would be revenue-neutral as a whole or revenue-neutral for underground mines, or it could be adjusted upward so that the program would be revenue-neutral for mines with active recovery projects.

For example, a program for all mines could be made revenue-neutral by funding the $.57 per Mcf subsidy for the 1.9 Tg of methane recovered with a $.36 per Mcf emission fee on the 3.0 Tg of residual emissions from underground and surface mines. In such a program, underground mines would gain $13.4 million or $.03 per ton of coal, while surface mines would lose $13.4 million or $.02 per ton of coal. A program limited to underground mines could be made revenue-neutral by funding the $.57 per Mcf subsidy with a $.47 per Mcf emission fee on the 2.3 Tg of residual emissions from underground mines; in this program there would be no net impact on the price of coal, but mines with recovery projects would gain at the expense of those without recovery projects.

In a program of subsidies funded by emission fees, the incentives would be stronger than with subsidies or emission fees alone, while the disadvantages would be neutralized. The combination of a subsidy and an emission fee would generate a double incentive for methane recovery, because each unit of methane recovered would lower the emission fee as well as generating a subsidy. Unlike a program of subsidies alone, there would be no net cost to taxpayers and no price distortion toward increased coal production. In comparison to a program of emission fees alone, the negative impact on the coal industry would be far smaller, and it could be eliminated entirely if the emission fees were reduced to achieve revenue-neutrality.

CONCLUSION

Recent studies of methane emissions from U.S. mines demonstrate that energy and environmental policy options should focus on promoting methane recovery at a relatively small number of large and very gassy mines. These mines, especially longwall mines and other mines with degas systems, account for the vast majority of U.S. methane emissions from mining.

Alternative policy options include command-and-control regulation (mandatory technology standards or performance standards) and economic incentives (tradeable emission rights, emission fees, subsidies, or deposit-refund systems).

Traditional command-and-control regulations are not likely to play a major role in promoting CBM recovery. The variability of mine-specific factors probably precludes regulations mandating use of particular technologies to capture and utilize CBM, except possibly for flaring of unutilized methane from degas wells. The variability of mine-specific factors also would preclude regulations establishing ceilings on methane emissions, except possibly for a ban on emissions from degas wells. *The government ought to begin funding research to develop technology for safe flaring of methane from degas wells.*

The best way to promote CBM recovery is through economic incentives. Recovery is already profitable at many mines, and economic incentives could provide the necessary profit margin to justify other large gassy mines to undertake recovery projects. Among the available fiscal policy instruments, none is ideal.

Systems of tradeable emissions rights within a ceiling on total emissions have been used for sulfur dioxide and have been proposed for carbon emissions, but they would not be feasible for CBM. While Section 1605(b) of the Energy Policy Act of 1992 promises credits for CBM recovery as offsets within a future system of tradeable emissions rights in carbon dioxide emissions, it is doubtful whether these credits will have much impact on the extent of CBM recovery. If the voluntary reporting program is not generating additional investment in CBM recovery, there would appear to be no reason to grant credits for current CBM recovery in any future program of tradeable emission rights for greenhouse gases that did not itself impose limits on methane emissions from mining.

In theory, the negative economic incentives from a methane emissions fee would be more practical and more efficient than direct regulation, but an emissions fee would be costly to administer and could have adverse secondary consequences. A deposit-refund system would be similar to a methane emission fee, with all of the same advantages and disadvantages.

Positive economic incentives in the form of subsidies or tax credits for CBM recovery would yield the same levels of methane recovery as emission fees, and with far less administrative cost. These subsidies would be expensive, however, and they could distort resource allocation to yield an increase in coal production and a net increase in greenhouse gas emissions.

Although none of the policy options is ideal, a program that funded a subsidy for methane recovery with a methane emission fee would appear to be the best alternative. In such a program, the positive incentives of emission fees and subsidies would be additive, yielding twice the incentives for methane recovery as an emission fee or subsidy alone. On the other hand, the negative attributes of emission fees and subsidies would tend to neutralize each other, thereby avoiding any net cost to taxpayers, minimizing the impact on the price of coal, and minimizing the distortion of resource allocation between underground and surface coal or between coal and other fuels.

ACKNOWLEDGMENTS

I especially want to thank my new colleague David Hodas for his insightful comments on an earlier draft of this paper. Research support for some of my early work on this project was provided by grants from the National Research Center for Coal and Energy at West Virginia University and by the Arthur D. Hodges Educational Trust of the West Virginia University College of Law.

REFERENCES CITED

1. Lewin J.L., Siriwardane H.J., Ameri S. and Peng S.S., 1992: "Unlocking the Fire: A Proposal for Judicial or Legislative Determination of the Ownership of Coalbed Methane"; West Virginia Law Review, V. 94, No. 3, p. 563-691.

2. Lewin J.L., Siriwardane, H.J. and Ameri S., 1993: "New Perspectives on the Indeterminacy of Coalbed Methane Ownership"; Proceedings of the 1993 International Coalbed Methane Symposium, V. 1, p. 305-316.

3. Lewin J.L., 1994: "Coalbed Methane: Recent Court Decisions Leave Ownership 'Up in the Air,' But New Federal and State Legislation Should Facilitate Production"; West Virginia Law Review, V. 96, No. 3, p. 631-684.

4. Southern Ute Indian Tribe v. Amoco Production Co., No. 91-B-2273 (D. Colo. 1994) (granting summary judgment to defendant gas owners; appeal pending).

5. Carbon County v. Baird, No. DV 90-120, 1992 WL 464786 (Dist. Ct., Carbon County, Mont. Dec. 14, 1992) (verdict for coal owners; appeal pending).

6. NCNB Texas Bank, N.A. v. West, 631 So. 2d 212 (Ala. 1993).

7. Section 1339 of the Energy Policy Act of 1992, Pub. L. No. 102-486, § 1339. 106 Stat. 2986 (codified at 42 U.S. Code § 13368 (Supp. 1994).

8. H.B. 4371, enacted March 13, 1994, codified as W. Va. Code ch. 22, Art. 21.

9. USEPA, Kruger D., ed. (prepared by DePasquale M. and Ricci S. of ICF, Inc.), 1994: Identifying Opportunities for Methane Recovery at U.S. Coal Mines: Draft Profiles of Selected Gassy Underground Coal Mines: Washington, DC, USEPA Office of Air and Radiation, EPA 430/R-94/012.

10. USEPA, Hogan K.B., ed., 1993: Opportunities to Reduce Anthropogenic Methane Emissions in the United States: Washington, DC, USEPA Office of Air and Radiation, EPA/430/R-93/012.

11. International Energy Agency, Coal Industry Advisory Board, Global Climate Committee, 1994 Global Methane and the Coal Industry: Paris (Fr.), Organisation for Economic Co-Operation and Development, 67 p.

12. Guidelines for Voluntary Reporting of Greenhouse Gas Emissions and Reductions, and Carbon Sequestration, 59 Fed. Reg. 52769-03, Oct. 19, 1994.

13. Form EIA-1605, Voluntary Reporting of Greenhouse Gases, 59 Fed. Reg. 55258-01, Nov. 4, 1994.

14. Intergovernmental Panel on Climate Change, Working Group 1, Houghton J.T., Jenkins G.J. and Ephraums J.J., eds., 1990, Climate Change: The IPCC Scientific Assessment: Cambridge (U.K.), Cambridge University Press, 365 p.

15. Intergovernmental Panel on Climate Change, Working Group 1, Houghton J.T., Callander B.A. and Varney S.K. eds., 1992, Climate Change 1992: The Supplementary Report to the IPCC Scientific Assessment: Cambridge (U.K.) Cambridge University Press, 200 p.

16. International Energy Agency, Coal Industry Advisory Board, 1994, Global Methane and the Coal Industry: Paris (Fr.), Organisation for Economic Co-Operation and Development, 67 p.

17. USEPA, Hogan K.B., ed., 1993: Options for Reducing Methane Emissions Internationally, Vol. II: International Opportunities for Reducing Methane Emissions: Washington, DC, USEPA Office of Air and Radiation, EPA/430/R-93/006B.

18. USEPA, Hogan K.B., ed., 1993: Anthropogenic Methane Emissions in the United States, Estimates for 1990: Washington, DC, USEPA Office of Air and Radiation, EPA/430/R-93/003.

19. Irani, M.C., Thimmons E.D., Bobick T.G., Duel M. and Zabetakis M.G., 1972: Methane Emission From U.S. Coal Mines, A Survey, Washington, DC, US BOM, IC 8558, 58 p.

20. Irani, M.C., Jeran P.W. and Duel M., 1974: Methane Emission From U.S. Coal Mines in 1973, A Survey, Washington, DC, US BOM, IC 8559, 47 p.

21. Irani, M.C., Jansky J.H., Jeran P.W. and Hassett G.L., 1977: Methane Emission From U.S. Coal Mines in 1975, A Survey, Washington, DC, US BOM, IC 8559, 47 p.

22. Grau III, R.H. and LaScola J.C., 1984: Methane Emissions From U.S. Coal Mines in 1980, A Survey, Washington, DC, US BOM, IC 8987, 13 p.

23. Grau R.H., 1987: "An Overview of Methane Liberations From US Coal Mines in the Last 15 Years"; Proceedings of the Third U.S. Mine Ventilation Symposium, SME-AIME, p. 251-255.

24. Trevits M.A., Finfinger G.L. and LaScola J.C., 1991; "Evaluation of U.S. Coal Mine Emissions"; Proceedings of the Fifth U.S. Mine Ventilation Symposium, SME-AIME, p. 177-182.

25. USEPA, Kruger D., ed. (prepared by Boyer C.M., Kelafant, J.R., Kuuskraa V.A., and Manger K.C. of ICF Resources Inc.), 1990: Methane Emissions from Coal Mining: Issues and Opportunities for Reduction: Washington, DC, USEPA Office of Air and Radiation, EPA/430/9-90/008.

26. Sprouls M.W., 1990: "Longwall Census '90"; Coal, Feb. 1990, p. 36-47.

27. Merritt P.C., 1991: "As Time Changes, So Do Longwalls" (Longwall Census); Coal, Feb. 1991, p. 40-49.

28. Pearce D.W. & Turner R.K., 1990: Economics of Natural Resources and the Environment: Baltimore, MD, The Johns Hopkins University Press, 378 p.

29. Lewin J.L., "Toward a New Ecological Law & Economics"; Ch. 8, p. 249-293, in Malloy R.P. and Braun C.K., eds., 1995: Law and Economics: New and Critical Perspectives: New York, Peter Lang, 456 p.

30. USDOE, 1989: A Compendium of Options for Government Policy to Encourage Private Sector Responses to Potential Climate Changes: Washington, DC, USDOE, Office of Environmental Analysis, DOE/EH-0102 (executive summary 94 p.) & 0103 (2 vol.)

31. Cline W.R., 1992: The Economics of Global Warming: Washington, DC, Institute for International Economics, 399 p.

32. Ottinger R.L., Wooley D.R., Robinson N.A., Hodas D.R. and Babb S.E., 1990: Environmental Costs of Electricity: New York, Oceana Publications, Inc., 769 p.

33. Ackerman B.A. and Stewart R.B., 1985: "Reforming Environmental Law"; Stanford Law Review, V. 37, p. 1333-1365.

34. Hahn R.W. and Stavins R.N., 1991: "Incentive-Based Environmental Regulation: A New Era From an Old Idea?"; Ecology Law Quarterly, Vol. 18, No. 1, p. 1-42.

35. USEPA, Hogan K.B., ed., 1993: Options for Reducing Methane Emissions Internationally, Vol. I: Technological Options for Reducing Methane Emissions: USEPA Office of Air and Radiation, Washington, DC, EPA/430/R-93/006.

36. Opschoor J.B. & Vos H.B., 1989: Economic Instruments for Environmental Protection: Washington, DC, Organisation for Economic Co-Operation and Development, 131 p.

37. Tietenberg T.H., 1985: Emissions Trading: An Exercise in Reforming Pollution Policy: Washington, DC, Resources for the Future, Inc., by the John Hopkins University Press, Baltimore, MD, 222 p.

38. Helme H., Popovich, M.G. and Gille J., 1993: Cooling the Greenhouse Effect: Options and Costs for Reducing CO_2 Emissions from the American Electric Power Company: Washington, DC, Center for Clean Air Policy, 55 p.

39. Bohm, P., 1981: Deposit-Refund Systems: Theory and Applications to Environmental, Conservation and Consumer Policy: Washington, DC, Resources for the Future, Inc., by the Johns Hopkins University Press, Baltimore, MD, 175 p.

TABLE 1 - ANALYSIS OF METHANE EMISSIONS FROM SELECTED GASSY MINES IN EPA STUDY

Category Daily Emissions Exceed (MMcf/d)	# Mines	Total Emissions (Vent+Degas) Per Day (MMcf/d)	Per Year (Bcf/yr)	(Tg/yr)
0.1	84	430.8	157.2	2.99
1.0	57	418.3	152.7	2.90
2.0	40	395.9	144.5	2.75
4.0	25	355.3	129.7	2.47
10.0	13	264.9	96.7	1.84
20.0	6	147.3	53.8	1.02

Totals include .28 Tg (40 MMcf/d = 14.6 Bcf/yr) of methane recovered for pipeline sales from six mines in Alabama and Utah, all of which were among the top 25 mines, five of which were among the top 13, and three of which were among the top six.

All data from EPA [9].

INTERGAS '95

May 15-19, 1995
The University of Alabama
Tuscaloosa, Alabama USA

9545

Mine Methane and Environment: Ways of Methane Utilization

E.A. Yelchainov, Skochinsky Institute of Mining, Russia

ABSTRACT

The paper considers the effect of coal-bed methane on the environment as well as technical possibilities of its utilization.

It describes technical and engineering approach to the methane-air mixture preparation and enrichment resorting to gas separation and cleaning.

Methane-air mixture separation is important for protection of environment and for utilization in various fields of application. The experimental installations make use of membranes, natural and artificial zeolites, gravity, low temperature, vortex and combined methods.

Coal-bed methane recovery and utilization should help solving the economical, ecological and even social problems in the coal-mining regions of Russia.

* * *

Investigations of gas and aerosol conditions of the atmosphere have shown considerable changes in its composition under the anthropogeneous influence which results in great changes in the globe and regional climate.

At present the atmosphere contains about $7.75 \cdot 10^{-5}$ per cent of methane - not very much, indeed - but taking into account that its radiative properties are but by twenty times more efficient than those of carbon dioxide as far as the Earth's heat emission absorption is concerned, this gas plays an important role in maintaining certain climate on our planet.

Economic activities of mankind are responsible for over 59 per cent of the volume of methane in the atmosphere and one of the sources is the methane emission during underground coal mining. According to the latest data every year the collieries provide about 32 milliard cu.m of methane for the atmosphere. In future this figure is going to grow because of the concentration of mining operations, increasing depths of extraction and growing natural content of methane in the rock massif.

During underground coal mining Russian collieries add 6-7.5 milliard cu.m of methane to the atmosphere every year including 0.7-0.8 milliard cu.m of gas pumped out with the degassing systems, the methane concentration reaching 10-60 per cent, while the rest is transported with the ventilation where the methane concentration is 0.1-1.0 per cent. Due to constant increase of depth of mining and concentration of the mining operations, the intensity of methane emission becomes greater, the gas being removed with the ventilation flows.

Taking into consideration the greater methane emission from the collieries and its concentration in the atmosphere of the coal-mining regions, absence of scientific estimates for the methane influence on the environment, on the social aspects of human activity as well as unsolved problems of utilization of the coal-bed methane and uninvestigated methane properties as anthropogenic source of influence on the environment and the climate, in particular, we have studied possible changes in climate in these regions. Such a task was set for the first time. It was necessary to find out to what degree the coal-bed methane provides for the hotbed effect and how this phenomenon influences the ecological and economic indices of the industrial area.

Two factors are assumed for investigations such as:

- average annual temperature of the near-surface atmospheric layer of the region to be investigated,
- amount of methane emitted in the atmosphere from collieries of the region to be investigated.

As the changes in climate due to the hot-bed gases in the atmosphere are taking place slowly, then, the investigations have to embrace a long period of time. We considered 35 years from 1955 to 1990 to calculate average values of temperature and methane emission. The experiment was carried out on the basis of the data available for the principal coalfields of the former Soviet Union such as: Kouznetsky, Pechorsky, Karagandinsky and Donetsky.

To determine the air temperature we resorted to the reference data of the hydro-meteorological stations. Only areas with high methane content of the collieries were to be investigated. All in all there were chosen 11 areas.

The included Vorkouta district in Pechorsky coalfield, Donetsk and Lougansk districts in Donetsky coalfield, Saransky, Abaysky, Promyshlenny and Shakhtinsky districts in Karagandinsky coalfield and Kemerovsky, Kiselyovsky, Novokouznetsky and Mezhdurechensky districts in Kouznetsky coalfield.

When calculating the increasing methane concentrations in the atmosphere for every coal field such factor as the period of methane stay in the atmosphere which usually takes from 3 to 11 years has not been taken into account. As there are no measurements of methane content above

the coal-mining areas, it is impossible to consider the changes in the vertical methane column relative to the Earth's surface, the column being conditioned by the time of its stay.

A release of the methane-air mixture in the atmosphere causes global damage because it ruins the ozone layer and provides for the «hot-bed» effect.

It was established by the investigations that the greater the methane content of the collieries, the higher the average annual temperature of the air near the surface (Fig. 1, 2, 3, and 4).

Methane is a noxious admixture to the mine air which affects the health of miners and inhabitants of these industrial areas.

Until now many researchers attribute methane to the physiologically indifferent gases, believing that it dilutes the oxygen concentration in mine air when emitting from the coal seams, thus, the methane effect is reduced to acute hypoxia and asphyxia. However, some scientists indicate that in great concentrations methane acts as narcotic. Subjected to sharp and quick intoxication the victims fall into a short-term state of «pleasant peace and quiet and wish for sleep». Motive activities get slower, muscle feebleness, apathy, asthenia and swooning take place. As the consciousness is getting recovered, a sharp motive stimulation is observed, often the victims experience the syndrome of «the morning after the night before» or hangover. With a normal amount of oxygen (21%) after inhaling methane there appear the inhibit reflexes and processes in the nervous system while respiratrion and circulation of the blood are decreased, i.e. the symptoms of narcotic origin are demonstrated.

At present the scope of unfavourable changes in the atmosphere of the coal-mining areas considerably exceeds the possibilities of their elimination (overcoming) and the consequences of the environment degradation tell upon the entire social and economic development of the regions.

Utilization of methane must include not only the economical profit because of its consumption, but also elimination of all kinds of damage caused by methane release in the atmosphere which not always can be measured and economically expressed.

Under the present conditions it is not the limitations of the raw materials and fuels but the environment pollution that is a decisive factor for the economic development. It becomes more and more obvious. Methods and directions for the methane utilization depend to a great extent on its concentration and volumes, that is why it is desirable first of all in the collieries to improve the existing and develop more efficient methods for its capture.

Provided the present tendency for transfer to the market is preserved, any enterprise (no matter to what kind of property it belongs) is sure to avoid its own expenses and costs for improving the quality of environment which is but common good and weal consumed by everybody. Within the framework of the market mechanism it is necessary first of all to be guided by the economic stimuli due to utilization of the secondary raw materials and then, to the reduction of damage caused by environment pollution. Experience for methane utilization indicates exactly a wide prospect and high economic efficiency of the gas utilization. This problem can be solved both in global and regional scale by working out new technologies for the secondary resource utilization. In this respect a most revealing and demonstrative example is the coal-mining industry of Kouznetsky and Pechorsky coalfields.

METHANE OUTPUT

Years	Kouznetsky coalfield	Pechorsky coalfield
1953	442 852	106 264
1960	546 244	158 691
1965	685 846	160 533
1970	956 470	315 582
1975	1 032 712	385 791
1980	1 484 234	579 661
1985	1 895 813	809 000
1990	2 071 080	896 898

At present there is accumulated certain experience for utilization of methane obtained from collieries during degassing but there are no proved solutions for utilization of methane transported with outgoing ventilation flow. For the industrial utilization of methane out of mine ventilation flows it is necessary to work out some methods of its utilization including development of technical means and technologies to increase its concentration up to 2.5-3.0 per cent in the air-methane mixtures. Development of technology, equipment and a chain of devices to control the utilization processes must provide for not only rational utilization of the resources, but also for protection of the environment.

In Russia the mine safety regulations allow up to 0.75% of methane in the mine outgoing ventilation flow that is why its direct utilization as an energy carrier is not economical.

The problem of concentration of the methane-air mixture can be solved in several ways such as:

- methane concentration can be increased by adding methane from state gas pipelines,
- binary gas flow can be parted by separation of methane and air flow,
- binary gas flow can be parted by separation of a part of the air flow with increased concentration of methane in it.

The first way is the simplest, but it cannot be widely applied because there are no state gas pipelines within the regions of collieries in operation.

As far as the second way of concentration of the methane-air mixtures is concerned, we consider two kinds of technology such as:

- obtaining methane gas-hydrates out of the gas-air mixture with a low methane content in it,
- separating methane-air mixture under low temperature in order to obtain the gaseous or liquid 98-99% methane.

The third way of the methane-air mixture concentration technologies includes development of several installations based on different principles for separation of a part of air flow with an increased methane concentration. For this purpose there have been created some experimental

prototypes of equipment based on the following principles:

- membrane separation
- vortex separation
- separation of gas mixture
- adsorption - desorption
- combined methods with additional coercion of artificial gravitation and ultrasound on the process of separation.

Concentration of methane from the state gas pipelines can be carried out only in case the gas is brought to the collieries. Most collieries have no supply of gas from such pipelines, so this way can be realized but in single isolated instances.

Obtaining gas-hydrates is technically possible, but it does not pay economically now. As the prices for power carriers change, it is obvious that this way of concentration and utilization of methane out of the methane-air mixture is sure to find its field of application.

As our investigations have shown, the installations operating according to the principles of molecular membrane are hardly efficient to separate methane and oxygen. The same can be said about the adsorption ways for separation of methane and oxygen. These installations can give a reliable result only in case of forming the basic process with additional technological measures.

A maximum effect can be obtained with the help of centrifugal vortex apparatus. The existing centrifugal apparatus for enriching the methane-air mixtures is not economically acceptable.

Upon estimating all possible ways for equipment to enrich the methane-air mixtures, we have begun development of the apparatus based on combination of principles such as membrane-centrifugal, vortex-centrifugal and separation-centrifugal in order to increase the methane concentration in outgoing mine air flows up to 2.5-3.5% to utilize them in the gas turbines to produce heat and electric power. The methane concentration from the degassing systems can reach as high as 33-65%.

For utilization of the methane-air mixture concentrated up to 2.5-3.5% some verifying calculations have been carried out for a gas turbine and reliability of its operation. Practically any of the gas turbines known with rated power from 0.5 to 3.5 kWt can be run with a 2.5-3.5% methane concentration provided a special combustion chamber is designed to provide for clean and continuous burning of methane. Today there are some difficulties in solving this problem. The existing combustion chambers do not meet the requirements for a constant temperature of the outgoing gases when burning the 2.5-3.5% concentration methane.

In order to provide the combustion efficiency there have been developed several chambers based on the principle of burning a methane-air mixture of stoichiometric composition, the vortex principle and the filtration burning principle.

There is a necessity of enriching the methane-air mixture from the degassing network with a methane concentration below 25%. This can be solved by a non-heating adsorption method to obtain the methane concentration up to 33-65%. Artificial zeolites with preset parameters serve as adsorbents. The methane-air mixture obtained can be utilized for burning in the boiler-rooms, heat-aggrigates, diesels, turbines, but it cannot be turned over to the state gas pipelines and accepted for transportation for a considerable distance. That is why we have worked out a technological scheme for a low-temperature separation of the mixture in order to obtain the gaseous methane concentrated up to 98-99% under pressure of 0.4 MPa to be increased to 25 MPa with the help of an automatic gas-inflating compressor station AGNKS type to utilize this methane as motor fuel. There is a second variant of the mixture low-temperature separation technology to obtain the liquid methane for its re-gasification to follow:

- either with pressure of 25 MPa to utilize it as motor fuel, or
- with pressure of 0.6 MPa to be supplied to the populated areas and settlments.

The technological line is equipped with standard equipments. Power consumption of the installation reaches 800 kWt. 925cu.m/h of methane and 425 cu.m/h of nitrogen can be obtained from the methane-air mixture. Cost of one cu.m. of methane is as high as US$ 2.00-2.50. Such an installation can produce up to 21,000t of conventional liquid motor fuel annually.

When there is a growing deficit of energy carriers they have every reason to utilize any quantity of the highly calorific and ecologically clean fuel. The work being carried out provides for a solution of important ecological problem with good economical efficiency.

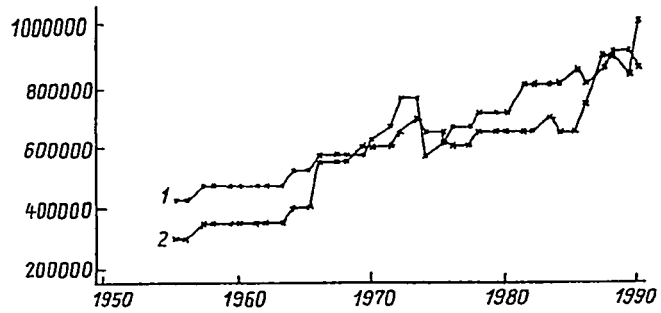


Fig. 1. Methane emission out of collieries.
1 - Kouznetsky coalfield
2 - Donetsky coalfield (Russian section)

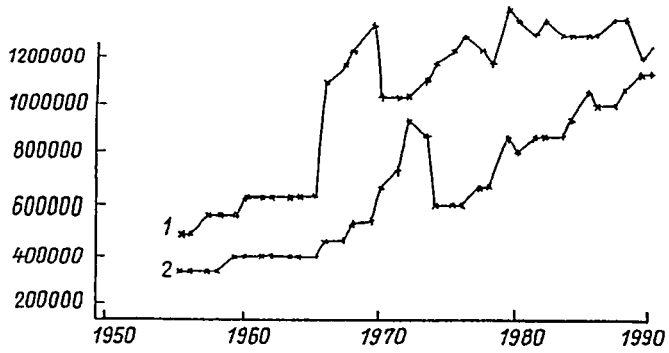


Fig. 2. Methane emission out of collieries.
1 - Karagandinsky coalfield
2 - Pechorsky coalfield

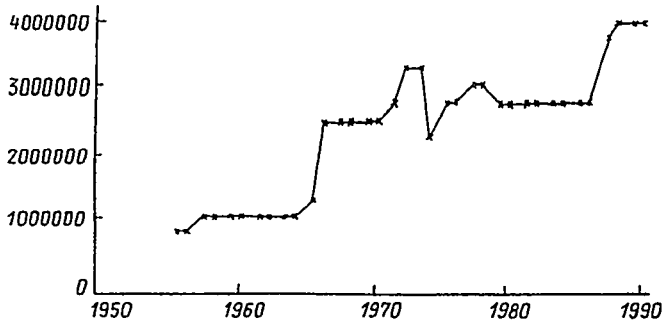


Fig. 3. Methane emission out of collieries.
Donetsky coalfield (Ukranian section).

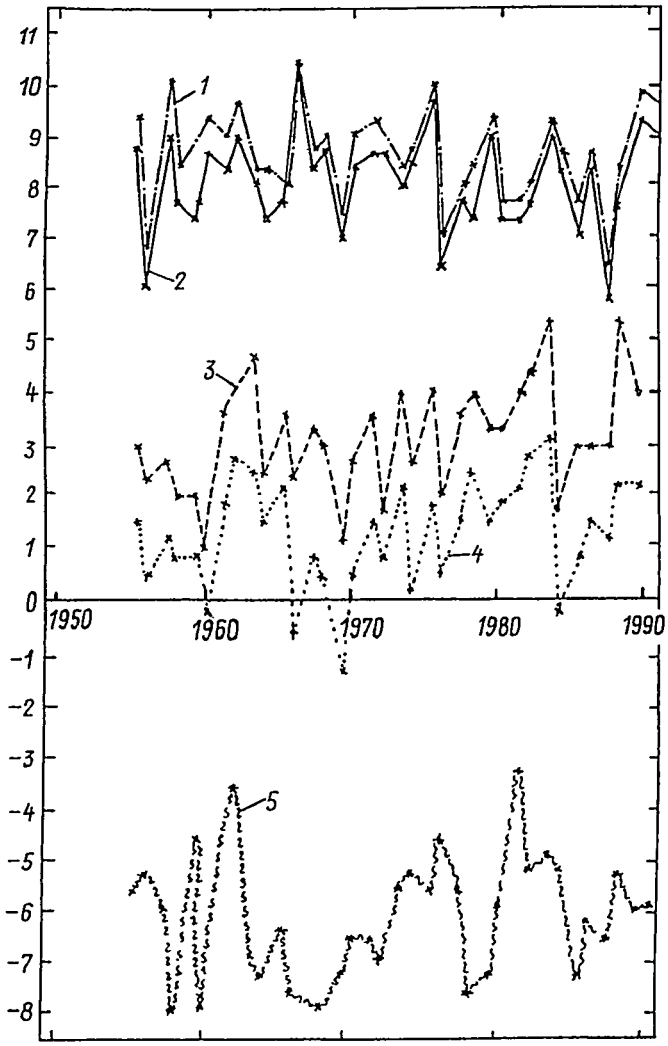


Fig.4. Average annual temperature of «just-above-the surface» air.

1 - Lougansky region of Donetzky coalfield
2 - Donetsky region of Donetsky coalfield
3 - Karagandinsky coalfield
4 - Koyznetsky coalfield
5 - «Vorkoutaugol» Production Unit (Vorkoutinsky coalfield)

INTERGAS '95

May 15-19, 1995
The University of Alabama
Tuscaloosa, Alabama USA

9552

Evolution of Severance Tax Policy by Litigation: The Coalbed Methane Industry vs. The State of Alabama

C.D. Haynes, The University of Alabama; and K.P. Hanby, Tom Joiner and Associates

ABSTRACT

Several recent oil and gas severance tax audits in the State of Alabama have been appealed by the producing companies and subsequently litigated. The rulings from each litigation have resulted in the evolution of severance tax policy now being implemented by the Alabama Department of Revenue (ADR). This exemplifies "placing the cart before the horse."

Alabama oil and gas severance tax law *Code of Alabama 40-20-1 (3) (1975)* and *Section 9-17-25 Code of Alabama* [1] established that severance tax be applied to the value of the product *at the wellhead* by direct sale or comparable sale. In practice, however, coalbed methane is not valued at the wellhead, therefore eliminating the determination of severance tax by either method in the Code. Coalbed methane in Alabama is typically sold at some point downstream of the wellhead, thus establishing value at a point other than the wellhead.

Rulings from *State of Alabama v. Petro-Lewis Corporation* [2], *Unocal Exploration Corporation, Appellant vs. State of Alabama* [3] and *State of Alabama v. Phillips Petroleum Company* [4] determined that in the absence of direct or comparable sale, the "workback method" could be used to determine the wellhead value of natural gas for severance tax calculation. Workback is a method to calculate the applicable costs from the point of sale upstream to the wellhead. These costs, which include direct and indirect expenditures, return on investment, and cost of capital, are deducted from the value of the gas at the point of sale to obtain its wellhead value. Applicable costs for workback calculations have been a source of controversy in the auditing of severance tax returns by the ADR, with inconsistent application being widespread.

The Coalbed Methane Association of Alabama proposed certain guidelines to the ADR for the workback method in order to ensure uniform application of the method [5]. These guidelines proposed operating cost categories as well as return on investment, depreciation, and overhead. The ADR did not consider these guidelines in their audit of the Black Warrior Methane Company (BWM) severance tax returns. Instead, they made partial reference to the "Onshore Proposal" [6] previously submitted to the ADR by conventional oil and gas producers in south Alabama. BWM subsequently appealed the severance tax audit, and after several negotiated adjustments, filed suit against the ADR to set aside the additional tax.

Black Warrior Methane Corporation v. State of Alabama [7] was tried in the Circuit Court of Tuscaloosa County, Alabama on July 20, 1994. Several rulings from this case complemented the guidelines proposed by the Coalbed Methane Association.

The majority of these rulings were incorporated into ADR procedures by memorandum from the Chief of the Natural Resources & License Tax Division dated May 27, 1994 [8]. This memorandum was significant in that it contained the first published set of severance tax guidelines from the ADR.

OIL AND GAS SEVERANCE TAX IN ALABAMA

Severance tax rates for coalbed methane ("gas" or "occluded natural gas") are given in *§40-20-2 Code of Alabama* and *Section 9-17-25 Code of Alabama*. The language of these Codes is given in several subdivisions, but in essence, explains that coalbed methane is taxed as follows:

1. Any well which begins commercial production of occluded natural gas after June 7, 1984 shall be taxed at the rate of two (2) percent of gross value from coal seams *at the point of production* for a period of five (5) years after production is initiated. After 5 years, the rate increases to six (6) percent if the well was permitted after July 1, 1988, and eight (8) percent if permitted prior to July 1, 1988.

2. All wells producing 200,000 cubic feet or less of gas per day shall be taxed at the rate of four (4) percent of gross value.

3. In addition to severance taxes, there is also a production tax which is two (2) percent of gross value.

The primary problems with severance tax calculations and establishment of value concern the point of production and the fact that the tax is applied to the gas in its natural, unrefined, or unmanufactured condition. If a gas sales contract specifies the wellhead as the point of production, there is no problem in calculating the severance tax. If the point of sale is somewhere other than the wellhead, however, an interpretation must be made for the value of gas at the point of production, usually meaning the wellhead. The nature of coalbed methane production does not lend itself to wellhead sale. The gas is at a very low pressure, usually 20-50 pounds per square inch-gauge (psig), and essentially saturated with water vapor. In order to make the gas salable, dehydration and pressure increase are minimum requirements, and these are applied somewhere downstream of the wellhead. Therefore, an inherent problem in severance tax calculations for coalbed methane operations requires determination of *value* at the *point of production.*

COMPARABLE SALE AND THE WORKBACK METHOD

The "workback method" is defined as *a method for calculating market value of oil or gas at the wellhead when value cannot be calculated on the basis of comparable sales. Under this method, costs of transportation, processing, and treatment are deducted from the ultimate proceeds of sale of oil*

or gas and any extracted or processed products to ascertain wellhead value [9]. Other costs would include the return on investment and cost of capital.

The workback method was initially tested in *State of Alabama v. Petro-Lewis Corporation* in 1987. This case involved gas processed at the Womack Hill and Big Escambia Creek Plants. The gas subject to the dispute was owned by Petro-Lewis and others. These associated owners had financial interest in both the producing wells and processing plants. Petro-Lewis valued their gas using casinghead gas contracts, establishing the value of gas at the wellhead for identical gas owned by the nonassociated owners at Womack Hill. They also valued their gas using gas contracts for sale of like-quality gas of others at Big Escambia Creek. The gas contracts were from the adjacent Little Escambia Creek. The casinghead gas contracts at Womack Hill provided that the well owners be paid 50% of the natural gas liquid (NGL) sales proceeds and 60% of the residue gas sales proceeds from the processing plant. The Big Escambia Creek contract stipulated 50% NGL and 100% of residue gas sales proceeds, respectively.

The ADR claimed that the associated well owners were not selling their gas at arms-length, therefore using the workback method, allowing a 21% deduction to NGL sales and no deduction to residue gas from both fields. The 21% processing fee deduction allowed on the NGLs was based on a prior audit agreement between the ADR and an unrelated company.

The court held the ADR's contention that the associated well owners were not selling their gas at arms-length to the plant at Womack Hill to be incorrect. The court further found that if the contracts were not considered arms-length, then they should be used to establish the value for identical gas for the ADR in satisfying *§40-20-1 (3)* pertaining to the sale of gas of like quality. Regarding Big Escambia Creek, the court found that the gas sales contracts used for like-quality gas provided the value of the gas sold by Petro-Lewis and satisfied the requirements of *§40-20-1 (3)* for the sale of like-quality gas.

Unocal Exploration Corporation, Appellant vs. State of Alabama presented a case wherein the point of sale was other than the wellhead. In this February 13, 1992 hearing, it was found that Unocal held interest in both the producing wells and a central treating plant to remove hydrogen sulfide and other contaminants. Unocal had previously signed an agreement with joint owners that determined the value of the raw gas at the wellhead by the workback method. Curiously, the ADR had accepted this arms-length agreement with the non-plant owners, but refused to accept the same agreement for a well owner who was also a plant owner. This mixed interpretation of arms-length agreements would be repeated several times thereafter in the litigation of severance tax issues.

The ADR claimed that the contract with non-plant owners did, in fact, establish the true value of the raw gas, and that this value was corroborated by comparison with similar quality gas from nearby fields in southwest Alabama. The Court held that the severance tax judgement be put aside, and that no additional tax be paid. Besides ruling against the ADR, the Court approved several "expenses" relating to Unocal's workback calculations. For example, a depreciation charge of 7.69%, a return on investment (ROI) of 16.65%, and an interest charge of 8% were approved as reasonable expenses of operation. As later seen, the ROI deduction had significant meaning as a precedent-setter. The Court held that the Unocal return of 83% of gas plant tailgate values to the well owners was considerably better than the 70% or less returned to owners in comparable operations.

As a sidelight in the Unocal case, the ADR had assessed Unocal taxes for gas flared during well testing. The Court held that the flared gas is exempt from taxation under the provisions of *§40-20-2(a) Code of Alabama (1975)* which exempts natural gas which is "lawfully vented or flared in connection with production of oil." This issue became important once again during coalbed methane severance tax litigation.

The workback method was to be tested again in *State of Alabama v. Phillips Petroleum Company* heard in the Supreme Court of Alabama during its October 1992-93 term. In this case, the court was to determine if the workback method, earlier prohibited by the Appeals Court, could in fact be used by the ADR in calculating the value of natural gas at the wellhead pursuant to *§40-20-2(a) Code of Alabama*. The Court of Civil Appeals had held previously that the ADR was prohibited from computing value by any method other than by the actual sale price of the raw gas or the sale price for comparable gas. The Supreme Court reversed the Court of Civil Appeals and determined that the workback method could be used to determine value in the absence of wellhead contracts or comparable sale.

THE ONSHORE PROPOSAL

In April 1989, several producers of natural gas in Alabama (Chevron, Exxon, LL&E, Mobil, Mosbacher, Murphy, and Texaco) presented a proposal to ADR to settle outstanding severance tax issues. This proposal set forth a method of calculating taxable value at the wellhead where produced gas is run through a treating facility and processing plant prior to sale. Further, this method would not apply to gas produced offshore.

Subscribers to this proposal would agree to pay severance tax on:

1. 100% of residue gas sales price as market value at the tailgate of the plant, less substantiated actual costs necessary to make the gas marketable.

2. 100% of the condensate sales price as market value at the point of sale, less substantiated actual costs necessary to make the condensate marketable.

3. In lieu of paying tax on 100% of the market value of natural gas liquids (NGL) less the applicable substantiated actual costs of processing gas for extraction of plant products, taxpayers would pay tax on 79% of sales value of NGL.

4. Actual substantiated costs as given above were interpreted as the costs and deductions allowed under Generally Accepted Accounting Principles, as documented in the taxpayer's books and records, including but not limited to the following:
   - ad valorem taxes
   - insurance
   - direct operating and maintenance expenses
   - overhead
   - employee benefits
   - depreciation
   - purchased fuel
   - return on investment.

5. Although it was conceded that residue gas would be taxable, it was proposed that the cost of the fuel be deducted as an operating expense when the fuel was used in processing operations.

6. An 8% return on investment (ROI) would be calculated on the average annual undepreciated investment balance of the treating facility. ROI for extraction of NGLs would be included in the 21% blanket deduction as referenced in (4) above.

7. Hydrogen sulfide gas and/or sulfur would not be taxable. Accordingly, costs associated with the recovery of sulfur from hydrogen sulfide gas will not be allowed as a marketing cost deduction against taxable hydrocarbons.

COALBED METHANE ASSOCIATION PROPOSAL

Shortly after the Onshore Proposal was submitted to the ADR, the Coalbed Methane Association of Alabama (CMA) proposed a method of calculating wellhead value as a basis for settling pending and future audits as well as future tax returns. The CMA was attempting to offer a standardized procedure instead of continuing to accommodate changes in auditing procedures of ADR audits.

The CMA proposal described the uniqueness of coalbed methane operations as compared to conventional natural gas operations. For example, the dewatering of wells and the low pressure of the coalbed methane as it is being produced were mentioned. It also emphasized that ceratin "marketing costs" were necessary to make the coalbed methane attain value.

The specific proposal contained three components:

1. severance tax to be paid on 100% of the gross receipts if the point of sale between non-related parties is at the wellhead.

2. if the first sale is not at the wellhead between non-related parties, severance tax will be based on 100% of the gross sales revenue less certain "marketing" costs (as defined below).

3. as a substitute to paying tax above, a simplified alternative of 79% of the gross sales price be used as a basis for calculating severance tax.

"Marketing costs" were listed as usual and customary for industry practice in transporting and conditioning gas from the wellhead to point of sale. These costs included the following:

- marketing
- dehydration
- treating
- gathering
- processing
- metering
- transporting (includes tariff charged by non-related party).

The proposal contained costs that were not considered marketing:

- production costs to extract coalbed methane from coal seams and bring it to the wellhead;
- normal lease separation of oil or condensate from gas.

Further, the proposal defined elements of marketing cost:

- ad valorem taxes
- insurance
- direct operating and maintenance expenses such as labor, materials, supplies, maintenance repairs, fuel and power, rent, supervision, and fees
- employee benefits and payroll taxes
- depreciation or equipment lease costs
- ROI equal to 8% per annum on the average undepreciated investment balance
- lease use gas other than pumping unit fuel
- overhead from field, district, administrative, and warehousing activities limited to 15% of the itemized costs listed above.

BLACK WARRIOR METHANE V. STATE OF ALABAMA

Black Warrior Methane Corporation v. State of Alabama was tried in the Circuit Court of Tuscaloosa County, Alabama, on July 20, 1994. This trial resulted from an audit of Black Warrior Methane Corporation (BWM) and Black Warrior Transmission Corporation (BWT) for the period June 1988 through August 1990.

BWM is equally co-owned by Jim Walter Resources, Inc. and SONAT Coal Gas, Inc. BWM produces coalbed methane in association with Jim Walter Resources, Inc. underground mining activity. Basically, gas is produced by BWM three ways:

1. "conventional" vertical coalbed methane wells drilled ahead of mining activities.

2. horizontal boreholes in coal blocks prior to being mined by longwall methods.

3. so-called "gob" wells directly above and behind the retreating longwall coal mining face.

An affiliated entity named Black Warrior Transmission, Inc. (BWT) transports the BWM coalbed methane in a sole-purpose pipeline system for a tariff of $0.46 per mcf. The severance tax audit determined that additional severance taxes were due as follows:

- vented gas, Jim Walter Resources No. 3 mine
- disallowing the BWT tariff
- disallowing a compressor fuel gas charge
- disallowing BWM administrative charges from BWT.

Although gas vented in oil and gas operations is clearly defined as non-taxable by *§40-20-2 Code of Alabama*, the ADR maintained that since no oil was being produced from coalbed methane operations, vented gas could not be given tax relief by the language of the Code. BWM contended that gas venting served two functions, both of which were indispensable to its operations:

- it removed the dangerous methane from underground coal mines as a safety measure;
- it provided prudent well testing before pipeline connections were committed.

The ADR argued that the $0.46/mcf transportation charge paid by BWM to BWT was not arms-length in nature because it was between affiliated entities. BWM countered by providing evidence that similar agreements between nearby non-affiliated parties were at higher tariffs.

The disallowing of compressor fuel gas by the ADR was perhaps the most illogical of their contentions. When questioned at the trial, the ADR auditor could not reconcile the similarity between purchased fuel gas from non-affiliated entities and the use of BWM fuel gas in marketing activities. In other words, the ADR would allow a fuel gas exemption if the fuel was purchased from a nonaffiliated entity, *but not from an affiliated entity at the identical price*!

The affiliated entity relationship between BWM and BWT caused the ADR to "collapse" both entities for the audit. Although upheld by the Court, this action resulted in several inconsistencies in the audit. For example, no uniform overhead for the combined entities was given by the ADR in the audit.

Over the course of the trial, BWM presented several inconsistencies in the ADR audit. These were:

- exempting vented gas from severance tax.
- failure to use a uniform overhead for the combined BWM/BWT entity.
- disallowing depreciation before the 15% overhead cap was applied.
- no deduction for fuel gas.
- disallowing the BWT tariff even though it was less than a similar tariff in the area.
- not differentiating between the cost and value of coalbed methane in allowing a deduction for fuel gas.
- using guidelines from the onshore agreement, although BWT was not a party to the agreement and the ADR never announcing its adoption.

The latter deficiency was particularly onerous to operators, because the ADR had not formally responded to either the

Onshore Proposal or the proposed guidelines submitted by the CMA. Essentially, the ADR appeared to be "flying blind" on every audit, having no uniform audit guidelines. They appeared to either adopt portions of the proposals submitted or simply made up new rules for each audit.

The ADR typically conducted an audit, then followed the audit with a notice of additional severance tax owed. This notice requested the operator to furnish additional information for potentially reducing the additional tax levy. Typically, the ADR would reduce the additional tax amount in stages after negotiation with the operator. At some point, the operator would balance the remaining tax levy against the technical/legal effort necessary to reduce the tax even further, then send a check to the ADR for the balance owed. Interest and penalties accompanied these late payments.

The Court found that the ADR failed to promulgate written rules and regulations for properly utilizing the workback method in determining wellhead value of coalbed methane as required by the Alabama Administrative Procedure Act. Therefore, the ADR violated BWM's due process rights by attempting the workback method without published rules and regulations.

In addition, the Court found that in applying the workback method to BWM wellhead value, it was appropriate to deduct from the coalbed methane sales price all actual expenses associated with the transportation, processing, and treatment of the gas, including the following elements:

- gathering costs at $0.68/mcf.
- all operating expenses claimed by BWM on their returns.
- all administrative expenses directly related to the processing, treatment, or transportation of the gas.
- ROI as an element of the workback method according to case law, therefore allowing a 10% value as a compromise between the ADR recommended 8% and BWM's recommended 16-25%.
- disallowing severance tax on vented gas, since it was not sold, transported, or stored.
- compressor fuel valued at the "spot" market price prevailing on the dates of severance.

CHANGES IN ADR SEVERANCE TAX POLICY

On May 27, 1994, the Chief of the Natural Resources & License Tax Division of the ADR issued a memorandum to oil and gas producers and purchasers entitled *Changes in Determining Taxable Value of Hydrocarbons*. This memorandum stated that the Circuit Court determination in *Black Warrior Methane Corporation v. State of Alabama* was to be applied on a statewide basis. The following deductions were to be effective on the memo date:

- the costs of any fuel used to transport, process, and/or treat hydrocarbons (previously disallowed).
- administrative expenses of personnel involved in the processing, transporting, and treating of hydrocarbons.
- ROI to be increased from 8% to 10% of the average undepreciated balances of the assets.
- vented and/or flared gas to be exempted from severance tax if the gas well was not connected to a gathering system (previously subject to severance taxes).

This memorandum was quite significant in that it provided the first public notification of ADR rules and regulations. While seemingly obvious from the operator's standpoint, this represented a significant departure from traditional ADR procedures.

SUMMARY

The State of Alabama Department of Revenue has been a continual source of frustration to Alabama oil and gas operators by their refusal to promulgate rules and regulations for conducting severance tax audits. By refusing to provide this basic service to taxpayers, the Court determined the ADR violated due process as explained in the Alabama Administrative Procedure Act. Typically, auditors were assigned complicated tasks without formal training in oil and gas operations, simply adhering to ADR customs regardless of their sensibility or applicability to a given situation. *State of Alabama v. Petro-Lewis Corporation, Unocal Exploration Corporation vs. State of Alabama, State of Alabama v. Phillips Petroleum Company*, and *Black Warrior Methane Corporation v. State of Alabama* were instrumental in shaping severance tax policy in Alabama through litigation.

Oil and gas operators in Alabama will find that the frustration of severance tax audits, while not likely to disappear, will be reduced significantly in the future as a result of these cases. It is expected that future litigation will be necessary to continue refining the ADR severance tax policy.

The evolution of workback guidelines by litigation should be carefully studied by coalbed methane operators in Alabama to plan their severance tax strategy. Wellhead contracts may be desired to avoid the difficulties in workback-based audits.

The planning and execution of severance tax strategy can result in significant cost savings through the knowledgeable application of workback components. Knowledge of these guidelines will also reduce the cost of legal representation if and when audit appeals are necessary.

ACKNOWLEDGEMENTS

The authors wish to express their appreciation to Mr. Jerry Sanders and Ms. Dona Sulzmann for their assistance in preparing this paper.

REFERENCES

1. *Code of Alabama 40-20-1 (3) (1975)* and *Section 9-17-25 Code of Alabama.*

2. *State of Alabama v. Petro-Lewis Corporation*, Department of Revenue Administrative Law Division, Dorbet No. Misc. 86-228, July 22, 1987.

3. *Unocal Exploration Corporation, Appellant vs. State of Alabama*, Circuit Court of Mobile County, Alabama CV91-000812, *Findings of Fact*, August 5, 1992, 8 pp.

4. *State of Alabama v. Phillips Petroleum Company*, Supreme Court of Alabama, 1910797, October 1992-93 Term, 9 pp.

5. *Proposal to Settle Outstanding Alabama Severance Tax Issues*, May 6, 1989, 4 pp.

6. *Proposal, Calculation of Wellhead Value, Alabama Coalbed Methane Severance Taxes*, Coalbed Methane Association of Alabama, (undated), 20 pp.

7. *Black Warrior Methane Corporation, Appellant v. State of Alabama*, Circuit Court of Tuscaloosa County, Alabama CV92-1923, *Findings of Fact*, December 30, 1993.

8. Pridgin, D.W., *Changes in Determining Taxable Value of Hydrocarbons*, memorandum dated May 27, 1994, State of Alabama Department of Revenue, 1pp.

9. Williams, H.R. and Meyers, C.J., *Manual of Oil and Gas Terms*, 8th edition, Matthew Bender, 1991, p. 1374.

INTERGAS '95

May 15-19, 1995
The University of Alabama
Tuscaloosa, Alabama USA

9563

Degassing of Methane Bearing Geologic Structures in the Donbass Coal Basin by the Donetsk Coal Association

V.V. Pudak, Donetskugol Coal Association, Ukraine

ABSTRACT

Coal fields of the Donetsk Coal Association are of different geological structures with high gas content; flexure folds and closed dome systems; thick, lithologically uniform, crack-porous sandstones and overlap faults.

Geological factors plus the gas content increasing with depth hold back the growth of underground coal production.

With these conditions, major emphasis is placed on controlling gas emissions from the coal-rock strata in order to more effectively use mining equipment, improve work conditions and better exploit energy resources.

Traditional methods of in-mine degassification become less effective with going deeper in mining. Gas content in a borehole over a mined seam reaches 60 to 80%.

Nevertheless, the concentration of methane captured in the air/gas mixture is so low due to long pipelines and insufficient sealing, that it cannot be utilized without preliminary enrichment.

The Association now uses more extensively surface drilling to degas methane bearing strata by employing different techniques to boost up gas recovery.

Certain methods have been elaborated to recover up to 4 million cubic meters of methane through one well from coal-rock strata. The lifetime of gas wells has been increased an additional 2-3 years. Surface wells capture up to 55% of the gas from underground workings.

The stable chemical composition of recovered gas with 90 to 99% of combustible hydrocarbons and the absence of sulphur compounds enable us to utilize methane gas as a high-octane motor fuel as well as fuel for municipal needs. The utilization of coalbed methane saves oil fuels and improves the environmental situation in the Donetsk region.

The mines in the region have been working on utilizing methane gas as a motor fuel for three years. there have been designs , manufacturing and installation of gas filled compressor stations of different sizes. These stations maintain a capacity to fill 10 to 60 automobiles on a daily basis. Gas, recovered from gob wells drilled from the surface. There also exists stations with a capacity to fill 100-200 autos a day, utilizing gas captured from field wells in advance of mine construction.

Both types of stations successfully operate in the Donetsk region. Gas from distant wells are transported by truck mounted filling stations directly to automobile companies.

The work done at the association on degassification of geological structures, recovering high content methane with its further utilization enables the region to better use the energy resources within the allocated field and, at the same time, improve the environmental situation in the Donetsk region.

RECOVERY AND UTILIZATION

In Donbass the depth of coal mining increases every year by 5-8 m and, at present, it is at a maximum of 1,400 m. With the depth of mining increasing gas content in coal/rock strata goes up.

The methane resources in the Donetsk coal basis at the depths of 500-1,800 m are estimated as 12 to 22 trillion cu.m., of which 3 to 4 trillion cu.m. are recoverable.

The research to evaluate the gas energy potential in "Donetskugol" mines indicated that there are 26.5 billion cu.m. of methane contained in recoverable coal seams and gob areas.

The range of methane content varies from mine to mine from 0.2 to 4 billion cu.m. (e.g., Skochinsky mine has 4.7 billion cu.m., Zasyadko mine--3.6 cu.m., Yuzhnodonbasskaya No. 3 mine--3.5 billion cu.m.) (Fig. 3).

Extensive resources of coalbed methane change the whole idea of their value as an energy source. For this reason, Donbass is to

be classified as a major coal/gas deposit, and a comprehensive approach to utilize fully its energy potential should take place. By means of such a comprehensive approach, the following can be achieved:

- safety improvement in coal mining;
- environmental situation improvement;
- use of low-cost methane as an energy source; and
- coal production increase,

Until recently methane liberated at coal mining has been treated in a simplified way as "enemy No. 1." With rare exceptions, it is extracted basically due to safety requirements. It is well illustrated by the diagram (Fig. 4) and numbers per sources of methane extraction while mining coal at "Donetskugol" Association (Figs. 5 and 6).

Statistics of the recent decade indicate that out of 4.5 billion cu.m. of methane extracted from the mines, 80% is vented into the atmosphere as a low-methane content gas mixture by mines of mine ventilation; 18% of methane is recovered by in-mine degassing technique, and 2% of methane is extracted through surface degassing wells.

Ventilation methane has not been used until now in "Donetskugol" because of its low concentration. In-mine degassing pipelines in some cases have methane content up to 60%. Only 5 mines out of 14 that have in-mine degassing systems utilized methane of over 25% concentration in their boilers.

With the rest of the mines, methane content in the pipelines is low beyond the limit due to air infiltration, so the gas is vented into the atmosphere.

As a result, only 9% of extracted methane has been used as an energy source. The increase of methane use in the near future depends on new technologies that enable the recovery of gas with high methane content.

The most promising technique, in this respect, is to degas coal/rock strata with wells drilled from the survace, which produce gas of high methane content. In the 10-year period, methane capture through surface wells has increased from 0.7% to 3.8% of the total gas amount extracted in the Association. Surface degassing technologies have been developed in the Association based upon modern views on gas states in coal/rock strata. Methane in coal resources is in three states (Fig. 7):

- free in open and closed pores;
- absorbed on pore surface; and
- dissolved in coal organics (solid solution).

With the change of thermodynamic state, methane goes from solid solution to absorbed and free state. Closed pores are filled with methane due to solid diffusion. When methane contained in closed pores and in coal solid solution is taken into account, gas content of coal fields is 1.5 times higher than that calculated by standard methods.

Within the Association coal fields, methane is contained in three types of collectors in absorbed and free states:

- in coal seams of different thicknesses;
- in coal matter scattered in embedded rock strata; and
- in free-gas accumulations in gas-bearing sandstones, geological "traps" and microdeposits.

Depending on the gas collector type, corresponding methods to recover methane have been developed.

1. While degassing in advance of mining hydrofracking technique has been applied with the use of surfactants and chemicals to stimulate surface wells. This technique has been tested at Skochinsky, Zasyadko, and Kalinin mines. The essence of this method is to create channels that transport gas to a well. This technique was thoroughly developed in collaboration with Moscow Mining Institute and Makeevka Research Institute, but has not been used in recent years because of the lack of equipment.

2. To degas coal/rock strata embedded in coal seams, scattered coal matter and gas-bearing sandstones, the methods of using gob fracking as a result of mining have been developed. The most effective method to deplete gas is to drill directional degassing wells.

This method consists in the disposition of a well in accordance with the structure of strata being displaced after mining (Figs. 8, 9 and 10). This method makes it possible to increase the service life of a well by 2 or 3 times and, accordingly, the amount of methane recovered from a well (Fig 11.). This technique has been implemented at Kalinin, Zasyadko, and Yuzhnodonbasskaya No. 3 mines.

3. Pre-mining degassing technique is applicable only in cases when the geological structures include dome and flexure systems, that have gas-bearing sands coated with gas-tight rock, i.e., gas traps. The

essence of this method is to drill a pre-mining degassing well in the most productive point of a gas trap. This technique has been used to degas in advance of mining the coal field of a would-be mine "Yuzhnodonbasskaya" No. 12, where there are dome geological structures with the reserves of 3 to 26 million cu.m. of free gas.

Gas recovered through the above methods is utilized in four ways (Fig. 12). To implement these ideas, the Association set up an experimental plant operating on the following scheme: gas filling compressor station (GFCS)--truck-mounted gas filling station (TGFS)--automobile (Fig. 13).

This experimental plant (Fig. 14) producing 1,000 cu.m. of compressed gas a day (equivalent of 1 tone of high-quality gasoline) has been in successful operation for three years by nos. Through this period, 325 thousand cu.m. of compressed methane have been produced, thus economizing 325 t of gasoline.

The importance of this small GFCS consists in that the Association could test and improve in practice the methods of utilizing methane produced from degassing wells and also the technique of cleaning and drying gas, compressing it to fuel automobiles on the spot or through TGFSes delivering gas to automobile companies. The personnel has been trained to operate such station, and work and safety procedures have been developed. All the above has made it possible to begin commercial use of gas as a motor fuel.

The first commercial GFCS has been set up to utilize methane recovered from pre-mining degassing wells located in the field of a would-be mine "Yuzhnodonbasskaya" No. 12 (Fig, 15).

For this purpose, a vertical well has been drilled in the area of Lavrentyev dome, which is located nearly in the center of the coal field, completed with pipes of 114 mm. diameter and tested under 120 kg./sq/cm. (Fig 16). The gas-bearing strata have been fractured by explosions at the depths of 704-714 m., 716-726m., and 936-945 m. The test results indicated that gas in the strata is under the pressure of 72 kg. sq.cm., and the total volume of it in the degassing zone is estimated as 26 million cu.m. this, in its turn, means that the expected discharge flow can be of about 10 thousand cu.m. a day.

The GFCS was built by the construction companies of the Association in August 1994. the production rate of it is up to 2000 fueled automobiles a day or 3.5 million cu.m. of gas a year (Fig. 17). It is also designed to fill TGFS that deliver gas to automobile companies of the Association. There are 6 of them working on a shuttle scheme between the GFCS and truck companies (Fig. 13).

The facilities comprise the following modules:

- three compressor units generating the pressure of 250 kg/sq.cm. handling up to 400 cu.m. of gas per hour;
- drying and gas accumulating unit;
- control room;
- electrical substation and commutation unit; and
- employee support facilities.

The gas filling area has one filling station to fuel automobiles on the spot and 5 stations to fill truck-mounted gas filling units at the pressure of 250 kg/sq.cm. The station is designed to operate for 8 years in accordance with the estimated gas reserves. Even by now the operation of this station has saved 1,000 tons of gasoline.

The "Gas" program from 1995 envisages:

methane recover --10 million cu.m.;
utilizing it as motor fuel--4 million cu.m.;
methane use for electricity production--1 million cu.m.;
put into operation a station to fill 45 TGFS a day--1 unit; and
gas-fueled electric generators--2 sets.

At present the work is underway to set up the facilities for the production line: gas well--electrical generator--coal mine, i.e., power supply for a mine by means of pre-mining degassing.

The Association is going on in collaboration with research groups to bring about promising technologies that widen the scope of methane utilization, low-content methane mixtures included.

Certain experiments have been done to turn methane into a hydrate state, which promises to develop the technology to purify in-mine water in a low-cost way, to cool the underground mine air, to generate super-high pressures for industrial processes.

Fig. 1 - DYNAMICS OF COAL MINING DEPTHS IN DONETSK COAL ASSOCIATION MINES

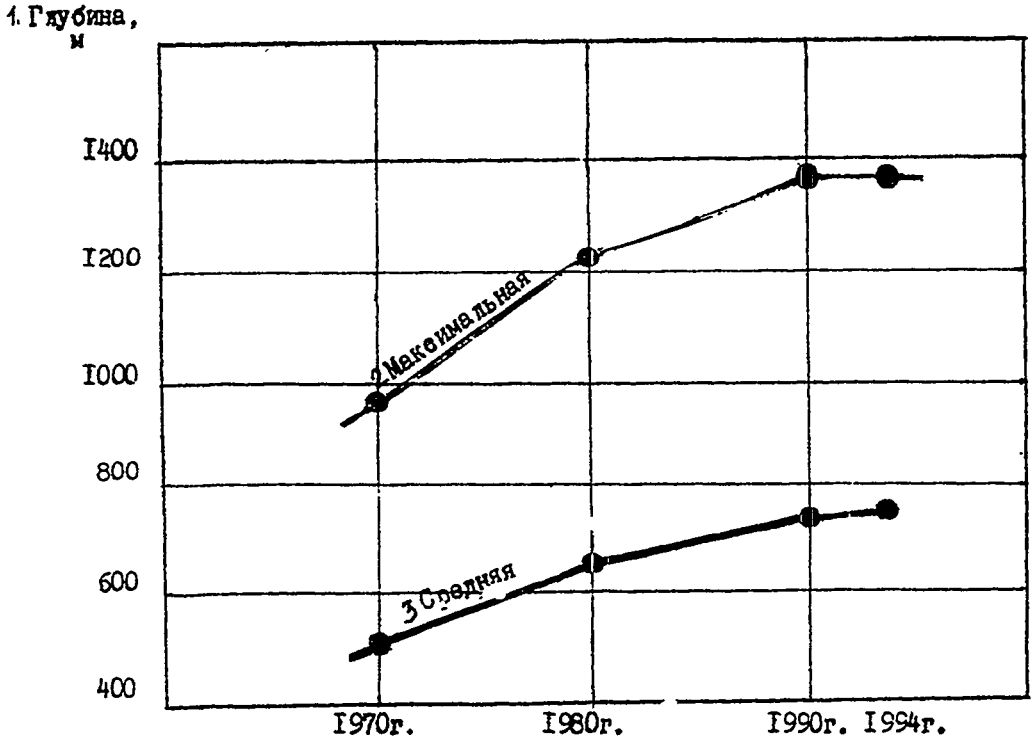


Fig. 2 - GROWTH OF COALBED METHANE CONTENT WITH THE DEPTH OF COAL SEAMS BEING MINED

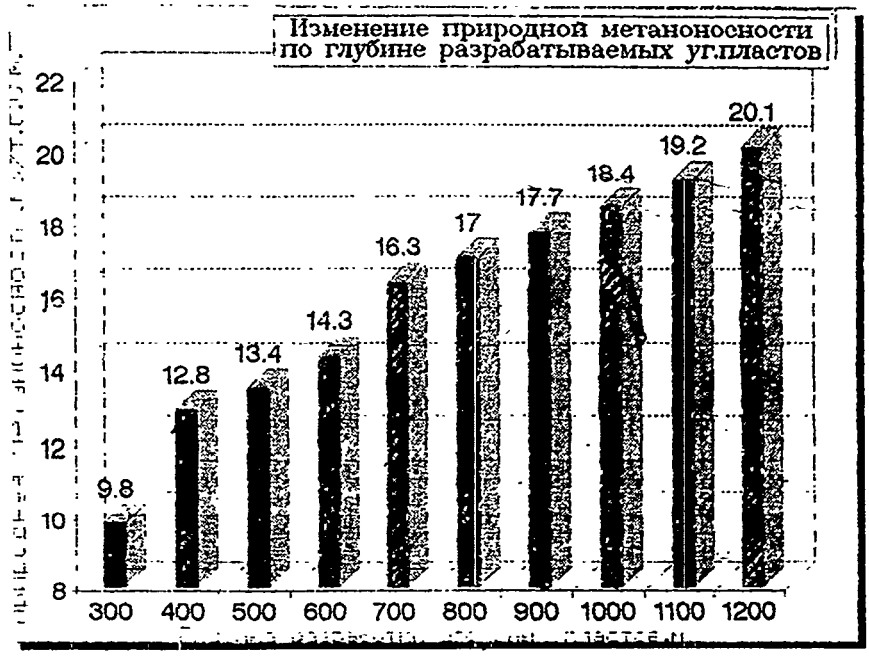


Fig. 3 - SCHEMATIC MAP OF GAS CONTENT OF DONETSK COAL ASSOCIATION MINE FIELDS

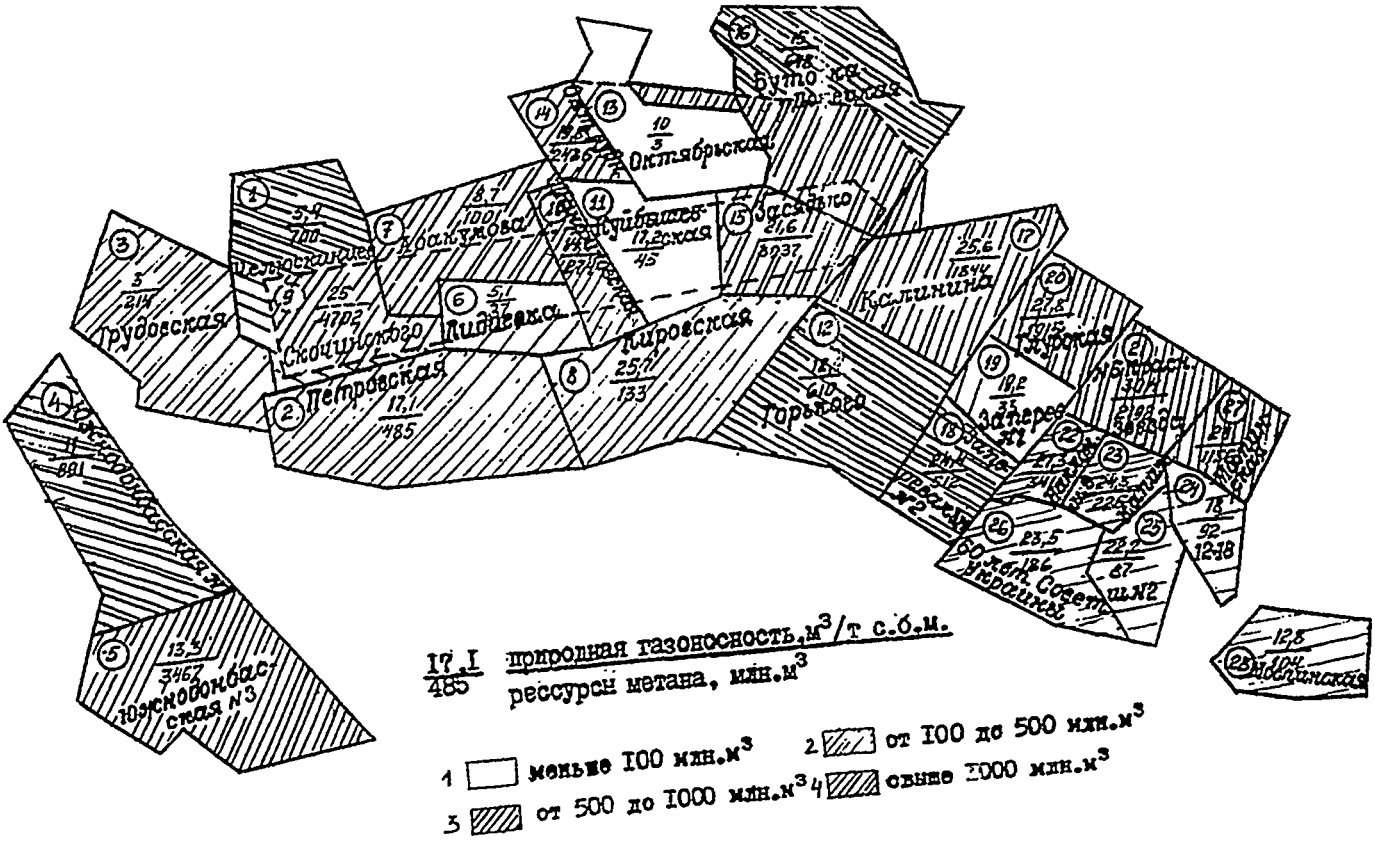


Fig. 4 - VOLUME OF METHANE RECOVERED FROM DONETSK COAL ASSOCIATION MINES

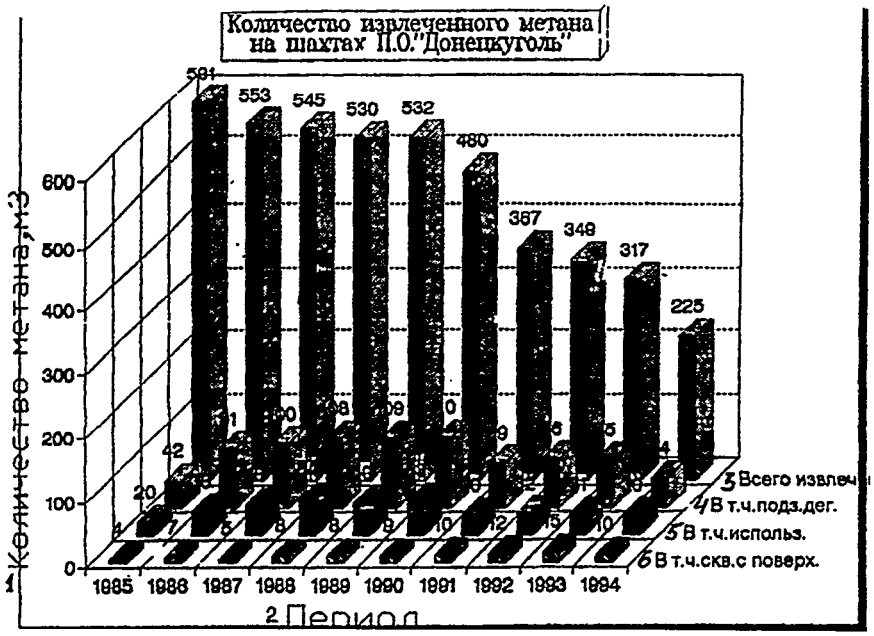


Fig. 5 - EXTRACTED METHANE VOLUME AS A RESULT OF DONETSK COAL ASSOCIATION MINES' ACTIVITIES IN 1985-1994

1 Год	2 Добыча	3 Всего извлечено метана		4 в том числе						8 Использование метана			
				5 Системами вентиляции		6 Системами подземной дегазации		7 Скважинами с поверхности		9 всего		10 в т.ч. из скважин с поверхности	
	11 млн.т	13 млн.м3	%	млн.м3	%	млн.м3	%	млн.м3	%	млн.м3	%	млн.м3	%
1985	21376	591	100	545	92.3	42	7.0	4	0.7	19.6	3.3	–	–
1986	21542	553	100	455	82.2	91	16.5	7	1.3	36.0	6.5	1.0	3.0
1987	21027	545	100	440	80.8	100	18.3	5	0.9	46.0	8.4	1.0	2.2
1988	20732	530	100	414	78.1	108	20.3	8	1.5	54.0	10.2	1.0	1.9
1989	20212	532	100	415	78.1	109	20.4	8	1.5	50.0	9.4	–	–
1990	18728	480	100	361	75.2	110	22.9	9	1.9	53.0	11.0	–	–
1991	14383	367	100	288	78.5	69	18.8	10	2.7	30.3	8.3	–	–
1992	14961	349	100	261	74.8	76	21.8	10	3.4	32.4	9.3	0.3	0.9
1993	13092	317	100	227	73.1	75	23.7	10	3.2	31.2	9.8	0.3	1.0
1994	11260	329	100	243	74.0	74	22.2	12	3.8	35.3	13.3	1.3	4.3
12 за 10 лет	177313	4593	100	3649	79.6	854	18.6	83	1.8	387.8	8.4	4.9	1.3

Fig. 6 - QUANTITY OF RECOVERED AND UTILIZED METHANE GAS IN DONETSK COAL ASSOCIATION as referred to 1 ton of daily production

1 Год	2 По объединению м3/т сут.доб.	3 в том числе, м3/т сут.доб.			7 Использование метана м3/т сут.доб.	
		4 Системами вентиляции	5 Системами подземной дегазации	6 Скважинами с поверхности	8 всего	9 из скважин с поверхности
1993	24.2	17.6	5.6	1.0	2.4	0.02
1994	29.2	21.6	6.5	1.1	3.1	0.13

Fig. 7 - GAS MOLECULES DISTRIBUTION MODEL IN COAL SUBSTANCE IN THE VICINITY OF AN OPEN PORE AND IN A PORE ITSELF

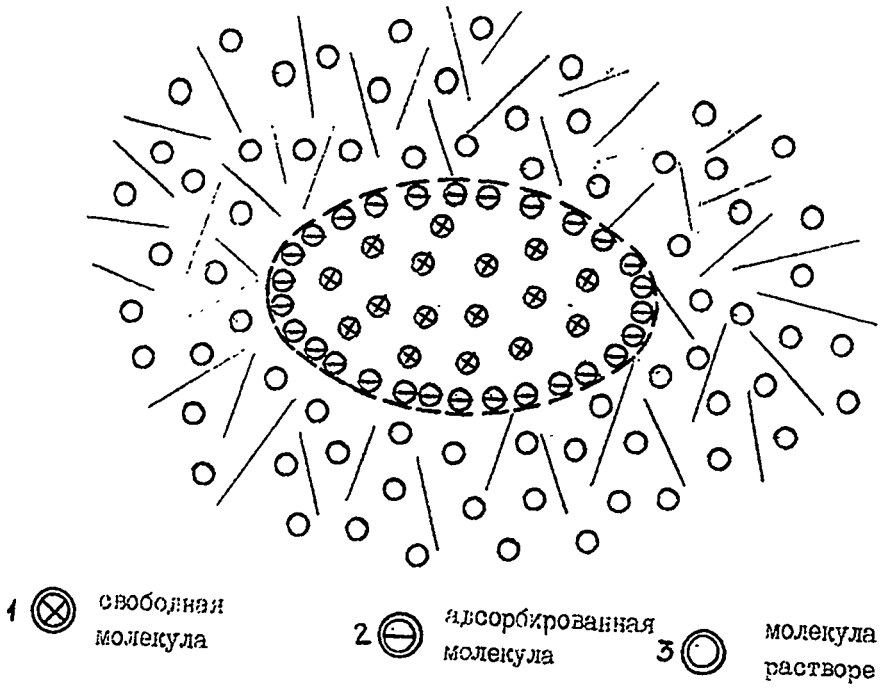


Fig. 8 - VERSIONS OF DIRECTIONAL WELLS

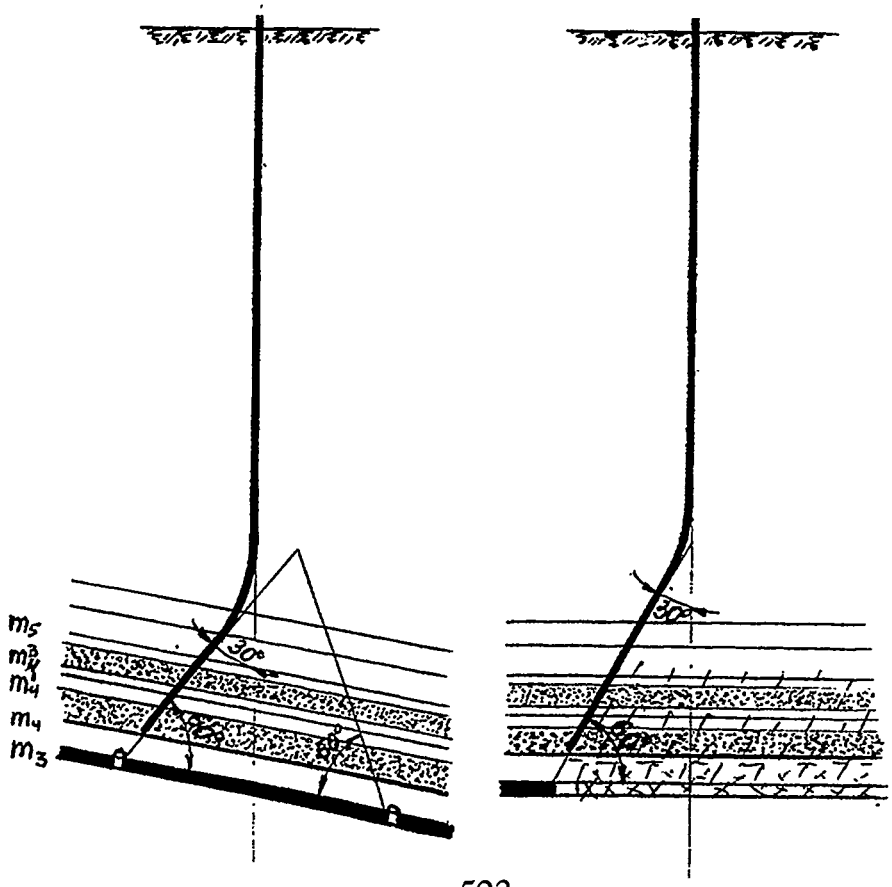


Fig. 9 - DESIGN DIAGRAM OF A DIRECTIONAL WELL

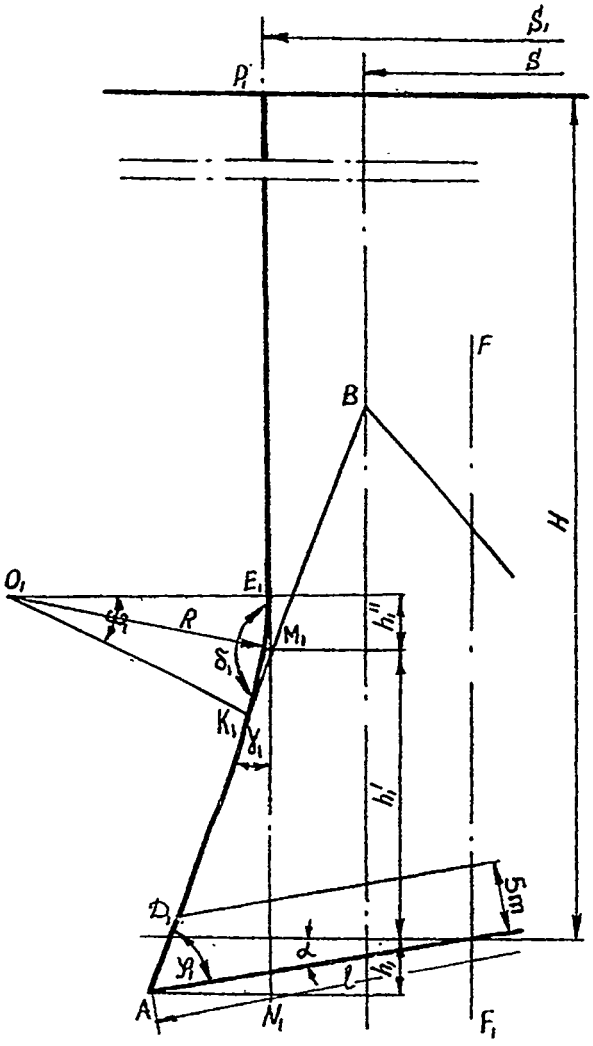


Fig. 10 - CONSTRUCTION OF A DIRECTIONAL WELL

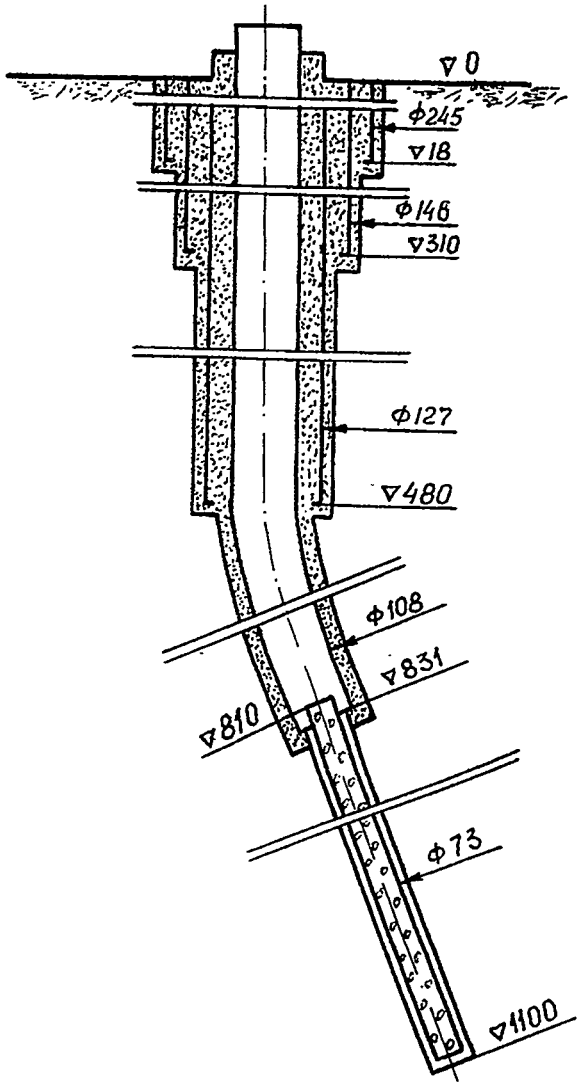
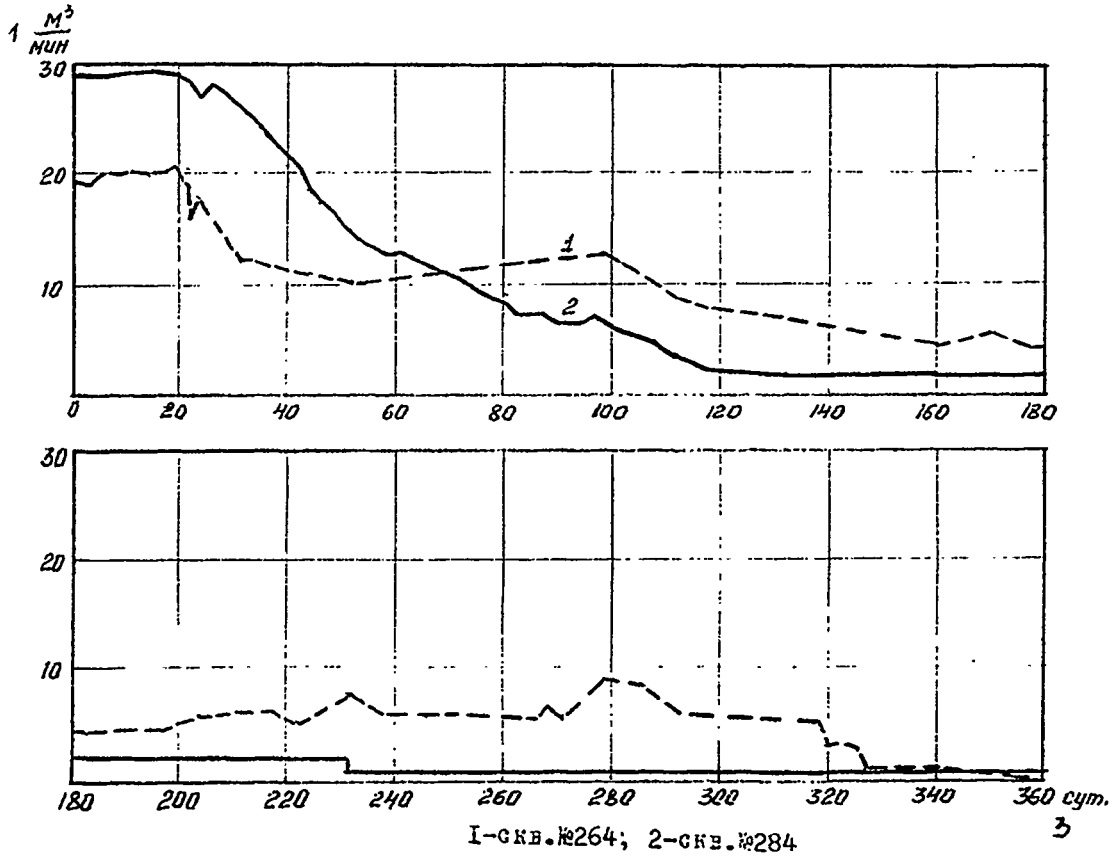


Fig. 11 - GAS WELL PRODUCTION IN ZASYADHKO MINE



I-скв.№264; 2-скв.№284

Fig. 12 - FIELDS OF METHANE GAS UTILIZATION
in Donetsk Coal Association

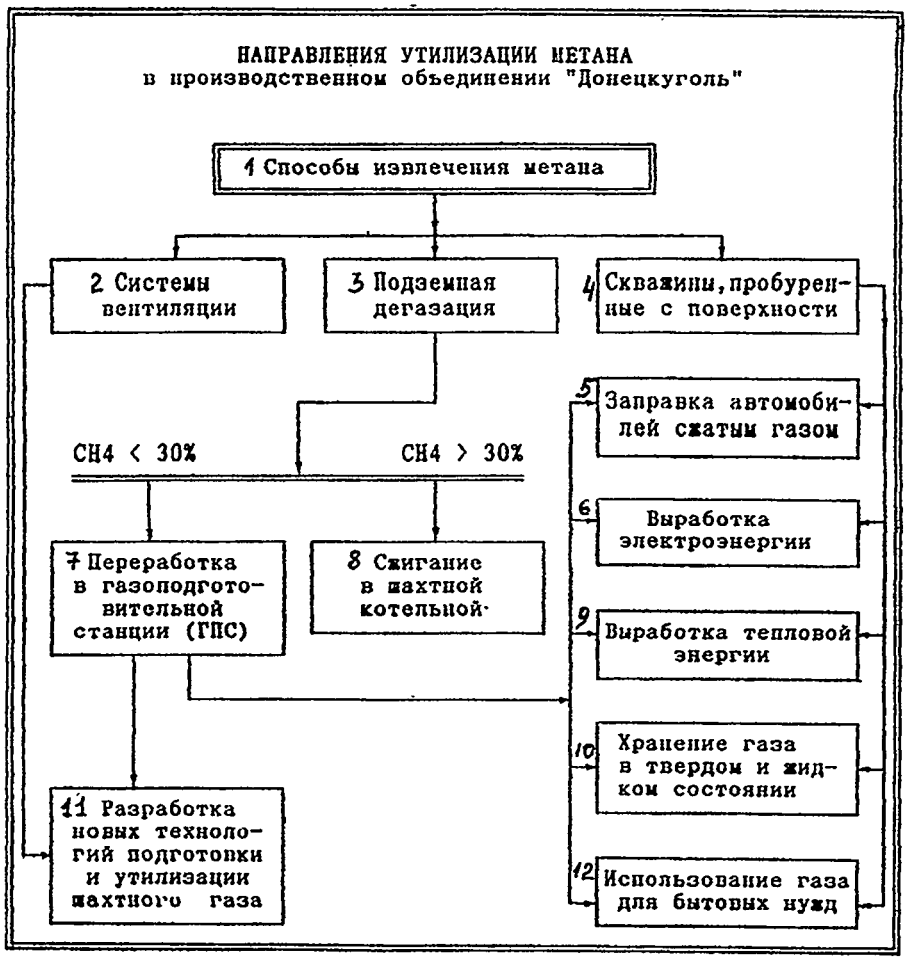
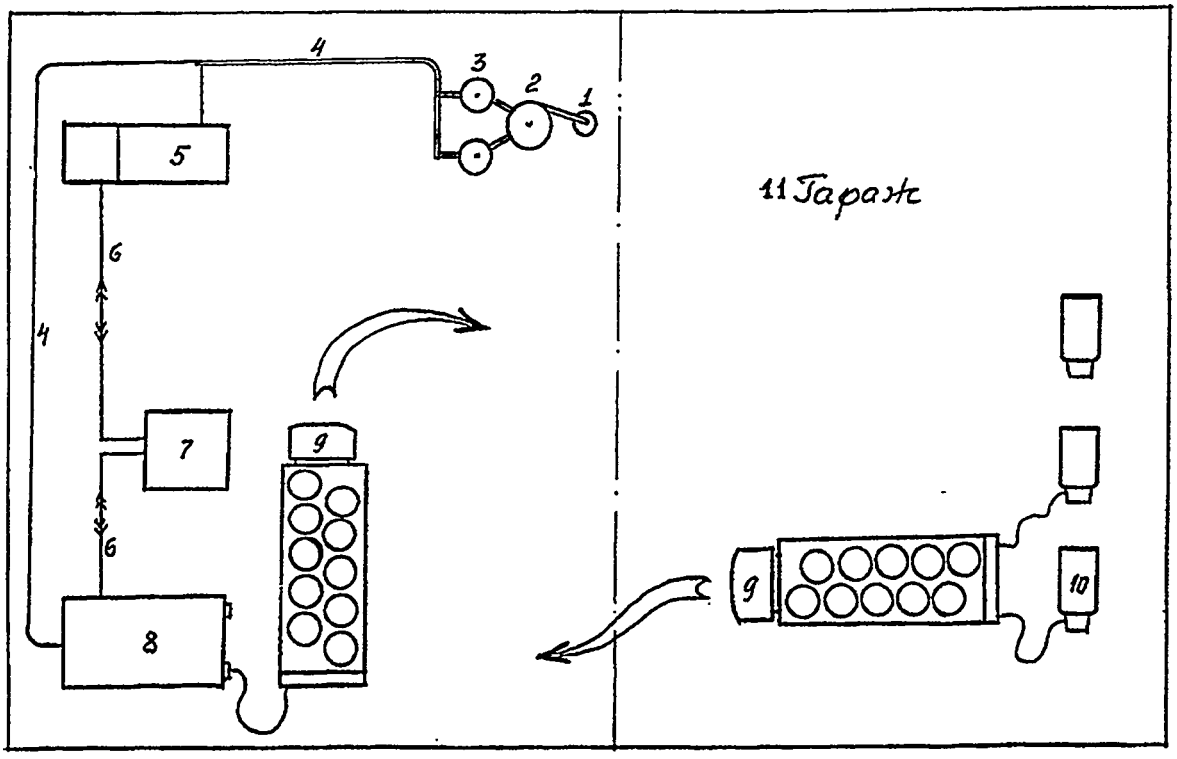
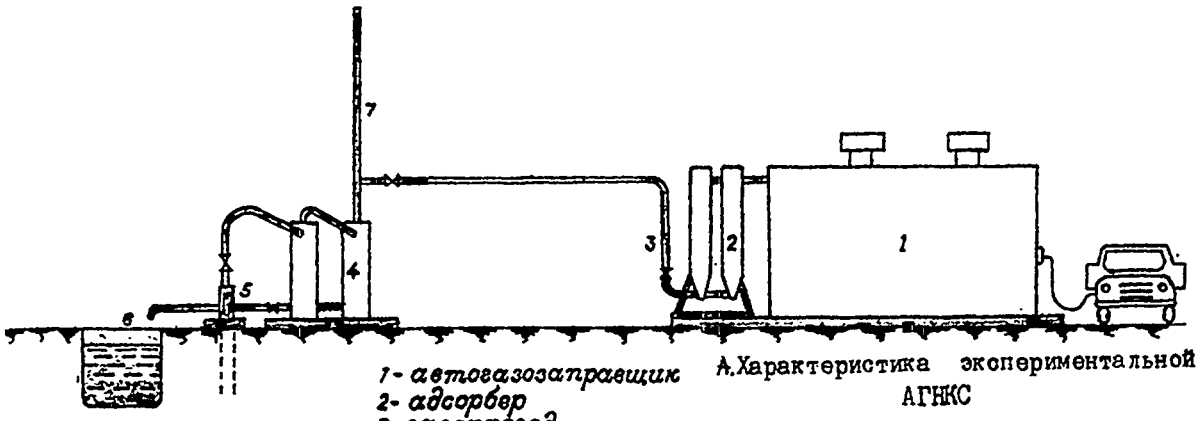


Fig. 13 - COMPLEX: GAS WELL - GAS FILLING COMPRESSOR STATION - TRUCK-MOUNTED GAS FILLING STATION - TRUCK



1. Скважина
2. Водоотделитель
3. Адсорберы влаги
4. Газопровод
5. Электроподстанция газотурбинная
6. Электросеть
7. Блок управления
8. Газонаполнительная компрессорная станция АГНКС
9. Автогазозаправщик передвижной ПАГЗ
10. Автомобиль

Fig. 14 - UTILIZATION DIAGRAM OF METHANE EXTRACTED FROM COAL AND ROCK STRATA IN DONETSK COAL ASSOCIATION



1- автогазозаправщик
2- адсорбер
3-газопровод
4-водоотделитель
5-скважина
6-отстойник
7-свеча

A. Характеристика экспериментальной АГНКС

B. Производительность 1000 м³/сут.

C. Давление 20 МПа

D Количество заправляемых автомобилей в сут. 10-12

Fig. 15 - STRUCTURAL MAP OF COALBED GAS SECTION OF LAVRENTYEV DOME

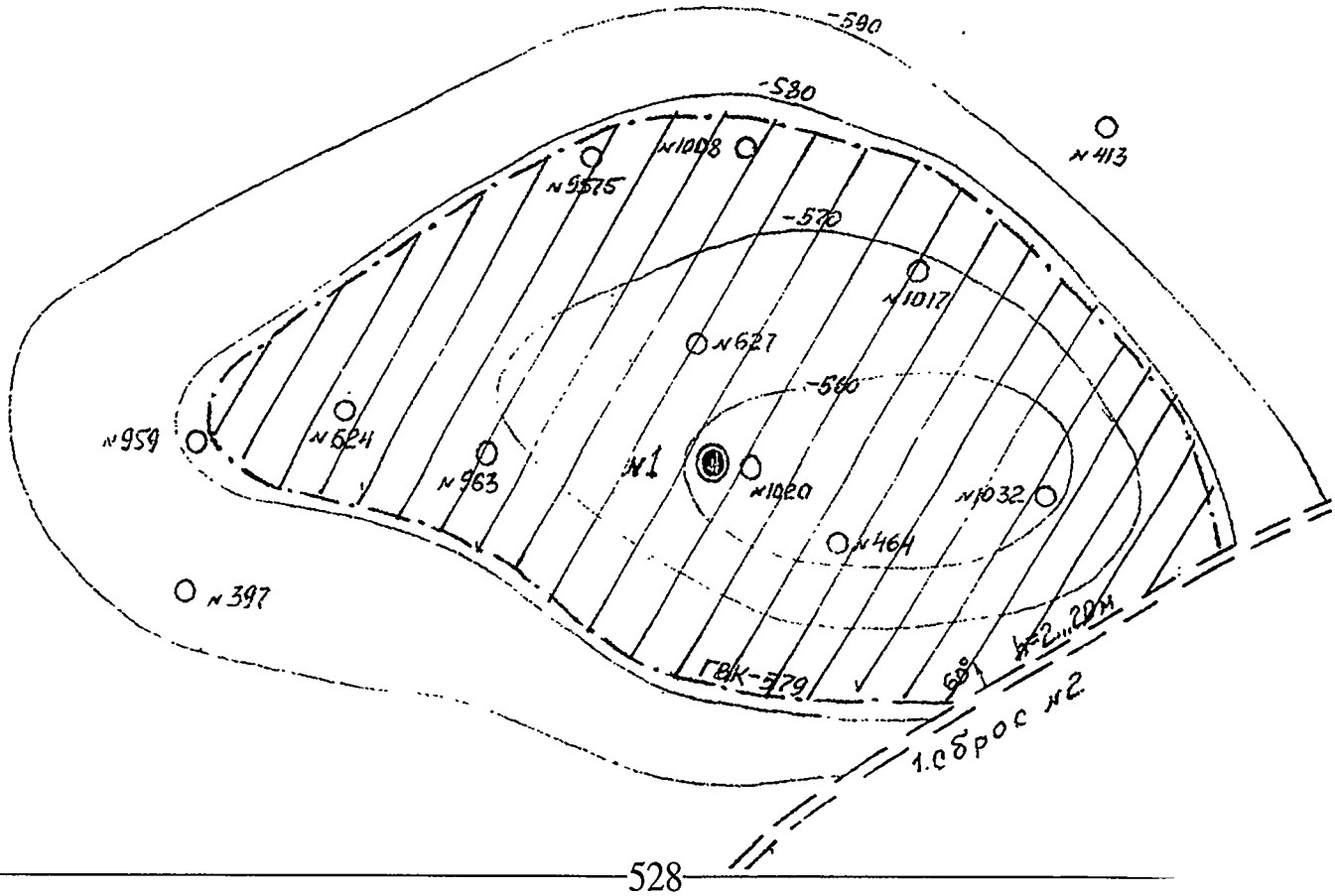
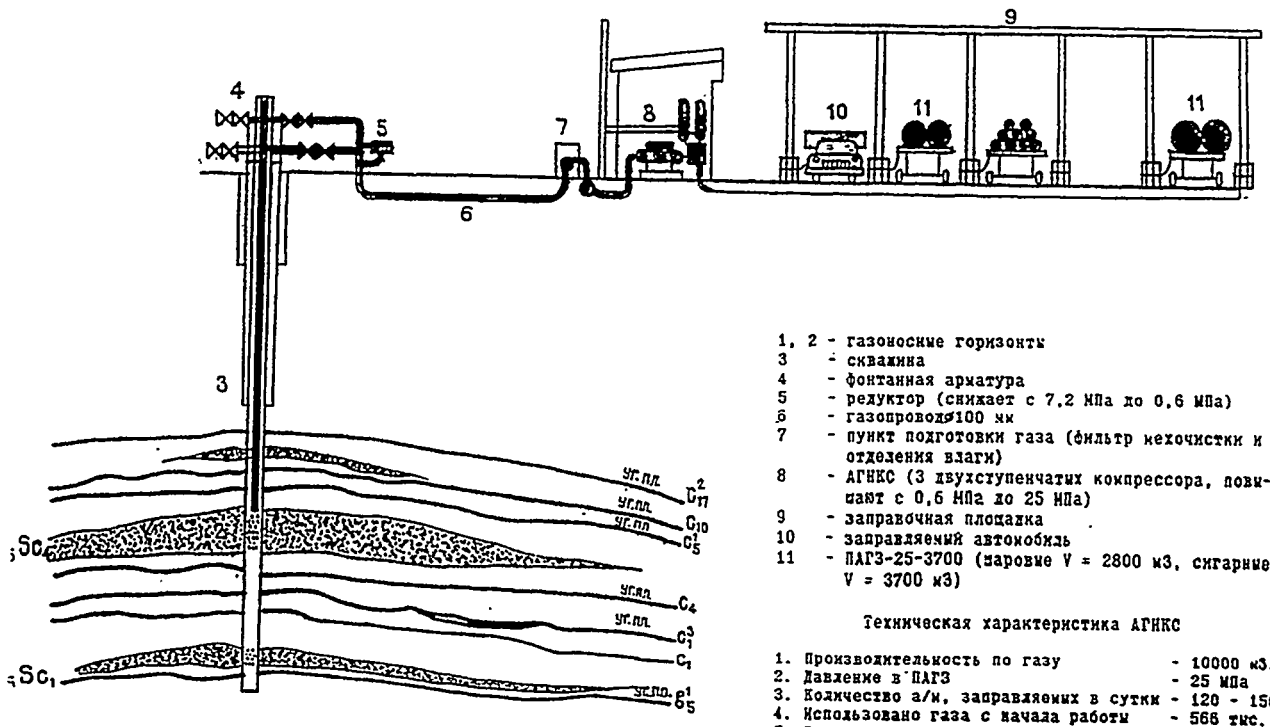


Fig. 17 - PRE-MINING DEGASSING AND METHANE UTILIZATION DIAGRAM IN YUZHNODONBASSKAYA No 12 MINE FIELD (LAVRENTYEVSKY DOME)



1, 2 - газоносные горизонты
3 - скважина
4 - фонтанная арматура
5 - редуктор (снижает с 7,2 МПа до 0,6 МПа)
6 - газопровод Ø100 мм
7 - пункт подготовки газа (фильтр мехочистки и отделения влаги)
8 - АГНКС (3 двухступенчатых компрессора, повышают с 0,6 МПа до 25 МПа)
9 - заправочная площадка
10 - заправляемый автомобиль
11 - ПАГЗ-25-3700 (наровые V = 2800 м3, сигарные V = 3700 м3)

Техническая характеристика АГНКС

1. Производительность по газу	- 10000 м3/сутк
2. Давление в ПАГЗ	- 25 МПа
3. Количество а/м, заправляемых в сутки	- 120 - 150
4. Использовано газа с начала работы	- 566 тыс. м3
5. Проведено заправок а/машин	- 9175



NOTES

INTERGAS '95

May 15-19, 1995
The University of Alabama
Tuscaloosa, Alabama USA

9554

Technical and Economic Feasibility of Coalbed Methane Production and Utilization in the Ukraine

V.L. Saprykin, Gas Institute, Academy of Sciences, Ukraine; Y.A. Boxerman, I.N. Karp and A.I. Pyatnichko, Academy of Sciences of Ukraine

INTRODUCTION

The fuel and energy complex of the Ukraine is presently in a state of crisis.The reason for this situation is a consiederable deficiency of indigenous resources and of the production of oil and gas.

The development concept for the fuel and energy sector of the Ukraine for the period until the year 2010 forecasts a level of energy consumption from domestic resources (i.e.from organic fuel, nuclear and hydro energy), equivalent to 190.6 million SCE per year (SCE = Standard Coal Equivalent, 1 SCE = 1 metric ton of hard coal, with calorifle value of 6879 kcal/kg, equal to 12382 Btu/pound).This volume corresponds to 56,6% of the total prime energy consumption of the contry. Domestic demand for coal will be satisfied to 100% from indigenous resources, oil to 13.8%, and gas to 29.6%.The predicted level of oil imports at that time will be at 44.8 million tons per year(about 314 million bbl/y), and for gas at 71.7 billion cubic meters (2.53 Tcf) per year.

The situation of the fuel and energy sector of the Ukraine economy can be improved by restructuring the industry, developing new techniques for saving energy and materials, and by modernization of oil and gas industry.Untraditional types of energy resources, in the first place coalbed methane (CBM), tone an importout place for overcoming the energy problems of the country in the future.

The authors thank the following scientists and experts, whose investigation results and ideas were used in this report: Zabigajlo V.E., Bulat A.F., Bikov G.A., Saprikin V.L. (National Academy of Sciences of Ukraine); Hrapkin S.G., Golubev O.A. (The State Committee of Ukraine for Geology) Kabanov A.I., Lestchinsky A.A., Gershun O.S. (Ministry of Coalmining of Ukraine); Terdovidov A.S., Dzhamalova H.F. (The State Committee of Ukraine for oil and gas).

ABSTRACT

Coalbed methane is regarded as an enemy to the miners.It causes large cost

for fighting it to prevent accidents and for preserving the safety of the miners at work.Annual emissions of CBM in the ventilation air of coal mining regions of the Ukraine reached a level of 3.0-3.5 billion cubic meters (0.11 - 0.12 Tcf).So large volume is the reason, wny CBM cannot simply be ragarded as only a by - product of coal mining, but rather as an independent fuel. The recovery and utilization of CBM would allow to solve the following problems:

- To improve the supply of gas to the Ukraine;
- To increase the safety and productivity of miners and coal mine construction personel at work;
- To improve the quality of the environment by reducing CBM emissions to the atmosphere.

The Ukraine has considerable resources of CBM in the Donetzk and Lvov-Volin basins. The CBM potential of the Ukraine is rated quite high using internationally accepted methods:

According to the opinion of our experts, the CBM resources in the Donetzk basin amount to 1200 Bcm (42.4 Tcf).This includes 970 Bcm (34.2 Tcf) within the limits of mine fields (as registered by "Gasbalanse"), and 208 Bcm (7.3 Tcf) within the area of coal assessments.

In 1993, 87 coal mines in the Donetzk basin were degassing their underground works to increase the safety in their ventilation systems.From such degassing, about 400 million cubic meters (14.1 Bcf) of CBM were produced, representing 14% of the total emissions.Additionally, 50 million cu.m (1.76 Bcf) were produced by vertical surface wells.The average efficiency of degassing reached 25%. Only 60-80 million cu.m (2.1-2.8 Bcf) of the CBM were utilized, mainly in the boilers of 17 of the coal mines.

From these figures follows, that only 15-20% of the CBM captured were being utilized. This is less than one third of the utilization coefficient in European countries with coal mines, and it is approximately 4-5% of the total amount of methane released from coal mining operations in the Ukraine.

Total resources of methane in the Lvov-Volin basin are about 10 Bcm (353 Bcf). There are 18 coal mines there, and degassing is applied in 4 of them.But in none of them is the gas captured being used.

World experience with CBM production confirms, that methane can be considered both as a potential fuel where it is being produced in connection with coal mining, and as an independent, additional fuel where it is produced outside of coal fields.

The new approach for solving the problem of methane released during coal production and regarded as a complicating factor, is to provide better safety to the work of the miners by applying degassing prior to the start of construction work at the mines, during the construction period and also during the mining operations.

According to the calculations

Table 1

The distribution of methane resources according to the investigating and settling level in Donezk basin.

The level of investigating and settling	Methane resources, bil.c.m.		
	total	including	
		in working layers	in un working layers
Mines in action and under construction	491	191	300
Investigated and begin investigated areas	430	209	221
Inside of limits of assés-sment and of predicated coal fossil	162	162	-
Total for basin	1083	562	521

Table 2

The distribution of methane resoerces among the geology and industry regions of Donezk basin

Geology and industry region	Methane resources, bil.c.m.			
	total	mines in action and under construc-tion	investi-gated and being in-vestiga-ted areas	inside the limits of assessment and of predicated coal fossil
West Donezk basin	30.8	10.2	20.6	-
Krasnoarmeisky	187.3	94.4	58.6	38.1
South Donezk basin	34.7	10.4	9.9	14.4
Donezk-Makeevsky	172.1	117.4	39.5	15.2
Central	71.6	39.8	30.2	1.6
Torez-Snezhniansky	142.6	71.9	64.7	6.0
Lisichansk	42.2	15.5	9.9	16.8
Almazo-Marjevsky	118.4	31.5	71.5	15.4
Seleznevsky	103.0	38.4	52.8	11.8
Krasnodonsky	39.5	2.9	24.4	12.2
Orekhovsky	9.3	4.0	-	5.3
Bokovo-Khrustalsky	60.8	25.5	25.6	9.7
Dolzhano-Rovenetsky	3.5	-	-	3.5
Total for basin	1083	491	430	162

Table 3

The distribution of methane resources according to the investigating and settling level in Lvov-Volin basin

The level of investigating and settling	Total	Krasnograd region		South-West region	
		including			
		main working layers	under main working layers	main working layers	under main working layers
Working mines	1946	958	988	-	-
Investigated and begin investigated areas	5746	-	1978	2895	873
Perspective areas	3219	-	-	3076	143
Total for basin	10911	958	2966	5971	1016

methane - as a passing fossil at the coefficient of recovery on level 70-80% (as in USA) - can be recovered by all operating and construction coal mines in amount 300-400 Bcm (10,5-14 Tcf)

The degasation technology must allow to receive condicioned mine gas with methane content above 25% both during in-mine degasation and using vertical surfase wells.Those technologies are known in Ukraine, they can be developed, if need, and can be realzed in short time. Besides this, the foreign experience can be used, for example Germany, where CBM production is very successful.

The CBM, as an independent fossil, can be produced by the wells, drilled from surface outside mine fields. Those technologies don't use in Ukraine due to few different causes, first of all geological.In this case, the experience of the USA can be used, because the USA are world leader in out-of-mine methods of CBM production.

The production of CBM from coal seams of working mines connects with unstability of debit and low concentrations of methane - air mixtures, there is the local position of wells inside the mine fields, the production outside the mine fields is local too. In this case the concentration of methane is 90-95% the debits are relative stable, but are small by volume.

Due to the above and to small development of pipeline network in Ukraine, the most perspective derection of CBM utilization seams uncentralized energy production. According to the quality of captured gas, may be realized different technologies of utilization : electricity and heat production by gas-diesel and gas-turbine units, as a motor fuel, for supplying of houses with heat and gas.

Having a skilled personal and high technical potential, Ukraine can in short time settle those technologies of CBM utilization.

For creating of CBM industry in Ukraine, from technical and economical view points, four next problems must be soluted: geology, production, utilization and economics.

1.GEOLOGY

Donetzk and Lvov-Volin coal basins have a coal with high methane content (10-35 cubic meters per 1 ton of dry ashless mass). The present situation with methane resources vs investigation level for few geology and industry regions of Donetsk basin is shown in tables 1 and 2, for Lvov-Volin basin - in table 3.

The analysis of investigating and settling levels of methane stocks for Donezk and Lvov-Volin basins at 1995, 2000 and 2005 years will be made according to "The Programme of Ukraine coal industry development".

During the making of geology and industry assessments of gas content for coal deposits, it will be necessary to assume these deposits as methane and as coal.The coal mining must necessary be with recovery and utilization of CBM.In this case methane can be mentioned both

as a passing fossil , which recovery is necessary for safety of mining of coal (the main fossil), or as main fossil, which recovery in independent from coal mining, with an aim of predegasation of coal massive.

Due to the new assumption of CBM to be an independent fossil, must be new understanding of study gas contents of coal fossil, during it's investigation. The aim of comlex study of coal fossil gas contents now is not only receiving of data for solution of problems security of mining works, but for making the assessment of perspectives of settling of deposits by passing or independent recovery of methane.This aim stands some new scientifical and engineer problems:

- to make predicative productive assessment for methane both as passing and main fossil;

- to investigate the sorbtion properties of coal in a wide range of temperatures, pressures and humidities in connection with the perspective depth of mining works, kinetics of desorbtion process, residual methane content of coal;

- to study the macro- and micro porosity of coal, it's molecular structure and diffusion properties;

- to measure the gas pressure in coal s eams by developed technology with using the data on step-by-step gas lost of coal layers;

- to study the filtration properties (permeability) of coal layers in natural state, to predicate the splif

- to study the filtration properties (permeability) of coal layers in natural state, to predicate the splif of layers by kern;

- to study surrounding strains not only from view point of defination of free gases (the sources of sudden gas pollutions) content, but from the position of possibility of their influence on methane production from coal layers;

- to create the maps of constant coal lauers thickness, those maps are necessary for the assissment of methane recovery levels.

2.RECOVERY

Main part (about 95%) of hydrocarbon resources in coal basins of Ukraine is methane, sorbed on coal layers. The technologies, using now in Ukraine , don't allow to recover the hudrocarbons with high efficient as main fossil. So those gases recover by degasation as a passing fossil.

At present time the single source of CBM is degasation systems of working mines. Those systems exit on 87 mines from 195 mines, where coal consists methane. At 01.01.1994 one took from underground to a surface away about 400 million cubic meters per year (14% from all in-mine gas emissions, equal app. 2,9 billion cubic meters per eyar). The main part of this gas was recorved by the wells, drilled from underground or from surface to discharged zone.Due to high cost of surface technology and low permeability of ukranian coals, the

technology of recovery of methane from underground works must be prefered at the nearest time.The increasing of production level of methane and its concentration in methane-air mixture can be reached by next:

1. Systematic parameter correction for degasation systems and their reconstruction according to the change technical conditions of mining, the increasing of wells and pipeline germetization quality.

2. The creation of in-mine recovery technologies for acting mining by degasation of undischarged mining layers. Must be made a pilot and productive areas for control of developed chart function.

3.The development of technologies for methane recovery with using of wells, drilled from surface to discharged zone. Donezk basin has the same experience. The life time of pilot wells was minute 250 days, methane debit was 3 - 3.5 cubic meters per minute, total amonut of methane per well was - 0.7-4.0 million cubic meters.First results of wells investigation show that, after optimization of well positions of construction and of regime of vacuum creating system work, the efficent of wells can achieve 50%.

4.The development of recovery technologies for microdeposits. Four pilot wells at a field of "Chaikino" mine (Makeevcoal) have produced 4.3 million cubic meters of gas during 1986-1989.

5.The investigation, directed to study of the recovery methods for small technogen deposits (i.e. from zones which are under the coal was taken away).Due to the desorbtion, in these zones free gas collected.The gas pressure in zones was 1,1 MN/m2 (11 kg/cm2).

6.The development of recovery technologies for unworking mines with using of experience of England, Belgium, France and Germany.In this countries the productivity is 13 to 20 cubic meters of gas per minute (about 25% from productivity during the period when mines were in action). Possible lifetime of those recovery methods is 6 - 16 years. In Donezk basin from unworking mine "Tsentralnaya-Pervomaiskaya" methane emission continues from 1972, debit in 1993 was 3 cubic meter per minute.

7.The development of special CBM recovery technologies with using of mechanical, physical, physico-chemical, hydro-dinamical and other methods of treatment on coal massive, with an aim of increasing gas return.

8.Using in wide range the foreign (first of all the USA) experience in recovery of gas by the wells, drilled from surface to undischarged zone long time before mining.

3.UTILIZATION

After sollution of geology and recovery problems, it will become real and advisable the solution of utilization problems. The most efficient kinds of CBM utilization are industry, transport and heatsuppling.The next directions of CBM utilization are preferable for real conditions:

- production of electricity and heat for industrial and householding aims by autonomy energy agregates of small capacity;

- the substitution of liquid motor fuels in transport engines;

- burning for supplying with heat of industrial, agricaltural and communal objects.

Due to the fact, that CBM recovery objects are usually outside populated points, the electricity generation must become the prefer method of CBM utilization.The industry of Ukraine can already now supple with necessary equipment this direction of use. Considerable perspectives are in using of electrical and heat agregates, which include the combined free-piston gas diesel, electric generator and equipment for supplying with heat. From the economic point of wiev, by this method must be utilized about 70% of all CBM, which will be produced in Ukraine.

The good perspectives has the using of CBM for automobile transport.In fact, automobile park of Donezk region includes 170 thousand lorries (18% of total amount in Ukraine), 33 thousand buses (25%), above 910 thousand of cars (24%) and 60 thousand of special transport units. The annual amount of petroleum fuel (gasoline and diesel fuel) is above 3 million tons per year. It seems to be real to displace 30% of this amount, the total price of which is above 750 million USD.

The difficulties at this way are:

- absence in Ukraine of production of gas-fuel automobil equipment;
- impossibility of direct method of CBM utilization with the changing component content without corrections in construction of standard gas-fuel equipment, which had made in Russia.

For soluting of this problem, it's necessary to create a complex of investigations, to make necessary correction of automobil equipment design, and then to begin in Ukraine the serial production of equipment.

The development of technologies of practical CBM utilization must include the next directions of uncentralized economics:

1.The creating of technologies and requirements of CBM preparation for using by different users.For soluting of this problem Institute of gas and Institute o f cybernetics (National Akademy of Sceinces of Ukraine) are created new informational and calculative computer system for definition of optimal technological and economical parameters of constructing of objects for recovery, preparation and utilization of CBM.

2.Design and organization of production of fuel equipment for automobil engines, which are using CBM as motor fuel.Institute of gas and Kiev Aviation Plant designed, built and succesful tested the research unit of this equipment.

3.Design and organization of production of gas-diesel engines for electrical stations with capacities 500,

1000 and 1600 kW.

4.Design and settling of fuel equipment for electrical ministations with capacities 5, 50 and 100 kW.

5.Creating of the network of mobil container automobil CBM-filling compressor ministations with capasity 40-50 refuelings per day.This way of CBM utilization is now succesful using in few mines of Donezk basin.

6.Creating of general scheme of bringing CBM to working pipelines of low and high pressures.Design and creating of CBM pipeline network for predication methane treatment industry of Ukraine.

7.Design and creation of gas full equipment for burning of CBM with defferent methane content.

8.Development of utilization technologies for mine ventilation gas. If debit of ventilation flow is 900 cubic meters per minute and methane concentration in mixture with air is 1%, the chemical catalysis conversion capasity will be equal about 6000 kW. Due to the low methane concentration in ventilation flow, it will be very difficult to realize this way.Our opinion is that more perspectively will be the using of ventilation flow as a blowing for furnaces of electrical stations and mine boilers.

9.The development of normative base for CBM.It is necessary for the realization of main part of all above direction of CBM utilization.

4.ECONOMICS

Our calculations show, when expendeture is 12 million USD (included in prime cost of coal) and when CBM production is 1 billion cubic meters per year, the prime cost of CBM can be as small as 9 USD per 1000 cubic meters.

Already now in mine boilers of Ukraine about 200 thousand tons of coal per eyar are substituting by CBM.

The calculations also show, that by using of CBM as motor fuel mine can receive profit 20 thousand USD allready at first year of utilizating. At the next years the profit will increase. The time of paying for itself will be about 1 eyar, relative profit 135%. The other directions of use cannot be calculated, because there is not any working units or real projects. At the whole, if annual rise of recovery level will be 600 million cubic meters, total profit during 5 years will be 30 million USD, the time of paying for itself will be 1 - 1,5 year.

Thus, the utilization of the CBM in Ukraine is profitable. Besides this, in above examples,we didn't show those profits, as decreasing of mine in cidents, connected with methane explosions, increasingof work productivity, decreasing of ventilation cost and expendeture, connected with enviromental damage, social effect, decreasing of the expendeture, connected with gas import, etc.

CONCLUSIONS

1.From the view point of sceintifical and technical readiness the problem of CBM utilization by

possibility of realization (only local) leave behind the geological and production problems.

2.Analysis of methane resources assessments and methane recovery and utilization levels allows to propose the development of works for creating ukranian industry for CBM recovery to be on 3 periods.

During the first period (1995 - 1997) will define values of CBM deposits inside limits of working and being builit mines.The level of recovery as passing fossil must be 1.0-1.2 billion cubic meters (0.035-0.042 Tcf) per eyar.Besides this, must be made the complex of works, conneted with recovery of CBM as an independent fossil.

During the second period (1998-2000) the recovery level of CBM both as passing and as independent fossil must reach 4-5 billion cubic meters (0.14-0.17 Tcf) per year.

During the third period (2000-2005) will take place a wide range using of progressive technologies. The CBM recovery level as independant fossil must reach 8-10 billion cubic meters (0.28-0.34 Tcf) per year.

3.As calculations show, the soluting of these problem demands the following cost:

- the first period, for reaching of CBM recovery level 0.7-0.8 billion cubic meters (0.025-0.028 Tcf) per year due to the development of degasation technology for working mines, and for increasing of mine works safety - 4,0-4,5 million USD;

- the second period - 80-100 million USD;

- the third period - 80-100 million USD;

The expendeture for CBM utilization equipment during 12 years will be about 1 - 1,25 billion USD.

Total expendeture for creating of CBM recovery industry in Ukraine is on level 1,2 - 1,5 billion USD. The price of methane is 62.2 USD per 1000 cubic meters. If gas production will be equal 10 billion cubic meters (0.35 Tcf) per year, the expendeture for recovery of CBM will pay for itself about 2,2 eyars.

4.The social effect of CBM utilization is increasing of safety of mining works, decreasing of incindent number, creating of new work places, all of this are very important for Ukraine, where the level of soluting of those problems is not enongh.

CBM utilization, especially inside limits of working mines, allows to decrease the methane atmosphere emission, to decrease content of soils in atmosphere and the velosity of ozone layer destruction, allows to prevent the rising of hotbed effect.

INTERGAS '95

May 15-19, 1995
The University of Alabama
Tuscaloosa, Alabama USA

9512

International Prospects for Coalbed Methane Recovery at Coal Mines: An Overview of Methane Emissions, Recovery Practices and Key Opportunities

D.W. Kruger, Methane Energy Programs, U.S. Environmental Protection Agency

ABSTRACT

This paper summarizes the results of work done by the U.S. Environmental Protection Agency to quantify international methane emissions from coal mining and to identify key countries that could profitably reduce their emissions in the future. A variety of activities should be undertaken to better characterize and promote these opportunities for coalbed methane recovery and use internationally, as further described in the paper.

Global methane emissions from coal mining are estimated to account for about 10 percent of total methane emissions from human sources. Given the availability of technologies to degasify coal mines and to use the recovered methane as fuel, there are many opportunities to reduce these emissions. Given the potential magnitude of the coalbed methane resource, attention should focus on the countries of China, the former Soviet Union, and Eastern Europe (particularly Poland). If programs to encourage the recovery of methane from coal mines are successful in these and other countries, it is estimated that emissions could be reduced by up to 7 teragrams (10 billion cubic meters, 360 billion cubic feet) in the near-term and, perhaps, by more than 11 teragrams (16 billion cubic meters, 575 billion cubic feet) in the longer-term.

INTRODUCTION

Recent evaluations by the U.S. Environmental Protection Agency (EPA) and others have indicated that countries other than the United States account for approximately 85 percent of global methane emissions from the coal fuel cycle. Several of these countries--most notably the People's Republic of China, the former Soviet Union, and Poland--have many gassy mines with significant opportunities for methane recovery. Numerous other countries--including India, the Czech Republic, South Africa--also appear to have strong project opportunities at their gassy coal mines.

The development of methane recovery projects at gassy coal mines should be encouraged internationally for several reasons. First, reducing methane emissions will result in significant environmental benefits because methane is a potent greenhouse gas and a clean-burning fuel. Second, methane recovery projects can improve the safety and productivity of mining operations. Third, U.S. companies are well positioned to capture significant coalbed methane market share, and with effectively targeted development assistance, could move rapidly into these markets.

The three sections of this paper describe the current state of knowledge regarding international opportunities to reduce methane emissions at coal mines. The first section summarizes global emission estimates from the coal fuel cycle (both mining and combustion) and identifies those countries which contribute most significantly to emissions from this source. The second section describes some of the most promising opportunities to reduce methane emissions at coal mines in selected countries. Section three outlines a variety of mechanisms for promoting these types of projects.

GLOBAL METHANE EMISSION FROM THE COAL FUEL CYCLE

Over the last several years, attention has focused on quantifying methane emissions from a variety of sources because of methane's potency as a greenhouse gas. Methane is currently estimated to be 24.5 times more effective than carbon dioxide at trapping heat in the atmosphere [1]. The contribution of methane to potential global warming, moreover, is approximately 18 percent [2], making it the second most significant greenhouse gas after carbon dioxide, as shown in Figure 1.

Methane has a short atmospheric lifetime--about 10 years, compared with 120 years or more for carbon dioxide [3]. This short lifetime means that programs and policies to reduce methane emissions can help to mitigate the rate of climate change faster than reductions in emission of carbon dioxide and other longer-lived greenhouse gases. In fact, it is estimated that the impact of a 10-percent reduction in methane emissions from human activities (which would stabilize

atmospheric concentrations) would have the same impact in terms of mitigating global warming between now and the year 2050 as capping carbon dioxide emissions at 1990 levels over the same period [4].

Methane emissions associated with human activities are estimated at approximately 354 Tg, with an uncertainty range of 277 - 477 Tg [5]. This estimate indicates that approximately 70 percent of current methane emissions are associated with human activities ("anthropogenic"). Figure 2 depicts the principal anthropogenic sources of methane. As the figure indicates, the largest sources of emissions are ruminant livestock (i.e., emissions from the digestive systems of ruminants) and rice cultivation.

The coal fuel cycle, representing emissions from both coal mining and combustion, is estimated to account for about 10 percent of global methane emissions from human activities, as shown in Figure 2. Current EPA estimates indicate that the world's coal production and combustion emits between 24 and 40 Tg (35 to 60 billion cubic meters, 1.2 to 2.1 Tcf) of methane annually, with a "best estimate" of 30 Tg (45 billion cubic meters, 1.6 Tcf) [5]. More than 90 percent of these emissions are associated with coal mining, primarily in underground mines [5].

Although the methane emissions associated with the coal cycle are lower than several other sources, coal mining is very significant emission source in many countries. Figure 3 summarizes the key methane emission sources for the five highest emitting countries--China, the former Soviet Union, India, the United States and Brazil. The coal cycle is estimated to be the second largest source of methane emissions in China, after rice cultivation, and the third largest source of emissions in both the former Soviet Union (after natural gas and oil production and ruminant livestock) and the United States (after landfills and ruminant livestock).

Taken together, China, the former Soviet Union and the United States account for almost 75 percent of global methane emissions from the coal cycle [5]. In fact, emissions from China alone are estimated to represent more than 30 percent of global emissions from this source, although there is significant uncertainty in this estimate. Further, as shown in Table 1, the ten countries with the highest emissions of methane from the coal cycle are estimated to account for more than 90 percent of global emissions [5].

Table 2 compares EPA's estimate of methane emissions from the coal cycle to other recent estimates for this sector [5-16]. As the table indicates, estimates have covered large ranges over time. Many of the early estimates addressed the emissions associated with hard coal mining only and were not transparent with respect to the emission factors assumed per ton of coal mined. More recent studies, particularly EPA's 1994 study [5] and a 1992 report of the Coal Industry Advisory Board [16], were prepared using country-specific, and often mine-by-mine, data where available. The CIAB estimate, which is consistent with the low-end of the range presented in EPA's study, uses conservative emission factor assumptions for certain key emitting countries (such as China) as well as for emissions from surface mining and post-mining activities. In addition, it does not estimate the methane emissions from coal combustion.

Figure 4 indicates that underground mining is estimated to be responsible for the bulk of emissions from the coal cycle, with its share ranging from 70 to 85 percent. Surface mining and post-mining emissions account for another 10 to 20 percent. Coal combustion is estimated to emit the remaining 5 to 10 percent. About 90 percent of the coal combustion emissions are estimated to come from China, where large amounts of coal are burned in small, inefficient domestic stoves. Figure 4 also indicates the ranges of uncertainty associated with the emission estimates presented in EPA's study. The key uncertainties include:

Lack of data for underground mining emissions in certain countries: Several countries have published mine-by-mine emissions data for their underground coal mines which include estimates of emissions from both ventilation and degasification systems. Where these data are available, the reliability of emissions estimates can be significantly improved. Such data are still unavailable for certain key countries, such as China, however, and in other countries it is unclear whether these data accurately reflect the total methane emissions from the mines. In the United States, moreover, mine-by-mine data is only available for ventilation system emissions; emissions from degasification systems must be estimated for the gassiest U.S. mines.

Lack of data on emissions from surface mining and post-mining activities: Detailed emissions estimates for surface mines and post-mining activities are generally unavailable, although there are several measurement studies currently underway both in the United States and internationally which should further improve understanding of these sources. Current estimates are based on extremely rough data and the range of emissions potentially associated with these sources is large. In spite of the uncertainty, however, it should be noted that these sources are believed to emit much less methane than underground mining.

In the future, methane emissions from coal mining are expected to increase as coal production grows and mines become deeper and gassier. The rate of increase in methane emissions from the coal cycle is uncertain, however, due to questions about future coal production levels and difficulty predicting future coal characteristics, including mine gassiness. In 1990,

world coal production was over 4.7 billion tonnes; future coal production could be significantly higher, perhaps reaching 5.3 to 5.9 billion tonnes in 2010 [17]. In addition, the proportion of underground mining could increase as surface-mined coal seams are depleted. At forecasted production levels, emissions could range from 27 to 50 Tg (40 to 75 billion cubic meters, 1.4 to 2.6 Tcf) in 2000 and 30 to 58 Tg (45 to 85 billion cubic meters, 1.6 to 3 Tcf) in 2010, assuming methane emission factors remain constant [5]. If mine gassiness increases as a result of the mining of deeper, gassier coal seams, or if the proportion of underground mining increases relative to surface mining, however, emissions could be even higher than these projections.

Increased methane emissions are particularly likely in countries like China, where coal production is forecast to grow by more than 2 percent annually between 1988 and 2000, and growth is expected to continue beyond 2000 as well. A recent study by the World Bank, for example, forecast that Chinese coal production could grow from 1.1 billion tonnes in 1990 to over 3 billion tonnes in 2020, which could result in methane emissions growing substantially over the same period [18].

In the future, the use of mine degasification systems may expand to cope with increasing mine gassiness. To the extent that additional recovered methane is used, the growth in methane emissions would be moderated. Several countries already use a substantial fraction of the methane recovered by mine degasification systems, while others do not. In 1990, for example, a reported 1.3 Tg (1.9 billion cubic meters, 68 bcf) of methane from coal mines was used globally, in the countries of Australia, China, the Czech Republic, Germany, Poland, the former Soviet Union, the United Kingdom and the United States [5]. Some methane is also recovered and used in Japan, and perhaps other countries, but the amounts are unknown. The amount of methane likely to be recovered by mine degasification systems and the extent to which methane use could increase in the future are uncertain. There is, however, the potential for significant reductions in emissions from coal mines, as discussed in the next section.

OPPORTUNITIES TO REDUCE METHANE EMISSIONS

Many countries are evaluating opportunities to reduce methane emissions from coal mining. This source represents an attractive reduction opportunity because of the availability of technologies to expand methane recovery and use at coal mines, and because of the many benefits associated with such projects. In many countries, methane recovery could be increased by degasifying coal seams in advance of mining, using vertical or in-mine recovery methods. Mine degasification could occur well in advance of mining activities and could be fairly independent of coal production. The recovered methane could then be used for power generation or industrial and residential uses. In addition to reducing the amount of methane vented to the atmosphere, such projects would also improve mine productivity and safety, which are of great importance to the coal industry. In many countries, moreover, there is potential for coalbed methane to make a large contribution to primary energy supply.

Currently, many countries use degasification technologies to maintain mine safety, but only a fraction of the recovered methane is used as fuel. As shown in Table 3 [11,19-27], for example, in 1990 an estimated 2.8 to 3.9 Tg (4.2 to 5.8 billion cubic meters, 145 to 200 bcf) of methane was recovered by mine degasification systems but only 1.3 Tg (1.9 billion cubic meters, 68 bcf) was used [5]. The remaining 1.5 to 2.6 Tg (2.2 to 3.9 billion cubic meters, 78 to 135 bcf) of methane was vented to the atmosphere, wasting a valuable fuel and contributing to the greenhouse effect. This currently vented methane represents a major near-term opportunity for reducing methane emissions in many countries. Developing uses for this gas will require investments in improved methane recovery as well as gas utilization equipment and infrastructure.

Overall, EPA estimates that methane emissions from coal mining could be reduced by 4 to 7 Tg (6 to 10.4 billion cubic meters, 205 to 365 bcf) in the near-term and 7 to 11 Tg (10.4 to 16.4 billion cubic meters, 205 to 575 bcf) in the longer term [27]. As shown in Table 4, the largest emitting countries--China, the former Soviet Union, and the United States--are believed to have the strongest potential for reducing their methane emissions. This assessment is based on their overall emission levels, current and expected mining practices, and local conditions. The potential for methane reductions in China, Russia and Ukraine (two key coal mining republics of the Former Soviet Union), and Poland are discussed briefly below.

China

China is the world's largest coal producer, and in 1990, it produced more than 1 billion tonnes of coal [28], which met about 75 percent of its total energy needs. Natural gas, by contrast represented less than 2 percent of China's energy use in 1990; total natural gas consumption was only 15 billion cubic meters (525 bcf). Not surprisingly, China is also the world's largest emitter of methane from coal mining. It's estimated coal mining emissions (not including coal combustion) were 8.5 to 13.0 Tg (12.7 to 19.4 billion cubic meters, 440 to 675 bcf) in 1990, which represented about one-third of the world's total emissions from this source. Coal combustion could increase emissions by anywhere from 1 to 3.6 Tg [5]. More than 97 percent of China's coal is mined in underground mines, many of which are extremely gassy. Of the roughly 600 state-owned coal mines, for example, more than 300 were classified as gassy and/or outburst-prone in 1990 [29].

Currently, more than 100 Chinese mines have

mine degasification systems, which together recovered about 434 million cubic meters (15.2 bcf) of methane in 1990 [21]. This represented less than 5 percent of estimated total methane emissions from underground mines, however, with the rest being emitted by ventilation systems. About 65 percent of this gas was used, primarily for residential cooking and heating and local industrial uses in the vicinity of the coal mines.

Methane recovery and use at Chinese mines could be significantly expanded with the introduction of better technologies, the development of appropriate economic and regulatory policies, and a focused effort at the local level and internationally to raise awareness of the potential of this resource to increase China's gas supplies. There is strong interest in encouraging the expanded use of methane within Chinese government agencies and among key municipalities. Many regions of China confront serious coal shortages and would benefit from access to additional local energy sources. In addition, the widespread use of coal for cooking and heating has generated extensive interest at the municipal level in developing clean-burning natura gas resources. In fact, some of the most successful coalbed methane projects in China have been initiated by municipalities interested in providing natural gas to their citizens.

Over the near- to mid-term, key opportunities exist to improve the recovery of methane at those Chinese mines with existing degasification systems by employing improved methane recovery technologies. These technologies should also be introduced at the many gassy mines that do not currently have degasification systems. Through the widespread implementation of such technologies, China could increase its average methane recovery efficiency from less than 5 percent to 25 percent at its state-owned mines, which would result in emission reductions of 1.2 to 1.6 Tg annually (1.8 to 2.4 billion cubic meters, 60 to 86 bcf) if all of this gas is used [27]. Even higher recovery efficiencies could be achieved in the longer term, particularly if China is successful in introducing market prices for energy commodities and continues to develop policies to encourage foreign investment in the development of its energy resources. Achieving a recovery efficiency of 40 percent at state-owned Chinese coal mines would result in emission reductions of 2.8 to 3.4 Tg annually (4.2 to 5.1 billion cubic meters, 145 to 175 bcf) [27].

Russia

Russia has abundant resources of coal, oil and natural gas, and has historically produced large quantities of all of these fuels. In 1990, Russia produced about 640 billion cubic meters (22 Tcf) of natural gas and about 260 million tonnes of hard coal [30]. It accounted for about 80 percent of the natural gas produced in the former Soviet Union and more than 50 percent of the coal. Most of the coal was consumed domestically, but about 25 percent of the gas was exported to Western and Eastern Europe [24].

Russia's coal is produced in several coal basins, including the Kuznetsk, the Pechora, and the Eastern Donetsk. The Kuznetsk is the largest coal basin in Russia, in terms of both surface and underground coal production. It is located in Western Siberia and is a center of heavy industry. The Donetsk basin in located primarily in Ukraine, but has several underground mines in Russia. The Pechora basin is north of the Arctic Circle, far from major population and industrial centers.

In 1990, reported methane liberations in Russia were 1.7 Tg (2.5 billion cubic meters, 88 bcf), of which more than 80 percent was emitted in ventilation air. Almost all of the remaining 20 percent which was recovered by mine degasification systems was also emitted to the atmosphere. The Pechora basin is the only region currently using significant amounts of the methane recovered by mine degasification, primarily for on-site heating of buildings and mine air.

There is significant near-term potential to reduce methane emissions from coal mining in Russia by encouraging the utilization of methane currently being vented by mine degasification systems. About 0.2 Tg (300 million cubic meters, 10 bcf) of this methane is currently vented, which could be recovered with appropriate investments in pipelines and gas utilization equipment. Over the longer-term, even larger emission reductions could be achieved if methane recovery programs were expanded. According to Russian data, current methane recovery efficiencies are about 23 percent at gassy mines [32]. If recovery efficiencies were improved to an average of 30 percent, an additional 0.3 to 0.5 Tg (450 to 750 million cubic meters, 15 to 26 bcf) of methane could be recovered. Reaching an average recovery efficiency of 40 percent, moreover, could increase recovery to 0.4 to 0.6 Tg (600 to 900 billion cubic meters, 20 to 30 bcf) [27].

Coalbed methane production could make an important contribution to the energy economies of the key coal mining regions of Russia. Currently, these regions have relatively limited supplies of natural gas and must rely on highly polluting, low-quality coal to meet many local energy needs. In addition, coal production levels have fallen substantially in recent years, due to high production costs and difficult mining conditions. It is expected that many coal mines, particularly in the Kuznetsk region, may close for economic reasons in coming years, which will necessitate the development of new fuel sources. To the extent that coalbed methane can meet local energy needs its development should be strongly supported by the Russian government.

Ukraine

Ukraine is one of the largest coal producing republics in the former Soviet Union; in 1991, it produced 127 million tonnes of coal, primarily from

mines in the Donetsk basin. Ukraine is a net importer of oil and natural gas, however. In 1991, for example, it met only 25 percent of its natural gas needs through domestic production, importing more than 90 billion cubic meters (3.1 Tcf) of gas from Russia.

Most Ukrainian coal mines are very deep and gassy, and mining conditions are dangerous. In 1990, reported methane liberations were 2.3 Tg (3.4 billion cubic meters, 120 bcf) [31]. About 100 of Ukraine's 319 underground coal mines have degasification systems, which recovered an estimated 600 million cubic meters (21 bcf) of methane in 1990. Only about 25 percent of this recovered gas was used, however, mostly in industrial boilers located near the mines [24].

In the near-term, methane emissions could be significantly reduced by using the methane that is already recovered by mine degasification systems. Developing such uses could reduce emissions by 0.3 Tg (450 million cubic meters, 15 bcf) per year [27]. Additional reductions could be achieved over the medium- to longer-term, moreover, by improving the average recovery efficiency of gassy mines from the current levels of 23 percent. Achieving an average recovery efficiency of 30 percent, for example, could produce as much as 0.4 to 0.6 Tg (600 to 900 million cubic meters, 20 to 30 bcf) of methane, and a recovery efficiency of 40 percent would result in emission reductions of 0.6 to 0.8 Tg (0.9 to 1.2 billion cubic meters, 30 to 40 bcf), if all of the gas was used [27].

The Ukrainian government strongly desires programs to increase domestic gas production, due to their current dependence on natural gas from Russia and their uncertain future in terms of coal production. Despite government support of the coal industry, coal production has been falling in recent years. Production costs are very high in Ukraine's underground mines and future prospects are not promising, given the difficult mining conditions. It appears that Ukraine will need to cease production at many of the more unprofitable mines in the coming years, but this decision is complicated by the need to obtain secure energy supplies to replace coal and need to find alternative employment for those currently working in the mining industry. Coalbed methane represents at least a partial solution to both of these problems. Because it is another resource located in the coal basin, it should be able to provide an additional source of fuel for the region and employ some of the displaced coal miners.

Poland

As in China, coal dominates Poland's energy supply mix. In 1992, coal met more than 75 percent of Poland's energy needs, with more than 130 million tonnes being mined [32]. Coal production has declined significantly from peak levels, however, primarily due to increasing extraction costs and a deep economic recession. Coal production peaked in 1979 at more than 200 million tonnes, and had fallen to only 130 million tonnes by 1993 [30,33].

Declining coal production has increased demand for both oil and natural gas in Poland. Unlike coal, however, known domestic conventional reserves of both of these fuels are small. In 1993, for example, Poland satisfied approximately 45 percent of its natural gas demand with domestic sources, and the rest was imported from Russia [30,33]. This dependence on Russia is a source of concern in Poland due to the difficulty of paying for imported gas and the possible uncertainty of supply.

Currently, 18 of Poland's 65 underground coal mines have degasification systems in place. In 1993, these mines recovered an estimated 213 million cubic meters (7.5 bcf) of methane, of which almost 80 percent was used [34]. The principal uses were for industrial purposes and on-site coal drying plants and boilers [32]. Total methane emissions to the atmosphere in 1993 were estimated at 0.4 Tg (600 million cubic meters, 20 bcf) from Poland's underground coal mines.

Coalbed methane represents an attractive option for increasing domestic natural gas supplies, and, as a result, the Polish government has actively encouraged the development of this resource. The government has held concession bidding rounds for the rights to develop coalbed methane in non-mining areas of the Upper Silesian Coal Basin, for example, and has also actively encouraged the development of joint venture projects with Polish mines.

Over the near-term, developing uses for all of the gas currently recovered from Polish mines would reduce methane emissions by about 0.03 Tg (45 million cubic meters or 1.6 bcf). Over the longer term, projects could be developed to degasify coal reserves in advance of mining. Focusing on projects to increase methane recovery efficiencies from their current level of 27 percent to 40 percent at gassy mines, could recover an additional 0.2 to 0.4 Tg (300 to 600 million cubic meters, 10 to 20 bcf) [27]. This recovered coalbed methane would represent 3 to 5 percent of current Polish gas demand, not including the coalbed methane that could be produced in the non-mining coal reserve areas. The most promising utilization options for the recovered methane in Poland are likely to be direct use in industrial applications, power generation and district heating.

HOW TO PROMOTE INTERNATIONAL COAL MINE METHANE PROJECTS

Encouraging the development of international projects to reduce methane emissions at coal mines will require a concerted, and multi-faceted effort. For centuries, methane has been perceived as a safety hazard in underground mining that can be most effectively addressed by venting to the atmosphere. In addition, many of the key methane emitting countries

are heavily dependent on coal as their major energy source and may not be fully prepared to exploit methane recovered from coal mines for fuel.

Facilitating the development of projects to expand methane recovery and use at the world's gassy coal mines will require aggressive programs directed at removing barriers. Key actions should include information exchange, technical assistance, and technology transfer. In order to deliver near-term results, moreover, these actions must involve at least three separate groups: (1) the host country; (2) key development assistance organizations; and (3) U.S. companies. By focusing the attention of these three groups on coalbed methane potential and encouraging the development of progressive policies and programs within foreign governments and development assistance agencies, U.S. companies should be able to participate in coalbed methane projects worldwide.

Table 5 summarizes the key types of barriers that may exist to different degrees in various countries, and which may have to be overcome to encourage methane recovery and use at underground coal mines. This table also highlights the types of programs that could be implemented to remove these barriers. Of course, the conditions in a specific country or at a specific coal mine will be unique, and the programs developed should address the particular conditions and needs of the target country. The overall types of issues that can hamper coalbed methane development and the most promising activities to address them can be generalized among countries, however.

Table 6 refers to several broad types of activities that are described briefly below. In many cases, these programs will be most effective if some of the components are implemented sequentially, as indicated in the table.

National or Basin Assessments

In many countries, preparing a national or basin-level assessment of the coalbed methane resource should be the first step in initiating an emission reduction program. This assessment should evaluate the magnitude of the coalbed methane resource, the potential role for coalbed methane in the country or region's energy economy, and the types of barriers that may be constraining development. Particular attention should be paid to the compatibility of coalbed methane development with the nation's energy or environmental goals. Current practices with respect to coalbed methane recovery and use should also be assessed and some of the more promising project types identified.

Policy Analysis and Assistance

One of the objectives of the national assessment is to identify policy, regulatory or other barriers to coalbed methane development. Examples of such barriers could include uncertain coalbed methane ownership laws, unclear project development requirements or regulations for coalbed methane development, or uneconomic state-mandated prices for coalbed methane produced by mines. Where such barriers are identified, it may be necessary to assess the implications of policy reforms and develop recommendations for removing the barriers.

For the most part, policy reform activities should be undertaken by in-country government personnel. Policy reform assistance may be useful to such personnel, however, to provide information about how various barriers have been addressed in other countries. Such advice could be provided by expert consultants, through seminars on various issues organized in the country, or by arranging for training opportunities for government personnel either internationally or in-country.

Information Exchange

Creating institutions within countries to disseminate information about domestic and international accomplishments in coalbed methane will be an important part of any program to encourage coalbed methane recovery. One effective means of exchanging information may be through the creation of coalbed methane technical information centers (or "clearinghouses") in target countries. The clearinghouse concept has been modelled on a domestic U.S. information exchange program that was initiated by the Gas Research Institute to support the U.S. coalbed methane industry in the early 1980s. Coalbed methane clearinghouses have been supported by the U.S. EPA in Poland, Russia, and China to serve the important functions of organizing the domestic coalbed methane industry and promoting U.S. business opportunities in coalbed methane development.

Technical Assistance

Technical assistance includes many activities, such as training and cooperative work on studies and pre-feasibility assessments. Typical activities could include arranging in-country seminars on technical issues taught by international experts, arranging international training opportunities and study tours, and organizing domestic and international teams to undertake project development activities, such as pre-feasibility studies.

Technology Transfer

Technology transfer activities can include research activities and pilot projects. In the research area, possible activities could include drilling and mining through vertical wells to test the impact of hydraulic fracturing on coal mine safety. Pilot projects could be implemented to demonstrate advanced mine degasification technologies, new utilization options, water disposal technologies, and innovative uses of mine ventilation air.

Commercialization

The successful implementation of the types of activities described above should lead to commercialization of coalbed methane development over a multi-year period in those countries that demonstrate strong potential. The combination of these activities is geared towards generating support for resource development in-country and focusing government attention on developing legal and regulatory frameworks that encourage coalbed methane production. At the same time, the local mining industry can receive technical information and training necessary to understand resource development issues and become effective partners in commercial projects. These activities can provide U.S. companies with critical information on resource potential, moreover, as well as with the potential to obtain financial support for the early phases of project development from international agencies.

CONCLUSION

In many countries, the potential to develop coalbed methane recovery and use projects at coal mines represents an opportunity that should not be overlooked. These projects are important not only because of their potential to protect the global environment by reducing emissions of methane, a potent greenhouse gas. They are important also because they can contribute to a better quality of life in mining communities by improving mine safety and by providing a local source of clean-burning fuel. Furthermore, these projects represent significant business opportunities for those U.S. companies with technologies that can be employed to recover and use methane from mines.

There are hundreds of mines throughout the world that may have the potential to profitably recover and use some of the methane they are currently venting to the atmosphere. Given the multiple benefits of such projects, a concerted effort should be made to identify these mines and provide the assistance necessary to reduce their methane emissions. With a strong focus on identifying key opportunities and an emphasis on developing assistance programs that can meet the needs of all of the parties that will be involved in project development--including in-country government and technical personnel, U.S. companies, and international development agencies--methane emissions could be significantly reduced over the near-term, thereby mitigating the risk of global warming.

REFERENCES

1. IPCC (Intergovernmental Panel on Climate Change), 1994: Radiative Forcing of Climate Change: The 1994 Report of the Scientific Assessment Working Group of the IPCC, Cambridge University Press, Cambridge, United Kingdom.

2. IPCC (Intergovernmental Panel on Climate Change), 1990: Climate Change: The IPCC Scientific Assessment, Cambridge University Press, Cambridge, United Kingdom.

3. IPCC (Intergovernmental Panel on Climate Change), 1992: Climate Change 1992: The Supplementary Report to the IPCC Scientific Assessment, Cambridge University Press, Cambridge, United Kingdom.

4. Hogan, K. B., J. S. Hoffman, and A. M. Thompson, 1991: "Methane on the Greenhouse Agenda," in Nature, No. 354, November 21, 1991, p. 181-182.

5. US EPA (United States Environmental Protection Agency), 1994: International Anthropogenic Methane Emissions for 1990, EPA-230-R-93-010, Office of Policy, Planning and Evaluation, Washington, D.C.

6. Koyama, T., 1963: "Gaseous metabolism in lake sediment and paddy soils and the production of atmospheric methane and hydrogen," in Journal of Geophysical Research, 68(13):3,971.

7. Hitchcock, D. R. and A. E. Wechsler, 1972: Biological Cycling of Atmospheric Trace Gases, Final Report, NASW-2128, p. 154-177.

8. Seiler, W., 1984: "Contribution of biological processes to the global budget of methane in the atmosphere," in Klug, M. and C. Reddy, eds., Current Perspectives in Microbial Ecology, American Society for Microbiology, Washington, D.C., p. 468-477.

9. Crutzen, P. J., 1987: "Geophysiology in Amazonia," in Dickenson, R., ed., Role of the Tropics in Atmospheric Chemistry, John Wiley, New York, New York, p. 107-132.

10. Okken, P. A. and T. Kram, 1988: "CH4/CO - Emission from fossil fuels global warming potential," ESC-WR-89-12, paper presented at the IEA/ETSAP Workshop, June 1989, Paris, France, Energy Study Center: Netherlands Energy Research Foundation, Petten, the Netherlands.

11. Zimmermeyer, 1991: "Recovery and Use of Coalbed Methane (Replies to the Questionnaire transmitted by the Federal Republic of Germany)," United Nations Economic Commission for Europe.

12. Selzer, H. and W. Zittel, 1990: Emissions of Methane Gas Affecting the Climate: An Investigation of Global Methane Emissions from the Use of Fossil Fuels, LBST-Report No. 10/90, Ludwig-Bolkow-Systemtechnik GmbH, Ottobrunn, Germany.

13. Barns, D. W. and J. A. Edmonds, 1990: An Evaluation of the Relationship between the Production and Use of Energy and Atmospheric Methane Emissions, TR047, USDOE/NBB0088P, prepared for the U.S. Department of Energy, Washington, D.C.

14. Boyer, C. M. et al, 1990: Methane Emissions from Coal Mining: Issues and Opportunities for Reduction, EPA-400/9-90/008, prepared for the U.S. Environmental Protection Agency, Office of Air and Radiation, Washington, D.C.

15. Kirchgessner, D. A., S. D. Piccot, and J. D. Winkler, 1993: "Estimates of global methane emissions from coal mines," in Chemosphere, 26(1-4), p. 453-472.

16. CIAB (Coal Industry Advisory Board), 1992: Global Methane Emissions in the Coal Industry, prepared for the Global Climate Committee, International Energy Agency, Paris, France.

17. US EIA (U.S. Energy Information Administration), 1991: International Energy Annual, Washington, D.C.

18. World Bank, 1994: China: Issues and Options for Greenhouse Gas Emissions Control, prepared by a joint study team from the National Environmental Protection Agency of China, the State Planning Commission of China, the United Nations Development Program and the World Bank, Washington, D.C.

19. Lama, R. D., 1991: "Methane Gas Emissions from Coal Mining in Australia: Estimates and Control Strategies," in Proceedings of the IEA/OECD Conference on Coal, the Environment, and Development: Technologies to Reduce Greenhouse Gas Emissions, IEA/OECD, Paris, France, p. 256-266.

20. Saghafi, A. and D. Williams, 1992: "Estimates of methane emissions from Australian coal mines," paper presented at symposium sponsored by Institute of Minerals, Energy and Construction, Division of Coal and Energy Technology, on Coalbed Methane Research and Development, November 1992, Townsville, Queensland, Australia.

21. MOE (Ministry of Energy of China), 1991: Coalbed Methane Recovery in China: an Information Report for the Consultants of UNDP, November 1991.

22. Bibler, C. J., et al., 1992: Assessment of the Potential for Economic Development and Utilization of Coalbed Methane in Czechoslovakia, EPA/430/R-92/1008, prepared for the U.S. Environmental Protection Agency, Office of Air and Radiation, Washington, D.C.

23. Pilcher, R.C., et al., 1991: Assessment of the Potential for Economic Development and Utilization of Coalbed Methane in Poland, EPA/400/1-91/032, prepared for the U.S. Environmental Protection Agency, Office of Air and Radiation, Washington, D.C.

24. Marshall, J., R. C. Pilcher, and D. W. Kruger, 1993: Assessment of the Potential for Economic Development and Utilization of Coalbed Methane in Russia and Ukraine, EPA 430-K-94-003, prepared for the U.S. Environmental Protection Agency, Office of Air and Radiation, Washington, D.C.

25. Airuni, A. T., 1992: personal communication with A. T. Airuni, Russian Institute of Comprehensive Mineral Resources Exploitation, Moscow, Russia, March 1992.

26. Creedy, D. P., 1992: personal communication with D. P. Creedy, British Coal Corp., Coal Research Establishment Technical Services, Gloucestershire, United Kingdom.

27. US EPA (United States Environmental Protection Agency), 1993: Options for Reducing Methane Emissions Internationally -- Volume II: International Opportunities for Reducing Methane Emissions (Report to Congress), EPA 430-R-93-006 B, Office of Air and Radiation, Washington, D.C.

28. Sinton, J. E., ed., 1992: China Energy Databook, Lawrence Berkeley Laboratories, LBL-32822/US-350.

29. UNDP (United Nations Development Program), 1992: Project of the Government of the People's Republic of China: Development of Coalbed Methane Resources in China, CPR/92/G32/A/IG.

30. PlanEcon, 1992: PlanEcon Energy Report, Vol. 2, No. 1, Washington, D.C., 84 pp.

31. Zabourdyaev, V. S., 1992: personal communication, Skochinsky Institute of Mining, Moscow, Russia, March 1992.

32. Pilcher, R. C., et al., 1994: Reducing Methane Emissions from Coal Mines in Poland: Expanding Coalbed Methane Recovery and Utilization in the Upper Silesian Coal Basin, draft, prepared for the U.S. Environmental Protection Agency, Office of Air and Radiation, Washington, D.C.

33. PlanEcon, 1994: PlanEcon Energy Report, Vol. 2, No. 1, Washington, D.C.

34. Coalbed Methane Clearinghouse, 1994: unpublished data provided to Raven Ridge Resources.

TABLES

Table 1

1990 ESTIMATED METHANE EMISSIONS FROM THE COAL FUEL CYCLE FOR THE TOP-10 EMITTING COUNTRIES

	Coal Production (million tonnes)			Estimated CH_4 Emissions (Tg)	
Country	Underground	Surface	Total	Low	High
China	1,024	43	1,066	9.5	16.6
United States	385	548	934	3.6	5.7
Former Soviet Union	393	309	701	4.8	6.0
Germany	77	359	436	1.0	1.2
India	109	129	238	0.4	0.4
Poland	154	58	212	0.6	1.5
Australia	52	154	206	0.5	0.8
South Africa	112	63	175	0.8	2.3
Former Czechoslovakia	22	85	107	0.3	0.5
United Kingdom	75	14	89	0.6	0.9
Subtotal -- Top 10	*2,043*	*1,762*	*4,164*	*22.1*	*35.9*
World Total			4,740	24.4	39.6

Source: [5]

Table 2

EMISSION ESTIMATES FROM SELECTED STUDIES

Study Author	Emission Estimate (Tg)	Year of Estimate	Methodological Issues
Koyama (1963)	20	1960	Hard coal only; no emission estimates for surface mining or post-mining activities. 1960 coal production data.
Hitchcock & Wechsler (1972)	8 - 28	1967	Post-mining not included. Source of emission factors, particularly low end, unspecified. 1967 coal production data.
Seiler (1984)	30	1975	Based on Koyama, with 1975 coal production data.
Crutzen (1987)	34	n/a	Source of emission factors unclear. Hard coal only; no emission estimates for surface mining or post-mining activities.
Okken & Kram (1989)	15 - 45	n/a	Source of emission factors unclear. Hard coal only; no emission estimates for surface mining or post-mining activities.
Zimmermeyer (1991)	24	n/a	Only underground mining considered; no emissions estimates for surface mines or post-mining activities.
Selzer & Zittel (1990)	23	n/a	Adjusted Zimmermeyer by: (1) including surface mines; (2) assuming that 15% of underground mining emissions (3.6 Tg) not emitted to the atmosphere due to CH_4 utilization.
Barns & Edmonds for U.S. DOE (1990)	25	1986	Assumed mathematical relationship between coal rank and depth and that in-situ CH_4 content was equal to the mining emission factor.
Boyer et al. for U.S. EPA (1990)	33 - 64	1988	Statistical approach related CH_4 emissions to in-situ CH_4 content. Correlation based on U.S. data only. Large uncertainty in application of results for global estimates.
Kirchgessner (1993)	47	1988	Statistical approach related coal characteristics to in-situ gas content and in-situ gas content to emissions. Correlation based on U.S. data only. No uncertainty analysis conducted.
CIAB (1992)	24	1990	Country-specific data used where available. Emission factor assumptions tend to be conservative, compared to present study. No uncertainty analysis.
Present study	24 - 40	1990	Country-specific data used where available to prepare best estimates. Global average emission factors used for rest of countries. Only study to include emission estimate for coal combustion.

Sources: [5 - 16]

Table 3

METHANE RECOVERY BY DEGASIFICATION SYSTEMS FOR KEY COUNTRIES (Tg)

	Degasification Emissions			
Country	Recovered	Used	Emitted	Year
Australia	0.10	0.05-0.08	0.02-0.05	1989
China	0.29	0.18	0.11	1990
Former Czechoslovakia	0.09	0.08	0.01	1990
Germany	0.35	0.25	0.10	1990
Poland	0.19	0.14	0.05	1989
Former Soviet Union	0.83	0.19	0.64	1990
United Kingdom	0.20	0.14	0.06	1990
United States	0.7-1.8	0.25	0.45-1.55	1988

Sources: [5, 19 - 26]

Table 4
Estimates of Potential Economically Viable Reductions in Methane Emissions from Coal Mining

Country	Estimated Emissions (Tg/yr)	Near Term Reductions		Longer Term Reductions (Tg/yr)	
		Tg/yr[1]	%	Tg/yr	%
China	9.5 -16.6	1.2 - 1.6 (0.1)	10 - 15	2.8 - 3.4	25 - 35
United States	3.6 - 5.7	1.0 - 2.2 (0.4 - 1.5)	35 - 40	1.7 - 3.1	45 - 55
CIS[2]	4.8 - 6.0	0.7 - 1.1 (0.6)	10 - 20	1.0 - 1.4	20 - 25
Poland	0.6 - 1.5	0.1 - 0.3 (0.1)	15 - 20	0.2 - 0.4	25 - 35
Former Czechoslovakia	0.3 - 0.5	0.1 - 0.2	30 - 40	0.2 - 0.3	60 - 65
Others[3]	3.3 - 5.6	0.9 - 1.8 (0.2)	20 - 30	1.5 - 2.8	35 - 45
TOTAL	22.1 - 35.9	4.0 - 7.2 (1.5 - 2.6)	15 - 25	7.4 - 11.4	30 - 40

1 Emission reduction estimates in parentheses can be achieved by utilizing gas currently recovered and vented to the atmosphere.
2 Emissions estimates are for entire CIS; reductions estimates include Russia and Ukraine.
3 Emissions estimates include several important coal-producers, such as Australia, Germany, India, South Africa, and the United Kingdom.

Source: [27]

Table 5
Key Barriers and Possible Responses - Coal Mining

Key Barriers	Possible Responses
Legal Systems: · Gas ownership uncertain · Concession system undeveloped · Joint venture project requirements unclear	· Resolve ownership legally or legislatively · Develop resource leasing mechanisms · Develop system for foreign investment, repatriation of profits, etc.
Regulatory Issues: · Project approval process unclear · Mine safety regulations inappropriate for gas recovery · No produced water regulations for CBM development · No specialized "field rules" for CBM development	· Streamline and clarify project approval/permit requirements · Determine how to incorporate gas recovery with mine safety regulations · Develop produced water regulations and industry "field rules" specific to CBM development
Information Issues: · Lack of awareness on part of government, mining personnel and others about magnitude and value of resource · Lack of awareness on part of potential project developers regarding potential in various countries	· Provide information to countries on resource, appropriate policies, technologies, etc. · Provide information to development companies and lending agencies regarding potential attractiveness of projects
Technical Issues: · Lack of access to new technologies, such as advanced drill rigs, reservoir simulators, etc. · Lack of familiarity with new methane recovery approaches, such as vertical pre-mine drainage or in-mine fracturing of longholes · Lack of familiarity with new methane utilization technologies, such as power generation · Need to demonstrate utilization options for low-concentration methane in ventilation air	· Encourage the development of joint ventures to introduce new approaches · Fund demonstration projects in key technical areas · Organize study tours and training trips for key personnel to advanced CBM projects · Establish technology centers to disseminate information on appropriate technologies and techniques
Financial Issues: · Lack of capital for investment in methane recovery projects · Poor financial condition of coal mines and historic dependence on heavy subsidies · Low subsidized energy prices reduce economic attractiveness	· Foster joint ventures · Raise awareness on part of international development agencies about coalbed methane potential · Encourage development of methane recovery and use projects that can improve coal productivity and mining economics

Source: [27]

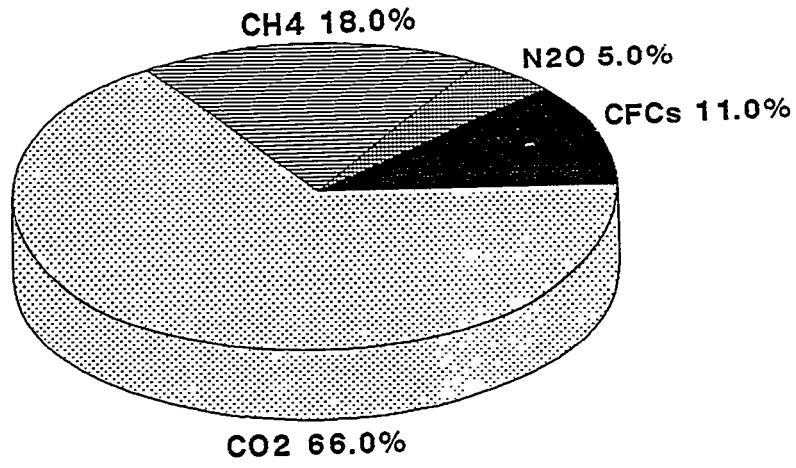
Table 6
Summary of Project Types

Project Type	Phase 1	Phase2	Phase 3	Cost
National or Basin Assessment	■■			$100K-1M per country
Policy Analysis and Assistance		■■■■■■■■■■■■		$25-100K per country, depending on types of activities
Information Exchange		■■■■■■■■■■■■■■		Varies; $75-100K/year to manage clearinghouse in developing/ transitional economies
Technical Assistance		■■■■■■■■■■■■■■		$25-50K per country for seminars; $25-150K for prefeasibility studies; $50K or more for study tours
Technology Transfer		■■■■■■		$1-15M or more, depending on scope of project
Commercialization		■■■■■■■■■■		Varies, depending on magnitude of project ($25-300M in U.S.)

Source: [27]

FIGURES

Figure 1
Global Contribution to Integrated Radiative Forcing by Gas for 1990[1]
CO_2-Equivalent Basis Using IPCC 1990 GWPs for a 100-Year Time Horizon



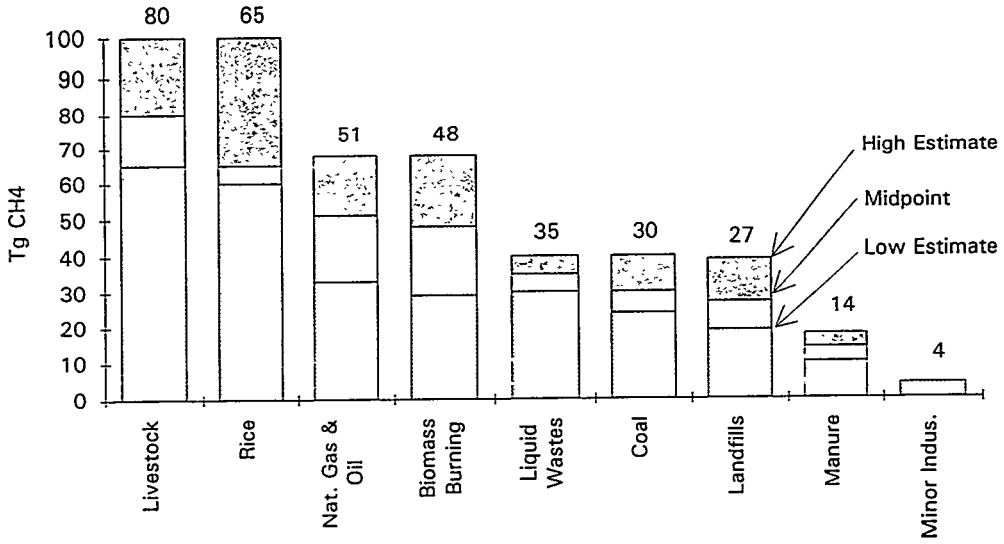
Note: Estimated on a carbon dioxide equivalent basis using IPCC (1990a) global warming potentials (GWPs) for a 100-year time horizon. Anthropogenic emissions only.

1 This chart is used to present a general understanding of methane's contribution to future warming based on the GWPs presented in IPCC (1990a). However, these GWPs are constantly being revised due to a variety of scientific and methodological issues. It is likely that the contribution of CFCs presented will decrease and that the contribution of other gases will be about the same or greater upon further investigation.

Source: [2]

Figure 2

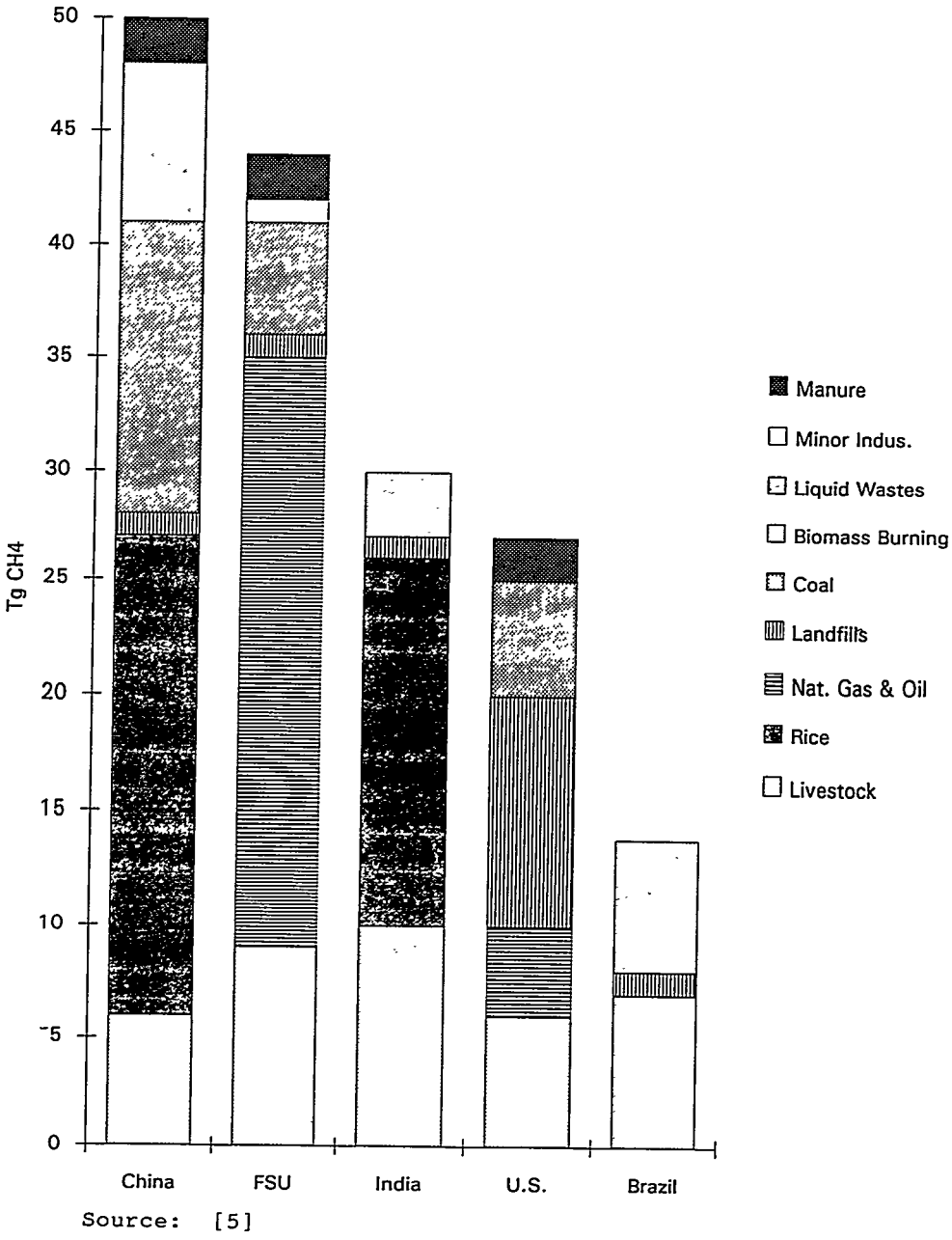
GLOBAL ANTHROPOGENIC METHANE EMISSIONS BY SOURCE (1990)
(Midpoints of ranges given above bars)



Source: [5]

Figure 3

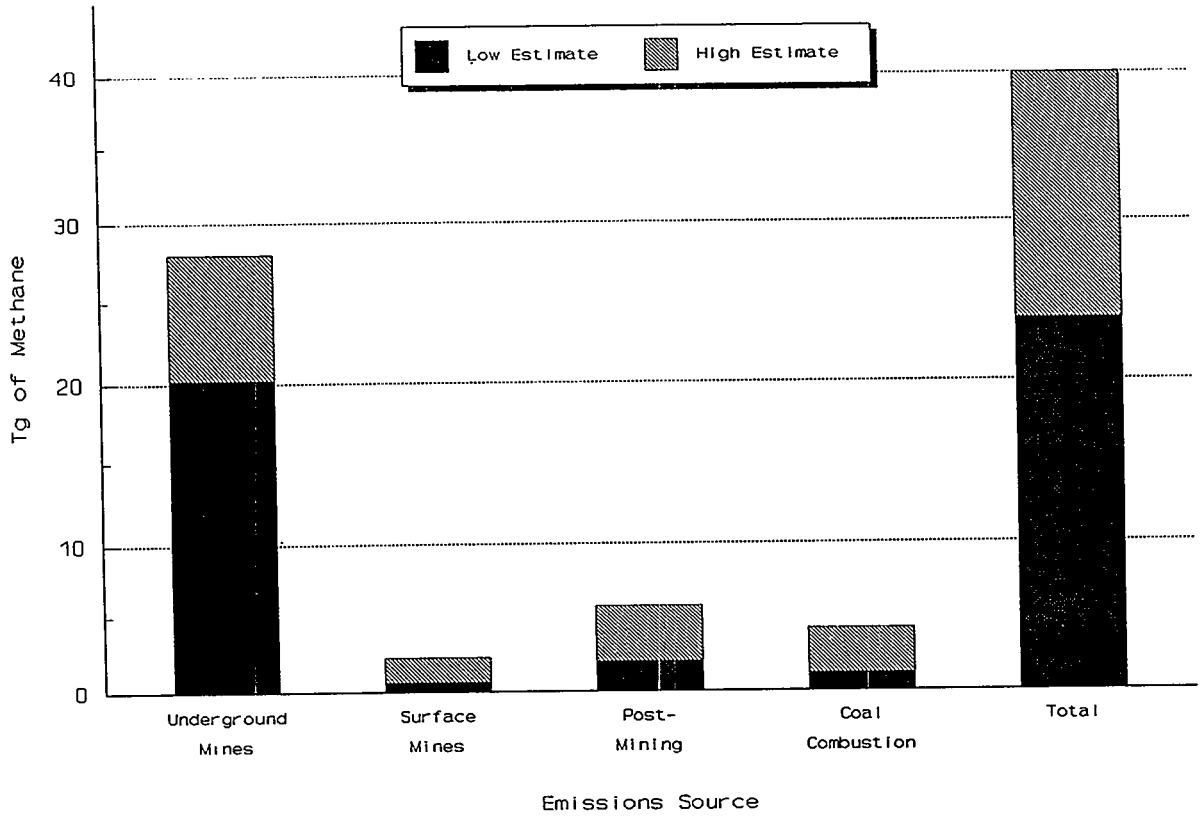
METHANE EMISSIONS OF THE FIVE LARGEST EMITTING COUNTRIES (1990)



Source: [5]

Figure 4

1990 METHANE EMISSIONS FROM THE COAL FUEL CYCLE



Source: [5]

AUTHOR INDEX

Adams, Q. 287

Almisned, O.A. 259

Bezdek, J. 361

Bibler, C.J. 203, 351

Bolshinsky, I. 189

Boxerman, Y.A. 531

Bukhantsov, A.I. 185

Byrer, C.W. 483

Calder, J.H. 311

Choi, S.K. 219

Conway, M.W. 229

Cooper, J.L. 341

Daltaban, T.S. 413

Day, S. 401

Deb, D. 151

Decker, A.D. 77, 97, 461

Dikolenko, E.Y. 173

Duhrkopf, D. 265

Durucan, S. 413

Enever, J.R. 321

Gamson, P.D. 451

Gotai Deguchi 163

Griff, M.T. 489

Groshong, Jr., R.H. 39

Guthrie, H.D. 483

Hamilton, D.S. 23

Hanby, K.P. 513

Haynes, C.D. 513

Herrington, M.R. 331

Hoak, T.E. 53, 77, 97

Holland, J.R. 115

Huang, S. 203

Huddleston, J.C. 389

Jiang, Y. 151

Kaiser, W.R. 23, 247

Karp, I.N. 531

Kasimov, O.I. 185

Kasyanov, V.V. 185

Khodaverdian, M. 237

Khoudin, Y.L. 197

Killingley, J. 401

Kimmons, J.W. 115

Kiyoshi Higuchi 163

Klawitter, A.L. 53, 97, 461

Kloisner, S. 189

Koenig, R.A. 219

Kotaro Ohga 163

Kruger, D.W. 541

Kumar, P. 341

Kuuskraa, V.A. 461

Layne, A.W. 483

Levy, J. 401

Lewin, J.L. 497

Lottman-Craigg, L. 203

MacDonald, D.J. 297, 311
Marinello, S.A. 441
Markowski, A.K. 125
Marshall, J.S. 351, 389
Mavor, M.J. 379
McLennan, J.D. 237
Meaney, K.T.A. 219
Morev, A. 189
Mukhopadhyay, P.K. 311
Nelson, C.R. 379
Novak, T. 151
Palmer, I.D. 237
Park, D. 151
Pashin, J.C. 39
Patton, S. 151
Pilcher, R.C. 203, 351, 389
Pratt, T.J. 379
Pudak, V.V. 517
Puri, R. 265
Pyatnichko, A.I. 531
Quinn, J.C. 441
Richardson, C.P. 275
Russell, C. 275
Saprykin, V.L. 531
Schraufnagel, R.A. 229
Schultz, K. 477
Scott, A.R. 23, 247, 423
Semmelbeck, M. 141
Sergeev, I.V. 173
Serov, V.I. 179
Shi, J.Q. 413
Smith, T.N. 1
Souhei Shimada 163
Su Xiaopeng 369
Sun, M. 203
Takla, G. 361
Tarabbia, P.J. 451
Thrasher, R.L. 259
Tyler, R. 23
Vavrusak, Z. 361
Vaziri, H.H. 237
Volz, R. 265
Wang, J.M. 413
Wang, S. 39
Warren, J.K. 451
Yelchainov, E.A. 509
Zabourdyaev, V.S. 207
Zebrowitz, M. 331
Zhang Xinmin 433
Zhong Lingwen 433
Zhu, C. 203
Zuber, M.D. 141

COMMITTEES

EXECUTIVE COMMITTEE

Dan A. Thompson
Symposium Chairman, College of Continuing Studies, The University of Alabama

Charles M. Boyer, II
Director/Owner, Dominion Energy Advisors

Maurice Deul
Visiting Professor Emeritus, Department of Geology & Planetary Science, University of Pittsburgh

Charles D. Haynes
Professor and Head, Department of Mineral Engineering, The University of Alabama

J. Read Holland
President, J.R. Holland & Associates

Kenneth T. Howard
Director of Technical Support, U.S. Department of Labor, Mine Safety & Health Administration

Dina W. Kruger
Manager, Methane Energy Programs, U.S. Environmental Protection Agency,

James S. Marshall
Executive Vice President
Raven Ridge Resources, Incorporated

Jack C. Pashin
Director, Energy and Minerals Section
Geological Survey of Alabama

R.G. Sanders
President, Black Warrior Methane Corporation

Richard A. Schraufnagel
Senior Technology Manager, Gas Research Institute

ABSTRACT REVIEW COMMITTEE

Igor Bolshinsky
Special Term Appointee, Argonne National Laboratory

Charles W. Byrer
Project Manager, U.S. Department of Energy
Morgantown Energy Technology Center

Joseph L. Cooper
Chief Coalbed Methane Geologist
Amoco India Petroleum Company

William P. Diamond
Senior Geologist, U.S. Bureau of Mines
Pittsburgh Research Center

Marvin T. Griff
Berkowitz, Lefkovits, Isom & Kushner
A Professional Corporation

Stephen A. Holditch
President, S.A. Holditch & Associates, Inc.

Enrico H.K. Kempter
Director/Owner, RICO RESEARCH, Switzerland

John Killingley
Senior Research Scientist, Division of Coal and Energy Technology, Lucas Heights Research Laboratories, CSIRO Australia

Stephen W. Lambert
General Manager, Methane Technical Service
Taurus Exploration, Inc.

Ben E. Law
Research Geologist, Branch of Petroleum Geology, Office of Energy & Marine Geology, U.S. Geological Survey

Jeffrey R. Levine
Consulting Geologist

Matthew J. Mavor
President, Petroleum Engineer, Tesseract Corporation

Ed Miller
U.S. Department of Labor, Mine Safety and Health Administration

D. Jack MacDonald
Senior Petroleum Geologist, Nova Scotia
Department of Natural Resources

Vladimir Saprykin
Senior Scientist, The Gas Institute
Academy of Sciences of Ukraine

Thomas E. Simpson
Senior Environmental Scientist, CH2M Hill

Pramod Thakur
Senior Research Associate
Consol, Inc. Research & Development

Bruce D. Thomas
North America Technical Manager
Halliburton Energy Services

Charles Willis
Vice President, Special Projects
The River Gas Corporation



NOTES

GeoMet, Inc.

GeoMet Operating Company, Inc.

GeoMet de Colombia

Worldwide Coalbed Methane Exploration and Development

Experience in Coalbed Methane since 1975

1826 Third Avenue North, Suite 301, Bessemer, Alabama 35020

Phone: (205) 425-3855 FAX: (205) 425-4711

Let EPA's Coalbed Methane Outreach Program Help You Identify Technologies, Markets and Finance Sources.

How It Works.



The Coalbed Methane Outreach Program is a flexible program that works with the coal industry on a mine-by-mine basis to identify attractive methane recovery projects and encourage their development. The program focuses on methane recovery projects at the gassiest mines in the United States.

The Bottom Line. Turning Waste Into Profit.

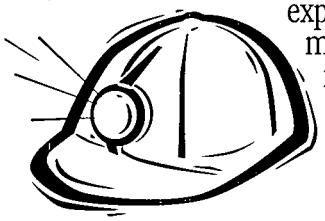
In today's tight coal market, mines cannot afford to throw away money unnecessarily by venting a valued commidity to the atmosphere. Coalbed methane recovery improves a coal mine's "bottom line" by turning a cost center into a revenue source. This saves energy, improves coal mining productivity, by reducing down time, and can reduce ventilation system capital and operating costs.

What's more, the gas can be sold or used as energy, which means more revenue for your mine.



Improving Safety.

By reducing concentrations of methane, an explosive gas, coalbed methane recovery improves mine safety.



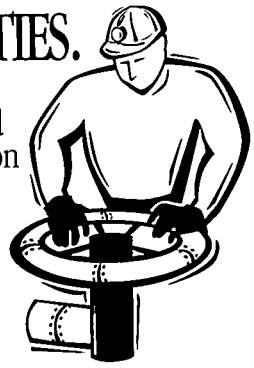
Helping The Environment.

We know coalbed methane recovery benefits the environment. The methane released by coal mines is a potent greenhouse gas that contributes to global warming and wastes energy. In the U.S., coal mines are the third largest methane emitters after landfills and domestic livestock. EPA estimates that more than 50 Bcf of methane currently being released to the atmosphere could be recovered at a profit!



Creating Job Opportunities.

An EPA study concluded that aggressive development of coalbed methane in the Appalachian region alone will create an estimated 7,500 jobs by 2010.



For More Information.

Call Karl Schultz, EPA's Coalbed Methane Program Manager, at **(202) 233-9468**, contact him at Internet address **schultz.karl@epamail.epa.gov** or send a fax to **(202) 233-9569**. You will learn how the Coalbed Methane Outreach Program's technical, market, and financing identification services can help the bottom line at your mine.

EPA
COALBED METHANE OUTREACH PROGRAM

INTERNATIONAL COALBED METHANE GROUP, INC.

The Consortium for Coalbed Methane Development

mine degasification	*econ. & environ. evaluation*	*standard well development*
Black Warrior Methane Corp.	**E. L. Lasseter & Assoc., Inc.**	**River Gas Energy Consultants, Inc.**
Post Office Box 140 Brookwood, Alabama, USA 35444 ph. 205-554-6270, fax 554-6285	3610 Watermelon Road, Suite 104 Northport, Alabama, USA 35476 ph. 205-759-2046, fax 759-2051	511 Energy Center Blvd. Northport, Alabama, USA 35476 ph. 205-759-3282, fax 759-3188

The ICMG was formed to provide services to the international coalbed methane industry, and it brings together both proven performance and a broad spectrum of expertise. Our members include a world leader in mine degasification, the operator of one of the largest and most successful projects in the Black Warrior Basin and a leader of industry-related environmental systems.

RGC

RIVER GAS CORPORATION is actively seeking new ventures and acquisitions in coalbed methane both domestically and abroad. An example of our expertise in exploration, implementation, and lowcost operations can be seen right here in the Black Warrior Basin. Please contact Charles Willis for more information.

River Gas Corporation, 511 Energy Center Blvd., Northport, AL 35476. ph: (205) 759-3283, fax: (205) 759-3188

Mathematical & Computer Services, Inc.

Walter K. Sawyer **Reservoir Simulation Consultant**

Reservoir Modeling Studies

Secondary Recovery
Miscible Displacement
Gas Storage

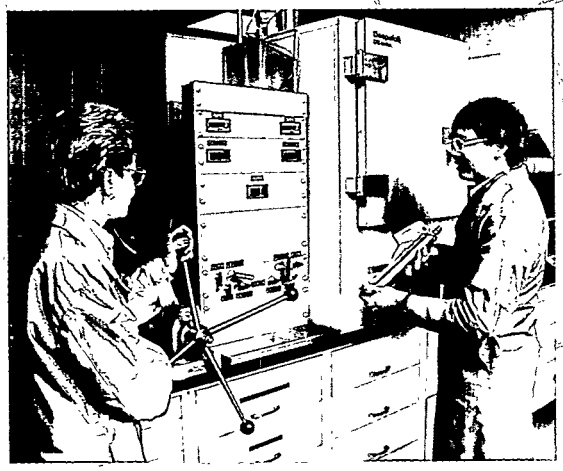
---- Specializing in Fractured Reservoirs ----

- **Tight Sands**
- **Devonian Shale**
- **Antrim Shale**
- **Coalbed Methane**

325 Seminole Trail Danville, VA 24540 (804) 836-9727

Amoco's successful business relationships...

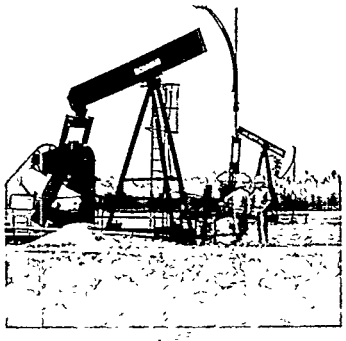
...have kept it a worldwide energy leader for the last 105 years.



With interests in all sectors of the petroleum industry — exploration, production, refining, marketing, power generation, and petrochemicals — Amoco brings key expertise to its partnerships. Amoco also brings the financial strength of U.S. $28 billion in total annual revenues and the experience of exploration and production ventures in over 30 countries.

These combined strengths make Amoco the preferred partner in coalbed methane:

- Current coalbed methane production of 13 million cubic metres/day (470 mmcf/day),
- Agreements in China, India, Australia, and Poland,
- Operating expertise with over 900 coalbed methane wells in three basins and over U.S. $600 million invested,
- Technological leadership with 15 issued U.S. patents and several pending patent applications,
- Patented and field-tested rate and reserve enhancement by gas injection (ECBM).





AMOCO

Amoco Corporation
Share Amoco technology to improve profitability.
Please contact:
U.S.A.: Raj Puri, Denver, CO, USA
Tel. 303-830-5064 Fax 303-830-4276
or
International: Dr. Bill Hanson, Houston, TX, USA
Tel. 713-366-5071 Fax 713-366-7574



"The Alternative Power Source"

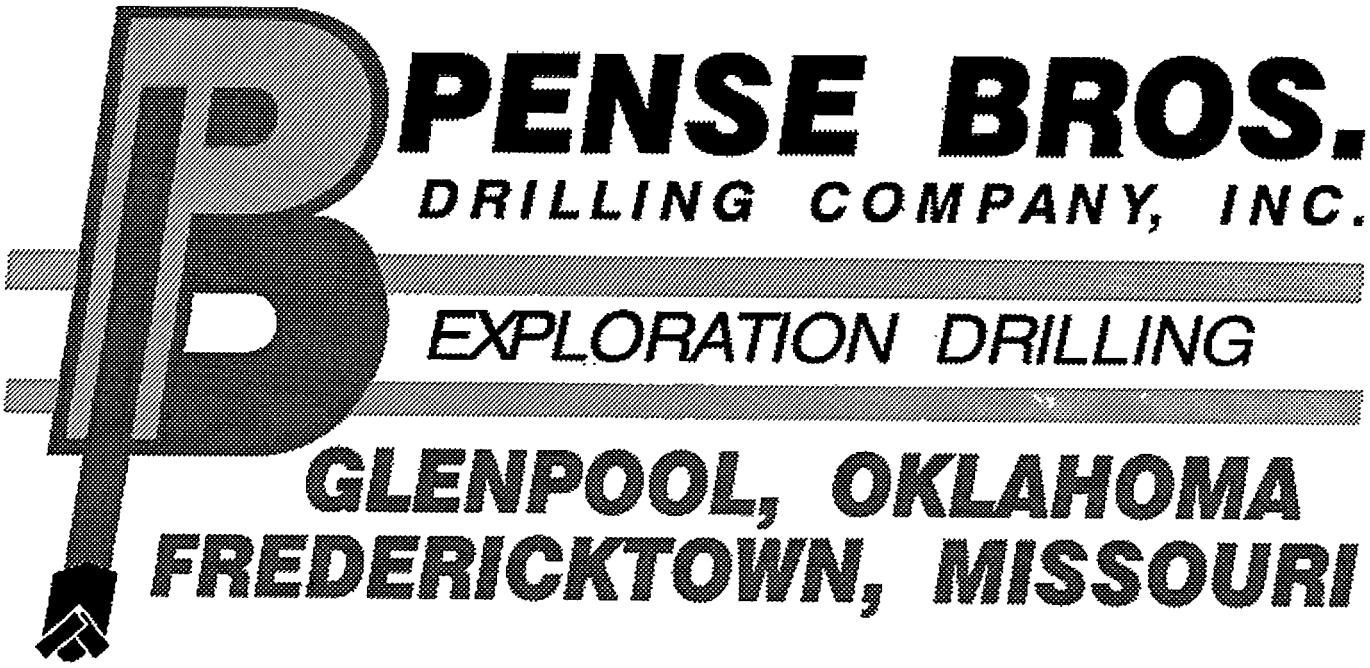
The P-Series Electric Generation System is the advent of induction technology. It will enhance the bottom-line economics of any operation to which it is applied. The P-Series Systems have the lowest operating costs of any electric generation system available and they are OIL FIELD TOUGH.

ELECTRIC GENERATION SYSTEMS THAT SUBSTANTIALLY REDUCE OR TOTALLY OFFSET YOUR ELECTRIC POWER COSTS

- New induction technology -- totally capable of paralleling the utility company without any additional ancillary equipment.
- Utilizes raw field gas as fuel from 400 btu/scf and up
- Extremely low operation & maintenance costs
- Extremely long life cycle components
- All-weather enclosures, including all controls
- Wet sleeved prime mover -- complete overhauls in the field

(713) 893-2020

One Cornerstone Plaza • 3845 FM 1960 West, Suite 270 • Houston, TX 77068 • FAX 893-2059





NOTES

PROCEEDINGS ORDER FORM

Mail this order form to:
InterGas '95 Proceedings
College of Continuing Studies/P&MD
The University of Alabama
Box 870388
Tuscaloosa, Alabama 35487-0388

To order by telephone:
(205)-348-6222

Or FAX order to:
(205)-348-9276

[ ] I enclose $_____for_____additional copies of the Proceedings ($75/copy) for pickup at the University. Please call ahead and your proceedings will be waiting.

[ ] I enclose $_____for_____copies of the Proceedings ($100/copy) to be airmailed to U.S.A., Canada or Mexico address; or surface mailed to other countries.

[ ] I enclose $_____for_____copies of the Proceedings ($135/copy) to be airmailed to other countries.

[ ] I enclose $_____for_____copies of the Proceedings ($175/copy) to be expressed to any address served by major couriers.

Total Payment:

[ ] Check enclosed for $_____Please make check payable to **THE UNIVERSITY OF ALABAMA.** (Checks must be drawn on a U.S.A. bank.)

[ ] Please bill my Company Purchase Order No._____for $_____. P.O. must accompany order.

[ ] Charge $_____ to my credit card.
[ ] MasterCard [ ] VISA [ ] Discover

Card #_____

Expiration Date_____

Authorizing Signature_____

Please mail Proceedings to:
Attach business card here in lieu of completing the following.

Name_____

Company_____

Street Address_____
(No Post Office Box #'s please)

City_____

State_____ZIP/Postal Code_____

Country_____

Phone #_____FAX #_____

LIMITED TIME SPECIAL OFFER

Buy **2 or more** copies of the 1995 Proceedings and receive a 1993 or 1995 proceedings at no additional cost while quantities last.

I prefer [ ] 1993 [ ] 1995

The views and opinions of the authors expressed herein do not necessarily state or reflect those of the sponsors. All papers are subject to correction by the authors.

The sponsors make no warranty or representation, expressed or implied, with respect to the accuracy, completeness, or usefulness of information contained in the publication, or that the use of any apparatus, method, or process disclosed may not infringe privately owned rights.

The sponsors assume no liability with respect to the use of, or for damages resulting from the use of, any information, apparatus, method or process disclosed.

Any use of material contained in this publication in relation to any specific application should be based on independent examination and verification of its unrestricted applicability for such use and on a determination of suitability for the application by professionally qualified personnel.

END DATE

8-28-95